VOLUME 29 / NUMBER 21
NOVEMBER 8, 1991
ACC. NOS. N91-29139 TO N91-30073

STAR
AN ABSTRACT JOURNAL

Scientific and Technical Aerospace Reports

PRODUCED BY THE
SCIENTIFIC AND TECHNICAL
INFORMATION
PROGRAM

NASA

NATIONAL AERONAUTICS AND SPACE ADMINISTRATION

***Scientific and Technical Aerospace Reports* (*STAR*)** is an abstract journal that provides comprehensive coverage of worldwide aerospace-related reports. It is a major product of the International Aerospace Database managed by the NASA Scientific and Technical Information (STI) Program. The coverage includes reports on aeronautics, space, and supporting disciplines. *STAR* lists current, publicly available reports entered into the NASA STI Database during the 2-week period preceding publication. A typical citation and abstract appear on page viii. They explain how to read the items that are announced in this journal.

NASA sponsors a companion journal, *International Aerospace Abstracts* (*IAA*), that lists abstracts of the open literature on aerospace subjects available worldwide. *IAA* is available through the American Institute of Aeronautics and Astronautics.

Entries found in *STAR* and *IAA* are available through NASA's online service, RECON, as the International Aerospace Database and through DIALOG as the Aerospace Database.

Information on aerospace and related subjects is gathered by the NASA STI Program through national and international agreements and exchanges and is made available to the NASA community as well as to the public in many forms through various outlets. The section on NASA STI Program Products and Services contains additional information.

US ISSN 0036-8741

Volume 29 Number 21 / NOVEMBER 8, 1991

TABLE OF CONTENTS

AERONAUTICS For related information see also *Astronautics.*

01 AERONAUTICS (GENERAL) **3451**

02 AERODYNAMICS **3452**
Includes aerodynamics of bodies, combinations, wings, rotors, and control surfaces; and internal flow in ducts and turbomachinery. For related information see also *34 Fluid Mechanics and Heat Transfer.*

03 AIR TRANSPORTATION AND SAFETY **3453**
Includes passenger and cargo air transport operations; and aircraft accidents. For related information see also *16 Space Transportation* and *85 Urban Technology and Transportation.*

04 AIRCRAFT COMMUNICATIONS AND NAVIGATION **3454**
Includes digital and voice communication with aircraft; air navigation systems (satellite and ground based); and air traffic control. For related information see also *17 Space Communications, Spacecraft Communications, Command and Tracking* and *32 Communications and Radar.*

05 AIRCRAFT DESIGN, TESTING AND PERFORMANCE **3455**
Includes aircraft simulation technology. For related information see also *18 Spacecraft Design, Testing and Performance* and *39 Structural Mechanics.* For land transportation vehicles see *85 Urban Technology and Transportation.*

06 AIRCRAFT INSTRUMENTATION ..... **N.A.**
Includes cockpit and cabin display devices; and flight instruments. For related information see also *19 Space craft Instrumentation* and *35 Instrumentation and Photography.*

07 AIRCRAFT PROPULSION AND POWER **3458**
Includes prime propulsion systems and systems components, e.g., gas turbine engines and compressors; and onboard auxiliary power plants for aircraft. For related information see also *20 Spacecraft Propulsion and Power, 28 Propellants and Fuels,* and *44 Energy Production and Conversion.*

08 AIRCRAFT STABILITY AND CONTROL **3460**
Includes aircraft handling qualities; piloting; flight controls; and autopilots. For related information see also *05 Aircraft Design, Testing and Performance.*

09 RESEARCH AND SUPPORT FACILITIES (AIR) **3461**
Includes airports, hangars and runways; aircraft repair and overhaul facilities; wind tunnels; shock tubes; and aircraft engine test stands. For related information see also *14 Ground Support Systems and Facilities (Space).*

ASTRONAUTICS For related information see also *Aeronautics.*

12 ASTRONAUTICS (GENERAL) **3462**
For extraterrestrial exploration see *91 Lunar and Planetary Exploration.*

13 ASTRODYNAMICS **3462**
Includes powered and free-flight trajectories; and orbital and launching dynamics.

14 GROUND SUPPORT SYSTEMS AND FACILITIES (SPACE) **3463**
Includes launch complexes, research and production facilities; ground support equipment, e.g., mobile transporters; and simulators. For related information see also *09 Research and Support Facilities (Air).*

15 LAUNCH VEHICLES AND SPACE VEHICLES **3464**
Includes boosters; operating problems of launch/space vehicle systems; and reusable vehicles. For related information see also *20 Spacecraft Propulsion and Power.*

16 SPACE TRANSPORTATION **3464**
Includes passenger and cargo space transportation, e.g., shuttle operations; and space rescue techniques. For related information see also *03 Air Transportation and Safety* and *18 Spacecraft Design, Testing and Performance.* For space suits see *54 Man/System Technology and Life Support.*

17 SPACE COMMUNICATIONS, SPACECRAFT COMMUNICATIONS, COMMAND AND TRACKING . **N.A.**
Includes telemetry; space communications networks; astronavigation and guidance; and radio blackout. For related information see also *04 Aircraft Communications and Navigation* and *32 Communications and Radar.*

N.A.—no abstracts were assigned to this category for this issue.

18 SPACECRAFT DESIGN, TESTING AND PERFORMANCE **3464**
Includes satellites; space platforms; space stations; spacecraft systems and components such as thermal and environmental controls; and attitude controls. For life support systems see *54 Man/System Technology and Life Support.* For related information see also *05 Aircraft Design, Testing and Performance, 39 Structural Mechanics,* and *16 Space Transportation.*

19 SPACECRAFT INSTRUMENTATION **3466**
For related information see also *06 Aircraft Instrumentation* and *35 Instrumentation and Photography.*

20 SPACECRAFT PROPULSION AND POWER **3466**
Includes main propulsion systems and components, e.g., rocket engines; and spacecraft auxiliary power sources. For related information see also *07 Aircraft Propulsion and Power, 28 Propellants and Fuels, 44 Energy Production and Conversion,* and *15 Launch Vehicles and Space Vehicles.*

CHEMISTRY AND MATERIALS

23 CHEMISTRY AND MATERIALS (GENERAL) **3468**

24 COMPOSITE MATERIALS **3469**
Includes physical, chemical, and mechanical properties of laminates and other composite materials. For ceramic materials see *27 Nonmetallic Materials.*

25 INORGANIC AND PHYSICAL CHEMISTRY **3472**
Includes chemical analysis, e.g., chromatography; combustion theory; electrochemistry; and photochemistry. For related information see also *77 Thermodynamics and Statistical Physics.*

26 METALLIC MATERIALS **3478**
Includes physical, chemical, and mechanical properties of metals, e.g., corrosion; and metallurgy.

27 NONMETALLIC MATERIALS **3484**
Includes physical, chemical, and mechanical properties of plastics, elastomers, lubricants, polymers, textiles, adhesives, and ceramic materials. For composite materials see *24 Composite Materials.*

28 PROPELLANTS AND FUELS **3492**
Includes rocket propellants, igniters and oxidizers; their storage and handling procedures; and aircraft fuels. For related information see also *07 Aircraft Propulsion and Power, 20 Spacecraft Propulsion and Power,* and *44 Energy Production and Conversion.*

29 MATERIALS PROCESSING **3494**
Includes space-based development of products and processes for commercial application. For biological materials see *55 Space Biology.*

ENGINEERING For related information see also *Physics.*

31 ENGINEERING (GENERAL) **3494**
Includes vacuum technology; control engineering; display engineering; cryogenics; and fire prevention.

32 COMMUNICATIONS AND RADAR **3495**
Includes radar; land and global communications; communications theory; and optical communications. For related information see also *04 Aircraft Communications and Navigation* and *17 Space Communications, Spacecraft Communications, Command and Tracking.* For search and rescue see *03 Air Transportation and Safety,* and *16 Space Transportation.*

33 ELECTRONICS AND ELECTRICAL ENGINEERING **3502**
Includes test equipment and maintainability; components, e.g., tunnel diodes and transistors; microminiaturization; and integrated circuitry. For related information see also *60 Computer Operations and Hardware* and *76 Solid-State Physics.*

34 FLUID MECHANICS AND HEAT TRANSFER **3510**
Includes boundary layers; hydrodynamics; fluidics; mass transfer and ablation cooling. For related information see also *02 Aerodynamics* and *77 Thermodynamics and Statistical Physics.*

35 INSTRUMENTATION AND PHOTOGRAPHY **3517**
Includes remote sensors; measuring instruments and gauges; detectors; cameras and photographic supplies; and holography. For aerial photography see *43 Earth Resources and Remote Sensing.* For related information see also *06 Aircraft Instrumentation* and *19 Spacecraft Instrumentation.*

36 LASERS AND MASERS **3520**
Includes parametric amplifiers. For related information see also *76 Solid-State Physics.*

37 MECHANICAL ENGINEERING **3526**
Includes auxiliary systems (nonpower); machine elements and processes; and mechanical equipment.

38 QUALITY ASSURANCE AND RELIABILITY **3529**
Includes product sampling procedures and techniques; and quality control.

39 STRUCTURAL MECHANICS **3530**
Includes structural element design and weight analysis; fatigue; and thermal stress. For applications see *05 Aircraft Design, Testing and Performance* and *18 Spacecraft Design, Testing and Performance.*

GEOSCIENCES For related information see also *Space Sciences.*

42 GEOSCIENCES (GENERAL) ..... **N.A.**

43 EARTH RESOURCES AND REMOTE SENSING **3534**
Includes remote sensing of earth resources by aircraft and spacecraft; photogrammetry; and aerial photography. For instrumentation see *35 Instrumentation and Photography.*

44 ENERGY PRODUCTION AND CONVERSION **3535**
Includes specific energy conversion systems, e.g., fuel cells; global sources of energy; geophysical conversion; and windpower. For related information see also *07 Aircraft Propulsion and Power, 20 Spacecraft Propulsion and Power,* and *28 Propellants and Fuels.*

45 ENVIRONMENT POLLUTION **3537**
Includes atmospheric, noise, thermal, and water pollution.

46 GEOPHYSICS **3540**
Includes aeronomy; upper and lower atmosphere studies; ionospheric and magnetospheric physics; and geomagnetism. For space radiation see *93 Space Radiation.*

47 METEOROLOGY AND CLIMATOLOGY **3542**
Includes weather forecasting and modification.

48 OCEANOGRAPHY **3545**
Includes biological, dynamic, and physical oceanography; and marine resources. For related information see also *43 Earth Resources and Remote Sensing.*

LIFE SCIENCES

51 LIFE SCIENCES (GENERAL) **3547**

52 AEROSPACE MEDICINE **3548**
Includes physiological factors; biological effects of radiation; and effects of weightlessness on man and animals.

53 BEHAVIORAL SCIENCES **3550**
Includes psychological factors; individual and group behavior; crew training and evaluation; and psychiatric research.

54 MAN/SYSTEM TECHNOLOGY AND LIFE SUPPORT **3551**
Includes human engineering; biotechnology; and space suits and protective clothing. For related information see also *16 Space Transportation.*

55 SPACE BIOLOGY ..... **N.A.**
Includes exobiology; planetary biology; and extraterrestrial life.

MATHEMATICAL AND COMPUTER SCIENCES

59 MATHEMATICAL AND COMPUTER SCIENCES (GENERAL) ..... **N.A.**

60 COMPUTER OPERATIONS AND HARDWARE **3552**
Includes hardware for computer graphics, firmware, and data processing. For components see *33 Electronics and Electrical Engineering.*

61 COMPUTER PROGRAMMING AND SOFTWARE **3553**
Includes computer programs, routines, algorithms, and specific applications, e.g., CAD/CAM.

62 COMPUTER SYSTEMS **3559**
Includes computer networks and special application computer systems.

63 CYBERNETICS **3562**
Includes feedback and control theory, artificial intelligence, robotics and expert systems. For related information see also *54 Man/System Technology and Life Support.*

64 NUMERICAL ANALYSIS **3564**
Includes iteration, difference equations, and numerical approximation.

65 STATISTICS AND PROBABILITY **3567**
Includes data sampling and smoothing; Monte Carlo method; and stochastic processes.

66 SYSTEMS ANALYSIS **3570**
Includes mathematical modeling; network analysis; and operations research.

67 THEORETICAL MATHEMATICS ..... **N.A.**
Includes topology and number theory.

PHYSICS For related information see also *Engineering.*

70 PHYSICS (GENERAL) **3571**
For precision time and time interval (PTTI) see *35 Instrumentation and Photography;* for geophysics, astrophysics or solar physics see *46 Geophysics, 90 Astrophysics,* or *92 Solar Physics.*

71 ACOUSTICS **3572**
Includes sound generation, transmission, and attenuation. For noise pollution see *45 Environment Pollution.*

72 ATOMIC AND MOLECULAR PHYSICS **3573**
Includes atomic structure, electron properties, and molecular spectra.

73 NUCLEAR AND HIGH-ENERGY PHYSICS **3579**
Includes elementary and nuclear particles; and reactor theory. For space radiation see *93 Space Radiation.*

74 OPTICS **3580**
Includes light phenomena and optical devices. For lasers see *36 Lasers and Masers.*

75 PLASMA PHYSICS **3584**
Includes magnetohydrodynamics and plasma fusion. For ionospheric plasmas see *46 Geophysics.* For space plasmas see *90 Astrophysics.*

76 SOLID-STATE PHYSICS **3590**
Includes superconductivity. For related information see also *33 Electronics and Electrical Engineering* and *36 Lasers and Masers.*

77 THERMODYNAMICS AND STATISTICAL PHYSICS **3601**
Includes quantum mechanics; theoretical physics; and Bose and Fermi statistics. For related information see also *25 Inorganic and Physical Chemistry* and *34 Fluid Mechanics and Heat Transfer.*

SOCIAL SCIENCES

80 SOCIAL SCIENCES (GENERAL) **3602**
Includes educational matters.

81 ADMINISTRATION AND MANAGEMENT **3602**
Includes management planning and research.

82 DOCUMENTATION AND INFORMATION SCIENCE **3603**
Includes information management; information storage and retrieval technology; technical writing; graphic arts; and micrography. For computer documentation see *61 Computer Programming and Software.*

83 ECONOMICS AND COST ANALYSIS ..... **N.A.**
Includes cost effectiveness studies.

84 LAW, POLITICAL SCIENCE AND SPACE POLICY ..... **N.A.**
Includes NASA appropriation hearings; aviation law; space law and policy; international law; international cooperation; and patent policy.

85 URBAN TECHNOLOGY AND TRANSPORTATION **3605**
Includes applications of space technology to urban problems; technology transfer; technology assessment; and surface and mass transportation. For related information see *03 Air Transportation and Safety, 16 Space Transportation,* and *44 Energy Production and Conversion.*

SPACE SCIENCES For related information see also *Geosciences.*

88 SPACE SCIENCES (GENERAL) ..... **N.A.**

89 ASTRONOMY **3605**
Includes radio, gamma-ray, and infrared astronomy; and astrometry.

90 ASTROPHYSICS **3605**
Includes cosmology; celestial mechanics; space plasmas; and interstellar and interplanetary gases and dust. For related information see also *75 Plasma Physics.*

91 LUNAR AND PLANETARY EXPLORATION **3606**
Includes planetology; and manned and unmanned flights. For spacecraft design or space stations see *18 Spacecraft Design, Testing and Performance.*

92 SOLAR PHYSICS **3607**
Includes solar activity, solar flares, solar radiation and sunspots. For related information see *93 Space Radiation.*

93 SPACE RADIATION ..... **N.A.**
Includes cosmic radiation; and inner and outer earth's radiation belts. For biological effects of radiation see *52 Aerospace Medicine.* For theory see *73 Nuclear and High-Energy Physics.*

GENERAL

Includes aeronautical, astronautical, and space science related histories, biographies, and pertinent reports too broad for categorization; histories or broad overviews of NASA programs.

99 GENERAL **3607**

SUBJECT INDEX **I-1**

PERSONAL AUTHOR INDEX **I-69**

CORPORATE SOURCE INDEX **I-77**

CONTRACT NUMBER INDEX **I-89**

REPORT/ACCESSION NUMBER INDEX **I-93**

APPENDIX **A-1**

TYPICAL CITATION AND ABSTRACT

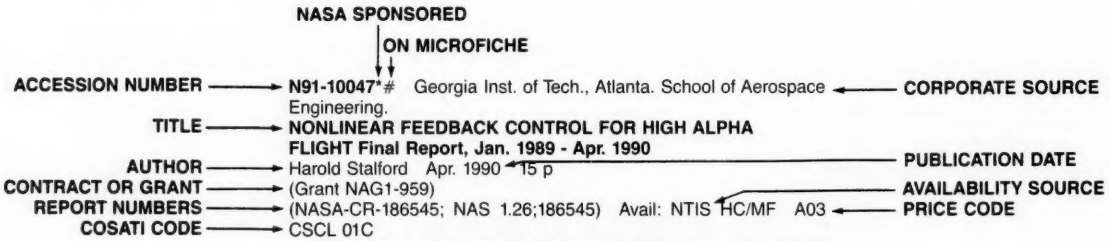

Analytical aerodynamic models are derived from a high alpha 6 DOF wind tunnel model. One detail model requires some interpolation between nonlinear functions of alpha. One analytical model requires no interpolation and as such is a completely continuous model. Flight path optimization is conducted on the basic maneuvers: half-loop, 90 degree pitch-up, and level turn. The optimal control analysis uses the derived analytical model in the equations of motion and is based on both moment and force equations. The maximum principle solution for the half-loop is poststall trajectory performing the half-loop in 13.6 seconds. The agility induced by thrust vectoring capability provided a minimum effect on reducing the maneuver time. By means of thrust vectoring control the 90 degrees pitch-up maneuver can be executed in a small place over a short time interval. The agility capability of thrust vectoring is quite beneficial for pitch-up maneuvers. The level turn results are based currently on only outer layer solutions of singular pertrubation. Poststall solutions provide high turn rates but generate higher losses of energy than that of classical sustained solutions.

Author

VOLUME 29 NUMBER 21 / NOVEMBER 8, 1991

Scientific and Technical Aerospace Reports

A Semimonthly Publication of the National Aeronautics and Space Administration

01 AERONAUTICS (GENERAL)

N91-29139# National Aeronautical Establishment, Ottawa (Ontario).
COMMONWEALTH ADVISORY AERONAUTICAL RESEARCH COUNCIL. FIRST CANADIAN NEWSLETTER ON SYSTEMS, 1989
John B. Croll Jul. 1989 45 p
(NAE-LTR-FR-108; CTN-91-60083) Copyright Avail: NTIS HC/MF A03

The Commonwealth Advisory Aeronautical Research Council (CAARC) exists to encourage and coordinate aeronautical research among four member countries: Australia, Canada, India and the United Kingdom. The five fields of colaboration within CAARC are aerodynamics, human engineering, propulsion, structures and systems. The field of systems includes display systems including night visioning systems, direct voice input/output systems, control technology (parameter estimation and mathematical modelling), integrayed flight control, satellite based systems, integrated navigation systems, and simulators. Brief descriptions are given of current Canadian research and development efforts relating to these areas. Reports are presented which were provided by universities, industry, and government agencies involved in aerospace systems research. A list of contributors and of Canadian companies involved in the manufacture of avionics and electronics products related to the selected systems topics is included.
CISTI

N91-29140# National Aeronautical Establishment, Ottawa (Ontario).
[FLIGHT RESEARCH LABORATORY. INSTITUTE FOR AEROSPACE RESEARCH] Annual Progress Report, April 1989 - March 1990
Jun. 1990 163 p
(CTN-91-60105) Copyright Avail: NTIS HC/MF A08

A summary is presented of progress in the research project of the Flight Research Laboratory (formerly the National Aeronautical Establishment) of the National Research Council of Canada, with a brief indication of plans for continuing and new projects. Flight Research Lab facilities include a fleet of five research aircraft, including a Twin Otter aircraft instrumented for atmospheric research, a Bell 205A airborne simulator used to simulate control systems in helicopters and other aircraft, a Convair 580 multipurpose flying laboratory, a T-33 platform for use in microgravity studies, and a Falcon 20 jet which was recently added to the research fleet. This aircraft is currently being prepared for applications in the areas of microgravity research, microwave landing system studies and atmospheric sensing. The Flight Recorder Playback Centre provides a facility for playback of cockpit flight recorders, flight data recorders, air traffic control tapes, and video tape recorders. The Speech Research Centre is equipped to study voice I/O technology and to support aircraft crash investigations on the research program of the Flight Research Laboratory. Most research is carried out as joint projects with collaborators from industry, universities and cooperating government agencies.
CISTI

N91-29141# Air Force Systems Command, Wright-Patterson AFB, OH. Foreign Technology Div.
INTERNATIONAL AVIATION (SELECTED ARTICLES)
25 Apr. 1991 71 p Transl. into ENGLISH from Guoji Hangkong (Peoples Rep. of China), no. 6, 1989 p 7-27
(AD-A237175; FTD-ID(RS)T-0533-90) Avail: NTIS HC/MF A04 CSCL 01/1

Translations are presented of articles from Chinese publication. Some topics of discussion are as follows: China's Developing Flight Test Research Center; Civilian Aircraft Flight Testing Technology; The BW-1 Longitudinal Variable Stability Aircraft; Experiments to Measure Flight Test Vibration and Flutter; by Guan Peifang; Thirty Years of Powerplant Flight Test Research; The Test Flight Center's Flight Simulation Devices; Aircraft Engine Environmental and Ingestion Testing; Test Flight Technology for Aviation Electronics Equipment; Flight Testing of Ejection Seat Systems, Remote Sensing for Aerial Photography; Feilundi TRANSLITERATION Produces an Optical Communications Installation for Helicopters; Flight Testing Aircraft Fire Control, Special Equipment and Electronic and Automatic Control System.
GRA

N91-29142# Air Force Systems Command, Wright-Patterson AFB, OH. Foreign Technology Div.
INTERNATIONAL AVIATION (SELECTED ARTICLES)
19 Mar. 1991 21 p Transl. into ENGLISH from Guoji Hangkong (Peoples Rep. of China), no. 314, Apr. 1989 p 52-56
(AD-A237232; FTD-ID(RS)T-0691-90) Avail: NTIS HC/MF A03 CSCL 01/3

Airborne Equipment and Systems are discussed. The following topics are included: (1) Model 10 Series Aerodynamic-Panel Emergency Escape Parachute, and (2) China-Made Liquid Cooling Vest for Pilots.
GRA

N91-29143# Pennsylvania State Univ., University Park. Applied Research Lab.
TRANSLATION OF AIRFOIL TRAILING EDGE NOISE ARTICLE FROM REVUE D'ACOUSTIQUE
R. C. Marboe and R. M. Weyer 25 Jun. 1991 31 p Transl. into ENGLISH from Revue d'Acoustique (France), no. 73, 1985 p 3
(Contract N00039-88-C-0051)
(AD-A237811; PSU-ARL-TM-91-120) Avail: NTIS HC/MF A03 CSCL 01/1

The paper Bruit d'un profil dans un e'coulement, by P. Garcia and P. Gerard, has been translated into English. The paper originally was published in Revue d'Acoustique, No 73, 1985 2/2 by Office National d'Etudes et de Recherches Aerospatiales (ONERA). The work, Airfoil noise in air flow, describes measurements of the wave number spectrum of the turbulent boundary layer induced pressure field in the vicinity of the airfoil trailing edge. An estimate of radiated noise using modifications to the theories of Howe and Hogdson is made. The paper is significant because of the good agreement between the measurements of Brooks and Hogdson (1980) and a predicted radiated noise level based on a measured trailing edge fluctuating pressure wave number spectrum with measured far field radiated noise. An effect of array element separation distance on measured convection velocity is also shown.
GRA

02 AERODYNAMICS

Includes aerodynamics of bodies, combinations, wings, rotors, and control surfaces; and internal flow in ducts and turbomachinery.

For related information see also *34 Fluid Mechanics and Heat Transfer.*

N91-29144# National Aeronautical Establishment, Ottawa (Ontario). Unsteady Aerodynamics Lab.
SUBSONIC AERODYNAMIC COEFFICIENTS OF THE SDM AT ANGLES OF ATTACK UP TO 90 DEG
X. Z. Huang and M. E. Beyers Jan. 1990 55 p
(NAE-LTR-UA-93; CTN-91-60006) Copyright Avail: NTIS HC/MF A04

Static aerodynamic coefficients were obtained for the Standard Dynamics Model (SDM), a generic fighter aircraft model, at angles of attack up to 90 deg. Effects of sideslip angle, wind speed and sting diameter were investigated under conditions of very low wall interference. The aerodynamic characteristics of the SDM are consistent with asymmetrical vortex shedding becoming dominant at angles of attack between 26 and 53 deg, and asymmetrical vortex breakdown occurring on the wing at higher angles of attack between 53 and 69 deg. The lateral-directional coefficients exhibited nonlinear dependence on angle of sideslip as well as angle of attack. The variations with angle of sideslip of the longitudinal aerodymanic and rolling moment coefficients are asymmetrical at angle of attack equals 36 deg. There was no distinct effect of velocity/Reynolds number for wind speeds between 69 and 100 m/s. Sting diameter effects were negligible at low angles of attack. Small but measurable effects of sting diameter on the side-force and moment coefficients were observed in angles of attack between 28 and 63 deg. Author (CISTI)

N91-29145# National Aeronautical Lab., Bangalore (India).
PERFORMANCE OF AN AIRFOIL AT LOW REYNOLDS NUMBER
Premalatha and P. Ramamoorthy Mar. 1991 83 p
(NAL-PD-CF-9102) Avail: NTIS HC/MF A05

A new airfoil performance software was developed by combining two independent codes. The first one is based on Theodorsen's thick airfoil theory, and the second is a boundary layer code based on the integral method. The lift and pitching moment coefficients are obtained by Theodorsen's theory, suitably modified for the viscous effects. The comparison between this code and the NCSU code and experiments for a few low drag airfoils show good correlation. Hence, the code has great potential for further development. Author

N91-29146# National Aeronautical Lab., Bangalore (India).
AEROWING - THE SOFTWARE FOR AERODYNAMIC ANALYSIS OF A LARGE ASPECT-RATIO FINITE WING AT LOW SPEEDS
P. Ramamoorthy and B. K. Premageetha Mar. 1991 17 p
(NAL-PD-CF-9101) Avail: NTIS HC/MF A03

An existing computer software package for the determination of lift, drag, and pitching moment of the finite wing is ported onto PS 386/387 system and validated against known examples. This software, is presently designated as AEROWING and is used to obtain the loads on the wing of an remotely piloted vehicle. The results prove that the software can provide a tool for the wing analysis and design. Author

N91-29147*# Akron Univ., OH. Dept. of Electrical Engineering.
EXACT AND APPROXIMATE SOLUTIONS TO THE OBLIQUE SHOCK EQUATIONS FOR REAL-TIME APPLICATIONS Final Report
T. T. Hartley, R. Brandis, and F. Mossayebi Aug. 1991 9 p
(Grant NAG3-904)
(NASA-CR-187173; NAS 1.26:187173) Avail: NTIS HC/MF A02 CSCL 01A

The derivation of exact solutions for determining the characteristics of an oblique shock wave in a supersonic flow is investigated. Specifically, an explicit expression for the oblique shock angle in terms of the free stream Mach number, the centerbody deflection angle, and the ratio of the specific heats, is derived. A simpler approximate solution is obtained and compared to the exact solution. The primary objectives of obtaining these solutions is to provide a fast algorithm that can run in a real time environment. Author

N91-29148# McDonnell-Douglas Missile Systems Co., Saint Louis, MO.
MISSILE DATCOM: USER'S MANUAL Final Report, May 1987 - Apr. 1991
Kevin D. Bruns, Marvin E. Moore, Stan L. Stoy, Steven R. Vukelich, and William B. Blake Apr. 1991 133 p Revised Supersedes AD-A210128
(Contract F33615-87-C-3604)
(AD-A237817; WL-TR-91-3039; AD-A210128) Avail: NTIS HC/MF A07 CSCL 16/2

In missile preliminary design it is necessary to quickly and economically estimate the aerodynamics of a wide variety of missile configuration designs. Since the ultimate shape and aerodynamic performance are so dependent upon the subsystems used, such as payload size, propulsion system selection and launch mechanism, the designer must be capable of predicting a wide variety of configurations accurately. The fundamental purpose of Missile Datcom is to provide an aerodynamic design tool which has the predictive accuracy suitable for preliminary design, and the capability for the user to easily substitute methods to fit specific applications. GRA

N91-29149# Department of the Navy, Washington, DC.
STABILIZED SQUARE PARACHUTE Patent Application
Carl Calianno, inventor (to Navy) 19 Apr. 1990 13 p
(AD-D014946; US-Patent-Appl-SN-518619) Avail: NTIS HC/MF A03 CSCL 01/1

This invention relates generally to aerodynamic decelerators and more particularly to the aerodynamic stabilization of parachutes having square canopies. When dropping a store such as a sonobuoy into the ocean from a high altitude it is necessary to assure proper orientation upon impact. This requires the use of a parachute which has high drag to slow the store's descent and stability to minimize its oscillations. Parachute instability, caused by destabilizing aerodynamic side forces on the canopy, is translated to the store through the parachute's suspension lines, causing the store to oscillate, adversely affecting impact orientation. An air-deployed payload which has a video camera mounted therein for transmission during air descent also requires a parachute with high drag efficiency and extreme stability to prevent oscillation of the payload during descent. GRA

N91-29150*# National Aeronautics and Space Administration. Lewis Research Center, Cleveland, OH.
PROGRESS TOWARD SYNERGISTIC HYPERMIXING NOZZLES
D. O. Davis and W. R. Hingst 1991 11 p Presented at the 27th Joint Propulsion Conference, Sacramento, CA, 24-27 Jun. 1991; sponsored by AIAA, SAE, ASME, and ASEE Previously announced as A91-45800
(NASA-TM-105169; E-6461; NAS 1.15:105169; AIAA-91-2264)
Copyright Avail: NTIS HC/MF A03 CSCL 01A

Mean flow measurements were obtained for air-to-air mixing downstream of swept and unswept ramp wall mounted hypermixing nozzle configurations. Aside from the sweep of the ramps, the two nozzle configurations studied are identical. The nozzles inject three parallel supersonic jets at a 15 deg angle (relative to the wind tunnel wall) into a supersonic freestream. Mach number and volume fraction distributions in a transverse plane 11.1 nozzle heights downstream from the nozzle exit plane were measured. Data are presented for a freestream Mach number of three at a matched static pressure condition and also at underexpanded static pressure condition (pressure ratio = 5). Surface oil flow visualization was used to study the near wall flow behavior. The results indicate that the swept ramp injectors produce stronger and larger vortex pairs than the unswept ramp injectors. The

increased interaction between the swept ramp model's larger vortex pairs yields better mixing characteristics for this model. Author

N91-29151# Sandia National Labs., Albuquerque, NM.
THE FUNCTIONAL DEPENDENCE OF TRAJECTORY DISPERSION ON INITIAL CONDITION ERRORS
R. A. LaFarge and R. S. Baty 1991 9 p Presented at the American Institute of Aeronautics and Astronautics (AIAA) Guidance, Navigation, and Control Conference, New Orleans, LA, 12-14 Aug. 1991
(Contract DE-AC04-76DP-00789)
(DE91-014661; SAND-91-0062C; CONF-910847-2) Avail: NTIS HC/MF A02

Six-degree-of-freedom (6DOF) trajectory codes are used for a wide range of pre-flight and post-flight tasks to compute the flight behavior of most vehicles. Some of the pre-flight tasks include investigations of resonance conditions, predictions of nominal downrange and crossrange values, and estimates of dispersion for range safety studies. Engineers involved in fuze effectiveness studies also apply 6DOF codes with scoring codes to determine the probability of kill (P(sub k)) of a given fuze. The scoring codes investigate multiple trajectories and actually count now many of the burst locations killed the target. The trajectories simulated in these fuze studies use computationally expensive Monte Carlo techniques. There are occasions, however, when a ballpark estimate of the maximum bounds of the burst points is quite adequate. In the present paper, a technique for estimating burst dispersion based on computing just a few trajectories is proposed. This approach is based on the property that the equations of motion produce solutions that vary continuously with initial conditions. Results from numerical experiments that simulate a fuze effectiveness study are compared to the dispersion bounds predicted by the approach. The agreement is excellent. DOE

03 AIR TRANSPORTATION AND SAFETY

Includes passenger and cargo air transport operations; and aircraft accidents.

For related information see also *16 Space Transportation* and *85 Urban Technology and Transportation.*

N91-29152# Idaho National Engineering Lab., Idaho Falls.
ENVIRONMENTAL ASSESSMENT FOR THE FAA EXPLOSIVE DETECTION SYSTEM INDEPENDENT VALIDATION AND VERIFICATION PROGRAM
May 1991 17 p Prepared in cooperation with Department of Energy, Idaho Falls, ID
(Contract DE-AC07-76ID-01570)
(DE91-013190; DOE/EA-0507) Avail: NTIS HC/MF A03

The urgent development, fabrication, and operation of advanced explosive detection systems are needed by the Federal Aviation Agency (FAA) to counteract potential terrorist threats. The Department of Energy (DOE) proposes to provide independent testing of such devices at the Idaho National Engineering Laboratory (INEL) to evaluate their effectiveness. Testing of explosive detection devices at the INEL would provide data from which explosive detection devices may be chosen for deployment by the FAA. The potential risks posed by the explosive handling and storage can be managed by safe administrative controls and proper training of personnel. The facility proposed for the action is in an isolated location and requires minimum renovations. Environmental impacts resulting from the proposed validation and verification tests would be minimal. DOE

N91-29153# Federal Aviation Administration, Washington, DC. Office of Aviation Medicine.
DONNING TIMES AND FLOTATION CHARACTERISTICS OF INFANT LIFE PRESERVERS: FOUR REPRESENTATIVE TYPES Final Report
Gordon E. Funkhouser and Gregory W. Fairlie Apr. 1991 12 p
(AD-A237120; DOT/FAA/AM-91/6) Avail: NTIS HC/MF A03 CSCL 06/11

Four currently available representative types of infant life preservers were tested to assess the donning times and flotation characteristics for infant subjects (6 months to 2 years old). Two of the four devices tested were fixed-foam recreational devices and two were inflatable, dual-chambered devices that met TSO C-13d requirements. The parent received video-taped donning instructions prior to the timed donning trials. Donning times were recorded from the time the unwrapped device was handed to the parent until the last connection or adjustment was made. The device that was most quickly donned was an inflatable type with a vest attached to the top of the upper chamber (median donning time was 28.8 seconds). This infant life preserver also exhibited good body support with the head well above the water. The two fixed-foam devices were designed to have approximately one-third of the buoyancy of the two inflatable types and relied on assistance from an adult to maintain the infant in a safe flotation attitude. It appears that the fixed-foam infant life preservers would provide more thermal protection than the inflatable life preservers. GRA

N91-29154# Gates Learjet Corp., Wichita, KS.
AIRCRAFT ICING HANDBOOK, VOLUME 1 Final Report, Feb. 1985 - Mar. 1991
A. Heinrich, Richard Ross, Glen Zumwalt, John Provorse, and Viswa Padmanabhan Mar. 1991 393 p
(Contract DTFA03-85-C-00007)
(AD-A238039; DOT/FAA/CT-88/8-1-Vol-1) Avail: NTIS HC/MF A17 CSCL 01/3

The design and validation of adequate aircraft ice protection has evolved into a specialized and technically complex area were many engineering disciplines are involved; namely, aeronautical, electrical, mechanical, electronics, chemical simulations, mathematical modeling, airframe/engine systems design, atmospheric physics, and meteorology. Research advances in any one discipline have a direct effect on updating the procedural technology used in the design and validation of ice protection configurations, equipment, and systems. Periodically the Federal Aviation Administration (FAA) provides documentation to assist regulatory certification teams and industry design engineers in standardizing testing and validating procedures. Examples of such documentation are Engineering Summary of Airframe Icing Technical Data, FAA Report No. ADS-4 dated December 1968, and Engineering Summary of Powerplant Icing Technical Data, FAA Report No. RD-77-76 dated July 1977. Although most of the information contained in these reports is still valid, some is outdated, and more usable information is now available through recent research and experience. Therefore, this work was directed towards developing an updated and more comprehensive combined version of Report ADS-4 and RD-77-76 that includes reference material on ground and airborne icing facilities, simulation procedures, and analytical techniques. This document represents all types and classes of aircraft and is intended as a working tool for GRA

N91-29155# Gates Learjet Corp., Wichita, KS.
AIRCRAFT ICING HANDBOOK, VOLUME 2 Final Report, Feb. 1985 - Mar. 1991
A. Heinrich, Richard Ross, Glen Zumwalt, John Provorse, and Viswa Padmanabhan Mar. 1991 604 p
(Contract DTFA03-85-C-00007)
(AD-A238040; DOT/FAA/CT-88/8-2-Vol-2) Avail: NTIS HC/MF A99 CSCL 01/3

The design and validation of adequate aircraft ice protection has evolved into a specialized and technically complex area where many engineering disciplines are involved; namely, aeronautical, electrical, mechanical, electronics, chemical simulations, mathematical modeling, airframe/engine systems design, atmospheric physics, and meteorology. Research advances in any one discipline have a direct effect on updating the procedural technology used in the design and validation of ice protection configurations, equipment, and systems. Periodically the Federal Aviation Administration (FAA) provides documentation to assist

regulatory certification teams and industry design engineers in standardizing testing and validating procedures. Examples of such documentation are Engineering Summary of Airframe Icing Technical Data, FAA Report No. ADS-4 dated December 1968, and Engineering Summary of Powerplant Icing Technical Data, FAA Report No. RD-77-76 dated July 1977. Although most of the information contained in these reports is still valid, some is outdated, and more usable information is now available through recent research and experience. Therefore, this work was directed towards developing an updated and more comprehensive combined version of Report ADS-4 adn RD-77-76 that includes reference material on ground and airborne icing facilities, simulation procedures, and analytical techniques. This document represents all types and classes of aircraft and is intended as a working too GRA

N91-29156# Gates Learjet Corp., Wichita, KS.
AIRCRAFT ICING HANDBOOK, VOLUME 3 Final Report, Feb. 1985 - Mar. 1991
A. Heinrich, Richard Ross, Glen Zumwalt, John Provorse, and Viswa Padmanabhan Mar. 1991 242 p
(Contract DTFA03-85-C-00007)
(AD-A238041; DOT/FAA/CT-88/8-3-Vol-3) Avail: NTIS HC/MF A11 CSCL 01/3

The design and validation of adequate aircraft ice protection has evolved into a specialized and technical complex area where many engineering disciplines are involved; namely, aeronautical, electrical, mechanical, electronics, chemical simulations, mathematical modeling, airframe/engine systems design, atmospheric physics, and meteorology. Research advances in any one discipline have a direct effect on updating the procedural technology used in the design and validation of ice protection configurations, equipment, and systems. Periodically the Federal Aviation Administration (FAA) provides documentation to assist regulatory certification teams and industry design engineers in standardizing testing and validating procedures. Examples of such documentation are Engineering Summary of Airframe Icing Technical Data, FAA Report No. ADS-4 dated December 1968, and Engineering Summary of Powerplant Icing Technical Data, FAA Report No. RD-77-76 dated July 1977. Although most of the information contained in these reports is still valid, some is outdated, and more usable information is now available through recent research and experience. Therefore, this work was directed towards developing an updated and more comprehensive combined version of Report ADS-4 and RD-77-76 that includes reference material on ground and airborne icing facilities, simulation procedures, and analytical techniques. This document represents all types and classes of aircraft and is intended as a working tool for GRA

N91-29157# National Transportation Safety Board, Washington, DC. Bureau of Accident Investigation.
AIRCRAFT ACCIDENT REPORTS: BRIEF FORMAT US CIVIL AND FOREIGN AVIATION ISSUE NUMBER 1 OF 1989 ACCIDENTS
18 Dec. 1990 413 p
(PB90-916901; NTSB/AAB-90/01) Avail: NTIS HC/MF A18; Paper copy also avail.on Standing Order deposit account required (minimum deposit $100 US, Canada, and Mexico; all others $200) CSCL 01C

Selected aircraft accident reports for both U.S and foreign aviation operations in 1989 are briefly reported. The approximately 200 accidents presented here represent a random selection. Facts, conditions, circumstances, and probable causes for each accident are given. Author

04 AIRCRAFT COMMUNICATIONS AND NAVIGATION

Includes digital and voice communication with aircraft; air navigation systems (satellite and ground based); and air traffic control.

For related information see also *17 Space Communications, Spacecraft Communications, Command and Tracking* and *Communications and Radar.*

N91-29158# National Aeronautical Establishment, Ottawa (Ontario).
EVALUATION OF A PRE-PRODUCTION VERSION OF CANADIAN MARCONI CMA-786 GPS RECEIVER
T. Onno and C. D. Hardwick Mar. 1989 36 p
(NAE-LTR-FR-106; CTN-91-60030) Copyright Avail: NTIS HC/MF A03

An evaluation of suitability of the Canadian Marconi Company's (CMC) CMA-786 GPs receiver for accurately positioning an in-flight aircraft with data from the U.S. Global Positioning System is described. Receivers were tested in a variety of static and dynamic conditions. A number of performance limitations were identified, the most significant being the inability to maintain satellite tracking under highly dynamic flight conditions. Changes made by CMC resulted in reliable tracking up to Rate 2 turns (6 degrees per second turn rates). The use of two receivers for differential correction of position bias was evaluated. The method will correct for slow drift errors in dynamic operation where only minimum filtering is allowable. In the present version of the CMC Kalman filter differential correction program, any gaps in the data can cause large transient errors in output position. The satellites have occasionally given indications of erratic behavior, and crosschecking of results is essential if high accuracy is required. Within these limitations, the CMA-786 receiver has demonstrated the potential for a radically improved accuracy of aircraft navigation. Evaluation during one flight gave comparison within 20 meters against a high precision microwave transponder system during most of the steady parts of the flight. CISTI

N91-29159# National Aeronautical Establishment, Ottawa (Ontario). Inst. for Aerospace Research
FLIGHT EVALUATION OF COMPLEX APPROACHES IN A TWIN OTTER AIRCRAFT USING A MICROWAVE LANDING SYSTEM
John B. Croll Jul. 1990 111 p
(NAE-LTR-FR-114; CTN-91-60103) Copyright Avail: NTIS HC/MF A06

Flight testing of curved, segmented approaches using a microwave landing system (MLS) was conducted on a Twin Otter aircraft. Algorithms were written to define several different approach configurations and to provide precision guidance to both straight and curved segments. These algorithms were developed and validated in flight during the software development phase of the project. A pilot evaluation phase was subsequently flown to assess the tracking accuracies and pilot workload associated with flying these approaches. Seven experienced pilots flew several different approaches each. Standard aircraft electro-mechanical flight instruments were modified slightly to assist the pilots. All approaches were flown successfully using instruments only, despite some problems in the performance of the lateral flight director. Approach track deviations and pilot workload were found to increase as a direct function of the track angle changes on the curved segments, though influenced by the limitations of the lateral flight director. Automatic course updating was rated as most essential and the heading index presentations had some use. The normal radio magnetic indicator was not generally used and the distance measuring equipment was rated as occasionally useful. All pilots felt that a plan view of the approach should be displayed for approaches with five or more segments and that a presentation of the next waypoint number, its bearing and distance, and the along track distance to touchdown should be mounted on the instrument panel. Author (CISTI)

N91-29160# National Aeronautical Establishment, Ottawa (Ontario).
NAE PARTICIPATION IN THE UNITED STATES FAA VERTICAL SEPARATION STUDY
J. Aitken Jan. 1989 21 p
(NAE-LTR-FR-105; CTN-91-60124) Copyright Avail: NTIS HC/MF A03

In order to assess the safety implications of reducing the vertical separation above flight level of 29,000 feet (FL290) from 2000 to 1000 feet, a number of International Civil Aviation Organization (ICAO) countries have conducted studies pertaining to aircraft height keeping performance. The National Aeronautical Establishment (NAE) of Canada participation in the United States Federal Aviation Administration Vertical Separation Study over the period of December 1984 to January 1987 is described. The NAE T-33 C-FSKH was flown a total of 289 hours. In conjunction with a NASA height finding radar, C-FSKH was used to determine accurate flight level heights in five study locations, one in Canada and four in the US. Extensive calibration studies were performed on the aircraft in support of the program. The studies included direct intercomparison flights with the program's second pacer aircraft, the NCAR Sabrelliner N307D. The study objectives are described along with the data collection procedures, the aircraft and instrumentation, the calibration procedures, and data transfer methods. It is reported that the major conclusion of the ICAO report is that 1000 vertical separation above FL290 is not feasible globally but may be feasible regionally. CISTI

N91-29161 Newcastle-upon-Tyne Univ. (England).
GPS: ASPECTS OF PSEUDO-RANGE POSITIONING OFFSHORE Ph.D. Thesis
Adrian A. Drewett 1989 180 p
Avail: Univ. Microfilms Order No. BRDX91851

A Global Positioning System (GPS), in particular its pseudo-range observable in the context of the offshore environment, is studied. The basic components of satellite motion and position computation are examined within the various coordinate systems used. A computer program which predicts the location of the GPS satellites and determines whether they are visible from a given receiver location was developed. It includes the algorithms for predicting the precision with which the receiver position can be computed given any particular satellite/receiver geometry. The effect of holding a station height fixed to an incorrect height is studied. Differential GPS is proposed as the main way in which GPS will be used on a dynamic platform such as a survey vessel. The accuracy which can be expected from differential GPS is studied and a new dilution of precision figure (DDOP) is developed to indicate the expected precision of the differential correction, and this is illustrated with DDOP contour plots. Through a study carried out on data captured in the North Sea, it is shown that GPS can be an efficient calibration tool which enhances the operational capabilities of the Pulse/8 system in the North Sea and enhances the number of costly reruns of seismic survey lines. Dissert. Abstr.

N91-29162# Mitre Corp., Bedford, MA.
MOBILE MICROWAVE LANDING SYSTEM (MMLS) USER INTERFACE Final Report
S. K. Verma May 1991 26 p
(Contract F19628-89-0001-5420)
(AD-A237470; MTR-11051; ESD-TR-91-205) Avail: NTIS HC/MF A03 CSCL 17/7

This paper describes a user friendly Mobile Microwave Landing System (MMLS) interface design, based on menu schemes, that needs only a small number of function keys and limited display size. Although the design was developed for consideration in the local and remote control units for the MMLS, it is suitable for implementation on other control system interfaces where weight, display size, and/or the number of keys be kept to a minimum. GRA

N91-29163# Massachusetts Inst. of Tech., Cambridge.
MILLIMETER-ACCURACY SATELLITE NAVIGATION Technical Report, 29 Apr. 1986 - 8 Apr. 1991
C. C. Counselman 8 Apr. 1991 24 p
(Contract F19628-86-K-0009)
(AD-A237736; PL-TR-91-2087) Avail: NTIS HC/MF A03 CSCL 17/7

Millimeter-accuracy satellite navigation, defined as the determination of instantaneous position coordinates of a point on a moving platform (land/sea/air/space vehicle) with respect to a reference frame defined by points fixed on the ground, with millimeter-level uncertainties, is possible using the satellite radio interferometry techniques. These techniques include use of doubly-differenced, dual-band, reconstructed-carrier phase observations of the NAVSTAR GPS satellites simultaneously from the unknown point and from fixed reference points suitably arrayed on the ground so that the integer-cycle ambiguities of their observations can be resolved to reduce satellite orbit uncertainties. For instantaneous ambiguity resolution of the moving-platform observations, at least seven satellites must be observed simultaneously. If the available number of NAVSTAR satellites is insufficient, GLONASS satellites may be used. Other options for ambiguity resolution are also available. GRA

N91-29164# Maryland Univ., College Park. Center for Automation Research.
VISION-BASED NAVIGATION AND PARALLEL COMPUTING Annual Report No. 2, May 1989 - May 1990
Larry S. Davis, Daniel DeMenthon, and Thor Bestul Aug. 1990 53 p
(Contract DACA76-88-C-0008)
(AD-A238570; ETL-0572) Avail: NTIS HC/MF A04 CSCL 17/7

This report summarizes the research performed under Contract DACA76-88-C-0008 during the period May 1989 to May 1990, the first year of the contract period. The focus of the research program is visual navigation, with an emphasis on the use of massively parallel algorithms to support basic navigational tasks in vision and planning. The first section describes research performed on a project called RAMBO. (RAMBO is an acronym for Robot Acting on Moving BOdies). The project attempts to develop and integrate Connection Machine algorithms for low-level vision, intermediate level vision and visual planning to allow a mobile robot to pursue (in simulation) a moving three dimensional target through space in order to maintain visual contact with points on surface of the target. The next selection describes our past year's work on cross-country navigation. We first describe massively parallel algorithms for route planning in digital terrain maps. Then we describe our research on the problem of filling in range shadows. We discuss why classical interpolation methods are not appropriate for this problem, and present methods. The last section presents brief descriptions of other research projects whose results were reported under this contract during the past year. GRA

05 AIRCRAFT DESIGN, TESTING AND PERFORMANCE

Includes aircraft simulation technology.

For related information see also *18 Spacecraft Design, Testing and Performance* and *39 Structural Mechanics*.For land transportation vehicles see *85 Urban Technology and Transportation.*

N91-29165# National Aeronautical Establishment, Ottawa (Ontario). Structures and Materials Lab.
REVIEW OF CANADIAN AERONAUTICAL FATIGUE WORK: 1987-1989
D. L. Simpson 15 May 1989 50 p Presented at the 21st Conference of the International Committee on Aeronautical Fatigue
(NAE-LTR-ST-1706; CTN-91-60024) Copyright Avail: NTIS HC/MF A03

A review is provided of Canadian work associated with fatigue of aeronautical structures during the period 1987 to 1988. Brief descriptions of each research project are provided, including the main results to date and future research plans. All aspects of structural technology are covered including full scale tests, loads monitoring, fracture mechanics, composite materials, and engine fatigue. The review covers work being performed by Canadian industry, universities, and governmental agencies involved in aeronautical fatigue studies. CISTI

N91-29166# National Aeronautical Establishment, Ottawa (Ontario). Structures and Materials Lab.
A FULL FUNCTION CHECKOUT TEST FOR THE NAE FULL SCALE STRUCTURAL TEST CONTROL AND DATA ACQUISITION SYSTEM
R. L. Hewitt and B. E. Shaver Feb. 1989 70 p Sponsored by Department of National Defense
(NAE-LTR-ST-1696; CTN-91-60029) Copyright Avail: NTIS HC/MF A04

A test of a control and data acquisition system for full scale aircraft structural fatigue testing is described. The test attempted to duplicate all the conditions that would be encountered in a full scale test of an aircraft structure by using a large structure with 4 controlled actuators and 6 additional channels of data acquisition. The test rig consisted of two aluminum beams attached at right angles loosely simulating an aircraft fuselage and wings. The aircraft was suspended from the wing tips and was also pivoted about the nose. It was loaded with four actuators, located at the tail, the center of the fuselage and at each wingtip. The wing actuators could apply only tension while the other could apply both tension and compression. Five different types of loads were considered corresponding to the maximum bending moments in the wing or fuselage, maximum shears in the fuselage, and maximum up and down tail loads. System fault simulations included hydraulic failure or loss of power to the pumps; total power failure; servo-valve failure, loss of computer or loss of loadcell; structural failure; and loss of strain gauge channel. A number of problems were encountered and solved. Some critical problems became apparent only after extensive testing. It was concluded that checkout tests were very useful and should be continued as long as is feasible. With suitable system changes all options expected to be used in a full scale fatigue test worked successfully. CISTI

N91-29167# National Aeronautical Establishment, Ottawa (Ontario). Structures and Materials Lab.
TUTOR AFT FUSELAGE AND EMPENNAGE FULL-SCALE TEST: PROCEDURES FOR CREATING A DAMAGE LOG
B. Shaver Feb. 1990 10 p Sponsored by Department of National Defence
(NAE-ST-576; CTN-91-60061) Copyright Avail: NTIS HC/MF A02

Full scale fatigue tests are being performed on the aft fuselage and empennage of a Canadian Forces CT-114 Tutor aircraft as part of a technology development program. Several logbooks are to be maintained during the test, including a damage logbook, whose purpose is to provide comprehensive, accurate information on the effects of the test on the specimen. The specific procedures for damage reporting, recording, and presentation of information during this test are described. A typical damage log entry is included for illustration. CISTI

N91-29168# National Aeronautical Establishment, Ottawa (Ontario). Unsteady Aerodynamics Lab.
A NEW LOOK AT THE TOBAK-SCHIFF MODEL OF NONPLANAR AIRCRAFT DYNAMICS
M. E. Beyers Dec. 1989 38 p
(NAE-LTR-UA-101; CTN-91-60082) Copyright Avail: NTIS HC/MF A03

Tobak and Schiff have developed an elegant model of nonlinear aerodynamic phenomena observed on aircraft at high angles of attack. The fundamental premise underlying this model is that the total aerodynamic reactions experienced by the aircraft in flight may be synthesized from the individual reactions to a small number of elementary characteristic motions. The underlying assumptions were that the aerodynamic reactions to a steady motion are themselves steady and single valued functions of the attitude of the aircraft. These assumptions are analyzed. The formulations restricted to linear dependence on the motion rates are derived in detail. Analysis of the kinematical relationships shows that the body axes formulations are expressed exactly in terms of the measured fixed axis derivatives. A formulation of the restricted nonplanar model in body axes is derived explicitly in terms of the aerodynamic angles. An interpretation is given of the identity linking the formulations in the aerodynamic and body axes systems. The derivation of the restricted nonplanar model was verified independently by comparing formulations in two systems of notation. The formulations in the aerodynamic and body axes systems, as well as the identity linking the formulations in the two systems, express the oscillatory derivative terms exactly in the form of measured fixed axis derivatives. The body axes formulation can be expressed in terms of conventional angles of attack and sideslip and the freestream velocity. The identity may be viewed as an equality between an effective rotary parameter and a resultant, planar damping parameter. CISTI

N91-29169*# National Aeronautical Establishment, Ottawa (Ontario). Inst. for Aerospace Research
NAE TWIN OTTER OPERATIONS IN FIFE 1989
J. I. MacPherson Jun. 1990 83 p Sponsored by NASA, Washington
(NASA-CR-188770; NAS 1.26:188770; NAE-LTR-FR-113; CTN-91-60102) Copyright Avail: NTIS HC/MF A05 CSCL 01C

During the summer of 1989, the National Aeronautical Establishment (Canada) Twin Otter Atmospheric Research Aircraft was flow in support of the NASA sponsored First ISLSCP (International Satellite Land Surface Climatology Project) Field Experiment called FIFE-89. Airborne measurements of the fluxes of heat, momentum, water vapor and carbon dioxide were made during 16 flow-altitude flights over the FIFE project area in central Kansas. The Twin Otter operations in FIFE are documented and details are included on the instrumentation, software, flight procedures, atmospheric conditions and analysis methods. Comparisons of Twin Otter measured fluxes are made with those determined at several surface sites and with those made by other instrumented aircraft in the FIFE-87 measurements. Airborne flux measurements are related to run length, altitude, and environmental parameters such as vegetation type, temperature, and wind speed. One night flight was run in an attempt to measure the respiration component of the CO2 flux. The use of aircraft was studied for regional observations of fluxes and to relate these to satellite radiance measurements. Run average data are presented for all 285 flux runs flown by the Twin Otter in FIFE-89. This should serve as as a working reference for scientists utilizing Twin Otter data either directly of through the FIFE data archive. CISTI

N91-29170 Georgia Inst. of Tech., Atlanta.
UNSTEADY COMPRESSIBLE LIFTING SURFACE ANALYSIS FOR ROTARY WINGS USING VELOCITY POTENTIAL MODES Ph.D. Thesis
Vasudevan Mundakizhi Kaladi 1990 136 p
Avail: Univ. Microfilms Order No. DA9115382

The compressible, unsteady lifting surface problem of a helicopter blade in hover using the velocity potential formulation is solved using a modal expansion technique. The mathematical formulation of the problem is presented and a panel method which has previously been applied to its solution is described. The model approach is offered as an alternate solution method.
Dissert. Abstr.

N91-29171# Wright Research Development Center, Wright-Patterson AFB, OH.
AIRCRAFT OPERATIONS FROM RUNWAYS WITH INCLINED RAMPS (SKI-JUMP)
Elijah W. Turner May 1991 19 p

(AF Proj. 2401)
(AD-A237265; WRDC-TM-90-337-FIBE) Avail: NTIS HC/MF A03 CSCL 01/5

The use of inclined ramps to launch aircraft from short runways is proposed as a possible solution to the runway denial problem in Europe. Past efforts to launch aircraft in this manner, including a very successful program conducted by the U.S. Navy to launch the T-2C, F-14, and F-18 aircraft, are reviewed. An analytical study was conducted for the launch of the F-16, F-15, A-10, A-7D and F-4E from inclined ramps. The takeoff ground roll, stabilizer trim setting, landing gear loads and flight trajectory are reported. The F-15 was selected as a candidate aircraft for a USAF flight test program to be patterned after the Navy program and additional studies were performed. Perturbations in center of gravity, thrust, and ramp exit angle were investigated. A ramp contour was designed for launch of the F-15, F-16, A-7D and A-10 which minimized the length and height of the ramp while maintaining the landing gear loads below 90 percent of their design limit. GRA

N91-29172# Army Aviation Test Board, Fort Rucker, AL.
METHODOLOGY INVESTIGATION, AVIATION TEST MANAGEMENT SYSTEM CONCEPT DEVELOPMENT Final Report, 1 Aug. 1989 - 30 Sep. 1990
Larry Wise Nov. 1990 17 p
(AD-A237349) Avail: NTIS HC/MF A03 CSCL 01/3

The United States Army Aviation Technical Test Center (ATTC), Fort Rucker, Alabama, conducted this methodology investigation on Aviation Test Management System Concept Development. The objectives were: (1) to investigate the feasibility of implementing a computerized project management system at ATTC; (2) to investigate the current project management concept to determine a list of requirements and specifications to consider in the selection of a state-of-the-art project management software package; (3) to investigate the necessary changes in the current project management concept to more effectively utilize a computerized project management system; and (4) to review, test run, select, and procure a state-of-the-art project management software package that most nearly meets the needs at ATTC. GRA

N91-29173# Naval Postgraduate School, Monterey, CA.
THE DESIGN AND CONSTRUCTION OF A SHIPLAUNCHED VTOL UNMANNED AIR VEHICLE M.S. Thesis
Bryan M. Blanchette Jun. 1990 103 p
(AD-A238053) Avail: NTIS HC/MF A06 CSCL 01/3

A Vertical Takeoff and Landing (VTOL) Unmanned Air Vehicle (UAV) was designed to serve as a shiplaunched reconnaissance and over the horizon targeting aircraft. Modeled after the U.S. Army's Aquila, the aircraft features a unique tilting ducted fan propulsion unit. The duct contains the engine, propeller, and control vanes used to provide the VTOL capability and is designed to be rotated as a unit for transition into horizontal flight. The duct also provides a measure of shipboard safety by eliminating the potential propeller blade and other hazards associated with the launch and recovery cycle currently experienced by topside personnel. The advantage of using tilting ducted fan technology is that it allows the vehicle to operate off any ship and to have the dash speed to arrive on station in a timely manner. A 1/2 scale model was built using composite wet lay-up techniques as a technology demonstrator and flight test vehicle. The engine system was tested but failed to produce enough static thrust for vertical takeoff. Research is continuing in the development of a propeller that will provide the necessary thrust. GRA

N91-29174# Air Force Inst. of Tech., Wright-Patterson AFB, OH. School of Engineering.
AGILITY: PRESENTATION AND FLIGHT TEST METHODS FOR THE OPERATIONAL FIGHTER PILOT M.S. Thesis
William R. Langdon Mar. 1991 114 p
(AD-A238456; AFIT/GAE/ENY/91M-2) Avail: NTIS HC/MF A06 CSCL 01/1

This thesis develops both metrics and flight test techniques to measure agility. During development of both the agility metrics and the flight test techniques, previous work conducted by the agility community and the Flight Test Center at Edwards Air Force Base was used as a lessons learned tool to insure favorable results. Both simulator and flight testing was performed to validate the flight test techniques. During simulator testing several problems with the original flight test techniques were noted. Flight testing on the pitch agility flight test technique solved most of its problems but problems found during roll testing in the simulator were not flight tested. Flight testing was limited to pitch agility testing only due to time and resource constraints. Results from the flight test were impressive showing a significant advantage using post-stall agility in the A-37B aircraft. Up to 40 deg of heading change was obtained in approximately one second. This turn rate exceeds all maximum instantaneous turn rates for current front line fighters. These results were analytically applied to 180 deg turn maneuvers and resulted in up to a 20 percent time savings from conventional turn methods. This will ultimately allow the fighter pilot to make an educated decision which flight condition is best to defeat a threat. GRA

N91-29175# Rensselaer Polytechnic Inst., Troy, NY. Dept. Engineering and Mechanics.
RESPONSE AND STABILITY ANALYSIS OF HELICOPTER ROTOR BLADES USING COMPUTERIZED SYMBOLIC MANIPULATION Final Report, 20 Sep. 1987 - 19 Mar. 1991
Marcelo R. CrespodaSilva May 1991 9 p
(Contract DAAL03-87-K-0116)
(AD-A238660; ARO-24456.5-EG) Avail: NTIS HC/MF A02 CSCL 20/4

The importance of nonlinearities, and of certain approximations, in the analysis of beams and rotor blades has been addressed in detail. For this, special care was taken in formulating the differential equations of motion of rotor blades in order to be able to identify sources of problematic approximations. In addition, the response of a rotor blade was analyzed by a methodology using an essentially exact solution for the equilibrium state of the blade and by subsequently determining the essentially exact eigenfunctions and eigenvalues associated with the perturbed motion of the blade. The results obtained could serve as a gauge for validating approximate results such as those obtained by a Galerkin procedure. A perturbation methodology was also used to analyze the response of a blade that is either in hover or in forward flight. GRA

N91-29176*# Research Triangle Inst., Research Triangle Park, NC. Center for Digital Systems Research.
ASSESSMENT TEAM REPORT ON FLIGHT-CRITICAL SYSTEMS RESEARCH AT NASA LANGLEY RESEARCH CENTER
Daniel P. Siewiorek, comp. and Janet R. Dunham, comp. Aug. 1989 71 p
(Contract NAS1-17964)
(NASA-CR-181850; NAS 1.26:181850) Avail: NTIS HC/MF A04 CSCL 01C

The quality, coverage, and distribution of effort of the flight-critical systems research program at NASA Langley Research Center was assessed. Within the scope of the Assessment Team's review, the research program was found to be very sound. All tasks under the current research program were at least partially addressing the industry needs. General recommendations made were to expand the program resources to provide additional coverage of high priority industry needs, including operations and maintenance, and to focus the program on an actual hardware and software system that is under development. Author

N91-29177*# National Aeronautics and Space Administration. Hugh L. Dryden Flight Research Facility, Edwards, CA.
PRELIMINARY FLIGHT-DETERMINED SUBSONIC LIFT AND DRAG CHARACTERISTICS OF THE X-29A FORWARD-SWEPT-WING AIRPLANE
John W. Hicks and Thomas Huckabine Aug. 1989 43 p
(NASA-TM-100409; H-1431; NAS 1.15:100409) Avail: NTIS HC/MF A03 CSCL 01C

The X-29A subsonic lift and drag characteristics determined, met, or exceeded predictions, particularly with respect to the drag polar shapes. Induced drag levels were as great as 20 percent less than wind tunnel estimates, particularly at coefficients of lift above 0.8. Drag polar shape comparisons with other modern fighter aircraft showed the X-29A to have a better overall aircraft aerodynamic Oswald efficiency factor for the same aspect ratio. Two significant problems arose in the data reduction and analysis process. These included uncertainties in angle of attack upwash calibration and effects of maneuver dynamics on drag levels. The latter problem resulted from significantly improper control surface automatic camber control scheduling. Supersonic drag polar results were not obtained during this phase because of a lack of engine instrumentation to measure afterburner fuel flow. Author

06 AIRCRAFT INSTRUMENTATION

Includes cockpit and cabin display devices; and flight instruments.

For related information see also *19 Spacecraft Instrumentation* and *35 Instrumentation and Photography.*

No abstracts in this category.

07 AIRCRAFT PROPULSION AND POWER

Includes prime propulsion systems and systems components, e.g., gas turbine engines and compressors; and onboard auxilliary power plants for aircraft.

For related information see also *20 Spacecraft Propulsion and Power, 28 Propellants and Fuels,* and *44 Energy Production and Conversion.*

N91-29178# National Research Council of Canada, Ottawa (Ontario). Engine Lab.

COMPRESSOR FAULT MODELLING FOR ENGINE HEALTH MONITORING: REVIEW AND RECOMMENDATIONS

P. J. Turyk Apr. 1989 147 p

(NRC-TR-ENG-004; NRC-31204; CTN-91-60034) Copyright Avail: NTIS HC/MF A07

A critical literature review was carried out concerning methods of gas turbine compressor performance calculations, and performance loss sources in compressors caused by rotor blade tip clearance, airfoil surface roughness and leading edge deterioration. The focus of the review was on engine health monitoring (EHM) requirements for accurate and reliable calculation procedures, and on engine performance losses related to damage to gas-path turbomachinery components. The performance calculation methods and loss sources in the literature were then evaluated in EHM engine simulation component models. The major conclusions were as follows: (1) Performance analysis methods are generally superior to design analysis procedures in calculating compressor performance; (2) The reliability and accuracy of computational methods increased with modelling sophistication, that is from one dimensional (1-D) to 3-D; (3) 3-D methods are well suited to fluid mechanics investigations while 1- and 2-D methods are suited to calculation of compressor maps for EHM component simulation; (4) A 2 to 3 percent loss in efficiency is experienced in a compressor stage for each 1 pct. increase in tip clearance relative to blade height (An engine scale effect was noted); and (5) Surface roughness losses depend on Reynolds number of the flow, and on the roughness characteristics. Few numerical expressions exist which relate performance losses to surface roughness. CISTI

N91-29179# National Aeronautical Establishment, Ottawa (Ontario). Structures and Materials Lab.

REJUVENATION OF SERVICE EXPOSED ALLOY 713C TURBINE BLADES

T. M. Maccagno, A. K. Koul, J.-P. Immarigeon, L. Cutler, R. Allem, and G. LEsperance (Ecole Polytechnique, Montreal, Quebec) 26 Jul. 1989 32 p Presented at the 28th Annual CIN Conference of Metallurgists, Halifax, Nova Scotia, 23 Aug. 1989 Sponsored by Department of National Defence

(NAE-LTR-ST-1716; CTN-91-60039) Copyright Avail: NTIS HC/MF A03

A detailed study was carried out on the microstructure and creep properties of aero engine first stage turbine blades made from Allow 713C nickle-base superalloy. The investigation was on new blades, service exposed blades, and service exposed blades that had been subjected to one of two rejuvenation treatments: a simulated recoating treatment, or a hot isostatic pressing (HIP) plus simulated recoating treatment. Several microstructural changes were found to take place during service exposure, and these led to a substantial loss in creep properties. Service exposure also led to a untwisting of the blade airfoil section. Good correlations were observed between the amount of untwisting and the measured creep properties. The simulated recoating treatment was moderately successful, and the HIP plus recoating treatment was very successful, in restoring the microstructure and creep properties of the service exposed blades. Author (CISTI)

N91-29180# National Aeronautical Establishment, Ottawa (Ontario). Inst. for Aerospace Research

THE FAILURE OF COMPONENTS IN POWER GENERATION EQUIPMENT

W. Wallace, J.-P. Immarigeon, and A. K. Koul 15 Jun. 1990 52 p Presented at a Short Course on Failure Analysis, Doha, Qatar, Oct. 1990 Prepared for Qatar Univ., Doha

(NAE-LTR-ST-1774; CTN-91-60099) Copyright Avail: NTIS HC/MF A04

The modern gas turbine engine is described in terms of the functions and operating conditions of the main sections including fan and compressor, combustion chamber, and the turbine section. Materials used for the primary structural components are indicated and the modes of deterioration affecting these components in service are reviewed. Failure of structural components may be due to material or manufacturing defects, to improper design or maintenance, or to insufficient knowledge of the modes and rates of damage accumulation in service. The need to understand the physical metallurgy of gas turbine materials and the way alloys respond to different engine operating conditions is emphasized. There is a need to control microstructures in all stages of processing since microstructures determine how the materials perform in service. Physical defects such as cavities, and microstructural discontinuities such as plate-like inclusions or precipitates must be avoided. The response to engine operation conditions in terms of the life limiting modes of degradation and their rates of damage accumulation must be known. Parts with finite lives must be withdrawn from service and either replaced or repaired before damage becomes critical. CISTI

N91-29181*# National Aeronautics and Space Administration. Lewis Research Center, Cleveland, OH.

DIVERGENCE THRUST LOSS CALCULATIONS FOR CONVERGENT-DIVERGENT NOZZLES: EXTENSIONS TO THE CLASSICAL CASE

Jeffrey J. Berton Aug. 1991 19 p

(NASA-TM-105176; E-6472; NAS 1.15:105176) Avail: NTIS HC/MF A03 CSCL 21E

The analytical derivations of the non-axial thrust divergence losses for convergent-divergent nozzles are described as well as how these calculations are embodied in the Navy/NASA engine computer program. The convergent-divergent geometries considered are simple classic axisymmetric nozzles, two dimensional rectangular nozzles, and axisymmetric and two dimensional plug nozzles. A simple, traditional, inviscid

mathematical approach is used to deduce the influence of the ineffectual non-axial thrust as a function of the nozzle exit divergence angle. Author

N91-29182# Air Force Inst. of Tech., Wright-Patterson AFB, OH. Foreign Technology Div.
GENERALIZED SIMPLIFIED ANALYTIC SOLUTION OF OPTIMUM CYCLE PARAMETERS FOR LAND AND AIRCRAFT GAS TURBINE ENGINES AND ITS APPLICATIONS
Jiya Cui 3 May 1991 20 p Transl. into ENGLISH from Jixie Gongcheng Xuebao (China), v. 25, no. 2, Jun. 1989 p 85-92
(AD-A237414; FTD-ID(RS)T-0647-90) Avail: NTIS HC/MF A03 CSCL 21/5

Nearly half a century has elapsed since the advent of gas turbines. In cycle analysis, there are equations for deriving power or thrust from the specific heat, thermal efficiency, and various optimal (optimal reheating or increase in stress) pressure ratios of turbine exit pressures. However, there are no equations for the optimal pressure ratios of the fuel consumption rate with more complex relations. By using the parameter section simplified method system, the paper derives the simplified solution of the optimal pressure ratios; in addition, examples are cited in comparing the results of calculations and the precise solutions of the variable specific heat in order to have a correct evaluation of the extent of approximation and applications. GRA

N91-29183# United Technologies Research Center, East Hartford, CT.
HYDROGEN-FUELED SCRAMJET INVESTIGATION Final Report, Feb. 1987 - Apr. 1990
W. T. Peschke, T. J. Barber, L. Chiappetta, T. J. Anderson, and W. J. Eckerle Feb. 1991 384 p
(Contract F33615-86-C-2695)
(AD-A237569; UTRC/R90-957663-1; WRDC-TR-90-2065) Avail: NTIS HC/MF A17 CSCL 21/2

An experimental and analytical study of the supersonic mixing and combustion processes associated with a free-shear layer is examined. A specific objective comprised quantifying the effects on the mixing and combustion processes of pressure gradients associated with the production of shock waves in the flow field. An experiment was conducted in a generic supersonic combustion configuration that incorporated the essential characteristics of scramjet combustors currently being considered for flight application. The objective of the analytical effort was to evaluate mixing and combustion models in state-of-the-art computational fluid dynamics (CFD) codes. The experiments provided accurate data used to formulate code input conditions and to evaluate codes that were formulated for application in current high speed propulsion design activities. Species concentration, total and static temperature, and pitot pressure profiles were measured in a shear layer experiment in which gaseous hydrogen was injected tangentially into a Mach 3 (nominal) vitiated air stream. In this experiment, hydrogen was injected adjacent to the upperwall of the test section. A nonintrusive optical diagnostic technique was used in conjunction with intrusive probing to define the flow field initial conditions and to characterize the detailed features of the flow field subsequent to hydrogen injection and combustion. GRA

N91-29184# Naval Postgraduate School, Monterey, CA.
EVALUATION OF AIRCRAFT TURBINE ENGINE REDESIGNS M.S. Thesis
Eugene G. Sudol, Jr. and Larry D. Price Jun. 1990 70 p
(AD-A237599) Avail: NTIS HC/MF A04 CSCL 21/5

This study of the Aircraft Turbine Engine Component Improvement Program (CIP) examines some of the problems associated with determining benefits accrued from CIP. The major emphasis of the thesis was developing a component selection method and an analysis procedure for detecting changes in logistics parameters. The data for this report come from aviation organizational level maintenance activities and squadrons. The thesis reached the conclusion that the effects of CIP are more effectively assessed at the component level rather than at the system level. The thesis further demonstrated the logical and data collection difficulties encountered in the process of isolating and measuring the incremental benefits obtained from CIP expenditures. GRA

N91-29185# Aeronautical Research Labs., Melbourne (Australia).
AN IMPROVED METHOD OF INVESTIGATION OF COMPRESSOR BLADE FIT USING HOLOGRAPHIC INTERFEROMETRY
J. Gordon and D. E. Rowlands Jan. 1991 21 p
(AD-A238182; ARL-STRUC-TM-577; DODA-AR-006-128) Avail: NTIS HC/MF A03 CSCL 14/2

Holography is a technique which has many scientific applications, and is now gaining acceptance in industry. It enables the recording of three-dimensional information about an object on a two-dimensional medium. Currently used methods of taking holograms rely on the recording the interference pattern which is generated when light from a coherent monochromatic source is split into two, (or sometimes more) beams, and they are recombined at the recording medium. One of the beams is reflected, or scattered from the object. As the source is coherent, the recombined beams interfere, and the resulting interference pattern is stored by the recording medium. The stored interference pattern can be used to reconstruct a three-dimensional optical field of the object. The light reaching the recording medium after reflection by the object is called the object or subject beam, the split off portion with which it interferes at the recording medium is called the reference beam. GRA

N91-29186# Iowa State Univ. of Science and Technology, Ames. Dept. of Mechanical Engineering.
MODIFICATION OF AXIAL-FLOW COMPRESSOR STALL MARGIN BY VARIATION OF STATIONARY BLADE SETTING ANGLES Final Technical Report
John P. Rukavina and Theodore H. Okiishi Apr. 1991 193 p
(Contract F33615-87-C-2739)
(AD-A238406) Avail: NTIS HC/MF A09 CSCL 13/7

The useful operating range of the multistage, axial-flow compressor component of a gas turbine engine limits the extent of operation of that engine. Generally, the compressor stalls or surges at a low flow rate and chokes a a high flow rate. Thus, any improvement in the range between these compressor aerodynamic limits is normally of benefit to the engine also. An idea for delaying the onset of rotating stall in a multistage, axial-flow compressor which involved circumferentially varying the blade setting angles of stationary blades upstream of the compressor rotors was investigated. Tests involving two low-speed, multistage, axial-flow compressors and an intermediate-speed, three-stage, axial-flow compressor were completed. Comparisons between baseline compressor (circumferentially uniform setting angles) and modified compressor (circumferentially varying setting angles) performance data were made. A variety of blade setting angle circumferential variation patterns were tested. GRA

N91-29187*# National Aeronautics and Space Administration. Lewis Research Center, Cleveland, OH.
EXPERIMENTAL STUDY OF CROSS-STREAM MIXING IN A CYLINDRICAL DUCT
A. Vranos, D. S. Liscinsky, B. True (United Technologies Research Center, East Hartford, CT.), and J. D. Holdeman 1991 15 p
Presented at the 27th Joint Propulsion Conference, Sacramento, CA, 24-27 Jun. 1991; sponsored by AIAA, SAE, ASME, and ASEE Previously announced as A91-45815
(Contract NAS3-25967)
(NASA-TM-105180; E-6478; NAS 1.15:105180; AIAA-91-2459)
Avail: NTIS HC/MF A03 CSCL 21E

An experimental investigation of cross stream injection and mixing was conducted with application to a low NO sub x combustor for the High Speed Civil Transport (HSCT). Mixing in a cylindrical chamber was studied for transverse injection from slanted slot and round orifice injectors. Momentum ratio, density ratio, and number were studied. Quantitative measurement of injectant

concentration distributions were obtained by planar digital imaging of the Mie scattered light from an aerosol seed uniformly mixed with the injectant. The unmixedness, defined as the ratio of the r.m.s. concentration fluctuation to mean concentration in a plane perpendicular to the main flow direction, was found to be primarily a function of momentum ratio and injector spacing. An optimum spacing is indicated. Unmixedness is also a function of orifice size, or mass flow ratio, but the mass flow dependence can be accounted for by normalizing the unmixedness with its maximum theoretical value. The data indicate that a density ratio greater than unity retards mixing. It was found that above a certain momentum flux ratio, mixing with slanted slot injectors was better than with round hole injectors. Author

N91-29188*# National Aeronautics and Space Administration. Lewis Research Center, Cleveland, OH.
A LINEAR CONTROL DESIGN STRUCTURE TO MAINTAIN LOOP PROPERTIES DURING LIMIT OPERATION IN A MULTI-NOZZLE TURBOFAN ENGINE
Duane Mattern (Sverdrup Technology, Inc., Brook Park, OH.) and Peter Ouzts 1991 28 p Presented at the 27th Joint Propulsion Conference, Sacramento, CA, 24-27 Jun. 1991; sponsored by AIAA, SAE, ASME, and ASEE Previously announced as A91-45780
(Contract NAS3-25266)
(NASA-TM-105163; E-6452; NAS 1.15:105163; AIAA-91-1997)
Avail: NTIS HC/MF A03 CSCL 21E

The implementation of multi-variable control systems on turbofan engines requires the use of limit protection to maintain safe engine operation. Since a turbofan engine typically encounters limits during transient operation, the use of a limit protection scheme that modifies the feedback loop may void the desired 'guarantees' associated with linear multi-variable control design methods, necessitating considerable simulation to validate the control with limited protection. An alternative control design structure is proposed that maintains the desired linear feedback properties when certain safety limits are encountered by moving the limit protection scheme outside the feedback loop. This proposed structure is compared to a structure with a limit protection scheme that modifies the feedback loop properties. The two design structures are compared using both linear and nonlinear simulations. The evaluation emphasizes responses where the fan surge margin limit is encountered. Author

08 AIRCRAFT STABILITY AND CONTROL

Includes aircraft handling qualities; piloting; flight controls; and autopilots.

For related information see also *05 Aircraft Design, Testing and Performance.*

N91-29189# National Aeronautical Establishment, Ottawa (Ontario).
WIND AND FLUX CALCULATIONS OF THE NAE TWIN OTTER
J. Ian MacPherson 26 Jan. 1990 40 p
(NAE-LTR-FR-109; CTN-91-60080) Copyright Avail: NTIS HC/MF A03

The National Aeronautical Establishment (NAE) of Canada Twin Otter Atmospheric Research Aircraft is instrumented to measure the means and turbulent components of atmospheric motion and the fluxes of trace gases such as water vapor and CO2. The methods of analysis are provided along with the derivations of the equations used in computing winds and fluxes. CO2 and water vapor concentrations are measured by infrared absorption (IRA). The measuring instrument has a CO2 range sensitivity of 0 to 700 mg/cu m with an accuracy of 0.5 mg/cu m and a H2O range sensitivity of 0 to 30 g/cu m with an accuracy of 0.05 g/cu m. Visible incident and reflected radiation is measured by pyranometer with a range of 0 to 1100 W/sq m. The vegetation index is measured by reflected radiation at 660 and 730 nanometers. The primary gust sensor is a Rosemont 858 50-hole probe mounted at the tip of the noseboom. There are two inertial velocity sensing systems on the aircraft, one a Litton LTN 90 to 100 inertial reference system utilizing ring laser gyros, and a second based on an NAE assembled system of accelerometers and rate gyros and a three axis Doppler radar. Approximate values for measured quantities are calculated on a microprocessor and displayed in flight. Accurate flux measurements are calculated on ground on the MicroVAX II ground playback system during post flight analysis. CISTI

N91-29190# National Research Council of Canada, Ottawa (Ontario). Inst. for Aerospace Research
AN INVESTIGATION INTO THE USE OF SIDE-ARM CONTROL FOR CIVIL ROTORCRAFT APPLICATIONS
S. W. Baillie and S. Kereliuk Jun. 1990 39 p
(AD-A226628; NRC-32133; IAR-AN-67; CTN-91-60100)
Copyright Avail: NTIS HC/MF A03

An evaluation of the handling qualities of civil rotocraft incorporating force or displacement sensing side arm controllers with varying levels of control integration was carried out on the Institute for Aeronautical Research of the National Research Council of Canada Bell 205 Airborne Simulator. Evaluators were certified pilots from the FAA or Transport Canada. Pilot workload level and performance for configurations with the force sensing 4 + 0 controller was as good or better than with conventional controls for most tasks and there is a good potential for improvement. The breakout gradient force characteristics and sensitivities of side arm controllers may dominate aircraft handling qualities. A systematic evaluation of a range of these characteristics for all representative tasks is required to establish satisfactory boundaries for both force sensing and deflection sensing controllers. Several certification issues are suggested. These include: fault failure analysis to ensure redundance, provision for monitoring coupled systems, and testing for electromagnetic interference. Overall, the force sensing 4 + 0 controller was preferred for most manoeuvres over the conventional configuration. CISTI

N91-29191*# National Aeronautics and Space Administration. Hugh L. Dryden Flight Research Facility, Edwards, CA.
CONTROLLING CRIPPLED AIRCRAFT-WITH THROTTLES
Frank W. Burcham, Jr. and C. Gordon Fullerton Sep. 1991 30 p Prepared for presentation at the 44th International Air Safety Seminar, Singapore, 12-14 Nov. 1991
(NASA-TM-104238; H-1747; NAS 1.15:104238) Avail: NTIS HC/MF A03 CSCL 01C

A multiengine crippled aircraft, with most or all of the flight control system inoperative, may use engine thrust for control. A study was conducted of the capability and techniques for emergency flight control. Included were light twin engine piston powered airplanes, an executive jet transport, commercial jet transports, and a high performance fighter. Piloted simulations of the B-720, B-747, B-727, MD-11, C-402, and F-15 airplanes were studied, and the Lear 24, PA-30, and F-15 airplanes were flight tested. All aircraft showed some control capability with throttles and could be kept under control in up-and-away flight for an extended period of time. Using piloted simulators, landings with manual throttles-only control were extremely difficult. However, there are techniques that improve the chances of making a survivable landing. In addition, augmented control systems provide major improvements in control capability and make repeatable landings possible. Control capabilities and techniques are discussed. Author

N91-29192# Lawrence Livermore National Lab., CA.
FLUTTER CONSIDERATION OF A CRASH-TEST AIRCRAFT
T. F. Chen 28 Feb. 1991 33 p
(Contract W-7405-eng-48)
(DE91-015094; UCRL-ID-107239) Avail: NTIS HC/MF A03

The Plutonium Air Transport Certification (PATC) project is currently being conducted by the Nuclear Systems Safety Program (NSSP) for the US Nuclear Regulatory Commission. Developing aircraft crash test criteria is part of this effort. One objective is to assess whether a researcher can safely control the aircraft and to evaluate the likelihood that the aircraft can be successfully

crash tested. Due to the extraordinarily high velocity of 925 fts required at aircraft impact, the likelihood for the crash test aircraft to undergo flutter in the final stages of flight is substantially increased. A fundamental understanding is gained of the aircraft flutter phenomenon in order to successfully determine the scope of and prepare for an aircraft crash test. This documentation includes: (1) a general description of the aircraft flutter phenomenon, its structural representation, and some of the commonly used unsteady oscillatory aerodynamic loading approximations; (2) a brief summary of the flutter equation solution techniques; (3) the input requirements for conducting a successful flutter prediction; (4) some of the main aircraft flutter characteristics and prevention considerations; and (5) an outline for future work on the aircraft flutter phenomenon. DOE

N91-29193*# Pennsylvania State Univ., University Park. Mechanical Engineering Dept.

COMPENSATION OF DISTRIBUTED DELAYS IN INTEGRATED COMMUNICATION AND CONTROL SYSTEMS Final Report

Asok Ray and Rogelio Luck Aug. 1991 74 p

(Grant NAG3-823)

(NASA-CR-187136; NAS 1.26:187136) Avail: NTIS HC/MF A04 CSCL 01C

The concept, analysis, implementation, and verification of a method for compensating delays that are distributed between the sensors, controller, and actuators within a control loop are discussed. With the objective of mitigating the detrimental effects of these network induced delays, a predictor-controller algorithm was formulated and analyzed. Robustness of the delay compensation algorithm was investigated relative to parametric uncertainties in plant modeling. The delay compensator was experimentally verified on an IEEE 802.4 network testbed for velocity control of a DC servomotor. Author

N91-29194*# National Aeronautics and Space Administration. Hugh L. Dryden Flight Research Facility, Edwards, CA.

A SIMULATION EVALUATION OF A FOUR-ENGINE JET TRANSPORT USING ENGINE THRUST MODULATION FOR FLIGHTPATH CONTROL

Glenn B. Gilyard, Joseph L. Conley, Jeanette Le, and Frank W. Burcham, Jr. Washington Sep. 1991 22 p Presented at the AIAA/ASME/SAE/ASEE 27th Joint Propulsion Conference, Sacramento, CA, 24-26 Jun. 1991

(NASA-TM-4324; H-1741; NAS 1.15:4324) Avail: NTIS HC/MF A03 CSCL 01C

The use of throttle control laws to provide adequate flying qualities for flight path control in the event of a total loss of conventional flight control surface use was evaluated. The results are based on a simulation evaluation by transport research pilots of a B-720 transport with visual display. Throttle augmentation control laws can provide flight path control capable of landing a transport-type aircraft with up to moderate levels of turbulence. The throttle augmentation mode dramatically improves the pilots' ability to control flight path for the approach and landing flight condition using only throttle modulation. For light turbulence, the average Cooper-Harper pilot rating improved from unacceptable to acceptable (a pilot rating improvement of 4.5) in going from manual to augmented control. The low frequency response characteristics of the engines require a considerably different piloting technique. The various techniques used by the pilot resulted in considerable scatter in data. Many pilots readily adapted to a good piloting technique while some had difficulty. A new viable approach is shown to provide independent means of redundancy of transport aircraft flight path control. Author

09 RESEARCH AND SUPPORT FACILITIES (AIR)

Includes airports, hangars and runways; aircraft repair and overhaul facilities; wind tunnels; shock tubes; and aircraft engine test stands.

For related information see also *14 Ground Support Systems and Facilities (Space).*

N91-29195# National Aeronautical Establishment, Ottawa (Ontario). Low Speed Aerodynamics Lab.

A WIND TUNNEL SMOKE GENERATOR

Todd R. Brown Mar. 1990 25 p

(NAE-LTR-LA-312; CTN-91-60005) Copyright Avail: NTIS HC/MF A03

The construction and operation is described of a flow visualization smoke generator used in the wind tunnels of the Low Speed Aerodynamics Lab. The smoke generator produces output when hot vaporized mineral oil condenses in cool ambient air. The oil is stored in a 1.5 liter pressure vessel. Compressed air at 700 kPA is supplied to an adjustable regulator that pressurizes the vessel. The mineral oil is delivered from the vessel to the wand through a shut-off valve and one of two needle valves with quick-connect couplings. The two needle valves have different flow ranges to accommodate different probes. The oil travels the length of the wand through 1.57 mm O.D. by 0.20 mm wall stainless steel tubing. Electric current is passed along the steel tube wall which acts as an electrical resistance heating element. The oil is heated and vaporizes by the time it reaches the end of the wand. A dense white plume is produced as the mineral oil condenses in the ambient air at the exit of the tube. This smoke generator has several advantages. It is portable, requiring only 110 VAC power and compressed air to operate. It starts to generate smoke within 15 seconds of being turned on. It uses non-toxic, deodorized, high flashpoint mineral oil that evaporates without residue or odor. The plume of particles produced is a continuous, dense, white, warm condensate that, when properly illuminated, is readily photographed or videotaped. The condensate disappears at a convenient rate, so that smoke does not make a complete circuit of the 2 m by 3 m wind tunnel. CISTI

N91-29196# National Aeronautical Establishment, Ottawa (Ontario). Structures and Materials Lab.

AN ASSESSMENT OF THE ACOUSTIC NOISE IN THE WORKING SECTION OF THE NAE 6 FT X 9 FT LOW SPEED WIND TUNNEL

V. K. Nguyen, R. Westley, and G. Basso 26 Jan. 1990 162 p

(NAE-LTR-ST-1744; CTN-91-60007) Copyright Avail: NTIS HC/MF A08

Detailed information is provided on the sound pressure level spectra of the ambient noise in the working section of the National Aeronautical Establishment (NEA) 6 ft by 9 ft Low Speed Wind Tunnel to aid in the selection of a wind tunnel that could be used for measuring the forward speed effects of model aeroacoustic noise sources. A comprehensive set of measurements, covering the full range of working section speeds from 0 to 350 ft/sec, is given of the overall sound pressure levels and the 1/24 and 1/3 octave spectra. It was concluded that the NAE wind tunnel is suitable for measuring the noise fields of those model propellors that have blade passing frequencies which are greater than 400 to 500 Hz and, for forward speeds above 165 ft/sec, which are limited to the two speed ranges of approximately 195 to 240 ft/sec and 300 to 340 ft/sec. An additional requirement is likely to be that the propellor noise levels in 1/24 octave frequency bands should be significantly greater than the background sound pressure levels of 100 dB. The side walls should be treated with material that will provide high sound absorption at sound frequencies emitted by the propellors. The fan from the working section should be acoustically isolated if low background noise levels are necessary. CISTI

N91-29197# National Aeronautical Lab., Bangalore (India). Flight Mechanics and Controls Div.
INSTRUMENTATION FOR ASE EXPERIMENTS IN THE DYNAMIC WIND TUNNEL
L. Poornima and K. Seshadri Jun. 1991 13 p
(PD-FC-9112) Avail: NTIS HC/MF A03

The instrumentation package developed for use with flexible wing models was tested in the dynamic wind tunnel for aeroservoelastic studies. This approach uses geometrically scaled elastic wings which are mounted with sensors to measure dynamic response. Strain gages and accelerometers were used. Author

N91-29198# Army Cold Regions Research and Engineering Lab., Hanover, NH.
PERFORMANCE OF ASPHALT CONCRETE AIRPORT PAVEMENTS DURING THAW WEAKENING PERIODS: A FIELD STUDY
Vincent C. Janoo and Richard L. Berg Apr. 1991 70 p
(Contract DTFA-01-84-2-02038)
(AD-A237441; CRREL-91-7; DOT/FAA/RD-91/16) Avail: NTIS HC/MF A04 CSCL 11/2

It is accepted that in the winter the load-carrying capacity of pavements increases dramatically because of freezing of the pavement structure. This is more striking in asphalt concrete pavements because of the stiffening of the asphalt at low temperatures. In the spring, the pavement structure below the asphalt layer thaws and can become saturated with water from the melting ice lenses, reducing the strength of the bases subbase and subgrades. In the spring of 1986, CRREL conducted Falling Weight Deflectometer (FWD) measurements at an airfield in Wisconsin, which had pavements that were primarily asphalt concrete, to determine the change in the load bearing strength of these pavement structures in a seasonal frost area during thaw weakening periods. In addition to FWD measurements, surface and subsurface pavement temperatures were measured at selected sites. This report gives a general description of the airfield and the pavement structure and a comprehensive analysis of the FWD measurements. GRA

N91-29199*# National Aeronautics and Space Administration. Lewis Research Center, Cleveland, OH.
CALCULATED PERFORMANCE OF THE NASA LEWIS ICING RESEARCH TUNNEL
Larry A. Viterna Aug. 1991 23 p
(NASA-TM-105173; E-6469; NAS 1.15:105173) Avail: NTIS HC/MF A03 CSCL 14B

The Icing Research Tunnel is used extensively to test many classes of aircraft under atmospheric icing conditions. Because of the need to test models at higher Reynolds numbers, a new fan rotor was designed to increase test section wind speed. A preliminary study was made of the present fan rotor to suggest possible methods to increase tunnel wind speed. The results of that study are presented. Author

12 ASTRONAUTICS (GENERAL)

For extraterrestrial exploration see *91 Lunar and Planetary Exploration.*

N91-29200# Los Alamos National Lab., NM.
NUCLEAR DATA NEEDS FOR THE SPACE EXPLORATION INITIATIVE
S. D. Howe and G. Auchampaugh 1991 5 p Presented at the International Conference on Nuclear Data for Science and Technology, Juelich, Fed. Republic of Germany, 13-17 May 1991
(Contract W-7405-eng-36)
(DE91-013231; LA-UR-91-1595; CONF-910503-13) Avail: NTIS HC/MF A01

On July 20, 1989, the President of the United States announced a new direction for the U.S. Space Program. The new Space Exploration Initiative (SEI) is intended to emplace a permanent base on the Lunar surface and a manned outpost on the Mars surface by 2019. In order to achieve this ambitious challenge, new, innovative, and robust technologies will have to be developed to support crew operations. Nuclear power and propulsion have been recognized as technologies that are at least mission enhancing and, in some scenarios, mission enabling. Because of the extreme operating conditions present in a nuclear rocket core, accurate modeling of the rocket will require cross section data sets which do not currently exist. In order to successfully achieve the goals of the SEI, major obstacles inherent in long duration space travel will have to be overcome. One of these obstacles is the radiation environment to which the astronauts will be exposed. In general, an unshielded crew will be exposed to roughly one REM per week in free space. For missions to Mars, the total dose could exceed more than one-half the total allowed lifetime level. Shielding of the crew may be possible, but accurate assessments of shield composition and thickness are critical if shield masses are to be kept at acceptable levels. In addition, the entire ship design may be altered by the differential neutron production by heavy ions (galactic cosmic rays) incident on ship structures. The components of the radiation environment, current modeling capability, and envisioned experiments will be discussed. DOE

N91-29201*# National Aeronautics and Space Administration. Goddard Space Flight Center, Greenbelt, MD.
THE HIGH ENERGY SOLAR PHYSICS MISSION (HESP): SCIENTIFIC OBJECTIVES AND TECHNICAL DESCRIPTION
Carol Crannell, Brian Dennis, John Davis, Gordon Emslie, Gerhard Haerendel, High Hudson, Gordon Hurford, Robert Lin, James Ling, and Monique Pick (Observatoire de Paris-Meudon, France) et al Jul. 1991 70 p
(NASA-TM-105033; NAS 1.15:105033) Avail: NTIS HC/MF A04 CSCL 22A

The High Energy Solar Physics mission offers the opportunity for major breakthroughs in the understanding of the fundamental energy release and particle acceleration processes at the core of the solar flare problem. The following subject areas are covered: the scientific objectives of HESP; what we can expect from the HESP observations; the high energy imaging spectrometer (HEISPEC); the HESP spacecraft; and budget and schedule. Author

13 ASTRODYNAMICS

Includes powered and free-flight trajectories; and orbital and launching dynamics.

N91-29202 Texas Univ., Austin.
SEASONAL AIR AND WATER MASS REDISTRIBUTION AND ITS EFFECT ON SATELLITE AND POLAR MOTION Ph.D. Thesis
Roberto Gutierrez 1990 130 p
Avail: Univ. Microfilms Order No. DA9116862

The laser geodetic satellites Lageos and Starlette exhibit residual orbital motion with an unexplained seasonal component. In addition, recognized polar motion excitation sources do not account for a large portion of observed polar motion. It is hypothesized that air and ocean mass redistribution is the primary source of seasonal perturbations in satellite motion, and that wind-driven ocean mass redistribution is a major source for polar motion excitation. Comparison of predicted polar motion with observations suggest that the effect of ocean mass redistribution is significant, and second only to air pressure in magnitude. Lageos ascending mode perturbations predicted from ocean mass redistribution indicate that non-isostatic sea level fluctuations should be readily observable by satellite laser ranging. Dissert. Abstr.

14 GROUND SUPPORT SYSTEMS AND FACILITIES (SPACE)

Includes launch complexes, research and production facilities; ground support equipment, e.g., mobile transporters; and simulators.

For related information see also *09 Research and Support Facilities (Air).*

N91-29203# Sandia National Labs., Albuquerque, NM.
LAUNCH CAPABILITIES TO OVER 10 km/s
L. C. Chhabildas, L. M. Barker, J. R. Asay, T. G. Trucano, G. I. Kerley, and J. E. Dunn 1991 11 p Presented at the 1991 American Physical Society (APS) Conference on Shock Compression of Condensed Matter, Williamsburg, 17-20 Jul. 1991
(Contract DE-AC04-76DP-00789)
(DE91-014657; SAND-90-3190C; CONF-9107105-33) Avail: NTIS HC/MF A03

A systematic study is described which addresses the technical issues associated with launching flier-plates to hypervelocities. Structured, time-dependent, uniform, high-pressure, pulses are needed to drive flier plates to hypervelocities without melting or fracturing the plate. This is achieved by using a graded-density impactor to impact a flier plate at high velocities on a two-stage light-gas gun. We have used this method to launch titanium and aluminum alloy plates to velocities of 9.5 km/s and 10.4 km/s, respectively. A method is proposed to extend the launch capabilities to velocities in excess of 14 km/s. DOE

N91-29204# California Univ., Berkeley. Lawrence Berkeley Lab.
THE ASTROMAG SUPERCONDUCTING MAGNET FACILITY CONFIGURED FOR A FREE FLYING SATELLITE
M. A. Green and G. F. Smoot Jun. 1991 18 p Presented at the Space Cryogenics Workshop, Cleveland, OH, 18-20 Jun. 1991
(Contract DE-AC03-76SF-00098)
(DE91-014710; LBL-30773; CONF-9106134-1; ASTROMAG-034)
Avail: NTIS HC/MF A03

ASTROMAG is a particle astrophysics facility that was originally configured for the Space Station. The heart of the ASTROMAG facility is a large superconducting magnet which is cooled using superfluid helium. The task of resizing the facility so that it will fly in a satellite in a high angle of inclination orbit is driven by the launch weight capability of the launch rocket and the desire to be able to do nearly the same physics as the Space Station version of ASTROMAG. In order to reduce the launch weight, the magnet and its cryogenic system had to be downsized, yet the integrated field generated by the magnet in the particle detectors has to match the Space Station version of the magnet. The use of aluminum matrix superconductor and oriented composite materials in the magnet insulation permits one to achieve this goal. The net magnetic dipole moment from the ASTROMAG magnet must be small to minimize the torque due to interaction with the earth's magnetic field. The ASTROMAG magnet consists of identical two coils 1.67 meters apart. The two coils are connected in series in persistent mode. Each coil is designed to carry 2.34 million ampere turns. Both coils are mounted on the same magnetic axis and they operate at opposite polarity. This reduces the dipole moment by a factor of more than 1000. This is tolerable for the Space Station version of the magnet. A magnet operating on a free flying satellite requires additional compensation. This report presents the magnet parameters of a free flying version of ASTROMAG and the parameters of the space cryogenic system for the magnet. DOE

N91-29205# Army Armament Research, Development and Engineering Center, Picatinny Arsenal, NJ.
BASIC SIMPLE MODELING OF BALLOTING MOTION OF RAILGUN PROJECTILES
Szu H. Chu Jul. 1991 23 p
(AD-A237938; ARFSD-TR-90029) Avail: NTIS HC/MF A03
CSCL 19/6

This is the second of three basic reports dealing with the in-bore balloting motion of a projectile launched in an electromagnetic railgun. The first report addressed axial projectile motion without cocking and was titled, A Basic Single Model of In-bore Motion of Railgun Projectiles. Understanding the inbore motion of a projectile is important to its design and its ability to hit a target with some effectiveness. Analysis of in-bore motion is a complicated problem since many parameters are involved and the interacting relationships between them must be determined. To make the problem easier to understand, it was analyzed on several levels beginning with the basic simple model which computed only the axial motion and followed by more complicated models in the upper analysis levels that included as many lateral forces and gun tube vibration effects as possible. This report deals with the second basic or zero level of balloting analysis. A basic simple model considering only the effect of the propulsion force, the friction force of the armature, and the clearance between the projectile and the barrel is presented. The computation of the axial projectile motion with a certain cocking angle is the goal of this analysis. Equations of motion are derived and solved. A sample computation with available data is performed and the results plotted to give a clearer understanding of balloting action. GRA

N91-29206# Army Armament Research, Development and Engineering Center, Picatinny Arsenal, NJ.
AN APPROXIMATE ANALYSIS OF BALLOTING MOTION OF RAILGUN PROJECTILES
Szu H. Chu Jul. 1991 27 p
(AD-A237942; ARFSD-TR-90030) Avail: NTIS HC/MF A03
CSCL 19/10

This is the final of three reports dealing with the in-bore balloting motion of a projectile fired from an electromagnetic railgun. Knowledge of projectile in-bore motion is important to its design and the design of the railgun. It is a complicated problem since many parameters are involved and it is not easy to determine the interacting relationships between them. To make the problem easier to understand it was analyzed on several levels. Beginning from the basic simple model which computed only the axial motion, more complicated models were introduced in upper levels that included the more significant lateral forces and gun tube vibration effects. This report deals with the approximate analysis of balloting motion. This model considers the effects of the propulsion force, the friction force of the projectile package (projectile and armature), air resistance, gravity, the elastic forces, and the projectile/barrel clearance. To simplify the modeling, a plane motion configuration is assumed. Though the projectile is moving with a varying yaw angle, the axes of the barrel and the projectile package, and the projectile center of gravity are always considered in a plane containing the centerlines of the rails. Equations of motion are derived and solved. A sample computation is performed and the results plotted to give a clearer understanding of projectile in-bore motion. GRA

N91-29207# Army Armament Research, Development and Engineering Center, Picatinny Arsenal, NJ. Fire Support Armament.
BASIC SIMPLE MODELING OF IN-BORE MOTION OF RAILGUN PROJECTILES
Szu H. Chu Jul. 1991 18 p
(AD-A238064; ARFSD-TR-90028) Avail: NTIS HC/MF A03
CSCL 19/10

In an electromagnetic railgun a projectile encounters a complex force environment during launch. A thorough understanding of these forces is critical to projectile and gun tube design. There are many parameters involved and interacting relationships which must be determined. To better understand and establish the in-bore force models, we begin with a basic simple model which computes only the axial motion. More complicated models will be introduced in subsequent reports which will include lateral forces and gun tube vibration effects. This report deals with a very simple axial motion model. Only the effects of the propulsion force, projectile package mass, air resistance, and the friction forces are presented.

Equations of motion are derived and solved. A sample computation with available data is performed and curves plotted to give clearer understanding of the results. GRA

N91-29208# Sandia National Labs., Albuquerque, NM.
THE USE OF HIGH VELOCITY LAUNCHERS FOR SCIENTIFIC AND ENGINEERING STUDIES
J. R. Asay, L. C. Chhabildas, and M. D. Furnish 1991 65 p Presented at the 18th International Symposium on Shock Waves, Sendai (Japan), 21-26 Jul. 1991
(Contract DE-AC04-76DP-00789)
(DE91-015564; SAND-91-0711C; CONF-9107138-1) Avail: NTIS HC/MF A04

Shockwave techniques have been used for decades to study the dynamic states of matter in temperature and pressure regimes inaccessible by other methods. These techniques have been employed in a wide variety of scientific, military, and commercial applications. A principal scientific objective has been to determine high-pressure equations of state (EOS) to ultra-high pressures; pressures of tens of Mbar have been reported for several materials. Most recently, these methods have been used for studies of thermophysical properties under shock compression, including phase transition kinetics, and mechanical properties, such as the high-pressure yield strength. In this paper, a brief discussion of recent developments in high velocity launchers is given. Advances in techniques for subjecting materials to a wide range of loading conditions is presented, including selected illustrations of shockwave measurements to Mbar pressures. DOE

15 LAUNCH VEHICLES AND SPACE VEHICLES

Includes boosters; operating problems of launch/space vehicle systems; and reusable vehicles.

For related information see also *20 Spacecraft Propulsion and Power.*

N91-29209*# National Aeronautics and Space Administration. Marshall Space Flight Center, Huntsville, AL.
RESOURCE ENVELOPE CONCEPTS FOR MISSION PLANNING
K. Y. Ibrahim, J. D. Weiler, and J. C. Tokaz (Sverdrup Technology, Inc., Huntsville, AL.) Aug. 1991 74 p
(NASA-TP-3139; M-666; NAS 1.60:3139) Avail: NTIS HC/MF A04 CSCL 22B

Seven proposed methods for creating resource envelopes for Space Station Freedom mission planning are detailed. Four reference science activity models are used to illustrate the effect of adding operational flexibility to mission timelines. For each method, a brief explanation is given along with graphs to illustrate the application of the envelopes to the power and crew resources. The benefits and costs of each method are analyzed in terms of resource utilization. In addition to the effect on individual activities, resource envelopes are analyzed at the experiment level. Author

16 SPACE TRANSPORTATION

Includes passenger and cargo space transportation, e.g., shuttle operations; and space rescue techniques.

For related information see also *03 Air Transportation and Safety* and *18 Spacecraft Design, Testing and Performance.* For space suits see *54 Man/System Technology and Life Support.*

N91-29210*# National Aeronautics and Space Administration. John F. Kennedy Space Center, Cocoa Beach, FL.
DEBRIS/ICE/TPS ASSESSMENT AND PHOTOGRAPHIC ANALYSIS FOR SHUTTLE MISSION STS-40
Gregory N. Katnik, Scott A. Higginbotham, and J. Bradley Davis Jul. 1991 195 p Original contains color illustrations
(NASA-TM-103822; NAS 1.15:103822) Avail: NTIS HC/MF A09; 79 functional color pages CSCL 22B

A debris, ice, Thermal Protection System (TPS) assessment and photographic analysis for Space Shuttle Mission STS-40 was conducted. Debris inspections of the flight elements and launch pad were performed before and after launch. Ice and frost conditions on the External Tank were assessed by the use of computer programs, nomographs, and infrared scanner data during cryogenic loading of the vehicle, followed by on-pad visual inspection. High speed photography was analyzed after launch to identify ice and debris sources and to evaluate potential vehicle damage and/or in-flight anomalies. Author

17 SPACE COMM., SPACECRAFT COMM., COMMAND & TRACKING

Includes telemetry; space communications networks; astronavigation and guidance; and radio blackout.

For related information see also *04 Aircraft Communications and Navigation* and *32 Communications and Radar.*

No abstracts in this category.

18 SPACECRAFT DESIGN, TESTING AND PERFORMANCE

Includes satellites; space platforms; space stations; spacecraft systems and components such as thermal and environmental controls; and attitude controls.

For life support systems see *54 Man/System Technology and Life Support.* For related information see also *05 Aircraft Design, Testing and Performance, 39 Structural Mechanics,* and *16 Space Transportation.*

N91-29211*# Draper (Charles Stark) Lab., Inc., Cambridge, MA.
EQUATIONS OF MOTION FOR A FLEXIBLE SPACECRAFT-LUMPED PARAMETER IDEALIZATION
Joel Storch and Stephen Gates Sep. 1982 71 p
(Contract NAS9-16023)
(NASA-CR-188727; NAS 1.26:188727; CSDL-R-1582) Avail: NTIS HC/MF A04 CSCL 22B

The equations of motion for a flexible vehicle capable of arbitrary translational and rotational motions in inertial space accompanied by small elastic deformations are derived in an unabridged form. The vehicle is idealized as consisting of a single rigid body with an ensemble of mass particles interconnected by massless elastic structure. The internal elastic restoring forces are quantified in terms of a stiffness matrix. A transformation and truncation of elastic degrees of freedom is made in the interest of numerical integration efficiency. Deformation dependent terms are partitioned into a hierarchy of significance. The final set of motion equations are brought to a fully assembled first order form suitable for direct digital implementation. A FORTRAN program implementing the equations is given and its salient features described. Author

N91-29212*# Arizona State Univ., Tempe. Dept. of Mechanical and Aerospace Engineering.
EXPERIMENTAL DEMONSTRATION OF A CLASSICAL APPROACH FOR FLEXIBLE SPACE STRUCTURE CONTROL: NASA CSI TESTBEDS Final Report
Wie Bond 31 Aug. 1991 54 p
(Grants NAG1-965; NAG1-1083)
(NASA-CR-188724; NAS 1.26:188724) Avail: NTIS HC/MF A04 CSCL 22B

The results of active control experiments performed for the Mini-Mast truss structure are presented. The primary research objectives were: (1) to develop active structural control concepts and/or techniques; (2) to verify the concept of robust non-minimum-phase compensation for a certain class of non-colocated structural control problems through ground

experiments; (3) to verify a 'dipole' concept for persistent disturbance rejection control of flexible structures; and (4) to identify CSI (Control Structure Interaction) issues and areas of emphasis for the next generation of large flexible spacecraft. The classical SISO (Single Input and Single Output) control design approach was employed. Author

N91-29213*# National Aeronautics and Space Administration. Marshall Space Flight Center, Huntsville, AL.
WHIPPLE BUMPER SHIELD SIMULATIONS
E. S. Hertel, L. C. Chhabildas (Sandia National Labs., Albuquerque, NM.), and S. A. Hill 1991 4 p Presented at the 1991 American Physical Society (APS) Conference on Shock Compression of Condensed Matter, Williamsburg, 17-20 Jul. 1991 (Contract DE-AC04-76DP-00789)
(NASA-TM-105089; NAS 1.15:105089; DE91-014896; SAND-91-1227C; CONF-9107105-45) Avail: NTIS HC/MF A01 CSCL 22B

The Whipple bumper is a space shield designed to protect a space station from the most hazardous orbital space debris environment. A series of numerical simulations has been performed using the multi-dimensional hydrodynamics code CTH to estimate the effectiveness of the thin Whipple bumper design. These simulations are performed for impact velocities of (approximately)10 km/s which are now accessible by experiments using the Sandia hypervelocity launcher facility. For a (approximately)10 km/s impact by a 0.7 gm aluminum flier plate, the experimental results indicate that the debris cloud resulting upon impact of the bumper shield by the flier plate, completely penetrates the sub-structure. The CTH simulations also predict complete penetration by the subsequent debris cloud. DOE

N91-29214# Harris Corp., Melbourne, FL. Government Aerospace Systems Div.
EXPERIMENTAL VERIFICATION OF AN INNOVATIVE PERFORMANCE-VALIDATION METHODOLOGY FOR LARGE SPACE SYSTEMS Final Report, 15 Aug. 1987 - 14 Feb. 1991
David C. Hyland 9 Feb. 1991 171 p
(Contract F49620-87-C-0108)
(AD-A237864; AFOSR-91-0232TR) Avail: NTIS HC/MF A08 CSCL 22/2

A technology gap exists in verifying performance of large space systems. To fill that gap the proposed program seeks to develop and validate an efficient pre-flight performance verification methodology. The approach involves selective component testing along with analysis of subsystem interactions. The methodology exploits MEOP (Maximum Entropy/Optimal Projection) Control System Design and Majorant Robustness Analysis. The approach is formulated for several representative large space systems and experimentally verified on a 3-meter diameter multi-hex panel ground-based active control tested. GRA

N91-29215# Naval Postgraduate School, Monterey, CA.
ABLATIVE HEAT SHIELD STUDIES FOR NASA MARS/EARTH RETURN ENTRY VEHICLES M.S. Thesis
Michael K. Hamm Sep. 1990 111 p
(AD-A238159) Avail: NTIS HC/MF A06 CSCL 11/2

A material that behaves likes a glassy ablator on the surface, has a low thermal conductivity, is structurally tough, lightweight, and is in some sense reusable, would be desirable for the protective heat shield used on Earth entry vehicles. A material for this purpose has been developed that uses silicon dioxide (fused quartz) in a fibrous packed matrix, forming blocks which can behave as a glassy ablator on the surface when subject to very high surface heat fluxes. These fibrous silicon dioxide blocks are called Reusable Surface Insulation (RSI). The primary constituent of the RSI material is silicon dioxide, but may contain other compounds (e.g., alumina borosilicate) to affect the thermal and physical properties. The research performed in this thesis is to determine the ablative behavior of ceramic RSI materials in a hypersonic high enthalpy flow that is used to simulate entry into Earth atmosphere. Actual arc jet experiments were performed to measure mass loss, melt run off, and fiber collapse of these materials and compare the experimental results with predicted theoretical values. The tests were performed to ascertain if RSI type materials could be used for entry vehicles proposed in NASA Mars missions. GRA

N91-29216# Air Force Inst. of Tech., Wright-Patterson AFB, OH. School of Engineering.
THE OPTIMAL LOCATION OF GEODSS SENSORS IN CANADA M.S. Thesis
Pierre J. Forgues Feb. 1991 317 p
(AD-A238444; AFIT/GSO/ENS/91M-1) Avail: NTIS HC/MF A14 CSCL 17/8

This thesis studies the maximal coverage p-median and the set covering facility location problems as applied to the GEODSS location problem. The classical single-objective mathematical formulations of the p-median and set covering problems are converted into network-flow formulations and various solution methods are developed using a scaled-down version of the GEODSS problem. The next step is the introduction of a second criterion function into the problem. This second function consists of minimizing the sum of the variance in coverage at the selected locations. Research reveals the deficiencies of MOLP (multiobjective linear programming) techniques in generating the efficient frontier of an integer problem. A brute-force solution algorithm is developed and programmed in FORTRAN 77 to generate all feasible alternatives, determine which of these are non-dominated, and then provide an ordered list of alternatives using paired comparisons with the ideal. A case study is presented which shows the difficulty in finding a feasible one-site solution given the need to observe a wide segment of the geostationary belt. The example also shows that, for a given satellite population, the optimal alternative must for similar reasons include two southerly locations. The example reveals that while two-site solutions therefore exclude northerly locations, three-site solutions will usually include a northerly location. GRA

N91-29217# Naval Postgraduate School, Monterey, CA.
OPERATIONAL PROCEDURES FOR POWERING UP, POWERING DOWN, AND CONFIGURING THE QUALIFICATION MODEL OF THE FLTSATCOM SATELLITE M.S. Thesis
H. Lawson, Jr. Sep. 1990 163 p
(AD-A238485) Avail: NTIS HC/MF A08 CSCL 22/2

The engineering qualification model of the Fleet Satellite Communications (FLTSATCOM) satellite was donated and is to be used for instructional laboratories and research. With the acquisition of this spacecraft, a course was established on spacecraft testing with the intent of using the qualification model as a lab device. The course requirement calls for the ability to power up, power down, and configure the satellite within a reasonable time frame. The objective of this thesis is to produce a single source implementation guide which will fully document the step-by-step procedures for powering up, powering down, and configuring the qualification model of the FLTSATCOM satellite in its current modified configuration. GRA

N91-29218# Calspan Field Services, Inc., Arnold AFS, TN.
CARINA AEROTHERMAL TEST AT MACH 8 Final Report, 16-18 Apr. 1991
M. G. Hammond Jul. 1991 50 p Prepared in cooperation with AEDC
(AD-A238561; AEDC-TSR-91-V12) Avail: NTIS HC/MF A03 CSCL 22/2

The test articles were scale models of the Carina Space Recovery Vehicle. Carina is an axisymmetric model of a blunt, low lift-to-drag reentry vehicle. Surface pressure, heat transfer, force and moment, base pressure, and oil flow visualization data were acquired on four model configurations of the Carina Space Recovery Vehicle. The test was conducted in the AEDC Hypersonic Wind Tunnel B at Mach 8 and free-stream Reynolds number of 0.75, 1.0, and 2.0 million per foot. Angle of attack was varied from 0 to 20 deg at roll angles of -180 to 180 deg. GRA

19 SPACECRAFT INSTRUMENTATION

For related information see also *06 Aircraft Instrumentation* and *35 Instrumentation and Photography.*

N91-29219*# Arizona Univ., Tucson. Lunar and Planetary Lab.
PLANETARY INSTRUMENT DEFINITION AND DEVELOPMENT PROGRAM: 'MINIATURE MONOCHROMATIC IMAGER' Final Technical Report
A. L. Broadfoot 12 Aug. 1991 111 p Submitted for publication Original contains color illustrations
(Contracts NASw-4245; NAG5-637; F19628-86-K-0040; NSF ATM-88-14440)
(NASA-CR-186550; NAS 1.26:186550) Avail: NTIS HC/MF A06; 7 functional color pages CSCL 14B

The miniature monochromatic imager (MMI) development work became the basis for the preparation of several instruments which were built and flown on the shuttle STS-39 as well as being used in ground based experiments. The following subject areas are covered: (1) applications of the ICCD to airglow and auroral measurements and (2) a panchromatic spectrograph with supporting monochromatic imagers. Author

20 SPACECRAFT PROPULSION AND POWER

Includes main propulsion systems and components, e.g., rocket engines; and spacecraft auxilliary power sources.

For related information see also *07 Aircraft Propulsion and Power, 28 Propellants and Fuels, 44 Energy Production and Conversion,* and *15 Launch Vehicles and Space Vehicles.*

N91-29220*# National Aeronautics and Space Administration. Lewis Research Center, Cleveland, OH.
DESIGN ISSUES FOR PROPULSION SYSTEMS USING METALLIZED PROPELLANTS
Bryan Palaszewski and Douglas Rapp (Sverdrup Technology, Inc., Brook Park, OH.) 1991 27 p Presented at the Advanced Space Exploration Initiative Technologies, Cleveland, OH, 4-6 Sep. 1991; cosponsored by AIAA and OAI
(NASA-TM-105190; E-6492; NAS 1.15:105190; AIAA-91-3484)
Avail: NTIS HC/MF A03 CSCL 21H

Metallized propellants are liquid propellants that contain metal particles. These particles are suspended in a gelled fuel or oxidizer. Aluminum is used as the metal additive. The addition of metal to conventional propellants can increase their specific impulse and their density over conventional propellants, and consequently, the payload delivered on Mars and lunar transportation vehicles, Earth-to-Orbit vehicles and upper stages for robotic planetary missions. Gelled fuels also provide increased safety during accidental propellant leakage or spills. To take full advantage of these potential performance increases, there are changes that must be made to the vehicle design. The differences are discussed between metallized propellant and traditional liquid propellants and their effect on the propulsion system design. These differences include the propellant density, mixture ratio, engine performance, and propellant rheology. Missions related to the Space Exploration Initiative are considered as design examples to illustrate these issues. Author

N91-29221*# National Aeronautics and Space Administration. Lewis Research Center, Cleveland, OH.
NUMERICAL PROPULSION SYSTEM SIMULATION: AN INTERDISCIPLINARY APPROACH
Lester D. Nichols and Christos C. Chamis 1991 16 p Presented at the Conference on Advanced Space Exploration Initiative Technologies, Clevelend, OH, 4-6 Sep. 1991; cosponsored by AIAA and OAI
(NASA-TM-105181; E-6359; NAS 1.15:105181; AIAA-91-3554)
Avail: NTIS HC/MF A03 CSCL 21H

The tremendous progress being made in computational engineering and the rapid growth in computing power that is resulting from parallel processing now make it feasible to consider the use of computer simulations to gain insights into the complex interactions in aerospace propulsion systems and to evaluate new concepts early in the design process before a commitment to hardware is made. Described here is a NASA initiative to develop a Numerical Propulsion System Simulation (NPSS) capability. Author

N91-29222*# National Aeronautics and Space Administration. Lewis Research Center, Cleveland, OH.
PRODUCTION AND USE OF METALS AND OXYGEN FOR LUNAR PROPULSION
Aloysius F. Hepp, Diane L. Linne, Geoffrey A. Landis, Mary F. Groth, and James E. Colvin (Arizona Univ., Tucson.) 1991 13 p Presented at the Conference on Advanced Space Exploration Initiative Technologies, Cleveland, OH, 4-6 Sep. 1991; cosponsored by AIAA and OAI
(NASA-TM-105195; E-6496; NAS 1.15:105195; AIAA-91-3481)
Avail: NTIS HC/MF A03 CSCL 21H

Production, power, and propulsion technologies for using oxygen and metals derived from lunar resources are discussed. The production process is described, and several of the more developed processes are discussed. Power requirements for chemical, thermal, and electrical production methods are compared. The discussion includes potential impact of ongoing power technology programs on lunar production requirements. The performance potential of several possible metal fuels including aluminum, silicon, iron, and titanium are compared. Space propulsion technology in the area of metal/oxygen rocket engines is discussed. Author

N91-29223# Georgia Inst. of Tech., Atlanta. School of Aerospace Engineering.
INVESTIGATION OF THE FLAME-ACOUSTIC WAVE INTERACTION DURING AXIAL SOLID ROCKET INSTABILITIES Final Report, 1 Mar. 1989 - 28 Feb. 1991
Ben T. Zinn and Brady R. Daniel 30 Apr. 1991 47 p
(Grant AF-AFOSR-0290-89; AF Proj. 2308)
(AD-A237851; AFOSR-91-0600TR) Avail: NTIS HC/MF A03 CSCL 21/2

Primary research objectives are to: (1) investigate mechanisms responsible for driving of axial instabilities by solid propellant flames; (2) determine whether state-of-the-art theoretical models can predict characteristics of the flame driving mechanisms; and (3) investigate the effect of flow turning upon axial instabilities in solid propellant rocket motors. To attain these objectives, the response of diffusion flames, stabilized on the side wall of a duct, to imposed acoustic waves was investigated by using flame radiation measurements and laser Doppler velocimetry (LDV). Flame radiation measurements revealed that the presence of an acoustic field produced space dependent oscillatory heat release rates which deperd upon characteristics of the flame and the excited acoustic field. Measurements of flame radiation and velocity field both showed that at a given instant some sections of the flame drive the acoustic field while others damp it. The net effect of the flame upon the acoustic field depends on the relative magnitude of these driving and damping regions. Validity of a previously developed flame response model was investigated by comparing measured and predicted oscillatory velocity components in the flame region. Using measured values of the acoustic admittance of the burner, flame shape, and steady state temperature distribution in the flame region, the model was used to predict oscillatory vertical velocity distributions in the flame region. GRA

N91-29224# Veritay Technology, Inc., Amherst, NY.
TWENTY FIRST CENTURY PROPULSION CONCEPT Final Report, 7 Feb. 1989 - 7 Jul. 1990
Robert L. Talley May 1991 102 p
(Contract F04611-89-C-0023)
(AD-A237853; F06-9-1; PL-TR-91-3009) Avail: NTIS HC/MF A06 CSCL 21/3

This contract explored the Biefield-Brown effect which allegedly converts electrostatic energy directly into a propulsive force in a

vacuum environment. The program emphasized the experimental exploration of this electrostatic thrust-generation concept to confirm or deny its existence, to verify its operation under high vacuum conditions, and to establish an experimental database via tests with candidate devices to permit the nature and magnitude of its thrust to be determined. An improved laboratory test configuration was developed for quantifying electrostatically induced propulsive forces on selected devices. This configuration used a vacuum chamber and diffusion pump arrangement which extended conditions to the 1 microtorr range. While attempts were made to increase the driving DC voltage to 50 kV or more, the driving voltages were generally limited to about 19 kV to avoid electrical breakdown problems. Boundary effects arising from the presence of induced surface charges on the walls of the vacuum chamber surrounding the test devices were significant, and had to be taken into account in using the torsion pendulum system to make thrust force measurements. Direct experimental results indicate that no detectable propulsive force was electrostatically induced by applying a static potential difference up to 19 kV between the electrodes of test devices under conditions in which electrical breakdowns did not occur. GRA

N91-29225# Forward Unltd., Oxnard, CA.
TWENTY FIRST CENTURY SPACE PROPULSION STUDY ADDENDUM Final Report, 25 Sep. 1990 - 15 Jan. 1991
Robert L. Forward Jun. 1991 40 p
(Contract F04611-87-C-0029)
(AD-A238011; PL-TR-91-3022-Add) Avail: NTIS HC/MF A03 CSCL 21/3

This addendum to the final report on the contract (AL-TR-90-030, 21st Century Space Propulsion Study, (Oct. 1990, AD A229279) evaluates a number of new space propulsion and sensor concepts. The major topics covered were coherent neutrino scattering and its application to neutrino sensors, the use of tethers for power and propulsion in space, the application of high pressure, high energy density materials, specifically metallic hydrogen, to divert velocity thrusters, and the use of solar sails to provide a non-orbiting space platform for surveillance and space-to-surface missiles. Two technical papers, included as appendices, are entitled: Surgical strikes from space using solar sail satellites; The Weber effect experiments. GRA

N91-29226# Aeronautical Research Labs., Melbourne (Australia).
A COMPUTER PROGRAM FOR PREDICTION OF INTERNAL PERFORMANCE OF A RAMROCKET
Lincoln P. Erm Apr. 1991 23 p
(AD-A238179; ARL-PROP-TM-452; DODA-AR-006-599) Avail: NTIS HC/MF A03 CSCL 12/5

The operation of a computer program to predict idealized ramrocket performance is described. The program predicts performance for chosen aerodynamic and thermodynamic variables and contains provisions for varying the gas generator propellant formulation. GRA

N91-29227# Aerospace Corp., El Segundo, CA. Vehicle and Control Systems Div.
SLAG AND THERMAL ENVIRONMENT OF A SPINNING ROCKET MOTOR Technical Report, Jun. 1988 - Jul. 1990
I-Shih Chang May 1991 28 p
(Contract F04701-88-C-0089)
(AD-A238557; TR-0091(6464-05)-1; SSD-TR-91-15) Avail: NTIS HC/MF A03 CSCL 21/2

It has been demonstrated that an increase in radial and/or axial acceleration results in an increase in the amount of slag accumulated in the chamber of a motor with a submerged nozzle design. The slag is composed of aluminum and alumina residue from the combustion of aluminized solid propellants. The presence of slag in the chamber influences motor burnout weight, soak-out thermal environment, residual thrust, and motor performance. An excessive amount of slag in the chamber also could affect mission success. This report studies the effect of slag in the chamber on the motor case thermal environment of a spinning rocket motor. Very good agreement between analysis results and ground test data is obtained for motor case temperature histories throughout the motor firing and heat soak period of the spinning payload assist module (Star-48) qualification motors. In the area in which the insulation is exposed to combustion products during motor firing, the insulation erosion rate is a function of motor spinning rate. During heat soak, the slag mass is considered to be the single parameter that influences the thermal environment of a spinning rocket motor. Available data from a flight motor are analyzed and compared with the analysis results. The thermal environment for the PAM-S/Ulysses flight motor is predicted. For a spinning flight motor, the analysis reveals that the insulation erosion rate and the amount of slag in the chamber of a spinning flight motor can be assessed or sensed from monitoring the temperature history on the outside surface of the motor case. GRA

N91-29228*# National Aeronautics and Space Administration. Lewis Research Center, Cleveland, OH.
PRESSURE MEASUREMENTS IN A LOW-DENSITY NOZZLE PLUME FOR CODE VERIFICATION
Paul F. Penko, Iain D. Boyd, Dana L. Meissner, and Kenneth J. DeWitt (Toledo Univ., OH.) 1991 18 p Presented at the 27th Joint Propulsion Conference, Sacramento, CA, 24-27 Jun. 1991; sponsored by AIAA, SAE, ASME, and ASEE Previously announced as A91-45783
(NASA-TM-105170; E-6463; NAS 1.15:105170; AIAA-91-2110)
Avail: NTIS HC/MF A03 CSCL 21H

Measurements of Pitot pressure were made in the exit plane and plume of a low-density, nitrogen nozzle flow. Two numerical computer codes were used to analyze the flow, including one based on continuum theory using the explicit MacCormack method, and the other on kinetic theory using the method of direct-simulation Monte Carlo (DSMC). The continuum analysis was carried to the nozzle exit plane and the results were compared to the measurements. The DSMC analysis was extended into the plume of the nozzle flow and the results were compared with measurements at the exit plane and axial stations 12, 24 and 36 mm into the near-field plume. Two experimental apparatus were used that differed in design and gave slightly different profiles of pressure measurements. The DSMC method compared well with the measurements from each apparatus at all axial stations and provided a more accurate prediction of the flow than the continuum method, verifying the validity of DSMC for such calculations. Author

N91-29229*# National Aeronautics and Space Administration. Lewis Research Center, Cleveland, OH.
PERFORMANCE AND OPTIMIZATION OF A DERATED ION THRUSTER FOR AUXILIARY PROPULSION
Michael J. Patterson and John E. Foster (Jackson State Univ., MS.) 1991 18 p Presented at the 27th Joint Propulsion Conference, Sacramento, CA, 24-27 Jun. 1991; sponsored by AIAA, SAE, ASME and ASEE Previously announced as A91-45809
(NASA-TM-105144; E-6419; NAS 1.15:105144; AIAA-91-2350)
Avail: NTIS HC/MF A03 CSCL 21H

The characteristics and implications of use of a derated ion thruster for north-south stationkeeping (NSSK) propulsion are discussed. A derated thruster is a 30 cm diameter primary propulsion ion thruster operated at highly throttled conditions appropriate to NSSK functions. The performance characteristics of a 30 cm ion thruster are presented, emphasizing throttled operation at low specific impulse and high thrust-to-power ratio. Performance data and component erosion are compared to other NSSK ion thrusters. Operations benefits derived from the performance advantages of the derated approach are examined assuming an INTELSAT 7-type spacecraft. Minimum ground test facility pumping capabilities required to maintain facility enhanced accelerator grid erosion at acceptable levels in a lifetest are quantified as a function of thruster operating condition. Approaches to reducing the derated thruster mass and volume are also discussed. Author

N91-29230*# National Aeronautics and Space Administration. Lewis Research Center, Cleveland, OH.
EXPERIMENTAL AND ANALYTICAL COMPARISON OF FLOWFIELDS IN A 110 N (25 lbf) H2/O2 ROCKET
Brian D. Reed, Paul F. Penko, Steven J. Schneider, and Suk C. Kim (Sverdrup Technology, Inc., Brook Park, OH.) 1991 17 p Presented at the 27th Joint Propulsion Conference, Sacramento, CA, 24-27 Jun. 1991; sponsored by AIAA, SAE, ASME, and ASEE Previously announced as A91-45802
(Contract NAS3-25266)
(NASA-TM-105175; E-6471; NAS 1.15:105175) Avail: NTIS HC/MF A03 CSCL 21H

A gaseous hydrogen/gaseous oxygen 110 N (25 lbf) rocket was examined through the RPLUS code using the full Navier-Stokes equations with finite rate chemistry. Performance tests were conducted on the rocket in an altitude test facility. Preliminary parametric analyses were performed for a range of mixture ratios and fuel film cooling pcts. It is shown that the computed values of specific impulse and characteristic exhaust velocity follow the trend of the experimental data. Specific impulse computed by the code is lower than the comparable test values by about two to three percent. The computed characteristic exhaust velocity values are lower than the comparable test values by three to four pct. Thrust coefficients computed by the code are found to be within two pct. of the measured values. It is concluded that the discrepancy between computed and experimental performance values could not be attributed to experimental uncertainty.
Author

N91-29231*# National Aeronautics and Space Administration. Lewis Research Center, Cleveland, OH.
ARCJET THERMAL CHARACTERISTICS
John M. Sankovic and Francis M. Curran 1991 31 p Presented at the 27th Joint Propulsion Conference, Sacramento, CA, 24-27 Jun. 1991; sponsored by AIAA, SAE, ASME, and ASEE Previously announced as A91-45814
(NASA-TM-105156; E-6442; NAS 1.15:105156; AIAA-91-2456)
Copyright Avail: NTIS HC/MF A03 CSCL 21H

The performance of water-cooled and radiation cooled arcjet thrusters operating on both 1:2 nitrogen/hydrogen mixtures at 1 to 2 kW and on pure hydrogen at 1 to 4 kW are compared. To investigate the effects of test facility background pressure on performance, data were taken for both thruster operating on nitrogen/hydrogen mixtures at facility background pressures nominally at 0.20 Pa and 20 Pa. It is shown that increasing the background pressure decreased the thruster performance, and simple pressure area corrections alone could not account for observed degradation in performance. Author

N91-29232# Brookhaven National Lab., Upton, NY.
LIGHT WEIGHT SPACE POWER REACTORS FOR NUCLEAR ELECTRIC PROPULSION
H. Ludewig, S. Mughabghab, O. Lazareth, K. Perkins, E. Schmidt, and J. R. Powell 1991 11 p Presented at the 6th International Conference on Emerging Nuclear Energy Systems, Monterey, CA, 16-21 Jun. 1991
(Contract DE-AC02-76CH-00016)
(DE91-014803; BNL-46235; CONF-910626-2) Avail: NTIS HC/MF A03

A Nuclear Electric Propulsion (NEP) unit capable of propelling a manned vehicle to Mars will be required to have a value of alpha (kg/kWe) which is less than five. In order to meet this goal the reactor mass, and thus its contribution to the value of alpha will have to be minimized. In this paper a candidate for such a reactor is described. It consists of a gas cooled Particle Bed Reactor (PBR), with specially chosen materials which allow it to operate at an exit temperature of approximately 2000 K. One of the unique features of a PBR is the direct cooling of particulate fuel by the working fluid. This feature allows for high power densities, highest possible gas exit temperatures, for a given fuel temperature and because of the thin particle bed a low pressure drop. The PBR's described in this paper will have a ceramic moderator (Be2C), ZrC coated fuel particles and a carbon/carbon hot frit. All the reactors will be designed with sufficient fissile loading to operate at full power for seven years. The burn up possible with particulate fuel is approximately 30 to 50 percent. These reactor designs achieve a value of alpha less than unity in the power range of interest (5 MWe). DOE

N91-29233*# Aerojet TechSystems Co., Sacramento, CA.
ALS ROCKET ENGINE COMBUSTION DEVICES DESIGN AND DEMONSTRATION Interim Study Report
Steve Arreguin 29 Sep. 1989 301 p
(NAS8-38080)
(NASA-CR-183824; NAS 1.26:183824) Avail: NTIS HC/MF A14 CSCL 21H

Work performed during Phase one is summarized and the significant technical and programmatic accomplishments occurring during this period are documented. Besides a summary of the results, methodologies, trade studies, design, fabrication, and hardware conditions; the following are included: the evolving Maintainability Plan, Reliability Program Plan, Failure Summary and Analysis Report, and the Failure Mode and Effect Analysis.
Author

23 CHEMISTRY AND MATERIALS (GENERAL)

N91-29234# Army Armament Research, Development and Engineering Center, Picatinny Arsenal, NJ.
METHODS TO DETERMINE THE COMPATIBILITY AND DEGRADATION OF ORGANIC MATERIALS Final Report
Robert B. Bonk, Linda J. Morlan, and Kathleen A. Chabot Jul. 1991 31 p
(AD-A237940; ARAED-TR-91012) Avail: NTIS HC/MF A03 CSCL 19/1

Some of the various methods used to evaluate the compatibility and degradation of organics when exposed directly or indirectly to energetic and nonenergetic materials is described in this report. The compatibility and degradation of materials has been and will continue to be a repeated problem with both developmental and field commodities. The deterioration process is due to numerous factors, i.e., time, temperature, humidity, heat, types of exposure (storage - direct or indirect), materials involved, etc. If this type of information is not available prior to fielding an item, catastrophic failures could result. Therefore, it is imperative that information on the compatibility of systems be known or generated prior to fielding. GRA

N91-29235*# National Aeronautics and Space Administration. Lewis Research Center, Cleveland, OH.
AN ANALYSIS OF THE WEAR BEHAVIOR OF SiC WHISKER REINFORCED ALUMINA FROM 25 TO 1200 C
Christopher DellaCorte Aug. 1991 19 p
(NASA-TM-104489; E-6337; NAS 1.15:104489) Avail: NTIS HC/MF A03 CSCL 11D

A model is described for predicting the wear behavior of whisker reinforced ceramics. The model was successfully applied to a silicon carbide whisker reinforced alumina ceramic composite subjected to sliding contact. The model compares the friction forces on the whiskers due to sliding, which act to pull or push them out of the matrix, to the clamping or compressive forces on the whiskers due to the matrix, which act to hold the whiskers in the composite. At low temperatures, the whiskers are held strongly in the matrix and are fractured into pieces during the wear process along with the matrix. At elevated temperatures differential thermal expansion between the whiskers and matrix can cause loosening of the whiskers and lead to pullout during the wear process and to higher wear. The model, which represents the combination of elastic stress analysis and a friction heating analysis, predicts a transition temperature at which the strength of the whiskers equals the clamping force holding them in the matrix. Above the transition the whiskers are pulled out of the matrix during sliding, and below

the transition the whiskers are simply fractured. The existence of the transition gives rise to a dual wear mode or mechanism behavior for this material which was observed in laboratory experiments. The results from this model correlate well with experimentally observed behavior indicating that the model may be useful in obtaining a better understanding of material behavior and in making material improvements. Author

24 COMPOSITE MATERIALS

Includes physical, chemical, and mechanical properties of laminates and other composite materials.

For ceramic materials see *27 Nonmetallic Materials*.

N91-29236# National Aeronautical Establishment, Ottawa (Ontario). Structures and Materials Lab.

ASSESSMENT OF IMPACT DAMAGE IN TOUGHENED RESIN COMPOSITES

C. Poon, T. Benak, and R. Gould 8 Mar. 1989 42 p Presented at CAARC Specialists Symposium, Melbourne, Australia, 18-19 May 1988

(NAE-LTR-ST-1695; CTN-91-60025) Copyright Avail: NTIS HC/MF A03

Low energy impact can produce internal delaminations in carbon/epoxy composites with little visible surface damage. This barely visible impact damage is of major concern in the design of composite aircraft structures from a damage tolerance viewpoint because it causes a significant reduction in compressive strength and it reduces fatigue strength as a result of delamination growth under compression cyclic loading. An evaluation of the impact performance of three commercial toughened resin systems against the baseline T300/5208 material was performed using an instrumented dropweight impact method. The following conclusions were reached: (1) The toughened resin systems can absorb a much higher level of elastic energy than the baseline system; (2) Toughened resin systems absorb inelastic energy by a damage process that involves delaminations and intralaminar transverse shear cracks (The baseline system absorbs inelastic energy by fiber and matrix fractures that coalesce to form a major through-the-thickness crack with extensive delaminations in every ply of the laminate); (3) Toughened resin systems have better resistance to impact loading as evidenced by the production of barely visible impact damage in contrast to the production of easily visible impact damage in the baseline system for the same impact energy; (4) Results of the compression-after-impact tests have indicated that the residual compressive properties for the toughened resin systems are higher than those for the baseline system. Author (CISTI)

N91-29237# National Aeronautical Establishment, Ottawa (Ontario). Structures and Materials Lab.

EFFECT OF FORTIFIER ON COMPRESSION-AFTER-IMPACT STRENGTH OF CARBON FABRIC REINFORCED EPOXY

R. F. Scott, P. C. Gaudert, C. Poon, S. Lee, R. Gould, and W. H. Ubbink Jan. 1990 45 p Sponsored by Department of National Defence

(NAE-LTR-ST-1736; CTN-91-60081) Copyright Avail: NTIS HC/MF A03

An investigation was conducted to determine the effect of fortifier additions on behavior during impact and compression-after-impact properties of carbon fabric reinforced epoxy composites. The experimental materials included three matrix compositions: two with different fortifier contents and one with no fortifier as a base for comparison. The experimental work included determining absorbed impact energies, damage areas and compression-after-impact strengths for two impact energy levels as well as compression strength of nonimpacted specimens. It was found that all prepreg materials used were easy to process and produced high quality laminates. The compressive strength of the nonimpacted carbon fabric reinforced material was found to increase with the addition of fortifier while the compressive moduli when normalized to a fiber content by volume of 60 pct. showed minor increases. The addition of fortifier reduced the absorbed energy and damage areas in the specimens and also increased the compression-after-impact strength significantly. Changes in strain at failure of the material associated with the addition of fortified were not significant. Author (CISTI)

N91-29238 Ohio State Univ., Columbus.

ULTRASONIC EVALUATION OF ELASTIC AND INTERFACIAL PROPERTIES OF COMPOSITE MATERIALS AND LAMINATES Ph.D. Thesis

Weicheng David Wang 1990 253 p

Avail: Univ. Microfilms Order No. DA9111812

Discussed here are new ultrasonic techniques developed for the determination of elastic constants of composite materials and interfacial properties of composite laminates with application to the evaluation of adhesive joints. For the determination of elastic constants, both bulk wave and plate wave techniques are included. Two bulk wave techniques are used for evaluation of thick composite materials, namely, a critical angle technique and a double transmission time delay technique. A plate mode antiresonance technique is developed for evaluation of thin composites. For evaluation of the interfacial properties of composite laminates, an algorithm is developed for computation of coefficients of reflection and transmission of an obliquely incident sound wave onto a layered anisotropic system bounded by two solid semispaces. Dissert. Abstr.

N91-29239*# National Aeronautics and Space Administration. Langley Research Center, Hampton, VA.

EFFECT OF FIBER-MATRIX DEBONDING ON NOTCHED STRENGTH OF TITANIUM METAL MATRIX COMPOSITES

C. A. Bigelow and W. S. Johnson Aug. 1991 33 p Presented at the ASTM 23rd National Symposium on Fracture Mechanics, College Station, TX, 18-20 Jun. 1991

(NASA-TM-104131; NAS 1.15:104131) Avail: NTIS HC/MF A03 CSCL 11D

Two specimen configuration of a (0/90)2s SCS-6/Ti-15-3 laminate were tested and analyzed: a center hole (CH) specimen and a double edge notch (DEN) specimen. The two specimen configurations failed at simular stress levels. Two analytical techniques, a 3-D finite-element analysis and a macro-micromechanical analysis were used to predict the overall stress-deformation behavior and the notch-tip fiber-matrix interface stresses in both configurations. Author

N91-29240*# National Aeronautics and Space Administration. Langley Research Center, Hampton, VA.

NASA WORKSHOP ON IMPACT DAMAGE TO COMPOSITES

C. C. Poe, Jr. Jul. 1991 476 p Workshop held in Hampton, Va, 19-20 Mar. 1991

(NASA-CP-10075; NAS 1.55:10075) Avail: NTIS HC/MF A21 CSCL 11D

A compilation of slides presented at the NASA Workshop on Impact Damage to Composites held on March 19 and 20, 1991, at the Langley Research Center, Hampton, Virginia is given. The objective of the workshop was to review technology for evaluating impact damage tolerance of composite structures and identify deficiencies. Research, development, design methods, and design criteria were addressed. Actions to eliminate technology deficiencies were developed. A list of those actions and a list of attendees are also included. Author

N91-29241# Wichita State Univ., KS. National Inst. for Aviation Research.

IMPACT CHARACTERIZATION OF GRAPHITE FIBER REINFORCED THERMOPLASTIC LAMINATES

J. Chaudhuri, G. H. Choe, and J. R. Vinson (Delaware Univ., Newark.) 1991 12 p

(NIAR-91-16) Avail: NTIS HC/MF A03

Instrumented drop weight impact testings were conducted in conjunction with the ultrasonic C-scan and scanning electron microscopy to characterize the impact response at low velocities. Thermoplastic composite materials in the simply supported case

showed dramatic improvements in impact damage resistance compared to the thermoset composite materials as reported. Scanning electron microscopy examination of the fracture surface revealed fiber matrix debonding, fiber pull-out, and a few delaminations. Matrix behavior can be characterized by a hackly appearance. On the other hand, the fracture mechanisms of the transverse normal compression and shear punch were matrix cracking and grouped lamina delamination, respectively. Author

N91-29242# Lasergenics Corp., San Jose, CA.
VERY HIGH TEMPERATURE FIBERS OF TiC AND TiB2 Final Report, Apr. 1988 - Aug. 1990
Richard G. Schlecht May 1991 52 p
(Contract F33615-88-C-5478)
(AD-A237423; WL-TR-91-4041) Avail: NTIS HC/MF A04 CSCL 11/4

The purpose of this work is to demonstrate the value of single crystal fibers of titanium carbide and titanium boride as fibers for strengthening elements in matrix composite materials. LaserGenics has used the laser-heated pedestal-growth technique to grow short lengths of these materials in fiber form. We were not able to reduce the oxygen content in the growth chamber to a low enough of a level that would ensure single crystal growth. The fibers grown were multicrystalline and, therefore, did not possess the hoped for strength. It is clear from these early growths that single crystal fibers of these matrix materials can be grown. Growth in a reduced level of oxygen should be done and then fibers of significant length should be grown. GRA

N91-29243# California Univ., San Diego, La Jolla. Dept. of Applied Mechanics and Engineering Sciences.
DEVELOPMENT OF A MIXTURE FOR NONLINEAR WAVE PROPAGATION IN FIBER-REINFORCED COMPOSITES Final Report, 1 Feb. 1987 - 30 Jun. 1989
Hidenori Murakami, T. J. Impelluso, and G. A. Hegemier 31 May 1991 40 p
(Contract N00014-87-K-0176)
(AD-A237471) Avail: NTIS HC/MF A03 CSCL 11/4

A method for constructing dispersive, nonlinear mixture models for unidirectionally fiber-reinforced composites is described herein. System nonlinearities in the treated example result from nonlinear material properties of the constituents. The proposed model is a nonlinear generalization of the linear model developed by Murakami and Hegemier (1986) for elastic constituents. Model construction is based upon a homogenization technique which employs multivariable asymptotic expansions in conjunction with certain weighted residual procedures. The methodology furnishes the equations of motion, the appropriate initial and boundary conditions, and a set of consistent rate constitutive relations. Model validation for linear and nonlinear dynamic responses is accomplished by comparing predicted results for waveguide and wave-reflect problems with the available experimental data or the data obtained by use of a detailed finite element (FE) analysis. GRA

N91-29244# Naval Postgraduate School, Monterey, CA.
ANISOTROPIC TENSILE PROBABILISTIC FAILURE CRITERION FOR COMPOSITES M.S. Thesis
Scott J. McKernan Jun. 1990 161 p
(AD-A237601) Avail: NTIS HC/MF A08 CSCL 11/4

A probabilistic failure criterion is needed to quantitatively predict reliability in critical applications, such as man-safe, deep-sea and air structures, and as an objective function for use in optimum design. Composites are multi-phased and anisotropic, which gives rise to failure in different modes with different probabilistic occurrences that are dependent on the applied stress tensor. Statistical representation of combined stress failure is practically impossible. Probabilistic modeling must be based on the failure modes. This investigation examines the underlying features required in a probabilistic failure criterion for unidirectional fiber-composite structures via Monte Carlo simulations. The interdependencies of the intrinsic strengths (associated with uniaxial loadings) and of the failure modes in a composite structure under combined tensile loadings are elucidated. The joint distribution function for composite failure due to a proportional loading regime is derived starting from the representation of the physical failure process in Boolean operations which, in turn, is represented by probability functions. GRA

N91-29245# Naval Postgraduate School, Monterey, CA.
STATISTICAL CHARACTERIZATION OF GRAPHITE FIBER FOR PREDICTION OF COMPOSITE STRUCTURE RELIABILITY M.S. Thesis
Carl R. Engelbert Jun. 1990 87 p
(AD-A238020) Avail: NTIS HC/MF A05 CSCL 11/4

The increased use of composite materials in Navy applications brings with it the need to know quantitatively the reliability of composite structures. Traditional methods of reliability prediction cannot be used. Therefore, analytical modeling is required, and experimental methods with which to assess the model are needed. This research refined experimental methods and obtained benchmark statistical data on the strength of graphite fibers. With the Chain-of-Bundles local load sharing model, the data were then used as a guide to perform a parametric influence study on the sensitivity of composite structure reliability to the statistical distribution of its constituent graphite fibers. The results indicate a strong influence by the lower tail of the single fiber statistical distribution, which has important implications for design, acceptance testing, and other Navy procurement functions. GRA

N91-29246# Naval Postgraduate School, Monterey, CA.
EFFECT OF ALUMINA PARTICLE ADDITIONS ON THE AGING KINETICS OF 6061 ALUMINUM MATRIX COMPOSITES M.S. Thesis
Susan M. Allen Jun. 1990 62 p
(AD-A238052) Avail: NTIS HC/MF A04 CSCL 11/4

Differential scanning calorimetry (DSC) was conducted using a monolithic 6061 aluminum material and two 6061 aluminum matrix composite materials. The composite materials were reinforced with 10 volume percent and 15 volume percent alumina particles. Electrical resistivity and hardness measurements during isothermal aging treatments were also conducted. The effects of prior aging and alumina particle additions on the growth kinetics and the thermal stability of the metastable phases in each material were studied. The results were used to characterize the effect of reinforcement on the aging kinetics of composite materials. GRA

N91-29247# Materials Sciences Corp., Blue Bell, PA.
COMPOSITE SPECIMEN DESIGN ANALYSIS. VOLUME 2: EXPERIMENTAL EFFORTS Final Report, 12 Jun. 1987 - 30 Jun. 1990
Jeff A. Keesler and Donald F. Adams Jan. 1991 156 p Prepared in cooperation with Wyoming Univ., Laramie
(Contract DAAL04-87-C-0064; DA Proj. 1L6-65502-MM-40)
(AD-A238277; MSC-TFR-2110/1705-Vol-2; UW-CMRG-R-90-101-Vol-2; MTL-TR-91-5-Vol-2) Avail: NTIS HC/MF A08 CSCL 11/4

This composite material test methods investigation involved the performance of seventeen different types of mechanical tests, all of which fell into one of five primary categories: axial tension, axial compression, in-plane shear, interlaminar shear, or combined shear stress. All test specimens were fabricated from Hercules AS4/3501-6 carbon/epoxy prepreg tape. In most cases, several different laminate configurations were tested using each method. The influence of potentially important test parameters such as specimen dimensions, ply angles, etc., on the results of a particular test was determined by testing specimens of slightly different configurations while maintaining the same basic methodology. It was therefore possible to compare results from a basic test method with those from a slight variation of the same method, as well as with other basic methods from within the same primary category. GRA

N91-29248# Northwestern Univ., Evanston, IL. Center for Advanced Cement-Based Materials.
WORKSHOP PROCEEDINGS: TOUGHENING MECHANISMS IN QU ASI-BRITTLE MATERIALS Final Report, Jul. - 1 Nov. 1990

Surendra P. Shah 5 May 1991 569 p Workshop held in Evanston, IL, 16-20 Jul. 1990
(Grant AF-AFOSR-0290-90; AF Proj. 2302)
(AD-A238289; AFOSR-91-0546TR) Avail: NTIS HC/MF A24 CSCL 11/4

Recently, considerable interest has been developing in understanding and modeling the fracture processes in these quasi-brittle materials as well as in designing materials with improved toughness. The research activities in these groups of materials: ceramics, cement and rock can be substantially enhanced with the exchange of information between these three groups of investigators. Since the field is relatively new, it is likely that the researchers working with one set of materials are not aware of similar developments with other sets of materials. Although each material has its own set of specific characteristics, many common aspects can be shared among these quasi-brittle materials. These include: (1) application of nonlinear fracture mechanics, (2) experimental and theoretical considerations of strain localization, (3) microscopic observation of fracture process zone, (4) nondestructive evaluation of damage, (5) models to relate microstructure with macroscopic response, and (6) development of experimental and theoretical tools. The purpose of this workshop was to bring together researchers addressing the problem of fracture in cement, ceramics, and rock so that they can share their knowledge and develop a more general syntheses of the problem. GRA

N91-29249# Northwestern Univ., Evanston, IL. Dept. of Materials Science.
DETERMINING STRESSES IN COMPOSITES
J. B. Cohen Jul. 1991 12 p
(Contract N00014-80-C-1116)
(AD-A238618; TR-31) Avail: NTIS HC/MF A03 CSCL 20/6

The basic diffraction techniques for the stress tensor analysis are reviewed, with particular emphasis on what can be done without knowing the unstressed lattice parameters(s). Examples are given of the residual stresses in thin films, how to measure the bonding and yield stress in composites and separating the micro and macrostresses to examine load sharing between phases. In this paper the term composite includes thin films on substrates, and steel, as well as other phase mixtures i.e., to include any arrangement where one phase has its properties affected by the presence of another. GRA

N91-29250*# National Aeronautics and Space Administration. Lewis Research Center, Cleveland, OH.
MICROSTRUCTURAL AND STRENGTH STABILITY OF CVD SiC FIBERS IN ARGON ENVIRONMENT
Ramakrishna T. Bhatt and David R. Hull 1991 19 p Presented at the 15th Annual Conference on Composites and Advanced Ceramics, Cocoa Beach, FL, 13-16 Jan. 1991; sponsored by the American Ceramic Society
(DA Proj. 1L1-61102-AH-45)
(NASA-TM-103772; E-5957; NAS 1.15:103772; AVSCOM-TR-91-C-014) Avail: NTIS HC/MF A03 CSCL 11D

The room temperature tensile strength and microstructure of three types of commercially available chemically vapor deposited silicon carbide fibers were measured after 1, 10, and 100 hour heat treatments under argon pressures of 0.1 to 310 MPa at temperatures to 2100 C. Two types of fiber had carbon-rich surface coatings and the other contained no coating. All three fiber types showed strength degradation beyond 1400 C. Time and temperature of exposure had greater influence on strength degradation than argon pressure. Recrystallization and growth of near stoichiometric SiC grains appears to be the dominant mechanism for the strength degradation. Author

N91-29251# National Inst. of Standards and Technology, Boulder, CO. Materials Reliability Div.
EFFECT OF A FREE SURFACE ON STRESS DISTRIBUTION IN A BIMATERIAL COMPOSITE
V. K. Tewary and R. D. Kriz Mar. 1991 186 p
(PB91-185116; NIST/SP-802) Avail: NTIS HC/MF A09; also available SOD HC $10.00 as 003-003-03080-5 CSCL 11D

The SI Green's function is calculated and applied to the plane-strain problems in cubic solids. Also, an extension of the Green's function method to the generalized-plain-strain problem is described, which enables the calculation of the elastic response of a solid to a prescribed out-of-plane strain. It is applied to calculate the stress distribution in a composite solid subjected to an out-of-plane load. The final results are in the form of an analytical closed integral representation which can be calculated numerically as well as analytically. The analytical evaluation of the integral by using the contour integration method gives the result in the form of series. The series contains singular as well as non-singular terms. In general, it is difficult to ascertain the convergence of the series representation. The analytical series representation can be used to identify precisely the nature and the weight of each singularity in the stress distribution. Author

N91-29252# Sandia National Labs., Albuquerque, NM.
EFFECTS OF HIGH-INTENSITY SOLAR RADIATION ON CARBON FIBERS
G. J. Kolb, J. D. Shutt, G. B. Freeman, and D. J. ONeil (Georgia Inst. of Tech., Atlanta.) Apr. 1991 126 p
(Contract DE-AC04-76DP-00789)
(DE91-015485; SAND-90-7034) Avail: NTIS HC/MF A07

Very large thermal gradients have been developed in the areas of metals processing, and high-energy incoherent light is currently in use for rapid thermal annealing in the semiconductor processing industry. The combination of the large thermal gradient that is characteristic of the solar furnace, coupled with the wide spectral distribution of solar radiation was thought to lead to unique and useful modifications of materials. Thus, the objective of this project was to develop carbon fibers with improved oxidation resistance or novel properties through the use of the unique characteristics of concentrated solar energy. In the course of this project, a method and apparatus for continuous roll-to-roll exposure of carbon fibers (or other materials) to high-intensity solar radiation were developed. As a result of this project it has been proven that the exposure to high-intensity solar radiation conducted in the Georgia Tech solar furnace is not a conventional graphitization heat treatment. However, it was not possible to conclude with statistical confidence as a result of the tests conducted here that solar exposure of carbon fibers affects oxidation resistance. DOE

N91-29253*# Lockheed Aeronautical Systems Co., Burbank, CA.
COMPOSITE TRANSPORT WING TECHNOLOGY DEVELOPMENT: DESIGN DEVELOPMENT TESTS AND ADVANCED STRUCTURAL CONCEPTS
Charles F. Griffin and William E. Harvill Washington NASA Sep. 1988 111 p
(NAS1-17699)
(NASA-CR-4177; NAS 1.26:4177) Avail: NTIS HC/MF A06 CSCL 11D

Numerous design concepts, materials, and manufacturing methods were investigated for the covers and spars of a transport box wing. Cover panels and spar segments were fabricated and tested to verify the structural integrity of design concepts and fabrication techniques. Compression tests on stiffened panels demonstrated the ability of graphite/epoxy wing upper cover designs to achieve a 35 percent weight savings compared to the aluminum baseline. The impact damage tolerance of the designs and materials used for these panels limits the allowable compression strain and therefore the maximum achievable weight savings. Bending and shear tests on various spar designs verified an average weight savings of 37 percent compared to the aluminum baseline. Impact damage to spar webs did not significantly degrade structural performance. Predictions of spar web shear instability correlated well with measured performance. The structural integrity of spars manufactured by filament winding equalled or exceeded those fabricated by hand lay-up. The information obtained will be applied to the design, fabrication, and test of a full-scale section

of a wing box. When completed, the tests on the technology integration box beam will demonstrate the structural integrity of an advanced composite wing design which is 25 percent lighter than the metal baseline. Author

N91-29254*# Douglas Aircraft Co., Inc., Long Beach, CA.
TEST RESULTS FOR COMPOSITE SPECIMENS AND ELEMENTS CONTAINING JOINTS AND CUTOUTS Final Report
P. T. Sumida, R. C. Madan, and A. V. Hawley Aug. 1988 100 p
(NAS1-17701)
(NASA-CR-178246; NAS 1.26:178246; ACEE-30-FR-3610) Avail: NTIS HC/MF A05 CSCL 11D

A program was conducted to develop the technology for joints and cutouts in a composite fuselage that meets all design requirements of a large transport aircraft for the 1990s. An advanced trijet derivative of the DC-10 was selected as the baseline aircraft. Design and analysis of a 30-foot-long composite fuselage barrel provided a realistic basis for the test effort. The primary composite material was Hexcel F584 resin on 12 K IM6 fiber, in tape and broadgoods form. Fiberglass broadgoods were used in E-glass and S-glass fiber form in the cutout region of some panels. Additionally, injection-molded chopped graphite fiber/PEEK was used for longeron-to-frame shear clips. The test effort included four groups of test specimens, beginning with coupon specimens of mono-layer and cross-piled laminates, progressing through increasingly larger and more complex specimens, and ending with two 4- by 5-foot curved fuselage side panels. One of the side panels incorporated a transverse skin splice, while the second included two cabin window cutouts. Author

25 INORGANIC AND PHYSICAL CHEMISTRY

Includes chemical analysis, e.g., chromatography; combustion theory; electrochemistry; and photochemistry.

For related information see also *77 Thermodynamics and Statistical Physics.*.

N91-29255# United Technologies Research Center, East Hartford, CT.
INVESTIGATION OF PARTICULATE FORMATION DURING DIESEL SPRAY COMBUSTION
L. R. Boedeker 1990 4 p
(Contract DE-AC04-87AL-43058)
(DE90-008282; DOE/AL-43058/T1) Avail: NTIS HC/MF A01

The objective of the contract is to conduct an experimental and analytical research program to investigate strategies for using coherent anti-Stokes Raman scattering (CARS) laser diagnostic techniques for detecting the degree of fuel pyrolysis and determining fuel-air ratio. Smoke and NO(x) production rates depend in a complex way on the local temperature, the evaporation of the diesel spray, the local fuel-air ratio, and the pyrolysis history of the fuel. Furthering the ability of CARS to provide more of this information may give engine designers more insight into the combustion process and allow them to create engines which produce fewer particulates or lower amounts of NO(x). Controlling the production rates is preferable to processing emissions. If they cannot both be suppressed simultaneously, adjusting the tradeoff between producing particulates or NO(x) may be helpful if an exhaust processing method is available for one of them. DOE

N91-29256# California Univ., Berkeley. Lawrence Berkeley Lab.
MOLECULAR BEAM STUDIES OF REACTION DYNAMICS
Y. T. Lee Mar. 1990 12 p Presented at the 1990 Combustion Research Contractors' Meeting, Granlibakken, 6-8 Jun. 1990
(Contract DE-AC03-76SF-00098)
(DE90-011600; LBL-28713-Abs; CONF-9006187-1) Avail: NTIS HC/MF A03

The major thrust of this research project is to elucidate detailed dynamics of simple reactions that are theoretically important and to unravel the mechanism of complex chemical reactions or photochemical processes that play important roles in many macroscopic processes. Molecular beams of reactants are used to study individual reactive encounters between molecules or to monitor photodissociation events in a collision-free environment. Most of the information is derived from measurement of the product fragment energy, angular, and state distributions. Recent activities are centered on the mechanisms of elementary chemical reactions involving oxygen atoms with unsaturated hydrocarbons, the dynamics of endothermic substitution reactions, the dependence of the chemical reactivity of electronically excited atoms on the alignment of excited orbitals, the primary photochemical processes of polyatomic molecules, intramolecular energy transfer of chemically activated and locally excited molecules, the energetics of free radicals that are important to combustion processes, the infrared-absorption spectra of carbonium ions and hydrated hydronium ions, and bond-selective photodissociation through electric excitation. DOE

N91-29257# Brown Univ., Providence, RI.
A MODEL OF MULTICOMPONENT DROPLET EVAPORATION WITH LIQUID PHASE REACTIONS Ph.D. Thesis
Y. Sezen 1990 226 p
(Contract DE-FG22-85PC-80527)
(DE90-012535; DOE/PC-80527/T2) Avail: NTIS HC/MF A11

Research on the dynamics of fuel droplets is of fundamental interest to energy and combustion science. Petroleum plays a significant role in supply the world energy. Since these fuel oils are usually introduced into the combustor as sprays of droplets, it is reasonable to investigate individual droplets which would intimately influence the bulk spray vaporization characteristics, which in turn determines the combustor performance. As interest grows in the use of heavier, synthetic fuels for combustion processes, researchers must re-examine the fuel droplet vaporization problem, both because lower rates of evaporation may pose design problems, and also may lead to greater emissions of unburned coke from combustors. These processes are of interest in connection with the pyrolysis of softening coals. It is experimentally observed that most softening coals exhibit liquid-like behavior during the pyrolysis process, especially under elevated temperature conditions (i.e., 650K and above). The fluidity and plasticity characteristics of softening coals lead us to consider and analogy between liquid fuel droplet combustion and softening coals at elevated temperatures. The present study discusses of pyrolysis of softening bituminous coal particles, and evaporating, coking, heavy oil droplets. A mathematical model for multicomponent droplet evaporation is discussed. With consideration of liquid phase reactions is presented. The model is applicable to coal particles undergoing a pyrolysis process which exhibit liquid-like behavior at elevated temperatures. DOE

N91-29258# National Research Council of Canada, Ottawa (Ontario). Inst. for Mechanical Engineering
AN OVERVIEW OF AEROTHERMAL MODELING
M. K. Y. Lai Jun. 1990 89 p Sponsored in part by Department of National Defence
(NRC-32088; TR-GD-016; CTN-91-60104) Copyright Avail: NTIS HC/MF A05

Recent advances in aerothermal modelings of combustion are reviewed. Although particular attention is devoted to 3-D, steady gas turbine combustor flows, the modelings considered are also applicable to other combustion systems and burners. Constituent components of aerothermal modelings, based on the numerical solution of conservation equations of mass, momentum, energy, and chemical species in turbulent combusting flows, are described. The closure physical submodels of turbulence, gaseous and liquid fuel combustion, NOx and soot emissions, and thermal and particulate radiation are described, formulated, and discussed. State-of-the-art physical submodels are identified. Different aerothermal modelings, used by gas turbine industries, universities, and research organizations, are also presented. The models described are adequate for design and perturbation studies. All

physical submodels discussed are suitable for incorporation into the TURCOM code. However, since these submodels were developed for limited conditions, a wide range evaluation of them is needed before the most economical, accurate, reliable submodels can be recommended. Author (CISTI)

N91-29259# California Univ., Berkeley. Lawrence Berkeley Lab.
PERFORMANCE OF MULTIPLE STREAM PULSED JET COMBUSTION SYSTEMS
J. A. Maxson, D. M. Hensinger, K. Hom, and A. K. Oppenheim Dec. 1990 11 p Presented at the 1991 Annual Congress of the Society of Automotive Engineers (SAE), Detroit, 26 - 27 Feb. 1991
(Contract DE-AC03-76SF-00098)
(DE91-012338; LBL-30021; CONF-9102106-2) Avail: NTIS HC/MF A03

In the course of our studies on pulsed jet combustion (PJC) a series of tests were carried out to determine the performance of multi-stream systems. This included multi-jet efflux, as well as dual-generator aggregates. The essential performance indicator of a PJC system is the pressure transducer record, yielding, in particular, data on the rise time and amplitude of the pressure pulse, as well as the rate of pressure rise. Concomitantly with pressure measurements, a sequence of schlieren records were obtained to reveal the salient features of the fluid mechanical phenomena of the PJC process. Elucidated thereby are the effects of entrainment induced by large scale vortex structures of turbulent jet plumes, and their decisive role in governing the process of combustion, as influenced by their particular configuration. Our tests demonstrated the capability of multiple stream PJC systems to shorten the rise time and increase the amplitude of the pressure pulse, both effects of obvious potential benefit to engine performance. DOE

N91-29260# Sandia National Labs., Albuquerque, NM.
STRUCTURE OF ICOSAHEDRAL BORIDES BY RAMAN SPECTROSCOPY
D. R. Tallant, T. L. Aselage, and D. Emin 1991 11 p Presented at the 10th International Symposium on Boron, Borides and Related Compounds, Albuquerque, 27-30 Aug. 1991
(Contract DE-AC04-76DP-00789)
(DE91-010872; SAND-91-0236C; CONF-910885-1) Avail: NTIS HC/MF A03

We have obtained Raman spectra of icosahedral boron-rich solids. The spectra of alpha-rhombohedral boron, boron arsenides, and boron phosphide are consistent with highly-ordered materials. Polarization studies have resulted in symmetry assignments for most of the Raman bands of alpha-rhombohedral boron. In contrast, the Raman spectra of the boron carbides reveal local substitutional disorder. They also change progressively as a function of carbon content. A structural model for the boron carbides has been developed to explain the Raman and infrared absorption spectra, x-ray data, and electrical and thermal transport properties. Raman spectra of boron carbide samples enriched in B-10, B-11, and C-13 reveal details of the atomic motions. The vibrational frequencies and exceptionally narrow linewidths of certain Raman modes are discussed in terms of a strong bond model. In this model certain vibrational modes involving relatively stiff bonds between chain atoms, chain and icosahedral atoms, and atoms on different icosahedral are decoupled from the boride lattice by weak, intraicosahedral bonds. DOE

N91-29261# Pacific Northwest Lab., Richland, WA.
A THEORETICAL AND EXPERIMENTAL STUDY OF UNIMOLECULAR AND BIOMOLECULAR RADICAL HYDROGEN TRANSFER REACTIONS
J. A. Franz, T. Autrey, G. J. Gleicher, D. M Camaioni, and K. F. Ferris Apr. 1991 9 p Presented at the 201st American Chemical Society (ACS) National Meeting, Atlanta, 14-19 Apr. 1991
(Contract DE-AC06-76RL-01830)
(DE91-012607; PNL-SA-19111; CONF-910402-17) Avail: NTIS HC/MF A02

We have examined the intramolecular radical hydrogen transfer (RHT) reaction of the 2- (2- phenyl ethyl) cyclohexadienyl radical. Intramolecular hydrogen shift from the cyclohexadienyl ring to the ipso position of the phenyl ring, followed by beta-scission would have given benzene and ethylbenzene as products. Competing with this reaction is beta-scission to give benzyl radical and isotoluene, or hydrogen loss to give bibenzyl. Studies to date suggest a barrier for thermoneutral hydrogen transfer in the RHT reaction between aromatic systems of ca. 18 kcal/mole. None of the studies of RHT or equivalent mechanisms have attempted to directly observe H2, and direct determination of Arrhenius parameters and a detailed examination of the pathway of the hydrogen transfer process remains to be carried out. To better understand the structural and energetic aspects of RHT, we have carried out a semiempirical molecular orbital study of bimolecular and intramolecular RHT reactions for a variety of aromatic systems. We also examined in detail the energetics of hydrogen transfer between ethyl radical and ethylene via RHT, an addition/metathesis/scission pathway, and a hybrid concerted pathway. DOE

N91-29262 Michigan Univ., Ann Arbor.
COMBUSTION STABILITY LIMITS AND PLANAR IMAGING OF SWIRL-STABILIZED FLAMES Ph.D. Thesis
Douglas Alan Feikema 1990 154 p
Avail: Univ. Microfilms Order No. DA9116177

The blowout limits of a number of swirl stabilized nonpremixed flames were measured, and the observed trends are successfully explained by applying certain concepts which previously have been applied only to nonswirling flames. It is shown that swirl flame blowout limits can be compared to well known limits for nonswirling simple diffusion flames by using the proper nondimensional parameter, i.e., the first Damkohler number. Results show that for zero swirl the blowout curves agree with curves predicted by the previous analysis of Dahm and Mayman. However, as swirl is added, the flame becomes more stable. To explain the effect of swirl, a simple analysis is presented which is an extension of previous nonswirling flame blowout theory. It shows that the conventional swirl number is not the appropriate governing parameter. Instead, a first Damkohler number which is suggested by the analysis is found to help collapse the data at the rich blowout limit to a single, general linear curve. Swirl causes a jet-vortex interaction to occur; the recirculation vortex reduces the fuel jet velocity on centerline, which strongly stabilizes the lifted flame. Dissert. Abstr.

N91-29263# Wichita State Univ., KS. National Inst. for Aviation Research.
TGA EXPERIMENTAL DATA ANALYZED BY TRANSPIRATION THEORY
P. G. Wahlbeck 1991 13 p
(NIAR-91-21) Avail: NTIS HC/MF A03

Thermogravimetric analysis (TGA), measurements of sample mass vs. temperature, is a frequently used laboratory technique in the analysis of materials, and commercial computer-automated equipment is available. The TGA experiment is designed much the same as a transpiration experiment which was theoretically analyzed using a transport mechanism coupling diffusion and viscous flow. This coupled flow analysis as applied to the TGA experiment is discussed. The analysis allows one to calculate equilibrium vapor pressures and related thermodynamic properties. As an example, data for the vaporization of TI2O3 are discussed. Author

N91-29264# California Univ., Berkeley. Lawrence Berkeley Lab.
HOT ATOM REACTIVE SCATTERING AND PHOTODISSOCIATION EXPERIMENTS WITH ACETYLENE AND ETHYLENE Ph.D. Thesis
B. A. Balko (California Univ., Berkeley.) Apr. 1991 268 p

(Contract DE-AC03-76SF-00098)
(DE91-013755; LBL-30655) Avail: NTIS HC/MF A12

Two different experimental techniques, chemical activation and photofragment translational spectroscopy, are used to study acetylene, ethylene, and their associated radicals: C2, C2H, C2H3, and C2H5. The experiments are done on a molecular beams apparatus with mass spectrometric detection. The first type of experiment uses a photolytic D atom source to look at the dynamics of the D + C2H2/C2H4 yields (C2H2D/C2H4D) yields C2HD/C2H3D + H substitution reactions at 20 kcal/mole collision energy. The derived product center-of-mass angular and translational energy distributions show that, for both hydrocarbons, the reaction is direct and has an exit barrier. These observations are compared with RRKM estimates of the lifetimes of the complexes. The other type of experiment involves 193 nm photodissociation of C2H2, C2H4, and C2H2F2. The acetylene photodissociation studies give a new measurement for the H-CCH bond energy. The H atom time-of-flight spectrum shows structure from the formation of vibrationally and electronically excited C2H. It is also found that internally excited C2H preferentially absorbs a photon and dissociates to yield C2 photofragments in high electronic states. DOE

N91-29265# Pacific Northwest Lab., Richland, WA.
ION TRANSMISSION STUDIES OF MULITPLE-SECTOR ISOTOPE-RATIO MASS SPECTROMETERS
J. J. Stoffels and H. J. Laue (Purdue Univ., West Lafayette, IN.) May 1991 36 p Presented at the Symposium on Inorganic Mass Spectrometry, Durango, CO, 7-9 May 1991
(Contract DE-AC06-76RL-01830)
(DE91-014253; PNL-SA-19175; CONF-9105216-1) Avail: NTIS HC/MF A03

Theoretical and experimental studies were conducted to determine the ion transmission efficiency of multiple-sector isotope ratio mass spectrometers with tandem magnets of normal geometry. The computer program GIOS (General Ion Optical Systems) was used to perform theoretical calculations of focusing properties and ion transmission efficiency. Actual transmission through multiple-sector instruments was determined from measurements of the ion beam vertical profile at the focus of each sector. Transmission was found to be strongly dependent on source filament geometry. The studies also determined a way to significantly increase ion transmission without changing the basic geometry of existing instruments. A cylindrical einzel lens located near the focus between the magnets provides vertical focusing of the ion beam without perturbing focal properties in the plane of mass dispersion. With a single V-filament ion source, a transmission increase from approx. 75 to approx. 100 pct. was achieved. DOE

N91-29266# Cornell Univ., Ithaca, NY. Dept. of Materials Science and Engineering.
DEFECTS AND TRANSPORT IN MIXED OXIDES
R. Dieckmann 24 Apr. 1991 16 p
(Contract DE-FG02-88ER-45357)
(DE91-014537; DOE/ER-45357/5) Avail: NTIS HC/MF A03

In the following, only results obtained after the progress report of September 26, 1990 are reported. Areas of research covered are Monte Carlo simulation of cation diffusion; stabilities of oxides in the system Co-Fe-Mn-O at 1200 C; electrical conduction in mixed oxides; point defect structure of pure cobaltous oxide; and cation tracer diffusion in mixed spinels. DOE

N91-29267# EG and G Rocky Flats, Inc., Golden, CO. Rocky Flats Plant.
CALCULATION OF INTRA-RARE EARTH BINARY PHASE DIAGRAMS
J. E. Selle 3 May 1991 34 p
(Contract DE-AC34-90DP-62349)
(DE91-014950; RFP-4423) Avail: NTIS HC/MF A03

A modification was made to the Kaufman method of calculating binary phase diagrams to permit calculation of intra-rare earth diagrams. Atomic volumes for all phases, real or hypothetical, are necessary to determine interaction parameters for calculation of complete diagrams. The procedures used to determine unknown atomic volumes are described. Also, procedures are described for determining lattice stability parameters for unknown transformations. Results are presented on the calculation of intra-rare earth diagrams between both trivalent and divalent rare earths. DOE

N91-29268# Oregon Univ., Eugene. Dept. of Chemistry.
STRUCTURE AND STABILITY OF UNDERPOTENTIALLY DEPOSITIED LAYERS ON Au(111) STUDIED BY OPTICAL SECOND HARMONIC GENERATION Technical Report No. 5, Sep. 1989 - Jun. 1991
D. A. Koos and G. L. Richmond 17 May 1991 29 p
(Contract N00014-89-J-1261)
(AD-A237087) Avail: NTIS HC/MF A03 CSCL 07/4

This report details changes in the second harmonic optical response from Au(111) during the underpotential deposition of Cu, Ag, Pb, and Tl. The signal from Au(111) exhibits a strong anisotropy that is assigned to a coupling of the SH photons with interband transitions. Underpotential deposition is used to form overlayers of foreign metals with precise control of the surface concentration of adatoms, and the participation of the d-like electronic states in binding of metal adsorbates is evidenced in the optical response. We compare the results from the Au(111)/Cu and the Au(111)/Ag interface with those from the (111) surface of the single crystal adsorbates and find that the results are consistent with the known electronic structure of the metals and geometric structures of the overlayers. In the case of lead and thallium deposition, a strong perturbation of anisotropic second harmonic signal is observed and attributed to the inability of the large adatoms to lattice match with the substrate. The consideration of domain effects is important for the optical results to be consistent with recent structural determinations. GRA

N91-29269# IBM Research Lab., San Jose, CA.
ELECTROCHEMICAL CONTACT ADSORPTION SITE CHANGES DRIVEN BY FIELD AND CHARGE FACT AND THEORY
Michael R. Philpott 19 Apr. 1991 19 p
(Contract N00014-82-C-0583)
(AD-A237127; TR-29) Avail: NTIS HC/MF A03 CSCL 07/4

When solvated anions like chloride or cyanide adsorb on metal electrodes from aqueous media they lost part of their solvation shell yielding a direct metal-ion bond. For certain anions this contact adsorption can occur even when the electrode carries net negative charge. On the basis of classical electrochemical measurements and deductive reasoning using simple models, electrochemists have evolved a detailed standard model of the disposition of ions, water, and organics adsorbed on the electrode in the range of potentials where the electric double layer is thermodynamically stable. There is evidence that the anions are physisorbed. However, it is only in more recent years through a variety of in situ probes of vibrational properties (ftir and raman) and geometry (sexafs and gixs) that this model is being really tested. GRA

N91-29270# Massachusetts Inst. of Tech., Cambridge.
SIMULATION OF THE STRUCTURE OF DENSE, AMORPHOUS BISPHENOL-A POLYCARBONATE Abstract Only
Michelle Hutnik, Ali S. Argon, Frank T. Gentile, Peter J. Ludovice, and Ulrich W. Suter 31 May 1991 3 p
(AD-A237222) Avail: NTIS HC/MF A01 CSCL 07/6

A detailed static atomistic model has been developed to generate dense, glassy microstructures of bisphenol-A polycarbonate (PC). Microstructures of edge length 18 and 30 A were generated using periodic continuation conditions and a potential energy minimization. The analysis of these microstructures has yielded insight into various experimental properties of PC. The conformation of the individual chains in the bulk were studied, and although analysis of short range structure did not show any strong spacial correlations, there is a tendency for carbonyl bonds to orient parallel at short distances of about 3 A. No long range was visible due to the small size of the microstructure. GRA

N91-29271# Naval Surface Warfare Center, Silver Spring, MD.
SPECTRAL ESTIMATION TECHNIQUES WITH EMPHASIS ON SHORT DATA RECORDS: A PRIMER
Manfred K. Pruessner 29 Jun. 1990 149 p
(AD-A237486; NAVSWC-TR-90-236) Avail: NTIS HC/MF A07 CSCL 12/1

A vast amount of literature exists that concerns itself with spectrum analysis. In particular, the last two decades have seen a great increase of published theoretical work as well as applications of so-called modern spectral estimation techniques based on nontraditional parametric approaches. Many papers dealing with this subject make it difficult even for the initiated to make the connection to his well known and routinely applied methods based on the Fourier Transform when he reads about modeling a random process to obtain a parametric spectrum of the observed data. The report attempts to show the transition from the classical approach of spectral estimation to the basic parametric methods. It also shows the results of these new techniques when applied to short data records and demonstrates their capabilities and limitations. GRA

N91-29272# Purdue Univ., West Lafayette, IN. Dept. of Chemistry.
SOLVENT-DEPENDENT REDOX THERMODYNAMICS OF METAL AMINE COMPLEXES. THE DELINEATION OF SPECIFIC SOLVATION EFFECTS
P. A. Lay, N. S. McAlpine, J. T. Hupp, M. J. Weaver, and A. M. Sargeson 31 May 1991 30 p
(Contract N00014-91-J-1409)
(AD-A237503; TR-103) Avail: NTIS HC/MF A03 CSCL 07/4

Solvent dependent formal potentials, Ef, and reaction entropies, for four reversible Co(III)/(II) couples featuring macrobicyclic cage ligands were obtained. These are utilized, together with corresponding data for other Co(III)/(II) and Ru(III)/(II) amine couples and for M(III)/(II) polypyridine couples, to unravel effects on the redox thermodynamics arising from specific ligand-solvent and other interactions. The solvent dependencies of Ef (vs. ferrocenium-ferrocene) for each redox couple are fitted by using a multiparameter approach, incorporating various well known empirical quantities describing solvent basicity, acidity, polarity, and internal ordering. For most amine couples, solvent basicity appears to play a prevailing role, associated with interactions involving the amine hydrogens, although solvent polarity also exerts a substantial, albeit less solvent dependent, influence upon EfD. GRA

N91-29273# North Carolina Univ., Chapel Hill. Dept. of Chemistry.
ELECTRICAL, MAGNETIC, AND SPECTROSCOPIC PROPERTIES OF TETRATHIAFULVALENE CHARGE TRANSFER COMPOUNDS WITH IRON, RUTHENIUM, RHODIUM, AND IRIDIUM HALIDES
Young I. Kim and William E. Hatfield 10 Jun. 1991 39 p
(Contract N00014-89-J-1734)
(AD-A237607; TR-43) Avail: NTIS HC/MF A03 CSCL 07/4

The charge transfer compounds (TTF)2FeCl3, (TTF)3FeBr3, (TTF)RuCl3.2H2O, (TTF)RhCl3.H2O, and (TTF)IrCl4.CH3OH were prepared from reaction of solutions of TTF (tetrathiafulvalence) and the metal halide. Magnetic susceptibility and spectroscopic (electronic, vibrational, XPS, and EPR) evidence indicate that there is incomplete charge transfer from the TTF donor to iron, and that there is essentially complete charge transfer to ruthenium, rhodium, and iridium. The experimental evidence indicates that two electrons are transferred in the rhodium compound. The electrical conductivities of powered samples of the iron compounds are five orders of magnitude greater than those of the ruthenium, rhodium, and iridium compounds. GRA

N91-29274# Crystallume, Menlo Park, CA.
THERMOCHEMISTRY OF HYDROCARBON DECOMPOSITION AND RELATIONSHIP TO PROPERTIES OF PECVD DIAMOND FILMS Final Report, 1 Nov. 1988 - 31 Jan. 1991
Linda S. Plano 31 Mar. 1991 47 p
(Contract F49620-89-C-0009)
(AD-A237793; AFOSR-91-0569TR) Avail: NTIS HC/MF A03 CSCL 07/4

Considerable empirical research has been performed in the field of diamond film growth over the past fifteen years. However, this approach has proven insufficient in optimizing the deposition process. Also, no deposition mechanism has become universally accepted. A combination of in situ plasma diagnostic instruments, diamond film characterization, and computer modeling was used to produce a self-consistent model of diamond-producing DC plasmas and to optimize the deposition process in terms of bonding type (i.e., graphite vs. diamond) and growth rate. The effects of important deposition parameters including methane concentration in hydrogen, current, electrode spacing, and pressure on both film and plasma characteristics were analyzed. The presence of a negative electric field at the anode (or substrate electrode) was determined to be necessary for the growth of high quality diamond films. The magnitude of this field is strongly dependent on pressure. Control of this field will be possible by monitoring with a Langmuir probe and controlling pressure, leading to in situ process control. GRA

N91-29275# Columbia Univ., New York, NY. Dept. of Chemistry.
PICOSECOND STUDIES OF CHEMICAL INTERMEDIATES Final Technical Report, Nov. 1983 - Mar. 1991
K. B. Eisenthal May 1991 59 p
(Grant AF-AFOSR-0014-88)
(AD-A237859; AFOSR-91-0549TR) Avail: NTIS HC/MF A04 CSCL 20/13

Surface second harmonic generation (SSHG) was used to study the chemical and physical properties of liquid interfaces. Information about the thermodynamics of neat liquid surfaces was found by observing the SH signal as a function of temperature. Extensive studies using monolayers at the air/water interface were undertaken. Studies of acid/base equilibrium and monolayer phase transitions were performed. The gas-liquid coexistence region and an orientational phase transition was observed. SHG was used to study the interface properties of fused silica/electrolyte solution. Orientational relaxation was observed on the picosecond time scale at the air/water interface by time resolved second harmonic generation. The data suggests that the ground and excited state of Rhodamine 6G have different equilibrium orientational distributions. Femtosecond studies of electrons in liquids have characterized the geminate recombination and solvation dynamics of electrons in polar and nonpolar liquids. Photodetachment of electrons from halide ions in aqueous solution was also studied. Picosecond studies of chemical intermediates have examined the role of restricted geometries on elementary chemical processes. GRA

N91-29276# Ballistic Research Labs., Aberdeen Proving Ground, MD.
SPECTRAL STUDIES OF SOLID PROPELLANT COMBUSTION. 3: EMISSION AND ABSORPTION RESULTS FOR HMX2 PROPELLANT Final Report, Jun. - Dec. 1990
M. W. Teague and John A. Vanderhoff May 1991 23 p
(DA Proj. 1L1-61102-AH-43)
(AD-A237958; BRL-MR-3911) Avail: NTIS HC/MF A03 CSCL 21/2

The propellant under study in this investigation is HMX2. Low pressure characteristics of HMX2 are quite different from either HMX1 or M-30. Propellants similar to HMX2 will find application for rockets where slow burning rates and low flame temperatures are desirable and for tank guns where low vulnerability is extremely important. Optical absorption and emission spectroscopy has been applied to HMX2 (a nitramine propellant exhibiting a dark zone) burning over a pressure range of 1.2 to 1.8 MPa nitrogen. Emission signals from CN have been observed and profiled, as well as absorption signals from NO. Large broadband absorptions occurred in the wavelength range appropriate for NO absorption. There was significant NO present in the dark zone as evidenced by 100

percent absorption occurring in the (0,0) vibrational band of the A 2Sigma - x 2Pi transition. GRA

N91-29277# Yale Univ., New Haven, CT.
NONLINEAR SPECTROSCOPY OF MULTICOMPONENT DROPLETS AND TWO- AND THREE-DIMENSIONAL MEASUREMENTS IN FLAMES Final Report, 1 Jan. 1988 - 31 Jan. 1991
Richard K. Chang and Marshall B. Long 15 May 1991 24 p
(Grant AF-AFOSR-0100-88; AF Proj. 2308)
(AD-A238028; AFOSR-91-0599TR) Avail: NTIS HC/MF A03 CSCL 20/5

Significant progress has been made in the following two research areas: (1) nonlinear spectroscopy of micrometer-size droplets; and (2) development and application of two- and three-dimensional scalar measurement techniques in flames. In the nonlinear spectroscopy area, the following achievements are reported: (1) laser-induced shape deformation of transparent droplets by electrostriction, which pushes against the surface tension force and causes the droplet to bulge; (2) laser-induced shape deformation by heating of absorbing droplets, which were imaged with fluorescence photography; (3) laser-induced breakdown which quenches the stimulated Raman scattering (SRS); (4) excitation of SRS with single-mode and multimode Q-switched lasers; and (5) four-wave mixing processes in droplets, such as third-order sum frequency generation. Achievements in multidimensional scalar imaging include the following: (1) measurement of the time evolution in premixed H2-air flames using imaging techniques: (2) development of new techniques for following the time evolution of flow structures in three dimensions; (3) introduction of a technique for visualizing supersonic flows using Rayleigh scattering from condensed-phase droplets; (4) measurement of the complete scalar gradient in a nonreacting flow, which allows calculation of the scalar dissipation; (5) simultaneous CH and CH4 mapping in a turbulent nonpremixed flame, and (6) investigation of differential diffusion effects. GRA

N91-29278# Naval Medical Research Inst., Bethesda, MD.
A TECHNIQUE FOR MEASURING THE SOLUBILITIES OF GASES IN LIQUIDS Technical Report, Feb. 1988 - Dec. 1989
Gary Albin, Julie Thai, George Tresansky, and William Mints Dec. 1990 41 p
(AD-A238071; NMRI-90-138) Avail: NTIS HC/MF A03 CSCL 07/4

Experiments are planned for measuring the solubilities of nitrogen, helium, and hydrogen in water, blood, and other tissues at 37 C and pressures ranging from 1 to 10 ATA. We describe a protocol for these experiments, which consists of measuring the change in total pressure that occurs during equilibration of the gas phase with the condensed phase in a closed container after an abrupt elevation of the partial pressure of the test gas. We derive the equations to compute the Henry's coefficient or the Ostwald coefficient from the results of that experiment. Experimental conditions are optimized based on a formal propagation of error. The error analysis shows that gas leakage is by far the most serious potential source of error. The technique for measuring leakage is discussed; actual solubility measurements will proceed when the error from this source is deemed acceptably small. GRA

N91-29279# Naval Weapons Center, China Lake, CA.
LITHIUM COMBUSTION: A REVIEW Final Report, Feb. - Jun. 1990
Robet A. Rhein Dec. 1990 62 p
(AD-A238154; NWC-TP-7087) Avail: NTIS HC/MF A04 CSCL 07/4

This review deals with the chemical reactions, ignition, and combustion of lithium combustion in air and in the components of air, including oxygen, nitrogen, water, and carbon dioxide. It was found that lithium reacts vigorously with these substances. In addition, a review of extinguishing lithium fires is included. Of the extinguishing agents, carbon has been found to be the most effective. GRA

N91-29280# Oregon State Univ., Corvallis. Dept. of Electrical and Computer Engineering.
ATOMIC APPROACHES TO DEFECT THERMOCHEMISTRY Annual Technical Report, 1 Apr. 1990 - 31 Mar. 1991
James A. VanVechten and John F. Wager 15 Apr. 1991 15 p
(Grant AF-AFOSR-0309-89; AF Proj. 2306)
(AD-A238260; AFOSR-91-0574TR) Avail: NTIS HC/MF A03 CSCL 07/4

The goal of the research program described herein was to apply atomistic thermodynamic theory, Monte Carlo simulation, and experimental analysis to elucidate the identity of point defects in semiconductors as well as to understand their static and dynamic properties. Significant progress has been made in the following nine areas: (1) Direct simulation of atomic diffusion including the effects of realistic boundary conditions, carrier injection and mis-fit strain, (2) Independent measurement of vacancy concentration and diffusivity, (3) Effects of temperature and strain on band offsets and atomic diffusion, (4) Elimination of DX centers from AlGaAs by optically stimulated dislocation climb, (5) Proper analysis of the capacitance-transient due to multiple carrier emission from a highly compensating deep level, (6) C-V analysis and SPICE modeling of ACTFEL devices, (7) DX in AlGaAs, (8) Statistical thermodynamics of ballistic hopping, and (9) Energetics of self-diffusion in GaAs. GRA

N91-29281# Los Alamos National Lab., NM.
SUPERSONIC COMBUSTION OF A TRANSVERSE INJECTED H2 JET IN A RADIO FREQUENCY HEATED FLOW
P. J. Wantuck, R. A. Tennant, and H. H. Watanabe 1991 17 p
Presented at the 27th Propulsion Conference and Exhibition, Sacramento, CA, 24-26 Jun. 1991
(Contract W-7405-eng-36)
(DE91-014739; LA-UR-91-1995; CONF-910605-1; AIAA-91-2393)
Avail: NTIS HC/MF A03

The combustion of a single hydrogen jet, normally injected into a radio frequency (RF) heated, oxidant-containing, supersonic flow, has been established to characterize the chemical and fluid dynamic phenomena associated with the reaction process and ultimately validate the predictive capability of computational fluid dynamic (CFD) codes. The experimental system employed for this study is unique in that it uses an electrodeless, inductively coupled plasma tube to generate the high temperature oxidant-containing gas for subsequent nozzle expansion. Advantages of an RF heated flow system include reduced free-stream chemical contamination, continuous operation, and relative ease of integration into a typical flow laboratory environment. A description of the system utilized for this study is presented including preliminary results of the reactive flow characterization. In addition, the use of the laser-based diagnostic techniques, such as planar laser-induced fluorescence (PLIF), for measuring flow properties is also discussed. DOE

N91-29282# Ames Lab., IA.
SYNTHESIS AND CHARACTERIZATION OF REDUCED TUNGSTEN SULFIDE CLUSTER COMPLEXES Ph.D. Thesis
Xiang Zhang 27 Jun. 1991 158 p
(Contract W-7405-eng-82)
(DE91-014916; IS-T-1534) Avail: NTIS HC/MF A08

Reduction of tungsten(IV) chloride with metals was studied in order to find a high-yield and convenient preparation of (alpha)-tungsten (II) chloride. The reduction of tungsten(IV) chloride with iron metal proved to be the most convenient and reliable synthesis, with a good yield of 60 percent. The reactions between (alpha)-tungsten(II) chloride and sodium hydrosulfide were investigated. Complete substitution of sulfide for chloride in W(sub 6)Cl(sub 8)(sup 4+) was achieved in the presence of sodium n-butoxide in pyridine solution. Single crystals were grown at elevated temperature (200 C) in pyridine, and the structure of W(sub 6)S(sub 8)(py)(sub 6) was determined by single crystal x-ray techniques. The triethylphosphine (PEt(sub 3)) and tetrahydrothiophene (THT) complexes of W(sub 6)S(sub 8) were established by ligand displacement of pyridine in W(sub 6)S(sub 8)(py)(sub 6). Structures for both W(sub 6)S(sub 8)(PEt(sub 3))(sub 6). 1.44CH(sub 2)Cl(sub 2) and W(sub 6)S(sub 8)(THT)(sub 6)

were determined by single crystal x-ray diffraction. These molecular complexes of the W(sub 6)S(sub 8) cluster were also characterized by infrared spectroscopy. DOE

N91-29283# Pennsylvania Univ., Philadelphia. Board of Trustees.
CATALYTIC HYDROGENATION OF CARBON MONOXIDE
B. B. Wayland 1991 7 p
(Contract DE-FG02-86ER-13615)
(DE91-015452; DOE/ER-13615/5) Avail: NTIS HC/MF A02

The primary focus of this project is on developing new approaches for the hydrogenation of carbon monoxide at mild conditions. Our strategies are based on the favorable thermodynamics of rhodium macrocycles implicated in the catalytic hydrogenation of CO. Metalloformyl complexes and CO reductive coupling provide alternate routes to organic oxygenates that utilize these species as intermediates. Thermodynamic and kinetic-mechanistic studies are used in guiding the design of new metallospecies to improve the thermodynamic and kinetic factors for individual steps in the overall process. Electronic and steric effects associated with the ligand arrays along with the influences of the reaction medium provide the chemical tools for tuning these factors. Non-macrocyclic ligand complexes that emulate rhodium macrocycles, but with improved reaction kinetics are promising materials for future development. DOE

N91-29284# Argonne National Lab., IL.
MOLECULAR DYNAMICS SIMULATION OF THE EFFECT OF INTERFACES IN MELTING AND SOLID-STATE AMORPHIZATION
D. Wolf and S. Yip (Massachusetts Inst. of Tech., Cambridge.) May 1991 13 p Presented at the Spring Meeting of the Materials Research Society (MRS), Anaheim, CA, 29 Apr. - 3 May 1991
(Contract W-31-109-eng-38)
(DE91-015550; ANL/CP-72361; CONF-910406-30) Avail: NTIS HC/MF A03

A newly developed molecular dynamics code was used to study the effect of free surfaces, grain boundaries and voids in the process of melting. It was found that conventional thermodynamic melting occurs via nucleation of the liquid at the extended defects with subsequent growth into the crystal. In the absence of interfaces, or when this transition is kinetically hindered, however, a second type of melting transition can be triggered by an elastic instability first described by Born (mechanical melting). It is suggested that the distinct characteristic features associated with the two types of melting are actually observed in solid-state amorphization experiments. A unified thermodynamics-based description, in the form of an extended phase diagram, of melting and solid-state amorphization is proposed which brings out the parallels between these two phenomena and suggests that their underlying causes are apparently the same. By investigating the effect of surface stresses on the structure and elastic behavior of free-standing thin films, we discuss how these concepts need to be modified in thin-film and small-grained materials. DOE

N91-29285# Brigham Young Univ., Provo, UT.
DEACTIVATION BY CARBON OF IRON CATALYSTS FOR INDIRECT LIQUEFACTION
C. H. Bartholomew 14 Feb. 1991 46 p
(Contract DE-FG22-86PC-90533)
(DE91-011276; DOE/PC-90533/16) Avail: NTIS HC/MF A03

Progress is reported for a four-year fundamental investigation of carbon formation and its effects on the activity and selectivity of promoted iron catalysts for Fischer-Tropsch (FT) synthesis, the objectives of which were to (1) determine rates and mechanisms of carbon deactivation of unsupported Fe and Fe/K catalysts during CO hydrogenation, and (2) model the global rates of deactivation at the surface of the catalyst for the same catalysts. A computer-automated reactor system to be used in the kinetic and deactivation studies was designed, constructed and tested. Kinetic data for CO hydrogenation on unsupported, unpromoted iron, 99 percent Fe/1 percent Al2O3, and K-promoted 99 percent Fe/1 percent Al2O3 catalysts were obtained as functions of temperature, reactant particle pressures and time. The activity/selectivity and kinetic data are consistent with those previously reported for supported, unpromoted and promoted iron. Two kinds of deactivation were observed during FT synthesis on these samples: (1) loss of surface area after reduction of unsupported, unpromoted iron at 400 C, and (2) loss of activity with time due to carbon deposition, especially in the case of K-promoted 99 percent Fe/1 percent Al2O3. Deactivation rate data were obtained for CO hydrogenation on promoted Fe as a function of time, temperature, and H2/CO ratio. DOE

N91-29286# California Univ., Berkeley. Lawrence Berkeley Lab.
EQUATION OF STATE FOR PURE SODIUM CHLORIDE
A. Anderko and K. S. Pitzer Jun. 1991 13 p Presented at the 11th Symposium on Thermophysical Properties, Boulder, CO, 23-27 Jun. 1991
(Contract DE-AC03-76SF-00098)
(DE91-014618; LBL-30861; CONF-9106176-2) Avail: NTIS HC/MF A03

An equation of state for pure sodium chloride has been developed on the basis of experimental data and results of Monte Carlo simulations for the restricted primitive model (RPM). The experimental data base included limited vapor pressure and saturated liquid density data as well as dimerization equilibrium constants. The liquid densities have been extrapolated to the supercooled region using liquid-phase Monte Carlo data. For this purpose, the parameters of the primitive model have been calculated by assuming that sodium chloride and RPM obey the corresponding states principle over a limited range of conditions. In the near-critical region Monte Carlo data as well as results of cluster calculations have been used with parameters scaled to reproduce the critical temperature obtained by extrapolating saturation data. The RPM parameters employed in the calculations are close to those for crystalline NaCl. The experimental and scaled Monte Carlo data have been reproduced within their accuracy using a van der Waals-type equation of state with two temperature-dependent parameters a and b. The functions representing the temperature dependence of the parameters have been designed to ensure reliable extrapolation to lower and higher temperatures. Dimerization of sodium chloride has been allowed for by using a closed-form term representing the effect of association on the compressibility factor. The performance of the equation has been additionally verified by predicting compressibility factors at low reduced temperatures outside the saturation region and comparing them with scaled Monte Carlo data. DOE

N91-29287# Massachusetts Univ., Amherst. Dept. of Chemical Engineering.
THEORETICAL STUDIES OF SOLID-FLUID PHASE EQUILIBRIA
P. A. Monson Jun. 1991 5 p
(Contract DE-FG02-90ER-14150)
(DE91-014811; DOE/ER-14150/1) Avail: NTIS HC/MF A01

Research is summarized of the molecular theory of solid-fluid phase equilibria. Research has focused principally upon the influence of molecular shape upon solid-fluid coexistence. The cell model was extended to the case of hard diatomic molecules to develop a first approximation for the free energy of these systems. Preliminary estimates of the solid-fluid coexistence properties were made. Monte Carlo simulations studies of solids of hard nonspherical molecules were initiated to provide accurate data for the free energy of these systems. These results are being used to develop a picture of how molecular shape influences solid-fluid coexistence and as the basis for a generalized van der Waals treatment of solid-fluid equilibria. DOE

26 METALLIC MATERIALS

Includes physical, chemical, and mechanical properties of metals, e.g., corrosion; and metallurgy.

N91-29288# National Aeronautical Establishment, Ottawa (Ontario). Structures and Materials Lab.
INTERMETALLICS: CANADIAN PERSPECTIVE
V. R. Parameswaran, J.-P. Immarigeon, and W. Wallace 4 Jun. 1990 43 p Presented at the TTCP-P-TP1 Workshop on Intermetallics, Vancouver, British Columbia, 25 Jun. 1990
(NAE-LTR-ST-1771; CTN-91-60011) Copyright Avail: NTIS HC/MF A03

Ordered intermetallic alloys have unique properties such as the retention of order to temperatures close to their melting or transition points, and their high strength and resistance to creep and oxidation at elevated temperatures. These materials offer the potential for high temperature structural applications, in particular, for engine components of advanced aerospace vehicles. A brief overview of the Canadian research on intermetallics is presented. Although not much work has been done in Canada on high temperature intermetallic such as aluminides for aerospace applications, a large number of studies have been carried out on Zr3Al for nuclear applications and some studies on other intermetallics such as Al3Ti and composites containing Ni3(Al, Zr, B) in Al matrix. Application oriented studies on intermetallic alloys of aluminum with Ni and Ti are reported at CANMET and the University of Waterloo. Fundamental studies on the formation and properties of intermetallics are being carried out at Bell Northern Reseach Laboratories, Hydro Quebec, Queens University and the Universities of Waterloo and Manitoba. High temperature coatings based on intermetallics such as aluminides are commonly used to protect components and structures exposed to elevated temperatures. Several Canadian companies are actively engaged in the development of aluminide coatings for gas turbine engines. CISTI

N91-29289# National Aeronautical Establishment, Ottawa (Ontario). Structures and Materials Lab.
METAL INJECTION MOULDING: A BRIEF REVIEW
Yu-Ning Ng, J.-P. Immarigeon, and V. R. Parameswaran 9 Mar. 1989 34 p
(NAE-LTR-ST-531; CTN-91-60091) Copyright Avail: NTIS HC/MF A03

Powder metal injection molding (MIM) is briefly reviewed and the advantages and disadvantages of the technology are discussed. In this process, fine metal powders are mixed with a thermoplastic or organic binder; the binder is injected into a mold and the binder is removed (debinding) by heating or solvent extraction; the debound compact is sintered to consolidate the powder into a nearly fully dense part of the desired shape. Small parts of intricate shape can be formed. Typical applications include precision parts manufacture as for aircraft and automotive applications. Advantages of the process include the following: parts can be produced with thin walls, threads, knurls, undercuts, and transverse holes; the need for post sinter machining is eliminated or reduced; MIM parts can be sintered to at least 90 percent density giving good machining properties. Disadvantages of the technology include the following: tolerances of sintered MIM parts are +/- 0.3 percent compared with +/- 0.1 percent for conventional powder metallurgy parts; it is difficult to form parts having internal cavities by MIM; abrupt changes in cross section may lead to stress concentrations and cracking; cross sections should be between 0.5 mm and 6 mm; weight should be in the range of 0.1 to 150 g; costs may be high due to the requirement for fine metal powders and precision control of debinding times; and carbon content is difficult to control. CISTI

N91-29290# Materials Research Labs., Melbourne (Australia).
HIGH TEMPERATURE MASS SPECTROMETRIC STUDY OF THE THERMODYNAMICS OF LIQUID NICKEL-ALUMINIUM ALLOYS AT 2000 K
Peter L. Mart and Warren D. Reid 1991 30 p
(MRL-TR-91-15; AR-006-366) Avail: NTIS HC/MF A03

A study of the thermodynamic properties of liquid nickel-aluminum alloys, using the technique of Knudsen effusion mass spectrometry is described. In the concentration range studied, 0.55 less than or = x(sub Ni) less than or = 0.89, the activity of nickel at 2000 K shows large negative deviations from Raoult's Law, which is indicative of the strong attraction between the nickel and aluminum atoms. The role of container interactions in affecting thermodynamic parameters derived from Knudsen cell measurements is highlighted, and inconsistencies in earlier investigations are discussed. Author

N91-29291# Joint Publications Research Service, Arlington, VA.
JPRS REPORT: SCIENCE AND TECHNOLOGY. USSR: MATERIALS SCIENCE
28 Jan. 1991 35 p Transl. into ENGLISH from various Russian articles
(JPRS-UMS-91-001) Avail: NTIS HC/MF A03

Abstracts of U.S.S.R. materials science research are given. Topics covered include composite materials, ferrous and nonferrous metals, alloys, solders, welding, brazing, soldering, and the effects of laser radiation on thin metal films. Author

N91-29292# Sandia National Labs., Livermore, CA.
COMPENDIUM OF MATERIAL TEST RESULTS ON HY-100 AND PSEUDO HY-100 METALS IN SUPPORT OF US NAVY PROGRAMS Interim Report
S. L. Brandon and K. L. Lee Apr. 1991 33 p
(Contract DE-AC04-76DR-00789)
(DE91-013134; SAND-91-8213) Avail: NTIS HC/MF A03

This report documents the status of ongoing tests performed to construct a material database for use in structural analysis codes. Room temperature uniaxial tension and compression tests were performed to quantify isotropy and strain-rate sensitivity at static rates. Notched tensile tests were performed to support development of the damage portion of coupled flow-damage constitutive models. Plate perforation tests were also performed to be compared with future analytical predictions. Limited quantities of the pseudo HY-100 material permitted only a subset of such tests. Future tests are to include high-rate compression for improved strain-rate sensitivity modeling at anticipated service conditions, and elevated temperature compression testing for improved modeling of potential material softening due to adiabatic heating. DOE

N91-29293# Northwestern Univ., Evanston, IL. Dept. of Materials Science and Engineering.
MECHANISMS OF TRANSFORMATION TOUGHENING
G. B. Olson 1991 70 p
(Contract DE-FG02-88ER-45365)
(DE91-013151; DOE/ER-45365/2) Avail: NTIS HC/MF A04

The operation of structural transformation as a deformation mechanism occurs widely throughout materials. By far the most studied prototypical case is the transformation plasticity associated with martensitic transformations, an area of intense recent interest stimulated by the achievement of record fracture toughness levels in both metals and ceramics. Developing a broad view of transformation plasticity and toughening phenomena, the current DOE-sponsored research program, originally organized at MIT, has been underway since 1983 addressing these phenomena in high-strength materials based on both homogeneous and dispersed-phase systems and involving toughening interactions with both ductile and brittle failure mechanisms. Research reviewed here includes continuation of transformation toughening studies in ultrahigh-strength austenitic steels as well as a new effort directed at enhancement of uniform ductility in multiphase high-strength low-alloy steels of interest for automotive applications. Concepts which have evolved from this research program have had an important role in the multi-institutional Steel Research Group (SRG) program which focusses on the fundamental principles allowing design of new classes of advanced steels with high toughness and ductility. Excerpts from a comprehensive review of our steel research reporting results of our DOE-sponsored transformation

plasticity studies and their role in our design approach are included. DOE

N91-29294# Argonne National Lab., IL.
CHARACTERISTICS OF AUTOCLAVE AND IN-REACTOR NODULAR CORROSION OF ZIRCALOYS
Y. H. Jeong, K. S. Rheem (Korean Atomic Energy Research Inst., Seoul, Republic of Korea), and H. M. Chung Nov. 1990 54 p Presented at the 9th American Society for Testing and Materials (ASTM) International Symposium on Zirconium in the Nuclear Industry, Kobe (Japan), 5-8 Nov. 1990
(Contract W-31-109-eng-38)
(DE91-013600; ANL/CP-69633; CONF-901107-1) Avail: NTIS HC/MF A04

Nodular corrosion characteristics of recrystallized Zircaloy-4 were investigated in static autoclave tests at 500 C and 10.3 MPa. The roles of annealing temperature, cooling rate after beta-treating at 1050 C, cold work, and surface treatment in corrosion tests were correlated with the results of microstructural characterization by scanning and transmission electron microscopies. A good correlation was obtained between average size of intermetallic precipitates and weight gain, in contrast to nodule coverage and nodule number density. These results could be best explained by the hypothesis that nodules nucleate in local regions that are depleted of Fe and Cr alloying elements. Some observations were inconsistent with the premise that nodules nucleate on or near intermetallic precipitates. Nodular corrosion characteristics and microstructures of commercial Zircaloy-2 cladding of fuel and gadolinia rods, obtained from several BWRs after burnup of 11 to 30 MWd/kgU, were also examined. Partial amorphization of intermetallic precipitates in BWR Zircaloy-2, and virtual dissolution and in an extreme case spinodal-like fluctuations of dissolved alloying elements in PWR Zircaloy-4 cladding were observed. Occurrence of nodular oxidation of Zircaloy-2 in BWRs could best be correlated to average size of intermetallic precipitates before irradiation and to fuel cladding operating temperature. For an intermetallic size range of 250 to 700 nm, nodular oxides were observed at 288 C, but only thick uniform oxide was observed at 307 C. DOE

N91-29295# Pacific Northwest Lab., Richland, WA.
POSTIRRADIATION DEFORMATION OF FERRITIC Fe-Cr BINARY ALLOYS
M. L. Hamilton and D. S. Gelles Jun. 1991 16 p Presented at the 15th International Symposium on Effects of Radiation on Materials, Nashville, 17-22 Jun. 1990
(Contract DE-AC06-76RL-01830)
(DE91-014856; PNL-SA-17478; CONF-900623-26) Avail: NTIS HC/MF A03

Six binary Fe-Cr alloys ranging from 3 to 18 percent chromium were irradiated in the form of miniature tensile specimens in the Fast Flux Test Facility and tested at room temperature. The irradiation conditions produced 7 to 30 dpa at 365 to 574 C. The major purpose of the experiment was to compare the behavior of these simple alloys with that of more complex commercial alloys. The tensile data obtained on these specimens at room temperature are discussed with appropriate fractographic and microstructural support. Previous studies on similar materials had revealed the presence of a feature typically exhibited in channel fractures: elongated voids were evident in shear bands of an irradiated and deformed TEM disk of a binary Fe-6Cr alloy. An additional purpose of the experiment was therefore to provide a better understanding of the potential contribution of channel fracture to deformation in ferritic alloys. No evidence for channel fracture was found, however. DOE

N91-29296# Oak Ridge National Lab., TN.
[A BRIEF OVERVIEW OF THE ACTIVITIES AND ACCOMPLISHMENTS OF THE METALS AND CERAMICS DIVISION] Progress Report, period ending 30 Sep. 1990
Apr. 1991 174 p
(Contract DE-AC05-84OR-21400)
(DE91-014955; ORNL-6653) Avail: NTIS HC/MF A08

This report provides a brief overview of the activities and accomplishments of the Metals and Ceramics (M and C) Division during fiscal year (FY) 1990. The division is organized to provide technical support, primarily in the area of structural materials, for the various technologies being developed by the U.S. Department of Energy (DOE). Activities span the range from basic research (through applied research and engineering development) to industrial research (through cooperative research and a strong technology transfer program). The division is organized in functional groups that encompass nearly all of the disciplines needed to develop and to apply materials in structural applications. Sections 1 through 4 describe the different functional groups; Section 5 provides an alternative view of the division in terms of the major programs, most of which cross group lines; and Section 6 summarizes external interactions including cooperative research programs and technology transfer activities. Appendices describe the organizational structure, note personnel changes, present honors and awards received by division members, and contain listings of publications completed and presentations made at technical meetings. DOE

N91-29297*# University of Eastern Kentucky, Richmond. Dept. of Physics and Astronomy.
STUDY OF ACTIVATION OF METAL SAMPLES FROM LDEF-1 AND SPACELAB-2 Final Report
C. E. Laird Jul. 1991 62 p
(Contract NAS8-36649)
(NASA-CR-184171; NAS 1.26:184171) Avail: NTIS HC/MF A04 CSCL 11F

The activation of metal samples and other material orbited onboard the Long Duration Exposure Facility (LDEF) and Spacelab-2 were studied. Measurements of the radioactivities of spacecraft materials were made, and corrections for self-absorption and efficiency were calculated. Activation cross sections for specific metal samples were updated while cross sections for other materials were tabulated from the scientific literature. Activation cross sections for 200 MeV neutrons were experimentally determined. Linear absorption coefficients, half lives, branching ratios and other pertinent technical data needed for LDEF sample analyses were tabulated. The status of the sample counting at low background facilities at national laboratories is reported. Author

N91-29298*# National Aeronautics and Space Administration. Lewis Research Center, Cleveland, OH.
ADVANCED MATERIALS FOR SPACE NUCLEAR POWER SYSTEMS Final Report
Robert H. Titran, Toni L. Grobstein, and David L. Ellis (Case Western Reserve Univ., Cleveland, OH.) 1991 21 p Presented at the Conference on Advanced Space Exploration Initiative Technologies, Cleveland, OH, 4-6 Sep. 1991; sponsored by AIAA, NASA, and OAI
(Contract DE-AI03-86SF-16310)
(NASA-TM-105171; DOE/NASA/16310-16; E-6464; NAS 1.15:105171; AIAA-91-3530) Avail: NTIS HC/MF A03 CSCL 11F

The overall philosophy of the research was to develop and characterize new high temperature power conversion and radiator materials and to provide spacecraft designers with material selection options and design information. Research on three candidate materials (carbide strengthened niobium alloy PWC-11 for fuel cladding, graphite fiber reinforced copper matrix composites for heat rejection fins, and tungsten fiber reinforced niobium matrix composites for fuel containment and structural supports considered for space power system applications is discussed. Each of these types of materials offers unique advantages for space power applications. Author

N91-29299# Edgerton, Germeshausen and Grier, Inc., Idaho Falls, ID.
TENSILE PROPERTIES AND MICROSTRUCTURE OF ALLOY 718 THERMALLY AGED TO 50,000 h
G. E. Korth and C. L. Trybus 1991 21 p Presented at the

Special Emphasis Symposium on Superalloys 718, 625, and Various Derivatives, Pittsburgh, 23-26 Jun. 1991
(Contract DE-AC07-76ID-01570)
(DE91-014099; EGG-M-90293; CONF-910614-5) Avail: NTIS HC/MF A03

Samples of Alloy 718 given the standard heat treatment were thermally aged from 538 to 704 C for times up to 25,000 h and aged at temperatures of 593 and 649 C up to 50,000 h. Tensile properties and microstructures of these samples show that extending the thermal exposure from 25,000 to 50,000 h at 593 and 649 C has very little additional effect, and further illustrates the long time stability of this aged hardened alloy. DOE

N91-29300# Argonne National Lab., IL.
BIOFOULING AND CORROSION FOULING OF PLAIN AND ENHANCED ALUMINUM SURFACES
C. Panchal and D. Sasscer (Northwestern Univ., Evanston, IL.) 1991 7 p Presented at the ASME/AIChE/ANS National Heat Transfer Conference, Minneapolis, MN, 26-31 Jul. 1991
(Contract W-31-109-eng-38)
(DE91-014464; ANL/CP-71781; CONF-910739-20) Avail: NTIS HC/MF A02

A long-term experimental research was carried out for the qualification of aluminum alloys for marine applications as a part of the Ocean Thermal Energy Conversion (OTEC) program. This paper presents the short- and long-term biofouling and corrosion-fouling results for a rectangular-flow channel and for the spirally fluted tube, and compares these results with that for a plain tube. The rectangular-flow channel tested in the present experimental program represents a typical flow passage for brazed-aluminum heat exchangers. The effectiveness of biofouling control methods such as chlorination and brush cleaning were also evaluated. DOE

N91-29301# Oak Ridge National Lab., TN.
ANALYSIS OF WELD METAL SOLIDIFICATION AND MICROSTRUCTURES
S. A. David and J. M. Vitek 1991 30 p Presented at the 1991 International Institute of Welding (IIW) Annual Workshop, Hague (Netherlands), 30 Jun. - 5 Jul. 1991
(Contract DE-AC05-84OR-21400)
(DE91-014574; CONF-9106229-1) Avail: NTIS HC/MF A03

Solidification is a critical phase change occurring during welding that controls weld metal microstructure, properties, and ultimately weldability of alloys. In recent years, significant advances have been made in the solidification theories that relate to castings and rapidly solidified materials. A critical need exists to understand weld pool solidification in the light of these new theories. This paper will describe the solidification behavior of weld pools, incorporating some recent advances in solidification theories. Basic principles from ingot, single crystal, and rapid solidification processes will be used to understand and explain observed weld-metal microstructures. DOE

N91-29302# Sandia National Labs., Albuquerque, NM.
POSTSHOCK SPECTRAL RADIANCE MEASUREMENTS IN NICKEL AND NICKEL/ALUMINUM POWDERS
M. B. Boslough 1991 4 p Presented at the 1991 American Physical Society (APS) Conference on Shock Compression of Condensed Matter, Williamsburg, VA, 17-20 Jul. 1991
(Contract DE-AC04-76DP-00789)
(DE91-014695; SAND-91-1197C; CONF-9107105-35) Avail: NTIS HC/MF A01

Because of complications associated with temperature heterogeneities in shocked metal powders, time-resolved radiation pyrometer measurements of shock temperatures in powders with particle sizes greater than a few tens of microns cannot be made under normal laboratory conditions with uniaxial loading durations limited to about one microsecond. Fortunately, for highly porous, reactive powders, the difference between shock and postshock temperature is negligible. For loading conditions similar to those that have yielded reaction products in recovery experiments, there is no evidence of any chemical reaction in a coarse (325 mesh) nickel/aluminum powder mixture within the first 6 microsec of shock arrival, based on constraints on postshock temperatures provided by thermal radiation measurements. This result is in contrast to that for a micron-sized nickel/aluminum mixture, for which there is evidence of significant reaction on a time scale of 100 ns under similar shock loading conditions. DOE

N91-29303# Sandia National Labs., Albuquerque, NM.
HIGH-ENERGY BACKSCATTERED ELECTRON IMAGING OF VOIDS IN ALUMINUM METALLIZATIONS
D. M. Follstaedt, J. A. VandenAvyle, A. D. Romig, Jr., and J. A. Knapp 1991 6 p Presented at the Spring Meeting of the Materials Research Society (MRS), Anaheim, 29 Apr. - 3 May 1991
(Contract DE-AC04-76DP-00789)
(DE91-014895; SAND-90-3000C; CONF-910406-26) Avail: NTIS HC/MF A02

Backscattered electron imaging of microcircuits in scanning transmission electron microscopes at 120 kV is shown to produce improved images of voids in passivated Al metallization lines relative to those obtained with scanning electron microscopes at less than or equal to 40 kV. At 120 kV, resolutions of about 0.1 microns are achieved for voids imaged beneath 1.0 microns glass overlayers. This technique allows improved characterization of microstructures for basic investigations of void formation and more accurate counting of voids in microcircuits without removing glass overlayers. Smaller voids should also be detectable with higher voltage. DOE

N91-29304# Sandia National Labs., Albuquerque, NM.
DYNAMIC BEHAVIOR OF FULLY DENSE MOLYBDENUM
M. D. Furnish, L. C. Chhabildas, D. J. Steinberg, and G. T. Gray, III (Los Alamos National Lab., NM.) 1991 4 p Presented at the 1991 American Physical Society (APS) Conference on Shock Compression of Condensed Matter, Williamsburg, 17-20 Jul. 1991
(Contract DE-AC04-76DP-00789)
(DE91-014902; SAND-91-0081C; CONF-9107105-44) Avail: NTIS HC/MF A01

We have performed a series of dynamic impact tests on molybdenum to determine its high-pressure yield and viscoelastic properties. Nine experiments, performed with a compressed gas gun and VISAR diagnostics, produced a variety of combinations of shocks, reshocks and releases. Pressure ranges from 6.5 to 15 GPa were investigated, and specimen thicknesses ranged from 6 to 13 mm. The Hugoniot elastic limit appears to be independent of sample thickness and final stress levels over the ranges reported in this study. Strengths at the HEL and the Hugoniot state, approximately 1.3 GPa, are within the range observed for lower strain rates of 10(exp -3)/sec to 5 x 10(exp 3)/sec. As with other metals, release waves do not show clean elastic-plastic behavior. Lagrangian sound velocities for singly shocked states are 6.30 to 7.40 km/sec over the pressure range tested. Strain tests behaves as approximately as the fourth power of stress, although it appears to decrease with propagation distance over the specimen thickness range used. DOE

N91-29305# Oak Ridge National Lab., TN.
DEFORMATION AND THERMAL FATIGUE IN HIGH TEMPERATURE AUSTENITIC ALLOYS
P. D. Ferro, B. Yost, R. W. Swindeman, and Che-Yu Li 1 Mar. 1991 31 p Prepared in cooperation with Cornell Univ., Ithaca, NY
(Contract DE-AC05-84OR-21400)
(DE91-014981; ORNL/Sub-85-27488/05) Avail: NTIS HC/MF A03

The flow properties of modified austenitic alloys are reviewed. The important strengthening mechanisms discussed include precipitation hardening produced by a combination of cold work and aging and by creep aging. Grain boundary sliding enhanced by reduced grain size is shown to reduce the flow strength of these alloys. DOE

N91-29306# Lawrence Livermore National Lab., CA.
THE MAGNETRON-ENHANCED ETCHING OF DOUBLE-LEVEL TUNGSTEN INTERCONNECT
R. Hsu, C. Y. Fu, and B. Law 28 May 1991 7 p Presented at the 3rd International Symposium on Ultra Large Scale Integration Science and Technology, Washington, 5-10 May 1991
(Contract W-7405-eng-48)
(DE91-014984; UCRL-JC-105487; CONF-9105224-1) Avail: NTIS HC/MF A02

The DC magnetron sputtered tungsten (W) and molybdenum (Mo) were evaluated for double level interconnect. The combined Cl2 and NF3 chemistry was chosen over either gas or SiCl4 for magnetron enhanced etching to achieve better etch selectivity and profile. Tungsten was picked over Mo for more vertical walls. The etch rate of W depended strongly on sputtering conditions. Reasonably high etch rate at 400 nm/min was obtained with selectivity to resist at about 1.4 to 1 Adhesion layer of 30 nm of TiW or Ta added to either M1 or M2 could be etched by the same recipe. The vertical profile achieved was found independent of feature size and had a large window in RF power, temperature and over etch time. This process has been successfully applied to define patterns for a double- level interconnect structure. DOE

N91-29307# Oak Ridge National Lab., TN.
X RAY REFLECTIVITY STUDIES OF Au SURFACES
D. L. Abernathy, S. G. J. Mochrie, A. R. Sandy, D. Gibbs, G. Gruebel, K. G. Huang, B. M. Ocko (Brookhaven National Lab., Upton, NY.), and D. M. Zehner 1991 14 p Presented at the 2nd International Conference on Surface X Ray and Neutron Scattering, Bad Honnes, Fed. Republic of Germany, 25-28 Jun. 1991
(Contracts DE-AC05-84OR-21400; DE-AC02-76CH-00016)
(DE91-015308; CONF-9106241-1) Avail: NTIS HC/MF A03

We briefly review the results of x ray scattering studies of the Au(001) surface between 300 K and the bulk melting temperature Tm = 1337 K. The specular reflectivities of the Au(001), (110), and (111) surfaces obtained at 300 K are compared. DOE

N91-29308# Harvard Univ., Cambridge, MA. Div. of Applied Sciences.
THE ROLE OF MICROORGANISMS IN MARINE CORROSION Final Report
Ralph Mitchell 30 Nov. 1990 4 p
(AD-A237062) Avail: NTIS HC/MF A01 CSCL 06/13

Our research under this contract was designed to investigate the role of microorganisms in hydrogen embrittlement. Specific objectives included the quantification of the amounts of microbially produced hydrogen absorbed by sensitive metals; the effect of competition from microbially produced hydrogen between metal surfaces and hydrogen consuming bacteria; and the effect of microbial metabolites on hydrogen absorption by metals. The first stage of this research involved the adaptation of a conventional electrochemical technique in order to provide a quantitative assay of hydrogen production in anaerobic zones between biofilms and metal surfaces. In this first stage of the work, we calculated hydrogen production on a per-cell basis. In all cases we used palladium foil. The advantage of this metal is that hydrogen permeation is not complicated by secondary phases within the metal, and absorption efficiency is very high. Maximum production of hydrogen was calculated at 6.5 x 10 - 11 moles per cell. GRA

N91-29309# Pratt and Whitney Aircraft, West Palm Beach, FL.
LIGHTWEIGHT DISK ALLOY DEVELOPMENT Final Report, Sep. 1986 - Apr. 1990
S. M. Russell, C. C. Law, M. J. Blackburn, P. C. Clapp, and D. M. Pease Apr. 1991 223 p
(Contract F33615-86-C-5037)
(AD-A237064; PWA-FR-21413; WRDC-TR-90-4125) Avail: NTIS HC/MF A10 CSCL 11/6

A 3-year program was conducted with the intention of developing NiAl-base alloys with mechanical and physical properties suitable for use as a lightweight turbine disk material. The program emphasized overcoming the room temperature brittleness problem and enhancing high temperature strength and creep resistance. Two approaches were utilized to address the room temperature brittleness problem: alloying to change the ordering energy to modify the slip behavior and exploiting a variety of martensitic transformation mechanisms. Ternary additions of chromium, cobalt, iron, and vanadium were studied at a variety of NiAl compositions. Both Cr and Co additions modify the room temperature slip behavior of NiAl toward one more favorable with respect to Von Mises criterion. However, a change in slip system alone is apparently insufficient for room temperature ductility. Therefore, this approach requires further study. The martensitic transformation mechanisms in Co-modified NiAl alloys were also studies as a means of overcoming the room temperature brittleness problem. The mechanisms of stress-induced martensite, nucleation of additional martensitic variants under stress, and rearrangement of twin lamellae within existing martensitic variants were beneficial and enhance the room temperature ductility and toughness. In addition to the alloy development studies, this program contained fundamental studies of the atomic bond characteristics of B2 compounds as well as computer simulation of flow and fracture of stoichiometric NiAl. GRA

N91-29310# Air Force Systems Command, Wright-Patterson AFB, OH. Foreign Technology Div.
POWDER METALLURGY TECHNOLOGY (SELECTED ARTICLES)
11 Apr. 1991 43 p Transl. into ENGLISH from P/M Technology (Peoples Rep. of China), v. 7, no. 4, 1989 p 213-219, 253-261
(AD-A237176; FTD-ID(RS)T-1058-90) Avail: NTIS HC/MF A03 CSCL 11/6

The effect is studied of various pre-HIP heating, isostatic pressure heat treatment on the size and distribution of prior particle boundary (PPB) carbide precipitates, volume fraction and grain size of HIP billets of Rene 95 P/M powder metallurgy alloy. The possibility of reducing the PPB carbide segregation by using pre-HIP heat treatment was explored. The results show that pre-HIP treatment can reduce the degree of PPB carbide segregation, increase the volume fraction, but leave grain size unchanged. This is due mainly to the improvement of pre-HIP powder surface state and the precipitating environment of carbides on PPB. GRA

N91-29311# Naval Postgraduate School, Monterey, CA.
AN INVESTIGATION OF THE AS-QUENCHED AND EARLY AGING CHARACTERISTICS OF A Al - 4.1 WT. PERCENT Li BINARY ALLOY BY X RAY DIFFRACTION M.S. Thesis
Scott J. Fuller Jun. 1990 62 p
(AD-A237598) Avail: NTIS HC/MF A04 CSCL 07/4

The as-quenched and early aging characteristics of an as-cast binary, Al-4.1 wt. percent Li alloy has been studied by X-ray diffraction. Flat plate samples were solution heat treated at 540 C under argon and ice-brine quenched. Powder samples were made from flat plate samples in the as-quenched condition by filing at liquid nitrogen temperatures. Aging was conducted at 200 C on both plate and powder samples. The presence of very broadened 100 superlattice reflections of delta' Al3Li(Ll2 structure) and small reflections of delta AlLi(B32 structure) were observed in the as-quenched condition for the plate sample. The powder sample showed the additional 110 superlattice peak of delta' and 220 delta peak. peak. This clearly showed the preferred orientation effects of the plate. From as-quenched powder, a volume fraction of 77 percent delta' with an average particle diameter of 53 angstroms was calculated. GRA

N91-29312# California Univ., Los Angeles. Dept. of Materials Science and Engineering.
DEVELOPMENT OF THE MICROSTRUCTURE BASED STOCHASTIC LIFE PREDICTION MODELS Progress Report
Marek A. Przystupa 27 Jun. 1991 9 p
(Contract N00014-91-J-1299)
(AD-A237768) Avail: NTIS HC/MF A02 CSCL 11/6

The purpose of the fatigue prediction program is to characterize

statistical changes taking place in the microstructure during fatigue of metallic alloys and to develop stochastic life prediction models based on these characterizations. In Phase 1 of the program, the microstructures and fatigue behaviors of 7050 and 8090 aluminum alloys will be studied. This will be followed by Phase 2, during which the life prediction models developed for the aluminum alloys will be generalized to predict fatigue limits in steels and superalloys. During this stage of the program also an expert system for an easy access to all results will be developed. GRA

N91-29313# California Univ., Davis. Div. of Materials Science and Engineering.
STRENGTHENING MECHANISMS, CREEP, AND FATIGUE PROCESSES IN DISPERSION HARDENED NIOBIUM ALLOY Annual Technical Report, 1 Feb. 1990 - 31 Jan. 1991
Amiya K. Mukherjee and Jeffery C. Gibeling 1 May 1991 24 p (AF Proj. 2306)
(AD-A237784) Avail: NTIS HC/MF A03 CSCL 11/6

The creep properties of Nb-1 pct. Zr alloy was investigated at intermediate temperatures. A model is proposed based on the operation of two parallel mechanisms. The first mechanism is based on dislocation glide controlled creep and controls creep rate at higher stresses where the influence of the threshold stress due to the particles is negligible. At lower stresses (below 135 MPa), the threshold stress of the particles come into play and becomes the rate controlling mechanism. The resultant effect of the operation of these two parallel mechanisms produced quite satisfactory correlation between theoretical predictions and experimental data. The cyclic deformation was also studied of commercially pure niobium and Nb-1Zr at ambient temperature. Tests were conducted at slow strain rates, where these materials exhibit high temperature dislocation glide kinetics, and at fast strain rates, where the behavior is characteristic of the low temperature regime. Additonal aspects are being explored of the fatigue response using a Bauschinger analysis and by testing at very low plastic strain amplitudes to see if a fatigue limit is observed. Refractory metals are developed and characterized for advanced aerospace craft and structural applications at elevated temperatures. These applications include space nuclear power reactors and hypersonic vehicles such as the National Aerospace Plane. GRA

N91-29314# California Univ., Los Angeles. Dept. of Chemistry and Biochemistry.
THE MIXED METALLIC-IONIC CLUSTERS OF THE SILVER/SILVER IODIDE
Clifton K. Fagerquist, Dilip K. Sensharma, and A. El-Sayed 5 Jul. 1991 47 p
(Contract N00014-89-J-1350)
(AD-A237883; TR-70) Avail: NTIS HC/MF A03 CSCL 07/4

We have sputtered isotopicall enriched silver foil (107) Ag in the source of a double-focusing mass spectrometer (reverse geometry) in the presence of methyl iodide vapor. We have detected the formation of a series of iodinated positively and negatively charged silver clusters of formula (AgXIY)k along with the purely metallic charged clusters. GRA

N91-29315# Pennsylvania State Univ., University Park.
MICROSTRUCTURAL DEVELOPMENT IN HSLA-100 STEEL WELD METALS Final Report
Paul R. Howell 1991 68 p
(Contract N00014-89-J-1958)
(AD-A237931) Avail: NTIS HC/MF A04 CSCL 11/6

In order to check the validity of the data from the as-received plate samples were re-austenitized, quenched and subsequently tempered for up to 3 hours at 605 C. In order to document the long term, high temperature stability of HSLA-100, tempering times were increased up to 48 hours. The microstructures that develop in the coarse-grained heat affected zone (CG-HAZ) of the welds are discussed in this document. At this point, it should be noted that all of the results reported herein are for the 0.04 percent C version of HSLA-100. We have also examined an 0.02 percent C version, and the results of these studies (primarily with respect to quenching/tempering and the CG-HAZ) will be submitted shortly. GRA

N91-29316# Royal Signals and Radar Establishment, Malvern (England).
A STUDY OF COPPER SEGREGATION IN SPUTTERED Al-Si-Cu FILMS USING AUGER ELECTRON SPECTROSCOPY
M. A. Green and D. C. Rodway Jan. 1991 34 p
(AD-A238130; RSRE-Memo-4281; DRIC-BR-301751) Avail: NTIS HC/MF A03 CSCL 11/6

A study has been made, using Auger Electron Spectroscopy (AES), of copper copper segregation in Aluminum Silicon Copper films processed in the Silicon Processing and Evaluation Laboratory (SPEL). The AES technique and its interpretation are briefly discussed. A description of the Auger Spectrometer and experimental details are also provided. The effects of variations in layer thickness and annealing temperatures on the interface between the Al-Si-Cu and the silicon substrate were studied. Results obtained from other samples from British Telecom research laboratories, and alternative analysis methods such as Rutherford Backscattering (RBS) are also discussed and conclusions drawn as to the nature of this segregation. GRA

N91-29317# California Univ., Berkeley. Dept. of Materials Science and Mineral Engineering.
MICROMECHANISMS OF MONOTONIC AND CYCLIC SUBCRITICAL CRACK GROWTH IN ADVANCED HIGH MELTING POINT LOW-DUCTILITY INTERMETALLICS Annual Report No. 1, 15 Apr. 1990 - 14 Apr. 1991
K. T. Rao, L. Murugesh, and L. C. DeJonghe 1 May 1991 49 p
(Grant AF-AFOSR-0167-90; AF Proj. 2306)
(AD-A238151; UCB/R/91/A1072; AFOSR-91-0576TR) Avail: NTIS HC/MF A03 CSCL 11/6

The next generation of high-performance jet engines will require markedly stiffer materials, operating at higher stress levels and capable of withstanding temperatures of up to 1650 C. Prime candidates for such applications include ordered intermetallics, ceramics and composites based on metal, intermetallic and ceramic or carbon matrices, all of which are currently of limited use due to their low ductility and fracture properties. Moreover, there is a lack of fundamental understanding on the micromechanisms influencing crack growth in these materials, particularly intermetallics. Accordingly, the present study is aimed at exploring the potential of intermetallic alloys and their composites as advanced structural materials by identifying the critical factors influencing the crack-propagation resistance under monotonic and cyclic loads. Attention is focused on the Nb3Al and TiAl intermetallic systems. In both cases, the principal mechanism of toughening is to impede crack advance from crack bridging by ductile second phase particles. Reactive sintering and vacuum hot pressing techniques are successful is processing Nb3Al intermetallics and duplex Nb/Nb3Al microstructure with a stringy niobium phase can be achieved through thermal treatments. Characterization of mechanical properties will commence in the second year. GRA

N91-29318*# National Aeronautics and Space Administration. Marshall Space Flight Center, Huntsville, AL.
THE INTERACTION OF HYDROGEN WITH METAL ALLOYS
M. D. Danford and J. W. Montano Aug. 1991 38 p
(NASA-TP-3128; M-664; NAS 1.60:3128) Avail: NTIS HC/MF A03 CSCL 11F

Hydrogen diffusion coefficients were measured for several alloys, and these were determined to be about the same at 25 C for all alloys investigated. The relation of structure, both metallurgical and crystallographic, to the observed hydrogen distribution on charging was investigated, as well as the role of hydride formation in the hydrogen resistance of metal alloys. An attempt was made to correlate the structures and compositions of metal alloys as well as other parameters with the ratios of their notched tensile strengths in hydrogen to that in helium, R(H2/He), which are believed to represent a measure of their

hydrogen resistance. Evidence supports the belief that hydrogen permeability and hydrogen resistance are increased by smaller grain sizes for a given alloy composition. Author

N91-29319# Oregon Graduate Inst. of Science and Technology, Beaverton.
DEFORMATION INDUCED MICROSTRUCTURAL AND MICROCHEMICAL CHANGES DURING THERMOMECHANICAL TREATMENT
D. G. Atteridge, L. E. Murr, W. E. Wood, and S. M. Bruemmer (Pacific Northwest Lab., Richland, WA.) 1990 55 p
(Contract DE-AC06-86NE-37963)
(DE91-014862; DOE/NE-37963/15) Avail: NTIS HC/MF A04

An important aspect of this program has been the continued study into the effects of deformation on isothermally induced grain boundary chromium depletion (GBCD) in mill annealed (MA) and solution annealed (SA) stainless steel (SS) material. An understanding of this subject is academically important to this program as well as commercially important to the industrial community. This quarterly report presents an overview of programmatic research in this area. DOE

N91-29320# Sandia National Labs., Albuquerque, NM.
LEAD-FREE SOLDERS FOR ELECTRONICS APPLICATIONS: WETTING ANALYSIS
P. T. Vianco, F. M. Hosking, and D. R. Frear 1991 8 p Presented at the 4th Electronic Materials Processing Congress, Montreal (Canada), 19-23 Aug. 1991
(Contract DE-AC04-76DP-00789)
(DE91-014900; SAND-91-0031C; CONF-9108110-1) Avail: NTIS HC/MF A02

The fabrication of electronic systems has relied upon eutectic tin-lead solder for the attachment of components to printed wiring boards. Higher service temperatures are approaching the durability limits of the eutectic solder. The tin-rich, lead-free solders are being actively studied as alternate alloys. Experiments that examined the wettability of 95Sn-5Sb (wt. pct.), 95.5Sn-4.0Cu-0.5Ag, 96.5Sn-3.5Ag, and the control solder, 60Sn-40Pb, on oxygen-free, high conductivity copper were performed. A rosin-based, mildly activated (RMA) flux and three water soluble, organic acid fluxes were used in the wetting balance/meniscometer measurements. The 95.5Sn-4.0Cu-0.5Ag and 95Sn-5Sb alloys exhibited good wetting, with contact angles of 35 degree less than (theta)(sub c) less than 55(degree) as compared to the excellent performance of the 60Sn-40Pb material (20(degree) less than (theta)(sub c) less than 35(degree)). The fair wettability observed with the 96.5Sn-3.5Ag solder (60(degree) less than (theta)(sub c) less than 75(degree)) was due in large part to the inability of the fluxes to significantly lower the solder-flux interfacial tension. The wetting rates of the 95.5Sn-4.0Cu-0.5Ag and 95Sn-5Sb solders were comparable to those of the control; the 96. 5Sn-3.5Ag alloy wetting rate was slower than the other candidates. The solder film formed on the substrate surface by the 95.5Sn-4.0Cu-0. 5Ag alloy was very grainy. The water soluble fluxes exhibited a larger degree of residue formation than did the RMA flux. DOE

N91-29321# Oak Ridge National Lab., TN.
REQUIREMENTS FOR THE OBSERVATION OF FERMI SURFACES IN DISORDERED ALLOYS
J. S. Faulkner (Florida Atlantic Univ., Boca Raton.) and G. M. Stocks 1991 12 p Presented at the Physical Phenomena At High Magnetic Fields, Tallahassee, FL, 15-18 May 1991
(Contract DE-AC05-84OR-21400)
(DE91-014578; CONF-9105151-6) Avail: NTIS HC/MF A03

The proposal is made that it may be possible to use de Haas-van Alphen measurements to gain a deeper understanding of the electronic states in concentrated, disordered, substitutional, metallic alloys. The reasons for this are the increased availability of high magnetic fields and the development of a quantitative alloy theory. DOE

N91-29322# Lawrence Livermore National Lab., CA.
LASER SURFACE MODIFICATION FOR SELECTIVE ELECTROPLATING OF METAL: A 2.5 m/s LASER DIRECT-WRITE PROCESS
V. Malba and A. F. Bernhardt 20 May 1991 14 p Presented at the Lasers 1991, Munich, Fed. Republic of Germany, 12-14 Jun. 1991
(Contract W-7405-eng-48)
(DE91-014988; UCRL-JC-106375; CONF-9106231-1) Avail: NTIS HC/MF A03

A very fast laser direct write process is described. The process involves laser modification of an insulating seed multilayer to form a conducting surface which can be electroplated. The seed layer is composed of an adhesion layer of TiW, a conducting layer of Au, and a top insulating layer of a-Si. The laser forms a Au-Si mixture without substantially affecting the adhesion layer. Writing speeds of 2.5 m/s were been demonstrated. The laser patterning can be performed in air, and the process works over a broad range of laser power (P sub max/P sub min approx. 5). DOE

N91-29323# Brookhaven National Lab., Upton, NY.
FIRST PRINCIPLES SIMULATIONS OF METALLIC ALLOYS AND LIQUIDS
J. W. Davenport, G. W. Fernando, G. X. Qian, R. E. Watson, and M. Weinert 1991 8 p Presented at the Power Supercomputer Users Meeting, Gaithersburg, MD, 21-22 May 1991
(Contract DE-AC02-76CH-00016)
(DE91-015171; BNL-46239; CONF-9105202-7) Avail: NTIS HC/MF A02

In recent years it has become possible to calculate the structural and thermodynamic properties of materials from first principles. The words first principles refer to the fact that there are no adjustable parameters in these theories. The calculator need only specify the atomic constituents; the rest is handled by the computer. In this sense the calculations are unbiased and can be used to search for new materials with interesting new properties. The search for new alloys by traditional techniques (based largely on trial and error) has become much too costly. Being both accurate and cheaper, guidance from computational and analytical theory is needed to narrow the search. In addition, it is important to extend these calculations to nonzero temperature, including the liquid phase. First principles calculations are nearly all based on the local density approximation (LDA). This is a technique for solving the quantum mechanical motion of the electrons in solids. It resembles the Hartree Fock approximation in the sense that a single particle Schrodinger equation must be solved and the resulting wave functions used to construct the electronic charge density. As an example of this method, platinum-titanium alloys are discussed. DOE

N91-29324# Oak Ridge National Lab., TN.
MECHANICAL PROPERTIES OF Fe3Al-BASED ALLOYS
V. K. Sikka, B. G. Gieseke, and R. H. Baldwin 1991 9 p Presented at the 1st International Conference on Heat-Resistant Materials, Lake Geneva, WI, 22-26 Sep. 1991
(Contract DE-AC05-84OR-21400)
(DE91-015322; CONF-910909-8) Avail: NTIS HC/MF A02

The Fe3Al-based alloys are ordered intermetallic that offer excellent corrosion resistance in molten salts. They also show excellent resistance to high temperature oxidation and sulfidation. Because of these properties, Fe3Al-based alloys were identified for many potential applications. Tensile, creep, and fatigue properties of selected iron aluminides are presented. Tensile data range from room temperature to 800 C. Creep properties vary from 450 to 750 C, and fatigue data at 600 C. Low temperature tensile properties of these alloys are sensitive to the composition, thermomechanical processing, and the final heat treatment. DOE

N91-29325# Oak Ridge National Lab., TN.
DEVELOPMENT OF NICKEL AND IRON ALUMINIDES AND THEIR APPLICATIONS
V. K. Sikka 1991 15 p Presented at the 30th Annual Canadian

Institute of Metallurgist (CIM) Conference, Ottawa (Canada), 18-21 Aug. 1991
(Contract DE-AC05-84OR-21400)
(DE91-015323; CONF-9108111-1) Avail: NTIS HC/MF A03

Alloys based on the intermetallic compounds Ni3Al and Fe3Al were developed. Intermetallic compounds are characteristically brittle at room temperature, and some are also brittle at elevated temperatures. Nickel-aluminide alloys were made ductile by alloying with a small amount of boron (200 ppM by weight) and adjusting the aluminum content to 24 at. pct. or less. Iron-aluminide alloys are ductile when chromium is added (greater than wt. 2 pct.) and the aluminum is adjusted to 28 at. pct. These alloys begin ordering upon solidification; therefore, a greater shrinkage must be accommodated during casting. The hot working temperature window for the nickel-aluminide alloy is very narrow; however, the alloy can be cold worked large amounts. Iron-aluminide alloys have a very broad hot working temperature range but have limited ductility (greater than 20 pct.) at room temperature. The strength and oxidation resistance of these alloys are such that many potential applications exist. Commercialization is in progress.
DOE

27 NONMETALLIC MATERIALS

Includes physical, chemical, and mechanical properties of plastics, elastomers, lubricants, polymers, textiles, adhesives, and ceramic materials.

For composite materials see *24 Composite Materials.*

N91-29326# Materials Research Labs., Ascot Vale (Australia).
A NOVEL EPOXY LACQUER FOR HIGH STRENGTH STEEL IN F-111 AIRCRAFT DURING OVERHAUL
L. V. Wake May 1991 11 p
(AD-A236828; MRL-TN-590; DODA-AR-006-362) Avail: NTIS HC/MF A03 CSCL 01/3

The corrosion inhibiting paint used on high strength steel (D6AC) components of RAAF F-111 aircraft is removed from the wing carry thru box and lower trap tank during deseal/reseal of integral fuel tanks and from the fuel flow holes and stiffener runouts during crack inspection of the wing pivot fittings. Following paint removal, a protective lubricant is applied to the exposed components during overhaul to inhibit corrosion and pitting of the D6AC steel. Adhesive paint failures have subsequently occurred following recoating of this steel in a number of F-111 aircraft as a result of incomplete removal of the lubricant. This report describes the development of an alternative temporary corrosion prevention coating to replace the protective grease. The replacement coating is an inhibited uncured epoxy resin system which is smear resistant, solvent removable and chemically compatible with the D6AC protective coating. Coating problems associated with the overhaul procedures are no longer being experienced since introduction of the epoxy lacquer into service by RAAF.
GRA

N91-29327# Oak Ridge National Lab., TN.
ANNEALING EFFECTS ON THE MICROSTRUCTURE OF TITANIUM ELECTRICAL CONTACTS ON DIAMOND FILMS
G. H. M. Ma, T. Tachibana, J. T. Glass, N. D. Evans (Oak Ridge Associated Universities, Inc., TN.), and R. E. Clausing 1991 4 p Presented at the 49th Electron Microscopy Society of America (EMSA) Annual Meeting, San Jose, 4-9 Aug. 1991
(Contracts DE-AC05-84OR-21400; DE-AC05-76OR-00033)
(DE91 010150; CONF-910870-8) Avail: NTIS HC/MF A01

With its large band gap and a unique combination of many excellent properties, diamond is regarded as an excellent candidate for making electronic devices for operation at high temperature. In order to fabricate diamond devices, suitable electrical contacts and appropriate deposition techniques must be developed. Titanium is considered a suitable electrical candidate material for diamond electrical contacts based on its properties. Recent current-voltage (I-V) measurements showed that as-deposited Ti contacts on boron-doped semiconducting diamond are rectifying in nature. However, upon post-deposition annealing at 430 C, these contacts became ohmic. Surface analysis by X-ray photoelectron spectroscopy (XPS) of these annealed metal contacts showed interfacial metal carbide formation at the metal/diamond interface. Therefore, the microstructural evolution causing these metal contacts to change from rectifying to ohmic in nature is the primary purpose of the present research.
DOE

N91-29328# Edgerton, Germeshausen and Grier, Inc., Idaho Falls, ID.
AN EVALUATION OF NICKEL-ALUMINUM COATINGS FABRICATED WITH THE PLASMA-SPRAY PROCESS
D. J. Varacalle, Jr., J. R. Knibloe, V. L. Smith-Wackerle, J. A. Walter, and G. Irons 1990 9 p Presented at the Expert Systems Analysis Meeting, Los Angeles, 8 Nov. 1990
(Contract DE-AC07-76ID-01570)
(DE91-013208; EGG-M-90391; CONF-9011207-1) Avail: NTIS HC/MF A02

As part of an investigation of the dynamics that occur in the plasma-spray process, an experimental study of the plasma spraying of nickel-aluminum powder was conducted. The coating experiments used typical process parameters that were varied in a Taguchi fractional factorial design parametric study. Operating parameters were varied around the typical spray parameters in a systematic design of experiments to display the range of plasma-processing conditions and their effect on the resultant coating. Parameters varied include the working gas mixture, power, powder injection location, spray distance, traverse rate, and powder feed rate. Typical operating conditions for the torch of this study were 35 V, 800 A, 100 standard ft(exp 3)/h (scfh) argon primary gas flow, 47 scfh helium secondary gas flow, and 7 lb/h powder feedrate. These parameter settings were used with a 3-in. spray distance and a gun traverse rate of 20 in./sec. The statistical scheme varied around these nominal parameter settings. The coatings were fabricated with ten passes, which yielded relatively even coatings that ranged in thickness from 187 to 603 microns. The coatings were characterized by hardness tests, optical metallography, and x-ray diffraction. Coating qualities are discussed with respect to thickness, hardness, porosity, and phase content.
DOE

N91-29329# Utah Univ., Salt Lake City. Dept. of Materials Science and Engineering.
FABRICATION, PHASE TRANSFORMATION STUDIES AND CHARACTERIZATION OF SiC-AlN-Al2OC CERAMICS
A. N. Virkar 11 Jan. 1991 16 p
(Contract DE-FG02-87ER-45286)
(DE91-013296; DOE/ER-45286/4) Avail: NTIS HC/MF A03

The principal objective of the work has been to examine phase relations, phase transformations, the resulting precipitate morphologies, and their influence on high temperature creep of the SiC-AlN-Al2OC ceramics. This system was chosen as prior work has shown the existence of extensive solid solubility at elevated temperatures and tendency for phase separation at lower temperatures. Phase separation by cellular precipitation as well as by the formation of modulated structures has been documented. The directions of modulations can be rationalized in terms of elastic strain energy considerations of the coherent precipitates. The shapes of the precipitates are also in accord with theoretical predictions. This report briefly describes the mechanisms of phase decomposition with particular emphasis on the role of elastic strain energy, the work on electron microscopic examination of modulated structures, and results of creep studies.
DOE

N91-29330# Battelle Columbus Labs., OH.
APPLICATION OF CERAMICS TO INDUSTRIAL GAS TURBINES
D. Anson, K. S. Ramesh, and M. DeCorso Mar. 1991 197 p
(Contract DE-AC02-89CE-40878)
(DE91-013140; DOE/CE-40878/1) Avail: NTIS HC/MF A09

The efficiency of any heat engine depends on the addition of heat at some elevated temperature, expansion of the working fluid under near-adiabatic conditions, and heat rejection at a lower temperature. The adiabatic temperature ratio during expansion

defines the useful work done and depends on the pressure ratio. The dependence of thermal efficiency on pressure ratio and turbine inlet temperature (TIT) is known. In considering industrial cogeneration units, raising the TIT also increases the turbine exhaust temperature and enhances the recovery of useful heat (typically above 150 C). Thus the overall fuel efficiency can be further improved by adopting higher turbine temperature. This report, is a review of the status of ceramic materials in the context of gas turbine engine development. The underlying features of ceramic materials, and the processes involved in production of ceramic components, are described in some detail. Overall, it is concluded that the present status of ceramic materials, together with the experience gained in past government sponsored programs, are such that the development of ceramic components for industrial gas turbines appears timely. DOE

N91-29331*# State Univ. of New York, Buffalo. Lab. for Ceramic and Reaction Engineering.
SYNTHESIS OF MULTIFILAMENT SILICON CARBIDE FIBERS BY CHEMICAL VAPOR DEPOSITION Final Technial Report, 1988 - 1991
Vithal Revankar and Vladimir Hlavacek May 1991 100 p
(Grant NAG3-863)
(NASA-CR-188725; NAS 1.26:188725) Avail: NTIS HC/MF A05 CSCL 11C

A process for development of clean silicon carbide fiber with a small diameter and high reliability is presented. An experimental evaluation of operating conditions for SiC fibers of good mechanical properties and devising an efficient technique which will prevent welding together of individual filaments are discussed. The thermodynamic analysis of a different precursor system was analyzed vigorously. Thermodynamically optimum conditions for stoichiometric SiC deposit were obtained. Author

N91-29332*# National Aeronautics and Space Administration. Lewis Research Center, Cleveland, OH.
THERMAL EMITTANCE ENHANCEMENT OF GRAPHITE-COPPER COMPOSITES FOR HIGH TEMPERATURE SPACE BASED RADIATORS
Sharon K. Rutledge, Mark J. Forkapa, and Jill M. Cooper (Cleveland State Univ., OH.) 1991 9 p Presented at the Conference on Advanced Space Exploration Initiative Technologies, Cleveland, OH, 4-6 Sep. 1991; cosponsored by AIAA and OAI
(NASA-TM-105178; E-6475; NAS 1.15:105178; AIAA-91-3527)
Avail: NTIS HC/MF A02 CSCL 11C

Graphite-copper composites are candidate materials for space based radiators. The thermal emittance of this material, however, is a factor of two lower than the desired emittance for these systems of greater than or equal to 0.85. Arc texturing was investigated as a surface modification technique for enhancing the emittance of the composite. Since the outer surface of the composite is copper, and samples of the composite could not be readily obtained for testing, copper was used for optimization testing Samples were exposed to various frequencies and currents of arcs during texturing. Emittances near the desired goal were achieved at frequencies less than 500 Hz. Arc current did not appear to play a major role under 15 amps. Particulate carbon was observed on the surface, and was easily removed by vibration and handling. In order to determine morphology adherence, ultrasonic cleaning was used to remove the loosely adherent material. This reduced the emittance significantly. Emittance was found to increase with increasing frequency for the cleaned samples up to 500 Hz. The highest emittance achieved on these samples over the temperature range of interest was 0.5 to 0.6, which is approximately a factor of 25 increase over the untextured copper emittance. Author

N91-29333# Clark-Atlanta Univ., GA. Dept. of Chemistry.
PRECURSORS TO Si-N-C-O CERAMICS: A REINVESTIGATION OF THE POLY METHYLVINYL SILYLETHYL ENEDIAMINE SYSTEMS
K. Feng and Y. H. Mariam Dec. 1990 12 p Presented at the 200th American Chemical Society (ACS) National Meeting, Washington, DC, 26-31 Aug. 1990
(Contract DE-FG05-87ER-45306)
(DE91-013722; DOE/ER-45306/5; CONF-900802-20) Avail: NTIS HC/MF A03

Since condensation of dichlorosilanes and diamines are known to result in mixed cyclic and acyclic structures, the various conditions under which cyclic structures would predominate over acyclic ones and vice versa were explored. The results reported here not only clarify the misleading results reported earlier, but they further corroborate some of the earlier findings that suggested that recipe-type procedures could be developed to at least partially control the microstructures of the polymers that can be prepared from dichlorosilanes and diamines. DOE

N91-29334# Los Alamos National Lab., NM.
THERMOPHYSICAL PROPERTIES OF POCO AXF-5Q GRAPHITE UP TO MELTING
G. Pottlacher, S. Melnitzky, E. Kaschnitz, H. Jaeger (Technische Univ., Graz, Austria), R. S. Hixson, and M. A. Winkler 1991 11 p Presented at the 11th Symposium on Thermophysical Properties, Boulder, 23-27 Jun. 1991
(Contract W-7405-eng-36)
(DE91-014751; LA-UR-91-1954; CONF-9106176-3) Avail: NTIS HC/MF A03

Measurements of the thermophysical properties of a particular POCO graphite (AXF-5Q) have been made up to melting. We obtained results in two different laboratories using two heating rates. We present data for temperature, volume, enthalpy, and electrical resistivity. Our measured melting point was found to be 4900 K +/- 200 K. DOE

N91-29335# MSE, Inc., Butte, MT.
CERAMIC FABRICATION R/D
1990 35 p
(Contract DE-AC07-88ID-12735)
(DE91-014758; DOE/ID-12735/T15) Avail: NTIS HC/MF A03

This project is separated into three tasks. The first task is a design and modelling effort to be carried out by MSE, Inc. The purpose of this task is to develop and analyze designs for various cohesive ceramic fabrication (CCF) components, principally an MHD electrode for strategic defense initiative (SDI) applications. A high stress, low cost, ceramic component is to be selected, designed and, if possible, analyzed. The final design for the MHD electrode comprised a layered structure of molybdenum disilicide graded with quartz glass. The design demonstrates the fabrication capabilities of the CCF process. The high stress component was targeted at armor applications and will be thick alumina plate. Silicon carbide reinforcement of the alumina will be explored. Task 2 is directed at establishing a mechanical properties data base for monolithic and laminated alumina fabricated using the CCF process. Task 3 involved production of a solid oxide fuel cell model electrode; however, work ceased when it became apparent that successful integration of the electrode modules would require additional time. Currently, work is principally focused on the production of thick CCF alumina plates; three test plates were ballistically tested and showed a very satisfactory performance. Silicon carbide reinforcement of the CCF alumina is being explored. Effort on the CCF processing of molybdenum disilicide (a nonoxide material) continued at a reduced level. Sinter aids were explored, and densities of 87 percent theoretical density on pressureless sintered dry pressed pellets were achieved. DOE

N91-29336# Argonne National Lab., IL.
ANL'S DEVELOPMENT OF CONDUCTIVE CERAMIC COMPONENTS FOR MCFC
G. H. Kucera and A. P. Brown 1991 7 p Presented at the Morgantown Energy Technology Center (METC) Contractors Review Meeting, Morgantown, WV, 5-6 Jan. 1991
(Contract W-31-109-eng-38)
(DE91-015557; ANL/CP-73155; CONF-9101102-3) Avail: NTIS HC/MF A02

The emphasis of this project is to develop new, conductive ceramic materials and to produce structures from these materials

for use as the components in the molten carbonate fuel cell (MCFC). The components under study include the cathode, anode, and interconnect, each of which is at a different stage of development. The cathode work focuses on assessing the viability of LiFeO2 as a replacement for the state-of-the-art NiO; this assessment relies on cell testing, with the performance data serving as the bases for component improvement. The anode studies seek to develop the required conductivity in a stable compound that exhibits little sensitivity to the range of anode oxygen partial pressures; this can be achieved through doping. The interconnect work emphasizes determining the effect of fuel and oxidant on conductivity, material properties, and structural integrity. DOE

N91-29337# California Inst. of Tech., Pasadena. Dept. of Chemistry.
MECHANISTIC INVESTIGATION OF NANOMETER-SCALE/LITHOGRAPHY AT LIQUID-COVERED GRAPHITE SURFACES Technical Report No. 11, Jun. 1990 - Jun. 1991
Reginald M. Penner, Michael J. Heben, and Nathan S. Lewis 31 May 1991 21 p Submitted for publication
(Contract N00014-88-K-0482)
(AD-A237085) Avail: NTIS HC/MF A03 CSCL 07/4

Pulse-induced nanometer-scale lithography has been performed on graphite surfaces that are in contact with pure water or other organic liquids. Very reproducible control over the pit diameter was observed in aqueous solutions, and a well-defined voltage threshold was also apparent. Near the threshold voltage, 7 angstroms dia. x 2 angstroms high protrusions were formed, while larger initial pulse voltages resulted in pits of diameter 20 angstroms. The protrusions were stable to imaging, but could be transformed into pits with the application of a subsequent voltage pulse. These protrusions are probable metastable intermediates in the pit formation process that operates both in liquid and gaseous ambients. Dissert. Abstr.

N91-29338# California Inst. of Tech., Pasadena. Dept. of Chemistry.
PULSE INDUCED NANLITHOGRAPHY OF GRAPHITE IN H2O: A ROAD TO CHEMICAL LINKAGES TO THE SURFACE? Technical Report, Jun. 1990 - Jun. 1991
Rik Blumenthal, Reginald M. Penner, Michael J. Heben, and Nathan S. Lewis 31 May 1991 8 p
(Contract N00014-88-K-0482)
(AD-A237086; TR-12) Avail: NTIS HC/MF A02 CSCL 07/4

The effects of tip-sample bias pulses while within tunneling distances have been investigated for graphite surfaces in contact with dry fluids, fluids containing water, and liquid water. In dry ambients, no surface modifications were observed at pulse voltages in excess of 10 V. In fluids containing water, bias pulses exceeding a threshold voltage produced pits in the graphite surface, but the threshold voltage exhibited daily fluctuations of as much as 5 V. At the threshold for surface modification, a typical pit was found to have a diameter of approximately 30 angstrom and was 3 angstrom in depth. The diameter and depth of the pits increased with pulse amplitude above the observed threshold. In pure water, a reproducible bias pulse threshold was observed, and such pulses yielded dome-like features on the surface. GRA

N91-29339# Air Force Systems Command, Wright-Patterson AFB, OH. Foreign Technology Div.
METHOD OF OBTAINING CURRENT-CONDUCTING POLYMERIC MATERIALS
L. K. Derez and B. S. Tulchinskiy 21 May 1991 9 p Transl. into ENGLISH of Russian Patent No. 328153, Nov. 1972 p 1-2
(AD-A237174; FTD-ID(RS)T-0470-91) Avail: NTIS HC/MF A02 CSCL 07/6

Invention refers to technology of obtaining polymeric materials, which possess low electrical resistance. Method of obtaining current-conducting polymers by solidifaction of a suspension of ferromagnetic filler, for example powder of carbonyl iron in epoxy, in a permanent magnetic field is known. However, high expenditure of filler decreases physicomechanical properties of material, and materials, obtained using this method, possess significant specific electric resistance. Target of invention is an increase of electroconductivity of polymeric compositions and reduction in expenditure of filler. GRA

N91-29340# Massachusetts Inst. of Tech., Cambridge.
SIMULATION OF LARGE DEFORMATION IN GLASSY ATACTIC POLYPROPYLENE Abstract Only
Peter H. Mott, Ali S. Argon, and Ulrich W. Suter 31 May 1991 3 p
(AD-A237223) Avail: NTIS HC/MF A01 CSCL 07/3

A static, atomistic model has been used to study the stress-strain behavior of glassy, atactic polypropylene well beyond the yield point. The polymer is modelled as a single chain of carbon atoms with pendant hydrogen atoms and methyl groups, packed using a periodic parallelepiped continuation condition (initially an 18.5 angstrom cube) at a potential energy minimum. Deformation is simulated by imposing small strain steps on the periodic box, minimizing the system energy at the end of each step, which causes the polymer to seek a new conformation. Molecular movement can occur only by rotation around the skeletal C-C bonds; all bond lengths and angles are fixed. GRA

N91-29341# Naval Ocean Systems Center, San Diego, CA.
SYNTHESIS OF DIAMOND FILMS BY MICROWAVE GENERATED PULSED PLASMAS
M. Aklufi and D. Brock May 1991 4 p
(AD-A237228) Avail: NTIS HC/MF A01 CSCL 20/2

The metastable growth of diamond films has been achieved by a number of continuous plasma-enhanced chemical vapor deposition (CVD) methods. Of these, none have gained more attention than the CW microwave plasma-enhanced chemical vapor deposition technique. In this technique the amount of microwave power used is typically limited by the extent of substrate heating induced by plasma and microwave heating. Concomitantly, the restriction in the amount of microwave power that can be used also reduces the amount of reactants that are dissociated and hence the film's growth rate. The use of pulsed radio-frequency discharges of very high power to deposit thin films as recently been reported. This paper investigates the use of microwave induced pulsed plasma in the growth of diamond films. GRA

N91-29342# Massachusetts Inst. of Tech., Cambridge.
MODELLING OF DEFORMATION TEXTURES EVOLUTION IN SEMI-CRYSTALLINE POLYMERS Interim Technical Report No. 26, 1990 - 1991
S. Ahzi, D. M. Parks, and A. S. Argon 31 May 1991 7 p
(Contract N00014-86-K-0768)
(AD-A237288) Avail: NTIS HC/MF A02 CSCL 07/6

A composite model for plastic deformation of semi-crystalline polymers is used to simulate deformation textures evolution in these two-phase materials. Three types of textures are simulated: crystallographic texture, morphological texture, and molecular alignment within the amorphous domains. Predictions of these textures in deformed high density polyethylene (HDPE) are shown for a uniaxial tension test. GRA

N91-29343# Massachusetts Inst. of Tech., Cambridge.
QUASI-STATIC MODELING OF CHAIN-DYNAMICS IN THE AMORPHOUS GLASSY POLYCARBONATE OF 4,4'-ISOPROPYLEDENEDIPHENOL Interim Technical Report No. 31, 1990 - 1991
H. Hutnik, A. S. Argon, and U. W. Suter 31 May 1991 49 p
(Contract N00014-86-K-0768)
(AD-A237289) Avail: NTIS HC/MF A03 CSCL 11/9

A detailed static atomistic model of the defense, glassy polycarbonate of 4,4'-isopropylidenediphenol (bisphenol-A polycarbonate, PC) is used for a quasi-static simulation of localized motions. These motions include the phenylene ring flip, conformational changes of the carbonate group, and cooperative main chain motion. The frequency distributions for both simulated motions cover several orders of magnitude. The average energy barrier to phenylene ring flip is calculated as 10.4 kcal/mol. No

significant reorientation of the ring axis was observed in the simulations, with 90 percent of the axes changing less than 15. A slight main chain motion was found superimposed upon the ring flip and the carbonate group conformational changes. GRA

N91-29344# Massachusetts Inst. of Tech., Cambridge.
INELASTIC DEFORMATION AND FRACTURE OF GLASSY SOLIDS Interim Technical Report No. 32, 1990 - 1991
A. S. Argon 31 May 1991 72 p
(Contract N00014-86-K-0768)
(AD-A237290) Avail: NTIS HC/MF A04 CSCL 11/2

A general unified treatment of the phenomeriology and mechanisms on inelastic deformation in glassy media, ranging from polymers to metals to ceramics. GRA

N91-29345# Massachusetts Inst. of Tech., Cambridge.
AN ATOMISTIC MODEL OF THE AMORPHOUS GLASSY POLYCARBONATE OF 4,4'-ISOPROPYLIDENEDIPHENOL Interim Technical Report No. 30, 1990 - 1991
M. Hutnik, F. T. Gentile, P. J. Ludovice, U. W. Suter, and A. S. Argon 31 May 1991 39 p
(Contract N00014-86-K-0768)
(AD-A237291) Avail: NTIS HC/MF A03 CSCL 11/9

A detailed static atomistic model of the dense, glassy polycarbonate of 4,4'-isopropylidenediphenol (bisphenol-A polycarbonate, PC) is simulated using a well established technique that previously proved successful for simple vinyl polymers. Initial chain conformations, which are generated using a Monte Carlo technique including periodic continuation conditions, are relaxed using a potential energy minimization. Two sizes of microstructures at densities of 1.20 g/cu cm were obtained, one with cube edge length of 18 angstrom and the other with an edge length of 30 angstrom. Detailed analysis of the minimized structures indicate intermolecular packing influences create a large variation of chain conformations different from the purely intramolecular ground states, but that it is the intramolecular energy contributions that determine which combinations can or cannot occur. The systems are amorphous, exhibiting random coil behavior, with some weak intermolecular correlations that exist on a very small scale. GRA

N91-29346# Massachusetts Inst. of Tech., Cambridge.
THE MOLECULAR VIEW OF PLASTIC DEFORMATION AND PRECURSOR PROCESSES OF CRAZING IN GLASSY POLYPROPYLENE AND POLYCARBONATE Interim Technical Report No. 33, 1990 - 1991
Ali S. Argon, M. Hutnik, P. Mott, and U. W. Suter 31 May 1991 6 p
(Contract N00014-86-K-0768)
(AD-A237333) Avail: NTIS HC/MF A02 CSCL 07/6

The kinematics and energetics of the anelastic processes of phenylene ring rotation and carbonate group rearrangements in polycarbonate, and the nature of coherent plastic relaxations under imposed conditions of pure shear to large plastic strains in polypropylene have been computationally simulated on computer generated molecular structure models of these polymers in glassy form. In addition, simulations have also been performed on the inelastic dilatational response of polypropylene to probe precursor processes to crazing. Results on these simulations will be presented. GRA

N91-29347# Massachusetts Inst. of Tech., Cambridge.
CONFORMATIONAL CHARACTERISTICS OF THE POLYCARBONATE 4,4'-ISOPROPYLIDENEDIPHENOL Interim Technical Report No. 29, 1990 - 1991
M. Hutnik, Ali S. Argon, and U. W. Suter 31 May 1991 32 p
(Contract N00014-86-K-0768)
(AD-A237334) Avail: NTIS HC/MF A03 CSCL 11/9

A classical force field has been developed to represent the conformational characteristics of the polycarbonate of 4,4'-isopropylidene diphenol (bisphenol-A polycarbonate, PC) based upon recent experimental and quantum mechanical data reported for diphenylcarbonate and diphenylpropane. This force field is an improvement upon previously published molecular mechanics force fields because it allows for rotation about all the single bonds in the PC repeat unit. A rotational isomeric state model PC has been obtained using the force field results; the computer unperturbed chain dimensions agree well with reported experimental values. GRA

N91-29348# Lowell Univ., MA. Dept. of Chemistry.
DESIGN, SYNTHESIS AND CHARACTERIZATION OF NOVEL POLYDIACETYLENES USING NEW ANALYTICAL TECHNIQUES Final Report
Sukant Tripathy 28 May 1991 22 p
(Contract N00014-90-J-1148)
(AD-A237362) Avail: NTIS HC/MF A03 CSCL 07/4

The principal focus of the project is to develop new materials chemistry based on molecular level design and solid state chemistry. The goals have been to develop electroactive polymers with novel electronic, optical, and nonlinear optical properties. Second and third order nonlinear optical materials have been developed based on conjugated macromolecules and asymmetric anharmonic molecular electronic dipolar oscillators. In this multidisciplinary research effort, starting from first principle, polymeric systems have been developed with stable large nonlinear optical coefficients, ultrathin electroactive redox monolayers, molecular superlattices, etc.. Photochemical crosslinking and photopolymerization have been employed as engineering tools in materials fabrication and to elicit new phenomenon. GRA

N91-29349# University of Southern California, Los Angeles. Dept. of Chemical Engineering.
MODEL FILLED POLYMERS 8: SYNTHESIS OF CROSSLINKED POLYMERIC BEADS BY SEED POLYMERIZATION Technical Report No. 8, 1 Sep. 1990 - 1 May 1991
Dezhong Zou, Liqing Sun, J. J. Aklonis, and R. Salovey 31 May 1991 37 p
(Contract N00014-88-K-0302)
(AD-A237429) Avail: NTIS HC/MF A03 CSCL 07/6

Monodisperse crosslinked polystyrene (PS) and polymethacrylate (PMA) beads of sizes greater than 1 micron in diameter are prepared by particle nucleation onto pre-existing polymer seeds in a multistage emulsion polymerization, in the absence of emulsifier. An adequate seed concentration, which decreases with increasing seed size, is necessary to achieve monodisperse beads. Monodisperse multicomposition beads are prepared by polymerizing styrene onto PMA seeds, but not by polymerizing methyl methacrylate onto PS seeds. Free radical capture by growing seed particles with surface polymerization may lead to the formation of asymmetric shaped particles. GRA

N91-29350# University of Southern California, Los Angeles. Dept. of Chemical Engineering.
MODEL FILLED POLYMER 7: FLOW BEHAVIOR OF POLYMERS CONTAINING MONODISPERSE CROSSLINKED POLYMERIC BEADS Technical Report No. 7, 1 Sep. 1990 - 1 May 1991
Liqing Sun, Moonsoo Park, J. J. Aklonis, and R. Salovey 10 May 1991 42 p
(Contract N00014-88-K-0302)
(AD-A237430) Avail: NTIS HC/MF A03 CSCL 07/6

Steady shear viscosities and dynamic moduli of polymer composites, consisting of combinations of crosslinked beads and matrices of polystyrene (PS) and polymethacryiates (PMA), are measured in a cone and plate rheometer. Viscosities and moduli were very sensitive to chemical composition. Crosslinked beads of identical composition to the matrix exhibited the lowest viscosity enhancements at low shear rates and the lowest moduli in dynamic mechanical properties analysis. The effects of bead concentration on rheological behavior were compared for PS and PMMA beads in a PMMA matrix. PMMA beads produce small effects, whereas, PS beads yielded highly non-Newtonian systems in PMMA, showing a yield stress of 1100 Pa at 30 wt percent filler loading, and dynamic moduli independent of frequency. We suggest that rheological behavior reflects the state of dispersion of beads in

the matrix. Beads identical in composition to the matrix yield uniform dispersions. We propose that uniform and stable bead dispersions exhibit the lowest viscosity and moduli. GRA

N91-29351# Maine Univ., Orono. Lab. for Surface Science and Technology.
EFFECT OF EXCESS OXYDIANILINE ON THE PROPERTIES OF POLYIMIDE Technical Report, 1 Jun. 1990 - 31 May 1991
R. G. Pethe, W. N. Unertl, and C. M. Carlin 15 May 1991 20 p
(Contract N00014-89-J-1314)
(AD-A237467) Avail: NTIS HC/MF A03 CSCL 07/6

Thin films of the polymer polyimide (PI) can be grown in ultra-high vacuum by codeposition of pyromellitic dianhydride (PMDA) and oxydianiline (ODA). Raman spectroscopy was used to characterize the effects of non-stoichiometric deposition rates and substrate temperature on the chemical properties of the resulting PI film. Low fluxes and excess PMDA yield PI formation. High fluxes and excess PMDA thus ruling out the possibility of a one step process for PI formation. Defects that develop during processing of the polymer polyimide can adversely alter the dielectric properties and adhesion of polyimide thin films which are widely used, for semiconductors. Polyimide films can be cast or spin coated from solution or formed by direct vapor deposition. GRA

N91-29352# University of Southern California, Los Angeles. Dept. of Chemical Engineering.
MODEL FILLED POLYMERS 9: SYNTHESIS OF UNIFORMLY CROSSLINKED POLYSTYRENE MICROBEADS Technical Report No. 9, 1 Sep. 1990 - 1 Jun. 1991
Zheng-You Ding, Shenmin Ma, Dennis Kriz, J. J. Aklonis, and R. Salovey 10 Jun. 1991 28 p
(Contract N00014-88-K-0302)
(AD-A237472) Avail: NTIS HC/MF A03 CSCL 07/6

Monodisperse sized crosslinked polystyrene (PS) beads by reaction of styrene (S) and divinylbenzene (DVB), in batch emulsion copolymerization in the absence of emulsifiers, are not uniformly crosslinked, because DVB is more reactive than S. For copolymerization of 1 to 10 mole percent DVB and S, within each crosslinked PS microbead, 7 crosslink density varies by a factor exceeding two and decreases with uniformity crosslinked PS beads. For both copolymerization techniques, T8 correlates well with crosslink density and PS beads are spherical and monodisperse in size. GRA

N91-29353# University of Southern California, Los Angeles. Hydrocarbon Research Inst.
MECHANISM OF ANIONIC RING-OPENING POLYMERIZATION OF SILACYCLOPENT 3-ENES Interim Technical Report
William P. Weber, Young T. Park, and Stephen Q. Zhou 1 Jul. 1991 11 p Submitted for publication
(Contract N00014-89-J-1961)
(AD-A237538) Avail: NTIS HC/MF A03 CSCL 07/3

Anionic ring opening polymerization of silacyclopent-3-enes has characteristics which are different from those of anionic living polymerizations of 1,3-dienes. High molecular weights are obtained in most cases but generally with most probable molecular weight distributions. The polymerization is stereospecific. Poly (1-sila-cis-pent-3-enes) are obtained. Ring opening polymerization of 1,1,3-trimethy1 1-silacyclo pent-3-ene is found to be regioselective at -78 C to yield a polymer in which cis-1,4-isoprene units are joined to diethylsilylene units almost exclusively in a head to tail orientation. Finally, anionic polymerization of 1-methy1 1-silacyclo pent-3-ene is found to yield poly(1-methy1 1-silacyclo pent-3-ene is found to yield poly(1-methy1 1-sila cis-pent-3-ene) of low molecular weight. This permits end group analysis by H-1, C-13, and Si-29 NMR spectroscopy. Signals are observed which are consistent with the presence of 1-methy1 1-silacyclo pent-3-ene rings. These are probably end groups. A mechanism consistent with the above is discussed. GRA

N91-29354# Rockwell International Science Center, Thousand Oaks, CA.
EFFECTS OF INTERFACIAL MODIFICATION ON DIAMOND FILM ADHESION
J. F. DeNatale, J. F. Flintoff, and A. B. Harker 1991 5 p Sponsored by ONR
(AD-A237750) Avail: NTIS HC/MF A01 CSCL 20/12

Microlithographic surface patterning has been investigated as a means of improving diamond film adhesion on noncompatible substrates. This technique produces significant improvements in film adhesion beyond identical unpatterned substrates, although sufficient film stresses can develop to induce subsurface substrate fracture. The substrate etching geometry can be chosen to simultaneously produce an antireflective surface relief. Polycrystalline diamond thin films offer a unique combination of physical properties highly desirable for optical device applications: high hardness, wideband transparency, chemical inertness, and high laser damage thresholds. Application of these coatings to optical device structures, however, is often impeded by poor film adherence and surface roughness. While the film's substantial thickness can be produced routinely on Si, films grown on numerous other optical materials under equivalent conditions often delaminate at thickness of only a few microns due to lack of interfacial chemical bonding, intrinsic growth stresses and thermal expansion mismatch. To fully exploit the potential of the diamond films in optical applications, fabrication on less-compatible substrates must be addressed. Additionally, the highly faceted polycrystalline diamond films cause high levels of scattering and normally must be polished to achieve good optical transmission. GRA

N91-29355# Rensselaer Polytechnic Inst., Troy, NY. Dept. of Chemistry.
ORGANOMETALLIC PRECURSOR ROUTES TO Si-C-Al-O-N CERAMICS Final Report, 1 Jul. 1989 - 31 Mar. 1991
Leonard V. Interrante 15 May 1991 78 p
(Grant AF-AFOSR-0439-89; AF Proj. 2303)
(AD-A237753; AFOSR-91-0586TR) Avail: NTIS HC/MF A05 CSCL 07/4

This report describes the results of a research program directed at the development of improved methods for the preparation of Si-C-Al-O-N ceramics using organometallic precursors. Two main approaches were employed in these studies: (1) co-pyrolysis of homogeneous mixtures of organosilicon and organoaluminum precursors; and (2) pyrolysis of specially designed, single-component precursors containing both Si and Al. Depending on the choice of precursors and the pyrolysis atmosphere employed, nanocrystalline Beta-SiC/2H-AlN and Si3N4/AlN composites, 2H-SiC/AlN solid solutions, and various crystalline SiAlON phases were obtained as final ceramic products after annealing at 1400 to 1800 C the initially amorphous pre-ceramic phases obtained on pyrolysis to 1000 C. GRA

N91-29356# Naval Civil Engineering Lab., Port Hueneme, CA.
ENERGY CONSERVING COATING: PIGMENT RESEARCH Final Report, Sep. 1988 - Apr. 1991
Thomas Novinson May 1991 48 p
(AD-A237841; NCEL-TN-1831) Avail: NTIS HC/MF A03 CSCL 20/13

This report documents research into novel experimental paints made from color-reversible pigments. These pigments are of two types: photochromic and thermochromic. The first group changes color on exposure to light, and the second changes color when subjected to a change in temperature. If successfully incorporated into a coating and applied to walls and roofs, these pigments could reduce heating and cooling costs by presenting a more absorbent color in the winter and a more reflective color in the summer. GRA

N91-29357# Vermont Univ., Burlington.
ORGANO- BORAZINES.3.HOMO- AND COPOLYMERIZATION OF P-VINYLPHENYL- CYCLOTRI- BORAZINES
Logan A. Jackson and Christopher W. Allen 1 Jul. 1991 15 p

(Contract N00014-89-J-1041)
(AD-A237881; TR-17) Avail: NTIS HC/MF A03 CSCL 07/6

The polymerization and copolymerization with styrene of a series of unsymmetrically B-p-vinylphenyl-N-methyl, and N-phenyl borazines (R3(R2)2B3N3(R1)3; R1 = methyl, phenyl, R2 = methyl phenyl, R3 = p-vinylphenyl) has been studied. The polymerization of these monomers yielded both tractable and crosslinked materials. The polymers obtained were characterized by 1H and 13C nuclear magnetic resonance (NMR) spectroscopy, elemental analysis, gel permeation chromatography and thermogravimetric analysis. The reactivity ratios for the copolymerization reaction were calculated by the Mortimer-Tidewell method. GRA

N91-29358# Army Lab. Command, Watertown, MA. Material Technology Lab.
STUDIES OF POLYMERS FOR SHOCK ABSORPTION APPLICATIONS Final Report
Catherine A. Byrne and Walter X. Zukas May 1991 32 p
(AD-A237925; MTL-TR-91-21) Avail: NTIS HC/MF A03 CSCL 11/10

The purpose of this study was to evaluate polymers with potential shock damping properties. Many soft polyurethane elastomers were prepared in the laboratory and evaluated by thermal and mechanical analysis; these include mostly poly(propylene oxide) and polythioether-based elastomers prepared with toluene diisocyanate. Tri- and tetrafunctional chain extenders were used in all cases, as well as some unusual secondary diamines. The objective was to soften the polymers, disorganize the hard phase, and broaden the soft segment glass transition temperature while still allowing a rather broad use temperature. Comparisons were made to commercially available shock absorbing polymers. The synthesis of the polyurethanes is discussed in detail and the results of characterization of all of the polymers are described. The polymers exhibit T sub g's ranging from -68 C to -19 C, final softening temperatures between 115 C and 246 C, Shore A hardness values ranging from 13 to 87, tensile strengths of 0.7 MPa to 20 MPa and elongations of 175 to 2900 percent. Several display low Bashore rebound values in the temperature range of interest. Dynamic mechanical data were extrapolated to high frequency through the assembly of master curves and revealed that the polymers evaluated probably would exhibit good high frequency shock absorbing properties at room temperature or somewhat above room temperature, but that they would not display satisfactory behavior at temperatures significantly below room temperature. GRA

N91-29359# Wien Univ. (Austria).
BORON NITRIDE AND SILICON NITRIDE SYSTEMS Final Report, Jun. 1990 - Feb. 1991
Peter Rogl and Julius C. Schuster Feb. 1991 224 p
(Contract DAJA45-90-C-0002)
(AD-A238080) Avail: NTIS HC/MF A10 CSCL 07/4

Information on phase equilibria and compound formation in the Li-B-N system all agree on the existence of a ternary compound Li3Bn2 with several pressure modifications. Heating powder compacts of Li3N + BN in a Mo-boat in a stream of nitrogen between 650 to 700 C was claimed as optimal conditions to obtain Li3BN2, the reaction being strongly exothermic. Melting of Li3BN2 was reported at 870 C. Based on earlier preliminary data, the p-T diagram of Li3BN2 was investigated over the pressure and temperature range from 1.0 to 6.5 GPa and 300 to 1900 C employing optical and x-ray powder diffraction analysis. GRA

N91-29360# California Univ., Los Angeles. Dept. of Materials Science and Engineering.
PREPARATION AND PROPERTIES OF NEW INORGANIC GLASSES AND GEL-DERIVED SOLIDS Final Technical Report, 1 Nov. 1987 - 30 Oct. 1990
John D. Mackenzie Apr. 1991 36 p
(Grant AF-AFOSR-0066-88; AF Proj. 2303)
(AD-A233095; AFOSR-91-0614TR) Avail: NTIS HC/MF A03 CSCL 11/2

Research has been carried out on two families of solids. The first one involves solids made by the sol-gel process and includes composites. The second one involves non-oxide glasses based on fluorides, chalcogenides, and chalcohalides. The structures of oxide gels were studied by x-ray photoelectron spectroscopy, liquid and solid state NMR. A new theory was developed on gel transformations. A number of new composites made by the sol-gel route were examined, including the use of silicon carbide and diamond powder as fillers and some triphasic solids. Many ferroelectric thin films were prepared and their properties measured. An inorganic-organic gel material named ORMOSIL was developed which exhibited rubbery elasticity. The viscosity and viscoelasticity of fluorozirconate glasses and glass fibers have been studied. New chalcohalide glasses were prepared and their optical properties evaluated. Structural information was derived from Raman spectroscopy. The interaction of ultraviolet radiation on chalcogenide fibers was investigated. GRA

N91-29361# State Univ. of New York, Buffalo.
FIRST INTERNATIONAL CONFERENCE ON FRONTIERS OF POLYMER RESEARCH Final Report, period ending 21 Jan. 1991
Paras N. Prasad and J. E. Mark Apr. 1991 11 p Conference held in New Delhi, India, 20-25 Jan. 1991
(Contract DAAL03-91-G-0057)
(AD-A238112; ARO-28836.1-MS-CF) Avail: NTIS HC/MF A03 CSCL 07/6

The focus of the conference was on three important areas of polymer research: polymers for photonics, polymers for electronics, and high-performance polymers. The conference emphasized the cross-fertilization of these areas, which traditionally have been covered in separate scientific meetings. Review talks were presented on the first day, after the inaugural session, to familiarize people with developments in each area. A unique feature of the conference was the session on Emerging New Technologies, in which high-level industrial representatives from many countries presented their views on the applications of polymeric materials in new future technologies. GRA

N91-29362# Texas Univ., Arlington. Center for Advanced Polymer Research.
ELECTRONIC AND IONIC TRANSPORT IN PROCESSABLE CONDUCTING POLYMERS End-of-the-Year Report, 1 Jun. 1990 - 31 May 1991
Martin Pomerantz, John R. Reynolds, Krishnan Rajeshwar, and Dennis S. Marynick 28 May 1991 12 p
(Contract N00014-90-J-1320)
(AD-A238175; TR-31) Avail: NTIS HC/MF A03 CSCL 07/6

Research carried out on this grant includes studies of water soluble polyelectrolyte polypyrrole composites, conducting polymer/dopant ion interactions, symmetrically and asymmetrically substituted, poly 5-decylisothianaphthene, polyrrole containing luminescent ions, the use of cyclic voltammetry coupled with UV-vis and Raman spectroscopy, the preparation of polypyrrole films containing nm-sized platinum particles, the neutral-polaron-bipolaron sequence of oxidation states of polypyrrole in the presence of Oxygen, melt spun fibers of blends of poly 3-dicylthiophene with polyethylene and the development of a new modification of the Extended Huckel band structure methodology which, when combined with geometries calculated by the PRDDO method, produces very accurate calculated band gaps. GRA

N91-29363# McGill Univ., Montreal (Quebec). Dept. of Chemistry.
PHYSICAL PROPERTIES AND STRUCTURE OF ION-CONTAINING POLYMERS Final Report, 1 Oct. 1987 - 31 May 1991
Adi Eisenberg Jun. 1991 19 p
(Contract DAAL03-87-K-0065)
(AD-A238196; ARO-24073.11-CH) Avail: NTIS HC/MF A03 CSCL 07/6

This report describes the progress made under the present contract. It is presented in three main sections dealing, respectively,

with structure-property relations, with blends, and with block copolymers. In the area of structure-property relations, one paper is particularly noteworthy in that it presents a new model for the morphology of ionomers which is consistent with all known experimental results, including small angle X-ray scattering and mechanical properties, among many others. In the blend area, the most notable result pertains to the achievement of controlled miscibility between nylon and polystyrene. Finally, in the block copolymer area, a completely new two dimensional micelle morphology was discovered at air-water interfaces. These studies represent the highlights of the broad investigation of the effect of coulombic interactions on the properties of polymer in the bulk, in solution, and on surfaces. GRA

N91-29364# Maine Univ., Orono. Lab. for Surface Science and Technology.
PROPERTIES AND ADHESION OF POLYIMIDES IN MICROELECTRONIC DEVICES Technical Report, 1 Jun. 1990 - 31 May 1991
M. Grunze 15 May 1991 7 p
(Contract N00014-89-J-1314)
(AD-A238204) Avail: NTIS HC/MF A02 CSCL 11/9

This paper gives a summary on the properties of polyimide films used in microelectronic devices and on recent research efforts to understand the adhesion between polyimides and inorganic materials. One of the major concerns in the application of polyimides is the integrity and reliability of the laminar structures. Surface sensitive spectroscopies have been recently applied to identify the nature of the chemical bond for metals evaporated onto cured polyimide surfaces and for spun-on and subsequently imidized polyamic acid films on metal surfaces. Depending on the preparation of the interface, e.g., metal on polymer or polymer on bulk metal, different phenomena are observed. GRA

N91-29365# Ohio State Univ., Columbus.
HIGH STRAIN RATE CHARACTERIZATION OF CERAMICS IN SHEAR Final Report
Amos Gilat Jun. 1991 58 p
(Contract N00014-88-K-0733)
(AD-A238319) Avail: NTIS HC/MF A04 CSCL 11/2

Ceramic materials are being used in applications that involve high rates of loading. Examples are jet engines and protective armor components. Most of the available data with regard to dynamic response of ceramics have been obtained from experiments that involve compressive loading. Two techniques, the normal plate impact and the compression split Hopkinson bar, are most commonly used for testing under high rate loading in compression. Results from normal plate impact tests generally show a increase in the yield strength when the Hogionot Elastic Limit (HEL) is transformed to uniaxial stress and compared with the static uniaxial yield stess. Tests on commercial aluminum oxides show a dynamic yield strength of 43 Kbars compared to a quasi-static yield strength of 19.3 Kbars. High strain rate tests with the compression split Hopkinson bar have been conducted. Results on aluminum oxides at various temperatures show an increase in the compressive strength with increasing strain rate. GRA

N91-29366# Maine Univ., Orono. Lab. for Surface Science and Technology.
COMPARISON BETWEEN THE INTERFACIAL CHEMISTRY OF METALLIZED POLYIMIDES AND POLYMIDE Technical Report No. 19, 6 Jan. 1990 - 31 May 1991
M. Grunze, A. Killinger, C. Nainka, C. Hahn, and T. Strunskus 31 May 1991 13 p
(Contract N00014-89-J-1314)
(AD-A238400) Avail: NTIS HC/MF A03 CSCL 11/4

In this short overview the pertinent differences in the chemical interactions of differently prepared polymide/metal interfaces are summarized. Considered are the cases for metals deposited onto cured polyimide surfaces, interfaces prepared by spin coating polyamic acid onto bulk substrates and subsequent thermal imidization (Cu), vapor deposited polyamic acid with subsequent thermal imidization (Cu, Ag, Si, Cr), and deposition of polyamic acid in the form of mono- and multilayers by Langmuir Blodgett (LB) techniques onto a silicon (100) surface. New FTIR and XPS data are presented for copper deposition onto polyimide suggesting that initial interaction leads to elimination of carbon monoxide molecules from the polymer surface. Aromatic linear polyimides are a class of organic polymers with favorable mechanical properties and dielectric properties for application in electronic devices which can easily be processed into planar films. Today they are used routinely in VSLI devices as multilevel dielectric insulation. GRA

N91-29367# State Univ. of New York, Stony Brook. Dept. of Chemistry.
LIGHT SCATTERING CHARACTERIZATION OF POLYMER ADDITIVES AND CORRELATION OF MOLECULAR PROPERTIES OF POLYMER FLUIDS Final Report, 1 Oct. 1987 - 31 Jan. 1991
Ben Chu 27 Mar. 1991 9 p
(Contract DAAL03-87-K-0136)
(AD-A238547; ARO-24559.15-CH) Avail: NTIS HC/MF A02 CSCL 07/6

In the ARO project, we have succeeded in characterizing a random copolymer of poly(isobutyl methacrylate-co-tertbutyl aminoethyl methacrylate), abbreviated as poly(iBMA-tBAEMA) in polar and protic solvents by means of laser light scattering (LLS) and viscosimetry. Intra- and intermolecular interactions could be used to explain the aggregation behavior which dominates the rheological properties of a large variety of such polymer solutions, making poly(iBMA-tBAEMA) a useful polymer additive/thickening agent. By adding another polymer which can complex with poly(iBMA-tBEAMA), we have found that the polymer can be used as a viscosity enhancer for the polymer additive, poly(iBMA-tBEAMA). With sulfonated polystyrenes, the enhancement could reach a factor of 20. GRA

N91-29368# Massachusetts Univ., Amherst. Dept. of Polymer Science and Engineering.
PHASE TRANSFORMATIONS, ULTRASTRUCTURE, AND PROPERTIES OF RIGID-ROD POLYMERS Final Report, 1 Jun. 1989 - 30 Nov. 1990
Edwin L. Thomas May 1991 9 p
(Contract F49620-89-C-0073)
(AD-A238643; AFOSR-91-0666TR) Avail: NTIS HC/MF A02 CSCL 11/4

The structure and properties of PBZT and PBO fibers and films depend critically in the detailed processing. Investigation of the coagulation process is of significant interest because this is where the initial solid state polymer structure forms and the starting point from which all other post treatment microstructures evolve. An analysis was made of crystal solvates in a PBZT/PPA/water system, a general geometrical classification scheme for grain boundaries in PBZO, the analysis of compressive strength of PBZT/PEEK film laminates after sol-gel microcomposite processing, a morphological study of kink bands in PBZT and PBZO fibers to determine the cause of the relative weakness of the fibers in compression, and a microstructural examination of PBZO fibers as a function of heat treatment processing. GRA

N91-29369# Minnesota Mining and Mfg. Co., Saint Paul. Corporate Research Labs.
DUAL CURE PHOTOCATALYST SYSTEMS
S. J. Keipert 1990 6 p Presented at the USAF/DOE Workshop on Solvent Substitution, Phoenix, AZ, Dec. 1990
(Contract DE-AC07-88ID-12692)
(DE91-014174; EGG-M-90520; CONF-901285-4) Avail: NTIS HC/MF A02

The 3M Dual Cure process is a method for producing radiation cured polymer compositions via a solventless coating process. The process involves the simulations cure of two different monomer types. The first type may be either an epoxy monomer, or the polyol and polyisocyanate precursors to a urethane polymer. These are polymerized by use of an iron based organometallic

photocatalyst which gives a Lewis acid upon irradiation. The second monomer type consists of acrylate monomers, which are polymerized via a free radical photoinitiator to give acrylate polymers. The two polymerization types procede separately to give substantially independent, interpenetrating polymer networks. The properties of the resulting Dual Cure compositions are often found to be superior to either component alone. The objective of the Dual Cure program is to eliminate solvents from coating composition, while simultaneously maintaining or improving the physical properties of the coating and the processing conditions used to prepare them. This will lead to reductions in solvent use, with a resulting reduction in energy consumption and solvent emissions. DOE

N91-29370# Oak Ridge National Lab., TN.
CORROSION BEHAVIOR OF CONTINUOUS-FILAMENT-WOUND CERAMIC COMPOSITE TUBES
J. I. Federer May 1991 49 p
(Contract DE-AC05-84OR-21400)
(DE91-014959; ORNL/TM-11691) Avail: NTIS HC/MF A03

Ceramic composites are being developed for heat exchanger tubes in industrial furnaces. Because industrial furnace atmospheres often contain alkali compounds, the corrosion behavior of ceramic composites was investigated in an oxidizing atmosphere containing Na(sub 2)CO(sub 3) vapor. The composites, the form of tubes, consisted of Al(sub 2)O(sub 3)-20 wt. percent ZrO(sub 2) continuous-filament-wound bodies impregnated with Al(sub 2)O(sub 3) or ZrO(sub 2) matrices. The matrices contained 20 to 30 percent porosity. The tubes were thermally cycled three or four times between 20 and 1150 C with cumulative holding times at 1150 C, of 300 or 500 h. One set of specimens was thermally cycled in air for comparison with a similar set thermally cycled in the Na(sub 2)Co(sub 3)-containing atmosphere. Specimens heat-treated in air had almost no visual evidence of degradation, but specimens exposed to the corrosive atmosphere exhibited bending, nonuniform expansion, cracking, and spalling. Dimensional changes in specimens heat-treated in air were less than (plus or minus) 0.5 percent compared to values up to + 6 percent in specimens exposed to the corrosive atmosphere. In specimens with ZrO(sub 2) matrices, Na was found to be concentrated at the interfaces between matrix and filaments, indicating that the matrix porosity allowed access of the atmosphere to the filaments. In the specimen with an Al(sub 2)O(sub 3) matrix, Na was concentrated on the outer surface, indicating high reactivity between Na and Al(sub 2)O(sub 3). X-ray diffraction analysis showed that several sodium aluminates had formed by reaction of Na(sub 2)CO(sub 3) with the Al(sub 2)O(sub 3) matrix and high Al(sub 2)O(sub 3) filaments, but no sodium zirconates were detected. The degradation of the specimens was attributed to the volume increases associated with formation of sodium aluminates. DOE

N91-29371# Northwestern Univ., Evanston, IL. Dept. of Physics and Astronomy.
NMR CHARACTERIZATION OF POROUS CERAMICS
W. P. Halperin Jun. 1991 14 p
(Contract DE-FG02-86ER-45251)
(DE91-015051; DOE/ER-45251/3) Avail: NTIS HC/MF A03

Investigation of nuclear magnetic resonance relaxation analysis (MRRA) of pore structures was carried out to study the development of pore structure following sintering of SiC samples, and porous glasses. The mechanisms for fast surface NMR relaxation that is at the heart of the MRRA method were determined. Diffusion coefficient measurements of water at full and partial saturation were made on xerogel glasses showing evidence for a new transport mechanism for enhanced molecular diffusion. These studies have shown that this enhanced diffusion process can be attributed to a two phase mechanism involving vapor and liquid components with fast molecular exchange between them. Investigation of the dynamical properties of water in submonolayer coverages of a borosilicate porous glass have shown that diffusion decreases with decreasing coverage. The applicability of the NMR method to the study of porosity and pore size distributions in a wide range of porous materials including glasses, ceramics and sandstones has been completed. DOE

N91-29372# California Univ., Davis. Dept. of Mechanical Engineering.
CERAMIC DECOMPOSITION UNDER IRRADIATION
D. G. Howitt 1991 8 p
(Contract DE-FG03-86ER-45279)
(DE91-015061; DOE/ER-45279/T2) Avail: NTIS HC/MF A02

Under this program fundamental investigations are being conducted on the physical and chemical processes associated with radiation damage in dielectric and semiconducting materials to both understand the mechanisms involved and to provide improved methodologies for the analysis of these materials by electron microscopy. The research has shown that there are at least two distinct processes which give rise to the deomposition of ceramics under irradiation. The first is a diffusion effect that is induced by the charge imbalance associated with ionization processes while the second is associated with a very short atomic displacement caused by elastic interactions. DOE

N91-29373# Oak Ridge National Lab., TN.
FABRICATION OF SILICON NITRIDE CERAMICS BY MICROWAVE HEATING
T. N. Tiegs and J. O. Kiggans 1991 7 p Presented at the 4th International Symposium on Ceramic Materials and Components for Engines, Goeteborg, Sweden, 10-12 Jun. 1991
(Contract DE-AC05-84OR-21400)
(DE91-015312; CONF-910617-3) Avail: NTIS HC/MF A02

Microwave processing of silicon nitride-based ceramics is currently being examined to identify aspects that may accelerate densification or produce unique microstructures. Because the microwaves preferentially couple with the sintering additives and the intergranular phases, relatively high additive contents are required to produce samples that will densify and are crack-free. Improved densification of green powder compacts and enhanced weight losses are observed during microwave heating. DOE

N91-29374# Oak Ridge National Lab., TN.
FUNDAMENTAL STUDIES OF CHEMICAL VAPOR DEPOSITION DIAMOND GROWTH PROCESSES
R. W. Shaw, W. B. Whitten, J. M. Ramsey, and L. Heatherly 1991 5 p Presented at the Society of Photo-Optical Instrumentation Engineers (SPIE) Meeting, San Diego, CA, 21-26 Jul. 1991
(Contract DE-AC05-84OR-21400)
(DE91-015324; CONF-9107115-10) Avail: NTIS HC/MF A01

We are developing laser spectroscopic techniques to foster a fundamental understanding of diamond film growth by hot filament chemical vapor deposition (CVD). Several spectroscopic techniques are under investigation to identify intermediate species present in the bulk reactor volume, the thin active volume immediately above the growing film, and the actual growing surface. Such a comprehensive examination of the overall deposition process is necessary because a combination of gas phase and surface chemistry is probably operating. Resonantly enhanced multiphoton ionization (REMPI) techniques have been emphasized. A growth rector that permits through-the-substrate gas sampling for REMPI/time of flight mass spectroscopy has been developed. DOE

N91-29375# Argonne National Lab., IL.
THE 3-D NMR IMAGING: A CHEMICAL MICROSCOPE FOR ANALYSIS OF HETEROGENEOUS MACROMOLECULAR NETWORKS
D. C. French, S. L. Dieckman, N. Gopalsami, and R. E. Botto 1991 8 p Presented at the 1991 Nondestructive Evaluation Subcommittee Meeting, Kennedy Space Center, FL, 13-16 May 1991
(Contract W-31-109-eng-38)
(DE91-015109; ANL/CP-73537; CONF-9105227-1) Avail: NTIS HC/MF A02

A new three-dimensional (3-D) nuclear magnetic resonance (NMR) imaging technique is presented for spatially mapping proton distributions in heterogeneous organic macromolecular networks and solvent treated samples. The technique is based on a 3-D back projection protocol for data acquisition, and a reconstruction technique based on 3-D Radon transform inversion. In principle, the 3-D methodology provides higher spatial resolution of solid materials than is possible with conventional slice selection protocols. The applicability of 3-D NMR imaging was demonstrated by mapping heterogeneous phases in a polymer sample and the distribution of mobile phases in a specimen imbibed with deuterated pyridine. DOE

N91-29376# Pacific Northwest Lab., Richland, WA.
ADVANCES IN THE DRAINED SHAPING OF CERAMICS
C. H. Schilling, W. H. Shih, and I. A. Aksay (Washington Univ., Seattle.) Jun. 1991 15 p Presented at the 4th International Conference on Ceramic Powder Processing Science, Nagoya (Japan), 12-15 Mar. 1991
(Contract DE-AC06-76RL-01830)
(DE91-015429; PNL-SA-19754; CONF-910397-1) Avail: NTIS HC/MF A03

Drained and undrained shaping are standard designations adapted from the soil mechanics field to classify differences in plastic behavior that arise in saturated granular media from changes in the pore liquid pressure. Packing density gradients that occur during drained shaping (e.g., slip casting, pressure filtration) primarily depend on two factors: spatial variations of effective stress inherent in the shaping process and surface chemistry variations that control yield behavior through particle surface forces. Radiography analysis during pressure filtration of flocculated alumina reveals that significant density gradients are caused by the collapse of the particle network against the model surface. This collapse results in the consolidation of a low permeability layer that restricts the casting rate. The evolution of the cake structure is explained by reviewing basic relationships between the dissipation of pore pressure and the resulting nonuniform accumulation of effective stress. We then show that shape forming by expression eliminates density gradients by altering the profile of the effective stress. We also review key aspects of drained compressibility behavior with an emphasis on studies elucidating the role of particle surface forces on micromechanisms of rearrangement. DOE

N91-29377# Pacific Northwest Lab., Richland, WA.
THE 0-G EXPERIMENTS WITH ADVANCED CERAMIC FABRIC WICK STRUCTURES
Z. I. Antoniak, B. J. Webb, J. M. Bates, M. F. Cooper, and K. A. Pauley Jul. 1991 17 p Presented at the ASME/AIChE/ANS National Heat Transfer Conference, Minneapolis, MN, 26-31 Jul. 1991
(Contract DE-AC06-76RL-01830)
(DE91-015531; PNL-SA-18880; CONF-910739-26) Avail: NTIS HC/MF A03

Both Air Force and NASA future spacecraft thermal management needs span the temperature range from cryogenic to liquid metals. Many of these needs are changing and not well defined and will remain so until goals, technology, and missions converge. Nevertheless, it is certain that high-temperature (less than 800 K) and medium-temperature (about 450 K) radiator systems will have to be developed that offer significant improvements over current designs. This paper discusses experiments performed in the lower temperature regime as part of a comprehensive advanced ceramic fabric (ACF) heat pipe development program. These experiments encompassed wicking tests with various ceramic fabric samples, and heat transfer tests with a 1-m long prototype ACF water heat pipe. A prototype ceramic fabric/titanium water heat pipe has been constructed and tested; it transported up to 60 W of power at about 390 K. Startup and operation both with and against gravity examined. Wick testing was begun to aid in the design and construction of an improved prototype heat pipe, with a 38 micron stainless steel linear covered by a biaxially-braided Nextel (trademark of the 3M Co., St. Paul, Minnesota) sleeve that is approximately 300 microns thick. Wick testing took place in 1-g; limited testing in 0-g was initiated, and results to date suggest that in 0-g, wick performance improves over that in 1-g. DOE

N91-29378# Argonne National Lab., IL.
MATERIALS RESEARCH FOR SODIUM ENGINE DEVELOPMENT
D. S. Kupperman, S. Majumdar, J. S. Gregar, J. P. Singh, S. Doris, N. Gopalsami, S. Dieckman, and A. C. Raptis Mar. 1991 36 p Presented at the 26th Intersociety Energy Conversion Engineering (IECE) Conference, Boston, MA, 3-9 Aug. 1991
(Contract W-31-109-eng-38)
(DE91-015715; ANL/CP-73108; CONF-910801-10) Avail: NTIS HC/MF A03

Experience has shown that the major reason for failure of the sodium heat engine (SHE) is breakage of the beta (double prime)-Al2O3 electrolytes (BASE). The life-limiting flaws in BASE tubes are generally found to be large grains and voids. These flaws are thought to originate from inhomogeneities and impurities in the beta (double prime)-Al2O3 powder. As a result of mechanical failures the issue of beta(double prime)-alumina solid electrolyte (BASE) durability is being addressed. Effective and mechanical and microstructural characterization were carried out. The strengths of rings from tubes from two sources were 175(+ or -)16 MPa, 204(+ or -)14 MPa, 279(+ or -)26 MPa, 238(+ or -)25 MPa for one source and 155(+ or -)34 MPa and 190(+ or -)27 MPa for the other. These values are adequate for operation of the sodium heat engine as estimated by analytical modeling. Anisotropic expansion of grains can create internal stresses even in a specimen that has a homogeneous distribution of neutral sodium. Further, in the Beta(double prime) alumina tubes, there is a gradient of the neutral sodium concentration, i.e., strain, from a maximum at the ID (inner diameter) surface to a minimum at the OD (outer diameter) surface. This strain gradient will lead to additional stresses in the tubes. Results from analytical efforts suggest the maximum tensile stress at the OD surface of tubes can vary from 14 MPa to 30 MPa depending on the sodium distribution. A fracture mechanics analysis indicates that in order to minimize the potential for cracking due to anisotropic expansion and contraction due to neutral sodium uptake and cooldown after sintering, the grain size of the material should be reduced to less than or = to 20 microns. DOE

N91-29379# Sandia National Labs., Albuquerque, NM.
THE CURE OF RIGID POLYURETHANE ENCAPSULATING FOAM
D. Adolf and C. Childress May 1991 25 p
(Contract DE-AC04-76DP-00789)
(DE91-016059; SAND-91-0328) Avail: NTIS HC/MF A03

The disappearance of isocyanate groups in 20 lb/cu ft rigid polyurethane encapsulating foam (44402-20) was monitored by Fourier Transform Infrared (FTIR) spectroscopy leading to an activation energy of 4 kcal/mole. The disappearance of isocyanates can be due to either crosslinking reactions or gas production. Attempting to separate these two reaction paths, we measured the gel time and volume change during cure leading to activation energies of 5 and 6 kcal/mole for the crosslinking and foaming mechanisms respectively. DOE

28 PROPELLANTS AND FUELS

Includes rocket propellants, igniters, and oxidizers; their storage and handling procedures; and aircraft fuels.

For related information see also *07 Aircraft Propulsion and Power, 20 Spacecraft Propulsion and Power,* and *44 Energy Production and Conversion.*

N91-29380# Oak Ridge National Lab., TN.
HYDROGEN PRODUCTIVITY BY PHOTOSYNTHETIC WATER SPLITTING
E. Greenbaum 1990 12 p Presented at the 8th World

Hydrogen Energy Conference, Honolulu, 22-27 Jul. 1990
(Contract DE-AC05-84OR-21400)
(DE90-012211; CONF-900705-4) Avail: NTIS HC/MF A03

This paper reviews recent progress in the field of hydrogen production by photosynthetic water splitting for both in vitro and in vivo systems. Absolute thermodynamic efficiencies of conversion of light energy into energy of molecular hydrogen by intact microalgae have been measured with an original physical measuring technique using a tin-oxide semiconducting gas sensor. Thin films of microalgae comprising 5 to 20 cellular monolayers have been entrapped on filter paper, thereby constraining them in a well-defined circular geometry. Based on absolute light absorption of visible polychromatic illumination in the low-intensity region of the light saturation curve, conversion efficiencies of 6 to 24 percent have been obtained. These values are the highest ever measured for hydrogen evolution by green algae. DOE

N91-29381# Georgia Inst. of Tech., Atlanta. School of Aerospace Engineering.

INVESTIGATION OF THE COMBUSTION OF LIQUID FUELS IN RIJKE TYPE PULSE COMBUSTORS

B. T. Zinn, B. R. Daniel, and T. Bai 1990 7 p
(Contract DE-AS04-85AL-31881)
(DE90-012490; DOE/AL-31881/T2) Avail: NTIS HC/MF A02

The synopsis summarizes the accomplishments of DOE Contract NO. AS04-85AL31881, which investigated the combustion of different liquid fuels in Rijke type pulse combustors. Interest in the development of a Rijke pulse combustor capable of burning liquid fuels was stimulated by earlier studies by the investigators of this program which had demonstrated that various coals can be burned efficiently and with low pollutant emissions in Rijke type pulse combustors. This research program consisted of three tasks. Task A was concerned with the development of a Rijke pulse combustor design capable of burning different liquid fuels, and determination of the performances of uninsulated and insulated versions of the developed Rijke pulse combustor when burning different liquid fuels under different operating conditions. Task B was concerned with the elucidation of the mechanisms responsible for driving the pulsations in the developed combustors, and Task C was concerned with the determination of the dependence of the combustor performance upon the amplitude of pulsations. The results of these studies are briefly discussed. DOE

N91-29382# EG and G Mound Applied Technologies, Miamisburg, OH.

FEASIBILITY OF A LASER-IGNITED HMX DEFLAGRATION-TO-DETONATION TRANSITION DEVICE FOR THE US NAVY LITES PROGRAM

D. W. Ewick, T. M. Beckman, and D. P. Kramer 18 Jun. 1991 20 p
(Contract DE-AC04-88DP-43495)
(DE91-015210; MLM-3691) Avail: NTIS HC/MF A03

Laser-ignited deflagration-to-detonation transition (DDT) devices using the secondary explosive HMX were fabricated and tested for application in the U.S. Navy's Laser-Initiated Transfer Energy Subsystem (LITES). A high density (1.55 g/cu cm) blend of 7460 sq cm/g HMX with 3 percent carbon black by weight was used for the ignition charge. Deflagration-to-detonation transition was achieved with transition charges of undoped 7460 sq cm/g HMX at densities of 1.0 and 1.2 g/cu cm. Thin (0.25 mm) Ti-6Al-4V confinement plates were found to drive the reaction to detonation more efficiently than thicker (0.75 mm) 6061-T6 aluminum confinement plates, which have a similar shear strength. Using a 10-ms laser diode pulse coupled to the test device via a 100-microns diameter optical fiber, the ignition threshold was determined to be approximately 1.3 mJ. Hermetic optical window devices were also built and tested. Ignition of the HMX/carbon black blend using a laser diode was achieved through optical windows up to 0.97 mm thick. Finally, several successful tests were conducted using the LITES Nd:glass laser to fire the devices. Test results demonstrated the feasibility of using a laser-ignited all-HMX deflagration-to-detonation transition detonator for the LITES program. DOE

N91-29383# Ballistic Research Labs., Aberdeen Proving Ground, MD.

REPORT ON USING EXPERT SYSTEMS FOR COMPUTER-AIDED FORMULATION AND PROPERTY ESTIMATION OF PROPELLANTS. 1: EXPERT SYSTEM SHELL SELECTION AND INITIAL PACKAGE DESIGN Final Report, Oct. 1989 - Sep. 1990

Jeffrey B. Morris and Robert A. Fifer Jun. 1991 63 p
(AD-A237567; BRL-TR-3239) Avail: NTIS HC/MF A04 CSCL 12/5

An expert system based computer assisted design (CAD) package for propellant formulation design was created for use on an Intel 80286/80386-based workstation (PC). This CAD package is intended for use by propellant formulators as a tool to aid in the design of, and properties estimation for, new rocket and gun propellants. A backward-chaining expert system shell (Level 5), dBase III-compatible databases, and a PC version of the NASA-Lewis thermochemical code CET89 are linked together into one package. Properties estimation is accomplished via the use of both the expert system shell and the CET89 code; the thermochemical code options RKT=T (rocket calculation) and UV=T (constant volume) are supported. The initial version of this expert system was implemented for a propellant formulation consisting of three ingredients (binder, plasticizer, and energetic material). Current research efforts are going into the design of a more comprehensive package for use with up to 21 propellant ingredients. GRA

N91-29384# Ballistic Research Labs., Aberdeen Proving Ground, MD.

EXPERIMENTAL HYPERVELOCITY FIRINGS USING STICK AND GRANULAR PROPELLANT CONFIGURATIONS Final Report, Jan. - Dec. 1989

Carl R. Ruth, Frederick W. Robbins, and Albert W. Horst Jun. 1991 44 p
(DA Proj. 1L1-61102-AH-43)
(AD-A238628; BRL-MR-3921) Avail: NTIS HC/MF A03 CSCL 19/1

The suitability of lumped-parameter interior ballistic models for prediction of the interior ballistic performance of very high velocity guns is limited by use of a predetermined pressure gradient which is superimposed on the solution to approximate the relationship between space-mean, breech and projectile base pressures. Even modern two-phase flow interior ballistic models, specifically formulated to address the hydrodynamics of the problem, have not been extensively exercised in this regime. Only recently have limited, large-caliber gun firings with realistic projectile masses been conducted to provide required data in this velocity regime. In this study, firings were conducted in a long 120-mm gun at propellant charge to projectile mass ratios (C/M) of about 3 to 6, yielding muzzle velocities in the 2 to 2.7 km/s range. The tube was instrumented with pressure gages at various locations along its length to provide data for comparison to predictions of various interior ballistic codes. GRA

N91-29385# Environmental Protection Agency, Research Triangle Park, NC. Atmospheric Research and Exposure Assessment Lab.

OVERVIEW OF THE TECHNICAL IMPLICATIONS OF METHANOL AND ETHANOL AS HIGHWAY MOTOR VEHICLE FUELS

F. M. Black 1991 32 p
(PB91-182881; EPA/600/D-91/076) Avail: NTIS HC/MF A03 CSCL 21D

The characteristics of methanol and ethanol as highway motor vehicle fuels are contrasted with those of conventional gasolines and diesel fuels. The implications of the physical and chemical differences of these fuels for motor vehicle design and emissions are discussed. Potential material compatibility concerns, such as elastomer swelling and metal corrosion, and safety concerns, such as fire hazard, flame luminosity, and human toxicity are examined. A number of possible air quality impacts are examined including changes in ozone, carbon monoxide, oxides of nitrogen, particulate

matter, toxic compounds (benzene, aldehydes, and 1,3- butadiene), and global climate 'greenhouse' gases (carbon dioxide, methane, and nitrous oxide). Author

N91-29386# Sandia National Labs., Albuquerque, NM.
DEVELOPMENT OF AN EXPLOSIVE VAPOR GENERATOR
D. Ingersoll and P. J. Rodacy 1991 9 p Presented at the 32nd Institute of Nuclear Materials Management (INMM) Annual Meeting, New Orleans, LA, 28-31 Jul. 1991
(Contract DE-AC04-76DP-00789)
(DE91-015700; SAND-91-1589C; CONF-910774-15) Avail: NTIS HC/MF A02

In order to critically evaluate explosive vapor detection systems, a calibrated explosive vapor source is required. A prototype source was developed and built, and it is currently being evaluated. This source was designed to be portable. The weight of the main unit is less than 20 pounds, and its size is comparable to a small briefcase. The design allows for easy interchange of explosive vapor sources. This prototype source is currently being evaluated for the generation of calibrated gas streams containing NG, EGDN, and TNT. The design and operational characteristics of the prototype unit is described. The possibility of extending this technology to other explosives is also described. DOE

N91-29387# Lawrence Livermore National Lab., CA.
THE EFFECTS OF HMX PARTICLE SIZE AND BINDER STIFFNESS ON THE BURNING MECHANISM AND REGRESSION RATE OF A SERIES OF FAST BURNING PROPELLANTS
W. C. Tao, M. S. Costantino, D. L. Ornellas, L. G. Green, and E. S. Jessop 3 Jun. 1991 13 p Presented at the 27th JANNAF Combustion Meeting, Cheyenne, WY, 5-9 Nov. 1990
(Contract W-7405-eng-48)
(DE91-015785; UCRL-JC-104515; CONF-9011119-4) Avail: NTIS HC/MF A03

The combustion behavior and average surface-regression rate of four low vulnerability explosives (LOVEX) formulation, RX-35-BG, -BH,-BI, and -BJ, are investigated to pressures to one GPa. In these propellant-type formulations, we vary the initial particle-size distribution of the HMX and the binder/plasticizer ratio, while maintaining the same HMX solids loading, binder/plasticizer type, and method of formulation. Nitroglycerin/Triacetin (75/25) and polyethylene glycol (PEG) are used as the energetic plasticizer and polymeric binder, respectively. The HMX solids loading in each formulation is 60 wt. percent, consisting of a narrow particle size distribution of 6-8 microns for RX-35-BG and -BI, and LX-04 grade HMX (a bimodal distribution with a 60/6 micron median particle sizes) for RX-35-BH and -BJ. Within each pair of formulations with the same HMX particle size, we varied the ratio of the NG/TA plasticizer to the PEG polymeric binder such that the mechanical properties ranged from rubbery to very stiff. In general, the regression rates for the larger particle size formulations are 20 to 50 percent faster than those for the 6 micron formulations. Comparing formulations in which the HMX particle size was kept constant, we observed that the formulation with the more compressible (and more energetic) binder burned faster than that with the stiff binder. Up to 950 MPa and independent of the initial confinement pressure, all of the formulations exhibited a planar burning mechanism with the regression rates obeying the classical aP(sup n) formalism. Comparison of the pressure-time and wire reporting-time curves indicates that there is no significant entrainment of still-burning condensed phase in the region behind the flame front. DOE

29 MATERIALS PROCESSING

Includes space-based development of products and processes for commercial applications.
For biological materials see *55 Space Biology*.

N91-29388# National Aeronautical Establishment, Ottawa (Ontario).
BUBBLE GENERATION AND MOVEMENT UNDER MICROGRAVITY CONDITIONS
John Aitken 7 Mar. 1990 102 p
(NAE-LTR-FR-110; CTN-91-60022) Copyright Avail: NTIS HC/MF A06

The NAE T-33 C-FSKH was used to provide several short periods of microgravity conditions for an experiment designed to permit comparison of actual and mathematical predictions of air bubble formation and motion in a liquid under low gravity conditions. During the five flight experiment, a total of 55 microgravity parabolas, each averaging 20 to 25 seconds long, were flown. The NAE T-33 C-FSKH proved to be a useful platform for producing short periods of near zero gravity for this series of experiments. Although varying from run to run, the 20 to 25 second periods provided vertical G values in the +/- 0.02 to 0.05 G range, longitudinal G on the order of +/- 0.02 G and lateral G between +/- 0.01 to 0.02 G. Constant ammeter readings observed during the tests indicated that the current output of the magnetohydrodynamic pump constant current source was unaffected by electrolysis bubble buildup. Very small bubbles were relatively unaffected by the +/- 0.02 to 0.05 vertical and +/- 0.02 longitudinal G, whereas during runs under similar G loadings the movements of larger bubbles showed definite buoyancy effects. The effects of off zero longtudinal G can be seen in the path plots of individual bubbles. Similar effects due to off zero vertical G were more difficult to visualize from the plots. The results of comparisons with mathematical predictions are not included in the report. CISTI

31 ENGINEERING (GENERAL)

Includes vacuum technology; control engineering; display engineering; cryogenics; and fire prevention.

N91-29389# Stevens Inst. of Tech., Hoboken, NJ.
INJECTION MOLDING OF ENGINEERING PLASTICS Final Report, 1986 - 1991
Dilhan M. Kalyon 1 Mar. 1991 14 p
(Contract DAAL03-86-G-0048)
(AD-A238583; ARO-23810.7-MS) Avail: NTIS HC/MF A03
CSCL 11/9

This final report summarizes the findings of a study in injection molding of engineering plastics. Two engineering plastic resins, i.e., unmodified grades of a polyetherimide and a poly (2,6-dimethyl-1,4-phenylene ether) were thoroughly characterized. The characterization included rheology, thermal properties and P-V-T behavior. The data were employed to predict various microstructural distributions including density, residual stress and birefringence distributions in compression and injection molded specimens of these two engineering plastics. The detailed microstructural distributions were also studied experimentally upon processing the two engineering plastics, employing instrumented machines and industrial practices. The experimental findings were elucidated under the light of the numerical simulation results. Overall, this study should furnish a first order understanding of the microstructure development in articles injection molded from amorphous engineering plastic resins. GRA

N91-29390*# Clemson Univ., SC. Dept. of Mechanical Engineering.
AN INVESTIGATION TO DETERMINE THE PRODUCIBILITY OF A 3-D BRAIDER AND BIAS DIRECTION WEAVING LOOM Final Report
Cecil O. Huey, Jr. Sep. 1991 269 p Original contains color illustrations

(Contract NCC1-128)
(NASA-CR-188741; NAS 1.26:188741) Avail: NTIS HC/MF A12; 15 functional color pages CSCL 13H

The development of prototype machines for the production of generalized braid patterns is described. Mechanical operating principles and control strategies are presented for two prototype machines which were fabricated and evaluated. Both machines represent advances over current techniques for forming composite material preforms by enabling near ideal control of fiber orientation. Furthermore, they overcome both the lack of general control of produced fiber architectures and the complexity of other weaving processes that were produced for the same purpose. One prototype, the modified Farley braider, consists of an array of turntables which can be rotated 90 degrees and returned; hence, they can form tracks in the x and y axis. Yarn ends are transported about the surface formed by the turntables using motorized tractors. These tractors are controlled using an optical link with a control circuit and host computer. The tractors are powered through electrical contact with the turntables. The necessary relative motions are produced by a series of linear tractor moves combined with a sequence of turntable rotations. The movement of the tractors about the surface causes the yarns to produce the desired braiding pattern. The second device, the shuttle plate braider, consists of a braiding surface formed by an array of square elements, each separated from its neighbor by a gap. Beneath this surface lies a shuttle plate, which reciprocates first in one axis and then in the other. As this movement takes place, yarn carrying shuttles engage and disengage the plate by means of solenoid activated pins. By selective engagement and disengagement, the shuttles can move the yarn ends in any desired pattern, forming the desired braid. Control power, and control signals, are transmitted from the electronic interface circuit and host computer, via the braiding surface through electrical contact with the shuttles. Motive power is proved to the shuttles by motion of the shuttle plate, which is passively driven using pneumatic rams. Each shuttle is a simple device that uses only a solenoid to engage the plate and is a simple device that uses only a solenoid to engage the plate and is independently controllable. When compared with each other, the modified Farley braider has the advantage of speed, and the shuttle plate braider the advantage of mechanical control and simplicity. Author

N91-29391# National Inst. of Standards and Technology, Gaithersburg, MD.
CONFIGURATION MANAGEMENT CONCEPTS DOCUMENT. NATIONAL PDES TESTBED REPORT SERIES
S. B. Katz Apr. 1991 33 p
(PB91-194480; NISTIR-4538) Avail: NTIS HC/MF A03 CSCL 13B

The purpose is to establish Configuration Management (CM) concepts to be applied in support of the development of the Standard for the Exchange of Product Model Data (STEP). Configuration management is the management of change. It is a formal discipline which provides methods and tools to: identify components, versions and baselines of selected items; and control changes to those items. CM provides a method for logically grouping related components throughout the various stages of product development. It also provides visibility and traceability for the evolving status of each item. An effective CM system thus identifies, controls, records, and reports on any functional, physical or status changes to the controlled items. Author

N91-29392# Argonne National Lab., IL.
MINIMIZATION OF REFRIGERATION POWER REQUIREMENTS FOR MECHANICAL SUPPORTS IN CRYOGENIC SYSTEMS
S. Y. Seol, M. C. Chyu (Texas Technological Univ., Lubbock.), T. M. Kuzay, and J. R. Hull 1991 7 p Presented at the 26th Intersociety Energy Conversion Engineering (IECE) Conference, Boston, MA, 3-9 Aug. 1991
(Contract W-31-109-eng-38)
(DE91-015720; ANL/CP-73209; CONF-910801-12) Avail: NTIS HC/MF A02

A solution scheme is presented for minimization of refrigeration power required for mechanical supports in cryogenic systems where refrigeration shields at intermediate temperatures are installed along the supports. The total refrigeration power requirement is minimized in terms of the temperatures and locations of the shields. The scheme involves the simulations solution of algebraic equations and is simpler than previous methods. Closed-form solutions for optimal shield temperatures and locations are presented for several specific cases of engineering interest. DOE

N91-29393# Allied-Signal Aerospace Co., Kansas City, MO.
LIQUID HONING EVALUATION
J. T. Slanina Jul. 1991 74 p
(Contract DE-AC04-76DP-00613)
(DE91-015749; KCP-613-4394) Avail: NTIS HC/MF A04

The conveyorized wetblast machine was characterized for epoxy/glass and polyimide/glass multilayers using a 12-run Plackett-Burman screening experiment and a four-variable factorial experiment. Test panels were processed using slurry and water mixtures and water only. Plated-through-holes were evaluated after wetblasting and copper plating for plating characteristics. Test panels were wetblasted and processed through photolithography operations. Photoresist adhesion characteristics were evaluated. As a result, the optimum production conditions were determined for slurry concentration, blast pressure, oscillator speed, conveyor speed, and blast gun distance. DOE

32 COMMUNICATIONS AND RADAR

Includes radar; land and global communications; communications theory; and optical communications.

For related information see also *04 Aircraft Communications and Navigation* and *17 Space Communications, Spacecraft Communications, Command and Tracking.* For search and rescue see *03 Air Transportation and Safety,* and *16 Space Transportation.*

N91-29394# National Aeronautical Establishment, Ottawa (Ontario). Flight Research Lab.
DISTANCE MEASURES FOR SPEECH RECOGNITION
M. J. Hunt and C. Lefebvre Mar. 1989 37 p Sponsored in part by Department of National Defence
(NAE-AN-57; NRC-30144; CTN-91-60008) Copyright Avail: NTIS HC/MF A03

The application is examined of aspects of statistical pattern classification to speech recognition. An extension is presented of linear discriminant analysis to the case where the classes are unknown. This extension provides solutions to the interrelated problems of the design of acoustic representations and spectral distance measures, and allows the efficient combination of heterogeneous sets of parameters. In particular, a representation called IMELDA based on the output of a filter-bank and its changes in time is introduced. Other approaches to distance measures are discussed. It is noted that these other methods lack the ability to make efficient combinations of heterogeneous parameters, and that they require empirical adjustments in order to give good results. Tests indicate that IMELDA provides markedly superior recognition performance compared to the alternatives. The transformations derived by the technique described are likely to be effective in Hidden Markov Modelling based speech recognition systems as well as those using dynamic programming template matching.
Author (CISTI)

N91-29395# Queens Univ., Kingston (Ontario). Dept. of Electrical Engineering.
THE STUDY OF SPACE COMMUNICATIONS SPREAD SPECTRUM SYSTEMS. PART 1: SAW-BASED JOINT GROUP DEMODULATION OF FREQUENCY SHIFT KEYED AND DIFFERENTIAL PHASE SHIFT KEYED SIGNALS Final Report
Peter T. Traynor and Peter J. McLane 26 Mar. 1990 169 p
(Contract DSS-36001-8-3528/01-SS)
(QU-90-1-Pt-1; CTN-91-60074) Copyright Avail: NTIS HC/MF A08

A surface acoustic wave (SAW) device based processor, capable of the joint group demodulation of frequency shift keying (FSK) and differential phase shift keying (DPSK) signals, and intended for use in the Canadian extremely high frequency (EHF) Satcom system is proposed. The processor is based on the ability of SAW filters to implement wideband, real time, Fourier transforms with an observation interval corresponding to the hop period of the system. The background for such an implementation is given. The SAW-based transforms are simulated using digital Fourier transforms, and a quasi-analytical technique is applied to determine bit error rate performance of both binary and quaternary differential phase shift keying in the presence of narrow band Gaussian noise. Signal parameters such as windowing, carrier separation, user bandwidth allocations, and nonlinear characteristics of the SAW devices are also considered. Based on the results determined, the SAW-based processor is capable of performing group binary DPSK demodulation. The maximum number of DPSK users depends on the time-bandwidth (TB) product of the SAW devices used in the implementation, varying from 3 users for TB=512 to 12 users for TB=2048. It is also shown that binary DPSK consistently out-performs quaternary DPSK for this application.
Author (CISTI)

N91-29396# Queens Univ., Kingston (Ontario). Dept. of Electrical Engineering.
A STUDY OF SPACE COMMUNICATIONS SPREAD-SPECTRUM SYSTEMS, PHASE 5 AND 6. PART 2: CODING AND MODULATION Final Progress Report
P. H. Wittke, M. Schefter, and Y. M. Lam 26 Mar. 1990 55 p
(Contract DSS-36001-8-3528/01-SS)
(QU-90-2-Pt-2; CTN-91-60075) Copyright Avail: NTIS HC/MF A04

Trellis codes are obtained for use with noncoherent M-ary frequency shift keying (FSK) transmission as would be used in a hopped spread spectrum system. These codes give improved performance in additive noise but do not require an increase bandwidth. In the trellis coding, the signal set of uniformly spaced tones is expanded from noncoherently orthogonal M-ary FSK to 2M-ary noncoherent FSK. To avoid significant bandwidth expansion, nonorthogonal tone spacing is permitted. The effects on error performance of tone spacing and of the number of states in the code is investigated. Performance in the presence of noise is analyzed and it is concluded that a coding gain of from 2 to 4 dB can be achieved with a simple 4-state trellis code. The exact gain depends on the choice of signal spacing. In a jamming environment, the coding gains are much more dramatic. New results on the error performance of trellis codes in noise and in partial-band jamming, with noncoherent detection and signal sets that are not orthogonal, are presented. Simulations were carried out which yield performance within a fraction of a dB of that predicted by the theory. A practical self-normalizing decoding metric is shown to give performance very close to that predicted by the idealized jamming bound considerations. There appears to be significant improvement in the 4-state over the 2-state codes, but little improvement is seen in going from 4-state to 8-state codes.
Author (CISTI)

N91-29397# Queens Univ., Kingston (Ontario). Dept. of Electrical Engineering.
THE STUDY OF SPACE COMMUNICATIONS SPREAD SPECTRUM SYSTEMS. PART 3: UPLINK SYNCHRONIZATION IN AN EHF FREQUENCY-HOPPED SATELLITE SYSTEM Final Report
Stanley J. Simmons and Paul Lamers 31 Mar. 1990 87 p
(Contract DSS-36001-8-3528/01-SS)
(QU-90-3-Pt-3; CTN-91-60076) Copyright Avail: NTIS HC/MF A05

The problem of users first attempting to synchronize their M-ary frequency shift keying (FSK) transmissions to the dehopper of a signal processing satellite in a multi-user frequency division multiple access (FDMA) frequency hopped extremely high frequency (EHF) satellite system is considered. Users send uplink sync probe signals and monitor downlink returns on the corresponding data detections at the satellite in order to receive feedback on the state or quality of their alignment. Users adjust their alignments in steps across the initial region of uncertainty. A simple and robust scheme is investigated based on using one of the FSK tones as the sync probe, and comparing its energy to that seen in M(prime) minus 1 other tone bins during each hop (best 1-of-M(prime) detection strategy). This simple scheme is invariant with respect to the (faded) signal levels received at the satellite, is invariant with respect to jammer strategy, and yields a probability of false sync tone detection which is also independent of jammer strategy or power. Strategies for detection of coarse sync acquisition are explored, beginning with a simple serial sweep, and ending with a multiple pass adaptive search scheme. Multi-tone jamming at signal to jamming ratio (SJR)=0 dB (and higher) with background noise is considered. It is shown that coarse sync (correct alignment to within a fraction of a hop period) can be quickly established (average time to acquisition on the order of 0.5 to 2 seconds) for all but the very highest jammer powers (larger by almost the full processing gain). Author (CISTI)

N91-29398# Victoria Univ. (British Columbia). Dept. of Electrical and Computer Engineering.
CODING FOR FREQUENCY HOPPED SPREAD SPECTRUM SATELLITE COMMUNICATIONS Final Report, 13 Oct. 1988 - 31 Mar. 1989
V. K. Bhargava, Ian F. Blake (Waterloo Univ., Ontario), T. A. Gulliver, G. Li, Q. Wang, and B. Weeks 15 Apr. 1990 112 p
(Contract DSS-36001-8-3529/01-SS)
(ECE-89-1; CTN-91-60078) Copyright Avail: NTIS HC/MF A06

Work on improving jamming resistance of satellite communications using slow frequency hopping systems are presented. A modified self normalizing combiner is presented and its performance is analyzed under partial band jamming. This is compared with other nonlinear combining schemes including adaptive gain control combining, product combining, and clipping combining. The throughput performance of a coded fast frequency hopped M-ary frequency shift keying (FFH/MFSK) system with a fixed hop rate is evaluated using the cutoff rate argument. The analysis derives upper bounds for the gains which can be realized using coding for various system parameters. As a prelude to the study of coding for slow frequency hopped differential phase shift keying (SFH/DPSK), the effects of jamming without coding are analyzed. The main result is the derivation of the probability distribution of DPSK in tone interference with applications to SFH/DPSK. The choice of the best DPSK scheme, and decision regions, is dependent on the relative strength of the noise and tone jamming. A comparison of two powerful DSP integrated circuit processors for implementation of a four error correcting BCH code decoder is presented. CISTI

N91-29399 Department of the Army, Washington, DC.
RANGE-ONLY MULTISTATIC RADAR SYSTEM Patent
D. M. Montana, inventor (to Air Force) and R. S. Herd, inventor (to Air Force) 6 Oct. 1985 1 p Filed 21 Apr. 1982 Supersedes AD-D011201
(AD-D011645; US-Patent-4,499-468; US-Patent-Appl-SN-370234; US-Patent-Class-343-15) Avail: US Patent and Trademark Office

A range-only multistatic radar system has a plurality of radar stations located in a square grid pattern. Each radar station has a plurality of low power pulsed transmitters and receivers that operate on omnidirection whip antennas. Echo information received by the receivers is transmitted to a computer wherein a technique is employed to deghost and identify real targets. The computer applies a range difference similarity test, a uniqueness test, and a position test to determine real targets from the plurality of echo returns received. Author

N91-29400# Department of the Navy, Washington, DC.
HARDWARE INTERFACE FOR HIGH SPEED VIDEO IMAGING Patent Application
David Sass, inventor (to Navy) and Steven Shepard, inventor (to

Navy) 28 Mar. 1991 33 p
(AD-D014902; US-Patent-Appl-SN-676669) Avail: NTIS HC/MF A03 CSCL 25/5

The invention is synchronization hardware for assisting the processing of video signals in a high speed imaging system. The hardware has logic circuitry for selecting acceptable pictorial units from within frames of a video signal. The synchronization hardware also has circuits for electronically coordinating a camera, a frame grabber, a host compugrabber, a host computer for the frame grabber, and a flagging signal generator. Author (GRA)

N91-29401# Oak Ridge National Lab., TN.
IMPACTS OF A NOMINAL NUCLEAR ELECTROMAGNETIC PULSE ON ELECTRIC POWER SYSTEMS
V. J. Kruse, D. L. Nickel, J. J. Bonk, and E. R. Taylor, Jr. Apr. 1991 92 p
(Contract DE-AC05-84OR-21400)
(DE91-012991; ORNL/Sub-83-43374/2) Avail: NTIS HC/MF A05

A high-altitude nuclear detonation several hundred kilometers above the central United States will subject much of the nation to an electromagnetic pulse (EMP) consisting of intense steep-front short-duration transient electromagnetic fields followed by a geomagnetic disturbance with a duration of tens of seconds. Since 1983, the Department of Energy has been actively pursuing a research program to assess the potential impacts of one or more EMP events on the nation's electric energy supply. A nominal EMP environmental suitable for assessing geographically large systems has been used to provide an indication of EMP impacts on electric power systems. It was found that a single high-altitude burst, which significantly disturbs the geomagnetic field, could cause significant load and generation loss, but permanent damage would be isolated. Multiple bursts would increase the disturbance. Nevertheless, based on the effects of a nominal EMP environment, a long-term blackout is not expected since major components such as power transformers are not likely to be damaged. DOE

N91-29402# Sandia National Labs., Albuquerque, NM.
A DIHEDRAL CORNER REFLECTOR MODEL FOR FULL POLARIZATION CALIBRATION OF RCS MEASUREMENTS
K. W. Sorensen 1991 14 p Presented at the 1991 Institute of Electrical and Electronics Engineers (IEEE) AP-S Symposium, Ontario (Canada), 24-28 Jun. 1991
(Contract DE-AC04-76DP-00789)
(DE91-013572; SAND-90-3125C; CONF-9106118-4) Avail: NTIS HC/MF A03

While the backscattered field as a function of angular incidence of a plane wave for dihedral corner reflectors having right, acute, and obtuse angles has been studied extensively, it has generally been stated that the RCS of a 90(degree) dihedral corner reflector oriented for maximum backscattered return to a radar is given by the expression (sigma) = 8(pi)a(sup 2)b(sup 2)/(lambda)(sup 2). The intent of this paper is to present experimental results which demonstrate that not only does the RCS of a dihedral corner reflector oriented for maximum backscattered return differ significantly from this value, but that high range resolution measurements of the dihedral can serve to identify the dominant contributors to the backscattered field. Further, inclusion of these backscattered components in an analytical calculation will allow an accurate calibration model to be generated. DOE

N91-29403# Grumman Aerospace Corp., Princeton, NJ. Corporate Research Center.
ICRF EDGE MODELING
23 May 1991 20 p
(Contract DE-FG02-86ER-53236)
(DE91-014401; DOE/ER-53236/11) Avail: NTIS HC/MF A03

This report describes the technical progress for the DOE sponsored ICRF edge modeling grant. An emphasis is placed on the progress since the Technical Progress Report (January 10, 1990) was submitted to the Department of Energy. The design of ICRF antennas for C-Mod and TFTR was investigated during this period. In addition, quasilinear models for electron heating were refined and applied to the design of ICRF antennas. The relevant professional activities sponsored by this grant are given. DOE

N91-29404*# National Aeronautics and Space Administration. Lewis Research Center, Cleveland, OH.
COMBINATORIAL FSK MODULATION FOR POWER-EFFICIENT HIGH-RATE COMMUNICATIONS
Paul K. Wagner, James M. Budinger, and Mark J. Vanderaar (Sverdrup Technology, Inc., Brook Park, OH.) 1991 10 p Presented at the Conference on Advanced Space Exploration Initiative Technologies, Cleveland, OH, 4-6 Sep. 1991; cosponsored by AIAA and OAI
(Contract NAS3-25266)
(NASA-TM-105188; E-6490; NAS 1.15:105188; AIAA-91-3532)
Avail: NTIS HC/MF A02 CSCL 17B

Deep-space and satellite communications systems must be capable of conveying high-rate data accurately with low transmitter power, often through dispersive channels. A class of noncoherent Combinatorial Frequency Shift Keying (CFSK) modulation schemes is investigated which address these needs. The bit error rate performance of this class of modulation formats is analyzed and compared to the more traditional modulation types. Candidate modulator, demodulator, and digital signal processing (DSP) hardware structures are examined in detail. System-level issues are also discussed. Author

N91-29405*# National Aeronautics and Space Administration. Lewis Research Center, Cleveland, OH.
QUATERNARY PULSE POSITION MODULATION ELECTRONICS FOR FREE-SPACE LASER COMMUNICATIONS
J. M. Budinger, S. D. Kerslake, L. A. Nagy, M. J. Shalkhauser, N. J. Soni, M. A. Cauley, J. H. Mohamed, J. B. Stover, R. R. Romanofsky, and P. J. Lizanich (Analex Corp., Brook Park, OH.) et al 1991 21 p Presented at the Conference on Advanced Space Exploration Initiative Technologies, Cleveland, OH, 4-6 Sep. 1991; cosponsored by AIAA and OAI
(NASA-TM-104502; E-6362; NAS 1.15:104502; AIAA-91-3471)
Avail: NTIS HC/MF A03 CSCL 17B

The development of a high data-rate communications electronic subsystem for future application in free-space, direct-detection laser communications is described. The dual channel subsystem uses quaternary pulse position modulation (QPPM) and operates at a throughput of 650 megabits per second. Transmitting functions described include source data multiplexing, channel data multiplexing, and QPPM symbol encoding. Implementation of a prototype version in discrete gallium arsenide logic, radiofrequency components, and microstrip circuitry is presented. Author

N91-29406# Sandia National Labs., Albuquerque, NM.
COMPARISON OF SYNTHETIC APERTURE RADAR AUTOFOCUS TECHNIQUES: PHASE GRADIENT VS SUBAPERTURE
T. M. Calloway, C. V. Jakowatz, Jr., P. A. Thompson, and P. H. Eichel 1991 12 p Presented at the Society of Photo-Optical Instrumentation Engineers (SPIE) Meeting, San Diego, 21-26 Jul. 1991
(Contract DE-AC04-76DP-00789)
(DE91-014696; SAND-91-0057C; CONF-9107115-5) Avail: NTIS HC/MF A03

Two methods of focusing synthetic aperture radar (SAR) images are compared. Both a conventional subaperture cross-correlation method and a new phase gradient autofocus (PGA) algorithm developed at Sandia National Laboratories are shown to perform well if high-order phase errors are not present. With the introduction of significant high-order phase errors (e.g., due to uncompensated platform motion), both algorithms suffer a loss in performance. However, relative performance degradation is less for PGA than for the subaperture focusing technique. An explanation is presented for the observed behavior of the two autofocus techniques. DOE

N91-29407# Fermi National Accelerator Lab., Batavia, IL.
CONFORMAL FDTD MODELING WAKE FIELDS
T. Jurgens and F. Harfoush May 1991 4 p Presented at the 1991 Institute of Electrical and Electronics Engineers (IEEE) Particle Accelerator Conference (PAC), San Francisco, CA, 6-9 May 1991
(Contract DE-AC02-76CH-03000)
(DE91-015129; FNAL/C-91/145; CONF-910505-359) Avail: NTIS HC/MF A01

Many computer codes have been written to model wake fields. The use is described of the Conformal Finite Difference Time Domain (CFDTD) method to model the wake fields generated by a rigid beam traveling through various accelerating structures. The noncylindrical symmetry of some of the problems considered here requires the use of a three dimensional code. In traditional FDTD codes, curved surfaces are approximated by rectangular steps. The errors introduced in wake field calculations by such an approximation can be reduced by increasing the mesh size, therefore increasing the cost of computing. Another approach, validated here, deforms Ampere and Faraday contours near a media interface so as to conform to the interface. These improvements of the FDTD method result in better accuracy of the fields at asymptotically no computational cost. This method is also capable of modeling thin wires as found in beam profile monitors, and slots and cracks as found in resistive wall motions. DOE

N91-29408# Fermi National Accelerator Lab., Batavia, IL.
VISUALIZATION OF WAKE FIELDS
F. Harfoush and T. Jurgens May 1991 4 p Presented at the 1991 Institute of Electrical and Electronics Engineers (IEEE) Particle Accelerator Conference (PAC), San Francisco, 6-9 May 1991
(Contract DE-AC02-76CH-03000)
(DE91-015130; FNAL/C-91/144; CONF-910505-360) Avail: NTIS HC/MF A01

Rapid advancements in computing capability, such as supercomputers, are enabling scientists and engineers to use numerical modeling tools to analyze large scale problems of volumetric complexity never considered before, and which are impossible to solve analytically. The Finite Difference Time Domain method (FDTD) is widely used to model different electromagnetic interaction problems. The large amount of information obtained from 3-D simulations makes global data analysis difficult. Visualization allows this analysis to be done in a more efficient manner. This technique is implemented here, using the FDTD code. For this purpose, a short video was generated to observe the 3-D time evolution of the wake fields, as a beam travelling in a cylindrical pipe encounters two structures: a cylindrically shaped pillbox cavity with and without parallel flat plates. DOE

N91-29409# Sandia National Labs., Albuquerque, NM.
VERY LOW BIT RATE VOICE FOR PACKETIZED MOBILE APPLICATIONS
C. D. Knittle and K. T. Malone 1991 7 p Presented at the 32nd Institute of Nuclear Materials Management (INMM) Annual Meeting, New Orleans, LA, 28-31 Jul. 1991
(Contract DE-AC04-76DP-00789)
(DE91-015333; SAND-91-1565C; CONF-910774-4) Avail: NTIS HC/MF A02

Transmitting digital voice via packetized mobile communications systems that employ relatively short packet lengths and narrow bandwidths often necessitates very low bit rate coding of the voice data. Sandia National Laboratories is currently developing an efficient voice coding system operating at 800 bits per second (bps). The coding scheme is a modified version of the 2400 bps NSA LPC-10e standard. The most significant modification to the LPC-10e scheme is the vector quantization of the line spectrum frequencies associated with the synthesis filters. An outline of a hardware implementation for the 800 bps coder is presented. The speech quality of the coder is generally good, although speaker recognition is not possible. Further research is being conducted to reduce the memory requirements and complexity of the vector quantizer, and to increase the quality of the reconstructed speech. DOE

N91-29410# Superconducting Super Collider Lab., Dallas, TX.
SLIDING MODE CONTROLLER OF RF CAVITY TUNING LOOP
L. K. Mestha and K. S. Yeung (Texas Univ., Arlington.) May 1991 4 p Presented at the 1991 Institute of Electrical and Electronics Engineers (IEEE) Particle Accelerator Conference (PAC), San Francisco, CA, 6-9 May 1991
(Contract DE-AC02-89ER-40486)
(DE91-015461; SSCL-452; CONF-910505-383) Avail: NTIS HC/MF A01

Ferrite tuned cavities must operate under a wide range of accelerating frequencies. The tuning is done by modulating the current in the coil surrounding the ferrite. Feedback controllers are used to improve the tuning condition by sensing the phase error. The design of controllers currently in use is based on classical frequency domain techniques. Classical controllers in this application are sensitive to variations in the tuning system parameters. Also, these controllers generally fail to provide correct transient response when there is beam in the cavity, since the beam loading changes the transfer function of the system. We have designed a robust and adaptive controller based on sliding mode techniques for a cavity tuning system on the ISIS synchrotron. The techniques are extendable to other systems. DOE

N91-29411# Rockwell International Corp., Anaheim, CA.
MULTI-SENSOR FEATURE LEVEL FUSION Final Report
22 May 1991 15 p
(Contract DAAB07-88-C-F205)
(AD-A237106) Avail: NTIS HC/MF A03 CSCL 17/9

The Multi-Sensor Feature Level Fusion (MSFLF) program is intended to improve automatic target recognition (ATR) performance by the use of multi-sensor feature techniques. MSFLF algorithms are evaluated using multi-sensor (8-12m FLIR, 94GHz MMW radar and 10.6 micron CO2 laser radar) data and imagery. This report gives the results of target detection and identification using the MSFLF training IR imagery. A set of image quality measures are defined and computed over the imagery. These quality measures suggest that performance should be better for the training imagery than for the test imagery. An overview of the FLIR and MMW radar algorithms, detailed descriptions of the IR target detection and identification algorithms are presented in a separate proprietary report. GRA

N91-29412# Environmental Research Inst. of Michigan, Ann Arbor.
P-3 SAR CALIBRATION ACTIVITY AT ANDROS ISLAND
Dan Sheen, Denise Gineris, and Eric Kasischke Feb. 1991 57 p
(Contract N00014-90-C-0117)
(AD-A237357; ERIM-226900-1-T) Avail: NTIS HC/MF A04 CSCL 17/9

From 26 May 1990 through 9 June 1990 the NADC/ERIM P-3/SAR collected calibration data over Andros Island. Several calibration reflectors were deployed on the ground at Andros town. The P-3/SAR typically imaged the reflectors during one pass at the start of each day's flight and one pass at the end of the day. These images were quickly processed to verify focussing and linearity of the SAR. The calibration activity demonstrated that the P-3/SAR was operating properly during the mission and that the data is calibratable. Author (GRA)

N91-29413# Naval Underwater Systems Center, New London, CT.
SPECTRA AND COVARIANCES FOR CLASSICAL NONLINEAR SIGNAL PROCESSING PROBLEMS INVOLVING CLASS A NON-GAUSSIAN NOISE Progress Report
Albert H. Nuttall and David Middleton 21 May 1991 87 p
(AD-A237388; NUSC-TR-8887) Avail: NTIS HC/MF A05 CSCL 12/9

Because of the critical role of non-Gaussian noise processes in modern signal processing, which usually involves nonlinear operations, it is important to examine the effects of the latter on such noise and the extension to added signal inputs. Here, only non-Gaussian (specifically class A) noise inputs, with an additive

Gaussian component, are considered. The classical problems of zero-memory nonlinear (ZMNL) devices serve to illustrate the approach and to provide a variety of useful output statistical quantities, e.g., mean or dc values, mean intensities, covariances, and their associated spectra. Here, Gaussian and non-Gaussian noise fields are introduced, and their respective temporal and spatial outputs are described and numerically evaluated for representative parameters of the noise and the ZMNL devices. GRA

N91-29414# Naval Ocean Systems Center, San Diego, CA.
DETECTION OF TARGETS IN TERRAIN CLUTTER BY USING MULTISPECTRAL INFRARED IMAGE PROCESSING Final Report, Oct. 1989 - Dec. 1990
L. E. Hoff, J. R. Evans, and L. E. Bunney Dec. 1990 56 p
(AD-A237436; NOSC/TR-1404) Avail: NTIS HC/MF A04 CSCL 17/5

A weighted-difference signal-processing algorithm for detecting ground targets by using dual-band IR data was investigated. Three variations of the algorithm were evaluated: (1) simple difference; (2) minimum noise; and (3) maximum SNR. The theoretical performance was compared to measured performance for two scenes collected by the NASA TIMS sensor over a rural area near Adelaide, Australia, and over a wooded area near the Redstone Arsenal. The theoretical and measured results agreed extremely well. For a given correlation coefficient and color ratio, the amount of signal-to-noise ratio gain can be predicted. However, target input SNRs and color ratios can vary considerably. For the targets and scenes evaluated here, the typical gains achieved ranged from a few dB loss (targets without color) to a maximum of approximately 20 dB. Author (GRA)

N91-29415# Oregon State Univ., Corvallis. Dept. of Electrical and Computer Engineering.
NONLINEAR COMPUTERIZED METHODOLOGY. A: ANGLE OF ARRIVAL ESTIMATION. B: DATA MODELING AND IDENTIFICATION Final Report
R. R. Mohler 10 Jun. 1991 17 p
(Contract N00014-90-J-1236)
(AD-A237564) Avail: NTIS HC/MF A03 CSCL 17/9

Multiple convolution of signals (sonar or radar) was analyzed as a nonlinear preprocessing technique for source localization from arrays of receivers, for time-delay estimation in general, and for spectral estimation of nonstationary signals. The method has proved successful by computer simulation for many troublesome cases as a supplement to MUSIC (and its adaptations) and as a simple alternative (or representation of) the Wigner-Ville distribution. Also, a new 2-D (image) processing method is being investigated by a transformed two-term Volterra series algorithm. The method appears promising for such applications as underwater green-laser data processing and other cases involving spatially coherent light and related nonlinear terms. GRA

N91-29416# Georgia Inst. of Tech., Atlanta. School of Electrical Engineering.
SIGNAL PROCESSING IN IMPULSIVE ELECTROMAGNETIC INTERFERENCE Progress Report
Serena M. Zabin 30 Jun. 1991 5 p
(Contract N00014-91-J-1334)
(AD-A237612) Avail: NTIS HC/MF A01 CSCL 20/14

Statistical signal processing functions such as signal detection, estimating, and identification play a key role in the development of effective communications, radar, and sonar systems. For example, advanced statistical methods are emerging as being particularly important in digital communications systems operating in channels corrupted by interference from such phenomena as multiple-access noise, intentional jamming, and impulsive noise sources. Conventional demodulation methods, such as coherent matched filtering, often suffer serious performance degradation when subjected to interference of these types; however, this degradation can frequently be eliminated through the use of more sophisticated signal processing techniques. A central issue in the design of effective signal processing procedures for system operating in channels such as those noted above is that of channel identification. Although certain aspects of channel identification have been studied extensively, one area in which there is a pressing need for further research is that of identification of impulsive channels. Communication systems are seldom interfered with by white Gaussian noise alone, yet receiving systems in general use are those which are optimum for white Gaussian noise. GRA

N91-29417# R and D Associates, Los Angeles, CA.
IMPACT OF IONOSPHERIC SCINTILLATIONS ON SPACE-BASED SURVEILLANCE RADARS Technical Report, 3 Jan. - 31 Dec. 1989
Lester L. DeRaad, Jr. and Brian Lamb 1 Jun. 1991 71 p
(Contract DNA001-88-C-0046)
(AD-A237673; RDA-TR-161603-001; DNA-TR-90-78) Avail: NTIS HC/MF A04 CSCL 20/14

A model is developed to analyze propagation effects on space-based radars (SBRs) with pulse-Doppler processing and with a displaced phase center antenna (DPCA) for rejection of surface clutter. It is found that nuclear-distributed ionospheric effects can significantly affect radar performance. Depending on the radar design parameters, similar, but less severe, problems may also occur in ambient auroral and equatorial ionospheres. The ionospheric effects degrade the DPCA clutter rejection and target Doppler processing functions of the radar. GRA

N91-29418# Defence Research Establishment, Ottawa (Ontario).
A DOPPLER BIN BLANKING CFAR PROCESSOR FOR AIRBORNE RADARS
G. Vrckovnik and D. Faubert Apr. 1991 44 p
(AD-A237890; DREO-1073) Avail: NTIS HC/MF A03 CSCL 17/9

Constant false alarm rate (CFAR) processors are used to prevent automatic detection radar systems from becoming overloaded with false targets, in the presence of time varying or unknown interference environments. They maintain the number of false alarms at a level consistent with the design goals. Unfortunately, large clutter returns can cause severe degradation in the performance of these processors. The degradation manifests itself as a reduction in the ability to detect targets of a given signal to noise ratio, while maintaining the overall system false alarm rate. As well, the constant multiplying factor used in CFAR processors tends to vary as the range-Doppler resolution cell map changes. In this report a novel adaptive algorithm to exclude the range-Doppler cells which contain clutter is developed. This algorithm, when used in conjunction with a CFAR processor, greatly enhances the system's sensitivity to targets which reside in the clutter free region of the range-Doppler map. It is also shown that the CFAR multiplier is relatively invariant to changes in the geometric conditions of the radar, when the adaptive Doppler bin blanking scheme is used. This blanking scheme could lead to a simple CFAR processor which would be effective in any possible clutter environment. GRA

N91-29419# Naval Postgraduate School, Monterey, CA.
ANALYSIS OF RADIO FREQUENCY RADIATION FROM A PROPAGATING ELECTRON BEAM M.S. Thesis
Richard W. Lally Jun. 1990 94 p
(AD-A237941) Avail: NTIS HC/MF A05 CSCL 20/7

An experiment was conducted which measured the Radio Frequency (RF) radiation from the PHERMEX accelerator, capable of 30 MeV and 600 A. This was accomplished by placing TEM horn antennae at varying angles from the path of the electron beam. The signals received by the antennae were then recorded by using a Digitizing Camera System (DCS). Measurements were taken of the radiation from propagating and non-propagating beams, beams with energy above and below Cherenkov threshold, and beams with varied currents. The captured RF signals and their corresponding frequency spectra were then analyzed. This analysis showed that the radio frequency radiation from the beams below the cherenkov threshold contained primarily transition radiation; when above, diffracted Cherenkov radiation was

observed. Non-propagating beams produced larger-angle radiation and had less definition in their spectrum. All electric fields measured were proportional to the beam current. Lastly, the electron beam pulse width and separation were determined by both the received signals and their spectrum. GRA

N91-29420# Pennsylvania State Univ., University Park. Coll. of Engineering.
PENN STATE/ONR MID FREQUENCY WORKSHOP
Victor W. Sparrow 24 May 1991 62 p Workshop held in State College, PA, 12-14 Mar. 1991
(Contract N00014-91-J-1459)
(AD-A237982) Avail: NTIS HC/MF A04 CSCL 20/1

The outcomes are presented of a workshop on the topic of scattering in the mid frequency range. Three of the major problems which persist in mid frequency scattering research are: the complexity of internal structures, a lack of understanding as to what physical variables correspond to appropriate observables, and a lack of standard model problems and benchmark problems. It is suggested that many avenues of research must be followed in parallel to meet these challenges. Traditional finite element/ boundary element method research should continue. Newer methods such as wavelets, decomposition techniques, and time domain techniques should be explored further, as well as the extension of high frequency methods down to mid frequency. Modeling the internal structures of realistic scatterers using probabilistic and other non traditional techniques should be pursued vigorously. Also, computations should be validated by appropriate experimental results. In addition, new experiments should be performed which specifically focus on the problems of complexity, observables, and the establishment of mid frequency model problems. GRA

N91-29421# Naval Weapons Center, China Lake, CA.
PORTABLE 45-GIGAHERTZ RADAR FOR GLINT AND SCINTILLATION STUDIES Final Report, Oct. 1988 - Sep. 1990
Robert J. Dinger, David R. Gagnon, David J. Banks, and Erik vanBronkhorst Dec. 1990 28 p
(AD-A238005; NWC-TP-7121) Avail: NTIS HC/MF A03 CSCL 17/9

A 45-gigahertz radar was developed that yields full polarization inverse synthetic aperture radar images and instantaneous angle-of-arrival measurements for angular scintillation studies. The system is portable, self-contained, and suitable for measurements of radar cross section ranges and open, unprepared sites. Measurements were made successfully on large scale model targets (8 meters in extent) at ranges up to 1000 meters. GRA

N91-29422# Naval Postgraduate School, Monterey, CA.
APPLICATION OF MULTI-FREQUENCY MODULATION (MFM) FOR HIGH-SPEED DATA COMMUNICATIONS TO A VOICE FREQUENCY CHANNEL M.S. Thesis
Charles P. Salsman Jun. 1990 103 p
(AD-A238019) Avail: NTIS HC/MF A06 CSCL 25/4

Multi-Frequency Modulation (MFM) has been developed at NPS using both differential quadrature-phase-shift-keying (DQPSK) and differential-quadrature-amplitude-modulation (DQAM) encoding formats. Previous applications of these encoding formats were on industry standard computers (PC) over a 16 to 20 kHz channel. This report discusses the implementation of MFM to a voice frequency channel of 200 to 3400 Hz, for possible future use with high-speed modems over switched telephone networks. Research and testing for this report included the DQPSK and differential 16 quadrature-amplitude-modulation (D16-QAM) encoding formats implemented on PCs. Experimental results of the implemented MFM signal were comparable to theory with acceptable bit error rates for input signal-to-noise ratios (SNR) of 15 dB and higher. GRA

N91-29423# Photometrics, Inc., Woburn, MA.
A PROGRAM TO OPERATE AND UPGRADE THE GL LOW ALTITUDE LIDAR SYSTEMS Final Report, 15 Jun. 1986 - 30 Sep. 1990
Richard C. Garner, Patrick J. McNicholl, Christian A. Trowbridge, and Gilbert Davidson 15 Jan. 1991 22 p
(Contract F19628-86-C-0102)
(AD-A238081; PHM-TR-91-10; PL-TR-91-2039) Avail: NTIS HC/MF A03 CSCL 17/5

This report describes work performed under a four year program to operate, upgrade, and maintain the GL/OP low altitude slant-path extinction mobile lidar system and the high altitude mobile and fixed lidar systems. In addition, certain instruments associated with the Mobile Atmospheric Optical Laboratory were to be operated, maintained, and upgraded. During the latter part of the program the responsibility to assist in development and operation of the GL/OP CO2 low altitude lidar system was added. GRA

N91-29424# Photometrics, Inc., Woburn, MA.
SCATTERING AND POLARIZATION MEASUREMENTS USING THE PL/OPA LOW ALTITUDE LIDAR Report, 15 Jun. 1986 - 30 Sep. 1990
Richard C. Garner 20 Dec. 1990 79 p
(Contract F19628-86-C-0102)
(AD-A238082; PHM-TR-91-06; PL-TR-91-2013; SR-2) Avail: NTIS HC/MF A05 CSCL 17/5

This report describes the background theory, experimental techniques, and results of research relating to lidar polarization, scattering, and absorption effects using the GL/OP low altitude lidar system. The work, which is aimed at improving the understanding of lidar as a diagnostic tool for studying the atmosphere, has concentrated on understanding multiple scattering and scattering from irregularly shaped particles, and deducing the extinction coefficient from lidar data. We present results of polarization measurements in snow, Mie scattering calculations, extinction coefficient calculations and preliminary modeling of multiple scattering effects as applied to lidar experiments. GRA

N91-29425# California Inst. of Tech., Pasadena. Dept. of Electrical Engineering.
CODING FOR SPREAD-SPECTRUM CHANNELS IN THE PRESENCE OF JAMMING Final Technical Report, 1 Jul. 1988 - 30 Sep. 1990
Robert J. McEliece 30 Sep. 1990 5 p
(Grant AF-AFOSR-0247-88; AF Proj. 2304)
(AD-A238233; AFOSR-91-0616TR) Avail: NTIS HC/MF A01 CSCL 17/4

Multi-user communication systems have been studied. There are systems in which many simultaneous two-way conversations have common frequencies. The maximum number of such conversations can be computed by a fairly simple linear program. A class of multi-user communication systems can, in some cases, be computed by a fairly simple linear program. GRA

N91-29426# Rockwell International Science Center, Thousand Oaks, CA.
NUMERICAL METHODS FOR SCATTERING FROM ELECTRICALLY LARGE OBJECTS Final Report, 1 Apr. 1989 - 31 Mar. 1991
Bjorn Enguist, W. D. Murphy, Vladimir Rokhlin, and Marius S. Vassiliou 31 May 1991 92 p
(Contract F49620-89-C-0048)
(AD-A238262; SC71004.FR; AFOSR-91-0612TR) Avail: NTIS HC/MF A05 CSCL 12/1

A new and computationally very efficient integral equation numerical method for computing electromagnetic scattering and radar cross section (RCS) was developed. A theory of higher order impedance boundary conditions was derived to handle single and multiple dielectric coatings around conductors. The method was tested in two dimensions using a 14,000-line FORTRAN program and was found to be very promising for electrically large objects. Initial ideas for extensions to three dimensions were explored. Treatments of trailing edge and corner singularities were developed. GRA

N91-29427# Arcon Corp., Waltham, MA.
RESEARCH AND DEVELOPMENT FOR DIGITAL VOICE PROCESSING (DVP) Final Technical Report, Feb. 1986 - Jun. 1988
J. D. Tardelli, P. A. LaFollette, C. M. Walter, J. LeBlanc, and P. D. Gatewood Jul. 1991 141 p
(Contract F19628-86-C-0057)
(AD-A238280; RL-TR-91-93) Avail: NTIS HC/MF A07 CSCL 25/4

This technical report covers a variety of topics and research areas. An update of the Canonical Coordinate (CC) Transformation process for digital speech compression based on non-Euclidean error minimization criteria is given. A method of transforming empirical filter sets to unitary error metrics is introduced and a sample error metric is developed. Research into frequency shift invarient transformation is presented and its utility for developing CC error metrics is discussed. A study into the relationship between CC analysis and Linear Predictive Coding is presented. An improved AP120-B implementation of the CC algorithm is given along with a fully parallel CC implementation on a systolic array processor. The latest developments in processor hardware, operating systems, and program development software at RADC/EEV are documented. Custom additions to the Interactive Laboratory System (ILS) analysis and display package are covered along with its relationship to the Speech Data Base Library used at RADC/EEV. Data Base input/output programs, analysis tools, search/sort programs are all presented. The status of a communicability testbed system at the Speech Processing Facility is presented. GRA

N91-29428# Ballistic Research Labs., Aberdeen Proving Ground, MD.
DESCRIPTION OF A COMPUTER FAULT DETECTOR AND NET ISOLATOR Final Report, 4-29 Mar. 1991
Mark D. Kregel Jun. 1991 13 p
(AD-A238387; BRL-TR-3240) Avail: NTIS HC/MF A03 CSCL 12/7

The reliability of a simple network can be improved by the use of highly reliable devices that monitor all sending elements attached to it. Such devices block network access if special electrical keys are not present before network communications are initiated. Such devices can also lock out network access for messages that exceed preset time limits. This report describes the construction of a simple device that serves these functions, termed a computer fault detector and net isolator, and describes the philosophy of its operation. The use of monitors of this type prevents the possible failure of a single sending element or node from disrupting the operation of an entire network. GRA

N91-29429# Naval Ocean Systems Center, San Diego, CA.
A NEW SYSTEM FOR MEASUREMENT OF LOW FREQUENCY RADIO TRANSMITTING ANTENNA PARAMETERS IN NEAR REAL TIME
S. C. Tietsworth Jun. 1991 5 p
(AD-A238555) Avail: NTIS HC/MF A01 CSCL 25/2

Fixed site very low frequency (VLF) and low frequency (LF) transmit antenna systems are used as the primary means of communication to submarine at sea. Until now there has not been a system to measure important antenna parameters on these low frequency transmit antennas in near real time while the antenna is being driven by frequency shift modulation. This paper describes a new system which can be used to measure several important antenna and tuning system parameters on these transmit antennas while the antennas are in normal operation. The measurements are made by sampling and processing the antenna voltage and current signals to calculate the antenna system resistance, capacitance, inductance, voltage, current and power which can then be displayed and stored on a personal computer. All of these measurements are made while the antenna is being driven by FSK or MSK signals. The paper includes a model of a typical low frequency transmit antenna as well as the associated equations. The response of the antenna system to frequency shift keying signals is then presented. In addition, the algorithms, hardware, and software used by the measurement system, called the VLF/LF antenna monitor system (AMOS), are discussed along with a summary of results obtained during initial testing of the AMOS system. GRA

N91-29430# Department of the Navy, Washington, DC.
A HIGH DATA RATE COMMUNICATIONS SYSTEM USING LONG PULSES Patent Application
W. M. Waters, inventor (to Navy) and G. J. Linde, inventor (to Navy) 31 Jan. 1990 32 p
(AD-D014947; US-Patent-Appl-SN-648696) Avail: NTIS HC/MF A03 CSCL 17/2

A communications system which decreases noise errors and increases information rate without sacrificing bandwidth is formed by a transmitter and a receiver designed to handle long pulse compression waveforms. An encoder connected to the transmitter converts a voice message into digitized voice words, encodes the digitized voice words into time shifted code sequences, and phase modulates the long pulse compression waveform, producing a M-ary coded signal at the output of the transmitter. The receiver is connected to a decoder which includes at least one convolver for computing the correlation of received digitally coded words with independently generated time shifted code sequences, and a controller for generating a plurality of data values according to the largest correlation values, and a transducer responsive to the data values. Author (GRA)

N91-29431*# National Aeronautics and Space Administration. Lewis Research Center, Cleveland, OH.
OPTICAL MULTIPLE ACCESS NETWORK (OMAN) FOR ADVANCED PROCESSING SATELLITE APPLICATIONS
Antonio J. Mendez, Robert M. Gagliardi, Eugene Park, William D. Ivancic, and Bradley D. Sherman (McDonnell-Douglas Corp., Long Beach, CA.) 1991 4 p Presented at the Summer Topical Meetings on Spacebourne Photonics: Aerospace Applications of Lasers and Electro-Optics, Newport Beach, CA, 22-24 Jul. 1991; sponsored by IEEE
(NASA-TM-105167; E-6458; NAS 1.15:105167) Avail: NTIS HC/MF A01 CSCL 17B

An OMAN breadboard for exploring advanced processing satellite circuit switch applications is introduced. Network architecture, hardware trade offs, and multiple user interference issues are presented. The breadboard test set up and experimental results are discussed. Author

N91-29432# National Inst. of Standards and Technology, Boulder, CO. Electromagnetic Fields Div.
NIST CALIBRATION PROCEDURE FOR VERTICALLY POLARIZED MONOPOLE ANTENNAS 30 kHz TO 300 MHz
D. G. Carnell, E. B. Larsen, J. E. Cruz, and D. A. Hill Jan. 1991 26 p
(PB91-185124; NIST/TN-1347) Avail: NTIS HC/MF A03; also available SOD HC $1.75 as 003-003-03077-5 CSCL 20N

The theoretical basis and test procedure are described for vertically polarized monopole antenna calibrations at the National Institute if Standards and Technology (NIST). The standard field method applies the theoretical equations of a vertical monopole antenna to calculate the vertical electric field. The method is used at the NIST open field site in the frequency range of 30 kHz to 300 MHz. The uncertainty in the antenna factor of the antenna under test (AUT) is now plus or minus 1 dB. Author

N91-29433# Sandia National Labs., Albuquerque, NM.
A METHOD FOR COMPUTING FIELDS NEAR THE ORIGIN OF A CYLINDRICAL COORDINATE SYSTEM IN TIME DOMAIN FINITE-DIFFERENCE ELECTROMAGNETIC SIMULATIONS
M. F. Pasik, D. B. Seidel, M. L. Kiefer, R. S. Coats, T. D. Pointon, and J. P. Quintenz 1991 3 p Presented at the 14th Conference on Numerical Simulation of Plasmas, Annapolis, MD, 4-6 Sep. 1991
(Contract DE-AC04-76DP-00789)
(DE91-015431; SAND-91-1514C; CONF-9109108-2) Avail: NTIS HC/MF A01

One problem with electromagnetic time domain finite-difference

simulations in cylindrical coordinates is the rapidly decreasing characteristic dimension of the cells as r approaches zero. In order to satisfy the Courant stability condition, a small time step is needed to insure stability, which is undesirable because it increases the cost of the simulation. In our presentation, we will describe a method which uses a rectangular grid and an annular cylindrical grid which overlap to perform electromagnetic simulations of cylindrical geometries. The two grids are connected by interpolating the field at the grid points of one grid using field values from the second grid. DOE

N91-29434# Argonne National Lab., IL.
THE APS RADIO FREQUENCY TEST STAND CONTROL SYSTEM
R. T. Daly, F. C. Vong, and M. R. Kraimer 1991 6 p Presented at the 7th International Conference on Real Time Computer Applications in Nuclear, Particle and Plasma Physics, Juelich, Fed. Republic of Germany, 18-21 Jun. 1991
(Contract W-31-109-eng-38)
(DE91-015711; ANL/CP-73512; CONF-9106122-3) Avail: NTIS HC/MF A02

A 7 GeV Advanced Photon Source is being designed for use as a synchrotron radiation source in basic and applied research. An RF Test Stand that uses a 250 kW RF source is being constructed to test the 352-MHz cavities and other high power RF components. How EPICS (Experimental Physics and Industrial Control System) is being used for control, monitoring and data acquisition in the RF Test Stand control system is described. Applications are discussed to demonstrate the use of the EPICS software tools. DOE

N91-29435# Lawrence Livermore National Lab., CA.
COMPUTATION OF BROADBAND, HIGH-POWER ELECTROMAGNETIC PULSE GENERATION FROM AN AIR GAS AVALANCHE SWITCH
D. J. Mayhall and J. H. Yee 1991 6 p Presented at the 8th IEEE Pulsed Power Conference, San Diego, CA, 17-19 Jun. 1991
(Contract W-7405-eng-48)
(DE91-015793; UCRL-JC-105249; CONF-910640-29) Avail: NTIS HC/MF A02

A two-dimensional, electromagnetic, electron fluid computer code predicts picosecond-scale electromagnetic wave generation in a simple air avalanche switch. Similar pulses occur from kilovolts to megavolts for proper scaling of the pressure. At fixed voltage, the pulse width varies with pressure. At fixed pressure, the pulse width varies with voltage. The pulse width can be reduced to 1 to 2 ps by operation in the wave interference model. In this mode, one air gap fires with a slight delay from the other air gap. This delay is some fraction of a picosecond. DOE

33 ELECTRONICS AND ELECTRICAL ENGINEERING

Includes test equipment and maintainability; components, e.g., tunnel diodes and transistors; microminiaturization; and integrated circuitry.

For related information see also *60 Computer Operations and Hardware* and *76 Solid-State Physics.*

N91-29436# Great Lakes Research Corp., Elizabethton, TN.
LONG-TERM TESTING AND EVALUATION OF CATHODE COMPONENTS IN A COMMERCIAL ALUMINUM CELL, VOLUME 1 Final Report Addendum
K. D. Church, E. G. Morris, L. A. Joo, D. V. Stewart, W. R. Morgan, and A. Tabereaux (Reynolds Metals Co., Sheffield, AL.) Apr. 1990 127 p
(Contract DE-AC07-87ID-12689)
(DE90-010896; DOE/ID-12689/1-Vol-1-Add) Avail: NTIS HC/MF A08

Since 1886, essentially all primary aluminum has been produced in Hall-Heroult electrolytic cells which electrochemically reduce alumina to the metal in an energy/capital intensive process. Nearly five per cent of the electrical energy generated in the United States in consumed in this Hall-Heroult process, at the rate of 6 to 8 kwh/lb. of aluminum produced. It has been in the aluminum industry's interest for the past several decades to utilize titanium diboride in some capacity as the cell cathode, either with conventional consumable carbon anodes or ultimately with nonconsumable, inert anodes. Eventual achievement of either or both of these goals will represent a technological breakthrough and make possible a significant reduction in the energy requirement to produce aluminum. The overall objective and achievement of this program was to better define the technical and economic viability of graphite-containing titanium diboride materials in low-cost shapes for use as cathodes in aluminum electrolytic cells as a precursor to subsequent demonstration and commercial application. This report covers the development of possible failure mechanisms, evaluations of the thermal shock resistance of non-cylindrical shapes, and an assessment of energy savings and technical/economic viability. In this program, titanium diboride-graphite (TiB2-G) materials were demonstrated to be superior to dense TiB2 materials which had been previously evaluated in studies by others in terms of longevity, thermal shock properties, and the ability to manufacture large, complex components. DOE

N91-29437# Tufts Univ., Medford, MA. Dept. of Chemical Engineering.
ELECTROCATALYTIC STUDY OF AMMONIA SYNTHESIS AND METHANE DIMERIZATION IN HIGH TEMPERATURE SOLID ELECTROLYTE CELLS
M. Stoukides 25 Jan. 1990 6 p
(Contract DE-FG02-89CE-90048)
(DE90-012496; DOE/CE-90048/1) Avail: NTIS HC/MF A02

The present report covers the first year of the three year project. The work is funded 50-50 by the National Science Foundation and the Department of Energy. The NSF support started on February 15, 1989 while the DOE support started on September 15, 1989. This created some minor difficulties in the budget distribution but hopefully within the second year everything will be smoothed out. The personnel involved in the project includes the principal investigator (M. Stoukides) who devotes 25 to 30 percent of his time during the year. Douglas Eng is going to work as a research scientist in the project on a full-time basis. Dr. Eng worked under the P.I. in the area of methane oxidation and he is probably the most qualified person for this position. Mr. Po-Hung Chiang has started working as a Ph.D. candidate in the H(sup +) solid electrolyte aided study of methane dimerization. Mr. Hyatham Algahtang, a new graduate student, is the most favorite candidate for the study of NH3 synthesis. He is already examining preliminary aspects of the project. Most of the equipment required for this research was in operating condition in the laboratory. Additional equipment purchased included a Lindberg furnace that could reach as high as 1500 C for fabrication of the solid electrolyte and a Rosemount Analytical hydrogen analyzer for continuous measurement of the concentration of hydrogen on either the cathodic or the anodic side. DOE

N91-29438# Department of the Navy, Washington, DC.
CABLE TESTER Patent Application
Robert L. Rammage, inventor (to Navy) 2 Oct. 1990 17 p
(AD-D014904; US-Patent-Appl-SN-591924) Avail: NTIS HC/MF A03 CSCL 14/2

A device for sequentially testing the plurality of connectors in a wiring harness is disclosed. The harness is attached to the tester by means of adapter cables and a rotary switch is used to sequentially, individually test the connectors by passing a current through the connector. If the connector is unbroken, a light will flash to show it is electrically sound. The adapters allow a large number of cable configurations to be tested using a single tester configuration. Author (GRA)

N91-29439 Department of the Navy, Washington, DC.
UNIVERSAL GROUND ADAPTER ASSEMBLY Patent
David S. Dixon, inventor (to Navy) and Nicholas Schade, inventor

(to Navy) 16 Apr. 1991 6 p Filed 18 Jun. 1990
(AD-D014908; US-Patent-5,007,847; US-Patent-Appl-SN-539954; US-Patent-Class-439-100) Avail: US Patent and Trademark Office CSCL 09/7

An electromagnetically shielded connector assembly is presented that enables connection from any one of conduit and cable to any one of conduit, cable and ground plane irrespective of the particular sizes of the members to be connected. GRA

N91-29440# Sandia National Labs., Albuquerque, NM.
PROCEEDINGS OF THE FIRST SWITCH TUBE ADVANCED TECHNOLOGY MEETING
A. Shuman and L. Beavis May 1991 189 p Meeting held in Salem, MA, 23 May 1990
(Contract DE-AC04-76DP-00789)
(DE91-012634; SAND-90-2172) Avail: NTIS HC/MF A09

Early in 1990, J. A. Wilder, Supervisor of Sandia National Laboratories (SNLA), Division 2565 requested that a meeting of the scientists and engineers responsible for developing and producing switch tubes be set up to discuss in a semi-formal way the science and technology of switch tubes. Programmatic and administrative issues were specifically exempted from the discussions. L. Beavis, Division 7471, SNL and A. Shuman, EG and G, Salem were made responsible for organizing a program including the materials and processes of switch tubes. The purpose of the Switch Tube Advanced Technology Meeting was to allow personnel from Allied Signal Kansas City Division (AS/KCD); EG and G, Salem, and Sandia National Laboratories (SNL) to discuss a variety of issues involved in the development and production of switch tubes. It was intended that the formal and informal discussions would allow a better understanding of the production problems by material and process engineers and of the materials and processes by production engineers. This program consisted of formal presentations on May 23 and informal discussions on May 24. The topics chosen for formal presentation were suggested by the people of AS/KCD, EG and G, Salem, and SNL involved with the design, development, and production of switch tubes. The topics selected were generic. They were not directed to any specific switch tube but rather to all switch tubes in production and development. This document includes summaries of the material presented at the formal presentation on May 23. DOE

N91-29441# Stanford Linear Accelerator Center, CA.
A HIGH POWER CROSS-FIELD AMPLIFIER AT X-BAND
K. Eppley, J. Feinstein, K. Ko, N. Kroll, T. Lee, and E. Nelson May 1991 3 p Presented at the 1991 Institute of Electrical and Electronics Engineers (IEEE) Particle Accelerator Conference (PAC), San Francisco, 6-9 May 1991
(Contract DE-AC03-76SF-00515)
(DE91-013277; SU-SLAC-PUB-5559; CONF-910505-115) Avail: NTIS HC/MF A01

A high power cross-field amplifier (CFA) is under development with the objective of providing sufficient peak power to feed a section of an X-Band (11.424 GHz) accelerator without the need for pulse compression. The CFA being designed employs a conventional distributed secondary emission cathode but a novel anode structure which consists of an array of vane resonators alternatively coupled to a rectangular waveguide. The waveguide impedance (width) is tapered linearly from input to output so as to provide a constant RF voltage at the vane tips, leading to uniform power generation along the structure. Nominal design for this tube calls for 300 MW output power, 20 dB gain, DC voltage 142 KV, magnetic field 5 KG, anode-cathode gap 3.6 mm and total interaction length of about 60 cm. These specifications have been supported by computer simulations of both the RF slow wave structure as well as the electron space charge wave interaction. We have used ARGUS to model the cold circuit properties and CONDOR to model the electronic power conversion. An efficiency of 60 percent can be expected. We will discuss the details of the design effort. DOE

N91-29442# Sandia National Labs., Albuquerque, NM.
THE 2ND WORKSHOP ON HIGH TEMPERTURE ELECTRONICS (METALLIZATION AND PACKAGING) Final Report
F. V. Thome, D. B. King, and C. W. Severt (Air Force Wright Research and Development Center, Wright-Patterson AFB, OH.) May 1991 654 p Workshop held in Albuquerque, NM, 6-8 Jun. 1989
(Contract DE-AC04-76DP-00789)
(DE91-014332; SAND-91-0370; CONF-8906408) Avail: NTIS HC/MF A99

This is a synopsis of a workshop on high temperature electronics. Their use could be in various fields to include supersonic aircraft, automobiles, or solar cells. The first session of the workshop examined user needs, impacts, and applications. The second session covered metallization with silicon, diamond, silicon carbide, and gallium arsenide. The third and final session dealt with packaging to include reliability, microelectronics, alloys, enclosures, ceramics, metal/glass, ceramic/glass, and plastic. This report consists of the presenters' abstracts and selected self-explanatory viewgraphs. DOE

N91-29443# Los Alamos National Lab., NM.
REX: A 5-MV PULSED-POWER SOURCE FOR DRIVING HIGH-BRIGHTNESS ELECTRON BEAM DIODES
R. L. Carlson, T. J. Kauppila, and R. N. Ridlon 1991 5 p Presented at the 8th IEEE Pulsed Power Conference, San Diego, CA, 17-19 Jun. 1991
(Contract W-7405-eng-36)
(DE91-014604; LA-UR-91-2050; CONF-910640-19) Avail: NTIS HC/MF A01

The Relativistic Electron-beam Experiment, or REX accelerator, is a pulsed-power source capable of driving a 100-ohm load at 5 MV, 50 kA, 45 ns (FWHM) with less than a 10-ns rise and 15-ns fall time. This paper describes the pulsed-power modifications, modelling, and extensive measurements on REX to allow it to drive high impedance (100s of ohms) diode loads with a shaped voltage pulse. A major component of REX is the 1.83-m-diam times 25.4-cm-thick Lucite insulator with embedded grading rings that separates the output oil transmission line from the vacuum vessel that contains the re-entrant anode and cathode assemblies. A radially tailored, liquid-based resistor provides a stiff voltage source that is insensitive to small variations of the diode current and, in addition, optimizes the electric field stress across the vacuum side of the insulator. The high-current operation of REX employs both multichannel peaking and point-plane diverter switches. This mode reduces the prepulse to less than 2 kV and the postpulse to less than 5 percent of the energy delivered to the load. Pulse shaping for the present diode load is done through two L-C transmission line filters and a tapered, glycol-based line adjacent to the water PFL and output switch. This has allowed REX to drive a diode producing a 4-MV, 4.5-kA, 55-ns flat-top electron beam with a normalized Lapostolle emittance of 0.96 mm-rad corresponding to a beam brightness in excess of 4.4 times 10(exp 8) A/m(sup 2) minus rad(sup 2). DOE

N91-29444# California Univ., Berkeley. Lawrence Berkeley Lab.
MEASUREMENTS OF RETRACTABLE GAS-COOLED 6061 ALUMINUM ELECTRICAL LEADS OPERATING IN A VACUUM
M. A. Green, H. Aguiar, M. J. Bensadoun, J. H. Gibson, D. L. Heine, S. Levin, M. Limon, G. F. Smoot, and C. Witebsky Jun. 1991 7 p Presented at the Cryogenic Engineering Conference and International Cryogenic Materials Conference, Huntsville, AL, 11-14 Jun. 1991
(Contract DE-AC03-76SF-00098)
(DE91-014617; LRL-30785; CONF-910635-3; ASTROMAG-035) Avail: NTIS HC/MF A02

To charge and discharge the ASTROMAG superconducting magnet in space requires retractable gas-cooled leads which must operate in a vacuum. This report describes the design and test of 500 ampere retractable gas-cooled leads made from 6061-T4 aluminum tubes. Aluminum is attractive for gas-cooled electrical

leads in space because of its low mass density and the desire for short leads. Initial tests showed that retractable gas-cooled leads could operate in a vacuum from a source of normal helium. The pressure drop through the leads was low enough to permit a superconducting magnet to be charged and discharged while the leads vent into space. The leads were stable at currents above 700 amperes. The voltage drop across the contact between the upper and lower leads was as low as 1.2 mV per lead out of a total voltage drop of 42 mV per lead when the leads carried 714 amperes. The gas required for cooling was comparable to the more conventional copper gas-cooled current leads. In a second test seven months later, the contact resistance between the lead sections had increased considerably. In the second test, the contact resistance was rep eatable for one lead but not for the other.
DOE

N91-29445# Sandia National Labs., Albuquerque, NM.
DESIGN AND TEST OF A CONTINUOUS DUTY PULSED ac GENERATOR
R. M. Calfo, D. J. Scott, D. W. Scherbarth (Westinghouse Electric Corp., Pittsburgh, PA.), M. T. Bubbtram, and H. C. Harjes 1991 5 p Presented at the 8th IEEE Pulsed Power Conference, San Diego, CA, 17-19 Jun. 1991
(Contract DE-AC04-76DP-00789)
(DE91-014664; SAND-90-3073C; CONF-910640-27) Avail: NTIS HC/MF A01

Specially designed synchronous ac generators can provide a high energy pulse power source capable of supplying energy to various pulse forming networks. One such generator, which is the subject of this paper, is presently being used as the prime power source for the Repetitive High Energy Pulsed Power Module (RHEPP) at Sandia National Laboratories. The generator has been designed to operate continuously in two distinct modes. In the first mode the generator can supply 50-kJ, 9.5-kV, 11,000-amp, 1-msec pulses continuously (500 kW average power) with a rep rate from 1 to 10 Hs. In the second mode, 20.8-kJ, 9.5-kV, 1052-amp, 4-msec pulses can be supplied continuously (5000 kW average power) at a rep rate of 240 pulses per second. The latter mode is being used in the RHEPP application at a reduced energy and voltage level. The generator was successfully tested in 9/89 to verify the performance at its maximum rating. Test results are presented along with details of the generator design and its applications. DOE

N91-29446# Sandia National Labs., Albuquerque, NM.
PHYSICS AND APPLICATIONS OF THE LOCK-ON EFFECT
G. M. Loubriel, F. J. Zutavern, W. D. Helgeson, D. L. McLaughlin, M. W. OMalley, and T. Burke (Army Electronics Technology and Devices Lab., Fort Monmouth, NJ.) 1991 4 p Presented at the 8th IEEE Pulsed Power Conference, San Diego, CA, 17-19 Jun. 1991
(Contract DE-AC04-76DP-00789)
(DE91-014670; SAND-90-3072C; CONF-910640-11) Avail: NTIS HC/MF A01

The lock-on effect is a high gain, high field switching mechanism that has been observed in GaAs and InP. This switching mode is exciting because the amount of light required to trigger it is small when compared to triggering the same switch at low fields. For this reason we can use laser diode arrays to trigger high voltages, currents and power. This paper will describe the lock-on effect, and our recent experiments to understand the effect. We will show that impact ionization from deep levels cannot account for the observed current densities, delays, and rise times unless a second mechanism is invoked. We will also describe our applications for laser diode array triggered lock-on switches, the best results that illustrate our potential for the application, and the studies carried out to improve the lifetime and current carrying capability of the switches. DOE

N91-29447# Sandia National Labs., Albuquerque, NM.
APPLICATION OF THE NUCLEAR MICROPROBE TO THE IMAGING OF SINGLE EVENT UPSETS IN INTEGRATED CIRCUITS
K. M. Horn, B. L. Doyle, D. S. Walsh, and F. W. Sexton 20 Jun. 1991 20 p Presented at the Scanning Microscopy Meeting, Bethesda, MD, 3-9 May 1991
(Contract DE-AC04-76DP-00789)
(DE91-014701; SAND-91-0799C; CONF-9105197-2) Avail: NTIS HC/MF A03

A new form of microscopy has been developed which produces micron-resolution maps of where single event upsets occur during ion irradiation of integrated circuits. Utilizing a nuclear microprobe, this imaging technique can irradiate, in isolation, the lowest functional units of an integrated circuit (e.g., transistor drains, gates, and feedback resistors) and measure immediately the effect of a high energy ion strike on circuit performance. Such detailed circuit characterization can provide heretofore inaccessible information to the designers of integrated circuits that are to be used in space or other radiation environments. DOE

N91-29448# Naval Ocean Systems Center, San Diego, CA.
THE DESIGN OF A REAL-TIME ADAPTIVE FILTER DEVELOPMENT SYSTEM
Terence R. Albert, Michael D. Juniper, Richard C. North, and Walter H. Ku May 1991 7 p
(AD-A237134) Avail: NTIS HC/MF A02 CSCL 12/6

A hardware test platform is described which was designed to implement adaptive lattice filters in real time. To achieve real time processing speeds, algorithm complexity was accomplished by custom designing the computation engines with respect to the lattice data flow. Execution speeds of the computation engines were dramatically increased by a memory architecture that supports efficient addressing and by providing a floating point ALU with numerous data paths and efficient implementation of division. Performance is further enhanced by pipelining multiple computation engines. In addition, the architecture is flexible enough to support other filter structures and to allow observation of filter variables as they adapt. With this system, various Adaptive Filter algorithms are being tested in real time implementation of Adaptive Line Enhancers (ALEs) and Adaptive Noise Cancelers (ANCs) in order to characterize their performance and behavior, especially long term stability and the ability to track nonstationary signals. GRA

N91-29449# Institute for Defense Analyses, Alexandria, VA.
DIGITAL SPC SWITCHING TECHNOLOGY: FOREIGN TECHNOLOGY ASSESSMENT Final Report, Jun. - Dec. 1990
Kurt Fischman and Norman D. Jorstad Dec. 1990 59 p
(Contract MDA903-89-C-0003)
(AD-A237258; AD-E501393; IDA-P-2498; IDA/HQ-90-36322)
Avail: NTIS HC/MF A04 CSCL 25/2

This paper provides a foreign technology assessment of digital switching technology. Leading suppliers of digital switching technology are identified; although the United States holds a large part of the market, major companies in France, Sweden, Japan, the U.K., and Germany are also important. These countries, along with Belgium and Canada, are the most innovative and technically advanced. A listing is provided of transfers of digital switching technology to non-COCOM countries through licensing and joint ventures which reflects the widespread dissemination of this technology. Detailed technical specifications are provided for selected digital switching systems worldwide. The report concludes that considering the degree to which the technology is in place, that control of digital switching technology may not be feasible.
GRA

N91-29450# Naval Research Lab., Washington, DC.
ANALYSIS OF FIN LINE FEASIBILITY FOR W-BAND ATTENUATOR APPLICATIONS Final Report
J. A. Molnar 11 Jun. 1991 68 p
(AD-A237271; NRL-MR-6843) Avail: NTIS HC/MF A04 CSCL 09/1

A study was performed that examines the feasibility of developing an electronically adjustable attenuator for W-band instrumentation applications. All common transmission line structures are considered. An analysis of the merits of each transmission line structure is presented. A fin line structure is

presented as having the greatest probability for success. PIN diodes are presented as the most frequently used device for attenuation and control applications. An analysis of the structural, electromagnetic and circuit characteristics was performed. The analysis presented indicates that forward biased, shunt mounted PIN diodes in a fin line structure is a viable approach for continuing investigation for the specified instrumentation application. The conclusions are supported by earlier works that are reviewed in this report. GRA

N91-29451# General Electric Co., Syracuse, NY.
FAILURE MECHANISMS ON GaAs INTEGRATED CIRCUITS: ELECTROMIGRATION ON GaAs Final Technical Report, Apr. 1988 - Jun. 1990
Donald J. LaCombe, Earl L. Parks, and David Widay Jun. 1991 73 p
(Contract F30602-88-C-0052)
(AD-A237352; RL-TR-91-81) Avail: NTIS HC/MF A04 CSCL 09/1

The objective of this program was to investigate two aspects of electromigration on GaAs devices: (1) the rate of electromigration of typical metallizations on GaAs; and (2) the occurrence of electromigration assisted interdiffusion of the gate metal and the GaAs in GaAs FETs. A life test was conducted, and the rate of electromigration was found to be influenced by the type of barrier metallization used. It was found that electromigration is no worse on GaAs than on silicon. It was found that interdiffusion of the gate metal into the GaAs was not significant at the test conditions used during the life test. GRA

N91-29452# Texas Instruments, Inc., Dallas.
SILICON WAFER ADVANCED PACKAGING (SWAP). MULTICHIP MODULE (MCM) FOUNDRY STUDY, VERSION 2 Final Report, Oct. 1990 - Mar. 1991
Larry Mowatt, Frank Henry, Mark Avery, Porter Sadler, and Mark Eskew 8 Apr. 1991 244 p
(Contract MDA972-90-C-0045; ARPA Order 7549)
(AD-A237412; SWAP001-AC) Avail: NTIS HC/MF A11 CSCL 09/1

MCM technology is crucial to maintaining the competitive position of the U.S. electronics industry - military and commercial. The driving force is performance, and MCM users will seek off-shore suppliers if capabilities are lacking. In the long term, low-cost overseas capabilities will make their way into the U.S. military market and put it at risk. The proven GE-HDI MCM technology was developed with combined government and Ge funding, and its chips first approach offers the lowest non-recurring cost. Rapid prototyping, high performance, and technology flexibility are characteristic, and the potential exists for extension to high-volume. GRA

N91-29453# Naval Surface Warfare Center, Silver Spring, MD.
AN ALTERNATIVE TO OPERATIONAL AMPLIFIERS Final Report
Arthur D. Delagrange 1 Jun. 1990 49 p
(AD-A237439; NAVSWC-TR-90-180) Avail: NTIS HC/MF A03 CSCL 09/1

Operational amplifiers are the mainstay of analog (linear) electronics. Alternatives have never been seriously considered. Today there is an increasing push for high speed. This report argues that operational amplifiers are not well suited to high speed and presents an alternative, fixed-gain amplifier. Typical applications are shown and an approach for designing them suggested. GRA

N91-29454# Georgia Inst. of Tech., Atlanta. School of Physics.
NONLINEAR DYNAMICS OF JOSEPHSON JUNCTION PARAMETRIC AMPLIFIER ARRAYS Final Report
Kurt Wiesenfeld 19 Jun. 1991 10 p
(Contract N00014-88-K-0494)
(AD-A237451) Avail: NTIS HC/MF A02 CSCL 09/1

For practical applications, it is most desirable to operate arrays in the in-phase state, so that each oscillator has precisely the same waveform, and all oscillators are in perfect synchrony. Consequently, the first order of business is to determine the conditions under which stable in-phase operation is possible. The stability regions for a variety of circuit configurations has been mapped out, first via numerical simulations and then via approximate analytic calculations. In fact, we discovered that for certain circuit designs, the dynamics possessed a fundamental symmetry that prohibits stable in-phase orbits. We conclude immediately that such designs should be avoided for any practical application. (For example, this applies to small capacitance point contact junctions shunted by a purely resistive load.) GRA

N91-29455# Purdue Univ., West Lafayette, IN. Dept. of Chemistry.
CYCLIC VOLTAMMETRIC WAVE-SHAPES FOR MICRODISK ELECTRODES: COUPLED EFFECTS OF SOLUTION RESISTANCE, DOUBLE-LAYER CAPACITANCE, AND FINITE ELECTROCHEMICAL KINETICS
L. K. Sattord and M. J. Weaver 31 May 1991 52 p
(Contract N00014-91-J-1409)
(AD-A237505; TR-104) Avail: NTIS HC/MF A04 CSCL 14/2

Cyclic voltammograms at microdisk electrodes that account for the effects of solution resistivity rho(Omega), double layer capacitance, C(dl), and electrochemical kinetics were simulated by using the explicit Hopscotch algorithm and a conformally mapped space-grid. The latter procedure, in particular, provides an efficient means of simulating voltammograms at slower potential scan rates where radial, rather than linear, diffusion predominates. Simulated voltammetric waveshapes as a function of scan rate are reported for systematic variations in rho(Omega), C(dl), and the standard electrochemical rate constant ks, both separately and together. The waveshape description utilizes both the anodic-cathodic potential peak separation, Delta E(p), and the halfwave potential for the forward scan in relation to the voltammograms where the influence of radial diffusion is sufficient to yield largely sigmoidal, rather than peaked, waveshapes. GRA

N91-29456# Army Lab. Command, Fort Monmouth, NJ. Electronics Technology and Devices Lab.
A CALORIMETRIC INVESTIGATION OF DEUTERATED PALLADIUM ELECTRODES Technical Report, Apr. - Sep. 1989
T. R. Jow, Steven Slane, Edward J. Plichta, Charles W. Walker, Jr., and Sol Gilman May 1991 22 p
(DA Proj. 1L1-611102-H-47)
(AD-A237571; SLCET-TR-91-17) Avail: NTIS HC/MF A03 CSCL 09/1

Calorimetric experiments were conducted to verify the caloric claims by Fleischmann and Pons. A twin-cell heat conduction calorimeter was used, rather than the quasi-adiabatic instrumentation of the original investigation. Under similar electro-chemical conditions, the output of heat powers from experimental cells of Pd in 0.1 M LiOD/D2O and that from control cells of Pd in 0.1 M LiOH/H2O and Pt in 0.1 M LiOD/D2O were all in close agreement with input heat powers using simple theory. These results show no anomalous excess heat, as claimed. GRA

N91-29457# Army Lab. Command, Fort Monmouth, NJ. Electronics Technology and Devices Lab.
MEASUREMENT OF LITHIUM CYCLING EFFICIENCY IN ORGANIC ELECTROLYTES Technical Report, Oct. 1990 - Feb. 1991
Steven Slane May 1991 17 p
(AD-A237632; SLCET-TR-91-15) Avail: NTIS HC/MF A03 CSCL 10/3

An experiment to measure the average lithium cycling efficiency of organic electrolytes has been developed. Lithium cycling efficiency is an important parameter in the research and development of rechargeable lithium batteries. The safety, shelf life, and cycle life of lithium batteries are direct consequences of hoe electrochemically stable the lithium anode is in the organic electrolyte used. Detailed within this report is the method of measurement and its advantages and disadvantages. Also reported

are results of lithium cycling efficiencies in various ester solvent-based electrolytes. The effects of cosolvents and electrolyte additives have been investigated. GRA

N91-29458# Massachusetts Inst. of Tech., Cambridge. Research Lab. of Electronics.
THE RESEARCH LABORATORY OF ELECTRONICS Progress Report No. 133, 1 Jan. - 31 Dec. 1990
Jonathan Allen and Daniel Kleppner 31 Dec. 1990 406 p
(AD-A237670) Avail: NTIS HC/MF A18 CSCL 09/1

The following subject areas are covered: (1) Solid State Physics, Electronics and Optics (Materials and Fabrication; Optics and Devices; and Surfaces and Interfaces); (2) Applied Physics (Atomic, Molecular and Optical Physics; Plasma Physics; Electromagnetics; and Radio Astronomy); (3) Systems and Signals (Digital Signal Processing); and (4) Language, Speech and Hearing (Speech Communication, Sensory Communication, Auditory Physiology, and Linguistics). GRA

N91-29459# University of Northern Illinois, De Kalb. Dept. of Chemistry.
ELECTRIFIED MICROSCOPIC AND CONVENTIONAL INTERFACES BETWEEN TWO IMMISCIBLE ELECTROLYTE SOLUTIONS Technical Report No. 40, 16 Oct. 1990 - 30 Jun. 1991
Petr Vanysek 24 Jun. 1991 40 p
(Contract N00014-91-J-1058; NR Proj. RR0-4108)
(AD-A237695) Avail: NTIS HC/MF A03 CSCL 09/1

Transport studies on interfaces between immiscible phases bridges the field of heterogeneous electrode electrochemistry and that of homogeneous solution chemistry. Early work on liquid/liquid boundary was concerned with large area (order of a square centimeter) interfaces. Recent studies investigate phenomena on interfaces rendered in pores, capillaries, and small holes. The behavior of such interfaces in the presence of dodecyl sulfate, forming micelles, is investigated. Voltammetry and amperometry on these small interfaces reveals that the accompanying voltammetric characteristics are similar to that of metal ultramicroelectrodes. Potentiometric studies of dodecyl sulfate on water/nitrobenzene and aqueous polymer immiscible interfaces allow determination of critical micelle concentration. GRA

N91-29460# Kansas State Univ., Manhattan. Dept. of Physics.
PERSISTENT PHOTOCONDUCTIVITY IN II-VI MIXED SEMICONDUCTORS RELATED CRITICAL PHENOMENA AND APPLICATIONS Final Report, 1 Aug. 1990 - 31 Mar. 1991
Hongxing Jing 31 Mar. 1991 29 p
(Grant AF-AFOSR-0318-90; AF Proj. 2306)
(AD-A237792; AFOSR-91-0582TR) Avail: NTIS HC/MF A03 CSCL 09/5

Persistent photoconductivity (PPC) was studied in II-VI mixed semiconductors and related device applications: (1) New Type of Materials; (2) PPC in II-VI Semiconductor Thin Films; (3) Comparison Between II-VI and III-V Semiconductors; and (4) PCC Transient Behavior. Author (GRA)

N91-29461# Stanford Univ., CA. Physics Lab.
MILLIMETER-WAVE CHARACTERIZATION OF GaAs DEVICES AND IC'S
David M. Bloom Jun. 1991 21 p
(Contract N00014-89-J-1842)
(AD-A237843; SU-GL-4841) Avail: NTIS HC/MF A03 CSCL 07/2

Coplanar waveguide transmission line (CPW) passive probes have become very popular for on-wafer characterization of integrated circuits. Since this transmission line has all conductors on one side of the substrate, it is a low parasitic medium for transmission from the input connector to the device under test. The entire line can be formed with one mask step and does not require backside metalization or via holes. Since the CPW formed on a semi-insulating substrate (e.g., GaAs) has a characteristic impedance which only depends on the center conductor width-to-ground gap, the impedance which only depends on the center conductor width-to-ground gap, the impedance can easily be changed. We have improved upon our ultra-short pulse generating capabilities with highly optimized non-linear transmission lines incorporated into the design of very wide-bandwidth electrical samples and also into an integrated circuit directional bridge. Since these integrated circuits are small, they can be mounted directly on an IC probe tip. This capability, by bringing the measurement instrument into contact with the circuit to be tested almost completely solves the interconnect losses. By placing the MMICs in an alumina tip package, we are able to measure s-parameters up to 85 GHz. Above 100 GHz, the parasitics of the connection between the MMIC samplers and the alumina probe tip become intolerable and the alumina tip must be eliminated. GRA

N91-29462# Northwestern Univ., Evanston, IL. Dept. of Materials Science and Engineering.
INFRARED AND RAMAN SPECTRA OF C60 AND C70 SOLID FILMS AT ROOM TEMPERATURE
R. J. Meilunas, R. P. Chang, S. Liu, and M. M. Kappes 1 Jul. 1991 12 p
(Contract N00014-89-J-1848)
(AD-A237880; TR-4) Avail: NTIS HC/MF A03 CSCL 09/1

Infrared and high resolution Raman spectroscopic probes of thin films of C60 and C70 are presented and discussed in terms of previous measurements, semi-empirical calculations and plausible molecular geometries. GRA

N91-29463# Syracuse Univ., NY. Dept. of Electrical and Computer Engineering.
THEORETICAL, EXPERIMENTAL, AND NUMERICAL STUDIES ON HYBRID ACOUSTOOPTIC BISTABLE DEVICES Final Report, Jun. - Dec. 1988
Partha P. Banerjee Jun. 1991 68 p
(Contract F30602-88-D-0027)
(AD-A237885; RL-TR-91-83) Avail: NTIS HC/MF A04 CSCL 09/6

This final report provides a short summary of various bistable optical devices, with emphasis on the acoustooptic bistable device. Difference equations describing an acoustooptic system have been defined along with numerical simulations to study the system dynamics. A summary of experimental work performed to verify some of the effects of hysteresis and bistability is included. A study of some of the characteristics of the underlying dynamical system using conventional methods is also included. This report also gives an alternative explanation of hysteresis and indicates how to study the behavior of the system for time varying inputs. GRA

N91-29464# Naval Research Lab., Washington, DC.
THE CHARGE-EXCHANGE NEUTRAL PROBLEM AND THE CODE NEUTRAL Interim Report
John M. Les and Robert E. Terry 26 Jun. 1991 67 p
(AD-A237889; NRL-MR-6779) Avail: NTIS HC/MF A04 CSCL 09/1

The code named NEUTRAL was developed to simulate the problem of charge-exchange neutrals, which has been proposed to explain the anamolous gap closure in a Reflex Switch. NEUTRAL is one dimensional in position and velocity space and includes a static electric field. Monte Carlo techniques are used to model the charge-exchange process. Analytic expressions are derived using the one dimensional Boltzmann equation, assuming a constant charge-exchange cross section, and they are compared against the NEUTRAL simulation runs. Good agreement is found between the two results. Some parameters were also varied independently to test the response of NEUTRAL. It was found that the code gives reasonable answers for a wide range of the input. From these bench-mark tests it is concluded that NEUTRAL is operating correctly. GRA

N91-29465# Naval Postgraduate School, Monterey, CA.
INTRODUCTION OF A CURRENT WAVEFORM, WAVESHAPING TECHNIQUE TO LIMIT CONDUCTION LOSS IN HIGH-FREQUENCY dc-dc CONVERTERS SUITABLE FOR SPACE POWER M.S. Thesis
Douglas P. Miller Jun. 1990 160 p
(AD-A237903) Avail: NTIS HC/MF A08 CSCL 10/2

Space power supply manufacturers have tried to increase power density and construct smaller, highly efficient power supplies by increasing switching frequency. Incorporation of a power MOSFET as a switching element alleviates switching loss. However, values of R sub DS(on) (drain-to-source resistance in the on-state) for MOSFET's are of such magnitude to produce greater on-state losses than an equivalent BJT operated in saturation. This research serves to introduce a design concept, pertinent to low-voltage relatively-high-current applications, that minimizes the peak current through the switching element in order to reduce average power loss. Basic waveforms produced by different PWM and resonant mode topologies were examined. Theoretical analysis reveals that a ramp-sine current waveform could cut conduction power loss by at least 18 percent over a conventional Buck switching converter. A 14V, 14W combination quasi-resonant Buck/ZCS, Quasi-Resonant Buck dc-dc converter with an unregulated input voltage of 28 V was built for simplicity to demonstrate one particular waveshaping technique. This converter represents a useful example of an actual circuit which is capable of producing the desired ramp-sine switch-current waveform. Final results confirm improvement in conduction loss enhancing existing power MOSFET technology for use in dc-dc power conversion. GRA

N91-29466# Naval Postgraduate School, Monterey, CA.
A CIRCUIT MODEL FOR AN INDUCTIVE STRIP IN HOMOGENEOUS FINLINE M.S. Thesis
Michael L. Morua Jun. 1990 110 p
(AD-A238001) Avail: NTIS HC/MF A06 CSCL 09/1

A CAD compatible circuit model is described for an infinitesimally thin inductive strip centered in homogeneous finline for 0.1 less than or = w over b less than or = 1.0. The model is shown to predict scattering data which agrees with data computed using the spectral domain method. Results were generated for strips of length T greater than or = 10 mils in X-band. By applying the scaling principle, the model is valid for any waveguide band over the normal frequency range for the dominant TE sub 10 mode. GRA

N91-29467# Naval Weapons Center, China Lake, CA.
ANNUAL ELECTRONICS MANUFACTURING SEMINAR PROCEEDINGS
Feb. 1991 303 p Seminar held in Ridgecrest, CA, 20-22 Feb. 1991
(AD-A238017) Avail: NTIS HC/MF A14 CSCL 13/8

The proceedings of the 15th Annual Electronics Manufacturing Seminar, held on 20-22 February 1991, in Ridgecrest, California are presented. The proceedings include the papers presented at the seminar and cover all aspects of soldering technology and electronics manufacturing. The proceedings are a compilation of information provided by both nongovernment and government sources. The proceedings are published in the interest of furthering communication and broadening awareness of current activities among soldering technology and electronics manufacturing specialists. GRA

N91-29468# Stanford Univ., CA.
VLSI CIRCUIT TECHNIQUES AND TECHNOLOGIES FOR ULTRAHIGH SPEED DATA CONVERSION INTERFACES Final Report, 28 Sep. 1987 - 28 Feb. 1991
Bruce A. Wooley 29 Apr. 1991 9 p
(Contract DAAL03-87-K-0111)
(AD-A238115; ARO-25156.12-EL) Avail: NTIS HC/MF A02 CSCL 09/1

The performance of digital VLSI signal processing and communications systems is often limited by the data conversion interfaces between digital system-level components and the analog environment in which those components are embedded. The focus of this program has been research into the fundamental nature of such interfaces in systems that digitally process high-bandwidth signals for purposes such as radar imaging, high-resolution graphics, high-definition video, mobile and fiber-optic communications, and broadband instrumentation. Effort has been devoted to the study of both generic circuit functions, such as sampling and comparison, and architectural alternatives relevant to the implementation of high-speed data converters in present and emerging VLSI technologies. Specific results of the research include the design and realization of novel low-power CMOS and BiCMOS sampled-data comparators operating at rates as high as 200 MHz, the exploration of various design approaches to the implementation of high-speed sample-and-hold circuits in CMOS and BiCMOS technologies, and the design of a subranging CMOS analog-to-digital converter that provides 12-bit resolution at a conversion rate of 10 MHz. GRA

N91-29469# Rockwell International Science Center, Thousand Oaks, CA.
ELECTRODEPOSITION OF HIGH TEMPERATURE SUPERCONDUCTORS Quarterly Status Report No. 3, 1 Mar. - 30 Jun. 1991
30 Jun. 1991 7 p
(Contract N00014-90-C-0225)
(AD-A238227) Avail: NTIS HC/MF A02 CSCL 09/1

The overall objective of this project is to develop a process for direct electrodeposition of Y-Ba-Cu superconducting oxides from a molten salt at relatively low temperatures (300 to 550 C). The approach entails establishing a sequence of electrochemical steps for the layered deposition of the Y, Ba, Cu oxide species from a molten Na-K nitrate eutectic. In this reporting period, the electrochemical behavior of Y in the molten nitrate has been characterized. The results show that Y, like Cu, can also be electrochemically injected as a soluble species in the melt. A Y foil electrode was found to be very electrochemically active throughout the entire region of stability of the melt as shown by the current vs voltage curves in Fig. 2. Hence the material can readily dissolve by anodic electrolysis in the melt for voltages above-1 V. Note that a relatively low cathodic current occurs for potentials from -1 V to -1.9 V since the overvoltage for the solvent breakdown (-1.4 V on Pt) is dramatically shifted to more negative potentials at the Y surface. GRA

N91-29470# Naval Postgraduate School, Monterey, CA.
LITHIUM ION SOURCE FOR SATELLITE CHARGE CONTROL M.S. Thesis
Tae I. Song Jun. 1990 59 p
(AD-A238272) Avail: NTIS HC/MF A04 CSCL 09/1

A lithium ion source using thermal emission from mineral beta-eucryptite was investigated as a possible control device for spacecraft charging. This source can be used for control of positively charged spacecraft potentials in sunlight and differentially charged spacecraft surfaces in shadow. The dependence is studied of the emitted ion current on several parameters: source temperature (power input), source bias potentials and potentials applied to simulated spacecraft geometries. Saturation current of about 5.8 micro amp were measured at an extraction potentials of 100 Volts from a source of 0.317 sq cm surface area with a power input of 18 Watts. The lifetime due to ion exhaustion was found to be approx. 200 hours for this compact source. The results indicate that this type of ion source may represent an effective charge control device for spacecraft. GRA

N91-29471# Harry Diamond Labs., Adelphi, MD.
SPIKE LEAKAGE AND BURNOUT OF SILICON PIN DIODE MICROWAVE LIMITERS Summary Report, Oct. 1988 - Nov. 1990
Alford L. Ward, Robert J. Tan, and Roger Kaul Jun. 1991 57 p
(AD-A238392; HDL-TR-2195) Avail: NTIS HC/MF A04 CSCL 09/1

Microwave limiters are used to protect sensitive electronics

from damage due to exposure to high levels of RF radiation. The two major limitations to the operation of PIN diode limiters are spike leakage, power transmitted before limiting action begins, and damage to the limiter itself due to high power. A combined theoretical and experimental study of spike leakage and burnout has been made for silicon PIN diodes. The diodes ranged in intrinsic-level thickness from 0.5 to 50 micron. Thin diodes, emphasized in this study, have little spike leakage but are damaged at relatively low power. Thick diodes withstand very high powers but have large spike leakage. Although qualitative agreement between the calculations and measurements is excellent, there are important areas of quantitative disagreement. Reasons for the disagreement are suggested. The computer program DIODE, used for the calculations, is described, as are the methods used in the experimental measurements. Useful comparisons have also been made of dc transients and of the forward-biased RF conductivity of the PIN diodes. Suggestions for further work are made.
Author (GRA)

N91-29472# Stanford Univ., CA. Lab. of Physics.
PHYSICAL CONCEPTS AND MODELING PROCEDURES FOR PICOSECOND AND SUBPICOSECOND DISTRIBUTED CIRCUITS Final Report
D. M. Bloom and B. A. Auld Jun. 1991 97 p
(Contract N00014-85-K-0381)
(AD-A238592; SU-GL-4840) Avail: NTIS HC/MF A05 CSCL 09/1

The development of advanced high-speed digital devices and integrated circuits has been spurred by a number of applications, including fiber-optic digital data transmission at gigahertz rates, high-throughput computing, and wideband signal processing. Military interest in high-speed digital electronics stems from the need to rapidly acquire, digitize, and process very large amounts of data in EW systems. Associated with the needs for high-speed logic are commensurate demands for broadband analog signal processing, interface, and I/O electronics. Such circuits include correlators, broadband adaptive filters, picosecond-resolution sample-and-hold gates, and multigigahertz-rate D/A and A/D converters. For the digital and analog circuits mentioned, ultra-wide bandwidth instrumentation of superior speed is required for measuring the devices to be employed. It is primarily this critical need for ultra-wide bandwidth instrumentation that has been addressed through the work done under this contract. Without such a capability for performing picosecond and subpicosecond measurements of electrical phenomena, it will be impossible to correctly engineer and characterize devices and circuits required for the applications listed above. GRA

N91-29473# Naval Ocean Systems Center, San Diego, CA.
InP AND InGaAs SUBMICRON GATE MICROWAVE POWER TRANSISTORS FOR 20 GHz APPLICATIONS
G. A. Johnson, M. D. Biendender, and V. J. Kapoor Jun. 1991 5 p
(AD-A238595) Avail: NTIS HC/MF A01 CSCL 09/1

In GaAs, MISFET's with 0.7 micron gate lengths and 0.2 mm gate widths have demonstrated an output power density of 0.92 W/mm at 18 GHz with a corresponding power gain and power-added efficiency of 3.2 dB and 29 percent, respectively. At 20 GHz, an output power density of 0.79 W/mm was obtained with a corresponding gain and power-added efficiency of 3.0 dB and 23 percent, respectively. GRA

N91-29474# Naval Postgraduate School, Monterey, CA.
USE OF AN EXTENDED KALMAN FILTER M.S. Thesis
Juan J. Sanchez Sep. 1990 92 p
(AD-A238639) Avail: NTIS HC/MF A05 CSCL 17/11

The error introduced by the DF accuracy of three direction finding equipments used on board two surface units providing bearing measurements is used to evaluate the performance of the ESM systems through the Extended Kalman Filter equations, and to appreciate the result in the estimation process by evaluating how the improvement of the tracking process is reduced as the error introduced by the DF accuracy of the ESM systems is increased. The process is conducted at three different scenarios involving a change in course of 0, 45 and 90 degrees, and it can be seen how the maneuver detection algorithm stop working when the DF accuracy reaches 4.6 deg. for the second scenario and 9.6 deg. for the scenario Nr 3. GRA

N91-29475# Department of the Navy, Washington, DC.
PYRITE CATHODE MATERIAL FOR A THERMAL BATTERY Patent Application
J. P. Pemsler, inventor (to Navy) and J. K. Litchfield, inventor (to Navy) 7 Feb. 1991 11 p
(AD-D014945; US-Patent-Appl-SN-652156) Avail: NTIS HC/MF A03 CSCL 10/3

The present invention relates in general to a synthetic cathode material for a molten salt battery and, more particularly, to a process of providing and using synthetic pyrite for use as a cathode in a thermal battery. These batteries, which have been successfully used in a number of military applications, include iron disulfide cathode material obtained as benefacted or from natural occurring pyrite deposits, or as a byproduct of flotation concentrate from the processing of base or noble metal ores. GRA

N91-29476# National Inst. of Standards and Technology, Gaithersburg, MD. Center for Electronics and Electrical Engineering.
TECHNICAL PUBLICATION ANNOUNCEMENTS COVERING CENTER PROGRAMS, JULY TO SEPTEMBER 1990, WITH 1991 CEEE EVENTS CALENDAR
J. A. Gonzalez Apr. 1991 31 p
(PB91-184754; NISTIR-4537) Avail: NTIS HC/MF A03 CSCL 09C

Information is given on the technical work of the National Institute of Standards and Technology. The third quarter of the calendar year 1990 is covered. Topics discussed include the semiconductor technology program; the signals and systems metrology program; fast signal acquisition, processing, and transmission; electrical systems; and electromagnetic interference.
Author

N91-29477# Los Alamos National Lab., NM.
EFFECTS OF DOPING ON HYBRIDIZATION GAPPED MATERIALS
P. C. Canfield, J. D. Thompson, M. F. Hundley, A. Lacerda, and Z. Fisk Jun. 1991 12 p Presented at the International Conference on Magnetism, Edinburgh, Scotland, 1-7 Sep. 1991
(Contract W-7405-eng-36)
(DE91-014611; LA-UR-91-2014; CONF-910903-1) Avail: NTIS HC/MF A03

Doping studies are presented on three materials exhibiting hybridization gaps: Ce3Bi4Pt3, U3Sb4Pt3, and CeRhSb. In the case of trivalent La, Y, or Lu substituting for Ce or U, there is a suppression of the low temperature gap and an increase in the electronic specific heat, gamma. In the case of tetravalent Th substitutions for U there is no change in gamma and in the case of tetravalent Zr substitution for Ce in CeRhSb, there is an enhanced semiconductor-like behavior in the electrical resistance. These results are discussed in the light of a simple model of hybridization gapped systems. DOE

N91-29478# Sandia National Labs., Albuquerque, NM.
HIGH GAIN PHOTOCONDUCTIVE SEMICONDUCTOR SWITCHING
F. J. Zutavern, G. M. Loubriel, M. W. OMalley, W. D. Helgeson, and D. L. McLaughlin 1991 6 p Presented at the 8th IEEE Pulsed Power Conference, San Diego, CA, 17-19 Jun. 1991
(Contract DE-AC04-76DP-00789)
(DE91-014668; SAND-90-2813C; CONF-910640-12) Avail: NTIS HC/MF A02

Switching properties are reported for high gain photoconductive semiconductor switches (PCSS). A 200 ps pulse width laser was used in tests to examine the relations between electric field, rise time, delay, and minimum optical trigger energy for switches which reached 80 kV in a 50 ohm transmission line with rise times as

short as 600 ps. Infrared photoluminescence was imaged during high gain switching providing direct evidence for current filamentation. Implications of these measurements for the theoretical understanding and practical development of these switches are discussed. DOE

N91-29479# Sandia National Labs., Albuquerque, NM.
A COMPACT 200 kV PULSE TRANSFORMER SYSTEM
G. J. Rohwein, R. N. Lawson, and M. C. Clark 1991 3 p Presented at the 8th IEEE Pulsed Power Conference, San Diego, CA, 17-19 Jun. 1991
(Contract DE-AC04-76DP-00789)
(DE91-014669; SAND-90-2815C; CONF-910640-13) Avail: NTIS HC/MF A01

Compact, lightweight pulse power systems are being developed to drive RF generators. The most feasible method of meeting these requirements is with high voltage PFN-Pulse Transformer (PPT) systems capable of driving the microwave tubes directly from the ouput of the transformer. To test the feasibility of this approach, a PPT system was designed and tested with an Split Cavity Oscillator (SCO) microwave generator. Results of the tests demonstrated satisfactory performance with this load and driver combination. The PPT system was designed with a 10X voltage step-up transformer and a 0.5 ohm, 2 micro-s PFN. The maximum rated output voltage of the transformer was 200 kV with a 50 ohm load. DOE

N91-29480# Los Alamos National Lab., NM.
COMPUTATIONAL SIMULATIONS OF PLASMA FLOW SWITCHES AND IMPLODING LOADS
D. L. Peterson, R. L. Bowers, J. H. Brownell, A. E. Greene, and N. F. Roderick 29 May 1991 13 p Presented at the 8th IEEE Pulsed Power Conference, San Diego, CA, 17-19 Jun. 1991
(Contract W-7405-eng-36)
(DE91-014768; LA-UR-91-1924; CONF-910640-24) Avail: NTIS HC/MF A03

The Procyon system in the Los Alamos Trailmaster foil implosion project is intended to produce soft x-ray radiation by delivering about 1 MJ of kinetic energy to an imploding plasma liner. The final switching stage of this system will be a Plasma Flow Switch (PFS) which delivers current to the cylindrical foil load. 1-D and 2-D simulations are now being conducted to examine: the initiation of the PFS plasma: the dynamics of the PFS and its switching efficiency; the load implosion and resulting radiation output. Considered here, for the PFS and imploding load, are the effects of electrode walls, perturbations, and radiation. Comparisons with experiments (using the 1.5 MJ Pegasus capacitor bank) are also described. DOE

N91-29481# Oak Ridge National Lab., TN.
SUPERCONDUCTIVITY INDUCED BY VERY HIGH MAGNETIC FIELDS: THERMODYNAMIC AND TRANSPORT PROPERTIES
M. Rasolt Jun. 1991 38 p Presented at the Gordon Godfrey Workshop on Condensed Matter Physics: Strongly Correlated Electron Systems, Sydney, Australia, 1-5 Jul. 1991
(Contract DE-AC05-84OR-21400)
(DE91-015327; CONF-910795-1) Avail: NTIS HC/MF A03

We discuss the progress made in the last few years in understanding the properties of superconductors in very high magnetic fields. A key point we wish to emphasize is that the usual frustration of a superconductor, reflected in diamagnetic pair breaking, is completely obviated when all electrons reside in only a few Landau levels. A new relation between the superconducting order parameter and the magnetic field now exists which permits a strong enhancement of the critical temperature with increasing magnetic field. The issue of Pauli pair breaking and the effect of impurities in this new state are also discussed along with the important observation that the attractive component of the effective electron-electron interaction is enhanced with increasing magnetic field. DOE

N91-29482# Argonne National Lab., IL.
PERFORMANCE AND LIFE EVALUATION OF ADVANCED BATTERY TECHNOLOGIES FOR ELECTRIC VEHICLE APPLICATIONS
W. H. DeLuca, K. R. Gillie, J. E. Kulaga, J. A. Smaga, A. F. Tummillo, and C. E. Webster 1991 11 p Presented at the 1991 Society of Automotive Engineers (SAE) Future Transportation Technology Conference, Portland, OR, 5-8 Aug. 1991
(Contract W-31-109-eng-38)
(DE91-015671; ANL/CP-72919; CONF-9108115-1) Avail: NTIS HC/MF A03

Advanced battery technology evaluations are performed under simulated electric vehicle (EV) operating conditions at the Argonne Analysis and Diagnostic Laboratory (ADL). The ADL provides a common basis for both performance characterization and life evaluation with unbiased application of tests and analyses. This paper summarizes the performance characterizations and life evaluations conducted in 1990 on nine single cells and fifteen 3- to 360-cell modules that encompass six technologies: (Na/S, Zn/Br, Ni/Fe, Ni/Cd, Ni-metal hydride, and lead-acid). These evaluations were performed for the Department of Energy and Electric Power Research Institute. The results provide battery users, developers, and program managers an interim measure of the progress being made in battery R and D programs, a comparison of battery technologies, and a source of basic data for modelling and continuing R and D. DOE

N91-29483# Sandia National Labs., Albuquerque, NM.
EXPERIMENTAL AND ANALYTICAL STUDY OF LASER-TRIGGERING IN THE RIMFIRE SWITCH
B. N. Turman, A. E. Rodriguez, and K. J. Touryan (Tetra Corp., Albuquerque, NM.) 1991 4 p Presented at the 8th IEEE Pulsed Power Conference, San Diego, CA, 17-19 Jun. 1991
(Contract DE-AC04-76DP-00789)
(DE91-014662; SAND-90-3020C; CONF-910640-25) Avail: NTIS HC/MF A01

The Rimfire multi-stage gas switch is a low-jitter switch that was developed to meet high-voltage and low-jitter requirements for the PBFA-2 pulsed power accelerator. The first stage is laser-triggered. Streak and framing camera data have been collected to determine the closure time, jitter, and optimum parameters for laser triggering. Three phases of closure are observed: (1) fast discharge phase, (2) channel heating phase, and (3) current conduction phase. Gap closure time and jitter are measured as a function of voltage laser energy, and focal position. A computer model has been developed with sufficient physics detail to provide good agreement with these data. SF(sub 6) Boltzmann kinetics, multi-photon laser ionization, and photodetachment are included. The photodetachment rate is shown to be a critical parameter in determining the minimum trigger energy for an undervolted SF(sub 6) gap. The model gives good agreement with experimental closure times and minimum laser energy requirements. DOE

N91-29484# Sandia National Labs., Albuquerque, NM.
ASPECTS OF FATIGUE AND RAPID DEPOLARIZATION IN THE FILM PZT CAPACITORS
R. D. Nasby, J. R. Schwank, M. S. Rodgers, and S. L. Miller 1991 14 p Presented at the 3rd International Symposium on Integrated Ferroelectrics, Colorado Springs, CO, 3-5 Apr. 1991
(Contract DE-AC04-76DP-00789)
(DE91-014904; SAND-91-0237C; CONF-9104274-1) Avail: NTIS HC/MF A03

Discrepancies in switched polarization values obtained with pulse measurements and hysteresis measurements were observed in ferroelectric PZT thin film capacitors. The differences are partially attributed to the effects of rapid depolarization. To measure rapid depolarization a pulse was applied to pole a ferroelectric capacitor; and then a second identical pulse of the same polarity was applied after a specified time. Significant switched charge was observed after the second pulse. This depolarization was observed to occur in the time frame from microseconds to seconds. Secondly, the effect of cycling voltage on fatigue was studied on several samples

processed by different vendors. A strong dependence on voltage was obtained for one sample which can be characterized using a voltage activation approach. A second sample showed no appreciable effect of cycling voltage on fatigue. The difference in behavior demonstrates that the dependence of the fatigue mechanism on voltage can vary significantly depending on sample preparation. DOE

N91-29485# Ames Lab., IA.
THE ac LOSSES IN TYPE-2 SUPERCONDUCTORS
J. R. Clem 1991 35 p Presented at the Three-Day International Workshop on AC Susceptibility, Coolfont, WV, 20-22 May 1991
(Contract W-7405-eng-82)
(DE91-015201; IS-M-669; CONF-9105147-1) Avail: NTIS HC/MF A03

This paper discusses the physics of ac losses in type-2 superconductors and in multifilamentary superconducting-normal composite conductors. As an introduction, the ac eddy-current losses in a homogeneous normal conducting cylindrical specimen subjected to an alternating applied magnetic field are briefly reviewed. The ac losses in a superconducting cylindrical specimen are discussed in detail, with emphasis on the losses in a specimen subjected to an alternating applied longitudinal magnetic field. In general, dissipation occurs via both flux-flow losses, which are analogous to eddy-current losses in the normal state, and hysteretic losses, which arise from bulk and surface pinning as well as annihilation of vortices of the opposite sense. Tests are suggested by which the dominant loss mechanisms can be identified. Special considerations are noted for the case of the high-temperature superconductors. Finally, the losses in multifilamentary superconducting-normal composite conductors are discussed. DOE

N91-29486# Lawrence Livermore National Lab., CA.
SIMULATION OF THE GROWTH OF Mo/Si MULTILAYERS
D. B. Boercker and W. L. Morgan (Kinema Research, Monument, CO.) Jul. 1991 12 p Presented at the Society of Photo-Optical Instrumentation Engineers (SPIE) Meeting, San Diego, CA, 21-26 Jul. 1991
(Contract W-7405-eng-48)
(DE91-015679; UCRL-JC-107890; CONF-9107115-13) Avail: NTIS HC/MF A03

The successful development of soft x ray projection lithography will depend heavily on the production of efficient, durable optical components. A leading candidate for x ray mirrors near 130A is multilayer structures made of alternating thin layers of Mo and Si. High resolution electron microscopy reveals that the interface created by deposition of Mo on Si is much more diffuse than that produced by depositing Si on Mo. Molecular dynamics simulations were performed of the deposition process and observe significant penetration of the Si substrates by incident Mo atoms, while Si atoms remain on the surface of the Mo substrates. DOE

N91-29487# Sandia National Labs., Albuquerque, NM.
GASEOUS PREBREAKDOWN PROCESSES THAT ARE IMPORTANT FOR PULSED POWER SWITCHING
T. H. Martin, J. F. Seamen, D. O. Jobe, and G. E. Pena (Ktech Corp., Albuquerque, NM.) 1991 5 p Presented at the 8th IEEE Pulsed Power Conference, San Diego, CA, 17-19 Jun. 1991
(Contract DE-AC04-76DP-00789)
(DE91-015902; SAND-91-1102C; CONF-910640-30) Avail: NTIS HC/MF A01

This paper is the latest in a series of papers that attempt to relate the multiple observed gas breakdown phenomena to useful switch design parameters. This series started when the gas density, not the gas type, was observed to give a power law relationship for the breakdown delay time delays of several gases to the applied electric field. This paper will show that this triggering or breakdown initiating process is similar to, if not the same as, a corona discharge. A hypothesis is made and a simple voltage breakdown relationship is shown to exist for air gaps between 1 and 1000 cm for sharp electrodes to a plane. DOE

34 FLUID MECHANICS AND HEAT TRANSFER

Includes boundary layers; hydrodynamics; fluidics; mass transfer; and ablation cooling.

For related information see also *02 Aerodynamics* and *77 Thermodynamics and Statistical Physics.*

N91-29488*# Tennessee Univ. Space Inst., Tullahoma.
A FINITE ELEMENT SOLVER FOR 3-D COMPRESSIBLE VISCOUS FLOWS Final Report
K. C. Reddy, J. N. Reddy, and S. Nayani Jan. 1990 72 p
(Contract NAS8-36555)
(NASA-CR-184175; NAS 1.26:184175) Avail: NTIS HC/MF A04 CSCL 20D

Computation of the flow field inside a space shuttle main engine (SSME) requires the application of state of the art computational fluid dynamic (CFD) technology. Several computer codes are under development to solve 3-D flow through the hot gas manifold. Some algorithms were designed to solve the unsteady compressible Navier-Stokes equations, either by implicit or explicit factorization methods, using several hundred or thousands of time steps to reach a steady state solution. A new iterative algorithm is being developed for the solution of the implicit finite element equations without assembling global matrices. It is an efficient iteration scheme based on a modified nonlinear Gauss-Seidel iteration with symmetric sweeps. The algorithm is analyzed for a model equation and is shown to be unconditionally stable. Results from a series of test problems are presented. The finite element code was tested for couette flow, which is flow under a pressure gradient between two parallel plates in relative motion. Another problem that was solved is viscous laminar flow over a flat plate. The general 3-D finite element code was used to compute the flow in an axisymmetric turnaround duct at low Mach numbers. Author

N91-29489# Lawrence Livermore National Lab., CA.
NUMERICAL SIMULATION OF A VISCOUS VORTEX RING INTERACTION WITH A DENSITY INTERFACE
D. L. Marcus and J. B. Bell 1991 12 p Presented at the 10th AIAA Computational Fluid Dynamics Conference in Conjunction with the 22nd AIAA Fluid Dynamics, Plasma Dynamics and Lasers Conference and the 26th AIAA Thermophysics Conference, Honolulu, 24-26 Jun. 1991
(Contract W-7405-eng-48)
(DE91-011532; UCRL-JC-105183-Rev-1; CONF-910651-2-Rev-1) Avail: NTIS HC/MF A03

The incompressible Navier-Stokes equations are solved for the interaction of a vortex ring with a density interface. Axisymmetric and three-dimensional calculations are performed for a range of interface strengths, for both Boussinesq and finite-amplitude density jumps. Secondary and tertiary ring formation, vortex rebound, and backflow jets are some of the features observed in the interactions. DOE

N91-29490# National Research Council of Canada, Ottawa (Ontario).
COMPUTATIONAL FLUID DYNAMICS AT NRC: A DIRECTORY OF PRACTITIONERS AND ACTIVITIES
Jun. 1989 15 p
(NRC-TTP-02-89; CTN-91-60018) Copyright Avail: NTIS HC/MF A03

Computational Fluid Dynamics (CFD) involves numerical solutions to the equations which describe the motions of fluids. Analytical routines can provide rapid and cost-effective means of studying a broad range of flow phenomena and design options. This directory provides a very brief overview of the people, the problems, and the programs currently active in the CFD field at the National Research Council Canada. Author (CISTI)

N91-29491# Pittsburgh Energy Technology Center, PA.
STEADY FLOW OF A FLUID-SOLID MIXTURE BETWEEN PARALLEL PLATES

G. Johnson, K. R. Rajagopal (Pittsburgh Univ., PA.), M. Masoudi, and M. P. Mathur May 1991 77 p
(DE91-013114; DOE/PETC-TR/91/7) Avail: NTIS HC/MF A05

In Part 1, a mathematical description for a flowing mixture of solid particulates and a fluid is developed within the context of Mixture Theory. Specifically, the equations governing the flow of a two-component mixture of a Newtonian fluid and granular solid are derived. These relatively general equations are then reduced to a system of coupled ordinary differential equations describing steady flow of the mixture between flat plates. The resulting boundary value problem is solved numerically and results are presented for cases in which drag and lift interactions are important. Part 2 gives an overview of the methods used to obtain the numerical solutions. Multiple shooting, finite difference, and collocation methods for solving boundary value problems involving ordinary differential equations are discussed. A method for applying integral boundary conditions is then presented. Finally, the relative efficiency and effectiveness of the methods is discussed. DOE

N91-29492# Johns Hopkins Univ., Baltimore, MD.
NUMERICAL AND PHYSICAL MODELLING OF BUBBLY FLOW PHENOMENA
A. Prosperetti Apr. 1991 4 p
(Contract DE-FG02-89ER-14043)
(DE91-013646; DOE/ER-14043/2) Avail: NTIS HC/MF A01

The work carried out in the period 1 Apr. 1990 - 31 Mar. 1991 has primarily been concerned with two problems related to the direct numerical simulation of the motion of spheres or bubbles in a liquid. The first problem is the calculation of the coefficients of added mass and drag for randomly placed bubble subject to an imposed oscillatory flow. The principal finding of this work has been the remarkable insensitivity of these coefficients to details of the flow and the surprisingly good performance of simple estimates already available in the literature. The second aspect of the work has been the development of a mathematical and numerical approach to the simulation of the transport of spheres by a liquid flow. Thirdly, we have implemented numerically a two-phase flow model based on averaged equations that will be used for comparisons with the direct numerical simulation results. DOE

N91-29493# Royal Aircraft Establishment, Farnborough (England).
THEORETICAL STUDY OF THE FLOW IN A ROTATING DUCT. EXPERIMENTAL STUDY THROUGH FLOW VISUALIZATION IN A CURVED DUCT
Joel Guidez, Pierre-Jaques Michard, Denis Dutoya, and Jean Perucchini Jan. 1991 24 p Previously announced as N90-21032 Original language document announced as A90-11153
(RAE-Trans-2189; BR-302896) Avail: NTIS HC/MF A03

An experimental and theoretical study of heat transfer and flow in a rotating duct is under development. The duct simulates an internal cooling passage of the blade of a turbine rotor. It was experimentally demonstrated that the rotational velocity causes an increase in thermal exchange by convection in the duct. This phenomenon is explained by secondary flows due to Coriolis force. The theoretical aspect of the work involves the solution of the Navier-Stokes equations in three dimensions. For both laminar and turbulent flows, the results obtained demonstrate the significance of secondary structures (having both two and four vortices). Also, by using a rotation-curvature analogy, visualization of the flow with air or hydrogen bubbles in a water duct gives rise to the same flow structures. Author

N91-29494# National Aeronautical Lab., Bangalore (India).
SOLUTIONS OF TWO-DIMENSIONAL EULER EQUATIONS WITH MULTIGRID ACCELERATION
S. Mahajan and A. Kumar Mar. 1990 29 p
(NAL-PD-CF-9006) Avail: NTIS HC/MF A03

A multigrid scheme is applied to accelerate the convergence of a solution of two-dimensional Euler equations to steady state. Results for flow over airfoils are presented. Author

N91-29495 Ohio State Univ., Columbus.
SECONDARY STABILITY AND THREE-DIMENSIONAL NATURAL CONVECTION IN A SHALLOW CAVITY Ph.D. Thesis
Tzyy-Ming Wang 1990 152 p
Avail: Univ. Microfilms Order No. DA9105233

Natural convection in a shallow cavity whose top and bottom boundaries are made of insulated material is considered. The length and width of the cavity are considered to be much larger than its height. With the right wall heated, flow along it is driven upward by a bouyancy force. In the cold end on the left, cooler fluid sinks to the bottom. Because the lid and the base constrain the fluid to flow horizontally to the cold end through the top half and back to the hot end through the bottom half of the cavity, parallel fully viscous flow develops in the center. For low Prandtl number fluids, the central parallel flow region occupies most of the cavity. Since researchers were interested in the flow of liquid metals, they take the horizontal extent to be infinite for theoretical purposes and focus on the parallel flow in the central part of the cavity. Direct three dimensional simulations were carried out for a flow resulting from subharmonic resonance. The migration of the axes of the transverse cells as a result of tertiary flow changing in the spanwise direction is described. Dissert. Abstr.

N91-29496# Pittsburgh Energy Technology Center, PA.
MODIFICATION OF THE 'TEACH' COMPUTER CODE FOR USE IN A STUDY OF SWIRLING TURBULENT FLOWS
C. C. Hwang, Genxing Zhu (Pittsburgh Univ., PA.), M. Massoudi, and J. M. Ekmann Mar. 1991 172 p
(DE91-010492; DOE/PETC-TR/91/3) Avail: NTIS HC/MF A08

For high-intensity pressurized combustors, swirl has been used to improve the flame stability and to produce higher rate of entrainment of the ambient fluid and fast mixing. Traditionally, designers relied heavily on experiments to design combustors. This approach is now being supplemented with theoretical and computational modeling techniques. Typical of the present generation of fluid dynamic computer codes being developed for combustor simulation is the TEACH solution procedure. The TEACH code uses the two-equations k-epsilon turbulence model for turbulent flow prediction. It has been suggested that the assumptions leading to the formulation of the k-epsilon model are inadequate for the modeling of turbulence in high swirling flows. Recently, Speziale (1987) has developed a non-linear k-epsilon model which extends the range of validity of the standard k-epsilon model while maintaining most of the interesting feature of the k-epsilon model, for example, the ease of application in existing Computational Fluid Dynamics (CFD) codes. The objectives of this work is to evaluate a modified version of the TEACH code (STARPIC) for its value in analyzing swirling flows in devices such as high-intensity combustors. Additional modifications include: (1) non-linear k-epsilon model, (2) cyclone geometry, and (3) particle trajectory submodel. Simple computational tests have been run to compare results from this code with other computational and experimental data. DOE

N91-29497 Pennsylvania State Univ., University Park.
A NUMERICAL STUDY OF FLOW PAST A CYLINDRICAL BODY Ph.D. Thesis
Jiahn-Horng Chen 1990 134 p
Avail: Univ. Microfilms Order No. DA9117663

The nature of the flow past a circular cylinder was a classic problem. A closely related flow was considered in which the cylinder is located in a 2-D channel with a steady fully developed velocity distribution far upstream and downstream of the body. Through the use of numerical computations, some fundamental phenomena were investigated associated with the motion, such as formation of the recirculating flow to the rear of the cylinder and the stability of the symmetric steady flow that is found at small Reynolds numbers. The effect of the blockage ratio of the cylinder to the channel width on the flow development is investigated. One of the main conclusions of the study is that the unique branch of flows at small Reynolds numbers loses stability through a Hopf

bifurcation to a time-periodic flow, rather than through a symmetry-breaking bifurcation to an asymmetrical steady flow. Dissert. Abstr.

N91-29498 California Inst. of Tech., Pasadena.
STATISTICAL MECHANICS OF TWO-DIMENSIONAL EULER EQUATIONS AND JUPITER'S GREAT RED SPOT Ph.D. Thesis
Jonathan Miller 1991 101 p
Avail: Univ. Microfilms Order No. DA9113609

For the first time, a statistical mechanics is constructed for the 2-D Euler fluid which respects all conservation laws. Mean field equations are derived for the equilibrium, and it is shown that they are exact. The methods ought to apply to a wide variety of Hamiltonian systems possessing an infinite family of Casimirs. The theory is illustrated by a comparison to numerical simulations of Jupiter's Great Red Spot. Dissert. Abstr.

N91-29499 Stanford Univ., CA.
THE EVOLUTION AND STRUCTURE OF HOMOGENEOUS STABLY STRATIFIED SHEARED TURBULENCE Ph.D. Thesis
Steven E. Holt 1991 205 p
Avail: Univ. Microfilms Order No. DA9115784

The structure and evolution of homogeneous stably stratified sheared turbulence was investigated through direct numerical simulation. In these simulations the primary dimensionless parameter is the Richardson number which measures the relative importance of stratification and mean shear. The effects of other dimensionless parameters were investigated. Dissert. Abstr.

N91-29500# Argonne National Lab., IL.
ANALYSIS OF CONDENSATION AND EVAPORATION OF AMMONIA/WATER MIXTURES IN MATRIX HEAT-EXCHANGERS
C. B. Panchal and B. Arman 1991 9 p Presented at the ASME/AIChE/ANS National Heat Transfer Conference, Minneapolis, 26-31 Jul. 1991
(Contract W-31-109-eng-38)
(DE91-014461; ANL/CP-71621; CONF-910739-23) Avail: NTIS HC/MF A02

A theoretical analysis is carried out for the condensation and evaporation of water/ammonia mixtures in matrix heat-exchangers. A set of equations is formulated and a calculation algorithm is developed to predict the local rate of heat and mass transfer for binary-component systems. A thermodynamic property model is developed for ammonia/water mixtures on the basis of the Peng-Robinson equation of state. The two-phase flow heat-transfer coefficient for matrix heat-exchangers is calculated by using the analytical method developed in a previous study. The experimental data are analyzed to determine the effects of small amounts of water in ammonia on the rate of evaporation. The role of diffusion in simultaneous heat and mass transfer associated with condensation and evaporation processes are analyzed by comparing the results from three limiting cases, which include equilibrium conditions, and liquid-phase diffusion- resistance of finite and infinite values. The results show that the vapor-phase mass-transfer resistance is the controlling mechanism for condensation, and the liquid-phase mass-transfer resistance is the controlling mechanism for evaporation. DOE

N91-29501# Argonne National Lab., IL.
ADIABATIC TWO-PHASE FLOW FRICTIONAL PRESSURE DROP. PART 2: A GENERALIZED METHOD FOR DATA CORRELATION
N. T. Obot, M. W. Wambsganss, J. A. Jendrzejczyk (Illinois Univ., Chicago.), and D. M. France 1991 21 p Presented at the ASME/AIChE/ANS National Heat Transfer Conference, Minneapolis, MN, 26-31 Jul. 1991
(Contract W-31-109-eng-38)
(DE91-014462; ANL/CP-72529-Pt-2; CONF-910739-22-Pt-2)
Avail: NTIS HC/MF A03

A generalized method, based on the frictional law of corresponding states, is proposed for the correlation of two-phase flow frictional pressure drop data. It is validated using air-water data obtained on narrow rectangular channels and a circular tube for valves of total mass flux (G) in the 50 to 2000 kg/sq meter range. As with single phase flow, the results indicate that two-phase pressure drop for air-water mixture can be predicted from the proposed correlations provided the critical parameters are known. The fact that the critical parameters are observed to occur for values of quality (x) less than 0.01 for 50 (le) G (le) 2000 kg/sq meters makes it clear that pressure drop data for the x less than 0.01 range are needed in order to apply the proposed method, just as laminar flow data are needed for the single phase counterpart. DOE

N91-29502# Argonne National Lab., IL.
ADIABATIC TWO-PHASE FLOW FRICTIONAL PRESSURE DROP. PART 1: CRITICAL PARAMETERS AND FRICTION FACTORS FOR AIR-WATER MIXTURE
N. T. Obot, M. W. Wambsganss, J. A. Jendrzejczyk (Illinois Univ., Chicago.), and D. M. France 1991 25 p Presented at the ASME/AIChE/ANS National Heat Transfer Conference, Minneapolis, 26-31 Jul. 1991
(Contract W-31-109-eng-38)
(DE91-014463; ANL/CP-72528-Pt-1; CONF-910739-21-Pt-1)
Avail: NTIS HC/MF A03

An analysis of air-water frictional pressure drop data for horizontal ducts was made. For small diameter, circular tubes and narrow rectangular channels, it is established that the frictional pressure deep profiles with increasing mixture quality (or superficial gas velocity) are characterized by critical values for gas Reynolds number, quality and friction factor. These characteristic features are in evidence for tests in which the total mass flux of the mixture is held fixed with increasing quality or superficial gas velocity. The effects of duct geometry and total mass flux on the critical parameters are documented and discussed. The results for two-phase flow friction factors are also presented. DOE

N91-29503# Argonne National Lab., IL.
PREDICTION OF THE PRESSURE DROP IN TRANSVERSE, REPEATED-RIB TUBES WITH NUMERICAL MODELING
B. Arman and T. Rabas 1991 8 p Presented at the ASME/AIChE/ANS National Heat Transfer Conference, Minneapolis, 26-31 Jul. 1991
(Contract W-31-109-eng-38)
(DE91-014465; ANL/CP-73141; CONF-910739-19) Avail: NTIS HC/MF A02

The obvious advantages resulting from the improved thermal performance achieved with enhanced heat-exchanger tubes are a reduction of the energy consumption and/or a reduction in the heat-exchanger size and cost. On the other hand, the improvement in the heat-transfer performance comes with an increased pressure-drop penalty. It is equally important to be able to predict both the pressure-drop and the heat-transfer performance of enhanced tubes in order to properly evaluate their effectiveness. The purpose of this paper is to demonstrate that numerical modeling can be used to predict the pressure drop in heat-exchanger tubes with transverse, repeated ribs. The maximum departure from experimental results was about 50 percent but for most cases the departures were much less, especially for the smaller rib heights and larger rib spacings. This successful demonstration of numerical modeling was obtained, however, for one of least complicated enhancement flow fields. DOE

N91-29504# Pittsburgh Univ., PA. Dept. of Physics and Astronomy.
THE PHYSICS OF PATTERN FORMATION AT LIQUID INTERFACES
J. V. Maher Jun. 1991 13 p
(Contract DE-FG02-84ER-45131)
(DE91-014529; DOE/ER-45131/9) Avail: NTIS HC/MF A03

This report discusses the following physics of liquid interfaces: pattern formation; perturbing Saffman-Taylor flow with a small gap-gradient; scaling of radial patterns in a viscoelastic solution; dynamic surface tension at an interface between miscible liquids; and random systems. DOE

N91-29505# Los Alamos National Lab., NM.
SHOCK ACCELERATION WITH TURBULENCE MINIMIZATION
N. M. Hoffman 1991 20 p Presented at the Workshop on Physics of Compressible, Turbulent Mixing, Royaumont (France), 17-19 Jun. 1991
(Contract W-7405-eng-36)
(DE91-014741; LA-UR-91-1993; CONF-9106222-1) Avail: NTIS HC/MF A03

We investigate whether there is an optimum way to accelerate an interface so as to minimize the generation of turbulence at the interface, using a k-(var epsilon) simplification of a one-point turbulence model. The problem is to use a finite number of shock waves to bring an interface, initially at rest, to a final velocity V after it has traveled a distance x. We restrict attention to the case of two shock waves, and treat the problem in three phases. The first phase is the initialization of turbulence at the discontinuous interface by the first shock wave, seeded by a spectrum of perturbations on the interface. This sets the initial conditions for the second phase, which is the transport of turbulence and growth of the interface's thickness during the period between shocks. The third phase is the arrival at the interface of the next shock wave, generating turbulence from finite density self-correlation, density-velocity correlation, and turbulence kinetic energy. We assume dissipation of turbulence is negligible, and use a configurational approximation for the density self-correlation, rather than solving an evolution equation for this quantity. We derive an expression for the total turbulence energy after the passage of the second shock wave, as a function of the two variables V(sub 1) (the interface velocity after the passage of the first shock) and t(sub 2) (the time of arrival of the second shock), parametric in the final velocity V, a scale S characterizing the initial perturbation, and the Atwood number A. We find that in the high-Atwood-number, small-perturbation-scale limit, the turbulence energy is maximized if the first shock is somewhat weaker than the second. For accelerations in which 60 percent or more of the final velocity V is acquired in the first shock, the turbulence energy is less than half what it is when only 25 percent of the final velocity is acquired in the first shock. DOE

N91-29506# Lawrence Livermore National Lab., CA.
SHOCKWAVE CONSIDERATIONS FOR SUB-GRID CLOSURE MODELING IN TURBULENT LARGE EDDY SIMULATIONS
A. C. Buckingham 1991 21 p Presented at the 7th International Conference on Numerical Methods in Laminar and Turbulent Flow, Stanford, 15-19 Jul. 1991
(Contract W-7405-eng-48)
(DE91-015142; UCRL-JC-105843; CONF-910720-1) Avail: NTIS HC/MF A03

The development is continued of sub-grid closure procedures tailored specifically for large eddy simulations (LES) in strongly compressible turbulent flow. A time explicit finite difference calculation is used to simulate the resolvable large scale features. The influence of the nonresolvable sub-grid scales on the large, computable scale range are modeled through application of a grid scale dependent, nonlinear eddy viscosity of the classical Smagorinsky form, nu sub t(exp v) = C sub s lambda (exp 2)S, but modified for dynamic viscoelasticity. Here S is the locally evaluated resolvable scale magnitude of the mean strain rate tensor, lambda is a grid length scale, and C sub s is the appropriate Smagorinsky constant. Extended for simulating dynamic viscoelasticity, the sub-grid model mimics the well established (and physically substantial) viscoelastic response of a turbulent field to the influence of an imbedded, interacting shock wave. The model viscoelastic parameters are developed separately from statistical realizations obtained independently from stochastic numerical simulations of shock turbulence interactions. DOE

N91-29507# Lehigh Univ., Bethlehem, PA.
THREE-DIMENSIONAL VORTEX DYNAMICS AND INTERACTIONS IN NEAR-WALL TURBULENT BOUNDARY LAYERS Final Report, 1 Nov. 1988 - 1 Mar. 1991
C. R. Smith and J. D. Walker 30 Mar. 1991 97 p
(Grant AF-AFOSR-0065-89; AF Proj. 2307)
(AD-A237413; AFOSR-91-0504TR) Avail: NTIS HC/MF A05 CSCL 20/4

A model of the three-dimensional dynamic physical processes that occur in the near-wall region of a turbulent flow at high Reynolds numbers is developed. The hairpin vortex is postulated to be the basic flow structure of the turbulent boundary layer. It is shown that the central features of the near-wall flow can be explained in terms of how asymmetric hairpin vortices interact with the background shear flow, with each other, and with the surface layer near the wall. The physical process that leads to the regeneration of new hairpin vortices near the surface is described, as well as the processes of evolution of such vortices to larger-scale motions farther from the surface. The model is supported by important developments in the theory of unsteady surface-layer separation and a number of kernel experiments which demonstrate basic fluid mechanics phenomena relevant to the turbulent boundary layer. Explanations for the kinematical behavior observed in direct numerical simulations of low Reynolds number boundary-layer and channel flows are given. GRA

N91-29508# United Technologies Research Center, East Hartford, CT.
EXPERIMENTAL AND ANALYTICAL STUDY OF RIPPLED TRAILING EDGE AIRFOILS FOR COMPRESSOR APPLICATION Final Report
Bruce L. Morin and Thomas J. Barber May 1991 95 p
(Contract N00014-86-C-0663)
(AD-A237425; UTRC/R89-957707) Avail: NTIS HC/MF A05 CSCL 13/7

Research was conducted to assess potential benefits of using the Rippled Trailing Edge (RTE) concept on compressor airfoils for separation alleviation and wake mixing enhancement. An empirically designed RTE was tested in a highly loaded, simulated compressor cascade that had demonstrated large scale suction side separation with a baseline circular trailing edge. The original RTE design resulted in a 50 percent increase of the chordwise extent of the separated flow compared to the baseline trailing edge. Extensive modifications to the RTE resulted in a fairing that eliminated separation, indicating that RTEs have potential for separation alleviation on compressor trailing edges. However, failure of the first design shows the weaknesses of the empirical RTE design procedure that was used, and that many unknowns still exist regarding the 3-D boundary layer relief concept. Further testing of ripples on more basic, isolated airfoils is suggested to develop further understanding of the 3-D boundary layer relief mechanism, without having to consider the inherent problems associated with the cascade testing. After developing such a data base, RTEs can then be evaluated for application to the more complex case where curvature and three-dimensional effects are significant. GRA

N91-29509# Naval Postgraduate School, Monterey, CA.
NEAR-STALL LOSS MEASUREMENTS IN A CD COMPRESSOR CASCADE WITH EXPLORATORY LEADING EDGE FLOW CONTROL M.S. Thesis
Jeffrey H. Armstrong Jun. 1990 166 p
(AD-A237497) Avail: NTIS HC/MF A08 CSCL 20/4

Loss measurements were conducted using a five-hole conical pneumatic probe in a subsonic wind tunnel containing a modeled cascade of controlled diffusion (CD) stator blades. Following reference measurements at high incidence one blade was modified (slotted at the leading edge) in an attempt to (passively) reduce the size of the leading edge separation bubble and thereby improve performance. Prior to the surveys, the acquisition and reduction software was modified to provide loss calculations using both mass-averaged and fully-mixed-out conditions for the upstream and downstream flows. Results showed that the mass-averaged method provided the more consistent results, and this was explained. The slotted leading edge blade was found to produce less loss than the reference blade, and it was concluded that the control concept should be explored in more detail. GRA

N91-29510# Purdue Univ., West Lafayette, IN. School of Mechanical Engineering.
POLYMER DRAG REDUCTION OF A ZERO PRESSURE GRADIENT BOUNDARY LAYER Technical Report, 1 Dec. 1989 - 30 Nov. 1990
John E. Koskie and William G. Tiederman Feb. 1991 59 p
(Contract N00014-83-K-0183)
(AD-A237572; PME-FM-91-1) Avail: NTIS HC/MF A04 CSCL 20/4

The objective was to determine the response of a zero pressure gradient boundary layer to slot injection of drag reducing polymer solution. Attention was focused on the region far downstream of the injector. Two-component velocity data were acquired with a laser Doppler velocimeter. Mean concentration data were measured using a laser induced fluorescence technique. A 1000 ppm solution of Separan AP-273 was injected into the boundary layer at 1 and 2 times the flow rate of the linear sublayer. Results are based on two component velocity profiles and concentration profiles at four locations downstream of the slot. These locations correspond to momentum thickness Reynolds numbers of 2478, 2978, 3527 and 3935 in an unmodified Newtonian boundary layer. In dimensionless distance from the slot they vary from 52 to 144 times the boundary layer thickness at the slot and 29000 to 81000 wall units using the unmodified Newtonian inner variables at the slot. There are two major conclusions from the present data. First, the sum of the viscous shear and Reynolds stresses in polymer drag reduced boundary layers does not always account for the total shear stress in the inner region of the boundary layer. Some additional stress which is due to the polymer is present. The second conclusion is that the slope of the logarithmic region of the mean velocity profile in a polymer drag reduced flow may increase over the Newtonian slope. The latter feature may depend on the type of polymer additive. GRA

N91-29511# Rensselaer Polytechnic Inst., Troy, NY.
AN EXPERIMENTAL STUDY OF PLUNGING LIQUID JET INDUCED AIR CARRYUNDER AND DISPERSION Quarterly Progress Report
20 Jun. 1991 10 p
(Contract N00014-91-J-1271)
(AD-A237757) Avail: NTIS HC/MF A02 CSCL 20/4

Preliminary analysis was performed on two-phase jet spreading phenomena. Appropriate equations of motion were derived by assembling the relevant equations and adding the appropriate term representing the action of surface tension, which was not originally included. These equations were nondimensionalized for a long, narrow jet. The resulting equations are parabolic, so that numerical solution should be straightforward. The equations of motion are approximated by assuming that the gas volume fraction is small. This allows one use of the known solution for the velocity field in a planar jet for the liquid. If one further approximate the momentum equation for the bubbles by neglecting all effects except drag, virtual mass, and liquid pressure gradient, one can solve the resulting equations for bubble trajectories in the known liquid velocity field. It was assumed that the bubbles do not affect the liquid velocity field and that the gas density is negligible. The resulting equation in Lagrangian form is given with the Tollmein solution for a planar jet used for the liquid velocity. GRA

N91-29512# Wisconsin Univ., Madison. Center for Mathematical Sciences.
PROBLEMS IN NONLINEAR CONTINUUM DYNAMICS Final Report, 15 Sep. 1987 - 14 Apr. 1991
Marshall Slemrod 14 May 1991 7 p
(Grant AF-AFOSR-0315-87; AF Proj. 2304)
(AD-A237844; AFOSR-91-0594TR) Avail: NTIS HC/MF A02 CSCL 20/4

Slemrod's research in 1990 to 1991 centered on two issues: (1) the kinetics of coagulation processes, and (2) behavior of discrete velocity models in the kinetic theory of gases. In the first area Slemrod has given a new method for solving the special class of coagulation equations which exhibit gelatin, and derived and proved existences of similarity solutions for coagulation equations with diffusion. In the second area Slemrod has used his relaxed invariance principle method to prove weak decay to equilibrium for the Broadwell model of gas dynamics in the case of specularly reflective boundary conditions. GRA

N91-29513# David Taylor Research Center, Bethesda, MD. Computation Mathematics/Logistics Dept.
AN EVALUATION OF THE NEKTON PROGRAM Final Report, Oct. 1989 - Sep. 1990
Bill H. Cheng, Janet S. Dean, and Ronald W. Miller Sep. 1990 24 p
(NR Proj. BR0-2301)
(AD-A237888; DTRC/CMLD-90/014) Avail: NTIS HC/MF A03 CSCL 20/4

This report describes the David Taylor Research Center's experiences with the NEKTON program, a computational fluid dynamics tool developed at the Massachusetts Institute of Technology. The theory and applications of the program are reviewed in a literature survey. A number of test cases were run successfully at DTRC and the results are promising. The applicability of NEKTON to high Reynolds number flows with three-dimensional complex geometries will require further study. GRA

N91-29514# Ballistic Research Labs., Aberdeen Proving Ground, MD.
A METHOD OF INVESTIGATING SCALES OF MOTION IN A TURBULENT WAKE Final Report, Dec. 1989 - Aug. 1990
Phillip C. Dykstra and John D. Kuzan Jun. 1991 38 p
(DA Proj. 1L1-62618-AH-80)
(AD-A237923; BRL-MR-3922) Avail: NTIS HC/MF A03 CSCL 20/4

Knowledge of the scales of motion in the flow around a body is important for accurate turbulence modeling in computational fluid dynamic calculations. Useful data can be measured in wind tunnel experiments, but often not for the free flight conditions of interest. This report examines the possibility of determining such information from shadowgraphs taken in a ballistic range. The application of digital scanning machines and spatial correlation interrogation to shadowgraphs are described. One method of analyzing a shadowgraph to extract information about turbulence structures in the flow field is discussed. Results are shown for the analysis of two regions in the wake of a projectile. This method might be used to quantify the effects of various projectile modifications on a turbulent structure, for example the introduction of a base burn unit. GRA

N91-29515# Pennsylvania State Univ., University Park. Applied Research Lab.
UNSTEADY FORCE CALCULATIONS IN TURBOMACHINERY
William C. Zierke Jul. 1991 57 p Sponsored by Naval Sea Systems Command
(AD-A237937; ARL/PSU/TR-91-008) Avail: NTIS HC/MF A04 CSCL 20/4

This report gives a review of the various types of unsteady flow phenomena that occur within a turbomachine and examines existing methods for computing several of these flows. Then, we discuss a method for applying two-dimensional, unsteady, thin airfoil theory in a stripwise manner to compute the unsteady forces and moments on the shaft of a rotor operating within a nonuniform inflow. Techniques for computing these unsteady forces and moments on a rotor blade row with rake and skew are included. GRA

N91-29516# National Taiwan Univ., Taipei. Inst. of Applied Mechanics.
INTERNATIONAL UNION OF THEORETICAL AND APPLIED MECHANICS (IUTAM) SYMPOSIUM ON AEROTHERMODYNAMICS IN COMBUSTORS
Richard S. Lee, J. H. Whitelaw, and T.-S. Wung Jun. 1991 175 p
(AD-A237943; R/D-6636-AN-02) Avail: NTIS HC/MF A08 CSCL 20/4

The subject of aerothermodynamics is playing an ever increasingly critical role in a variety of important industrial and technical problems in the design of combustors. In recent years, it has become the focus of attention among investigators from research laboratories and industries around the world resulting in a large number of meetings on its various aspects every year. However, most of these meetings deal with a certain problem area, for instance that of the global combustion of fuel droplets in a flow. Because of the inherent complexities involved in such flows, the analytical effort has been mostly confined to over-simplified and over-idealized flow systems while the experimental effort has been mostly directed towards global measurements of flows found in industrial applications. With the rapid and phenomenal developments of key research tools mostly in the last two decades, in particular those of modern digital computers, laser optics, and electronics, many of the previously unthinkable, rigorous investigations in real-life flows have gradually become feasible. It is against this background that this international conference on the aerothermodynamics in combustors is being held at this point in time. This symposium involves the presentation of papers concerned with flow and thermodynamic characteristics of combustors, with emphasis on gas-turbine combustors and including information relevant to rocket motors, internal combustion engines and furnaces. GRA

N91-29517# Naval Postgraduate School, Monterey, CA.
EFFECTS OF 1, 2, 3, AND 4 Hz IMPOSED BULK FLOW OSCILLATIONS ON TRANSITION IN A STRAIGHT CHANNEL WITH 40 TO 1 ASPECT RATIO M.S. Thesis
Howard E. Koth Jun. 1990 243 p
(AD-A237988) Avail: NTIS HC/MF A11 CSCL 20/4

A channel with 40 to 1 aspect ratio and rectangular cross section is used to study the effects of imposed oscillations on transition from laminar to turbulent flow. Oscillations are imposed using a single rotating vane located in the flow downstream of the test section. Flows with Reynolds numbers ranging from 1100 to 3580 and Strouhal numbers from 0.0211 to 0.2418 are studied. For all cases, time averaged velocity profiles are unaffected by imposed oscillations. Imposed oscillations have a destabilizing effect on the flow near the edge of the Stokes layer. Turbulence intensity magnitudes with imposed oscillations show that transition to turbulence begins at lower Reynolds numbers and extends over a wider range of Reynolds numbers than when no imposed oscillations are present. In addition, higher levels of intermittency are present with imposed oscillations for Reynolds numbers 1900 to 2200 at y/d = 0.90. At Reynolds numbers from 1450 to 1800, frequency spectra evidence high intensity intermittent turbulent fluctuations, followed and preceded by quiescent flow, both with and without imposed oscillations. A center mode of secondary instability is evidenced by high values of normalized longitudinal turbulence intensity measured in the channel center when no oscillations are imposed on the flow. Imposed oscillations are found to suppress this center mode of secondary instability, as evidenced by reductions in longitudinal turbulence intensity values near the channel center. GRA

N91-29518# Arizona State Univ., Tempe. Dept. of Mechanical and Aerospace Engineering.
SEPARATION-BUBBLE VELOCITY MEASUREMENTS USING AN OSCILLATING-HOT-WIRE SYSTEM Final Technical Report
William S. Saric Jun. 1991 27 p
(Contract N00014-85-K-0527)
(AD-A237997) Avail: NTIS HC/MF A03 CSCL 20/4

A system is developed to allow measurement of both the mean and disturbance flow velocities in separated regions. An oscillating arm assembly provides a directional bias to the hot-wire probe, along with a iinear step assembly, which steps the probe through the boundary layer. This system is used to investigate the flow field associated with laminar separation bubbles. A series of velocity profiles are measured on an FX63-137 airfoil in the chord-Reynolds number range: 150,000 less than or = R sub c less than or = 300,000, at angles of attack of alpha = 12 deg and alpha = 14 deg. Data are presented on the size of the separation bubble and on the location of transition to turbulence. GRA

N91-29519# Naval Postgraduate School, Monterey, CA.
NUMERICAL STUDY OF NON-IMPULSIVELY STARTED FLOW AROUND A CIRCULAR CYLINDER M.S. Thesis
Kent A. Fredrickson Sep. 1990 78 p
(AD-A238051) Avail: NTIS HC/MF A05 CSCL 20/4

The effect of constant acceleration, prior to the establishment of a steady uniform flow, on some of the characteristics of the resulting time-dependent flow about a circular cylinder has been investigated numerically. It is shown that the occurrence of a local maximum drag is dependent on the parameters characterizing the non-impulsive nature of the ambient flow. However, the onset of the wake asymmetry and the evolution of the lift and drag forces during the transient period depend on the characteristics of the numerical perturbation used to initiate the asymmetric vortex shedding. It is concluded that the numerical methods can predict, to varying degrees of accuracy, the behavior of the symmetric state and the quasi-steady-state, but not of the intermediate state. GRA

N91-29520# University of Southern Illinois, Carbondale. Dept. of Physics.
ELECTRO-RHEOLOGY FLUIDS AND LIQUID FUEL FLOW Annual Report, 1 Jul. 1990 - 30 Jun. 1991
Rongjia Tao, Narendra K. Jaggi, and Robert N. Zitter 30 Jun. 1991 18 p
(Contract N00014-90-J-4041)
(AD-A238600) Avail: NTIS HC/MF A03 CSCL 20/4

The goals of this research are: to understand and clarify the physical mechanism underlying the electrorheological (ER) response of fluids and establish an ab initio theory for the phenomenon; to study the structure of ER fluids and their properties in order to investigate the change of viscosity of ER fluids with an applied electric field; to apply the ER phenomenon to liquid fuel flows in order to control their viscosity and hence their velocity; and to examine the necessary theoretical and technique problems associated to the design of a new class of liquid fuel control devices which are based on the ER phenomenon. GRA

N91-29521# Naval Postgraduate School, Monterey, CA.
CONTROL OF FLOW OVER A BACKWARD FACING STEP M.S. Thesis
J. V. Healey Sep. 1990 92 p
(AD-A238638) Avail: NTIS HC/MF A05 CSCL 20/4

The poor aerodynamic design of the superstructures of today's Navy ships create a highly turbulent airwake that can make shipboard helicopter operations quite hazardous. This study is part of a longer-term project to tailor airflow over a ship's helicopter deck in order to improve the poor quality of the airflow. This airflow is thought to be largely responsible for several costly blade strike mishaps involving H-46 helicopters during start-up and shut down. Numerous computer simulations were conducted using the Phoenics Computational Fluid Dynamics code to simulate airflow over a backward-facing-step. The latter represents a simple 2-d model of flow behind a typical hangar/flight deck combination. In each run a deflector of different size, orientation or porosity was placed in a specific location in an attempt to reduce the size of the recirculation zone, the velocities and the turbulence levels. Of the studies involved, a vertical deflector offset downstream with its lower edge at the top of the step produced the best overall results. GRA

N91-29522# Arnold Engineering Development Center, Arnold Air Force Station, TN.
EFFECT OF GEOMETRIC PARAMETERS ON THE PERFORMANCE OF SECOND THROAT ANNULAR STEAM EJECTORS Final Report, 28 Feb. - 30 Sep. 1990
S. E. Stephens and L. B. Bates Jul. 1991 69 p Prepared in cooperation with Sverdrup Technology, Inc., Arnold AFS, TN
(AD-A238645; AEDC-TR-91-2) Avail: NTIS HC/MF A04 CSCL 20/4

Steam ejectors are simple pumps that, among many possible applications, are used in altitude simulation rocket motor testing. Of the two main types of ejectors, annular and centerbody, the latter has been the subject of most previous research. Less is known about the operation of annular ejectors. For example, ejector diffusers that contain a contraction known as a second throat have been studied widely for centerbody configurations; however, very little work has been conducted to determine the effects of specific design variables. The design variables investigated were second throat area ratio has a strong impact on system operation, as expected. The second throat axial position appears to have a mild impact on the overall pressure recovery of the system over most of the range investigated, but with a strong effect when the second throat ramp is moved forward to the steam nozzle outlet. At the point, there is a large degradation in cell pressure. Ramp angle over the range investigated does not have a significant effect on cell pressure. A computational study was also conducted to evaluate the suitability of a single-phase Navier-Stokes computational fluid dynamics (CFD) code for prediction of stream ejector flow fields. The results of the study concluded that the state of the art (circa 1989) was insufficient for the successful prediction of ejector performance. The inability to model the condensation effects is indicated as a major cause of a deficiency. GRA

N91-29523# Department of the Navy, Washington, DC.
TRANSIENT FLOWMETER CALIBRATION FACILITY Patent Application
Paul Lefebvre, inventor (to Navy) 19 Dec. 1990 8 p
(AD-D014937; US-Patent-Appl-SN-632707) Avail: NTIS HC/MF A02 CSCL 13/7

An apparatus for defining the free surface of a moving column of a fluid in a vertical pipe to enhance the accuracy of measurements of transient rate of flow of the fluid using electromagnetic flowmeter is described. It provides a neutrally buoyant plug which stays in contact with the free surface of the column of the fluid at all times and thus defines the free surface of the fluid moving in the vertical pipe accurately and reduces the oscillations of the free surface of the fluid. GRA

N91-29524*# Minnesota Univ., Minneapolis. Dept. of Mechanical Engineering.
NUMERICAL PREDICTION OF TURBULENT OSCILLATING FLOW AND ASSOCIATED HEAT TRANSFER Final Report
W. J. Koehler, S. V. Patankar, and W. E. Ibele Aug. 1991 247 p
(Grant NAG3-1024)
(NASA-CR-187177; NAS 1.26:187177) Avail: NTIS HC/MF A11 CSCL 20D

A crucial point for further development of engines is the optimization of its heat exchangers which operate under oscillatory flow conditions. It has been found that the most important thermodynamic uncertainties in the Stirling engine designs for space power are in the heat transfer between gas and metal in all engine components and in the pressure drop across the heat exchanger components. So far, performance codes cannot predict the power output of a Stirling engine reasonably enough if used for a wide variety of engines. Thus, there is a strong need for better performance codes. However, a performance code is not concerned with the details of the flow. This information must be provided externally. While analytical relationships exist for laminar oscillating flow, there has been hardly any information about transitional and turbulent oscillating flow, which could be introduced into the performance codes. In 1986, a survey by Seume and Simon revealed that most Stirling engine heat exchangers operate in the transitional and turbulent regime. Consequently, research has since focused on the unresolved issue of transitional and turbulent oscillating flow and heat transfer. Since 1988, the University of Minnesota oscillating flow facility has obtained experimental data about transitional and turbulent oscillating flow. However, since the experiments in this field are extremely difficult, lengthy, and expensive, it is advantageous to numerically simulate the flow and heat transfer accurately from first principles. Work done at the University of Minnesota on the development of such a numerical simulation is summarized. Author

N91-29525*# National Aeronautics and Space Administration. Lewis Research Center, Cleveland, OH.
QUALITATIVE INVESTIGATION OF CRYOGENIC INJECTED SHOCK DISSIPATION
R. C. Hendricks 1991 8 p Presented at the Cryogenic Engineering Conference, Huntsville, AL, 11-14 Jun. 1991; sponsored by Univ. of Alabama at Huntsville, and NASA, Huntsville
(NASA-TM-105140; E-6244; NAS 1.15:105140) Avail: NTIS HC/MF A02 CSCL 20D

The injection of fluid nitrogen into the flow discharged from a two-dimensional, ambient, static-temperature and static pressure Mach = 2.7 nitrogen flow tunnel was observed. A bow shock stands approximately one diameter off the end of the 3.2 mm o.d. x 1.6 mm i.d. injection tube placed directly into the tunnel exhaust. Cryogenic injection creates a high density region in the injected region and within the bow shock wake but the standoff distance remains unchanged. However as the temperature reaches a critical value the sharp shock interface begins to fade resembling the density gradient seen at the interface of a supercritical fluid and the shock interface begins to move into the supersonic stream. As the injection temperature decreases, the interface continues to move into the supersonic stream and becomes more diffuse; the shock interface can not be distinguished. The phenomena is completely reversible. Author

N91-29526# Environmental Protection Agency, Ada, OK. Environmental Research Lab.
APPROXIMATE MULTIPHASE FLOW MODELING BY CHARACTERISTIC METHODS Summary Report, Oct. 1988 - Sep. 1990
J. W. Weaver May 1991 129 p
(PB91-190959; EPA/600/2-91/015) Avail: NTIS HC/MF A07 CSCL 20D

The flow of petroleum hydrocarbons, organic solvents and other liquids that are immiscible with water presents the nation with some of the most difficult subsurface remediation problems. One aspect of contaminant transport associated releases of such liquids is the transport as a water-immiscible liquid phase. Approximate models of immiscible flow are presented for two- and three-phase flow. The approximations are constructed by representing the flow by hyperbolic equations which have method of characteristics solutions. This approximation has the additional benefit of being based on the fundamental wave behavior of the flow, which is revealed by the solutions of the models. An important result is that for three-phase flow, two flow regimes exist. The first is characterized by the displacement of one of the liquids into a bank which moves ahead of the other liquid. The second is characterized by almost complete bypassing of a liquid by the other. The occurrence of the flow regimes is dependent on the organic liquid properties, soil type and the initial amounts of the fluids present. Author

N91-29527*# National Inst. of Standards and Technology, Boulder, CO. Chemical Engineering Div.
HEAT TRANSFER AND PRESSURE DROP IN A COMPACT PIN-FIN HEAT EXCHANGER WITH PIN ORIENTATION AT 18 DEG TO THE FLOW DIRECTION
D. A. Olson Feb. 1991 78 p Sponsored by NASA. Langley Research Center
(NASA-CR-186544; NAS 1.26:186544; PB91-194464; NISTIR-3965) Avail: NTIS HC/MF A05 CSCL 20D

The heat transfer and pressure drop characteristics of a novel, compact heat exchanger in helium gas were measured at 3.5 MPa and Reynolds numbers of 450 to 12,000. The pin-fin specimen consisted of pins, 0.51 mm high and spaced 2.03 mm on centers, spanning a channel through which the helium flows; the angle of the row of pins to the flow direction was 18 deg. The specimen was radiatively heated on the top side at heat fluxes up to 74

W/sq cm and insulated on the back side. Correlations were developed for the friction factor and Nusselt number. The Nusselt number compares favorably to those of past studies of staggered pin-fins, when the measured temperatures are extrapolated to the temperature of the wall-fluid interface. Author

N91-29528# Lawrence Livermore National Lab., CA.
ELECTROFORMING THIN CHANNEL HEAT EXCHANGERS
C. P. Steffani Jun. 1991 10 p Presented at the SURFIN 1991, Toronto (Canada), 24-28 Jun. 1991
(Contract W-7405-eng-48)
(DE91-015114; UCRL-JC-106908; CONF-9106238-1) Avail: NTIS HC/MF A02

Research at Lawrence Livermore National Laboratory has shown that thin channel heat exchangers can be produced on bimetallic mandrels by the stack and plate method. Depth to width ratios of 100 to 1 are easily produced, with other ratios dependent on heating or cooling requirements. Mass production of these plates may be possible using reel to reel methods. Future generations of heat exchangers may be produced via composite electroforming, chemical vapor deposition (CVD) or physical vapor deposition (PVD). DOE

N91-29529# Doty Scientific, Inc., Columbia, SC.
MICROTUBE STRIP HEAT EXCHANGER
F. D. Doty Jul. 1991 8 p
(Contract DE-FG01-90CE-15440)
(DE91-015223; DOE/CE-15440/T3) Avail: NTIS HC/MF A02

During the last quarter, Doty Scientific, Inc. (DSI) continued to make progress on the microtube strip (MTS) heat exchanger. The DSI completed a heat exchanger stress analysis of the ten-module heat exchanger bank; and performed a shell-side flow inhomogeneity analysis of the three-module heat exchanger bank. The company produced 50 tubestrips using an in-house CNC milling machine and began pressing them onto tube arrays. The DSI revised some of the tooling required to encapsulate a tube array and press tubestrips into the array to improve some of the prototype tooling. DOE

N91-29530# Lawrence Livermore National Lab., CA.
ENERGY GENERATION BY A SHOCK CROSSING A PERTURBED INTERFACE
W. P. Crowley and E. W. Burke 29 May 1991 19 p Presented at the Workshop on Physics of Compressible, Turbulent Mixing, Royaumont (France), 17-19 Jun. 1991
(Contract W-7405-eng-48)
(DE91-015678; UCRL-JC-107409; CONF-9106222-3) Avail: NTIS HC/MF A03

The investigation is directed toward determining, computationally, the amount of perturbed kinetic energy that is generated by a shock passing over a perturbed interface. The traditional experimental approach is to make measurements on a perturbed flow, obtain mean values from these data and to define the difference between the mean and the instantaneous as the perturbed energy. The approach is amenable to numerical simulations as well and the fluctuating kinetic energy (FKE) obtained from it was described by Besnard. Another approach is to obtain two computational results, one perturbed and the other unperturbed and to define the perturbed energy as the difference between these two. This approach is not amenable to physical experiments; from it was derived perturbed kinetic energy (PKE) defined below. Results from the two methods are compared. DOE

N91-29531# Rensselaer Polytechnic Inst., Troy, NY. Center for Multiphase Research.
USE OF ELECTRICAL IMPEDANCE IMAGING IN TWO-PHASE, GAS-LIQUID FLOWS
J. T. Lin, L. Ovacik, O. C. Jones, J. C. Newell, M. Cheney, and H. Suzuki (Hitachi Ltd., Japan) 1991 12 p Presented at the ASME/AIChE/ANS National Heat Transfer Conference, Minneapolis, MN, 26-31 Jul. 1991
(Contract DE-FG07-90ER-13032)
(DE91-015914; CONF-910739-27) Avail: NTIS HC/MF A03

The determination of interfacial area density in two-phase, gas-liquid flows is one of the major elements impeding significant development of predictive tools based on the two-fluid model. Currently, these models require coupling of liquid and vapor at interfaces using constitutive equations which do not exist in any but the most rudimentary form. Work described herein represents the first step towards the development of electrical impedance computed tomography (EICT) for nonintrusive determination of interfacial structure and evolution in such flows. DOE

35 INSTRUMENTATION AND PHOTOGRAPHY

Includes remote sensors; measuring instruments and gages; detectors; cameras and photographic supplies; and holography.

For aerial photography see *43 Earth Resources and Remote Sensing*. For related information see also *06 Aircraft Instrumentation*, and *19 Spacecraft Instrumentation*.

N91-29532# National Bureau of Standards, Washington, DC.
STANDARD NIM INSTRUMENTATION SYSTEM
May 1990 66 p Revised
(DE90-010387; DOE/ER-0457T) Avail: NTIS HC/MF A04

The Nuclear Instrument Module (NIM) is a standard modular instrumentation system that is in wide use throughout the world. As the NIM system developed and accommodations were made to a dynamic instrumentation field and a rapidly advancing technology, additions, revisions and clarifications were made. These were incorporated into the standard in the form of addenda and errata. This standard is a revision of the NIM document, AEC Report TID-20893 (Rev. 4) dated July 1974. It includes all the addenda and errata items that were previously issued as well as numerous additional items to make the standard current with modern technology and manufacturing practice. DOE

N91-29533# National Aeronautical Establishment, Ottawa (Ontario). Unsteady Aerodynamics Lab.
LABORATORY EVALUATION OF PORTABLE AND WALK-THROUGH EXPLOSIVES VAPOUR DETECTORS
Lorne Elias and Pavel Neudorfl Mar. 1990 26 p Presented at the 3rd Symposium on Analysis and Detection of Explosives, Mannheim, Fed. Republic of Germany, 10-13 Jul. 1989 Sponsored in part by Transport Canada
(NAE-LTR-UA-104; CTN-91-60015) Copyright Avail: NTIS HC/MF A03

Thirteen different explosives vapor detectors (EVD) were quantitatively tested for their response to certain nitroorganics, particularly ethylene glycol dinitrate (EGDN), as part of an assessment of their overall efficacy in field use. Eleven of these instruments are housed in carrying cases for portability, two are designed as fixed-installation portals for personal screening. Instruments tested were of two types: (1) continuous, fast acting devices based on electron capture detection (ECD) or ion mobility spectrometry (IMS), usually in conjunction with semi-permeable membranes; and (2) slower, batch sampling, gas chromatographic equipment with ECD using vapor preconcentrators. Sensitivity was measured by subjecting the instrument under test to known controllable levels of exposives vapors from a dynamic vapor source. The continuous EVDs had response times of a few seconds, poor to good selectivity, and a lower detection limit in the 1 to 100 ppb range; the GC based instruments were 100 times more sensitive, considerably more specific, but required 0.5 to 3 minutes per analysis. CISTI

N91-29534# National Aeronautical Establishment, Ottawa (Ontario). Structures and Materials Lab.
STRAIN GAUGE CABLING, CONDITIONING, AND SENSITIVITY CALCULATIONS FOR THE CT-114 (TUTOR) AIRCRAFT AFT FUSELAGE AND EMPENNAGE FULL-SCALE FATIGUE TEST
P. A. Adams and R. A. Brackett 22 Feb. 1990 36 p Sponsored

by Department of National Defense
(NAE-LTR-ST-1758; CTN-91-60021) Copyright Avail: NTIS HC/MF A03

The monitoring of strain on the aft fuselage and empennnage of the CT-114 is accomplished by the cabling, conditioning and sensitivity calculations described. Gauge types and locations simulate a subset of those which formed part of the CL-41 flight load survey strain gauge report by Canadair. Eighty-eight bridges are monitored. Eight of those include original flight load survey gauges. The effect of lead resistances are figured into the calculations of shunt strain simulation. Two data acquisition systems were employed. Sixty out of a 64 channel system manufactured by MTS Systems Corp QUAD system were used along with 30 channels on a Hewlett Packard system. Cabling and calculations spreadsheets as well as schematics of quarter, half and full bridge set-ups are included for each system. Author (CISTI)

N91-29535# National Aeronautical Establishment, Ottawa (Ontario). Structures and Materials Lab.
LOAD TABLES FOR THE AVERY AND GILMORE STANDARD FORCE MACHINES CORRECTED FOR GRAVITY, 1989
C. W. MacKenzie 5 Jun. 1989 44 p
(NAE-LTR-ST-1703; CTN-91-60028) Copyright Avail: NTIS HC/MF A03

The actual forces exerted by the weights in the Avery and Gilmore Standard Force machines in the National Aeronautical Establishment are dependent on the local gravitational acceleration. The last gravitational measurements were made in 1966. In preparation for updating the gravity effect values, the Geophysics Divison obtained new measurements based on gravity ties to two absolute gravity sites used in the Canadian Gravity Standardization Network. The new gravity measurements were used to correct the applied force values for both standard force machines. The correction procedures and tables of corrected forces are detailed. A QuickBasic program is provided for the calculation of a table of forces for Avery deadweights in kgt, newtons, lbf (at standard gravity) and lbf (corrected for machine height). CISTI

N91-29536# Oak Ridge National Lab., TN.
MATERIALS SCIENCE APPLICATIONS OF A 120 kV FEG TEM/STEM: TRISKAIDEKAPHILIA
J. Bentley, A. T. Fisher, E. A. Kenik, and Z. L. Wang 1991 2 p Presented at the 49th Electron Microscopy Society of America (EMSA) Annual Meeting, San Jose, 4-9 Aug. 1991
(Contract DE-AC05-84OR-21400)
(DE91-010136; CONF-910870-7) Avail: NTIS HC/MF A01

The introduction by several manufacturers of 200kV transmission electron microscopes (TEM) equipped with field emission guns affords the opportunity to assess their potential impact on materials science by examining applications of similar 100-120kV instruments that have been in use for more than a decade. This summary is based on results from a Philips EM400T/FEG configured as an analytical electron microscope (AEM) with a 6,585 scanning transmission (STEM) unit, EDAX 9100/70 or 9900 energy dispersive X-ray spectroscopy (EDS) systems, and Gatan 607 serial- or 666 parallel-detection electron energy-loss spectrometers (EELS). Examples in four areas that illustrate applications that are impossible or so difficult as to be impracticable with conventional thermionic electron guns are described. DOE

N91-29537# Sandia National Labs., Albuquerque, NM.
USING QUARTZ CRYSTAL MICROBALANCES TO SIMULTANEOUSLY SENSE MASS ACCUMULATION AND SOLUTION PROPERTIES
S. J. Martin, V. E. Granstaff, G. C. Frye, and A. J. Ricco 1991 8 p Presented at the Transducers 1991 Conference, San Francisco, 23-27 Jun. 1991
(Contract DE-AC04-76DP-00789)
(DE91-011501; SAND-91-0064C; CONF-9106116-4) Avail: NTIS HC/MF A02

A lumped-element equivalent circuit model is presented that describes the near resonance electrical characteristics of a quartz crystal microbalance (QCM) simultaneously loaded by a surface mass layer and a contacting liquid. The model was derived by solving the boundary-value problem for coupled mechanical displacement and electrical potential; this results in circuit elements that are explicitly related to physical properties of the quartz, the perturbing mass layer, and the contacting liquid. The effects of mass and/or liquid loading on the admittance-vs-frequency behavior are predicted from the model and compared with experimental impedance analyzer measurements. Surface mass accumulation causes a simple translation in frequency of the resonance peak, while increasing the density-viscosity product of the contacting solution causes both a translation and damping of the resonance peak. Using the model, changes in surface mass can be differentiated from changes in solution properties. DOE

N91-29538# Los Alamos National Lab., NM.
A SLIT APERTURE FOR THE MONITORING X RAY EXPERIMENT (MOXE)
J. C. Lochner and W. C. Priedhorsky 1991 13 p Presented at the Society of Photo-Optical Instrumentation Engineers (SPIE) Meeting, San Diego, 21-26 Jul. 1991
(Contract W-7405-eng-36)
(DE91-013317; LA-UR-91-1654; CONF-9107115-1) Avail: NTIS HC/MF A03

We have investigated a slit aperture as an alternative to the square pinhole aperture for the MOXE detectors, which are to be put on the Soviet satellite Spectrum X-Gamma. A slit offers advantages for better discrimination of sources in crowded regions, eliminates the need for support structures for the aperture window, and does not compromise the signal-to-noise ratio (S/N) of a point source. We find that in a single 24 hr pointing of the satellite, MOXE can determine the position of a 10 mCrab source to better than 0.5 degrees with the slit. The structure of a titanium grate which supports the detector's beryllium window constrains the slit to be 0.5 cm x 2.56 cm, oriented at an angle of 26.6 degrees to either side of the center lines of the detector. We illustrate an arrangement of the slits on each of the six detectors which optimizes source localization for a number of pointings. DOE

N91-29539 Texas Univ., Austin.
MEASUREMENT OF A THREE-DIMENSIONAL HYPERSONIC DENSITY FIELD USING HOLOGRAPHIC INTERFEROMETRY Ph.D. Thesis
Stephen Eugene Doerr 1990 184 p
Avail: Univ. Microfilms Order No. DA9116847

The objective of this work was to develop a holographic interferometry system to measure and analyze density distributions about a generic maneuvering reentry vehicle in a hypersonic wind tunnel. This data is needed to understand the flow physics better so that accurate models of the processes that govern the dynamics and thermodynamics of the flow can be developed and validated. A dual-plate holographic interferometry system, providing full-field, non-intrusive measurements, was developed to acquire data at a given projection angle. The phase of the modulated laser wave was determined from the interferograms using a digital phase shifting method with a measurement resolution of 100 microns. Cross sectional distributions were then recovered from the phase measurements using an algebraic reconstruction technique. The data base obtained consisted of a series of density distributions at axial locations of interest. The interferometric data was supplemented with surface measurements, schlieren and oil flow photographs. Analysis of the data showed an extensive region of separated flow around the control surfaces, resulting in loss of control effectiveness and severe localized heating, which could not be modeled by the computational solution used for comparison. Holographic interferometry was shown to be a viable measurement technique for obtaining accurate, 3D density distributions in a hypersonic wind tunnel. Dissert. Abstr.

N91-29540# Los Alamos National Lab., NM.
FULL-FIELD FABRY-PEROT INTERFEROMETER
A. R. Mathews, R. M. Boat, W. F. Hemsing, R. H. Warnes, and G. R. Whittemore 1991 5 p Presented at the 1991 American

Physical Society (APS) Conference on Shock Compression of Condensed Matter, Williamsburg, VA, 17-20 Jul. 1991
(Contract W-7405-eng-36)
(DE91-014610; LA-UR-91-2020; CONF-9107105-42) Avail: NTIS HC/MF A01

This paper describes the use of a Fabry-Perot interferometer for simultaneously measuring velocity at many points on the surface of a shock-loaded solid. The method is based upon work reported by S. Gidon and G. Behar in 1986, but the data analysis has been improved by the application of image-processing techniques. Light from a pulsed single-frequency laser is focused onto a moving target and the returned Doppler-shifted image passed through a Fabry-Perot interferometer. Output of the interferometer is a set of fringes that are formed for specific combinations of wavelength and light angle. These fringes are recorded on film for subsequent analysis. Fringe position determines the velocity for each point on the target that forms a fringe. A method for determining the velocity as a function of both position and time will also be discussed. DOE

N91-29541# Sandia National Labs., Albuquerque, NM.
SUPERCONDUCTING INSTRUMENTATION FOR PRECISION MEASUREMENT AND CONTROL
R. V. Duncan 1991 4 p Presented at the International Conference on Superconducting and Quantum Effect Devices and Their Applications, Berlin, Fed. Republic of Germany, 18-21 Jun. 1991
(Contract DE-AC04-76DP-00789)
(DE91-014650; SAND-91-0725; CONF-910661-1) Avail: NTIS HC/MF A01

The Josephson series-array voltage standard (JAVS) has dramatically improved the level to which high-accuracy electrical equipment may be monitored and stabilized. For example, a small pressure dependence in the output of some solid-state voltage standards has been measured with the JAVS. The use of two such series-arrays in a superconductive loop promises to be a new method of ultra-small frequency difference measurement. The accuracy of these new measurement configurations is set by the superconductive loop inductance and the Josephson junction parameters. DOE

N91-29542# Los Alamos National Lab., NM.
VISAR: LINE-IMAGING INTERFEROMETER
W. F. Hemsing, A. R. Mathews, R. H. Warnes, M. J. George, and G. R. Whittemore 1991 5 p Presented at the 1991 American Physical Society (APS) Conference on Shock Compression of Condensed Matter, Williamsburg, VA, 17-20 Jul. 1991
(Contract W-7405-eng-36)
(DE91-014749; LA-UR-91-1973; CONF-9107105-39) Avail: NTIS HC/MF A01

A line-imaging Velocity Interferometer System for Any Reflector (VISAR) was applied to measure velocity across the diameter of a metal plate explosively accelerated to 5.5 km/s. Amplified, single-frequency laser light was focused to illuminate a line on the metal surface. The line's image was focused through the interferometer to a streak camera that swept in time and recorded directly on film. During the experiment, the Doppler-shift caused motion of the interference fringes. Analysis of the digitized film record yielded a continuum of time-resolved velocity histories. Velocity gradients across the plate that first swept radially inward, then reflected outward, were clearly measured. Increased power provided by the laser amplifier greatly improved the signal-to-noise ratio compared to our previous line VISAR experiments. DOE

N91-29543# Virginia Univ., Charlottesville. Dept. of Electrical Engineering.
DESIGN AND ANALYSIS OF MULTI-SENSOR SEQUENTIAL DETECTION SYSTEM Final Report, Jan. - Dec. 1989
Quan-Ming Chang and Demetrios Kazakos Jul. 1991 116 p
(Contract F30602-81-C-0169)
(AD-A238012; RL-TR-91-92) Avail: NTIS HC/MF A06 CSCL 17/9

A multiple sensor system is considered under binary hypothesis environments. All sensors are assumed independent, and the observed data is also independent. Received data is quantized and then sent to the fusion center to determine whether a target is present. The Sequential Probability Ratio Test is employed in the fusion center. The objective to find an optimal system by minimizing the expected number of observations. Both two-level and four-level quantizer are used in the process of finding the optimal system. Numerical evaluations are made to find the quantizer which minimize the expected number of observations that are required to decide the presence of the target. System simulations are also performed to confirm the results. GRA

N91-29544# Michigan Univ., Ann Arbor. Dept. of Electrical Engineering and Computer Science.
INVESTIGATION OF SUPERRESOLUTION BY INCOHERENT TO COHERENT CONVERSION Final Report, Jul. 1988 - Mar. 1991
Emmett N. Leith 22 May 1991 6 p
(Contract DAAL03-88-K-0177)
(AD-A238111; Rept-88-1316-PI; ARO-25896.1-PH) Avail: NTIS HC/MF A02 CSCL 14/1

The superresolution method was applied to the problem of imaging through inhomogeneities. The process was combined with phase conjugation imaging, thereby producing a very generalized process for imaging through inhomogeneities. In particular, a one-pass phase conjugation process is effectively converted into a two-phase conjugation process. In addition, various other related methods for imaging through inhomogeneities were invented, the most successful being a process that combines electronic holography with femtosecond pulse technology. GRA

N91-29545# Battelle Memorial Inst., Research Triangle Park, NC.
THE DEVELOPMENT OF A FIBER-OPTIC READOUT PRESSURE TRANSDUCER Final Report, Jun. 1990 - Jan. 1991
Joseph H. Haritonidis Jun. 1991 18 p
(Contract DAAL03-86-D-0001)
(AD-A238393; BRL-CR-665) Avail: NTIS HC/MF A03 CSCL 14/2

An all-optical pressure measurement system has been developed that uses a highly reflective diaphragm as the sensing element for a pressure transducer. This type of pressure transducer offers improved sensitivity, free from electrical and magnetic disturbances. Laser light is reflected off of the fiber's end and from the diaphragm. The reflections travel back into the same fiber and are combined interferometrically to create interference fringes. These fringes shift proportionally to the diaphragm's deflection. The return signal is sent to a photodetector and analyzed for pressure variations. Author (GRA)

N91-29546# Universal Energy Systems, Inc., Dayton, OH.
COUNTERDOPED HIGH TEMPERATURE, SILICON ARRAY INFRARED DETECTOR Final Report, Apr. 1986 - Apr. 1987
John A. Baker May 1991 88 p
(Contract F33615-86-C-5091)
(AD-A238483; WL-TR-91-4048) Avail: NTIS HC/MF A05 CSCL 17/5

A counterdoped infrared detector system consisting of a silicon substrate doped with boron and divacancies has been created. High purity polycrystalline silicon was further purified by float zoning to reduce the impurity levels still present; it was then back doped with boron. Electron irradiation was used to create the divacancies which become the active infrared centers. Boron served to compensate the newly created divacancies thus producing only positively charged divacancies; these positively charged divacancies are stable under illumination. The experimental results thus verify the theoretical model postulated by Elliott for counterdoping. A theoretical analysis of multivalent statistics as applied to counterdoped detectors has developed an extended model for counterdoped detectors. This model has identified the relevant parameters which control the operating temperature and figure of merit for the counterdoped detector. The model may be

used to optimize doping concentration for the highest background limited infrared photoconductor (BLIP) operating temperature.
Author (GRA)

N91-29547# Naval Postgraduate School, Monterey, CA.
EXPERIMENTAL ANALYSIS OF B-DOT SENSORS M.S. Thesis
Holly L. Nye Jun. 1990 165 p
(AD-A238487) Avail: NTIS HC/MF A08 CSCL 14/2

A new design for non-self integrating magnetic-loop sensors (B-dots) has been developed at Los Alamos National Laboratory. Experiments and tests were performed using the Relativistic Electron Beam Experiment (REX) machine to compare the B-dot sensors to optical beam diagnostics (streak camera). The B-dots were assessed to have the capability of measuring the REX electron beam's position to within 0.25mm with 2 percent error, and its transverse oscillatory movement to within 0.5mm amplitude with 7 percent error, over a 1 GHz bandwidth. Many calibration parameters and factors affecting sensor signals were examined during the experiment. The experimental calibration of the B-dots, and the resulting certified accuracy of their remote, non-intrusive measurements of relativistic electron beam parameters should have a wide range of application to many other electron beam machines. Author (GRA)

N91-29548# Lawrence Livermore National Lab., CA.
AN ELEVATED TEMPERATURE TITRATION CALORIMETER
J. R. Smith, P. L. Zanonato, and G. R. Choppin (Florida State Univ., Tallahassee.) Jun. 1991 19 p
(Contract W-7405-eng-48)
(DE91-015765; UCRL-CR-107905) Avail: NTIS HC/MF A03

A variable-temperature (313 K to 353 K) titration calorimeter of high sensitivity has been constructed. The purpose of the calorimeter is to study temperature effects on the enthalpies of complex formation and of other reactions of metal cations such as hydrolysis and precipitation. Operation of the calorimetric system, including that final calculation of the heat released during titration, is automatic via computer control. Calibration tests of the calorimeter using 2-amino 2-hydroxymethyl 1,3-propanediol gave -(46.0 +/- 0.3) kJ/mol and -(46.2 +/- 0.2) kJ/mol for the enthalpy of protonation, at 318 K and at 343 K, respectively. For titrations of 2-bis(2-hydroxyethyl) amino 2-hydroxymethyl 1,3-propanediol, enthalpy of protonation values of -(28.4 +/- 0.3) kJ/mol and -(29.3 +/- 0.2) kJ/mol were obtained at 318 K and at 343 K, respectively. DOE

N91-29549# Sandia National Labs., Albuquerque, NM.
VIDEO FRAME STORE: AN ADVANCED SOLID STATE RECORDER
Tan Thai and J. Walker 1991 9 p Presented at the 32nd Institute of Nuclear Materials Management (INMM) Annual Meeting, New Orleans, LA, 28-31 Jul. 1991
(Contract DE-AC04-76DP-00789)
(DE91-015709; SAND-91-1667C; CONF-910774-9) Avail: NTIS HC/MF A02

In many security applications, solid state recorders (SSRs) have been used to quickly record and playback video images of a scene when an alarm occurs in that scene. Unlike video cassette recorders (VCRs) which take a second or two to start, SSRs can respond to a command from a host computer in less than 1/30th of a second. Therefore, they can be a very useful tool for assessing video alarms. Current commercial SSRs, however, have four major drawbacks: high cost; inability to record asynchronous videos; inflexible system configuration; and inability to guarantee the integrity of the response to the host's commands. The Video Frame Store (VFS) is an advanced SSR that provides an effective solution to the above problems. The VFS consists of commercial hardware products and Sandia-developed software. A VFS unit that stores 128 video frames costs less than half of a typical SSR. In addition to the many basic features of a typical SSR, the VFS also provides a number of advanced features: user friendly menu for system configuration and setup; expandable video memory size from a minimum of 32 frames to a maximum of 512 frames; image pan, scroll and zoom; and reduction of image resolution to increase storage capacity. The hardware and software implementation as well as the advanced features is discussed. DOE

36 LASERS AND MASERS

Includes parametric amplifiers.
For related information see also *76 Solid-State Physics.*

N91-29550# Lawrence Livermore National Lab., CA.
SDIO LASER PROPULSION WORKSHOP Summary Report
J. T. Kare Jun. 1989 32 p Workshop held in Stanford, CA, 17-18 Oct. 1988
(Contract W-7405-eng-48)
(DE90-011758; UCID-21719; CONF-8810506-1) Avail: NTIS HC/MF A03

The workshop concentrated on the double-pulse planar thruster. Theoretical and computer modelling results were presented by Physical Sciences, Inc. (PSI) and by the Stanford University group. Several groups presented new results from small scale experiments. The double-pulse concept illustrated has been shown to work, in that two closely spaced pulses do remove less mass and produce more thrust with higher efficiency than a single pulse (or two widely spaced pulses) with the same total energy. However, the best efficiencies reported are still only about 10 percent (kinetic energy of exhaust/total laser energy in), although specific impulses of 600 to 1000 seconds appear to be easy to achieve. Both the theoretical and the experimental results point to a strong need for longer pulse experiments; some of these are already planned, and were discussed in detail. Various alternative thrusters were discussed briefly; groups working on CW laser thrusters were invited to the workshop but were unable to attend. Systems issues were discussed only very briefly. DOE

N91-29551# Lawrence Livermore National Lab., CA.
PROGRAM AND APPLICATIONS FOR A NEAR-TERM LASER LAUNCH SYSTEM
J. T. Kare Jun. 1989 10 p
(Contract W-7405-eng-48)
(DE90-011760; UCID-21718) Avail: NTIS HC/MF A02

This note discusses possible applications of a minimum-size laser launch system capable of launching 20 kg payloads into orbit. Such a launcher could greatly reduce the cost, and increase the capability, of space-based system, particularly in connection with Brilliant Pebbles technology. The ongoing SDIO Laser Propulsion Program has experimentally demonstrated the basic properties of a laser propulsion thruster, and analyzed many of the physics and technology issues involved in building a launcher. This note also presents the outline of a 5 year program to build such a launcher, starting with a modest extension of the current SDIO Program. DOE

N91-29552# Advanced Research and Applications Corp., Sunnyvale, CA.
DIAGNOSTIC SUPPORT SERVICES FOR LLNL (LAWRENCE LIVERMORE NATIONAL LABORATORY) NOVA LASER EXPERIMENTS Final Report, 1 Nov. 1988 - 31 Mar. 1990
10 Apr. 1990 6 p
(Contract W-7405-eng-48)
(DE90-012125; UCRL-CR-103900) Avail: NTIS HC/MF A02

Advanced Research and Applications Corporation (ARACOR) provided diagnostic support services to the NOVA Laser Experimental Program. The support services consisted of personnel attending to the fielding, analysis, and calibration of diagnostic instruments on the NOVA Laser system. The specific systems supported were the DANTE, FFLEX, and HENWAY spectrometers. Particular services for each diagnostic system fell into four support categories: (1) generation of setup and data acquisition configuration data; (2) availability during experimental series to address real time contingencies; (3) instrument calibration; and (4) software generation as directed by the cognizant contract

technical monitor. This is a final report for the period 1 November 1988 through 31 March 1990. DOE

N91-29553# Sandia National Labs., Albuquerque, NM.
DIODE LASER IGNITION OF EXPLOSIVE AND PYROTECHNIC COMPONENTS
R. G. Jungst and F. J. Salas 1990 23 p Presented at the Optoelectronics 1990, Albuquerque, 5-7 Jun. 1990
(Contract DE-AC04-76DP-00789)
(DE90-012227; SAND-90-0641C; CONF-9006190-2) Avail: NTIS HC/MF A03

The Laser Diode Ignition (LDI) program at Sandia Laboratories has as its objective the development of optically ignited analogs to the presently used low energy, hot wire igniters, DDT detonators, and actuators. In our concept, optical energy would be transmitted from a diode laser to the explosive or pyrotechnic power via a fiber optic. The laser energy is coupled to the energetic powder through a hermetically sealed optical feedthrough in the charge cavity. Optical ignition has many advantages, most of which are related to the removal of electrical leads to the powder interface. This eliminates concerns such as sensitivity to electrostatic discharge and electromagnetic radiation, conductance after fire, and isolation resistance. The optical interface would also not have the corrosion tendency that has occasionally been a problem with bridgewires. Another convenient property of diode laser sources is that the current and voltage needed to drive them are quite similar to those now applied to bridgewires for hot wire ignition. Therefore LDI devices would have an overall electrical requirement which is nearly identical to that of the hot wire components they are replacing. DOE

N91-29554*# Simpson Weather Associates, Inc., Charlottesville, VA.
SPACE-BASED DOPPLER LIDAR SAMPLING STRATEGIES: ALGORITHM DEVELOPMENT AND SIMULATED OBSERVATION EXPERIMENTS Final Report
G. D. Emmitt, S. A. Wood, and M. Morris 15 Jul. 1990 111 p
(Contract NAS8-37779)
(NASA-CR-184172; NAS 1.26:184172) Avail: NTIS HC/MF A06 CSCL 20E

Lidar Atmospheric Wind Sounder (LAWS) Simulation Models (LSM) were developed to evaluate the potential impact of global wind observations on the basic understanding of the Earth's atmosphere and on the predictive skills of current forecast models (GCM and regional scale). Fully integrated top to bottom LAWS Simulation Models for global and regional scale simulations were developed. The algorithm development incorporated the effects of aerosols, water vapor, clouds, terrain, and atmospheric turbulence into the models. Other additions include a new satellite orbiter, signal processor, line of sight uncertainty model, new Multi-Paired Algorithm and wind error analysis code. An atmospheric wind field library containing control fields, meteorological fields, phenomena fields, and new European Center for Medium Range Weather Forecasting (ECMWF) data was also added. The LSM was used to address some key LAWS issues and trades such as accuracy and interpretation of LAWS information, data density, signal strength, cloud obscuration, and temporal data resolution. Author

N91-29555# Columbia Univ., New York, NY. Dept. of Chemistry.
LASER ENHANCED CHEMICAL REACTION STUDIES
G. Flynn 1 Dec. 1990 20 p
(Contract DE-FG02-88ER-13937)
(DE91-013021; DOE/ER-13937/3) Avail: NTIS HC/MF A03

Experimental studies of dynamic molecular processes are described with particular emphasis on the use of a powerful infrared diode laser probe technique developed in our laboratory. This technique allows us to determine the final states of CO2 (and other molecules) produced by collisions, photofragmentation, or chemical reactions with a spectral resolution of 0.0003 cm(exp -1) and a time resolution of 10(exp -7) sec. Such high spectral resolution provides a detailed picture of the vibrational and rotational states of molecules produced by these dynamic events. We have used this experimental method to probe collisions between hot hydrogen/deuterium atoms and CO2, between O(D-1) atoms and CO2, to study the final states of DCl molecules produced as a result of the reactions of hot Cl atoms, and to investigate the dynamics of the reaction between OH and CO molecules. Advances in our technique over the past two years have allowed us to identify and study more than 200 final rotational states in ten different vibrational levels of CO2 encompassing all 3 normal modes, many overtones, and combination states of the molecule. We have extended the technique to probe a variety of new molecules such as OCS, N2O, DCl, CS2 and Cl atoms (via the (sup 2)P(sub 3/2) yields (sup 2)P(sub 1/2) atomic transition). All of this work is aimed at providing experimental tests for polyatomic molecule potential energy surfaces, chemical transition states in complex systems, and theories of reaction dynamics in molecules with more than 3 atoms. We hope through these experiments to provide dynamical and mechanistic information of fundamental interest for combustion and atmospheric reaction processes. DOE

N91-29556# Rochester Univ., NY. Lab. for Laser Energetics.
INERTIAL FUSION PROGRAM AND NATIONAL LASER USERS FACILITY PROGRAM Annual Report, 1 Oct. 1989 - 30 Sep. 1990
Jan. 1991 263 p
(Contract DE-FC03-85DP-40200)
(DE91-013164; DOE/DP-40200/146) Avail: NTIS HC/MF A12

This report summarizes research at the Laboratory for Laser Energetics (LLE) for FY 1990 (1 October 1989 to 30 September 1990). During the year, a number of important reviews of the U.S. effort in inertial fusion were concluded. Some of the major findings as they relate to LLE and the high quality of our laser fusion research effort are summarized. A review of LLE's progress on the OMEGA upgrade is offered next, followed by a summary of the Laboratory's role and activities in education this year. A brief review of the activities of the National Laser Users Facility is provided, followed by a summary of progress in advanced technology at LLE. DOE

N91-29557# Sandia National Labs., Albuquerque, NM.
LASER TRIGGERED SPARK GAP MODELING
A. E. Rodriguez, K. J. Touryan, W. M. Moeny, and W. L. Morgan (Tetra Corp., Albuquerque, NM.) Aug. 1990 142 p
(Contract DE-AC04-76DP-00789)
(DE91-014831; SAND-91-7065) Avail: NTIS HC/MF A07

This report describes the work done by Tetra Corporation in modeling laser triggered spark gaps in air and SF6. The objective was to develop a model that describes the physics of the laser triggered spark gap in sufficient detail to improve our understanding of the important physical processes involved in switch closure time and compare it with experimental data. The model would help determine the sensitivity of switch closure time to key parameters, such as laser energy loading into the spark, the electric field shaping in the gap and the properties of the gas mixture, and thus help guide the design of laser triggered spark gaps. The work was accomplished in five tasks, outlined in the report. Our approach was to adapt the ELF electrostatic field codes developed at Tetra Corporation to the laser triggered spark gap closure problem and use a Boltzmann solver (ELENDIF) to describe the kinetics of the discharge. DOE

N91-29558 Stanford Univ., CA.
PHOTOELECTRON AND PHOTOIONIZATION PUMPING OF XUV LASERS BY LASER-PRODUCED PLASMAS Ph.D. Thesis
Christopher Peter Ja Barty 1991 161 p
Avail: Univ. Microfilms Order No. DA9115739

An experimental and theoretical investigation is presented of several photo-electron and photoionization pumped lasers in the extreme ultraviolet (XUV). In the systems studied, soft x-ray emission from a laser produced plasma is used to excite an ambient atomic or molecular vapor. In photoionization pumped systems, differing photoionization cross sections allow for the preferential

ionization of inner shell electrons by soft x-ray photons. The resulting ionic species are either inverted with respect to the ground state of the first ion or are energetically unstable and undergo rapid, selective Auger decay into inverted states in the second ion. Studies of photoionization pumped systems in atomic xenon, krypton, zinc, cesium, lithium, and potassium were conducted.
Dissert. Abstr.

N91-29559# Lawrence Livermore National Lab., CA.
BLACKBODY PUMPED CO2 LASERS USING GAUSSIAN AND WAVEGUIDE CAVITIES
J. J. C. Chang and W. H. Christiansen (Washington Univ., Seattle.) 19 Dec. 1990 15 p Presented at the OE/LASE 1991: 4th Society of Photo-Optical Instrumentation Engineers (SPIE) International Symposium, Los Angeles, CA, 20-25 Jan. 1991
(Contract W-7405-eng-48)
(DE91-012494; UCRL-JC-104237; CONF-910123-31) Avail: NTIS HC/MF A03

A large scale pulsed laser system with heated tantalum foils as the blackbody pumping source was built in the laboratory. A deeper understanding of the effects of pumping configurations and laser modes on the blackbody pumped CO2 laser has been achieved through parametric studies using this system. Theoretical analysis and experimental investigation show the feasibility of a slab pumping scheme which may be applied to large scale transverse flow laser systems. The use of an 8mm tube with waveguide quality enable us to generate both Gaussian and waveguide modes in the same structure with different optics setup. The experiment demonstrates that high waveguide cavity losses can be prevented with large bore structure (greater than 4mm) and the advantage of better filling of the laser gain region by waveguide modes is clearly observed. The size scaling studies also indicate that there are similarity relations of the optimum laser parameters between different sizes of tube in optically pumped gas lasers. DOE

N91-29560# Los Alamos National Lab., NM.
MEASUREMENT OF LONGITUDINAL EMITTANCE GROWTH USING A LASER-INDUCED NEUTRALIZATION METHOD
V. W. Yuan, R. Garcia, K. F. Johnson, K. Saadatmand, O. R. Sander, D. Sandoval, and M. Shinas 1991 4 p Presented at the 1991 Institute of Electrical and Electronics Engineers (IEEE) Particle Accelerator Conference (PAC), San Francisco, 6-9 May 1991
(Contract W-7405-eng-36)
(DE91-013500; LA-UR-91-1523; CONF-910505-173) Avail: NTIS HC/MF A01

A laser-induced neutralization technique, LINDA, has been used to study the longitudinal emittance of the 5-MeV H(-) beam exiting the drift-tube Linac (DTL) of the Los Alamos Accelerator Test Stand (ATS). By using multiple laser intersection points, longitudinal emittance growths over drift distances of 23.6 and 30.6 cm were measured. Subsequently, a beam transport line, which consisted of one arm of a beam funnel, was substituted for the drift space. Measurements show that the elements of the funnel constrain emittance growth while the H(-) beam is contained within these transport elements. DOE

N91-29561# Lawrence Livermore National Lab., CA.
ADJUSTABLE MAGNIFICATION ANAMORPHIC BEAM EXPANDER
S. R. Escobar Aug. 1990 47 p
(Contract W-7405-eng-48)
(DE91-014110; UCRL-ID-106488) Avail: NTIS HC/MF A03

A visible laser diode package is proposed to substitute a Krpton-Ion laser for alignment purposes. The proposed system uses 5 Melles Griot AR coated stock lenses. Tests performed to the optics reveal some undesirable properties, such as, astigmatism and spherical aberration; however, the interference pattern and star test reveals what seems to be a good quality wavefront. The interference fringes seem to be very good, but there still is a small presence of a comalike aberration at the fringes extreme. The star test revealed the system to be about 3 times diffraction limited. The system has yet to be tested in an alignment situation. As for now, it is ready to be tested with some minor alignment adjustments necessary for a good wavefront quality. A safety memo was written for testing the prototype system at the alignment lab. The initial laser diode system alignment method suggested, uses a reverse alignment procedure. In this procedure, the expected output (30 mm diameter beam) is input into the system output and alignment is performed by moving the components until the desired system input is found; an elliptical beam with 1 mm in the horizontal axis and 4 mm in the vertical axis. Once this reverse alignment procedure is completed the laser diode is placed at the system input. Fine alignment is done with the help of shear plate interference patterns in both, the 1 mm axis and 4 mm axis. The proposed final opto-mechanical packaging of this system is formed with squared adapter plates that are connected by means of four support rods where the center of the plate becomes the optical axis. These components are commercially available and provide high mechanical stability. DOE

N91-29562# Los Alamos National Lab., NM.
LOW-JITTER, HIGH-VOLTAGE, INFRARED, LASER-TRIGGERED, VACUUM SWITCH
L. M. Earley and G. A. Barnes 1991 5 p Presented at the 8th IEEE Pulsed Power Conference, San Diego, CA, 17-19 Jun. 1991
(Contract W-7405-eng-36)
(DE91-014602; LA-UR-91-2052; CONF-910640-21) Avail: NTIS HC/MF A01

A laser-triggered, high-voltage vacuum switch using a triggering pellet embedded in the cathode has been developed. The switch was constructed with tungsten electrodes and used either KC1 or Poco graphite pellets. An aperture in the anode allowed the laser beam to strike the pellet on the cathode surface. Reliable triggering was achieved with only 200 mu J of laser energy at a wavelength of 1064 nm. The switch was operated with an A-K gap voltage ranging from 5- to 30-kV with switching currents up to 15 kA peak. The delay time of the switch vaired from 70 plus or minus) 3 ns at 25 kv to 500 plus or minus 100 ns at 5 kV. DOE

N91-29563# Los Alamos National Lab., NM.
ABLATION OF MATERIAL BY FRONT SURFACE SPALLATION
R. S. Dingus and R. J. Scammon 1991 12 p Presented at the HASRD Workshop on Laser Ablation: Mechanisms and Application, Oak Ridge, TN, 8-10 Apr. 1991
(Contract W-7405-eng-36)
(DE91-014773; LA-UR-91-1911; CONF-9104192-12) Avail: NTIS HC/MF A03

Laser irradiation can be utilized to remove (i.e., ablate) material in a controlled manner by a hydrodynamic process, referred to as front surface spallation. In this process, a thin layer next to a free surface is heated to a level (below vaporization) so rapidly that it cannot undergo thermal expansion during laser heating. This generates a stress pulse, which propagates both inward and toward the free surface, with an initial amplitude that can be calculated using the Grueneisen coefficient. As the pulse reflects from the free surface, a tensile tail can develop of sufficient amplitude, exceeding the material strength, that a layer will be spalled off, taking much of the laser-deposited energy with it. To achieve spallation conditions, the laser wavelength, pulselength and fluence must be tailored to the absorption depth, Grueneisen coefficient, and spall strength. Hydrodynamic calculations and analytical modeling are presented to explain the process and illustrate conditions under which it should be expected to occur. Under some conditions, front surface spallation can have advantages over ablation by thermal vaporization, where residual temperatures are generally higher. DOE

N91-29564# Air Force Systems Command, Wright-Patterson AFB, OH. Foreign Technology Div.
SECOND-HARMONIC GENERATION OF TEA CO2 10.6 MICROMETER LASER LIGHT IN AgGaS2 CRYSTALS
Zhang Bangmin and Wang Dinghua 3 May 1991 13 p Transl.

into ENGLISH from Zhongguo Jiguang (Peoples Rep. of China) v. 10, no. 6, 1983 p 339-342
(AD-A237169; FTD-ID(RS)T-0742-90) Avail: NTIS HC/MF A03 CSCL 09/3

Characteristics of AgGaS2 crystal for frequency doubling of TEA CO2 10.6 micrometer laser light were investigated. When the crystal was 4.3mm long, the maximum conversion frequency was 0.122 percent. In recent years, much progress was made in expanding the range of laser wavebands by utilizing the nonlinear effects. In the medium infrared waveband, the CO2 laser is a relatively ideal light source and can output tens of laser spectral lines within the range 8.7 to 11.8 micrometers. With double frequency, tunable output can be obtained within the range 4.3 to 5.9 micrometers. Since the advent of CO2 lasers, researchers have conducted numerous research tasks in this area. However, since it is relatively difficult to obtain high quality and large infrared nonlinear optical crystals, such work still remains at the laboratory research stage without practical applications. GRA

N91-29565# Air Force Systems Command, Wright-Patterson AFB, OH. Foreign Technology Div.
EXPERIMENTAL STUDY OF GAS KINETICS OF A FAST-AXIAL FLOW KILOWATT CO2 LASER
Gao Yungui, Ma Shuyun, Meng Ping, and Wang Ruxiang 3 May 1991 17 p Transl. into ENGLISH from Jiguang Zazhi (Peoples Rep. of China), v. 10, no. 6, 1989 p 246-250
(AD-A237178; FTD-ID(RS)T-0720-90) Avail: NTIS HC/MF A03 CSCL 09/3

The rapid flow is described of a gas mixture in a fast axial flow kilowatt level CO2 laser. A high flow velocity wind tunnel is introduced. Gas pressure, gas flow velocity, and its method of measurement are analyzed. A wind tunnel was constructed and gas experiments were conducted. The gas flow velocity was as high as the speed of sound. Experimental data are given. Worldwide, it is accepted that the kilowatt level, fast axial flow CO2 lasers are an ideal light source, with high efficiency and good quality of light beam for high power laser industrial processing. Within the range of 1 and 3 kW abroad, these lasers have replaced most lateral direction flow and slow speed axial flow devices. In China, the study of these devices is just beginning with this experiment. The results are preented of experimental studies of gasdynamics of a kilowatt level, fast axial flow CO2 laser. GRA

N91-29566# Air Force Systems Command, Wright-Patterson AFB, OH. Foreign Technology Div.
DEVELOPMENT OF LOW-THRESHOLD VALUE, HIGH-POWER SEMICONDUCTOR LASER
Li Yudong, Zhu Donghai, Shu Schihang, and Zhang Shuzhi 27 Mar. 1991 9 p Transl. into ENGLISH from Jilian Dafve Liran Kefue Xuebao (Peoples Rep. of China), no. 1, 1990 p 75-77
(AD-A237183; FTD-ID(RS)T-1135-90) Avail: NTIS HC/MF A02 CSCL 09/3

The concept and experimental results are presented of a novel large optical cavity structure semiconductor laser. GRA

N91-29567# Air Force Systems Command, Wright-Patterson AFB, OH. Foreign Technology Div.
CHINESE PHYSICS LASERS (SELECTED ARTICLES)
11 Apr. 1991 90 p Transl. into ENGLISH from Zhong Guo Jiguang (Peoples Rep. of China), v. 16, no. 11, 1989 p 675-703
(AD-A237263; FTD-ID(RS)T-0811-90) Avail: NTIS HC/MF A05 CSCL 09/3

The following contents are included in this report: Successful Target Hit by China's First High-Power Double-Frequency Laser; Optical Bistability in Nematic Liquid Crystals; Binocular Stereoscopic Holograms for Three Dimensional Display; Study of Phosphate Laser Glass with High Neodymium Concentration; Stress Strain State of Slab Amplifiers; Gain Saturation Parameters and Their Variation in Transverse-Flow Discharge CO2 Lasers; Influence of Electrode Material on Operating Life of Line Selection CO-CO2 Compound Lasers; Space Variant Optical Logic Operation with Theta Modulation; XeCl-Laser-Induced Oxidation Reaction of Cerium Separation; Resonance Fluorescence Shift in Mg Atomic Isotopes with Ultraviolet Laser; and Ideal Size of Laser Spot in Laser Printing and its Measurement. GRA

N91-29568# Naval Research Lab., Washington, DC.
EVOLUTION OF A FINITE PULSE OF RADIATION IN A HIGH-POWER FREE-ELECTRON LASER Memorandum Report
A. Ting, B. Hafizi, P. Sprangle, and C. M. Tang 20 Jun. 1991 51 p
(AD-A237427; NRL-MR-6844) Avail: NTIS HC/MF A04 CSCL 09/3

The development of an optical pulse of finite axial extent is studied by means of an axisymmetric, time-dependent, particle simulation code for different rates of tapering of the wiggler field. The results illustrate a number of the physical phenomena underlying the free-electron laser mechanism. These include: suppression of the sideband instability; the role of gain focusing versus that of refractive guiding; efficiency enhancement; and pulse slippage. It is found that a significant reduction in the sideband modulation of the optical field can be achieved with a faster tapering of the wiggler parameters. Increasing the tapering rate also reduces refractive guiding, causing the optical wavefronts to become more convex, thus spreading the optical field into a large cross-section. The corresponding enhancement of the peak output power is associated with an increased lateral extent of the optical field rather than an increase in the field amplitude. Author (GRA)

N91-29569# Puerto Rico Univ., Rio Piedras. Dept. of Chemistry.
THE LASER ABLATION OF ALUMINUM AT 193, 248, AND 351 NM
Hongxin Wang, A. P. Salzberg, and Brad R. Weiner May 1991 15 p
(Contract N00014-89-J-1829)
(AD-A237574; TR-2) Avail: NTIS HC/MF A03 CSCL 20/5

Pulsed laser ablation of an aluminum target at 193, 248 and 351 nm was investigated by laser induced fluorescence (LIF) spectroscopy. Velocity distributions of the ablated Al atoms were measured directly by monitoring their flight times from the target to the probe laser beam, and by Doppler laser spectroscopy. The velocity distributions resulting from the three wavelengths can all be characterized as hyperthermal, with average velocities of between 4.5 x 10(exp 5) cm/s and 6.5 x 10(exp 5) cm/s over a fluence range of 0.3 to 6.5 J/sq cm. Average values of the Al atom distribution can also be derived by measuring the AlO internal energy distribution of the hot Al atom reaction with low pressures of O2. GRA

N91-29570# California Univ., Berkeley.
STRUCTURES, PROPERTIES, AND DYNAMICS OF METAL CLUSTERS FROM INFRARED LASER SPECTROSCOPY Final Report, 1 Jan. 1987 - 31 Dec. 1989
Richard J. Saykally 21 Jun. 1991 4 p
(Contract N00014-87-K-0270)
(AD-A237669) Avail: NTIS HC/MF A01 CSCL 14/2

Two new types of infrared spectrometers have been developed for the study of gas-phase cluster species. A tunable far-infrared (FIR) laser was combined with an apparatus for producing planar supersonic beams of laser vaporized clusters, and used in the measurement of the 64.1 cm(exp -1) bending vibration of C3. A mid-IR diode laser system was constructed with a similar cluster source, and used in studies of the C4, C5, C7, and C9 clusters. Structures and internal dynamics of the clusters were determined. Extensions to metal cluster systems are currently underway. A new type of spectrometer was developed for measuring electronic spectra of supersonic metal clusters. Cavity Ringdown Laser Absorption Spectroscopy (CRLAS) was utilized in a study of the Cu3 cluster in the initial application of the method. GRA

N91-29571# Utah Univ., Salt Lake City. Dept. of Physics.
RESEARCH IN THE PHYSICAL SCIENCES WITH APPLICATION TO THE FREE ELECTRON LASER Final Report, May 1986 - Dec. 1989

P. C. Taylor, G. B. Stringfellow, R. M. Cohen, C. A. Wright, and W. Gellerman 3 Jul. 1991 16 p
(Contract N00014-86-K-0710)
(AD-A237884) Avail: NTIS HC/MF A03 CSCL 05/1

The goals of this research are to perform research in the physical sciences (chemistry, electrical engineering, materials science, physics) with direct application to Free Electron Laser technology. Recent progress includes: (1) infrared modulation spectroscopy of III-V quantum wells and superlattices; (2) subpicosecond spectroscopy of conducting polymers, metals and amorphous multilayers; (3) new tunable infrared lasers based on defects in alkali halides; (4) laser induced photolysis of small hydrocarbons, organometallics nitrosyls and formaldehyde; (5) modeling of eigenstates in semiconductor quantum wells; and (6) theory of disordered solids. GRA

N91-29572# Massachusetts Inst. of Tech., Cambridge.
CHARACTERIZATION OF A SUB-PICOSECOND DYE LASER FOR THE STUDY OF ATOM-PERTURBER COLLISIONS M.S. Thesis
Scott A. Fedorchak Jun. 1991 102 p
(AD-A238099) Avail: NTIS HC/MF A06 CSCL 09/3

This thesis covers an in-depth analysis of the pulsed laser system to be used in the developing a linear technique for the time domain study of the change in coherence of atomic superposition states for the Ytterbrium atom due to phase-interrupting collisions. The hybrid synchronously pumped dye laser yielded optimally shaped sub-picosecond pulses at the 555.6 nanometer wavelength. Comparison of the results for the experimental trials at the 576 and 555.6 nanometer wavelengths yielded an experimental value for the dephasing time, T sub 2 = 621 picoseconds, of the DMETCI dye used as a saturable absorber dye for the first time. GRA

N91-29573# Massachusetts Inst. of Tech., Cambridge. Research Lab. of Electronics.
MULTIPIXEL MULTIDIMENSIONAL LASER RADAR SYSTEM THEORY Final Report, 1 Oct. 1987 - 31 May 1991
Jeffrey H. Shapiro 6 Jul. 1991 15 p
(Contract DAAL03-87-K-0117)
(AD-A238110; ARO-25299.12-PH) Avail: NTIS HC/MF A03 CSCL 17/9

Coherent laser radars for tactical sensor applications are under development at a number of laboratories, based on the mid-infrared technology of CO2 lasers and HgCdTe photodetectors. Test bed radars of this class have already demonstrated that tactical targets may be resolved in any combination of the modalities of space, angle, range, and velocity. Under U.S. Army Research Office Contract DAAL03-87-K-0117, a program of research was pursued to advance the system theory of such multipixel, multidimensional laser radars, and to corroborate these advances through experiments performed using the test bed coherent lasers radars of the MIT Lincoln Laboratory Opto-Radar Systems Group. Major progress was made on the problem of target detection during the course of this work: quasi-optimal detection processors were derived for various 2-D and 3-D pulsed imagers; performance results for these processors were developed from computer simulation; and 2-D detection performance was confirmed experimentally. Substantial progress was also made on the problem of resolved-target tracking: generalized Kalman filter was derived for linear-least-squares operation in a track-while-image mode, with tracking performance studied both analytically and through simulation. GRA

N91-29574# Westinghouse Defense and Electronic Systems Center, Baltimore, MD. Advanced Technology Div.
STABLE INTEGRATED MICROWAVE TO OPTICAL MODULATOR Technical Financial Report, 2 Mar. - 1 Jun. 1991
Jun. 1991 11 p
(Contract N00014-90-C-0073)
(AD-A238166) Avail: NTIS HC/MF A03 CSCL 09/1

The key technical objective for this research program is to integrate quantum well lasers (QWLs), detectors and GaAs MESFET's to produce a monolithic integrated microwave to optical modulator on semi-insulating GaAs substrates. GRA

N91-29575# Yale Univ., New Haven, CT. Dept. of Applied Physics.
HIGH-INTENSITY AND HIGH-ENERGY LASER INTERACTIONS WITH SINGLE DROPLETS Final Report, 1 Feb. 1988 - 31 Jan. 1991
Richard K. Chang Apr. 1991 13 p
(Contract DAAL03-88-K-0040)
(AD-A238197; ARO-25670.8-GS) Avail: NTIS HC/MF A03 CSCL 20/6

During the three years of ARO support, significant progress has been made toward furthering the understanding of high-intensity laser beam interactions with single liquid droplets with radius, a, much larger than the input laser wavelength (input). Our research efforts can be divided into two parts: (1) laser-induced breakdown (LIB) of droplets; and (2) nonlinear optical effects in droplets. One part of our research was directed toward the optical diagnostics of the plasma associated with the laser-induced breakdown (LIB) processes. We developed several spectroscopic techniques that are capable of providing spatially and temporally resolved measurements of the plasma emission and transmission. The propagation speed and the optical transmission of the breakout plasma from the droplet shadow face and from the illuminated face are determined. The relative heating of the atoms in the plasma is extracted from atomic emission intensities at two different wavelengths. The other part of our research was directed toward the following nonlinear optical effects: (1) the generation of stimulated Brillouin scattering (SBS) in simple droplets; (2) the determination of the angular pattern of stimulated Raman scattering (SRS); (3) the two-photon excitation of lasing droplets; and (4) the modification of the standard nonlinear wave equations to describe the growth and decay of nonlinear waves in droplets. GRA

N91-29576# Texas Univ., Austin. Computer and Vision Research Center.
MULTI-SENSOR IMAGE INTERPRETATION USING LASER RADAR AND THERMAL IMAGES Interim Technical Report
Chen-Chau Chu and J. K. Aggarwal Mar. 1991 25 p
(Contract DAAL03-91-G-0050)
(AD-A238245; TR-91-6-70; ARO-28258.4-PH) Avail: NTIS HC/MF A03 CSCL 17/9

A knowledge based system is presented which interprets registered laser radar and thermal images. The object is to detect and recognize man-made objects at kilometer range in outdoor scenes. The multisensor fusion approach is applied to various sensing modalities (range, intensity, velocity, and thermal) to improve both image segmentation and interpretation. The ability to use multiple sensors greatly helps an intelligent platform to understand and interact with its environment. The knowledge-based interpretation system, AIMS, is constructed using KEE and Lisp. Low-level attributes of image segments (regions) are computed by the segmentation modules and then converted into the KEE format. The interpretation system applies forward chaining in a bottom-up fashion to derive object-level interpretations from data bases generated by low-level processing modules. Segments are grouped into objects and then objects are classified into predefined categories. AIMS employs a two tiered software structure. The efficiency of AIMS is enhanced by transferring nonsymbolic processing tasks to a concurrent service manager (program). Therefore, tasks with different characteristics are executed using different software tools and methodologies. Author (GRA)

N91-29577# Naval Postgraduate School, Monterey, CA.
DESIGN OF A STABILIZED, dc-POWERED ANALOG LASER DIODE DRIVER M.S. Thesis
John J. Bradunas Sep. 1990 116 p
(AD-A238596) Avail: NTIS HC/MF A06 CSCL 10/2

This thesis presents the design, implementation, and evaluation of a depowered, stabilized-output laser diode drive unit for use in

an analog fiber-optic communication transmitter. The driver circuits provide for a stable temperature-controlled operating environment by monitoring the thermistor in the laser diode module and by controlling the current to the module's integral thermoelectric cooler. Output optical power is maintained at desired bias and peak-to-peak levels by processing the signal from the monitor photodiode and amplifying (if necessary) the ac and dc drive units. These efforts offset the degradation of the laser diode's capabilities due to heat and age. GRA

N91-29578# Lawrence Livermore National Lab., CA.
DEGRADATION OF BRIGHTNESS BY RESONANT PARTICLE EFFECTS
Y. J. Chen, G. J. Caporaso, A. G. Cole, A. C. Paul, and W. C. Turner Jun. 1991 5 p Presented at the Institute of Electrical and Electronics Engineers (IEEE) Particle Accelerator Conference (PAC), San Francisco, CA, 6-9 May 1991
(Contract W-7405-eng-48)
(DE91-015181; UCRL-JC-105558; CONF-910505-366) Avail: NTIS HC/MF A01

A resonance between the periodic focusing force and the envelope oscillations or the particle orbits can lead to beam halo formation and a dramatic decrease in brightness. We have developed a theoretical model for this parametric transport instability. We have also investigated the instability on the Experimental Test Accelerator II (ETA-II). The instability can be excited by altering the excitation of just one solenoid. DOE

N91-29579# Los Alamos National Lab., NM.
KINETICS OF DARK REACTION IN CHEMICAL LASER GASES
R. C. Heaton, R. C. Feber, J. H. Sullivan, N. R. Greiner, and W. F. Sandoval Jul. 1991 42 p
(Contract W-7405-eng-36)
(DE91-015320; LA-12018-MS) Avail: NTIS HC/MF A03

We experimentally measured rates of formation of DF in gas mixtures containing F2, D2, O2, CO2, and argon in various initial proportions. The gas mixtures were mostly stable, and the measurements were made without igniting the gas whenever possible. We compared the measured rates with those calculated by using a computer model similar to those used to describe chemical laser systems. The rate constants used in the model were critically evaluated, and in many cases the model gave results consistent with the experimental data. We also derived a steady-state kinetic model that predicts the DF formation rate at long times and is useful in understanding the relative importance of some of the reactions. Heterogeneous chemical reactions are important in explaining the experimental results. We postulate two such reactions: the formation of fluorine atoms on the chamber wall and an equilibrium between fluorine atoms adsorbed on the wall and fluorine atoms in the gas phase. Rate and equilibrium constants for these reactions were obtained. Because of the postulated wall reactions, the materials and geometry associated with the reaction vessel may be important in determining whether the gas mixtures are stable. We obtained evidence that the important chain-branching reaction, D2 + F2 yields DF + D + F, is driven by D2 in its first vibrational state and is not strongly dependent on D2 in its vibrational ground state. Agents that promote vibrational relaxation of DF, such as COP2, may improve the stability of the gas mixture by indirectly limiting the amount of excited D2 in the gas mixture. Gas mixtures containing 45 torr F2, 15 torr D2, 45 torr CO2, and 650 torr argon were stable for O2 pressures greater than approximately 1 torr in the reaction vessel we used. DOE

N91-29580# Massachusetts Inst. of Tech., Cambridge.
SHORT-PULSE GLASS SLAB AMPLIFIER
M. Muendel and P. Hagelstein 1990 11 p Presented at the International Conference on Lasers '90, San Diego, CA, 10-14 Dec. 1990
(Contract DE-FG02-89ER-14012)
(DE91-015385; CONF-901263-9-Vugraphs) Avail: NTIS HC/MF A03

This work is comprised of viewgraphs from a talk at the LASERS 1990 conference. The design and specifications of the phosphate glass slab are examined, along with the components of the optical, electrical, and cooling systems. The gain, efficiency, uniformity, apodization, thermal behavior, and a double pass test are presented as measures of the performance of the system. DOE

N91-29581# Argonne National Lab., IL.
DEVELOPMENT OF LASER OPTICS FOR THE AWA PHOTOCATHODE
J. Norem and W. Gai 1991 3 p Presented at the 1991 Institute of Electrical and Electronics Engineers (IEEE) Particle Accelerator Conference (PAC), San Francisco, CA, 6-9 May 1991
(Contract W-31-109-eng-38)
(DE91-015552; ANL-HEP-CP-91-43; CONF-910505-386) Avail: NTIS HC/MF A01

A photocathode electron source for the Argonne Wakefield accelerator is being designed to produce a number of short (10 psec), 100 nC bunches per rf pulse. Possible sources of fluctuations in the position and energy of these bunches are variations in the initial intensity, position and profile of the bunches which are amplified by wakefields. Since high pulse power lasers have historically produced large fluctuations in pulse to pulse energy and transverse beam profiles, we have been concerned about the stability of the RF photocathode as an injector for the linac. Unfortunately, there is no commercial devices that will minimize those fluctuations. In order to minimize these problems, we have designed and begun to test systems which should reduce the initial fluctuations of the beam by stabilizing the laser pulse energy and beam profile. DOE

N91-29582# Massachusetts Inst. of Tech., Cambridge. Research Lab. of Electronics.
THE MIT SHORT-WAVELENGTH LASER PROJECT
P. Hagelstein, S. Basu, M. Muendel, J. P. Braud, S. Kaushik, and D. Tauber 1991 21 p
(Contract DE-FG02-89ER-14012)
(DE91-015357; DOE/ER-14012/2) Avail: NTIS HC/MF A03

The present status of the project follows: the Nd:glass power amplifier was constructed and brought from LLNL to MIT; gain measurements were performed, and work on the associated optics is currently underway. The vacuum chamber was built and successfully tested. The optics for the target alignment system were redesigned, fabricated, and partially assembled; the electronics are now being brought together. EUV spectrometers for use as laser diagnostics are under development; these incorporate both commercially available gratings as well as novel, in-house designs. Work on laser cavities has yielded an greatly improved understanding of the difficulties involved in using whispering gallery optics. An earlier analysis of soft x ray frequency conversion was refined. A numerical study of plasma kinetics has elucidated the physics of transiently pumped x ray lasers. DOE

N91-29583# Lawrence Livermore National Lab., CA.
RF TRANSFER IN THE COUPLED-CAVITY FREE-ELECTRON LASER TWO-BEAM ACCELERATOR
M. A. Makowski 1991 5 p Presented at the 1991 Institute of Electrical and Electronics Engineers (IEEE) Particle Accelerator Conference (PAC), San Francisco, CA, 6-9 May 1991
(Contract W-7405-eng-48)
(DE91-015676; UCRL-JC-105604; CONF-910505-387) Avail: NTIS HC/MF A01

A significant technical problem associated with the Coupled-Cavity Free Electron Laser Two Beam Accelerator is the transfer of RF energy from the drive accelerator to the high gradient accelerator. Several concepts have been advanced to solve this problem. One possible solution is examined in which the drive and high gradient cavities are directly coupled to one another by means of holes in the cavity walls or coupled indirectly through a third intermediate transfer cavity. Energy cascades through the cavities on a beat frequency time scale which must be made small compared to the cavity skin time but large compared to the FEL pulse length. The transfer is complicated by the fact that each of the cavities in the system can support many resonant

modes near the chosen frequency of operation. A generalized set of coupled-cavity equations was developed to model the energy transfer between the various modes in each of the cavities. For a two cavity case transfer efficiencies in excess of 95 pct. can be achieved. DOE

37 MECHANICAL ENGINEERING

Includes auxiliary systems (nonpower); machine elements and processes; and mechanical equipment.

N91-29584# California Univ., Berkeley. Lawrence Berkeley Lab.
A METHODOLOGY FOR INHIBITING THE FORMATION OF POLLUTANTS IN DIESEL ENGINES
A. K. Oppenheim, K. Hom, J. A. Maxson, N. J. Beck, and H. E. Stewart (California Univ., Berkeley.) Jan. 1990 13 p Presented at the Society of Automotive Engineers International Congress and Exhibition, Detroit, 26 Feb. - 2 Mar. 1990
(Contract DE-AC03-76SF-00098)
(DE90-011615; LBL-28270; CONF-9002115-1) Avail: NTIS HC/MF A03

The methodology put forth in this paper stems from the premise that the primary reason for the generation of major pollutants by diesel engines, particulates and nitric oxides, is associated with over-reliance upon diffusion flames to carry out the process of combustion. Specific means are, therefore, proposed to inhibit their formation. This consists of refinements involving the use of either hollow cone spray injectors or air blast atomizers. Concomitantly, the process of combustion is staged by either regulating the rate of injection or employing a number of consecutively activated injectors per cylinder under a microprocessor command, while regions of high temperature peaks are distributed throughout the charge and kept at a relatively low level by exploiting the large scale vortex structure of turbulent pulsed jets combined with residual gas recirculation. Most appropriate for the realization of these concepts is a two-stroke, loop scavenged engine with special provisions included to curb emission of unburned hydrocarbon due to lubricating oil. DOE

N91-29585# Oak Ridge National Lab., TN.
FORCE-REFLECTING CONTROL OF A TELEOPERATED SYSTEM COUPLING A NONREDUNDANT MASTER WITH A REDUNDANT SLAVE
R. Kress, J. Jansen, F. DePiero, and S. Babcock 1990 7 p Presented at the ISRAM 1990: International Symposium on Robotics and Automation, Vancouver (Canada), 18-20 Jul. 1990
(Contract DE-AC05-84OR-21400)
(DE90-012137; CONF-900780-6) Avail: NTIS HC/MF A02

A bilateral, force-reflecting controller was formulated for a 6-Degree-of-Freedom (6-DOF) master operating a 7-DOF slave. Six degrees of freedom are required to arbitrarily position and orient a manipulator end effector. A 7-DOF slave manipulator is desirable because the additional (or redundant) degree of freedom potentially allows for an infinite number of manipulator configurations for a given end effector position and orientation, thus permitting the manipulator to reach around obstacles to perform a task, to avoid joint limits, or to optimize its configuration in some other manner. A master/slave control system was formulated using a stiffness controller for the master and a gradient-projection algorithm for the slave. The complete control system provides scaled position tracking and indexing between slave and master and force reflection between master and slave. DOE

N91-29586# Carnegie-Mellon Univ., Pittsburgh, PA. Robotics Inst.
MODELING OF A 3-D LIGHT-WEIGHT SPACE MANIPULATOR
Hiroshi Ueno and Yangsheng Xu Apr. 1991 24 p
(AD-A236823; CMU-RI-TR-91-08) Avail: NTIS HC/MF A03 CSCL 23/2

This report addresses the problem of modeling a 3-D flexible robot. First, the flexibility of each link is modeled by a lumped system assuming the bending deflection is not too large compared to the length of the link. The the kinematics of a serial-chain flexible mechanism is obtained by using a transform of rigid coordinates and flexible coordinates. The flexible coordinated frame is defined to represent deflections of each link. Based on the kinematics, overall dynamics are derived by Lagrangian method. To obtain transfer functions from the joint torque to the tip displacements, the inertial matrix must be invertible. We defined a set of new variables by which the inertial matrix is invertible. This provides a general approach for modeling a large class of multi-joint flexible robot, and the resultant model is easy to implement in a real-time model, and the experimental results have been compared to the analytical results. GRA

N91-29587 Pennsylvania Univ., Philadelphia.
A GENERAL PURPOSE, COMPREHENSIVE DYNAMICS SIMULATION OF SERIAL ROBOT MANIPULATORS Ph.D. Thesis
Chi-Kai Lo 1990 225 p
Avail: Univ. Microfilms Order No. DA9112599

A systematic method for the efficient and comprehensive simulation of the dynamics of robot manipulators was created. Researchers were able to determine the motion of any open chain, serial-link robot with arbitrary geometry. The simulator includes a number of phenomena which are known to influence the dynamic response of the manipulator. Phenomena include joint compliance (including gear train deformations), geometric errors, power amplifier nonlinearities, and actuator saturation. The researchers model the kinematic structure of the manipulator by the modified Paul-Rosa representation (MPR), which uses an internal algorithm to extract the kinematic parameter from the convenient Paul Rosa representation. The MPR method compares favorably with the commonly used Denavit-Hartenberg notation in terms of computational efficiency and user friendliness. Many by-products of the efficient kinematic analysis are directly applied towards the formulation of the dynamics equations of motions, via the d'Alembert-Lagrange virtual work approach. Dissert. Abstr.

N91-29588 Pennsylvania Univ., Philadelphia.
SINGULARITY AVOIDANCE AND THE KINEMATICS OF AN EIGHT-REVOLUTE-JOINT MANIPULATOR Ph.D. Thesis
Gregory Lynn Long 1990 150 p
Avail: Univ. Microfilms Order No. DA9112601

A geometrically optimum six-revolute-joint robot manipulator, which is decoupled into a regional structure and an orientation structure is discussed. Since this 6R manipulator is kinematically decoupled, the regional and orientation structures comprise two separate screw systems, both of third order. When the order of either of these systems falls below three, the 6R manipulator will be at a configuration singularity. With the three actuator screws of the orientation structure placed in a configuration singularity, researchers found the screw that is instantaneously reciprocal to this system. With this screw they located a fourth redundant actuator screw best suited for returning freedom to the orientation structure. With the regional structure placed in its configuration singularity, researchers did likewise by adding to it the actuator screw best suited for returning the lost freedom. Hence, the orientation and regional structures form two separate 4R structures which, taken together, form an 8R manipulator. Dissert. Abstr.

N91-29589 Ohio State Univ., Columbus.
KINEMATICS OF SERIAL MANIPULATORS AND THEIR PARALLEL DUALS Ph.D. Thesis
Vasudeva S. Murthy 1990 124 p
Avail: Univ. Microfilms Order No. DA9111775

The relationship in the kinematics of serial manipulators and their parallel duals are discussed. An open kinematic chain with joints connected in series is referred to as a serial manipulator. Its parallel dual is generated based on the duality between force and angular velocity and between moment and linear velocity. The parallel dual of a serial manipulator turns out to be a multi-loop closed kinematic chain. There exists a well established symmetry

in the rate kinematics of serial manipulators and their parallel duals. The equations for the direct (inverse) rate kinematics of serial manipulators bear a symmetry with the equations for the inverse (direct) rate kinematics of their parallel duals and vice versa. A new solution to the inverse position kinematics problem of the Lobster arm is presented which takes advantage of its special geometry. A new solution procedure for the direct position kinematics of its parallel dual is also given. The equations for the two problems are shown to have a strong resemblance and both problems have sixteen solutions. Dissert. Abstr.

N91-29590 Michigan Univ., Ann Arbor.
PERFORMANCE MODELS FOR ROBOT MANIPULATORS Ph.D. Thesis
Chek-Peng Foo 1990 217 p
Avail: Univ. Microfilms Order No. DA9116180

The concept of performance models for manipulators is introduced and defined. Performance models are used to reduce the computational burden associated with the motion planning of manipulators where manipulator dynamics and actuator constraints have to be taken into account. A performance model for a robot manipulator is a mathematical representation of a subset of the feasible motions of the manipulator, i.e., all those motions which satisfy the manipulator dynamics and meet the actuator constraints. A performance model for a robot manipulator is conservative if it concludes only a small subset of the feasible motions. There are many performance models that can be constructed, each with varying degrees of conservativeness and computational complexity. Generally, these two qualities are contradictory. Dissert. Abstr.

N91-29591 Stanford Univ., CA.
QUASISTATIC MANIPULATION WITH COMPLIANCE AND FRICTION Ph.D. Thesis
Imin Kao 1991 189 p
Avail: Univ. Microfilms Order No. DA9115793

Grasp compliance and the friction properties of robotic fingers are first explored individually and then combined to provide a method for planning and predicting the sliding motions of the fingers with respect to a grasped object. The compliance of a grasp is expressed as a function of grasp geometry, contact conditions between the fingers and the grasped object, and kinetic properties of the fingers. The resulting compliance and stiffness matrices are useful for characterizing the grasp of a robotic hand on a tool or workpiece when small motions and low velocities are involved. The results depend on structural compliance and small changes in the grasp geometry. Friction models of point-contact and soft fingers are studied. Finally, the grasp compliance and friction limit surfaces are combined in a method for modeling manipulation with sliding fingers. Dissert. Abstr.

N91-29592 Stanford Univ., CA.
MOTION PLANNING FOR MANIPULATORS WITH EXCESSIVE DEGREES OF FREEDOM Ph.D. Thesis
Heow-Pueh Lee 1991 170 p
Avail: Univ. Microfilms Order No. DA9115804

Several algorithms were developed for global resolution of redundancy of a mechanical manipulator with excessive degrees of freedom for a prescribed end effector motion. The first few methods presented are for resolving the redundancy of a manipulator without the notion of optimal motions. The objective of these methods is to produce smooth and desired variations for joint angles, joint torques or performance functions such as rate of energy dissipation and rate of change of kinetic energy, rather than producing optimal motions with respect to some optimization criterion. Moreover, singular configurations which lead to unstable behavior in the form of unacceptably large joint speeds and joint torques are to be avoided during manipulator motions. An algorithm based on the Calculus of Variations and the use of Lagrange multipliers is presented to produce manipulator motions free from singularities or singular configurations. Dissert. Abstr.

N91-29593 Connecticut Univ., Storrs.
GLOBAL OPTIMALITY, CONSERVATIVITY AND SINGULARITY IN REDUNDANCY RESOLUTION OF ROBOTIC MANIPULATORS Ph.D. Thesis
Zhaoyu Wang 1990 148 p
Avail: Univ. Microfilms Order No. DA9115588

In redundant robotics, global optimality, conservativity, and singularity are three of the most challenging problems which essentially prohibit any practical implementation of the previously developed control algorithm for optimal redundant manipulation. Instead of resolving them separately, the resolutions of global optimality, conservativity and singularity are combined in this work by formulating redundant manipulation as a problem of the calculus of variations and, more generally, as the Lagrange problem of optimal control. Based on these formulations, the conditions on conservativity and algorithmic singularities are studied and resolved for the first time. Dissert. Abstr.

N91-29594 Stanford Univ., CA.
EXPERIMENTS IN ADAPTIVE CONTROL OF COOPERATING MANIPULATORS Ph.D. Thesis
Roberto Ernesto Zanutta 1991 117 p
Avail: Univ. Microfilms Order No. DA9115869

A robot's capability to carry out complex tasks can be greatly increased by the use of multiple cooperating manipulators. To make the control of such robots robust the robots must have the capability to identify the dynamic properties of the objects under manipulation and based thereon, continually select control-parameter values appropriately, all in real time. This can be done using adaptive control. Presented here are strategies developed for adaptive control using cooperative manipulators. Experimental results are presented for each strategy.
Dissert. Abstr.

N91-29595# Naval Ocean Systems Center, San Diego, CA.
OBJECTIVE ASSESSMENTS OF MOBILITY WITH AN EARLY UNMANNED GROUND VEHICLE (UGV) PROTOTYPE VIEWING SYSTEM
E. H. Spain and T. W. Hughes May 1991 16 p
(AD-A237317) Avail: NTIS HC/MF A03 CSCL 25/3

To guide development of a mobility sensor for an unmanned ground vehicle (UGV), a field testing program was established in which alternate mobility viewing system options were objectively compared with regard to their impact on driving under controlled field testing conditions. This report describes the procedures and specific tasks used in making comparisons across the 4 viewing system options that were compared: (1) direct view; (2) direct view 40 deg x 30 deg; (3) monoscopic helmet-mounted display (HMD); and (4) stereoscopic HMD. Testing was conducted with two groups of drivers: (1) an experienced group who were well practiced on courses run and tested with each of the four alternate viewing system options; and (2) an inexperienced group who were unfamiliar with courses and tested with a single mobility sensor system option on a one-time basis. Specific results in terms of relative driving efficiencies on six driving courses are reported and discussed with respect to their general implications for design of the man-machine interface for safe and efficient driving of UGVs in the teleoperated mode. GRA

N91-29596# Cambridge Univ. (England).
BASIC MECHANISMS OF DIESEL LUBRICATION CORRELATION OF BENCH AND ENGINE TESTS Final Report, Dec. 1985 - Jan. 1991
A. Cameron, J. A. Greenwood, A. F. Alliston-Greiner, and D. Cameron 25 Mar. 1991 226 p
(Contract DAJA45-86-C-0007; DA Proj. 1L1-61102-BH-57)
(AD-A237685; R/D-5305-AN-01) Avail: NTIS HC/MF A11 CSCL 11/8

The lubrication behavior of a cylinder liner/piston ring contact in a diesel engine has been simulated in a point contact reciprocating rig. When lubricants containing ZDDP additives are used, electrical contact resistance measurements establish that a thick reaction film quickly forms in the rubbed region, protecting

the metal surfaces. Electrical capacitance measurements show that the film thickness can vary from 0.1 to 1 micrometer: the film appears to be a solid organic polymer with a shear strength of 50 to 100 MPa. Using segments of diesel engine cylinder liners from various manufacturers in the reciprocating rig, the changes in surface roughness during the running-in process were monitored. The induction time needed for the formation of the reaction film as well as the coherence of the film was studied as a function of load and temperature (in the range 150 to 250 C). A theoretical analysis of flash temperatures in reciprocating contacts confirms that these are small under the conditions in this rig, so that the measured temperatures are those actually responsible for the reactions. GRA

N91-29597# Illinois Univ., Chicago. Dept. of Mechanical Engineering.
PERFORMANCE AND STABILITY IN HIGH SPEED ARTICULATED STRUCTURES UNDERGOING QUICK MANEUVERS: THEORY AND APPLICATIONS Final Report, 1 Sep. - 31 Dec. 1991
Farid M. Amirouche Jan. 1991 46 p
(Contract F49620-89-C-0114)
(AD-A237857; AFOSR-91-0535TR) Avail: NTIS HC/MF A03 CSCL 13/9

The proposed research is divided into two phases. The first introduces the PUTD (Pseudo Uptriangular Decomposition) to reduce the governing equations of motion of articulated mechanical systems. This investigation proposes a new method, which allows the constrained systems to operate in the presence of singularities. This is achieved by regularization technique which makes use of a new representation of the kinematical and geometrical constraint equations at singular positions. This method of stability analysis is compared with the asymptotic stability presented by Baumgarte. The PUTD is extended to accommodate the dynamics of such systems. An illustration of the utility and effectiveness of the method proposed is shown through a two arm planar robot undergoing large motions and driven through singularities. The driving torques are then compared to check for discontinuities and jerks. The second phase of the research project set the stage for the testing of the proposed method when the articulated structures are composed of flexible bodies. GRA

N91-29598# Department of the Navy, Washington, DC.
QUICK DISCONNECT PRESSURE CAP Patent Application
Peter Machado, inventor (to Navy) and James Muzaca, inventor (to Navy) 28 Sep. 1990 9 p
(AD-D014936; US-Patent-Appl-SN-590182) Avail: NTIS HC/MF A02 CSCL 13/5

A closure for the end of a male quick disconnect fluid coupling has an internal plug that displaces the plug normally provided in the male quick disconnect coupling, and the closure also has an outer plug wall with balls that can be radially cammed inwardly by a rotatable sleeve on the closure. GRA

N91-29599*# National Aeronautics and Space Administration. Lewis Research Center, Cleveland, OH.
EFFECT OF TWO SYNTHETIC LUBRICANTS ON LIFE OF AISI 9310 SPUR GEARS
Dennis P. Townsend and John Shimski (Naval Air Propulsion Test Center, Trenton, NJ.) Jun. 1991 16 p
(DA Proj. 1L1-62211-A-47A)
(NASA-TM-104352; E-6004; NAS 1.15:104352;
AVSCOM-TR-91-C-011) Avail: NTIS HC/MF A03 CSCL 13I

Spur-gear fatigue tests were conducted with two lubricants using a single lot of consumable-electrode vacuum-melted (CVM) AISI 9310 spur gears. The gears were case carburized and hardened to Rockwell C60. The gear pitch diameter was 8.89 cm. The lot of gears was divided into two groups, each of which was tested with a different lubricant. The test lubricants can be classified as synthetic polyol-ester-based lubricants. One lubricant was 30 percent more viscous that the other. Both lubricants have similar pressure viscosity coefficients. Test conditions included a bulk gear temperature of 350 K, a maximum Hertz stress of 1.71 GPa at the pitch line, and a speed of 10,000 rpm. The surface fatigue life of gears tested with one lubricant was approximately 2.4 times that for gears tested with the other lubricant. The lubricant with the 30 percent higher viscosity gave a calculated elastohydrodynamic (EHD) film thickness that was 20 percent higher than the other lubricant. This increased EHD film thickness is the most probable reason for the improvement in surface fatigue life of gears tested with this lubricant over gears tested with the less viscous lubricant. Author

N91-29600*# National Aeronautics and Space Administration. Lewis Research Center, Cleveland, OH.
LOCAL SYNTHESIS AND TOOTH CONTACT ANALYSIS OF FACE-MILLED SPIRAL BEVEL GEARS
F. L. Litvin, Y. Zhang (Illinois Univ., Chicago.), and R. F. Handschuh 1991 6 p Presented at the 1991 International Conference on Motion and Power Transmissions, Hiroshima, Japan, 24-26 Nov. 1991; sponsored by the Japan Society of Mechanical Engineers
(Grant NAG3-1263; DA Proj. 1L1-62211-A-47A)
(NASA-TM-105182; E-6349; NAS 1.15:105182;
AVSCOM-TR-91-C-039) Avail: NTIS HC/MF A02 CSCL 13I

A new approach is proposed for the local synthesis of spiral bevel gears. The approach provides contact at the mean contact point with the desired deviation of the transmission error function by a predesigned parabolic function. The orientation of the contact path on the gear tooth surface and the length of the major axis of the instantaneous contact ellipse are also included in the analysis. A tooth contact analysis (TCA) computer program was developed to simulate meshing and contact of the gear tooth surfaces. A numerical example of the process is given. Author

N91-29601# Solar Turbines, Inc. San Diego, CA.
ULTRA-LOW NOx GAS TURBINE COMBUSTOR Final Report, Oct. 1985 - Jun. 1990
Kenneth O. Smith Jul. 1991 48 p
(Contract GRI-5083-251-1000)
(PB91-184994; SR90-R-5357; GRI-90/0158) Avail: NTIS HC/MF A03 CSCL 21B

The design and rig testing of a lean premixed, low emissions, gas turbine combustor prototype are described. The combustor evaluated was a 90 degree sector of a full-scale annular combustor for a 3.7 Mw, natural gas-fired, industrial gas turbine. The combustor sector represented an intermediate development step in extending the lean premixed combustor technology from a can combustor configuration with a single fuel injector to an annular geometry with multiple injectors. In a parallel effort, a rich/lean combustor sector was also evaluated. This effort provided a direct comparison of the NO(x) reduction capabilities of the rich/lean and lean premixed concepts. Testing at typical gas turbine operating pressures (122 psig) demonstrated that both the lean premixed and rich/lean combustor sectors were capable of meeting the program NO(x) goal of 25 ppm (15 percent O2) while maintaining CO emissions below 50 ppm. The testing indicated that variable geometry and fuel staging will be required for low emissions range extension and low part load operation, respectively. GRA

N91-29602# Environmental Protection Agency, Ann Arbor, MI. Control Technology and Applications Branch.
CONVERSION OF METHANOL-FUELED 16-VALVE, 4-CYLINDER ENGINE TO OPERATION ON GASEOUS 2H2/CO FUEL Interim Report No. 3
R. M. Schaefer, G. K. Piotrowski, and J. C. Martin Apr. 1991 27 p
(PB91-195941; EPA/AA/CTAB-91/01) Avail: NTIS HC/MF A03 CSCL 13I

The aim of this project is to convert a Nissan CA18ED engine, previously modified for operation on M100 neat methanol, to operation on dissociated gaseous fuel. The modifications made to the engine are described. The results of testing are summarized. Author

N91-29603*# Spectra Research Systems, Inc., Huntsville, AL. Systems Technology Div.
BEARING TESTER DATA COMPILATION ANALYSIS, AND REPORTING AND BEARING MATH MODELING Quarterly Progress Report, Jul. - Sep. 1985
1985 63 p
(Contract NAS8-36183)
(NASA-CR-178883; NAS 1.26:178883; SRS/STD-PR-535/11; Rept-535) Avail: NTIS HC/MF A04 CSCL 13I

The magnitude and direction of fluid induced torques and forces on the 57 mm bearing cage is considered to be a contributing factor in possible cage instabilities that can produce intermittent high heating in the bearing. Analyses of the fluid forces and torques are presented. Heat generated by viscous fluid work was estimated for two flow diverter configurations and a coolant flow of 10 lbs/sec to support the thermal evaluation of the LOX Bearing Materials Tester. Results of the analysis of the LOX turbopump turbine end bearings are discussed. Coolant velocities for the no. 4 LOX turbopump turbine end bearings were estimated as a function of shaft speed and coolant flow rate. Contact angles and track width data were developed for the 57 mm bearing as functions of shaft speed, and axial and radial loads. The Advanced Dynamics of Rolling Elements (ADORE) computer program was installed on the MSFC UNIVAC 1100 and a test case successfully run. Both the text output and the plotting output were verified. The Bearing Seal and Materials Tester - Test Condition Data Base was developed. The parametric analysis of the operating characteristics of the LOX turbopump pump end bearing using the 45 mm bearing thermal model was begun. B.G.

38 QUALITY ASSURANCE AND RELIABILITY

Includes product sampling procedures and techniques; and quality control.

N91-29604# National Aeronautical Establishment, Ottawa (Ontario). Structures and Materials Lab.
EVALUATION OF SHADOW MOIRE FOR SURFACE DEFORMATION DETECTION AND MEASUREMENT
A. R. Kotanen and J. P. Komorowski 23 Jan. 1990 31 p Sponsored by Department of National Defence
(NAE-LTR-ST-1737; CTN-91-60033) Copyright Avail: NTIS HC/MF A03

As part of an investigation into various inspection methods for the detection and measurement of low energy impact damage on composite materials, an investigation was undertaken of a shadow moire topographical inspection system. This system combines a collimated light source, a camera, and a moire grating to provide topographical information regarding an object's surface. Shadow moire employs a single grating. The moire pattern is created on the test object by projecting a collimated light beam through the grating at a selected angle and then viewing the object through the same grating normal to the object surface. The results of tests indicate a number of disadvantages to the method. It requires a well collimated light source and a rigid setup; is usable only on light colored, external surfaces; has difficulty determining surface-slope direction in recorded images; and requires that high density gratings be placed in close proximity to objects being measured. Advangages include the following: surface discontinuities can be determined rapidly; it can carry out noncontact measurement; integration with a computer based image acquisition system is possible; the surface slope can be determined in real time; and the equipment is portable. The method shows promise for the rapid nondestructive, noncontact identification of deformed areas for further investigation by other test measures. CISTI

N91-29605# Sandia National Labs., Albuquerque, NM.
CHARACTERIZATION OF SURFACE CONTAMINANTS USING INFRARED MICROSPECTROSCOPY
D. S. Blair and K. J. Ward 1991 10 p Presented at the OE/LASE '91: 4th Society of Photo-Optical Instrumentation Engineers (SPIE) International Symposium, Los Angeles, 20-25 Jan. 1991
(Contract DE-AC04-76DP-00789)
(DE91-009405; SAND-91-0162C; CONF-910123-17) Avail: NTIS HC/MF A02

Coupling microscopes and infrared spectrometers results in the technique called microscopy/Fourier-transform infrared spectroscopy (microscopy/FT-IR), which makes it possible to examine samples, such as particles, droplets, smears, fibers, crystals, inclusions, bubbles, or additives, as small as 10 microns in diameter. This minimum size limitation is a physical constraint based on the diffraction limit of light in the mid-infrared region. Microscopy/FT-IR, when combined with repetitive microscopy stage movements, can be used to both locate and help identify chemical species. This infrared micro-profiling provides an infrared spectrum for each stage position or pixel element. The information is used to map, chemically identify and spatially resolve, a sample. Recent work using this technique includes mapping a thin film of solder flux rosin, identifying individual polymers present in a multilayer polymer structure, and identifying a fluid inclusion. This technique, in general, generates a large number of spectra that must be manipulated so that relevant information can be extracted to produce a spatial image. An efficient method for estimating this information is to compress the spectral data at each pixel to a single intensity value and plot this value as a function of pixel position. The method of compressing spectral data by integrating absorbance intensity over a characteristics frequency range was used to manipulate data generated during IR micro-profiling of a single cellulose acetate fiber placed on a gold coated glass slide. DOE

N91-29606# Allied-Signal Aerospace Co., Kansas City, MO.
INVESTIGATION OF ULTRASONIC EVALUATION OF SOLID-STATE METAL BOND
F. L. Robinson Jun. 1991 16 p
(Contract DE-AC04-76DP-00613)
(DE91-014996; BDX-613-3962) Avail: NTIS HC/MF A03

It was determined whether ultrasonic examination would be useful in evaluating solid state bonds in selected test assemblies. Useful information which might be obtainable by ultrasonic methods includes detection of bond line defects, detection of mismatch at the hidden surface of the bond, and evaluation of microstructural changes which may correlate with bond strength. DOE

N91-29607# Army Materials Technology Lab., Watertown, MA.
A LAYERED BEAM THEORY FOR SINGLE LAP JOINTS Final Report
Donald W. Oplinger Jun. 1991 53 p
(AD-A237324; MTL-TR-91-23) Avail: NTIS HC/MF A04 CSCL 20/11

Analysis of the single lap joint by Goland and Reissner provided important contributions to the literature on stress analysis of adhesive joints by clarifying not only the importance of adhesive peel stresses and peel strength in joint failure, but also the role of bending deflections of the joint in controlling the level of the stresses in the adhesive layer. Subsequent efforts have suggested the need for corrections to the Goland and Reissner analysis because of what have been conceived as deficiencies in the model used to describe bending deflections of the central part of the joint where a classical homogeneous beam model without shear or thickness normal deflections were used. The present paper addresses the issue through the use of a more realistic model in which adhesive layer deflections are allowed to decouple the two halves of the joint in the overlap region in the bending deflection analysis, as well as in Goland and Reissner. It is found that many of the predictions of the Goland and Reissner analysis are recovered in the limit of large adherend-to-adhesive layer thickness ratios, although substantial differences from the Goland and Reissner analysis can occur for relatively thin adherends. GRA

N91-29608# Army Lab. Command, Watertown, MA. Material Technology Lab.
ULTRASONIC EVALUATION OF SILICON NITRIDE GREEN BODIES Final Report
Janet Quinn and Lisa Tardiff May 1991 17 p
(AD-A237924; MTL-TR-91-19) Avail: NTIS HC/MF A03 CSCL 11/2

Advances in ultrasonic materials evaluation technology have greatly expanded the potential usefulness of this nondestructive testing technique to the ceramics industry. The development of dry coupling transducers has been especially beneficial to the early stages of ceramic processing with processing with increasing application to green body evaluation. In this study, ultrasonic techniques are utilized to determine property relationships in silicon nitride green bodies. A correlation of ultrasonic velocities with green body densities was found to be affected by a commercial plasticizer utilized in processing the slurries. This correlation was further investigated with photomicrographs, porosimetry, and a BET analysis. GRA

N91-29609# Netrologic, Inc., San Diego, CA.
NEURAL NETWORKS AND ROBOTICS APPLIED TO THE NON-DESTRUCTIVE INSPECTION OF AIRCRAFT Status Report
Dan Greenwood 1 Jul. 1991 2 p
(Contract N00014-91-C-0095)
(AD-A238312) Avail: NTIS HC/MF A01 CSCL 12/9

We are converting the in phase and quadrature measurements into an image and then using the image to classify fault or no fault eddy current. This has been done using old OCR features developed to recognize handwritten numerical characters which are applicable to this situation. The raw data was first smoothed out by taking the average of the nearest 10 measurements, then plotted on a 50 by 50 grid. The X axis is the in phase measurement normalized to accommodate the maximum and minimum in phase values in the data set. The same was done for quadrature values on the Y axis. An efficient path planning method for collision avoidance has been developed. Fast path planning is achieved by decomposing the 3-dimensional space into a number of 2-dimensional subspaces. A method is devised to work directly with arm postures (configurations) instead of dealing with individual joint angles. These two aspects, namely decomposition and posture control, greatly speed up the path finding procedure and make it possible to perform near real-time planning in a moderately cluttered environment. Meetings were held at McDonnell Douglas, McClelland AFB, and Physical Research Inc., manufacturers of Magneto-Optic Crack Detectors, to assess the utility of our research and plans for prototyping during Phase 2. Discussions have begun with United Technologies concerning the use of our research for a large Air Force NDI program. Prospects for Phase 3 follow-on look promising. GRA

N91-29610*# National Aeronautics and Space Administration. Lewis Research Center, Cleveland, OH.
NDE OF CERAMICS AND CERAMIC COMPOSITES
Alex Vary and Stanley J. Klima (Sverdrup Technology, Inc., Brook Park, OH.) Jul. 1991 15 p
(NASA-TM-104520; E-6390; NAS 1.15:104520) Avail: NTIS HC/MF A03 CSCL 14D

Although nondestructive evaluation (NDE) techniques for ceramics are fairly well developed, they are difficult to apply in many cases for high probability detection of the minute flaws that can cause failure in monolithic ceramics. Conventional NDE techniques are available for monolithic and fiber reinforced ceramic matrix composites, but more exact quantitative techniques needed are still being investigated and developed. Needs range from flaw detection to below 100 micron levels in monolithic ceramics to global imaging of fiber architecture and matrix densification anomalies in ceramic composites. NDE techniques that will ultimately be applicable to production and quality control of ceramic structures are still emerging from the lab. Needs are different depending on the processing stage, fabrication method, and nature of the finished product. NDE techniques are being developed in concert with materials processing research where they can provide feedback information to processing development and quality improvement. NDE techniques also serve as research tools for materials characterization and for understanding failure processes, e.g., during thermomechanical testing. Author

39 STRUCTURAL MECHANICS

Includes structural element design and weight analysis; fatigue; and thermal stress.

For applications see *05 Aircraft Design, Testing and Performance* and *18 Spacecraft Design, Testing and Performance.*

N91-29611# National Aeronautical Establishment, Ottawa (Ontario).
REVIEW OF LITERATURE ON THE DAMAGE, LOSS OF STIFFNESS, AND RESIDUAL STRENGTH OF GRAPHITE/EPOXY LAMINATES SUBJECTED TO CYCLIC LOADING
Luc Dupont, Clermont Roy (Sherbrooke Univ., Quebec), and Jerzy P. Komorowski 6 Jul. 1989 48 p In FRENCH; ENGLISH summary
(NAE-LTR-ST(CR)-1711; CTN-91-60073) Copyright Avail: NTIS HC/MF A03

The review is focused on fatigue testing of laminates subjected to cyclic loading especially where compressive loads were present. There is presently no standard or generally accepted method of compression fatigue testing of composite specimens. Works on specimen design, on the design of grips and buckling guides used to transfer loads to the test samples, loading conditions, methods of data acquisition, and empirical methods and models used in data analysis are reviewed. The process of damage leading to final rupture can be divided into distinct stages. The final rupture of a composite specimen is not governed by a single dominating crack but by a multitude of cracks or delaminations. The lay-up as well as the stacking sequence influences the damage mode and life of a specimen. Composite materials demonstrate good resistance to fatigue, however this is closely tied with a large scatter in the number of cycles to failure. In tests where compressive loads are included, greatly reduced specimen lives were observed. Spectrum loading tests have shown that the cycles with the highest loads have the greatest effect on specimen life.
Author (CISTI)

N91-29612# Sandia National Labs., Albuquerque, NM.
ELASTIC-PLASTIC CONSTITUTIVE RELATIONS AT LARGE STRAIN
W. Herrmann 1991 5 p Presented at the 1991 American Physical Society (APS) Conference on Shock Compression of Condensed Matter, Williamsburg, 17-20 Jul. 1991
(Contract DE-AC04-76DP-00789)
(DE91-013195; SAND-91-1169C; CONF-9107105-17) Avail: NTIS HC/MF A01

Present practice in most computer codes intended for the solution of dynamic mechanics problems is to use the classical infinitesimal plasticity relations together with the Jaumann stress rate to account for finite rotations. Use of the Jaumann stress rate is known to lead to oscillating stress-strain response in simple shear at large deformations for elastic and some plastic relations, and is limited to isotropic material descriptions. Formulations of finite deformation plasticity based on the Lagrangian reference configuration and an unrotated configuration have been proposed which, in principle, should overcome these limitations. The latter has been implemented in a finite element computer code. In this paper, it is shown how a Lagrangian description based on the reference configuration may be implemented in computer codes, and how it may be translated into a corresponding Eulerian description based on the current configuration and a description based on the unrotated configuration for comparison with currently used descriptions. DOE

N91-29613 Washington Univ., Seattle.
HIERARCHIC EXTENSIONS IN THE STATIC AND DYNAMIC ANALYSIS OF ELASTIC BEAMS Ph.D. Thesis
Robert A. Watson 1990 317 p
Avail: Univ. Microfilms Order No. DA9114724

Approximate solutions of static and dynamic beam problems by the p-version of the finite element method are investigated. Within a hierarchy of engineering beam idealizations, rigorous formulations of the strain and kinetic energies for straight and circular beam elements are presented. These formulations include rotating coordinate system effects and geometric nonlinearities to allow for the evaluation of vertical axis wind turbines - the motivating problem for this research. Hierarchic finite element spaces, based on extensions the polynomial orders used to approximate the displacement variables, are constructed. The developed models are implemented into a general purpose computer program for evaluation. Quality control procedures are examined for a diverse set of sample problems. Sequential eigensolutions of problems utilizing hierarchic extensions allow for algorithmic enhancements of some iterative eigensolver techniques. The study details the theoretical basis for these improvements and documents the resulting computational benefits. Dissert. Abstr.

N91-29614 Connecticut Univ., Storrs.
PREDICTION OF EDGE STRESSES IN LAYERED MEDIA USING THE SURFACE INTEGRAL-FINITE ELEMENT TECHNIQUE Ph.D. Thesis
Michael Bak 1990 267 p
Avail: Univ. Microfilms Order No. DA9115570

A method for predicting the state of stress of a body consisting of two isotropic materials including the intersection of the interface with a stress free boundary is presented. The prediction of the so-called free edge stress is accomplished using a stress intensity parameter. The solution, which addresses arbitrary two-dimensional geometries with mechanical and thermal loading and plane strain or plane stress behavior, couples the finite element method to a singular integral representation of a dislocation. The finite element solution of the two layers, which allows for independent displacement of the two layers based on the applied loading, is added to the solution of distributed dislocations along the interface of two semi-infinite layers. Coupling of the two solutions occurs along the interface and at the finite boundary. Dissert. Abstr.

N91-29615 Virginia Polytechnic Inst. and State Univ., Blacksburg.
MODELING AND RESPONSE ANALYSIS OF THIN-WALLED BEAM STRUCTURES CONSTRUCTED OF ADVANCED COMPOSITE MATERIALS Ph.D. Thesis
Ohseop Song 1990 194 p
Avail: Univ. Microfilms Order No. DA9116645

The objective is to incorporate several essential effects which have a considerable importance for the rational design of composite thin-walled beam structures. These effects are the transverse shear deformation, the warping constraint, the secondary warping as well as the hygrothermal and the dynamic ones. The field equations of laminated composite thin-walled beams of either open or closed single and multicell cross-sections are derived through the application of Hamilton's variational principle. The Laplace Transform technique is used to obtain exact solutions. The aeroelastic divergence instability of aircraft wings modelled as thin-walled beams as well as the eigenfrequency problem of cantilevered composite thin-walled beams of closed cross-section are considered in the framework of a refined theory incorporating non-classical effects. Author

N91-29616 Michigan Univ., Ann Arbor.
STRUCTURAL OPTIMIZATION WITH PSEUDO-LOAD APPROACH EXPLOITING DESIGN LENGTH SCALES Ph.D. Thesis
Jianhong Zhang 1990 121 p
Avail: Univ. Microfilms Order No. DA9116337

Numerical optimization techniques are lagging in acceptance by the engineering community. One of the most serious problems is the high computational costs associated with repeated evaluation of constraint functions and their derivatives. To reduce costs, an approximate method exploiting design length scales is devised and built into the analysis and optimization programs. This approach is called the pseudo-load approach. Most practical structures are divided into naturally occurring regions by manufacturers and engineers. Design variable linking is used for variables in each region. Pseudo loads are applied on each region; the response to these loads provides certain mode shapes, called pseudo-load modes. These are used to approximate the behavior of the modified structures by a Rayleigh-Ritz technique. A structural synthesis program was developed by coupling the numerical optimization program ADS to the widely used finite element program MSC/NASTRAN. Dissert. Abstr.

N91-29617 Stanford Univ., CA.
INTEGRATED STRUCTURAL DAMPING AND CONTROL SYSTEM DESIGN FOR HIGH-ORDER FLEXIBLE SYSTEMS Ph.D. Thesis
Frank Anthony McLoughlin 1991 291 p
Avail: Univ. Microfilms Order No. DA9115819

A novel design methodology that integrates both control system and structural design activities was developed and applied to an experimental apparatus. The modular design procedure, which is automated in software, identifies an optical allocation of damping for controlled linear structures. The procedure is unique in that it modifies both structural topology and structural parameters to identify effective locations and levels of damping. In doing so, the procedure quantifies the payoff of damping a controlled structure. The principal application of this procedure was the vibration isolation system of the Stanford Gravity Wave Experiment. This isolation system is a complex, high-order, six degrees-of-freedom, very lightly damped structure which is maintained at low temperature near absolute zero. Dissert. Abstr.

N91-29618 Purdue Univ., West Lafayette, IN.
FINITE ELEMENT-BASED SYSTEM IDENTIFICATION FROM EXPERIMENTAL MODAL ANALYSIS RESULTS Ph.D. Thesis
David Edward Watts 1990 197 p
Avail: Univ. Microfilms Order No. DA9116478

A process is developed to determine the physical attributes of a structure from experimental measurements of the natural frequencies of vibration and the corresponding mode shapes of the structure. The process is based upon minimization of a least squares measure of the difference between the measured vibrational characteristics and those characteristics determined from a finite element model of the structure. The solution is given by the parameters of the finite element model which yield a minimum least squares difference in the two sets of modal data. Author

N91-29619# Sandia National Labs., Albuquerque, NM.
HYPERVELOCITY IMPACT JET FORMATION
J. A. Ang 1991 8 p Presented at the 1991 American Physical Society (APS) Conference on Shock Compression of Condensed Matter, Williamsburg, VA, 17-20 Jul. 1991
(Contract DE-AC04-76DP-00789)
(DE91-014651; SAND-91-0146C; CONF-9107105-36) Avail: NTIS HC/MF A02

The hypervelocity impact of a particle on a surface generates a jet of shocked material which is thrown from the impact site. A simple analytic model has been developed to obtain expressions for the evolution of this jet of ejecta. The analysis is based on applying the conservation equations of mass and momentum to the problem of a normal impact of a sphere against a semi-infinite flat target. Expressions are developed for the evolution of the jet velocity, jet release point and the locus of points which describe the ejecta envelope. These analytical ejecta profiles are compared with high speed photographs of impact jet formation. DOE

N91-29620# Lawrence Livermore National Lab., CA.
DEFORMATION BEHAVIOR OF PRE-SHOCKED COPPER AS A FUNCTION OF STRAIN RATE AND TEMPERATURE

W. H. Gourdin and D. H. Lassila May 1991 6 p Presented at the 7th American Physical Society (APS) Topical Conference on Shock Compression of Condensed Matter, Williamsburg, 17-20 Jun. 1991
(Contract W-7405-eng-48)
(DE91-015180; UCRL-JC-106130; CONF-910654-3) Avail: NTIS HC/MF A02

From quasi-static compression data for 30 micron grain size samples of oxygen free electronic (OFE) grade copper shocked to 10 GPa for 1 microsec, a value is derived for the thermal component of the mechanical threshold stress (MTS). It is shown that model calculations of the flow stress based on this value provide an excellent description of the uniaxial deformation of preshocked specimens tested in compression at low and high strain rates. Excellent agreement is shown with data obtained from electromagnetically launched expanding ring experiments, during which excursions of both temperature and strain rate are large. DOE

N91-29621# Brown Univ., Providence, RI. Div. of Engineering.
FUNDAMENTAL STUDIES IN DYNAMIC PLASTICITY Final Report
R. J. Clifton 10 Jun. 1991 6 p
(Contract N00014-87-K-0118)
(AD-A237114) Avail: NTIS HC/MF A02 CSCL 20/11

The principal objective of the research on this project has been to develop improved understanding of the plastic response of metals at strain rates of 100000 1/s and higher. This objective has been pursued primarily by the development of a strain-rate change test for probing the plastic response of a metal being sheared at strain rates of 105 1/s to 106 1/s in a pressure-shear plate impact experiment. Such a test makes it possible to distinguish between the rate sensitivity of the flow stress at fixed dislocation structure, and the rate sensitivity of strain hardening. These effects cannot be distinguished in the usual tests at constant strain rates. A second objective arises from the main result of the research on the principal objective; namely, that the rate sensitivity at high strain rates is associated primarily with the rate sensitivity of strain hardening. Consequently, improved understanding of strain hardening takes on greater importance and had been addressed as a second objective. Quasi-static compression tests have been conducted on aluminum single crystals to clarify the interaction between slip on one slip system and hardening on another. Such clarification is required to allow the development of reliable models for plastic flow based on slip on multiple slip systems. GRA

N91-29622# Massachusetts Inst. of Tech., Cambridge.
MORPHOLOGY OF BULK NYLON 6 SUBJECTED TO PLANE STRAIN COMPRESSION Interim Technical Report, No. 28, 1990 - 1991
A. Galeski, Ali S. Argon, and R. E. Cohen 31 May 1991 36 p
(Contract N00014-86-K-0768)
(AD-A237331) Avail: NTIS HC/MF A03 CSCL 11/5

The mechanics of deformation of nylon 6 in plane strain compression were elucidated by density measurements, differential scanning calorimetry, polarized light microscopy, x ray diffraction and x ray diffraction pole figures. A deconvolution procedure for separating overlapping x ray diffraction peaks and the amorphous halo was used to generate pole figures for the various alpha and gamma phase reflections exhibited by nylon 6. At compression ratios above 1.6, specimens experienced intense shear stresses at -45 deg and +45 deg with respect to the flow direction. Shear bands were formed most frequently at interspherulitic boundaries. This shearing produced a small volume fraction of gamma phase crystals in samples which originally contained only alpha crystallinity. The x ray diffraction studies showed that gamma phase crystals were oriented with their macromolecular chains along the directions of shear bands. The alpha crystals of nylon 6 underwent extensive deterioration in compression by a chain slip mechanism along the (0 0 2) planes containing hydrogen bonds. Slip also caused the rotation of fragmented lamellae that lead, at high compression ratios, to a peculiar bifurcated orientation state resembling a twinned monocrystal. GRA

N91-29623# Massachusetts Inst. of Tech., Cambridge.
DECONVOLUTION OF X RAY DIFFRACTION DATA TO ELUCIDATE PLASTIC DEFORMATION MECHANISMS IN THE UNIAXIAL EXTENSION OF BULK NYLON-6 Interim Technical Report No. 27, 1990 - 1991
A. Galeski, Ali S. Argon, and R. E. Cohen 31 May 1991 26 p
(Contract N00014-86-K-0768)
(AD-A237332) Avail: NTIS HC/MF A03 CSCL 20/5

A least square peak deconvolution procedure was applied to wide angle x ray diffraction data on uniaxially drawn nylon 6 so that pole figures could be generated from clearly separated crystallographic reflections. Beside peak total intensity pole figures, a new type of pole figure, based on peak widths, was proposed and proved to be useful in elucidating the mechanisms of plastic deformation in the nylon 6 samples. In uniaxial tension, alpha and gamma crystals of nylon 6 become oriented with macromolecular chains parallel to the drawing direction. In contrast to gamma crystals, alpha crystals experience a large amount of breakdown between planes containing hydrogen bonds. Macromolecules which are in the amorphous phase are mostly aligned along the drawing direction and that fraction of amorphous phase are mostly aligned along the drawing direction and that fraction of amorphous phase which is so oriented shows the best close packing. GRA

N91-29624# General Physics Corp., Cape Canaveral AFS, FL. Space Coast Office.
PRESSURE VESSEL BURST TEST PROGRAM Progress Paper No. 2
M. Cain, D. Sharp, and M. Coleman 17 Jun. 1991 12 p
Previously announced as A90-40623 Sponsored by AFSC
(AD-A237845; ESMC-TR-91-1) Avail: NTIS HC/MF A03 CSCL 13/4

An updated progress report is provided on a program developed to study through test and analysis, the characteristics of blast waves and fragmentation generated by ruptured gas filled pressure vessels. The initial paper on this USAF/NASA/General Physics program was presented to the AIAA in July 1990. Since the initial paper, several pressure vessels have been burst characteristics and utilized a well instrumented arena. Data trends for current experiments are presented. This paper is the second progress report on the program and addresses (1) a brief review of current methods for assessing vessel safety and burst parameters; (2) a review of pneumatic burst testing operations and testing results, including a comparison to current methods for burst assessment; and (3) a review of the basis for the current test program including planned testing. GRA

N91-29625# Metz Univ. (France). Lab. of Physics and Mechanics of Materials.
EXPERIMENTAL INVESTIGATION OF ADIABATIC SHEAR BANDING AT DIFFERENT IMPACT VELOCITIES Interim Report No. 2, 19 Jan. - 18 May 1991
J. R. Klepaczko 10 May 1991 5 p
(Contract DAJA45-90-C-0052)
(AD-A237901; R/D-614B-MS-01) Avail: NTIS HC/MF A01 CSCL 19/10

A new experimental technique to study adiabatic shear bands at different displacement velocities has been pursued. The technique is in its early stage of development, i.e., the mechanical parts have been machined and the experimental setup has been assembled. The measuring techniques are in preparation. GRA

N91-29626# Northwestern Univ., Evanston, IL. Dept. of Civil Engineering.
FISSION-FUSION ADAPTIVITY IN FINITE ELEMENTS FOR NONLINEAR DYNAMICS OF SHELLS Final Technical Report, 1 Oct. 1987 - 30 Aug. 1990
Ted Belytschko 30 Aug. 1990 48 p
(Contract F49620-88-C-0011)
(AD-A238029; AFOSR-91-0602TR) Avail: NTIS HC/MF A03 CSCL 13/13

The objective of this work was to develop adaptive finite element analysis methods for nonlinear structural dynamics.

Adaptive methods are particularly promising for nonlinear problems involving failure, because in failure and near-failure states of structures, three predominant phenomena are; buckling, shear banding, and fracture. These phenomena are associated with localization of the deformation, by which is meant the development of large strains in small regions of the structure, which is accompanied by large gradients in the strain. While strains are distributed in elastic buckling, once plasticity develops a large part of the deformation of beams or shells usually occurs over narrow zone called hingelines. Shear banding is a result of strain softening material behavior and is also associated with narrow bands of highly strained material. In fracture, high strain gradients occur at the crack tip, and in addition the displacement field is discontinuous behind the crack tip. In this work, adaptive methods are developed for the nonlinear dynamics of shells with both geometric and material nonlinearities. The localization phenomenon which is of primary interest in this class of problems is hingeline formation, but aspects of this work should be applicable to other localization phenomena in structural dynamics. GRA

N91-29627# Georgia Inst. of Tech., Atlanta. Mechanical Properties Research Lab.

A STUDY OF THE RELATIONSHIP BETWEEN MACROSCOPIC MEASURES AND PHYSICAL PROCESSES OCCURRING DURING N00014-89-J-1708 Annual Report

Stephen D. Antolovich and Stuart R. Stock 1991 41 p
(Contract N00014-89-J-1708)
(AD-A238423) Avail: NTIS HC/MF A03 CSCL 20/11

The principal experimental accomplishments during the second year of the program were two sets of x-ray tomographic microscopy (XTM) measurements on notched tensile samples. Fatigue crack growth was in a conventional servo-hydraulic machine before the samples were mounted in the in situ load frame. The choice of the extremely small (by fracture mechanics standards) samples was dictated by the need to have good sample transparency at the synchrotron x-ray energies with the highest fluxes (typically up to about 25 keV before the flux starts to drop dramatically). A second consideration limiting the sample diameter is the number of detector elements and the maximum cross-sectional dimension of the sample: a 10 mm diameter sample sampled with 10 to the third power detector elements yield a minimum pixel dimension of 10 um; closure measurements requires pixels smaller than this. GRA

N91-29628# Florida Univ., Gainesville. Dept. of Aerospace Engineering.

VIBRATION CONTROL AND OPTIMIZATION IN COMPOSITE STRUCTURAL ELEMENTS BY USE OF ADD-ON VISCOELASTIC MATERIALS

C. T. Sun and P. Hajela 26 Apr. 1991 15 p
(Contract DAAL03-88-K-0013)
(AD-A238533) Avail: NTIS HC/MF A03 CSCL 11/4

Three areas of study are presented: (1) development of new and efficient models for accurate prediction of structural damping ability; (2) development and application of new strategies to the associated optimization problem, i.e., damping layer redistribution for maximizing damping subject to static stiffness, stress, weight and frequency constraints; and (3) experimental quantification for comparison with analytical predictions. GRA

N91-29629*# Texas Univ., San Antonio. Engineering Div.

PROBABILISTIC LIFETIME STRENGTH OF AEROSPACE MATERIALS VIA COMPUTATIONAL SIMULATION Final Report, Jan. - Dec. 1989

Lola Boyce, Jerome P. Keating, Thomas B. Lovelace, and Callie C. Bast Aug. 1991 280 p
(Grant NAG3-867)
(NASA-CR-187178; NAS 1.26:187178) Avail: NTIS HC/MF A13 CSCL 20K

The results of a second year effort of a research program are presented. The research included development of methodology that provides probabilistic lifetime strength of aerospace materials via computational simulation. A probabilistic phenomenological constitutive relationship, in the form of a randomized multifactor interaction equation, is postulated for strength degradation of structural components of aerospace propulsion systems subjected to a number of effects of primitive variables. These primitive variables often originate in the environment and may include stress from loading, temperature, chemical, or radiation attack. This multifactor interaction constitutive equation is included in the cornputer program, PROMISS. Also included in the research is the development of methodology to calibrate the constitutive equation using actual experimental materials data together with the multiple linear regression of that data. Author

N91-29630# Massachusetts Inst. of Tech., Cambridge. Sea Grant Coll. Program.

DIMENSIONLESS PARAMETERS IMPORTANT TO THE PREDICTION OF VORTEX-INDUCED VIBRATION OF LONG, FLEXIBLE CYLINDERS IN OCEAN CURRENTS

J. K. Vandiver 1991 55 p Sponsored in part by the National Sea Grant Coll. Program, Silver Spring, MD
(Grant NA86AA-D-SG089)
(PB91-184713; MITSG-91-13) Avail: NTIS HC/MF A04 CSCL 20K

Case studies drawn from 15 years of field and laboratory experiments are used to demonstrate and explain why the flow induced vibration of long cylinders in ocean currents varies from single mode locking to broadband random vibration. It is shown that the range of observed behavior is predictable, with careful consideration of a few dimensionless parameters. New interpretations are given to the significance of familiar parameters such as mass ratio, and reduced damping. In addition, the fractional variation in flow velocity over the length of the cylinder and the number of natural frequencies within the bandwidth of the vortex shedding frequencies are shown to be of considerable importance. Author

N91-29631# Sandia National Labs., Albuquerque, NM.

EXPLOSIVELY DRIVEN MISSILE TRAJECTORY PARAMETERS FOR VARIOUS FRAGMENT MATERIALS AND VELOCITIES

M. G. Vigil Jun. 1991 71 p
(Contract DE-AC04-76DP-00789)
(DE91-014330; SAND-91-0277) Avail: NTIS HC/MF A04

Analyses are presented for explosively driven missile fragment trajectories resultant from cased explosive configurations. Fragment trajectory parameter data are presented in graphical form for three different fragment materials (aluminum, steel, and uranium), initial velocities between 0.6 to 4.3 mm/microns, various launch angles (0 to 45 degrees), various drag coefficients, several elevations above sea level, and for various geometries. This trajectory information can be used to determine safe distances for spectators or site personnel observing a test or to address potential fragment damage to structures at impact. DOE

N91-29632# Los Alamos National Lab., NM.

EFFECTS OF ANISOTROPY ON DYNAMIC TENSILE BEHAVIOR

S. K. Schifert, R. F. Davidson, and P. J. Maudlin 1991 5 p Presented at the 1991 American Physical Society (APS) Conference on Shock Compression of Condensed Matter, Williamsburg, VA, 17-20 Jul. 1991
(Contract W-7405-eng-36)
(DE91-014748; LA-UR-91-1976; CONF-9107105-38) Avail: NTIS HC/MF A01

A stability analysis for an anisotropic stretching rod is presented. We consider the particular case of a rapidly stretching titanium jet using a continuum code to examine anisotropic plastic response in the finite-neck regime. It was found that the classical analysis (yield strength is inversely proportional to stability) is insufficient; anisotropic jets can be more or less stable than their maximum or minimum yield strengths, depending on initial perturbations and the orientation of the anisotropy. One particular anisotropy - with the weak direction along the jet axis - appears to be generally stabilizing. DOE

N91-29633# Lawrence Livermore National Lab., CA.
A SIMPLE MODEL FOR LOW L/D PENETRATION PHYSICS
K. E. Froeschner 25 Jan. 1991 12 p
(Contract W-7405-eng-48)
(DE91-015747; UCRL-ID-107610) Avail: NTIS HC/MF A03

There are references in the Terminal Ballistics literature concerning experiments in which very high values of penetration efficiency are seen when the penetrator has a very low length to diameter ratio, i.e., is disc-like. In this paper we present a simple theoretical model which might explain these results in terms of shock hydrodynamics and the results of experiments with low L/D impactors in our ballistics range. DOE

N91-29634# Lawrence Livermore National Lab., CA.
NIKE2D: A NONLINEAR, IMPLICIT, TWO-DIMENSIONAL FINITE ELEMENT CODE FOR SOLID MECHANICS
B. Engelmann and J. O. Hallquist Apr. 1991 206 p
(Contract W-7405-eng-48)
(DE91-015734; UCRL-MA-105413) Avail: NTIS HC/MF A10

An updated user manual is presented to the 1991 version of NIKE2D, and serves as a temporary theoretical manual. NIKE2D is an implicit finite element code for analyzing the finite deformation, static and dynamic response of 2-D, axisymmetric, plane strain, and plane stress solids. The code is fully vectorized and available on several computer platforms. A number of material models are incorporated to simulate a wide range of material behavior including elastoplasticity, anisotropy, creep, thermal effects, and rate dependence. Slideline algorithms model gaps and sliding along material interfaces, including interface friction and single surface contact. Interactive graphics and rezoning is included for analyses with large mesh distortions. In addition to quasinewton and arc-length procedures, adaptive algorithms can be defined to solve the implicit equations using the solution language ISLAND. Each of these capabilities and more make NIKE2D a robust analysis tool. DOE

42 GEOSCIENCES (GENERAL)

No abstracts in this category.

43 EARTH RESOURCES AND REMOTE SENSING

Includes remote sensing of earth resources by aircraft and spacecraft; photogrammetry; and aerial photography.

For instrumentation see *35 Instrumentation and Photography.*

N91-29635# Instituto de Pesquisas Espaciais, Sao Jose dos Campos (Brazil).
A PRACTICAL EXAMPLE OF FOREST MAPPING AND TIMBER VOLUME ESTIMATION USING LANDSAT-5 TM IMAGERY
David Chung Liang Lee, Rene Antonio Novaes, Pedro Hernandez Filho, and Flavio Jorge Ponzoni Jan. 1991 12 p Presented at the State of the Art Methodology of Forest Inventory, Syracuse, NY, 30 Jul. - 5 Aug. 1989
(INPE-5244-PRE/1675) Avail: NTIS HC/MF A03

The main objective was to obtain basic forest information of Uruguay. A methodology is described which used LANDSAT TM data as a first segment of a two-stage sampling plan designed to produce typical forest inventory information for plantations (pine and eucalypt) and to map forest areas. From all the results obtained, it can be concluded that LANDSAT-5 TM imagery, at a scale of 1:100,000, served well as the primary source of data for forest area mapping and timber inventory over a nation-wide level. Author

N91-29636*# Georgia Univ., Athens. School of Forest Resources.
USING THE TIMS TO ESTIMATE EVAPOTRANSPIRATION FROM A FOREST Final Technical Report, 1 Feb. 1987 - 30 Sep. 1989
Robert Teskey 30 Aug. 1991 10 p
(Grant NAGw-1034)
(NASA-CR-188729; NAS 1.26:188729) Avail: NTIS HC/MF A02 CSCL 08F

The main goals were: (1) to characterize the evapotranspiration (Et) of two forested watersheds using direct measurement techniques, and (2) to evaluate if remotely sensed surface temperatures could be used to estimate Et from the same watersheds. Two independent approaches for estimating the Et from watersheds were used. The first was derived using the Penman-Monteith Equation. This model requires the direct measurement of the microclimate of the site as well as biological measurements, i.e., stomatal conductance to water vapor and the leaf area of the stand. The primary limitation of this approach is that the measurement of stomatal conductance is time consuming, and in large trees, access to the foliage is difficult so the sample must be limited to the small number of trees. In the study, the sample was limited to the trees which could be measured from a single tower in each stand. Author

N91-29637# Naval Oceanographic and Atmospheric Research Lab., Bay Saint Louis, MS.
AN AVHRR DATA SET FOR THE ARCTIC LEADS ARI Final Report
F. M. Fetterer and J. D. Hawkins Apr. 1991 56 p
(AD-A237221; AD-E040005; NOARL-TN-118) Avail: NTIS HC/MF A04 CSCL 08/12

The Naval Oceanographic and Atmospheric Research Laboratory (NOARL) Remote sensing Branch is selecting and processing Advanced Very High Resolution Radiometer (AVHRR) data to support the science objectives of the Office of Naval Research Arctic Leads Accelerated Research Initiative (Arctic Leads ARI). Imagery was selected using hard copy prints from the Navy/National Oceanic and Atmospheric Administrative (NOAA) Joint Ice Center. An attempt is made to select imagery so that most of the Arctic was covered every 3 days. Imagery from NOAA's Satellite Data Services Division was calibrated and mapped to a stereographic projection identical to that used for Special Sensor Microwave Imager (SSM/I) data by the National Snow and Ice Data Center. The Arctic was covered in 2 grids of 1 km pixel size. Three years worth of imagery will be processed. At present, processing for 1989 is underway. GRA

N91-29638# Naval Oceanographic and Atmospheric Research Lab., Bay Saint Louis, MS.
ALGORITHMS FOR CONVERTING GEODETIC EARTH LOCATION TO SATELLITE TIME AND SWATH PIXEL COORDINATES FOR THE DMSP SATELLITE SYSTEM Final Report
A. K. Goroch Mar. 1991 20 p
(AD-A237589; AD-E040060; NOARL-TN-105) Avail: NTIS HC/MF A03 CSCL 17/7

Archived DMSP Operational Line Scanner data are stored in a satellite projection consisting of contiguous blocks of line and pixel information. The transformation from the satellite line and pixel coordinates to the conventional geodetic latitude and longitude are derived. A program suitable for use on a personal computer is provided. The program can be used for fast registration of an image in the line pixel coordinate system to any other projection. GRA

N91-29639# Army Cold Regions Research and Engineering Lab., Hanover, NH.
REMOTE SENSING OF SNOW COVERS USING THE GAMMA RAY TECHNIQUE
Elmer L. Offenbacher and Samuel C. Colbeck Apr. 1991 25 p
(DA Proj. 4A7-62784-AT-42; DA Proj. 4A7-62730-AT-42)

(AD-A238016; CRREL-91-9) Avail: NTIS HC/MF A03 CSCL 08/12

This report reviews various aspects of the use of natural gamma-ray emissions to determine the mass of snow covering the ground. The interactions of gamma rays with water mass are described, along with the various sources of gamma radiation from the ground. Different possible techniques for measuring gamma radiation are described. Each has advantages and disadvantages in obtaining the desired result. The sources of error and the use of this method are described. GRA

N91-29640# Minnesota Univ., Minneapolis. Inst. of Child Development.

TOPOGRAPHIC MAP READING Final Report, 1 May 1988 - 31 Dec. 1990

Herbert L. Pick, Jr. and William B. Thompson 12 May 1991 60 p

(Grant AF-AFOSR-0187-88; AF Proj. 2313)

(AD-A238026; AFOSR-91-0590TR) Avail: NTIS HC/MF A04 CSCL 08/2

Work completed includes a field study and protocol analysis of experienced map readers solving a localization problem. The analysis focused on identifying both the features the map readers attended to and the information processes involved in solving the problem. The information processes identified were reconnaissance, map orientation, feature matching, relation or configuration matching, and hypothesis generation and evaluation. The laboratory simulation studies were conducted on the basis of the field study. They both involved matching a photographic scene to a station point and direction of view on a topographic map. Results of these studies tended to confirm the description of the features and processes from the field study. Two supplementary studies were carried out. One used an alternative laboratory map reading task and provided converging evidence for the effects of manipulation of the amount of information available in the map. The other study was carried out to determine the precision with which map readers could judge physical distance and slope from photographic scenes and maps. This ability would constrain the possibility of using metric information in map reading. Preliminary specification for a computational architecture for the problem solving aspects of the drop-off site problem was completed. The model includes both knowledge bases for features and hypothesized solutions as well as a control structure for guiding problem solving activity. GRA

N91-29641# Pennsylvania State Univ., University Park. Dept. of Meteorology.

REMOTE DETERMINATION OF SOIL MOISTURE AND EVAPOTRANSPIRATION FROM THERMAL INFRARED MEASUREMENTS: DETECTION OF A DRYING THRESHOLD Final Report, 1 Sep. 1987 - 28 Feb. 1991

T. N. Carlson and J. M. Russo Mar. 1991 22 p

(Grant DI-14-08-0001-G1490)

(PB91-195818; USGS/G-1490) Avail: NTIS HC/MF A03 CSCL 08M

Important objectives in the work were to: (1) model the water movement through the soil/plant/atmosphere system; (2) use, in conjunction with this model, remote measurement of infrared surface temperature and vegetation index to calculate soil water content; and (3) determine whether water stress can be detected radiometrically over vegetation, specifically to identify the threshold at which these measurements for remotely estimating soil water content over both bare soil and vegetation, and to specify the limits of accuracy in the soil water content estimates. Much of the modeling efforts were devoted to improving the vegetation component of the model. Sensitivity tests with the vegetation model suggest that water stress in vegetation may be detectable for a period of a few days prior to wilting, provided that the atmospheric demand is large, an appropriate threshold leaf water potential exists and plant storage capacity is not large. Horizontal variations in radiometric surface temperature over sparse vegetation may simply reflect horizontal variations in canopy density rather than horizontal variations in soil water content. GRA

44 ENERGY PRODUCTION AND CONVERSION

Includes specific energy conversion systems, e.g., fuel cells; global sources of energy; geophysical conversion; and windpower.

For related information see also *07 Aircraft Propulsion and Power, 20 Spacecraft Propulsion and Power,* and *28 Propellants and Fuels.*

N91-29642# National Aeronautical Establishment, Ottawa (Ontario).

EXPERIMENTAL STRESS MEASUREMENTS FOR THE MODIFIED INDAL SERIES 6400 VAWT

P. J. Penna Sep. 1989 77 p Prepared for Indal Technologies, Inc., Mississauga, Ontario

(NAE-LTR-LA-310; CTN-91-60115) Copyright Avail: NTIS HC/MF A05

The results are presented of a measurement campaign on the INDAL Technologies Series 6400 vertical axis wind turbine (VAWT) at the Atlantic Wind Test Site. The instrumentation and data acquisition is discussed along with the turbine's structural response and the cycle counting method which was applied to the time-series stress measurements. The cycle counting method used was based on a rainflow counting algorithm. For a given stress measurement location on the turbine, it was found that the maximum stress range increased with wind speed and the location of peaks in the histograms of rainflow counted cycles were shifted, but the general shape of the histogram remained the same. This feature allowed a normalization procedure to be applied to the histograms. The histograms for a given stress measurement location were then found to collapse onto a single curve. The effect of wind turbulence intensity on the maximum cyclic stress was also studied. The results confirmed the generally held view that increases in turbulence intensity lead to higher cyclic stresses. Author (CISTI)

N91-29643# Midwest Research Inst., Golden, CO.

WORLDWIDE WIND/DIESEL HYBRID POWER SYSTEM STUDY: POTENTIAL APPLICATIONS AND TECHNICAL ISSUES

W. R. King and B. L. Johnson, III (Science Applications International Corp., McLean, VA.) Apr. 1991 104 p

(Contract DE-AC02-83CH-10093)

(DE91-002160; SERI/TP-257-3757) Avail: NTIS HC/MF A06

The world market potential for wind/diesel hybrid technology is a function of the need for electric power, the availability of sufficient wind resource to support wind/diesel power, and the existence of buyers with the financial means to invest in the technology. This study includes data related to each of these three factors. This study does not address market penetration, which would require analysis of application specific wind/diesel economics. Buyer purchase criteria, which are vital to assessing market penetration, are discussed only generally. Countries were screened for a country-specific market analysis based on indicators of need and wind resource. Both developed countries and less developed countries (LDCs) were screened for wind/diesel market potential. Based on the results of the screening, ten countries showing high market potential were selected for more extensive market analyses. These analyses provide country-specific market data to guide wind/diesel technology developers in making design decisions that will lead to a competitive product. Section 4 presents the country-specific data developed for these analyses, including more extensive wind resource characterization, application-specific market opportunities, business conditions, and energy market characterizations. An attempt was made to identify the potential buyers with ability to pay for wind/diesel technology required to meet the application-specific market opportunities identified for each country. Additionally, the country-specific data are extended to corollary opportunities in countries not covered by the study. Section 2 gives recommendations for wind/diesel research based on the findings of the study. DOE

N91-29644# Pacific Northwest Lab., Richland, WA.
ELECTRIC RATE STRUCTURES FOR THERMAL ENERGY STORAGE EVALUATION
D. R. Brown, S. M. Garrett, and J. M. Sedgewick May 1991 36 p
(Contract DE-AC06-76RL-01830)
(DE91-013168; PNL-7697) Avail: NTIS HC/MF A03

Future electric rate structures are critical to thermal energy storage (TES) technologies that are specifically designed to take advantage of electric energy costs that vary depending on the magnitude, duration, and timing of power demand (e.g., cool storage). In fact, rate structure characteristics may affect the TES system design and operating approach as well as economic feasibility. The objective of this study, conducted by the Pacific Northwest Laboratory for the U.S. Department of Energy, was to define reference electric utility rate structures to be used in technical assessments of TES technologies. Electric rate structures were characterized for residential, commercial, and industrial sectors. A range of conditions for several alternative rate structures was identified for each sector to capture the variability of likely conditions. Individual rate structure characteristics include demand charges and energy charges applicable during different months of the year, days of the week, and hours of the day. DOE

N91-29645# Argonne National Lab., IL.
DEVELOPMENTAL STATUS AND SYSTEM STUDIES OF THE MONOLITHIC SOLID OXIDE FUEL CELL
K. M. Myles 1991 8 p Presented at the 2nd International Symposium on Solid Oxide Fuel Cells, Athens, Greece, 2-5 Jul. 1991
(Contract W-31-109-eng-38)
(DE91-014389; ANL/CP-72346; CONF-9107106-1) Avail: NTIS HC/MF A02

The monolithic solid oxide fuel cell (MSOFC) was invented at the Argonne National Laboratory in 1983 and is currently being developed by a team consisting of Argonne National Laboratory and Allied-Signal Aerospace/AiResearch. The MSOFC is an oxide ceramic structure in which appropriate electronic and ionic conductors are fabricated in a honeycomb shape similar to a block of corrugated paperboard. The electrolyte, which conducts oxygens ions from the air side to the fuel side, is yttria-stabilized zirconia (YSZ). All the other materials, that is, the nickel-YSZ anode, the strontium-doped lanthanum manganite cathode, and the doped lanthanum chromite interconnect (bipolar plate), are electronic conductors. These electronic and ionic conductors are arranged to provide short conduction paths to minimize resistive losses. The power density achievable with the MSOFC is expected to be about 8 kW/kg or 4 kW/l at fuel efficiencies over 50 percent, because of small cell size and low resistive losses in the materials. These performances have been approached in laboratory test fuel cell stacks of nominal 125-W capacities. DOE

N91-29646# Midwest Research Inst., Golden, CO.
ANALYSIS OF A TEETERED, VARIABLE-SPEED ROTOR
T. L. Weber, R. E. Wilson, and S. N. Walker (Oregon State Univ., Corvallis.) Jun. 1991 59 p
(Contract DE-AC02-83CH-10093)
(DE91-002190; SERI/TP-257-4366) Avail: NTIS HC/MF A04

A computer model of a horizontal axis wind turbine (HOOT) with four structural degrees of freedom has been derived and verified. The four degrees of freedom include flapwise motion of the blades, teeter motion, and variable rotor speed. Options for the variable rotor speed include synchronous, induction, and constant-tip speed generator models with either start, stop, or normal operations. Verification is made by comparison with analytical solutions and mean and cyclic ESI-80 data. The Veers full-field turbulence model is used as a wind input for a synchronous and induction generator test case during normal operation. As a result of the comparison, it is concluded that the computer model can be used to predict accurately mean and cyclic loads with a turbulent wind input. DOE

N91-29647# L'Garde, Inc., Tustin, CA.
CONCENTRATOR FLIGHT TEST EXPERIMENT Final Report, 23 Sep. 1987 - 17 May 1990
C. Thompsen, S. Dalbey, G. Friese, E. Zaccardelli, and B. McDaniel May 1991 91 p
(Contract F04611-87-C-0072)
(AD-A237390; LTR-90-SD-011; AL-TR-90-066) Avail: NTIS HC/MF A05 CSCL 22/1

The goal of this Phase 2 Small Business Innovation Research (SBIR) effort was to take the conceptual design begun under the Phase 1 SBIR flight test planning effort and accomplish the preliminary design of a subscale inflatable solar collector system. The preliminary design was then to be experimentally verified and a detail design generated. The inflatable portion of the collector was to be an adaptation of the inflatable collector produced on the Deployable Solar Collector Experiment. The entire collector system was to be designed to be packaged into a Get Away Special Canister launched from the Space Shuttle. No experimentation was done in this effort. This final report covers the preliminary design and the analysis supporting that design. GRA

N91-29648# Air Force Occupational and Environmental Health Lab., Brooks AFB, TX.
ACOUSTIC TESTS ON A NEW MOTOR GENERATOR SYSTEM FOR THE MINUTEMAN LAUNCH CONTROL CENTERS AT ALPHA 01 AND SIERRA 00, MALMSTROM AFB, MONTANA Final Report, 23 Apr. - 4 May 1990
Terry M. Fairman May 1991 121 p
(AD-A237944; AL-TR-91-0061) Avail: NTIS HC/MF A06 CSCL 10/2

Field tests of the acoustic performance of a new motor generator system (MGS) were performed at Minuteman Launch Control Centers (LCC) Alpha 01 and Sierra 00, Malmstrom AFB, MT. This same MGS unit was accepted for use after the Hill Engineering Test Facilities (HETF) acoustic performance studies conducted in 1988. Rivet Mile from the Ogden ALC began installation of the new MGS at Malmstrom in the spring of 1990. Performance tests were requested by 00-ALC/MMGRMM, and SAC, to compare with the HETF data and document the LCC acoustic environment with the new MGS operating in a field setting. This report presents our findings. GRA

N91-29649# Midwest Research Inst., Golden, CO.
THE DEPARTMENT OF ENERGY'S SOLAR INDUSTRIAL PROGRAM: NEW IDEAS FOR AMERICAN INDUSTRY
J. V. Anderson, S. G. Hauser, and R. J. Clyne Jul. 1991 8 p Presented at the 26th Intersociety Energy Conversion Engineering (IECE) Conference, Boston, MA, 3-9 Aug. 1991
(Contract DE-AC02-83CH-10093)
(DE91-002197; SERI-TP-250-4256; CONF-910801-15) Avail: NTIS HC/MF A02

As society becomes more and more sensitive to the environment, and energy supplies become scarcer, the application of solar energy is expanding into new areas. The industrial sector is one of the most difficult for solar energy to impact because of its technical diversity and economic requirements. However, the opportunities are still abundant. The Department of Energy's Solar Industrial Program is dedicated to advancing the applications of solar energy in this sector. Research and technology development activities are currently focused in three areas: solar process heat, advanced materials manufacturing, and destruction of chemical wastes. The Solar Energy Research Institute manages these activities for DOE with close interactions with other Federal agencies, private industry, and universities. DOE

N91-29650# Midwest Research Inst., Golden, CO.
HORIZONTAL AXIS WIND TURBINE POST STALL AIRFOIL CHARACTERISTICS SYNTHESIZATION
J. L. Tangler and C. Ostowari (Texas A&M Univ., College Station.) Jun. 1991 7 p Presented at the Horizontal-Axis Wind Turbine Technology Conference, Cleveland, OH, 8-10 May 1984

(Contracts DE-AC02-83CH-10093; DE-AC04-76DP-03533)
(DE91-002198; SERI/TP-257-4400; CONF-8405153-6) Avail: NTIS HC/MF A02

Blade-element/momentum performance prediction codes are routinely used for wind turbine design and analysis. A weakness of these codes is their inability to consistently predict peak power upon which the machine structural design and cost are strongly dependent. The purpose of this study was to compare post-stall airfoil characteristics synthesization theory to a systematically acquired wind tunnel data set in which the effects of aspect ratio, airfoil thickness, and Reynolds number were investigated. The results of this comparison identified discrepancies between current theory and the wind tunnel data which could not be resolved. Other factors not previously investigated may account for these discrepancies and have a significant effect on peak power prediction. DOE

45 ENVIRONMENT POLLUTION

Includes atmospheric, noise, thermal, and water pollution.

N91-29651# National Aeronautical Establishment, Ottawa (Ontario).
NAE TWIN OTTER OPERATIONS IN THE 1988 EULERIAN MODEL EVALUATION FIELD STUDY
J. I. MacPherson Apr. 1989 90 p
(NAE-LTR-FR-107; CTN-91-60027) Copyright Avail: NTIS HC/MF A05

From July 18 to August 31, 1988, the NAE Twin Otter Atmospheric Research Aircraft was operated from Muskoka, Ontario in an experiment designed to test a new computer model for the long range transport of atmospheric pollutants. The 1988 Eulerian Model Evaluation Field Study was a collaborative effort with the Atmospheric Environment Service of Canada and the Ontario Ministry of the Environment. The Twin Otter flew 50 flights and 122.8 hours in support of this study. Scientists using Twin Otter data will find this a working reference. Flight summaries, atmospheric profile data, and details on the instrumentation, software, and flight procedures used is included. A discussion is presented on tests conducted on the wind measuring systems on the aircraft and recommendations are given for improvements in instrumentation and operational procedures for the next in this series of atmospheric pollution experiments. During this flight program the instrumentation computed and recorded three wind estimates, the Doppler/inertial wind measure which uses a National Aeronautical Establishment accelerometer and gyro package, and 3-axis Doppler radar; Litton winds which used inertial components taken directly from the Litton inertial reference system in earth-fixed axes; and Litton/Doppler winds using the 3-axis Doppler data with the Litton system supplying accelerometer and gyro data, and the Litton heading and attitude data to resolve the computed wind component into earth-axis. The best results were obtained from the Litton/Doppler system with the Doppler/inertial system only slightly less accurate. The Litton winds values were unacceptable.
Author (CISTI)

N91-29652# Lawrence Livermore National Lab., CA.
NUMERICAL MODELING OF TURBULENT DISPERSION AROUND STRUCTURES USING A PARTICLE-IN-CELL METHOD
R. L. Lee and J. M. Leone, Jr. Apr. 1991 18 p Presented at the 84th Annual Meeting and Exhibition of the Air and Waste Management Association (AWMA), Vancouver (Canada), 16-21 Jun. 1991 Revised
(Contract W-7405-eng-48)
(DE91-012035; UCRL-JC-105271-Rev-1; CONF-910659-5-Rev-1) Avail: NTIS HC/MF A03

Prediction of the transport and dispersion of air pollutants around structures is of interest in environmental applications ranging from the assessment of roadway emissions within street canyons to the siting of containment enclosures for limiting the spread of accidental releases of hazardous gases. However, the fate of the pollutants within these settings is greatly complicated by the presence of multiple obstructions such as buildings, trees and wall barriers. In this paper, a methodology is described wherein two numerical models are exercised in order to predict the turbulent transport and dispersion around a surface-mounted rectangular block. This methodology can be expanded in the future to treat more irregularly-shaped single buildings or clusters of buildings.
DOE

N91-29653# Oak Ridge National Lab., TN.
DIRECT-SAMPLING MS MEASUREMENT OF VOLATILES IN ENVIRONMENTAL SAMPLES
G. B. Hurst, C. V. Thompson, D. L. Theobald, and M. B. Wise 1991 3 p Presented at the American Society for Mass Spectrometry (ASMS) Meeting, Nashville, 19-24 May 1991
(Contract DE-AC05-84OR-21400)
(DE91-013417; CONF-9105181-13) Avail: NTIS HC/MF A01

We are developing methods for detecting volatile organics in water and soil samples. Our twofold goal is to develop rapid, fieldable screening procedures to identify contaminated samples that will require full analysis by EPA-approved methods, and to scope the utility of direct sampling MS for quantitating volatiles in the low ppb range. The apparatus consists of a Finnigan ion trap mass spectrometer (ITMS) connected via an open-split interface with a purge device. The sample, contained in a standard 40 mL VOA vital, attaches to the purge device. The sample is sparged with helium at a flow rate of 100 to 150 mL/min. A portion of the purge gas flows into the ITMS through a restricting capillary. Mass spectra are obtained under EI conditions. Direct sampling ITMS is useful for screening environmental samples for volatiles. Our results show that quantitation is feasible, despite some matrix effects. We plan to study other matrices and investigate alternative methods for troublesome compounds such as water-soluble ketones.
DOE

N91-29654# Lawrence Livermore National Lab., CA.
ATMOSPHERIC DISPERSION MODELS FOR DENSE GAS RELEASES
D. L. Ermak 18 Jun. 1991 8 p Presented at the 10th International System Safety Society (SSS) Conference, Dallas, 18-22 Jul. 1991
(Contract W-7405-eng-48)
(DE91-015144; UCRL-JC-107536; CONF-9107114-3) Avail: NTIS HC/MF A02

In this paper we present a limited review of atmospheric dispersion models that were specifically developed to treat denser-than-air releases. We separate the models into the two classes: three-dimensional, conservation equation models and one-dimensional (quasi-three-dimensional) similarity models. These two classes of models differ considerably in physical completeness, numerical complexity, computer capability required to run the models, and ease of use. For each class of models, we present a brief description of their distinguishing features, examples of models developed in the past decade, their advantages and disadvantages as a class, and some preliminary results from independent model evaluations. Special attention is given to the FEM3 and SLAB models developed at Lawrence Livermore National Laboratory. DOE

N91-29655# Sandia National Labs., Albuquerque, NM.
ON-LINE MONITORING OF VOLATILE ORGANIC SPECIES
G. C. Frye and S. J. Martin 1990 9 p Presented at the USAF/DOE Workshop on Solvent Substitution, Phoenix, Dec. 1990
(Contract DE-AC04-76DP-00789)
(DE91-014655; SAND-91-0659C; CONF-901285-5) Avail: NTIS HC/MF A02

On-line chemical monitoring systems can help ensure safe, environmentally sound operation of industrial processes using hazardous chemicals. Using polymer-coated surface acoustic wave (SAW) sensors, we have demonstrated monitors that are capable of detecting dilute concentrations of volatile organic species. Using

changes in both wave velocity and wave attenuation, the identity and concentration of an isolated chemical species can be determined. A polysiloxane coating has been found to provide unique properties for monitoring chlorinated hydrocarbons (CHCs) such as trichloroethylene: good discrimination of CHCs from most other organic species, rapid and reversible sensor response, and low detection limits. Using this technology, a portable acoustic wave sensor (PAWS) system has been constructed. DOE

N91-29656# Brookhaven National Lab., Upton, NY.
METHODS FOR DETERMINATION OF LOW-MOLECULAR WEIGHT CARBONYL COMPOUNDS IN THE AMBIENT ATMOSPHERE
A. Vairavamurthy, J. M. Roberts, and L. Newman Jan. 1991 98 p Presented at the Symposium on Measurement of Airborne Compounds: Sampling, Analysis, and Data Interpretation, Washington, DC, 26-31 Aug. 1990
(Contract DE-AC02-76CH-00016)
(DE91-015188; BNL-46244; CONF-9008162-3) Avail: NTIS HC/MF A05

Determination of carbonyl compounds in the ambient atmosphere is receiving increasing attention because of the critical role these compounds play in tropospheric organic chemistry. Currently, field measurements are very limited mainly because of the analytical challenges posed by trace concentrations and interferences arising from atmospheric copollutants. The methods used for determination of carbonyl compounds are reviewed, from an atmospheric chemistry perspective, emphasizing the principles, advantages, and limitations. Since a large number of varied types of methods have been used specifically for determination of formaldehyde, it is considered separately from other carbonyls. It is clear that despite more than a decade of work, many problems related to sampling, interferences, and artifacts have not been resolved. Because of the increasing demand for time-series measurements in field studies, and automated method for continuous sampling and analysis of carbonyls is very much required. The widely used liquid chromatographic method based on 2,4-dinitrophenylhydrazine derivatization appears unsuitable for this purpose because of the lengthy collection times required to achieve sub-ppbv detection limits. Important issues to be considered in the development of a suitable field method and potential approaches are discussed. DOE

N91-29657# Naval Postgraduate School, Monterey, CA.
EQUATORIAL ENTRAINMENT ZONE SIMULATIONS M.S. Thesis
Chi-Shao Chen Jun. 1990 88 p
(AD-A237234) Avail: NTIS HC/MF A05 CSCL 08/3

The equatorial entrainment zone model of Garwood et al. (1989) is employed along with data collected by Moum et al. (1984) during the Tropic Heat I Experiment to explain how the dissipation of turbulence is related to surface forcing of wind stress and net heat flux. Four numerical experiments with different atmospheric conditions are conducted with the entrainment zone model. Solar radiation is diurnally repeated, and wind stress is held constant in the first case. The model is forced with linearly varied wind speed in the second case and uses observed winds for the third cases. The first three cases demonstrated the effects of wind stress on the dissipation of turbulence. In the final case both observed wind and observed solar radiation were applied to the model to simulate the effect of realistic forcing, allowing a comparison between model-predicted and observed values of dissipation. Numerical solutions qualitatively agree with the observations, and the time and depth dependence of the diurnal dissipation cycle are well reproduced by the model. GRA

N91-29658# Pittsburgh Univ., PA. Dept. of Materials Science and Engineering.
ENVIRONMENTAL EFFECTS IN NIOBIUM BASE ALLOYS AND OTHER SELECTED INTERMETALLIC COMPOUNDS Final Report, 1 Jan. 1987 - 31 Oct. 1990
G. H. Meier and A. W. Thompson 30 Apr. 1991 186 p Prepared in cooperation with Carnegie-Mellon Univ., Pittsburgh, PA
(Contract F49620-88-C-0013; DARPA Order 6155)
(AD-A237535; AFOSR-91-0568TR) Avail: NTIS HC A09/MF A01 CSCL 07/2

Niobium aluminides and silicides as well as other intermetallic compounds have potential for use in advanced gas turbines where increased operating temperatures are necessary to obtain the targeted performance goals. These materials will be subjected to a variety of environments over a range of temperatures. Two of the principal reactants in these environments are oxygen and hydrogen. This program is concerned with the effects of oxygen and hydrogen on niobium alloys and other selected intermetallic compounds. The investigations involving oxygen examined the mechanisms by which intermetallic compounds are degraded in oxidizing environments. Emphasis was placed upon the conditions which must be achieved in order to obtain sufficient oxidation resistance for use at temperatures above approx. 1100 C. Oxidation was investigated at temperatures between 500 and 1400 C in oxygen and in air. Investigations involving hydrogen have emphasized brittle fracture, crack growth and the behavior of hydrides in Ti-24Al-11Nb (at. pct). Some work of this type was also performed on TiAl. The mechanical properties of these alloys were determined after exposure to hydrogen. Mechanical tests included simple tensile and compression tests, and notched bend and precracked compact tension specimens. Properties such as yield strength and ultimate strength, tensile strength, ductility, and fracture toughness were determined as a function of both hydrogen (hydride) content and temperature. GRA

N91-29659# Army Lab. Command, Fort Monmouth, NJ. Electronics Technology and Devices Lab.
PROTECTING THE OZONE SHIELD: A NEW PUBLIC POLICY Technical Report, Jan. - Dec. 1990
Paul C. Manz Apr. 1991 11 p
(AD-A237640; SLCET-TR-91-10) Avail: NTIS HC/MF A03 CSCL 13/2

Throughout the 1980's, public attention and concern have become increasingly focused on a number of specific environmental issues including the consequences of stratospheric ozone depletion cause by the release of CFC's and halons into the environment. This report discusses the policy issues relating to the use of CFC's and halons and their long-term impact on the environment. Stratospheric ozone protects the earth, and the life that dwells on it, from the sun's harmful ultraviolet radiation (UVb). A prolonged increase in UVb radiation exposure can cause suppression of the immune system and an increase in the incidence of skin cancer and cataracts in human beings. High levels of UVb radiation can damage land and water based plant life including major food crops, and can cause an increase in smog formation, which has become a major problem in many urban areas. GRA

N91-29660# Institute for Defense Analyses, Alexandria, VA.
IDA STUDIES ON NATURAL SPACE ENVIRONMENTAL EFFECTS ON MATERIALS FOR SDIO Final Report, Nov. 1987 - Dec. 1990
Janet M. Sater, Charles F. Bersch, and William S. Hong Dec. 1990 109 p
(Contract MDA903-89-C-0003)
(AD-A237974; IDA-P-2432; IDA/HQ-90-35736; AD-E501404)
Avail: NTIS HC/MF A06 CSCL 15/3

The background is provided of IDA's role in the area of space environmental effects (SEE) for Strategic Defense Initiative Organization (SDIO), particularly the Materials and Structures program. Included in these efforts are establishing and co-chairing the NASA/SDIO Workshop on Space Environmental Effects on Materials (June 1988). This workshop, in part, led to the recovery of the NASA Long Duration Exposure Facility (LDEF) after more than 5 years in space as well as to the appointment of the M and S Office as the SDIO focal point for SEE. A technical assessment of the utility of various LDEF experiments to SDI is highlighted. Results of the assessment were presented at an SDIO Workshop in August 1989 and copies were provided to appropriate, interested groups. The study provided the basis for preparation of

detailed SDIO sample/analysis information packages for the NASA-LDEF Office. Continuing involvement in LDEF post-retrieval activities is noted as well. GRA

N91-29661# Harvard Univ., Cambridge, MA.
THEORETICAL STUDIES OF LONG-RANGE TRANSPORT OF OXIDANTS Final Report
D. J. Jacob, S. C. Wofsy, C. M. Spivakovsky, J. A. Logan, and R. M. Yevich Mar. 1991 51 p
(PB91-182360; CRC-APRAC-AP-9-A) Avail: NTIS HC/MF A04 CSCL 13B

A 3-D chemical trace model (CTM) was developed for the long-range transport of oxidants that can predict ozone levels in rural areas. Ozone episodes occur each summer, during which a significant fraction of the U.S. may experience concentrations of oxidants more than the National Ambient Air Quality Standard (120 ppb). The CTM was constructed to simulate production, transport, and deposition of O3, NO(x), and other reactive species in regions of North America. Subgrid models were implemented to account for different chemical regimes in areas defined as rural, urban, urban plumes, and power plant plumes. Model simulations reproduce key features of available observations, indicating that the model provides a realistic climatology for concentrations of O3 and O3 precursors. The CTM represents an analytical tool uniquely suited for analysis of problems associated with means and extremes of pollutant concentrations over large areas of North America, including interactions between urban and rural environments. GRA

N91-29662# Environmental Protection Agency, Research Triangle Park, NC. Office of Air Quality Planning and Standards.
CRITERIA FOR ASSESSING THE ROLE OF TRANSPORTED OZONE/PRECURSORS IN OZONE NONATTAINMENT AREAS
May 1991 55 p
(PB91-195958; EPA/450/4-91/015) Avail: NTIS HC/MF A04 CSCL 13B

A series of modeling analyses appropriate for characterizing transport of ozone and its precursors into nonattainment areas is discussed. Air quality and meteorological measurements needed to characterize transport in identified modeling techniques are identified. Author

N91-29663# Midwest Research Inst., Golden, CO.
ULTRAVIOLET REFLECTOR MATERIALS FOR SOLAR DETOXIFICATION OF HAZARDOUS WASTE
G. Jorgensen and R. Govindarajan Jul. 1991 14 p Presented at the Society of Photo-Optical Instrumentation Engineers (SPIE) Meeting, San Diego, CA, 21-26 Jul. 1991
(Contract DE-AC02-83CH-10093)
(DE91-002196; SERI/TP-257-4418; CONF-9107115-9) Avail: NTIS HC/MF A03

Organic waste detoxification requires cleavage of carbon bonds. Such reactions can be photo-driven by light that is energetic enough to disrupt such bonds. Alternately, light can be used to activate catalyst materials, which in turn can break organic bonds. In either case, photons with wavelengths less than 400 nm are required. Because the terrestrial solar resource below 400 nm is so small (roughly 3 percent of the available spectrum), highly efficient optical concentrators are needed that can withstand outdoor service conditions. In the past, optical elements for solar application have been designed to prevent ultraviolet (UV) radiation from reaching the reflective layer to avoid the potentially harmful effects of such light on the collector materials themselves. This effectively forfeits the UV part of the spectrum in return for some measure of protection against optical degradation. To optimize the cost/performance benefit of photochemical reaction systems, optical materials must be developed that are not only highly efficient but also inherently stable against the radiation they are designed to concentrate. The requirements of UV optical elements in terms of appropriate spectral bands and level of reflectance are established based upon the needs of photochemical applications. Relevant literature on UV reflector materials is reviewed which, along with discussions with industrial contacts, allows the establishment of a data base of currently available materials. Although a number of related technologies exist that require UV reflectors, to date little attention has been paid to achieving outdoor durability required for solar applications. DOE

N91-29664# Oak Ridge National Lab., TN. Carbon Dioxide Information Analysis Center.
ATMOSPHERIC METHANE CONCENTRATIONS: THE NOAA/CMDL GLOBAL COOPERATIVE FLASK SAMPLING NETWORK, 1983 - 1988
L. P. Steele, P. M. Lang (National Oceanic and Atmospheric Administration, Boulder, CO.), and R. J. Sepanski May 1991 295 p
(Contract DE-AC05-84OR-21400)
(DE91-014942; ORNL/CDIAC-42; NDP-038; ESD-Publ-3642)
Avail: NTIS HC/MF A13

This document presents monthly averages and sampling statistics for atmospheric methane (CH(sub 4)) concentrations (mixing ratios) from the National Oceanic and Atmospheric Administration Climate Monitoring and Diagnostics Laboratory (NOAA/CMDL) global cooperative flask sampling network from 1983 to 1988. The data are derived from a network of 31 stations (27 of which were still active at the end of 1988), which collected air samples in flasks approximately once per week for measurement of both methane and carbon dioxide. The samples were analyzed for atmospheric methane on a gas chromatograph (fitted with a flame ionization detector) at the NOAA/CMDL Laboratory in Boulder, Colorado. These data represent the most spatially comprehensive atmospheric methane record available in the world. They have been used to study the temporal and spatial variations in atmospheric methane concentration and have applications in modeling, projections, and global mass balance calculations. The data consist of station identification code; year; and, for each month, mean monthly methane concentration, standard deviation, and number of samples contributing to the mean. This document provides sample listings of the NOAA/CMDL atmospheric methane data as they appear on magnetic tape, as well as a complete listing of the methane data (statistics excluded) in tabular form. This document also offers retrieval program listings, furnishes information on sampling and analysis methods and on data selection, defines limitations and restrictions of the data, and provides reprints of pertinent literature. DOE

N91-29665# Department of Energy, Washington, DC. Office of Health and Environmental Research.
SUBSURFACE SCIENCE PROGRAM
Jun. 1991 43 p
(DE91-015480; DOE/ER-0501T) Avail: NTIS HC/MF A03

The Office and Health and Environmental Research (OHER) within the Department of Energy's (DOE's) Office of Energy Research conducts long-term fundamental research in the physical, chemical, and biological sciences. OHER Subsurface Science Program, summarized in this document, supports a university and national laboratory research program that is interdisciplinary, covering such disciplines as geochemistry, microbiology, and hydrology. Departmental needs in environmental restoration, a major issue of that DOE will face several decades, are emphasized. The Subsurface Science Program emphasizes research on subsoils and ground water, i.e., the natural subsurface environments that are most significantly affected by past DOE waste-disposal practices. More specifically, research is being conducted in hydrogeology, in subsurface microbiology, and on the biogeochemistry of chemical mixtures in the subsurface environment. The program is organized into interdisciplinary subprograms, or areas of research emphases, with each subprogram conducting basic research of interest to DOE. For example, fundamental scientific research in several subprograms on microbial distribution, function, and effects is laying a foundation for cost-effective in situ mitigation of contamination at DOE sites. Research on the behavior of organic- radionuclide mixtures in ground water will be used by DOE sites, other Federal agencies, and the international community to assess environmental risks and to establish effective remedial procedures. DOE

N91-29666# Pacific Northwest Lab., Richland, WA.
THE OBSERVATIONAL APPROACH IN ENVIRONMENTAL RESTORATION
J. D. Smyth and R. D. Quinn Jul. 1991 9 p Presented at the 1991 American Society of Civil Engineers (ASCE) National Conference on Environmental Engineering, Reno, NV, 8-10 Jul. 1991
(Contract DE-AC06-76RL-01830)
(DE91-015528; PNL-SA-18817; CONF-9107139-1) Avail: NTIS HC/MF A02

The U.S. Department of Energy (DOE) has committed to completing environmental restoration of its facilities within the next 28 years (DOE 1990b). In order to achieve this, DOE must ensure that its restoration activities are both effective and efficient. A key aspect of fulfilling this commitment is the recognition and management of uncertainty that is inherent in waste-site clean-up actions. The DOE Office of Environmental Restoration (DOE-ER) requested Pacific Northwest Laboratory (PNL) to investigate the applicability and implementation of what is known as the observational approach to better address these needs. PNL's initial investigation resulted in the positive conclusion that the observational approach had potential benefit to DOE during environmental restoration. In a follow-on effort, PNL supported by CH2M HILL, has been providing guidance to DOE field-offices on observational approach fundamentals, implementation, and application to waste-site remediation. This paper outlines the fundamentals of the observational approach and discusses the progress in integrating the observational approach in DOE's environmental restoration efforts. DOE

N91-29667# Pacific Northwest Lab., Richland, WA.
A CLIMATOLOGICAL MODEL FOR RISK COMPUTATIONS INCORPORATING SITE-SPECIFIC DRY DEPOSITION INFLUENCES
J. G. Droppo, Jr. Jul. 1991 12 p Presented at the 5th International Conference on Precipitation Scavenging and Atmosphere Surface Exchange Process, Richland, WA, 15-19 Jul. 1991
(Contract DE-AC06-76RL-01830)
(DE91-015536; PNL-SA-19548; CONF-9107104-9) Avail: NTIS HC/MF A03

A gradient-flux dry deposition module was developed for use in a climatological atmospheric transport model, the Multimedia Environmental Pollutant Assessment System (MEPAS). The atmospheric pathway model computes long-term average contaminant air concentration and surface deposition patterns surrounding a potential release site incorporating location-specific dry deposition influences. Gradient-flux formulations are used to incorporate site and regional data in the dry deposition module for this atmospheric sector-average climatological model. Application of these formulations provide an effective means of accounting for local surface roughness in deposition computations. Linkage to a risk computation module resulted in a need for separate regional and specific surface deposition computations. DOE

46 GEOPHYSICS

Includes aeronomy; upper and lower atmosphere studies; ionospheric and magnetospheric physics; and geomagnetism.

For space radiation see *93 Space Radiation.*

N91-29668# Pacific Northwest Lab., Richland, WA.
THREE-DIMENSIONAL VISUALIZATION FOR EVALUATING AUTOMATED, GEOMORPHIC PATTERN-RECOGNITION ANALYSES OF CRUSTAL STRUCTURES
M. G. Foley Feb. 1991 7 p Presented at the 8th Thematic Conference on Geologic Remote Sensing: Exploration, Engineering and Environment, Denver, 29 Apr. - 2 May 1991
(Contract DE-AC06-76RL-01830)
(DE91-012929; PNL-SA-18442; CONF-910432-1) Avail: NTIS HC/MF A02

We are developing and applying a suite of automated remote geologic analysis (RGA) methods at Pacific Northwest Laboratory (PNL) for extracting structural and tectonic patterns from digital models of topography and other spatially registered geophysical data. In analyzing a map area, the geologist employs a variety of spatial representations (e.g., topographic maps; oblique, vertical and vertical stereographic aerial photographs; satellite-sensor images) in addition to actual field observations to provide a basis for recognizing features (patterns) diagnostic or suggestive of various geologic and geomorphic features. We intend that our automated analyses of digital models of elevation use the same photogeologic pattern-recognition methods as the geologist's; otherwise there is no direct basis for manually evaluating results of the automated analysis. Any system for automating geologic analysis should extend the geologist's pattern-recognition abilities and quantify them, rather than replace them. This requirement means that results of automated structural pattern-recognition analyses must be evaluated by geologists using the same method that would be employed in manual field checking: visual examination of the three-dimensional relationships among rocks, erosional patterns, and identifiable structures. Interactive computer-graphics in quantitative (i.e., spatially registered), simulated three-dimensional perspective and stereo are thus critical to the integration and interpretation of topography, imagery, point data, RGA-identified fracture/fault planes, stratigraphy, contoured geophysical data, nonplanar surfaces, boreholes, and three-dimensional zones (e.g., crush zones at fracture intersections). This graphical interaction presents the megabytes of digital geologic and geophysical data to the geologist in the same spatial format that field observations would take, permitting direct evaluation of RGA methods and results. DOE

N91-29669 California Univ., Los Angeles.
REGIONAL TECTONIC DEFORMATION IN SOUTHERN CALIFORNIA, INFERRED FROM TERRESTRIAL GEODESY AND THE GLOBAL POSITIONING SYSTEM Ph.D. Thesis
Zhengkang Shen 1991 175 p
Avail: Univ. Microfilms Order No. DA9115442

Tectonic deformation in two regions in Southern California, the Southern Coast Ranges and the Los Angeles Basin, was studied. Results show that in the Southern Coast Ranges, regional deformation is predominantly controlled by deep strike slip motion along the San Andreas Fault, at a rate of 32 plus or minus 2 mm/yr. The deep slip along the San Gregorio-Hosgri Fault is about 1-3 mm/yr, assuming a locked fault depth of 20 km. Convergence normal to the San Andreas Fault in the Southern Coast ranges is not significantly different from zero. About 5 mm/yr convergence is detected from the Santa Maria Basin. In the Los Angeles Basin area, this study demonstrates about 10 mm/yr relative motion trending northwest from San Pedro Hill to the San Gabriel Mountains. The direction of motion closely parallels to the trend of the frontal fault system at the southern margin of the San Gabriel Mountains. The basin suffers from north-south convergence and east-west extension, at a rate of about 0.07 mu rad/yr for either components. The convergence rate normal to the San Andreas across the basin is 4 plus or minus 3 mm/yr, implying smaller compression than previous estimates (e.g., Cline et al. 1984). Dissert. Abstr.

N91-29670 Pennsylvania State Univ., University Park.
ON THE APPLICATION OF EDGE WAVE THEORY TO TERRAIN-BOUNDED COLD SURGES: A NUMERICAL STUDY Ph.D. Thesis
Jeffrey Scott Tilley 1990 377 p
Avail: Univ. Microfilms Order No. DA9117748

A theory based upon topographically trapped edge waves is developed to explain the phenomenology of shallow cold surges adjacent to major topographic features of the earth's surface. It is proposed that a trapped response, composed of baroclinic Kelvin modes, shelf modes, and coupled motions, is a dominant mechanism within the surge regime. Three case studies, concerning

events near the Himalayas, Rockies, and the Great Dividing Range were examined using the NCAR/PSU mesoscale model. The control experiments, with full terrain and physical parameterizations, implied the existence of a shallow multiscale structure, as well as other characteristics expected of edge waves, in the regions affected by surges. Sensitivity studies strongly pointed to the topography as the key dynamic forcing agent for the three cases.
Dissert. Abstr.

N91-29671# Spectral Sciences, Inc., Burlington, MA.
DESCRIPTION OF THE STRATEGIC HIGH-ALTITUDE ATMOSPHERIC RADIATION CODE (SHARC) Scientific Report, Jan. 1989 - Oct. 1990
J. W. Duff, R. L. Sundberg, J. H. Gruninger, L. S. Bernstein, D. C. Robertson, and R. J. Healey 27 Nov. 1990 131 p
(Contract F19628-87-C-0130)
(AD-A237089; SSI-TR-176; GL-TR-90-0315; SR-4) Avail: NTIS HC/MF A07 CSCL 04/1

The report describes an upgraded version of the strategic high-altitude radiance code, SHARC-2. The SHARC calculates atmospheric radiance and transmittance over the 2 to 40 micrometer spectral region for arbitrary paths within 50 and 300 km altitude, including space viewing. It models radiation due to non-local thermodynamic equilibrium (NLTE) molecular emissions which are the dominant sources at these altitudes. This new version, which is now ready for distribution, has been upgraded to include a fully integrated auroral model with time-dependent chemistry, extention down to 50 km altitude, and radiation from the minor isotopes of CO2. In addition, there have been numerous internal upgrades to the various modules. These include a Voigt lineshape for the radiative excitation module; embedding of the auroral region into a quiescent atmosphere; and improvements in the radiation transport algorithms. GRA

N91-29672# Naval Surface Warfare Center, Dahlgren, VA.
WORLDWIDE MARITIME INFRARED ATMOSPHERIC TRANSMITTANCE DATA Final Report
Stephen B. Rogers and David E. Troyer Aug. 1990 220 p
(AD-A237292; NAVSWC-MP-90-409) Avail: NTIS HC/MF A10 CSCL 04/1

This report provides extinction coefficients which model infrared atmospheric transmittance. A pair of coefficients define a decaying exponential from a two-parameter curve fit to transmittance values for 10 and 20-km path lengths. Each location has approximately 700 individual sets of weather observations with a corresponding set of extinction coefficients. These coefficients are calculated from actual maritime meteorological conditions and the LOWTRAN 7 atmospheric transmittance model. There is a total of 9,833 sets of parameters worldwide. The meteorological conditions were measured over a 10-year period in the 1960s and early 1970s and are evenly distributed throughout the seasons. The weather parameters used as inputs to the LOWTRAN 7 model are relative humidity, air temperature and pressure, current and 24-hr average wind speed, and a calculated rain rate. GRA

N91-29673# Naval Postgraduate School, Monterey, CA.
ANALYSIS OF THE ULTRAVIOLET EMISSIONS OF NITRIC OXIDE FROM MID-LATITUDE ROCKET OBSERVATIONS M.S. Thesis
Michael J. Clayton Jun. 1990 67 p
(AD-A237340) Avail: NTIS HC/MF A04 CSCL 04/1

Ultraviolet emissions of the Earth's ionosphere in the wavelength range of 2000 to 2500 A are analyzed. These data were obtained by a rocket-borne spectrograph flown on March 30, 1990 from the White Sands Missile Range, New Mexico. The gamma and epsilon bands of nitric oxide dominate this portion of the spectrum. Column densities of nitric oxide are determined by fitting eleven of the most prominent bands with synthetic spectra. Additionally, a temperature profile is found between the altitudes of 145 and 195 km. From the data, corrections to the Franck-Condon factors are determined for three v (Z primes) progressions of the nitric oxide gamma bands. GRA

N91-29674# Army Lab. Command, White Sands Missile Range, NM. Atmospheric Sciences Lab.
XTRAN: AN ATMOSPHERIC TRANSMITTANCE CODE BASED ON XSCALE Final Report
Ricardo Pena Apr. 1991 38 p
(AD-A237624; ASL-TR-0294) Avail: NTIS HC/MF A03 CSCL 04/1

Several Electro-Optical Systems Atmospheric Effects Library modules require the use of XSCALE for calculation of the natural atmospheric transmittance value. XSCALE is a large (over 1600 lines of code) algorithm, which, in some cases, requires other external modules or data files for execution. XTRAN, a comparatively smaller (less than 240 lines) computer code, was developed for use with the KWIK (crosswind integrated concentration) munition expenditure stand-alone versions (SKWIK and IKWIK). XTRAN computes horizontal extinction and transmittance values based on the XSCALE module for visible, near-, mid-, and far-infrared wavelengths by using estimated values of visibility and polynomial regression equations for aerosol extinction as a function of relative humidity. This report shows the usefulness and practicality of the XTRAN code as a horizontal transmittance model. GRA

N91-29675# Army Lab. Command, White Sands Missile Range, NM. Atmospheric Sciences Lab.
A MANUAL METHOD FOR DETERMINING THE FRACTIONAL STABILITY CATEGORY Final Report
Ricardo Pena Apr. 1991 93 p
(DA Proj. 1L1-62111-AH-71)
(AD-A237627; ASL-TR-0296) Avail: NTIS HC/MF A05 CSCL 04/1

A simplistic manual method has been developed for determining the atmospheric stability based on FSCAT, a computer code that calculates the fractional stability category. The FSCAT algorithm retains the simplicity of the well-known Pasquill stability category scheme, and it also allows a much finer semicontinuous resolution of the stability of the surface boundary layer. The manual method allows the user to obtain the same results as with FSCAT, using cloud, wind, and solar angle data with a decision tree method, to determine the insolation class number, the net radiation index, and the fractional stability category. This practical method can be a useful tool for field operations where use of computers may not be possible. GRA

N91-29676# Boston Univ., MA. Center for Space Physics.
MAGNETOSPHERIC STRUCTURE AND DYNAMICS: A MULTISATELLITE APPROACH
W. J. Hughes 20 Mar. 1991 13 p
(Contract F19628-90-K-0003)
(AD-A237674; PL-TR-91-2063) Avail: NTIS HC/MF A03 CSCL 04/1

This report reviews progress during the first year of a contract to study magnetospheric structure and dynamics. Four areas of scientific investigation are highlighted. Pressure gradients form in the geotail because ions drift preferentially toward the dusk flank. These pressure gradients drive field aligned currents that close in the ionosphere and which provide a natural explanation of the Harang discontinuity when the full electrodynamics are modelled. Observations made during a passage by DE 2 through the dayside cusp at a time when the IMF was directed northwards are consistent with magnetic merging occurring on field line that map to the poleward cusp boundary. We infer that tail lobe field lines were merging with magnetosheath field lines at the magnetopause tailward of the external cusp. During the March 1989 magnetic storm, the DMSP F9 spacecraft observed extensive substantial decreases in equatorial ion density in the post-dusk sector. Modelling calculations show that the depletions were caused by unusually large upward flows moving the equatorial F region peak above 850 km. Calculations of ion cyclotron wave group velocities show that they are sensitive to both the hot and cold plasma populations. Calculated group delays agree with our earlier observations. GRA

N91-29677# Sparta, Inc., Lexington, MA.
EFFECTS OF SOLAR HEATING BY AEROSOLS AND TRACE GASES ON THE TEMPERATURE STRUCTURE CONSTANT Scientific Report No. 6, 1 Jul. 1988 - 31 Dec. 1990
J. R. Hummel and E. P. Shettle 9 Aug. 1990 24 p
(Contract F19628-88-C-0038)
(AD-A237675; LTR90-009; GL-TR-90-0349) Avail: NTIS HC/MF A03 CSCL 13/1

Thermosonde measurements made in the stratosphere indicate an increase in the temperature structure constant, C 2/T during daylight hours. Simplified calculations indicate that temperature perturbations resulting from solar heating by thin layers of aerosols and ozone could provide the mechanism for the observed day-night differences in C 2/T. Estimates of the vertical variations in ozone and aerosol abundances on spatial scales between a few tens of meters of about a kilometer have been used with mean ozone and aerosol profiles to make detailed calculations of the solar heating rates by ozone and aerosols. The calculations have utilized the temperature dependent ozone absorption cross sections and the aerosol properties from the AFGL model atmospheres. Perturbations of various amounts and at different altitudes have been applied to the mean ozone and aerosol profiles to study the impact on the heating rates with the goal of trying to understand the stratospheric thermosonde measurements. GRA

N91-29678# Wisconsin Univ., Madison.
THREE-DIMENSIONAL MAPPING OF ATMOSPHERIC BOUNDARY LAYER STRUCTURE AND WINDS WITH A HIGH PERFORMANCE LIDAR Final Report, 15 Dec. 1985 - 31 Jan. 1990
Edwin W. Eloranta Apr. 1991 260 p
(Contract DAAL03-86-K-0024)
(AD-A238098; ARO-23217.4-GS) Avail: NTIS HC/MF A12 CSCL 17/5

Initial work under this grant concentrated on construction of the Volume Imaging Lidar (VIL). While the major mechanical structures were completed on the previous contract most of the system integration and testing remained when this grant began. The result of this work is an instrument with unmatched capabilities; no existing lidar system approaches its ability to map the three-dimensional structure of the atmosphere. A brief description of the VIL is supplied as appendix A. GRA

N91-29679# Technology International Corp., Bedford, MA.
DNA OPTICAL SUPPORT PROGRAM SUMMARY FOR 1989 Technical Report, 1 Jan. 1989 - 1 Jan. 1990
Wallace P. Boquist 1 Jul. 1991 32 p
(Contract DNA001-88-C-0033)
(AD-A238397; TIC-864; DNA-TR-90-115) Avail: NTIS HC/MF A03 CSCL 04/1

This annual report summarizes the technical work performed in the planning and preparation of the ground optics instrumentation planned for use on the EXCEDE III upper atmospheric research experiment scheduled for the spring 1990. A summary of this effort, the resulting instrument plan, and the completion status of the optical instrumentation are contained in this report. During this same period, the vendor continued to provide data, measurements, and data film copies relating to atmospheric effects topics. The EXCEDE III experiment was designed to quantitatively measure the optical emissions associated with the collisional excitations of the upper atmosphere by a rocket borne electron beam accelerator. Observations of the real time and decaying emissions brightness and spectral characteristics will be analyzed to provide data on the atmospheric composition and reaction/rates of the beam excited species. GRA

N91-29680# Scripps Institution of Oceanography, La Jolla, CA. Marine Physical Lab.
TEST OF NEWTONIAN GRAVITY USING DSV SEA CLIFF Final Report, 1 Oct. 1988 - 31 Dec. 1991
John A. Hildebrand and Mark A. Zumgerge Jun. 1991 5 p
(Contract N00014-90J-1063)
(AD-A238558; MPL-U-48/91) Avail: NTIS HC/MF A01 CSCL 08/5

Several recent geophysical measurements have searched for deviations from Newton's inverse square law by testing for range dependence of the gravitational constant G. One group of these experiments observes the vertical gravity gradient above the earth using measurements on tall towers and tests for deviations from Newtonian gravity but provides no direct estimate of G. Another group of geophysical experiments observes gravity from material slabs of known density by measuring within mines and boreholes or above fluctuating lakes. Collectively, these experiments offer little evidence for deviations from Newtonian gravity in the scale range 10 m to 1200 m. GRA

47 METEOROLOGY AND CLIMATOLOGY

Includes weather forecasting and modification.

N91-29681# Brookhaven National Lab., Upton, NY.
AN OBSERVATIONAL STUDY OF THE EFFICIENCY OF ACTIVATION OF ACCUMULATION-MODE PARTICLES IN WARM CONTINENTAL STRATIFORM CLOUDS
N. V. Gillani, P. H. Daum, S. E. Schwartz, W. R. Leaitch, J. W. Strapp, and G. A. Isaac (Atmospheric Environment Service, Downsview, Ontario) Apr. 1991 13 p Presented at the 5th International Conference on Precipitation Scavenging and Atmosphere Surface Exchange Process, Richland, 15-19 Jul. 1991
(Contract DE-AC02-76CH-00016)
(DE91-013335; BNL-46115; CONF-9107104-5) Avail: NTIS HC/MF A03

Continuous aircraft measurements of the in-cloud number concentrations (N) of cloud droplets (CD, 2 to 35 microns diameter) and accumulation-mode particles (AMP, 0.17 to 2.07 microns diameter) have been used to study the efficiency of activation of AMP in warm continental stratiform clouds near Syracuse, NY during Fall 1984. The efficiency is defined as the activated fraction (F) of all measured particles. Thus, F (equivalent to) N(sub cd)/N(sub tot), where N(sub tot) = N(sub cd) + N(sub amp). The primary focus in this paper is on the dependence of F on N(sub tot). In the interior of clouds, two distinct regimes of the state of activation of AMP were observed. For N(sub tot) less than 600 cm(exp -3), F was largely close to unity and relatively insensitive to N(sub tot). Such conditions prevailed in relatively cold airmasses of northerly origin. For N(sub tot) greater than 800 cm(exp -3), F tended to decrease with increasing N(sub tot). This decrease was greatest in a stable stratus deck embedded in a warm, moist airmass of southerly origin. The spatial variation of F is used to explore the non-uniform state of activation in the clouds. In general, F was lower in cloud edges and in the upper portions of the clouds. DOE

N91-29682# Oak Ridge National Lab., TN. Carbon Dioxide Information Analysis Center.
A GLOBAL GEOGRAPHIC INFORMATION SYSTEM DATA BASE OF STORM OCCURRENCES AND OTHER CLIMATIC PHENOMENA AFFECTING COASTAL ZONES
K. R. Birdwell and R. C. Daniels (Miami Univ., Oxford, OH.) May 1991 304 p
(Contract DE-AC05-84OR-21400)
(DE91-014949; ORNL/CDIAC-40; NDP-035; ESDP-3656) Avail: NTIS HC/MF A14

This document describes the contents of a digital climatological data set that may be used by raster or vector geographic information systems (GISs). The primary focus of the data set is the quantification of the occurrence of synoptic storms and other climatological factors that affect coastlines. However, recent demands for new and/or improved climatologies of storm events as well as an increase in the availability of source data have made it useful to extend the domain of most of the data variables to that of regional and/or global coverage. The expansion of the data makes the data set applicable in several areas of climatic

research. The data set contains eight data groups. Spatial coverage of data varies by data group. All data groups except one are referred to 1 deg x 1 deg or 5 deg x 5 deg grid cells of latitude and longitude. DOE

N91-29683# Hawaii Univ., Manoa.
TROPICAL CYCLONE MOTION IN THE NORTHWEST PACIFIC OCEAN, PHASE 1 Final Report
Thomas A. Schroeder Jun. 1991 4 p
(Contract N00014-88-K-0249)
(AD-A237455) Avail: NTIS HC/MF A01 CSCL 04/2

Our program involved observational studies of tropical cyclone cases, numerical simulation of a real-case, numerical studies of the beta drift using a three dimensional model and post-doctoral visitations to the Joint Typhoon Warning Center (JTWC). The principal investigator and post-doctoral researcher each participated in detailed planning for the Tropical Cyclone Motion 1990 (TCM 90) experiment. This entailed participation in workshops in Rainbow Beach, Australia and San Diego as well a substantial amount of time at JTWC. Research included work on surface station network augmentation and on synoptic forecasting in support of operations. GRA

N91-29684# Naval Postgraduate School, Monterey, CA.
AN INVESTIGATION OF THE ERICA IOP-2 CYCLONE USING THE NORAPS MODEL M.S. Thesis
Ronald J. Miller Jun. 1990 86 p
(AD-A237683) Avail: NTIS HC/MF A05 CSCL 04/2

Rapid cyclogenesis is studied using the Naval Operational Regional Atmospheric Prediction System (NORAPS) numerical model. The cyclone studied occurred during the second Intensive Observation Period (IOP-2) of the Experiment on Rapidly Intensifying Cyclones over the Atlantic (ERICA). Several simulations were run to examine the inability of this and other models to correctly predict development movement, and other characteristics of this cyclone. The experiments consisted of varying the cumulus parameterization and the initial low-level temperature and moisture fields. The exact cumulus specification did not appear to have a significant effect on the forecast sea level pressure. Although convective precipitation amounts varied with different parameterizations, the stable precipitation recovered the difference resulting in a nearly equivalent amount of latent heating. A dry simulation showed that the latent heat released from precipitation is necessary to achieve the observed deepening rate. A poor analysis over the data-sparse ocean and lack of a moisture analysis caused the modeled atmosphere to be too potentially unstable, resulting in much more precipitation and development than was observed early in the forecast period. A simulation using the global analysis fields for initialization, which were somewhat cooler and drier than the NORAPS initial fields, resulted in a better forecast, although the observed deepening rate was not achieved. GRA

N91-29685# Naval Oceanographic and Atmospheric Research Lab., Bay Saint Louis, MS.
DEPENDENCE OF RADAR BACKSCATTER ON THE ENERGETICS OF THE AIR-SEA INTERFACE Final Report
Marie C. Colton Jul. 1990 325 p
(AD-A237818; AD-E040062; NOARL-6) Avail: NTIS HC/MF A14 CSCL 04/2

In these times scientists are challenged to reverse dangerous climatic trends. U.S. military strategy will evolve to more passive defense measures. The role of remote sensing satellites cannot be underestimated at this early stage of a whole Earth philosophy. Satellites will provide surveillance data needed to verify arms treaties and the synoptic geophysical data required for either realtime monitoring of environmental conditions or data assimilation into prognostic models. Quality of these remotely sensed data will be limited by our understanding of the physical mechanisms which produced the signals. Surface wind over oceans is a physical phenomenon which can be sensed from remote platforms and which is paramount in monitoring the types of global changes described. Wind affects both strategic and tactical naval operations, drives ocean currents and determines air-sea fluxes important for climate modeling. In 1978 a microwave radar scatterometer onboard SEASAT used an algorithm, SASS1, to infer wind velocity from measured radar returns. Twelve years later, scatterometer data from this mission are still being analyzed to confirm the instrument as a breakthrough in maritime meteorology and oceanography and to reveal short comings of the SASS1 algorithm and the possibility that the radar return is sensitive to environmental parameters other than wind. This study evaluates environmental effects on the functional form, which relates radar echoes from sea surface to sea surface wind vector. GRA

N91-29686# Naval Postgraduate School, Monterey, CA.
TOVS SATELLITE SOUNDINGS OF THE ERICA IOP-2 CYCLONE M.S. Thesis
John J. Pereira Jun. 1990 76 p
(AD-A237998) Avail: NTIS HC/MF A05 CSCL 04/2

Satellite soundings from the TIROS/N Operational Vertical Sounder (TOVS) are used to study the Experiment on Rapidly Intensifying Cyclones over the Atlantic (ERICA) Intensive Observation Period-2 (IOP-2), 13 to 14 Dec. 88. TOVS data are compared with dropwindsondes and coastal rawinsondes, and Spectral Grid Model (SGM) analyses of stability, geopotential height, and temperature. The impact of the first guess on the TOVS retrieval is studied by comparing four first guess methods: (1) regression without surface data; (2) regression with surface data; (3) climatology with surface data; and (4) SGM analyses with surface data. Ship reports and moored and drifting buoys were objectively analyzed to obtain the surface data for the first guess. The retrievals with 6-h old SGM analyses as a first guess best best captured the low level structure of the in situ soundings. The TOVS stability analyses defined the rapid cyclogenesis environment, in advance of the developing cyclone. The TOVS height and temperature analyses successfully described the structure of the developing cyclone, in reasonable agreement with experimental data and synoptic scale analyses. GRA

N91-29687# Naval Postgraduate School, Monterey, CA.
MULTIPLE CHANNEL SATELLITE ANALYSIS OF CIRRUS M.S. Thesis
Sharon A. Wieman Jun. 1990 58 p
(AD-A238054) Avail: NTIS HC/MF A04 CSCL 04/2

The split-window technique is based on the varying radiative properties of clouds and the atmosphere in different wavelengths of the primary infrared (IF) window. Channels 4 (11 micron) and 5 (12 micron) on the NOAA Advance Very High Resolution Radiometer (AVHRR) are used to apply the technique to determine the differences between thick and thin cirrus and multiple layered clouds. The brightness temperature from channel 5 was subtracted from the brightness temperature from channel 4, resulting in a brightness temperature difference (BTD) image. The technique was applied to ten subscenes over mid-latitude land areas for both summer and winter cases. The BTD values were compared to surface observations of the same time period as the images. The cases were grouped into five and then three cloud groups based on the surface observations. The analysis of variance showed that the average showed that the average BTD values for the three cloud groups were statistically different for the summer cases but not for the winter cases. The BTD thresholds estimated from these cases are: (1) Multiple layered clouds--0.00 to 0.80; (2) Thick cirrus--0.81 to 1.50; and (3) Thin cirrus--1.51 and greater. The split-window technique is successful in distinguishing the varying cirrus thicknesses when the surface temperature is warmer than 285 K. GRA

N91-29688# Naval Oceanographic and Atmospheric Research Lab., Bay Saint Louis, MS.
AN EXPERT SYSTEM APPROACH FOR PREDICTION OF MARITIME VISIBILITY OBSCURATION Proceedings Report
James A. Peak Jul. 1990 8 p Presented at the Armed Forces Communications and Electronics Association Conference, Dayton, OH, 18-20 Jul. 1990
(NR Proj. RM3-5-G-80)

(AD-A238305; AD-E040019; NOARL-PR-90-073-401) Avail: NTIS HC/MF A02 CSCL 04/2

An Expert system for Shipboard Obscuration Prediction (AESOP) and Artificial Intelligence (AI) approach to forecasting maritime visibility obscurations has been designed, developed, and tested. AESOP is rule-based, using backward chaining. The current version, AESOP 2.1, has 290 rules and has been designed in terms of nowcasts (0 to 1 hr) and forecasts (1 to 6 hr). An extensive explanation feature allows the user to understand the reasoning process behind a particular forecast. AESOP has been evaluated against 100 independent test cases, in which clear, hazy, or foggy conditions are predicted. The overall performance of AESOP is 68 percent correct. This value indicates considerable forecast skill when compared to 36 percent for random chance. When the distinction between clear and haze is ignored, the expert system correctly forecasts 79 percent of the Fog/No fog situations.

GRA

N91-29689# Naval Postgraduate School, Monterey, CA.
FORECASTING TROPICAL CYCLONE RECURVATURE USING AN EMPIRICAL OTHOGONAL FUNCTION REPRESENTATION OF VORTICITY FIELDS M.S. Thesis
Debra M. Ford Sep. 1990 84 p
(AD-A238489) Avail: NTIS HC/MF A05 CSCL 04/2

An empirical orthogonal function (EOF) representation of relative vorticity is used to forecast recurvature (change in storm heading from west to east of 000 deg N) of western North Pacific tropical cyclones. The time-dependent coefficients of the first and second EOF eigenvectors vary in a systematic manner as the tropical cyclone recurves around the subtropical ridge and tend to cluster in a different region in EOF space. Exploiting this Euclidean distance approach, additional EOF coefficients are identified that best represent the vorticity fields of recurving and straight-moving storms. Classification of an individual case is then into the closest time-to-recurvature in 12-h intervals or straight-moving storm category as measured in multidimensional EOF space. Although rather subjective, the Euclidean method demonstrates skill relative to climatological forecasts. A more objective discriminant analysis technique is also tested. A final version that involves the first six EOF coefficients of the 250 mb vorticity field is useful (72 percent correct) in identifying recurvers or straight-movers during the 72-h forecast period. Skill in classifying situations within 12-h time-to-recurvature groups is low, but might be improved using other analysis techniques or in combination with other predictors.

GRA

N91-29690# METSAT, Inc., Fort Collins, CO.
CLOUD DATA COLLECTION, COMPOSITES AND ANALYSIS FOR WHOLE-SKY IMAGER (WSI) STUDIES Final Report
Thomas H. Haar Jul. 1991 75 p
(Contract N00014-86-C-0463)
(AD-A238531) Avail: NTIS HC/MF A04 CSCL 04/2

The objectives are to combine knowledge of cloud and atmospheric physics, the physics of detection systems and new microprocessor technology to determine ways to quickly derive information about cloud amounts, location, height, existence of holes and other parameters suitable for characterizing clouds as background. The results presented have contributed much to the accomplishment of those objectives, and have broken new ground in the general area of satellite cloud analysis. Areas of discussion are as follow: New Cloud Composite Climatologies Using Meteorological Satellite Imagery; New Cloud Composite Climatologies Using Meteorological Satellite Imagery; High Resolution Space/Time Cloud Climatologies From Satellite Data; Interannual Variability in Cloud Frequency as Determined from GOES Satellite; Persistence Forecasts From High Resolution Cloud Composite Climatologies; and Technique for Cloud Discrimination on GOES Infrared Imagery.

GRA

N91-29691# Chicago Univ., IL.
PERFORMANCE REPORT OF THE WIND RESEARCH LAB.
T. T. Fujita 8 Jul. 1991 26 p
(Contract N00014-90-J-1526)
(AD-A238575) Avail: NTIS HC/MF A03 CSCL 04/2

The purpose of this research is to generate the data base of all cyclones in the northern hemisphere, north of the latitude 20 North for determining the oceanic regions where cyclones develop (deepening of the central pressure) and weaken (filling of the central pressure). Specific regions of the Navy's interest are The North Pacific Ocean, North Atlantic Ocean, and Arctic Oceans. The data base is obtained by examining the 6-hourly National Meteorological Center surface maps and the 12-hourly surface maps from The Japan Meteorological Agency. The input data for generating the magnetic cyclone tape are latitude, longitude, central pressure (PC*) and the radii of the PC* + 16 mb and PC* + 8 mb isobars surrounding or in the vicinity of the cyclone center. After smoothing, the input values are used in computing the differencial values (finite differences) such as pressure deepening in mb/6hrs, pressure filling and the windspeed intensification m/sec in 6 hours. These parameters, both input and computed, are tabulated along with the consecutive number of each cyclone.

GRA

N91-29692# Naval Postgraduate School, Monterey, CA.
THE NATURE OF THE PROPAGATION OF SEA BREEZE FRONTS IN CENTRAL CALIFORNIA M.S. Thesis
Joseph A. Yetter, Jr. Sep. 1990 78 p
(AD-A238635) Avail: NTIS HC/MF A05 CSCL 04/2

An examination is made of the nature of propagation of sea breeze fronts in central California. From 15 to 30 September, 1987, the Land/Sea Breeze Experiment (LASBEX) provided a series of meteorological observations including sodar, lidar, rawinsonde, radiosonde and surface observations. Surface observations of opportunity were also available from local marine labs and airports. Using a very simple linear model, the speed and direction of the sea breeze front is investigated. The speed of frontal propagation varied from 1 m/s to 3 m/s. A correlation between the speed of frontal propagation and estimated surface heat flux is observed. The direction of frontal propagation tends to be up valley. Comparison of the frontal propagation vector with stations in the southern portion of Monterey Bay shows that the front is curved on the mesoscale.

GRA

N91-29693# National Oceanic and Atmospheric Administration, Boulder, CO. Forecast Systems Lab.
DAR(3)E-1 EVALUATION: ASSESSMENT OF WEATHER FORECASTS MADE USING THE DAR(3)E-1 WORKSTATION
Mary M. Cairns Dec. 1990 36 p
(PB91-181701; NOAA-TR-ERL-443; FSL-5) Avail: NTIS HC/MF A03 CSCL 04B

The evaluation of the Denver AWIPS-90 Risk Reduction and Requirements Evaluation, Part 1 (DAR3E-1) system compares the forecast accuracy of severe storm warnings, probability of precipitation (POP), and maximum and minimum temperature forecasts issued before and after the system was installed in the Denver National Weather Service Office (WSFO) in Septemper, 1986. Twenty years of POP and temperature forecasts for Denver and Grand Junction, Colorado are compared to those forecasts issued in the year following installation, whereas severe storm warnings issued by the Denver WSFO for the Colorado Front-Range were evaluated for a three- and five-year period. For the evaluation, tornado warnings showed the most improvement in the false alarm ratio (FAR). Increased lead time and the decreased size of the warning area indicate a marked potential for improved service to the public. Severe thunderstorm warnings also showed similar, but not as noticeable improvements. The probability of detection (POD) scores declined for both tornado and severe thunderstorm warnings. The precipitation forecasts show little change in skill and reliability, while there is suggested improvement in the cool- and warm-season 0 to 12 hour temperature forecasts after the installation of DAR3E-1.

GRA

N91-29694# National Academy of Sciences - National Research Council, Washington, DC. Commission on National Weather Service Modernization.
TOWARD A NEW NATIONAL WEATHER SERVICE: A FIRST REPORT Annual Report, 1990
Mar. 1991 80 p
(Contract NOAA-50-DGNW-0-00041)
(PB91-184077) Avail: NTIS HC/MF A05 CSCL 04B

The status and plans are reviewed for the modernization and associated reconstructing of the National Weather Service (NWS) of the National Oceanic and Atmospheric Administration, U.S. Department of Commerce. The major elements of the modernization include the next-generation Doppler Radar (NEXRAD), Automated Surface Observing System, next-generation Geostationary Operational Environmental Satellites, and Advanced Weather Interactive Processing System. Author

N91-29695# Pacific Northwest Lab., Richland, WA.
MESOSCALE MODELING OF PRECIPITATION SCAVENGING BY A COLD-FRONTAL SQUALL LINE
R. C. Easter, W. R. Cotton, M. Nicholls, R. Walko, and C. Tremback (ASTeR, Inc., Fort Collins, CO.) Jun. 1991 11 p Presented at the 5th International Conference on Precipitation Scavenging and Atmosphere Surface Exchange Process, Richland, WA, 15-19 Jul. 1991
(Contract DE-AC06-76RL-01830)
(DE91-015534; PNL-SA-19712; CONF-9107104-12) Avail: NTIS HC/MF A03

A cold-frontal squall line that was observed during the PRE-STORM/PRECP-2 experiment has been simulated using a mesoscale model operated in a three-dimensional channel mode. Measurements obtained during the experiment included a network of nine wet-only precipitation chemistry samplers, two air chemistry aircraft, surface and airborne Doppler radar, an upper-air sounding network, and a surface meteorological network. Model-simulated concentrations of SO4(2-) and NH4(+) in precipitation agreed well with observations, both in terms of mean values and spatial variability. Wet deposition amounts of these species were underpredicted by a factor of two, as was the event precipitation amount, and this is attributed to an underprediction of the inflow of water vapor and pollutants to the storm. Concentrations of NO3(-) in precipitation were underpredicted by a factor of two, and this is attributed to either measurement errors of NO3(-) aerosol and HNO3 in inflow air or to an unaccounted source for NO3(-) in precipitation. DOE

N91-29696# Argonne National Lab., IL.
PARAMETERIZATIONS OF MICROPHYSICAL PROCESSES FOR SIMULATION OF REGIONAL-SCALE CLOUDS
In Young Lee 1991 26 p Presented at the Symposium on Cloud Physics and Mesoscale Dynamics, Seoul (Republic of Korea) 2-5 Jul. 1991
(Contract W-31-109-eng-38)
(DE91-015554; ANL/CP-73289; CONF-9107142-1) Avail: NTIS HC/MF A03

Cloud physics parameterizations are comprehensively reviewed to examine their theoretical bases and to evaluate their applicability to mesoscale modeling. The constant distribution functions of hydrometeors assumed in previous work are found to be unrealistic. New parameterizations are developed for mixing ratios of water vapor, cloud water, rainwater, cloud ice, graupel, and snowflakes. Equations are derived from theoretical considerations and multiple regression applied to results of simulations with a cloud model that incorporates sophisticated treatments of microphysics and dynamics. In the detailed simulations from which they were derived, the parameterizations generally give better results than do the existing parameterizations tested. In a Lagrangian air parcel model under variable atmospheric conditions, the new parameterizations give consistent results and are computationally more efficient than previously available formulas. DOE

48 OCEANOGRAPHY

Includes biological, dynamic, and physical oceanography; and marine resources.

For related information see also *43 Earth Resources and Remote Sensing.*

N91-29697# Woods Hole Oceanographic Inst., MA.
STOCHASTIC MODELLING OF SEAFLOOR MORPHOLOGY Ph.D. Thesis
John A. Goff Jun. 1990 269 p
(AD-A237063; WHOI-90-24) Avail: NTIS HC/MF A12 CSCL 12/3

At scale lengths less than 100 km or so, statistical descriptions of seafloor morphology can be usefully employed to characterize processes which form and reshape abyssal hills, including ridge crest volcanism, off-axis tectonics and volcanism, mass wasting, sedimentation, and post-depositional transport. The objectives of this thesis are threefold: (1) to identify stochastic parameterizations of small-scale topography that are geologically useful, (2) to implement procedures for estimating these parameters from multibeam and side-scan sonar surveys that take into account the finite precision, resolution, and sampling of real data sets, and (3) to apply these techniques to the study of marine geological problems. The seafloor is initially modeled as a stationary, zero-mean, Gaussian random field completely specified by its two-point covariance function. An anisotropic two-point covariance function is introduced that has five free parameters describing the amplitude, orientation, characteristic width and length, and Hausdorff (fractal) dimension of seafloor topography. The general forward problem is then formulated relating this model to the statistics of an ideal multibeam echo sounder, in particular the along-track autocovariance functions of individual beams and the cross-covariance functions between beams of arbitrary separation. GRA

N91-29698# Naval Postgraduate School, Monterey, CA.
ACOUSTIC TOMOGRAPHIC ESTIMATE OF OCEAN ADVECTIVE HEAT FLUX: A NUMERICAL ASSESSMENT IN THE NORWEGIAN SEA M.S. Thesis
Richard T. Barock Jun. 1990 108 p
(AD-A237100) Avail: NTIS HC/MF A06 CSCL 08/3

In a computer simulation experiment, acoustic tomography is assessed as a means of measuring the seasonal flux of heat advected by the Norwegian Atlantic Current. Oceanic heat flux has traditionally been measured by various direct or indirect techniques that are prone to error or large uncertainty. The tomographic technique offers distinct advantages over conventional methods in that temperature and current fields, that combine to yield heat flux in the ocean, can be determined at various spatial and temporal scales. The adequacy of the tomographic technique thus hinges on the question of how well can the temperature and current by resolved spatially? The spatial resolution of tomography varies with array size, number of transceivers used and the characteristics of the sound channel. In the assessment we use the General Digital Environmental Model (GDEM), a climatological data base, to simulate an ocean area 550 x 550 km squared off the Norwegian Coast. Resolution and variance analysis are performed on two circular arrays consisting of six transceivers. An important finding is that the horizontal resolution lengths of the current and temperature fields differ. For a six element array the horizontal resolution length is approximately one fifth the array diameter for the current field, whereas for the temperature field it is one sixth the array diameter. GRA

N91-29699# Naval Underwater Systems Center, Newport, RI.
RELATING OCEAN ACOUSTIC AMBIENT TO OCEAN SURFACE DYNAMICS
R. M. Kennedy 29 May 1991 26 p
(AD-A237167; NUSC-TD-8879) Avail: NTIS HC/MF A03 CSCL 20/1

The acoustical significance of ocean surface dynamics is well known. Motivation for establishing the casual relations between these two physical processes has both underwater acoustic system

noise reduction and oceanographic remote sensing objectives. The goal has eluded investigators because of the complexity of both the acoustic and oceanographic mechanisms involved. Progression is discussed in spatial scales by utilizing a relatively deep water basin (The Tongue of the Ocean, the Bahamas) in a quasi-controlled environment which made a broadband measurement (40 to 4000 Hz) of the vertical directional spectrum are dominated by local (fetch limited) water surface conditions over a wide range of environmental conditions. While the exploratory nature of the experiment limited the amount of supporting meteorological and oceanographic measurements made, the results give additional credence to the role of entrapped air bubbles and bubble clouds in the generation of acoustic ambient. Sea surface generated acoustics is shown to be dependent on a fundamental nondimensional variable describing the air-sea boundary process and the rate of energy dissipation caused by wave breaking in the gravity wave equilibrium range. GRA

N91-29700# Washington Univ., Seattle. Applied Physics Lab.
HAMILTONIAN 3-D RAY TRACING IN THE OCEANIC WAVEGUIDE ON THE ELLIPSOIDAL EARTH
George Dworski and James A. Mercer Dec. 1990 78 p
(Contract N00014-89-J-1979)
(AD-A237458; APL-UW-TR-8929) Avail: NTIS HC/MF A05 CSCL 17/10

Ray equations based on an acoustic Hamiltonian, and formulated by Jones et al. (1986) for spherical coordinates in NOAA's three dimensional ray tracer HARPO, are adapted to ellipsoidal coordinates in the oceanic waveguide. The ensuing modified HARPO is used to model very long range (up to antipodal) acoustic paths in which the difference between geodesics and great circles is measurable. The eventual objective of this modeling is to extract the predictable part of the travel time trend and fluctuations along several long paths that will be used to monitor hypothetical global warming effects. The requirements for easy assimilation and representation of realistic environmental inputs are discussed. These requirements, when coupled with the possibility of classical chaos in the ray paths, dictate a new software architecture. We use the existing software, however, to breadboard and test features of new ray tracers in the global boundary layer, and to support the experimental design of a forthcoming pilot experiment that will use a transmitter located at Heard Island in the Indian Ocean near Antarctica. GRA

N91-29701# Old Dominion Univ., Norfolk, VA. Dept. of Oceanography.
MESOSCALE CHARACTERISTICS AND THE ROLE OF DEFORMATION ON OCEAN DYNAMICS Final Report, 15 Dec. 1988 - 30 Sep. 1990
Albert D. Kirwan, Jr. 5 Jun. 1991 61 p
(Contract N00014-89-J-1595)
(AD-A237577; TR-91-7) Avail: NTIS HC/MF A04 CSCL 08/3

The bulk of the activities consisted of basic research on ocean flow dynamics as it pertains to the prediction of ocean motions. Results from the research were published in refereed scientific literature. The following articles are included: (1) Evolution of a warm-core ring in the Gulf of Mexico: Lagrangian observations; (2) Fractal drifter trajectories in the Kuroshio Extension; (3) Observed and simulated kinematic properties of loop current rings; and (4) Dynamics of warm-core mesoscale eddies. GRA

N91-29702# Naval Postgraduate School, Monterey, CA.
MODELING A RAIN-INDUCED MIXED LAYER M.S. Thesis
Hong B. Hur Jun. 1990 63 p
(AD-A238022) Avail: NTIS HC/MF A04 CSCL 08/3

With the development of ocean surface remote sensing, air sea interaction theory and the theory of underwater sound generation at the ocean surface, the potential calming effect on surface gravity waves by raindrop induced mixing has become important. The rain induced mixed layer was studied with models based on the turbulent kinetic energy budget. A bulk mixed layer model was tuned with laboratory experimental data. The turbulent kinetic energy going into subsurface mixing was found to be less than 10 percent of the total raindrop kinetic energy. The length scale for mixing is proportional to both raindrop size and rain intensity. Furthermore, there is some indication of an initial penetration depth for raindrops. Although the available data was inadequate to complete model development and verification, a prediction for a hypothetical situation in the North Pacific is proposed. The diffusion processes are illustrated by solving for the diffusion and dissipation terms of the turbulent kinetic energy equation with a finite difference scheme. New experiments are suggested to allow future model development and testing. GRA

N91-29703# Delaware Univ., Newark.
OCEAN THERMAL FEATURE RECOGNITION, DISCRIMINATION AND TRACKING USING INFRARED SATELLITE IMAGERY M.S. Thesis
James A. Holland, II 1 Jun. 1991 93 p
(AD-A238138) Avail: NTIS HC/MF A05 CSCL 17/5

This paper presents a method to quantitatively measure ocean surface movement, using 10.5 micron band AVHRR images. An ordered statistical edge detection algorithm is used to select thermal pattern features, at the same time discriminating between the water surface, clouds and land. A constrained statistical correlation based recognition scheme is then used to find the best match to the pattern feature in a subsequent image. Study Areas off the Delaware and New Jersey coast were analysed using the method, with results comparing favorably with in situ anchored buoy measurements. All relevent algorithms are included in the paper with key program code included in appendices. GRA

N91-29704# Naval Oceanographic and Atmospheric Research Lab., Bay Saint Louis, MS.
FITTING SEASONAL AVERAGES WITH A CONTINUOUS FUNCTION Final Report
Daniel N. Fox Apr. 1991 24 p
(NR Proj. RM3-5-G-84)
(AD-A238300; AD-E040041; NORDA-246) Avail: NTIS HC/MF A03 CSCL 08/3

A large-scale, integrated program in ocean circulation model development has been pursued by the ocean modeling and prediction branch, ocean sensing and prediction division, naval ocean research and development activity. This program will provide the navy with accurate nowcasts and forecasts of the state of the ocean on global, regional and tactical scales. One of the constraints that has been applied to this research is the development of circulation models that accurately reproduce the measured climatologies of south quantities as the dynamic height, thermocline depth, and depth-averaged density. These fields are derived using in situ data that have been acquired over many decades, but are so irregularly distributed that in most regions only annual or seasonal mean fields have been derived. Comparisons between model and data climatologies are facilitated if both are available as continuous time series, but the standard Levitus climatology is generally available at time scales no shorter than seasonal. This report describes several methods for converting the existing seasonal quantities into a continuous time series of fields, and also notes an amplitude error and bias present in the seasonal values as presently derived. GRA

N91-29705# National Oceanic and Atmospheric Administration, Seattle, WA. Pacific Marine Environmental Lab.
SEA LEVEL AND BOTTOM PRESSURE MEASUREMENTS IN THE NORTHERN GULF OF ALASKA
S. J. Bograd Mar. 1991 64 p
(PB91-184135; NOAA-DR-ERL-PMEL-29; CONTRIB-1277) Avail: NTIS HC/MF A04 CSCL 08C

The data presented here gives information on the spatial and temporal variability of the sea level along the Alaska coast. The study contributed to the understanding of the physical environment in the experimental region of the Fisheries Oceanography Coordinated Investigations (FOCI). Author

N91-29706# Delaware Univ., Newark. Sea Grant Coll. Program.
OCEANOGRAPHIC DATA REPORT NUMBER 7: DATA FROM THE DELAWARE ESTUARY SCENIC CRUISES, APRIL 1986 - SEPTEMBER 1988
M. E. Lebo, L. A. Cifuentes, M. L. Fogel, and M. P. Hoch Oct. 1990 153 p Sponsored in part by National Sea Grant Coll. Program, Silver Spring, MD and by NSF
(Grant NA86AA-D-SG040)
(PB91-183582; DEL-SG-06-90) Avail: NTIS HC/MF A08
CSCL 08C

Physical, chemical, and biological data collected during cruises on the Delaware Estuary from April 1986 to September 1988 are given. The cruise series, designated SCENIC, report data from the entire estuary from the tidal river near Trenton, NJ to the mouth of the bay. In addition, three cruises report data from the adjacent continental shelf. The data collected on each cruise is accompanied by a cruise report outlining the objectives and events of that cruise. Author

N91-29707# Delaware Univ., Newark. Sea Grant Coll. Program.
OCEANOGRAPHIC DATA REPORT NUMBER 8: DENSITY PROFILES FROM THE DELAWARE ESTUARY, OCTOBER 1986 - SEPTEMBER 1988
M. Kawabe, J. H. Sharp, K. C. Wong, and M. E. Lebo Oct. 1990 126 p Sponsored in part by National Sea Grant Coll. Program, Silver Spring, MD and by NSF
(Grant NA86AA-D-SG040)
(PB91-183608; DEL-SG-07-90) Avail: NTIS HC/MF A07
CSCL 08C

An analysis of physical oceanographic data collected on the SCENIC cruise series on the Delaware Estuary between October 1986 and September 1988 is presented. Detailed biological, chemical, and physical data from discrete samples are published in a separate report. The data used here were collected by a computer controlled conductivity, temperature, and depth sensor system (CTD). Due to missing or incomplete CTD records, results are presented from only 17 of the 24 cruises. Author

N91-29708# Lamont-Doherty Geological Observatory, Palisades, NY.
CO2 MEASUREMENTS ALONG THE WOCE P-16 AND 19 SECTIONS IN THE SOUTH PACIFIC OCEAN: A JOINT LDGO/WHOI PROGRAM
D. W. Chipman and Taro Takahashi 18 Jul. 1991 8 p
(Contract DE-FG02-90ER-60983)
(DE91-015742; DOE/ER-60983/2) Avail: NTIS HC/MF A02

Due to substantial delays in the refitting of the R/V KNORR, the field work which was originally scheduled to begin in October, 1990, had to be delayed by seven months and modified. In late May, 1991, the analytical equipment and personnel were loaded on the R/V THOMAS WASHINGTON to Tahiti. During the 40-day first leg of the expedition, the CO2 analyses were carried out. Approximately 1500 seawater samples were analyzed for the total CO2 concentration and about 1/3 as many for alkalinity. Additional water samples were collected for land-based manometric measurements of total CO2 concentration. The second leg of this expedition is in progress. The data obtained during the expedition will be analyzed and interpreted during the third year of this grant. The coulometer and gas chromatograph was further tested and improved. The nature of the improvements and the results of tests are described. DOE

51 LIFE SCIENCES (GENERAL)

N91-29709# Pacific Northwest Lab., Richland, WA.
BIOLOGICAL INTERACTIONS OF EXTREMELY-LOW-FREQUENCY ELECTRIC AND MAGNETIC FIELDS
T. S. Tenforde Mar. 1990 30 p Presented at the 10th International Conference on Bioelectrochemistry and Bioenergetics, Pont-a-Mousson (France), 24-30 Sep. 1989
(Contract DE-AC06-76RL-01830)
(DE90-011927; PNL-SA-17147; CONF-8909334-1) Avail: NTIS HC/MF A03

A description is given of the fundamental physical properties of extremely-low frequency (ELF) electromagnetic fields, and the mechanisms through which these fields interact with the human body at a macroscopic level. The mechanisms through which ELF electric and magnetic fields induce currents in humans and other living objects are described. Evidence is presented that cell membranes play an important role in transducing ELF signals. Both experimental evidence and theoretical models are described that relate pericellular currents and electrochemical events at the outer membrane surface to transmembrane signaling pathways and cytoplasmic responses. Biological responses to ELF fields at the tissue, cellular and molecular levels are summarized, including new evidence that ELF field exposure produces alterations in messenger RNA synthesis, gene expression and the cytoplasmic concentrations of specific proteins. DOE

N91-29710# Army Research Inst. of Environmental Medicine, Natick, MA.
DATA ACQUISITION SYSTEM FOR COLLECTING BIOPHYSICAL AND PHYSIOLOGICAL DATA
K. W. Stephen and M. S. Chang Apr. 1991 249 p
(DA Proj. 3M1-62787-A-878)
(AD-A237654; USARIEM-T9-91) Avail: NTIS HC/MF A11
CSCL 12/5

The Biophysics and Biomedical Modeling Division general purpose data acquisition system (AC128) is designed to sample up to 128 channels of input data, using an IBM-AT compatible personal computer (PC). The most recent set of sampled data are displayed in real time on the PC monitor. All data are also temporarily stored in the PC memory. Options to save the collected data onto other more permanent storage devices are provided. In this report the term AC128 represents the entire data acquisition system, comprising both the hardware and the software. The software portion alone will be referred to as the SoS. The AC128 SoS does not replace the PC Disk Operating System (DOS). The SoS runs within the PC DOS and calls many DOS provided functions. The primary types of input supported include thermocouples, thermistors, and voltages. All standard thermocouple types (T, E, J, K, B, R, S) are allowed. Thermistors which subscribe to the Steinhart-Hart conversion equation are supported. GRA

N91-29711# Arizona State Univ., Tempe. Dept. of Botany.
SPECIFIC MUTAGENESIS OF A CHLOROPHYLL-BINDING PROTEIN
W. F.J. Vermaas Jan. 1991 6 p
(Contract DE-FG02-89ER-14031)
(DE91-014813; DOE/ER-14031/3) Avail: NTIS HC/MF A02

Chlorophyll, absorbing light energy for use in photosynthesis, is bound by specific proteins in thylakoid membranes such as CP47. His residues have been suggested to serve as chlorophyll ligands. To test the necessity of His residues in CP47, specific His residues have been altered to Tyr or Asn, and the effects of these mutations are now studied in vivo in the cyanobacterium Synechocystis sp. PCC 6803. Most mutations lead to a decreased photoautotrophic growth rate of the cyanobacterium, due in part to a decreased stability of the photosystem 2 complex. The effective relative antenna size of photosystem 2 in the various CP47 mutants is now being measured. The CP47 protein may also be involved in events at the donor side of photosystem 2. We have identified a region which can be deleted without obvious ill effects, and a domain which appears crucial for photosystem 2 structure and function. Residues of particular importance will be defined by further mutagenesis experiments. DOE

N91-29712# Georgia Univ., Athens.
MICROBIOLOGY AND PHYSIOLOGY OF ANAEROBIC FERMENTATIONS OF CELLULOSE
J. Wiegel May 1991 23 p
(Contract DE-FG09-86ER-13614)
(DE91-015239; DOE/ER-13614/4) Avail: NTIS HC/MF A03

The biochemistry and physiology of four major groups of anaerobic bacteria involved in the conversion of cellulose to methane or chemical feedstocks are examined. Aspects of metabolism which are relevant to the interactions and bioenergetics of consortia are being studied. Properties of the cellulolytic enzyme cluster of Clostridium thermocellum are investigated. Five different hydrogenases have been characterized in detail from anaerobic bacteria. Genes for different hydrogenases are being cloned and sequenced to determine their structural relationships. The role of metal clusters in activation of H2 is being investigated, as is the structure and role of metal clusters in formate metabolism. The function of formate in the total synthesis of acetate from CO2 and the role of this primary in anaerobes will be examined as well. Finally, these enzyme studies will be performed on thermophilic bacteria, and pertinent species will be isolated.
DOE

N91-29713# Duke Univ., Durham, NC.
STABLE ISOTOPE FRACTIONATION IN PHOTOSYNTHESIS: ANALYSIS OF AUTOTROPHIC COMPETENCE FOLLOWING TRANSFORMATION OF THE CHLOROPLAST GENOME OF CHLAMYDOMONAS
J. E. Boynton, N. W. Gillham, and C. B. Osmond 15 Jun. 1991 12 p
(Contract DE-FG05-89ER-14005)
(DE91-015792; DOE/ER-14005/T1) Avail: NTIS HC/MF A03

Isotopic techniques needed to assess the interactions between photosynthesis and respiration in Chlamydomonas have been devised for C-13, using plate and liquid cultures. The effectiveness of various transformation strategies for the chloroplast psbA gene has been evaluated with respect to their utility in constructing and characterizing strains homoplasmic for site-directed mutations in an otherwise isogenic background. Our analysis of the first site-directed change in the D-1 protein of Chlamydomonas indicates that a second site mutation (arg(sub 238) greater than lys) in the loop between transmembrane helices IV -- V can partially compensate for the reduced photosynthetic performance that accompanies the atrazine resistant mutation (ser(sub 264) greater than ala/gly) in this alga and in higher plants grown under high light intensities.
DOE

52 AEROSPACE MEDICINE

Includes physiological factors; biological effects of radiation; and effects of weightlessness on man and animals.

N91-29714*# National Aeronautics and Space Administration. Goddard Space Flight Center, Greenbelt, MD.
COMPLIANT WALKER Patent Application
James J. Kerley, inventor (to NASA), Wayne Eklund, inventor (to NASA), and J. Allen Crane, inventor (to NASA) (NSI, Inc., Greenbelt, MD.) 3 Jul. 1991 21 p
(NASA-Case-GSC-13348-2; NAS 1.71:GSC-13348-2; US-Patent-Appl-SN-725111) Avail: NTIS HC/MF A03 CSCL 06L

A compliant walker is provided for humans having limited use of their legs and lower back. It includes an upright wheel frame which at least partially surrounds an upright user wearing a partial body harness. It is attached to the frame by means of cable compliant apparatus consisting of sets of cable segments and angle bracket members connected between opposite side members of the frame and adjacent side portions of the harness. Novelty is believed to exist in the combination of a wheeled frame including a side support structure, a body harness, and compliance means connecting the body harness to the side support structure for flexibility holding and supporting a person in a substantially upright position when the user sags in the frame when taking weight off the lower extremities.
NASA

N91-29715# Washington Univ., Seattle. Dept. of Applied Mathematics.
PERTURBATION TECHNIQUES FOR MODELS OF BURSTING ELECTRICAL ACTIVITY IN PANCREATIC (BETA)-CELLS
M. Pernarowski, R. M. Muira (British Columbia Univ., Vancouver.), and J. Kevorkian 1991 46 p
(Contract DE-FG06-86ER-25019)
(DE91-013901; DOE/ER-25019/21) Avail: NTIS HC/MF A03

Pancreatic beta-cells exhibit periodic bursting electrical activity consisting of active and silent phases. Experimentally, the ratio, (rho sub f), of the active phase duration to the overall period is correlated to the insulin response of these cells to glucose concentration. Several different mathematical models of the beta-cell were developed to describe changes in the intracellular ionic concentrations and the ionic flow through the cellular membrane. The membrane potential in each of these models exhibits the same active and silent phase bursting patterns observed experimentally and, therefore, these models can be used to predict the value of the plateau fraction, (rho sub f). The Sherman-Rinzel-Keizer (SRK) model of this phenomenon consists of three coupled first-order nonlinear differential equations which describe the dynamics of the membrane potential, the activation parameter for the voltage gated potassium channel, and the intracellular calcium concentration. These equations are transformed into a Lienard differential equation coupled to a single first-order differential equation for the slowly changing nondimensional calcium concentration. Leading order perturbation problems for the silent phase and the transition regions are reduced to quadrature. The solution of the leading order active phase problem is a limit cycle which depends on the value of the intracellular calcium concentration. Since the active phase equations exhibit weak damping, Melnikov's method can be applied to determine the bifurcation point of these equations. Thus, an explicit expression for the active phase duration is obtained. Together with the silent phase analysis, an approximation of the plateau fraction, (rho sub f), is derived and its value compared to the plateau fraction numerically obtained from the SRK model.
DOE

N91-29716# Army Research Inst. of Environmental Medicine, Natick, MA.
PHYSIOLOGICAL RESPONSES TO INTERMITTENT EXERCISE AS MODIFIED BY HEAT STRESS AND PROTECTIVE CLOTHING
Kenneth K. Kraning, II and Richard R. Gonzalez May 1991 34 p
(AD-A237447; USARIEM-12-91) Avail: NTIS HC/MF A03 CSCL 06/10

Time-weighted averaging is a method employed in heat stress analyses to consolidate the rate of heat production (M) from complex intermittent exercise patterns into a single continuous level of heat production. Physiological responses during intermittent and continuous exercise were studied in 4 subjects exposed to heat stress in which evaporation was either free or severely restricted. Intermittent work consisted of repeated 10 min exercise/rest patterns. Continuous work was at the time weighted average of intermittent exercise. When heat stress was uncompensable, intermittent work induced more physiological strain than continuous work: endurance time was 14 min less (p less than 0.05), core temperature at 60 min was 0.40 C higher (p less than 0.05), and the rate of core temperature rise was 33 percent greater. The difference in the rate of heat storage was not satisfactorily explained by a discrepancy in average M or in the calculated rate of surface heat loss. Alternatively, results may be explained by interruptions in the rate of heat transport via the cutaneous circulation. These interruptions may be associated with postural and workload transitions. While the mechanisms are not totally understood, it is clear that application of the time-weighted averaging method should be applied with discretion.
GRA

N91-29717# California Inst. of Tech., Pasadena.
STUDIES IN NEURAL NETWORKS Final Report
1991 5 p
(Contract N00014-87-K-0377)
(AD-A237452) Avail: NTIS HC/MF A01 CSCL 06/4

Research performed under this grant centered on the computations done by biological networks of nerve cells, and on the theoretical and engineering of neurobiological computation. The biological studies were in greatest part theoretical analysis of the olfactory (smell) system. This is a very old and simple sensory system, and is highly conserved. Animals as different as snails and humans have strong anatomical similarities in their olfactory systems. In addition, the basic architecture of much of old cortex is claimed to be related to that of olfactory cortex, so understandings gained in the olfactory system are potentially applicable to other areas of brain. GRA

N91-29718# Pennsylvania Univ., Philadelphia. School of Medicine.
HARDWARE IMPLEMENTATION OF NEURON NETS AND SYNAPSES WORKSHOP Final Report
Paul Mueller 26 May 1991 3 p Workshop held in San Diego, CA, 13-15 Jan. 1988
(Contract N00014-88-J-1050)
(AD-A237704) Avail: NTIS HC/MF A01 CSCL 06/5

The workshop brought together 35 key investigators in this area and several representatives from funding agencies, with the aim to assess the current state of the field, to explore the potential for existing and new approaches and to identify those areas that provide currently the greatest opportunities and may need particular emphasis. It was evident from the high quality of the presentations that the field is making excellent and rapid progress. This is especially so for the special purpose systems that are modeled after biological sensory input systems such as retinas, cochleas, and networks for sound localization. The development of larger systems for more complex problems such as vision, speech recognition, tactile sensing, and robotics lies still in the more distant future. It was agreed that the field should make use of currently available technologies although research into new materials, devices, and interconnection methodology should be continued at an active level. GRA

N91-29719# Naval Aerospace Medical Research Lab., Pensacola, FL.
MICRO SAINT MODELING OF PHYSIOLOGICAL AND HUMAN PERFORMANCE IN THE HEAT
S. Shamma, R. Stanny, E. A. Molina, and W. A. Morey Mar. 1991 28 p
(DA Proj. 3M4-637648995)
(AD-A238659; NAMRL-MONOGRAPH-42) Avail: NTIS HC/MF A03 CSCL 06/5

This report documents a Micro SAINT implementation of a heat-stress model developed by the U.S. Army Research Institute of Environmental Medicine. The model incorporates equations that relate deep-body temperature, heart rate, and sweat loss for clothed soldiers performing physical work in various environments. The Micro SAINT program might be used to help reduce casualties associated with extremes of environmental heat, to calculate appropriate work-rest cycles, and to estimate the drinking-water requirements associated with various levels of sweat loss. GRA

N91-29720# Smith-Kettlewell Inst. of Visual Sciences, San Francisco, CA.
PSYCHOPHYSICAL STUDIES OF VISUAL CORTICAL FUNCTION Final Technical Report, 1 Sep. 1988 - 31 Dec. 1990
Ken Nakayama 28 Jun. 1991 4 p
(Grant AF-AFOSR-0326-88; AF Proj. 2313)
(AD-A238663; AFOSR-91-0639TR) Avail: NTIS HC/MF A01 CSCL 06/5

Our work explored a variety of research areas, all directed towards obtaining an understanding of visual cortical function using psychophysical techniques. In particular, we examined visual search, visual attention, the encoding of occluding surfaces, and color filling-in. With respect to visual search, we found a new unexpected relation between distractor number and reaction time, showing that for particular tasks, performance improved when distractor number increased. With respect to visual attention we obtained new information to support the specific hypothesis which proposed that express saccades were due to a rapid disengagement of attention from the fixation. With respect to occluded surfaces, we provided a new theoretical framework to understand the large number of new results collected, suggesting the generic view principle. Finally, with respect to color filling-in, we found evidence that such a hypothetical process can be interrupted after the presentation of a stimulus and we evaluated its spatio-temporal time course. GRA

N91-29721# Retina Foundation, Boston, MA. Eye Research Inst.
EYE MOVEMENTS AND SPATIAL PATTERN VISION Annual Report, 1 May 1990 - 30 Apr. 1991
Lawrence E. Arend 1 Jul. 1991 16 p
(Grant AF-AFOSR-0377-89; AF Proj. 2313)
(AD-A238664; AFOSR-91-0651TR) Avail: NTIS HC/MF A03 CSCL 06/5

Models of human lightness and color perception must take account of color constancy, a tendency for apparent surface color to be relatively independent of the color and intensity of the illuminating light source. Our observers matched the lightnesses (apparent reflectances) and brightnesses (apparent luminances) of regions in simple and complex achromatic spatial patterns. The data showed that the observers' knowledge of the surface reflectances was unaffected by brightness changes due to varying illuminance. A third perceptual dimension, local brightness contrast, was different from both lightness and brightness. In further experiments, we found that moving a patch from a black background to a white background could produce an error of apparent surface color of about 1.5 Munsell Value steps. Similar experiments at mesopic mean luminances revealed that the brightness contrast produced by a fixed luminance contrast declines with mean luminance. GRA

N91-29722# Michigan Univ., Ann Arbor. Transportation Research Inst.
METHODS FOR EVALUATING DISCOMFORT GLARE
D. J. Weintraub, A. W. Gellatly, M. Sivak, and M. Flannagan Apr. 1991 24 p
(PB91-185132; UMTRI-91-13) Avail: NTIS HC/MF A03 CSCL 05H

The ratings obtained from the de Boer scale were compared to ratings from three alternative discomfort glare scales. Of additional interest was the relation between discomfort glare ratings and brightness ratings for the same stimuli. The scales evaluated were the de Boer scale, the DANDY scale (a newly developed categorical scale), an anchored magnitude estimation scale, a free magnitude estimation scale, and a brightness magnitude estimation scale. There are two main findings: (1) the discomfort ratings from the four tested discomfort glare scales were highly intercorrelated, and (2) brightness ratings from a magnitude estimation scale were highly correlated with ratings from an analogous discomfort glare scale. An implication of these findings is that brightness ratings provided essentially the same information as discomfort ratings using any of the four tested discomfort glare scales. Consequently, to the extent that brightness is a concept that is easier to communicate to subjects than is discomfort, researchers interested in discomfort glare might consider using brightness scales.
Author

53 BEHAVIORAL SCIENCES

Includes psychological factors; individual and group behavior; crew training and evaluation; and psychiatric research.

N91-29723# California Univ., Berkeley. Lawrence Berkeley Lab.
QUANTUM MEASUREMENT AND THE MIND-BRAIN CONNECTION
H. P. Stapp 17 Oct. 1990 28 p Presented at the Symposium on the Foundations of Modern Physics, Joensuu (Finland), 13-17 Aug. 1990
(Contract DE-AC03-76SF-00098)
(DE91-012343; LBL-29594; CONF-900862-2) Avail: NTIS HC/MF A03

It is argued that quantum measurements do pose a problem, within the context created by the fundamental aim of science, which is identified as the construction of a cohesive, comprehensive, and rationally coherent idea of the nature of the world in which we live. Models of nature are divided into two classes: (1) those in which there is a selection process that, for any possible measurement, would, if that measurement were to be performed, pick out one single outcome, and (2) all others. It is proved that any model of class that reproduces the predictions of quantum theory must violate the condition that there be no faster-than-light influences of any kind. This result is used to motivate the study of models in which unitary evolution is maintained and there is no selection of unique outcomes. A consideration of ontic probabilities, historical records, and the form of the mind-brain connection leads to an elaboration of the Everett many-worlds interpretation that appears to provide the basis of satisfactory solution of the measurement problem. DOE

N91-29724# Naval Medical Research and Development Command, Bethesda, MD.
DEVELOPMENT AND EVALUATION OF A HUMAN PERFORMANCE ASSESSMENT BATTERY Final Report, 21 Apr. 1984 - 30 Sep. 1989
John Schrot 1 Sep. 1990 13 p
(DA Proj. 3M4-63807-D-993)
(AD-A237391) Avail: NTIS HC/MF A03 CSCL 06/5

The antihistamine-PAB validation study was completed during the reporting period. Preliminary analysis of the results indicates that Benadryl and Seldane produced different effects on different tests of the battery. Benadryl produced more profound effects than Seldane on both accuracy and speed of responding. This laboratory also participated in the testing and evaluation of version 2.1 of the UTC-PAB software systems. The information obtained, along with standards specifications for certain PAB component tasks was provided to the Director, JWGD3 MILPERF. GRA

N91-29725# Reading Univ. (England).
PREDICTING PERFORMANCE BREAKDOWN IN PILOTS THROUGH OBJECTIVE MEASURES OF STRESS SENSITIVITY Final Report, Oct. 1988 - Oct. 1990
Frank P. McKenna and Dinkbar Sharma Apr. 1991 56 p
(Contract DAJA45-88-C-0024; DA Proj. 2Q1-61102-B-74-F)
(AD-A237540; ARI-RN-91-40) Avail: NTIS HC/MF A04 CSCL 05/8

It is well known that stress can have an adverse effect on performance and that individual differences in responses to stress are varied. The potential is explored of developing an objective measure of stress resistance and the possibility of developing a laboratory model of the effects of stress on performance. The paradigm developed reveals that (1) emotional stimuli disrupt performance, (2) the disruption is exacerbated by time pressure and task difficulty, (3) repetition of the emotional stimuli (habituation) eliminates the disruptive effect, (4) it is not the emotionality of the stimulus, but rather the threat component that is critical to the disruptive effect. These results parallel effects in everyday life and suggest that the paradigm shows great promise for developing a measure of stress resistance and a laboratory model of the effects of stress. GRA

N91-29726# Indiana Univ., Bloomington.
INSTITUTE FOR THE STUDY OF HUMAN CAPABILITIES: SUMMARY DESCRIPTIONS OF RESEARCH FOR THE PERIOD DECEMBER 1989 THROUGH SEPTEMBER 1990 Final Report, 1 Nov. 1986 - 30 Sep. 1990
Charles S. Watson 30 May 1991 61 p
(Grant AF-AFOSR-0089-87; AF Proj. 3484)
(AD-A237767; AFOSR-91-0564TR) Avail: NTIS HC/MF A04 CSCL 05/8

Two new psychophysical testing stations were used in cross-modality sensory and cognitive research and a third was constructed for auditory-visual projects. Initial experiments underway with these systems include a visual detection task with auditory cuing, a tactile-visual identification experiment, and a basic investigation of cross modality temporal acuity. A conference was planned on the subject of Human Error. GRA

N91-29727# New York Univ., New York. Neuromagnetism Lab.
COGNITION AND THE BRAIN Annual Technical Report, 15 Feb. 1990 - 14 Feb. 1991
Lloyd Kaufman and Samuel J. Williamson 10 May 1991 62 p
(Grant AF-AFOSR-0221-90; AF Proj. 2313)
(AD-A237846; AFOSR-91-0571TR) Avail: NTIS HC/MF A04 CSCL 05/8

Using an array of 14 superconducting magnetic field sensors we succeeded in establishing the locations of neuronal activity that produce the dominant alpha rhythm recorded in the electroencephalogram and magnetoencephalogram. Of particular interest is our observation that spontaneous alpha activity is suppressed over the visual area when a person is engaged in mental imagery, and over other functional areas when appropriate cognitive tasks are performed. Computer simulations of the changes in patterns of alpha field power reveal how the power map is related to the underlying cortical topography when suppression occurs. In studies of sensory evoked cortical activity, an analysis of published current source density measurements on animals provides information from which we obtain the first realistic measure for the spatial extent of cortical activity in human cortex when responding to sensory stimuli. Measurements with a 5-sensor system for chrominance and luminance stimuli shows that the sites of response in visual cortex coincide. The separation of color information processing apparently takes place at a later stage, if at all. Responses in human auditory cortex to appropriate sound stimuli reveal activity not previously identified, which has characteristics that suggest it is related to sensory memory functions. GRA

N91-29728# Naval Aerospace Medical Research Lab., Pensacola, FL.
ANALYSIS OF NAVAL AVIATION SELECTION TEST DATA WITH NONLINEAR MODELS. PART 1: PARAMETER ESTIMATION Interim Report, Dec. 1988 - Dec. 1989
David J. Blower Dec. 1990 34 p
(AD-A238244; NAMRL-TM-90-2) Avail: NTIS HC/MF A03 CSCL 12/1

An algorithm is described for estimating the parameters of a nonlinear model. This algorithm is called simulated annealing. The actual workings of this algorithm are examined in some detail. The reason for studying this algorithm is because statistical analysis of naval aviation selection test data has always relied on the use of linear regression models. Linear models represent only a small subset of possible mathematical models that could be used as an empirical tool to predict aviator performance. Specifically, the whole class of nonlinear models was not addressed. Recent research into neural networks and parallel distributed processing has uncovered some interesting nonlinear models. The test scores of student naval aviators will be reanalyzed with a nonlinear model borrowed from the neural network literature. It is hoped that this new class of nonlinear models will be a more powerful tool in predicting aviator performance and will result in an improved naval aviator selection test battery. GRA

N91-29729# Naval Aerospace Medical Research Lab., Pensacola, FL.
PERFORMANCE OF MARINE AV-8B (HARRIER) PILOTS ON A COGNITIVE/PSYCHOMOTOR TEST BATTERY: COMPARISON AND PREDICTION Interim Report, Jan. - Jul. 1990
R. N. Shull Dec. 1990 15 p
(AD-A238563; NAMRL-1362) Avail: NTIS HC/MF A03 CSCL 05/9

Several studies have suggested the possibility of predicting pilot flight performance in various aviation environments. The current report concerns the use of an automated performance-based test battery, measuring various aspects of cognitive and psychomotor function, to eventually predict the flight performance of Marine jet pilots during various stages of flight training while comparing their test results to those of other aviation communities. A group of Marine jet pilots assigned to operate the AV-8B vertical takeoff/landing attack jet were tested. No significant differences in test performance were found among the various subgroups of student and experienced AV-8B pilots tested. The subject group, as a whole, performed most like pilots of other types of jet aircraft on some tests and more like helicopter pilots on other tests. GRA

N91-29730# Naval Aerospace Medical Research Lab., Pensacola, FL.
PERFORMANCE OF SEVERAL DIFFERENT NAVAL AVIATOR COMMUNITIES ON A COGNITIVE/PSYCHOMOTOR TEST BATTERY: PIPELINE COMPARISON AND PREDICITON Interim Report, Dec. 1988 - Dec. 1989
R. N. Shuli and G. R. Griffin Dec. 1990 18 p
(AD-A238564; NAMRL-1361) Avail: NTIS HC/MF A03 CSCL 05/8

Research is currently being conducted to develop reliable predictor tests which might aid in the making of decisions concerning aircrew assignment. The current approach involves comparing the performance of several different aviator communities on a test battery measuring various aspects of cognitive and psychomotor functioning. Four groups of pilots (two experienced jet groups, one experienced helicopter (helo) group, and one untrained student group) were tested on this battery. Overall, the jet groups performed in general. Within this student group, pilot trainees who were assigned to the jet pipeline did significantly better on several of these tests than those trainees who were assigned to either helicopter or land-based fixed-wing pipelines. Many of the test performance differences seen between these jet and helo student pipeline groups were also seen between the experienced jet and helo pilots tested. GRA

N91-29731# Reading Univ. (England).
PREDICTING PERFORMANCE BREAKDOWN IN PILOTS THROUGH OBJECTIVE MEASURES OF STRESS SENSITIVITY Annual Report, Oct. 1988 - Oct. 1989
Apr. 1991 39 p
(Contract DAJA45-88-C-0024)
(AD-A238597; ARI-RN-91-39) Avail: NTIS HC/MF A03 CSCL 05/8

While the adverse effects of stress are widely recognized, researchers have difficulty in developing appropriate measures. Previous research has rested heavily on subjective measures. The present approach is based on development of a simple objective performance-based measure. By showing that emotional stimuli disrupt performance, the basis of a test of stress resistance is formed. Major progress has been made by putting the test on a computer, where a more detailed investigation reveals that: (1) the performance decrement due to emotional stimuli occurs early in the test; and (2) the time pressure results in large fatigue effects. Both these findings have implications for future developments of the test. GRA

N91-29732# Carnegie-Mellon Univ., Pittsburgh, PA.
THE FUNCTIONAL ARCHITECTURE OF VISUAL OBJECT RECOGNITION Final Report, 1 May 1989 - 31 Dec. 1990
Martha J. Farah Jul. 1991 10 p
(Contract N00014-89-J-3016; NR Proj. RR0-4206)
(AD-A238617) Avail: NTIS HC/MF A02 CSCL 05/8

The goal of this grant was to constrain our theories of visual object recognition, including face and printed word recognition, using evidence from brain-damaged and normal subjects. By observing the patterns of association and dissociation among abilities after brain damage, one can infer the architecture of those abilities in the normal brain. In the case of object recognition, the different forms of agnosia can provide clues to the representations underlying normal object recognition. GRA

54 MAN/SYSTEM TECHNOLOGY AND LIFE SUPPORT

Includes human engineering; biotechnology; and space suits and protective clothing.

For related information see also *16 Space Transportation.*

N91-29733# Department of Transportation, Cambridge, MA. National Transportation Systems Center.
THE USE AND DESIGN OF FLIGHTCREW CHECKLISTS AND MANUALS Final Report, Sep. 1988 - Jan. 1990
John W. Turner and M. S. Huntley, Jr. Apr. 1991 71 p
(AD-A237206; DOT/FAA/AM-91/7) Avail: NTIS HC/MF A04 CSCL 06/11

A survey of aircraft checklists and flight manuals was conducted to identify impediments to their use and to determine if standards or guidelines for their design were needed. Information for this purpose was collected through the review of checklists and manuals from six Part 121 and nine Part 135 carriers, review of NTSB and ASRS reports, analysis of an ALPA survey of air carrier pilots, and by direct observation in air carrier cockpits. The survey revealed that some checklists and manuals were difficult to locate and were poorly designed for use in the cockpit environment, the use of checklists by flight crews was not always well defined, the use of checklists interfered with other flight operations, and flight operations often made it difficult to use checklists effectively. Recommendations are made for the formatting and content of checklists and manuals, their use by flight crews, and areas of research relevant to checklist design. GRA

N91-29734# Chemical Research and Development Center, Aberdeen Proving Ground, MD.
VENTILATION KINETICS TESTING OF A STEEL FRAME/RUBBER FABRIC UNDERGROUND SHELTER Final Report, Aug. 1989 - Aug. 1990
Alan T. Seitzinger May 1991 24 p
(AD-A237469; CRDEC-TR-278) Avail: NTIS HC/MF A03 CSCL 13/13

Design modifications were implemented on a respectively new steel frame/rubber fabric underground shelter to improve its collective protection characteristics for usage in an NBC warfare environment. Design changes were evaluated by analyzing volumetric air flow and pressure data collected from ventilation tests conducted for each design modification. Modifications to doors within the shelter proved to have significant impact on its performance. One door modification utilized velcro and rubber adhesives to attach the doorflap on the positive pressure side of the doorway. This modification increased maximum overpressure attained by the shelter from 0.125 inches of water (in.WG) to 1.8 in.WG over its original design. Test results indicated that this was due to a substantial decrease in the effective leakage areas associated with all of the doorways. At this higher overpressure, the risk of airborne nuclear fallout, biological agents, or vapors from chemical agents or aerosols penetrating into the shelter during exit/entry operations would be greatly reduced. GRA

N91-29735# Army Aeromedical Research Lab., Fort Rucker, AL.
HUMAN FACTORS OF NIGHT VISION DEVICES: ANECDOTES FROM THE FIELD CONCERNING VISUAL ILLUSIONS AND OTHER EFFECTS Final Report
John S. Crowley May 1991 49 p
(AD-A237641; USAARL-91-15) Avail: NTIS HC/MF A03
CSCL 23/2

To investigate the breadth of visual illusions experienced by aviators flying with night vision devices (NVDs), an open-ended questionnaire was distributed to the military helicopter community in the fall of 1989. Of the 242 returned questionnaires, there were 221 night vision goggle (NVG) reports and 21 thermal imaging system (FLIR) reports. Most sensory events occurred at night, during low illumination, good weather, and over varied terrain. Contributing factors included inexperience, division of attention, and fatigue. Frequently reported illusions were misjudgements of drift, clearance, height above the terrain, and attitude. Also reported were illusions due to external lights, and distributed depth perception caused by differences in brightness between NVG tubes. Other respondents cited hardware problems and physiological effects. There were no obvious differences between the experiences of NVG users and FLIR users. Although incidence rates cannot be inferred from these data, the variety of expected aviator anecdotes in this report will be useful to all those concerned with human factors and safety of NVDs. GRA

N91-29736# Naval Aerospace Medical Research Lab., Pensacola, FL.
THE EFFECT OF THREE LEVELS OF LASER GLARE ON THE SPEED AND ACCURACY OF TARGET LOCATION PERFORMANCE WHEN VIEWING A BRIEFLY PRESENTED VISUAL ARRAY Interim Report, 1 Oct. 1989 - 30 Sep. 1990
M. D. Reddix, T. L. DeVietti, J. C. Knepton, and J. A. DAndrea
Nov. 1990 20 p
(AD-A238565; NAMRL-1359) Avail: NTIS HC/MF A03 CSCL 09/3

The effect of three levels of low-intensity laser glare on the visual search performance of student aviators was investigated. Subjects were exposed to laser glare while seated in a cockpit simulation trainer with attached F/15 windscreen assembly. The experimental task was designed to maximize visual attentional demands to a degree that might be expected in normal flight. Thus, speed and accuracy of performance were monitored while subjects located targets in a complex, briefly presented (about 1 s), visual array under simulated dusk conditions. Low-level argon laser-induced glare (a factor 3700 times below the ANSI maximum permissible exposure for a 902-ms laser presentation) caused significant decrements in visual search performance for briefly displayed visual information. Subjects identified significantly fewer targets when experiencing low-intensity laser glare relative to a no-glare control. In addition, the speed with which correctly identified targets were located was significantly reduced relative to a no-glare control. As incident laser glare increased, significant decrements in the speed and accuracy of target location responses were observed at target eccentricities up to 8.1 deg from the center of the beam path. GRA

N91-29737*# Alabama Univ., Huntsville. Coll. of Science.
CHEMICAL WASTE DISPOSAL IN SPACE BY PLASMA DISCHARGE Final Report
James K. Baird 31 Mar. 1991 68 p
(Contract NAS8-37195)
(NASA-CR-184169; NAS 1.26:184169) Avail: NTIS HC/MF A04
CSCL 06K

An inductively coupled plasma discharge apparatus operating at 13.56 MHz and with electrical power up to 2.5 kW was constructed. The efficiency of this device to destroy various gases expected to be carried aboard the Space Station was tested. By expressing the efficiency of the device in terms of G-value (the number of molecules decomposed per 100 eV of energy absorbed), the results are compared with known efficiencies of ionizing radiation to destroy these same gases. In the case of ammonia, it was found that in the inductively coupled device, the destruction efficiency, G(-NH3) varied from 6.0 to 32.0 molecules/100 eV, depending on conditions. It was also found that capacitatively coupled discharges were less efficient in destroying NH2 than the inductively coupled discharge. In the case NH2 destruction, it was found that the G(-NH3) was a qualitative guide to the efficiencies of plasmas. The plasma device was also used to destroy nitrous oxide and methane. It is shown how the G-value for the destruction of any gas can be computed theoretically from a knowledge of the electron velocity distribution, the various electron molecule scattering cross sections, and the rate constants for the reactions of secondary species. Author

55 SPACE BIOLOGY

Includes exobiology; planetary biology; and extraterrestrial life.

No abstracts in this category.

59 MATHEMATICAL AND COMPUTER SCIENCES (GENERAL)

No abstracts in this category.

60 COMPUTER OPERATIONS AND HARDWARE

Includes hardware for computer graphics, firmware, and data processing.

For components see *33 Electronics and Electrical Engineering.*

N91-29738# National Computing Centre Ltd., Manchester (England).
ALSYS LIMITED, ALSYCOMP 017, VERSION 5.2, MICRO VAX 2 UNDER MICRO VMS V5.3 (HOST) TO INMOS T425 TRANSPUTER IMPLEMENTED ON A B403 TRAM (TARGET), 901118N1.11064 Final Report
15 Aug. 1990 96 p Sponsored by DOD
(AD-A237411) Avail: NTIS HC/MF A05 CSCL 12/5

This Validation Summary Report describes the extent to which a specific ADA compiler conforms to the Ada Standard, ANSI/MIL-STD-1815A. This report explains all technical terms used within it and thoroughly reports the results of testing this compiler using the Ada Compiler Validation Capability. An Ada compiler must be implemented according to the Ada Standard, and any implementation-dependent features must conform to the requirements of the Ada Standard. The Ada Standard must be implemented in its entirety, and nothing can be implemented that is not in the Standard. Even though all validated Ada compilers conform to the Ada Standard, it must be understood that some differences do exist between implementations. The Ada Standard permits some implementation dependencies - for example, the maximum length of identifiers or the maximum values of integer types. Other differences between compilers result from the characteristics of particular operating systems, hardware, or implementation strategies. All the dependencies observed during the process of testing this compiler are given in this report. The information in this report is derived from the test results produced during validation testing. The validation process includes submitting

a suite of standardized tests, the ACVC, as inputs to an Ada compiler and evaluating the results. GRA

N91-29739# Massachusetts Inst. of Tech., Cambridge. Lab. for Computer Science.
APRIL: A PROCESSOR ARCHITECTURE FOR MULTIPROCESSING
Anant Agarwal, Beng-Hong Lim, David Kranz, and John Kubiatowicz Jun. 1991 16 p
(Contract N00014-87-K-0825)
(AD-A237476; MIT/LCS/TM-450) Avail: NTIS HC/MF A03 CSCL 12/6

Processors in large scale multiprocessors must be able to tolerate large communication latencies and synchronization delays. This paper describes the architecture of a rapid-context-switching processor called APRIL with support for fine-grain threads and synchronization. APRIL achieves high single-thread performance and supports virtual dynamic threads. A commercial RISC-based implementation of APRIL and a run time software system that can switch contexts in about 10 cycles is described. Measurements taken for several parallel applications on an APRIL simulator show that the overhead for supporting parallel tasks based on futures is reduced by a factor of two over a corresponding implementation on the Encore Multimax. The scalability of a multiprocessor based on APRIL is explored using a performance model. We show that the SPARC-based implementation of APRIL can achieve close to 80 percent processor utilization with as few as three resident threads per processor in a large-scale cache-based machine with an average base network latency of 55 cycles. GRA

N91-29740# Calspan-Buffalo Univ. Research Center, NY.
DISCRETIONARY SECURITY FOR OBJECT-ORIENTED DATABASE SYSTEMS Final Report, Mar. 1989 - Aug. 1990
Teresa F. Lung Mar. 1991 50 p Prepared in cooperation with SRI International Corp., Menlo Park, CA
(Contract F30602-88-D-0026)
(AD-A237573; RL-TR-91-17) Avail: NTIS HC/MF A03 CSCL 12/8

The discretionary access controls in today's computer systems are designed to enforce a specific access control policy. An application whose access control policies do not easily match the policy that is wired into the system is forced to work around that wired-in policy. As a result, the application itself must enforce discretionary security and cannot make use of the assurances of the computer system's discretionary access controls. A flexible approach is presented to discretionary access control that allows the implementation of arbitrary access control policies. The generality of the approach allows a user to implement a discretionary access control policy that is tailored to an application, rather than having to work around a specific policy that is wired into the computer system. Discretionary controls for object-oriented systems are examined. Object-oriented systems are an emerging technology of great import for applications in business, industry, and the military. Many of these applications must share information among users with different needs and authorizations. The specific access rules desired will vary from application to application. Thus, a flexible approach to discretionary access control for such systems is proposed. GRA

N91-29741# Air Force Inst. of Tech., Wright-Patterson AFB, OH.
A PROLOG SYSTEM FOR CONVERTING VHDL-BASED MODELS TO GENERALIZED EXTRACTION SYSTEM (GES) RULES Final Report, Jun. - Dec. 1990
Michael A. Dukes, Frank M. Brown, and Joanne E. DeGroat Jun. 1991 44 p
(AF Proj. 6096)
(AD-A238545; WL-TR-91-5018) Avail: NTIS HC/MF A03 CSCL 12/3

With the advent of the VHDL language accurate documentation of hardware designs is a practical reality. In the past, schematics were typically used for documentation of hardware designs. However, these schematics would usually become obsolete as the hardware design was being constructed. Deviations in the hardware design would sometimes not be reflected in the schematics. For design groups, failure to update schematics could lead to different parts of a hardware design becoming incompatible. A system to ensure compliance of hardware with its VHDL documentation is presented in this paper. The system, vhdl2ges, is meant to help guide the development of hardware by pointing out where hardware deviates from its VHDL documentation. A tool is used to parse the VHDL description into a Prolog-type intermediate form. A customized GES is constructed that checks a netlist derived from a layout description for deviations from the components and interconnections specified in the structural VHDL documentation. GRA

61 COMPUTER PROGRAMMING AND SOFTWARE

Includes computer programs, routines, alogorithms, and specific applications, e.g., CAD/CAM.

N91-29742# National Aeronautical Establishment, Ottawa (Ontario). Structures and Material Lab.
QBDATAMT: A COMPUTER PROGRAM TO READ DATAMYTE RECORDER DATA INTO AN IBM PC OR COMPATIBLE COMPUTER Preliminary Report
Colin W. MacKenzie 1 Mar. 1989 56 p Revised
(NAE-LTR-ST-547; CTN-91-60023) Copyright Avail: NTIS HC/MF A04

A description of QBDATAMT: a QuickBASIC based computer program designed to read Datamyte recorder data into an IBM PC and for initializing the memory packs is given. Datamyte can do several types of recording, depending on the plug-in program pack installed in the recorder. QBDATAMT has been written and tested for the 451 and 458 Rainflow packs. Program pack 451 is used to handle data from an accelerometer mounted vertically at the center of gravity of a fixed wing aircraft, and pack 458 is used for data collected from a strain gage bridge mounted in the longitudinal pitch link of both the forward and the aft main rotor heads of the CH-113 Voyageur helicopter. The code itself and abbreviated installation instructions are included. CISTI

N91-29743# National Research Council of Canada, Ottawa (Ontario). Div. of Electrical Engineering.
MATCHING OF COMPLEX 3-D SURFACES USING DYNAMIC PROGRAMMING
Hiromitsu Yamada, Pierre Boulanger, and Katsuhiko Sakaue Jul. 1989 20 p Prepared in cooperation with Electrotechnical Lab,, Ibaraki, Japan
(ERB-1022; NRC-30411; CTN-91-60036) Copyright Avail: NTIS HC/MF A03

A preliminary study is described of the potential use of dynamic programming techniques to perform the matching of 3-D images. The matching technique uses the segmentation produced by the differential geometry method. Using the signs of the Gaussian and mean curvatures one can segment a range image into regions corresponding to one of the eight fundamental surfaces such as peak, pit, ridge, flat, valley, saddle ridge, minimal surface, and saddle valley. This segmentation produces a labeled image called a topographic primal sketch. The result of this segmentation is an adjacency graph of regions of similar curvature signs. How the graphs produced by this segmentation technique can be matched to a model graph using dynamic programming (DP) is described. The mathematical formulation is presented of the matching process and describes how the graph produced by this segmentation technique can be matched to a model graph using DP.
Author (CISTI)

N91-29744# National Aeronautical Establishment, Ottawa (Ontario). Structures and Materials Lab.
DESCRIPTION OF COMPUTER PROGRAMS USED TO ANALYZE AND PLOT SPECTRAPOT DATA FILES

C. W. Mackenzie 13 Jun. 1989 30 p
(NAE-ST-557; CTN-91-60047) Copyright Avail: NTIS HC/MF A03

A program designed to plot Spectrapot data files is described. Four CL-41 Tutor aircraft were instrumented with strain gages located in the aft-fuselage upper longeron, horizontal stabilizer rear spar cap, and the vertical stabilizer rear spar cap. The aircraft were then flown through various maneuvers while recording strain gage data. The Spectrapot data collector was used to record and process data from the strain gages in one of two formats: rainflow or sequential peak valley (SPV). The internal SPV program of the data collector collects peak and valley points which are separated by a specified hysteresis value that is set during initialization of the memory module. Two computer programs, QBSPEC and SPECPM, were developed to provide a means of plotting strain gage data gathered by the Spectrapot-1C data collection system. QBSPEC is written in QuickBASIC and allows the user to: plot sequential valleys and peaks; calculate and print class average; edit a data file; and select a printer. SPECPM, written in GWBASIC, is similar to QBSPEC except that it plots only one point in a 30 second interval, while QBSPEC plots a complete data set. The programs, although written for use by the Tutor fatigue test spectrum development teams, can be used with any Spectrapot data processed using the SPV method. Computer coding for these programs is provided. CISTI

N91-29745*# National Aeronautics and Space Administration. Langley Research Center, Hampton, VA.
A GENERAL GRAPHICAL USER INTERFACE FOR AUTOMATIC RELIABILITY MODELING
Carlos A. Liceaga and Daniel P. Siewiorek (Carnegie-Mellon Univ., Pittsburgh, PA.) May 1991 57 p
(NASA-TM-104068; NAS 1.15:104068) Avail: NTIS HC/MF A04 CSCL 09B

Reported here is a general Graphical User Interface (GUI) for automatic reliability modeling of Processor Memory Switch (PMS) structures using a Markov model. This GUI is based on a hierarchy of windows. One window has graphical editing capabilities for specifying the system's communication structure, hierarchy, reconfiguration capabilities, and requirements. Other windows have field texts, popup menus, and buttons for specifying parameters and selecting actions. An example application of the GUI is given. Author

N91-29746# Superconducting Super Collider Lab., Dallas, TX.
ZLIB: A NUMERICAL LIBRARY FOR DIFFERENTIAL ALGEBRA AND LIE ALGEBRAIC TREATMENT OF BEAM DYNAMICS
Yiton T. Yan May 1991 4 p Presented at the 1991 Institute of Electrical and Electronics Engineers (IEEE) Particle Accelerator Conference (PAC), San Francisco, 6-9 May 1991
(Contract DE-AC02-89ER-40486)
(DE91-014875; SSCL-464; CONF-910505-335) Avail: NTIS HC/MF A01

A dynamic-memory numerical library, ZLIB, has been developed in an attempt to offer efficient numerical routines on supercomputers for differential algebra and the relevant Lie algebraic techniques for mapping studies of beam dynamics. Optimization of ZLIB has been attempted for vector computing as well as scalar computing. Parallel computing (multi-tasking) can also be easily employed. Currently, ZLIB contains more than 200 subroutines. DOE

N91-29747# Sandia National Labs., Albuquerque, NM.
A FAST, ONE PASS ALGORITHM TO LABEL OBJECTS AND COMPUTE THEIR FEATURES
Tan Thai 1991 9 p Presented at the Society of Photo-Optical Instrumentation Engineers (SPIE) Meeting, San Diego, CA, 21-26 Jul. 1991
(Contract DE-AC04-76DP-00789)
(DE91-015441; SAND-91-1324C; CONF-9107115-11) Avail: NTIS HC/MF A02

In many image processing applications, labeling objects and computing their features for recognition are crucial steps for further analysis. In general these two steps are done separately. This paper proposes a new approach to label all objects and compute their features (such as moments, best fit ellipse, major and minor axis) in one pass. The basic idea of the algorithm is to detect interval overlaps among the line segments as the image is scanned from left to right, top to bottom. Ambiguity about an object's connectivity can also be resolved with the proposed algorithm. It is a fast algorithm and can be implemented on either serial or parallel processors. DOE

N91-29748# Vexcel Corp., Boulder, CO.
AN AUTOMATED SOFTWARE SYSTEM FOR UPDATING DIGITAL TERRAIN DATABASES FROM ALL-SOURCE IMAGERY, PHASE 1
J. Curlander, W. Kober, J. Thomas, and A. Stocker Feb. 1991 130 p
(Contract DACA76-90-C-0013)
(AD-A237105; ETL-0584) Avail: NTIS HC/MF A07 CSCL 12/5

VEXCEL Corporation's Phase 1 SBIR research effort for U.S. Army's Engineer Topographic Laboratories concentrated on the feasibility of creating the primary tools for the prototype development in Phase II of a digital change detection work station. This system in intended to be capable of detecting long-term (6 months to 1 year) and/or seasonal changes from all-source imagery. The system is intended to be hosted on a SUN-4 platform operating under a UNIX/C software environment. The emphasis of the present Phase 1 effort was on the two major technical challenges for the development of such a system: precision image registration and robust change detection and analysis. Most of this effort was directed toward automated SAR-optical image registration and automated change cueing experiments. Change cueing is an initial step in change detection for identifying regions where possible change events may have occurred. The automated registration and cueing efforts were successful over the data sets tested. These data sets did not contain appreciable terrain-induced distortions. Theoretical improvements for algorithms are recommended for addressing such terrain-induced registration complications in Phase 2. Recommendations are also made for the inclusion of interactive capabilities to supplement the automated registration techniques. GRA

N91-29749# Washington Univ., Seattle. Dept. of Computer Science.
NW LAB FOR INTEGRATED SYSTEMS Final Report, 5 Feb. 1988 - 30 Sep. 1990
Larry Snyder 24 May 1991 42 p
(Contract N00014-88-K-0453)
(AD-A237118) Avail: NTIS HC/MF A03 CSCL 12/5

This report gives an overview of the research and development projects supported by the VLSI Architectures and CAD contract between DARPA and the University of Washington's Northwest Laboratory for Integrated Systems. Because most of these scientific and engineering accomplishments have been reported on in the technical literature, this report serves primarily as a introduction to the topics. Emphasis here is on overall directions, motivation, and describing what has been achieved. References are provided to the appropriate papers, where the full details can be found. As the name VLSI Architectures and CAD suggests, the contract addressed many topics that generally fall into the architecture related topics and computer aided design topics. GRA

N91-29750# Aerospace Corp., El Segundo, CA. Engineering Group.
THE LANGUAGE FOR DENOTE (DENOTATIONAL SEMANTICS TRANSLATION ENVIRONMENT)
J. V. Cook 31 Aug. 1990 35 p
(Contract F04701-88-C-0089)
(AD-A237144; TR-0090(5920-07)-02; SSD-TR-90-49) Avail: NTIS HC/MF A03 CSCL 12/5

The State Delta Verification System (SDVS) is a proof checker for correctness proofs of properties expressed in the state delta logic. When one proves correctness properties of a computer

program within SDVS, one must first translate the program into the language of the state delta logic. The translation semantics of a computer language can be specified formally by means of denotational semantics. An automated environment is described for specifying and implementing denotational semantics, called DENOTE (Denotational Semantics Translation Environment). The language accepted by DENOTE is called the DENOTE language (DL). DL is a language in which formal denotational semantic specifications can be written. DL specifications can be transformed by DENOTE into text suitable for input to the Scribe and LaTEX formatters, as well as into Common Lisp code that implements the specified semantics. GRA

N91-29751# Department of the Air Force, Washington, DC. Command Control Communications/Computers.
SLAYING THE SOFTWARE DRAGON: A LOOK AT HOW SOFTWARE ENGINEERING, THE Ada PROGRAMMING LANGUAGE AND PROCESS MATURITY ARE CHANGING SOFTWARE DEVELOPMENT Final Report
David R. Dick 1 Jun. 1991 71 p
(AD-A237156) Avail: NTIS HC/MF A04 CSCL 12/5

The cost of software today consumes over ten percent of the DoD budget. Software costs, complexity, and size continue to rise because of the ever increasing dependence of weapons and general purpose systems on computers. Software engineering, the Ada programming language, and efforts to determine the performance and risk of software development organizations by measuring process maturity represent key initiatives by the DoD to improve the quality, reliability, and maintainability of the software DoD buys. Each of these areas are examined and described which are based on current literature and interviews with officers of 37 companies engaged in software development for command, control, and communications systems. GRA

N91-29752# Harry Diamond Labs., Adelphi, MD.
USER'S MANUAL FOR DIODE Interim Report, 1 Jul. - 31 Dec. 1988
Alford L. Ward and Steven L. Kaplan Jun. 1991 75 p
(DA Proj. 1L1-62120-A-140)
(AD-A237190; HDL-SR-91-1) Avail: NTIS HC/MF A04 CSCL 12/5

The DIODE computer program at the Harry Diamond Laboratories (HDL) is used to compute current and voltage characteristics in semiconductors or gases. This user's manual serves two main purposes: (1) to document the present DIODE computer program in preparation for proposed improvements; and (2) to allow others to use the program without personal instruction. Included are a brief history of the origin of the DIODE computer program, input data requirements, description of the computer code, output, and a discussion of the material parameters. Detailed instructions are included for the use of a remote IBM terminal on the Harry Diamond Laboratories site. Also included is a list of over 100 papers, reports, and oral presentations based on the DIODE program. GRA

N91-29753# Carnegie-Mellon Univ., Pittsburgh, PA. Management Sciences Research Group.
AN EXACT ALGORITHM FOR FUNDING UNDIRECTED HAMILTONIAN CYCLES BASED ON A TWO-MATCHING PROBLEM RELAXATION
D. L. Miller, J. F. Pekny, and G. L. Thompson 22 Mar. 1991 13 p Prepared in cooperation with E. I. du Pont de Nemours and Co., Inc., Wilmington, DE and Purdue Univ., West Lafayette, IN
(Contracts N00014-85-K-0198; DE-FG02-85ER-13396)
(AD-A237241; MSRR-565; WP-1991-18) Avail: NTIS HC/MF A03 CSCL 12/1

We describe an algorithm for finding two matchings in undirected graphs. This algorithm is used as a basis for a simple exact algorithm for determining the hamiltonicity of undirected graphs. Results are presented for random graphs with up to 30,000 vertices and for knight's tour problems having up to 10,000 vertices. GRA

N91-29754# Institute for Defense Analyses, Alexandria, VA.
REAL-TIME Ada DESIGN METHODOLOGIES AND THEIR IMPACT ON PERFORMANCE Final Report
Norman R. Howes Jun. 1991 41 p
(AD-A237259; AD-E501397; IDA-P-2488; IDA/HQ-91-37919)
Avail: NTIS HC/MF A03 CSCL 12/5

This paper, written as part of an IDA Central Research Project, provides an overview of the existing state of Ada real-time design methodologies and qualifies the impact on performance of some of the best known and widely used Ada real-time design methodologies. The paper also discusses the limitations of these methodologies and indicates some alternative principles upon which a better design methodology might be based. GRA

N91-29755# Aerojet-General Corp., El Monte, CA. Microwave Div.
Ada 9X REQUIREMENTS RATIONALE
May 1991 165 p
(AD-A237350) Avail: NTIS HC/MF A08 CSCL 12/5

For those revision requests (RR's) whose request was met (at least in part), there is a reference to the Requirements Document that points to the place in that document (a Requirement or a Study Topic) where the topic of the RR or the draft Ada commentary is dealt with. Such a reference indicates that the request was met to at least some extent, even if it was not met in its entirety. Some requests, usually requests for no change in a specific area, are marked as having been met, with no reference. Some requests are marked as rejected, with a brief explanation and a reference to a section of this document. GRA

N91-29756# Stanford Univ., CA. Systems Optimization Lab.
PRIMAL-DUAL METHODS FOR LINEAR PROGRAMMING
Philip E. Gill, Walter Murray, Dulce B. Ponceleon, and Michael A. Saunders May 1991 24 p
(Contract N00014-90-J-1242)
(AD-A237418; SU-SOL-91-3) Avail: NTIS HC/MF A03 CSCL 12/4

Many interior-point methods for linear programming are based on the properties of the logarithmic barrier function. We first give a convergence proof for the (primal) projected Newton barrier method. We then analyze three types of barrier method that can be categorized as primal, dual and primal-dual. All three approaches may be derived from the application of Newton's method to different variants of the same system of nonlinear equations. A fourth variant of the same equations leads to a new primal-dual algorithm. In each of the methods discussed, covergence is demonstrated without the need for a nondegeneracy assumption. In particular, convergence is established for a primal-dual algorithm that allows a different step in the primal and dual variables. Finally, we describe a new method for treating free variables. GRA

N91-29757# California Univ., Berkeley. Dept. of Electrical Engineering and Computer Science.
[SOFTWARE DEVELOPMENT OF THE COCHLEAR FILTER AND EIGHTH-NERVE MODEL] Semiannual Report, 1 Jan. - 31 Jun. 1991
24 Jun. 1991 3 p
(Contract N00014-91-J-1333)
(AD-A237454) Avail: NTIS HC/MF A01 CSCL 12/5

Our software development comprised the following steps: (1) transport of our previously-developed code for modeling cochlear and 8th-nerve signal processing from PCAT DOS format to the SUN, UNIX format in an X-Windows environment; (2) modification of this code to improve modularity-- cochlear signal processing and 8th-nerve signal processing (spike initiation) now are completely independent; (3) development of a new spike-initiator module (based on the Hill model); (4) development of display software for three-dimensional presentation of neural response data and user-interactive manipulation of those presentations; (5) development of a cochlear filter module based on FFT computation; and (6) development of user-interactive software to smooth REVCOR-derived cochlear filter functions so that they can be used in cochlear-filter modules. GRA

N91-29758# Army Construction Engineering Research Lab., Champaign, IL.
THE PC DUGOUT MICRO-MAINFRAME INTEGRATION SYSTEM: PAX IMPLEMENTATION Final Report
Edward J. Japel, J. R. Murphy, Wayne J. Schmidt, and Connie L. Raaymakers May 1991 51 p
(AD-A237480; CERL-TR-P-91/34) Avail: NTIS HC/MF A04 CSCL 12/5

This report describes the research and development of PC Dugout, a transparent software application for the distribution and control of applications on the Programming, Administration, and Execution (PAX) system. PC Dugout is designed to aid in the productive use of personal computers connected to PAX. The program enables previously centralized processing tasks to be distributed to personal computers, resulting in lower operating costs and improved user interfaces. PC Dugout automatically distributes and maintains personal computer applications developed to support the Military Construction, Army program. The design of PC Dugout addresses the challenge of providing an efficient, reliable method for distributing and updating PC applications while exercising an effective level of system management for a group of users that constantly changes and possesses varying degrees of computer proficiency. PC Dugout employs a menu interface, takes advantage of the PC interface with which new Dugout users are already familiar, and transparently manages tasks for multiuser applications. GRA

N91-29759# Naval Research Lab., Washington, DC.
MODIFICATION OF PROGRAMS CHIEF AND CID TO COMPUTE SOUND RADIATION FROM AN ARBITRARY BODY WITH MIXED BOUNDARY CONDITIONS Final Report
W. Thompson, Jr., B. Dubus, and C. M. Siders 1 Jun. 1991 67 p
(AD-A237502; NRL-MR-6813) Avail: NTIS HC/MF A04 CSCL 20/1

The computer program CHIEF developed over the last two decades by Naval Ocean Systems Center, San Diego, was recently modified to allow the computation of sound radiation from arbitrarily shaped body where the normal velocity is prescribed on only part of its surface while one or two locally reacting complex impedances are assumed to cover the remainder of the surface. These impedances can range in value from zero to essentially infinity with any complex value in between. Results of some computations of far field directivity pattern and radiation loading on simple shaped radiators with the mixed boundary conditions were compared with results available in the literature with generally good agreement. Author (GRA)

N91-29760# Tulane Univ., New Orleans, LA.
THE 6TH WORKSHOP ON THE MATHEMATICAL FOUNDATIONS OF PROGRAMMING SEMANTICS Final Project Report
Michael W. Mislove 30 Jun. 1991 5 p Workshop held in Kingston, Ontario, 16-19 May 1990
(Contract N00014-90-J-1809)
(AD-A237754) Avail: NTIS HC/MF A01 CSCL 12/5

There were seven invited lectures and 25 contributed talks at the meeting. The invited talks were on three broad topics: polymorphism; applications of category theory to programming semantics; and concurrency. The specific topics included polymorphism and type theory; the use of functor categories to model ALGOL like languages; linear logic; the semantics of dataflow networks; semantic models of CSP; and the use of probability theory to model nondeterminism. GRA

N91-29761# Rensselaer Polytechnic Inst., Troy, NY. Dept. of Mathematical Sciences.
IMPLEMENTATION OF AN EXACT PENALTY FUNCTION FORMULATION TO SOLVE CONVEX NONLINEAR PROGRAMMING PROBLEMS M.S. Thesis Final Report
Christopher W. Fowler 8 Apr. 1991 37 p
(AD-A237905) Avail: NTIS HC/MF A03 CSCL 12/4

A convex nonlinear programming problem (NLP) can be reformulated using an exact penalty function. One such function is the L1 exact penalty function examined by Zangwill. The result of this reformulation is an unconstrained optimization problem. Unfortunately, this nonlinear, convex function is not a continuously differentiable function. Most computer methods/algorithms are based on the condition that the functions involved are differentiable. One exception is the Ellipsoid Algorithm, EA3, by Ecker and Kupferschmid. This algorithm, while demonstrating only linear convergence, has been shown to be robust in solving problems with nondifferentiable functions. The problem reduces to the following question. Is it better to solve the original, constrainted problem, or the reformulated unconstrained problem? Here, better is defined as faster and more accurate. After demonstrating that the exact penalty formulation will always solve the convex NLP, comparisons are made, using the ellipsoid algorithm, of accuracy of solution and solution time for several example problems. GRA

N91-29762# Naval Weapons Center, China Lake, CA.
ANALOG DESIGN VERIFICATION WITH PSPICE AND MICRO-CAP 3 Summary Report, Jan. - Mar. 1990
Melody Witham Aug. 1990 59 p
(AD-A237922; NWC-TP-7075) Avail: NTIS HC/MF A04 CSCL 09/1

Computer simulation has become very important in the design world. Few engineers design a circuit and send it right to the shop to be built. Instead, some level of simulation is used. Because fewer prototype boards need to be built, simulation saves a designer many hours of debugging time in the lab and quite a bit of money. Digital simulators are considered to be very accurate and indispensable tools. However, analog and mixed analog analog and digital simulators have not been perfected. With a digital chip, everything is black and white (or one and zero). Only the timing raises some questions. Within an analog circuit, the model is one of the most important items. Without good device model, the simulation is worthless. Two bipolar models are most popular: Gummel-Poon and Ebers-Moll. In this document the operation of PSpice is explained. The capabilities of PSpice and MICRO-CAP III are discussed. Two example circuits were designed, built, and tested in the lab and on the computer using PSpice and MICRO-CAP III. Calculations done by hand are compared to those obtained in the lab and on the computer. GRA

N91-29763# Naval Postgraduate School, Monterey, CA.
THE USE OF SEARCHING ALGORITHMS FOR THE MINIMIZATION OF MULTI-VALUED LOGIC FUNCTIONS M.S. Thesis
Alan W. Watts Jun. 1990 45 p
(AD-A238018) Avail: NTIS HC/MF A03 CSCL 12/5

The goal of this thesis was to develop a searching algorithm for simplifying Multi-Valued Logic (MVL) functions. The algorithm was implemented as a program written in C for the UNIX operating system. The algorithm accepts an MVL function in the format required by HAMLET, an MVL computer aided design tool, and produces a minimal or near-minimal realization. The output also conforms to that required by HAMLET to produce a layout of a programmable logic array (PLA) integrated circuit that realized the given function. The advantage of the algorithm is that it allows backtracking to investigate alternate solutions, producing a greater expectation of minimal results. It stops upon finding a solution, thus producing results much faster than an exhaustive search of all possible solutions. GRA

N91-29764# George Mason Univ., Fairfax, VA.
HYPERDIMENSIONAL DATA ANALYSIS AND STRUCTURAL INFERENCE Final Report, 1 Jul. 1987 - 31 Jan. 1991
Edward J. Wegman 25 May 1991 11 p
(Contract DAAL03-87-K-0087)
(AD-A238097; ARO-24105.19-MA) Avail: NTIS HC/MF A03 CSCL 12/6

This project focused on exploratory and structural inference for high dimensional data. Exploratory techniques focused mainly on the parallel coordinate technique which was exploited on

graphical computing platforms. A MS-DOS package was developed using this and other dynamical graphics techniques. Several refinements of the parallel coordinate technique were made including scintillation, parallel coordinate density plots and grand tours in d-dimensions. The structural inference work is nonparametric in character and focuses on high dimensional density estimation and ridge estimation. These ideas are currently still under development and promising techniques involved random tessellations, the trajectory method for finding ridges and the gradient density plot. GRA

N91-29765# Stanford Univ., CA. Dept. of Operations Research.
SIMULATION METHODOLOGY Final Report, 1 Apr. 1988 - 31 Mar. 1991
Peter W. Glynn and Donald L. Iglehart May 1991 10 p
(Contract DAAL03-88-K-0063)
(AD-A238113; ARO-25839.36-MA) Avail: NTIS HC/MF A02
CSCL 12/5

The main thrust of this research has been in developing new statistical methods for analyzing the output from computer simulations. The technical work can be divided into three areas: simulation output analysis, variance reduction, stochastic optimization, and generalized semiMarkov processes. Below we mention some of the most important results in each area. GRA

N91-29766# Naval Postgraduate School, Monterey, CA.
A TYPE CALCULUS FOR MATHEMATICAL PROGRAMMING MODELING LANGUAGES Ph.D. Thesis
Robert D. Clemence, Jr. Sep. 1990 141 p
(AD-A238160) Avail: NTIS HC/MF A07 CSCL 12/5

The issue of model validation is critical in the formulation and interpretation of mathematical programming models, yet this problem is largely ignored by contemporary modeling languages and the systems they support. This research advanced modeling languages for mathematical programming by providing a formalism and defining a language for specifying a dimensional complement, called typing, to the algebraic representation of models. Typing is a formal specification used to determine automatically whether the algebraic model is well-formed in the sense that its objective junction and constraints are composed of homogeneous components and that operations junction and constraints are composed of homogeneous components and that operations performed using indices are meaningful. A provision is made for the definition of dimensional axioms that can be applied automatically to resolve dimensional differences. The addiction of formal typing to mathematical programming models also yields a powerful abstraction mechanism for integrated modeling. GRA

N91-29767# Naval Postgraduate School, Monterey, CA.
VALIDATION OF THE SCHWARTZ AND HON ALGORITHM AT LOW GRAZING ANGLES M.S. Thesis
Gregory M. Lawler Sep. 1990 115 p
(AD-A238162; NPS-61-90-006) Avail: NTIS HC/MF A06
CSCL 08/3

An experimental validation of the Schwartz-Hon computer code for emissivity of the rough sea surface in the grazing angle region was carried out using an AGEMA 780 thermovision radiometric sensor. The experimental measurements were made in Monterey Bay using a meteorological suite mounted on the Research Vessel Point Sur, with coordinated radiosonde launches. Predicted sea surface radiance was computer from reflected sky radiance and thermal sea emission, using the Schwartz-Hon algorithm for sea emissivity and equivalent specular incidence angle. AGEMA sea radiance measurements were compared with the model predictions as a function of observation angle and were found to agree within 8 pct. for elevation angles from zero to 5 degrees. PC-TRAN sky radiance computations for the grazing angle region agreed with AGEMA measurements within approximately 12 pct. GRA

N91-29768# Qualcomm, Inc., San Diego, CA.
RESEARCH IN MATHEMATICS AND COMPUTER SCIENCE: CALCULATION OF THE PROBABILITY OF UNDETECTED ERROR FOR CERTAIN ERROR DETECTION CODES, PHASE 2 Final Technical Report, 1 Apr. 1990 - 31 May 1991
Andrew J. Viterbi, Jack K. Wolf, Lyle J. Fredrickson, Jeff A. Levin, and Robert D. Blakeney 31 May 1991 32 p
(Contract F49620-90-C-0017)
(AD-A238234; AFOSR-91-0596TR) Avail: NTIS HC/MF A03
CSCL 12/5

Cyclic Redundancy Check (CRC) codes have become the standard means for detecting error in messages that have been transmitted over a noisy communications channel. Unfortunately, even the very best CRC codes cannot detect all transmission errors. A hardware device is described which is capable of evaluating the random error performance of an important class of CRC codes that are generated by polynomials of the form $g(x) = (x+1)\,p(x)$, where $p(x)$ is a primitive polynomial of degree (R-1). A new burst error model is introduced and an equivalence is established between the burst and random error performance of cyclic codes. From this, the random error test results obtained from the hardware device is extended to include burst errors. Also included is an intuitive look at the factors which lead to good code performance, and an overview of a supplemental hardware device to measure the performance of cyclic codes that are generated by arbitrary polynomials. GRA

N91-29769*# Illinois Univ., Urbana. Center for Reliable and High-Performance Computing.
FAULT-TOLERANT COMPUTING: AN OVERVIEW
R. K. Iyer, J. H. Patel, W. K. Fuchs, P. Banerjee, and R. Horst Jun. 1991 59 p
(Contract NAG1-613; N00014-90-J-1270)
(NASA-CR-188793; NAS 1.26:188793; AD-A238266;
UILU-ENG-91-2232; CRHC-91-22) Avail: NTIS HC/MF A04
CSCL 09/2

The purpose of this report is to outline the major concepts and developments in the area of fault tolerant computing. Both hardware and software fault tolerance issues are addressed. The topics covered include module function and system-level fault detection methods, redundancy and reconfiguration strategies, valid fault models, and coding and checking in computer systems. Software fault tolerance methods such as recovery blocks, design diversity, and checkpointing and recovery are also discussed. Major issues in modeling and evaluation of fault-tolerant systems are outlined. The design of two successful commercial systems is discussed. GRA

N91-29770# Air Force Inst. of Tech., Wright-Patterson AFB, OH. School of Engineering.
A COMMON INTERFACE REAL-TIME MULTIPROCESSOR OPERATING SYSTEM FOR EMBEDDED SYSTEMS M.S. Thesis
Michael S. Rottman 4 Mar. 1991 227 p
(AD-A238445; AFIT/GCE/ENG/91M-04) Avail: NTIS HC/MF A11 CSCL 12/5

Large real time applications such as aerospace avionics systems, battle management, and factory automation place many demands and constraints on the computing system not found in other applications. Software development is hindered by software dependence on the computer architecture and the lack of portability between systems. This thesis specifies and designs a real time multiprocessor operating system (RTMOS) that implements a consistent programming model, enabling the development of real time parallel software independent of the target architecture. The RTMOS defines the core functionality required to demonstrate the programming model. The RTMOS functional requirements are specified using Structured Analysis and Design Technique (SADT). A hybrid of the Design Approach for Real-Time Software (DARTS) is used to perform the preliminary and detailed designs. The preliminary design is architecture-independent; the detailed design phase maps the design to a specific parallel system, the Intel iPSC/2 hypercube. The modular RTMOS design partitions operating

system operations and data structures from hardware-dependent functions for portability. GRA

N91-29771# Air Force Inst. of Tech., Wright-Patterson AFB, OH.
TRANSFER OF 4GL APPLICATION FROM INGRES TO ORACLE M.S. Thesis
Adnan Altunisik Mar. 1991 85 p
(AD-A238448; AFIT/GCE/ENG/91M-01) Avail: NTIS HC/MF A05 CSCL 12/5

This paper documents the transfer of 4GL applications from INGRES to ORACLE. As a result of a fast and conceptual change in computer languages, 4GLs were developed and evolved. These are programming support tools whose goal is, basically, to make the programs more efficient by reducing the number of instructions. Both ORACLE and INGRES database systems use 4GLs to develop applications. Their 4GL environments and their facilities for application development are investigated and explained in depth in this effort. The TWX application, which was originally implemented in INGRES by using its 4GL, is designed and reimplemented in ORACLE. This is accomplished in ORACLE SQL *Forms. Totally eight forms are built to accommodate the new application. The data, itself, was easily transferred to ORACLE apriori. The TWX applications now runs on a Sun386i stand-alone computer interactively. GRA

N91-29772# State Univ. of New York, Buffalo. Dept. of Biophysical Sciences.
ALIGNMENT OF TOMOGRAPHIC PROJECTIONS USING AN INCOMPLETE SET OF FIDUCIAL MARKERS
Zhongqi Jing and Frederick Sachs 1991 8 p Submitted for publication
(Contract DAAL03-89-K-0064)
(AD-A238536; ARO-26099.4-LS) Avail: NTIS HC/MF A02 CSCL 12/3

Reconstruction of three-dimensional images using tomography requires that the projections be aligned along a common rotational axis. We present here a solution to the problem of alignment for single-axis tomography using fiducial markers. The algorithm is based on iterative linearization of the projection equations and is least-squares optimized by a linear least-squares solution instead of a gradient search. The algorithm does not require markers to be available in every projection, and initial estimates are unnecessary. Program execution is robust, fast, and can quickly align large data sets containing 256 or more projections. The three-dimensional reconstruction of objects from projections had been widely used for medical imaging and more recently for electron microscopy imaging. Because the HVEM has a depth of focus larger than the thickness of many specimens, it can create images that approximate the projections of the object. GRA

N91-29773# Stanford Univ., CA. Systems Optimization Lab.
BARRIER METHODS FOR LARGE-SCALE QUADRATIC PROGRAMMING
Dulce B. Ponceleon Jun. 1991 129 p
(Contract N00014-90-J-1242)
(AD-A238554; SU-SOL-91-2) Avail: NTIS HC/MF A07 CSCL 12/4

We present several new algorithms for solving the general large-scale quadratic programming (QP) problem. A feature of QP problems is the presence of linear inequality constraints, which introduce a combinatorial aspect to the problem. Currently the most common approach to solving QP problems is to apply active-set methods, in which only some of the inequalities are used to produce a search direction at each stage. The combinatorial element is therefore inherent. As problems become larger, there is a potential for an excessive number of iterations and consequent inefficiency. In contrast, we use the new familiar barrier function approach, which circumvents the combinatorial aspect by introducing a barrier transformation involving all of the inequalities. The barrier term enforces satisfaction of the inequalities by modifying the objective function. The transformed problem is solved by a modified Newton method applied to the nonlinear equations defining feasibility and optimality. The main computation at each iteration of the new algorithms is the solution of an indefinite system of linear equations. Barrier methods are known to lead to ill-conditioned systems. However, we show by a special sensitivity analysis that the particular manner in which we have formulated the barrier transformation leads to ill-conditioning that is benign. GRA

N91-29774# State Univ. of New York, Albany. Dept. of Computer Science.
A WORKSHOP ON THE INTEGRATION OF NUMERICAL AND SYMBOLIC COMPUTING METHODS Final Report, May 1990 - Apr. 1991
Deepak Kapur Apr. 1991 10 p Workshop held in Saratoga Springs, NY, 9-11 Jul. 1990
(Grant AF-AFOSR-0052-90)
(AD-A238601; AFOSR-91-0556TR) Avail: NTIS HC/MF A02 CSCL 12/4

A workshop on the integration of symbolic and numerical computing methods was held on July 9 to 11, 1990 in Saratoga Springs, New York. The workshop was supported by a grant from the Air Force Office of Scientific Research and the National Science Foundation along with partial funding from G.E. Corporate Research and Development, and the State University of New York at Albany. The workshop was hosted by the Institute of Programming and Logics, the State University of New York at Albany. Twenty five research papers on symbolic methods, numerical methods, interface between symbolic and numerical methods, applications of symbolics methods in machine vision, robotics, computer aided design, computational geometry, and related topics were presented. Over forty researchers and students participated in the workshop. GRA

N91-29775# Johns Hopkins Univ., Baltimore, MD. Dept. of Electrical and Computer Engineering.
STOCHASTIC SIMULATION TECHNIQUES FOR PARTITION FUNCTION APPROXIMATION OF GIBBS RANDOM FIELD IMAGES Technical Report, 1 Jan. 1990 - 30 Jun. 1991
Gerasimos Potamianos and John Goutsias Jun. 1991 70 p
(Contract N00014-90-J-1345)
(AD-A238611) Avail: NTIS HC/MF A04 CSCL 12/3

A Monte Carlo simulation technique for the calculation of the partition function of a general Gibbs random field is presented. We show that the partition function of a general Gibbs random field is equivalent to an expectation. This observation allows us to develop an importance sampling approach for estimating this expectation by using Monte-Carlo simulations. Two different methods are proposed for this task. We show that the resulting estimators are unbiased and consistent. Computations are performed iteratively, by using a simple, Metropolis-like, Monte-Carlo algorithm with remarkable success, as it is demonstrated by our simulations. Our work concentrates on binary, second-order Gibbs random fields defined on a rectangular lattice. GRA

N91-29776# Technische Hogeschool Twente, Enschede (Netherlands). Dept. of Applied Mathematics.
NEGATION IN KNOWLEDGE GRAPHS
H. vandenBerg Oct. 1990 32 p
(PB91-185421; MEMO-893; ISSN-0169-2690) Avail: NTIS HC/MF A03 CSCL 09B

One encounters negation in many ways in natural language. Two ways in which negation can be brought into the system of knowledge graphs are investigated. One way is to define a frame negation, which behaves as a kind of context. The other way is to define a new relation DIS, expressing the two concepts are distinct. Both methods have their advantages and disadvantages. A representation of negation is given that combines the advantages of both methods. GRA

62 COMPUTER SYSTEMS

Includes computer networks and special application computer systems.

N91-29777*# ORA Corp., Ithaca, NY.
VERIFICATION OF THE FTCAYUGA FAULT-TOLERANT MICROPROCESSOR SYSTEM. VOLUME 2: FORMAL SPECIFICATION AND CORRECTNESS THEOREMS Final Report
Mark Bickford and Mandayam Srivas Jul. 1991 74 p
(Contract NAS1-18972)
(NASA-CR-187574; NAS 1.26:187574) Avail: NTIS HC/MF A04 CSCL 09B

Presented here is a formal specification and verification of a property of a quadruplicately redundant fault tolerant microprocessor system design. A complete listing of the formal specification of the system and the correctness theorems that are proved are given. The system performs the task of obtaining interactive consistency among the processors using a special instruction on the processors. The design is based on an algorithm proposed by Pease, Shostak, and Lamport. The property verified insures that an execution of the special instruction by the processors correctly accomplishes interactive consistency, providing certain preconditions hold, using a computer aided design verification tool, Spectool, and the theorem prover, Clio. A major contribution of the work is the demonstration of a significant fault tolerant hardware design that is mechanically verified by a theorem prover. Author

N91-29778*# ORA Corp., Ithaca, NY.
VERIFICATION OF THE FTCAYUGA FAULT-TOLERANT MICROPROCESSOR SYSTEM. VOLUME 1: A CASE STUDY IN THEOREM PROVER-BASED VERIFICATION Final Report
Mandayam Srivas and Mark Bickford Washington Jul. 1991 61 p
(Contract NAS1-18972)
(NASA-CR-4381; NAS 1.26:4381) Avail: NTIS HC/MF A04 CSCL 09B

The design and formal verification of a hardware system for a task that is an important component of a fault tolerant computer architecture for flight control systems is presented. The hardware system implements an algorithm for obtaining interactive consistancy (byzantine agreement) among four microprocessors as a special instruction on the processors. The property verified insures that an execution of the special instruction by the processors correctly accomplishes interactive consistency, provided certain preconditions hold. An assumption is made that the processors execute synchronously. For verification, the authors used a computer aided design hardware design verification tool, Spectool, and the theorem prover, Clio. A major contribution of the work is the demonstration of a significant fault tolerant hardware design that is mechanically verified by a theorem prover. Author

N91-29779# Massachusetts Inst. of Tech., Cambridge. Lab. for Computer Science.
A HIGH-PERFORMANCE RETARGETABLE SIMULATOR FOR PARALLEL ARCHITECTURES
Chrysanthos N. Dellarocas Jun. 1991 100 p
(Contract N00014-89-J-1988)
(AD-A237354; MIT/LCS/TR-505) Avail: NTIS HC/MF A05 CSCL 12/6

In this thesis, we describe Proteus, a high-performance simulation-based system for the evaluation of parallel algorithms and system software. Proteus is built around a retargetable parallel architecture simulator and a flexible data collection and display component. The simulator uses a combination of simulation and direct execution to achieve high performance, while retaining simulation accuracy. Proteus can be configured to simulate a wide range of shared memory and message passing MIMD architectures and the level of simulation detail can be chosen by the user. Detailed memory, cache and network simulation is supported. Parallel programs can be written using a programming model based on C and a set of runtime system calls for thread and memory management. The system allows nonintrusive monitoring of arbitrary information about an execution, and provides flexible graphical utilities for displaying recorded data. To validate the accuracy of the system, a number of published experiments were reproduced on Proteus. In all cases the results obtained by simulation are very close to those published, a fact that provides support for the reliability of the system. Performance measurements demonstrate that the simulator is one to two orders of magnitude faster than other similar multiprocessor simulators. GRA

N91-29780# Massachusetts Inst. of Tech., Cambridge. Lab. for Computer Science.
COUNTING NETWORKS
James Aspnes, Maurice Herlihy, and Nir Shavit Jun. 1991 35 p
(Contract N00014-91-J-1046)
(AD-A237475; MIT/LCS/TM-451) Avail: NTIS HC/MF A03 CSCL 12/7

Many fundamental multiprocessor coordination problems can be expressed as counting problems: processes must cooperate to assign successive values from a given range, such as addresses in memory or destinations on an interconnection network. Conventional solutions to these problems perform poorly because of synchronization bottlenecks and high memory contention. Motivated by observations on the behavior of sorting networks, we offer a completely new approach to solving such problems. We introduce a new class of networks called counting networks, i.e., networks that can be used to count. We give two counting network constructions of depth log square n, using n log square n gates, avoiding the sequential bottlenecks inherent to former solutions, and substantially lowering the memory contention. Finally, to show that counting networks are not merely mathematical creatures, we provide experimental evidence that they outperform conventional synchronization techniques under a variety of circumstances. GRA

N91-29781# Massachusetts Inst. of Tech., Cambridge. Lab. for Computer Science.
LAZY TASK CREATION: A TECHNIQUE FOR INCREASING THE GRANULARITY OF PARALLEL PROGRAMS
Eric Mohr, David Kranz, and Robert H. Halstead, Jr. Jun. 1991 25 p
(Contract N00014-87-K-0825)
(AD-A237477; MIT/LCS/TM-449) Avail: NTIS HC/MF A03 CSCL 12/5

Many parallel algorithms are naturally expressed at a fine level of granularity, often finer than a MIMD parallel system can exploit efficiently. Most builders of parallel systems have looked to either the programmer or a parallelizing compiler to increase the granularity of such algorithms. In this paper, we explore a third approach to the granularity problem by analyzing two strategies for combining parallel tasks dynamically at run-time. We reject the simpler load-based inlining method, where tasks are combined based on dynamic load level, in favor of the safer and more robust lazy task creation method, where tasks are created only retroactively as processing resources become available. These strategies grew out of work on Mul-T 17, an efficient parallel implementation of Scheme, but could be used with other languages as well. We describe our Mul-T implementations of lazy task creation for two contrasting machines, and present performance statistics which show the method's effectiveness. Lazy task creation allows efficient execution of naturally expressed algorithms of a substantially finer grain than possible with previous parallel Lisp systems. GRA

N91-29782# Naval Underwater Systems Center, Newport, RI.
OPERATIONAL CONCEPT DOCUMENT FOR THE NEXT GENERATION COMPUTER RESOURCES (NGCR) OPERATING SYSTEMS INTERFACE STANDARD BASELINE
1 Apr. 1991 159 p
(AD-A237501; NUSC-TD-6998) Avail: NTIS HC/MF A08 CSCL 12/5

The purpose of this Operational Concept Document (OCD) is

to present the operational concept of the Operating Systems Interface (OSIF) Standart, which was derived through a consensus amoung Navy agencies, industry, and academia. This OCD will identify the requirements for services, interfaces, and protocols to be supported by the OSIF. The purpose of the OSIF is to establish a set of interfaces that controls the operation of all computing system hardware and software elements of a platform. These elements are coordinated in a uniform manner that is consistent with the mission of the platform. The OSIF is an interface specification; it does not specify an operating system implementation. The objective of the baseline specification is to select a commercially available OSIF or family of interface baseline requirements and modify them as little as possible. GRA

N91-29783# Stanford Univ., CA.
ASYNCHRONOUS DESIGN FOR PARALLEL PROCESSING ARCHITECTURES Semiannual Report, Jan. - Jul. 1991
Teresa H. Meng Jul. 1991 3 p
(Contract N00014-89-J-3036)
(AD-A237696) Avail: NTIS HC/MF A01 CSCL 12/6

The objective of this research is to provide an interconnect synthesis methodology which facilitates a modular design approach without compromising the global performance. The main tasks of this effort will be the development of the theory for optimal interconnect circuit synthesis from a high level specification, with emphasis on testability and fault tolerance asynchronous interface among concurrently computing hardware, and the application of this design methodology to physical implementations of parallel processing systems. GRA

N91-29784# Massachusetts Inst. of Tech., Cambridge. Lab. for Computer Science.
THE MIT ALEWIFE MACHINE: A LARGE-SCALE DISTRIBUTED-MEMORY MULTIPROCESSOR
Anant Agarwal, David Chaiken, Kirk Johnson, David Kranz, and John Kubiatowicz Jun. 1991 26 p
(Contract N00014-87-K-0825)
(AD-A237705; MIT/LCS/TR-454) Avail: NTIS HC/MF A03 CSCL 12/6

The Alewife multiprocessor project focuses on the architecture and design of a large-scale parallel machine. The machine uses a low dimension direct interconnection network to provide scalable communication band-width, while allowing the exploitation of locality. Despite its distributed memory architecture, Alewife allows efficient shared memory programming through a multilayered approach to locality management. A new scalable cache coherence scheme called LimitLESS directories allows the use of caches for reducing communication latency and network bandwidth requirements. Alewife also employs run-time and compile-time methods for partitioning and placement of data and processes to enhance communication locality. While the above methods attempt to minimize communication latency, remote communications with distant processors cannot be completely avoided. Alewife's processor, Sparcle, is designed to tolerate these latencies by rapidly switching between threads of computation. This paper describes the Alewife architecture and concentrates on the novel hardware features of the machine including LimitLESS directories and the rapid context switching processor. GRA

N91-29785# Princeton Univ., NJ. Dept. of Electrical Engineering and Computer Science.
ANALOG COMPUTATION IN NEURAL SYSTEMS: ARCHITECTURES AND COMPLEXITY Final Technical Report, 1 Aug. 1988 - 31 Jul. 1990
Bradley W. Dickinson 17 May 1991 12 p
(Grant AF-AFOSR-0227-88; AF Proj. 2304)
(AD-A237856; AFOSR-91-0554TR) Avail: NTIS HC/MF A03 CSCL 12/4

First, we studied the representation problem for the class of single-hidden-layer feedforward networks, which is fundamental for understanding limitations of learning algorithms, and which also contributed to understanding the behavior of learning algorithms in applications involving low-complexity networks. The second kind of problem studied concerns dynamics behavior in neural networks containing feedback (trellis-structured networks in one particular application). Our work focused on studying stability issues and exploring the implications of computational complexity theory. Third, the PAC learning paradigm (probably almost correct) was analyzed with the goal of characterizing the effects of statistically dependent sequences of training examples on learning performance. The goal of all these efforts was to discover and explore insights about fundamental limitations on the computational capabilities of analog neural systems and, where possible, of more general classes of physical systems as well. GRA

N91-29786# Stanford Univ., CA. Knowledge Systems Lab.
EXPERT SYSTEMS ON MULTIPROCESSOR ARCHITECTURES. VOLUME 1: SUMMARY Final Report, Mar. 1985 - Oct. 1990
Edward A. Feigenbaum, Robert Engelmore, H. P. Nii, and James P. Rice Jun. 1991 55 p
(Contract F30602-85-C-0012)
(AD-A238046; RL-TR-91-76-Vol-1) Avail: NTIS HC/MF A04 CSCL 12/5

This final report documents the results of a five-year investigation of methods for achieving higher performance for knowledge based systems through the design of innovative software and hardware systems architectures. Volume 1 summarizes the work performed and lessons learned, and serves as an annotated index to the set of over 50 project technical reports. Volumes 2 through 4 contain the project technical reports. GRA

N91-29787# Stanford Univ., CA. Knowledge Systems Lab.
EXPERT SYSTEMS ON MULTIPROCESSOR ARCHITECTURES. VOLUME 2: TECHNICAL REPORTS Final Report, Mar. 1985 - Oct. 1990
Edward A. Feigenbaum, Robert Engelmore, H. P. Nii, and James P. Rice Jun. 1991 474 p
(Contract F30602-85-C-0012)
(AD-A238047; SU-RL-TR-91-76-Vol-2) Avail: NTIS HC/MF A20 CSCL 12/5

This final report documents the results of a five-year investigation of methods for achieving higher performance for knowledge-based systems through the design of innovative software and hardware systems architectures. Volume 1 summarizes the work performed and lessons learned, and serves as an annotated index to the set of over 50 project technical reports. Volumes 2 through 4 contain the project technical reports. GRA

N91-29788# Stanford Univ., CA. Knowledge Systems Lab.
EXPERT SYSTEMS ON MULTIPROCESSOR ARCHITECTURES, VOLUME 3 Final Report, Mar. 1985 - Oct. 1990
Edward A. Feigenbaum, Robert Engelmore, H. P. Nii, and James P. Rice Jun. 1991 465 p
(Contract F30602-85-C-0012)
(AD-A238048; SU-RL-TR-91-76-Vol-3) Avail: NTIS HC/MF A20 CSCL 12/5

This final report documents the results of a five-year investigation of methods for achieving higher performance for knowledge based systems through the design of innovative software and hardware systems architectures. Volume 1 summarizes the work performed and lessons learned, and serves as an annotated index to the set of over 50 project technical reports. Volumes 2 through 4 contain the project technical reports. GRA

N91-29789# Stanford Univ., CA. Knowledge Systems Lab.
EXPERT SYSTEMS ON MULTIPROCESSOR ARCHITECTURES, VOLUME 4 Final Report, Mar. 1985 - Oct. 1990
Edward A. Feigenbaum, Robert Engelmore, H. P. Nii, and James P. Rice Jun. 1991 554 p
(Contract F30602-85-C-0012)
(AD-A238049; SU-RL-TR-91-76-Vol-4) Avail: NTIS HC/MF A24 CSCL 12/5

This final report documents the results of a five-year

investigation of methods for achieving higher performance for knowledge based systems through the design of innovative software and hardware systems architectures. Volume 1 summarizes the work performed and lessons learned, and serves as an annotated index to the set of over 50 project technical reports. Volumes 2 through 4 contain the project technical reports. GRA

N91-29790# Illinois Univ., Urbana. Center for Reliable and High-Performance Computing.
PERFORMANCE IMPLICATIONS OF SYNCHRONIZATION SUPPORT FOR PARALLEL FORTRAN PROGRAMS
Sadun Anik and Wen-mei W. Hwu 17 Jun. 1991 47 p
(AD-A238493; UILU-ENG-91-1231; CRHC-91-21) Avail: NTIS HC/MF A03 CSCL 12/7

This paper studies the performance implications of architectural synchronization support for automatically parallelized numerical programs. As the basis for this work, we analyze the needs for synchronization in automatically parallelized numerical programs. The needs are due to task management, loop scheduling, barriers, and data dependency handling. We present synchronization algorithms for efficient execution of programs with nested parallel loops. Next, we identify how various hardware synchronization primitives can be used to satisfy these software synchronization needs. The synchronization primitives studied are test and set, fetch and add, exchange-byte and synchronization bus implementation of lock/unlock operations. Lastly, we ran experiments to quantify the impact of various architectural support on the performance of a bus-based shared memory multiprocessor running automatically parallelized numerical programs. We found that supporting an atomic fetch and add primitive in shared memory is as effective as supporting lock/unlock operations with a synchronization bus. Both achieve substantial performance improvement over the cases where atomic test and set and exchange-byte operations are supported in shared memory. GRA

N91-29791# Air Force Inst. of Tech., Wright-Patterson AFB, OH. School of Engineering.
OPTIMAL ITERATIVE TASK SCHEDULING FOR PARALLEL SIMULATIONS M.S. Thesis
JoAnn M. Sartor Mar. 1991 129 p
(AD-A238631; AFIT/GCS/ENG/91M-03) Avail: NTIS HC/MF A07 CSCL 12/4

The ultimate purpose of this research is to reduce the time needed for execution of parallel computer simulations. In particular, the impact of task assignment strategies is determined for parallel VHDL circuit simulations. The classical scheduling problem, which assigns n precedence-constrained tasks to m processors is NP-complete in all but the simplest cases. The problem of assigning simulation tasks is further complicated by the iterative nature of computer simulations: each task is required to execute multiple times as the simulation executes. This investigation develops a polynomial-time algorithm (the level strategy) which provides optimal assignment for iterative systems with specific constraints. A mathematical foundation for iterative task systems is proved. In particular, it is shown that restricted cases of iterative systems achieve minimal latency,(time between successive iterations of a given task), when the level strategy is used for task assignment. To verify the theoretical results, various task scheduling strategies are compared using VHDL logic-circuit simulations on the ipsc/2 hypercube computer. Tests are run with mappings based on the level strategy, the classical optimal assignment, a greedy technique for assignment, and an unbalanced assignment. The best results of these experiments, in terms of speedup, occur consistently in cases where the level strategy is used. GRA

N91-29792# Technische Hogeschool Twente, Enschede (Netherlands). Dept. of Computer Science.
THE CYK-APPROACH TO SERIAL AND PARALLEL PARSING
Anton Nijholt Mar. 1990 23 p
(PB91-185447; Memo-INF-90-13; ISSN-0923-1714) Avail: NTIS HC/MF A03 CSCL 09B

Traditional parsing methods for general context-free grammars were re-investigated in order to see whether they can be adapted to a parallel processing view. Sequential and parallel versions of the Cocke-Younger-Kasami (CYK) parsing algorithm are discussed. The algorithms that are considered turn out to be suitable for implementations ranging from environments with a small number of asynchronous processors to environments consisting of a large array of highly synchronized processors. Author

N91-29793# Oak Ridge National Lab., TN.
VISUALIZING PERFORMANCE OF PARALLEL PROGRAMS
M. T. Heath (Illinois Univ., Urbana.) and J. A. Etheridge May 1991 61 p
(Contract DE-AC05-84OR-21400)
(DE91-014966; ORNL/TM-11813) Avail: NTIS HC/MF A04

In this paper we describe a graphical display system for visualizing the behavior and performance of parallel programs on message-passing multiprocessor architectures. The visual animation is based on execution trace information monitored during an actual run of a parallel program on a message-passing parallel computer. The resulting trace data are replayed pictorially to provide a dynamic depiction of the behavior of the parallel program, as well as graphical summaries of its overall performance. Several distinct visual perspectives are provided from which to view the same performance data, in an attempt to gain insights that might be missed by an single view. We describe this visualization tool, outline the motivation and philosophy behind its design, and illustrate its usefulness in analyzing parallel programs. DOE

N91-29794# General Electric Co., Schenectady, NY.
PORTABLE PARALLEL PROGRAMMING
S. L. Fiedler Apr. 1991 69 p
(Contract DE-AC12-76SN-00052)
(DE91-015648; KAPL-4728) Avail: NTIS HC/MF A04

The Portable Parallel Programming Library (P(sup 3)Lib) provides a set of FORTRAN-callable routines that standardize the development of parallel programs. P(sup 3)Lib includes routines for message passing between independent sequential processes, and a standard means for instantiating the concurrent processes of the parallel application. The need for a standard in the area of parallel programming is widely recognized, as is the lack of a standard being offered by the parallel computer vendors. While parallel computers are designed for high performance, for portability there is a need to put limited software between the user's application program and the hardware. To assist application programmers so that they do not need to spend excessive time in converting thousands of lines of vendor specific code to new machines, the Portable Parallel Programming Library has been developed. The Portable Parallel Programming Library has been implemented on three different MIMD computers, the Meiko Computing Surface, the Intel iPSC/860 and the Cray YMP, and it is expected to be readily extensible to any MIMD computer with either shared or distributed memory. DOE

N91-29795# New York Univ., New York. Inst. of Mathematical Sciences.
ANALYTICAL AND NUMERICAL METHODS; ADVANCED COMPUTER CONCEPTS
P. D. Lax Mar. 1991 8 p
(Contract DE-AC02-76ER-03077)
(DE91-014526; DOE/ER-03077/284) Avail: NTIS HC/MF A02

This past year, two projects have been completed and a new one is under way. First, in joint work with R. Kohn, we developed a numerical algorithm to study the blowup of solutions to equations with certain similarity transformations. In the second project, the adaptive mesh refinement code of Berger and Colella for shock hydrodynamic calculations has been parallelized and numerical studies using two different shared memory machines have been done. My current effort is towards the development of Cartesian mesh methods to solve partial differential equations with complicated geometries. Most of the coming year will be spent on this project, which is joint work with Prof. Randy Leveque at the University of Washington in Seattle. DOE

N91-29796# Oak Ridge National Lab., TN.
SUPERNODAL SYMBOLIC CHOLESKY FACTORIZATION ON A L OCAL-MEMORY MULTIPROCESSOR
E. Ng Jun. 1991 16 p
(Contract DE-AC05-84OR-21400)
(DE91-014967; ORNL/TM-11836) Avail: NTIS HC/MF A03

The symbolic factorization step is considered in computing the Cholesky factorization of a sparse symmetric positive definite matrix on distributed memory multiprocessor systems. By exploiting the supernodal structure in the Cholesky factor, the performance of a previous parallel symbolic factorization algorithm is improved. Empirical tests demonstrate that there can be drastic reduction in the execution time required by the new algorithm on an Intel iPSC/2 hypercube. DOE

N91-29797# Argonne National Lab., IL.
THE ADVANCED SOFTWARE DEVELOPMENT AND COMMERCIALIZATION PROJECT
T. Canfield, ed., M. Minkoff, ed., and E. Plaskacz, ed. Apr. 1991 78 p
(Contract W-31-109-eng-38)
(DE91-015756; ANL/TM-488) Avail: NTIS HC/MF A05

Progress is reported in the Advanced Software Development and Commercialization Project, a collaborative effort between the Center for Supercomputing Research and Development of the University of Illinois and the Computing and Telecommunications Divisions of Argonne National Laboratory. Techniques are applied to parallel computing to mature computational fluid dynamics (CFD) and structural dynamics (SC) computer codes developed at Argonne. The collaboration in this project brings this unique combination of expertise to bear, for the first time, on industrially important problems. By so doing, it will expose the strengths and weaknesses of existing techniques for parallelizing programs and will identify those problems that need to be solved in order to enable widespread production use of parallel computers. Secondly, the increased efficiency of the CFD and SD codes themselves will enable the simulation of larger, more accurate engineering models that involve fluid and structural dynamics. Such an enhance capability is fundamental to industrial efficiency and competitiveness, and could serve as an exemplary model for similar future activities. DOE

N91-29798# Lawrence Livermore National Lab., CA.
THE PARALLEL BFGS METHOD FOR UNCONSTRAINED MINIMIZATION
C. H. Still Jun. 1991 19 p Presented at the 6th Distributed Memory Computing Conference, Portland, OR, 28 Apr. -2 May 1991
(Contract W-7405-eng-48)
(DE91-015784; UCRL-JC-107453; CONF-9104158-5) Avail: NTIS HC/MF A03

In this paper, we present a parallel formulation of the BFGS method for unconstrained minimization obtained by decomposing the iteration and update equations with an orthonormal basis. To aid in evaluating the performance of this method, numerical results are presented from experiments run on an nCUBE/1 hypercube and a Symult S2010. Finally, we present the theoretical performance analysis of the algorithm on these machines solving the test problems to substantiate the numerical testing. DOE

63 CYBERNETICS

Includes feedback and control theory, artificial intelligence, robotics and expert systems.

For related information see also *54 Man/System Technology and Life Support.*

N91-29799# National Research Council of Canada, Ottawa (Ontario). Div. of Electrical Engineering.
USING THE HARMONY OPERATING SYSTEM: RELEASE 3.0
W. M. Gentleman, S. A. MacKay, D. A. Stewart, and M. Wein Feb. 1989 70 p Supersedes ERB-966; NRC-27469
(ERA-377; ERB-966; NRC-30081; NRC-27469; CTN-91-60016)
Copyright Avail: NTIS HC/MF A04

A brief description of the Harmony operating system, version 3.0 is provided. A portable operating system is intended that lays the groundwork for local optimization but does not include it. Harmony is a multitasking, multiprocessing operating system for real time control (such as is required in sensor-based robotics). It can also be used to implement smart peripherals to be used with itself or with some other operating system, and it provides a simple and inexpensive vehicle for experimenting with parallel computation. It is portable in that with moderate effort it can be realized on any computer of appropriate architecture. Existing realizations are based on the Motorola 680X0 family of processors, the Atari 520, or 1040 ST, and on the DEC VAX. One such realization is based on the Macintosh personal computer and is described here. An overview is presented of the operating system along with the rationale for the design, and the abstractions used in creating applications that can be targeted to either a single processor or a multiprocessor. Also discussed is the principal mechanisms used for task management, and for intertask communication. Appendices include examples of both uniprocessor and multiprocessor programs, and listings of user callable functions. Program development must be completed on a host computer, and test executions are done by downloading the program to a target computer containing the Harmony system. Performance is dependant upon kernel tuning, compiler selection, the microprocessor instruction set, and other aspects of the operating hardware. Processing times achieved in test cases are commensurate with the best task context switching times achieved by other systems on similar hardware. Significant improvements could be achieved by writing several key kernel routines in assembly language. CISTI

N91-29800# National Research Council of Canada, Ottawa (Ontario). Div. of Electrical Engineering.
THEORY AND COMPUTER SIMULATION OF THE INTERACTIONAL NEURAL NETWORK
E. Porada, M. Rioux, and P. Boulanger Apr. 1989 27 p
(NRC-30269; ERB-1021; CTN-91-60042) Copyright Avail: NTIS HC/MF A03

Robot vision requires that image processing not only produce coherent representations but that it result in a proper reaction to the input stimulus. Thus image processing should result in the conversion of the image to a stimuli. The algorithm presented here appears to have the capability of processing data from the vision system of a mobile robot so as to provide the key outputs to produce the proper reactions in a behavior controller. An algorithm is presented for a given sequence of associations (I sub 1,Y sub 1), (I sub 2,Y sub 2),...,(I sub K,Y sub K) where I and Y are pairs of binary vectors. Find a matrix W which solves the equations, I sub k times W = rho sub k times Y sub k, where k = 1, 2,...,K and rho sub k is positive. The condition for existence of W is stated and the solution is found in an explicit form. If W is implemented as connectivity pattern (matrix of connection strengths in a two-layer neural network) then the unidirectional associations I(k) to Y(k) are executed infallibly. The FORTRAN programs are included along with a description of a computer simulation of the neural network based on W. With the inclusion of a layer of hidden neurons, the algorithm producing W can be implemented in the form of a self-programming of the network. The three-layer mathematical and interactional model and the process of self-programming are presented. Author (CISTI)

N91-29801# Lawrence Livermore National Lab., CA.
WORKSHOP ON AUTOMATION AND ROBOTICS: PROCEEDINGS
Feb. 1991 243 p Workshop held in Livermore, CA, 6 Feb. 1991
(Contract W-7405-eng-48)
(DE91-015175; CONF-910274) Avail: NTIS HC/MF A11

This workshop provided a forum in which Lawrence Livermore National Laboratory scientists and engineers exchanged ideas and

information on the latest internal developments in the field of robotic and automation technologies. The material presented constitutes most of the presentations given during the workshop. Presentations were given on the following session topics: robotics and automation in hazardous environments; laboratory and machine tool automation; neural networks, machine vision, and sensors; applied real time control; future technologies and applications; intelligent man-machine interaction issues. Individual papers have been cataloged separately. DOE

N91-29802# JAYCOR, Vienna, VA.
USER'S GUIDE TO THE (NCARAI) ARTIFICIAL INTELLIGENCE TECHNICAL LIBRARY
Cathy J. Wiley 12 Jun. 1991 12 p
(AD-A237270; NRL-MR-6842) Avail: NTIS HC/MF A03 CSCL 05/2

The Navy Center for Applied Research in Artificial Intelligence (NCARAI) Technical Library is a collection dedicated to the field of artificial intelligence research. This guide outlines services available at the library, which include a circulating and reference book collection, technical reports, journals, microfiche, and microcomputer software. The guide discusses briefly online search and retrieval systems available and provides a listing of current periodical holdings. GRA

N91-29803# Army Construction Engineering Research Lab., Champaign, IL.
ENGINEERING APPLICATIONS OF NEURAL COMPUTING: A STATE-OF-THE-ART SURVEY Final Report
Xiping Wu and James D. Westervelt May 1991 138 p
(DA Proj. 4A1-61102-AT-23)
(AD-A237628; CERL-SR-N-91/22) Avail: NTIS HC/MF A07 CSCL 12/7

Neural computing, as a paradigm of knowledge representation and information processing, has attracted tremendous enthusiasm and research interest recently. With advancing sophistication, neural computing technology has been successfully tailored for a wide range of applications, including some engineering fields. With the development of hardware based neural networks and neural computing theory, neural networks potentially provide efficient tools for solving some difficult engineering problems related to U.S. Army Construction Engineering Research Laboratories (USACERL) research. This report reviews and describes different types of neural networks including feedforward, feedback, and recurrent networks, their learning algorithms and recent developments. The emphasis is on the most frequently used multilayer feedforward neural networks. Representative publications on neural network applications to engineering problems related and/or of interest to research at USACERL, especially civil engineering problems, are also covered, and each modeling methodology identified. An extensive reference list is provided with each subject. The appendices list major technical journals dedicated to the theory and application of neural computing, some publicly available neural network simulators, and selected books and proceedings published on neural networks and genetic algorithms. GRA

N91-29804# Pennsylvania Univ., Philadelphia. School of Medicine.
DESIGN AND HARDWARE IMPLEMENTATION OF NEURAL SYSTEMS Final Report, 1 Oct. 1987 - 30 Sep. 1988
Paul Mueller 26 Jun. 1991 5 p
(Contract N00014-87-K-0780)
(AD-A237703) Avail: NTIS HC/MF A01 CSCL 06/4

This project had two major aims. One was is the design and computer simulation of specific neural circuits modeled after the early vision system of higher vertebrates. The second aim was the design and construction of electronic analog neural system that could be used for implementing such a vision system and possibly other neural systems. Our initial approach to the hardware implementation was to build an entirely hardwired system using Very Large Scale Integration assemblies of electronic neurons and separate resistive synapse connection matrices fabricated by chemical vapor deposition (CVD) of amorphous silicon. During further simulation studies of the vision system, it became clear that at this early state of development a completely hardwired system would incorporate modifiable synapses and a programmable connection architecture. Rather than restrict the design of such a system by tailoring it to the specific architectures of the vision system, we decided to design a general purpose programmable neural analog computer that would be useful not only for vision but also for other task of real world computation and other problems suitable for neural computation. GRA

N91-29805# Georgia Univ., Athens.
HIGH BANDWIDTH DIAGNOSIS WITHIN THE FRAMEWORK OF A MICROCOMPUTER-BASED INTELLIGENT TUTORING SYSTEM Final Report, Jun. - Oct. 1990
Michael A. Orey Apr. 1991 23 p Sponsored by Army Research Inst. for the Behavioral and Social Sciences
(AD-A237959; ARI-RN-91-45) Avail: NTIS HC/MF A03 CSCL 12/9

This paper describes a project undertaken with the U.S. Army Research Institute for the Behavioral and Social Sciences at Fort Gordon: The Advanced Learning for Mobile (ALM) Subscriber Equipment (MSE). This project resulted in the development of a system that operates in a 640K MS-DOS environment. The system has three major components: a hypermedia environment, a microworld, and a problem solving environment. The focus of this paper is the intelligent tutoring system capabilities of the problem-solving environment. The problem solving environment of ALM, which is MSE troubleshooting, has three emphases. The first emphasis is high bandwidth diagnosis using a model tracing technique for modeling. The second is a conceptual framework for the organization of MSE within a problem solving supported interface. The third is the integration of frame-based and rule-based representations. GRA

N91-29806# Wright State Univ., Dayton, OH. Dept. of Electrical Engineering.
ROBUST DESIGN OF MULTIVARIABLE CONTROL: AN INTERVAL ARITHMETIC APPROACH Final Report, Aug. 1988 - Sep. 1990
Pradeep Misra Jun. 1991 76 p
(Contract F33615-88-C-3605)
(AD-A238006; WRDC-TR-90-3080) Avail: NTIS HC/MF A05 CSCL 12/3

An important aspect of analysis and design of control laws for a dynamic system is the robustness of the control laws to uncertainties in the model parameters. Interval arithmetic is used to model dynamic systems whose parameters are not known exactly, but are known to lie within an interval. Analysis techniques for interval systems are developed, and include the solution of ordinary differential equations with interval coefficients and interval initial conditions, and the solution of linear interval equations. Feedback stabilization of interval systems by state feedback using interval Routh Hurwitz arrays is developed. GRA

N91-29807# Naval Surface Warfare Center, Dahlgren, VA.
INVARIANT TARGET RECOGNITION USING SELF-ORGANIZING NETWORKS Final Report
Beth Farrar, Ali Farsaie, and J. J. Fuller Oct. 1990 28 p
(AD-A238252; NAVSWC-TR-90-418) Avail: NTIS HC/MF A03 CSCL 12/9

This paper presents an overview of neural network technology and specifics of the self-organizing networks. An artificial neural network is described which recognizes objects regardless of their spatial orientation. This network is invariant to rotation, scale, and translation. Invariance is built into the network by introducing a unique set of features which were developed in-house. This overcame the two shortcomings of long training times and combinatorial explosion of terms often present in other networks. Preliminary results suggest that with further refinement and enhancement, the system described in this report will have the capability to reliably recognize targets under adverse environmental conditions. GRA

N91-29808# Charles River Analytics, Inc., Cambridge, MA.
AN EXPERT SYSTEM APPROACH TO GLOBAL FAULT DETECTION AND ISOLATION DESIGN Final Report, 26 Jun. - 26 Dec. 1989
S. M. Allen and A. K. Caglayan Jan. 1990 50 p
(Contract F33615-89-C-3606)
(AD-A238494; R9004; WL-TR-91-3007) Avail: NTIS HC/MF A03 CSCL 09/2

The primary objective of this research is the development and demonstration of a global Failure Detection and Identification (FDI) Design Assistant (DA) prototype based on expert system technology. A global FDI algorithm performs its detection, isolation and estimation function by assessing the global effects of a hardware fault and surface damage on the closed-loop aircraft dynamics. Since changes in the flight control law affect the signature of a hardware fault and surface damage, the design of a global FDI algorithm is dependent on the flight control law performance characteristics. Ideally, the flight control law and global FDI designs should be accomplished simultaneously, especially for a new aircraft design rather than the current practice of serial iterations on the two designs. Hence, automation of the global FDI design process is desirable in order to reduce development time, cost and risk for advanced flight control systems. A secondary study objective is to investigate how expert systems and neural networks can be integrated into the implementation of a global FDI system. We describe the implementation of the detection and isolation logic portions of the CRCA global FDI algorithm as a rule-based expert system so that symbolic knowledge representation and reasoning can be incorporated into the design. GRA

N91-29809# Pacific Northwest Lab., Richland, WA.
A METHODOLOGY FOR DEVELOPING PHYSICAL SYSTEM FAULT DIAGNOSTIC AIDS
R. C. Stratton and D. B. Jarrell Jul. 1991 6 p Presented at the AAAI-91 Model-Based Reasoning Workshop, Anaheim, CA, 14-18 Jul. 1991
(Contract DE-AC06-76RL-01830)
(DE91-015533; PNL-SA-19305; CONF-9107141-1) Avail: NTIS HC/MF A02

A methodology is presented for developing automated aids for diagnosing faults in complex physical systems, e.g., reactor cooling system. We undertook this research at the Pacific Northwest Laboratory (PNL) for the U.S. Department of Energy and the U.S. Nuclear Regulatory Commission. We have designed these aids as multilevel-multiagent diagnostic aids based on principles that should be generally applicable to any complex system. In this methodology, multilevel refers to information models described at successive levels of abstraction that are tied together in such a way that reasoning is directed to the appropriate level as determined by the problem solving requirements. The concept of multiagent refers to the method of information processing within the multilevel model network; each model network is an independent information processor, i.e., an intelligent agent. DOE

N91-29810# Oak Ridge National Lab., TN.
RESEARCH AND DEVELOPMENT AT ORNL/CESAR TOWARDS COOPERATING ROBOTIC SYSTEMS FOR HAZARDOUS ENVIRONMENTS
R. C. Mann, K. Fujimura, and M. A. Unseren 1991 6 p Presented at the Space Operations, Applications, and Research Symposium (SOAR 1991), Houston, TX, 9-11 Jul. 1991
(Contract DE-AC05-84OR-21400)
(DE91-015638; CONF-9107144-1) Avail: NTIS HC/MF A02

One of the frontiers in intelligent machine research is the understanding of how constructive cooperation among multiple autonomous agents can be effected. The effort at the Center for Engineering Systems Advanced Research (CESAR) at the Oak Ridge National Laboratory (ORNL) focuses on two problem areas: (1) cooperation by multiple mobile robots in dynamic, incompletely known environments; and (2) cooperating robotic manipulators. Particular emphasis is placed on experimental evaluation of research and developments using the CESAR robot system testbeds, including three mobile robots, and a seven-axis, kinematically redundant mobile manipulator. This paper summarizes initial results of research addressing the decoupling of position and force control for two manipulators holding a common object, and the path planning for multiple robots in a common workspace. DOE

64 NUMERICAL ANALYSIS

Includes iteration, difference equations, and numerical approximation.

N91-29811# National Research Council of Canada, Ottawa (Ontario). Div. of Electrical Engineering
PIECEWORK LINEAR LEAST-SQUARES APPROXIMATION PLANAR CURVES INCLUDING COMPUTER PROGRAMS
N. N. Abdelmalek May 1989 53 p
(NRC-31069; ERB-1020; CTN-91-60098) Copyright Avail: NTIS HC/MF A04

Piecewise approximation of plane curves is of interest in image processing, noise filtering, and data compression. Two algorithms for solving the piecewise linear least squares approximation problem of plane curves are presented. The first one is for the case when the L2 residual (error) norm in any segment is not to exceed a pre-assigned value. The second algorithm is for the case when the number of segments is given and a (balanced) L2 residual norm solution is required. The given curve is first digitized and either algorithm is then applied to the discrete points. For each segment, the upper triangular matrix R in the QR factorization of the (augmented) coefficient matrix of the resulting system of linear equations is obtained. The least squares solutions are calculated in terms of the R (and Q) matrices. The algorithms then work in an iterative manner by updating the least squares solutions for the segments via updating the R matrices. The calculation requires as little computational effort as possible. Numerical results and comments are given. Computer programs written in FORTRAN 77, for the above two algorithms are also included. Author (CISTI)

N91-29812# Los Alamos National Lab., NM.
LIMITATIONS TO THE METHOD OF POWER SPECTRUM ANALYSIS: NONSTATIONARITY, BIASED ESTIMATORS, AND WEAK CONVERGENCE TO NORMALITY
W. I. Newman, M. P. Haynes, and Y. Terzian (Cornell Univ., Ithaca, NY.) 1991 22 p Presented at the Statistical Challenges in Modern Astronomy Conference, University Park, 11-14 Aug. 1991
(Contract W-7405-eng-36)
(DE91-008583; LA-UR-91-477; CONF-910859-1) Avail: NTIS HC/MF A03

The Power Spectrum Analysis method developed by Yu and Peebles has been widely employed as a technique for establishing the existence of periodicities. This method generates a sequence of random numbers from observational data which, it was claimed, is exponentially distributed with unit mean and variance, essentially independent of the distribution of the original data. We show that the derived random process preserves a subtle imprint of the original distribution, rendering the derived process nonstationary and producing a small but systematic bias in the usual estimate of the mean and variance. Although the derived variable may be reasonably described by an exponential distribution, the tail of the distribution is far removed from that of an exponential, thereby rendering statistical inference and confidence testing based on the tail of the distribution completely unreliable. DOE

N91-29813# International Centre for Theoretical Physics, Trieste (Italy).
THE 'T HOOFT'S SOLUTION FOR ARBITRARY SEMISIMPLE LIE GROUP
A. N. Leznov and M. A. Mukhtarov (Academy of Sciences of the Azerbaijan SSR, Baku.) Jul. 1990 11 p
(DE91-617572; IC-90/163) Avail: NTIS HC/MF A03

The generalization of the 't Hooft's A(sub 1) solution for every

semisimple Lie algebra is found. The solution depends on r-independent chains of linear self-dual systems (Delta(sub s)(sup alpha))(sub z) = (Delta(sub s+1)(sup alpha))(sub bar-y), (Delta(sub s)(sup alpha))(sub bar-y) = -(Delta(sub s+1)(sup alpha))(sub z) (1 less than or equal to alpha less than or equal to r); the length of alpha chain is equal to 2 omega(sub alpha) + 1, where omega(sub alpha) are the indexes of the semisimple algebra and r is its rank. In the special case the O(4)-invariant solutions with instanton number equal to one arises. DOE

N91-29814# National Aeronautical Lab., Bangalore (India).
PARAMETER ESTIMATION VIA NONLINEAR DIFFERENTIAL CORRECTION LEAST SQUARE METHOD
V. Parameswaran, J. R. Raol, and Shaik Ismail Apr. 1991 26 p
(NAL-PD-FC-9110) Avail: NTIS HC/MF A03

Results of application of nonlinear least squares parameter estimation (NLSPE) method to flight data are discussed. The method is based on a differential correction technique and the partial differentiation is performed numerically by using finite difference method. It can be used for estimating of initial states and parameters of a nonlinear dynamic model. It is a batch-iterative procedure and can be regarded as complementary to other nonlinear parameter estimation procedures. It can also be used as a start-up procedure to estimate initial parameter values which are required for other methods, and also as a regression procedure required in estimation before modelling methodology. Author

N91-29815# Oak Ridge National Lab., TN.
PARALLELIZING THE SPECTRAL TRANSFORM METHOD
P. H. Worley, D. W. Walker, and J. B. Drake 1991 9 p Presented at the 6th Distributed Memory Computing Conference, Portland, 28 Apr. - 2 May 1991
(Contract DE-AC05-84OR-21400)
(DE91-013969; CONF-9104158-4) Avail: NTIS HC/MF A02

The spectral transform method is the standard numerical technique for solving partial differential equations on the sphere in global climate modeling. This paper describes the parallelization and performance of the spectral transform method for solving the nonlinear shallow water equations on the surface of a sphere using a 128-node Intel iPSC/860 hypercube. This work is part of a research program to develop climate models that are capable of much longer and more numerous simulations at a significantly finer resolution than are currently available. Such models are important in understanding the effects of the increasing atmospheric concentrations of greenhouse gases, and the computational requirements are such that massively parallel multiprocessors will be necessary to run such simulations in a reasonable amount of time. DOE

N91-29816# Fermi National Accelerator Lab., Batavia, IL.
A NOTE ON THE AUTOMATED DIFFERENTIATION OF IMPLICIT FUNCTIONS
L. Michelotti 27 Jun. 1991 9 p
(Contract DE-AC02-76CH-03000)
(DE91-015104; FNAL-TM-1742) Avail: NTIS HC/MF A02

The question, can automated differentiation be used on functions that are defined implicitly, recursively, or iteratively, is studied. Consider, for example, the simple function x(m) defined by the equation, x(m) = cos(m times x(m). DOE

N91-29817# Pittsburgh Univ., PA. Inst. for Computational Mathematics and Applications.
COMPUTATIONAL METHODS FOR BIFURCATION PROBLEMS WITH SYMMETRIES ON THE MANIFOLD
Bin Hong 3 Jun. 1991 22 p
(Contract N00014-90-J-1025; NSF CCR-89-07654)
(AD-A237146; ICMA-91-163) Avail: NTIS HC/MF A03 CSCL 12/1

Numerical methods are examined for the determination of bifurcation points of certain steady state multi-parameter problems in the presence of symmetries. A principal tool is the fact that under general conditions the solution set forms a manifold in the space of all state and parameter variables. The reduced manifold with respect to some subsymmetry is introduced. Methods are presented for the local computation of the submanifold of bifurcation points of the same symmetry. GRA

N91-29818# New Mexico State Univ., Las Cruces. Computing Research Lab.
PROCEEDINGS OF THE 1ST WORKSHOP ON PROXIMITY GRAPHS Report, 1 Dec. 1989 - 31 May 1991
Donald W. Dearholt and Frank W. Harary 31 May 1991 198 p Workshop held in Las Cruces, NM, 30 Nov. - 2 Dec. 1989
(Contract N00014-90-J-1323; NSF CCR-89-18729)
(AD-A237250; CRL-MCCS-91-224) Avail: NTIS HC/MF A09 CSCL 12/1

The motivations for holding this workshop came from the recently discovered associations between proximity graphs and Pathfinder networks. The elegant theoretical domain and the breadth of applications make this a very rich area indeed. The workshop was attended by several of the leading researchers in proximity graphs, and was organized so that there would be adequate opportunity for discussion of common interests. The presentation was organized into four sections: theoretical foundations, algorithms and computational aspects, applications, and graphics and unsolved problems. There were also demonstrations of three systems based on proximity graphs: information retrieval using Pathfinder networks, a robotic vision database system organized as a monotonic search network, and a UNIX help system on a Hypertext Browser organized as a Pathfinder network. A tool to display and manipulate large graphs was also demonstrated. The workshop brought together some mainstream graph theorists and the researchers who had been working on proximity graphs as a special case of graph theory, and the interchange was profitable for all. GRA

N91-29819# Naval Ocean Systems Center, San Diego, CA.
USE OF THE IMPLICIT-FINITE-DIFFERENCE METHOD TO IMPLEMENT THE PARABOLIC EQUATION MODEL Final Report, Oct. 1989 - Oct. 1990
C. H. Shellman Feb. 1991 14 p
(AD-A237437; NOSC/TR-1413) Avail: NTIS HC/MF A03 CSCL 12/1

An effort to investigate alternate means to the split step algorithm for determining radar coverage in the troposphere at gigahertz (GHz) frequencies is presented. The theory of the implicit-finite-difference method is summarized and the boundary conditions described. Examples indicate that, for sufficiently high signal levels, the IFD method is adequate at 9.6 GHz. However, the method did not give correct results beyond 35 km for the standard-atmosphere case in which signal level are very low. GRA

N91-29820# California Inst. of Tech., Pasadena. Flight Sciences Lab.
DIFFERENTIAL EQUATIONS AND CONTINUUM MECHANICS Final Report, 1 Aug. 1988 - 31 Jul. 1990
Donald S. Cohen 10 May 1991 7 p
(Grant AF-AFOSR-0269-88; AF Proj. 2304)
(AD-A237722; AFOSR-91-0557TR) Avail: NTIS HC/MF A02 CSCL 12/1

Models have been developed to attempt to realistically account for recent observations involving new classes of polymerpenetrant systems. The attempt has been to account for their properties as they are currently being used in certain emerging technologies such as novel pharmaceutical delivery systems and separating membranes. Since most of the new observations involve various aspects of non-Fickian diffusion coupled with viscoelastic mechanical properties, the mathematical models usually involve degenerate parabolic systems which give rise to new and fascinating types of mathematical behavior. They have provided the impetus to develop interesting analytical and numerical techniques. GRA

N91-29821# New Mexico State Univ., Las Cruces. Dept. of Physics.
A SURVEY OF NONLINEAR DYNAMICS (CHAOS THEORY) Final Report
Richard L. Ingraham Apr. 1991 103 p
(Contract DAAL03-86-D-0001)
(AD-A237802; ASL-CR-91-0001-1) Avail: NTIS HC/MF A06 CSCL 12/1

A survey is given of the whole field of nonlinear dynamics (chaos theory) in compressed form. The standard topics (such as stability and bifurcation of continuous and discrete time systems, Hamiltonian systems, measures of chaos through Lyapunov exponents, broad band power spectra, and algorithmic complexity and related entropies, and experimental realization of chaos) are covered. But in addition, some topics seldom seen in short surveys are included: basic sensitive dependence and a precise definition of chaos, absence of chaos in a large sector of quantum mechanics, renormalization group and critical phenomena theory, and the very important Galerkin approximation method in partial differential equation dynamics. Mathematical rigor is not emphasized; however, precise statements of the crucial, mainly topological, key concepts and theorems are insisted upon. GRA

N91-29822# University of Northern Illinois, De Kalb. Dept. of Mathematical Sciences.
ANALYSIS OF NONGAUSSIAN, NONLINEAR TIME SERIES WITH LONG-MEMORY Final Report, 30 Sep. 1988 - 31 Mar. 1991
Moshen Pourahmadi 31 Mar. 1991 6 p
(Grant AF-AFOSR-0284-88; AF Proj. 2304)
(AD-A237847; AFOSR-91-0617TR) Avail: NTIS HC/MF A02 CSCL 12/3

The project has been concerned with statistical analysis of certain time series and stochastic signals that are unusual, in that they have long memory and are nonGaussian. Standard statistical procedures, such as the Box Jenkins procedure which presumes Gaussianity and short range dependence, when applied to these series will certainly produce inferior and suboptimal results. The PI pursued two approaches to address the twin problems of long memory and nonGaussianity. The first approach is rather general and it uses the setup of the Kolmogorov Wiener prediction theory of stationary processes. The second approach is more specific and it uses a random coefficient stochastic difference equation, which has a stationary solution with long memory and nonGaussian marginal simulating time series data with aforementioned properties. Such simulated data are used in verifying empirically the more general results obtained via the first approach. GRA

N91-29823# Carnegie-Mellon Univ., Pittsburgh, PA. Graduate School of Industrial Administration.
AN EXACT TWO-MATCHING BASED BRANCH AND BOUND ALGORITHM FOR THE SYMMETRIC TRAVELING SALESMAN PROBLEM
D. L. Miller, J. F. Pekny, and G. L. Thompson Feb. 1991 13 p Prepared in cooperation with Du Pont de Nemours (E. I.) and Co., Wilmington, DE and Purdue Univ., West Lafayette, IN
(Contract N00014-85-K-0198)
(AD-A237878; MSRR-566; WP-1991-21) Avail: NTIS HC/MF A03 CSCL 12/4

An algorithm is described for the symmetric traveling salesman problem (TSP) based on a bipartite two-matching lower bounding technique. The lower bound is strengthened by using the bipartite two-matching as the basis for a heuristic algorithm for the dual of integer two-matching. We use this dual as a lower bound for the symmetric traveling salesman problem in a branch and bound algorithm. Results are presented for random symmetric TSPs with up to 3000 cities. On Euclidean problems the two-matching bound is weaker than on random problems and algorithm performance deteriorates as a result. The algorithm successfully solves 11 of 15 Euclidean problems from the literature with sizes ranging from 17 to 99 cities. GRA

N91-29824# Naval Weapons Center, China Lake, CA.
ON THE INTERPOLATION PROPERTIES OF FEEDFORWARD LAYERED NEURAL NETWORKS Final Report, Oct. 1988 - Jun. 1989
Jorge M. Martin Oct. 1990 34 p
(NR Proj. RR0-1404; NR Proj. RR0-5202)
(AD-A238035; NWC-TP-7094) Avail: NTIS HC/MF A03 CSCL 12/4

The characterization of the interconnection weights of an L layered feedforward neural net that interpolates through a set of points is considered. A closed form expression for the last layer of weights of a net that interpolates through m sub L - 1 + 1 points is derived in terms of the points of interpolation. These weights are a function of all the weights in the preceding layers which may be chosen at random, and m sub L -1 is the number of neurons in the layer preceding the output layer. Another method for determining all the weights of a net with only two layers of weights is also presented. This method produces a transfer function that interpolates through m sub o + 1 points or less, where m sub o is the number of inputs to the net. The norm of the Jacobian matrix of the transfer function at the interpolation points is introduced as a measure of the sensitivity of the transfer function to perturbations in the inputs of the interpolation points. The points suggest that small weights are required for low sensitivity. GRA

N91-29825# Naval Postgraduate School, Monterey, CA.
SUM OF DISTANCES IN NORMED SPACES Technical Report, Apr. 1990 - Oct. 1990
Mostafa Ghandehari 9 Oct. 1990 10 p
(AD-A238066; NPS-MA-001; NPS-MA-91-001) Avail: NTIS HC/MF A02 CSCL 12/1

A geometric proof for the following theorem due to Martelli and Busenberg is given. Integral geometry is used to discuss special cases and related results. Minkowski spaces are simply finite dimensional normed linear spaces. Smoothness assumptions on the boundary of the unit disk E for a Minkowski plane will enable us to use Crofton's simplest formula from integral geometry to give a proof for three points. If the unit ball for a 3-dimensional Minkowski space is a zonoid, then we used integral geometry for the case of four points forming a simplex. A zonoid is a limit of sums of segments. Bolker discusses equivalent conditions for a convex subset of Rn to be a zonoid. GRA

N91-29826# Wisconsin Univ., Madison. Center for Mathematical Sciences.
APPROXIMATION FROM SHIFT-INVARIANT SURFACES OF L2(IRd) Summary Report
Carl DeBoor, Ronald A. DeVore, and Amos Ron 6 Jul. 1991 22 p Prepared in cooperation with the University of South Carolina, Columbia
(Contracts N00014-90-C-1343; DAAL03-G-90-0090; AF-AFOSR-0455-89; NSF DMS-90-00053; NSF DMS-89-22154; NSF DMS-91-02857)
(AD-A238165; CMS-TSR-92-2) Avail: NTIS HC/MF A03 CSCL 12/1

A complete characterization is given of closed shift-invariant subspaces of which provide a specified approximation order. When such a space is principal (i.e., generated by a single function), then this characterization is in terms of the Fourier transform of the generator. As a special case, we obtain the classical Strang-Fix conditions, but without requiring the generating function to decay at infinity. The approximation order of a general closed shift-invariant space is shown to be already realized by a specifiable principal subspace. GRA

N91-29827# Air Force Inst. of Tech., Wright-Patterson AFB, OH. School of Engineering.
AN ALTERNATIVE ALGORITHM FOR DISCRETE-TIME FILTERING M.S. Thesis
Frederick H. Zeitz, III Jun. 1991 159 p
(AD-A238443; AFIT/GE/ENG-91J-06) Avail: NTIS HC/MF A08 CSCL 12/1

The discrete-time Kalman filter is a conditional mean estimator

of the states of a linear stochastic process, conditioned on the previous state and current measurements. It assumes that the states and noise inputs can be represented as jointly Gaussian random variables. The influence diagram is a decision analysis tool. Under certain conditions, it can represent continuous, jointly Gaussian random variables. The conditioning order of the random variables may be changed (using Bayes' rule) so that any random variable can be conditioned on any other subset of random variables in the diagram. Under these conditions, an influence diagram can represent the states, measurements, and initial conditions of a linear stochastic process. It too can be a conditional mean estimator of the states of a linear stochastic process, and is an alternative algorithm for the Kalman filter. The influence diagram algorithm for the Kalman filter uses a factored covariance matrix. It is similar to other factored forms of the Kalman filter such as the U-D filter. It can be faster than other factored forms of the Kalman filter, but retain their improved numerical properties. GRA

N91-29828# Air Force Inst. of Tech., Wright-Patterson AFB, OH. School of Engineering.
THE BOUNDARY ELEMENT METHOD APPLIED TO THE TWO DIMENSIONAL STEFAN MOVING BOUNDARY PROBLEM M.S. Thesis
Donald C. Vosika 15 Mar. 1991 68 p
(AD-A238458; AFIT/GCS/ENC/91M-1) Avail: NTIS HC/MF A04 CSCL 20/13

This thesis considers problems for which the boundary is not known before the problem is solved and must be determined as part of the solution. We consider a time dependent problem which results in a moving boundary. We look at the heat conduction/diffusion equation in one and two spatial dimensions. We use Green's Theorem to yield a Volterra boundary integral equation which involves an unknown function on the moving boundary. We use the boundary element method to obtain a solution. Graphical results for the two dimensional problem are presented. GRA

N91-29829# Wisconsin Univ., Madison.
COMPUTATIONAL AND THEORETICAL ASPECTS OF NONLINEAR PARTIAL DIFFERENTIAL EQUATIONS Final Report, 10 Feb. 1987 - 9 Feb. 1991
John C. Strikwerda and Bradley K. Plohr 8 Apr. 1991 6 p
(Contract DAAL03-87-K-0018)
(AD-A238495; ARO-23933.10-MA) Avail: NTIS HC/MF A02 CSCL 12/1

This research centered around three topics in computational fluid dynamics. These were: schemes for the time dependent Navier Stokes equations, improved methods for the steady Navier-Stokes equations, and domain decomposition methods. (In the original proposal, the domain decomposition methods were referred to as overlapping grid methods.) All of these topics are coupled to the development of faster algorithms for solving the systems of indefinite linear equations that arise from discretizations of the Navier Stokes equations. Significant results have been obtained in all of these areas. GRA

N91-29830# Princeton Univ., NJ. Dept. of Statistics.
COMBINING CL (CONFIDENCE LIMITS) AND PL (PARTIAL LIMITS) DISPLAYS
John W. Tukey Jun. 1990 28 p
(Contract DAAL03-88-K-0045)
(AD-A238507; ARO-26098.21-MA) Avail: NTIS HC/MF A03 CSCL 12/1

There are a variety of circumstances where we might want to show two (or even three) intervals of uncertainty around each measured data point. The most frequent involves a wider interval (between SCL's) for comparing values with a numerical scale and a narrower interval (between SPL's) for comparing results with one another. In that circumstance, the use of double open triangular arrowheads (a DOTAR display) is particularly useful. Having chosen a graphical style, we need quantitative insight and numerical tables to implement our choice. In particular, we need to recognize the distinction between severe simultaneous and tight simultaneous and the possibility of finding, and using, severe simultaneous SCL's and SPL's at large exception rates. Numerical tables that outline quantitative behavior are provided. GRA

N91-29831# Stanford Univ., CA. Dept. of Statistics.
THE ASYMPTOTIC DISTRIBUTIONS OF AUTOREGRESSIVE COEFFICIENTS
T. W. Anderson Apr. 1991 24 p
(Contract DAAL03-89-K-0033)
(AD-A238538; SU-TR-26; ARO-26394.5-MA) Avail: NTIS HC/MF A03 CSCL 12/1

The asymptotic distribution of a finite set of autocorrelations is obtained for a time series from a linear stochastic process. The disturbances (or innovations) are martingale differences with bounded variances and bounded mixed fourth-order moments satisfying a uniform conditional square integrability condition. The conditions are weaker than those used previously for such asymptotic distributions. Specific topics include: autocorrelations, asymptotic distributions, martingale differences, bounded second order moments. GRA

N91-29832*# Sverdrup Technology, Inc., Brook Park, OH.
NUMERICAL SIMULATION OF SELF-FIELD MPD THRUSTERS Final Report
Michael R. LaPointe Aug. 1991 37 p Presented at the 27th Joint Propulsion Conference, Sacramento, CA, 24-27 Jun. 1991; sponsored by AIAA, SAE, ASME, and ASEE Previously announced as A91-45805
(Contract NAS3-25266)
(NASA-CR-187168; E-6440; NAS 1.26:187168; AIAA-91-2341)
Avail: NTIS HC/MF A03 CSCL 12A

A fully two dimensional magnetohydrodynamics code was developed to predict self-field, steady-state MPD thruster performance. The governing equations are outlined, and methods of solution are presented. Model predictions are compared with experimental data for two thruster geometries over a range of discharge currents and mass flow rates. Model limitations are evaluated, and issues concerning quasi-steady versus steady-state thruster comparisons are discussed. Author

65 STATISTICS AND PROBABILITY

Includes data sampling and smoothing; Monte Carlo method; and stochastic processes.

N91-29833# Naval Ocean Systems Center, San Diego, CA.
LEAST-SQUARES LEARNING AND APPROXIMATION OF POSTERIOR PROBABILITIES ON CLASSIFICATION PROBLEMS BY NEURAL NETWORK MODELS
P. A. Shoemaker, M. J. Carlin, R. L. Shimabukuro, and C. E. Priebe May 1991 11 p
(AD-A237140) Avail: NTIS HC/MF A03 CSCL 12/9

Multilayer neural network models are considered which are applied to stochastic classification problems and are trained with error back propagation methods. Expectations for network outputs are weighted least squares approximations to posterior probabilities for the classes (Gish 1990; Shoemaker, forthcoming; White 1981). In an empirical study, networks were trained on small benchmark problems with known probability density functions, using training data comprising random samples generated according to those functions. Expected classification accuracy and goodness of fit of network outputs to posterior class probabilities were subsequently evaluated. Classification performance near the Bayes optimum was obtained for each problem, and fits to posterior class probabilities were judged resonable, with root-mean-expected-square differences between outputs and probabilities below 0.05 seen in individual networks for both problems. GRA

N91-29834# Naval Ocean Systems Center, San Diego, CA.
DEDUCTION AND INFERENCE USING CONDITIONAL LOGIC

AND PROBABILITY Professional Paper
P. G. Calabrese May 1991 32 p
(AD-A237285) Avail: NTIS HC/MF A03 CSCL 12/1

In contrast to the author's 1987 paper, which presented an algebraic synthesis of conditional logic and conditional probability starting with an initial Boolean algebra of propositions, this paper starts with an initial probability space of events and generates the associated propositions as measurable indicator functions (a la the approach of B. De Finetti). Conditional propositions are generated as measureable indicator functions restricted to subset of positive probability measure. The operations of and, or, not, and given are defined for arbitrary conditional propositions. The representation of the resulting conditional event algebra as a 3-valued logic (always possible according to a new theorem due to I. R. Goodman) is given in terms of 3-valued truth tables. Formulas for the conditional probability of complex conditional propositions such as (q/p) v (s/r) are proved. A second major theme of the paper concerns deductions in the realm of conditional propositions. It turns out that there are varieties of logical deduction for conditional propositions depending on the particular entailment relation (less than or equal to) chosen. These relations are explored including their lattice properties and properties and properties of non-monotonicity. Computational aspects for Artificial Intelligence are also discussed. GRA

N91-29835# Stanford Univ., CA. Dept. of Statistics.
CONFIDENCE BANDS FOR THE MEDIAN SURVIVAL TIME AS A FUNCTION OF THE COVARIATES IN THE COX MODEL
Deborah Burr and Hani Doss 25 Jun. 1991 38 p
(Contract N00014-89-J-1627)
(AD-A237626; SU-TR-443) Avail: NTIS HC/MF A03 CSCL 12/3

The proportional hazards model of Cox (1972) specifies that the hazard rate for an individual with covariate vector x is a certain equation where beta sub o is a vector of unknown-regression coefficients and lambda, and the underlying baseline hazard rate, is an unknown and unspecified nonnegative function. In most cases where this model is used, interest centers on the estimation of beta sub o. However, it is often also very useful to investigate the effect of the covariates on the median (or some other fixed quantile) of the survival time. GRA

N91-29836# Stanford Univ., CA. Dept. of Operations Research.
DIFFUSION APPROXIMATIONS FOR COMPLEX REPAIR SYSTEMS
Donald L. Iglehart and Atam Lalchandani Feb. 1991 30 p
(Contract DAAL03-88-K-0063)
(AD-A238100; ARO-25839.42-MA) Avail: NTIS HC/MF A03 CSCL 12/4

A wide variety of complex repair systems can be modeled as continuous time Markov chains. These systems are closed networks of queues with a total of n jobs circulating in the network. The process of interest is the number of jobs, X sub n (t), at the various repair centers at time t. After appropriate translation and scaling, we show that the processes (X sub n (t) : t greater than or = 0) converge weakly to a limiting multivariate Ornstein-Uhlenbeck process. This limit process is then used to obtain computable approximations for X sub n (t). Numerical results are presented for three specific repairman models and the approximations are compared with exact results obtained through product form formulae. In most cases the approximation is quite accurate. GRA

N91-29837# Electronics Research Lab., Adelaide (Australia).
A GENERAL LEASE-SQUARES FITTING PACKAGE FOR THE SUN WORKSTATION
S. C. Troedson and A. C. Lindsay Apr. 1991 52 p
(AD-A238180; ERL-0544-GD; DODA-AR-006-481) Avail: NTIS HC/MF A04 CSCL 12/5

This document introduces a user interface that provides fast and efficient general least-square analysis of experimental data. It is suitable for use in the Sunwindows environment on Sun UNIX workstation. The package is capable of providing solutions of both linear and non-linear least-squares models of experimental data, and incorporates full graphics and error analysis. Known uncertainties in the data are easily incorporated as weights for each experimental point if required. An overview of the operational details of the package is given in Section 2. Examples of how to use the package are given in Section 3. The linear least-squares analysis allows unweighted, y-weighted and x- and y-weighted optimization, and in the former cases either the slope or intercept may be fixed if required. Since the theory of unweighted and y-weighted linear least-squares is well known 1, 2, it will not be described in this document. The theory for the case where both the dependent and independent variables exhibit uncertainties is not well known however, and as such is outlined in Appendix A. Appendix B details the theory of non-linear least-squares optimisation using the Levenberg-Marquardt algorithm, which is the routine implemented in this package. GRA

N91-29838# Florida State Univ., Tallahassee. Dept. of Statistics.
ON THE ANALYSIS OF GROUPED SURVIVAL DATA USING CUMULATIVE OCCURRENCE/EXPOSURE RATES
Ian W. McKeague and Mei-Jie Zhang Mar. 1991 27 p
(Contract DAAL03-90-G-0103; AF-AFOSR-0040-88)
(AD-A238219; FSU-STATISTICS-M840; TR-91-257-AFOSR; ARO-27868.3-MA) Avail: NTIS HC/MF A03 CSCL 12/3

One may estimate a conditional hazard function from grouped (and possibly censored) survival data by the time and covariate specific occurrence/exposure rate. Asymptotic results for cumulative versions of this estimator are developed, utilizing the general frame-work of counting processes. In particular, a grouped data based goodness of fit test for Cox's proportional hazard model is given. Various constraints on the asymptotic behavior of the widths of the calendar periods and covariate strata employed in grouping the data are needed to prove the results. Actual performance of the estimators and test statistics is evaluated by Monte Carlo methods. GRA

N91-29839# Florida State Univ., Tallahassee. Dept. of Statistics.
SINGULARITIES IN GAUSSIAN RANDOM FIELDS
T. V. Kurien and Jayaram Sethuraman Nov. 1990 15 p
(Contract DAAL03-90-G-0103; AF-AFOSR-0221-89)
(AD-A238220; FSU-STATISTICS-M836; TR-90-256-AFOSR; ARO-27868.4-MA) Avail: NTIS HC/MF A03 CSCL 12/3

This paper discusses a Gaussian random field that arises in pattern analysis. This random field exhibits phase transitive behavior for a particular value of the temperature parameter. We analyze this kind of non singular behavior and the effect that it has on the field random variables. The limiting specific heat also exhibits a phase transition with a power law behavior. One of the principal aims of statistical mechanics is to derive the thermodynamic behavior of macroscopic bodies beginning from a description of their microscopic components. A good deal of work has been done on modelling ferromagnetic and antiferromagnetic behavior. A magnet can be considered to have a large number of magnetic domains, to each of which a magnetic spin is associated that represents the direction of magnetization at that domain. We usually assume that the spins take two values, 0 and 1. The physical models usually postulate that these domains are sites (or vertices) in a graph. GRA

N91-29840# Florida State Univ., Tallahassee. Dept. of Statistics.
A MIXED LIMIT THEOREM FOR STABLE RANDOM FIELDS
T. V. Kurien and J. Sethuraman Sep. 1990 12 p
(Contract DAAL03-90-G-0103; AF-AFOSR-0040-88)
(AD-A238222; FSU-STATISTICS-M832; TR-90-251-AFOSR; ARO-27868.5-MA) Avail: NTIS HC/MF A03 CSCL 12/3

A mixed distributional limit theorem for a stable random field of index 0 less than alpha less than 2 is derived. These random fields are of special interest in pattern analysis, in particular, in pattern synthesis. This paper considers the case when the

underlying graph that the random field is defined on is linear. This result is encouraging insofar as it shows that the mixed limit theorems do exist in the stable case. The final limiting distribution can be written in terms of the stable process of index alpha in D0, 1. GRA

N91-29841# Arizona Univ., Tucson. Dept. of Systems and Industrial Engineering.
HEURISTIC METHODS IN APPLIED PROBABILITY Final Report, 1 Dec. 1989 - 30 May 1990
Julia L. Higle 30 May 1991 8 p
(Grant AF-AFOSR-0076-88; AF Proj. 2304)
(AD-A238229; AFOSR-91-0615TR) Avail: NTIS HC/MF A02 CSCL 12/1

The purpose of this research program is the development of heuristic and algorithmic approaches to various problems of engineering and applied mathematical interest. This research program was initiated under the guidance of Professor Marcel F. Neuts. Unfortunately, a substantial revision of the project budget required his resignation from the project. Thus, in this report, we will summarize the work of Dr's Julia L. Higle, who investigates problems of stochastic optimization and develops non-accident based measures of vehicular traffic hazards, and Jeffrey B. Goldberg, who investigates problems of design for reliability and manufacturability, decision making in Just-In-Time manufacturing systems, and approximation models for spatially distributed queueing systems. These investigators and the students supported during the final year of this grant work in quite diverse areas, but share a strong interest in algorithmic methodology. GRA

N91-29842# Air Force Inst. of Tech., Wright-Patterson AFB, OH.
THE UTILITY OF ELLIPTICAL AND CIRCULAR CONFIDENCE REGIONS FOR HFDF RECEIVERS M.S. Thesis
Paul T. Nemec Mar. 1991 90 p
(AD-A238390; AFIT/GST/ENS/91M-2) Avail: NTIS HC/MF A05 CSCL 17/11

This thesis investigates High Frequency Direction Finding (HFDF) Confidence Region (CR) shape exhibited by geolocations in a search-and-rescue context. In Phase 1, a Keeney-Raiffa multiattribute utility function was developed which allowed an analytical measure of preference between elliptical and equivalent-probability circular CRs. Phase 2 utilized a likelihood approach to establish CR shape for sample operational geolocations having multiple points of bearing intersections. For 12 sample Phase 1 geolocations, the elliptical CR always had higher utility than its corresponding circular CR. For accepted sample geolocations, a preference condition was developed whereby a circular CR would only be preferred over the corresponding elliptical CR if the relative percent utility difference was less than some DOD-established threshold percentage. GRA

N91-29843# Army Strategic Defense Command, Huntsville, AL.
MANAGEMENT OF VARIATION AND TQM Final Report
William E. Hughes, Jr. Jul. 1991 35 p
(AD-A238399) Avail: NTIS HC/MF A03 CSCL 12/3

Variation has been studied by statisticians and scientists for decades. Although variation is not a new concept, what is new is the awareness that variation affects everyday activities in the workplace. Modern man is plagued with variation problems ranging from raw materials to finished products and services. No matter how precise our methods of producing products and providing services becomes, there will always be some degree of variation. Today's thrust toward the Total Quality Management (TQM) concept will include the understanding of variation. In fact, the concept of variation may be analyzed in each of Deming's 14 points. Future variation issues will include the understanding and management of people. GRA

N91-29844# Air Force Inst. of Tech., Wright-Patterson AFB, OH. School of Engineering.
EFFECTS OF COLOCATION AND NON-COLOCATION OF SENSORS AND ACTUATORS ON FLEXIBLE STRUCTURES M.S. Thesis
W. C. Lee Mar. 1991 137 p
(AD-A238457; AFIT/GA/ENY/91M-01) Avail: NTIS HC/MF A07 CSCL 22/1

This thesis compares the performance and robustness of colocated and non-colocated sensor/actuator pairs. Linear quadratic Gaussian and loop transfer recovery (LOG/LTR) procedures are used to design optimum controllers for three example problems. The first example is a single motion degree-of-freedom system having motion only about one axis. This type of system does not have any right half plane zeros for the non-colocated case; however, the thesis shows it behaves as a non minimum phase system. The second example is a Bernoulli-Euler beam which does not have RHP zeros. An optimum LOG/LTR controller can not improve the robustness of non minimum phase systems; whereas, colocated systems are easy to stabilize and make robust with LTR. However, this thesis shows that non colocated systems can achieve higher bandwidth and performance. So, each system has its own advantage. GRA

N91-29845# Princeton Univ., NJ. Dept. of Statistics.
SCRAWL STRIPS, AND LETTER OR B-LETTER STRIPS: DEPICTING MARGINALS OF SCATTER PLOTS Technical Report No. 299, 1 May 1986 - 31 Dec. 1990
John W. Tukey and James G. Veitch Dec. 1990 23 p
(Contracts DAAL03-86-K-0073; DAAG29-82-K-0178)
(AD-A238556; ARO-23360.17-MA) Avail: NTIS HC/MF A03 CSCL 12/3

Data from a bivariate distribution is often graphically presented by using a scatter plot. Adding a suitable depiction of the marginal data distributions to the edges of the scatter plot allows interesting features of the marginal data distributions to be seen alongside the original bivariate data. We propose providing these marginal depictions by a modification of Quantile-Quantile plots (QQ plots) we call scrawl strips. We also propose adding a strip or axis showing location of the letter values, or the broadened letter values, which we call a letter strip, or b-letter strip, respectively. These two strips can be combined. Since scrawl strips are modified QQ plots, they inherit useful features of QQ plots. These features include information about the shape of the marginal distribution, the presence and type of skewness, the presence of heavy tails, gaps and ties in the ordered data, appearances of bimodality or high shoulders, and assumptions of normality. This type of information is often either absent or depicted poorly, both in univariate competitors to the QQ plot and in the basic scatter plot. GRA

N91-29846# Air Force Inst. of Tech., Wright-Patterson AFB, OH. School of Engineering.
NEW MODIFIED ANDERSON-DARLING AND CRAMER-VON MISES GOODNESS-OF-FIT TESTS FOR A NORMAL DISTRIBUTION WITH SPECIFIED PARAMETERS M.S. Thesis
Goksel Kahya Mar. 1991 109 p
(AD-A238630; AFIT/GOR/ENC/91M-3) Avail: NTIS HC/MF A06 CSCL 12/3

This thesis improves the powers of the Anderson-Darling and Cramer-von Mises goodness-of-fit tests using the mean rank and the median rank plotting positions. A Monte Carlo simulation of 5000 repetitions is used to generate the critical values from $n = 4$ through $n = 80$ for certain significance levels. An extensive power study is performed to compare the powers of the modified tests to the known tests for the uniform, the exponential, the double exponential, the lognormal, and the Weibull distributions. The power of the A-D tests modified by the median rank plotting and the mean rank plotting position are approximately 0.01% higher than the unmodified tests. The power of the C-VM test is 10% higher than the unmodified C-VM test for the Weibull, the lognormal, the exponential, and the double exponential distributions when the median rank plotting position also improves the power of the C-VM

test for the uniform and the Weibull distributions; while it reduces the power for the exponential, the double exponential, and the lognormal distributions. GRA

N91-29847# Air Force Inst. of Tech., Wright-Patterson AFB, OH. School of Engineering.
A GOODNESS-OF-FIT TEST FOR A FAMILY OF TWO PARAMETER WEIBULLS WITH KNOWN SHAPE USING MINIMUM DISTANCE ESTIMATION OF PARAMETERS M.S. Thesis
John S. Crown Mar. 1991 83 p
(AD-A238633; AFIT/GOR/ENC/91M-4) Avail: NTIS HC/MF A05 CSCL 12/3

This research is to produce a modified Anderson-Darling goodness of fit test for the Weibull distribution when the location parameter is found by minimum distance estimation, the shape parameter is assumed known, and the MLE is used for the scale parameter. The critical values for the Anderson-Darling test are generated via Monte Carlo simulation when both the Anderson-Darling and Cramer-Von Mises distance statistics are minimized. These critical values are then used for a power study. The Monte Carlo simulation used 5000 repetitions for sample sizes of 5,8,12,15,16,20 and 25 with the Weibull shape parameter of .5(.5)4.0. The power study is made for the same sample sizes as above with the hypothesized Weibull shape parameter of 1.0 and 3.5 against ten alternate hypothesized distributions. For small sample sizes, improvement can be seen over tests which use MLEs for the location and scale parameters. However, for larger sample sizes, more than 20, the power is similar to other goodness-of-fit tests for the Weibull. In most cases, minimizing the Anderson-Darling distance statistic to estimate the Weibull location parameter had more power than minimizing the Cramer-Von Mises distance statistic. GRA

66 SYSTEMS ANALYSIS

Includes mathematical modeling; network analysis; and operations research.

N91-29848# Lawrence Livermore National Lab., CA.
PLAN FOR A LASER WEAPON VERIFICATION RESEARCH PROGRAM
T. J. Karr 1 Mar. 1990 26 p
(Contract W-7405-eng-48)
(DE90-012123; UCID-21956) Avail: NTIS HC/MF A03

Currently there is great interest in the question of how, or even whether, a treaty limiting the development and deployment of laser weapons could be verified. The concept of cooperative laser weapon verification is that each party would place monitoring stations near the other party's declared or suspect laser weapon facilities. The monitoring stations would measure the primary laser observables such as power or energy, either directly or by collecting laser radiation scattered from the air or the target, and would verify that the laser is operated within treaty limits. This concept is modeled along the lines of the seismic network recently activated in the USSR as a joint project of the United States Geologic Survey and the Soviet Academy of Sciences. The seismic data, gathered cooperatively, can be used by each party as it wishes, including to support verification of future nuclear test ban treaties. For laser weapon verification the monitoring stations are envisioned as ground-based, and would verify treaty limitations on ground-based laser anti-satellite (ASAT) weapons and on the ground-based development of other laser weapons. They would also contribute to verification of limitations on air-, sea- and space-based laser weapons, and the technology developed for cooperative verification could also be used in national technical means of verification. DOE

N91-29849# Lawrence Livermore National Lab., CA.
SDI PERFORMANCE AND START CONSTRAINTS: MODELING PHASE-1 DEFENSE ENGAGEMENTS
C. Cunningham 20 Mar. 1991 10 p Presented at the The Role of Nuclear Weapons in the Year 2000, San Ramon, 22-24 Oct. 1990
(Contract W-7405-eng-48)
(DE91-013305; UCRL-JC-106498; CTS-19-90; CONF-9010247-4)
Avail: NTIS HC/MF A02

My interest has been the performance of near-term Strategic Defense Initiative (SDI) systems rather than the kinds of questions discussed at this Workshop (e.g., implications of U.S. force structure). It is clear, though, that the two issues are closely related. Arms control along with treaties that impact the force structure of the Soviet Union will greatly affect the performance of SDI systems. Similarly, the U.S. intention to pursue SDI will be a driver in arms control negotiations, as well it should be. Indeed, the implications of SDI for Strategic Arms Reduction Treaty (START)-constrained Soviet forces are the focus of my discussion. To put this in some context, I will begin with the premises underlying my results: the United States and the Soviet Union reach an arms control agreement limiting strategic forces below current levels. The United States decides to pursue defense deployments to limit damage to the U.S. and, eventually, to provide robust protection against ballistic missile attack. The Soviet Union responds by improving its forces within the numerical bounds of the treaty. My basic calculations are: Under START and in the absence of defenses, the offenses has sufficient weapons to attack 10,000 targets with strong value contrast. START constraints are severely limiting against an adaptive preferential defense, even with adaptive targeting. The adaptive preferential defense may contain a random-subtractive space based interceptor (SBI) tier. Post boost vehicle (PBV) redesign alone is insufficient to stress the SBI. Offload penalties to defeat endoatmospheric interceptors appear significant. Despite increased flexibility to modernize, a small attacking force is vulnerable to a small defense. DOE

N91-29850# Lawrence Livermore National Lab., CA.
ASAT MONITORING PROJECT AT LLNL
Lawrence F. Jelsma and Asher S. Blum May 1991 8 p Presented at the 1990 Sensor Technical Conference, Cocoa, 29 Apr. - 2 May 1991
(Contract W-7405-eng-48)
(DE91-013247; UCRL-JC-106819; CONF-9104238-2) Avail: NTIS HC/MF A02

LLNL, in conjunction with LANL, SNL and Argonne National Laboratories, is currently involved in the development of a Anti-Satellite (ASAT) monitoring system which is supported by Defense Advanced Research Projects Agency (DARPA). LLNL is responsible for the development of the image acquisition hardware data analysis and data storage. The first year's effort at LLNL has been directed towards modeling IR imaging systems for ASAT monitors and experimentally imaging the output of the MIRACL laser at White Sands test range. Using a model of the scattering and infrared detection process we have estimated the minimum detectable laser energy for currently available cameras. The minimum detectable laser energy during a frame time is dependent on background radiation, saturation charge and only weakly dependent on the noise floor of the array. To enhance the sensitivity of the monitor we have adapted the Hough algorithm to our requirements. DOE

N91-29851# Los Alamos National Lab., NM.
ON SATELLITE CONSTELLATION SELECTION
G. H. Canavan May 1991 9 p
(Contract W-7405-eng-36)
(DE91-014562; LA-12059-MS) Avail: NTIS HC/MF A02

Analytical estimates can be used to produce and discuss optimal constellations. They are in close agreement with phase-space estimates and exact solutions. They suggest that distributions of inclined orbits could reduce satellite numbers by factors of 2 to 3 while improving uniformity. DOE

N91-29852# Naval Postgraduate School, Monterey, CA.
A FRAMEWORK FOR UNDERSTANDING THE STRATEGIC

DEFENSE INITIATIVES' SOFTWARE DEBATES M.S. Thesis
Reginald C. Adams Jun. 1990 95 p
(AD-A237193) Avail: NTIS HC/MF A05 CSCL 12/5

On March 23, 1983, then-President Ronald Reagan challenged a group of engineers and scientists to make nuclear weapons impotent and obsolete. This challenge led to the beginning of a new era in space technology and strategic defense, thus creating the Strategic Defense Initiative (SDI), better known as Star Wars. By 1984, several studies had begun to show that software in conjunction with Battle Management/Command, Control, and Communications techniques would play a major role in determining the effectiveness of the SDI. The results from these studies caused numerous controversial debates on the reliability, dependability, and trustworthiness of the software. A framework is provided for understanding the complexities of the SDI software and some of the major issues involved in the software debates are pointed out. The structure is based on presenting the opinions of various computer scientists and engineers, indicating the issues that are controversial and those that have been defined as a necessity for the SDI program. One of the major highlights is the SDI summary chart that provides a very brief narrative of each individual's opinion on the software issues discussed. GRA

N91-29853# Analytic Sciences Corp., Arlington, VA.
REPORT TO THE CONGRESS ON THE STRATEGIC DEFENSE INITIATIVE, 1991 Final Report
May 1991 215 p
(Contract SDI084-88-C-0018)
(AD-A237658) Avail: NTIS HC/MF A10 CSCL 15/3

This report details progress and changes in SDI during the past year. It examines SDI's role in the changing international threat environment, particularly the use of SDI technologies in global protection against limited strikes (GPALS). This report also details current research and development strategy, allied participation in the program and compliance of SDI with the ABM Treaty. The report summarizes program funding and provides Congressional Descriptive Summary Extracts in the appendix. GRA

N91-29854# General Accounting Office, Washington, DC. National Security and International Affairs Div.
STRATEGIC DEFENSE INITIATIVE: NEED TO EXAMINE CONCURRENCY IN DEVELOPMENT OF BRILLIANT PEBBLES
Mar. 1991 30 p
(AD-A238292; GAO/NSIAD-91-154) Avail: NTIS HC/MF A03 CSCL 15/3

In the summer of 1989, the Strategic Defense Initiative Organization (SDIO) initiated studies to identify the best spacebased weapon concept, and in February 1990 it announced that Brilliant Pebbles was replacing the Space-Based Interceptor. The Brilliant Pebbles concept consists of several thousand interceptors orbiting the earth with the capability to detect and destroy targets by smashing into them at high speed. Each interceptor will be housed in a lifejacket that will provide, among other things, communications and the necessary on-orbit protection. SDIO has established two concurrent Brilliant Pebbles research and development programs to enable the President to make a decision not later than the summer of 1993 on deployment of strategic defenses. Both programs are part of the demonstration and validation phase, which precedes full-scale development. One program consists of a series of flight and underground tests to demonstrate that Brilliant Pebbles technology can intercept ballistic missiles and survive in wartime conditions. GRA

67 THEORETICAL MATHEMATICS

Includes topology and number theory.

No abstracts in this category.

70 PHYSICS (GENERAL)

For precision time and time interval (PTTI) see *35 Instrumentation and Photography;* for geophysics, astrophysics or solar physics see *46 Geophysics, 90 Astrophysics,* or *92 Solar Physics.*

N91-29855# International Centre for Theoretical Physics, Trieste (Italy).
THE KRAMERS PROBLEM: FIFTY YEARS OF DEVELOPMENT
V. O. Melnikov Sep. 1990 72 p
(DE91-617583; IC-90/262) Avail: NTIS HC/MF A04

In the last fifty years the seminal work by Kramers of 1940 has been greatly extended both by elaboration of new theoretical approaches and through applications to new experimental systems. The most interesting case turns out to be the regime of weak-to-medium damping, in which case the Fokker-Planck equation can be reduced to an equation or to a system of integral equations of the Wiener-Hopf type. Exact solutions can then be given for the escape rate from single- and double-well potentials. This general scheme can be naturally extended to include quantum penetration through a semiclassical barrier and the effect of quantum noise. Finally, we consider the Brownian motion in a tilted washboard potential using Josephson junctions as an illustrative example. In that context we calculate fluctuation-induced voltage-current characteristics, the lifetime of a zero-voltage state, the lifetime of the running state, partial probabilities of the phase jumps by 2(pi)n (n is an integer) and (v) retrapping current distribution in both classical and quantum regimes. DOE

N91-29856# Naval Research Lab., Washington, DC.
NRL REVIEW, 1989-1990
Jun. 1990 300 p
(AD-A238612; NRL-158-4831) Avail: NTIS HC/MF A13 CSCL 05/2

The Naval Research Laboratory Review includes the following topics: solid-state supercomputing; new frontiers in electronics; global weather observations; parallel algorithms for real-time tracking; behavior and properties of materials; chemical research and biotechnology; electromagnetic systems; electronics research; energetic particles and beams; information technology and communications; numerical simulating, computing, and modeling; ocean acoustics and surfaces, optical systems, space research and technology, excellence in research for tomorrow's Navy. GRA

N91-29857# Naval Research Lab., Washington, DC.
NRL REVIEW, 1991 Annual Report, FY 1990
May 1991 272 p
(AD-A238665; NRL-Pub-181-4830) Avail: NTIS HC/MF A12 CSCL 05/2

Topics of the major articles in this report include: Adaptive radar; Synthesis and structures of new energetic materials; and Synchrotron x-radiation research. Summary articles are included in the following topics: Acoustics; Chemical/biochemical research; Electronics and electromagnetics; Energetic particles, plasmas, and beams; Information technology and communication, Marine technology; Materials science and technology; Numerical simulating, computing, and modeling; Optics; and Space research and satellite technology. GRA

N91-29858# National Inst. of Standards and Technology, Gaithersburg, MD.
TECHNICAL ACTIVITIES 1990, ELECTRON AND OPTICAL PHYSICS DIV.
C. W. Clark May 1991 72 p
(PB91-194423; NISTIR-4553) Avail: NTIS HC/MF A04 CSCL 20C

Technical activities of the NIST Electron and Optical Physics Division during fiscal year 1990 are summarized. These fall into five general areas: soft x ray radiometry; operation of the SURF-2 synchrotron storage ring; electron microscopy and basic surface physics; soft x ray emission studies; and multiphoton processes.

A listing is given of calibration services, publications, talks, and other relevant activities of the division's staff. GRA

N91-29859# Brookhaven National Lab., Upton, NY.
MONTE CARLO AND MEAN FIELD CALCULATIONS OF THE MAGNETOCALORIC EFFECT OF FERROMAGNETICALLY INTERACTING CLUSTERS
L. H. Bennett, R. D. McMichael, L. J. Swartzendruber, R. D. Shull (National Inst. of Standards and Technology, Gaithersburg, MD.), and R. E. Watson 1991 8 p Presented at the International Conference on Magnetism, Edinburgh, Scotland, 1-7 Sep. 1991
(Contract DE-AC02-76CH-00016)
(DE91-014792; BNL-46292; CONF-910903-3) Avail: NTIS HC/MF A02

The magnetic entropy change of a ferromagnet induced by an application of a magnetic field is greatest in the temperature region near the Curie point, and the magnitude of the effect is expected to rise monotonically with the size of individual moments which make up the material. We explore the case of nanocomposite materials with ferromagnetically interacting clusters having large cluster magnetic moments as a function of cluster size. As cluster size increases, both Monte Carlo and mean field calculations show a decrease in the entropy change at (Tc) for a given applied field and constant total magnetic moment, and an increase in the entropy change well over (Tc). In addition, for the first time, we present a comparison of the results of mean field and Monte Carlo calculations of the magnetocaloric effect in classical Heisenberg ferromagnets. Previous calculations of the magnetocaloric effect have taken the mean field approach, which is known to underestimate the spontaneous magnetization below (Tc). These issues are relevant to devices employing magnetic refrigeration. DOE

N91-29860# Argonne National Lab., IL.
MAGLEV SYSTEM CONCEPT USING 20-K HIGH-TEMPERATURE SUPERCONDUCTORS AND HYPERCONDUCTORS
J. R. Hull and Jianliang He 1991 7 p Presented at the 26th Intersociety Energy Conversion Engineering (IECE) Conference, Boston, MA, 3-9 Aug. 1991
(Contract W-31-109-eng-38)
(DE91-015714; ANL/CP-72217; CONF-910801-11) Avail: NTIS HC/MF A02

A magnetically levitated high-speed ground transportation concept is proposed that uses high-temperature superconductors or hyperconductors, cooled by liquid hydrogen at 20 K, to provide levitation. An on-board hydrogen-powered turbine/generator provides electricity for propulsion by linear induction motors. The liquid hydrogen is used to cool the superconductors and the windings of the generator and motors before combusting in the turbine. The principal advantage of this system is the potential to greatly reduce the cost of the guideway, which is completely passive. DOE

N91-29861# Westinghouse Hanford Co., Richland, WA.
PARAMETRIC DESIGN CALCULATIONS USING GREEN'S FUNCTION TO DETERMINE UNIQUE SOURCE
L. L. Carter and J. S. Lan Jan. 1991 9 p Presented at the International Topical Meeting on Advances in Mathematics, Computation and Reactor Physics, Pittsburgh, PA, 28 Apr. - 2 May 1991
(Contract DE-AC06-87RL-10930)
(DE91-014683; WHC-SA-0986; CONF-910414-37) Avail: NTIS HC/MF A02

The energy dependence of the current incident on a macrocell can in principle be determined if the Green's function and the interior flux due to the total current are known. The Green's function is the flux within some portion of the macrocell due to a unit source in each energy group. It was demonstrated that the appropriate solution for the current is obtained for the higher energy groups in a fast reactor example. However, the lower energy groups are very sensitive to the downscattering and the solution even led to negative values for the incident partial current in some energy groups, which is not physical. In this particular example, the preliminary design study was insensitive to the incident current of the lower energy groups. For problems where the lower groups are important, it would seem prudent to abandon the exact solution and use a weighted least squares solution. Such a weighted least squares solution could assign importance for obtaining nearly the exact solution for as many energy groups as possible, while simultaneously making slight adjustments in the higher energy currents to obtain downscatter contributions that will approximately perserve the flux in the lower energy groups. DOE

71 ACOUSTICS

Includes sound generation, transmission and attenuation. For noise pollution see *45 Environmental Pollution.*

N91-29862# Loyola Univ., Chicago, IL. Hearing Inst.
AUDITORY PROCESSING OF COMPLEX SOUNDS ACROSS FREQUENCY CHANNELS Annual Technical Report, 1 May 1990 - 1 May 1991
William P. Shofner, Raymond H. Dye, William A. Yost, and Stanley Sheft 31 May 1991 8 p
(Grant AF-AFOSR-0335-89; AF Proj. 2313)
(AD-A238023; AFOSR-91-0604TR) Avail: NTIS HC/MF A02 CSCL 09/1

Our work has centered on the discovery of the MDI or Modulation Detection Interference phenomenon, in which the modulation properties of tonal components in multi-tone complexes can not be processed when all the tones are modulated at the same low modulation rate as well as when the tones are not modulated or when the modulation rates differ for different components. We have argued that MDI results from the fact that the coherent modulation of all of the components fuse them into a single auditory image, and since coherent modulation was the basis of the perceptual fusion, temporal modulation for any one tone is not easily processed. We recently tested a corollary to this assumption. That is, when tonal complexes are fused into an auditory image based on coherent temporal modulation and MDI occurs, can subjects still process other attributes of the tones (e.g., changes in frequency and intensity) since these other attributes were not the basis for the tones being fused into a single image. GRA

N91-29863# Arcon Corp., Waltham, MA.
ACOUSTIC BACKGROUND NOISE VARIATION IN AIR FORCE PLATFORMS AND ITS EFFECT ON NOISE REMOVAL ALGORITHMS Interim Report, Aug. 1988 - Feb. 1990
Philip A. LaFollette Jun. 1991 110 p
(Contract F19628-88-C-0190)
(AD-A238279; RL-TR-91-97) Avail: NTIS HC/MF A06 CSCL 01/2

In this study of short-term noise variation in Air Force platforms, we followed two avenues of investigation. First, we applied quantitative measures of variation to individual noise recordings, and compared the results across various aircraft. Some measures used were simple descriptive statistics, but we also measured attenuation obtained by spectral restoration (spectral subtraction), applied to the noise signal alone. The noise attenuation obtained for real aircraft environments was in most cases about the same as predicted theoretically for white Gaussian noise, but in some instances was considerably higher, especially in the presence of propeller noise. Second, we applied the nonparametric Mann-Whitney statistic to test the stationarity of power spectrum estimates on time scales of 200 to 800 ms. There was little or no evidence of nonstationarity in large jet or turboprop aircraft. In fighter aircraft and helicopters, there was some evidence of nonstationarity confined to more or less narrow frequency ranges. The nonstationarity found did not appear to limit the performance of special restoration algorithms. The noise recordings used were taken from the RADC/EEV database of field recordings made in the E-3A, E-4B, EC-135, E-130, P-3C, F-15, F-16, F-4, A-10, HH-53 and Tornado aircraft. GRA

72 ATOMIC AND MOLECULAR PHYSICS

Includes atomic structure, electron properties, and molecular spectra.

N91-29864# Oak Ridge National Lab., TN.
DESIGN ASPECTS FOR A PULSED-MODE, HIGH-INTENSITY, HEAVY NEGATIVE ION SOURCE
G. D. Alton 1991 3 p Presented at the 1991 Institute of Electrical and Electronics Engineers (IEEE) Particle Accelerator Conference (PAC), San Francisco, 6-9 May 1991
(Contract DE-AC05-84OR-21400)
(DE91-011094; CONF-910505-4) Avail: NTIS HC/MF A01

A high-intensity, plasma-sputter, negative ion source, which utilizes multi-cusp, magnetic-field, plasma-confinement techniques, has been designed at the Oak Ridge National Laboratory (ORNL). The source is an axial-geometry version of the radial-geometry source which has demonstrated pulsed-mode peak intensity levels of several mA for a wide spectrum of heavy negative ion species. The mechanical design features include provisions for fast interchange of sputter samples, ease of maintenance, direct cooling of the discharge chamber, and the use of easily replaced coaxial LaB6 cathodes. DOE

N91-29865*# University of Eastern Kentucky, Richmond. Dept. of Physics and Astronomy.
ACTIVATION CALCULATIONS FOR TRAPPED PROTONS BELOW 200 MeV: APPENDIX Final Technical Report
C. E. Laird Jul. 1991 192 p
(Contract NAS8-36649)
(NASA-CR-184170; NAS 1.26:184170) Avail: NTIS HC/MF A09 CSCL 20H

Tables are given displaying of the results of the activation calculations of metal samples and other material aboard the Long Duration Exposure Facility-1 (LDEF-1) and Spacelab-2 with the computer program, PTRAP4. The computer printouts give the reaction, the reactant product, the proton reaction cross sections as a function of the energy of the incident protons, and the activation as a function of distance into the sample from the exposed surface. Author

N91-29866# Washington Univ., Seattle. Dept. of Physics.
NUCLEAR THEORY PROGRESS REPORT
1991 21 p
(Contract DE-FG06-88ER-40427)
(DE91-013908; DOE/ER-40427/11-N91) Avail: NTIS HC/MF A03

Research performed in nuclear theory is discussed. Some of the topics discussed are: nuclear astrophysics; symmetry; time reversal invariance; quark matter; superallowed beta decay; exclusive reactions; nuclear probes; soliton model; relativistic heavy ion collisions; supernova explosions; neutrino processes in dense matter; field theories; weak interaction physics; and nuclear structure. DOE

N91-29867# University of Southern California, Los Angeles. Dept. of Chemistry.
REACTIONS OF SMALL MOLECULAR SYSTEMS
C. Wittig 1991 5 p
(Contract DE-FG03-85ER-13363)
(DE91-014519; DOE/ER-13363/T2) Avail: NTIS HC/MF A01

In this report, we present the C2 H2 + hv(193.3 nm) yields H + C2 H translational energy distribution. A C2 H bending progression dominates the distribution. The Rydberg time of flight (TOF) method offers high resolution (10's of cm(exp -1)), which may ultimately be needed to establish D0 doubt. The method of detecting H atoms via 2-photon, 2-frequency excitation to a high-lying Rydberg state followed by efficient field ionization was used. Briefly an expansion of C2 H2 seeded in He is skimmed and crossed with the output from an ArF laser. H-atoms are excited by VUV radiation tuned to 121.6 nm (Lyman-(alpha). This is generated by tripling the output of a 364.7 nm dye laser in Kr. Another laser beam, overlapping the 121.6 nm beam, transfers population from the 2(exp 2)P level to a high-lying Rydberg level. Such levels are metastable and remain excited or many 10's of microns. These atoms travel to a detector 23.6 cm from the interaction region; since the atoms are neutral, they are not affected by space charge. As the atoms arrive at the detector, they are field-ionized and detected as ions. TOF spectra are recorded using a transient digitizer and a computer. DOE

N91-29868# California Univ., Berkeley. Lawrence Berkeley Lab.
MOLECULAR BEAM STUDIES OF REACTION DYNAMICS
Yuan T. Lee Mar. 1991 8 p Presented at the Department of Energy-Basic Energy Sciences (DOE-BES) Combustion Research Meeting, Lake Geneva, WI, 28-31 May 1991
(Contract DE-AC03-76SF-00098)
(DE91-014866; LBL-30436-Abs; CONF-9105162-4) Avail: NTIS HC/MF A02

The major thrust of this research project is to elucidate detailed dynamics of simple elementary reactions that are theoretically important and to unravel the mechanism of complex chemical reactions or photochemical processes that play important roles in many macroscopic processes. Molecular beams of reactants are used to study individual reactive encounters between molecules or to monitor photodissociation events in a collision-free environment. Most of the information is derived from measurement of the product fragment energy, angular, and state distributions. Recent activities are centered on the mechanisms of elementary chemical reactions involving oxygen atoms with unsaturated hydrocarbons, the dynamics of endothermic substitution reactions, the dependence of the chemical reactivity of electronically excited atoms on the alignment of excited orbitals, the primary photochemical processes of polyatomic molecules, intramolecular energy transfer of chemically activated and locally excited molecules, the energetics of free radicals that are important to combustion processes, the infrared-absorption spectra of carbonium ions and hydrated hydronium ions, and bond-selective photodissociation through electric excitation. DOE

N91-29869# Lawrence Livermore National Lab., CA.
SINGLE-SCATTER MONTE CARLO COMPARED TO CONDENSED HISTORY RESULTS FOR LOW ENERGY ELECTRONS
C. T. Ballinger, D. E. Cullen, S. T. Perkins, J. A. Rathkopf, W. R. Martin, and S. J. Wilderman (Michigan Univ., Ann Arbor.) May 1991 27 p Presented at the 5th International Symposium on Radiation Physics, Dubrovnik (Yugoslavia), 10-14 Jun. 1991
(Contract W-7405-eng-48)
(DE91-015176; UCRL-JC-107067; CONF-910606-1) Avail: NTIS HC/MF A03

A Monte Carlo code was developed to simulate individual electron interactions. The code was instrumental in determining the range of validity for the widely used condensed history method. This task was accomplished by isolating and testing the condensed history assumptions. The results show that the condensed history method fails for low energy electron transport due to inaccuracies in energy loss and spatial positioning. DOE

N91-29870# Brookhaven National Lab., Upton, NY.
ALGEBRAIC APPROACHES TO NUCLEAR STRUCTURE
R. F. Casten (Brookhaven National Lab., Upton, NY.) 1991 18 p Presented at the Nuclear Shapes and Nuclear Structure at Low Excitation Energies, Cargese (France), 3-7 Jun. 1991
(Contract DE-AC02-76CH-00016)
(DE91-015214; BNL-46279; CONF-9106196-2) Avail: NTIS HC/MF A03

The concept and application of algebraic models to nuclear structure is surveyed with emphasis on interpretations in terms of traditional geometric models. Recent studies relating to the relationship between (beta) and (gamma) vibrations in deformed nuclei, to the rigidity or softness of axial asymmetry, to signature splitting in octupole excitations, to O(6) quantum numbers and multi-phonon excitations, and to pseudo-SU(3) are discussed. DOE

N91-29871# Sandia National Labs., Albuquerque, NM.
ANALYZING PHOTOGRAPHICALLY RECORDED ATOMIC EMISSION SPECTRA USING AN AUTOMATED DENSITOMETER
W. A. Hareland Jul. 1991 20 p
(Contract DE-AC04-76DP-00789)
(DE91-015368; SAND-89-1371) Avail: NTIS HC/MF A03

This report describes a computer-controlled densitometer and software designed for qualitative and semiquantitative analyses of photographically recorded atomic emission spectra. The instrument provides a number of operational features and unique capabilities for spectrochemical analyses. The purpose of this research was the evaluation of the automated densitometer system and computer algorithms for identifying and measuring atomic emission spectra from photographs. DOE

N91-29872# Kansas Univ., Lawrence. Dept. of Chemistry.
ATOMIC PHYSICS IN STRONG FIELDS
Shih-I Chu Jun. 1991 9 p
(Contract DE-FG02-90ER-14159)
(DE91-015393; DOE/ER-14159/1) Avail: NTIS HC/MF A02

This report discusses the following topics: nonadiabatic geometric phases of multiphoton transitions; nonperturbative treatments of level shifts of excited states in strong fields; multiple high-order harmonic generation in intense laser fields; quantum fractal character of quasi-energy states in multi-color fields; complex scaling Fourier-grid Hamiltonian method for intense-field multiphoton resonances; and microwave driven multiphoton excitation dynamics in Rydberg atoms: Fast Fourier transformation propagation method. DOE

N91-29873# Stanford Linear Accelerator Center, CA.
STUDY OF NUCLEAR EFFECTS IN THE DEUTERON AND EXTRACTION OF NEUTRON TO PROTON STUCTURE FUNCTION RATIO
A. Bodek, S. Dasu, and S. E. Rock (American Univ., Washington, DC.) Jun. 1991 4 p Presented at the 4th Conference on the Intersections Between Particle and Nuclear Physics, Tucson, AZ, 23-29 May 1991
(Contract DE-AC03-76SF-00515)
(DE91-015484; SU-SLAC-PUB-5598; CONF-9105106-16) Avail: NTIS HC/MF A01

We performed a combined analysis of electron, muon, neutrino, and anti-neutrino deep inelastic scattering structure functions of hydrogen and deuterium, within the framework of a quark-parton model. The neutron to proton structure function ratio was obtained using three different techniques: electron and muon scattering experiments on deuterium and hydrogen by using traditional Fermi motion corrections; extrapolation of the EMC effect on heavy targets to deuterium and free nucleons; and using Be and C data. At high x there is a disagreement between these data. DOE

N91-29874# George Washington Univ., Washington, DC. Dept. of Chemistry.
QUANTITATIVE INTERPRETATION OF AUGER LINESHAPES AND ELECTRON/PHOTON STIMULATED DESORPTION Final Report, 1 Oct. 1988 - 28 Feb. 1991
David E. Ramaker 28 Feb. 1991 7 p
(Contract N00014-89-J-1103)
(AD-A237138) Avail: NTIS HC/MF A02 CSCL 20/5

This project has involved a quantitative theoretical interpretation of electron spectroscopic data with a view toward elucidating the chemical environment and electronic structure of atoms in the bulk and adsorbed on solid surfaces. XPS, XAS, and AES data was examined for the high temperature superconductors, and CEELS, AES, and NEXAFS data for chemisorbed carbon species on metals. Electron/photon stimulated desorption (ESD/PSD) was also of interest. Here, an interpretation of spectroscopic data allowed for the first quantitative determination of a dissociative attachment cross section on a surface and new knowledge about the trajectory of the desorbing atom. GRA

N91-29875# California Univ., Davis. Dept. of Chemistry.
SOLVENT EFFECTS ON SIMPLE ELECTRON TRANSFER REACTIONS. A COMPARISON OF RESULTS IN DEBYE AND NON-DEBYE SOLVENTS
W. R. Fawcett and Colby A. Foss, Jr. 20 May 1991 18 p
(Contract N00014-90-J-1235)
(AD-A237157; TR-10) Avail: NTIS HC/MF A03 CSCL 20/5

Estimation of the longitudinal relaxation time for non-Debye solvents is considered on the basis of Hynes' theory for solvents exhibiting more than one relaxation process. It is shown that the major portion of the solvent effect on electron transfer kinetics in these solvents follows that in Debye solvents when the high frequency limiting value is used. The solvent effect on the outer sphere contribution to the Gibbs energy of activation is then examined with respect to the variation in solvent permittivity. Analysis of the available data suggests that the reactants involved in electron transfer are solvated mainly by solvent monomers such that the dielectric constant in the vicinity of the reactant is considerably reduced in protic solvents. GRA

N91-29876# California Univ., Davis. Dept. of Chemistry.
ROLE OF THE SOLVENT IN KINETICS OF HETEROGENEOUS ELECTRON AND ION TRANSFER REACTIONS
W. R. Fawcett and Colby A. Foss, Jr. 20 May 1991 11 p
(Contract N00014-90-J-1235)
(AD-A237168; TR-12) Avail: NTIS HC/MF A03 CSCL 07/4

Solvent effects studied in simple heterogeneous redox reactions, and for amalgam formation reactions were reviewed. It is emphasized that on the basis of a regression analysis of the data, solvent effects relating to the pre-exponential factor of the electron transfer rate constant can be separated from those for the exponential term. Analysis of data in non-Debye solvents such as the alcohols shows that the parameters relating to the second dielectric relaxation process are more important than those for the first in determining the magnitude of the rate constant. Examination of solvent effects for amalgam formation reactions reveals that they are quite different from those observed in electron transfer processes. As a result, it is concluded that the rate determining step in the amalgam formation reaction is ion transfer, not electron transfer, and that this rate limiting step is often located in the inner part of the double layer. Data recently obtained for the electroreduction of Cu(I) in the nitrile solvents are presented and discussed with respect to solvent trends found for other systems. GRA

N91-29877# Massachusetts Inst. of Tech., Cambridge.
THE ATOMIC STRAIN TENSOR Technical Report, 1990 - 1991
Peter Mott, Ali S. Morgan, and Ulrich W. Sutter 31 May 1991 23 p
(Contract N00014-86-K-0768)
(AD-A237287; TR-23) Avail: NTIS HC/MF A03 CSCL 20/11

A definition of the local atomic strain increments in three dimensions and an algorithm for computing them is presented. An arbitrary arrangement of atoms is tessellated into Delaunay tetrahedra, identifying interstices, and Voronol polyhedra, identifying atomic domains. The deformation gradient increment tensor for interstitial space is obtained from the displacement increments of the corner atoms of Delaunay tetrahedra. The atomic site strain increment tensor is then obtained by finding the intersection of the Delaunay tetrahedra with the Voronol polyhedra, accumulating the individual deformation gradient contributions of the intersected Delaunay tetrahedra into the Voronol polyhedra. An example application is discussed, showing how the atomic strain clarifies the relative local atomic movement for a polymeric glass treated at the atomic level. GRA

N91-29878# Purdue Univ., West Lafayette, IN. Dept. of Chemistry.
THE EFFECTS OF DONOR-ACCEPTOR ELECTRONIC INTERACTIONS ON THE RATES OF GAS-PHASE METALLOCENE ELECTRON-EXCHANGE REACTIONS
D. K. Phelps, J. R. Gord, B. S. Freiser, and M. J. Weaver 31

May 1991 25 p
(Contract N00014-91-J-1409)
(AD-A237459; TR-99) Avail: NTIS HC/MF A03 CSCL 07/4

Rate constants for electron self exchange, kax, of five cobaltocenium-cobaltocene and ferrocenium-ferrocene couples in the gas phase have been measured by means of Fourier transform ion cyclotron resonance mass spectrometry in order to explore the possible effects of donor-acceptor electronic coupling on gas-phase redox reactivity. The systems studied were selected in view of the substantial variations in electronic coupling inferred on the basis of their solvent-dependent reactivities and on theoretical grounds. The sequence of kax values determined in the gas phase is roughly similar to that observed in solution, although the magnitude of the kax variations is smaller in the former case. The likely origins of these differences in gas-phase reactivity are discussed in light of the known variations in the electronic coupling matrix element H12, inner-shell reorganization energy. GRA

N91-29879# Purdue Univ., West Lafayette, IN. Dept. of Chemistry.
TEMPERATURE DEPENDENCE OF PROTON ELECTROREDUCTION KINETICS AT GOLD(111) AND (210) SURFACES
A. Hamelin, L. Stoicoviciu, S. C. Chang, and M. J. Weaver 31 May 1991 24 p
(Contract N00014-91-J-1409)
(AD-A237460; TR-98) Avail: NTIS HC/MF A03 CSCL 07/4

Rate-potential data are reported for proton electroreduction on Au(111) and (210) in acidic perchlorate electrolytes over the temperature range 0 to 60 C, and examined with regard to temperature dependence of the transfer coefficient alpha. Since the Tafel plots exhibit significant curvature the analysis requires information on the temperature-dependent thermodynamics (i.e., the reaction entropy) for the proton discharge step. This was estimated from temperature-dependent voltammetry of reversible proton discharge to form adsorbed hydrogen on platinum. When evaluated at a constant overpotential for the proton discharge step, alpha for this reaction on both Au(111) and (210) is independent of temperature. An effect of electrocatalysts for proton reduction on Au(111) engendered by prior voltametric oxide formation was also observed. This effect is attributed to formation of surface defects on the basis of recently reported scanning tunneling microscopy data. Surface structural changes are also evident in the morphology of cyclic voltammograms obtained in the double-layer region. Electrochemical effects disappear with time when potential is held in the double layer region, and more rapidly at higher temperatures. GRA

N91-29880# Purdue Univ., West Lafayette, IN. Dept. of Chemistry.
SOLVENT DYNAMICAL EFFECTS IN ELECTRON TRANSFER: THE SOLVENT INERTIAL LIMIT AND THE PREDICTED INFLUENCE OF QUANTUM EFFECTS
G. W. McManis, A. Gochev, and M. J. Weaver 31 May 1991 40 p
(Contract N00014-91-J-1409)
(AD-A237462; TR-101) Avail: NTIS HC/MF A03 CSCL 07/4

Analytical continuum formulations for the solvent inertial frequency, constituting the anticipated zero-friction limit for adiabatic barrier crossing in solvent-controlled electron-transfer processes, are derived and discussed. The role of the solvent inertia in solvent dynamical effects is discussed with emphasis on the likely modifications brought about by nuclear tunneling. Approximate formulations suitable for assessing the latter correction in the presence as well as absence of solvent friction are outlined and compared. Numerical calculations are provided that illustrate the partly compensatory influence on the rate-solvent friction dependence resulting from nuclear tunneling together with reaction nonadiabaticity. Such combined quantum effects are anticipated typically to mask the clearcut emergence of solvent inertial effects on electron-transfer reaction dynamics in common low-friction media. GRA

N91-29881# Oak Ridge National Lab., TN.
NEGATIVE ION FORMATION WITH ELECTRON IMPACT TO SIMULANTS Final Report, Jul. 1987 - Dec. 1990
P. G. Datskos, L. A. Pinaduwage, L. G. Christophorou, and J. G. Carter Dec. 1990 66 p
(MIPR-FY1455-88-N065; AF Proj. 2301)
(AD-A237478; WL-TR-91-2019) Avail: NTIS HC/MF A04 CSCL 15/6

The report describes the electron capture properties and ensuing fragmentation pattern of 11 chemical agent simulants: (1) DMMP; (2) DIMP; (3) nBM; (4) 2CLES; (5) MS; (6) TEP; (7) DMP; (8) DE3CLMP; (9) DECLP; (10) DECLMP; and (11) DECyMP. The electron attachment coefficient and drift velocity of the negative ions were measured by three techniques: (1) time of flight mass spectrometry, (2) electron swarm with pulse height analysis, and (3) electron swarm with pulsed Townsend method. GRA

N91-29882# Purdue Univ., West Lafayette, IN. Dept. of Chemistry.
ELECTRON-TRANSFER REACTIONS AT METAL-SOLUTION INTERFACES: AN INTRODUCTION TO SOME CONTEMPORARY ISSUES
M. J. Weaver 31 May 1991 18 p
(Contract N00014-91-J-1409)
(AD-A237506; TR-105) Avail: NTIS HC/MF A03 CSCL 07/4

Some pivotal aspects of the contemporary treatment of electrochemical kinetics for one electron redox couples are outlined, and some commonalities with homogeneous phase electron transfers are pointed out. Two illustrative examples of the interplay between theory and experiment are briefly discussed: specifically to the relation between the rates of electrochemical and homogeneous phase processes; and to the recognition and elucidation of dynamical solvent effects. Author (GRA)

N91-29883# Purdue Univ., West Lafayette, IN. Dept. of Chemistry.
COMPARISONS BETWEEN SCANNING TUNNELING MICROSCOPY AND OUTER-SPHERE ELECTRON-TRANSFER RATES AT Pt(111) SURFACES COATED WITH ORDERED IODINE ADLAYERS
S. C. Chang, S. L. Yau, B. C. Schardt, and M. J. Weaver 31 May 1991 40 p
(Contract N00014-91-J-1409)
(AD-A237507; TR-102) Avail: NTIS HC/MF A03 CSCL 09/1

Rate parameters are reported for the electroreduction of eight CoIII(NH3)5X complexes at ordered Pt(111) surfaces coated with iodine adlayers whose structures are characterized by scanning tunneling microscopy (STM) in order to explore possible correlations between the outer-sphere electron transfer kinetics and the spatially resolved adlattice properties as revealed by STM. The sixth ligands: acetates, and three cyclic organic carboxylates, were selected to vary the reactant charge, and hence the magnitude of electrostatic double layer effects, and to examine the effect of potential organic mediators. The ordered Pt(111) surfaces were prepared by flame annealing, followed by cooling in a stream of nitrogen over iodine crystals. GRA

N91-29884# Purdue Univ., West Lafayette, IN. Dept. of Chemistry.
ATOMIC-RESOLUTION SCANNING TUNNELING MICROSCOPY AND INFRARED SPECTROSCOPY AS COMBINED IN-SITU PROBES OF ELECTROCHEMICAL ADLAYER STRUCTURE: CARBON MONOXIDE ON RHODIUM(111)
S. L. Yau, X. Gao, S. C. Chang, B. C. Schardt, and M. J. Weaver 31 May 1991 48 p
(Contract N00014-91-J-1409)
(AD-A237508; TR-106) Avail: NTIS HC/MF A03 CSCL 20/5

In-situ scanning tunneling microscopy (STM) was combined with infrared reflection-absorption spectroscopy (IRRAS) to yield detailed atomic level adlayer structures for saturated coverages of CO on ordered Rh(111) in aqueous solutions. Two distinctly different structures were obtained in CO-containing 0.1 M NaClO4, depending on the electrode potential. At higher potentials, ca -0.1

to 0.3 V vs. SCE, atomic-resolution STM images were obtained that indicated the presence of a (2 x 2)-3CO unit cell, having a CO coverage in agreement with electrochemical and IRRAS measurements. The corresponding in-situ infrared spectra indicate the presence of two atop (or near-atop) and one twofold bridging CO in the unit cell. A real space structure is suggested that is related to the corresponding (2 x 2)-3CO adlattice on Rh(111) in uhv as deduced previously by low energy electron diffraction and vibrational spectroscopy. GRA

N91-29885# Harvard Univ., Cambridge, MA.
STUDY OF ENERGY LEVELS AND DECAY MECHANISMS FOR SINGLET RYDBERG STATES OF MOLECULAR NITROGEN Final Report, 4 Mar. 1987 - 4 Mar. 1991
F. M. Pipkin 4 Jun. 1991 73 p
(Contract F19628-87-K-0031)
(AD-A238156) Avail: NTIS HC/MF A04 CSCL 20/5

This report summarizes a series of investigations of the singlet Rydberg states of molecular nitrogen. The object of the research was to use laser excitation out of the metastable state of N2 to study the energy levels and decay mechanisms for the high lying singlet Rydberg and valence states. Two techniques were used to produce molecules in the metastable state -- electron excitation of N2 molecules in a thermal beam and charge capture by a fast beam of N2 ions. The first section summarizes the current knowledge of these states. The second section describes the measurements of the energy levels and lifetimes for individual notational levels. The third section describes the measurements of the lifetime of the metastable level which used a uv spectrometer and a pulsed electron beam. The fourth section summarizes a number of experiments which were not successful. GRA

N91-29886# State Univ. of New York, Buffalo. Dept. of Chemistry.
CHARGE MOTION EFFECTS IN IONIC CLUSTERS
Isidore Last and Thomas F. George Jul. 1991 16 p
(Contract N00014-90-J-1193)
(AD-A238178; WSU/DC/91/TR-53) Avail: NTIS HC/MF A03 CSCL 20/5

In ionic clusters, the polarization depends on the dynamics of charge delocalization. The polarization follows the charge motion when the characteristic time of motion is much longer than the polarization time (adiabatic polarization). For the opposite case (diabatic polarization), the polarization is determined by an average field. These two kinds of polarization are considered for the ionic clusters Xe2(+)R and benzene +R (R=He, Ne, Ar). GRA

N91-29887# Maryland Univ., College Park. Inst. for Physical Science and Technology.
LASER-ATOM INTERACTION AT HIGH INTENSITIES Final Report, 1 Jan. 1988 - 31 Dec. 1990
T. J. McIlrath and C. W. Clark 20 May 1991 7 p
(Grant AF-AFOSR-0098-88; AF Proj. 2301)
(AD-A238231; AFOSR-91-0593TR) Avail: NTIS HC/MF A02 CSCL 20/10

A general program has been developed to calculate multiphoton processes in atomic hydrogen to arbitrarily high order in perturbation theory. This program can be used to calculate quantities in intense field multiphoton processes, such as the generalized cross section of multiphoton absorption, the a.c. Stark effect (shift and the broadening of the level due to the field interaction), and the parameters in nonlinear optics such as the nonlinear index of refraction and the nonlinear susceptibility. Effective parametrization of high-order susceptibilities has been achieved over a wide range of frequencies, utilizing concepts from quantum defect theory to express the results of lengthy calculations in a compact form that also permits extrapolation across thresholds and resonance poles. Significant progress has been made in direct numerical solution of the time-dependent Schroedinger equation. In addition, contributions have been made in: understanding the role of spatial dimensionality in the solution of model systems (e.g., the one-dimensional delta-function potential); the development of a general R-matrix code for perturbative computations of multiphoton processes in many-electron atoms; and multiphoton ionization with two commensurate laser frequencies. GRA

N91-29888# California Univ., Los Angeles. Dept. of Chemistry and Biochemistry.
THE RELATIVE STABILITY AND POSSIBLE STRUCTURAL FORMULAE OF THE NEGATIVELY CHARGED SILVER MONOIODIDE CLUSTERS
Clifton K. Fagerquist, Dilip K. Sensharma, and Mostafa A. ElSayed 8 Jul. 1991 33 p
(Contract N00014-89-J-1350)
(AD-A238398; TR-71) Avail: NTIS HC/MF A03 CSCL 20/5

We have determined the relative mass peak intensities of Ag(X)(-) and (Ag(X)I)(-) clusters formed from the sputtering of isotopically enriched silver foil in the presence and absence of CH3I vapor. The important results can be summarized as follows: (1) the relative intensity of the Ag(X)(-) mass peaks showed a steady decrease with increasing X (due to the drop in their formation probability) with oscillations the correlate well with the previously published electron affinities of the corresponding Ag(X) neutral clusters (which is in agreement with the jellium model predictions) and thus reflects the relative stability of the Ag(X)(-) clusters; (2) an oscillatory correlation and the shell closing effect for eight delocalized electrons is found between the measured electron affinities (EA) for Ag(X) and mass peak intensities of the clusters (Ag(X+1)I)(-) and not with the (Ag(X)I)(-) mass peak intensities. GRA

N91-29889# Johns Hopkins Univ., Baltimore, MD.
STUDY OF ELEMENTARY REACTIONS AND ENERGY TRANSFER PROCESSES INVOLVING THE NH AND CN FREE RADICALS Final Report, 15 Apr. 1988 - 14 Apr. 1991
Paul J. Dagdigian and Millard H. Alexander 14 Jun. 1991 24 p
(Contract DAAL03-88-K-0031)
(AD-A238461; ARO-25425.21-CH) Avail: NTIS HC/MF A03 CSCL 20/5

Collaborative theoretical and experimental studies of a variety of elementary chemical reactions and collisional energy transfer processes involving small molecular free radicals, with particular emphasis on the NH and CN molecules, have been carried out. Specific topics studied include: molecular free radicals, collisional energy transfer, chemical reactions, excited states, and molecular decomposition. GRA

N91-29890# Cornell Univ., Ithaca, NY. Dept. of Chemistry.
REACTIONS OF HYDROGEN ATOMS IMPORTANT TO THE DECOMPOSITION OF ENERGETIC MATERIALS Final Report
Paul L. Houston 9 May 1991 15 p
(Contract DAAL03-88-K-0034)
(AD-A238482; ARO-25502.1-CH) Avail: NTIS HC/MF A03 CSCL 20/5

A new technique for characterizing the velocity distributions of state-selected reaction products was developed for analyzing the reactions of hydrogen atoms: the three dimensional velocity distribution of product fragments is determined by ionizing the appropriate species, waiting for a delay while the species separate along their trajectories, and then projecting the spatial distribution of ions onto a two-dimensional screen. The objectives of this work were to develop the new technique and, eventually, to use it to characterize the reactions of hydrogen atoms with NO2, CH3HNO2, and H2NNO2. GRA

N91-29891# California State Univ., Northridge.
SPIN-LABEL-SPIN-PROBE. STUDIES OF BIMOLECULAR ENCOUNTERS IN MICELLES Final Report, 15 Oct. 1987 - 31 Dec. 1990
Barney L. Bales 26 Feb. 1991 11 p
(Contract DAAL03-88-K-0006)
(AD-A238546; ARO-24944.8-CH) Avail: NTIS HC/MF A03 CSCL 12/1

A new method, based on EPR, to study the bimolecular collision rate between additives at the surface of micelles was developed.

In order to study the collision rate in these compartmentalized systems, a detailed understanding of the number distribution function of the additives is crucial. A completely random distribution of the additives is described by the Poisson distribution. A primary goal of this project was to develop a method to measure the collision rate between additives on the same micelle. This is accomplished by deducing the collision-induced linewidth broadening of the ESR spectrum. GRA

N91-29892# Brandeis Univ., Waltham, MA. Dept. of Physics.
RESEARCH IN ELEMENTARY PARTICLE PHYSICS
L. E. Kirsch, H. J. Schnitzer, L. F. Abbott, J. R. Bensinger, and C. A. Blocker 1991 29 p
(Contract DE-AC02-76ER-03230)
(DE91-015359; DOE/ER-03230/T10) Avail: NTIS HC/MF A03

This report discusses the following topics: Z neutral boson decay asymmetry; B-anti-B mixing; top quark search; measurement of the inclusive central jet cross section; search for pair produced leptoquarks at cdf; direct photon production; calibration of cdf; hadronic energy scale for the cdf central calorimeters; skyrme model; two and three dimensional field theory; the path integral on a branched manifold; and mean-field theory of neural networks. DOE

N91-29893# Pacific Northwest Lab., Richland, WA.
REEVALUATION OF S-VALUES CONSIDERING ELECTRON TRANSPORT
G. Akabani and J. W. Poston, Sr. (Texas A&M Univ., College Station.) May 1991 11 p Presented at the 5th International Radiopharmaceutical Dosimetry Symposium, Oak Ridge, TN, 7-10 May 1991
(Contracts DE-AC06-76RL-01830; DE-FG05-88ER-60707)
(DE91-015428; PNL-SA-19740; CONF-910529-4) Avail: NTIS HC/MF A03

Electron-specific absorbed fractions were calculated for selected organs and regions of the mathematical reference man. The organs or regions considered were those with high surface-to-volume ratio, organs with walls, and organs that have subdivisions. The calculated specific absorbed fractions for electrons are a complement to be used with the Medical Internal Radiation Dose (MIRD) methodology. New estimates of S-values for 80 radionuclides were calculated using the new electron-specific absorbed fractions for 21 combinations of source-target regions and were compared with those already published in MIRD Pamphlet No. 5 Revised. Small differences in S-values were found by using electron specific absorbed fractions when the source organ is the target organ. However, large differences in S-values were found for those organs with walls. DOE

N91-29894# Argonne National Lab., IL.
SUPERDEFORMATION: AN EXPERIMENTAL REVIEW
R. V. F. Janssens 1991 15 p Presented at the Nuclear Shapes and Nuclear Structure At Low Excitation Energies, Cargese, France, 3-7 Jun. 1991
(Contract W-31-109-eng-38)
(DE91-015566; ANL/CP-73370; CONF-9106196-3) Avail: NTIS HC/MF A03

The discovery of a superdeformed (SD) band of 19 discrete transitions in the nucleus Dy-152(1) is at the origin of the formidable experimental and theoretical effort which has allowed for much progress in the unraveling of the main properties of superdeformation. Over the last five years, many unexpected features have been discovered. In fact, just as soon as a new feature has been explained invariably the next observation has highlighted another surprising phenomenon. The net result of all the activity has been a dramatic increase of our understanding of rapidly rotating nuclei. The organizers of this conference have asked me to review the present status of the field: this is clearly an impossible task within the allowed space and time. Fortunately, the subject has recently been reviewed on several occasions, and therefore, I will only attempt to present here some of the general features that have emerged thus far, and discuss some of the important open questions. The discussion will be restricted to SD nuclei in the A=150 and A=190 regions, i.e., to the nuclei with the largest quadrupole deformations and will address four main issues. First, the evidence for the stiffness of the SD minimum will be reviewed. This section will be followed by discussions on the role of pairing and of specific quasiparticle configurations in the second well. Evidence for other effects at large deformation will be addressed in the section as well. The discussion will then address the issue of the so-called identical bands and will conclude with a brief presentation on the feeding and decay of SD nuclei. DOE

N91-29895# Brookhaven National Lab., Upton, NY.
STRANGE QUARKS IN NUCLEI
C. B. Dover Jun. 1991 16 p Presented at the 4th Conference on the Intersections Between Particle and Nuclear Physics, Tucson, AZ, 23-29 May 1991
(Contract DE-AC02-76CH-00016)
(DE91-015833; BNL-46322; CONF-9105106-20) Avail: NTIS HC/MF A03

We survey the field of strange particle nuclear physics, starting with the spectroscopy of strangeness S = -1 Lambda hypernuclei, proceeding to an interpretation of recent data on S = -2 Lambda Lambda hypernuclear production and decay, and finishing with some speculations on the production of multi-strange nuclear composites (hypernuclei or strangelets) in relativistic heavy ion collisions. DOE

N91-29896# Texas Univ., Austin. Inst. for Fusion Studies.
ANALYTICAL CALCULATION OF NEUTRAL TRANSPORT AND ITS EFFECT ON IONS
M. D. Calvin, R. D. Hazeltine, P. M. Valanju, and E. R. Solano Jun. 1991 26 p
(Contract DE-FG05-80ET-53088)
(DE91-015908; DOE/ET-53088/489; IFSR-489) Avail: NTIS HC/MF A03

We analytically calculate the neutral particle distribution and its effects on ion heat and momentum transport in three-dimensional plasmas with arbitrary temperature and density profiles. A general variational principle taking advantage of the simplicity of the charge-exchange (CX) operator is derived to solve self-consistently the neutral-plasma interaction problem. To facilitate an extremal solution, we use the short CX mean-free-path (lambda(sub x)) ordering. Further, a non-variational, analytical solution providing a full set of transport coefficient is derived by making the realistic assumption that the product of the CX cross section with relative velocity is constant. The effects of neutrals on plasma energy loss and rotation appear in simple, sensible forms. We find that neutral viscosity dominates ion viscosity everywhere, and in the edge region by a large factor. DOE

N91-29897# Alabama Univ., Huntsville. Dept. of Physics.
STUDY OF PARTICLE CORRELATIONS IN HIGH ENERGY S + Pb AND Pb + Pb INTERACTIONS WITH A MAGNETIC-INTERFEROMETRIC-EMULSION-CHAMBER
Yoshiyuki Takahashi Apr. 1991 8 p
(Contract DE-FG05-88ER-40467)
(DE91-014355; DOE/ER-40467/6) Avail: NTIS HC/MF A02

Exploratory investigations were made in 1986 with 200 GeV/AMU O-16, followed by the second phase experiments with S-32 ions in 1987, and again in 1990, by using the SPS accelerator of the European Center for Nuclear Research (CERN), Geneve, Switzerland. The UAH experimental nuclear group of the present project carries out studies on collisions of these heavy nuclei with target lead nucleus, using a newly invented instrument. This instrument, composed of emulsion films with spacer materials in a high magnetic field, provides spectroscopic details of particles produced in a collision. The instrument is called the Magnetic-Interferometric-Emulsion-Chamber, and has evolved further as a hybrid detector coupled with microstrip silicone ring counters. Within the past year a new, improved run with a 200 GeV/n sulfur beam was successfully carried out at the H3 beam line in the West Hall at CERN. The SPS Supercycle, being installed after July 1989, had caused some timing conflicts of heavy-ion

run with LEP operation. Due to the very limited kicker timing allowed, kicking out the unwanted beam particles after irradiating specified number of ions at each pulse was not perfectly achieved. Consequently, kicker failures frequently occurred for about 40 percent of the run. Nevertheless, the EMU05 provided a sufficiently large number of chambers to save the experiments from overdose damage. The EMU05 run used improved MAGIC detector, which gives a momentum resolution to 5.2 percent, while previous detectors were limited to 14 percent accuracy. DOE

N91-29898# Sandia National Labs., Albuquerque, NM.
NMR SPECTROSCOPY OF EXPERIMENTALLY SHOCKED SILICATE MINERALS
R. T. Cygan, M. B. Boslough, and R. J. Kirkpatrick (Illinois Univ., Urbana.) 1991 15 p Presented at the 1991 American Physical Society (APS) Conference on Compression of Condensed Matter, Houston, TX, 18-22 Mar. 1991
(Contract DE-AC04-76DP-00789)
(DE91-014897; SAND-91-0122C; CONF-9103186-1) Avail: NTIS HC/MF A03

Magic-angle spinning nuclear magnetic resonance (MAS NMR) techniques were used to analyze experimentally shocked quartz and feldspar powders. Si-29 NMR spectra were determined for quartz and labradorite feldspar and Al-27 and Na-23 spectra for labradorite. Both minerals were shocked to 7.5, 16.4, and 22 GPA using the Sandia Momma Bear recovery fixtures. The MAS NMR results for quartz are in full agreement with previous measurements, indicating a high degree of reproducibility. Numerical decomposition of quartz data are consistent with two distinct phases: a defective crystalline quartz and an amorphous-like silica phase. There is a strong correlation between the fraction of amorphous phase and the mean peak shock pressure. The labradorite data are much more complicated, consisting of multiple peaks with no obvious correlation with shock pressure. No amorphous phase was evident from the NMR spectra of the shocked labradorite, nor were high pressure phases detectable for either mineral. DOE

N91-29899# Lawrence Livermore National Lab., CA.
CHASING THE x(SUB f) DEPENDENCE OF J/PSI PRODUCTION
R. Vogt 10 Jun. 1991 8 p Presented at the 4th Conference on the Intersections Between Particle and Nuclear Physics, Tucson, AZ, 23-29 May 1991
(Contract W-7405-eng-48)
(DE91-015136; UCRL-JC-107505; CONF-9105106-12) Avail: NTIS HC/MF A02

The combined effects are discussed of hard scattering processes and intrinsic heavy-quark components in the hadron wavefunction on the x sub f dependence of J/psi production. The A dependence arises from nuclear absorption, comover interactions, shadowing of parton distributions, and intrinsic heavy quarks. DOE

N91-29900# Temple Univ., Philadelphia, PA. Dept. of Physics.
MIXED VALENT AND HEAVY FERMIONS AND RELATED SYSTEMS
P. Schlottmann 15 Apr. 1991 32 p
(Contract DE-FG02-87ER-45333)
(DE91-015454; DOE/ER-45333/1) Avail: NTIS HC/MF A03

The main objective of the project is to gain a better understanding of highly correlated fermion systems. High correlations appear in a variety of solid state phenomena: mixed-valence and heavy-fermions or Kondo systems; superfluid and normal He-3; high-temperature superconductors; magnetism in low dimensions; quantum Hall effect; spin-fluctuations in transition metals; giant magnetic moments; tunneling of an atom interacting with a degenerate electron gas; quantum dissipative systems; organic superconductors; etc. The primary focus of the work is on valence mixing and heavy fermions, but elated highly correlated systems are also studied. A brief summary of the achievements is presented under the following headings: (1) heavy fermions-mixed valence-Kondo; (2) magnetism in low dimensions; (3) narrow band phenomena/Hubbard model; and (4) collaborations with experimentalists. DOE

N91-29901# Massachusetts Univ., Amherst. Dept. of Physics and Astronomy.
MEDIUM ENERGY NUCLEAR PHYSICS RESEARCH
G. A. Peterson, J. F. Dubach, R. S. Hicks, and R. A. Miskimen Jun. 1991 62 p
(Contract DE-FG02-88ER-40415)
(DE91-015740; DOE/ER-40415/18) Avail: NTIS HC/MF A04

Research on the following topics is discussed: Transverse from factors of (Sn-117); Elastic magnetic electron scattering from C-13 at Q(exp 2) = 1 GeV(exp 2)/sq c; A reanalysis of C-13 elastic scattering; Deuteron threshold electrodisintegration; Measurement of the elastic magnetic form factor of He-3 at high momentum transfer; Coincidence measurement of the D(electron, electron proton) cross section at low excitation energy and high momentum transfer; Measurement of the quadrupole contribution to the N yields Delta excitation; measurement of the x-, Q(exp 2)-, and A-dependence of R = sigma sub L/sigma sub T; The PEGASYS project; PEP beam-gas event analysis; Plans for other experiments at SLAC, i.e., polarized electron scattering on polarized nuclei; Experiment PR-89-015 (study of coincidence reactions in the dip and delta resonance regions); Experiment PR-89-031 (multi-nulceon knockout using the CLAS detector); Drift chamber tests; A memorandum of understanding and test experiments; Photoprotons from (exp 10)B; And hadronic electroproduction at LEP. DOE

N91-29902# Pacific Northwest Lab., Richland, WA.
NEUTRON DOSIMETRY USING OPTICALLY STIMULATED LUMINESCENCE
S. D. Miller and P. A. Eschbach Jun. 1991 16 p Presented at the 11th Department of Energy Workshop on Personnel Neutron Dosimetry, Las Vegas, NV, 4-7 Jun. 1991
(Contract DE-AC06-76RL-01830)
(DE91-015781; PNL-SA-19592; CONF-9106235-3) Avail: NTIS HC/MF A03

The addition of thermoluminescent (TL) materials within hydrogenous matrices to detect neutron induced proton recoils for radiation dosimetry is a well known concept. Previous attempts to implement this technique have met with limited success, primarily due to the high temperatures required for TL readout and the low melting temperatures of hydrogen-rich plastics. Research in recent years PNL has produced a new Optically Stimulated Luminescence (OSL) technique known as the Cooled Optically Stimulated Luminescence (COSL) that offers, for the first time, the capability of performing extremely sensitive radiation dosimetry at low temperatures. In addition to its extreme sensitivity, the COSL technique offers multiple readout capability, limited fading in a one year period, and the capability of analyzing single grains within a hydrogenous matrix. DOE

N91-29903# Lawrence Livermore National Lab., CA.
ELECTRON-ION INTERACTION CROSS SECTIONS DETERMINED BY X RAY SPECTROSCOPY ON EBIT
P. Beiersdorfer, R. Cauble, S. Chantrenne, M. Chen, D. Knapp, R. Marrs, T. Phillips, K. Reed, M. Schneider, and J. Scofield et al 26 Jun. 1991 21 p Presented at the 17th International Conference on the Physics of Electronic and Atomic Collisions, Brisbane (Australia), 10-16 Jul. 1991
(Contract W-7405-eng-48)
(DE91-015786; UCRL-JC-107611; CONF-910746-2) Avail: NTIS HC/MF A03

The Livermore electron beam ion trap (EBIT) is used to measure electron-ion interactions with high-resolution x-ray spectroscopy. Measurements are presented of the K(alpha) x-ray emission of heliumlike Fe(24+) that demonstrate the effect of various processes on the spectrum of highly charged heliumlike ions. In particular, we have studied how dielectronic recombination into high-n Rydberg levels and resonance excitation processes contribute to the x-ray emission near threshold for direct electron-impact excitation. From these and other measurements we infer the cross sections for impact excitation of heliumlike

titanium, chromium, manganese, and iron. Comparing the results with theoretical cross sections from distorted-wave calculations we find excellent agreement for all transitions but the heliumlike resonance transition from 1s2p1 P1 to ground, whose excitation cross section is measured to be 10 to 20 percent smaller than calculated. DOE

73 NUCLEAR AND HIGH-ENERGY PHYSICS

Includes elementary and nuclear particles; and reactor theory.

For space radiation see *93 Space Radiation.*

N91-29904# Columbia Univ., New York, NY.
THEORETICAL HIGH ENERGY PHYSICS
T. D. Lee May 1990 30 p
(Contract DE-AC02-76ER-02271)
(DE90-012527; DOE/ER-02271/T5; COO-2271-113) Avail: NTIS HC/MF A03

This report discusses progress on theoretical high energy physics at Columbia University in New York City. Some of the topics covered are: Chern-Simons gauge field theories; dynamical fermion QCD calculations; lattice gauge theory; the standard model of weak and electromagnetic interactions; Boson-fermion model of cuprate superconductors; S-channel theory of superconductivity and axial anomaly and its relation to spin in the parton model. DOE

N91-29905# Columbia Univ., New York, NY.
THEORETICAL HIGH ENERGY PHYSICS
T. D. Lee 1991 33 p
(Contract DE-AC02-76ER-02271)
(DE91-013639; DOE/ER-02271/114; COO-2271-114) Avail: NTIS HC/MF A03

This report discusses theoretical research in high energy physics at Columbia University. Some of the research topics discussed are: quantum chromodynamics with dynamical fermions; lattice gauge theory; scattering of neutrinos by photons; atomic physics constraints on the properties of ultralight-ultraweak gauge bosons; black holes; Chern-Simons physics; S-channel theory of superconductivity; charged boson system; gluon-gluon interactions; high energy scattering in the presence of instantons; anyon physics; causality constraints on primordial magnetic manopoles; charged black holes with scalar hair; properties of Chern-Aimona-Higgs solitons; and extended inflationary universe. DOE

N91-29906# Ames Lab., IA.
ELECTROMAGNETIC DISSOCIATION OF Au AND Co TARGETS BY RELATIVISTIC HEAVY IONS Ph.D. Thesis
D. Schwellenbach 28 Jun. 1991 74 p
(Contract W-7405-eng-82)
(DE91-014915; IS-T-1500) Avail: NTIS HC/MF A04

This investigation is a part of ongoing series of experiments designed to extend the systematics of ED for various targets and projectiles. The goal of these experiments is to determine sigma(sub ED) for various combinations of projectile, projectile energy, and target. These cross sections are than compared to the theoretical predictions of a model based on the Weizsacker-Williams (WW) method. Determination of sigma(sub ED) entails first finding the total crossing section (sigma(sub tot)) for the reaction T(RHI,X)T', where T is the target RHI is the projectile, X is the remnant of the RHI after the reaction (the details of which are not studied in this series of experiments), and T' is the new state of the target (the target minus one neutron for the one-neutron removal reaction). Since sigma(sub tot) consists of contributions due to both ED and nuclear processes, sigma(sub nuc) must also be found for this reaction. Once sigma(sub tot) and sigma(sub nuc) are determined, sigma(sub ED) is given by sigma(sub ED) = sigma(sub tot) - sigma(sub nuc). In this investigation, Au-197 and Co-59 targets were irradiated by a beam of U-238 ions with an energy of 0.96 GeV per nucleon (0.96 GeV/A). The particular reactions of interest are Au-197(U-238,X)Au-196 and Co-59(U-238,X)Co-58. The cross sections for these reactions were found by studying the gamma-ray activity of Au-196 and Co-58 in the targets. The experimental value of sigma(sub ED) was compared to the value calculated using the WW method. Results of previous experiments are shown along with the results of the present study so that the systematics of ED can be studied. DOE

N91-29907# Brown Univ., Providence, RI. Dept. of Physics.
A RESEARCH PROGRAM IN EXPERIMENTAL AND THEORETICAL HIGH ENERGY PHYSICS
1 Jul. 1991 126 p
(Contract DE-AC02-76ER-03130)
(DE91-014728; DOE/ER-03130/821) Avail: NTIS HC/MF A07

This report discusses progress in high energy physics at Brown University. Some topics discussed are: quantum field theory; physics of the early universe; standard model and beyond; progress in computational physics; interactions of leptons and hadrons, with accelerator and astrophysical sources; and hadron collider and neutrino physics. DOE

N91-29908# Tufts Univ., Medford, MA. Dept. of Physics and Astronomy.
HIGH ENERGY PHYSICS AT TUFTS UNIVERSITY
R. H. Milburn and J. Schneps 15 Jun. 1991 129 p
(Contract DE-AC02-83ER-40085)
(DE91-015055; DOE/ER-40085/23) Avail: NTIS HC/MF A07

This report discusses Fermilab fixed target experiments; photoproduction at 20 GeV: exposures at a 40-inch hybrid hydrogen bubble chamber system to a 20 GeV polarized photon beam; the Soudan 2 nucleon decay project; physics at the antiproton-proton collider at (radical)s = 1.8 TeV; designing the solenoidal detector for the supercollider; charm physics; a neutrino telescope proposal; a general kinematic description of polarization in scattering processes; polarization in inclusive hyperon production and QCD subprocesses; measuring quark helicity underlying hadronic jets; scattering in extended skyrmion models and spin dependence; the diquark-quark model of the excited baryons; computation and networking; and the science and technology center. DOE

N91-29909# Oak Ridge National Lab., TN.
ELECTRON CAPTURE IN VERY LOW ENERGY COLLISIONS OF MULTICHARGED IONS WITH H AND D IN MERGED BEAMS
C. C. Havener, F. W. Meyer, and R. A. Phaneuf 1991 10 p Presented at the 17th International Conference on the Physics of Electronic and Atomic Collisions, Brisbane, Australia, 10-16 Jul. 1991
(Contract DE-AC05-84OR-21400)
(DE91-015617; CONF-910746-1) Avail: NTIS HC/MF A02

An ion-atom merged-beams technique is being used to measure total absolute electron-capture cross sections for multicharged ions in collisions with H (or D) in the energy range between 0.1 and 1000 eV/amu. Comparison between experiment and theory over such a large energy range constitutes a critical test for both experiment and theory. Total capture cross-section measurements for O(3+) + H(D) and O(5+) + H(D) are presented and compared to state selective and differential cross section calculations. Landau-Zener calculations show that for O(5+) the sharp increase in the measured cross section below 1 eV/amu is partly due to trajectory effects arising from the ion-induced dipole interaction between the reactants. DOE

N91-29910# Sandia National Labs., Albuquerque, NM.
TRITIUM-FIELD BETACELLS
R. J. Walko, R. C. Lincoln, W. E. Baca, S. H. Goods, and G. H. Negley (Astropower, Inc., Newark, DE.) 1991 16 p Presented at the 26th Intersociety Energy Conversion Engineering (IECE) Conference, Boston, MA, 3-9 Aug. 1991
(Contract DE-AC04-76DP-00789)
(DE91-014666; SAND-91-1364C; CONF-910801-8) Avail: NTIS HC/MF A03

Betavoltaic power sources operate by converting the nuclear decay energy of beta-emitting radioisotopes into electricity. Since they are not chemically driven, they could operate at temperatures which would either be too hot or too cold for typical chemical batteries. Further, for long lived isotopes, they offer the possibility of multi-decade active lifetimes. Two approaches are being investigated: direct and indirect conversion. Direct conversion cells consist of semiconductor diodes similar to photovoltaic cells. Beta particle directly bombard these cells, generating electron-hole pairs in the semiconductor which are converted to useful power. When using low power flux beta emitters, wide bandgap semiconductors are required to achieve useful conversion efficiencies. The combination of tritium, as the beta emitter, and gallium phosphide (GaP), as the semiconductor converter, was evaluated. Indirect conversion betacells first convert the beta energy to light with a phosphor, and then to electricity with photovoltaic cells. An indirect conversion power source using a tritium radioluminescent (RL) light is being investigated. Our analysis indicates that this approach has the potential for significant volume and cost savings over the direct conversion method. DOE

N91-29911# Lawrence Livermore National Lab., CA.
CONTROL OF ENERGY SWEEP AND TRANSVERSE BEAM MOTION IN INDUCTION LINACS
W. C. Turner 3 May 1991 7 p Presented at the 1991 Institute of Electrical and Electronics Engineers (IEEE) Particle Accelerator Conference (PAC), San Francisco, CA, 6-9 May 1991
(Contract W-7405-eng-48)
(DE91-015177; UCRL-JC-105566; CONF-910505-364) Avail: NTIS HC/MF A02

Recent interest in the electron induction accelerator has focussed on its application as a driver for high power radiation sources; free electron laser (FEL), relativistic klystron (RK) and cyclotron autoresonance maser (CARM). In the microwave regime where many successful experiments have been carried out, typical beam parameters are: beam energy 1 to 10 MeV, current 1 to 3 kA and pulse width 50 nsec. Radiation source applications impose conditions on electron beam quality, as characterized by three parameters; energy sweep, transverse beam motion and brightness. These conditions must be maintained for the full pulse duration to assure high efficiency conversion of beam power to radiation. The microwave FEL that has been analyzed in the greatest detail requires energy sweep less than (+ or -) 1 pct., transverse beam motion less than (+ or -) 1 mm and brightness approx. 1 x 10(exp 8)A/sq m sq rad. In the visible region the requirements on these parameters become roughly an order of magnitude more strigent. With the ETAII accelerator at LLNL the requirements were achieved for energy sweep, transverse beam motion and brightness. The recent data and the advances that have made the improved beam quality possible are discussed. The most important advances are: understanding of focussing magnetic field errors and improvements in alignment of the magnetic axis, a redesign of the high voltage pulse distribution system between the magnetic compression modulators and the accelerator cells, and exploitation of a beam tuning algorithm for minimizing transverse beam motion. The prospects are briefly described for increasing the pulse repetition frequency to the range of 5 kHz and a delayed feedback method of regulating beam energy over very long pulse bursts, thus making average power megawatt level microwave sources at 140 GHz and above a possibility. DOE

N91-29912# Wisconsin Univ., Madison. Dept. of Physics.
HIGH ENERGY PHYSICS: EXPERIMENTAL, THEORETICAL, AND PHENOMENOLOGY INSTITUTE
V. Barger, U. Camerini, D. Carlsmith, B. Durand, L. Durand, A. Erwin, W. Fry, C. Goebel, F. Halzen, and R. Loveless et al 1 May 1991 273 p
(Contract DE-AC02-76ER-00881)
(DE91-015737; DOE/ER-00881/T2) Avail: NTIS HC/MF A12

Research in the following areas are discussed: Hadron physics at Fermilab; Lepton hadron scattering; electromagnetic and weak interactions at the Stanford Linear Accelerator Center (SLAC); Hyperon beam program (hadroproduction of heavy beam flavors at Fermilab); Ultra high energy colliding beam physics; Institute for high energy physics phenomenology; Weak and electromagnetic interactions using PETRA at DESY and LEP at CERN; Theoretical high energy physics; DUMAND; Study of ultra high energy gamma rays; Data analysis facility; and R and D for major subsystems for the SSC detectors. DOE

N91-29913# Texas Univ., Austin.
A MESOSCOPIC LINEAR ACCELERATOR DRIVEN BY SUPERINTENSE SUBPICOSECOND LASER PULSES
B. Meerson (Hebrew Univ., Jerusalem, Israel) and T. Tajima Jun. 1991 14 p
(Contract DE-FG05-80ET-53088)
(DE91-015941; DOE/ET-53088/504; IFSR-504) Avail: NTIS HC/MF A03

We reconsider the idea of a solid-state laser-driven linac in view of the latest development in the creation of super-intense subpicosecond laser pulses and studying their interaction with surfaces. We suggest that by guiding such pulses in a disposable mesoscopic (several hundred nm diameter) hollow metal waveguide it will be possible to avoid deleterious effects of the breakdown and provide very high acceleration gradients. DOE

74 OPTICS

Includes light phenomena; and optical devices.
For lasers see *36 Lasers and Masers.*

N91-29914 Lawrence Livermore National Lab., CA.
A REAL TIME COLLIMATION SENSOR USING A SHEAR PLATE AND A SPATIAL LIGHT MODULATOR
J. T. Salmon and J. S. Toeppen 1990 7 p Presented at the Conference on Lasers and Electro-Optics, Anaheim, 21-25 May 1990
(Contract W-7405-eng-48)
(DE90-011362; UCRL-102524; CONF-900530-9) Avail: NTIS HC/MF A02

We have developed a sensor that optically processes interferograms from a shear plate to yield the radius of curvature or sag in the wavefront at video frame rates. Higher rates are achievable with a faster spatial light modulator and faster detectors. DOE

N91-29915# Los Alamos National Lab., NM.
DEVELOPMENT OF REFLECTIVE OPTICAL SYSTEMS FOR XUV PROJECTION LITHOGRAPHY
V. K. Viswanathan and B. E. Newnam 1991 5 p Presented at the Soft-X Ray Projection Lithography Topical Meeting, Monterey, 10-12 Apr. 1991
(Contract W-7405-eng-36)
(DE91-013167; LA-UR-91-1439; CONF-9104203-3) Avail: NTIS HC/MF A01

We describe two full-field reflective reduction systems (1 and 6.25 sq cm image area) and one scanning system (25 mm x scan length image size) that meet the performance requirements for 0.1-micron resolution projection lithography using extreme-ultraviolet (XUV) wavelengths from 10 to 15 nm. These systems consist of two centered, symmetric, annular aspheric mirrors with 35 to 40 percent central obscuration, providing a reduction ratio of 3.3 x. Outstanding features include the remarkably low distortion (less than or = 10 nm) over the entire image field and the comparatively liberal tolerances on the mirror radii and alignment. While optimized annular illumination can improve the performance, the required performance can be met with full illumination, thereby allowing a simpler system design. DOE

N91-29916# Lawrence Livermore National Lab., CA.
PREPARATION OF DAMAGE RESISTANT OPTICAL COATINGS ON FLAT SUBSTRATES
J. Otto, R. T. Kersten, V. Paquet, and R. Hochhaus (Schott Glaswerke, Mainz, Germany, F.R.) 14 Jan. 1991 24 p

(Contract W-7405-eng-48)
(DE91-013588; UCRL-CR-107094) Avail: NTIS HC/MF A03

A list of all the rugate filters that were made with the planar high temperature PICVD coater and shown to LLNL during the visit of Otto to Livermore in November 1990 are included. Those samples that have been left at LLNL are indicated. The process parameters are also added. It was demonstrated that the planar high temperature PICVD coater is in principle capable of making high reflectivity rugate mirrors. A deposition rate of up to 1.44 micron/min was obtained and thick layers (475 microns) with over 1000 periodes could be made. The deposition turns out to be non-uniform across the substrate with respect to reflectivity, band shape, peak width and film thickness. There are two types of thickness non-uniformities: bumps caused by a too small spacing between substrate and shower head, and an overall non-uniformity due to a marginal effect. The non-uniformity in reflection is probably due to a non-uniform feeding of microwave power into the plasma. It is therefore necessary to search for an improved antenna design to overcome the uniformity problems. The damage thresholds of all the coatings made with the flat coater turned out to be much lower (less than 20 J/sq cm) than for PICVD coatings i n cylindrical geometry (in tubes up to 63 J/sq cm) for unknown reasons. Possible measures for a reduction of the number of particulates in the films are discussed. DOE

N91-29917*# Sverdrup Technology, Inc., Brook Park, OH.
REVIEW OF NONDIFFRACTING BESSEL BEAMS
Michael R. LaPointe Aug. 1991 21 p Presented at the 36th Annual International Symposium on Optical and Optoelectronic Applied Science and Engineering, San Diego, CA, 21-26 Jul. 1991; sponsored in part by the Society of Photo-Optical Instrumentation Engineers
(Contract NAS3-25266)
(NASA-CR-187188; E-6480; NAS 1.26:187188) Avail: NTIS HC/MF A03 CSCL 20F

The theory of nondiffracting beam propagation and experimental evidence for nearly-nondiffractive Bessel beam propagation are reviewed. The experimental results are reinterpreted using simple optics formulas, which show that the observed propagation distances are characteristic of the optical systems used to generate the beams and do not depend upon the initial beam profiles. A set of simple experiments are described which support this interpretation. It is concluded that nondiffracting Bessel beam propagation has not yet been experimentally demonstrated.
Author

N91-29918# Carnegie-Mellon Univ., Pittsburgh, PA. Optical Data Processing.
MULTITARGET TRACKING USING OPTICAL PROCESSING Annual Report
David Casasent 1 Feb. 1991 157 p
(AD-A237107) Avail: NTIS HC/MF A08 CSCL 17/11

Our work concerns multitarget tracking (MTT) for SDI using optical processing. Our three layer system, detection, track initiation, and tracking, was detailed in prior reports. Our present work involves a modified optical correlator and a new algorithm for detection, Hough transform extensions for track initiation, and new MTT data and algorithms. We now provide an overview of this work with details given in associated chapters. GRA

N91-29919# California Univ., Irvine. Dept. of Electrical and Computer Engineering.
[MAJOR ACHIEVEMENTS DURING THE FIRST PROGRAM YEAR] Annual Report No. 1, 1 Jul. 1990 - 30 Jun. 1991
Chen S. Tsai 1 Jul. 1990 35 p
(Contract N00014-90-J-4039)
(AD-A237171) Avail: NTIS HC/MF A03 CSCL 20/6

Two major achievements were made: First, a compact magnetooptic forward volume wave based guided wave magnetooptic (MO) Bragg cell module was realized by utilizing a small permanent magnet together with a current carrying tuning coil. Performance characteristics comparable to those obtained using the bulk electromagnet have been obtained. Second, magnetostatic backward volume wave based guided wave MO Bragg cells were realized, for the first time, and used to perform wide angle light beam scanning by tuning the carrier frequency from UHF-to X-band. Although Magneto-optics in waveguide structures was among the areas actively pursued during the early phase of Guided Wave Optics research, research activity in this area was greatly reduced between the mid 70's and early 80's. However, a revival of interest in this area has taken place recently. One subject of this renewed interest concerns collinear and noncollinear (transverse Bragg) magnetooptic (MO) interactions between guided optical waves (GOW) and magnetostatic waves (MSW) in Yttrium Iron Garnet - Gadolinium Gallium Garnet (YIG-GGG) waveguides. GRA

N91-29920# Physical Sciences, Inc., Andover, MA.
A SURVEY OF OPTICAL DIAGNOSTIC METHODS FOR THE STUDY OF FUEL FOULING Final Report, 31 Jul. 1990 - 31 Jan. 1991
T. E. Parker, R. R. Foutter, and W. T. Rawlins Jun. 1991 49 p
(Contract F33615-90-C-2068)
(AD-A237361; PSI-2143/TR-1115; WL-TR-91-2064) Avail: NTIS HC/MF A03 CSCL 17/5

An experimental study of fuel fouling using optical measurement methods was performed. These measurements included absorption from 350 to 750 nm, scattering at 514.5 nm, and fluorescence using a probe wavelength of 514.5 nm. Measurements were performed using a constant temperature heating system which exited into an optical cell. Each of the measurements proved useful in monitoring changes in the test fuel, JP-4, at test temperatures up to 775 K and pressures of 400 Psig. Absorption measurements at temperatures between ambient and 860 K indicated dramatic changes in the thermally stressed fuel. These changes included indications of both molecular changes in the fuel composition and a dramatic increase in the particulate present in the flow. Relative kinetic behavior for the absorption measurement indicated that both temperature and residence time were controlling variables in the fouling process. Arrhenius plots of the absorption results illustrated that the fouling behavior could be grouped into two constant slope regions with a transition region near 525 K. Scattering measurements indicated room temperature fuel to contain particulates with average diameters greater than 0.1 micron while thermally stressed fuel contained much larger concentrations of particulates with sizes below 0.06 micron. Fluorescence signal intensities behaved, over the experimental temperature range, in a manner similar to scattering intensities, and displayed significant variations in spectral structure. GRA

N91-29921# Army Lab. Command, Watertown, MA. Material Technology Lab.
FATIGUE RESISTANT OPTICAL FIBERS Final Report
George G. Bryant May 1991 38 p
(AD-A237568; MTL-TR-91-7) Avail: NTIS HC/MF A03 CSCL 20/6

Certain requirements in commercial and military communications and guidance systems have prompted the development of high-strength, fatigue-resistant optical fibers for uncabled applications. The most significant environmental factors degrading the strength of glass fibers over time are stress and hydroxyl ion attack on glass surfaces. Several solutions have been formulated and attempted; these include increased bulk-strength glass and hermetic or passivating coatings. Test and evaluation of several commercially available fibers incorporating these promising solutions have been made using various fatigue and aging scenarios. Static-fatigue prediction from analysis of various constant extension rates to failure, termed in the literature and here as dynamic-fatigue, was also investigated. GRA

N91-29922# New Mexico Univ., Albuquerque. Center for High Technology Materials.
OPTOELECTRONIC MATERIALS CENTER Quarterly Report, 1 Oct. - 31 Dec. 1990
S. R. Brueck 11 Jun. 1991 9 p

(Contract MDA972-90-C-0046; ARPA Order 7526)
(AD-A237663) Avail: NTIS HC/MF A02 CSCL 20/6

The Optoelectronic Materials Center is a collaborative program involving the University of New Mexico, Stanford University, and the California Institute of Technology. Sandia National Laboratories and MIT Lincoln Laboratory are also involved in this program under separate contract vehicles. This program emphasizes three main areas: diode-based visible sources, two-dimensional optical interconnects, and high-speed optoelectronics. Progress on individual tasks is very briefly discussed below. Several of the tasks will impact more than one of the above areas. For simplicity, the tasks are arranged by institute in an order roughly determined by the above areas. GRA

N91-29923# Kaman Sciences Corp., Colorado Springs, CO.
TELESCOPE AND SENSOR INTERFACE PRELIMINARY REQUIREMENTS REPORT FOR THE PORTS CHAMBER
19 Jun. 1991 15 p
(AD-A237755; K91-21U(R)) Avail: NTIS HC/MF A03 CSCL 20/6

This report describes the interface requirements between the PORTS chamber and the LATS telescope or sensor. We have conceptually designed at LATS interface chamber which provides the mechanical interface needed between the LATS sensor and the PORTS chamber. The LATS interface provides alignment of the LATS sensor with the PORTS optical center line and then translates the sensor into the cryogenically cooled optical bench for testing. Also, the interface chamber allows the LATS sensor to be accessed without breaking the PORTS chamber vacuum. Under test configuration the LATS sensor will be placed in a high vacuum cryogenic environment inside of the PORTS chamber. While under test the LATS sensor will be cryogenically cooled and thermally isolated from the rest of the PORTS chamber. GRA

N91-29924# Sparta, Inc., Lexington, MA.
DEVELOPMENT OF OPTICAL SUBAPERTURES Final Report, 1 Sep. 1990 - 28 Feb. 1991
David E. Lees, Norman R. Guivens, Jr., and Philip D. Henshaw
17 Jun. 1991 56 p
(Contract N00014-90-C-0199)
(AD-A237759; SPARTA-LTR91-009) Avail: NTIS HC/MF A04 CSCL 20/6

Key issues are addressed for development of a multiple aperture imaging system which could perform high resolution imaging at very long ranges for surveillance or discrimination. Multiple aperture systems can be used to realize extremely large optical apertures required for long range, high resolution systems. The concept, which makes use of an array of intensity sensing subapertures (photon buckets), requires the simplest and potentially lowest cost hardware of any multiple aperture imaging system. A three part study is described: a study of subaperture fill factors; a subaperture design; and a discussion of issues which relate to the performance of phase retrievel algorithms. GRA

N91-29925# Harvard Univ., Cambridge, MA. Div. of Applied Sciences.
THE EFFECTS OF LUMINANCE BOUNDARIES ON COLOR PERCEPTION Annual Report, 15 Mar. 1990 - 14 Mar. 1991
Richard E. Kronauer, R. T. Eskewm, Jr., and C. F. Stromeyer, III
24 Apr. 1991 19 p
(Grant AF-AFOSR-0304-89; AF Proj. 2313)
(AD-A237794; AFOSR-91-0544TR) Avail: NTIS HC/MF A03 CSCL 20/6

When a suprathreshold luminance flash, presented as an increment on a large background field, accompanies a coincident equiluminant flash, the chromatic threshold is reduced. Early studies suggested that the chromatic facilitation grows large at small test size. Detection thresholds were measured for test spots with diameters from 5 min to 1 degree. Even for the smallest size the chromatic red-green sensitivity (specified in cone-contrast coordinates) is greater than luminance sensitivity, which has important implication for what the eye sees best. Facilitation by the luminance flash remains constant at 2x for all sizes contrary to other earlier studies. Further work with 1 degree flashes indicates that the facilitation results from a demarcation of the chromatic region by luminance features, and is not due to simple reduction of detection uncertainty. How the L and M cone signals combine in detecting motion was also studied. GRA

N91-29926# Arnold Engineering Development Center, Arnold Air Force Station, TN.
APPLICATION OF DIFFRACTION CORRECTION TO BLACKBODY SOURCES Final Report, Dec. 1990 - Mar. 1991
R. P. Young and C. B. Herron Jun. 1991 29 p
(AD-A237840; AEDC-TR-91-4) Avail: NTIS HC/MF A03 CSCL 20/6

Diffraction losses should be accounted for in calculating the radiometric output for all cavity-type blackbody sources in use. The theoretically predicted source diffraction losses were examined and compared to experimental data obtained during the calibration of a typical AEDC source. The results revealed that the experimental data do not support the use of currently available diffraction correction theories. At this time, the use of diffraction corrections is not recommended for the Arnold Engineering Development Center (AEDC) blackbody sources. GRA

N91-29927# University Coll. of North Wales, Bangor. School of Electronic Engineering Science.
FAST ACTING OPTICAL DEFLECTION Final Report No. 3, Dec. 1989 - Mar. 1991
D. K. Das-Gupta 13 May 1991 36 p
(Contract DAJA45-90-C-0005; DA Proj. 1L1-61102-BH-57)
(AD-A237904; R/D-6310-MS-01) Avail: NTIS HC/MF A03 CSCL 20/6

The spectral transmittance has been studied with sinusoidal phase transmission gratings with 600 lines per mm and of varying groove depths from 637nm to 776nm in order to obtain minimum optical transmission in the wavelength range of 500nm to 1000nm. All the gratings were formed on photo-resist materials on glass substrates using a holographic technique. A high degree of attenuation of the zero order beam over a small wavelength range is attainable with a single sinusoidal transmission grating of an appropriate groove depth, min at which the transmittance is minimum, being proportional to the magnitude of the groove depth. A superposition of two crossed gratings of two dissimilar groove depths either on two different glass substrate or on a single substrate can provide a very low optical transmittance in the band 400 to 1000nm although the visibility through such a system is poor. GRA

N91-29928# Naval Weapons Center, China Lake, CA.
EFFECT OF CLADDING THICKNESS ON ATTENUATION IN UNIFORMLY CURVED SINGLE-MODE OPTICAL FIBERS Final Report, Jan. - Aug. 1990
P. L. Overfelt and G. A. Hewer Sep. 1990 26 p
(AD-A238034; NWC-TP-7104) Avail: NTIS HC/MF A03 CSCL 20/6

This report analyzes the effect of finite cladding thickness on attenuation loss in uniformly curved single-mode optical fibers. An approximate electromagnetic analysis valid for relatively small cladding thicknesses and fiber radii of curvature in the centimeter to millimeter range is presented. Numerical results for fibers used in actual SKYRAY Fiber Optics Project field tests are presented and discussed. GRA

N91-29929# IBM Federal Systems Div., Manassas, VA.
SAFENET 2 FIBER OPTIC IMPLEMENTATION STUDY Final Report
V. W. Townsend, T. P. Sevinsky, and F. J. Owens 28 Jun. 1991 63 p
(Contract N00014-88-C-0745)
(AD-A238044) Avail: NTIS HC/MF A04 CSCL 20/6

The SAFENET II draft Military Handbook, MCCR-0036-DRAFT, establishes requirements and provides guidance for the implementation of a Survivable Adaptable Fiber Optic Network.

SAFENET II. The fiber optics communications channel essentially adopts the ANSI Fiber Distributed Data Interface (FDDI) Physical Layer Medium Dependent (PMD) Specification, modified by a requirement for increased transmitter optical output power and decreased minimum receiver optical input power (increased sensitivity) to provide a 21 dB overall optical flux budget between (and including) the equipment fiber optic interface connectors (FOIC). A network of cables, optical bypass switches, and spliced fiber joints is described in the Handbook which permit ring operation through up to 5 bypassed nodes while maintaining a minimum 6 dB link optical power margin. GRA

N91-29930# Air Force Inst. of Tech., Wright-Patterson AFB, OH. School of Engineering.
A VISION SYSTEM MODEL Ph.D. Thesis
Erik J. Fretheim Jun. 1991 273 p
(AD-A238459; AFIT/DS/ENG/91-1) Avail: NTIS HC/MF A12 CSCL 20/6

This dissertation provides four major contributions to the field of vision research. The first contribution is a general vision system model. The model, which blends biological as well as technological methods into a coherent approach to vision, will provide a basis for implementing vision systems. The second contribution of this dissertation is to demonstrate particular implementations of portions of the model. These implementations will include methods for using Gabor wavelets in edge detection, in preprocessing images for use as feature vectors in backpropagation neural networks, and as basis functions in a recognition/reconstruction network, as well as methods for integrating color into a vision system. The third major contribution is an investigation of attentional mechanisms using a two-part model with Gabor filters as a base attentional indicator. The second part of the model, the search mechanism, is only briefly studied. The final contribution is a description of an actual vision system for the analysis of VLSI circuits in terms of the general vision system model. This system provides a means of obtaining a logical circuit description from an actual physical circuit. GRA

N91-29931# Pennsylvania State Univ., University Park. Dept. of Electrical and Computer Engineering.
ADAPTIVE LIQUID CRYSTAL TV BASED JOINT TRANSFORM CORRELATOR AS APPLIED TO REAL-TIME PATTERN RECOGNITION Final Report, 1 Oct. 1987 - 31 Mar. 1991
Francis T. Yu 23 May 1991 168 p
(Contract DAAL03-87-K-0147)
(AD-A238576; ARO-25146.28-PH) Avail: NTIS HC/MF A08 CSCL 20/6

The primary goal of this research is to study a programmable joint-transform correlator (JTC) using liquid crystal television (LCTV) panels for adaptive real-time pattern recognition applications. The technique can improve the pattern recognition and identification technology that is of interest to the U.S. Army. The technique we studied is a real-time programmable electro-optical architecture. There are several reasons for selecting the optical technique over their digital and electronic counterparts, as follows: Optical technique is capable of handling a large space-bandwidth image; optical technique is capable of performing parallel operations; optics can perform massive interconnections; optical transformation can be operated at high speed, etc. By using the LCTV, the pattern under observation can be correlated with a large number of recallable image memories. In addition, the LCTV technique is rather simple and economical to operate. The LCTV-optical correlator, in principle, can be designed into a compact portable form for insitu application. Brief outlines of the major research findings and publications are provided in this report. GRA

N91-29932# Rochester Univ., NY. Inst. of Optics.
THE 23RD OPTOELECTRONIC WORKSHOP: OPTICAL SYSTEM ASSESSMENT FOR DESIGN AND SIMULATED ANNEALING
Gregory Forbes and Robert Spande 2 Aug. 1990 61 p
Workshop held in Rochester, NY, 2 Aug. 1990
(Contract DAAL03-86-K-0173)
(AD-A238588; ARO-24626.211-PH-UIR) Avail: NTIS HC/MF A04 CSCL 20/6

This workshop on Optical System Assessment for Design and Simulated Annealing represents the twenty-third of a series of intensive academic/government interactions in the field of advanced electro-optics, as part of the Army sponsored University Research Initiative. By documenting the associated technology status and dialogue it is hoped that this baseline will serve all interested parties towards providing a solution to high priority Army requirements. GRA

N91-29933# Department of the Navy, Washington, DC.
OPTICAL SOLITON SOURCE Patent Application
I. N. Duling, inventor (to Navy) 5 Nov. 1990 23 p
(AD-D014942; US-Patent-Appl-SN-608764) Avail: NTIS HC/MF A03 CSCL 20/6

An optical source for producing short optical pulses comprises first and second optical loops coupled together by a beam splitter so as to define a figure eight optical path in which a light beam propagating toward the beam splitter in one of the first and second loops is split by the beam splitter to form two light beams propagating in opposite directions around the other of the first and second loops. The first loop includes a direction dependent loss element for reducing the intensity of light propagating in predetermined direction around the first loop, and the second loop includes an element having an intensity dependent nonlinear optical transmission characteristic. One of the first and second loops includes an optical gain medium. Coupling apparatus is also provided for coupling pump light into the loop including the gain medium and for coupling optical pulses out of the source. GRA

N91-29934# Department of the Navy, Washington, DC.
ELECTRO-OPTIC LINE NARROWING OF OPTICAL PARAMETRIC OSCILLATORS Patent Application
Bruce P. Boczar, inventor (to Navy) 21 May 1990 18 p
(AD-D014944; US-Patent-Appl-SN-527966) Avail: NTIS HC/MF A03 CSCL 20/6

In the present invention a nonlinear crystal of an optical parametric oscillator is provided with a pump pulse and electrodes for applying a high voltage to the crystal during the pump pulse. The high voltage is switched from one level to another during the pump pulse duration. The initial value of the high voltage determines the position of the frequency center of the optical parametric oscillator gain profile because the indices of refraction are a function of the applied voltage due to the electro-optic effect. During the pump pulse, when the high voltage is switched to some other value, a new set of momentum and energy conservation conditions results. This causes a frequency shift in the gain profile. Thus the oscillator is provided with two differing gain profiles during the pump pulse. The output frequency of the oscillator is only those frequencies in both gain profiles. GRA

N91-29935*# CVD, Inc., Woburn, MA.
FABRICATION OF LIGHTWEIGHT Si/SiC LIDAR MIRRORS Final Report, 9 Jun. 1987 - 8 Dec. 1990
Jitendra S. Goela and Raymond L. Taylor Washington Aug. 1991 97 p
(Contract NAS1-18476)
(NASA-CR-4389; NAS 1.26:4389; CVD-TR-9081) Avail: NTIS HC/MF A05 CSCL 20F

A new, chemical vapor deposition (CVD) process was developed for fabricating lightweight, polycrystalline silicon/silicon-carbide (Si/SiC) mirrors. The process involves three CVD steps: (1) to produce the mirror faceplate; (2) to form the lightweight backstructure, which is deposited integral to the faceplate; and (3) to deposit a layer of optical-grade material, e.g., Si, onto the front surface of the faceplate. The mirror figure and finish are fabricated into the faceplate. Author

N91-29936# Purdue Univ., West Lafayette, IN. School of Electrical Engineering.
NONLINEAR OPTICAL INTERACTIONS INVOLVING THE REAL GAUSSIAN FIELD
D. S. Elliott 1991 7 p
(Contract DE-FG02-86ER-13576)
(DE91-015052; DOE/ER-13576/1) Avail: NTIS HC/MF A02

The effects were determined of the bandwidth of a laser on nonlinear interactions between the laser light and an atomic system. Atomic structure (or more specifically, atomic wave functions) can be probed very sensitively by examining the behavior of the atom when irradiated by laser radiation resonant with a transition between various energy eigenstates of the atom. When making these observations, it is important to know the features of the atomic response are caused by the intrinsic properties of the atom and what is caused by other influences, such as the bandwidth of the laser. A method was developed for generating the real Gaussian field and testing some of its statistical properties, the effect was calculated of a Fabry-Perot interferometer on the statistical properties of the transmitted light when the phase diffusion field, the real Gaussian field and the thermal field is incident upon it; and the same effect was measured for the real Gaussian field. Projects under way which are not yet complete are measurements of the effect of this field on two photon absorption and extension of this technique to the generation of the complex Gaussian field. DOE

75 PLASMA PHYSICS

Includes magnetohydrodynamics and plasma fusion.

For ionospheric plasmas see *46 Geophysics*. For space plasmas see *90 Astrophysics*.

N91-29937*# American Science and Engineering, Inc., Cambridge, MA.
PLASMA PROPERTIES OF HOT CORONAL LOOPS UTILIZING COORDINATED SMM AND SOLAR RESEARCH ROCKET OBSERVATIONS Final Report, 19 Oct. 1987 - 30 Nov. 1989
J. Daniel Moses 30 Nov. 1989 68 p Original contains color illustrations
(Contract NAS5-30141)
(NASA-CR-186094; NAS 1.26:186094; ASE-5600) Avail: NTIS HC/MF A04; 1 functional color page CSCL 20I

Three improvements in photographic x-ray imaging techniques for solar astronomy are presented. The testing and calibration of a new film processor was conducted; the resulting product will allow photometric development of sounding rocket flight film immediately upon recovery at the missile range. Two fine grained photographic films were calibrated and flight tested to provide alternative detector choices when the need for high resolution is greater than the need for high sensitivity. An analysis technique used to obtain the characteristic curve directly from photographs of UV solar spectra were applied to the analysis of soft x-ray photographic images. The resulting procedure provides a more complete and straightforward determination of the parameters describing the x-ray characteristic curve than previous techniques. These improvements fall into the category of refinements instead of revolutions, indicating the fundamental suitability of the photographic process for x-ray imaging in solar astronomy. Author

N91-29938# Columbia Univ., New York, NY. Plasma Physics Lab.
IDENTIFICATION OF, AND TRANSITION TO, THE SECOND REGION OF IDEAL MHD STABILITY IN TOKAMAKS Ph.D. Thesis
S. A. Sabbagh 1990 200 p
(Contracts DE-FG02-86ER-53222; DE-FG02-89ER-53297)
(DE90-010380; DOE/ER-53222/101) Avail: NTIS HC/MF A09

The second region of ideal magnetohydrodynamic stability in tokamaks is studied by considering the behavior of the second region boundary for self-consistently calculated, marginally stable, second region equilibria and the characteristics of numerically computed transport sequences that achieve second stability. Equilibria with pressure profiles, p(psi), that are marginally stable to the second region on each flux surface are generated numerically. This constraint eliminates p(psi) as an independent variable, and reduces the predictor variables to the tokamak parameters and the q profile. The primary response functions considered are the plasma figures of merit, (beta) and (var epsilon)(beta)(sub p), and the normalized pressure gradient, (alpha). Variations of the radial wavenumber in the ballooning equation negligibly affect the second region boundary for these equilibria. The second region boundary is sensitive to variations in the q profile at small aspect ratio, A, and will stabilize or destabilize depending on the balance of higher order (var epsilon) = A(exp -1) modifications of the normal field line curvature, (kappa)(sub n). These effects are a competition between the stabilizing geometric magnetic well of the toroidal field component of (kappa)(sub n) and the destabilizing poloidal field component of (kappa)(sub n). The latter term becomes competitive in high (var epsilon)(beta)(sub p) plasmas with large Shafranov shifts. Simple analytic models are presented that reproduce the scaling of the marginally stable second region values of (alpha) and (var epsilon)(beta)(sub p), and stability diagrams illustrating the behavior of the high-n unstable region for various parameters are shown. DOE

N91-29939# Ames Lab., IA.
FUNDAMENTAL STUDIES OF THE EXTRACTION PROCESS IN INDUCTIVELY COUPLED PLASMA MASS SPECTROMETRY Ph.D. Thesis
Heoungbin Lim Jan. 1990 154 p
(Contract W-7405-eng-82)
(DE90-011733; IS-T-1414) Avail: NTIS HC/MF A08

A reduced pressure jet extracted from an inductively coupled plasma (ICP) was studied for information about conditions during the extraction process in inductively coupled plasma mass spectrometry (ICP-MS). The background spectrum and intensity ratio of ion lines to atom lines were similar to those from the ICP, except the lines from the jet were much weaker. Gas kinetic temperature in the Mach disk region of the extracted plasma were of the order of 2200 K. Fluorescence studies indicated there was little neutral sodium inside the zone of silence of the free jet, which showed that little ion-electron recombination occurred during the initial extraction and supersonic expansion. DOE

N91-29940# Wisconsin Univ., Madison. Dept. of Physics.
MAGNETIC FLUCTUATIONS DUE TO THERMALLY EXCITED ALFVEN WAVES
Y. Z. Agim and S. C. Prager Jan. 1990 44 p
(Contract DE-FG02-85ER-53212)
(DE90-011790; DOE/ER-53212/152) Avail: NTIS HC/MF A03

Magnetic fluctuations due to the thermally excited magnetohydrodynamic (MHD) waves are investigated using fluid and kinetic models to describe a stable, uniform, compressible plasma in the range above the drift wave frequency and below the ion cyclotron frequency. It is shown that the fluid model with resistivity yields spectral densities which are roughly Lorentzian, exhibits equipartition with no apparent cutoff in wavenumber space, and a Bohm-type diffusion coefficient. Under certain conditions, the ensuing transport may be comparable to classical values. For a phenomenological cutoff imposed on the spectrum, the typical fluctuating-to-equilibrium magnetic field ratio is found to be of the order of 10(exp -10). Physical mechanisms to obtain decay profiles of the spectra with increasing wavenumber due to dispersion and/or different forms of damping are investigated analytically in a cold fluid approximation and numerically, with a kinetic model. The mode dispersion due to the finite ion-gyrofrequency is identified as the leading effect determining the spectral profile shapes. It is found that the amplitude of fluctuations may be within a factor of the value suggested by the cold plasma model. The results from both models are presented and compared in low- and high-beta regimes. DOE

N91-29941# California Univ., Davis.
MEASUREMENTS OF THE ION ACOUSTIC DECAY INSTABILITY AND THE RESULTANT THERMAL AND SUPRATHERMAL ELECTRON HEATING IN LASER-PLASMA INTERACTION EXPERIMENTS
K. Mizuno, J. S. DeGroot, and W. Seka (Rochester Univ., NY.)
Jun. 1989 16 p
(Contract DE-AS08-87NV-10652)
(DE90-012477; DOE/NV-10652/T1) Avail: NTIS HC/MF A03

We have made extensive studies of Ion Acoustic Decay Instabilities (IADI) in laser-pellet interactions under the program of the National Laser Users Facility at the Laboratory for Laser Energetics (LLE). We have observed well-defined IADI. It is shown that IADI is potentially important in laser fusion applications. The threshold decreased as the laser spot size increased. The measured threshold is an order of magnitude lower than previously reported values in small spot experiments. The threshold values for IR and short wavelength Green lasers are quite low, and reached homogeneous-plasma collisional values in a planar plasma produced by a large spot size laser irradiations. The results are explained in agreement with LASNEX calculations with a flux limit of f = 0.1. These low threshold values indicate that IADI is potentially important in a large scale plasma, and even in short-wavelength laser-pellet interactions which are applicable to laser fusion research. DOE

N91-29942# Oak Ridge National Lab., TN.
FUSION REACTOR MATERIALS Semiannual Progress Report, period ending 30 Sep. 1990
Apr. 1991 336 p
(Contract DE-AC05-84OR-21400)
(DE91-012984; ORNL/ER-0313/9; ORNL/M-1389) Avail: NTIS HC/MF A15

This is the ninth in a series of semiannual technical progress reports on fusion reactor materials. This report combines research and development activities which were previously reported separately in the following technical progress reports: Alloy Development of Irradiation Performance; Damage Analysis and Fundamental Studies; and Special Purpose Materials. These activities are concerned principally with the effects of the neutronic and chemical environment on the properties and performance of reactor materials; together they form one element of the overall materials program being conducted in support of the Magnetic Fusion Energy Program of the U.S. Department of Energy. The other major element of the program is concerned with the interactions between reactor materials and the plasma and is reported separately. The Fusion Reactor Materials Program is a national effort involving several national laboratories, universities, and industries. The purpose of this series of reports is to provide a working technical record for the use of the program participants, and to provide a means of communicating the efforts of materials scientists to the rest of the fusion community, both nationally and worldwide. DOE

N91-29943# Missouri Univ., Rolla. Dept. of Physics.
COLLISIONAL PROCESSES OF INTEREST IN MFE PLASMA RESEARCH
R. E. Olson 24 Apr. 1991 15 p
(Contract DE-FG02-84ER-53175)
(DE91-013023; DOE/ER-53175/6) Avail: NTIS HC/MF A03

Research on this grant is devoted to the calculation of heavy particle collision cross sections needed for diagnostic studies of magnetic fusion plasmas. This work requires the development and testing of new theoretical methods, with the implementation of benchmarked techniques to collisions pertinent to fusion reactors. Within the last context, we have provided charge-exchange-recombination cross sections of specific n,l-levels for diagnostic studies on TFTR and for major compilations for the IAEA. We have also completed a cross section study related to the planned neutral beam current drive for ITER. In addition, calculations were made to assess the use of He neutral atom angular scattering measurements for JT-60. Also, new theoretical methods have been developed to more accurately calculate cross sections involving either He or H2 targets and partially stripped multiply-charged ions. Our most recent work concentrates on alpha particle diagnostics and collision processes of helium ash in burning reactors. Here, we are providing atomic cross section data for the carbon pellet alpha particle diagnostic work at General Atomics and the neutral He beam alpha particle diagnostic under study by the IAEA. DOE

N91-29944# Wisconsin Univ., Madison. Center for Plasma Theory and Computation.
FLUIDLIKE STUDIES OF THE SHEATH AND PRESHEATH REGIONS OF A PLASMA Ph.D. Thesis
B. J. Lee 1991 67 p
(Contract DE-FG02-86ER-53218)
(DE91-013343; UW-CPTC-91-4) Avail: NTIS HC/MF A04

We investigate the problem of a collisional plasma flowing into a perfectly absorbing wall including the parallel viscosity and heat flux effects. Both the collisional presheath and the collisionless sheath regions are modelled by fluid-like moment equations that are derived from kinetic theory. Previous work has been based primarily on a collisionless kinetic theory or collisional Braginskii equations which have singularities at the sheath edge. The electron distribution function is obtained here from the solution of a Pastukhov type problem instead of a simple Boltzmann relation. For the ions a kinetic theory is required to determine the ion viscous stress tensor and heat flux because the collisional mean free path is comparable to the characteristic gradient scale length in the presheath region. A boundary layer analysis is applied for determining the distribution function of the ions in the velocity space region corresponding to no net return flux from the wall. This analysis provides a continuous solution over the entire region of interest. The viscous force deduced from this distribution function, which is a cutoff Maxwellian relaxed by collisions, is comparable to the electric field force everywhere and removes the singularity between the presheath and the sheath regions in the ion momentum equation. The total heat flux obtained using the same method as for the viscous force removes the singularity in the ion energy conservation equation. Four different numerical calculation cases are presented in this thesis. DOE

N91-29945# National Academy of Sciences - National Research Council, Washington, DC. Commission on Physical Sciences, Mathematics, and Applications.
SECOND REVIEW OF THE DEPARTMENT OF ENERGY'S INERTIAL CONFINEMENT FUSION PROGRAM
Sep. 1990 52 p
(Contract DE-AC01-89DP-20154)
(DE91-013157; DOE/DP-20154/T1) Avail: NTIS HC/MF A04

This report of the second review by the National Research Council of inertial confinement fusion (ICF) contains the appointed committee's final conclusions and recommendations. An interim report was issued in January 1990. The charge to the committee was as follows: determine whether the recommendations of the 1985 NAS review are still appropriate to advance the technology efficaciously. Provide an assessment of the most promising technologies for continuation of the program. Assess the potential contributions of the program under the following scenarios: a comprehensive test ban on underground nuclear testing and prohibition of underground nuclear testing to levels of 1 kiloton, 5 kilotons, and 10 kilotons. Assess the civilian energy potential of ICF. Assess the adequacy of the ICF target performance data base for supporting program plans and decision milestones. Identify major technical and programmatic issues facing the program. Determine the status of each major candidate inertial fusion driver, and specify the critical issues involved in the development of each. Recommend program priorities, particularly with regard to the Centurion/halite program, driver development, and laboratory experiments and theory. Recommend relative priorities of individual support laboratory activities. Examine the strategies and plans of the ICF Program, comment on their soundness, cohesiveness, and programmatic effectiveness, and recommend management initiatives that could improve the progress of the program toward achieving of its goals. The major difference between the 1985

and 1989 reviews is the request for greater attention to the energy potential of the ICF Program and the heavy-ion work being carried out by the Lawrence Berkeley Laboratory at the University of California. DOE

N91-29946# Lawrence Livermore National Lab., CA.
STAGNATION AND INTERPENETRATION OF LASER-CREATED COLLIDING PLASMAS
S. M. Pollaine, J. R. Albritton, R. Kauffman, C. J. Keane, R. L. Berger, R. Bosch, N. D. Delamerter, and B. H. Failor (KMS Fusion, Inc., Ann Arbor, MI.) 25 Feb. 1991 7 p Presented at the 21st Annual Anomalous Absorption Conference, Banff (Canada), 15-19 Apr. 1991 Revised
(Contract W-7405-eng-48)
(DE91-013244; UCRL-JC-104425-Rev-1; CONF-9104241-3-Rev-1) Avail: NTIS HC/MF A02

A KMS laser experiment collides Aluminum (Al) and Magnesium (Mg) plasmas. The measurements include electron density, time and space-resolved Ly(alpha) and He(alpha) lines of Al and Mg, and x-ray images. These measurements were analyzed with a two-fluid code OFIS and Keane's code DSP. The results suggest that at early times, the Al interpenetrates the counterstreaming Mg plasma and deposits in the dense Mg region. At late times, the Al plasma stagnates against the Mg plasma. DOE

N91-29947# Brookhaven National Lab., Upton, NY.
THE BNL TOROIDAL VOLUME H(-) SOURCE
J. G. Alessi and K. Prelec 1991 3 p Presented at the 1991 Institute of Electrical and Electronics Engineers (IEEE) Particle Accelerator Conference (PAC), San Francisco, 6-9 May 1991
(Contract DE-AC02-76CH-00016)
(DE91-013592; BNL-45445; CONF-910505-182) Avail: NTIS HC/MF A01

The BNL toroidal volume H(-) ion source, in pulsed operation is now producing up to 35 mA with an electron to H(-) ratio of less than 5, and a ratio of less than 3 for currents up to 20 mA. This improvement came about by increasing the strength of the conical filter field. The source has also been operated steady state at low arc currents, where up to 6 mA of H(-) was extracted. The electron to H(-) ratio is 2 to 3 times larger for dc operation. For dc currents up to 5 mA, the arc power efficiency was 5 mA/kW. Pulsed performance with Ta and W filaments were very similar, except for the large gas pumping observed with the Ta filament. In dc operation, the Ta filament performed somewhat better than W. Extraction from 7 apertures having a total area of 1 sq cm produced the same results as a single 1 sq cm aperture. DOE

N91-29948# Wisconsin Univ., Madison.
THE EFFECTS OF MAGNETIC FIELD ERRORS ON REVERSED FIELD PINCH PLASMA Ph.D. Thesis
A. F. Almagri Dec. 1990 63 p
(Contract DE-FG02-85ER-53198)
(DE91-013636; DOE/ER-53198/171) Avail: NTIS HC/MF A04

Studies of magnetic field error effects on Reversed Field Pinch plasma were carried out on the Madison Symmetric Torus. Magnetic field errors at the poloidal gap were reduced by 18 percent in rms value. This modest reduction of field errors resulted in improved plasma discharges. The plasma loop voltage was reduced by about 31 percent, and the plasma resistivity was reduced by 36 percent. Reversal duration increased by 16 percent. The character of the sawtooth activity as seen on the toroidal field at the wall changed considerably when field errors were reduced. These results suggest improved plasma confinement. Field errors were reduced further by a factor of six in rms value. With this reduction of field errors, plasma loop voltage was reduced by about a factor of two. The discharge duration doubled. At this low level of field errors, the plasma exhibited coherent magnetic fluctuations. These fluctuations have a poloidal mode number $m = 1$ and toroidal mode number $n = 5$ to 10. These modes are typically phase-locked to one another to form a localized perturbation. This perturbation rotates toroidally in the ion-diamagnetic drift direction with a speed of about 10(exp 6) cm/sec. Occasionally these modes are observed to lock to the conducting wall. This locking is believed to be caused by the poloidal gap field errors. These locked discharges tend to be much shorter in duration and to have larger loop voltage. The behavior of locked discharges can be explained by a field-error instability. Some estimates of the internal radial magnetic fields and the resulting magnetic islands are calculated. These calculations show that the field errors need to be reduced to less than 2 percent of the poloidal field at the wall to reduce islands overlap. DOE

N91-29949# Wisconsin Univ., Madison.
TOTAL MAGNETIC RECONNECTION DURING A TOKAMAK MAJOR DISRUPTION Ph.D. Thesis
J. A. Goetz Sep. 1990 66 p
(Contract DE-FG02-85ER-53198)
(DE91-013637; DOE/ER-53198/163) Avail: NTIS HC/MF A04

Magnetic reconnection has long been considered to be the cause of sawtooth oscillations and major disruptions in tokamak experiments. Experimental confirmation of reconnection models has been hampered by the difficulty of direct measurement of reconnection, which would involve tracing field lines for many transits around the tokamak. Perhaps the most stringent test of reconnection in a tokamak involves measurement of the safety factor q. Reconnection arising from a single helical disturbance with mode numbers m and n should raise q to m/n everywhere inside of the original resonant surface. Total reconnection should also flatten the temperature and current density profiles inside of this surface. Disruptive instabilities have been studied in the Tokapole 2, a poloidal divertor tokamak. When Tokapole 2 is operated in the material limiter configuration, a major disruption results in current termination as in most tokamaks. However, when operated in the magnetic limiter configuration current termination is suppressed and major disruptions appear as giant sawtooth oscillations. The objective of this thesis is to determine if total reconnection is occurring during major disruptions. To accomplish this goal, the poloidal magnetic field has been directly measured in Tokapole 2 with internal magnetic coils. A full two-dimensional measurement over the central current channel has been done. From these measurements, the poloidal magnetic flux function is obtained and the magnetic surfaces are plotted. The flux-surface-averaged safety factor is obtained by integrating the local magnetic field line pitch over the experimentally obtained magnetic surface. DOE

N91-29950# General Atomics Technologies Corp., San Diego, CA.
ADVANCED DIVERTOR EXPERIMENTS ON DIII-D
M. J. Schaffer, M. A. Mahdavi, T. Osborne, T. W. Petrie, R. D. Stambaugh, D. Buchenauer, D. N. Hill, and C. C. Klepper (Oak Ridge National Lab., TN.) Apr. 1991 5 p Presented at the 18th European Conference on Controlled Fusion and Plasma Physics, Berlin, Fed. Republic of Germany, 3-7 Jun. 1991
(Contracts DE-AC03-89ER-51114; DE-AC05-84OR-21400; DE-AC04-76DP-00789; W-7405-eng-48)
(DE91-011138; GA-A-20480; CONF-910609-10) Avail: NTIS HC/MF A01

The poloidal divertor is presently favored for next-step, high-power tokamaks. The DIII-D Advanced Divertor Program (ADP) aims to gain increased control over the divertor plasma and tokamak boundary conditions. This paper reports experiments done in the first phase of the ADP. The DIII-D lower divertor was modified by the addition of a toroidally symmetric, graphite-armoured, water-cooled divertor-biasing ring electrode at the entrance to a gas plenum. The plenum will eventually contain a He cryogenic loop for active divertor pumping. The separatrix strike position is controlled by the lower poloidal field shaping coils and can be varied smoothly from the ring electrode upper surface to the divertor floor far from the entrance aperture. External power, at up to 550 V and 8 kA separately, has been applied to the electrode to date. DOE

N91-29951# Los Alamos National Lab., NM.
FUTURE EXPLOSIVE PULSE-POWER TECHNOLOGY FOR HIGH-ENERGY PLASMA PHYSICS EXPERIMENTS
R. E. Reinovsky, I. R. Lindemuth, and S. P. Marsh 1991 9 p Presented at the 8. IEEE Pulsed Power Conference, San Diego, 17-19 Jun. 1991
(Contract W-7405-eng-36)
(DE91-014601; LA-UR-91-2054; CONF-910640-22) Avail: NTIS HC/MF A02

A variety of high-performance pulse-power systems in the 10 to 20-MJ class have been built in the last ten years or are planned in the next 3 to 5 years. Such systems, using capacitive energy storage, are employed in particle beam fusion, x-ray effects, x-ray physics, and plasma physics experiments. Advances in the technology of high-energy-density capacitors over the same time period has substantially decreased the cost per joule of the basic capacitor and kept the total parts count in large systems within reason. Overall, the savings in capacitor costs has about balanced the generally increasing system costs keeping the total cost of large, high-performance systems at $1 to 2 per joule over the period. The next step, to 100-MJ class systems, will profit from the improvements of the last decade, but there seems little reason to project a lowering of the cost per joule. In contrast, there is every reason to expect the continuously growing system costs to outstrip any savings to be realized from improvements in capacitor technology. Over the same period, explosive pulse power systems in the 10 to 20-MJ class have been employed, routinely, in plasma physics experiments. These one-shot systems currently cost about $100 K for the generator and switching and deliver energy to a plasma physics experiment in a few microseconds. Comparing only hardware costs, such systems are competitive with capacitor systems for developmental activities involving 100 to 200 shots -- but not for repetitive applications involving 1000's of shots. At this rate, explosive systems are competitive systems for applications involving up to 200 to 500 shots. In this paper, we discuss general concepts for generators and power-conditioning systems appropriate for high-energy applications. We scope two such applications and show how explosive pulse power can address those applications. DOE

N91-29952# Los Alamos National Lab., NM.
PLASMA AND ELECTRICAL DIAGNOSTICS FOR PROCYON EXPERIMENTS
H. Oona, B. G. Anderson, J. C. Cochrane, C. E. Findley, J. H. Goforth, A. E. Greene, H. W. Kruse, J. V. Parker, and D. G. Rickel 1991 5 p Presented at the 8th IEEE Pulsed Power Conference, San Diego, CA, 17-19 Jun. 1991
(Contract W-7405-eng-36)
(DE91-014736; LA-UR-91-2007; CONF-910640-10) Avail: NTIS HC/MF A01

The aim of the Trailmaster series of experiments is to generate an intense source of soft x-rays by imploding a thin (2000 Angstrom) aluminum cylinder. The present scheme incorporates a plasma flow switch for the final pulse shaping and requires careful diagnostic analysis. The emphasis of this work is to transfer the energy to the load area and to understand the dynamics of the plasma flow switch. The experiments are carried out in two facilities. Laboratory experiments that answer questions about the details of the plasma flow switch are done on the 1.5-MJ Pegasus capacitor bank. The higher energy experiments (Procyon series) utilize explosive pulsed power systems and are conducted at the Ancho Canyon firing site. It is the latter set of experiments that will eventually supply an x-ray radiation source at the megajoule level. At the present time, the emphasis of the Procyon experiments is to deliver energy from the generator to the plasma flow switch and the load area. The details of these experiments are given in other papers at this conference. In order to characterize these experiments one needs to diagnose the driver performance and the dynamics of the plasma and power flow in the plasma flow switch region. The difficulty of experiments in which high current high voltage, and high explosive are combined, leads to severe problems. Many of the diagnostics are unique and untested. Since only a limited number of experiments are done during a year, the effort is to maximize the information per shot. The aim in this report is to present some of the diagnostic techniques used in the adverse Trailmaster environment. DOE

N91-29953# Los Alamos National Lab., NM.
PROCYON EXPERIMENTS UTILIZING EXPLOSIVELY-FORMED FUSE OPENING SWITCHES
J. H. Goforth, H. Oona, J. H. Brownell, A. E. Greene, H. W. Kruse, I. R. Lindemuth, S. P. Marsh, J. V. Parker, R. E. Reinovsky, and D. G. Rickel et al 1991 5 p Presented at the 8th IEEE Pulsed Power Conference, San Diego, 17-19 Jun. 1991
(Contract W-7405-eng-36)
(DE91-014742; LA-UR-91-1992; CONF-910640-17) Avail: NTIS HC/MF A01

In this paper we describe results from tests of an explosive pulsed power system designed to deliver 15 to 16 MA to a plasma flow switch (PFS). The PFS, in turn, has the goal of switching current to a z-pinch load to produce a 1-MJ implosion for x-ray generation experiments. The system consists of a MK-IX magnetic flux-compression generator, a coaxial inductive store, an explosively formed fuse (EFF) opening switch, and a vacuum power flow/PFS assembly. A completed assembly ready to test is shown. We have performed two development tests of the Procyon system. A preliminary reduced energy test delivered approximately 13.6 MA to a 25-nH PFS load, and imposed a large voltage spike on the EFF at nominal pinch time without failure. In a full-energy test, the system delivered 20 MA to the EFF without suffering unexpected losses, and demonstrated the proper onset of EFF opening. In the 20-MA test, mistiming between the EFF and the load isolation switches led to transmission line failure that disguised late time opening switch performance and diverted most of the current pulse away from the PFS load. These two tests have provided important system characterization information. In some cases, design expectations are confirmed and in others, adjustments to initial expectations are needed. Performance details are presented below. DOE

N91-29954# Los Alamos National Lab., NM.
PLASMA FLOW SWITCH EXPERIMENTS ON THE PEGASUS FACILITY
J. C. Cochrane, Jr., B. Anderson, R. R. Bartsch, R. Bowers, C. Findley, A. Greene, H. Kruse, H. Oona, J. V. Parker, and D. Peterson et al 1991 4 p Presented at the 8th IEEE Pulsed Power Conference, San Diego, CA, 17-19 Jun. 1991
(Contract W-7405-eng-36)
(DE91-014744; LA-UR-91-1983; CONF-910640-23) Avail: NTIS HC/MF A01

Plasma flow switch experiments conducted on Pegasus have shown that a conducting layer of plasma shunts the load slot preventing efficient switching of current to the load. This effect is seen computationally. The magnitude of the effect depends on the specific parameters of the switch plasma and current level. Computations have also shown that a plasma boundary layer trap would effectively remove enough plasma from the inner conductor of the power flow channel so that efficient switching would occur. This plasma trap has been successfully demonstrated when used with a static load. It has not yet been tested with an imploding load. DOE

N91-29955# Los Alamos National Lab., NM.
COMPUTATIONAL MODELING OF THE TRAILMASTER PROCYON SYSTEM
A. E. Greene, R. L. Bowers, J. H. Brownell, D. L. Peterson, D. L. Weiss, H. Oona, J. H. Goforth, and D. G. Rickel 1991 23 p Presented at the 8th IEEE Pulsed Power Conference, San Diego, 17-19 Jun. 1991
(Contract W-7405-eng-36)
(DE91-014765; LA-UR-91-1946; CONF-910640-15) Avail: NTIS HC/MF A03

The goal of the Los Alamos Foil Implosion project (Trail-master) is the development of an intense source of soft x-rays for materials and fusion studies. The x-ray source in the Trailmaster project is a foil initiated z-pinch. The next system in the Trailmaster project

is designed to deliver 15 MA of current to the imploding linear creating approximately 1 MJ of soft x-ray radiation in a submicrosecond pulse. This system, designated Procyon, will consist of a Mark 9 helical explosive generator, an explosively formed fuse (EFF) opening switch, detonator closing switches, a vacuum powerflow channel, a plasma flow switch (PFS), and the imploding foil load. In the present paper we will focus on the computational modeling of the overall Procyon system. This effort includes circuit and zero-dimensional point mass (slug) modeling, 1-D and 2-D radiation MHD calculations and 3-D radiation transport and view factor modeling of the vacuum powerflow channel. DOE

N91-29956# Texas Univ., Austin. Inst. for Fusion Studies.
ESTABLISHMENT OF AN INSTITUTE FOR FUSION STUDIES
D. E. Baldwin Jun. 1991 26 p
(Contract DE-FG05-80ET-53088)
(DE91-014922; DOE/ET-53088/7) Avail: NTIS HC/MF A03

This report discusses the following research: tokamak magnetohydrodynamic behavior; turbulence theory and plasma transport; computational plasma physics; alpha particle physics; nonlinear dynamics and mathematical physics. DOE

N91-29957# General Atomic Co., San Diego, CA.
H-MODE ENERGY CONFINEMENT SCALING FROM THE ASDEX, DIII-D, AND JET TOKAMAKS
D. P. Schissel, J. C. DeBoo, F. Ryter, O. Gruber, O. Kardaun, and F. Wagner (Max-Planck-Inst. fuer Plasmaphysik, Garching, Germany, F.R.) May 1991 5 p Presented at the International Conference on Systems Analysis in Water Quality Management, Berlin, Fed. Republic of Germany, 3-7 Jun. 1991
(Contract DE-AC03-89ER-51114)
(DE91-015145; GA-A-20548; CONF-910609-18) Avail: NTIS HC/MF A01

The desire to reach ignition in future tokamaks makes the energy confinement time (tau sub E) a critical parameter. The most promising enhanced (over L-mode) confinement regime is the H-mode, discovered on ASDEX with neutral beam heating, and than confirmed with various auxiliary heating sources on numerous machines. The knowledge of how H-mode tau sub E depends on different parameters is of crucial importance to the performance predictions for next generation devices. Historically, the designs have made the unsatisfactory assumption that H-mode tau sub E will scale as L-mode tau sub E with an H-mode enhancement factor of order two. Recently, in an effort to reduce the uncertainty in the predicted H-mode tau sub E, studies have been undertaken to investigate the scaling of ELM-free thermal H-mode confinement (tau sub th) and global tau sub E. The tau sub th scaling study was a joint effort between the JET and DIII-D Research Teams and found the relationship tau sub th is proportional to I sub p (exp 1.0) P sub L(exp -0.5) L(exp 1.5) where I sub p is the plasma current, P sub L is the loss power, and L is a plasma linear dimension. In the latter work performed for ITER, global confinement data from six tokamaks was assembled and the confinement time was analyzed statistically; the DIII-D/JET data was a subset of this larger database. Unfortunately the results from this larger study were unclear since the toroidal field (B sub T) scaling was not well defined. The preliminary results are reported of an extension of the tau sub th work by adding ASDEX data and examining the dependence of tau sub th on major radius R, minor radius a, and plasma elongation (kappa). DOE

N91-29958# Lawrence Livermore National Lab., CA.
DETECTION OF COHERENT STRUCTURES IN THE EDGE OF THE TEXT TOKAMAK PLASMA
A. V. Filippas, Ch. P. Ritz, A. E. Koniges, J. A. Crotinger, and P. H. Diamond (California Univ., San Diego, La Jolla.) 26 Apr. 1991 6 p Presented at the International Conference on Systems Analysis in Water Quality Management, Berlin, Fed. Republic of Germany, 3-7 Jun. 1991
(Contract W-7405-eng-48)
(DE91-015183; UCRL-JC-107194; CONF-910609-19) Avail: NTIS HC/MF A02

The detection is discussed of coherent structures in the edge of the text tokamak plasma. DOE

N91-29959# Wisconsin Univ., Madison.
EDGE ELECTROSTATIC FLUCTUATIONS AND TRANSPORT IN THE MST REVERSED FIELD PINCH
T. D. Rempel, C. W. Spragins, S. C. Prager, S. Assadi, D. J. DenHartog, and S. Hokin Apr. 1991 20 p
(Contract DE-FG02-85ER-53198)
(DE91-015218; DOE/ER-53198/174) Avail: NTIS HC/MF A03

Electrostatic fluctuations have been measured in a large reversed field pinch, and are large (tilde n sub e)/n approx. 20 to 40 pct., (tilde T sub e)/T approx. 10 to 25 pct. Frequency and wave number spectra are broad Delta n approx. 70 to 150, Delta m approx. 3 to 6, and differ from measured magnetic fluctuation spectra. The transport inferred from correlation measurements indicates that electrostatic fluctuations can account for significant particle losses, but contribute less than 15 pct. to energy loss. DOE

N91-29960# Wisconsin Univ., Madison.
GLOBAL CONFINEMENT AND DISCRETE DYNAMO ACTIVITY IN THE MST REVERSED FIELD PINCH
S. Hokin, A. Almagri, S. Assadi, J. Beckstead, G. Chartas, N. Crocker, M. Cudzinovic, D. DenHartog, R. Dexter, and D. Holly et al Apr. 1991 26 p
(Contract DE-FG02-85ER-53198)
(DE91-015219; DOE/ER-53198/173) Avail: NTIS HC/MF A03

Results obtained on the Madison Symmetric Torus (MST) reversed field pinch after installation of the design poloidal field winding are presented. Values of (beta sub theta e0) (triple bond) 2 mu (sub 0)n(sub e0) T(sub e0)/B(sub theta sup 2)(a) approximately 12% are achieved in low-current (I = 220 kA) operation; here n(sub e0) and T(sub e0) are central electron density and temperature, and B(sub theta)(a) is the poloidal magnetic field at the plasma edge. An observed decrease in (beta sub theta e0) with increasing plasma current may be due to inadequate fueling, enhanced wall interaction, and the growth of a radial field error at the vertical cut in the shell at high current. Energy confinement time varies little with plasma current, lying in the range 0.5 minus 1.0 ms. Strong discrete dynamo activity is present, characterized by the coupling of m = 1, n = 5 minus 7 modes leading to an m = 0, n = 0 crash (m and n are poloidal and toroidal mode numbers). The m = 0 crash generates toroidal flux and produces a small 2.5% increase in plasma current. DOE

N91-29961# Naval Research Lab., Washington, DC.
VLASOV SIMULATIONS OF VERY-LARGE-AMPLITUDE WAVE GENERATION IN THE PLASMA WAKEFIELD ACCELERATOR
Memorandum Report
Jonathan Krall, Glenn Joyce, and Eric Esarey 17 Jun. 1991 31 p
(Contract DE-AI05-83ER-40017)
(AD-A237428; NRL-MR-6772) Avail: NTIS HC/MF A03 CSCL 20/7

Simulations of the plasma wakefield accelerator are carried out by following the time evolution of the plasma distribution function in one dimension via the Vlasov-Maxwell equations. Simulation results are compared to numerical solutions of the nonlinear relativistic cold plasma equations and to previous theoretical estimations of trapping and thermal effects on plasma waves. It is found that highly nonlinear wakes are obtainable in the vicinity of the driving beam, where the thermal velocity spread of the plasma is reduced. In this region, wake amplitudes can significantly exceed the expectations of relativistic warm plasma models and agree closely with cold fluid theory. In all cases, however, particle trapping and thermalization due to particle scattering from the large amplitude plasma wave reduce the wake to below the nonrelativistic wavebreaking limit after the initial accelerating peak. GRA

N91-29962# Lawrence Livermore National Lab., CA.
ELECTROMAGNETIC PIC SIMULATIONS USING FINITE ELEMENTS ON UNSTRUCTURED GRIDS
J. Ambrosiano, S. T. Brandon, and R. Loehner (George Washington Univ., Washington, DC.) Jun. 1991 6 p Presented at the 14th Conference on Numerical Simulation of Plasmas, Annapolis, MD, 4-6 Sep. 1991
(Contract W-7405-eng-48)
(DE91-015141; UCRL-JC-107684; CONF-9109108-1) Avail: NTIS HC/MF A02

There is an increasing demand to use kinetic plasma simulations to model real plasma devices such as e-beam diodes, plasma torches, opening switches, and so on. With this demands comes the realization that standard simulation tools based on rectangular structured meshes are often too inflexible to accommodate real device geometries. To gain geometric flexibility, one typically must abandon structured rectangular meshes. Some have had considerable success by distorting the grid to conform to boundary-fitted curvilinear coordinates. This gives substantial flexibility while retaining a logically rectangular data structure. However, to achieve the greatest flexibility, an unstructured mesh is necessary. For the last several years, we have been engaged in designing electromagnetic particle-in-cell (PIC) simulations that can be performed on unstructured grids of triangles. We feel this is a powerful strategy for matching kinetic plasma simulations to real problem geometries. Unstructured meshes not only accommodate complicated boundary shapes with ease, but also allow extreme local refinement without affecting resolution elsewhere. The basic challenges to overcome in formulating EM-PIC on these new meshes are: (1) grid generation; (2) particle interpolation and tracking, and (3) field solution. In this paper we briefly describe our techniques and give a simple example. DOE

N91-29963# Oak Ridge National Lab., TN.
THICK-SECTION WELDMENTS IN 21-6-9 AND 316LN STAINLESS STEEL FOR FUSION ENERGY APPLICATIONS
D. J. Alexander and G. M. Goodwin 1991 7 p Presented at the Cryogenic Engineering Conference and International Cryogenic Materials Conference, Huntsville, AL, 11-14 Jun. 1991
(Contract DE-AC05-84OR-21400)
(DE91-015307; CONF-910635-8) Avail: NTIS HC/MF A02

The Burning Plasma Experiment (BPX), formerly known as the Compact Ignition Tokomak, will be a major advance in the design of a fusion reactor. The successful construction of fusion reactors will require extensive welding of thick-section stainless steel plates. Severe service conditions will be experienced by the structure. Operating temperatures will range from room temperature (300 K) to liquid nitrogen temperature (77 K), and perhaps even lower. The structure will be highly stressed, and subject to sudden impact loads if plasma disruptions occur. This demands a combination of high strength and high toughness from the weldments. Significant portions of the welding will be done in the field, so preweld and postweld heat treatments will be difficult. The thick sections to be welded will require a high deposition rate process, and will result in significant residual stresses in the materials. Inspection of these thick sections in complex geometries will be very difficult. All of these constraints make it essential that the welding procedures and alloys be well understood, and the mechanical properties of the welds and their heat-affected zones must be adequately characterized. The candidate alloy for structural applications in the BPX such as the magnet cases was initially selected as 21-6-9 austenitic stainless steel, and later changed to 316LN stainless steel. This study examined several possible filler materials for thick-section (25 to 50 mm) weldments in these two materials. The tensile and Charpy V-notch properties were measured at room temperature and 77 K. The fracture toughness was measured for promising materials. DOE

N91-29964# Lodestar Research Corp., Boulder, CO.
FUNDAMENTAL STUDIES OF FUSION PLASMAS
R. E. Aamodt, P. J. Catto, D. A. Dlppolito, J. R Myra, and D. A. Russell 28 Jun. 1991 18 p
(Contract DE-FG02-88ER-53263)
(DE91-015656; DOE/ER-53263/16; LRC-91-28) Avail: NTIS HC/MF A03

This report discusses ion cyclotron range of frequencies (ICRF) impurity studies; ICRF convective cells; sheath plasma waves and anomalous ion-Bernstain-wave (IBW) loading; a quasilinear description for fast wave minority heating permitting off-magnetic axis heating in a tokamak; and runaway electrons studies in support of TEXT. DOE

N91-29965# Texas Univ., Austin. Inst. for Fusion Studies.
IMPURITY AND NEUTRAL EFFECTS ON THE DISSIPATIVE DRIFT WAVE IN TOKAMAK EDGE PLASMAS
Y. Z. Zhang and S. M. Mahajan May 1991 37 p
(Contracts DE-FG05-80ET-53088; DE-FG05-88ER-53266)
(DE91-015907; DOE/ET-53088/500; IFSR-500) Avail: NTIS HC/MF A03

Possible destabilizing mechanisms for the liner electrostatic dissipative drift waves (in tokamak edge plasmas) are investigated in slab geometry. The effects of processes such as ionization, charge exchange, radiation, and rippling are examined. In particular, the impurity condensation associated with radiation cooling is evaluated appropriately for the drift wave ordering, which is found to be an important driving mechanism in contrast to the results of earlier studies. It is also shown that the role of ionization is quite complicated, and depends strongly on the manner in which the equilibrium is achieved. The linear eigenmode equation is studied both analytically and numerically. For the range of parameters relevant to TEXT tokamak, both the charge exchange of the rippling effect are found to be unimportant for instability. DOE

N91-29966# Wisconsin Univ., Madison.
ANOMALOUS ION HEATING FROM THE DYNAMO IN A REVERSED FIELD PINCH
N. Mattor, P. W. Terry, and S. C. Prager Jul. 1991 13 p
(Contracts DE-FG02-85ER-53212; DE-FG02-89ER-53291)
(DE91-015586; DOE/ER-53212/177) Avail: NTIS HC/MF A03

It is shown that the anomalous ion temperatures observed in reversed field pinches can arise from the dynamo. The dynamo is driven by $m = 1$ tearing modes, the energy of which partly inverses the cascades to restore the resistively decaying equilibrium. In addition, the $m = 1$ modes contain an excess amount of energy, which can be calculated via elementary means. This excess energy gives an anomalous loop voltage, and cascades to shorter wavelength where, for RFP parameters, it dissipates partly to ion heat via ion cyclotron resonances. DOE

N91-29967# Lawrence Livermore National Lab., CA.
TOWARDS A REALISTIC PLASMA SIMULATION CODE
D. V. Anderson Jun. 1991 6 p Presented at the 14th Conference on Numerical Simulation of Plasmas, Annapolis, MD, 4-6 Sep. 1991
(Contract W-7405-eng-48)
(DE91-015698; UCRL-JC-107735; CONF-9109108-3) Avail: NTIS HC/MF A02

Several new developments in the technology of simulating plasmas, both in particle and fluid models, now allow a stage of synthesis in which many of these advances can be combined into one simulation model. Accuracy and efficiency are the criteria to be satisfied in this quest. The following research is built on: (1) The development of the delta f method of Barnes; (2) The moving node Galerkin model of Glasser, Miller and Carlson; (3) Particle moving schemes on unstructured grids by Ambrosiano and Bradon; and (4) Particle simulations using sorted particles Anderson and Shumaker. Rather than being competing developments,these presumably can be combined into one computational model. The physics model for the plasma is summarized. The Vlasov equation can be solved as an initial value problem by integrating the plasma distribution function forward in time. DOE

N91-29968# Argonne National Lab., IL.
INTERACTIONS OF TURBULENT EDDIES AND COMBUSTION IN AN MHD SECOND STAGE COMBUSTOR

S. L. Chang and S. A. Lottes 1991 7 p Presented at the 26th Intersociety Energy Conversion Engineering (IECE) Conference, Boston, MA, 3-9 Aug. 1991
(Contract W-31-109-eng-38)
(DE91-015722; ANL/CP-72035; CONF-910801-14-Draft) Avail: NTIS HC/MF A02

Computer simulation was used to aid in the design of a magnetohydrodynamic second stage combustor. A 2-D steady state computer model, based on mass, momentum, and energy conservation laws for multiple gas species, an integral combustion submodel, and a two parameter turbulence submodel, is used to simulate the turbulent flow and combustion patterns in the combustor in which opposed jets of oxidizer are injected into a confined cross stream of hot gas/fuel mixture entering from the first stage. The model computes flow and combustion variable distributions in the combustor and predicts turbulent eddy size, fluid mixing patterns, and combustion efficiency. The interactions of turbulent eddies and combustion are studied and the results show that: (1) parameters of a turbulence submodel may significantly affect fluid mixing and combustion performance; (2) turbulent eddy size is a function of turbulent kinetic energy and dissipation rate; and (3) intense combustion occurs in areas where turbulent eddy size is about one tenth of the combustor size.
DOE

76 SOLID-STATE PHYSICS

Includes superconductivity.

For related information, see also *33 Electronics and Electrical Engineering* and *36 Lasers and Masers.*

N91-29969# Lawrence Livermore National Lab., CA.
InGaAs/GaAs GRADED SUPERLATTICES IN PHOTODETECTORS FOR WAVELENGTHS BEYOND 1 MICRON
R. Mariella, Jr., J. Morse, and Z. Liliental-Weber (California Univ., Berkeley. Lawrence Berkeley Lab.) Apr. 1990 8 p Presented at the Spring Meeting of the Materials Research Society, San Francisco, 16-21 Apr. 1990
(Contract W-7405-eng-48)
(DE90-012073; UCRL-102563; CONF-900466-53) Avail: NTIS HC/MF A02

We have used molecular beam epitaxy (MBE) to grow graded In(x)Ga(1-x)As/GaAs superlattices on GaAs substrates as buffers for larger period, constant composition In(x)Ga(1-x)As/GaAs superlattices. Transmission electron microscopy (TEM) analysis shows that there are numerous crystal defects associated with the presence in strained layers, but, in many cases, the buffer layers confine these defects to areas outside of the strained-layer superlattices. PIN detectors fabricated from these structures show external quantum efficiencies up to 2.7 percent. DOE

N91-29970# Argonne National Lab., IL.
HIGH RESOLUTION ELECTRON MICROSCOPY OF GRAIN BOUNDARIES
K. L. Merkle and Y. Gao Mar. 1991 19 p Presented at the 25th Annual Microbeam Analysis Society Meeting, San Jose, 4-9 Aug. 1991
(Contract W-31-109-eng-38)
(DE91-010593; ANL/CP-72768; CONF-910872-1) Avail: NTIS HC/MF A03

Systematic High-Resolution Electron Microscopy (HREM) investigations have provided new insights into the atomic structure of grain boundaries (GBs). The application of this atomic-scale information to the understanding of GB properties may in the future allow for the possibility of prediction and modification of GB properties. HREM studies of a number of GBs in NiO and Au have clearly demonstrated that a general tendency exists to produce atomically well-matched structures and to preserve a high degree of coherency across the interface. HREM observations have established that misfit-dislocation-like defects are formed in large-misfit, incommensurate grain boundaries. We expect that these and other general structural features that have been investigated in NiO and Au are typical for other ceramic and metal GBs. Considerable progress has been made regarding the quantification of structural Gb parameters via HREM. Whereas several discrepancies between observed and calculated GB parameters remain, it is expected that the mutual feedback between HREM observations and GB computer simulation will serve as a stimulus to improve both the experimental and theoretical techniques and will lead to a better understanding of the complicated interrelations between GB structure and properties. Atomic structure information obtained from HREM observations on YBa2Cu3O(7-x) GBs has led to a much improved understanding of the critical current behavior in these systems. Direct correlations between atomic structure, including chemical composition, and property measurements on individual GBs will be important for a full understanding of many grain boundary properties. DOE

N91-29971# Sandia National Labs., Albuquerque, NM.
QUANTITATIVE ANALYSIS OF OXYGEN SEGREGATION ON INVERSION DOMAIN BOUNDARIES IN ALUMINUM NITRIDE
A. D. Westwood, M. R. Notis (Lehigh Univ., Bethlehem, PA.), and J. R. Michael 1991 15 p Presented at the 49th Electron Microscopy Society of America (EMSA) Annual Meeting, San Jose, 4-9 Aug. 1991
(Contract DE-AC04-76DP-00789)
(DE91-010869; SAND-91-0760C; CONF-910870-10) Avail: NTIS HC/MF A03

Curved and planar inversion domain boundaries (IDB) in aluminum nitride (AIN) form in sintered AIN ceramics containing oxygen, and oxygen is known to segregate to them. A number of interface models shown in Table 1, have been suggested based upon crystallographic constraints, chemical information and observed high resolution electron microscope (HREM) images. Until recently, problems with simulation of HREM images from AIN have made accurate determination of the structure of the IDB interface difficult. The aim of the present study was to use quantitative analytical electron microscopy (AEM) to determine the oxygen concentration at the IDBs, and then to compare the experimental results with calculated oxygen concentrations for each of the IDB models using a Monte Carlo electron trajectory simulation program. A match, if any, between the experimental and calculated oxygen concentrations would indicate the model which best described the IDB structure. The best match was obtained for Youngman's defect model. DOE

N91-29972# Lawrence Livermore National Lab., CA.
ELECTRON MICROSCOPY OF THICK 304 SS-COPPER MULTILAYERS
M. A. Wall and T. W. Barbee, Jr. Mar. 1991 6 p Presented at the 25th Annual Microbeam Analysis Society Meeting, San Jose, 4-9 Aug. 1991
(Contract W-7405-eng-48)
(DE91-011116; UCRL-JC-106765; CONF-910872-3) Avail: NTIS HC/MF A02

Multilayer nano-structures are dense synthetic ultrafine grained high interface concentration solids. Such material are of interest since their unique structures often result in new or enhanced physical properties. In this paper the results of a TEM characterization study of a series of thick 304 Stainless Steel (SS)-Copper (Cu) multilayered structures are presented. Magnetron sputter deposited SS films have a metastable BCC structure with the (110) planes parallel to the substrate. This occurs as the mean energy of an incident adatoms are approximately 9 eV; all this energy is absorbed at the deposition surface. The surface of the material passes through the delta BCC phase of SS during deposition and this structure is quench stabilized due to the large (greater than 10(exp 10) K/sec.) surface cooling rates. At multilayer periods of less than or equal to 200 A the epitaxial growth of SS on a FCC-Cu results in FCC-SS as deposited. Transformation of the FCC-SS to BCC is possibly held in check by coherency strains with the Cu lattice. For periods of greater than or equal to 500 A there is a bimodal FCC,BCC-SS structure. The FCC to BCC interface in the SS layer appears to lie at 50 to 100 A from the

SS on Cu interface. Since coherency strains are confined to regions near the interface, the retained FCC structure of the SS is limited to this region. The bimodal structure is believed to result from partial transformation of the SS during deposition in the larger period (greater than or equal to 500 A) multilayers. DOE

N91-29973# Argonne National Lab., IL.
RUDDLESDEN-POPPER PHASES A(n+1)M(n)O(3n+1): STRUCTURES AND PROPERTIES
J. S. Kim, J. Y. Lee, J. S. Swinnea, H. Steinfink, W. M. Reiff (Northeastern Univ., Boston, MA.), P. Lightfoot, S. Pei, and J. D. Jorgensen Mar. 1991 6 p Presented at the International Conference on the Chemistry of Electronic Ceramic Materials, Grand Teton National Park, 16-21 Aug. 1990
(Contract W-31-109-eng-38)
(DE91-011748; ANL/CP-72825; CONF-900813-2) Avail: NTIS HC/MF A02

Intergrowth crystal structures in inorganic systems have provide a fertile field of solid state chemical research for many years and the discovery of high-(Tc) superconducting cuprates has focused attention on intergrowth structures based on perovskite blocks. Ruddlesden and Popper (R-P hereafter) have described intergrowth structures with the general formula Sr(n+1)Ti(n)O(3n+1) where n is the number of perovskite layers separated by SrO layers. Indeed, La2CuO4 corresponds to the n = 1 phase in which the decreased ionic charge of the octahedral ion is compensated by the increased ionic charge of the dodecahedral ion. Numerous structures have been derived from the parent compounds by the replacement of Ti(4+) with lower valent transition metals and charge compensation with higher valent ions on the alkaline earth site. In this manner the series of compounds Ln2AM2O7 (Ln(3+) = La, Nd, Sm, Eu, Gd, Tb; A(2+) = Sr, Ba; M(3+) = Mn, Fe) has been synthesized and they are isomorphous with the n = 2 R-P phase. Relatively few compounds with n = 3 have been investigated. We have synthesized and investigated the properties of LaSr3Fe3O(9 +/- delta) and report here some of the results. DOE

N91-29974# California Univ., Berkeley. Lawrence Berkeley Lab.
SPECIFIC HEAT OF YBaCu3O7: VOLUME FRACTION OF SUPERCONDUCTIVITY; PARAMETERS CHARACTERISTIC OF THE IDEAL SUPERCONDUCTING STATE
N. E. Phillips and R. A. Fisher Jan. 1991 11 p Presented at the Workshop on Electronic Structures and Mechanisms for High Temperature Superconductivity, Miami, 3-9 Jan. 1991
(Contract DE-AC03-76SF-00098)
(DE91-011827; LBL-30435; CONF-910190-3) Avail: NTIS HC/MF A03

Experimentally determined parameters for YBa2Cu3O7 (YBCO) are strongly sample dependent. However correlations among parameters derived from the specific heat (C) suggest that the variation reflects a variation in the volume fraction of superconductivity, (f(sub s)). From these correlations f(sub s) can be quantitatively determined and values of parameters characteristic of fully superconducting material can be derived. With additional assumptions, it is also possible to estimate the Sommerfeld constant gamma for the fully normal state. Among the parameters of particular importance in establishing the correlations are the discontinuity in C (Delta C(Tc)) at the critical temperature (Tc) and concentration (n(sub 2)) of localized Cu(2+) magnetic moments. These are located on the YBCO lattice, at least in substantial measure, and are directly correlated with f(sub s). From an analysis of C in the vicinity of (Tc) it is possible to obtain information on the strength of the coupling responsible for the superconductivity; from a comparison of gamma with that calculated for the bare density of states (gamma(sub bs)) the electronphonon enhancement parameter (lambda) can be obtained. This linear term, gamma(0)T, has attracted much attention. It was recognized very early that it could be simply a manifestation of an incomplete transition to the superconducting state. However, independently of, and more or less simultaneously with, its experimental discovery , a linear term was predicted theoretically as one of the consequences of the resonant valence bond (RVB) theory. In the RVB model the excitations from the superconducting ground state re qualitatively different from those. DOE

N91-29975# Oak Ridge National Lab., TN.
PROPERTIES OF MATERIALS WITH A FINE LENGTH SCALE: MECHANICALLY ALLOYED METALS AND THE HIGH TEMPERATURE SUPERCONDUTOR Y1Ba2Cu3O7
J. R. Thompson, C. Politis, and Young Cheol Kim (Tennessee Univ., Knoxville.) 1991 8 p Presented at the International Symposium on Mechanical Alloying, Kyoto, Japan, 7-10 May 1991
(Contract DE-AC05-84OR-21400)
(DE91-012538; CONF-9105182-1) Avail: NTIS HC/MF A02

A variety of methods, particularly mechanical alloying, can be used to fabricate materials that have a fine length scale. As the relevant length scale and/or physical dimensions of a system are reduced, its structural, electronic, and other physical properties may change greatly. This paper reviews some features of materials processed by two quite different methods to achieve desired relative lengths. By ball milling mixtures of early and late transition metals in a high energy mill, one ternary and several binary metal systems were mechanically alloyed. This produced amorphous, microcrystalline, intermetallic, or mixed phase alloys of Ti-Pd, Ti-Pd-Cu, Hf-Ni, Hf-Cu, Hf-Ru, and Zr-Rh. In some cases, a wide compositional range of highly disordered or amorphous materials was obtained. X-ray diffraction and differential thermal analysis (DTA) were used for materials analysis. The resulting crystallization temperatures for different compositions are compared with model predictions. For comparison, fine powders of the superconductor Y1Ba2Cu3O7 produced by vapor phase pyrolysis were studied. DOE

N91-29976# International Centre for Theoretical Physics, Trieste (Italy).
DIELECTRIC FUNCTION OF SEMICONDUCTOR SUPERLATTICE
Guoyi Qin Aug. 1990 14 p
(DE91-617788; IC-90/227) Avail: NTIS HC/MF A03

We present a calculation of the dielectric function for semiconductor GaAs/Ga(1-x)Al(x)As superlattice taking account of the extension of the electron envelope function and the difference of both the dielectric constant and width between GaAs and Ga(1-x)Al(x)As layers. In the appropriate limits, our results exactly reduce to the well-known results of the quasi two-dimensional electron gas obtained by Lee and Spector and of the period array of two-dimensional electron layers obtained by Das Sarma and Quinn. By means of the dielectric function of the superlattice, the dispersion relation of the collective excitation and the screening property of semiconductor superlattice are discussed and compared with the results of the quasi two-dimensional system and with the results of the periodic array of the two-dimensional electron layers. DOE

N91-29977# International Centre for Theoretical Physics, Trieste (Italy).
ORBITALS, CORRELATION, VALENCIES IN HIGH-T(SUB c) SUPERCONDUCTORS
D. I. Khomskii Sep. 1990 19 p
(DE91-618099; IC-90/266) Avail: NTIS HC/MF A03

The survey is given of certain properties of high-Tc superconductors connected with the details of their electronic structure such as the kind of orbitals involved and the degree of correlation. Special attention is paid to the properties of cuprates at high doping level. The problem whether there exists a 'Mott transition' at high electron or a hole concentration is discussed. We also discuss physical factors (d-p Coulomb interaction, orbital mixing) leading to the partial occupation of copper d(sub x(exp 2))-orbital. In particular, we show that in localized picture (x(exp 2)-y(exp 2)) and z(exp 2)-levels in La(2-x)Sr(x)CuO4 may cross at x approx. 0.4 which may be responsible for a marked change of many properties at this doping. The possible role of x(exp 2)-electrons in pairing is discussed in connection with some recent experiments. DOE

N91-29978# Missouri Univ., Rolla.
DEFECT CHARACTERIZATION OF ELECTRONIC CONDUCTING PSEUDO-PEROVSKITE SYSTEMS
H. U. Anderson, M. M. Nasrallah, D. M. Sparlin, and P. E. Parris 1990 44 p
(Contract DE-FG02-85ER-45219)
(DE91-014385; DOE/ER-45219/5) Avail: NTIS HC/MF A03

The goal of the investigation presented in this report is to study the inter-relationship between electrical conductivity, oxidation-reduction kinetics, defect structure, and composition of n- and p- type binary and ternary transition metal oxides. The experimental part of the investigation included specimen preparation, thermogravimetric measurements, x ray diffraction, thermally stimulated current, oxygen diffusion, optical absorption, transmission electron microscopy, electrical conductivity, and Seebeck measurements. The systems studied or being studied are LaMnO3-LaCrO3-LaCoO3, Y(1-x)Ca(x)CrO3, Sr-doped LaMnO3, Y(1-x)Ca(x)MnO3, and Ba2YCu3O(7-x). DOE

N91-29979# Argonne National Lab., IL.
PHOTOEMISSION AND ELECTRONIC STRUCTURE STUDIES OF YBa2Cu3O(x)
R. Liu, B. W. Veal, A. P. Paulikas, J. W. Downey, H. Shi, C. G. Olson, C. Gu, A. J. Arko, J. J. Joyce, and R. J. Bartlett (Los Alamos National Lab., NM.) May 1991 11 p Presented at the Conference on Fermiology of High Tc Superconductors, Argonne, 25-27 Mar. 1991
(Contract W-31-109-eng-38)
(DE91-014469; ANL/CP-73357; CONF-9103112-2) Avail: NTIS HC/MF A03

High-resolution angle-resolved photoelectron spectroscopy measurements are reported for YBa2Cu3O(x) when the oxygen stoichiometry x is varied between 6.9 (92 K superconductor) and 6.2 (insulator). Fermi surfaces obtained from energy distribution curve measurements on a grid scanning the entire first Brillouin zone are reported for the x = 6.9 samples. Bands along the (Gamma)-S symmetry line were measured for samples with reduced oxygen stoichiometry. For superconducting samples, these bands are essentially independent of x. As the material becomes insulating (x less than 6.4), a dramatic falloff of spectral weight near E(sub F) is observed. Resonant spectral features also disappear. Efforts to observe a superconducting gap are reported. DOE

N91-29980# Missouri Univ., Columbia. Research Reactor Facility.
INELASTIC SCATTERING IN CONDENSED MATTER WITH HIGH INTENSITY MOESSBAUER RADIATION
W. B. Yelon and G. Schupp May 1991 24 p
(Contract DE-FG02-85ER-45200)
(DE91-014384; DOE/ER-45200/7) Avail: NTIS HC/MF A03

We give a progress report for the work which has been carried out in the last three years with DOE support. A facility for high-intensity Moessbauer scattering is not fully operational at the University of Missouri Research Reactor (MURR) as well as a facility at Purdue, using special isotopes produced at MURR. High precision, fundamental Moessbauer effect studies have been carried out using Bragg scattering filters to suppress unwanted radiation. These have led to a Fourier transform method for describing Moessbauer effect (ME) lineshape and a direct method of fitting ME data to the convolution integral. These methods allow, complete correction for source resonance self absorption and the accurate representation of interference effects that add an asymmetric component to the ME lines. We have begun applying these techniques to attenuated ME sources whose central peak has been attenuated by stationary resonant absorbers, to make a novel independent determination of interference parameters and line-shape behavior in the resonance asymptotic region. This analysis is important to both fundamental ME studies and to scattering studies for which a deconvolution is essential for extracting the correct recoilless fractions and interference parameters. A number of scattering studies have been successfully carried out including a study of the thermal diffuse scattering in Si, which led to an analysis of the resolution function for gamma-ray scattering. Also studied was the anharmonic motion in Na metal and the charge density wave satellite reflection Debye-Waller factor in TaS2, which indicate phason rather than phonon behavior. Using a specially constructed sample cell which enables us to vary temperatures from -10 C to 110 C, we have begun quasielastic diffusion studies in viscous liquids and current results are summarized. Included are the temperature and Q dependence of the scattering in pentadecane and diffusion in glycerol. DOE

N91-29981# Wichita State Univ., KS. National Inst. for Aviation Research.
HIGH TEMPERATURE KNUDSEN EFFUSION-MASS SPECTROMETRIC STUDIES OF THE Y-Ba-Cu-O SYSTEM Ph.D. Thesis
Dwight L. Myers and Phillip G. Wahlbeck 1991 122 p
(NIAR-91-23) Avail: NTIS HC/MF A06

The vaporization of copper from YBa2Cu3O(7-x) was studied by Knudsen Effusion Mass Spectrometry (KEMS). The oxygen content at the starting temperature of the vaporization studies was inferred to be 6.24. The vapor pressures yielded activities and chemical potential differences of Cu in equilibrium with YBa2Cu3O(6.24). The residues after the experiments were found by X-ray diffraction to be principally Y2BaCuO5. The relative merits of BaCO3 compared to Ba(NO3)2 as precursor in the synthesis of YBa2Cu3O(7-x) superconductor were examined. Samples of YBa2Cu3O(7-x) were prepared using Y2O3, CuO and either Ba(NO3)2 or BaCO3. These samples were studied using KEMS and SEM-EDAX to determine if levels of carbonate in the sample were reduced by using Ba(NO3)2 as a starting material. The results showed that samples prepared using the nitrate compound were significantly lower in carbonate than the samples prepared using the carbonate. Author

N91-29982*# National Aeronautics and Space Administration. Lewis Research Center, Cleveland, OH.
HIGH TEMPERATURE SUPERCONDUCTOR ANALOG ELECTRONICS FOR MILLIMETER-WAVELENGTH COMMUNICATIONS
R. R. Romanofsky and K. B. Bhasin 1991 8 p Presented at the Conference on Advanced Space Exploration Initiative Technologies, Cleveland, OH, 4-6 Sep. 1991; cosponsored by AIAA and OAI
(NASA-TM-105184; E-6481; NAS 1.15:105184; AIAA-91-3592)
Avail: NTIS HC/MF A02 CSCL 20L

The performance of high temperature superconductor (HTS) passive microwave circuits up to X-band was encouraging when compared to their metallic counterparts. The extremely low surface resistance of HTS films up to about 10 GHz enables a reduction in loss by as much as 100 times compared to copper when both materials are kept at about 77 K. However, a superconductor's surface resistance varies in proportion to the frequency squared. Consequently, the potential benefit of HTS materials to millimeter-wave communications requires careful analysis. A simple ring resonator was used to evaluate microstrip losses at Ka-band. Additional promising components were investigated such as antennas and phase shifters. Prospects for HTS to favorable impact millimeter-wave communications systems are discussed. Author

N91-29983# Midwest Research Inst., Golden, CO.
SCANNING TUNNELING MICROSCOPY STUDIES OF THE SURFACES OF a-Si:H AND a-SiGe:H FILMS
A. Gallagher, R. Ostrom, and D. Tannenbaum (National Inst. of Standards and Technology, Boulder, CO.) Jun. 1991 25 p
(Contract DE-AC02-83CH-10093)
(DE91-002169; SERI/TP-214-4409) Avail: NTIS HC/MF A03

The report contains a detailed description of the experimental complexities encountered in developing scanning tunneling microscope (STM) probing of atomic structure on the surface of freshly-grown hydrogenated-amorphous semiconductors. It also contains a speculative microscopic film-growth model that explains differences between the disorder in CVD grown a-Ge:H versus a-Si:H films. This model is derived from prior results obtained in the chemical analysis of GeH4 plasmas, combined with surface

reaction and thermodynamic considerations. The neutral radical fragments of silane, disilane and germane dissociation in discharges, which dominate the vapor and film-growth reactions, have been deduced from detailed analysis of prior data and are reported. DOE

N91-29984# Argonne National Lab., IL.
INVERSE PROBLEM IN NEUTRON REFLECTION
Xiao-Lin Zhou, G. P. Felcher, and Sow-Hsin Chen (Massachusetts Inst. of Tech., Cambridge.) May 1991 23 p Presented at the North Atlantic Treaty Organization (NATO) Advanced Research Workshop on Inverse Problems in Scattering and Imaging, North Falmouth, MA, 14-19 Apr. 1991
(Contract W-31-109-eng-38)
(DE91-014457; ANL/CP-73387; CONF-9104271-1) Avail: NTIS HC/MF A03

Reflectance and transmittance of neutrons from a thin film deposited on a bulk substrate are derived from solution of Schroedinger wave equation in the material medium with an optical potential. A closed-form solution for the complex reflectance and transmittance is obtained in an approximation where the curvature of the scattering length density profile in the film is small. This closed-form solution reduces to all the known approximations in various limiting cases and is shown to be more accurate than the existing approximations. The closed-form solution of the reflectance is used as a starting point for an inversion algorithm whereby the reflectance data are inverted by a matrix iteration scheme to obtain the scattering length density distribution in the film. A preliminary test showed that the inverted profile is accurate for the linear scattering length density distribution but falls short in the case of an exponential distribution. DOE

N91-29985# Sandia National Labs., Albuquerque, NM.
LARGE BIPOLARONS AND SUPERCONDUCTIVITY
D. Emin 1991 2 p Presented at the International Conference on Materials and Mechanisms of Superconductivity, Kanazawa (Japan), 22-26 Jul. 1991
(Contract DE-AC04-76DP-00789)
(DE91-014699; SAND-88-2554C; CONF-910736-3) Avail: NTIS HC/MF A01

With a strong electron-lattice interaction, charge carriers pair as bipolarons. In analogy with large (multisite) polarons, large bipolarons move itinerantly. Such mobile-charge bosons can condense into a superconducting state. Distinctive properties characterize large bipolarons. DOE

N91-29986# Los Alamos National Lab., NM.
GROWTH CONDITION DEPENDENCE OF RHEED PATTERN FROM GaAs(111)B SURFACE
K. Yang, W. Li, A. P. Taylor, L. J. Schowalter, Q. F. Xiao (State Univ. of New York, Albany.), B. K. Laurich, and D. L. Smith 1991 7 p Presented at the Spring Meeting of the Materials Research Society (MRS), Anaheim, CA, 29 Apr. - 3 May 1991
(Contract W-7405-eng-36)
(DE91-014770; LA-UR-91-1919; CONF-910406-24) Avail: NTIS HC/MF A02

A 3-D phase diagram is introduced to describe the dependence of the RHEED pattern from GaAs(111)B surface on growth conditions. The 2 x 2, transitional (1 x 1), and sq. root of 19 x sq. root of 19 surface reconstructions correspond to different zones in the phase diagram. A equation is given for the planes that separate these zones, which fit experimental data well. Homoepitaxial films on GaAs(111)B grown in the 2 x 2 region generally have bad crystal quality as determined by the ion channeling, and growth in the sq. root of 19 x sq. root of 19 region generally yields rough surface morphology. At higher substrate temperatures (approximately 650 C), featureless films with minimum ion channeling yields of less than 4 percent are achieved. DOE

N91-29987# Argonne National Lab., IL.
DE HAAS-VAN ALPHEN AND FERMI SURFACE STUDIES OF ORGANIC SUPERCONDUCTORS (ET)2X
J. Wosnitza, G. W. Crabtree, H. H. Wang, K. D. Carlson, and J. M. Williams May 1991 18 p Presented at the Physical Phenomena At High Magnetic Fields, Tallahassee, 15-18 May 1991
(Contract W-31-109-eng-38)
(DE91-015137; ANL/CP-73426; CONF-9105151-8) Avail: NTIS HC/MF A03

We report measurements of the de Haas-van Alphen (dHvA) effect in the organic superconductors ET (sub 2)X with X = Cu(NCS)(sub 2), NH(sub 4) Hg(SCN)(sub 4) and IBr2 in fields up to 15 T and temperatures down to 0.45 K. All three materials show a strong two-dimensionality of the Fermi surface (FS) as seen by the perfect 1/cos Theta behavior of the dHvA frequencies. Beating of the dHvA oscillations in X = IBr2 gives clear evidence of a warped structure of the FS cylinder. For the first time, we determine the angular dependence of the cyclotron effective mass, m(sub c). The 1/cos Theta dependence of m(sub c) causes directly observable spin slitting zeros for up to 5 angles. With our results it was possible to obtain the effective mass enhancement due to electron-phonon coupling. Estimates of (Tc) yield qualitative agreement with the observed values. DOE

N91-29988# Argonne National Lab., IL.
LOW TEMPERATURE FLUX CREEP IN HIGH-T(SUB c) SUPERCONDUCTORS
V. M. Vinokur, Ming Xu, G. W. Crabtree, M. V. Feigelman, V. B. Geshkenbein (Academy of Sciences, USSR, Moscow), and A. Umezawa 1991 14 p Presented at the Physical Phenomena At High Magnetic Fields, Tallahassee, 15-18 May 1991
(Contract W-31-109-eng-38)
(DE91-015193; ANL/CP-73508; CONF-9105151-9) Avail: NTIS HC/MF A03

An exact solution describing flux creep in high T sub c superconductors at low temperatures was found, assuming the creep activation barrier U grows logarithmically with decreasing current j: U = U sub 0 ln(j sub 0/j). The magnetic relaxation of single crystal Bi2Sr2CaCu2O8 was measured at moderate temperatures and magnetic fields. Two different regimes corresponding to the partial and full penetration of the magnetic field into the sample were found. The observed magnetic relaxation behavior is in a good agreement with the model proposed. DOE

N91-29989# Argonne National Lab., IL.
PHOTOEMISSION MEASUREMENT OF FERMI SURFACE, BAND DISPERSION, AND QUASIPARTICLE LIFETIME IN YBa2Cu3O6.9
J. C. Campuzano, G. Jennings, B. W. Veal, R. Benedek, A. J. Arko, and R. S. List (Los Alamos National Lab., NM.) Jun. 1991 8 p Presented at the Conference on Fermiology of High Tc Superconductors, Argonne, 25-27 Mar. 1991
(Contracts W-31-109-eng-38; DE-FG02-85ER-45222)
(DE91-015194; ANL/CP-73507; CONF-9103112-3) Avail: NTIS HC/MF A02

High resolution (20 MeV) angle-resolved photoemission measurements on single-crystals of YBa2Cu3O6.9 were analyzed to obtain band dispersion and quasiparticle lifetimes. The mass enhancement is 1.2 for a Cu-O plane band mass and 1.0 for the Pd(Pi) chain band. Fitting measured energy distribution curves to a model spectrum that includes self-energy corrections, we find that the imaginary part of the self-energy varies quadratically in the immediate vicinity of E(sub F), and becomes linear above approximately 20 MeV. DOE

N91-29990# Argonne National Lab., IL.
CORRELATIONS BETWEEN GRAIN BOUNDARY STRUCTURE AND ENERGY
K. L. Merkle and D. Wolf 1991 7 p Presented at the Spring Meeting of the Materials Research Society (MRS), 29 Apr. - 3 May 1991 and the International Symposium on Metal/Ceramic Interfaces, Anaheim, CA, 30 Jun. - 5 Jul. 1991
(Contract W-31-109-eng-38)
(DE91-015204; ANL/CP-71904; CONF-910406-27; CONF-9106236-1) Avail: NTIS HC/MF A02

High-resolution electron-microscopy (HREM) and computer simulations of (110) tilt grain boundaries (GBs) in Au are used to investigate correlations between atomic-scale GB structure and energy. The energies calculated for a variety of symmetric and asymmetric GBs suggest that asymmetric GB-plane orientations are often preferred over symmetric ones. The experimentally observed faceting behavior agrees with the computed energies. Computer simulations indicate general interrelations between GB energy and (1) volume expansion and (2) the number of broken bonds per unit area of GB. These atomic-scale microstructural GB parameters, as evaluated from observations, are compared to simulation results. DOE

N91-29991# Argonne National Lab., IL.
FABRICATION AND WIRE EXTRUSION OF CERAMIC SUPERCONDUCTORS
R. B. Poeppel, U. Balachandran, J. P. Singh, J. T. Dusek, J. J. Picciolo, S. E. Dorris, M. T. Lanagan, K. C. Goretta, C. A. Youngdahl, and J. R. Hull May 1991 8 p Presented at the 2nd Topical Conference on Emerging Technologies in Materials, San Francisco, CA, 6-9 Nov. 1989
(Contract W-31-109-eng-38)
(DE91-015207; ANL/CP-68452; CONF-891153-2) Avail: NTIS HC/MF A02

Many applications of high-temperature superconductors (HTSs) will depend on the ability to fabricate these materials into long lengths with suitable electrical and mechanical properties maintained over the entire length. The program described in this paper is focused on improvement of the relevant material properties of HTSs and on development of fabrication methods that can be transferred to industry for production of commercial conductors. Our research has resulted in advances in fabrication methods that improve the performance of long lengths of polycrystalline HTS wires and tapes. We have examined the Y-Ba-Cu-O (YBCO), Bi-Sr-Ca-Cu-O (BSCCO), and Tl- Ba-Ca-Cu-O (TBCCO) classes of HTSs. Significant results from our research and work by contemporaries are reported in the various sections of the paper. DOE

N91-29992# Argonne National Lab., IL.
SYNTHESIS AND SUPERCONDUCTIVITY IN Ba(1-x)K(x)BiO3
D. G. Hinks May 1991 5 p Presented at the 3rd International Superconductivity Technology Center Workshop on Superconductivity, Kumamoto City (Japan), 13-15 May 1991
(Contract W-31-109-eng-38)
(DE91-015254; ANL/CP-73493; CONF-9105226-1) Avail: NTIS HC/MF A01

The synthesis of Ba(1-x)K(x)BiO3 requires a two step process. In-situ neutron diffraction and thermogravimetric analysis (TGA) has been used to follow the synthesis process and shows that the superconducting material is metastable at room temperature. Recent work on point contact tunneling into high-density, melt processed material has shown almost ideal junction behavior unlike the behavior found in the copper-oxide compounds. DOE

N91-29993# Oak Ridge National Lab., TN.
AC SUSCEPTIBILITY OF SUPERCONDUCTIVE THIN FILMS
H. R. Kerchner, R. Feenstra, and J. O. Thomson (Tennessee Univ., Knoxville.) 1991 8 p Presented at the Cryogenic Engineering Conference and International Cryogenic Materials Conference, Huntsville, AL, 11-14 Jun. 1991
(Contract DE-AC05-84OR-21400)
(DE91-015273; CONF-910635-7) Avail: NTIS HC/MF A02

The magnetic transitions of superconductive materials are readily observed by the use of a mutual inductance bridge. The critical current density J(sub c) has long been deduced from ac-susceptibility measurements. Thermally activated giant flux creep and flux flow (TAFF) make the new, high-(Tc) materials respond to applied ac fields with lossy ac currents. Measurements of J(sub c), the effective penetration depth (lambda sub c), and the TAFF resistivity (rho sub TAFF) in YBa2Cu3O(7-delta) thin films are presented. A technique is described for deducing J(sub c) from moment changes with 10(exp -6)-emu sensitivity fr deducing J(sub c) from moment changes with 10(exp -6)-emu sensitivity. DOE

N91-29994# Oak Ridge National Lab., TN.
HIGH-RESOLUTION Z-CONTRAST IMAGING OF SUPERLATTICES AND HETEROSTRUCTURES
S. J. Pennycook, D. E. Jesson, and M. F. Chisholm Jun. 1991 10 p Presented at the 7th Oxford Conference on Microscopy of Semiconducting Materials, London, England, 25-28 Mar. 1991
(Contract DE-AC05-84OR-21400)
(DE91-015329; CONF-910322-2) Avail: NTIS HC/MF A02

The Z-contrast technique for high-resolution imaging provides incoherent images with column-by-column compositional sensitivity, therefore allowing a direct interpretation of interfacial structures to be made to first order. This capability is illustrated through studies of interfaces in epitaxial silicides and ultrathin Si(sub m)Fe(sub n)(sup p) superlattices. Interface defects observed at the (100) Si/CoSi2 interface are linked to Si surface defects preserved during growth of the thin silicide template. At Si/Ge interfaces grown by molecular beam epitaxy (MBE), new ordered arrangements have been observed and attributed to a Si/Ge atom exchange mechanism occurring during growth of Si over a 2 times 1 reconstructed Ge surface. Anticipated performance of a 300 kV high-resolution scanning transition electron microscope (STEM) is briefly discussed. DOE

N91-29995# Sandia National Labs., Albuquerque, NM.
SUPERCONDUCTING SUPEROXYGENATED La(2-x)Sr(x)CuO(4+DELTA): SEARCH FOR PHASE SEPARATION
B. Morosin, J. E. Schirber, J. A. Voigt, E. L. Venturini, G. H. Kwei, and J. A. Goldstone (Los Alamos National Lab., NM.) 1991 2 p Presented at the International Conference on Materials and Mechanisms of Superconductivity, Kanazawa (Japan), 22-26 Jul. 1991
(Contract DE-AC04-76DP-00789)
(DE91-015334; SAND-91-0773C; CONF-910736-5) Avail: NTIS HC/MF A01

High pressure (2.3 kbar) high temperature (575 C) oxygen annealed ceramic La(2-x)Sr(x)Cu(4+delta), with x = 0.1 and 0.16, have been studied by high-resolution neutron powder diffraction to determine their low temperature structural properties in comparison to similarly oxygenated La2CuO(4+delta). Unlike La2CuO(4+delta), these Sr-containing superconductors show no low temperature phase separation. Further, for x = 0.16, the interstitial oxygen appears to be located at (1/4, 1/4, z) with z = 0.163(5) and to have a value of delta consistent with La(1.84)Sr(0.16)CuO(4.019). Such a site is significantly displaced away from the interstitial location, (1/4, 1/4, z) with z (approx equal) 0.25 observed in La2CuO(4+delta). For x = 0.1, no interstitial oxygen is found and delta = 0.0. DOE

N91-29996# California Univ., Davis. Dept. of Chemistry.
DISCRETENESS-OF-SOLVENT EFFECTS IN MARCUS EQUATIONS IN THE MEAN SPHERICAL APPROXIMATION
L. Blum and W. R. Fawcett 20 May 1991 5 p
(Contract N00014-90-J-1235)
(AD-A237133; TR-14) Avail: NTIS HC/MF A01 CSCL 20/12

In the Marcus theory of electron transfer the outer sphere contribution to the free energy of activation G sub os is usually computed from Born continuum dielectric formula. The Mean Spherical Approximation gives systematic corrections to this quantity, which for a solvent of hard dipolar spheres can be explicitly calculated. The contributions are of two kinds: The polarization of the solvent by the charges, and the electrostriction effects, which usually are small. The effects of ion association are included using recent results for sticky potential models. These corrections also can be incorporated into the dynamical theories of solvation effects. GRA

N91-29997# Naval Ocean Systems Center, San Diego, CA.
RESPONSIVITY UNIFORMITY ENHANCEMENTS FOR BACKSIDE-ILLUMINATED CHARGE-COUPLED DEVICES (BICCDS) BY EXCIMER LASER-ASSISTED ETCHING Final Report, May 1990 - Apr. 1991
Stephen D. Russell and Douglas A. Sexton May 1991 44 p
(AD-A237435; NOSC/TD-2103) Avail: NTIS HC/MF A03
CSCL 17/5

BICCDs are solid-state electronic imaging devices which read out image charges from wells in an array of pixels. The substrate below the pixel array is typically thinned by chemically etching (100)-oriented silicon using a potassium hydroxide (KOH) etch. The potassium hydroxide anisotropically etches to the (111) crystallographic plane in silicon, leaving smooth sidewalls at an angle of 54.7 deg to the image plane. This smooth surface acts as a mirror to reflect extraneous light onto the image plane of the BICCD, causing spurious images and reducing the responsivity uniformity (RU) of the devices. We have developed a noncontact excimer laser-assisted process to promote a chemical reaction between a halocarbon ambient and the silicon. The laser-assisted chemical reaction results in a roughened (textured) surface which behaves as a light sink. The use of a nonreactive ambient allows us to texture the sidewalls of prepackaged and pretested devices. The sidewalls of fully functional BICCD die have been textured in a Freon-115 (chloropentafluoroethane) ambient by directing 5000 pulses with laser fluence of about 0.75 J/sq cm upon them. The RU of the devices as well as the background level (fat-zero) are dramatically improved. GRA

N91-29998# Massachusetts Inst. of Tech., Cambridge.
DEVELOPMENT OF MODEL BASED MAGNETIC LP-LEC GROWTH LARGE DIAMETER GaAs Final Report, 14 Aug. 1987 - 28 Nov. 1990
August F. Witt 28 Nov. 1990 105 p
(Contract F49620-87-C-0106)
(AD-A237456; AFOSR-91-0580TR) Avail: NTIS HC/MF A06
CSCL 20/2

The stated objectives of this research effort were directed at: (1) The establishment of magnetic liquid phase-liquid encapsulated Czochralski (LP-LEC) growth capability with diameters approaching 4 inches; (2) The design of heat and mass transfer control systems required for optimization of growth with magnetic melt stabilization, and (3) Development of a model-based growth control scheme which includes complementary knowledge-based system inputs for seeding, shouldering, and growth termination. A non-invasive wafer inspection system has been developed. It is based on near infrared (NIR) transmission microscopy with bright and dark field illumination. It provides for rapid quantitative characterization of doped and non-doped SI GaAs on both a macro- and selected microscale. Model-based control of thermal stresses in LEC growth of GaAs has been implemented. In this approach mathematical models of the growth process and a heat exchange system are used to control the temperature field in the crystal during growth and cooldown. Crystals grown in this configuration exhibit dislocation densities in the range of 1000/sq. cm. Also developed was a micro-mechanical constitutive law for high temperature creep and dislocation multiplication in GaAs. GRA

N91-29999# Arizona Univ., Tucson. Optical Sciences Center.
CENTER FOR THIN FILM STUDIES Final Report, 1 Oct. 1986 - 1 Jun. 1990
Robert R. Shannon 22 Jan. 1991 140 p
(AF Proj. 3484)
(AD-A237457; AFOSR-91-0565TR) Avail: NTIS HC/MF A07
CSCL 09/1

This report is for the entire term of operation of the URI Thin Film Center, including the six-month no-cost extension of the subject contract, and contains a summary of the research performed under this umbrella grant. Sections of this report address work on growth and characterization of thin films by various methods; modeling of thin film growth; and preparation and characterization of substrates for film growth. The Center for Thin Film Studies covered a wide range of research topics, from fundamental studies of growth to applications of processing methods. Also developed were new and improved analysis tools, such as Brillouin spectroscopy, Rutherford backscattering spectrometry, microreflectometry, and surface probes such as scanning tunneling microscopy. Practical properties of interest such as scattering and absorptive losses, surface roughness, and optical properties for a variety of materials have also been reported. The attached summary highlights the important advances of the three-and-a-half-year effort; for further details, the reader is referred to the bibliography and the articles listed therein. GRA

N91-30000# North Carolina State Univ., Raleigh.
GROWTH, CHARACTERIZATION, AND DEVICE DEVELOPMENT IN MONOCRYSTALLINE DIAMOND FILMS Quarterly Letter Report, 1 Apr. - 30 Jun. 1991
Robert F. Davis, Jeffrey T. Glass, Klaus J. Bachmann, and R. J. Trew 30 Jun. 1991 28 p
(Contract N00014-90-J-1604)
(AD-A237463) Avail: NTIS HC/MF A03 CSCL 20/2

Carbon has been implanted into monocrystalline (100) copper substrates. Owing to the low solubility of C in Cu, it was easily diffused to a clean Cu surface at 550 C in the form of graphite rather than the desired diamond, as shown by Auger electron spectroscopy measurements. Laser reflection interferometry has proven to be a useful technique in the study of diamond growth processes. Nucleation and growth rates were monitored in real time. The problem of surface roughness of the polycrystalline films was surmounted by growing diamond on a thin amorphous C or diamond-like film. The microwave performance of p-type diamond MESFETs operating at 10 GHz has been investigated. The moderate activation energy of the p-type dopant of B may force operation at elevated temperature. However this may result in a significantly degraded RF performance, since holes in diamond demonstrate a T to the -2.8 power temperature dependence. GRA

N91-30001# Maine Univ., Orono. Lab. for Surface Science and Technology.
SURFACE STRUCTURE AND SURFACE ORDER Technical Report, 6 Jan. 1990 - 15 May 1991
W. N. Unertl 15 May 1991 81 p
(Contract N00014-89-J-1314)
(AD-A237466) Avail: NTIS HC/MF A05 CSCL 20/2

This chapter provides an introduction to the current state of knowledge about the crystal structure of solid surfaces, phase transformations on surfaces, and defects on surfaces. Spatial arrangements of atoms near surfaces and interfaces determine the chemical, electronic and mechanical properties of materials. Processes such as epitaxial growth of thin films and catalytic reactions are sensitive functions of surface structure and composition. Significant gaps remain in understanding some materials and, in particular, real surfaces such as those of non-crystalline materials like polymers. Surface properties of oxides and carbides are dominated by the presence of defects and are only beginning to be understood. Real surfaces are often formed in metastable structural states rather than in thermodynamic equilibrium. With the recent introduction of direct imaging techniques like scanning tunneling microscopy (STM) and low energy electron microscopy (LEEM), there has been a rapid increase in research directed toward understanding the noncrystalline aspects of surface structure. Surface defects range from atomic scale defects such as impurities and vacancies to macroscopic imperfections such as grain boundaries. Diffusion, nucleation, growth, and chemical reactivity are sensitive to the presence of surface defects of both mesoscopic and microscopic extent. This chapter places emphasis on surface defects. GRA

N91-30002# Army Lab. Command, Watertown, MA. Material Technology Lab.
EFFECT OF HYDROGEN ON THE ELECTRONIC STRUCTURE OF A GRAIN BOUNDARY IN IRON Final Report
Genrich L. Krasko and Gregory B. Olson May 1991 16 p

(AD-A237499; MTL-TR-91-18) Avail: NTIS HC/MF A03 CSCL 11/6

Linear Muffin Tin Orbitals-Atomic Sphere Approximation (LMTO-ASA) calculations were performed on a 26 atom supercell model of a (111) grain boundary (GB) in bcc Fe. The supercell emulated two GBs with 11 (111) planes of Fe atoms between the GB planes. One of the GBs was clean, with a structural vacancy at the GB core in the center of a trigonal prism of Fe atoms, while on other GB site was occupied by an H atom. The interplanar spacings of the supercell were relaxed using a modified embedded atom method. As in the case of P and S in a similar GB environment in Fe, there is only a weak interaction between H and the nearest Fe atoms. Almost all the Fe d-states are nonbonding. A very weak covalent bond exists between H and Fe due to s-pd hybridization; the hybrid bonding band located far below the Fermi energy (Ef). This bond is mostly of sigma-type, connecting H with Fe atoms in the GB plane; the delta-component of this bond across the GB is weaker. GRA

N91-30003# California Inst. of Tech., Pasadena.
ELECTRON TUNNELING MICROSCOPY Final Report, 1 Dec. 1985 - 31 Mar. 1991
John D. Baldeschwieler 13 Jun. 1991 12 p
(Contract N00014-86-K-0214)
(AD-A237504) Avail: NTIS HC/MF A03 CSCL 20/7

The rapid development of the Scanning Tunneling Microscope (STM) and its derivatives in the past five years has created new techniques not only for examining surfaces and surface processes, but also for surface modification, lithography and performing surface chemistry and spectroscopy at microscopic levels never before attainable. Understanding the mechanisms involved in these processes will enable researchers to utilize fully the tremendous capabilities potentially available with this technology. STM is based on the phenomenon of quantum mechanical tunneling. A metal tip is brought within a few angstroms of a conducting sample by means of a 3-D piezoelectric ceramic positioner. A tunneling current whose magnitude depends exponentially on the tip-sample separation can be established and maintained by means of a feedback circuit to the positioner. By rastering the tip over the surface (x and y) and monitoring the feedback to the z position, a topographic image of the surface can be formed. A current image can also be obtained by rastering the tip over the surface at a high frequency so that a constant average height over the surface is maintained. The image contrast is produced by monitoring the fluctuation in current. The exponential dependence of the tunneling current upon the separation of the tip from the surface provides the exquisite resolution of the STM. Author (GRA)

N91-30004# Purdue Univ., West Lafayette, IN. Dept. of Chemistry.
THE INFLUENCE OF POTENTIAL ON METAL-ADSORBATE STRUCTURE: SOLVENT-INDEPENDENT NATURE OF INFRARED SPECTRA FOR Pt(111)/CO
S. C. Chang, X. Jiang, J. D. Roth, and M. J. Weaver 31 May 1991 21 p
(Contract N00014-91-J-1409)
(AD-A237509; TR-107) Avail: NTIS HC/MF A03 CSCL 20/2

In-situ infrared spectra are reported in the C-O stretching (nu sub co) region for saturated CO adlayers on Pt(111) in four nonaqueous solvents; acetonitrile, dimethylformamide, dichloromethane and tetra hydrofuran, each containing tetra alkylammonium cations, over wide electrode potential ranges, ca -2.0 to 1.5 V vs. SCE. Notably, the spectral features (nu sub co frequencies, CO site occupancies, etc) are sensitive only to the applied potential, being virtually independent of the solvating medium. Comparisons with spectra obtained in the presence of different cations, and in corresponding aqueous electrochemical and ultrahigh vacuum environments, demonstrate that the adlayer properties are controlled in each case by the surface potential drop across the adsorbate layer. GRA

N91-30005# North Carolina State Univ., Raleigh. Dept. of Electrical and Computer Engineering.
DEFECT REDUCTIONS IN EPITAXIAL GROWTH USING SUPERLATTICE BUFFER LAYERS Final Report, 1 Apr. 1988 - 30 Sep. 1990
Salah Bedair and N. El-Masry Dec. 1990 170 p
(Grant AF-AFOSR-0160-88; AF Proj. 2306)
(AD-A237710; AFOSR-91-0584TR) Avail: NTIS HC/MF A08 CSCL 20/2

This final report is in the area of defect reduction using strained layer superlattices. A variety of attempts to reduce the defects density in GaAs epitaxial films grown on Si substrates using annealing, InGaAs-GaAsP strained-layer superlattices, strained-layer superlattices combined with annealing, and the selective etching are presented. Both conventional furnace annealing/slow cooling and rapid thermal annealing were effective to eliminate microtwins and stacking faults. However, the conventional furnace annealing/slow cooling showed more promising results in terms of dislocations reduction. This conventional furnace annealing reduces dislocation density to about high 10(exp 7)/sq cm. GRA

N91-30006# Rockwell International Science Center, Thousand Oaks, CA.
PRESSURE EFFECTS IN THE MICROWAVE PLASMA GROWTH OF POLYCRYSTALLINE DIAMOND
A. B. Harker and J. F. DeNatale 1991 7 p Sponsored by ONR
(AD-A237751) Avail: NTIS HC/MF A02 CSCL 20/11

Microwave plasma deposition of polycrystalline diamond is being investigated over the pressure range 1 to 100 kPa. The conditions of growth, microstructure, and spectroscopic properties of the resulting materials are being compared. A phenomenological description of the dependence of diamond microstructure upon growth conditions has been developed. Diamond films were grown in two different flow systems both using an Applied Science 1.5kW, 2.45GHz magnetron source and waveguide arrangements. All substrate surfaces were prepared by diamond paste abrasion before deposition. Polycrystalline particles and films were examined by scanning electron microscopy and Raman spectroscopy. GRA

N91-30007# Advanced Fuel Research, Inc., East Hartford, CT.
EPITAXIAL GROWTH OF SINGLE CRYSTAL DIAMOND ON SILICON Progress Report No. 1, 15 May - 14 Nov. 1991
Philip W. Morrison, Jr., David B. Fenner, and Joseph E. Cosgrove 1991 3 p
(Contract N00014-91-C-0101)
(AD-A237758) Avail: NTIS HC/MF A01 CSCL 20/12

The oxyacetylene torch for diamond CVD is currently operating and available. Although another project is actively employing the spin etch system and the pulsed laser system for depositing high temperature superconductors, the spin etch system is available immediately and the laser system is available on demand in about a month. Work on the conversion of the plasma reactor to an ultraclean, hot filament CVD reactor has begun. The ultraclean system is designed and most of the parts are on order including a new chamber, resin purifiers, and new mass flow controllers. A future work schedule is included. GRA

N91-30008# Notre Dame Univ., IN. Dept. of Physics.
VIBRATIONAL, MECHANICAL, AND THERMAL PROPERTIES OF III-V SEMICONDUCTORS Final Report, 1 Nov. 1988 - 31 Oct. 1990
John Dow 20 Mar. 1991 8 p
(Grant AF-AFOSR-0063-89; AF Proj. 2306)
(AD-A237785; AFOSR-91-0583TR) Avail: NTIS HC/MF A02 CSCL 09/1

Theories of the mechanical, vibrational, and electronic properties of III-V semiconductors were developed and applied to the following conditions. The physics were studies which underlie the II-VI doping problem and suggesting band gap engineering schemes for circumventing the problem. Predictions are made of

how the character of deep and shallow impurities can be different in superlattices from in bulk materials. How surfaces of zincblende and wurtzite semiconductors relax was studied along with how this relaxation depends on the ionicity of the semiconductor. Better insight was gained into the properties of semiconducting alloys, both electronically and vibrationally, with attention paid to how ordering phenomena in these alloys affects their properties. GRA

N91-30009# Joint Inst. for Lab. Astrophysics, Boulder, CO.
LASER PROBING OF THE KINETICS AND DYNAMICS OF III -V SEMICONDUCTOR GROWTH Annual Report, 1 Feb. 1990 - 31 Jan. 1991
Stephen R. Leone 31 Jan. 1991 7 p
(Grant AF-AFOSR-0166-90; AF Proj. 2306)
(AD-A237795; AFOSR-91-0572TR) Avail: NTIS HC/MF A02 CSCL 20/2

Work is carried out on the dynamics of Ga, In, and As scattering, sticking, and desorption from silicon single crystals using laser induced fluorescence probing of the Ga and In atoms and As dimer gas phase species. Desorption kinetics are used to probe the InAs and GaAs heterostructures on silicon and the islanding behavior that occurs for the mixed systems. It is observed that islands form readily when In or Ga are grown on a prelayer of As on Si(100). State-resolved detection of As2 species is demonstrated by laser induced fluorescence probing for the first time. Laser multiphoton ionization detection of the III-V semiconductor species is also demonstrated. A technique is being developed to measure surface migration rates of epitaxial species by using a two laser, desorption and detection scheme. GRA

N91-30010# Columbia Univ., New York, NY. Dept. of Electrical Engineering.
MOLECULAR BEAM EPITAXIAL GROWTH AND CHARACTERIZATION OF METASTABLE COMPOUND SEMICONDUCTORS FOR INFRARED DETECTOR APPLICATIONS Final Report, 1 Feb. 1988 - 31 Jan. 1991
Wen I. Wang 19 Apr. 1991 12 p
(Grant AF-AFOSR-0126-88; AF Proj. 2306)
(AD-A237797; AFOSR-91-0566TR) Avail: NTIS HC/MF A03 CSCL 20/2

Single crystal metastable GeSn alloys were grown on lattice-matched GaSb and InP substrates. Surface structures of AlGaSb and alternating GaSb and AlSb layers were studied. Resonant tunneling an I interband tunneling in the polytype GaSb/AlSh.InAs material system was observed. On the basis of simple circuit modeling, these structures are shown to have potential for high frequency performance. An InAs-channel field effect transistor was fabricated and theoretically shown to have an order of magnitude higher transconductance than AlGaAs/-GaAs HEMT. The successful operation is reported of the first AlSbAs/GaSb p-channel MODFET with the highest transconductance at 77K achieved for any p-channel FET. The doping was studied of Ge and Sn for GaSb by MBE and found them well behaved up to very high doping levels. GRA

N91-30011# Minnesota Univ., Minneapolis. Dept. of Electrical Engineering.
THE GROWTH OF ULTRATHIN EPITAXIAL INTERMETALLIC FILMS Technical Report, 1 Aug. 1989 - 31 Jul. 1990
P. I. Cohen 11 Feb. 1991 9 p
(Grant AF-AFOSR-0494-89; AF Proj. 2306)
(AD-A237798; AFOSR-91-0575TR) Avail: NTIS HC/MF A02 CSCL 07/2

The growth of iron aluminide and NiAl intermetallic compounds on III-V substrates was studied using reflection high energy electron diffraction (RHEED), transmission electron diffraction (TEM), and selected area electron channeling patterns (SAECP). Procedures for the growth of both of these intermetallics with layer-by-layer control were developed. The quality of the films on indium phosphides (100) substrates exceeds those grown on gallium arsenides (100) substrates due to the lower lattice mismatch. The films are stable to at least 820 K. TEM measurements indicate that the burgers vector of misfit dislocations is a complete a(100). SACP, TEM, and TEM indicate that the film relaxation approximates the Matthews Blakeslee prediction. Even this was surprising in light of the layer by layer growth after relaxation since the type of dislocation that forms cannot glide to the interface to relieve the strain. Preliminary semiconductor intermetallic semiconductor structures were grown. The quality of the interfaces is being assessed. GRA

N91-30012# Honeywell, Inc., Bloomington, MN. Sensor and System Development Center.
MONOLITHIC INTEGRATION OF SEMICONDUCTOR AND SUPERCONDUCTOR COMPONENTS Report, 1 Apr. - 30 Jun. 1991
30 Jun. 1991 11 p
(Contract N00014-90-C-0226)
(AD-A237946) Avail: NTIS HC/MF A03 CSCL 14/2

The goal of the program is to develop transistor technology compatible with high transition temperature superconductor technology so that transistor pixel switches can be integrated with YBa2Cu3O7 superconducting microbolometers in the same silicon substrate. A 4x4 matrix-addressable superconducting microbolometer array will be delivered at the completion of the program. GRA

N91-30013# Surrey Univ., Guildford (England).
ION IMPLANTATION TECHNOLOGY: PROCEEDINGS OF THE 8TH INTERNATIONAL CONFERENCE ON ION IMPLANTATION TECHNOLOGY
K. G. Stephens, P. L. Hemment, K. J. Reeson, B. J. Sealy, and J. S. Colligon 1991 939 p Conference held in Guildford, England, 30 Jul. - 3 Aug. 1990
(Contract DAJA45-90-M-0185)
(AD-A237955; R/F-6461-EE-02) Avail: NTIS HC/MF A99 CSCL 09/1

The implantation of semiconductor devices as a manufacturing routine is a relatively recent development. But there is a much longer-standing tradition of scientific interest in the production of focussed beams of heavy ions and in the various ways in which they interact with surfaces. This has its origins in Goldstein's 1886 description of Kanalstrahlen in an electric discharge. However, the real significance of this - almost inadvertent - observation of collimated beams of energetic ions only became apparent in 1993 when J. J. Thomson described the detailed behavior of such positive rays in his parabola-ray apparatus. He gave a convincing explanation of the phenomenon of ionization and he provided a pioneering account of ion implantation when he noted that: some of the atoms constituting the positive rays seem to enter a metal against which they strike and either combine with the metal or get absorbed by it . The intensity of these ion beams was evidence by his description of the extent of the spluttering in his apparatus, as well as by his report of the effects of ion bombardment in the presence of reactive gases. GRA

N91-30014# California Univ., Santa Barbara. Dept. of Physics.
THE EMBEDDED ELECTRON-GAS BOUNDARY: A NEW STANDARD PROBLEM IN SURFACE PHYSICS Technical Report No. 36, 1 Jan. - 31 Dec. 1991
John Dobson Jul. 1991 18 p
(Contract N00014-89-J-1530)
(AD-A238152) Avail: NTIS HC/MF A03 CSCL 20/12

Consider a nonneutral system consisting of a broad but finite slab of immobile uniform positive charge interpenetrated by mobile interacting electrons of total charge less than that of the positive background. This idealized configuration, which is termed an embedded electron gas, is approximated by the wide parabolic quantum wells now being grown by molecular beam epitaxy in the GaAs/GaAlAs system. Compared with the electron density profile of the standard Lang-Kohn jellium edge, the boundary of the embedded electron gas is sharper as a result of the continuation of the jellium background outside the electron gas. This is expected to cause significant differences between the surface properties of the embedded electron gas and those of the regular jellium surface

model long used to study the surface properties of simple metals. Since the readily excited center-of-mass motions of the parabolic-well electronic density are now known to be insensitive to subband and many-body effects, surface properties such as those considered here may take on increased significance for the study of many-body phenomena in such systems. GRA

N91-30015# Colorado Univ., Boulder.
SEMICONDUCTOR DEPOSITION AND ETCHING INTERACTIONS OF LASER-GENERATED TRANSLATIONALLY HOT ATOMS AND RADICALS Final Report, 1 May 1988 - 30 Apr. 1991
Stephen R. Leone May 1991 19 p
(Contract DAAL03-88-K-0072)
(AD-A238198; ARO-25375.7-PH) Avail: NTIS HC/MF A03 CSCL 13/8

The goal in the work has been to investigate the microscopic basis for materials removal using neutral atoms and radicals at high kinetic energies (1 to 10 eV). With support from this ARO grant, it was possible to develop and characterize a new beam source of translationally fast atoms, radicals, and molecules. This beam source is based on a laser vaporization technique. The mechanisms of laser vaporization have been pioneered by many groups in the past several years; the method can be used to produce a variety of reactive neutral atoms, radicals, metal vapors, and other compounds with high kinetic energies. In this work, the laser vaporization process is used to produce a beam source of energetic, reactive neutral species which can be used to study collisions with semiconductor surfaces for fundamental investigations of etching and deposition. GRA

N91-30016*# Massachusetts Inst. of Tech., Lexington.
SOLID STATE RESEARCH Quarterly Technical Report, 1 Aug. - 31 Oct. 1990
Alan L. McWhorter 15 Nov. 1990 107 p Sponsored in part by NASA, Army, DARPA, Navy, SDIO, and DOE
(Contract F19628-90-C-0002)
(NASA-CR-188021; NAS 1.26:188021; AD-A238427; Rept-1990:4; ESD-TR-90-152) Avail: NTIS HC/MF A06 CSCL 20/12

The research work of the Solid State Division is detailed. The topics covered are Electrooptical Devices, Quantum Electronics, Materials Research, Submicrometer Technology, Microelectronics, and Analog Device Technology. Funding is provided primarily by the Air Force, with additional support provided by the Army, DARPA, Navy, SDIO, NASA, and DOE. GRA

N91-30017# North Carolina State Univ., Raleigh.
DEVICE PROCESSING OF II-VI SEMICONDUCTOR FILMS AND QUANTUM WELL STRUCTURES Final Report, 1987 - 1990
J. F. Schetzina 7 Mar. 1991 4 p
(Contract DAAL03-87-K-0153)
(AD-A238460; ARO-25541.1-PH) Avail: NTIS HC/MF A01 CSCL 20/10

The objective of this program is to develop a device having the technology necessary for proper utilization of Hg-based heterostructures and superlattices in device applications. The specific focus or long term goal guiding the direction of the program is to develop the devices and processing technology required for an IR focal plane integrated with on-board signal processing electronics. GRA

N91-30018# Columbia Univ., New York, NY. School of Mines.
ON THE ROLE OF CRYSTAL DEFECTS AS SOURCES OF RESONATOR FREQUENCY INSTABILITY Final Report, Jun. 1985 - Aug. 1988
A. S. Nowick Jul. 1991 38 p
(Contract F19628-85-C-0104)
(AD-A238505; RL-TR-91-95) Avail: NTIS HC/MF A03 CSCL 20/2

This work involved the study of defects in quartz crystals, primarily by the use of electrical measurements, viz. electrical conductivity and dielectric relaxation (DR) measurements. The latter has turned out to be a powerful tool since it is capable of detecting dipolar defects that other techniques, e.g., electron paramagnetic resonance (EPR) and infrared absorption (IR), cannot detect, as well as defects that EPR can also measure. DR peaks have been observed that are produced by Al-Na defects in two different configurations, by Al-hole defects, and by several types of defects involving Fe, in the case of Fe-containing crystals. In all cases, we have worked to identify the responsible defect, to correlate it with defects measured by EPR and IR techniques, and to determine the interactions of the defect with the lattice. Special attention has also been given to the role of ionizing radiation (X-ray and y-rays) and of subsequent annealing on these various defects. GRA

N91-30019# North Carolina State Univ., Raleigh.
ATOMIC LAYER EPITAXY GROUP IV MATERIALS: SURFACE PROCESSES, THIN FILMS, DEVICES AND THEIR CHARACTERIZATION Semiannual Report
Robert F. Davis and Salah Bedair Jun. 1991 17 p
(Contract N00014-91-J-1416)
(AD-A238506) Avail: NTIS HC/MF A03 CSCL 09/1

As the first step in the chemically-controlled atomic layer epitaxy (ALE) of SiC, research has been conducted regarding the ALE of Si. Good quality single crystal epitaxial films of Si on off-axis (100) Si have been produced in the Davis group. Equipment related to the deposition of high-quality Si only is virtually completed in the Bedair group. Dichlorosilane has been used (or is being considered) by both groups. A deposition system that will achieve ALE of CeO2 on Si has also been designed. GRA

N91-30020# North Carolina State Univ., Raleigh. Dept. of Materials Science and Engineering.
PSEUDOMORPHIC SEMICONDUCTING HETEROSTRUCTURES FROM COMBINATIONS OF AIN, GaN AND SELECED SiC POLYTYPES: THEORETICAL ADVANCEMENT AND ITS COORDINATION WITH EXPERIMENTAL STUDIES OF NUCLEATION, GROWTH, CHARACTERIZAITON AND DEVICE DEVELOPMENT Semiannual Letter Report, 1 Jan. - 30 Jun. 1991
Robert F. Davis Jun. 1991 28 p
(Contract N00014-90-J-1427)
(AD-A238520) Avail: NTIS HC/MF A03 CSCL 20/2

The initial stages of growth of AlN and GaN on the Si (0001) face of alpha(6H-SiC and the (0001) face of sapphire were studied. The growth of both nitrides on the alpha(6H)-SiC substrates occurred on a thin of Si3N4. No significant surface chemical changes were observed when the films were grown on sapphire. The deposition of GaN on sapphire appeared to follow a Stranski-Krastanov mode of growth that on SiC showed characteristics of 3-Dgrowth, possibly due to the Si3N4. The AlN grew on both substrates either layer-by-layer or, more likely, by the Stranski-Krastanov mode. The gas source MBE for the growth of SiC-AlN-GaN heterostructures was commissioned. Growth of single crystal (100) Beta-SiC on 3 degrees off axis Si(100) substrates at 1075 C was successful. Two classes of computer codes were also developed for theoretical modeling of pseudomorphic heterostructures of complex systems. GRA

N91-30021# North Carolina State Univ., Raleigh. Dept. of Materials Science and Engineering.
GROWTH, NITROGEN VACANCY REDUCTION AND SOLID SOLUTION FORMATION IN CUBIC GaN THIN FILMS AND THE SUBSEQUENT FABRICATION OF SUPERLATTICE STRUCTURES USING AlN AND InN Semiannual Letter Report, 1 Jan. - 30 Jun. 1991
Robert F. Davis Jun. 1991 44 p
(Contract N00014-86-K-0686)
(AD-A238521) Avail: NTIS HC/MF A03 CSCL 20/5

An Atomic Layer Epitaxy (ALE) deposition system, as well as the initial results of the ALE growth of GaN, are described. The deposition system was fabricated in-house. It is high vacuum capable and allows the introduction of up to 16 gases without mixing. The substrates travel under different zones, each of which allows the adsorption or decomposition of one gas species at a

time. Continuous crystalline GaN films were grown on (0001) alpha-SiC and analyzed by Auger spectroscopy, scanning electron microscopy and electron diffraction. Research concerned with the heteroepitaxial deposition of cubic boron nitride (c-BN) using different substrates and deposition technologies was also conducted. Films were deposited and analyzed using the techniques of reflection high energy electron diffraction (RHEED), x ray photoelectron spectroscopy (XPS), low energy electron diffraction (LEED), x ray diffraction (XRD), scanning electron microscopy (SEM), transmission electron microscopy (TEM), and Fourier transform infrared spectroscopy (FT-IE). GRA

N91-30022# Air Force Inst. of Tech., Wright-Patterson AFB, OH. School of Engineering.
A STUDY OF THE LIQUID-SOLID INTERFACE DURING RAPID RESOLIDIFICATION OF COOPER-TITANIUM USING MOLECULAR DYNAMICS M.S. Thesis
Craig L. Loisel Mar. 1991 55 p
(AD-A238634; AFIT/GNE/ENP/91M-4) Avail: NTIS HC/MF A04 CSCL 20/2

The behavior of the liquid-solid interface during resolidification of a condensed copper-titanium crystal is studied by atomistic simulation. A system of 1080 atoms (540 of each type) was simulated. The interface was created using Monte Carlo techniques and resolidification was performed by molecular dynamics. Resolidification was attempted at temperatures of 1200 K, 1100 K, 1000 K, 900 K, 818 K and 773 K. The liquid-solid interface was found to move only at 773 K, resulting in a chemically disordered crystal. The interface velocity observed in the simulation is 6.6 m/s which agrees well with the theoretical value of 5.5 m/s. The low interface velocity indicates the recrystallization is governed by diffusion-limited growth. GRA

N91-30023# Physical Optics Corp., Torrance, CA.
AN OPTICALLY ACTIVATED MODULATOR AND GaAs-GaAlAs COMPOUND SEMICONDUCTOR CHANNEL WAVEGUIDE Final Report, 1 Sep. Apr. 1991
Ray Chen 30 Apr. 1991 53 p
(Contract F49620-90-C-0068)
(AD-A238642; AFOSR-91-0664TR) Avail: NTIS HC/MF A04 CSCL 09/1

An optically activated modulator (OAM) and modulator array on GaAs-GaAlAs compound semiconductor channel waveguides was proposed and developed. A channel waveguide device with an optical activation window of 5 micron in diameter was fabricated. Optical activation was produced by using HeNe 631.8 nm wavelength as the free carrier generator and a 1.3 micron laser as the signal carrier. Thirty-three percent modulation depth was observed and 10-2 index modulation was experimentally confirmed on an OAM working in the phase modulation regime. OAMs working in both phase and cutoff modulation regimes were theoretically determined by considering the fluctuation of the waveguide confinement factor. The 8.2 dB modulation depth was observed on an OAM working at the cutoff regime. Furthermore, the activation source is in the mW power region which significantly reduces the size and cost of all optical switching devices. GRA

N91-30024# Indiana Univ., Bloomington.
HIGH RESOLUTION ELECTRON ENERGY LOSS STUDIES OF SURFACE VIBRATIONS
L. L. Kesmodel May 1991 6 p
(Contract DE-FG02-84ER-45147)
(DE91-014539; DOE/ER-45147/6) Avail: NTIS HC/MF A02

New experimental studies of surface vibrational properties of materials with high resolution electron energy loss spectroscopy (EELS) are reported. This document summarizes recent progress on surface phonon dispersion measurements on copper (001); aluminum on silicon (111); ultrathin films of nickel on copper (001); and oxygen adsorption on ultrathin films of cobalt and nickel. DOE

N91-30025# Michigan Univ., Ann Arbor.
SYNCHROTRON STUDIES OF NARROW BAND MATERIALS
1991 5 p
(Contract DE-FG02-90ER-45416)
(DE91-014826; DOE/ER-45416/1) Avail: NTIS HC/MF A01

At the time of writing this report, we have had 3 weeks of beamtime on the Ames/Montana beamline at the Wisconsin Synchrotron Radiation Center (SRC), working with Cliff Olson. This run was devoted to a mix of high temperature superconductors, heavy-Fermion and related uranium materials, and some heavy Fermion and other rare earth materials. The high (Tc) materials are very difficult because only a small fraction of samples yield high quality photoemission spectra, even if they have good bulk superconducting properties, as is the case for our samples. DOE

N91-30026# Brookhaven National Lab., Upton, NY.
INTERMETALLIC SUPERCONDUCTORS: THE STATE OF DEVELOPMENT IN 1991
E. B. Forsyth 1991 7 p Presented at the Technological Issues of Superconducting Maglev Transportation, Upton, NY, 23-24 May 1991
(Contract DE-AC02-76CH-00016)
(DE91-014844; BNL-46259; CONF-9105133-2) Avail: NTIS HC/MF A02

The commercial fabrication of intermetallic superconductors has reached a high degree of maturity in the past thirty years. The only significant, commercial requirement for superconducting wire is the construction of magnetic resonance imaging (MRI) devices for medical diagnosis. In addition to this demand there are one-time projects such as high energy particle accelerators which often need considerable quantities of superconducting material over the few years of construction. R and D projects also provide a fluctuating market for superconducting materials, in the past the projects have included power apparatus such as generators, motors, energy storage and transmission cables, and magnets for experimental fusion reactors. Superconducting magnetically levitated trains have undergone full scale trials in Japan and Germany. This is by no means a comprehensive list of all the possible applications. Virtually all the devices requiring a magnetic field to be produced by superconducting windings have used NbTi wire, but a few experimental Nb3Sn high field magnets have been constructed. This report briefly discusses development of intermetallic superconductors. DOE

N91-30027# Pacific Northwest Lab., Richland, WA.
AIR-SINTERING MECHANISMS OF CHROMITES
L. A. Chick, J. L. Bates, and G. D. Maupin Jul. 1991 9 p Presented at the 2nd International Symposium on Solid Oxide Fuel Cells, Athens, Greece, 2-5 Jul. 1991
(Contract DE-AC06-76RL-01830)
(DE91-015527; PNL-SA-19212; CONF-9107106-2) Avail: NTIS HC/MF A02

The sintering behaviors of La(1-x)Sr(x)CrO3 and Y(1-x)-Ca(x)CrO3 in air at 1550 C are described as functions of alkaline earth concentration and chromium enrichment or depletion. Vapor-, liquid-, and solid-phase mass transport mechanisms appear to be operative in both systems. Liquid-phase sintering appears dominant an Y(1-x)Ca(x)CrO3 with x = 0.15 to 0.40, especially with Cr enrichment. Either vapor- or solid-phase transport may dominate in the La(1-x)Sr(x)CrO3 system. Slight depletion or enrichment of Cr in both systems has dramatic effects on air-sintered density and microstructure, probably due to modulation of vapor-phase transport and liquid-phase formation. Substantial Cr depletion enhances sintering. DOE

N91-30028# Argonne National Lab., IL.
CONSOLIDATION AND PLASTICITY OF Bi-Sr-Ca-Cu-O SUPERCONDUCTORS
A. S. Nash, K. C. Goretta, R. Wheeler, B. M. Moon (Illinois Univ., Urbana.), C. T. Wu, and P. Nash May 1991 11 p Presented at the 1991 Powder Metallurgy Conference and Exhibition, Chicago, IL, 9-12 Jun. 1991
(Contract W-31-109-eng-38)

(DE91-015544; ANL/CP-71552; CONF-9106244-2) Avail: NTIS HC/MF A03

The Bi2Sr2CaCu2O(x) (2212) superconductor consists of platelike grains that grow up very rapidly in two directions at high temperature. The grain growth is so fast that this superconductor can not be sintered by conventional means. Densification can be achieved, however, by hot isostatic pressing by a combination of flat rolling and sintering. Results from 2212 and 2212 + 15 wt. percent Ag specimens produced by these consolidation methods are compared with those from sintering studies. Scanning and transmission electron microscopy were used to assess the mechanisms by which 2212 densifies. The superconducting properties of each type of specimen were measured. It was found that only forms in which the platelike grains exhibited substantial preferred orientation were capable of carrying large amounts of current. This result has important implications to the thermomechanical processing of Bi-Sr-Ca-Cu-O superconductors. DOE

N91-30029# Argonne National Lab., IL.
HIGH-(Tc) SUPERCONDUCTORS: FABRICATING TECHNOLOGIES AND FUTURE PERSPECTIVES
K. C. Goretta, W. Wu, C. T. Wu, D. Xu, C. A. Youngdahl, Donglu Shi, J. P. Singh, J. J. Picciolo, M. T. Lanagan, and J. R. Hull et al May 1991 19 p Presented at the 2nd Workshop on Basic and Applied Aspects of Rare Earths, Venice, Italy, 9-10 May 1991
(Contract W-31-109-eng-38)
(DE91-015553; ANL/CP-73053; CONF-9105233-1) Avail: NTIS HC/MF A03

Processing methods for production of bulk high-(Tc) superconductors are reviewed. Conductors made by conventional forming and sintering methods can generally carry only small current densities. Melting and powder-in-tube methods yield superior conductors, but further improvements are necessary before these superconductors can be employed in most large-scale applications. DOE

N91-30030# Argonne National Lab., IL.
CONNECTION BETWEEN GRAIN BOUNDARY STRUCTURE AND ENERGY
K. L. Merkle and D. Wolf 1991 7 p Presented at the International Conference on Grain Growth in Polycrystalline Materials, Rome, Italy, 18-21 Jun. 1991
(Contract W-31-109-eng-38)
(DE91-015558; ANL/CP-73327-Rev; CONF-9106101-1-Rev)
Avail: NTIS HC/MF A02

High-resolution electron-microscopy (HREM) experiments are combined with computer simulations of group of zone axes (110) tilt grain boundaries (GBs) in Au to investigate the correlations between atomic-scale GB structure and energy. The energies calculated for a variety of symmetric and asymmetric GBs suggest that asymmetric GB-plane orientations are often preferred over symmetric ones. Experimentally the observed faceting behavior agrees with the computed energies. Computer simulations suggest general interrelations between GB energy and (1) volume expansion and (2) the number of broken bonds per unit area of GB. These atomic-scale microstructural GB parameters, as evaluated from HREM observations, can be compared to simulation results. The fact that asymmetric GBs often are low in energy may be of considerable important for grain growth in polycrystalline materials. DOE

N91-30031# Argonne National Lab., IL.
DETERMINATION OF THERMODYNAMIC AND KINETIC PROPERTIES OF GRAIN BOUNDARIES USING HIGH TEMPERATURE CALORIMETRY
C. D. Terwilliger, Y. M. Chiang (Massachusetts Inst. of Tech., Cambridge.), J. A. Eastman, and Y. Liao Jun. 1991 9 p Presented at the 93rd Annual Meeting and Exposition of the American Ceramic Society (ACerS), Cincinnati, OH, 28 Apr. - 2 May 1991
(Contracts W-31-109-eng-38; DE-FG02-87ER-45307)
(DE91-015571; ANL/CP-72267; CONF-910430-17) Avail: NTIS HC/MF A02

This work explores the use of high temperature differential scanning calorimetry as a novel way in which to measure thermodynamic and kinetic properties of grain boundaries in ceramics. A calorimetric study of grain growth has become practical only recently, with the development of processing methods for nanocrystalline materials (10 to 50 nm grain size) that have enough grain boundary area and thus grain boundary excess properties to be detected by commercial calorimeters. Here we report results from experiments on nanocrystalline silicon and titanium dioxide. DOE

N91-30032# Los Alamos National Lab., NM.
ANISOTROPIC SPIN SUSCEPTIBILITY OF THE (Y,Ca),(Ba, La)2Cu4O8 SYSTEM
I. Tomeno, J. O. Willis, T. Machi, M. Kosuge, T. Miyakate, K. Tai, N. Koshizuka, and S. Tanaka (International Superconductivity Technology Center, Tokyo, Japan) 1991 3 p Presented at the International Conference on Materials and Mechanisms of Superconductivity, Kanazawa (Japan), 22-26 Jul. 1991
(Contract W-7405-eng-36)
(DE91-014593; LA-UR-91-2096; CONF-910736-2) Avail: NTIS HC/MF A01

The normal-state susceptibility, chi, for (Y,Ca)(Ba,La)2Cu4O8 (Y124) was determined up to 300 K. Comparison with the chi data for YBa2Cu3O(x) suggests that antiferromagnetic correlations also persist in undoped and La-substituted Y124. For the La substituted Y124, we measured chi for magnetic fields H parallel and perpendicular to the c axis. Both chi(sub c) for H parallel c and chi(sub ab) for H perpendicular c decrease gradually with decreasing temperature. The temperature-independent difference chi(sub c)-chi(sub ab) suggests that the Cu 3d spin susceptibility in Y124 is isotropic above T(sub c). DOE

N91-30033# Lawrence Livermore National Lab., CA.
UNIAXIAL STRESS STUDY OF THE QUANTUM TRANSITIONS IN A STRAINED LAYER (001) In0.2Ga0.8As/GaAs SINGLE QUANTUM WELL
H. Qiang, F. H. Pollak, C. Mailhiot, G. D. Pettit, and J. M. Woodall (International Business Machines Corp., Yorktown Heights, NY.) May 1991 12 p Presented at the 5th International Conference on Modulated Semiconductor Structures, Nara (Japan), 8-12 Jul. 1991
(Contract W-7405-eng-48)
(DE91-014990; UCRL-JC-106546; CONF-9107135-1) Avail: NTIS HC/MF A03

Uniaxial stress (T) has proven to be a powerful tool for the study of the electronic states of semiconductors. However, in spite of its utility little work has been done on the effects of external strain on the properties of semiconductor microstructures. The effects were studied of large, external uniaxial stress (T) along (100) and (110) on the optical properties of a strained layer (001) In(0.2)Ga(0.8)As/GaAS single quantum well. Because of the large stresses employed the observed energy shifts exhibit a nonlinear behavior due to the stress induced coupling with the spin orbit split band. For T(vert bar) (110) the piezoelectric coupling produces an electric field along (001) which has a significant effect on both the energies and intensities of the various intersubband transitions. DOE

N91-30034# Lawrence Livermore National Lab., CA.
OPTICAL AND ENVIRONMENTALLY PROTECTIVE COATINGS FOR POTASSIUM DIHYDROGEN PHOSPHATE (KDP) HARMONIC CONVERTER CRYSTALS
I. M. Thomas 24 Jun. 1991 15 p Presented at the Society of Photo-Optical Instrumentation Engineers (SPIE) Meeting, San Diego, CA, 21-26 Jul. 1991
(Contract W-7405-eng-48)
(DE91-015296; UCRL-JC-105836; CONF-9107115-8) Avail: NTIS HC/MF A03

Potassium dihydrogen phosphate (KDP) crystals have been used as harmonic converters on the Nova laser at LLNL for over

six years. All crystals were coated with a single layer, quarterwave antireflection (AR) coating of porous silica with a refractive index of 1.22. This was prepared by a sol-gel process and was applied from a colloidal suspension by spin coating at room temperature. A few crystals were also coated with a methyl silicone coating prior to the application of the AR coating for environmental protection. The initial optical performance of all crystals was very good but there has been some deterioration over the years because of environmental and laser damage degradation. The deterioration in the silicone samples was, however, much less than the others. All ten KDP arrays are being replaced with new crystals and the silicone undercoat will be applied to all samples. Recently, a new perfluorinated organic polymer coating which has a refractive index of 1.29, was evaluated. This material is soluble in fluorinated solvents and can be applied by dip coating from solution at room temperature. It is hoped that this can provide environmental protection when applied to KDP and also act as an AR coating at the same time. The optical performance is not as good as the porous silica because of the higher index; about 0.3 pct. reflection per surface is obtained. DOE

N91-30035# Lawrence Livermore National Lab., CA.
INFLUENCE OF DIAMOND TURNING AND SURFACE CLEANING PROCESSES ON THE DEGRADATION OF KDP CRYSTAL SURFACES
M. R. Kozlowski, I. Thomas, G. Edwards, K. Stanion, and B. Fuchs 24 Jun. 1991 13 p Presented at the Society of Photo-Optical Instrumentation Engineers (SPIE) Meeting, San Diego, CA, 21-26 Jul. 1991
(Contract W-7405-eng-48)
(DE91-015300; UCRL-JC-105835; CONF-9107115-7) Avail: NTIS HC/MF A03

One factor influencing the efficiency of KDP (potassium dihydrogen phosphate) frequency conversion arrays on the Nova laser system at LLNL has been environmental degradation, or fogging, of the crystal surfaces. Decreases in array transmission by as much as 20 pct. have been attributed to crystal fogging. The surfaces of the 27 sq cm Nova array crystals are prepared by a wet diamond turning process. The rate of surface fogging has been associated with several parameters of the diamond turning and subsequent cleaning processes. High humidity during diamond turning, storage, and use on the laser tends to accelerate the fogging. It is suspected that some of the additives present in the diamond turning oil increase the fogging rate and have found a machining oil which minimizes this surface degradation. Efficient removal of the machining oils from the crystal surface also minimizes the fogging problem. Care must be taken to use cleaning solvents which do not cause additional surface degradation. The fogging rate is sensitive to the crystallographic orientation of the material as well as to surface roughness related to the diamond turning process. Accelerated fogging at diamond turning artifacts may increase crystal surface roughness causing increased beam modulation and scattering losses. DOE

N91-30036# Oak Ridge National Lab., TN.
FORMATION OF CoSi2 IN SIMOX WAFERS BY HIGH DOSE Co IMPLANTATION
T. P. Sjoreen, R. Jebasinski, K. Schmidt, and S. Mantl (Kernforschungsanlage, Juelich, Germany, F.R.) 1991 11 p Presented at the International Conference on Advanced Materials (ICAM 91), Strasbourg (France), 27-31 May 1991
(Contract DE-AC05-84OR-21400)
(DE91-015639; CONF-910580-3) Avail: NTIS HC/MF A03

SIMOX wafers were implanted with high doses of Co and annealed at high temperatures in order to study the formation of buried single crystal CoSi2 layers in this material. SIMOX wafers of (100) oriented Si were implanted at 100 to 200 keV with doses of 1.2 to 2.0 x 10(exp 17) Co(+)/sq cm, and annealed in rapid thermal processor or tube furnace. As-implanted and annealed samples were analyzed by Rutherford backscattering channeling spectroscopy (RBS), cross sectional transmission electron microscopy (XTEM), secondary ion mass spectroscopy, and the Van der Pauw technique. The best buried CoSi2 layers were obtained at an implantation energy of 100 keV and by subsequent RTA. RBS minimum yields of approx. 6 pct. were obtained for the buried layer, this is the same as that reported for bulk (100) Si. The measured resistivity of 15 micro-Omega-cm and XTEM confirmed the continuity of the layer. Buried CoSi2 layers were successfully produced up to an implantation energy of 180 keV. However, as the energy was increased the quality of the CoSi2 layer degraded, with minimum yields increasing to 24 pct. at 180 keV, and with a corresponding degradation in the minimum yields in the top Si layer. At 200 keV a buried epitaxial layer was not produced. The degradation of crystal quality with ion implantation energy and the failure to produce a buried layer at 200 keV are discussed. DOE

N91-30037# Sandia National Labs., Albuquerque, NM.
HIGH TEMPERATURE THERMOELECTRIC PROPERTIES OF BORON CARBIDE
T. L. Aselage 1991 17 p Presented at the Spring Meeting of the Materials Research Society (MRS), Anaheim, CA, 29 Apr. - 3 May 1991
(Contract DE-AC04-76DP-00789)
(DE91-015848; SAND-90-3080C; CONF-910406-31) Avail: NTIS HC/MF A03

Boron carbides are refractory solids with potential for application as very high temperature p-type thermoelectrics in power conversion applications. The thermoelectric properties of boron carbides are unconventional. In particular, the electrical conductivity is consistent with the thermally activated hopping of a high density (approx 10(exp 21)/cu cm) of bipolarons; the Seebeck coefficient is anomalously large and increases with increasing temperature; and the thermal conductivity is surprisingly low. In this paper, these unusual properties and their relationship to the unusual structure and bonding present in boron carbides are reviewed. Finally, the potential for utilization of boron carbides at very high temperatures (up to 2200 C) and for preparing n-type materials is discussed. DOE

N91-30038# California Univ., Berkeley. Lawrence Berkeley Lab.
TEM CHARACTERIZATION OF GRAIN BOUNDARIES IN MIXED BICRYSTAL FILMS OF ALUMINUM
U. Dahmen and K. H. Westmacott Mar. 1991 18 p Presented at the Spring Meeting of the Materials Research Society (MRS), Anaheim, CA, 29 Apr. - 3 May 1991
(Contract DE-AC03-76SF-00098)
(DE91-016267; LBL-30694; CONF-910406-32) Avail: NTIS HC/MF A03

The structure and faceting behavior of near-90 degree (110) tilt grain boundaries in thin films of aluminum with a unique mazed bicrystal geometry is characterized by conventional, high-resolution and high-voltage electron microscopy. In this microstructure the absence of triple junctions allows grain boundaries to facet in optimum orientation (inclination) during annealing. The degree of anisotropy of the boundaries is expressed in the form of a rose plot. Small local deviations in misorientation are shown to be necessary to accommodate optimum boundary segments. The crystallographic symmetry inherent in this microstructure is apparent and utilized throughout the analysis. DOE

77 THERMODYNAMICS AND STATISTICAL PHYSICS

Includes quantum mechanics; theoretical physics; and Bose and Fermi statistics.

For related information see also *25 Inorganic and Physical Chemistry* and *34 Fluid Mechanics and Heat Transfer.*

N91-30039# Lawrence Livermore National Lab., CA.
SPATIAL PROPAGATION OF SQUEEZED LIGHT IN A DEGENERATE PARAMETRIC AMPLIFIER
I. H. Deutsch (California Univ., Berkeley.) and J. C. Garrison 1 Mar. 1991 11 p Presented at the Squeezed States and

Uncertainty Relations Conference, College Park, 28-30 Mar. 1991
(Contract W-7405-eng-48)
(DE91-014989; UCRL-JC-106950-Rev-1; CONF-9103184-2-Rev-1)
Avail: NTIS HC/MF A03

Differential equations which describe the steady state spatial evolution of nonclassical light are established using standard quantum field theoretic techniques. A Schrodinger equation for the state vector of the optical field is derived using the quantum analog of the lowly varying envelope approximation (SVEA). The steady sate solutions are those that satisfy the time independent Schrodinger equation. The resulting eigenvalue problem then leads to the spatial propagation equations. For the degenerate parametric amplifier this method shows that the squeezed state is the ground state of the squeezing Hamiltonian. The magnitude and phase of the squeezing parameter obey nonlinear differential equations coupled by the amplifier gain constant and phase mismatch. The solution to these differential equations is equivalent to one obtained from the classical three wave mixing steady solution to the parametric amplifier with a nondepleted pump. DOE

N91-30040# Los Alamos National Lab., NM.
SUPERCOHERENT STATES AND PHYSICAL SYSTEMS
B. W. Fatyga, V. A. Kostelecky, M. M. Nieto, and D. R. Truax (Calgary Univ., Alberta) 1991 8 p Presented at the Squeezed States and Uncertainty Relations Conference, College Park, 28-30 Mar. 1991
(Contracts W-7405-eng-36; DE-AC02-84ER-40125)
(DE91-014598; LA-UR-91-2074; CONF-9103184-1) Avail: NTIS HC/MF A02

A method is developed for obtaining coherent states of a system admitting a supersymmetry. These states are called supercoherent states. The approach presented in this talk is based on an extension to supergroups of the usual group-theoretic approach. The example of the supersymmetric harmonic oscillator is discussed, thereby illustrating some of the attractive features of the method. Supercoherent states of an electron moving in a constant magnetic field are also described. DOE

N91-30041# Maryland Univ., College Park. Inst. for Physical Science and Technology.
THERMOPHYSICAL PROPERTIES OF SUPERCRITICAL FLUIDS AND FLUID MIXTURES
J. V. Sengers Jul. 1991 13 p
(Contract DE-FG05-88ER-13902)
(DE91-015794; DOE/ER-13902/3) Avail: NTIS HC/MF A03

This research is concerned with the development of a quantitative scientific description of the thermodynamic and transport properties of supercritical and subcritical fluids and fluid mixtures. It is known that the thermophysical properties of fluids and fluid mixtures asymptotically close to the critical point satisfy scaling laws with universal critical exponents and universal scaling functions. However, the range of validity of these asymptotic scaling laws is quite small. As a consequence, the impact of the modern theory of critical phenomena on chemical engineering has been limited. On the other hand, an a priori estimate of the range of temperatures and densities, where critical fluctuations become significant, can be made on the basis of the so-called Ginzburg criterion. A recent analysis of this criterion suggests that this range is actually quite large and for a fluid like carbon dioxide can easily extend to 100 deg or so above the critical temperature. Hence, the use of traditional engineering equations like cubic equations is not scientifically justified in a very wide range of temperatures and densities around the critical point. We have therefore embarked on a scientific approach to deal with the global effects of critical fluctuations on the thermophysical properties of fluids and fluid mixtures. For this purpose it is not sufficient to consider the asymptotic critical fluctuations but we need to deal also with the nonasymptotic critical fluctuations. The goal is to develop scientifically based questions that account for the crossover of the thermophysical properties from their asymptotic singular behavior in the near vicinity of the critical point to their regular behavior very far away from the critical point. DOE

80 SOCIAL SCIENCES (GENERAL)

Includes educational matters.

N91-30042# Wichita State Univ., KS. National Inst. for Aviation Research.
MARKETING FOR COLLEGIATE AVIATION EDUCATION
Phillips W. Goodell, Brent D. Bowen, and Marla J. Holt 1991 34 p
(NIAR-91-18) Avail: NTIS HC/MF A03

The increased reliance on marketing and its ability to solve pressing concerns has allowed it to overcome its opposition and become an integral part of higher education. Educational marketing is a competitive tool which must now be utilized for mere survival in today's dynamic world. An educational institution must present its specialty niche in the marketplace much the same as business. Marketing offers many advantages other than student recruitment. Its principles can be applied to the selection of faculty, positioning within the marketplace (academic rankings) and in the resource allocation process. Marketing has been successfully applied to higher education as evidenced by increasing enrollments in a period of decreasing supply of traditional college age students. Forecasting student enrollment in a new academic program at a university is similar to forecasting the demand for a new product or service in a business environment. Marketing has legitimatized its necessity and purpose in the academic arena. The application of basic marketing principles will only enhance the success of collegiate aviation education programs. Author

81 ADMINISTRATION AND MANAGEMENT

Includes management planning and research.

N91-30043# Los Alamos National Lab., NM.
COMPARISON OF FOUR METHODS FOR AGGREGATING JUDGMENTS FROM MULTIPLE EXPERTS
J. M. Booker and R. R. Picard 1991 28 p Presented at the American Statistical Association (ASA) Annual Meeting, Atlanta, 18-22 Aug. 1991
(Contract W-7405-eng-36)
(DE91-013522; LA-UR-91-1512; CONF-9108100-2) Avail: NTIS HC/MF A03

This report describes a study that compares four different methods for aggregating expert judgment data given from multiple experts. These experts need not be a random sample of available experts. The experts estimate the same unknown parameter value. Their estimates need not be a representative set of sample values from an underlying distribution whose mean is an unknown parameter, theta. However, it is desired to combine the experts' estimates into a single aggregation estimate to reflect their amount of available knowledge about the unknown parameter. Many different aggregation estimators and methods have been proposed in the literature. However, few have been used, tested, or compared. Four different methods are chosen for this study which have been used or proposed for use in NRC studies. The set represents a cross section of the various types of methods. The results of this study do not indicate the use of any one method over another. Methods requiring minimal decision maker input are sensitive to the biases in the experts' responses. For these methods, there is no mechanism to adjust the experts' estimates to account for any known biases in the expert population such as optimism or pessimism. The results of this study indicate that these methods tend to perform poorly in all but the most ideal cases. Conversely, methods requiring extensive decision maker inputs are sensitive to misspecification. These methods perform poorly unless complete information is known about all the experts. That is, the decision maker's input parameters must nearly equal the actual values. DOE

N91-30044# National Academy of Sciences - National Research Council, Washington, DC.
THE GOVERNMENT-UNIVERSITY-INDUSTRY RESEARCH ROUNDTABLE
1991 32 p Prepared in cooperation with National Academy of Engineering, Washington, DC
(Contract DE-FG05-89ER-75498)
(DE91-015795; DOE/ER-75498/T2) Avail: NTIS HC/MF A03

The Government-University-Industry Research Roundtable in transition was the theme of 1990. During the past several years, the Roundtable has been evolving from an experimental venture into an established organization. While continuing self examination and adjustments will be required to ensure that the Roundtable maintains the vitality of an innovative enterprise, progression of the Roundtable through several transitions in 1990 indicate that the evolutionary process is complete. The Roundtable now is an established institution in national science and technology policy affairs. DOE

82 DOCUMENTATION AND INFORMATION SCIENCE

Includes information management; information storage and retrieval technology; technical writing; graphic arts; and micrography.

For computer documentation see *61 Computer Programming and Software*.

N91-30045# Sandia National Labs., Albuquerque, NM.
COMPILATION AND REPRESENTATION OF INTELLIGENT ELECTRONIC DOCUMENTS: AN ARCHITECTURE FOR REFERENCEABILITY
R. C. Hall May 1991 28 p
(Contract DE-AC04-76DP-00789)
(DE91-012635; SAND-90-3150) Avail: NTIS HC/MF A03

This report describes an architecture for compiling and representing electronic documents in a framework which accommodates knowledge about how the documents are composed, organized, and correlated. A general concept of referenceability is employed. While the concept is relevant to a wide range of application areas, it is described in familiar terms of an electronic document comprised of related textual information and graphics. The concept is applicable to all classes of objects which, together with their references, constitute the electronic document. The documents may themselves contain references to other documents, as well as to constituent object classes such as textual components, figures, footnotes, subject indexes, and the like. The objects and references can be dynamically combined according to a total logical structure representable within a window environment. The framework supports automatic resolution of references and display of related document objects through intercommunicating windows which constitute a relevant user view of a document. DOE

N91-30046# Sandia National Labs., Albuquerque, NM.
LEGAL AND RECORDS MANAGEMENT ISSUE OF OPTICAL DISK STORAGE MEDIA
A. Nusbaum 1991 16 p Presented at the Rio Grande Chapter of Association of Records Managers and Administrators (ARMA) Meeting, Albuquerque, 21 Aug. 1991
(Contract DE-AC04-76DP-00789)
(DE91-014898; SAND-91-1370C; CONF-9108109-1) Avail: NTIS HC/MF A03

The advent of optical storage has made the digital storage of documents a viable option from both a practical and legal perspective. However, the availability of Optical Disk Storage raises questions regarding the destruction of the stored records and standards of longevity, and the admissibility in court of records produced from optical storage has not been tested. This paper will attempt to address these issues. DOE

N91-30047# Massachusetts Inst. of Tech., Cambridge. Lab. for Computer Science.
SPECIFICATION AND VERIFICATION OF REAL-TIME CONSTRAINTS IN COARSE-GRAIN DATAFLOW
Dana S. Henry May 1991 105 p
(Contract N00014-89-J-1988)
(AD-A237355; MIT/LCS/TR-487) Avail: NTIS HC/MF A06 CSCL 12/5

We present a method for verifying real time constraints in a distributed, coarse-grain dataflow environment starting with a program which has already been allocated onto a machine. The user specifies the timing of each module together with real-time constraints; and we verify the constraints. To deduce program's timing, the user specifies all possible behaviors of each dataflow module and assigns timing costs to each module's behavior. We use the behavior and timing of individual modules to derive a data independent timing model for the entire program. User specifiable constraints include conditional constraints and constraints through non-deterministic paths. An event-driven verification verifies constraints. We justify the need for an event-driven verification, describe design issues, and offer a tagging scheme for sharing state among multiple verifications. GRA

N91-30048# SRI International Corp., Menlo Park, CA.
PERSISTENT DATA/KNOWLEDGE BASE Final Report, Oct. 1988 - Dec. 1990
Donovan Hsieh and Teresa Lunt Jun. 1991 71 p
(Contract F30602-88-C-0142)
(AD-A237498; RL-TR-91-72) Avail: NTIS HC/MF A04 CSCL 12/7

The Persistent Data/Knowledge Base (PDKB) project is a research effort funded by Rome Laboratory and conducted at the Computer Science Laboratory of SRI International. The main goal was to design/develop persistent object storage techniques capable of handling multiple data objects in a distributed information processing environment. The objective was to perform an investigation and evaluation and to develop and verify a top level system/segment design specification for a persistent object-oriented data/knowledge base system using techniques for (1) reliable and efficient access to data/Knowledge bases, (2) increased programmer/user productivity, and (3) integrated hyper-media data types. Techniques that were investigated include AI/DB workstations, object representation including multimedia databases, temporal change management, persistent object storage media, spatial databases, and massive memory data/knowledge systems. The contribution is a highly intelligent technique for managing very large main memory or traditional secondary storage domains in a multimedia information system environment. GRA

N91-30049# Naval Postgraduate School, Monterey, CA.
THREE CASE STUDIES OF MANAGEMENT INFORMATION SYSTEMS M.S. Thesis
Marc W. Theberge Sep. 1990 55 p
(AD-A238310) Avail: NTIS HC/MF A04 CSCL 05/1

The Naval Postgraduate School must, by default, make use of teaching cases in information technology case studies oriented or based upon corporations. It has been difficult for the school to obtain such studies oriented to the military, much less the United States Navy. This thesis provides the Naval Postgraduate School with three teaching cases concerning automated information systems serving the administrative and operational needs of unit-level command organizations. GRA

N91-30050# Ballistic Research Labs., Aberdeen Proving Ground, MD.
RANDOMIZATION PROCEDURES APPLIED TO ANALYSIS OF BALLISTIC DATA Final Report, Jun. 1990 - May 1991
Malcolm S. Taylor and Barry A. Bodt Jun. 1991 20 p
(DA Proj. 1L1-61102-AH-43)
(AD-A238389; BRL-TR-3245) Avail: NTIS HC/MF A03 CSCL 19/10

Randomization procedures are shown to offer a viable approach

to the analysis of ballistic data in a variety of settings. Distribution assumptions are unnecessary and, of even greater importance, random samples of data are not required. Small sample sizes, while never welcome, can also be accommodated. The price paid for randomization is increased computation, since every problem requires a tailored solution. Application of normal theory may only be valid to the extent that it approximates the results obtained from randomization. Reconciliation of some theoretical questions raised by the application of randomization procedures to ballistics data establishes this is an important and practical area of research. GRA

N91-30051# Air Force Systems Command, Eglin AFB, FL. Development Test Center.
SCIENTIFIC AND TECHNICAL INFORMATION HANDBOOK FOR TECHNICAL REPORT PREPARATION
L. Wargo 31 May 1991 41 p
(AD-A238548; AFDTC-TM-91-01; AFDTC-PAMPHLET-83-2)
Avail: NTIS HC/MF A03 CSCL 05/2

The contents of this publication describes the organization and format of a technical report, and is a compilation of standards, manuals and regulations pertaining to technical report publication. Attachments 1 through 4 contain report preparation and processing requirements. Attachments 5 through 18 contain examples of report content and format. GRA

N91-30052# Harry Diamond Labs., Adelphi, MD.
A SURVEY OF TECHNIQUES IN AIDED TARGET RECOGNITION (ATR) FROM DIGITAL AND OPTICAL PERSPECTIVES Progress Report, Jun. 1988 - Apr. 1989
Charles G. Garvin Jul. 1991 25 p
(AD-A238644; HDL-PR-91-1) Avail: NTIS HC/MF A03 CSCL 12/9

Since there is no generally applicable definition of the term aided target recognition (ATR), the author takes as a working definition the task of mapping scenes to representations and extracting information concerning specific elements from these representations, such as the physical attributes of objects in the scenes. This report presents a survey of a number of useful linear and nonlinear image processing techniques for aided target recognition tasks. A summary of the current progress with both digital and optical implementations of these techniques is also given. GRA

N91-30053# Technische Hogeschool Twente, Enschede (Netherlands). Dept. of Computer Science.
DATA ABSTRACTION, CONCURRENCY AND SYNCHRONIZATION IN SINA
M. Aksit and A. Tripathi Apr. 1990 70 p Prepared in cooperation with Minnesota Univ., Minneapolis
(PB91-185454; Memo-INF-90-15) Avail: NTIS HC/MF A04 CSCL 05B

The data abstraction, concurrency and synchronization mechanisms of the object oriented language, Sina, are described. The general idea behind the data abstraction mechanism is that, starting from a simple object-based model, one can implement various forms of abstractions without committing to a fixed number of techniques such as inheritance, delegations, and relations. The concurrent programming model of Sina provides the flexibility of implementing objects with different policies of synchronization. Author

N91-30054# National Inst. of Standards and Technology, Gaithersburg, MD.
GUIDE TO DESIGN, IMPLEMENTATION AND MANAGEMENT OF DISTRIBUTED DATABASES
E. N. Fong, C. L. Sheppard, and K. A. Harvill Feb. 1991 60 p
(PB91-187567; NIST/SP-500/185) Avail: NTIS HC/MF A04; also available SOD HC $3.50 as 003-003-03076-7 CSCL 05B

For an organization to operate in a distributed database environment, there are two related but distinct tasks that must be accomplished. First, the distributed database environment must be established. Then, a distributed database application can be designed and installed within the environment. The guide describes both of those activities based on a development life-cycle phase framework. The guide provides practical information and identifies skills needed for systems designers, application developers, database and data administrators who are interested in the effective planning, design, installation, and support for a distributed database environment. In addition, the guide instructs system analysts and application developers with a step-by-step procedure for the design, implementation and management of a distributed data base management system application. The guide also notes that truly heterogeneous distributed database technology is still a research consideration. Author

N91-30055# Environmental Protection Agency, Washington, DC. Office of Information Resources Management.
INFORMATION SYSTEMS INVENTORY (ISI)
May 1991 246 p
(PB91-172940) Avail: NTIS HC/MF A11 CSCL 05B

A hardcopy version of the EPA Information Systems Inventory (ISI) data base is presented. The ISI data base is maintained on an IBM PC and an Apple Macintosh and currently holds roughly 500 records. The ISI was developed to enhance the Agency's ability to track major information systems, facilitate the sharing of information across media and program boundaries and improve the Agency's oversight of information systems development. For each system in the Inventory, the following information is included: system identification, descriptors of data base content, and administrative data about access and legal authorities. Author

N91-30056# Executive Office of the President, Washington, DC. Office of Administration.
PUBLICATIONS OF THE EXECUTIVE OFFICE OF THE PRESIDENT, JANUARY 20, 1989 - MARCH 31, 1991
1991 10 p
(PB91-156828) Avail: NTIS HC/MF A02 CSCL 05B

Publications of the Executive Office of the President for the Bush administration for the period January 20, 1989 through March 31, 1991 are listed. Author

N91-30057# Sandia National Labs., Albuquerque, NM.
RECORDS MANAGEMENT AT THE DOE NATIONAL LABORATORIES: SANDIA NATIONAL LABORATORIES
N. J. Pruett 1991 5 p Presented at the 1991 Nuclear Information and Records Management Association (NIRMA) Symposium, Charlotte, NC, 25-28 Aug. 1991
(Contract DE-AC04-76DP-00789)
(DE91-015563; SAND-91-1581C; CONF-9108113-1) Avail: NTIS HC/MF A01

Sandia National Laboratories is a large multi-program DOE laboratory. The Recorded Information Management Division (RIM) has an expanding mission to meet Sandia's needs for cost-effective management in information from creation to final disposition in accordance with applicable regulations and requirements. An analysis based on the need to meet requirements and to improve business practice was successful in convincing management to allocate increased resources to the RIM Compliance Project. DOE

83 ECONOMICS AND COST ANALYSIS

Includes cost effectiveness studies.

No abstracts in this category.

84 LAW, POLITICAL SCIENCE AND SPACE POLICY

Includes NASA appropriation hearings; aviation law; space law and policy; international law; international cooperation; and patent policy.

No abstracts in this category.

85 URBAN TECHNOLOGY AND TRANSPORTATION

Includes applications of space technology to urban problems; technology transfer; technology assessment; and surface and mass transportation.

For related information see also *03 Air Transportation and Safety, 16 Space Transportation,* and *44 Energy Production and Conversion.*

N91-30058# Sandia National Labs., Albuquerque, NM.
TECHNOLOGY TRANSFER: A NEW PROGRAM BETWEEN SANDIA NATIONAL LABORATORIES AND THE UNIVERSITY OF NEW MEXICO
M. S. Allen 1991 2 p Presented at the 32nd Institute of Nuclear Material Management (INMM) Annual Meeting, New Orleans, 28-31 Jul. 1991
(Contract DE-AC04-76DP-00789)
(DE91-015439; SAND-91-1570C; CONF-910774-5) Avail: NTIS HC/MF A01

Sandia National Laboratories and the University of New Mexico's Anderson School of Management are developing a program which enables M.B.A. students to assist in commercializing Sandia developed technologies. Thus far, students have prepared detailed business plans (which include market analyses, design and development sections, and pro forma financials) for a wide range of technologies. Potential applications include waste management, cancer treatment, oil and gas transportation, coating of plastics, manufacturing and assembly, and parts inspections. By having graduate students conduct the research necessary to identify positive net-present-value projects, Sandia is able to interest private sector firms in its technologies. DOE

88 SPACE SCIENCES (GENERAL)

No abstracts in this category.

89 ASTRONOMY

Includes radio, gamma-ray, and infrared astronomy, and astrometry.

N91-30059 Council for National Academic Awards (England).
AN INVESTIGATION OF NOVA PERSEI (1901) AND ITS ENVIRONMENT Ph.D. Thesis
John Anthony Roberts 1989 160 p
Avail: Univ. Microfilms Order No. BRDX91968

The nature of the ambient medium about the classical nova GK Persei (Nova Persei 1901) was investigated using Infrared Astronomy Satellite (IRAS) far infrared and optical observations, coupled with detailed modeling of the optical light echoes. Measurements of the time dependent expansion of the nova ejecta show that significant deceleration is occurring in the SW quadrant; otherwise, the expansion appears fairly uniform at a velocity of around 1200 km s (sup -1). Interaction with the surrounding medium is the likely cause of thsi deceleration. Analysis of IRAS 12-100 micron raw data reveals that GK Per is centrally positioned on a saddle point between the two emission peaks of an isothermal (T equals 22 plus or minus 1K) bipolar nebulosity. This work has helped to elucidate the cause of some of the rare features associated with GK Per, and also to achieve a better understanding of the nova environment. Dissert. Abstr.

N91-30060*# National Aeronautics and Space Administration. Goddard Space Flight Center, Greenbelt, MD.
LOWELL PROPER MOTION SURVEY: SOUTHERN HEMISPHERE (GICLAS, BURNHAM, AND THOMAS 1978). DOCUMENTATION FOR THE MACHINE-READABLE VERSION
Wayne H. Warren, Jr. Aug. 1989 19 p
(NASA-TM-105069; NSSDC/WDC-A-R/S-89-15; NAS 1.15:105069) Avail: NTIS HC/MF A03 CSCL 03A

The machine-readable version of the catalog, as it is currently being distributed from the Astronomical Data Center, is described. The catalog is a summary compilation of the Lowell Proper Motion Survey for the Southern Hemisphere, as completed to mid-1978 and published in the Lowell Observatory Bulletins. This summary catalog serves as a Southern Hemisphere companion to the Lowell Proper Motion Survey, Northern Hemisphere. Author

N91-30061*# National Aeronautics and Space Administration. Marshall Space Flight Center, Huntsville, AL.
A SIMULATION OF THE INSTRUMENT POINTING SYSTEM FOR THE ASTRO-1 MISSION
M. Whorton, M. West, and J. Rakoczy Jul. 1991 30 p
(NASA-TM-103547; NAS 1.15:103547) Avail: NTIS HC/MF A03 CSCL 03A

NASA has recently completed a shuttle-borne stellar ultraviolet astronomy mission known as Astro-1. A three axis instrument pointing system (IPS) was employed to accurately point the science instruments. In order to analyze the pointing control system and verify pointing performance, a simulation of the IPS was developed using the multibody dynamics software TREETOPS. The TREETOPS IPS simulation is capable of accurately modeling the multibody IPS system undergoing large angle, nonlinear motion. The simulation is documented and example cases are presented demonstrating disturbance rejection, fine pointing operations, and multiple target pointing and slewing of the IPS. Author

N91-30062# Lawrence Livermore National Lab., CA.
DIFFRACTION-LIMITED IMAGING OF SATELLITES USING BISPECTRAL SPECKLE INTERFEROMETRY
T. W. Lawrence, D. M. Goodman, J. P. Fitch, and E. M. Johansson 21 Nov. 1990 9 p
(Contract W-7405-eng-48)
(DE91-015745; UCRL-ID-105574) Avail: NTIS HC/MF A02

We have developed and implemented a new technology for removing the effects of atmospheric turbulence from telescope images. This technology, bispectral speckle interferometry, permits imaging of astronomical objects and satellites to the diffraction limit of the collecting telescope. We have successfully applied this technique to speckle images we obtained with a 1.6 meter telescope at the Air Force Maui Optical Station on Mt. Haleakala, Maui. We have extracted diffraction-limited features of several satellites, including the Hubble Space Telescope. This technology should have a positive impact on both astronomical and defense imaging problems. DOE

90 ASTROPHYSICS

Includes cosmology; celestial mechanics; space plasmas; and interstellar and interplanetary gases and dust.

For related information see also *75 Plasma Physics.*

N91-30063 Illinois Univ., Urbana-Champaign.
PROTON DECELERATION NEAR THE SURFACE OF AN

ACCRETING NEUTRON STAR Ph.D. Thesis
Donald Dean Pakey 1990 131 p
Avail: Univ. Microfilms Order No. DA9114369

Presented here is a study of proton deceleration by multiple Coulomb collisions with electrons in a hot, strongly magnetized plasma. Th evolution of the proton velocity-space distribution function is followed by integrating a Fokker-Planck equation numerically. The Fokker-Planck coefficients are calculated for conditions in which the electrons have a thermal distribution of velocities parallel to the field and remain in their lowest magnetic Landau levels. Nonrelativistic Landau wavefunctions are used for both the electrons and the accreting protons. The significance of results for X-ray emission by accreting neutron stars is discussed and the reasons for the discrepancies among previous calculations are clarified. Dissert. Abstr.

N91-30064 California Inst. of Tech., Pasadena.
THE RELATIONSHIP BETWEEN THE DENSITY WAVE, MOLECULAR GAS AND STAR FORMATION IN M51 Ph.D. Thesis
Richard John Rand 1991 192 p
Avail: Univ. Microfilms Order No. DA9113617

A study is presented of the relationship between the density wave, molecular gas, and star formation in the molecule-rich, grand-design spiral galaxy M51. An interferometric map of CO emission from M51 is presented. A narrow, two-armed spiral pattern is seen in the molecular gas. Streaming motions indicate the presence of a density wave. Many apparently bound Giant Molecular Associations (GMAs) of typical mass are seen along the arms. A few unbounded GMAs are seen between the arms. Two consequences of star formation for the state of the Interstellar Medium (ISM) are discussed. Researchers find evidence of the idea that the HI is predominantly a product of dissociation in the star-forming regions. IRAS pointed observations are used to probe the origins of the infrared emission. Two independent tests indicate that a substantial portion of the infrared emission originates in a cirrus component, and not in star forming regions. A kinematic study of the old disk stars and various gaseous components is presented. Dissert. Abstr.

N91-30065# Fermi National Accelerator Lab., Batavia, IL.
DARK MATTER IN THE UNIVERSE
M. S. Turner Mar. 1991 40 p Presented at the International Conference on Trends in Astroparticle Physics, Santa Monica, CA, 26 Nov. - 1 Dec. 1990
(Contract DE-AC02-76CH-03000)
(DE91-014863; FNAL/C-91/78-A; CONF-901141-6) Avail: NTIS HC/MF A03

What is the quantity and composition of material in the universe? This is one of the most fundamental questions we can ask about the universe, and its answer bears on a number of important issues including the formation of structure in the universe, and the ultimate fate and the earliest history of the universe. Moreover, answering this question could lead to the discovery of new particles, as well as shedding light on the nature of the fundamental interactions. At present, only a partial answer is at hand: most of the material in the universe does not give off detectable radiation, i.e., is dark; the dark matter associated with bright galaxies contributes somewhere between 10 and 30 percent of the critical density (by comparison luminous matter contributes less than 1 percent); baryonic matter contributes between 1.1 and 12 percent of critical. The case for the spatially-flat, Einstein-de Sitter model is supported by three compelling theoretical arguments -- structure formation, the temporal Copernican principle, and inflation -- and by some observational data. If (Omega) is indeed unity--or even just significantly greater than 0.1--then there is a strong case for a universe comprised of nonbaryonic matter. There are three well motivated particle dark-matter candidates: an axion of mass 10(exp -6) eV to 10(exp -4) eV; a neutralino of mass 10 GeV to about 3 TeV; or a neutrino of mass 20 eV to 90 eV. All three possibilities can be tested by experiments that are either being planned or are underway. DOE

N91-30066# State Univ. of New York, Stony Brook.
RESEARCH IN NUCLEAR ASTROPHYSICS: STELLAR COLLAPSE AND SUPERNOVAE
J. M. Lattimer and A. Yahil 1991 15 p
(Contract DE-FG02-87ER-40317)
(DE91-015449; DOE/ER-40317/5) Avail: NTIS HC/MF A03

The interaction between nuclear theory and some outstanding problems in astrophysics is examined. We are actively researching the astrophysics of gravitational collapse, neutron star birth and neutrino emission, and neutron star cooling, on the one hand, and the nuclear physics of the equation of state of hot, dense matter on the other hand. There is close coupling between nuclear theory and supernova and neutron star phenomenon; some nuclear matter properties might be best delineated by astrophysical considerations. Our research has focused on the neutrinos emitted from supernovae, since they are the only available observables of the internal supernova mechanism. We are modifying our hydrodynamical code to use implicit differencing and to include multi-group neutrino diffusion and general relativity. In parallel, we are extending calculations of core collapse supernovae to long times after collapse by using a hybrid explicit-implicit hydrodynamical code and by using simplified neutrino transport. We hope to establish the existence or non-existence of the so-called long-term supernova mechanism. We are also extending models of the neutrino emission and cooling of neutron stars to include the effects of rotation and the direct Urca process that we recently discovered to be crucial. We have developed a rapid version of the dense matter equation of state for use in hydrodynamic codes that retains essentially all the physics of earlier, more detailed equations of state. This version also has the great advantage that nuclear physics inputs, such as the nuclear incompressibility, symmetry, energy, and specific heat, can be specified. DOE

91 LUNAR AND PLANETARY EXPLORATION

Includes planetology; and manned and unmanned flights. For spacecraft design or space stations see *18 Spacecraft Design, Testing and Performance.*

N91-30067 Arizona State Univ., Tempe.
INVESTIGATIONS IN MARTIAN GEOLOGY. PART 1: NATURE OF THE MANTLING DEPOSIT IN THE HEAVILY CRATERED TERRAIN OF NORTHEASTERN ARABIA, MARS. PART 2: EXPERIMENTAL STUDIES OF CLEAN AND DUST-OR-SAND-COVERED ICE SUBLIMATION UNDER MARS-LIKE CONDITIONS Ph.D. Thesis
Jeffrey Morgan Moore 1990 179 p
Avail: Univ. Microfilms Order No. DA9116769

The geomorphology is described of a portion of northeastern Arabia, Mars. This surface is covered by an extensive, layered deposit which has been, in places, substantially eroded. Speculative origins for the deposit include formation as a differentially welded pyroclastic tuff, or a differentially compacted, zonally indurated aeolian dust deposit. An experimental study was made of the sublimation rate of H2O ice, both from clean surfaces and from under thin layers of dust or sand, in a Mars-like environment. The major conclusions drawn from the results of this experiment are: (1) even very thin layers of dust greatly lower the sublimation rate of an underlaid ice substrate being heated from above; (2) thin layers of dust or sand only mildly suppress the sublimation rate of an underlaid ice substrate when a sample is wholly isothermal; (3) even a low flux, desicated gas flow over the sample surface greatly increases the sublimation rate of any given sample; (4) dry sublimation of ice underlying thin layers of dust or sand may modify the surface texture as a function of particle cohesion; and (5) the actual sublimation rate of clean ice is several factors lower than the sublimation rate predicted by a common formula.
Dissert. Abstr.

N91-30068*# National Aeronautics and Space Administration. Langley Research Center, Hampton, VA.
CONCEPTS FOR MANNED LUNAR HABITATS
W. D. Hypes, A. J. Butterfield, C. B. King, G. D. Qualls (Flight Mechanics and Control, Inc., Hampton, VA.), W. T. Davis, M. J. Gould, J. E. Nealy, and L. C. Simonsen Aug. 1991 103 p
(NASA-TM-104114; NAS 1.15:104114) Avail: NTIS HC/MF A06 CSCL 03B

The design philosophy that will guide the design of early lunar habitats will be based on a compromise between the desired capabilities of the base and the economics of its development and implantation. Preferred design will be simple, make use of existing technologies, require the least amount of lunar surface preparation, and minimize crew activity. Three concepts for an initial habitat supporting a crew of four for 28 to 30 days are proposed. Two of these are based on using Space Station Freedom structural elements modified for use in a lunar-gravity environment. A third concept is proposed that is based on an earlier technology based on expandable modules. The expandable modules offer significant advantages in launch mass and packaged volume reductions. It appears feasible to design a transport spacecraft lander that, once landed, can serve as a habitat and a stand-off for supporting a regolith environmental shield. A permanent lunar base habitat supporting a crew of twelve for an indefinite period can be evolved by using multiple initial habitats. There appears to be no compelling need for an entirely different structure of larger volume and increased complexity of implantation. Author

92 SOLAR PHYSICS

Includes solar activity, solar flares, solar radiation and sunspots.

For related information see *93 Space Radiation.*

N91-30069# Naval Observatory, Washington, DC.
CENTRAL SOLAR ECLIPSES OF 1992. ANNUAL SOLAR ECLIPSE OF 4-5 JANUARY 1992, TOTAL SOLAR ECLIPSE OF 30 JUNE 1992
John A. Bangert, Alan D. Fiala, and William T. Harris 1 Feb. 1991 51 p
(AD-A237614; NOBS-CIRC-176) Avail: NTIS HC/MF A04 CSCL 03/2

By coincidence, the two central solar eclipses of 1992 share a similar characteristic: both central paths will pass almost entirely over water, except for a very small portion at one end which will pass over land and include a major city. The first of the eclipses, an annular eclipse of the Sun, will occur on Saturday, 4 January 1992 and Sunday, 5 January 1992. It will be preceded by an associated partial lunar eclipse on 21 December 1991. The central path of this annular eclipse will include a number of small islands in the Pacific Ocean and end over the Los Angeles, California metropolitan area. At maximum over the central Pacific Ocean, approximately 84.4 percent of the Sun's disk will be obscured. The maximum duration of annularity will be about 11m 36s. Because the track will cross the International Date Line, by local times the eclipse will occur on the morning of 5 January at the beginning of the path and occur on the evening of 4 January at the end of the path. This eclipse belongs to saros series number 141. The last preceding eclipse in this series was the annular solar eclipse of 24 December 1973; the next eclipse in series will be the annular solar eclipse of 15 January 2010. GRA

N91-30070# Woods Hole Oceanographic Inst., MA.
COURSE LECTURES ABSTRACTS OF PARTICIPANTS FELLOWS PROJECT REPORTS
Rick Salmon Oct. 1990 373 p
(Grant NSF OCE-89-01012)
(AD-A237909; WHOI-91-03) Avail: NTIS HC/MF A16 CSCL 03/2

The 1990 program in Geophysical Fluid Dynamics (GFD) had as its special topic Stellar Fluid Dynamics. Introductory lectures paved the way for more specialized seminars on solar oscillations, neutron stars, stellar winds, solar convection, and flows with strong magnetic fields. The lectures ranged far beyond the special topic of the summer, with GFD filling its traditional role as a clearing house for information between the various fields that share an interest in rotating, differentially-heated flows. Relativistic fluctuation-dissipation theorems, radiative, hydrodynamics and galaxy formation, Solar acoustic oscillations, Convection and chaos, Very high resolution solar Xray imaging, Coherent structures and statistical theory of turbulence, Dynamics of localized structures with Galilean invariance, Polytropes and their perturbations, Hydromagnetic instability due to elliptical flow, Vortices in tight embrace, Catastrophe structure of thermohaline convection, simulations of solar convection and Fluid mechanics and melting.Fellows Project Reports include: Structure and stability of rapidly rotating polytropes, Nonlinear evolution of a perturbed axisymmetric eddy, Rise and fall of buoyant plumes, Transport of a chemical in stellar radiative zones, Magnetic flux tubes and convection, Diffusing in Poiseuille flow and Classification of similarity solutions of the two-dimensional convection equations. GRA

93 SPACE RADIATION

Includes cosmic radiation; and inner and outer earth's radiation belts.

For biological effects of radiation see *52 Aerospace Medicine.* For theory see *73 Nuclear and High-Energy Physics.*

No abstracts in this category.

99 GENERAL

N91-30071# National Research Council of Canada, Ottawa (Ontario). Div. of Electrical Engineering.
BULLETIN OF THE DIVISION OF ELECTRICAL ENGINEERING, 1988-1989
May 1989 177 p In ENGLISH and FRENCH
(NRC-30458; ISSN-0706-568X; CTN-91-60012) Copyright Avail: NTIS HC/MF A09

The activities of this division cover a spectrum of technologies. The major sections of the division are as follows: The Industrial Liaison Office supports R and D activities in collaboration with Canadian industry. The Laboratory of Biomedical Engineering has three primary strategic objectives: to develop assistive devices for those with physical and developmental disabilities; to do research on the health effects of non-ionizing radiation; and to develop therapeutic and diagnostic instrumentation. A Space Life Sciences project has been established to carry out work in collaboration with NRCCs Space Division. Two experiments was carried out on Soviet satellites in 1989. The Laboratory for Electromagnetic Power Engineering has a mandate to provide standards, testing procedures, and technology in the area of precision measurement, electomagnetic compatibility, and dielectrics. The Laboratory for Intelligent Systems has three major objectives: to develop computing and sensor technologies which will be applied to the building of autonomous systems; to develop computer based technology for the creation of advanced knowledge based systems; and to encourge the application and exploitation of advanced computer technologies by industry. It has been involved in the development of 3D vision systems, guided wave optics, sensor based robotics, and knowledge based systems. In 1989 a prototype diagnosis and troubleshooting advisor for acceleration faults in jet engines was developed. Use of a two-axis wrist-mounted scanner to determine the pose of a standard satellite grappling fixture was demonstrated. CISTI

N91-30072# National Research Council of Canada, Ottawa (Ontario).

NRC ANNUAL REPORT, 1988/1989

1989 104 p In ENGLISH and FRENCH

(NRC-30398; ISBN-0-662-56720-X; CTN-91-60013) Copyright

Avail: NTIS HC/MF A06

The National Research Council of Canada (NRCC) is Canada's leading science and technology agency. It provides national science and engineering facilities, expertise, assistance, and coordination in fundamental research and in the development of new technologies to solve immediate and practical problems. NRCC is involved in a broad spectrum of research areas in both the pure sciences and in enginering. The last year of a five year plan, 1989, focussed on improving the technological capabilities and competitiveness of Canadian companies. Consortia wave established in several technological areas. Cooperative programs were created with the audio equipment industry (to develop smart speakers), the microelectronics industry, and for the development of superconductors. Two new services were made available to Canadian companies: a calibration asessment service provides access to international standards in the calibration of equipment, and a Canadian Construction Materials Centre to provide a national evaluation service for all sectors of the construction industry. The construction of a new high speed communication link, NRNet, connecting research centers across Canada, is well underway. Descriptions of the major research divisions and their research projects are included. Divisions involved in work of high relevance to the aerospace industry include: the Space Division, which is involved in a number of collaborative projects with space agencies in other countries; National Aeronautical Establishment; the Hertzberg Institute of Astrophysics; the Mechanical Engineering Division; and the Division of Electrical Engineering. CISTI

N91-30073*# National Aeronautics and Space Administration. Lewis Research Center, Cleveland, OH.

NASA CRYOGENIC FLUID MANAGEMENT SPACE EXPERIMENT EFFORTS, 1960-1990

Daniel Glover 1991 29 p Presented at the Conference on Advanced Space Exploration Initiative Technologies, Cleveland, OH, 4-6 Sep. 1991; cosponsored by AIAA and OAI

(NASA-TM-103752; E-6005; NAS 1.15:103752; AIAA-91-3538)

Avail: NTIS HC/MF A03 CSCL 05D

A history of technological development for subcritical cryogenic fluid management (CFM) through space experiments is given for the period 1960 to 1990. Space experiments with liquid hydrogen were conducted in the early 1960's. Efforts since then have consisted of studies and designs of potential space experiments. A chronology of CFM space experiments and design efforts is included. Author

Typical Subject Index Listing

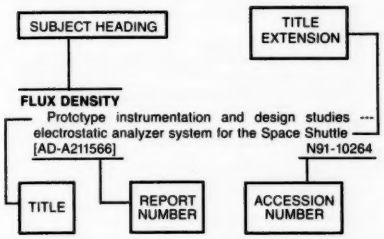

The subject heading is a key to the subject content of the document. Titles, report numbers, and accession numbers of pertinent documents are provided under each subject heading. When the title is insufficiently descriptive of the document content, a title extension has been added, separated from the title by three hyphens. The report number helps to indicate the type of document cited (e.g., NASA report, NASA translation, NASA contractor report). The accession number is the number by which the document abstracts are arranged in this journal and by which the document is sold or requested. The titles, with title extensions if present, are arranged under each subject heading in ascending accession number order. The subject headings have been selected from the latest revision of the *NASA Thesaurus* (NASA SP-7064).

A

ABLATION
Ablation of material by front surface spallation
[DE91-014773] N91-29563
The laser ablation of aluminum at 193, 248, and 351 nm
[AD-A237574] N91-29569

ABLATIVE MATERIALS
Ablative heat shield studies for NASA Mars/Earth return entry vehicles
[AD-A238159] N91-29215

ABSORPTION CROSS SECTIONS
Chasing the x(sub f) dependence of J/psi production
[DE91-015136] N91-29899

ABSORPTION SPECTROSCOPY
Structures, properties, and dynamics of metal clusters from infrared laser spectroscopy
[AD-A237669] N91-29570
Atomic-resolution scanning tunneling microscopy and infrared spectroscopy as combined in-situ probes of electrochemical adlayer structure: Carbon monoxide on rhodium(111)
[AD-A237508] N91-29884

AC GENERATORS
Design and test of a continuous duty pulsed ac generator
[DE91-014664] N91-29445

ACCELERATION (PHYSICS)
Shock acceleration with turbulence minimization
[DE91-014741] N91-29505
Numerical study of non-impulsively started flow around a circular cylinder
[AD-A238051] N91-29519

ACCELEROMETERS
Instrumentation for ASE experiments in the dynamic wind tunnel
[PD-FC-9112] N91-29197

ACCEPTABILITY
Statistical characterization of graphite fiber for prediction of composite structure reliability
[AD-A238020] N91-29245

ACCESS CONTROL
Discretionary security for object-oriented database systems
[AD-A237573] N91-29740

ACCIDENT PREVENTION
Methods to determine the compatibility and degradation of organic materials
[AD-A237940] N91-29234

ACETYLENE
Hot atom reactive scattering and photodissociation experiments with acetylene and ethylene
[DE91-013755] N91-29264
Reactions of small molecular systems
[DE91-014519] N91-29867

ACOUSTIC EMISSION
An assessment of the acoustic noise in the working section of the NAE 6 ft x 9 ft low speed wind tunnel
[NAE-LTR-ST-1744] N91-29196

ACOUSTIC INSTABILITY
Measurements of the ion acoustic decay instability and the resultant thermal and suprathermal electron heating in laser-plasma interaction experiments
[DE90-012477] N91-29941

ACOUSTIC MEASUREMENT
On-line monitoring of volatile organic species
[DE91-014655] N91-29655

ACOUSTIC PROPERTIES
Investigation of the flame-acoustic wave interaction during axial solid rocket instabilities
[AD-A237851] N91-29223
Acoustic tests on a new motor generator system for the Minuteman launch control centers at Alpha 01 and Sierra 00, Malmstrom AFB, Montana
[AD-A237944] N91-29648

ACOUSTIC VELOCITY
Ultrasonic evaluation of silicon nitride green bodies
[AD-A237924] N91-29608
Modification of programs CHIEF and CID to compute sound radiation from an arbitrary body with mixed boundary conditions
[AD-A237502] N91-29759

ACOUSTICS
Hamiltonian 3-D ray tracing in the oceanic waveguide on the ellipsoidal earth
[AD-A237458] N91-29700
NRL review, 1991
[AD-A238665] N91-29857

ACOUSTO-OPTICS
Theoretical, experimental, and numerical studies on hybrid acoustooptic bistable devices
[AD-A237885] N91-29463

ACRYLATES
Light scattering characterization of polymer additives and correlation of molecular properties of polymer fluids
[AD-A238547] N91-29367

ACRYLIC RESINS
Model filled polymer 7: Flow behavior of polymers containing monodisperse crosslinked polymeric beads
[AD-A237430] N91-29350
Light scattering characterization of polymer additives and correlation of molecular properties of polymer fluids
[AD-A238547] N91-29367

ACTIVATION
Activation calculations for trapped protons below 200 MeV: Appendix
[NASA-CR-184170] N91-29865

ACTIVATION ENERGY
Solvent effects on simple electron transfer reactions. A comparison of results in Debye and non-Debye solvents
[AD-A237157] N91-29875
Discreteness-of-solvent effects in Marcus equations in the mean spherical approximation
[AD-A237133] N91-29996

ACTIVE CONTROL
Experimental demonstration of a classical approach for flexible space structure control: NASA CSI testbeds
[NASA-CR-188724] N91-29212

ACTUATORS
Compensation of distributed delays in integrated communication and control systems
[NASA-CR-187136] N91-29193
Singularity avoidance and the kinematics of an eight-revolute-joint manipulator N91-29588
Effects of colocation and non-colocation of sensors and actuators on flexible structures
[AD-A238457] N91-29844

ADA (PROGRAMMING LANGUAGE)
Alsys Limited, Alsycomp 017, version 5.2, MICRO VAX 2 under Micro VMS V5.3 (host) to INMOS T425 transputer implemented on a B403 TRAM (target), 901118N1.11064
[AD-A237411] N91-29738
Slaying the software dragon: A look at how software engineering, the Ada programming language and process maturity are changing software development
[AD-A237156] N91-29751
Real-time Ada design methodologies and their impact on performance
[AD-A237259] N91-29754
Ada 9X requirements rationale
[AD-A237350] N91-29755

ADAPTATION
Fission-fusion adaptivity in finite elements for nonlinear dynamics of shells
[AD-A238029] N91-29626

ADAPTERS
Universal ground adapter assembly
[AD-D014908] N91-29439

ADAPTIVE CONTROL
Experiments in adaptive control of cooperating manipulators N91-29594

ADAPTIVE FILTERS
The design of a real-time adaptive filter development system
[AD-A237134] N91-29448

ADAPTIVE OPTICS
NRL review, 1991
[AD-A238665] N91-29857

ADDITIVES
Effect of alumina particle additions on the aging kinetics of 6061 aluminum matrix composites
[AD-A238052] N91-29246
Light scattering characterization of polymer additives and correlation of molecular properties of polymer fluids
[AD-A238547] N91-29367
Effects of doping on hybridization gapped materials
[DE91-014611] N91-29477
Basic mechanisms of diesel lubrication correlation of bench and engine tests
[AD-A237685] N91-29596

ADHESION
Effects of interfacial modification on diamond film adhesion
[AD-A237750] N91-29354
Liquid honing evaluation
[DE91-015749] N91-29393
A layered beam theory for single lap joints
[AD-A237324] N91-29607

ADHESIVE BONDING
Ultrasonic evaluation of elastic and interfacial properties of composite materials and laminates N91-29238
A layered beam theory for single lap joints
[AD-A237324] N91-29607

ADHESIVES
A layered beam theory for single lap joints
[AD-A237324] N91-29607
Ventilation kinetics testing of a steel frame/rubber fabric underground shelter
[AD-A237469] N91-29734

ADIABATIC CONDITIONS
Experimental investigation of adiabatic shear banding at different impact velocities
[AD-A237901] N91-29625
Charge motion effects in ionic clusters
[AD-A238178] N91-29886

ADIABATIC FLOW
Adiabatic two-phase flow frictional pressure drop. Part 2: A generalized method for data correlation
[DE91-014462] N91-29501

Adiabatic two-phase flow frictional pressure drop. Part 1: Critical parameters and friction factors for air-water mixture
[DE91-014463] N91-29502
ADSORPTION
Electrochemical contact adsorption site changes driven by field and charge fact and theory
[AD-A237127] N91-29269
High resolution electron energy loss studies of surface vibrations
[DE91-014539] N91-30024
ADVANCED LAUNCH SYSTEM (STS)
ALS rocket engine combustion devices design and demonstration
[NASA-CR-183824] N91-29233
ADVANCED VERY HIGH RESOLUTION RADIOMETER
An AVHRR data set for the arctic leads ARI
[AD-A237221] N91-29637
AERIAL RECONNAISSANCE
NAE Twin Otter operations in FIFE 1989
[NASA-CR-188770] N91-29169
AEROACOUSTICS
Translation of airfoil trailing edge noise article from Revue d'Acoustique
[AD-A237811] N91-29143
AERODYNAMIC BALANCE
A new look at the Tobak-Schiff model of nonplanar aircraft dynamics
[NAE-LTR-UA-101] N91-29168
AERODYNAMIC BRAKES
Stabilized square parachute
[AD-D014946] N91-29149
AERODYNAMIC CHARACTERISTICS
Missile Datcom: User's manual
[AD-A237817] N91-29148
A computer program for prediction of internal performance of a ramrocket
[AD-A238179] N91-29226
AERODYNAMIC COEFFICIENTS
Subsonic aerodynamic coefficients of the SDM at angles of attack up to 90 deg
[NAE-LTR-UA-93] N91-29144
AERODYNAMIC DRAG
Performance of an airfoil at low Reynolds number
[NAL-PD-CF-9102] N91-29145
Preliminary flight-determined subsonic lift and drag characteristics of the X-29A forward-swept-wing airplane
[NASA-TM-100409] N91-29177
An approximate analysis of balloting motion of railgun projectiles
[AD-A237942] N91-29206
Basic simple modeling of in-bore motion of railgun projectiles
[AD-A238064] N91-29207
AERODYNAMIC INTERFERENCE
Subsonic aerodynamic coefficients of the SDM at angles of attack up to 90 deg
[NAE-LTR-UA-93] N91-29144
Control of flow over a backward facing step
[AD-A238638] N91-29521
AERODYNAMIC LOADS
Strain gauge cabling, conditioning, and sensitivity calculations for the CT-114 (Tutor) aircraft aft fuselage and empennage full-scale fatigue test
[NAE-LTR-ST-1758] N91-29534
AERODYNAMIC NOISE
Translation of airfoil trailing edge noise article from Revue d'Acoustique
[AD-A237811] N91-29143
AERODYNAMIC STABILITY
Stabilized square parachute
[AD-D014946] N91-29149
AERODYNAMIC STALLING
Horizontal axis wind turbine post stall airfoil characteristics synthesization
[DE91-002198] N91-29650
AERODYNAMICS
Missile Datcom: User's manual
[AD-A237817] N91-29148
The functional dependence of trajectory dispersion on initial condition errors
[DE91-014661] N91-29151
Unsteady compressible lifting surface analysis for rotary wings using velocity potential modes N91-29170
Unsteady force calculations in turbomachinery
[AD-A237937] N91-29515
Analysis of a teetered, variable-speed rotor
[DE91-002190] N91-29646
Horizontal axis wind turbine post stall airfoil characteristics synthesization
[DE91-002198] N91-29650
AEROELASTICITY
Modeling and response analysis of thin-walled beam structures constructed of advanced composite materials N91-29615
AEROSOLS
XTRAN: An atmospheric transmittance code based on XSCALE
[AD-A237624] N91-29674
Effects of solar heating by aerosols and trace gases on the temperature structure constant
[AD-A237675] N91-29677
AEROSPACE ENVIRONMENTS
IDA studies on natural space environmental effects on materials for SDIO
[AD-A237974] N91-29660
AEROSPACE SAFETY
Nuclear data needs for the space exploration initiative
[DE91-013231] N91-29200
AEROSPACE SYSTEMS
Experimental verification of an innovative performance-validation methodology for large space systems
[AD-A237864] N91-29214
AEROSPACE VEHICLES
Ablative heat shield studies for NASA Mars/Earth return entry vehicles
[AD-A238159] N91-29215
AEROTHERMODYNAMICS
Carina aerothermal test at Mach 8
[AD-A238561] N91-29218
An overview of aerothermal modeling
[NRC-32088] N91-29258
International Union of Theoretical and Applied Mechanics (IUTAM) Symposium on Aerothermodynamics in Combustors
[AD-A237943] N91-29516
AGING (MATERIALS)
Effect of alumina particle additions on the aging kinetics of 6061 aluminum matrix composites
[AD-A238052] N91-29246
Tensile properties and microstructure of Alloy 718 thermally aged to 50,000 h
[DE91-014099] N91-29299
Deformation and thermal fatigue in high temperature austenitic alloys
[DE91-014981] N91-29305
Fatigue resistant optical fibers
[AD-A237568] N91-29921
AGING (METALLURGY)
Effect of alumina particle additions on the aging kinetics of 6061 aluminum matrix composites
[AD-A238052] N91-29246
AGREEMENTS
Plan for a laser weapon verification research program
[DE90-012123] N91-29848
AIR
Computation of broadband, high-power electromagnetic pulse generation from an air gas avalanche switch
[DE91-015793] N91-29435
AIR FLOW
Translation of airfoil trailing edge noise article from Revue d'Acoustique
[AD-A237811] N91-29143
Progress toward synergistic hypermixing nozzles
[NASA-TM-105169] N91-29150
Development of an explosive vapor generator
[DE91-015700] N91-29386
Adiabatic two-phase flow frictional pressure drop. Part 2: A generalized method for data correlation
[DE91-014462] N91-29501
Control of flow over a backward facing step
[AD-A238638] N91-29521
AIR JETS
An experimental study of plunging liquid jet induced air carryunder and dispersion
[AD-A237757] N91-29511
AIR LAW
NAE participation in the United States FAA vertical separation study
[NAE-LTR-FR-105] N91-29160
AIR NAVIGATION
Evaluation of a pre-production version of Canadian Marconi CMA-786 GPS receiver
[NAE-LTR-FR-106] N91-29158
AIR POLLUTION
Overview of the technical implications of methanol and ethanol as highway motor vehicle fuels
[PB91-182881] N91-29385
NAE Twin Otter operations in the 1988 Eulerian model evaluation field study
[NAE-LTR-FR-107] N91-29651
Numerical modeling of turbulent dispersion around structures using a particle-in-cell method
[DE91-012035] N91-29652
Methods for determination of low-molecular weight carbonyl compounds in the ambient atmosphere
[DE91-015188] N91-29656
Theoretical studies of long-range transport of oxidants
[PB91-182360] N91-29661
Atmospheric methane concentrations: The NOAA/CMDL global cooperative flask sampling network, 1983 - 1988
[DE91-014942] N91-29664
A climatological model for risk computations incorporating site-specific dry deposition influences
[DE91-015536] N91-29667
Mesoscale modeling of precipitation scavenging by a cold-frontal squall line
[DE91-015534] N91-29695
AIR QUALITY
Theoretical studies of long-range transport of oxidants
[PB91-182360] N91-29661
Criteria for assessing the role of transported ozone/precursors in ozone nonattainment areas
[PB91-195958] N91-29662
AIR WATER INTERACTIONS
Seasonal air and water mass redistribution and its effect on satellite and polar motion N91-29202
Dependence of radar backscatter on the energetics of the air-sea interface
[AD-A237818] N91-29685
Modeling a rain-induced mixed layer
[AD-A238022] N91-29702
AIRBORNE EQUIPMENT
International aviation (selected articles)
[AD-A237232] N91-29142
NAE Twin Otter operations in FIFE 1989
[NASA-CR-188770] N91-29169
Wind and flux calculations of the NAE Twin Otter
[NAE-LTR-FR-109] N91-29189
A Doppler bin blanking CFAR processor for airborne radars
[AD-A237890] N91-29418
NAE Twin Otter operations in the 1988 Eulerian model evaluation field study
[NAE-LTR-FR-107] N91-29651
AIRCRAFT ACCIDENT INVESTIGATION
Aircraft accident reports: Brief format US civil and foreign aviation issue Number 1 of 1989 accidents
[PB90-916901] N91-29157
AIRCRAFT ACCIDENTS
Aircraft accident reports: Brief format US civil and foreign aviation issue Number 1 of 1989 accidents
[PB90-916901] N91-29157
AIRCRAFT CARRIERS
Control of flow over a backward facing step
[AD-A238638] N91-29521
AIRCRAFT CONSTRUCTION MATERIALS
Assessment of impact damage in toughened resin composites
[NAE-LTR-ST-1695] N91-29236
Composite transport wing technology development: Design development tests and advanced structural concepts
[NASA-CR-4177] N91-29253
Test results for composite specimens and elements containing joints and cutouts
[NASA-CR-178246] N91-29254
Probabilistic lifetime strength of aerospace materials via computational simulation
[NASA-CR-187178] N91-29629
AIRCRAFT CONTROL
A full function checkout test for the NAE full scale structural test control and data acquisition system
[NAE-LTR-ST-1696] N91-29166
A linear control design structure to maintain loop properties during limit operation in a multi-nozzle turbofan engine
[NASA-TM-105163] N91-29188
Flutter consideration of a crash-test aircraft
[DE91-015094] N91-29192
AIRCRAFT DESIGN
AEROWING - The software for aerodynamic analysis of a large aspect-ratio finite wing at low speeds
[NAL-PD-CF-9101] N91-29146
The design and construction of a shiplaunched VTOL unmanned air vehicle
[AD-A238053] N91-29173
Composite transport wing technology development: Design development tests and advanced structural concepts
[NASA-CR-4177] N91-29253
Test results for composite specimens and elements containing joints and cutouts
[NASA-CR-178246] N91-29254
AIRCRAFT ENGINES
International aviation (selected articles)
[AD-A237175] N91-29141
Generalized simplified analytic solution of optimum cycle parameters for land and aircraft gas turbine engines and its applications
[AD-A237414] N91-29182
Evaluation of aircraft turbine engine redesigns
[AD-A237599] N91-29184

AIRCRAFT EQUIPMENT
Evaluation of aircraft turbine engine redesigns
[AD-A237599] N91-29184
AIRCRAFT GUIDANCE
Flight evaluation of complex approaches in a Twin Otter aircraft using a microwave landing system
[NAE-LTR-FR-114] N91-29159
AIRCRAFT HAZARDS
Aircraft icing handbook, volume 1
[AD-A238039] N91-29154
Aircraft icing handbook, volume 2
[AD-A238040] N91-29155
Calculated performance of the NASA Lewis icing research tunnel
[NASA-TM-105173] N91-29199
Laboratory evaluation of portable and walk-through explosives vapour detectors
[NAE-LTR-UA-104] N91-29533
AIRCRAFT INSTRUMENTS
Commonwealth Advisory Aeronautical Research Council. First Canadian newsletter on systems, 1989
[NAE-LTR-FR-108] N91-29139
P-3 SAR calibration activity at Andros Island
[AD-A237357] N91-29412
AIRCRAFT LAUNCHING DEVICES
Aircraft operations from runways with inclined ramps (ski-jump)
[AD-A237265] N91-29171
AIRCRAFT MODELS
Subsonic aerodynamic coefficients of the SDM at angles of attack up to 90 deg
[NAE-LTH-UA-93] N91-29144
AIRCRAFT PERFORMANCE
Aircraft operations from runways with inclined ramps (ski-jump)
[AD-A237265] N91-29171
AIRCRAFT PILOTS
Performance of several different Naval aviator communities on a cognitive/psychomotor test battery: Pipeline comparison and prediciton
[AD-A238564] N91-29730
The effect of three levels of laser glare on the speed and accuracy of target location performance when viewing a briefly presented visual array
[AD-A238565] N91-29736
AIRCRAFT SAFETY
Environmental assessment for the FAA explosive detection system independent validation and verification program
[DE91-013190] N91-29152
Aircraft icing handbook, volume 2
[AD-A238040] N91-29155
Aircraft icing handbook, volume 3
[AD-A238041] N91-29156
AIRCRAFT STABILITY
International aviation (selected articles)
[AD-A237175] N91-29141
A new look at the Tobak-Schiff model of nonplanar aircraft dynamics
[NAE-LTR-UA-101] N91-29168
AIRCRAFT STRUCTURES
A full function checkout test for the NAE full scale structural test control and data acquisition system
[NAE-LTR-ST-1696] N91-29166
Assessment of impact damage in toughened resin composites
[NAE-LTR-ST-1695] N91-29236
Composite transport wing technology development: Design development tests and advanced structural concepts
[NASA-CR-4177] N91-29253
AIRDROPS
Stabilized square parachute
[AD-D014946] N91-29149
AIRFOILS
Translation of airfoil trailing edge noise article from Revue d'Acoustique
[AD-A237611] N91-29143
Performance of an airfoil at low Reynolds number
[NAL-PD-CF-9102] N91-29145
Experimental and analytical study of rippled trailing edge airfoils for compressor application
[AD-A237425] N91-29508
Horizontal axis wind turbine post stall airfoil characteristics synthesization
[DE91-002198] N91-29650
AIRGLOW
Planetary instrument definition and development program: 'Miniature Monochromatic Imager'
[NASA-CR-186550] N91-29219
AIRPORTS
Performance of asphalt concrete airport pavements during thaw weakening periods: A field study
[AD-A237441] N91-29198
ALGAE
Hydrogen productivity by photosynthetic water splitting
[DE90-012211] N91-29380
Stable isotope fractionation in photosynthesis: Analysis of autotrophic competence following transformation of the chloroplast genome of Chlamydomonas
[DE91-015792] N91-29713
ALGEBRA
The 't Hooft's solution for arbitrary semisimple Lie group
[DE91-617572] N91-29813
Algebraic approaches to nuclear structure
[DE91-015214] N91-29870
ALGORITHMS
Flight evaluation of complex approaches in a Twin Otter aircraft using a microwave landing system
[NAE-LTR-FR-114] N91-29159
Vision-based navigation and parallel computing
[AD-A238570] N91-29164
Compensation of distributed delays in integrated communication and control systems
[NASA-CR-187136] N91-29193
Coding for frequency hopped spread spectrum satellite communications
[ECE-89-1] N91-29398
Multi-sensor feature level fusion
[AD-A237106] N91-29411
Nonlinear computerized methodology. A: Angle of arrival estimation. B: Data modeling and identification
[AD-A237564] N91-29415
The APS radio frequency test stand control system
[DE91-015711] N91-29434
The design of a real-time adaptive filter development system
[AD-A237134] N91-29448
Cyclic voltammetric wave-shapes for microdisk electrodes: Coupled effects of solution resistance, double-layer capacitance, and finite electrochemical kinetics
[AD-A237505] N91-29455
Use of an extended Kalman filter
[AD-A238639] N91-29474
A finite element solver for 3-D compressible viscous flows
[NASA-CR-184175] N91-29488
Space-based Doppler lidar sampling strategies: Algorithm development and simulated observation experiments
[NASA-CR-184172] N91-29554
Motion planning for manipulators with excessive degrees of freedom N91-29592
NIKE2D: A nonlinear, implicit, two-dimensional finite element code for solid mechanics
[DE91-015734] N91-29634
Description of the Strategic High-Altitude Atmospheric Radiation Code (SHARC)
[AD-A237089] N91-29671
XTRAN: An atmospheric transmittance code based on XSCALE
[AD-A237624] N91-29674
A manual method for determining the fractional stability category
[AD-A237627] N91-29675
A fast, one pass algorithm to label objects and compute their features
[DE91-015441] N91-29747
An exact algorithm for funding undirected Hamiltonian cycles based on a two-matching problem relaxation
[AD-A237241] N91-29753
Primal-dual methods for linear programming
[AD-A237418] N91-29756
The use of searching algorithms for the minimization of multi-valued logic functions
[AD-A238018] N91-29763
Alignment of tomographic projections using an incomplete set of fiducial markers
[AD-A238536] N91-29772
Barrier methods for large-scale quadratic programming
[AD-A238554] N91-29773
A high-performance retargetable simulator for parallel architectures
[AD-A237354] N91-29779
Lazy task creation: A technique for increasing the granularity of parallel programs
[AD-A237477] N91-29781
Analog computation in neural systems: Architectures and complexity
[AD-A237856] N91-29785
Performance implications of synchronization support for parallel FORTRAN programs
[AD-A238493] N91-29790
Analytical and numerical methods; advanced computer concepts
[DE91-014526] N91-29795
Supernodal symbolic Cholesky factorization on a local-memory multiprocessor
[DE91-014967] N91-29796
The parallel BFGS method for unconstrained minimization
[DE91-015784] N91-29798
Theory and computer simulation of the interactional neural network
[NRC-30269] N91-29800
An expert system approach to global fault detection and isolation design
[AD-A238494] N91-29808
Piecework linear least-squares approximation planar curves including computer programs
[NRC-31069] N91-29811
Proceedings of the 1st Workshop on Proximity Graphs
[AD-A237250] N91-29818
Use of the implicit-finite-difference method to implement the parabolic equation model
[AD-A237437] N91-29819
A survey of nonlinear dynamics (chaos theory)
[AD-A237802] N91-29821
An exact two-matching based branch and bound algorithm for the symmetric traveling salesman problem
[AD-A237878] N91-29823
Acoustic background noise variation in Air Force platforms and its effect on noise removal algorithms
[AD-A238279] N91-29863
Development of optical subapertures
[AD-A237759] N91-29924
Towards a realistic plasma simulation code
[DE91-015698] N91-29967
ALIGNMENT
Adjustable magnification anamorphic beam expander
[DE91-014110] N91-29561
Alignment of tomographic projections using an incomplete set of fiducial markers
[AD-A238536] N91-29772
ALIPHATIC HYDROCARBONS
On-line monitoring of volatile organic species
[DE91-014655] N91-29655
ALLOYING
Properties of materials with a fine length scale: Mechanically alloyed metals and the high temperature superconductor Y1Ba2Cu3O7
[DE91-012538] N91-29975
ALLOYS
The interaction of hydrogen with metal alloys
[NASA-TP-3128] N91-29318
ALTERNATING CURRENT
The ac losses in type-2 superconductors
[DE91-015201] N91-29485
Ac susceptibility of superconductive thin films
[DE91-015273] N91-29993
ALTITUDE CONTROL
NAE participation in the United States FAA vertical separation study
[NAE-LTR-FR-105] N91-29160
ALUMINIDES
Intermetallics: Canadian perspective
[NAE-LTR-ST-1771] N91-29288
Mechanical properties of Fe3Al-based alloys
[DE91-015322] N91-29324
Development of nickel and iron aluminides and their applications
[DE91-015323] N91-29325
Environmental effects in niobium base alloys and other selected intermetallic compounds
[AD-A237535] N91-29658
The growth of ultrathin epitaxial intermetallic films
[AD-A237798] N91-30011
ALUMINUM
Postshock spectral radiance measurements in nickel and nickel/aluminum powders
[DE91-014695] N91-29302
High-energy backscattered electron imaging of voids in aluminum metallizations
[DE91-014895] N91-29303
Long-term testing and evaluation of cathode components in a commercial aluminum cell, volume 1
[DE90-010896] N91-29436
The laser ablation of aluminum at 193, 248, and 351 nm
[AD-A237574] N91-29569
Fundamental studies in dynamic plasticity
[AD-A237114] N91-29621
Explosively driven missile trajectory parameters for various fragment materials and velocities
[DE91-014330] N91-29631
Plasma and electrical diagnostics for Procyon experiments
[DE91-014736] N91-29952
TEM characterization of grain boundaries in mixed bicrystal films of aluminum
[DE91-016267] N91-30038

ALUMINUM ALLOYS
High temperature mass spectrometric study of the thermodynamics of liquid nickel-aluminium alloys at 2000 K
[MRL-TR-91-15] N91-29290
Biofouling and corrosion fouling of plain and enhanced aluminum surfaces
[DE91-014464] N91-29300
Lightweight disk alloy development
[AD-A237064] N91-29309
An investigation of the as-quenched and early aging characteristics of a Al - 4.1 wt. percent Li binary alloy by x ray diffraction
[AD-A237598] N91-29311
Development of the microstructure based stochastic life prediction models
[AD-A237768] N91-29312
Mechanical properties of Fe3Al-based alloys
[DE91-015322] N91-29324
An evaluation of nickel-aluminum coatings fabricated with the plasma-spray process
[DE91-013208] N91-29328
Measurements of retractable gas-cooled 6061 aluminum electrical leads operating in a vacuum
[DE91-014617] N91-29444
ALUMINUM ARSENIDES
Dielectric function of semiconductor superlattice
[DE91-617788] N91-29976
ALUMINUM GALLIUM ARSENIDES
The embedded electron-gas boundary: A new standard problem in surface physics
[AD-A238152] N91-30014
An optically activated modulator and GaAs-GaAlAs compound semiconductor channel waveguide
[AD-A238642] N91-30023
ALUMINUM NITRIDES
Quantitative analysis of oxygen segregation on inversion domain boundaries in aluminum nitride
[DE91-010869] N91-29971
Pseudomorphic semiconducting heterostructures from combinations of AlN, GaN and seleced SiC polytypes: Theoretical advancement and its coordination with experimental studies of nucleation, growth, characterizaiton and device development
[AD-A238520] N91-30020
Growth, nitrogen vacancy reduction and solid solution formation in cubic GaN thin films and the subsequent fabrication of superlattice structures using AlN and InN
[AD-A238521] N91-30021
ALUMINUM OXIDES
Ablative heat shield studies for NASA Mars/Earth return entry vehicles
[AD-A238159] N91-29215
Slag and thermal environment of a spinning rocket motor
[AD-A238557] N91-29227
An analysis of the wear behavior of SiC whisker reinforced alumina from 25 to 1200 C
[NASA-TM-104489] N91-29235
Effect of alumina particle additions on the aging kinetics of 6061 aluminum matrix composites
[AD-A238052] N91-29246
Deactivation by carbon of iron catalysts for indirect liquefaction
[DE91-011276] N91-29285
Ceramic fabrication R/D
[DE91-014758] N91-29335
High strain rate characterization of ceramics in shear
[AD-A238319] N91-29365
Corrosion behavior of continuous-filament-wound ceramic composite tubes
[DE91-014959] N91-29370
Advances in the drained shaping of ceramics
[DE91-015429] N91-29376
Materials research for sodium engine development
[DE91-015715] N91-29378
Liquid honing evaluation
[DE91-015749] N91-29393
AMBIENT TEMPERATURE
Acoustic tomographic estimate of ocean advective heat flux: A numerical assessment in the Norwegian Sea
[AD-A237100] N91-29698
AMINES
Solvent-dependent redox thermodynamics of metal amine complexes. The delineation of specific solvation effects
[AD-A237503] N91-29272
Studies of polymers for shock absorption applications
[AD-A237925] N91-29358
An elevated temperature titration calorimeter
[DE91-015765] N91-29548
AMMONIA
Electrocatalytic study of ammonia synthesis and methane dimerization in high temperature solid electrolyte cells
[DE90-012496] N91-29437
Analysis of condensation and evaporation of ammonia/water mixtures in matrix heat-exchangers
[DE91-014461] N91-29500
Study of elementary reactions and energy transfer processes involving the NH and CN free radicals
[AD-A238461] N91-29889
AMORPHOUS MATERIALS
Simulation of the structure of dense, amorphous bisphenol-A polycarbonate
[AD-A237222] N91-29270
Molecular dynamics simulation of the effect of interfaces in melting and solid-state amorphization
[DE91-015550] N91-29284
Quasi-static modeling of chain-dynamics in the amorphous glassy polycarbonate of 4,4'-isopropyledenediphenol
[AD-A237289] N91-29343
An atomistic model of the amorphous glassy polycarbonate of 4,4'-isopropylidenediphenol
[AD-A237291] N91-29345
ANAEROBES
Microbiology and physiology of anaerobic fermentations of cellulose
[DE91-015239] N91-29712
ANALOG CIRCUITS
An alternative to operational amplifiers
[AD-A237439] N91-29453
VLSI circuit techniques and technologies for ultrahigh speed data conversion interfaces
[AD-A238115] N91-29468
Physical concepts and modeling procedures for picosecond and subpicosecond distributed circuits
[AD-A238592] N91-29472
Design of a stabilized, dc-powered analog laser diode driver
[AD-A238596] N91-29577
Analog design verification with PSpice and MICRO-CAP 3
[AD-A237922] N91-29762
High temperature superconductor analog electronics for millimeter-wavelength communications
[NASA-TM-105184] N91-29982
ANALOG COMPUTERS
Analog computation in neural systems: Architectures and complexity
[AD-A237856] N91-29785
ANALOG DATA
Analog computation in neural systems: Architectures and complexity
[AD-A237856] N91-29785
Design and hardware implementation of neural systems
[AD-A237703] N91-29804
ANALOG TO DIGITAL CONVERTERS
VLSI circuit techniques and technologies for ultrahigh speed data conversion interfaces
[AD-A238115] N91-29468
ANALYSIS (MATHEMATICS)
Generalized simplified analytic solution of optimum cycle parameters for land and aircraft gas turbine engines and its applications
[AD-A237414] N91-29182
ANGLE OF ATTACK
Subsonic aerodynamic coefficients of the SDM at angles of attack up to 90 deg
[NAE-LTR-UA-93] N91-29144
ANGULAR DISTRIBUTION
A dihedral corner reflector model for full polarization calibration of RCS measurements
[DE91-013572] N91-29402
ANIMALS
Biological interactions of extremely-low-frequency electric and magnetic fields
[DE90-011927] N91-29709
ANIONS
Electrochemical contact adsorption site changes driven by field and charge fact and theory
[AD-A237127] N91-29269
Mechanism of anionic ring-opening polymerization of silacyclopent 3-enes
[AD-A237538] N91-29353
ANISOTROPY
Effects of anisotropy on dynamic tensile behavior
[DE91-014748] N91-29632
Responsivity uniformity enhancements for Backside-Illuminated Charge-Coupled Devices (BICCDs) by excimer laser-assisted etching
[AD-A237435] N91-29997
Anisotropic spin susceptibility of the (Y,Ca),(Ba, La)2Cu4O8 system
[DE91-014593] N91-30032
ANNEALING
Characteristics of autoclave and in-reactor nodular corrosion of Zircaloys
[DE91-013600] N91-29294
Annealing effects on the microstructure of titanium electrical contacts on diamond films
[DE91-010150] N91-29327
The 23rd Optoelectronic Workshop: Optical System Assessment for Design and Simulated Annealing
[AD-A238588] N91-29932
On the role of crystal defects as sources of resonator frequency instability
[AD-A238505] N91-30018
ANNUAL VARIATIONS
Seasonal air and water mass redistribution and its effect on satellite and polar motion N91-29202
Fitting seasonal averages with a continuous function
[AD-A238300] N91-29704
An automated software system for updating digital terrain databases from all-source imagery, phase 1
[AD-A237105] N91-29748
ANODES
Low-jitter, high-voltage, infrared, laser-triggered, vacuum switch
[DE91-014602] N91-29562
ANODIC COATINGS
Electrodeposition of high temperature superconductors
[AD-A238227] N91-29469
ANTARCTIC REGIONS
Hamiltonian 3-D ray tracing in the oceanic waveguide on the ellipsoidal earth
[AD-A237458] N91-29700
ANTENNA ARRAYS
High temperature superconductor analog electronics for millimeter-wavelength communications
[NASA-TM-105184] N91-29982
ANTENNA DESIGN
ICRF edge modeling
[DE91-014401] N91-29403
A new system for measurement of low frequency radio transmitting antenna parameters in near real time
[AD-A238555] N91-29429
ANTENNA RADIATION PATTERNS
Range-only multistatic radar system
[AD-D011645] N91-29399
ANTENNAS
ICRF edge modeling
[DE91-014401] N91-29403
ANTHRACENE
A theoretical and experimental study of unimolecular and biomolecular radical hydrogen transfer reactions
[DE91-012607] N91-29261
ANTIHISTAMINICS
Development and evaluation of a human performance assessment battery
[AD-A237391] N91-29724
ANTIMATTER
The ASTROMAG superconducting magnet facility configured for a free flying satellite
[DE91-014710] N91-29204
ANTIMISSILE DEFENSE
The functional dependence of trajectory dispersion on initial condition errors
[DE91-014661] N91-29151
On satellite constellation selection
[DE91-014562] N91-29851
A framework for understanding the strategic defense initiatives' software debates
[AD-A237193] N91-29852
Report to the Congress on the Strategic Defense Initiative, 1991
[AD-A237658] N91-29853
Strategic defense initiative: Need to examine concurrency in development of brilliant pebbles
[AD-A238292] N91-29854
Multitarget tracking using optical processing
[AD-A237107] N91-29918
ANTIMONY ALLOYS
Lead-free solders for electronics applications: Wetting analysis
[DE91-014900] N91-29320
ANTIREFLECTION COATINGS
Effects of interfacial modification on diamond film adhesion
[AD-A237750] N91-29354
Preparation of damage resistant optical coatings on flat substrates
[DE91-013588] N91-29916
Optical and environmentally protective coatings for Potassium Dihydrogen Phosphate (KDP) harmonic converter crystals
[DE91-015296] N91-30034
APERTURES
A slit aperture for the Monitoring X ray Experiment (MOXE)
[DE91-013317] N91-29538
Development of optical subapertures
[AD-A237759] N91-29924

APPLICATIONS PROGRAMS (COMPUTERS)
AEROWING - The software for aerodynamic analysis of a large aspect-ratio finite wing at low speeds
| NAL-PD-CF-9101 | N91-29146
Distance measures for speech recognition
| NAE-AN-57 | N91-29394
Elastic-plastic constitutive relations at large strain
| DE91-013195 | N91-29612
Performance implications of synchronization support for parallel FORTRAN programs
| AD-A238493 | N91-29790
APPROACH CONTROL
Flight evaluation of complex approaches in a Twin Otter aircraft using a microwave landing system
| NAE-LTR-FR-114 | N91-29159
APPROXIMATION
Exact and approximate solutions to the oblique shock equations for real-time applications
| NASA-CR-187173 | N91-29147
Stochastic simulation techniques for partition function approximation of Gibbs random field images
| AD-A238611 | N91-29775
Approximation from shift-invariant surfaces of L2(IRd)
| AD-A238165 | N91-29826
Least-squares learning and approximation of posterior probabilities on classification problems by neural network models
| AD-A237140 | N91-29833
AQUEOUS SOLUTIONS
Mechanistic investigation of nanometer-scale/lithography at liquid-covered graphite surfaces
| AD-A237085 | N91-29337
ARC JET ENGINES
Ablative heat shield studies for NASA Mars/Earth return entry vehicles
| AD-A238159 | N91-29215
Arcjet thermal characteristics
| NASA-TM-105156 | N91-29231
ARCHITECTURE (COMPUTERS)
The design of a real-time adaptive filter development system
| AD-A237134 | N91-29448
Video frame store: An advanced solid state recorder
| DE91-015709 | N91-29549
Topographic map reading
| AD-A238026 | N91-29640
Studies in neural networks
| AD-A237452 | N91-29717
APRIL: A processor architecture for multiprocessing
| AD-A237476 | N91-29739
A fast, one pass algorithm to label objects and compute their features
| DE91-015441 | N91-29747
NW lab for integrated systems
| AD-A237118 | N91-29749
A common interface real-time multiprocessor operating system for embedded systems
| AD-A238445 | N91-29770
Verification of the FtCayuga fault-tolerant microprocessor system. Volume 1: A case study in theorem prover-based verification
| NASA-CR-4381 | N91-29778
A high-performance retargetable simulator for parallel architectures
| AD-A237354 | N91-29779
Asynchronous design for parallel processing architectures
| AD-A237696 | N91-29783
The MIT Alewife machine: A large-scale distributed-memory multiprocessor
| AD-A237705 | N91-29784
Analog computation in neural systems: Architectures and complexity
| AD-A237856 | N91-29785
Expert systems on multiprocessor architectures. Volume 1: Summary
| AD-A238046 | N91-29786
Expert systems on multiprocessor architectures. Volume 2: Technical reports
| AD-A238047 | N91-29787
Expert systems on multiprocessor architectures, volume 3
| AD-A238048 | N91-29788
Expert systems on multiprocessor architectures, volume 4
| AD-A238049 | N91-29789
Performance implications of synchronization support for parallel FORTRAN programs
| AD-A238493 | N91-29790
Using the Harmony operating system: Release 3.0
| ERA-377 | N91-29799
Design and hardware implementation of neural systems
| AD-A237703 | N91-29804
Compilation and representation of intelligent electronic documents: An architecture for referenceability
| DE91-012635 | N91-30045
ARCTIC REGIONS
An AVHRR data set for the arctic leads ARI
| AD-A237221 | N91-29637
Performance report of the Wind Research Lab.
| AD-A238575 | N91-29691
ARGON
Microstructural and strength stability of CVD SiC fibers in argon environment
| NASA-TM-103772 | N91-29250
ARMED FORCES (UNITED STATES)
Micro SAINT modeling of physiological and human performance in the heat
| AD-A238659 | N91-29719
ARMOR
Ceramic fabrication R/D
| DE91-014758 | N91-29335
High strain rate characterization of ceramics in shear
| AD-A238319 | N91-29365
ARRAYS
Microtube strip heat exchanger
| DE91-015223 | N91-29529
Counterdoped high temperature, silicon array infrared detector
| AD-A238483 | N91-29546
ARTIFICIAL INTELLIGENCE
Workshop on Automation and Robotics: Proceedings
| DE91-015175 | N91-29801
User's guide to the (NCARAI) artificial intelligence technical library
| AD-A237270 | N91-29802
ARTIFICIAL SATELLITES
The ASTROMAG superconducting magnet facility configured for a free flying satellite
| DE91-014710 | N91-29204
The optimal location of GEODSS sensors in Canada
| AD-A238444 | N91-29216
NRL review, 1991
| AD-A238665 | N91-29857
ASPECT RATIO
AEROWING - The software for aerodynamic analysis of a large aspect-ratio finite wing at low speeds
| NAL-PD-CF-9101 | N91-29146
Effects of 1, 2, 3, and 4 Hz imposed bulk flow oscillations on transition in a straight channel with 40 to 1 aspect ratio
| AD-A237988 | N91-29517
ASPHALT
Performance of asphalt concrete airport pavements during thaw weakening periods: A field study
| AD-A237441 | N91-29198
ASSAYING
The role of microorganisms in marine corrosion
| AD-A237062 | N91-29308
ASSEMBLING
Universal ground adapter assembly
| AD-D014908 | N91-29439
ASSESSMENTS
Assessment team report on flight-critical systems research at NASA Langley Research Center
| NASA-CR-181850 | N91-29176
ASTRO MISSIONS (STS)
A simulation of the instrument pointing system for the Astro-1 mission
| NASA-TM-103547 | N91-30061
ASTRONOMICAL CATALOGS
Lowell proper motion survey: Southern Hemisphere (Giclas, Burnham, and Thomas 1978). Documentation for the machine-readable version
| NASA-TM-105069 | N91-30060
ASTRONOMICAL SATELLITES
A slit aperture for the Monitoring X ray Experiment (MOXE)
| DE91-013317 | N91-29538
Diffraction-limited imaging of satellites using bispectral speckle interferometry
| DE91-015745 | N91-30062
ASTROPHYSICS
The ASTROMAG superconducting magnet facility configured for a free flying satellite
| DE91-014710 | N91-29204
Nuclear theory progress report
| DE91-013908 | N91-29866
A research program in experimental and theoretical high energy physics
| DE91-014728 | N91-29907
The relationship between the density wave, molecular gas and star formation in M51 N91-30064
ASYMPTOTIC SERIES
The asymptotic distributions of autoregressive coefficients
| AD-A238538 | N91-29831
On the analysis of grouped survival data using cumulative occurrence/exposure rates
| AD-A238219 | N91-29838
ATLANTIC OCEAN
Performance report of the Wind Research Lab.
| AD-A238575 | N91-29691
Acoustic tomographic estimate of ocean advective heat flux: A numerical assessment in the Norwegian Sea
| AD-A237100 | N91-29698
Oceanographic data report Number 7: Data from the Delaware Estuary SCENIC cruises, April 1986 - September 1988
| PB91-183582 | N91-29706
ATMOSPHERIC BOUNDARY LAYER
Three-dimensional mapping of atmospheric boundary layer structure and winds with a high performance lidar
| AD-A238098 | N91-29678
ATMOSPHERIC CHEMISTRY
NAE Twin Otter operations in FIFE 1989
| NASA-CR-188770 | N91-29169
Wind and flux calculations of the NAE Twin Otter
| NAE-LTR-FR-109 | N91-29189
Methods for determination of low-molecular weight carbonyl compounds in the ambient atmosphere
| DE91-015188 | N91-29656
Atmospheric methane concentrations: The NOAA/CMDL global cooperative flask sampling network, 1983 - 1988
| DE91-014942 | N91-29664
ATMOSPHERIC CIRCULATION
Wind and flux calculations of the NAE Twin Otter
| NAE-LTR-FR-109 | N91-29189
NAE Twin Otter operations in the 1988 Eulerian model evaluation field study
| NAE-LTR-FR-107 | N91-29651
Numerical modeling of turbulent dispersion around structures using a particle-in-cell method
| DE91-012035 | N91-29652
Criteria for assessing the role of transported ozone/precursors in ozone nonattainment areas
| PB91-195958 | N91-29662
A climatological model for risk computations incorporating site-specific dry deposition influences
| DE91-015536 | N91-29667
On the application of edge wave theory to terrain-bounded cold surges: A numerical study N91-29670
Tropical cyclone motion in the northwest Pacific Ocean, phase 1
| AD-A237455 | N91-29683
ATMOSPHERIC COMPOSITION
Wind and flux calculations of the NAE Twin Otter
| NAE-LTR-FR-109 | N91-29189
Methods for determination of low-molecular weight carbonyl compounds in the ambient atmosphere
| DE91-015188 | N91-29656
Protecting the ozone shield: A new public policy
| AD-A237640 | N91-29659
Criteria for assessing the role of transported ozone/precursors in ozone nonattainment areas
| PB91-195958 | N91-29662
Effects of solar heating by aerosols and trace gases on the temperature structure constant
| AD-A237675 | N91-29677
DNA optical support program summary for 1989
| AD-A238397 | N91-29679
Mesoscale modeling of precipitation scavenging by a cold-frontal squall line
| DE91-015534 | N91-29695
ATMOSPHERIC EFFECTS
DNA optical support program summary for 1989
| AD-A238397 | N91-29679
ATMOSPHERIC ENTRY
Ablative heat shield studies for NASA Mars/Earth return entry vehicles
| AD-A238159 | N91-29215
ATMOSPHERIC GENERAL CIRCULATION MODELS
Space-based Doppler lidar sampling strategies: Algorithm development and simulated observation experiments
| NASA-CR-184172 | N91-29554
ATMOSPHERIC MODELS
Atmospheric dispersion models for dense gas releases
| DE91-015144 | N91-29654
Atmospheric methane concentrations: The NOAA/CMDL global cooperative flask sampling network, 1983 - 1988
| DE91-014942 | N91-29664
A climatological model for risk computations incorporating site-specific dry deposition influences
| DE91-015536 | N91-29667
On the application of edge wave theory to terrain-bounded cold surges: A numerical study N91-29670

Description of the Strategic High-Altitude Atmospheric Radiation Code (SHARC)
[AD-A237089] N91-29671
Worldwide maritime infrared atmospheric transmittance data
[AD-A237292] N91-29672
Tropical cyclone motion in the northwest Pacific Ocean, phase 1
[AD-A237455] N91-29683
Dependence of radar backscatter on the energetics of the air-sea interface
[AD-A237818] N91-29685
Mesoscale modeling of precipitation scavenging by a cold-frontal squall line
[DE91-015534] N91-29695
Parameterizations of microphysical processes for simulation of regional-scale clouds
[DE91-015554] N91-29696
Parallelizing the spectral transform method
[DE91-013969] N91-29815

ATMOSPHERIC OPTICS
Worldwide maritime infrared atmospheric transmittance data
[AD-A237292] N91-29672
DNA optical support program summary for 1989
[AD-A238397] N91-29679

ATMOSPHERIC PHYSICS
Aircraft icing handbook, volume 1
[AD-A238039] N91-29154
Aircraft icing handbook, volume 2
[AD-A238040] N91-29155
Aircraft icing handbook, volume 3
[AD-A238041] N91-29156
Cloud data collection, composites and analysis for Whole-Sky Imager (WSI) studies
[AD-A238531] N91-29690

ATMOSPHERIC PRESSURE
Seasonal air and water mass redistribution and its effect on satellite and polar motion N91-29202
An investigation of the ERICA IOP-2 cyclone using the NORAPS model
[AD-A237683] N91-29684

ATMOSPHERIC RADIATION
Description of the Strategic High-Altitude Atmospheric Radiation Code (SHARC)
[AD-A237089] N91-29671
Analysis of the ultraviolet emissions of nitric oxide from mid-latitude rocket observations
[AD-A237340] N91-29673

ATMOSPHERIC SOUNDING
Analysis of the ultraviolet emissions of nitric oxide from mid-latitude rocket observations
[AD-A237340] N91-29673

ATMOSPHERIC TEMPERATURE
Worldwide maritime infrared atmospheric transmittance data
[AD-A237292] N91-29672
Effects of solar heating by aerosols and trace gases on the temperature structure constant
[AD-A237675] N91-29677
TOVS satellite soundings of the ERICA IOP-2 cyclone
[AD-A237998] N91-29686
DAR(3)E-1 evaluation: Assessment of weather forecasts made using the DAR(3)E-1 workstation
[PB91-181701] N91-29693

ATMOSPHERIC TURBULENCE
A simulation evaluation of a four-engine jet transport using engine thrust modulation for flightpath control
[NASA-TM-4324] N91-29194
Equatorial entrainment zone simulations
[AD-A237234] N91-29657

ATOMIC ENERGY LEVELS
The atomic strain tensor
[AD-A237287] N91-29877

ATOMIC PHYSICS
The Research Laboratory of Electronics
[AD-A237670] N91-29458
Atomic physics in strong fields
[DE91-015393] N91-29872
Theoretical high energy physics
[DE91-013639] N91-29905
Atomic layer epitaxy group IV materials: Surface processes, thin films, devices and their characterization
[AD-A238506] N91-30019

ATOMIC SPECTRA
Analyzing photographically recorded atomic emission spectra using an automated densitometer
[DE91-015368] N91-29871

ATOMIC STRUCTURE
Structure and stability of underpotentially depositied layers on Au(111) studied by optical second harmonic generation
[AD-A237087] N91-29268
Requirements for the observation of Fermi surfaces in disordered alloys
[DE91-014578] N91-29321
First principles simulations of metallic alloys and liquids
[DE91-015171] N91-29323
Quasi-static modeling of chain-dynamics in the amorphous glassy polycarbonate of 4,4'-isopropyledenediphenol
[AD-A237289] N91-29343
An atomistic model of the amorphous glassy polycarbonate of 4,4'-isopropylidenediphenol
[AD-A237291] N91-29345
Effects of doping on hybridization gapped materials
[DE91-014611] N91-29477
Quantitative interpretation of auger lineshapes and electron/photon stimulated desorption
[AD-A237138] N91-29874
The atomic strain tensor
[AD-A237287] N91-29877
Laser-atom interaction at high intensities
[AD-A238231] N91-29887
Nonlinear optical interactions involving the real Gaussian field
[DE91-015052] N91-29936
High resolution electron microscopy of grain boundaries
[DE91-010593] N91-29970
Photoemission and electronic structure studies of YBa2Cu3O(x)
[DE91-014469] N91-29979
Surface structure and surface order
[AD-A237466] N91-30001
Effect of hydrogen on the electronic structure of a grain boundary in iron
[AD-A237499] N91-30002
Device processing of II-VI semiconductor films and quantum well structures
[AD-A238460] N91-30017

ATOMIZING
A methodology for inhibiting the formation of pollutants in diesel engines
[DE90-011615] N91-29584

ATTENUATORS
Analysis of FIN line feasibility for W-band attenuator applications
[AD-A237271] N91-29450

AUDIO FREQUENCIES
Auditory processing of complex sounds across frequency channels
[AD-A238023] N91-29862

AUDITORY PERCEPTION
Institute for the Study of Human Capabilities: Summary descriptions of research for the period December 1989 through September 1990
[AD-A237767] N91-29726

AUDITORY SIGNALS
Auditory processing of complex sounds across frequency channels
[AD-A238023] N91-29862

AUGER EFFECT
Photoelectron and photoionization pumping of XUV lasers by laser-produced plasmas N91-29558

AUGER SPECTROSCOPY
A study of copper segregation in sputtered Al-Si-Cu films using Auger electron spectroscopy
[AD-A238130] N91-29316

AURORAS
Planetary instrument definition and development program: 'Miniature Monochromatic Imager'
[NASA-CR-186550] N91-29219

AUSTENITIC STAINLESS STEELS
Mechanisms of transformation toughening
[DE91-013151] N91-29293
Deformation and thermal fatigue in high temperature austenitic alloys
[DE91-014981] N91-29305

AUTOCLAVES
Characteristics of autoclave and in-reactor nodular corrosion of Zircaloys
[DE91-013600] N91-29294

AUTOCORRELATION
The asymptotic distributions of autoregressive coefficients
[AD-A238538] N91-29831

AUTOMATIC CONTROL
Multi-sensor feature level fusion
[AD-A237106] N91-29411
Theory and computer simulation of the interactional neural network
[NRC-30269] N91-29800
Workshop on Automation and Robotics: Proceedings
[DE91-015175] N91-29801
Research and development at ORNL/CESAR towards cooperating robotic systems for hazardous environments
[DE91-015638] N91-29810

AUTOMOBILE ENGINES
Conversion of methanol-fueled 16-valve, 4-cylinder engine to operation on gaseous 2H2/CO fuel
[PB91-195941] N91-29602

AUTONOMOUS NAVIGATION
Research and development at ORNL/CESAR towards cooperating robotic systems for hazardous environments
[DE91-015638] N91-29810

AUTOREGRESSIVE PROCESSES
The asymptotic distributions of autoregressive coefficients
[AD-A238538] N91-29831

AUXILIARY PROPULSION
Performance and optimization of a derated ion thruster for auxiliary propulsion
[NASA-TM-105144] N91-29229

AVIONICS
Commonwealth Advisory Aeronautical Research Council. First Canadian newsletter on systems, 1989
[NAE-LTR-FR-108] N91-29139

AXIAL FLOW
Experimental study of gas kinetics of a fast-axial flow kilowatt CO2 laser
[AD-A237178] N91-29565

AXIAL STRESS
High strain rate characterization of ceramics in shear
[AD-A238319] N91-29365
Uniaxial stress study of the quantum transitions in a strained layer (001) In0.2Ga0.8As/GaAs single quantum well
[DE91-014990] N91-30033

B

BACKGROUND NOISE
Acoustic background noise variation in Air Force platforms and its effect on noise removal algorithms
[AD-A238279] N91-29863

BACKGROUND RADIATION
ASAT monitoring project at LLNL
[DE91-013247] N91-29850
Dark matter in the universe
[DE91-014863] N91-30065

BACKSCATTERING
High-energy backscattered electron imaging of voids in aluminum metallizations
[DE91-014895] N91-29303
A dihedral corner reflector model for full polarization calibration of RCS measurements
[DE91-013572] N91-29402
Dependence of radar backscatter on the energetics of the air-sea interface
[AD-A237818] N91-29685
Single-scatter Monte Carlo compared to condensed history results for low energy electrons
[DE91-015176] N91-29869

BACTERIA
The role of microorganisms in marine corrosion
[AD-A237062] N91-29308
Microbiology and physiology of anaerobic fermentations of cellulose
[DE91-015239] N91-29712

BALLISTIC MISSILES
SDI performance and START constraints: Modeling phase-1 defense engagements
[DE91-013305] N91-29849

BALLISTICS
Randomization procedures applied to analysis of ballistic data
[AD-A238389] N91-30050

BAND STRUCTURE OF SOLIDS
Orbitals, correlation, valencies in high-T(sub c) superconductors
[DE91-618099] N91-29977

BANDPASS FILTERS
Development of optical subapertures
[AD-A237759] N91-29924

BARIUM OXIDES
Photoemission and electronic structure studies of YBa2Cu3O(x)
[DE91-014469] N91-29979
High temperature Knudsen effusion-mass spectrometric studies of the Y-Ba-Cu-O system
[NIAR-91-23] N91-29981
Photoemission measurement of Fermi surface, band dispersion, and quasiparticle lifetime in YBa2Cu3O6.9
[DE91-015194] N91-29989
Synthesis and superconductivity in Ba(1-x)K(x)BiO3
[DE91-015254] N91-29992

BAROCLINIC INSTABILITY
On the application of edge wave theory to terrain-bounded cold surges: A numerical study N91-29670

BATCH PROCESSING
Model filled polymers 9: Synthesis of uniformly crosslinked polystyrene microbeads
[AD-A237472] N91-29352
BEADS
Model filled polymers 8: Synthesis of crosslinked polymeric beads by seed polymerization
[AD-A237429] N91-29349
Model filled polymer 7: Flow behavior of polymers containing monodisperse crosslinked polymeric beads
[AD-A237430] N91-29350
BEAM CURRENTS
REX: A 5-MV pulsed-power source for driving high-brightness electron beam diodes
[DE91-014604] N91-29443
Control of energy sweep and transverse beam motion in induction linacs
[DE91-015177] N91-29911
Collisional processes of interest in MFE plasma research
[DE91-013023] N91-29943
BEAM INJECTION
REX: A 5-MV pulsed-power source for driving high-brightness electron beam diodes
[DE91-014604] N91-29443
BEAM INTERACTIONS
Visualization of wake fields
[DE91-015130] N91-29408
Electron capture in very low energy collisions of multicharged ions with H and D in merged beams
[DE91-015617] N91-29909
High energy physics: Experimental, Theoretical, and Phenomenology Institute
[DE91-015737] N91-29912
BEAM NEUTRALIZATION
Measurement of longitudinal emittance growth using a laser-induced neutralization method
[DE91-013500] N91-29560
BEAM SPLITTERS
An improved method of investigation of compressor blade fit using holographic interferometry
[AD-A238182] N91-29185
Measurement of longitudinal emittance growth using a laser-induced neutralization method
[DE91-013500] N91-29560
A real time collimation sensor using a shear plate and a spatial light modulator
[DE90-011362] N91-29914
Optical soliton source
[AD-D014942] N91-29933
BEAMS (RADIATION)
An improved method of investigation of compressor blade fit using holographic interferometry
[AD-A238182] N91-29185
Study of particle correlations in high energy S + Pb and Pb + Pb interactions with a magnetic-interferometric-emulsion-chamber
[DE91-014355] N91-29897
BEAMS (SUPPORTS)
A layered beam theory for single lap joints
[AD-A237324] N91-29607
Hierarchic extensions in the static and dynamic analysis of elastic beams N91-29613
Modeling and response analysis of thin-walled beam structures constructed of advanced composite materials N91-29615
BEARING (DIRECTION)
Use of an extended Kalman filter
[AD-A238639] N91-29474
BEARINGS
Bearing tester data compilation analysis, and reporting and bearing math modeling
[NASA-CR-178883] N91-29603
BENDING MOMENTS
A full function checkout test for the NAE full scale structural test control and data acquisition system
[NAE-LTR-ST-1696] N91-29166
BENDING THEORY
A layered beam theory for single lap joints
[AD-A237324] N91-29607
BENDING VIBRATION
Structures, properties, and dynamics of metal clusters from infrared laser spectroscopy
[AD-A237669] N91-29570
BENZENE
A theoretical and experimental study of unimolecular and biomolecular radical hydrogen transfer reactions
[DE91-012607] N91-29261
BETA PARTICLES
Tritium-field betacells
[DE91-014666] N91-29910
BIBLIOGRAPHIES
JPRS report: Science and technology. USSR: Materials science
[JPRS-UMS-91-001] N91-29291
Publications of the Executive Office of the President, January 20, 1989 - March 31, 1991
[PB91-156828] N91-30056
BICRYSTALS
TEM characterization of grain boundaries in mixed bicrystal films of aluminum
[DE91-016267] N91-30038
BIG BANG COSMOLOGY
Dark matter in the universe
[DE91-014863] N91-30065
BINARY ALLOYS
Postirradiation deformation of ferritic Fe-Cr binary alloys
[DE91-014856] N91-29295
An investigation of the as-quenched and early aging characteristics of a Al - 4.1 wt. percent Li binary alloy by x ray diffraction
[AD-A237598] N91-29311
Properties of materials with a fine length scale: Mechanically alloyed metals and the high temperature superconductor Y1Ba2Cu3O7
[DE91-012538] N91-29975
BINARY SYSTEMS (MATERIALS)
Effect of a free surface on stress distribution in a bimaterial composite
[PB91-185116] N91-29251
Calculation of intra-rare Earth binary phase diagrams
[DE91-014950] N91-29267
BIOCHEMISTRY
Microbiology and physiology of anaerobic fermentations of cellulose
[DE91-015239] N91-29712
NRL review, 1991
[AD-A238665] N91-29857
BIODEGRADATION
The role of microorganisms in marine corrosion
[AD-A237062] N91-29308
BIOELECTRICITY
Electrified microscopic and conventional interfaces between two immiscible electrolyte solutions
[AD-A237695] N91-29459
BIOGEOCHEMISTRY
Subsurface Science Program
[DE91-015480] N91-29665
BIOLOGICAL EFFECTS
Biofouling and corrosion fouling of plain and enhanced aluminum surfaces
[DE91-014464] N91-29300
BIOLOGICAL MODELS (MATHEMATICS)
Software development of the cochlear filter and eighth-nerve model
[AD-A237454] N91-29757
BIOLOGY
Oceanographic data report Number 7: Data from the Delaware Estuary SCENIC cruises, April 1986 - September 1988
[PB91-183582] N91-29706
BIOMAGNETISM
Biological interactions of extremely-low-frequency electric and magnetic fields
[DE90-011927] N91-29709
BIOPHYSICS
Data acquisition system for collecting biophysical and physiological data
[AD-A237654] N91-29710
BISMUTH OXIDES
Synthesis and superconductivity in Ba(1-x)K(x)BiO3
[DE91-015254] N91-29992
Consolidation and plasticity of Bi-Sr-Ca-Cu-O superconductors
[DE91-015544] N91-30028
BISPHENOLS
Conformational characteristics of the polycarbonate 4,4'-isopropylidenediphenol
[AD-A237334] N91-29347
BISTABLE CIRCUITS
Theoretical, experimental, and numerical studies on hybrid acoustooptic bistable devices
[AD-A237885] N91-29463
BIT ERROR RATE
Combinatorial FSK modulation for power-efficient high-rate communications
[NASA-TM-105188] N91-29404
BIVARIATE ANALYSIS
Scrawl strips, and letter or B-letter strips: Depicting marginals of scatter plots
[AD-A238556] N91-29845
BLACK BODY RADIATION
Application of diffraction correction to blackbody sources
[AD-A237840] N91-29926
BLOCK COPOLYMERS
Physical properties and structure of ion-containing polymers
[AD-A238196] N91-29363
BLOOD
A technique for measuring the solubilities of gases in liquids
[AD-A238071] N91-29278
BODY CENTERED CUBIC LATTICES
Electron microscopy of thick 304 SS-copper multilayers
[DE91-011116] N91-29972
BODY TEMPERATURE
Micro SAINT modeling of physiological and human performance in the heat
[AD-A238659] N91-29719
BOILING WATER REACTORS
Characteristics of autoclave and in-reactor nodular corrosion of Zircaloys
[DE91-013600] N91-29294
BORANES
Organo- borazines.3.homo- and copolymerization of p-vinylphenyl- cyclotri- borazines
[AD-A237881] N91-29357
BORIDES
Structure of icosahedral borides by Raman spectroscopy
[DE91-010872] N91-29260
Long-term testing and evaluation of cathode components in a commercial aluminum cell, volume 1
[DE90-010896] N91-29436
BORON
Counterdoped high temperature, silicon array infrared detector
[AD-A238483] N91-29546
BORON ALLOYS
Development of nickel and iron aluminides and their applications
[DE91-015323] N91-29325
BORON CARBIDES
High temperature thermoelectric properties of boron carbide
[DE91-015848] N91-30037
BORON COMPOUNDS
Structure of icosahedral borides by Raman spectroscopy
[DE91-010872] N91-29260
BORON ISOTOPES
Structure of icosahedral borides by Raman spectroscopy
[DE91-010872] N91-29260
BORON NITRIDES
Boron nitride and silicon nitride systems
[AD-A238080] N91-29359
BOROSILICATE GLASS
Ablative heat shield studies for NASA Mars/Earth return entry vehicles
[AD-A238159] N91-29215
NMR characterization of porous ceramics
[DE91-015051] N91-29371
BOSONS
Large bipolarons and superconductivity
[DE91-014699] N91-29985
BOUNDARY CONDITIONS
Numerical methods for scattering from electrically large objects
[AD-A238262] N91-29426
Modification of programs CHIEF and CID to compute sound radiation from an arbitrary body with mixed boundary conditions
[AD-A237502] N91-29759
Numerical simulation of self-field MPD thrusters
[NASA-CR-187168] N91-29832
Advanced divertor experiments on DIII-D
[DE91-011138] N91-29950
BOUNDARY ELEMENT METHOD
The boundary element method applied to the two dimensional Stefan moving boundary problem
[AD-A238458] N91-29828
BOUNDARY LAYER FLOW
A finite element solver for 3-D compressible viscous flows
[NASA-CR-184175] N91-29488
BOUNDARY LAYER SEPARATION
Experimental and analytical study of rippled trailing edge airfoils for compressor application
[AD-A237425] N91-29508
Near-stall loss measurements in a CD compressor cascade with exploratory leading edge flow control
[AD-A237497] N91-29509
Separation-bubble velocity measurements using an oscillating-hot-wire system
[AD-A237997] N91-29518
BOUNDARY LAYERS
Performance of an airfoil at low Reynolds number
[NAL-PD-CF-9102] N91-29145
A manual method for determining the fractional stability category
[AD-A237627] N91-29675

BOUNDARY VALUE PROBLEMS
Steady flow of a fluid-solid mixture between parallel plates
[DE91-013114] N91-29491
Using quartz crystal microbalances to simultaneously sense mass accumulation and solution properties
[DE91-011501] N91-29537
The boundary element method applied to the two dimensional Stefan moving boundary problem
[AD-A238458] N91-29828
BOW WAVES
Qualitative investigation of cryogenic injected shock dissipation
[NASA-TM-105140] N91-29525
BOX BEAMS
Composite transport wing technology development: Design development tests and advanced structural concepts
[NASA-CR-4177] N91-29253
BRAGG ANGLE
Inelastic scattering in condensed matter with high intensity Moessbauer radiation
[DE91-014384] N91-29980
BRAGG CELLS
Major achievements during the first program year
[AD-A237171] N91-29919
BRAIN
Psychophysical studies of visual cortical function
[AD-A238663] N91-29720
Cognition and the brain
[AD-A237846] N91-29727
BRAIN DAMAGE
The functional architecture of visual object recognition
[AD-A238617] N91-29732
BRANCHING (MATHEMATICS)
Computational methods for bifurcation problems with symmetries on the manifold
[AD-A237146] N91-29817
BRAZING
JPRS report: Science and technology. USSR: Materials science
[JPRS-UMS-91-001] N91-29291
BREADBOARD MODELS
Optical Multiple Access Network (OMAN) for advanced processing satellite applications
[NASA-TM-105167] N91-29431
BRIGHTNESS
Degradation of brightness by resonant particle effects
[DE91-015181] N91-29578
Methods for evaluating discomfort glare
[PB91-185132] N91-29722
BRIGHTNESS TEMPERATURE
Multiple channel satellite analysis of cirrus
[AD-A238054] N91-29687
BRILLOUIN ZONES
Center for thin film studies
[AD-A237457] N91-29999
BRITTLE MATERIALS
Workshop proceedings: Toughening Mechanisms in Quasi-Brittle Materials
[AD-A238289] N91-29248
BRITTLENESS
Lightweight disk alloy development
[AD-A237064] N91-29309
BROADBAND
Computation of broadband, high-power electromagnetic pulse generation from an air gas avalanche switch
[DE91-015793] N91-29435
BROWNIAN MOVEMENTS
The Kramers problem: Fifty years of development
[DE91-617583] N91-29855
BUBBLES
Bubble generation and movement under microgravity conditions
[NAE-LTR-FR-110] N91-29388
Numerical and physical modelling of bubbly flow phenomena
[DE91-013646] N91-29492
An experimental study of plunging liquid jet induced air carryunder and dispersion
[AD-A237757] N91-29511
Separation-bubble velocity measurements using an oscillating-hot-wire system
[AD-A237997] N91-29518
Relating ocean acoustic ambient to ocean surface dynamics
[AD-A237167] N91-29699
BUCKLING
Fission-fusion adaptivity in finite elements for nonlinear dynamics of shells
[AD-A238029] N91-29626
BUMPERS
Whipple bumper shield simulations
[NASA-TM-105089] N91-29213
BUOYANCY
Donning times and flotation characteristics of infant life preservers: Four representative types
[AD-A237120] N91-29153
Bubble generation and movement under microgravity conditions
[NAE-LTR-FR-110] N91-29388
Transient flowmeter calibration facility
[AD-D014937] N91-29523
BURNING RATE
Spectral studies of solid propellant combustion. 3: Emission and absorption results for HMX2 propellant
[AD-A237958] N91-29276
The effects of HMX particle size and binder stiffness on the burning mechanism and regression rate of a series of fast burning propellants
[DE91-015785] N91-29387
BURNOUT
Spike leakage and burnout of silicon PIN diode microwave limiters
[AD-A238392] N91-29471
BURST TESTS
Pressure vessel burst test program
[AD-A237845] N91-29624

C

C (PROGRAMMING LANGUAGE)
The use of searching algorithms for the minimization of multi-valued logic functions
[AD-A238018] N91-29763
CABLES
Cable tester
[AD-D014904] N91-29438
CALCIUM OXIDES
Consolidation and plasticity of Bi-Sr-Ca-Cu-O superconductors
[DE91-015544] N91-30028
CALCULUS
A type calculus for mathematical programming modeling languages
[AD-A238160] N91-29766
CALCULUS OF VARIATIONS
Motion planning for manipulators with excessive degrees of freedom N91-29592
CALIBRATING
GPS: Aspects of pseudo-range positioning offshore N91-29161
A dihedral corner reflector model for full polarization calibration of RCS measurements
[DE91-013572] N91-29402
P-3 SAR calibration activity at Andros Island
[AD-A237357] N91-29412
NIST calibration procedure for vertically polarized monopole antennas 30 kHz to 300 MHz
[PB91-185124] N91-29432
Transient flowmeter calibration facility
[AD-D014937] N91-29523
Experimental analysis of B-dot sensors
[AD-A238487] N91-29547
Diagnostic support services for LLNL (Lawrence Livermore National Laboratory) NOVA laser experiments
[DE90-012125] N91-29552
Application of diffraction correction to blackbody sources
[AD-A237840] N91-29926
CALIFORNIA
Regional tectonic deformation in Southern California, inferred from terrestrial geodesy and the global positioning system N91-29669
The nature of the propagation of sea breeze fronts in central California
[AD-A238635] N91-29692
CALORIMETERS
A calorimetric investigation of deuterated palladium electrodes
[AD-A237571] N91-29456
An elevated temperature titration calorimeter
[DE91-015765] N91-29548
CANADA
Commonwealth Advisory Aeronautical Research Council. First Canadian newsletter on systems, 1989
[NAE-LTR-FR-108] N91-29139
NRC annual report, 1988/1989
[NRC-30398] N91-30072
CAPACITANCE
Cyclic voltammetric wave-shapes for microdisk electrodes: Coupled effects of solution resistance, double-layer capacitance, and finite electrochemical kinetics
[AD-A237505] N91-29455
CAPACITORS
Aspects of fatigue and rapid depolarization in the film PZT capacitors
[DE91-014904] N91-29484
Future explosive pulse-power technology for high-energy plasma physics experiments
[DE91-014601] N91-29951
CAPILLARIES (ANATOMY)
Electrified microscopic and conventional interfaces between two immiscible electrolyte solutions
[AD-A237695] N91-29459
CARBIDES
Powder metallurgy technology (selected articles)
[AD-A237176] N91-29310
Deformation induced microstructural and microchemical changes during thermomechanical treatment
[DE91-014862] N91-29319
CARBON
Feasibility of a laser-ignited HMX deflagration-to-detonation transition device for the US Navy LITES Program
[DE91-015210] N91-29382
Structures, properties, and dynamics of metal clusters from infrared laser spectroscopy
[AD-A237669] N91-29570
Growth, characterization, and device development in monocrystalline diamond films
[AD-A237463] N91-30000
CARBON DIOXIDE
Lithium combustion: A review
[AD-A238154] N91-29279
Atmospheric methane concentrations: The NOAA/CMDL global cooperative flask sampling network, 1983 - 1988
[DE91-014942] N91-29664
CO2 measurements along the WOCE P-16 and 19 sections in the South Pacific Ocean: A joint LDGO/WHOI program
[DE91-015742] N91-29708
CARBON DIOXIDE LASERS
Multi-sensor feature level fusion
[AD-A237106] N91-29411
Program and applications for a near-term laser launch system
[DE90-011760] N91-29551
Blackbody pumped CO2 lasers using Gaussian and waveguide cavities
[DE91-012494] N91-29559
Second-harmonic generation of TEA CO2 10.6 micrometer laser light in AgGaS2 crystals
[AD-A237169] N91-29564
Experimental study of gas kinetics of a fast-axial flow kilowatt CO2 laser
[AD-A237178] N91-29565
Chinese physics lasers (selected articles)
[AD-A237263] N91-29567
CARBON FIBER REINFORCED PLASTICS
Effect of fortifier on compression-after-impact strength of carbon fabric reinforced epoxy
[NAE-LTR-ST-1736] N91-29237
CARBON FIBERS
Statistical characterization of graphite fiber for prediction of composite structure reliability
[AD-A238020] N91-29245
Effects of high-intensity solar radiation on carbon fibers
[DE91-015485] N91-29252
CARBON ISOTOPES
Structure of icosahedral borides by Raman spectroscopy
[DE91-010872] N91-29260
CARBON MONOXIDE
Catalytic hydrogenation of carbon monoxide
[DE91-015452] N91-29283
Deactivation by carbon of iron catalysts for indirect liquefaction
[DE91-011276] N91-29285
Comparison between the interfacial chemistry of metallized polyimides and polymide
[AD-A238400] N91-29366
Atomic-resolution scanning tunneling microscopy and infrared spectroscopy as combined in-situ probes of electrochemical adlayer structure: Carbon monoxide on rhodium(111)
[AD-A237508] N91-29884
The influence of potential on metal-adsorbate structure: Solvent-independent nature of infrared spectra for Pt(111)/CO
[AD-A237509] N91-30004
CARBON 13
Stable isotope fractionation in photosynthesis: Analysis of autotrophic competence following transformation of the chloroplast genome of Chlamydomonas
[DE91-015792] N91-29713
CARBONATES
ANL's development of conductive ceramic components for MCFC
[DE91-015557] N91-29336

CARBONYL COMPOUNDS
Simulation of the structure of dense, amorphous bisphenol-A polycarbonate
| AD-A237222 | N91-29270
Methods for determination of low-molecular weight carbonyl compounds in the ambient atmosphere
| DE91-015188 | N91-29656
CASCADE FLOW
Near-stall loss measurements in a CD compressor cascade with exploratory leading edge flow control
| AD-A237497 | N91-29509
CASE HISTORIES
Three case studies of management information systems
| AD-A238310 | N91-30049
CATALYSTS
Catalytic hydrogenation of carbon monoxide
| DE91-015452 | N91-29283
Deactivation by carbon of iron catalysts for indirect liquefaction
| DE91-011276 | N91-29285
Dual cure photocatalyst systems
| DE91-014174 | N91-29369
CATALYTIC ACTIVITY
Dual cure photocatalyst systems
| DE91-014174 | N91-29369
CATHODES
Pyrite cathode material for a thermal battery
| AD-D014945 | N91-29475
CAVITIES
Sliding mode controller of RF cavity tuning loop
| DE91-015461 | N91-29410
Secondary stability and three-dimensional natural convection in a shallow cavity N91-29495
CAVITY RESONATORS
Sliding mode controller of RF cavity tuning loop
| DE91-015461 | N91-29410
A compact 200 kV pulse transformer system
| DE91-014669 | N91-29479
Development of low-threshold value, high-power semiconductor laser
| AD-A237183 | N91-29566
RF transfer in the coupled-cavity free-electron laser two-beam accelerator
| DE91-015676 | N91-29583
CELL CATHODES
Long-term testing and evaluation of cathode components in a commercial aluminum cell, volume 1
| DE90-010896 | N91-29436
CELL MEMBRANES (BIOLOGY)
Electrified microscopic and conventional interfaces between two immiscible electrolyte solutions
| AD-A237695 | N91-29459
Perturbation techniques for models of bursting electrical activity in pancreatic (beta)-cells
| DE91-013901 | N91-29715
CELLS (BIOLOGY)
Studies in neural networks
| AD-A237452 | N91-29717
CELLULOSE
Microbiology and physiology of anaerobic fermentations of cellulose
| DE91-015239 | N91-29712
CEMENTS
Workshop proceedings: Toughening Mechanisms in Quasi-Brittle Materials
| AD-A238289 | N91-29248
CERAMIC COATINGS
Light weight space power reactors for nuclear electric propulsion
| DE91-014803 | N91-29232
CERAMIC FIBERS
Microstructural and strength stability of CVD SiC fibers in argon environment
| NASA-TM-103772 | N91-29250
Synthesis of multifilament silicon carbide fibers by chemical vapor deposition
| NASA-CR-188725 | N91-29331
CERAMIC MATRIX COMPOSITES
An analysis of the wear behavior of SiC whisker reinforced alumina from 25 to 1200 C
| NASA-TM-104489 | N91-29235
NDE of ceramics and ceramic composites
| NASA-TM-104520 | N91-29610
CERAMICS
Workshop proceedings: Toughening Mechanisms in Quasi-Brittle Materials
| AD-A238289 | N91-29248
A brief overview of the activities and accomplishments of the Metals and Ceramics Division
| DE91-014955 | N91-29296
Micromechanisms of monotonic and cyclic subcritical crack growth in advanced high melting point low-ductility intermetallics
| AD-A238151 | N91-29317
Fabrication, phase transformation studies and characterization of SiC-AlN-Al2OC ceramics
| DE91-013296 | N91-29329
Application of ceramics to industrial gas turbines
| DE91-013140 | N91-29330
Precursors to Si-N-C-O ceramics: A reinvestigation of the poly methylvinyl silylethyl enediamine systems
| DE91-013722 | N91-29333
Ceramic fabrication R/D
| DE91-014758 | N91-29335
ANL's development of conductive ceramic components for MCFC
| DE91-015557 | N91-29336
Organometallic precursor routes to Si-C-Al-O-N ceramics
| AD-A237753 | N91-29355
High strain rate characterization of ceramics in shear
| AD-A238319 | N91-29365
Corrosion behavior of continuous-filament-wound ceramic composite tubes
| DE91-014959 | N91-29370
NMR characterization of porous ceramics
| DE91-015051 | N91-29371
Ceramic decomposition under irradiation
| DE91-015061 | N91-29372
Fabrication of silicon nitride ceramics by microwave heating
| DE91-015312 | N91-29373
Advances in the drained shaping of ceramics
| DE91-015429 | N91-29376
The 0-G experiments with advanced ceramic fabric wick structures
| DE91-015531 | N91-29377
Ultrasonic evaluation of silicon nitride green bodies
| AD-A237924 | N91-29608
NDE of ceramics and ceramic composites
| NASA-TM-104520 | N91-29610
Developmental status and system studies of the monolithic solid oxide fuel cell
| DE91-014389 | N91-29645
Preparation of damage resistant optical coatings on flat substrates
| DE91-013588 | N91-29916
Fabrication and wire extrusion of ceramic superconductors
| DE91-015207 | N91-29991
Determination of thermodynamic and kinetic properties of grain boundaries using high temperature calorimetry
| DE91-015571 | N91-30031
CHAMBERS
Kinetics of dark reaction in chemical laser gases
| DE91-015320 | N91-29579
CHANNEL FLOW
Three-dimensional vortex dynamics and interactions in near-wall turbulent boundary layers
| AD-A237413 | N91-29507
Effects of 1, 2, 3, and 4 Hz imposed bulk flow oscillations on transition in a straight channel with 40 to 1 aspect ratio
| AD-A237988 | N91-29517
CHANNEL NOISE
Signal processing in impulsive electromagnetic interference
| AD-A237612 | N91-29416
CHANNELS (DATA TRANSMISSION)
Quaternary pulse position modulation electronics for free-space laser communications
| NASA-TM-104502 | N91-29405
Application of Multi-Frequency Modulation (MFM) for high-speed data communications to a voice frequency channel
| AD-A238019 | N91-29422
Acoustic tomographic estimate of ocean advective heat flux: A numerical assessment in the Norwegian Sea
| AD-A237100 | N91-29698
CHAOS
A survey of nonlinear dynamics (chaos theory)
| AD-A237802 | N91-29821
CHARACTERIZATION
Characterization of surface contaminants using infrared microspectroscopy
| DE91-009405 | N91-29605
CHARGE COUPLED DEVICES
Responsivity uniformity enhancements for Backside-Illuminated Charge-Coupled Devices (BICCDs) by excimer laser-assisted etching
| AD-A237435 | N91-29997
CHARGE TRANSFER
Electrical, magnetic, and spectroscopic properties of tetrathiafulvalene charge transfer compounds with iron, ruthenium, rhodium, and iridium halides
| AD-A237607 | N91-29273
The charge-exchange neutral problem and the code NEUTRAL
| AD-A237889 | N91-29464
Role of the solvent in kinetics of heterogeneous electron and ion transfer reactions
| AD-A237168 | N91-29876
Charge motion effects in ionic clusters
| AD-A238178 | N91-29886
Analytical calculation of neutral transport and its effect on ions
| DE91-015908 | N91-29896
CHARM (PARTICLE PHYSICS)
High energy physics at Tufts University
| DE91-015055 | N91-29908
CHECKOUT
The use and design of flightcrew checklists and manuals
| AD-A237206 | N91-29733
CHEMICAL BONDS
Pulse induced nanlithography of graphite in H2O: A road to chemical linkages to the surface?
| AD-A237086 | N91-29338
Conformational characteristics of the polycarbonate 4,4'-isopropylidenediphenol
| AD-A237334 | N91-29347
Effects of interfacial modification on diamond film adhesion
| AD-A237750 | N91-29354
Properties and adhesion of polyimides in microelectronic devices
| AD-A238204 | N91-29364
CHEMICAL COMPOSITION
Structure of icosahedral borides by Raman spectroscopy
| DE91-010872 | N91-29260
Development of nickel and iron aluminides and their applications
| DE91-015323 | N91-29325
Model filled polymer 7: Flow behavior of polymers containing monodisperse crosslinked polymeric beads
| AD-A237430 | N91-29350
Effects of doping on hybridization gapped materials
| DE91-014611 | N91-29477
Direct-sampling MS measurement of volatiles in environmental samples
| DE91-013417 | N91-29653
On-line monitoring of volatile organic species
| DE91-014655 | N91-29655
High resolution electron microscopy of grain boundaries
| DE91-010593 | N91-29970
Quantitative analysis of oxygen segregation on inversion domain boundaries in aluminum nitride
| DE91-010869 | N91-29971
High temperature Knudsen effusion-mass spectrometric studies of the Y-Ba-Cu-O system
| NIAR-91-23 | N91-29981
Air-sintering mechanisms of chromites
| DE91-015527 | N91-30027
CHEMICAL EXPLOSIONS
Feasibility of a laser-ignited HMX deflagration-to-detonation transition device for the US Navy LITES Program
| DE91-015210 | N91-29382
CHEMICAL LASERS
Kinetics of dark reaction in chemical laser gases
| DE91-015320 | N91-29579
CHEMICAL PROPULSION
Production and use of metals and oxygen for lunar propulsion
| NASA-TM-105195 | N91-29222
CHEMICAL REACTIONS
Lithium combustion: A review
| AD-A238154 | N91-29279
Postshock spectral radiance measurements in nickel and nickel/aluminum powders
| DE91-014695 | N91-29302
Organometallic precursor routes to Si-C-Al-O-N ceramics
| AD-A237753 | N91-29355
First International conference on Frontiers of Polmer Research
| AD-A238112 | N91-29361
Comparison between the interfacial chemistry of metallized polyimides and polymide
| AD-A238400 | N91-29366
The cure of rigid polyurethane encapsulating foam
| DE91-016059 | N91-29379
Laser enhanced chemical reaction studies
| DE91-013021 | N91-29555
Kinetics of dark reaction in chemical laser gases
| DE91-015320 | N91-29579
Study of elementary reactions and energy transfer processes involving the NH and CN free radicals
| AD-A238461 | N91-29889
CHEMICAL REACTORS
Synthesis of multifilament silicon carbide fibers by chemical vapor deposition
| NASA-CR-188725 | N91-29331

Electrocatalytic study of ammonia synthesis and methane dimerization in high temperature solid electrolyte cells
[DE90-012496] N91-29437

CHINA
Chinese physics lasers (selected articles)
[AD-A237263] N91-29567

CHIPS (ELECTRONICS)
Silicon Wafer Advanced Packaging (SWAP). Multichip Module (MCM) foundry study, version 2
[AD-A237412] N91-29452
Analog design verification with PSpice and MICRO-CAP 3
[AD-A237922] N91-29762

CHLORIDES
Electrochemical contact adsorption site changes driven by field and charge fact and theory
[AD-A237127] N91-29269

CHLOROCARBONS
On-line monitoring of volatile organic species
[DE91-014655] N91-29655

CHLOROPHYLLS
Specific mutagenesis of a chlorophyll-binding protein
[DE91-014813] N91-29711
Stable isotope fractionation in photosynthesis: Analysis of autotrophic competence following transformation of the chloroplast genome of Chlamydomonas
[DE91-015792] N91-29713

CHLOROPLASTS
Stable isotope fractionation in photosynthesis: Analysis of autotrophic competence following transformation of the chloroplast genome of Chlamydomonas
[DE91-015792] N91-29713

CHOLESKY FACTORIZATION
Supernodal symbolic Cholesky factorization on a l ocal-memory multiprocessor
[DE91-014967] N91-29796

CHROMITES
Air-sintering mechanisms of chromites
[DE91-015527] N91-30027

CHROMIUM ALLOYS
Postirradiation deformation of ferritic Fe-Cr binary alloys
[DE91-014856] N91-29295

CIRCUIT DIAGRAMS
A circuit model for an inductive strip in homogeneous finline
[AD-A238001] N91-29466

CIRCUITS
Physical concepts and modeling procedures for picosecond and subpicosecond distributed circuits
[AD-A238592] N91-29472

CIRCULAR CYLINDERS
A numerical study of flow past a cylindrical body
N91-29497
Numerical study of non-impulsively started flow around a circular cylinder
[AD-A238051] N91-29519
Dimensionless parameters important to the prediction of vortex-induced vibration of long, flexible cylinders in ocean currents
[PB91-184713] N91-29630

CIRRUS CLOUDS
Multiple channel satellite analysis of cirrus
[AD-A238054] N91-29687

CIVIL AVIATION
Aircraft accident reports: Brief format US civil and foreign aviation issue Number 1 of 1989 accidents
[PB90-916901] N91-29157

CLADDING
Advanced materials for space nuclear power systems
[NASA-TM-105171] N91-29298
Effect of cladding thickness on attenuation in uniformly curved single-mode optical fibers
[AD-A238034] N91-29928

CLEANING
Influence of diamond turning and surface cleaning processes on the degradation of KDP crystal surfaces
[DE91-015300] N91-30035

CLIMATE
A global geographic information system data base of storm occurrences and other climatic phenomena affecting coastal zones
[DE91-014949] N91-29682
Parallelizing the spectral transform method
[DE91-013969] N91-29815

CLIMATOLOGY
Theoretical studies of long-range transport of oxidants
[PB91-182360] N91-29661
A climatological model for risk computations incorporating site-specific dry deposition influences
[DE91-015536] N91-29667
Dependence of radar backscatter on the energetics of the air-sea interface
[AD-A237818] N91-29685
Forcasting tropical cyclone recurvature using an empirical othogonal function representation of vorticity fields
[AD-A238489] N91-29689
Cloud data collection, composites and analysis for Whole-Sky Imager (WSI) studies
[AD-A238531] N91-29690
Fitting seasonal averages with a continuous function
[AD-A238300] N91-29704
Parallelizing the spectral transform method
[DE91-013969] N91-29815

CLOSED CYCLES
Compensation of distributed delays in integrated communication and control systems
[NASA-CR-187136] N91-29193

CLOSURES
Quick disconnect pressure cap
[AD-D014936] N91-29598

CLOUD PHYSICS
Cloud data collection, composites and analysis for Whole-Sky Imager (WSI) studies
[AD-A238531] N91-29690
Parameterizations of microphysical processes for simulation of regional-scale clouds
[DE91-015554] N91-29696

CLOUDS (METEOROLOGY)
Cloud data collection, composites and analysis for Whole-Sky Imager (WSI) studies
[AD-A238531] N91-29690
Parameterizations of microphysical processes for simulation of regional-scale clouds
[DE91-015554] N91-29696
Ocean thermal feature recognition, discrimination and tracking using infrared satellite imagery
[AD-A238138] N91-29703

CLUMPS
Structures, properties, and dynamics of metal clusters from infrared laser spectroscopy
[AD-A237669] N91-29570

CLUSTERS
Charge motion effects in ionic clusters
[AD-A238178] N91-29886

CLUTTER
Impact of ionospheric scintillations on space-based surveillance radars
[AD-A237673] N91-29417
A Doppler bin blanking CFAR processor for airborne radars
[AD-A237890] N91-29418

COAGULATION
Problems in nonlinear continuum dynamics
[AD-A237844] N91-29512

COAL
A model of multicomponent droplet evaporation with liquid phase reactions
[DE90-012535] N91-29257

COASTS
Sea level and bottom pressure measurements in the Northern Gulf of Alaska
[PB91-184135] N91-29705

COATING
Rejuvenation of service exposed alloy 713C turbine blades
[NAE-LTR-ST-1716] N91-29179
Energy conserving coating: Pigment research
[AD-A237841] N91-29356

COATINGS
A novel epoxy lacquer for high strength steel in F-111 aircraft during overhaul
[AD-A236828] N91-29326
Energy conserving coating: Pigment research
[AD-A237841] N91-29356
Numerical methods for scattering from electrically large objects
[AD-A238262] N91-29426
Electroforming thin channel heat exchangers
[DE91-015114] N91-29528
Ultraviolet reflector materials for solar detoxification of hazardous waste
[DE91-002196] N91-29663
Comparisons between scanning tunneling microscopy and outer-sphere electron-transfer rates at Pt(111) surfaces coated with ordered iodine adlayers
[AD-A237507] N91-29883

COBALT
The effects of donor-acceptor electronic interactions on the rates of gas-phase metallocene electron-exchange reactions
[AD-A237459] N91-29878

COBALT COMPOUNDS
Formation of CoSi2 in SIMOX wafers by high dose Co implantation
[DE91-015639] N91-30036

COCHLEA
Software development of the cochlear filter and eighth-nerve model
[AD-A237454] N91-29757

COCKPITS
The use and design of flightcrew checklists and manuals
[AD-A237206] N91-29733

CODE DIVISION MULTIPLE ACCESS
Optical Multiple Access Network (OMAN) for advanced processing satellite applications
[NASA-TM-105167] N91-29431

CODERS
A study of space communications spread-spectrum systems, phase 5 and 6. Part 2: Coding and modulation
[QU-90-2-PT-2] N91-29396

CODING
Quaternary pulse position modulation electronics for free-space laser communications
[NASA-TM-104502] N91-29405
Research and development for Digital Voice Processing (DVP)
[AD-A238280] N91-29427
XTRAN: An atmospheric transmittance code based on XSCALE
[AD-A237624] N91-29674

COEFFICIENTS
Forcasting tropical cyclone recurvature using an empirical othogonal function representation of vorticity fields
[AD-A238489] N91-29689

COGNITION
Institute for the Study of Human Capabilities: Summary descriptions of research for the period December 1989 through September 1990
[AD-A237767] N91-29726
Cognition and the brain
[AD-A237846] N91-29727
Performance of Marine AV-8B (Harrier) pilots on a cognitive/psychomotor test battery: Comparison and prediction
[AD-A238563] N91-29729
Performance of several different Naval aviator communities on a cognitive/psychomotor test battery: Pipeline comparison and prediciton
[AD-A238564] N91-29730

COHERENCE
Detection of coherent structures in the edge of the TEXT tokamak plasma
[DE91-015183] N91-29958

COHERENT RADAR
Multipixel multidimensional laser radar system theory
[AD-A238110] N91-29573

COHERENT RADIATION
An improved method of investigation of compressor blade fit using holographic interferometry
[AD-A238182] N91-29185

COHERENT SCATTERING
Twenty first century space propulsion study addendum
[AD-A238011] N91-29225

COLD FRONTS
On the application of edge wave theory to terrain-bounded cold surges: A numerical study
N91-29670
Mesoscale modeling of precipitation scavenging by a cold-frontal squall line
[DE91-015534] N91-29695

COLD PLASMAS
Vlasov simulations of very-large-amplitude wave generation in the plasma wakefield accelerator
[AD-A237428] N91-29961

COLLIMATION
A real time collimation sensor using a shear plate and a spatial light modulator
[DE90-011362] N91-29914

COLLIMATORS
A real time collimation sensor using a shear plate and a spatial light modulator
[DE90-011362] N91-29914

COLLISION AVOIDANCE
NAE participation in the United States FAA vertical separation study
[NAE-LTR-FR-105] N91-29160

COLLISION PARAMETERS
Characterization of a sub-picosecond dye laser for the study of atom-perturber collisions
[AD-A238099] N91-29572
Electromagnetic dissociation of Au and Co targets by relativistic heavy ions
[DE91-014915] N91-29906

COLLISION RATES
Spin-Label-Spin-Probe. Studies of bimolecular encounters in micelles
[AD-A238546] N91-29891

COLLISIONAL PLASMAS
Hypervelocity impact jet formation
| DE91-014651 | N91-29619
Collisional processes of interest in MFE plasma research
| DE91-013023 | N91-29943
Fluidlike studies of the sheath and presheath regions of a plasma
| DE91-013343 | N91-29944
Stagnation and interpenetration of laser-created colliding plasmas
| DE91-013244 | N91-29946
COLLISIONS
Proton deceleration near the surface of an accreting neutron star N91-30063
COLLOCATION
Unsteady compressible lifting surface analysis for rotary wings using velocity potential modes N91-29170
COLLOIDS
Spin-Label-Spin-Probe. Studies of bimolecular encounters in micelles
| AD-A238546 | N91-29891
COLOR
Energy conserving coating: Pigment research
| AD-A237841 | N91-29356
Psychophysical studies of visual cortical function
| AD-A238663 | N91-29720
COLOR VISION
Eye movements and spatial pattern vision
| AD-A238664 | N91-29721
The effects of luminance boundaries on color perception
| AD-A237794 | N91-29925
COMBINATORIAL ANALYSIS
Invariant target recognition using self-organizing networks
| AD-A238252 | N91-29807
COMBUSTIBLE FLOW
International Union of Theoretical and Applied Mechanics (IUTAM) Symposium on Aerothermodynamics in Combustors
| AD-A237943 | N91-29516
COMBUSTION
An overview of aerothermal modeling
| NRC-32088 | N91-29258
Performance of multiple stream pulsed jet combustion systems
| DE91-012338 | N91-29259
Molecular beam studies of reaction dynamics
| DE91-014866 | N91-29868
COMBUSTION CHAMBERS
Experimental study of cross-stream mixing in a cylindrical duct
| NASA-TM-105180 | N91-29187
Performance of multiple stream pulsed jet combustion systems
| DE91-012338 | N91-29259
Investigation of the combustion of liquid fuels in Rijke type pulse combustors
| DE90-012490 | N91-29381
Modification of the 'TEACH' computer code for use in a study of swirling turbulent flows
| DE91-010492 | N91-29496
International Union of Theoretical and Applied Mechanics (IUTAM) Symposium on Aerothermodynamics in Combustors
| AD-A237943 | N91-29516
Ultra-low NOx gas turbine combustor
| PB91-184994 | N91-29601
Interactions of turbulent eddies and combustion in an MHD second stage combustor
| DE91-015722 | N91-29968
COMBUSTION CHEMISTRY
Supersonic combustion of a transverse injected H2 jet in a radio frequency heated flow
| DE91-014739 | N91-29281
COMBUSTION PHYSICS
Lithium combustion: A review
| AD-A238154 | N91-29279
Ultra-low NOx gas turbine combustor
| PB91-184994 | N91-29601
COMBUSTION PRODUCTS
An overview of aerothermal modeling
| NRC-32088 | N91-29258
COMFORT
Methods for evaluating discomfort glare
| PB91-185132 | N91-29722
COMMUNICATION NETWORKS
Description of a computer fault detector and net isolator
| AD-A238387 | N91-29428
Optical Multiple Access Network (OMAN) for advanced processing satellite applications
| NASA-TM-105167 | N91-29431
SAFENET 2 fiber optic implementation study
| AD-A238044 | N91-29929
COMMUNICATION THEORY
Application of Multi-Frequency Modulation (MFM) for high-speed data communications to a voice frequency channel
| AD-A238019 | N91-29422
COMPATIBILITY
Methods to determine the compatibility and degradation of organic materials
| AD-A237940 | N91-29234
COMPENSATORS
Compensation of distributed delays in integrated communication and control systems
| NASA-CR-187136 | N91-29193
COMPILERS
Alsys Limited, Alsycomp 017, version 5.2, MICRO VAX 2 under Micro VMS V5.3 (host) to INMOS T425 transputer implemented on a B403 TRAM (target), 901118N1.11064
| AD-A237411 | N91-29738
Lazy task creation: A technique for increasing the granularity of parallel programs
| AD-A237477 | N91-29781
COMPLEX SYSTEMS
Diffusion approximations for complex repair systems
| AD-A238100 | N91-29836
COMPOSITE MATERIALS
Review of Canadian aeronautical fatigue work: 1987-1989
| NAE-LTR-ST-1706 | N91-29165
Effect of a free surface on stress distribution in a bimaterial composite
| PB91-185116 | N91-29251
Micromechanisms of monotonic and cyclic subcritical crack growth in advanced high melting point low-ductility intermetallics
| AD-A238151 | N91-29317
Thermal emittance enhancement of graphite-copper composites for high temperature space based radiators
| NASA-TM-105178 | N91-29332
Ceramic fabrication R/D
| DE91-014758 | N91-29335
Preparation and properties of new inorganic glasses and gel-derived solids
| AD-A238095 | N91-29360
Evaluation of Shadow Moire for surface deformation detection and measurement
| NAE-LTR-ST-1737 | N91-29604
Modeling and response analysis of thin-walled beam structures constructed of advanced composite materials N91-29615
COMPOSITE STRUCTURES
NASA workshop on impact damage to composites
| NASA-CP-10075 | N91-29240
Anisotropic tensile probabilistic failure criterion for composites
| AD-A237601 | N91-29244
Modeling and response analysis of thin-walled beam structures constructed of advanced composite materials N91-29615
Vibration control and optimization in composite structural elements by use of add-on viscoelastic materials
| AD-A238533 | N91-29628
COMPRESSING
Composite specimen design analysis. Volume 2: Experimental efforts
| AD-A238277 | N91-29247
Morphology of bulk Nylon 6 subjected to plane strain compression
| AD-A237331 | N91-29622
COMPRESSION LOADS
Postshock spectral radiance measurements in nickel and nickel/aluminum powders
| DE91-014695 | N91-29302
COMPRESSION TESTS
Effect of fortifier on compression-after-impact strength of carbon fabric reinforced epoxy
| NAE-LTR-ST-1736 | N91-29237
Compendium of material test results on HY-100 and pseudo HY-100 metals in support of US Navy programs
| DE91-013134 | N91-29292
High strain rate characterization of ceramics in shear
| AD-A238319 | N91-29365
Review of literature on the damage, loss of stiffness, and residual strength of graphite/epoxy laminates subjected to cyclic loading
| NAE-LTR-ST(CR)-1711 | N91-29611
COMPRESSIVE STRENGTH
High strain rate characterization of ceramics in shear
| AD-A238319 | N91-29365
Phase transformations, ultrastructure, and properties of rigid-rod polymers
| AD-A238643 | N91-29368
COMPRESSOR BLADES
An improved method of investigation of compressor blade fit using holographic interferometry
| AD-A238182 | N91-29185
COMPRESSOR EFFICIENCY
Compressor fault modelling for engine health monitoring: Review and recommendations
| NRC-TR-ENG-004 | N91-29178
COMPRESSOR ROTORS
Modification of axial-flow compressor stall margin by variation of stationary blade setting angles
| AD-A238406 | N91-29186
COMPRESSORS
Experimental and analytical study of rippled trailing edge airfoils for compressor application
| AD-A237425 | N91-29508
Near-stall loss measurements in a CD compressor cascade with exploratory leading edge flow control
| AD-A237497 | N91-29509
COMPUTATION
Near-stall loss measurements in a CD compressor cascade with exploratory leading edge flow control
| AD-A237497 | N91-29509
Topographic map reading
| AD-A238026 | N91-29640
Barrier methods for large-scale quadratic programming
| AD-A238554 | N91-29773
Engineering applications of neural computing: A state-of-the-art survey
| AD-A237628 | N91-29803
Design and hardware implementation of neural systems
| AD-A237703 | N91-29804
COMPUTATIONAL FLUID DYNAMICS
Performance of an airfoil at low Reynolds number
| NAL-PD-CF-9102 | N91-29145
Computational fluid dynamics at NRC: A directory of practitioners and activities
| NRC-TTP-02-89 | N91-29490
Theoretical study of the flow in a rotating duct. Experimental study through flow visualization in a curved duct
| RAE-TRANS-2189 | N91-29493
An evaluation of the NEKTON program
| AD-A237888 | N91-29513
A method of investigating scales of motion in a turbulent wake
| AD-A237923 | N91-29514
The advanced software development and commercialization project
| DE91-015756 | N91-29797
Computational and theoretical aspects of nonlinear partial differential equations
| AD-A238495 | N91-29829
COMPUTATIONAL GRIDS
A method for computing fields near the origin of a cylindrical coordinate system in time domain finite-difference electromagnetic simulations
| DE91-015431 | N91-29433
Solutions of two-dimensional Euler equations with multigrid acceleration
| NAL-PD-CF-9006 | N91-29494
Electromagnetic PIC simulations using finite elements on unstructured grids
| DE91-015141 | N91-29962
COMPUTER AIDED DESIGN
AEROWING - The software for aerodynamic analysis of a large aspect-ratio finite wing at low speeds
| NAL-PD-CF-9101 | N91-29146
Missile Datcom: User's manual
| AD-A237817 | N91-29148
Report on using expert systems for computer-aided formulation and property estimation of propellants. 1: Expert system shell selection and initial package design
| AD-A237567 | N91-29383
A circuit model for an inductive strip in homogeneous finline
| AD-A238001 | N91-29466
Horizontal axis wind turbine post stall airfoil characteristics synthesization
| DE91-002198 | N91-29650
A prolog system for converting VHDL-based models to Generalized Extraction System (GES) rules
| AD-A238545 | N91-29741
NW lab for integrated systems
| AD-A237118 | N91-29749
The use of searching algorithms for the minimization of multi-valued logic functions
| AD-A238018 | N91-29763
Verification of the FtCayuga fault-tolerant microprocessor system. Volume 2: Formal specification and correctness theorems
| NASA-CR-187574 | N91-29777
COMPUTER AIDED TOMOGRAPHY
Use of electrical impedance imaging in two-phase, gas-liquid flows
| DE91-015914 | N91-29531

COMPUTER COMPATIBLE TAPES
Lowell proper motion survey: Southern Hemisphere (Giclas, Burnham, and Thomas 1978). Documentation for the machine-readable version
[NASA-TM-105069] N91-30060
COMPUTER GRAPHICS
Three-dimensional visualization for evaluating automated, geomorphic pattern-recognition analyses of crustal structures
[DE91-012929] N91-29668
A general graphical user interface for automatic reliability modeling
[NASA-TM-104068] N91-29745
A fast, one pass algorithm to label objects and compute their features
[DE91-015441] N91-29747
Visualizing performance of parallel programs
[DE91-014966] N91-29793
Proceedings of the 1st Workshop on Proximity Graphs
[AD-A237250] N91-29818
Compilation and representation of intelligent electronic documents: An architecture for referenceability
[DE91-012635] N91-30045
COMPUTER INFORMATION SECURITY
Discretionary security for object-oriented database systems
[AD-A237573] N91-29740
COMPUTER NETWORKS
Application of Multi-Frequency Modulation (MFM) for high-speed data communications to a voice frequency channel
[AD-A238019] N91-29422
Description of a computer fault detector and net isolator
[AD-A238387] N91-29428
APRIL: A processor architecture for multiprocessing
[AD-A237476] N91-29739
The language for DENOTE (Denotational Semantics Translation Environment)
[AD-A237144] N91-29750
Counting networks
[AD-A237475] N91-29780
Proceedings of the 1st Workshop on Proximity Graphs
[AD-A237250] N91-29818
COMPUTER PROGRAM INTEGRITY
Fault-tolerant computing: An overview
[NASA-CR-188793] N91-29769
COMPUTER PROGRAMMING
Slaying the software dragon: A look at how software engineering, the Ada programming language and process maturity are changing software development
[AD-A237156] N91-29751
Real-time Ada design methodologies and their impact on performance
[AD-A237259] N91-29754
Ada 9X requirements rationale
[AD-A237350] N91-29755
Software development of the cochlear filter and eighth-nerve model
[AD-A237454] N91-29757
The 6th Workshop on the Mathematical Foundations of Programming Semantics
[AD-A237754] N91-29760
A common interface real-time multiprocessor operating system for embedded systems
[AD-A238445] N91-29770
Transfer of 4GL application from INGRES to ORACLE
[AD-A238448] N91-29771
A Workshop on the Integration of Numerical and Symbolic Computing Methods
[AD-A238601] N91-29774
The MIT Alewife machine: A large-scale distributed-memory multiprocessor
[AD-A237705] N91-29784
Expert systems on multiprocessor architectures. Volume 1: Summary
[AD-A238046] N91-29786
The advanced software development and commercialization project
[DE91-015756] N91-29797
COMPUTER PROGRAMS
Missile Datcom: User's manual
[AD-A237817] N91-29148
The functional dependence of trajectory dispersion on initial condition errors
[DE91-014661] N91-29151
Methodology investigation, aviation test management system concept development
[AD-A237349] N91-29172
Divergence thrust loss calculations for convergent-divergent nozzles: Extensions to the classical case
[NASA-TM-105176] N91-29181
Calculated performance of the NASA Lewis icing research tunnel
[NASA-TM-105173] N91-29199
A computer program for prediction of internal performance of a ramrocket
[AD-A238179] N91-29226
Pressure measurements in a low-density nozzle plume for code verification
[NASA-TM-105170] N91-29228
ALS rocket engine combustion devices design and demonstration
[NASA-CR-183824] N91-29233
Molecular dynamics simulation of the effect of interfaces in melting and solid-state amorphization
[DE91-015550] N91-29284
Conformal FDTD modeling wake fields
[DE91-015129] N91-29407
Nonlinear computerized methodology. A: Angle of arrival estimation. B: Data modeling and identification
[AD-A237564] N91-29415
Research and development for Digital Voice Processing (DVP)
[AD-A238280] N91-29427
A method for computing fields near the origin of a cylindrical coordinate system in time domain finite-difference electromagnetic simulations
[DE91-015431] N91-29433
Modification of the 'TEACH' computer code for use in a study of swirling turbulent flows
[DE91-010492] N91-29496
Near-stall loss measurements in a CD compressor cascade with exploratory leading edge flow control
[AD-A237497] N91-29509
An evaluation of the NEKTON program
[AD-A237888] N91-29513
Local synthesis and tooth contact analysis of face-milled spiral bevel gears
[NASA-TM-105182] N91-29600
Analysis of a teetered, variable-speed rotor
[DE91-002190] N91-29646
Horizontal axis wind turbine post stall airfoil characteristics synthesization
[DE91-002198] N91-29650
Atmospheric methane concentrations: The NOAA/CMDL global cooperative flask sampling network, 1983 - 1988
[DE91-014942] N91-29664
Description of the Strategic High-Altitude Atmospheric Radiation Code (SHARC)
[AD-A237089] N91-29671
Worldwide maritime infrared atmospheric transmittance data
[AD-A237292] N91-29672
XTRAN: An atmospheric transmittance code based on XSCALE
[AD-A237624] N91-29674
A manual method for determining the fractional stability category
[AD-A237627] N91-29675
Hamiltonian 3-D ray tracing in the oceanic waveguide on the ellipsoidal earth
[AD-A237458] N91-29700
Data acquisition system for collecting biophysical and physiological data
[AD-A237654] N91-29710
Alsys Limited, Alsycomp 017, version 5.2, MICRO VAX 2 under Micro VMS V5.3 (host) to INMOS T425 transputer implemented on a B403 TRAM (target), 901118N1.11064
[AD-A237411] N91-29738
QBDATAMT: A computer program to read Datamyte recorder data into an IBM PC or compatible computer
[NAE-LTR-ST-547] N91-29742
Description of computer programs used to analyze and plot Spectrapot data files
[NAE-ST-557] N91-29744
Software development of the cochlear filter and eighth-nerve model
[AD-A237454] N91-29757
The PC Dugout micro-mainframe integration system: PAX implementation
[AD-A237480] N91-29758
Modification of programs CHIEF and CID to compute sound radiation from an arbitrary body with mixed boundary conditions
[AD-A237502] N91-29759
Implementation of an exact penalty function formulation to solve convex nonlinear programming problems
[AD-A237905] N91-29761
A common interface real-time multiprocessor operating system for embedded systems
[AD-A238445] N91-29770
Lazy task creation: A technique for increasing the granularity of parallel programs
[AD-A237477] N91-29781
Expert systems on multiprocessor architectures. Volume 1: Summary
[AD-A238046] N91-29786
Expert systems on multiprocessor architectures. Volume 2: Technical reports
[AD-A238047] N91-29787
The advanced software development and commercialization project
[DE91-015756] N91-29797
Piecework linear least-squares approximation planar curves including computer programs
[NRC-31069] N91-29811
A framework for understanding the strategic defense initiatives' software debates
[AD-A237193] N91-29852
Parametric design calculations using Green's function to determine unique source
[DE91-014683] N91-29861
A simulation of the instrument pointing system for the Astro-1 mission
[NASA-TM-103547] N91-30061
COMPUTER STORAGE DEVICES
A high-performance retargetable simulator for parallel architectures
[AD-A237354] N91-29779
Counting networks
[AD-A237475] N91-29780
The MIT Alewife machine: A large-scale distributed-memory multiprocessor
[AD-A237705] N91-29784
Performance implications of synchronization support for parallel FORTRAN programs
[AD-A238493] N91-29790
Persistent data/knowledge base
[AD-A237498] N91-30048
COMPUTER SYSTEMS DESIGN
A general graphical user interface for automatic reliability modeling
[NASA-TM-104068] N91-29745
COMPUTER SYSTEMS PERFORMANCE
The design of a real-time adaptive filter development system
[AD-A237134] N91-29448
Discretionary security for object-oriented database systems
[AD-A237573] N91-29740
Operational concept document for the Next Generation Computer Resources (NGCR) operating systems interface standard baseline
[AD-A237501] N91-29782
Using the Harmony operating system: Release 3.0
[ERA-377] N91-29799
COMPUTER SYSTEMS PROGRAMS
A high-performance retargetable simulator for parallel architectures
[AD-A237354] N91-29779
COMPUTER TECHNIQUES
Methodology investigation, aviation test management system concept development
[AD-A237349] N91-29172
The optimal location of GEODSS sensors in Canada
[AD-A238444] N91-29216
Coding for spread-spectrum channels in the presence of jamming
[AD-A238233] N91-29425
The PC Dugout micro-mainframe integration system: PAX implementation
[AD-A237480] N91-29758
Implementation of an exact penalty function formulation to solve convex nonlinear programming problems
[AD-A237905] N91-29761
Fault-tolerant computing: An overview
[NASA-CR-188793] N91-29769
Transfer of 4GL application from INGRES to ORACLE
[AD-A238448] N91-29771
User's guide to the (NCARAI) artificial intelligence technical library
[AD-A237270] N91-29802
High bandwidth diagnosis within the framework of a microcomputer-based intelligent tutoring system
[AD-A237959] N91-29805
Data abstraction, concurrency and synchronization in Sina
[PB91-185454] N91-30053
COMPUTER VISION
Vision-based navigation and parallel computing
[AD-A238570] N91-29164
Theory and computer simulation of the interactional neural network
[NRC-30269] N91-29800
Proceedings of the 1st Workshop on Proximity Graphs
[AD-A237250] N91-29818
COMPUTERIZED SIMULATION
Numerical propulsion system simulation: An interdisciplinary approach
[NASA-TM-105181] N91-29221
Pressure measurements in a low-density nozzle plume for code verification
[NASA-TM-105170] N91-29228

Supersonic combustion of a transverse injected H2 jet in a radio frequency heated flow
[DE91-014739] N91-29281
Molecular dynamics simulation of the effect of interfaces in melting and solid-state amorphization
[DE91-015550] N91-29284
Equation of state for pure sodium chloride
[DE91-014618] N91-29286
Quasi-static modeling of chain-dynamics in the amorphous glassy polycarbonate of 4,4'-isopropyledenediphenol
[AD-A237289] N91-29343
Nonlinear computerized methodology. A: Angle of arrival estimation. B: Data modeling and identification
[AD-A237564] N91-29415
Computational simulations of plasma flow switches and imploding loads
[DE91-014768] N91-29480
Modification of the 'TEACH' computer code for use in a study of swirling turbulent flows
[DE91-010492] N91-29496
A numerical study of flow past a cylindrical body N91-29497
Shockwave considerations for sub-grid closure modeling in turbulent large eddy simulations
[DE91-015142] N91-29506
Control of flow over a backward facing step
[AD-A238638] N91-29521
Multipixel multidimensional laser radar system theory
[AD-A238110] N91-29573
Probabilistic lifetime strength of aerospace materials via computational simulation
[NASA-CR-187178] N91-29629
Three-dimensional visualization for evaluating automated, geomorphic pattern-recognition analyses of crustal structures
[DE91-012929] N91-29668
Acoustic tomographic estimate of ocean advective heat flux: A numerical assessment in the Norwegian Sea
[AD-A237100] N91-29698
Cognition and the brain
[AD-A237846] N91-29727
Analog design verification with PSpice and MICRO-CAP 3
[AD-A237922] N91-29762
Simulation methodology
[AD-A238113] N91-29765
A high-performance retargetable simulator for parallel architectures
[AD-A237354] N91-29779
Optimal iterative task scheduling for parallel simulations
[AD-A238631] N91-29791
Visualizing performance of parallel programs
[DE91-014966] N91-29793
Design and hardware implementation of neural systems
[AD-A237703] N91-29804
Numerical simulation of self-field MPD thrusters
[NASA-CR-187168] N91-29832
The atomic strain tensor
[AD-A237287] N91-29877
Vlasov simulations of very-large-amplitude wave generation in the plasma wakefield accelerator
[AD-A237428] N91-29961
Electromagnetic PIC simulations using finite elements on unstructured grids
[DE91-015141] N91-29962
Towards a realistic plasma simulation code
[DE91-015699] N91-29967
High resolution electron microscopy of grain boundaries
[DE91-010593] N91-29970
Correlations between grain boundary structure and energy
[DE91-015204] N91-29990
Connection between grain boundary structure and energy
[DE91-015558] N91-30030

COMPUTERS

Strain gauge cabling, conditioning, and sensitivity calculations for the CT-114 (Tutor) aircraft aft fuselage and empennage full-scale fatigue test
[NAE-LTR-ST-1758] N91-29534
Alsys Limited, Alsycomp 017, version 5.2, MICRO VAX 2 under Micro VMS V5.3 (host) to INMOS T425 transputer implemented on a B403 TRAM (target), 901118N1.11064
[AD-A237411] N91-29738

CONCENTRATION (COMPOSITION)

CO2 measurements along the WOCE P-16 and 19 sections in the South Pacific Ocean: A joint LDGO/WHOI program
[DE91-015742] N91-29708

CONCRETES

Performance of asphalt concrete airport pavements during thaw weakening periods: A field study
[AD-A237441] N91-29198

CONCURRENT PROCESSING

Multi-sensor image interpretation using laser radar and thermal images
[AD-A238245] N91-29576
Data abstraction, concurrency and synchronization in Sina
[PB91-185454] N91-30053

CONDENSATION NUCLEI

An observational study of the efficiency of activation of accumulation-mode particles in warm continental stratiform clouds
[DE91-013335] N91-29681

CONDENSATION PUMPS

Effect of geometric parameters on the performance of second throat annular steam ejectors
[AD-A238645] N91-29522

CONDENSED MATTER PHYSICS

Inelastic scattering in condensed matter with high intensity Moessbauer radiation
[DE91-014384] N91-29980

CONDUCTING POLYMERS

Method of obtaining current-conducting polymeric materials
[AD-A237174] N91-29339
Electronic and ionic transport in processable conducting polymers
[AD-A238175] N91-29362

CONDUCTION ELECTRONS

Electrical, magnetic, and spectroscopic properties of tetrathiafulvalene charge transfer compounds with iron, ruthenium, rhodium, and iridium halides
[AD-A237607] N91-29273

CONDUCTORS

Numerical methods for scattering from electrically large objects
[AD-A238262] N91-29426
The ac losses in type-2 superconductors
[DE91-015201] N91-29485

CONFERENCES

Whipple bumper shield simulations
[NASA-TM-105089] N91-29213
NASA workshop on impact damage to composites
[NASA-CP-10075] N91-29240
Workshop proceedings: Toughening Mechanisms in Quasi-Brittle Materials
[AD-A238289] N91-29248
Proceedings of the First Switch Tube Advanced Technology Meeting
[DE91-012634] N91-29440
The 2nd Workshop on High Temperture Electronics (Metallization and Packaging)
[DE91-014332] N91-29442
Annual Electronics Manufacturing Seminar proceedings
[AD-A238017] N91-29467
Hardware Implementation of Neuron Nets and Synapses Workshop
[AD-A237704] N91-29718
The 6th Workshop on the Mathematical Foundations of Programming Semantics
[AD-A237754] N91-29760
A Workshop on the Integration of Numerical and Symbolic Computing Methods
[AD-A238601] N91-29774

CONFIDENCE LIMITS

Combining CL (Confidence Limits) and PL (Partial Limits) displays
[AD-A238507] N91-29830
Confidence bands for the median survival time as a function of the covariates in the Cox model
[AD-A237626] N91-29835
The utility of elliptical and circular confidence regions for HFDF receivers
[AD-A238390] N91-29842

CONFIGURATION MANAGEMENT

Configuration management concepts document. National PDES testbed report series
[PB91-194480] N91-29391

CONGRESSIONAL REPORTS

Report to the Congress on the Strategic Defense Initiative, 1991
[AD-A237658] N91-29853

CONSERVATION LAWS

Statistical mechanics of two-dimensional Euler equations and Jupiter's Great Red Spot N91-29498

CONSOLIDATION

Consolidation and plasticity of Bi-Sr-Ca-Cu-O superconductors
[DE91-015544] N91-30028

CONSTITUTIVE EQUATIONS

Probabilistic lifetime strength of aerospace materials via computational simulation
[NASA-CR-187178] N91-29629

CONTAINMENT

Advanced materials for space nuclear power systems
[NASA-TM-105171] N91-29298

CONTAMINANTS

A methodology for inhibiting the formation of pollutants in diesel engines
[DE90-011615] N91-29584
Characterization of surface contaminants using infrared microspectroscopy
[DE91-009405] N91-29605
Numerical modeling of turbulent dispersion around structures using a particle-in-cell method
[DE91-012035] N91-29652

CONTAMINATION

Characterization of surface contaminants using infrared microspectroscopy
[DE91-009405] N91-29605

CONTINUUM MECHANICS

Differential equations and continuum mechanics
[AD-A237722] N91-29820

CONTINUUMS

Problems in nonlinear continuum dynamics
[AD-A237844] N91-29512

CONTOURS

GPS: Aspects of pseudo-range positioning offshore N91-29161

CONTRAST

The effects of luminance boundaries on color perception
[AD-A237794] N91-29925

CONTROL EQUIPMENT

Sliding mode controller of RF cavity tuning loop
[DE91-015461] N91-29410

CONTROL SIMULATION

An investigation into the use of side-arm control for civil rotorcraft applications
[AD-A226628] N91-29190
A simulation evaluation of a four-engine jet transport using engine thrust modulation for flightpath control
[NASA-TM-4324] N91-29194
A simulation of the instrument pointing system for the Astro-1 mission
[NASA-TM-103547] N91-30061

CONTROL SYSTEMS DESIGN

A linear control design structure to maintain loop properties during limit operation in a multi-nozzle turbofan engine
[NASA-TM-105163] N91-29188
An investigation into the use of side-arm control for civil rotorcraft applications
[AD-A226628] N91-29190
Experimental demonstration of a classical approach for flexible space structure control: NASA CSI testbeds
[NASA-CR-188724] N91-29212
Integrated structural damping and control system design for high-order flexible systems N91-29617
Using the Harmony operating system: Release 3.0
[ERA-377] N91-29799

CONTROL THEORY

Controlling crippled aircraft-with throttles
[NASA-TM-104238] N91-29191
Compensation of distributed delays in integrated communication and control systems
[NASA-CR-187136] N91-29193
A simulation evaluation of a four-engine jet transport using engine thrust modulation for flightpath control
[NASA-TM-4324] N91-29194
Force-reflecting control of a teleoperated system coupling a nonredundant master with a redundant slave
[DE90-012137] N91-29585
Robust design of multivariable control: An interval arithmetic approach
[AD-A238006] N91-29806
An expert system approach to global fault detection and isolation design
[AD-A238494] N91-29808

CONTROLLABILITY

An investigation into the use of side-arm control for civil rotorcraft applications
[AD-A226628] N91-29190

CONTROLLED FUSION

Stagnation and interpenetration of laser-created colliding plasmas
[DE91-013244] N91-29946

CONTROLLERS

Compensation of distributed delays in integrated communication and control systems
[NASA-CR-187136] N91-29193
Sliding mode controller of RF cavity tuning loop
[DE91-015461] N91-29410

Force-reflecting control of a teleoperated system coupling a nonredundant master with a redundant slave [DE90-012137] N91-29585
Singularity avoidance and the kinematics of an eight-revolute-joint manipulator N91-29588
Effects of colocation and non-colocation of sensors and actuators on flexible structures [AD-A238457] N91-29844

CONVECTION
Secondary stability and three-dimensional natural convection in a shallow cavity N91-29495
An investigation of the ERICA IOP-2 cyclone using the NORAPS model [AD-A237683] N91-29684

CONVECTIVE FLOW
Course lectures abstracts of participants fellows project reports [AD-A237909] N91-30070

CONVERGENCE
Solutions of two-dimensional Euler equations with multigrid acceleration [NAL-PD-CF-9006] N91-29494
Primal-dual methods for linear programming [AD-A237418] N91-29756

CONVERGENT-DIVERGENT NOZZLES
Divergence thrust loss calculations for convergent-divergent nozzles: Extensions to the classical case [NASA-TM-105176] N91-29181

CONVERTERS
Physical concepts and modeling procedures for picosecond and subpicosecond distributed circuits [AD-A238592] N91-29472

COOLANTS
Bearing tester data compilation analysis, and reporting and bearing math modeling [NASA-CR-178883] N91-29603

COOLING
Energy conserving coating: Pigment research [AD-A237841] N91-29356

COOLING FINS
Heat transfer and pressure drop in a compact pin-fin heat exchanger with pin orientation at 18 deg to the flow direction [NASA-CR-186544] N91-29527

COOLING SYSTEMS
Light weight space power reactors for nuclear electric propulsion [DE91-014803] N91-29232
Short-pulse glass slab amplifier [DE91-015385] N91-29580
A methodology for developing physical system fault diagnostic aids [DE91-015533] N91-29809

COOPERATION
Experiments in adaptive control of cooperating manipulators N91-29594

COORDINATE TRANSFORMATIONS
Research and development for Digital Voice Processing (DVP) [AD-A238280] N91-29427

COORDINATES
GPS: Aspects of pseudo-range positioning offshore N91-29161
Hamiltonian 3-D ray tracing in the oceanic waveguide on the ellipsoidal earth [AD-A237458] N91-29700

COORDINATION
Counting networks [AD-A237475] N91-29780

COPOLYMERIZATION
Model filled polymers 9: Synthesis of uniformly crosslinked polystyrene microbeads [AD-A237472] N91-29352
Organo- borazines.3.homo- and copolymerization of p-vinylphenyl- cyclotri- borazines [AD-A237881] N91-29357

COPOLYMERS
Light scattering characterization of polymer additives and correlation of molecular properties of polymer fluids [AD-A238547] N91-29367

COPPER
Thermal emittance enhancement of graphite-copper composites for high temperature space based radiators [NASA-TM-105178] N91-29332
Deformation behavior of pre-shocked copper as a function of strain rate and temperature [DE91-015180] N91-29620
Electron microscopy of thick 304 SS-copper multilayers [DE91-011116] N91-29972

COPPER ALLOYS
Lead-free solders for electronics applications: Wetting analysis [DE91-014900] N91-29320

COPPER OXIDES
Photoemission and electronic structure studies of YBa2Cu3O(x) [DE91-014469] N91-29979
High temperature Knudsen effusion-mass spectrometric studies of the Y-Ba-Cu-O system [NIAR-91-23] N91-29981
Photoemission measurement of Fermi surface, band dispersion, and quasiparticle lifetime in YBa2Cu3O6.9 [DE91-015194] N91-29989
Consolidation and plasticity of Bi-Sr-Ca-Cu-O superconductors [DE91-015544] N91-30028

CORIOLIS EFFECT
Theoretical study of the flow in a rotating duct. Experimental study through flow visualization in a curved duct [RAE-TRANS-2189] N91-29493

CORONAL LOOPS
Plasma properties of hot coronal loops utilizing coordinated SMM and solar research rocket observations [NASA-CR-186094] N91-29937

CORRECTION
Parameter estimation via nonlinear differential correction least square method [NAL-PD-FC-9110] N91-29814
Application of diffraction correction to blackbody sources [AD-A237840] N91-29926

CORRELATION
Adiabatic two-phase flow frictional pressure drop. Part 2: A generalized method for data correlation [DE91-014462] N91-29501
Basic mechanisms of diesel lubrication correlation of bench and engine tests [AD-A237685] N91-29596
Correlations between grain boundary structure and energy [DE91-015204] N91-29990

CORROSION
Characteristics of autoclave and in-reactor nodular corrosion of Zircaloys [DE91-013600] N91-29294
Biofouling and corrosion fouling of plain and enhanced aluminum surfaces [DE91-014464] N91-29300
The role of microorganisms in marine corrosion [AD-A237062] N91-29308
Corrosion behavior of continuous-filament-wound ceramic composite tubes [DE91-014959] N91-29370

CORROSION PREVENTION
A novel epoxy lacquer for high strength steel in F-111 aircraft during overhaul [AD-A236828] N91-29326

CORROSION RESISTANCE
Biofouling and corrosion fouling of plain and enhanced aluminum surfaces [DE91-014464] N91-29300
Mechanical properties of Fe3Al-based alloys [DE91-015322] N91-29324

CORROSION TESTS
Characteristics of autoclave and in-reactor nodular corrosion of Zircaloys [DE91-013600] N91-29294

COSMIC RAYS
The ASTROMAG superconducting magnet facility configured for a free flying satellite [DE91-014710] N91-29204
Research in nuclear astrophysics: Stellar collapse and supernovae [DE91-015449] N91-30066

COSMOLOGY
The ASTROMAG superconducting magnet facility configured for a free flying satellite [DE91-014710] N91-29204

COST ANALYSIS
Resource envelope concepts for mission planning [NASA-TP-3139] N91-29209
ALS rocket engine combustion devices design and demonstration [NASA-CR-183824] N91-29233
Electric rate structures for thermal energy storage evaluation [DE91-013168] N91-29644
Slaying the software dragon: A look at how software engineering, the Ada programming language and process maturity are changing software development [AD-A237156] N91-29751

COUETTE FLOW
A finite element solver for 3-D compressible viscous flows [NASA-CR-184175] N91-29488

COULOMB COLLISIONS
Physical properties and structure of ion-containing polymers [AD-A238196] N91-29363

COUNTING
Counting networks [AD-A237475] N91-29780

COUPLING
Quick disconnect pressure cap [AD-D014936] N91-29598

COVARIANCE
Spectra and covariances for classical nonlinear signal processing problems involving class A non-Gaussian noise [AD-A237388] N91-29413
Confidence bands for the median survival time as a function of the covariates in the Cox model [AD-A237626] N91-29835

CRACK GEOMETRY
Fission-fusion adaptivity in finite elements for nonlinear dynamics of shells [AD-A238029] N91-29626

CRACK PROPAGATION
Micromechanisms of monotonic and cyclic subcritical crack growth in advanced high melting point low-ductility intermetallics [AD-A238151] N91-29317
A study of the relationship between macroscopic measures and physical processes occurring during N00014-89-J-1708 [AD-A238423] N91-29627

CRASHWORTHINESS
Flutter consideration of a crash-test aircraft [DE91-015094] N91-29192

CREEP PROPERTIES
Rejuvenation of service exposed alloy 713C turbine blades [NAE-LTR-ST-1716] N91-29179
Strengthening mechanisms, creep, and fatigue processes in dispersion hardened niobium alloy [AD-A237784] N91-29313
Low temperature flux creep in high-T(sub c) superconductors [DE91-015193] N91-29988

CREEP STRENGTH
Lightweight disk alloy development [AD-A237064] N91-29309

CRITICAL POINT
Thermophysical properties of supercritical fluids and fluid mixtures [DE91-015794] N91-30041

CRITICAL TEMPERATURE
Specific heat of YBaCu3O7: Volume fraction of superconductivity; parameters characteristic of the ideal superconducting state [DE91-011827] N91-29974
Thermophysical properties of supercritical fluids and fluid mixtures [DE91-015794] N91-30041

CROSS FLOW
Experimental study of cross-stream mixing in a cylindrical duct [NASA-TM-105180] N91-29187

CROSS SECTIONS
Electron-ion interaction cross sections determined by x ray spectroscopy on EBIT [DE91-015786] N91-29903
Electromagnetic dissociation of Au and Co targets by relativistic heavy ions [DE91-014915] N91-29906

CROSSED FIELDS
A high power cross-field amplifier at X-Band [DE91-013277] N91-29441

CROSSLINKING
Pulse induced nanlithography of graphite in H2O: A road to chemical linkages to the surface? [AD-A237086] N91-29338
Model filled polymers 8: Synthesis of crosslinked polymeric beads by seed polymerization [AD-A237429] N91-29349
Model filled polymer 7: Flow behavior of polymers containing monodisperse crosslinked polymeric beads [AD-A237430] N91-29350
Model filled polymers 9: Synthesis of uniformly crosslinked polystyrene microbeads [AD-A237472] N91-29352
The cure of rigid polyurethane encapsulating foam [DE91-016059] N91-29379

CRYOGENIC COOLING
Telescope and sensor interface preliminary requirements report for the PORTS chamber [AD-A237755] N91-29923

CRYOGENIC FLUIDS
NASA cryogenic fluid management space experiment efforts, 1960-1990 [NASA-TM-103752] N91-30073

CRYOGENICS
The ASTROMAG superconducting magnet facility configured for a free flying satellite
[DE91-014710] N91-29204
Minimization of refrigeration power requirements for mechanical supports in cryogenic systems
[DE91-015720] N91-29392
Qualitative investigation of cryogenic injected shock dissipation
[NASA-TM-105140] N91-29525
Advanced divertor experiments on DIII-D
[DE91-011138] N91-29950

CRYOPUMPING
Measurements of retractable gas-cooled 6061 aluminum electrical leads operating in a vacuum
[DE91-014617] N91-29444

CRYSTAL DEFECTS
Effect of excess oxydianiline on the properties of polyimide
[AD-A237467] N91-29351
NMR spectroscopy of experimentally shocked silicate minerals
[DE91-014897] N91-29898
High resolution electron microscopy of grain boundaries
[DE91-010593] N91-29970
Defect characterization of electronic conducting pseudo-perovskite systems
[DE91-014385] N91-29978
Defect reductions in epitaxial growth using superlattice buffer layers
[AD-A237710] N91-30005
On the role of crystal defects as sources of resonator frequency instability
[AD-A238505] N91-30018

CRYSTAL DISLOCATIONS
Fundamental studies in dynamic plasticity
[AD-A237114] N91-29621

CRYSTAL GROWTH
Thermochemistry of hydrocarbon decomposition and relationship to properties of PECVD diamond films
[AD-A237793] N91-29274
Effect of excess oxydianiline on the properties of polyimide
[AD-A237467] N91-29351
Fundamental studies of chemical vapor deposition diamond growth processes
[DE91-015324] N91-29374
Center for thin film studies
[AD-A237457] N91-29999
Growth, characterization, and device development in monocrystalline diamond films
[AD-A237463] N91-30000
Pressure effects in the microwave plasma growth of polycrystalline diamond
[AD-A237751] N91-30006

CRYSTAL LATTICES
Deconvolution of x ray diffraction data to elucidate plastic deformation mechanisms in the uniaxial extension of bulk Nylon-6
[AD-A237332] N91-29623
High resolution electron microscopy of grain boundaries
[DE91-010593] N91-29970

CRYSTAL OPTICS
Second-harmonic generation of TEA CO2 10.6 micrometer laser light in AgGaS2 crystals
[AD-A237169] N91-29564

CRYSTAL STRUCTURE
Theoretical studies of solid-fluid phase equilibria
[DE91-014811] N91-29287
Materials science applications of a 120 kV FEG TEM/STEM: Triskaidekaphilia
[DE91-010136] N91-29536
Deconvolution of x ray diffraction data to elucidate plastic deformation mechanisms in the uniaxial extension of bulk Nylon-6
[AD-A237332] N91-29623
Atomic-resolution scanning tunneling microscopy and infrared spectroscopy as combined in-situ probes of electrochemical adlayer structure: Carbon monoxide on rhodium(111)
[AD-A237508] N91-29884
Electron microscopy of thick 304 SS-copper multilayers
[DE91-011116] N91-29972
Ruddlesden-Popper phases $A(n+1)M(n)O(3n+1)$: Structures and properties
[DE91-011748] N91-29973
Defect characterization of electronic conducting pseudo-perovskite systems
[DE91-014385] N91-29978
Growth condition dependence of RHEED pattern from GaAs(111)B surface
[DE91-014770] N91-29986
High-resolution Z-contrast imaging of superlattices and heterostructures
[DE91-015329] N91-29994
Responsivity uniformity enhancements for Backside-Illuminated Charge-Coupled Devices (BICCDs) by excimer laser-assisted etching
[AD-A237435] N91-29997
Surface structure and surface order
[AD-A237466] N91-30001
A study of the liquid-solid interface during rapid resolidification of cooper-titanium using molecular dynamics
[AD-A238634] N91-30022
Connection between grain boundary structure and energy
[DE91-015558] N91-30030
Formation of CoSi2 in SIMOX wafers by high dose Co implantation
[DE91-015639] N91-30036

CRYSTAL SURFACES
Comparisons between scanning tunneling microscopy and outer-sphere electron-transfer rates at Pt(111) surfaces coated with ordered iodine adlayers
[AD-A237507] N91-29883
Atomic-resolution scanning tunneling microscopy and infrared spectroscopy as combined in-situ probes of electrochemical adlayer structure: Carbon monoxide on rhodium(111)
[AD-A237508] N91-29884
Growth condition dependence of RHEED pattern from GaAs(111)B surface
[DE91-014770] N91-29986
Influence of diamond turning and surface cleaning processes on the degradation of KDP crystal surfaces
[DE91-015300] N91-30035

CRYSTALLINITY
NMR spectroscopy of experimentally shocked silicate minerals
[DE91-014897] N91-29898

CRYSTALLIZATION
Inelastic deformation and fracture of glassy solids
[AD-A237290] N91-29344

CRYSTALLOGRAPHY
Responsivity uniformity enhancements for Backside-Illuminated Charge-Coupled Devices (BICCDs) by excimer laser-assisted etching
[AD-A237435] N91-29997
TEM characterization of grain boundaries in mixed bicrystal films of aluminum
[DE91-016267] N91-30038

CRYSTALS
Morphology of bulk Nylon 6 subjected to plane strain compression
[AD-A237331] N91-29622
Electro-optic line narrowing of optical parametric oscillators
[AD-D014944] N91-29934
Development of model based magnetic LP-LEC growth large diameter GaAs
[AD-A237456] N91-29998
Optical and environmentally protective coatings for Potassium Dihydrogen Phosphate (KDP) harmonic converter crystals
[DE91-015296] N91-30034

CUMULUS CLOUDS
An investigation of the ERICA IOP-2 cyclone using the NORAPS model
[AD-A237683] N91-29684

CURIE TEMPERATURE
Monte Carlo and mean field calculations of the magnetocaloric effect of ferromagnetically interacting clusters
[DE91-014792] N91-29859

CURING
Dual cure photocatalyst systems
[DE91-014174] N91-29369
The cure of rigid polyurethane encapsulating foam
[DE91-016059] N91-29379

CURVES (GEOMETRY)
Piecework linear least-squares approximation planar curves including computer programs
[NRC-31069] N91-29811

CYANIDES
Electrochemical contact adsorption site changes driven by field and charge fact and theory
[AD-A237127] N91-29269

CYANOGEN
Study of elementary reactions and energy transfer processes involving the NH and CN free radicals
[AD-A238461] N91-29889

CYCLIC HYDROCARBONS
Mechanism of anionic ring-opening polymerization of silacyclopent 3-enes
[AD-A237538] N91-29353

CYCLIC LOADS
Experimental stress measurements for the modified Indal Series 6400 VAWT
[NAE-LTR-LA-310] N91-29642

CYCLOGENESIS
An investigation of the ERICA IOP-2 cyclone using the NORAPS model
[AD-A237683] N91-29684
TOVS satellite soundings of the ERICA IOP-2 cyclone
[AD-A237998] N91-29686
Performance report of the Wind Research Lab.
[AD-A238575] N91-29691

CYCLONES
Tropical cyclone motion in the northwest Pacific Ocean, phase 1
[AD-A237455] N91-29683
TOVS satellite soundings of the ERICA IOP-2 cyclone
[AD-A237998] N91-29686
Forcasting tropical cyclone recurvature using an empirical othogonal function representation of vorticity fields
[AD-A238489] N91-29689
Performance report of the Wind Research Lab.
[AD-A238575] N91-29691

CYCLOTRON FREQUENCY
Fundamental studies of fusion plasmas
[DE91-015656] N91-29964

CYCLOTRON RESONANCE
Anomalous ion heating from the dynamo in a reversed field pinch
[DE91-015586] N91-29966

CYLINDRICAL BODIES
Experimental study of cross-stream mixing in a cylindrical duct
[NASA-TM-105180] N91-29187
The ac losses in type-2 superconductors
[DE91-015201] N91-29485
Plasma and electrical diagnostics for Procyon experiments
[DE91-014736] N91-29952

CYLINDRICAL COORDINATES
A method for computing fields near the origin of a cylindrical coordinate system in time domain finite-difference electromagnetic simulations
[DE91-015431] N91-29433

CYLINDRICAL SHELLS
Penn State/ONR Mid Frequency Workshop
[AD-A237982] N91-29420

CZOCHRALSKI METHOD
Development of model based magnetic LP-LEC growth large diameter GaAs
[AD-A237456] N91-29998

D

DAMAGE
Debris/ice/TPS assessment and photographic analysis for Shuttle Mission STS-40
[NASA-TM-103822] N91-29210
Preparation of damage resistant optical coatings on flat substrates
[DE91-013588] N91-29916

DAMAGE ASSESSMENT
Compendium of material test results on HY-100 and pseudo HY-100 metals in support of US Navy programs
[DE91-013134] N91-29292

DARK MATTER
The ASTROMAG superconducting magnet facility configured for a free flying satellite
[DE91-014710] N91-29204
Dark matter in the universe
[DE91-014863] N91-30065

DATA ACQUISITION
Evaluation of aircraft turbine engine redesigns
[AD-A237599] N91-29184
Strain gauge cabling, conditioning, and sensitivity calculations for the CT-114 (Tutor) aircraft aft fuselage and empennage full-scale fatigue test
[NAE-LTR-ST-1758] N91-29534
Oceanographic data report Number 8: Density profiles from the Delaware Estuary, October 1986 - September 1988
[PB91-183608] N91-29707
Data acquisition system for collecting biophysical and physiological data
[AD-A237654] N91-29710
Hyperdimensional data analysis and structural inference
[AD-A238097] N91-29764
A high-performance retargetable simulator for parallel architectures
[AD-A237354] N91-29779

Limitations to the method of power spectrum analysis: Nonstationarity, biased estimators, and weak convergence to normality
[DE91-008583] N91-29812

DATA BASE MANAGEMENT SYSTEMS

User's guide to the (NCARAI) artificial intelligence technical library
[AD-A237270] N91-29802

Guide to design, implementation and management of distributed databases
[PB91-187567] N91-30054

DATA BASES

Research and development for Digital Voice Processing (DVP)
[AD-A238280] N91-29427

Bearing tester data compilation analysis, and reporting and bearing math modeling
[NASA-CR-178883] N91-29603

An AVHRR data set for the arctic leads ARI
[AD-A237221] N91-29637

XTRAN: An atmospheric transmittance code based on XSCALE
[AD-A237624] N91-29674

DNA optical support program summary for 1989
[AD-A238397] N91-29679

A global geographic information system data base of storm occurrences and other climatic phenomena affecting coastal zones
[DE91-014949] N91-29682

Performance report of the Wind Research Lab.
[AD-A238575] N91-29691

Acoustic tomographic estimate of ocean advective heat flux: A numerical assessment in the Norwegian Sea
[AD-A237100] N91-29698

Discretionary security for object-oriented database systems
[AD-A237573] N91-29740

An automated software system for updating digital terrain databases from all-source imagery, phase 1
[AD-A237105] N91-29748

A common interface real-time multiprocessor operating system for embedded systems
[AD-A238445] N91-29770

Second Review of the Department of Energy's Inertial Confinement Fusion Program
[DE91-013157] N91-29945

Persistent data/knowledge base
[AD-A237498] N91-30048

Guide to design, implementation and management of distributed databases
[PB91-187567] N91-30054

Information Systems Inventory (ISI)
[PB91-172940] N91-30055

DATA CONVERSION ROUTINES

VLSI circuit techniques and technologies for ultrahigh speed data conversion interfaces
[AD-A238115] N91-29468

DATA FLOW ANALYSIS

Specification and verification of real-time constraints in coarse-grain dataflow
[AD-A237355] N91-30047

DATA MANAGEMENT

Configuration management concepts document. National PDES testbed report series
[PB91-194480] N91-29391

Specification and verification of real-time constraints in coarse-grain dataflow
[AD-A237355] N91-30047

Guide to design, implementation and management of distributed databases
[PB91-187567] N91-30054

Information Systems Inventory (ISI)
[PB91-172940] N91-30055

DATA PROCESSING

Diagnostic support services for LLNL (Lawrence Livermore National Laboratory) NOVA laser experiments
[DE90-012125] N91-29552

Randomization procedures applied to analysis of ballistic data
[AD-A238389] N91-30050

DATA PROCESSING TERMINALS

A general lease-squares fitting package for the sun workstation
[AD-A238180] N91-29837

DATA RECORDERS

QBDATAMT: A computer program to read Datamyte recorder data into an IBM PC or compatible computer
[NAE-LTR-ST-547] N91-29742

DATA REDUCTION

Randomization procedures applied to analysis of ballistic data
[AD-A238389] N91-30050

DATA SAMPLING

VLSI circuit techniques and technologies for ultrahigh speed data conversion interfaces
[AD-A238115] N91-29468

On the analysis of grouped survival data using cumulative occurrence/exposure rates
[AD-A238219] N91-29838

DATA STORAGE

Research and development for Digital Voice Processing (DVP)
[AD-A238280] N91-29427

Video frame store: An advanced solid state recorder
[DE91-015709] N91-29549

ASAT monitoring project at LLNL
[DE91-013247] N91-29850

DATA TRANSFER (COMPUTERS)

QBDATAMT: A computer program to read Datamyte recorder data into an IBM PC or compatible computer
[NAE-LTR-ST-547] N91-29742

DATA TRANSMISSION

Application of Multi-Frequency Modulation (MFM) for high-speed data communications to a voice frequency channel
[AD-A238019] N91-29422

Physical concepts and modeling procedures for picosecond and subpicosecond distributed circuits
[AD-A238592] N91-29472

Research in mathematics and computer science: Calculation of the probability of undetected error for certain error detection codes, phase 2
[AD-A238234] N91-29768

DEACTIVATION

Deactivation by carbon of iron catalysts for indirect liquefaction
[DE91-011276] N91-29285

DEBRIS

Debris/ice/TPS assessment and photographic analysis for Shuttle Mission STS-40
[NASA-TM-103822] N91-29210

DECELERATION

Proton deceleration near the surface of an accreting neutron star N91-30063

DECISION MAKING

An alternative algorithm for discrete-time filtering
[AD-A238443] N91-29827

Heuristic methods in applied probability
[AD-A238229] N91-29841

Comparison of four methods for aggregating judgments from multiple experts
[DE91-013522] N91-30043

DECISION THEORY

A manual method for determining the fractional stability category
[AD-A237627] N91-29675

An alternative algorithm for discrete-time filtering
[AD-A238443] N91-29827

DECODERS

A high data rate communications system using long pulses
[AD-D014947] N91-29430

DECOMPOSITION

Thermochemistry of hydrocarbon decomposition and relationship to properties of PECVD diamond films
[AD-A237793] N91-29274

Ceramic decomposition under irradiation
[DE91-015061] N91-29372

Computational and theoretical aspects of nonlinear partial differential equations
[AD-A238495] N91-29829

Reactions of hydrogen atoms important to the decomposition of energetic materials
[AD-A238482] N91-29890

DECONTAMINATION

The Department of Energy's solar industrial program: New ideas for American industry
[DE91-002197] N91-29649

Ultraviolet reflector materials for solar detoxification of hazardous waste
[DE91-002196] N91-29663

DEFENSE PROGRAM

Report to the Congress on the Strategic Defense Initiative, 1991
[AD-A237658] N91-29853

DEFORMATION

Mechanisms of transformation toughening
[DE91-013151] N91-29293

Postirradiation deformation of ferritic Fe-Cr binary alloys
[DE91-014856] N91-29295

Deformation and thermal fatigue in high temperature austenitic alloys
[DE91-014981] N91-29305

Deformation induced microstructural and microchemical changes during thermomechanical treatment
[DE91-014862] N91-29319

Modeling and response analysis of thin-walled beam structures constructed of advanced composite materials N91-29615

Deformation behavior of pre-shocked copper as a function of strain rate and temperature
[DE91-015180] N91-29620

Morphology of bulk Nylon 6 subjected to plane strain compression
[AD-A237331] N91-29622

NIKE2D: A nonlinear, implicit, two-dimensional finite element code for solid mechanics
[DE91-015734] N91-29634

Regional tectonic deformation in Southern California, inferred from terrestrial geodesy and the global positioning system N91-29669

Mesoscale characteristics and the role of deformation on ocean dynamics
[AD-A237577] N91-29701

The atomic strain tensor
[AD-A237287] N91-29877

DEGRADATION

Methods to determine the compatibility and degradation of organic materials
[AD-A237940] N91-29234

Effect of geometric parameters on the performance of second throat annular steam ejectors
[AD-A238645] N91-29522

DEGREES OF FREEDOM

The functional dependence of trajectory dispersion on initial condition errors
[DE91-014661] N91-29151

Force-reflecting control of a teleoperated system coupling a nonredundant master with a redundant slave
[DE90-012137] N91-29585

Motion planning for manipulators with excessive degrees of freedom N91-29592

DEICING

Debris/ice/TPS assessment and photographic analysis for Shuttle Mission STS-40
[NASA-TM-103822] N91-29210

DELAMINATING

Effect of fiber-matrix debonding on notched strength of titanium metal matrix composites
[NASA-TM-104131] N91-29239

Impact characterization of graphite fiber reinforced thermoplastic laminates
[NIAR-91-16] N91-29241

DEMODULATION

Signal processing in impulsive electromagnetic interference
[AD-A237612] N91-29416

DENSIFICATION

Fabrication of silicon nitride ceramics by microwave heating
[DE91-015312] N91-29373

DENSIMETERS

Test of Newtonian gravity using DSV sea cliff
[AD-A238558] N91-29680

DENSITOMETERS

Analyzing photographically recorded atomic emission spectra using an automated densitometer
[DE91-015368] N91-29871

DENSITY DISTRIBUTION

Measurement of a three-dimensional hypersonic density field using holographic interferometry N91-29539

DENSITY WAVE MODEL

The relationship between the density wave, molecular gas and star formation in M51 N91-30064

DEPLOYMENT

SDI performance and START constraints: Modeling phase-1 defense engagements
[DE91-013305] N91-29849

DEPOLARIZATION

Aspects of fatigue and rapid depolarization in the film PZT capacitors
[DE91-014904] N91-29484

DEPOSITION

Structure and stability of underpotentially depositied layers on Au(111) studied by optical second harmonic generation
[AD-A237087] N91-29268

Inverse problem in neutron reflection
[DE91-014457] N91-29984

Atomic layer epitaxy group IV materials: Surface processes, thin films, devices and their characterization
[AD-A238506] N91-30019

DESIGN ANALYSIS

AEROWING - The software for aerodynamic analysis of a large aspect-ratio finite wing at low speeds
[NAL-PD-CF-9101] N91-29146

Evaluation of aircraft turbine engine redesigns
[AD-A237599] N91-29184

ALS rocket engine combustion devices design and demonstration
[NASA-CR-183824] N91-29233

Composite specimen design analysis. Volume 2: Experimental efforts
[AD-A238277] N91-29247

A prolog system for converting VHDL-based models to Generalized Extraction System (GES) rules
[AD-A238545] N91-29741
Real-time Ada design methodologies and their impact on performance
[AD-A237259] N91-29754
The 23rd Optoelectronic Workshop: Optical System Assessment for Design and Simulated Annealing
[AD-A238588] N91-29932

DESORPTION
Electrochemical contact adsorption site changes driven by field and charge fact and theory
[AD-A237127] N91-29269
Quantitative interpretation of auger lineshapes and electron/photon stimulated desorption
[AD-A237138] N91-29874
Laser probing of the kinetics and dynamics of III -V semiconductor growth
[AD-A237795] N91-30009

DETECTION
Environmental assessment for the FAA explosive detection system independent validation and verification program
[DE91-013190] N91-29152
An expert system approach to global fault detection and isolation design
[AD-A238494] N91-29808
Plan for a laser weapon verification research program
[DE90-012123] N91-29848
Auditory processing of complex sounds across frequency channels
[AD-A238023] N91-29862

DETECTORS
Environmental assessment for the FAA explosive detection system independent validation and verification program
[DE91-013190] N91-29152

DETERIORATION
Morphology of bulk Nylon 6 subjected to plane strain compression
[AD-A237331] N91-29622

DETONATION
Feasibility of a laser-ignited HMX deflagration-to-detonation transition device for the US Navy LITES Program
[DE91-015210] N91-29382
Impacts of a nominal nuclear electromagnetic pulse on electric power systems
[DE91-012991] N91-29401
Diode laser ignition of explosive and pyrotechnic components
[DE90-012227] N91-29553

DETONATORS
Feasibility of a laser-ignited HMX deflagration-to-detonation transition device for the US Navy LITES Program
[DE91-015210] N91-29382
Diode laser ignition of explosive and pyrotechnic components
[DE90-012227] N91-29553

DEUTERIUM
Hot atom reactive scattering and photodissociation experiments with acetylene and ethylene
[DE91-013755] N91-29264
Study of nuclear effects in the deuteron and extraction of neutron to proton stucture function ratio
[DE91-015484] N91-29873
Electron capture in very low energy collisions of multicharged ions with H and D in merged beams
[DE91-015617] N91-29909

DEUTERIUM COMPOUNDS
A calorimetric investigation of deuterated palladium electrodes
[AD-A237571] N91-29456

DEUTERONS
Study of nuclear effects in the deuteron and extraction of neutron to proton stucture function ratio
[DE91-015484] N91-29873

DIAMONDS
Thermochemistry of hydrocarbon decomposition and relationship to properties of PECVD diamond films
[AD-A237793] N91-29274
Annealing effects on the microstructure of titanium electrical contacts on diamond films
[DE91-010150] N91-29327
Synthesis of diamond films by microwave generated pulsed plasmas
[AD-A237228] N91-29341
Effects of interfacial modification on diamond film adhesion
[AD-A237750] N91-29354
Fundamental studies of chemical vapor deposition diamond growth processes
[DE91-015324] N91-29374
Growth, characterization, and device development in monocrystalline diamond films
[AD-A237463] N91-30000
Pressure effects in the microwave plasma growth of polycrystalline diamond
[AD-A237751] N91-30006
Epitaxial growth of single crystal diamond on silicon
[AD-A237758] N91-30007
Influence of diamond turning and surface cleaning processes on the degradation of KDP crystal surfaces
[DE91-015300] N91-30035

DIATOMIC MOLECULES
Theoretical studies of solid-fluid phase equilibria
[DE91-014811] N91-29287

DIELECTRIC POLARIZATION
Discreteness-of-solvent effects in Marcus equations in the mean spherical approximation
[AD-A237133] N91-29996

DIELECTRIC PROPERTIES
Comparison between the interfacial chemistry of metallized polyimides and polymide
[AD-A238400] N91-29366
Dielectric function of semiconductor superlattice
[DE91-617788] N91-29976

DIELECTRICS
Numerical methods for scattering from electrically large objects
[AD-A238262] N91-29426
On the role of crystal defects as sources of resonator frequency instability
[AD-A238505] N91-30018

DIESEL ENGINES
Investigation of particulate formation during diesel spray combustion
[DE90-008282] N91-29255
A methodology for inhibiting the formation of pollutants in diesel engines
[DE90-011615] N91-29584
Basic mechanisms of diesel lubrication correlation of bench and engine tests
[AD-A237685] N91-29596
Worldwide wind/diesel hybrid power system study: Potential applications and technical issues
[DE91-002160] N91-29643

DIESEL FUELS
Investigation of particulate formation during diesel spray combustion
[DE90-008282] N91-29255
A methodology for inhibiting the formation of pollutants in diesel engines
[DE90-011615] N91-29584

DIFFERENTIAL CALCULUS
ZLIB: A numerical library for differential algebra and Lie algebraic treatment of beam dynamics
[DE91-014875] N91-29746
A note on the automated differentiation of implicit functions
[DE91-015104] N91-29816

DIFFERENTIAL EQUATIONS
Response and stability analysis of helicopter rotor blades using computerized symbolic manipulation
[AD-A238660] N91-29175
Differential equations and continuum mechanics
[AD-A237722] N91-29820
Spatial propagation of squeezed light in a degenerate parametric amplifier
[DE91-014989] N91-30039

DIFFRACTION
Application of diffraction correction to blackbody sources
[AD-A237840] N91-29926
Diffraction-limited imaging of satellites using bispectral speckle interferometry
[DE91-015745] N91-30062

DIFFRACTION PATTERNS
An improved method of investigation of compressor blade fit using holographic interferometry
[AD-A238182] N91-29185

DIFFUSION
Defects and transport in mixed oxides
[DE91-014537] N91-29266
NMR characterization of porous ceramics
[DE91-015051] N91-29371
Analysis of condensation and evaporation of ammonia/water mixtures in matrix heat-exchangers
[DE91-014461] N91-29500
Near-stall loss measurements in a CD compressor cascade with exploratory leading edge flow control
[AD-A237497] N91-29509
Numerical modeling of turbulent dispersion around structures using a particle-in-cell method
[DE91-012035] N91-29652
Modeling a rain-induced mixed layer
[AD-A238022] N91-29702
Identification of, and transition to, the second region of ideal MHD stability in tokamaks
[DE90-010380] N91-29938

DIFFUSION COEFFICIENT
Atomic approaches to defect thermochemistry
[AD-A238260] N91-29280

DIFFUSION ELECTRODES
Cyclic voltammetric wave-shapes for microdisk electrodes: Coupled effects of solution resistance, double-layer capacitance, and finite electrochemical kinetics
[AD-A237505] N91-29455

DIFFUSION FLAMES
Combustion stability limits and planar imaging of swirl-stabilized flames N91-29262

DIFFUSION PUMPS
Twenty first century propulsion concept
[AD-A237853] N91-29224

DIGITAL DATA
Physical concepts and modeling procedures for picosecond and subpicosecond distributed circuits
[AD-A238592] N91-29472
A global geographic information system data base of storm occurrences and other climatic phenomena affecting coastal zones
[DE91-014949] N91-29682

DIGITAL SIMULATION
Acoustic tomographic estimate of ocean advective heat flux: A numerical assessment in the Norwegian Sea
[AD-A237100] N91-29698
Analog design verification with PSpice and MICRO-CAP 3
[AD-A237922] N91-29762

DIGITAL SYSTEMS
Assessment team report on flight-critical systems research at NASA Langley Research Center
[NASA-CR-181850] N91-29176
Research and development for Digital Voice Processing (DVP)
[AD-A238280] N91-29427
Digital SPC switching technology: Foreign technology assessment
[AD-A237258] N91-29449
A method of investigating scales of motion in a turbulent wake
[AD-A237923] N91-29514
An automated software system for updating digital terrain databases from all-source imagery, phase 1
[AD-A237105] N91-29748
Analog design verification with PSpice and MICRO-CAP 3
[AD-A237922] N91-29762

DIGITAL TECHNIQUES
A global geographic information system data base of storm occurrences and other climatic phenomena affecting coastal zones
[DE91-014949] N91-29682

DIHEDRAL ANGLE
A dihedral corner reflector model for full polarization calibration of RCS measurements
[DE91-013572] N91-29402

DIMENSIONAL ANALYSIS
Three-dimensional mapping of atmospheric boundary layer structure and winds with a high performance lidar
[AD-A238098] N91-29678

DIMENSIONAL MEASUREMENT
A study of the relationship between macroscopic measures and physical processes occurring during N00014-89-J-1708
[AD-A238423] N91-29627

DIMERIZATION
Equation of state for pure sodium chloride
[DE91-014618] N91-29286

DIODES
REX: A 5-MV pulsed-power source for driving high-brightness electron beam diodes
[DE91-014604] N91-29443
Diode laser ignition of explosive and pyrotechnic components
[DE90-012227] N91-29553

DIRECTION FINDING
Use of an extended Kalman filter
[AD-A238639] N91-29474
The utility of elliptical and circular confidence regions for HFDF receivers
[AD-A238390] N91-29842

DIRECTORIES
Computational fluid dynamics at NRC: A directory of practitioners and activities
[NRC-TTP-02-89] N91-29490

DISABILITIES
Compliant walker
[NASA-CASE-GSC-13348-2] N91-29714

DISCONNECT DEVICES
Quick disconnect pressure cap
[AD-D014936] N91-29598

DISCRETE FUNCTIONS
An alternative algorithm for discrete-time filtering
[AD-A238443] N91-29827
DISCRIMINANT ANALYSIS (STATISTICS)
Distance measures for speech recognition
[NAE-AN-57] N91-29394
DISKS (SHAPES)
Lightweight disk alloy development
[AD-A237064] N91-29309
DISPLACEMENT
Using quartz crystal microbalances to simultaneously sense mass accumulation and solution properties
[DE91-011501] N91-29537
DISPLACEMENT MEASUREMENT
Experimental investigation of adiabatic shear banding at different impact velocities
[AD-A237901] N91-29625
DISPLAY DEVICES
Research and development for Digital Voice Processing (DVP)
[AD-A238280] N91-29427
The development of a fiber-optic readout pressure transducer
[AD-A238393] N91-29545
Visualizing performance of parallel programs
[DE91-014966] N91-29793
Combining CL (Confidence Limits) and PL (Partial Limits) displays
[AD-A238507] N91-29830
DISSOCIATION
Molecular beam studies of reaction dynamics
[DE90-011600] N91-29256
Reactions of small molecular systems
[DE91-014519] N91-29867
DISSOLVED GASES
A technique for measuring the solubilities of gases in liquids
[AD-A238071] N91-29278
DISTRIBUTED PROCESSING
The MIT Alewife machine: A large-scale distributed-memory multiprocessor
[AD-A237705] N91-29784
Supernodal symbolic Cholesky factorization on a l ocal-memory multiprocessor
[DE91-014967] N91-29796
SAFENET 2 fiber optic implementation study
[AD-A238044] N91-29929
Persistent data/knowledge base
[AD-A237498] N91-30048
Guide to design, implementation and management of distributed databases
[PB91-187567] N91-30054
DISTRIBUTION (PROPERTY)
A mixed limit theorem for stable random fields
[AD-A238222] N91-29840
DISTRIBUTION FUNCTIONS
Anisotropic tensile probabilistic failure criterion for composites
[AD-A237601] N91-29244
The Kramers problem: Fifty years of development
[DE91-617583] N91-29855
DIVERTERS
Total magnetic reconnection during a tokamak major disruption
[DE91-013637] N91-29949
Advanced divertor experiments on DIII-D
[DE91-011138] N91-29950
DMSP SATELLITES
Algorithms for converting geodetic Earth location to satellite time and swath pixel coordinates for the DMSP satellite system
[AD-A237589] N91-29638
Magnetospheric structure and dynamics: A multisatellite approach
[AD-A237674] N91-29676
DOCUMENTATION
Legal and records management issue of optical disk storage media
[DE91-014898] N91-30046
DOCUMENTS
Expert systems on multiprocessor architectures. Volume 1: Summary
[AD-A238046] N91-29786
Expert systems on multiprocessor architectures. Volume 2: Technical reports
[AD-A238047] N91-29787
User's guide to the (NCARAI) artificial intelligence technical library
[AD-A237270] N91-29802
Compilation and representation of intelligent electronic documents: An architecture for referenceability
[DE91-012635] N91-30045
DOPED CRYSTALS
Effects of doping on hybridization gapped materials
[DE91-014611] N91-29477
Developmental status and system studies of the monolithic solid oxide fuel cell
[DE91-014389] N91-29645
Development of model based magnetic LP-LEC growth large diameter GaAs
[AD-A237456] N91-29998
DOPPLER EFFECT
A Doppler bin blanking CFAR processor for airborne radars
[AD-A237890] N91-29418
Full-field Fabry-Perot interferometer
[DE91-014610] N91-29540
DOPPLER RADAR
Space-based Doppler lidar sampling strategies: Algorithm development and simulated observation experiments
[NASA-CR-184172] N91-29554
DOSIMETERS
Neutron dosimetry using optically stimulated luminescence
[DE91-015781] N91-29902
DRAG
Numerical study of non-impulsively started flow around a circular cylinder
[AD-A238051] N91-29519
DRAG CHUTES
Stabilized square parachute
[AD-D014946] N91-29149
DRAG REDUCTION
Polymer drag reduction of a zero pressure gradient boundary layer
[AD-A237572] N91-29510
DRAINAGE
Advances in the drained shaping of ceramics
[DE91-015429] N91-29376
DROPS (LIQUIDS)
A model of multicomponent droplet evaporation with liquid phase reactions
[DE90-012535] N91-29257
Nonlinear spectroscopy of multicomponent droplets and two- and three-dimensional measurements in flames
[AD-A238028] N91-29277
An observational study of the efficiency of activation of accumulation-mode particles in warm continental stratiform clouds
[DE91-013335] N91-29681
DROPSONDES
TOVS satellite soundings of the ERICA IOP-2 cyclone
[AD-A237998] N91-29686
DUCTED FAN ENGINES
The design and construction of a shiplaunched VTOL unmanned air vehicle
[AD-A238053] N91-29173
DUCTED FLOW
Experimental study of cross-stream mixing in a cylindrical duct
[NASA-TM-105180] N91-29187
A finite element solver for 3-D compressible viscous flows
[NASA-CR-184175] N91-29488
Theoretical study of the flow in a rotating duct. Experimental study through flow visualization in a curved duct
[RAE-TRANS-2189] N91-29493
Adiabatic two-phase flow frictional pressure drop. Part 1: Critical parameters and friction factors for air-water mixture
[DE91-014463] N91-29502
DUCTILITY
Lightweight disk alloy development
[AD-A237064] N91-29309
Development of nickel and iron aluminides and their applications
[DE91-015323] N91-29325
DUCTS
Adiabatic two-phase flow frictional pressure drop. Part 1: Critical parameters and friction factors for air-water mixture
[DE91-014463] N91-29502
DUST
Investigations in Martian geology. Part 1: Nature of the mantling deposit in the heavily cratered terrain of northeastern Arabia, Mars. Part 2: Experimental studies of clean and dust-or-sand-covered ice sublimation under Mars-like conditions N91-30067
DYE LASERS
Characterization of a sub-picosecond dye laser for the study of atom-perturber collisions
[AD-A238099] N91-29572
DYNAMIC CHARACTERISTICS
A new look at the Tobak-Schiff model of nonplanar aircraft dynamics
[NAE-LTR-UA-101] N91-29168
Atomic approaches to defect thermochemistry
[AD-A238260] N91-29280
Dynamic behavior of fully dense molybdenum
[DE91-014902] N91-29304
Studies of polymers for shock absorption applications
[AD-A237925] N91-29358
Experiments in adaptive control of cooperating manipulators N91-29594
Effects of anisotropy on dynamic tensile behavior
[DE91-014748] N91-29632
Solvent dynamical effects in electron transfer: The solvent inertial limit and the predicted influence of quantum effects
[AD-A237462] N91-29680
Charge motion effects in ionic clusters
[AD-A238178] N91-29886
DYNAMIC CONTROL
Experimental demonstration of a classical approach for flexible space structure control: NASA CSI testbeds
[NASA-CR-188724] N91-29212
Robust design of multivariable control: An interval arithmetic approach
[AD-A238006] N91-29806
DYNAMIC MODELS
Fundamental studies in dynamic plasticity
[AD-A237114] N91-29621
Robust design of multivariable control: An interval arithmetic approach
[AD-A238006] N91-29806
Parameter estimation via nonlinear differential correction least square method
[NAL-PD-FC-9110] N91-29814
DYNAMIC PROGRAMMING
Matching of complex 3-D surfaces using dynamic programming
[ERB-1022] N91-29743
DYNAMIC RESPONSE
Instrumentation for ASE experiments in the dynamic wind tunnel
[PD-FC-9112] N91-29197
High strain rate characterization of ceramics in shear
[AD-A238319] N91-29365
A general purpose, comprehensive dynamics simulation of serial robot manipulators N91-29587
DYNAMIC STABILITY
Performance and stability in high speed articulated structures undergoing quick maneuvers: Theory and applications
[AD-A237857] N91-29597
DYNAMIC STRUCTURAL ANALYSIS
Review of Canadian aeronautical fatigue work: 1987-1989
[NAE-LTR-ST-1706] N91-29165
Hierarchic extensions in the static and dynamic analysis of elastic beams N91-29613
Structural optimization with pseudo-load approach exploiting design length scales N91-29616
Integrated structural damping and control system design for high-order flexible systems N91-29617
Description of computer programs used to analyze and plot Spectrapot data files
[NAE-ST-557] N91-29744
The advanced software development and commercialization project
[DE91-015756] N91-29797
DYNAMIC TESTS
Dynamic behavior of fully dense molybdenum
[DE91-014902] N91-29304
DYNAMO THEORY
Anomalous ion heating from the dynamo in a reversed field pinch
[DE91-015586] N91-29966
DYSPROSIUM ISOTOPES
Superdeformation: An experimental review
[DE91-015566] N91-29894

E

EARTH (PLANET)
Hamiltonian 3-D ray tracing in the oceanic waveguide on the ellipsoidal earth
[AD-A237458] N91-29700
EARTH ATMOSPHERE
Flight Research Laboratory. Institute for Aerospace Research
[CTN-91-60105] N91-29140
NAE Twin Otter operations in FIFE 1989
[NASA-CR-188770] N91-29169
Wind and flux calculations of the NAE Twin Otter
[NAE-LTR-FR-109] N91-29189
Atmospheric methane concentrations: The NOAA/CMDL global cooperative flask sampling network, 1983 - 1988
[DE91-014942] N91-29664
XTRAN: An atmospheric transmittance code based on XSCALE
[AD-A237624] N91-29674

A manual method for determining the fractional stability category
[AD-A237627] N91-29675
Three-dimensional mapping of atmospheric boundary layer structure and winds with a high performance lidar
[AD-A238098] N91-29678
A global geographic information system data base of storm occurrences and other climatic phenomena affecting coastal zones
[DE91-014949] N91-29682
CO2 measurements along the WOCE P-16 and 19 sections in the South Pacific Ocean: A joint LDGO/WHOI program
[DE91-015742] N91-29708

EARTH ENVIRONMENT
Dependence of radar backscatter on the energetics of the air-sea interface
[AD-A237818] N91-29685

EARTH IONOSPHERE
Analysis of the ultraviolet emissions of nitric oxide from mid-latitude rocket observations
[AD-A237340] N91-29673

EARTH MAGNETOSPHERE
Magnetospheric structure and dynamics: A multisatellite approach
[AD-A237674] N91-29676

EARTH ORBITS
The optimal location of GEODSS sensors in Canada
[AD-A238444] N91-29216

ECONOMIC ANALYSIS
Electric rate structures for thermal energy storage evaluation
[DE91-013168] N91-29644

ECONOMIC DEVELOPMENT
The advanced software development and commercialization project
[DE91-015756] N91-29797
Technology transfer: A new program between Sandia National Laboratories and the University of New Mexico
[DE91-015439] N91-30058

EDDY CURRENTS
The ac losses in type-2 superconductors
[DE91-015201] N91-29485
Shockwave considerations for sub-grid closure modeling in turbulent large eddy simulations
[DE91-015142] N91-29506
Course lectures abstracts of participants fellows project reports
[AD-A237909] N91-30070

EDDY VISCOSITY
Shockwave considerations for sub-grid closure modeling in turbulent large eddy simulations
[DE91-015142] N91-29506

EDUCATION
Operational procedures for powering up, powering down, and configuring the qualification model of the FLTSATCOM satellite
[AD-A238485] N91-29217
Marketing for collegiate aviation education
[NIAR-91-18] N91-30042

EFFLUX
Performance of multiple stream pulsed jet combustion systems
[DE91-012338] N91-29259

EIGENVALUES
Response and stability analysis of helicopter rotor blades using computerized symbolic manipulation
[AD-A238660] N91-29175

EIGENVECTORS
Response and stability analysis of helicopter rotor blades using computerized symbolic manipulation
[AD-A238660] N91-29175

EJECTION SEATS
International aviation (selected articles)
[AD-A237175] N91-29141

EJECTORS
Effect of geometric parameters on the performance of second throat annular steam ejectors
[AD-A238645] N91-29522

ELASTIC DEFORMATION
Equations of motion for a flexible spacecraft-lumped parameter idealization
[NASA-CR-188727] N91-29211
Inelastic deformation and fracture of glassy solids
[AD-A237290] N91-29344
Fission-fusion adaptivity in finite elements for nonlinear dynamics of shells
[AD-A238029] N91-29626

ELASTIC PROPERTIES
Ultrasonic evaluation of elastic and interfacial properties of composite materials and laminates N91-29238
Preparation and properties of new inorganic glasses and gel-derived solids
[AD-A238095] N91-29360
Elastic-plastic constitutive relations at large strain
[DE91-013195] N91-29612

ELASTOMERS
Studies of polymers for shock absorption applications
[AD-A237925] N91-29358

ELASTOSTATICS
High strain rate characterization of ceramics in shear
[AD-A238319] N91-29365

ELECTRIC BATTERIES
Measurement of lithium cycling efficiency in organic electrolytes
[AD-A237632] N91-29457
Pyrite cathode material for a thermal battery
[AD-D014945] N91-29475

ELECTRIC CHARGE
The charge-exchange neutral problem and the code NEUTRAL
[AD-A237889] N91-29464
The embedded electron-gas boundary: A new standard problem in surface physics
[AD-A238152] N91-30014

ELECTRIC CONDUCTORS
Laser surface modification for selective electroplating of metal: A 2.5 m/s laser direct-write process
[DE91-014988] N91-29322
Cable tester
[AD-D014904] N91-29438
Measurements of retractable gas-cooled 6061 aluminum electrical leads operating in a vacuum
[DE91-014617] N91-29444

ELECTRIC CONNECTORS
Cable tester
[AD-D014904] N91-29438
Universal ground adapter assembly
[AD-D014908] N91-29439
On the interpolation properties of feedforward layered neural networks
[AD-A238035] N91-29824

ELECTRIC CONTACTS
Annealing effects on the microstructure of titanium electrical contacts on diamond films
[DE91-010150] N91-29327
Nonlinear dynamics of Josephson junction parametric amplifier arrays
[AD-A237451] N91-29454

ELECTRIC CORONA
Gaseous prebreakdown processes that are important for pulsed power switching
[DE91-015902] N91-29487

ELECTRIC CURRENT
Gaseous prebreakdown processes that are important for pulsed power switching
[DE91-015902] N91-29487
Parametric design calculations using Green's function to determine unique source
[DE91-014683] N91-29861

ELECTRIC DISCHARGES
Gaseous prebreakdown processes that are important for pulsed power switching
[DE91-015902] N91-29487
Ion Implantation Technology: Proceedings of the 8th International Conference on Ion Implantation Technology
[AD-A237955] N91-30013

ELECTRIC FIELDS
Thermochemistry of hydrocarbon decomposition and relationship to properties of PECVD diamond films
[AD-A237793] N91-29274
NIST calibration procedure for vertically polarized monopole antennas 30 kHz to 300 MHz
[PB91-185124] N91-29432
Gaseous prebreakdown processes that are important for pulsed power switching
[DE91-015902] N91-29487
Laser triggered spark gap modeling
[DE91-014831] N91-29557
Nonlinear optical interactions involving the real Gaussian field
[DE91-015052] N91-29936

ELECTRIC GENERATORS
A high power cross-field amplifier at X-Band
[DE91-013277] N91-29441
Acoustic tests on a new motor generator system for the Minuteman launch control centers at Alpha 01 and Sierra 00, Malmstrom AFB, Montana
[AD-A237944] N91-29648

ELECTRIC MOTOR VEHICLES
Performance and life evaluation of advanced battery technologies for electric vehicle applications
[DE91-015671] N91-29482

ELECTRIC POTENTIAL
Twenty first century propulsion concept
[AD-A237853] N91-29224
Cyclic voltammetric wave-shapes for microdisk electrodes: Coupled effects of solution resistance, double-layer capacitance, and finite electrochemical kinetics
[AD-A237505] N91-29455
Gaseous prebreakdown processes that are important for pulsed power switching
[DE91-015902] N91-29487
Standard NIM instrumentation system
[DE90-010387] N91-29532
Perturbation techniques for models of bursting electrical activity in pancreatic (beta)-cells
[DE91-013901] N91-29715
Edge electrostatic fluctuations and transport in the MST reversed field pinch
[DE91-015218] N91-29959
The influence of potential on metal-adsorbate structure: Solvent-independent nature of infrared spectra for Pt(111)/CO
[AD-A237509] N91-30004

ELECTRIC POWER
Electric rate structures for thermal energy storage evaluation
[DE91-013168] N91-29644

ELECTRIC POWER PLANTS
Worldwide wind/diesel hybrid power system study: Potential applications and technical issues
[DE91-002160] N91-29643

ELECTRIC POWER SUPPLIES
Impacts of a nominal nuclear electromagnetic pulse on electric power systems
[DE91-012991] N91-29401

ELECTRIC SWITCHES
Computation of broadband, high-power electromagnetic pulse generation from an air gas avalanche switch
[DE91-015793] N91-29435
Cable tester
[AD-D014904] N91-29438
Proceedings of the First Switch Tube Advanced Technology Meeting
[DE91-012634] N91-29440
Experimental and analytical study of laser-triggering in the Rimfire switch
[DE91-014662] N91-29483
Gaseous prebreakdown processes that are important for pulsed power switching
[DE91-015902] N91-29487
Laser triggered spark gap modeling
[DE91-014831] N91-29557
Low-jitter, high-voltage, infrared, laser-triggered, vacuum switch
[DE91-014602] N91-29562
Procyon experiments utilizing explosively-formed fuse opening switches
[DE91-014742] N91-29953
Plasma flow switch experiments on the Pegasus facility
[DE91-014744] N91-29954

ELECTRIC WIRE
Cable tester
[AD-D014904] N91-29438

ELECTRICAL ENGINEERING
Research in the physical sciences with application to the free electron laser
[AD-A237884] N91-29571
Bulletin of the Division of Electrical Engineering, 1988-1989
[NRC-30458] N91-30071

ELECTRICAL FAULTS
Twenty first century propulsion concept
[AD-A237853] N91-29224
Gaseous prebreakdown processes that are important for pulsed power switching
[DE91-015902] N91-29487

ELECTRICAL IMPEDANCE
Millimeter-wave characterization of GaAs devices and IC's
[AD-A237843] N91-29461
Use of electrical impedance imaging in two-phase, gas-liquid flows
[DE91-015914] N91-29531

ELECTRICAL MEASUREMENT
Basic mechanisms of diesel lubrication correlation of bench and engine tests
[AD-A237685] N91-29596

ELECTRICAL PROPERTIES
Electrical, magnetic, and spectroscopic properties of tetrathiafulvalene charge transfer compounds with iron, ruthenium, rhodium, and iridium halides
[AD-A237607] N91-29273
Design, synthesis and characterization of novel polydiacetylenes using new analytical techniques
[AD-A237362] N91-29348

ELECTRICAL RESISTANCE
Method of obtaining current-conducting polymeric materials
[AD-A237174] N91-29339
Basic mechanisms of diesel lubrication correlation of bench and engine tests
[AD-A237685] N91-29596

ELECTRICAL RESISTIVITY
Thermophysical properties of POCO AXF-5Q graphite up to melting
[DE91-014751] N91-29334
ANL's development of conductive ceramic components for MCFC
[DE91-015557] N91-29336
The Kramers problem: Fifty years of development
[DE91-617583] N91-29855
Defect characterization of electronic conducting pseudo-perovskite systems
[DE91-014385] N91-29978
Ac susceptibility of superconductive thin films
[DE91-015273] N91-29993
High temperature thermoelectric properties of boron carbide
[DE91-015848] N91-30037
ELECTRO-OPTICS
Optoelectronic Materials Center
[AD-A237663] N91-29922
The 23rd Optoelectronic Workshop: Optical System Assessment for Design and Simulated Annealing
[AD-A238588] N91-29932
Electro-optic line narrowing of optical parametric oscillators
[AD-D014944] N91-29934
Solid state research
[NASA-CR-188021] N91-30016
ELECTROCATALYSTS
Electrocatalytic study of ammonia synthesis and methane dimerization in high temperature solid electrolyte cells
[DE90-012496] N91-29437
ELECTROCHEMISTRY
Long-term testing and evaluation of cathode components in a commercial aluminum cell, volume 1
[DE90-010896] N91-29436
Electrocatalytic study of ammonia synthesis and methane dimerization in high temperature solid electrolyte cells
[DE90-012496] N91-29437
Cyclic voltammetric wave-shapes for microdisk electrodes: Coupled effects of solution resistance, double-layer capacitance, and finite electrochemical kinetics
[AD-A237505] N91-29455
Electrified microscopic and conventional interfaces between two immiscible electrolyte solutions
[AD-A237695] N91-29459
Electrodeposition of high temperature superconductors
[AD-A238227] N91-29469
Temperature dependence of proton electroreduction kinetics at gold(111) and (210) surfaces
[AD-A237460] N91-29879
Electron-transfer reactions at metal-solution interfaces: An introduction to some contemporary issues
[AD-A237506] N91-29882
The influence of potential on metal-adsorbate structure: Solvent-independent nature of infrared spectra for Pt(111)/CO
[AD-A237509] N91-30004
ELECTRODE MATERIALS
Pyrite cathode material for a thermal battery
[AD-D014945] N91-29475
Developmental status and system studies of the monolithic solid oxide fuel cell
[DE91-014389] N91-29645
ELECTRODEPOSITION
Electrodeposition of high temperature superconductors
[AD-A238227] N91-29469
Electroforming thin channel heat exchangers
[DE91-015114] N91-29528
ELECTRODES
Electrochemical contact adsorption site changes driven by field and charge fact and theory
[AD-A237127] N91-29269
Ceramic fabrication R/D
[DE91-014758] N91-29335
Computation of broadband, high-power electromagnetic pulse generation from an air gas avalanche switch
[DE91-015793] N91-29435
Electrified microscopic and conventional interfaces between two immiscible electrolyte solutions
[AD-A237695] N91-29459
Gaseous prebreakdown processes that are important for pulsed power switching
[DE91-015902] N91-29487
Electro-optic line narrowing of optical parametric oscillators
[AD-D014944] N91-29934
Advanced divertor experiments on DIII-D
[DE91-011138] N91-29950
ELECTROFORMING
Electroforming thin channel heat exchangers
[DE91-015114] N91-29528
ELECTROLYTES
Measurement of lithium cycling efficiency in organic electrolytes
[AD-A237632] N91-29457
Electrified microscopic and conventional interfaces between two immiscible electrolyte solutions
[AD-A237695] N91-29459
ELECTROLYTIC CELLS
Electrocatalytic study of ammonia synthesis and methane dimerization in high temperature solid electrolyte cells
[DE90-012496] N91-29437
ELECTROMAGNETIC ABSORPTION
Laser-atom interaction at high intensities
[AD-A238231] N91-29887
ELECTROMAGNETIC ACCELERATION
Basic simple modeling of balloting motion of railgun projectiles
[AD-A237938] N91-29205
An approximate analysis of balloting motion of railgun projectiles
[AD-A237942] N91-29206
Basic simple modeling of in-bore motion of railgun projectiles
[AD-A238064] N91-29207
ELECTROMAGNETIC FIELDS
Impacts of a nominal nuclear electromagnetic pulse on electric power systems
[DE91-012991] N91-29401
Visualization of wake fields
[DE91-015130] N91-29408
Biological interactions of extremely-low-frequency electric and magnetic fields
[DE90-011927] N91-29709
Electromagnetic PIC simulations using finite elements on unstructured grids
[DE91-015141] N91-29962
ELECTROMAGNETIC INTERACTIONS
Medium energy nuclear physics research
[DE91-015740] N91-29901
High energy physics: Experimental, Theoretical, and Phenomenology Institute
[DE91-015737] N91-29912
ELECTROMAGNETIC INTERFERENCE
Signal processing in impulsive electromagnetic interference
[AD-A237612] N91-29416
ELECTROMAGNETIC NOISE
Spectra and covariances for classical nonlinear signal processing problems involving class A non-Gaussian noise
[AD-A237388] N91-29413
ELECTROMAGNETIC PROPERTIES
Transient flowmeter calibration facility
[AD-D014937] N91-29523
Vibrational, mechanical, and thermal properties of III-V semiconductors
[AD-A237785] N91-30008
ELECTROMAGNETIC PULSES
Impacts of a nominal nuclear electromagnetic pulse on electric power systems
[DE91-012991] N91-29401
Computation of broadband, high-power electromagnetic pulse generation from an air gas avalanche switch
[DE91-015793] N91-29435
Evolution of a finite pulse of radiation in a high-power free-electron laser
[AD-A237427] N91-29568
Optical soliton source
[AD-D014942] N91-29933
ELECTROMAGNETIC SCATTERING
Numerical methods for scattering from electrically large objects
[AD-A238262] N91-29426
ELECTROMAGNETIC WAVE TRANSMISSION
Ion transmission studies of mulitple-sector isotope-ratio mass spectrometers
[DE91-014253] N91-29265
ELECTROMAGNETISM
A method for computing fields near the origin of a cylindrical coordinate system in time domain finite-difference electromagnetic simulations
[DE91-015431] N91-29433
The Research Laboratory of Electronics
[AD-A237670] N91-29458
ELECTROMAGNETS
Major achievements during the first program year
[AD-A237171] N91-29919
ELECTROMIGRATION
Failure mechanisms on GaAs integrated circuits: Electromigration on GaAs
[AD-A237352] N91-29451
ELECTRON ACCELERATORS
Analysis of radio frequency radiation from a propagating electron beam
[AD-A237941] N91-29419
ELECTRON AFFINITY
The relative stability and possible structural formulae of the negatively charged silver monoiodide clusters
[AD-A238398] N91-29888
ELECTRON BEAMS
Analysis of radio frequency radiation from a propagating electron beam
[AD-A237941] N91-29419
REX: A 5-MV pulsed-power source for driving high-brightness electron beam diodes
[DE91-014604] N91-29443
Study of energy levels and decay mechanisms for Singlet Rydberg states of molecular nitrogen
[AD-A238156] N91-29885
Electron-ion interaction cross sections determined by x ray spectroscopy on EBIT
[DE91-015786] N91-29903
Control of energy sweep and transverse beam motion in induction linacs
[DE91-015177] N91-29911
ELECTRON CAPTURE
Laboratory evaluation of portable and walk-through explosives vapour detectors
[NAE-LTR-UA-104] N91-29533
Negative ion formation with electron impact to simulants
[AD-A237478] N91-29881
Electron capture in very low energy collisions of multicharged ions with H and D in merged beams
[DE91-015617] N91-29909
ELECTRON DENSITY (CONCENTRATION)
First principles simulations of metallic alloys and liquids
[DE91-015171] N91-29323
ELECTRON DENSITY PROFILES
The embedded electron-gas boundary: A new standard problem in surface physics
[AD-A238152] N91-30014
ELECTRON DISTRIBUTION
Chemical waste disposal in space by plasma discharge
[NASA-CR-184169] N91-29737
Fluidlike studies of the sheath and presheath regions of a plasma
[DE91-013343] N91-29944
ELECTRON ENERGY
Edge electrostatic fluctuations and transport in the MST reversed field pinch
[DE91-015218] N91-29959
Global confinement and discrete dynamo activity in the MST reversed field pinch
[DE91-015219] N91-29960
Surface structure and surface order
[AD-A237466] N91-30001
High resolution electron energy loss studies of surface vibrations
[DE91-014539] N91-30024
ELECTRON GAS
Dielectric function of semiconductor superlattice
[DE91-617788] N91-29976
The embedded electron-gas boundary: A new standard problem in surface physics
[AD-A238152] N91-30014
ELECTRON IMPACT
Negative ion formation with electron impact to simulants
[AD-A237478] N91-29881
ELECTRON IRRADIATION
Counterdoped high temperature, silicon array infrared detector
[AD-A238483] N91-29546
ELECTRON MICROSCOPES
High-energy backscattered electron imaging of voids in aluminum metallizations
[DE91-014895] N91-29303
Materials science applications of a 120 kV FEG TEM/STEM: Triskaidekaphilia
[DE91-010136] N91-29536
ELECTRON MICROSCOPY
Technical activities 1990, Electron and Optical Physics Div.
[PB91-194423] N91-29858
Comparisons between scanning tunneling microscopy and outer-sphere electron-transfer rates at Pt(111) surfaces coated with ordered iodine adlayers
[AD-A237507] N91-29883
High resolution electron microscopy of grain boundaries
[DE91-010593] N91-29970
Electron microscopy of thick 304 SS-copper multilayers
[DE91-011116] N91-29972

Correlations between grain boundary structure and energy
[DE91-015204] N91-29990
Surface structure and surface order
[AD-A237466] N91-30001
Electron tunneling microscopy
[AD-A237504] N91-30003

ELECTRON PARAMAGNETIC RESONANCE
Spin-Label-Spin-Probe. Studies of bimolecular encounters in micelles
[AD-A238546] N91-29891
On the role of crystal defects as sources of resonator frequency instability
[AD-A238505] N91-30018

ELECTRON SCATTERING
Single-scatter Monte Carlo compared to condensed history results for low energy electrons
[DE91-015176] N91-29869
The effects of donor-acceptor electronic interactions on the rates of gas-phase metallocene electron-exchange reactions
[AD-A237459] N91-29878

ELECTRON SOURCES
REX: A 5-MV pulsed-power source for driving high-brightness electron beam diodes
[DE91-014604] N91-29443
Development of laser optics for the AWA photocathode
[DE91-015552] N91-29581

ELECTRON SPECTROSCOPY
A study of copper segregation in sputtered Al-Si-Cu films using Auger electron spectroscopy
[AD-A238130] N91-29316
Quantitative interpretation of auger lineshapes and electron/photon stimula'ed desorption
[AD-A237138] N91-29874

ELECTRON SPIN
Anisotropic spin susceptibility of the (Y,Ca),(Ba, La)2Cu4O8 system
[DE91-014593] N91-30032

ELECTRON STATES
Atomic physics in strong fields
[DE91-015393] N91-29872

ELECTRON TRANSFER
Solvent effects on simple electron transfer reactions. A comparison of results in Debye and non-Debye solvents
[AD-A237157] N91-29875
Role of the solvent in kinetics of heterogeneous electron and ion transfer reactions
[AD-A237168] N91-29876
Solvent dynamical effects in electron transfer: The solvent inertial limit and the predicted influence of quantum effects
[AD-A237462] N91-29880
Electron-transfer reactions at metal-solution interfaces: An introduction to some contemporary issues
[AD-A237506] N91-29882
Comparisons between scanning tunneling microscopy and outer-sphere electron-transfer rates at Pt(111) surfaces coated with ordered iodine adlayers
[AD-A237507] N91-29883
Reevaluation of S-values considering electron transport
[DE91-015428] N91-29893
Discreteness-of-solvent effects in Marcus equations in the mean spherical approximation
[AD-A237133] N91-29996

ELECTRON TRANSITIONS
Laser enhanced chemical reaction studies
[DE91-013021] N91-29555
Superdeformation: An experimental review
[DE91-015566] N91-29894

ELECTRON TUNNELING
Electron tunneling microscopy
[AD-A237504] N91-30003

ELECTRONIC CONTROL
Analysis of FIN line feasibility for W-band attenuator applications
[AD-A237271] N91-29450

ELECTRONIC EQUIPMENT
First International conference on Frontiers of Polmer Research
[AD-A238112] N91-29361
The 2nd Workshop on High Temperture Electronics (Metallization and Packaging)
[DE91-014332] N91-29442
Hyperdimensional data analysis and structural inference
[AD-A238097] N91-29764

ELECTRONIC PACKAGING
The 2nd Workshop on High Temperture Electronics (Metallization and Packaging)
[DE91-014332] N91-29442

ELECTRONIC SPECTRA
Structures, properties, and dynamics of metal clusters from infrared laser spectroscopy
[AD-A237669] N91-29570

ELECTRONICS
Annual Electronics Manufacturing Seminar proceedings
[AD-A238017] N91-29467
NRL review, 1989-1990
[AD-A238612] N91-29856

ELECTRONS
Quantitative interpretation of auger lineshapes and electron/photon stimulated desorption
[AD-A237138] N91-29874
The effects of donor-acceptor electronic interactions on the rates of gas-phase metallocene electron-exchange reactions
[AD-A237459] N91-29878
Negative ion formation with electron impact to simulants
[AD-A237478] N91-29881
Measurements of the ion acoustic decay instability and the resultant thermal and suprathermal electron heating in laser-plasma interaction experiments
[DE90-012477] N91-29941
Proton deceleration near the surface of an accreting neutron star N91-30063

ELECTROPHYSIOLOGY
Perturbation techniques for models of bursting electrical activity in pancreatic (beta)-cells
[DE91-013901] N91-29715

ELECTROPLATING
Laser surface modification for selective electroplating of metal: A 2.5 m/s laser direct-write process
[DE91-014988] N91-29322

ELECTRORHEOLOGICAL FLUIDS
Electro-rheology fluids and liquid fuel flow
[AD-A238600] N91-29520

ELECTROSTATIC PROBES
Edge electrostatic fluctuations and transport in the MST reversed field pinch
[DE91-015218] N91-29959

ELECTROSTATIC PROPULSION
Twenty first century propulsion concept
[AD-A237853] N91-29224

ELECTROSTATIC WAVES
Impurity and neutral effects on the dissipative drift wave in tokamak edge plasmas
[DE91-015907] N91-29965

ELECTROSTATICS
Edge electrostatic fluctuations and transport in the MST reversed field pinch
[DE91-015218] N91-29959

ELECTROSTRICTION
Discreteness-of-solvent effects in Marcus equations in the mean spherical approximation
[AD-A237133] N91-29996

ELEMENTARY PARTICLES
Research in elementary particle physics
[DE91-015359] N91-29892

ELEVATION ANGLE
Validation of the Schwartz and Hon algorithm at low grazing angles
[AD-A238162] N91-29767

ELLIPSOIDS
Hamiltonian 3-D ray tracing in the oceanic waveguide on the ellipsoidal earth
[AD-A237458] N91-29700

ELLIPTICAL GALAXIES
Course lectures abstracts of participants fellows project reports
[AD-A237909] N91-30070

EMERGENCIES
International aviation (selected articles)
[AD-A237232] N91-29142

EMISSION
Proton deceleration near the surface of an accreting neutron star N91-30063

EMISSION SPECTRA
Spectral estimation techniques with emphasis on short data records: A primer
[AD-A237486] N91-29271
Analysis of the ultraviolet emissions of nitric oxide from mid-latitude rocket observations
[AD-A237340] N91-29673
Technical activities 1990, Electron and Optical Physics Div.
[PB91-194423] N91-29858
Analyzing photographically recorded atomic emission spectra using an automated densitometer
[DE91-015368] N91-29871
Electron-ion interaction cross sections determined by x ray spectroscopy on EBIT
[DE91-015786] N91-29903
Fundamental studies of the extraction process in inductively coupled plasma mass spectrometry
[DE90-011733] N91-29939
Synchrotron studies of narrow band materials
[DE91-014826] N91-30025

EMITTANCE
Thermal emittance enhancement of graphite-copper composites for high temperature space based radiators
[NASA-TM-105178] N91-29332
Measurement of longitudinal emittance growth using a laser-induced neutralization method
[DE91-013500] N91-29560

EMOTIONS
Predicting performance breakdown in pilots through objective measures of stress sensitivity
[AD-A237540] N91-29725

EMULSIONS
Model filled polymers 8: Synthesis of crosslinked polymeric beads by seed polymerization
[AD-A237429] N91-29349

ENCAPSULATING
The cure of rigid polyurethane encapsulating foam
[DE91-016059] N91-29379

END EFFECTORS
Force-reflecting control of a teleoperated system coupling a nonredundant master with a redundant slave
[DE90-012137] N91-29585
Singularity avoidance and the kinematics of an eight-revolute-joint manipulator N91-29588
Quasistatic manipulation with compliance and friction N91-29591
Motion planning for manipulators with excessive degrees of freedom N91-29592

ENERGETIC PARTICLES
NRL review, 1991
[AD-A238665] N91-29857

ENERGY CONSERVATION
Fluidlike studies of the sheath and presheath regions of a plasma
[DE91-013343] N91-29944

ENERGY CONVERSION
Worldwide wind/diesel hybrid power system study: Potential applications and technical issues
[DE91-002160] N91-29643
Tritium-field betacells
[DE91-014666] N91-29910

ENERGY CONVERSION EFFICIENCY
Hydrogen productivity by photosynthetic water splitting
[DE90-012211] N91-29380

ENERGY DISSIPATION
Qualitative investigation of cryogenic injected shock dissipation
[NASA-TM-105140] N91-29525
Modeling a rain-induced mixed layer
[AD-A238022] N91-29702
Edge electrostatic fluctuations and transport in the MST reversed field pinch
[DE91-015218] N91-29959
Impurity and neutral effects on the dissipative drift wave in tokamak edge plasmas
[DE91-015907] N91-29965
High resolution electron energy loss studies of surface vibrations
[DE91-014539] N91-30024

ENERGY GAPS (SOLID STATE)
Electronic and ionic transport in processable conducting polymers
[AD-A238175] N91-29362
Vibrational, mechanical, and thermal properties of III-V semiconductors
[AD-A237785] N91-30008

ENERGY LEVELS
Design and test of a continuous duty pulsed ac generator
[DE91-014664] N91-29445
Superdeformation: An experimental review
[DE91-015566] N91-29894
Growth, nitrogen vacancy reduction and solid solution formation in cubic GaN thin films and the subsequent fabrication of superlattice structures using AlN and InN
[AD-A238521] N91-30021

ENERGY SPECTRA
Relating ocean acoustic ambient to ocean surface dynamics
[AD-A237167] N91-29699
Single-scatter Monte Carlo compared to condensed history results for low energy electrons
[DE91-015176] N91-29869

ENERGY TECHNOLOGY
Energy conserving coating: Pigment research
[AD-A237841] N91-29356

ENERGY TRANSFER
Molecular beam studies of reaction dynamics
[DE90-011600] N91-29256

RF transfer in the coupled-cavity free-electron laser two-beam accelerator
[DE91-015676] N91-29583
Reactions of small molecular systems
[DE91-014519] N91-29867
Study of elementary reactions and energy transfer processes involving the NH and CN free radicals
[AD-A238461] N91-29889

ENGINE CONTROL
Controlling crippled aircraft-with throttles
[NASA-TM-104238] N91-29191

ENGINE DESIGN
ALS rocket engine combustion devices design and demonstration
[NASA-CR-183824] N91-29233
Application of ceramics to industrial gas turbines
[DE91-013140] N91-29330
Materials research for sodium engine development
[DE91-015715] N91-29378
Numerical prediction of turbulent oscillating flow and associated heat transfer
[NASA-CR-187177] N91-29524

ENGINE MONITORING INSTRUMENTS
Compressor fault modelling for engine health monitoring: Review and recommendations
[NRC-TR-ENG-004] N91-29178

ENGINE PARTS
The failure of components in power generation equipment
[NAE-LTR-ST-1774] N91-29180

ENGINE TESTS
Compressor fault modelling for engine health monitoring: Review and recommendations
[NRC-TR-ENG-004] N91-29178
Experimental and analytical comparison of flowfields in a 110 N (25 lbf) H2/O2 rocket
[NASA-TM-105175] N91-29230
Basic mechanisms of diesel lubrication correlation of bench and engine tests
[AD-A237685] N91-29596

ENTHALPY
An elevated temperature titration calorimeter
[DE91-015765] N91-29548

ENTRAINMENT
Equatorial entrainment zone simulations
[AD-A237234] N91-29657

ENTROPY
Monte Carlo and mean field calculations of the magnetocaloric effect of ferromagnetically interacting clusters
[DE91-014792] N91-29859

ENVIRONMENT EFFECTS
Environmental assessment for the FAA explosive detection system independent validation and verification program
[DE91-013190] N91-29152
IDA studies on natural space environmental effects on materials for SDIO
[AD-A237974] N91-29660

ENVIRONMENT MANAGEMENT
The observational approach in environmental restoration
[DE91-015528] N91-29666

ENVIRONMENT MODELS
High bandwidth diagnosis within the framework of a microcomputer-based intelligent tutoring system
[AD-A237959] N91-29805

ENVIRONMENTAL LABORATORIES
An automated software system for updating digital terrain databases from all-source imagery, phase 1
[AD-A237105] N91-29748

ENVIRONMENTAL QUALITY
Publications of the Executive Office of the President, January 20, 1989 - March 31, 1991
[PB91-156828] N91-30056

EPITAXY
Growth condition dependence of RHEED pattern from GaAs(111)B surface
[DE91-014770] N91-29986
Defect reductions in epitaxial growth using superlattice buffer layers
[AD-A237710] N91-30005
Epitaxial growth of single crystal diamond on silicon
[AD-A237758] N91-30007
Laser probing of the kinetics and dynamics of III -V semiconductor growth
[AD-A237795] N91-30009
The growth of ultrathin epitaxial intermetallic films
[AD-A237798] N91-30011
Atomic layer epitaxy group IV materials: Surface processes, thin films, devices and their characterization
[AD-A238506] N91-30019
Growth, nitrogen vacancy reduction and solid solution formation in cubic GaN thin films and the subsequent fabrication of superlattice structures using AlN and InN
[AD-A238521] N91-30021

EPOXY MATRIX COMPOSITES
Effect of fortifier on compression-after-impact strength of carbon fabric reinforced epoxy
[NAE-LTR-ST-1736] N91-29237

EPOXY RESINS
A novel epoxy lacquer for high strength steel in F-111 aircraft during overhaul
[AD-A236828] N91-29326

EQUATIONS OF MOTION
The functional dependence of trajectory dispersion on initial condition errors
[DE91-014661] N91-29151
An approximate analysis of balloting motion of railgun projectiles
[AD-A237942] N91-29206
Equations of motion for a flexible spacecraft-lumped parameter idealization
[NASA-CR-188727] N91-29211
Computational fluid dynamics at NRC: A directory of practitioners and activities
[NRC-TTP-02-89] N91-29490
Performance and stability in high speed articulated structures undergoing quick maneuvers: Theory and applications
[AD-A237857] N91-29597

EQUATIONS OF STATE
The use of high velocity launchers for scientific and engineering studies
[DE91-015564] N91-29208

EQUILIBRIUM EQUATIONS
Problems in nonlinear continuum dynamics
[AD-A237844] N91-29512

EQUIVALENT CIRCUITS
Using quartz crystal microbalances to simultaneously sense mass accumulation and solution properties
[DE91-011501] N91-29537

ERROR ANALYSIS
A technique for measuring the solubilities of gases in liquids
[AD-A238071] N91-29278
Remote sensing of snow covers using the gamma ray technique
[AD-A238016] N91-29639
Research in mathematics and computer science: Calculation of the probability of undetected error for certain error detection codes, phase 2
[AD-A238234] N91-29768
A general lease-squares fitting package for the sun workstation
[AD-A238180] N91-29837

ERROR CORRECTING CODES
Coding for frequency hopped spread spectrum satellite communications
[ECE-89-1] N91-29398

ERROR DETECTION CODES
Research in mathematics and computer science: Calculation of the probability of undetected error for certain error detection codes, phase 2
[AD-A238234] N91-29768

ERROR FUNCTIONS
Local synthesis and tooth contact analysis of face-milled spiral bevel gears
[NASA-TM-105182] N91-29600

ERRORS
The functional dependence of trajectory dispersion on initial condition errors
[DE91-014661] N91-29151
A technique for measuring the solubilities of gases in liquids
[AD-A238071] N91-29278
An expert system approach to global fault detection and isolation design
[AD-A238494] N91-29808

ESTIMATING
Parameter estimation via nonlinear differential correction least square method
[NAL-PD-FC-9110] N91-29814

ESTUARIES
Oceanographic data report Number 7: Data from the Delaware Estuary SCENIC cruises, April 1986 - September 1988
[PB91-183582] N91-29706
Oceanographic data report Number 8: Density profiles from the Delaware Estuary, October 1986 - September 1988
[PB91-183608] N91-29707

ETCHING
The magnetron-enhanced etching of double-level tungsten interconnect
[DE91-014984] N91-29306
Effects of interfacial modification on diamond film adhesion
[AD-A237750] N91-29354
Scanning tunneling microscopy studies of the surfaces of a-Si:H and a-SiGe:H films
[DE91-002169] N91-29983
Responsivity uniformity enhancements for Backside-Illuminated Charge-Coupled Devices (BICCDs) by excimer laser-assisted etching
[AD-A237435] N91-29997
Defect reductions in epitaxial growth using superlattice buffer layers
[AD-A237710] N91-30005
Semiconductor deposition and etching interactions of laser-generated translationally hot atoms and radicals
[AD-A238198] N91-30015

ETHYL ALCOHOL
Overview of the technical implications of methanol and ethanol as highway motor vehicle fuels
[PB91-182881] N91-29385

ETHYL COMPOUNDS
Negative ion formation with electron impact to simulants
[AD-A237478] N91-29881

EULER EQUATIONS OF MOTION
Solutions of two-dimensional Euler equations with multigrid acceleration
[NAL-PD-CF-9006] N91-29494
Statistical mechanics of two-dimensional Euler equations and Jupiter's Great Red Spot N91-29498

EVALUATION
An evaluation of the NEKTON program
[AD-A237888] N91-29513

EVAPORATION
A model of multicomponent droplet evaporation with liquid phase reactions
[DE90-012535] N91-29257
Analysis of condensation and evaporation of ammonia/water mixtures in matrix heat-exchangers
[DE91-014461] N91-29500

EVAPOTRANSPIRATION
Using the TIMS to estimate evapotranspiration from a forest
[NASA-CR-188729] N91-29636
Remote determination of soil moisture and evapotranspiration from thermal infrared measurements: Detection of a drying threshold
[PB91-195818] N91-29641

EVOLUTION (DEVELOPMENT)
The evolution and structure of homogeneous stably stratified sheared turbulence N91-29499

EXCIMER LASERS
Responsivity uniformity enhancements for Backside-Illuminated Charge-Coupled Devices (BICCDs) by excimer laser-assisted etching
[AD-A237435] N91-29997

EXCITATION
Atomic physics in strong fields
[DE91-015393] N91-29872

EXHAUST EMISSION
Overview of the technical implications of methanol and ethanol as highway motor vehicle fuels
[PB91-182881] N91-29385

EXHAUST NOZZLES
Pressure measurements in a low-density nozzle plume for code verification
[NASA-TM-105170] N91-29228

EXHAUST VELOCITY
Experimental and analytical comparison of flowfields in a 110 N (25 lbf) H2/O2 rocket
[NASA-TM-105175] N91-29230

EXPERT SYSTEMS
Report on using expert systems for computer-aided formulation and property estimation of propellants. 1: Expert system shell selection and initial package design
[AD-A237567] N91-29383
Multi-sensor image interpretation using laser radar and thermal images
[AD-A238245] N91-29576
An expert system approach for prediction of maritime visibility obscuration
[AD-A238305] N91-29688
Expert systems on multiprocessor architectures. Volume 1: Summary
[AD-A238046] N91-29786
Expert systems on multiprocessor architectures. Volume 2: Technical reports
[AD-A238047] N91-29787
Expert systems on multiprocessor architectures, volume 3
[AD-A238048] N91-29788
Expert systems on multiprocessor architectures, volume 4
[AD-A238049] N91-29789
User's guide to the (NCARAI) artificial intelligence technical library
[AD-A237270] N91-29802
An expert system approach to global fault detection and isolation design
[AD-A238494] N91-29808

A methodology for developing physical system fault diagnostic aids
[DE91-015533] N91-29809
Proceedings of the 1st Workshop on Proximity Graphs
[AD-A237250] N91-29818
Persistent data/knowledge base
[AD-A237498] N91-30048

EXPLOSIONS
Explosively driven missile trajectory parameters for various fragment materials and velocities
[DE91-014330] N91-29631
Future explosive pulse-power technology for high-energy plasma physics experiments
[DE91-014601] N91-29951

EXPLOSIVE DEVICES
Environmental assessment for the FAA explosive detection system independent validation and verification program
[DE91-013190] N91-29152
.Laboratory evaluation of portable and walk-through explosives vapour detectors
[NAE-LTR-UA-104] N91-29533

EXPLOSIVES
Environmental assessment for the FAA explosive detection system independent validation and verification program
[DE91-013190] N91-29152
Development of an explosive vapor generator
[DE91-015700] N91-29386
Diode laser ignition of explosive and pyrotechnic components
[DE90-012227] N91-29553

EXPONENTIAL FUNCTIONS
New modified Anderson-Darling and Cramer-von Mises goodness-of-fit tests for a normal distribution with specified parameters
[AD-A238630] N91-29846

EXPOSURE
Study of activation of metal samples from LDEF-1 and Spacelab-2
[NASA-CR-184171] N91-29297

EXTERNAL TANKS
Debris/ice/TPS assessment and photographic analysis for Shuttle Mission STS-40
[NASA-TM-103822] N91-29210

EXTINCTION
XTRAN: An atmospheric transmittance code based on XSCALE
[AD-A237624] N91-29674

EXTRACTION
Fundamental studies of the extraction process in inductively coupled plasma mass spectrometry
[DE90-011733] N91-29939

EXTREME ULTRAVIOLET RADIATION
Photoelectron and photoionization pumping of XUV lasers by laser-produced plasmas N91-29558
Development of reflective optical systems for XUV projection lithography
[DE91-013167] N91-29915

EXTRUDING
Fabrication and wire extrusion of ceramic superconductors
[DE91-015207] N91-29991

EYE MOVEMENTS
Eye movements and spatial pattern vision
[AD-A238664] N91-29721

F

F REGION
Magnetospheric structure and dynamics: A multisatellite approach
[AD-A237674] N91-29676

F-111 AIRCRAFT
A novel epoxy lacquer for high strength steel in F-111 aircraft during overhaul
[AD-A236828] N91-29326

FABRICATION
Fabrication, phase transformation studies and characterization of SiC-AlN-Al2OC ceramics
[DE91-013296] N91-29329
Ceramic fabrication R/D
[DE91-014758] N91-29335
Fabrication of silicon nitride ceramics by microwave heating
[DE91-015312] N91-29373
The 0-G experiments with advanced ceramic fabric wick structures
[DE91-015531] N91-29377
An investigation to determine the producibility of a 3-D braider and bias direction weaving loom
[NASA-CR-188741] N91-29390
Electroforming thin channel heat exchangers
[DE91-015114] N91-29528
Fabrication and wire extrusion of ceramic superconductors
[DE91-015207] N91-29991
Intermetallic superconductors: The state of development in 1991
[DE91-014844] N91-30026
High-(Tc) superconductors: Fabricating technologies and future perspectives
[DE91-015553] N91-30029

FABRICS
Effect of fortifier on compression-after-impact strength of carbon fabric reinforced epoxy
[NAE-LTR-ST-1736] N91-29237
The 0-G experiments with advanced ceramic fabric wick structures
[DE91-015531] N91-29377

FABRY-PEROT INTERFEROMETERS
Full-field Fabry-Perot interferometer
[DE91-014610] N91-29540

FAILURE
Anisotropic tensile probabilistic failure criterion for composites
[AD-A237601] N91-29244
A layered beam theory for single lap joints
[AD-A237324] N91-29607
An expert system approach to global fault detection and isolation design
[AD-A238494] N91-29808

FAILURE ANALYSIS
The failure of components in power generation equipment
[NAE-LTR-ST-1774] N91-29180
ALS rocket engine combustion devices design and demonstration
[NASA-CR-183824] N91-29233
Mechanisms of transformation toughening
[DE91-013151] N91-29293
Failure mechanisms on GaAs integrated circuits: Electromigration on GaAs
[AD-A237352] N91-29451
A methodology for developing physical system fault diagnostic aids
[DE91-015533] N91-29809

FALSE ALARMS
A Doppler bin blanking CFAR processor for airborne radars
[AD-A237890] N91-29418

FAR FIELDS
Modification of programs CHIEF and CID to compute sound radiation from an arbitrary body with mixed boundary conditions
[AD-A237502] N91-29759

FAR INFRARED RADIATION
XTRAN: An atmospheric transmittance code based on XSCALE
[AD-A237624] N91-29674
An investigation of Nova Persei (1901) and its environment N91-30059

FAST FOURIER TRANSFORMATIONS
Parallelizing the spectral transform method
[DE91-013969] N91-29815

FATIGUE (MATERIALS)
Review of Canadian aeronautical fatigue work: 1987-1989
[NAE-LTR-ST-1706] N91-29165
The failure of components in power generation equipment
[NAE-LTR-ST-1774] N91-29180
A study of the relationship between macroscopic measures and physical processes occurring during N00014-89-J-1708
[AD-A238423] N91-29627
Fatigue resistant optical fibers
[AD-A237568] N91-29921

FATIGUE LIFE
Effect of two synthetic lubricants on life of AISI 9310 spur gears
[NASA-TM-104352] N91-29599

FATIGUE TESTING MACHINES
A full function checkout test for the NAE full scale structural test control and data acquisition system
[NAE-LTR-ST-1696] N91-29166

FATIGUE TESTS
A full function checkout test for the NAE full scale structural test control and data acquisition system
[NAE-LTR-ST-1696] N91-29166
Tutor aft fuselage and empennage full-scale test: Procedures for creating a damage log
[NAE-ST-576] N91-29167
Assessment of impact damage in toughened resin composites
[NAE-LTR-ST-1695] N91-29236
Strain gauge cabling, conditioning, and sensitivity calculations for the CT-114 (Tutor) aircraft aft fuselage and empennage full-scale fatigue test
[NAE-LTR-ST-1758] N91-29534
Effect of two synthetic lubricants on life of AISI 9310 spur gears
[NASA-TM-104352] N91-29599
Review of literature on the damage, loss of stiffness, and residual strength of graphite/epoxy laminates subjected to cyclic loading
[NAE-LTR-ST(CR)-1711] N91-29611
Description of computer programs used to analyze and plot Spectrapot data files
[NAE-ST-557] N91-29744

FATTY ACIDS
Spin-Label-Spin-Probe. Studies of bimolecular encounters in micelles
[AD-A238546] N91-29891

FAULT TOLERANCE
Fault-tolerant computing: An overview
[NASA-CR-188793] N91-29769
Verification of the FtCayuga fault-tolerant microprocessor system. Volume 2: Formal specification and correctness theorems
[NASA-CR-187574] N91-29777
Verification of the FtCayuga fault-tolerant microprocessor system. Volume 1: A case study in theorem prover-based verification
[NASA-CR-4381] N91-29778

FEASIBILITY ANALYSIS
Methodology investigation, aviation test management system concept development
[AD-A237349] N91-29172
Feasibility of a laser-ignited HMX deflagration-to-detonation transition device for the US Navy LITES Program
[DE91-015210] N91-29382

FEDERAL BUDGETS
Publications of the Executive Office of the President, January 20, 1989 - March 31, 1991
[PB91-156828] N91-30056

FEEDBACK
Sliding mode controller of RF cavity tuning loop
[DE91-015461] N91-29410

FEEDBACK CIRCUITS
Electron tunneling microscopy
[AD-A237504] N91-30003

FEEDBACK CONTROL
A linear control design structure to maintain loop properties during limit operation in a multi-nozzle turbofan engine
[NASA-TM-105163] N91-29188
An expert system approach to global fault detection and isolation design
[AD-A238494] N91-29808
Effects of colocation and non-colocation of sensors and actuators on flexible structures
[AD-A238457] N91-29844

FEEDFORWARD CONTROL
On the interpolation properties of feedforward layered neural networks
[AD-A238035] N91-29824

FELDSPARS
NMR spectroscopy of experimentally shocked silicate minerals
[DE91-014897] N91-29898

FERMENTATION
Microbiology and physiology of anaerobic fermentations of cellulose
[DE91-015239] N91-29712

FERMI SURFACES
Requirements for the observation of Fermi surfaces in disordered alloys
[DE91-014578] N91-29321
De Haas-van Alphen and Fermi surface studies of organic superconductors (ET)2X
[DE91-015137] N91-29987
Photoemission measurement of Fermi surface, band dispersion, and quasiparticle lifetime in YBa2Cu3O6.9
[DE91-015194] N91-29989

FERMIONS
Mixed valent and heavy fermons and related systems
[DE91-015454] N91-29900

FERROMAGNETIC MATERIALS
Method of obtaining current-conducting polymeric materials
[AD-A237174] N91-29339

FERROMAGNETISM
Monte Carlo and mean field calculations of the magnetocaloric effect of ferromagnetically interacting clusters
[DE91-014792] N91-29859

FERROUS METALS
JPRS report: Science and technology. USSR: Materials science
[JPRS-UMS-91-001] N91-29291

FEYNMAN DIAGRAMS
Sum of distances in normed spaces
[AD-A238066] N91-29825

FIBER COMPOSITES
Effect of fiber-matrix debonding on notched strength of titanium metal matrix composites
[NASA-TM-104131] N91-29239
Very high temperature fibers of TiC and TiB2
[AD-A237423] N91-29242
Development of a mixture for nonlinear wave propagation in fiber-reinforced composites
[AD-A237471] N91-29243
Statistical characterization of graphite fiber for prediction of composite structure reliability
[AD-A238020] N91-29245
Test results for composite specimens and elements containing joints and cutouts
[NASA-CR-178246] N91-29254
Advanced materials for space nuclear power systems
[NASA-TM-105171] N91-29298
An investigation to determine the producibility of a 3-D braider and bias direction weaving loom
[NASA-CR-188741] N91-29390
NDE of ceramics and ceramic composites
[NASA-TM-104520] N91-29610
FIBER OPTICS
Physical concepts and modeling procedures for picosecond and subpicosecond distributed circuits
[AD-A238592] N91-29472
VISAR: Line-imaging interferometer
[DE91-014749] N91-29542
The development of a fiber-optic readout pressure transducer
[AD-A238393] N91-29545
Diode laser ignition of explosive and pyrotechnic components
[DE90-012227] N91-29553
Design of a stabilized, dc-powered analog laser diode driver
[AD-A238596] N91-29577
Effect of cladding thickness on attenuation in uniformly curved single-mode optical fibers
[AD-A238034] N91-29928
SAFENET 2 fiber optic implementation study
[AD-A238044] N91-29929
FIELD COILS
Advanced divertor experiments on DIII-D
[DE91-011138] N91-29950
FIELD EFFECT TRANSISTORS
Introduction of a current waveform, waveshaping technique to limit conduction loss in high-frequency dc-dc converters suitable for space power
[AD-A237903] N91-29465
InP and InGaAs submicron gate microwave power transistors for 20 GHz applications
[AD-A238595] N91-29473
Stable integrated microwave to optical modulator
[AD-A238166] N91-29574
Growth, characterization, and device development in monocrystalline diamond films
[AD-A237463] N91-30000
Molecular beam epitaxial growth and characterization of metastable compound semiconductors for infrared detector applications
[AD-A237797] N91-30010
FIELD EMISSION
Materials science applications of a 120 kV FEG TEM/STEM: Triskaidekaphilia
[DE91-010136] N91-29536
FIELD THEORY (PHYSICS)
Research in elementary particle physics
[DE91-015359] N91-29892
A research program in experimental and theoretical high energy physics
[DE91-014728] N91-29907
FIGHTER AIRCRAFT
Agility: Presentation and flight test methods for the operational fighter pilot
[AD-A238456] N91-29174
Acoustic background noise variation in Air Force platforms and its effect on noise removal algorithms
[AD-A238279] N91-29863
FILAMENTS
Synthesis of multifilament silicon carbide fibers by chemical vapor deposition
[NASA-CR-188725] N91-29331
FILLERS
Model filled polymer 7: Flow behavior of polymers containing monodisperse crosslinked polymeric beads
[AD-A237430] N91-29350
FILM THICKNESS
Preparation of damage resistant optical coatings on flat substrates
[DE91-013588] N91-29916
FILTERS
Software development of the cochlear filter and eighth-nerve model
[AD-A237454] N91-29757
FINGERS
Quasistatic manipulation with compliance and friction N91-29591
FINITE DIFFERENCE THEORY
Conformal FDTD modeling wake fields
[DE91-015129] N91-29407
Visualization of wake fields
[DE91-015130] N91-29408
A method for computing fields near the origin of a cylindrical coordinate system in time domain finite-difference electromagnetic simulations
[DE91-015431] N91-29433
Use of the implicit-finite-difference method to implement the parabolic equation model
[AD-A237437] N91-29819
FINITE ELEMENT METHOD
Development of a mixture for nonlinear wave propagation in fiber-reinforced composites
[AD-A237471] N91-29243
A finite element solver for 3-D compressible viscous flows
[NASA-CR-184175] N91-29488
Hierarchic extensions in the static and dynamic analysis of elastic beams N91-29613
Prediction of edge stresses in layered media using the surface integral-finite element technique N91-29614
Structural optimization with pseudo-load approach exploiting design length scales N91-29616
Finite element-based system identification from experimental modal analysis results N91-29618
Fission-fusion adaptivity in finite elements for nonlinear dynamics of shells
[AD-A238029] N91-29626
NIKE2D: A nonlinear, implicit, two-dimensional finite element code for solid mechanics
[DE91-015734] N91-29634
Electromagnetic PIC simulations using finite elements on unstructured grids
[DE91-015141] N91-29962
FINS
Advanced materials for space nuclear power systems
[NASA-TM-105171] N91-29298
FISCHER-TROPSCH PROCESS
Deactivation by carbon of iron catalysts for indirect liquefaction
[DE91-011276] N91-29285
FITTING
A general lease-squares fitting package for the sun workstation
[AD-A238180] N91-29837
FITTINGS
Quick disconnect pressure cap
[AD-D014936] N91-29598
FLAME PROPAGATION
Investigation of the flame-acoustic wave interaction during axial solid rocket instabilities
[AD-A237851] N91-29223
FLAME STABILITY
Combustion stability limits and planar imaging of swirl-stabilized flames N91-29262
FLAMES
Investigation of the flame-acoustic wave interaction during axial solid rocket instabilities
[AD-A237851] N91-29223
Nonlinear spectroscopy of multicomponent droplets and two- and three-dimensional measurements in flames
[AD-A238028] N91-29277
FLAT PLATES
An investigation of the as-quenched and early aging characteristics of a Al - 4.1 wt. percent Li binary alloy by x ray diffraction
[AD-A237598] N91-29311
Steady flow of a fluid-solid mixture between parallel plates
[DE91-013114] N91-29491
FLEET SATELLITE COMMUNICATION SYSTEM
Operational procedures for powering up, powering down, and configuring the qualification model of the FLTSATCOM satellite
[AD-A238485] N91-29217
FLEXIBLE BODIES
Experimental demonstration of a classical approach for flexible space structure control: NASA CSI testbeds
[NASA-CR-188724] N91-29212
Modeling of a 3-D light-weight space manipulator
[AD-A236823] N91-29586
Dimensionless parameters important to the prediction of vortex-induced vibration of long, flexible cylinders in ocean currents
[PB91-184713] N91-29630
Effects of colocation and non-colocation of sensors and actuators on flexible structures
[AD-A238457] N91-29844
FLEXIBLE SPACECRAFT
Equations of motion for a flexible spacecraft-lumped parameter idealization
[NASA-CR-188727] N91-29211
FLEXIBLE WINGS
Instrumentation for ASE experiments in the dynamic wind tunnel
[PD-FC-9112] N91-29197
FLIGHT ALTITUDE
NAE participation in the United States FAA vertical separation study
[NAE-LTR-FR-105] N91-29160
FLIGHT CONDITIONS
Agility: Presentation and flight test methods for the operational fighter pilot
[AD-A238456] N91-29174
FLIGHT CONTROL
Assessment team report on flight-critical systems research at NASA Langley Research Center
[NASA-CR-181850] N91-29176
Controlling crippled aircraft-with throttles
[NASA-TM-104238] N91-29191
A simulation evaluation of a four-engine jet transport using engine thrust modulation for flightpath control
[NASA-TM-4324] N91-29194
Verification of the FtCayuga fault-tolerant microprocessor system. Volume 1: A case study in theorem prover-based verification
[NASA-CR-4381] N91-29778
An expert system approach to global fault detection and isolation design
[AD-A238494] N91-29808
FLIGHT CREWS
Performance of several different Naval aviator communities on a cognitive/psychomotor test battery: Pipeline comparison and prediciton
[AD-A238564] N91-29730
FLIGHT MECHANICS
Flight Research Laboratory. Institute for Aerospace Research
[CTN-91-60105] N91-29140
FLIGHT OPERATIONS
Aircraft operations from runways with inclined ramps (ski-jump)
[AD-A237265] N91-29171
The use and design of flightcrew checklists and manuals
[AD-A237206] N91-29733
FLIGHT OPTIMIZATION
Experimental verification of an innovative performance-validation methodology for large space systems
[AD-A237864] N91-29214
FLIGHT PATHS
Aircraft operations from runways with inclined ramps (ski-jump)
[AD-A237265] N91-29171
A simulation evaluation of a four-engine jet transport using engine thrust modulation for flightpath control
[NASA-TM-4324] N91-29194
FLIGHT RULES
NAE participation in the United States FAA vertical separation study
[NAE-LTR-FR-105] N91-29160
FLIGHT SIMULATION
Controlling crippled aircraft-with throttles
[NASA-TM-104238] N91-29191
FLIGHT SIMULATORS
Agility: Presentation and flight test methods for the operational fighter pilot
[AD-A238456] N91-29174
The effect of three levels of laser glare on the speed and accuracy of target location performance when viewing a briefly presented visual array
[AD-A238565] N91-29736
FLIGHT TEST VEHICLES
The design and construction of a shiplaunched VTOL unmanned air vehicle
[AD-A238053] N91-29173
FLIGHT TESTS
International aviation (selected articles)
[AD-A237175] N91-29141
Flight evaluation of complex approaches in a Twin Otter aircraft using a microwave landing system
[NAE-LTR-FR-114] N91-29159
Agility: Presentation and flight test methods for the operational fighter pilot
[AD-A238456] N91-29174
Preliminary flight-determined subsonic lift and drag characteristics of the X-29A forward-swept-wing airplane
[NASA-TM-100409] N91-29177
An investigation into the use of side-arm control for civil rotorcraft applications
[AD-A226628] N91-29190
Flutter consideration of a crash-test aircraft
[DE91-015094] N91-29192

Concentrator flight test experiment
[AD-A237390] N91-29647
Parameter estimation via nonlinear differential correction least square method
[NAL-PD-FC-9110] N91-29814

FLIGHT TIME
The laser ablation of aluminum at 193, 248, and 351 nm
[AD-A237574] N91-29569

FLIGHT TRAINING
Performance of Marine AV-8B (Harrier) pilots on a cognitive/psychomotor test battery: Comparison and prediction
[AD-A238563] N91-29729

FLIR DETECTORS
Multi-sensor feature level fusion
[AD-A237106] N91-29411
Human factors of night vision devices: Anecdotes from the field concerning visual illusions and other effects
[AD-A237641] N91-29735

FLOATS
Donning times and flotation characteristics of infant life preservers: Four representative types
[AD-A237120] N91-29153

FLOTATION
Donning times and flotation characteristics of infant life preservers: Four representative types
[AD-A237120] N91-29153

FLOW CHARACTERISTICS
Modification of axial-flow compressor stall margin by variation of stationary blade setting angles
[AD-A238406] N91-29186
Approximate multiphase flow modeling by characteristic methods
[PB91-190959] N91-29526

FLOW DISTRIBUTION
Hydrogen-fueled scramjet investigation
[AD-A237569] N91-29183
Experimental and analytical comparison of flowfields in a 110 N (25 lbf) H2/O2 rocket
[NASA-TM-105175] N91-29230
Conformal FDTD modeling wake fields
[DE91-015129] N91-29407
Visualization of wake fields
[DE91-015130] N91-29408
A finite element solver for 3-D compressible viscous flows
[NASA-CR-184175] N91-29488
Solutions of two-dimensional Euler equations with multigrid acceleration
[NAL-PD-CF-9006] N91-29494
A numerical study of flow past a cylindrical body N91-29497
An experimental study of plunging liquid jet induced air carryunder and dispersion
[AD-A237757] N91-29511
A method of investigating scales of motion in a turbulent wake
[AD-A237923] N91-29514
Effects of 1, 2, 3, and 4 Hz imposed bulk flow oscillations on transition in a straight channel with 40 to 1 aspect ratio
[AD-A237988] N91-29517
Separation-bubble velocity measurements using an oscillating-hot-wire system
[AD-A237997] N91-29518
Effect of geometric parameters on the performance of second throat annular steam ejectors
[AD-A238645] N91-29522
Interactions of turbulent eddies and combustion in an MHD second stage combustor
[DE91-015722] N91-29968

FLOW EQUATIONS
Approximate multiphase flow modeling by characteristic methods
[PB91-190959] N91-29526
Course lectures abstracts of participants fellows project reports
[AD-A237909] N91-30070

FLOW MEASUREMENT
Progress toward synergistic hypermixing nozzles
[NASA-TM-105169] N91-29150
Ablative heat shield studies for NASA Mars/Earth return entry vehicles
[AD-A238159] N91-29215
Near-stall loss measurements in a CD compressor cascade with exploratory leading edge flow control
[AD-A237497] N91-29509
International Union of Theoretical and Applied Mechanics (IUTAM) Symposium on Aerothermodynamics in Combustors
[AD-A237943] N91-29516

FLOW STABILITY
A numerical study of flow past a cylindrical body N91-29497
Course lectures abstracts of participants fellows project reports
[AD-A237909] N91-30070

FLOW VELOCITY
Polymer drag reduction of a zero pressure gradient boundary layer
[AD-A237572] N91-29510
Separation-bubble velocity measurements using an oscillating-hot-wire system
[AD-A237997] N91-29518
Experimental study of gas kinetics of a fast-axial flow kilowatt CO2 laser
[AD-A237178] N91-29565
Direct-sampling MS measurement of volatiles in environmental samples
[DE91-013417] N91-29653

FLOW VISUALIZATION
A wind tunnel smoke generator
[NAE-LTR-LA-312] N91-29195
Visualization of wake fields
[DE91-015130] N91-29408
Theoretical study of the flow in a rotating duct. Experimental study through flow visualization in a curved duct
[RAE-TRANS-2189] N91-29493

FLOWMETERS
Transient flowmeter calibration facility
[AD-D014937] N91-29523

FLUID DYNAMICS
The evolution and structure of homogeneous stably stratified sheared turbulence N91-29499
Numerical study of non-impulsively started flow around a circular cylinder
[AD-A238051] N91-29519

FLUID FLOW
Measurements of retractable gas-cooled 6061 aluminum electrical leads operating in a vacuum
[DE91-014617] N91-29444
Computational fluid dynamics at NRC: A directory of practitioners and activities
[NRC-TTP-02-89] N91-29490

FLUID MANAGEMENT
NASA cryogenic fluid management space experiment efforts, 1960-1990
[NASA-TM-103752] N91-30073

FLUID MECHANICS
Three-dimensional vortex dynamics and interactions in near-wall turbulent boundary layers
[AD-A237413] N91-29507

FLUID-SOLID INTERACTIONS
Steady flow of a fluid-solid mixture between parallel plates
[DE91-013114] N91-29491

FLUORESCENCE
A survey of optical diagnostic methods for the study of fuel fouling
[AD-A237361] N91-29920

FLUORINE COMPOUNDS
Preparation and properties of new inorganic glasses and gel-derived solids
[AD-A238095] N91-29360

FLUTTER
International aviation (selected articles)
[AD-A237175] N91-29141
Flutter consideration of a crash-test aircraft
[DE91-015094] N91-29192

FLUX QUANTIZATION
NAE Twin Otter operations in FIFE 1989
[NASA-CR-188770] N91-29169

FOAMS
The cure of rigid polyurethane encapsulating foam
[DE91-016059] N91-29379

FOCUSING
Comparison of synthetic aperture radar autofocus techniques: Phase gradient vs subaperture
[DE91-014696] N91-29406

FOILS (MATERIALS)
Electrodeposition of high temperature superconductors
[AD-A238227] N91-29469
Computational simulations of plasma flow switches and imploding loads
[DE91-014768] N91-29480
Computational modeling of the Trailmaster Procyon system
[DE91-014765] N91-29955

FOKKER-PLANCK EQUATION
The Kramers problem: Fifty years of development
[DE91-617583] N91-29855
Fluidlike studies of the sheath and presheath regions of a plasma
[DE91-013343] N91-29944

FORECASTING
Fitting seasonal averages with a continuous function
[AD-A238300] N91-29704
Marketing for collegiate aviation education
[NIAR-91-18] N91-30042

FOREST MANAGEMENT
A practical example of forest mapping and timber volume estimation using LANDSAT-5 TM imagery
[INPE-5244-PRE/1675] N91-29635

FORESTS
A practical example of forest mapping and timber volume estimation using LANDSAT-5 TM imagery
[INPE-5244-PRE/1675] N91-29635
Using the TIMS to estimate evapotranspiration from a forest
[NASA-CR-188729] N91-29636

FORMALISM
A type calculus for mathematical programming modeling languages
[AD-A238160] N91-29766

FORMING TECHNIQUES
Advances in the drained shaping of ceramics
[DE91-015429] N91-29376

FORMULATIONS
Report on using expert systems for computer-aided formulation and property estimation of propellants. 1: Expert system shell selection and initial package design
[AD-A237567] N91-29383

FORTRAN
Performance implications of synchronization support for parallel FORTRAN programs
[AD-A238493] N91-29790

FOULING
Biofouling and corrosion fouling of plain and enhanced aluminum surfaces
[DE91-014464] N91-29300
A survey of optical diagnostic methods for the study of fuel fouling
[AD-A237361] N91-29920

FOUNDRIES
Silicon Wafer Advanced Packaging (SWAP). Multichip Module (MCM) foundry study, version 2
[AD-A237412] N91-29452

FOURIER TRANSFORMATION
Spectral estimation techniques with emphasis on short data records: A primer
[AD-A237486] N91-29271
Approximation from shift-invariant surfaces of L2(IRd)
[AD-A238165] N91-29826

FRACTIONATION
Stable isotope fractionation in photosynthesis: Analysis of autotrophic competence following transformation of the chloroplast genome of Chlamydomonas
[DE91-015792] N91-29713

FRACTURE MECHANICS
Workshop proceedings: Toughening Mechanisms in Quasi-Brittle Materials
[AD-A238289] N91-29248
Fission-fusion adaptivity in finite elements for nonlinear dynamics of shells
[AD-A238029] N91-29626
A study of the relationship between macroscopic measures and physical processes occurring during N00014-89-J-1708
[AD-A238423] N91-29627

FRACTURE STRENGTH
Mechanisms of transformation toughening
[DE91-013151] N91-29293
Micromechanisms of monotonic and cyclic subcritical crack growth in advanced high melting point low-ductility intermetallics
[AD-A238151] N91-29317
Pressure vessel burst test program
[AD-A237845] N91-29624

FRACTURES (MATERIALS)
Workshop proceedings: Toughening Mechanisms in Quasi-Brittle Materials
[AD-A238289] N91-29248

FRACTURING
Launch capabilities to over 10 km/s
[DE91-014657] N91-29203
Impact characterization of graphite fiber reinforced thermoplastic laminates
[NIAR-91-16] N91-29241
Inelastic deformation and fracture of glassy solids
[AD-A237290] N91-29344

FRAGMENTATION
Pressure vessel burst test program
[AD-A237845] N91-29624
Negative ion formation with electron impact to simulants
[AD-A237478] N91-29881

FRAGMENTS
Explosively driven missile trajectory parameters for various fragment materials and velocities
[DE91-014330] N91-29631
Reactions of hydrogen atoms important to the decomposition of energetic materials
[AD-A238482] N91-29890

FRAMES (DATA PROCESSING)
Video frame store: An advanced solid state recorder
[DE91-015709] N91-29549
FREE CONVECTION
Theoretical study of the flow in a rotating duct. Experimental study through flow visualization in a curved duct
[RAE-TRANS-2189] N91-29493
FREE ELECTRON LASERS
Evolution of a finite pulse of radiation in a high-power free-electron laser
[AD-A237427] N91-29568
Research in the physical sciences with application to the free electron laser
[AD-A237884] N91-29571
Degradation of brightness by resonant particle effects
[DE91-015181] N91-29578
RF transfer in the coupled-cavity free-electron laser two-beam accelerator
[DE91-015676] N91-29583
Control of energy sweep and transverse beam motion in induction linacs
[DE91-015177] N91-29911
FREE FLIGHT
A method of investigating scales of motion in a turbulent wake
[AD-A237923] N91-29514
FREE FLOW
Exact and approximate solutions to the oblique shock equations for real-time applications
[NASA-CR-187173] N91-29147
FREE RADICALS
Model filled polymers 8: Synthesis of crosslinked polymeric beads by seed polymerization
[AD-A237429] N91-29349
Study of elementary reactions and energy transfer processes involving the NH and CN free radicals
[AD-A238461] N91-29889
FREEZING
Performance of asphalt concrete airport pavements during thaw weakening periods: A field study
[AD-A237441] N91-29198
FREQUENCIES
On the role of crystal defects as sources of resonator frequency instability
[AD-A238505] N91-30018
FREQUENCY DIVISION MULTIPLE ACCESS
The study of space communications spread spectrum systems. Part 1: Saw-based joint group demodulation of frequency shift keyed and differential phase shift keyed signals
[QU-90-1-PT-1] N91-29395
FREQUENCY HOPPING
A study of space communications spread-spectrum systems, phase 5 and 6. Part 2: Coding and modulation
[QU-90-2-PT-2] N91-29396
The study of space communications spread spectrum systems. Part 3: Uplink synchronization in an EHF frequency-hopped satellite system
[QU-90-3-PT-3] N91-29397
Coding for frequency hopped spread spectrum satellite communications
[ECE-89-1] N91-29398
FREQUENCY MEASUREMENT
A new system for measurement of low frequency radio transmitting antenna parameters in near real time
[AD-A238555] N91-29429
Superconducting instrumentation for precision measurement and control
[DE91-014650] N91-29541
FREQUENCY MODULATION
Combinatorial FSK modulation for power-efficient high-rate communications
[NASA-TM-105188] N91-29404
Application of Multi-Frequency Modulation (MFM) for high-speed data communications to a voice frequency channel
[AD-A238019] N91-29422
A new system for measurement of low frequency radio transmitting antenna parameters in near real time
[AD-A238555] N91-29429
Nonlinear optical interactions involving the real Gaussian field
[DE91-015052] N91-29936
FREQUENCY SHIFT
A new system for measurement of low frequency radio transmitting antenna parameters in near real time
[AD-A238555] N91-29429
FREQUENCY SHIFT KEYING
The study of space communications spread spectrum systems. Part 1: Saw-based joint group demodulation of frequency shift keyed and differential phase shift keyed signals
[QU-90-1-PT-1] N91-29395
A study of space communications spread-spectrum systems, phase 5 and 6. Part 2: Coding and modulation
[QU-90-2-PT-2] N91-29396
The study of space communications spread spectrum systems. Part 3: Uplink synchronization in an EHF frequency-hopped satellite system
[QU-90-3-PT-3] N91-29397
Coding for frequency hopped spread spectrum satellite communications
[ECE-89-1] N91-29398
Combinatorial FSK modulation for power-efficient high-rate communications
[NASA-TM-105188] N91-29404
FREQUENCY STABILITY
On the role of crystal defects as sources of resonator frequency instability
[AD-A238505] N91-30018
FRICTION
An approximate analysis of balloting motion of railgun projectiles
[AD-A237942] N91-29206
An analysis of the wear behavior of SiC whisker reinforced alumina from 25 to 1200 C
[NASA-TM-104489] N91-29235
Quasistatic manipulation with compliance and friction N91-29591
FRICTION FACTOR
Adiabatic two-phase flow frictional pressure drop. Part 2: A generalized method for data correlation
[DE91-014462] N91-29501
Adiabatic two-phase flow frictional pressure drop. Part 1: Critical parameters and friction factors for air-water mixture
[DE91-014463] N91-29502
FROST
Debris/ice/TPS assessment and photographic analysis for Shuttle Mission STS-40
[NASA-TM-103822] N91-29210
FUEL CELLS
ANL's development of conductive ceramic components for MCFC
[DE91-015557] N91-29336
Electrocatalytic study of ammonia synthesis and methane dimerization in high temperature solid electrolyte cells
[DE90-012496] N91-29437
Developmental status and system studies of the monolithic solid oxide fuel cell
[DE91-014389] N91-29645
FUEL COMBUSTION
Investigation of particulate formation during diesel spray combustion
[DE90-008282] N91-29255
A model of multicomponent droplet evaporation with liquid phase reactions
[DE90-012535] N91-29257
Investigation of the combustion of liquid fuels in Rijke type pulse combustors
[DE90-012490] N91-29381
A methodology for inhibiting the formation of pollutants in diesel engines
[DE90-011615] N91-29584
FUEL CORROSION
A novel epoxy lacquer for high strength steel in F-111 aircraft during overhaul
[AD-A236826] N91-29326
FUEL FLOW
Electro-rheology fluids and liquid fuel flow
[AD-A238600] N91-29520
FUEL INJECTION
Experimental study of cross-stream mixing in a cylindrical duct
[NASA-TM-105180] N91-29187
Supersonic combustion of a transverse injected H2 jet in a radio frequency heated flow
[DE91-014739] N91-29281
Ultra-low NOx gas turbine combustor
[PB91-184994] N91-29601
FUEL PRODUCTION
Production and use of metals and oxygen for lunar propulsion
[NASA-TM-105195] N91-29222
FUEL SPRAYS
Investigation of particulate formation during diesel spray combustion
[DE90-008282] N91-29255
A methodology for inhibiting the formation of pollutants in diesel engines
[DE90-011615] N91-29584
FUELS
Overview of the technical implications of methanol and ethanol as highway motor vehicle fuels
[PB91-182881] N91-29385
A survey of optical diagnostic methods for the study of fuel fouling
[AD-A237361] N91-29920
FUNCTIONAL DESIGN SPECIFICATIONS
A program to operate and upgrade the GL low altitude lidar systems
[AD-A238081] N91-29423
FUNCTIONS (MATHEMATICS)
Stochastic simulation techniques for partition function approximation of Gibbs random field images
[AD-A238611] N91-29775
A note on the automated differentiation of implicit functions
[DE91-015104] N91-29816
FUSELAGES
Tutor aft fuselage and empennage full-scale test: Procedures for creating a damage log
[NAE-ST-576] N91-29167
Test results for composite specimens and elements containing joints and cutouts
[NASA-CR-178246] N91-29254
FUSES (ORDNANCE)
The functional dependence of trajectory dispersion on initial condition errors
[DE91-014661] N91-29151
FUSION REACTORS
ICRF edge modeling
[DE91-014401] N91-29403
Inertial fusion program and National Laser Users Facility program
[DE91-013164] N91-29556
Fusion reactor materials
[DE91-012984] N91-29942
Collisional processes of interest in MFE plasma research
[DE91-013023] N91-29943
Thick-section weldments in 21-6-9 and 316LN stainless steel for fusion energy applications
[DE91-015307] N91-29963

G

GALACTIC EVOLUTION
Dark matter in the universe
[DE91-014863] N91-30065
Course lectures abstracts of participants fellows project reports
[AD-A237909] N91-30070
GALACTIC RADIATION
Course lectures abstracts of participants fellows project reports
[AD-A237909] N91-30070
GALLIUM ARSENIDES
Physics and applications of the lock-on effect
[DE91-014670] N91-29446
Failure mechanisms on GaAs integrated circuits: Electromigration on GaAs
[AD-A237352] N91-29451
Millimeter-wave characterization of GaAs devices and IC's
[AD-A237843] N91-29461
High gain photoconductive semiconductor switching
[DE91-014668] N91-29478
Stable integrated microwave to optical modulator
[AD-A238166] N91-29574
Dielectric function of semiconductor superlattice
[DE91-617788] N91-29976
Growth condition dependence of RHEED pattern from GaAs(111)B surface
[DE91-014770] N91-29986
Development of model based magnetic LP-LEC growth large diameter GaAs
[AD-A237456] N91-29998
Defect reductions in epitaxial growth using superlattice buffer layers
[AD-A237710] N91-30005
Laser probing of the kinetics and dynamics of III -V semiconductor growth
[AD-A237795] N91-30009
The embedded electron-gas boundary: A new standard problem in surface physics
[AD-A238152] N91-30014
GALLIUM NITRIDES
Pseudomorphic semiconducting heterostructures from combinations of AlN, GaN and seleced SiC polytypes: Theoretical advancement and its coordination with experimental studies of nucleation, growth, characterizaiton and device development
[AD-A238520] N91-30020
Growth, nitrogen vacancy reduction and solid solution formation in cubic GaN thin films and the subsequent fabrication of superlattice structures using AlN and InN
[AD-A238521] N91-30021
GALLIUM PHOSPHIDES
Tritium-field betacells
[DE91-014666] N91-29910

Defect reductions in epitaxial growth using superlattice buffer layers
[AD-A237710] N91-30005

GAMMA RAYS
Remote sensing of snow covers using the gamma ray technique
[AD-A238016] N91-29639
Inelastic scattering in condensed matter with high intensity Moessbauer radiation
[DE91-014384] N91-29980

GAS CHROMATOGRAPHY
CO2 measurements along the WOCE P-16 and 19 sections in the South Pacific Ocean: A joint LDGO/WHOI program
[DE91-015742] N91-29708

GAS COOLED REACTORS
Light weight space power reactors for nuclear electric propulsion
[DE91-014803] N91-29232

GAS DENSITY
Atmospheric dispersion models for dense gas releases
[DE91-015144] N91-29654

GAS DETECTORS
Laboratory evaluation of portable and walk-through explosives vapour detectors
[NAE-LTR-UA-104] N91-29533

GAS DYNAMICS
Problems in nonlinear continuum dynamics
[AD-A237844] N91-29512

GAS FLOW
Experimental study of gas kinetics of a fast-axial flow kilowatt CO2 laser
[AD-A237178] N91-29565
Direct-sampling MS measurement of volatiles in environmental samples
[DE91-013417] N91-29653

GAS GENERATORS
Development of an explosive vapor generator
[DE91-015700] N91-29386

GAS GUNS
The use of high velocity launchers for scientific and engineering studies
[DE91-015564] N91-29208
Dynamic behavior of fully dense molybdenum
[DE91-014902] N91-29304

GAS INJECTION
Hydrogen-fueled scramjet investigation
[AD-A237569] N91-29183
Qualitative investigation of cryogenic injected shock dissipation
[NASA-TM-105140] N91-29525

GAS JETS
Supersonic combustion of a transverse injected H2 jet in a radio frequency heated flow
[DE91-014739] N91-29281

GAS LASERS
Laser surface modification for selective electroplating of metal: A 2.5 m/s laser direct-write process
[DE91-014988] N91-29322

GAS MIXTURES
An evaluation of nickel-aluminum coatings fabricated with the plasma-spray process
[DE91-013208] N91-29328
Kinetics of dark reaction in chemical laser gases
[DE91-015320] N91-29579

GAS PRESSURE
Experimental study of gas kinetics of a fast-axial flow kilowatt CO2 laser
[AD-A237178] N91-29565

GAS TRANSPORT
Problems in nonlinear continuum dynamics
[AD-A237844] N91-29512
Criteria for assessing the role of transported ozone/precursors in ozone nonattainment areas
[PB91-195958] N91-29662

GAS TURBINE ENGINES
Compressor fault modelling for engine health monitoring: Review and recommendations
[NRC-TR-ENG-004] N91-29178
The failure of components in power generation equipment
[NAE-LTR-ST-1774] N91-29180
Generalized simplified analytic solution of optimum cycle parameters for land and aircraft gas turbine engines and its applications
[AD-A237414] N91-29182
Evaluation of aircraft turbine engine redesigns
[AD-A237599] N91-29184
Modification of axial-flow compressor stall margin by variation of stationary blade setting angles
[AD-A238406] N91-29186
Application of ceramics to industrial gas turbines
[DE91-013140] N91-29330

GAS TURBINES
Generalized simplified analytic solution of optimum cycle parameters for land and aircraft gas turbine engines and its applications
[AD-A237414] N91-29182
An overview of aerothermal modeling
[NRC-32088] N91-29258
Application of ceramics to industrial gas turbines
[DE91-013140] N91-29330
International Union of Theoretical and Applied Mechanics (IUTAM) Symposium on Aerothermodynamics in Combustors
[AD-A237943] N91-29516
Ultra-low NOx gas turbine combustor
[PB91-184994] N91-29601

GAS-METAL INTERACTIONS
The interaction of hydrogen with metal alloys
[NASA-TP-3128] N91-29318

GASEOUS DIFFUSION
The interaction of hydrogen with metal alloys
[NASA-TP-3128] N91-29318

GASEOUS FUELS
Conversion of methanol-fueled 16-valve, 4-cylinder engine to operation on gaseous 2H2/CO fuel
[PB91-195941] N91-29602

GASES
User's manual for DIODE
[AD-A237190] N91-29752

GATES (CIRCUITS)
InP and InGaAs submicron gate microwave power transistors for 20 GHz applications
[AD-A238595] N91-29473

GAUSSIAN ELIMINATION
Singularities in Gaussian random fields
[AD-A238220] N91-29839
Nonlinear optical interactions involving the real Gaussian field
[DE91-015052] N91-29936

GEAR TEETH
Local synthesis and tooth contact analysis of face-milled spiral bevel gears
[NASA-TM-105182] N91-29600

GEARS
Effect of two synthetic lubricants on life of AISI 9310 spur gears
[NASA-TM-104352] N91-29599
Local synthesis and tooth contact analysis of face-milled spiral bevel gears
[NASA-TM-105182] N91-29600

GELS
Preparation and properties of new inorganic glasses and gel-derived solids
[AD-A238095] N91-29360

GENETIC ENGINEERING
Microbiology and physiology of anaerobic fermentations of cellulose
[DE91-015239] N91-29712
Stable isotope fractionation in photosynthesis: Analysis of autotrophic competence following transformation of the chloroplast genome of Chlamydomonas
[DE91-015792] N91-29713

GEOCHEMISTRY
Subsurface Science Program
[DE91-015480] N91-29665

GEODESY
Regional tectonic deformation in Southern California, inferred from terrestrial geodesy and the global positioning system N91-29669

GEODETIC ACCURACY
The optimal location of GEODSS sensors in Canada
[AD-A238444] N91-29216

GEODETIC SATELLITES
Seasonal air and water mass redistribution and its effect on satellite and polar motion N91-29202
Algorithms for converting geodetic Earth location to satellite time and swath pixel coordinates for the DMSP satellite system
[AD-A237589] N91-29638

GEOGRAPHIC INFORMATION SYSTEMS
A global geographic information system data base of storm occurrences and other climatic phenomena affecting coastal zones
[DE91-014949] N91-29682

GEOLOGICAL SURVEYS
Three-dimensional visualization for evaluating automated, geomorphic pattern-recognition analyses of crustal structures
[DE91-012929] N91-29668

GEOLOGY
Stochastic modelling of seafloor morphology
[AD-A237063] N91-29697

GEOMAGNETISM
Impacts of a nominal nuclear electromagnetic pulse on electric power systems
[DE91-012991] N91-29401

GEOMETRY
Infrared and Raman spectra of C60 and C70 solid films at room temperature
[AD-A237880] N91-29462

GEOMORPHOLOGY
Three-dimensional visualization for evaluating automated, geomorphic pattern-recognition analyses of crustal structures
[DE91-012929] N91-29668
Investigations in Martian geology. Part 1: Nature of the mantling deposit in the heavily cratered terrain of northeastern Arabia, Mars. Part 2: Experimental studies of clean and dust-or-sand-covered ice sublimation under Mars-like conditions N91-30067

GEOPHYSICS
Test of Newtonian gravity using DSV sea cliff
[AD-A238558] N91-29680

GEOPOTENTIAL
Seasonal air and water mass redistribution and its effect on satellite and polar motion N91-29202

GERMANIUM COMPOUNDS
Scanning tunneling microscopy studies of the surfaces of a-Si:H and a-SiGe:H films
[DE91-002169] N91-29983

GET AWAY SPECIALS (STS)
Concentrator flight test experiment
[AD-A237390] N91-29647

GIBBS FREE ENERGY
Solvent effects on simple electron transfer reactions. A comparison of results in Debye and non-Debye solvents
[AD-A237157] N91-29875
Discreteness-of-solvent effects in Marcus equations in the mean spherical approximation
[AD-A237133] N91-29996

GLARE
Methods for evaluating discomfort glare
[PB91-185132] N91-29722
The effect of three levels of laser glare on the speed and accuracy of target location performance when viewing a briefly presented visual array
[AD-A238565] N91-29736

GLASS
Short-pulse glass slab amplifier
[DE91-015385] N91-29580
Fast acting optical deflection
[AD-A237904] N91-29927

GLASS FIBERS
Preparation and properties of new inorganic glasses and gel-derived solids
[AD-A238095] N91-29360
Fatigue resistant optical fibers
[AD-A237568] N91-29921

GLASS LASERS
The MIT short-wavelength laser project
[DE91-015357] N91-29582

GLINT
Portable 45-gigahertz radar for glint and scintillation studies
[AD-A238005] N91-29421

GLOBAL POSITIONING SYSTEM
Evaluation of a pre-production version of Canadian Marconi CMA-786 GPS receiver
[NAE-LTR-FR-106] N91-29158
GPS: Aspects of pseudo-range positioning offshore N91-29161
Regional tectonic deformation in Southern California, inferred from terrestrial geodesy and the global positioning system N91-29669

GOGGLES
Human factors of night vision devices: Anecdotes from the field concerning visual illusions and other effects
[AD-A237641] N91-29735

GOLD
X ray reflectivity studies of Au surfaces
[DE91-015308] N91-29307
Temperature dependence of proton electroreduction kinetics at gold(111) and (210) surfaces
[AD-A237460] N91-29879
Connection between grain boundary structure and energy
[DE91-015558] N91-30030

GOLD ISOTOPES
Structure and stability of underpotentially deposited layers on Au(111) studied by optical second harmonic generation
[AD-A237087] N91-29268

GOODNESS OF FIT
An improved method of investigation of compressor blade fit using holographic interferometry
[AD-A238182] N91-29185
New modified Anderson-Darling and Cramer-von Mises goodness-of-fit tests for a normal distribution with specified parameters
[AD-A238630] N91-29846

A goodness-of-fit test for a family of two parameter Weibulls with known shape using minimum distance estimation of parameters
[AD-A238633] N91-29847
GOVERNMENT PROCUREMENT
Statistical characterization of graphite fiber for prediction of composite structure reliability
[AD-A238020] N91-29245
GOVERNMENTS
The Government-University-Industry Research Roundtable
[DE91-015795] N91-30044
GRADIENTS
Comparison of synthetic aperture radar autofocus techniques: Phase gradient vs subaperture
[DE91-014696] N91-29406
GRAIN BOUNDARIES
Molecular dynamics simulation of the effect of interfaces in melting and solid-state amorphization
[DE91-015550] N91-29284
Deformation and thermal fatigue in high temperature austenitic alloys
[DE91-014981] N91-29305
Powder metallurgy technology (selected articles)
[AD-A237176] N91-29310
Deformation induced microstructural and microchemical changes during thermomechanical treatment
[DE91-014862] N91-29319
Phase transformations, ultrastructure, and properties of rigid-rod polymers
[AD-A238643] N91-29368
High resolution electron microscopy of grain boundaries
[DE91-010593] N91-29970
Quantitative analysis of oxygen segregation on inversion domain boundaries in aluminum nitride
[DE91-010869] N91-29971
Correlations between grain boundary structure and energy
[DE91-015204] N91-29990
Surface structure and surface order
[AD-A237466] N91-30001
Effect of hydrogen on the electronic structure of a grain boundary in iron
[AD-A237499] N91-30002
Connection between grain boundary structure and energy
[DE91-015558] N91-30030
Determination of thermodynamic and kinetic properties of grain boundaries using high temperature calorimetry
[DE91-015571] N91-30031
TEM characterization of grain boundaries in mixed bicrystal films of aluminum
[DE91-016267] N91-30038
GRAIN SIZE
Powder metallurgy technology (selected articles)
[AD-A237176] N91-29310
Materials research for sodium engine development
[DE91-015715] N91-29378
GRAMMARS
The CYK-approach to serial and parallel parsing
[PB91-185447] N91-29792
GRANULAR MATERIALS
Steady flow of a fluid-solid mixture between parallel plates
[DE91-013114] N91-29491
GRAPH THEORY
An exact algorithm for funding undirected Hamiltonian cycles based on a two-matching problem relaxation
[AD-A237241] N91-29753
Proceedings of the 1st Workshop on Proximity Graphs
[AD-A237250] N91-29818
GRAPHITE
Impact characterization of graphite fiber reinforced thermoplastic laminates
[NIAR-91-16] N91-29241
Statistical characterization of graphite fiber for prediction of composite structure reliability
[AD-A238020] N91-29245
Thermal emittance enhancement of graphite-copper composites for high temperature space based radiators
[NASA-TM-105178] N91-29332
Thermophysical properties of POCO AXF-5Q graphite up to melting
[DE91-014751] N91-29334
GRAPHITE-EPOXY COMPOSITES
Assessment of impact damage in toughened resin composites
[NAE-LTR-ST-1695] N91-29236
Composite transport wing technology development: Design development tests and advanced structural concepts
[NASA-CR-4177] N91-29253
Review of literature on the damage, loss of stiffness, and residual strength of graphite/epoxy laminates subjected to cyclic loading
[NAE-LTR-ST(CR)-1711] N91-29611
GRAPHS (CHARTS)
Negation in knowledge graphs
[PB91-185421] N91-29776
Scrawl strips, and letter or B-letter strips: Depicting marginals of scatter plots
[AD-A238556] N91-29845
GRATINGS (SPECTRA)
Fast acting optical deflection
[AD-A237904] N91-29927
GRAVITATION
Test of Newtonian gravity using DSV sea cliff
[AD-A238558] N91-29680
GRAVITATIONAL COLLAPSE
Research in nuclear astrophysics: Stellar collapse and supernovae
[DE91-015449] N91-30066
GRAVITATIONAL CONSTANT
Test of Newtonian gravity using DSV sea cliff
[AD-A238558] N91-29680
GRAVITATIONAL EFFECTS
Bubble generation and movement under microgravity conditions
[NAE-LTR-FR-110] N91-29388
Load tables for the Avery and Gilmore standard force machines corrected for gravity, 1989
[NAE-LTR-ST-1703] N91-29535
GREEN'S FUNCTIONS
Effect of a free surface on stress distribution in a bimaterial composite
[PB91-185116] N91-29251
The boundary element method applied to the two dimensional Stefan moving boundary problem
[AD-A238458] N91-29828
Parametric design calculations using Green's function to determine unique source
[DE91-014683] N91-29861
Research in elementary particle physics
[DE91-015359] N91-29892
GROUND BASED CONTROL
Acoustic tests on a new motor generator system for the Minuteman launch control centers at Alpha 01 and Sierra 00, Malmstrom AFB, Montana
[AD-A237944] N91-29648
GROUND WIND
Equatorial entrainment zone simulations
[AD-A237234] N91-29657
GROWTH
Simulation of the growth of Mo/Si multilayers
[DE91-015679] N91-29486
GULF OF ALASKA
Sea level and bottom pressure measurements in the Northern Gulf of Alaska
[PB91-184135] N91-29705
GUN LAUNCHERS
Experimental hypervelocity firings using stick and granular propellant configurations
[AD-A238628] N91-29384
GUN PROPELLANTS
Report on using expert systems for computer-aided formulation and property estimation of propellants. 1: Expert system shell selection and initial package design
[AD-A237567] N91-29383

H

HABITATS
Concepts for manned lunar habitats
[NASA-TM-104114] N91-30068
HADRONS
Chasing the x(sub f) dependence of J/psi production
[DE91-015136] N91-29899
HALF LIFE
Study of activation of metal samples from LDEF-1 and Spacelab-2
[NASA-CR-184171] N91-29297
HALIDES
Electrical, magnetic, and spectroscopic properties of tetrathiafulvalene charge transfer compounds with iron, ruthenium, rhodium, and iridium halides
[AD-A237607] N91-29273
HALL EFFECT
Mixed valent and heavy ferimons and related systems
[DE91-015454] N91-29900
HAMILTONIAN FUNCTIONS
An exact algorithm for funding undirected Hamiltonian cycles based on a two-matching problem relaxation
[AD-A237241] N91-29753
A survey of nonlinear dynamics (chaos theory)
[AD-A237802] N91-29821
HANDBOOKS
Aircraft icing handbook, volume 1
[AD-A238039] N91-29154
Aircraft icing handbook, volume 2
[AD-A238040] N91-29155
Aircraft icing handbook, volume 3
[AD-A238041] N91-29156
Scientific and technical information handbook for technical report preparation
[AD-A238548] N91-30051
HARDENING (MATERIALS)
Tensile properties and microstructure of Alloy 718 thermally aged to 50,000 h
[DE91-014099] N91-29299
Fundamental studies in dynamic plasticity
[AD-A237114] N91-29621
HARDWARE
Hardware interface for high speed video imaging
[AD-D014902] N91-29400
A prolog system for converting VHDL-based models to Generalized Extraction System (GES) rules
[AD-A238545] N91-29741
HARMONIC GENERATIONS
Picosecond studies of chemical intermediates
[AD-A237859] N91-29275
Atomic physics in strong fields
[DE91-015393] N91-29872
HARMONIC GENERATORS
Structure and stability of underpotentially depositied layers on Au(111) studied by optical second harmonic generation
[AD-A237087] N91-29268
HARMONIC OSCILLATORS
Supercoherent states and physical systems
[DE91-014598] N91-30040
HAZARDOUS MATERIAL DISPOSAL (IN SPACE)
Chemical waste disposal in space by plasma discharge
[NASA-CR-184169] N91-29737
HAZARDS
Confidence bands for the median survival time as a function of the covariates in the Cox model
[AD-A237626] N91-29835
HEARING
Auditory processing of complex sounds across frequency channels
[AD-A238023] N91-29862
HEART RATE
Micro SAINT modeling of physiological and human performance in the heat
[AD-A238659] N91-29719
HEAT EXCHANGERS
Application of ceramics to industrial gas turbines
[DE91-013140] N91-29330
Numerical prediction of turbulent oscillating flow and associated heat transfer
[NASA-CR-187177] N91-29524
Heat transfer and pressure drop in a compact pin-fin heat exchanger with pin orientation at 18 deg to the flow direction
[NASA-CR-186544] N91-29527
Electroforming thin channel heat exchangers
[DE91-015114] N91-29528
Microtube strip heat exchanger
[DE91-015223] N91-29529
HEAT FLUX
The nature of the propagation of sea breeze fronts in central California
[AD-A238635] N91-29692
Acoustic tomographic estimate of ocean advective heat flux: A numerical assessment in the Norwegian Sea
[AD-A237100] N91-29698
HEAT GENERATION
Bearing tester data compilation analysis, and reporting and bearing math modeling
[NASA-CR-178883] N91-29603
HEAT MEASUREMENT
A survey of optical diagnostic methods for the study of fuel fouling
[AD-A237361] N91-29920
Determination of thermodynamic and kinetic properties of grain boundaries using high temperature calorimetry
[DE91-015571] N91-30031
HEAT PIPES
The 0-G experiments with advanced ceramic fabric wick structures
[DE91-015531] N91-29377
HEAT RADIATORS
Thermal emittance enhancement of graphite-copper composites for high temperature space based radiators
[NASA-TM-105178] N91-29332
HEAT RESISTANT ALLOYS
Intermetallics: Canadian perspective
[NAE-LTR-ST-1771] N91-29288

Tensile properties and microstructure of Alloy 718 thermally aged to 50,000 h
[DE91-014099] N91-29299
Deformation and thermal fatigue in high temperature austenitic alloys
[DE91-014981] N91-29305
Lightweight disk alloy development
[AD-A237064] N91-29309

HEAT STORAGE
Electric rate structures for thermal energy storage evaluation
[DE91-013168] N91-29644

HEAT TOLERANCE
Physiological responses to intermittent exercise as modified by heat stress and protective clothing
[AD-A237447] N91-29716
Micro SAINT modeling of physiological and human performance in the heat
[AD-A238659] N91-29719

HEAT TRANSFER
Arcjet thermal characteristics
[NASA-TM-105156] N91-29231
Biofouling and corrosion fouling of plain and enhanced aluminum surfaces
[DE91-014464] N91-29300
The 0-G experiments with advanced ceramic fabric wick structures
[DE91-015531] N91-29377
Measurements of retractable gas-cooled 6061 aluminum electrical leads operating in a vacuum
[DE91-014617] N91-29444
Theoretical study of the flow in a rotating duct. Experimental study through flow visualization in a curved duct
[RAE-TRANS-2189] N91-29493
Analysis of condensation and evaporation of ammonia/water mixtures in matrix heat-exchangers
[DE91-014461] N91-29500
Prediction of the pressure drop in transverse, repeated-rib tubes with numerical modeling
[DE91-014465] N91-29503
Heat transfer and pressure drop in a compact pin-fin heat exchanger with pin orientation at 18 deg to the flow direction
[NASA-CR-186544] N91-29527

HEAT TREATMENT
Micromechanisms of monotonic and cyclic subcritical crack growth in advanced high melting point low-ductility intermetallics
[AD-A238151] N91-29317

HEATING
Generalized simplified analytic solution of optimum cycle parameters for land and aircraft gas turbine engines and its applications
[AD-A237414] N91-29182
Hamiltonian 3-D ray tracing in the oceanic waveguide on the ellipsoidal earth
[AD-A237458] N91-29700

HEAVY IONS
Design aspects for a pulsed-mode, high-intensity, heavy negative ion source
[DE91-011094] N91-29864
Strange quarks in nuclei
[DE91-015833] N91-29895
Study of particle correlations in high energy S + Pb and Pb + Pb interactions with a magnetic-interferometric-emulsion-chamber
[DE91-014355] N91-29897
Electromagnetic dissociation of Au and Co targets by relativistic heavy ions
[DE91-014915] N91-29906
Ion Implantation Technology: Proceedings of the 8th International Conference on Ion Implantation Technology
[AD-A237955] N91-30013

HELICOPTER CONTROL
An investigation into the use of side-arm control for civil rotorcraft applications
[AD-A226628] N91-29190

HELICOPTERS
Unsteady compressible lifting surface analysis for rotary wings using velocity potential modes N91-29170
Response and stability analysis of helicopter rotor blades using computerized symbolic manipulation
[AD-A238660] N91-29175
Control of flow over a backward facing step
[AD-A238638] N91-29521
Human factors of night vision devices: Anecdotes from the field concerning visual illusions and other effects
[AD-A237641] N91-29735
Acoustic background noise variation in Air Force platforms and its effect on noise removal algorithms
[AD-A238279] N91-29863

HELIUM
A technique for messuring the solubilities of gases in liquids
[AD-A238071] N91-29278
The interaction of hydrogen with metal alloys
[NASA-TP-3128] N91-29318
Heat transfer and pressure drop in a compact pin-fin heat exchanger with pin orientation at 18 deg to the flow direction
[NASA-CR-186544] N91-29527

HELIUM ISOTOPES
Mixed valent and heavy ferimons and related systems
[DE91-015454] N91-29900

HELMET MOUNTED DISPLAYS
Objective assessments of mobility with an early Unmanned Ground Vehicle (UGV) prototype viewing system
[AD-A237317] N91-29595

HETEROJUNCTION DEVICES
Laser probing of the kinetics and dynamics of III -V semiconductor growth
[AD-A237795] N91-30009

HETEROJUNCTIONS
Pseudomorphic semiconducting heterostructures from combinations of AlN, GaN and seleced SiC polytypes: Theoretical advancement and its coordination with experimental studies of nucleation, growth, characterizaiton and device development
[AD-A238520] N91-30020

HEURISTIC METHODS
An exact two-matching based branch and bound algorithm for the symmetric traveling salesman problem
[AD-A237878] N91-29823
Heuristic methods in applied probability
[AD-A238229] N91-29841

HIERARCHIES
Hierarchic extensions in the static and dynamic analysis of elastic beams N91-29613

HIGH ALTITUDE
Description of the Strategic High-Altitude Atmospheric Radiation Code (SHARC)
[AD-A237089] N91-29671

HIGH ENERGY INTERACTIONS
The High Energy Solar Physics mission (HESP): Scientific objectives and technical description
[NASA-TM-105033] N91-29201
Study of particle correlations in high energy S + Pb and Pb + Pb interactions with a magnetic-interferometric-emulsion-chamber
[DE91-014355] N91-29897
Theoretical high energy physics
[DE90-012527] N91-29904
Theoretical high energy physics
[DE91-013639] N91-29905
A research program in experimental and theoretical high energy physics
[DE91-014728] N91-29907
High energy physics at Tufts University
[DE91-015055] N91-29908
High energy physics: Experimental, Theoretical, and Phenomenology Institute
[DE91-015737] N91-29912

HIGH FREQUENCIES
Penn State/ONR Mid Frequency Workshop
[AD-A237982] N91-29420
Introduction of a current waveform, waveshaping technique to limit conduction loss in high-frequency dc-dc converters suitable for space power
[AD-A237903] N91-29465
The utility of elliptical and circular confidence regions for HFDF receivers
[AD-A238390] N91-29842

HIGH GAIN
High gain photoconductive semiconductor switching
[DE91-014668] N91-29478

HIGH POWER LASERS
Chinese physics lasers (selected articles)
[AD-A237263] N91-29567
Evolution of a finite pulse of radiation in a high-power free-electron laser
[AD-A237427] N91-29568
Development of laser optics for the AWA photocathode
[DE91-015552] N91-29581
Laser-atom interaction at high intensities
[AD-A238231] N91-29887

HIGH PRESSURE
The use of high velocity launchers for scientific and engineering studies
[DE91-015564] N91-29208

HIGH RESOLUTION
VLSI circuit techniques and technologies for ultrahigh speed data conversion interfaces
[AD-A238115] N91-29468
High resolution electron microscopy of grain boundaries
[DE91-010593] N91-29970
High-resolution Z-contrast imaging of superlattices and heterostructures
[DE91-015329] N91-29994
High resolution electron energy loss studies of surface vibrations
[DE91-014539] N91-30024

HIGH REYNOLDS NUMBER
Calculated performance of the NASA Lewis icing research tunnel
[NASA-TM-105173] N91-29199
An evaluation of the NEKTON program
[AD-A237888] N91-29513

HIGH SPEED
Hardware interface for high speed video imaging
[AD-D014902] N91-29400
Performance and stability in high speed articulated structures undergoing quick maneuvers: Theory and applications
[AD-A237857] N91-29597

HIGH SPEED PHOTOGRAPHY
Debris/ice/TPS assessment and photographic analysis for Shuttle Mission STS-40
[NASA-TM-103822] N91-29210

HIGH STRENGTH
Fatigue resistant optical fibers
[AD-A237568] N91-29921

HIGH STRENGTH ALLOYS
Probabilistic lifetime strength of aerospace materials via computational simulation
[NASA-CR-187178] N91-29629

HIGH STRENGTH STEELS
Microstructural development in HSLA-100 steel weld metals
[AD-A237931] N91-29315
A novel epoxy lacquer for high strength steel in F-111 aircraft during overhaul
[AD-A236828] N91-29326

HIGH TEMPERATURE
High temperature mass spectrometric study of the thermodynamics of liquid nickel-aluminium alloys at 2000 K
[MRL-TR-91-15] N91-29290
Advanced materials for space nuclear power systems
[NASA-TM-105171] N91-29298
Thermal emittance enhancement of graphite-copper composites for high temperature space based radiators
[NASA-TM-105178] N91-29332
The 2nd Workshop on High Temperture Electronics (Metallization and Packaging)
[DE91-014332] N91-29442
Counterdoped high temperature, silicon array infrared detector
[AD-A238483] N91-29546
An elevated temperature titration calorimeter
[DE91-015765] N91-29548
Determination of thermodynamic and kinetic properties of grain boundaries using high temperature calorimetry
[DE91-015571] N91-30031
High temperature thermoelectric properties of boron carbide
[DE91-015848] N91-30037

HIGH TEMPERATURE ENVIRONMENTS
Application of ceramics to industrial gas turbines
[DE91-013140] N91-29330
High temperature Knudsen effusion-mass spectrometric studies of the Y-Ba-Cu-O system
[NIAR-91-23] N91-29981
Air-sintering mechanisms of chromites
[DE91-015527] N91-30027

HIGH TEMPERATURE PLASMAS
Proton deceleration near the surface of an accreting neutron star N91-30063

HIGH TEMPERATURE SUPERCONDUCTORS
Electrodeposition of high temperature superconductors
[AD-A238227] N91-29469
The ac losses in type-2 superconductors
[DE91-015201] N91-29485
Maglev system concept using 20-K high-temperature superconductors and hyperconductors
[DE91-015714] N91-29860
Mixed valent and heavy ferimons and related systems
[DE91-015454] N91-29900
Ruddlesden-Popper phases A(n+1)M(n)O(3n+1): Structures and properties
[DE91-011748] N91-29973
Specific heat of YBaCu3O7: Volume fraction of superconductivity; parameters characteristic of the ideal superconducting state
[DE91-011827] N91-29974
Properties of materials with a fine length scale: Mechanically alloyed metals and the high temperature superconductor Y1Ba2Cu3O7
[DE91-012538] N91-29975
Orbitals, correlation, valencies in high-T(sub c) superconductors
[DE91-618099] N91-29977

Photoemission and electronic structure studies of YBa2Cu3O(x)
[DE91-014469] N91-29979
High temperature superconductor analog electronics for millimeter-wavelength communications
[NASA-TM-105184] N91-29982
Low temperature flux creep in high-T(sub c) superconductors
[DE91-015193] N91-29988
Fabrication and wire extrusion of ceramic superconductors
[DE91-015207] N91-29991
Synchrotron studies of narrow band materials
[DE91-014826] N91-30025
Consolidation and plasticity of Bi-Sr-Ca-Cu-O superconductors
[DE91-015544] N91-30028
High-(Tc) superconductors: Fabricating technologies and future perspectives
[DE91-015553] N91-30029

HIGH VACUUM
Twenty first century propulsion concept
[AD-A237853] N91-29224
Telescope and sensor interface preliminary requirements report for the PORTS chamber
[AD-A237755] N91-29923

HIGH VOLTAGES
Computation of broadband, high-power electromagnetic pulse generation from an air gas avalanche switch
[DE91-015793] N91-29435
A compact 200 kV pulse transformer system
[DE91-014669] N91-29479
Experimental and analytical study of laser-triggering in the Rimfire switch
[DE91-014662] N91-29483
Low-jitter, high-voltage, infrared, laser-triggered, vacuum switch
[DE91-014602] N91-29562
Computational modeling of the Trailmaster Procyon system
[DE91-014765] N91-29955

HMX
Feasibility of a laser-ignited HMX deflagration-to-detonation transition device for the US Navy LITES Program
[DE91-015210] N91-29382
The effects of HMX particle size and binder stiffness on the burning mechanism and regression rate of a series of fast burning propellants
[DE91-015785] N91-29387

HOLOGRAPHIC INTERFEROMETRY
An improved method of investigation of compressor blade fit using holographic interferometry
[AD-A238182] N91-29185
Measurement of a three-dimensional hypersonic density field using holographic interferometry N91-29539

HOLOGRAPHY
An improved method of investigation of compressor blade fit using holographic interferometry
[AD-A238182] N91-29185
Investigation of superresolution by incoherent to coherent conversion
[AD-A238111] N91-29544
Chinese physics lasers (selected articles)
[AD-A237263] N91-29567
Review of nondiffracting Bessel beams
[NASA-CR-187188] N91-29917
Fast acting optical deflection
[AD-A237904] N91-29927

HOMOGENEOUS TURBULENCE
The evolution and structure of homogeneous stably stratified sheared turbulence N91-29499

HONEYCOMB STRUCTURES
Developmental status and system studies of the monolithic solid oxide fuel cell
[DE91-014389] N91-29645

HONING
Liquid honing evaluation
[DE91-015749] N91-29393

HORIZONTAL FLIGHT
NAE participation in the United States FAA vertical separation study
[NAE-LTR-FR-105] N91-29160

HORSESHOE VORTICES
Three-dimensional vortex dynamics and interactions in near-wall turbulent boundary layers
[AD-A237413] N91-29507

HOT ATOMS
Laser enhanced chemical reaction studies
[DE91-013021] N91-29555

HOT ISOSTATIC PRESSING
Rejuvenation of service exposed alloy 713C turbine blades
[NAE-LTR-ST-1716] N91-29179
Powder metallurgy technology (selected articles)
[AD-A237176] N91-29310

HOT PRESSING
Micromechanisms of monotonic and cyclic subcritical crack growth in advanced high melting point low-ductility intermetallics
[AD-A238151] N91-29317

HOVERING
Unsteady compressible lifting surface analysis for rotary wings using velocity potential modes N91-29170
Response and stability analysis of helicopter rotor blades using computerized symbolic manipulation
[AD-A238660] N91-29175

HUBBLE SPACE TELESCOPE
Diffraction-limited imaging of satellites using bispectral speckle interferometry
[DE91-015745] N91-30062

HUMAN BEINGS
Donning times and flotation characteristics of infant life preservers: Four representative types
[AD-A237120] N91-29153
Protecting the ozone shield: A new public policy
[AD-A237640] N91-29659

HUMAN FACTORS ENGINEERING
Compliant walker
[NASA-CASE-GSC-13348-2] N91-29714
Human factors of night vision devices: Anecdotes from the field concerning visual illusions and other effects
[AD-A237641] N91-29735

HUMAN PERFORMANCE
Micro SAINT modeling of physiological and human performance in the heat
[AD-A238659] N91-29719
Development and evaluation of a human performance assessment battery
[AD-A237391] N91-29724
Institute for the Study of Human Capabilities: Summary descriptions of research for the period December 1989 through September 1990
[AD-A237767] N91-29726

HYDRODYNAMICS
Ablation of material by front surface spallation
[DE91-014773] N91-29563
A simple model for low L/D penetration physics
[DE91-015747] N91-29633
Analytical and numerical methods; advanced computer concepts
[DE91-014526] N91-29795

HYDROGEN
Arcjet thermal characteristics
[NASA-TM-105156] N91-29231
A theoretical and experimental study of unimolecular and biomolecular radical hydrogen transfer reactions
[DE91-012607] N91-29261
A technique for measuring the solubilities of gases in liquids
[AD-A238071] N91-29278
Supersonic combustion of a transverse injected H2 jet in a radio frequency heated flow
[DE91-014739] N91-29281
The interaction of hydrogen with metal alloys
[NASA-TP-3128] N91-29318
Hydrogen productivity by photosynthetic water splitting
[DE90-012211] N91-29380

HYDROGEN ATOMS
A theoretical and experimental study of unimolecular and biomolecular radical hydrogen transfer reactions
[DE91-012607] N91-29261
Simulation of large deformation in glassy atactic polypropylene
[AD-A237223] N91-29340
Reactions of hydrogen atoms important to the decomposition of energetic materials
[AD-A238482] N91-29890
Electron capture in very low energy collisions of multicharged ions with H and D in merged beams
[DE91-015617] N91-29909
Effect of hydrogen on the electronic structure of a grain boundary in iron
[AD-A237499] N91-30002

HYDROGEN COMPOUNDS
Scanning tunneling microscopy studies of the surfaces of a-Si:H and a-SiGe:H films
[DE91-002169] N91-29983

HYDROGEN EMBRITTLEMENT
The role of microorganisms in marine corrosion
[AD-A237062] N91-29308
The interaction of hydrogen with metal alloys
[NASA-TP-3128] N91-29318
Environmental effects in niobium base alloys and other selected intermetallic compounds
[AD-A237535] N91-29658

HYDROGEN IONS
Measurement of longitudinal emittance growth using a laser-induced neutralization method
[DE91-013500] N91-29560
Reactions of hydrogen atoms important to the decomposition of energetic materials
[AD-A238482] N91-29890
The BNL toroidal volume H(-) source
[DE91-013592] N91-29947

HYDROGEN OXYGEN ENGINES
Experimental and analytical comparison of flowfields in a 110 N (25 lbf) H2/O2 rocket
[NASA-TM-105175] N91-29230

HYDROGEN PRODUCTION
Hydrogen-fueled scramjet investigation
[AD-A237569] N91-29183
Hydrogen productivity by photosynthetic water splitting
[DE90-012211] N91-29380

HYDROGENATION
Catalytic hydrogenation of carbon monoxide
[DE91-015452] N91-29283
Deactivation by carbon of iron catalysts for indirect liquefaction
[DE91-011276] N91-29285

HYDROGEOLOGY
Subsurface Science Program
[DE91-015480] N91-29665

HYDROLOGY
Subsurface Science Program
[DE91-015480] N91-29665

HYDROLOGY MODELS
Remote determination of soil moisture and evapotranspiration from thermal infrared measurements: Detection of a drying threshold
[PB91-195818] N91-29641

HYPERCUBE MULTIPROCESSORS
Optimal iterative task scheduling for parallel simulations
[AD-A238631] N91-29791
Supernodal symbolic Cholesky factorization on a local-memory multiprocessor
[DE91-014967] N91-29796

HYPERFINE STRUCTURE
Inelastic scattering in condensed matter with high intensity Moessbauer radiation
[DE91-014384] N91-29980

HYPERNUCLEI
Strange quarks in nuclei
[DE91-015833] N91-29895

HYPERONS
High energy physics at Tufts University
[DE91-015055] N91-29908

HYPERSONIC SPEED
Carina aerothermal test at Mach 8
[AD-A238561] N91-29218
Experimental hypervelocity firings using stick and granular propellant configurations
[AD-A238628] N91-29384

HYPERSONIC WIND TUNNELS
Carina aerothermal test at Mach 8
[AD-A238561] N91-29218
Measurement of a three-dimensional hypersonic density field using holographic interferometry N91-29539

HYPERSONICS
Measurement of a three-dimensional hypersonic density field using holographic interferometry N91-29539

HYPERVELOCITY GUNS
Basic simple modeling of balloting motion of railgun projectiles
[AD-A237938] N91-29205
Basic simple modeling of in-bore motion of railgun projectiles
[AD-A238064] N91-29207
The use of high velocity launchers for scientific and engineering studies
[DE91-015564] N91-29208

HYPERVELOCITY IMPACT
Hypervelocity impact jet formation
[DE91-014651] N91-29619

HYPERVELOCITY LAUNCHERS
The use of high velocity launchers for scientific and engineering studies
[DE91-015564] N91-29208
Experimental hypervelocity firings using stick and granular propellant configurations
[AD-A238628] N91-29384

HYPERVELOCITY PROJECTILES
Basic simple modeling of balloting motion of railgun projectiles
[AD-A237938] N91-29205
Basic simple modeling of in-bore motion of railgun projectiles
[AD-A238064] N91-29207

HYSTERESIS
Theoretical, experimental, and numerical studies on hybrid acoustooptic bistable devices
[AD-A237885] N91-29463

I

ICE
Debris/ice/TPS assessment and photographic analysis for Shuttle Mission STS-40
[NASA-TM-103822] N91-29210
An AVHRR data set for the arctic leads ARI
[AD-A237221] N91-29637
ICE FORMATION
Aircraft icing handbook, volume 1
[AD-A238039] N91-29154
Aircraft icing handbook, volume 2
[AD-A238040] N91-29155
Aircraft icing handbook, volume 3
[AD-A238041] N91-29156
Calculated performance of the NASA Lewis icing research tunnel
[NASA-TM-105173] N91-29199
ICE PREVENTION
Aircraft icing handbook, volume 1
[AD-A238039] N91-29154
Aircraft icing handbook, volume 2
[AD-A238040] N91-29155
Aircraft icing handbook, volume 3
[AD-A238041] N91-29156
Debris/ice/TPS assessment and photographic analysis for Shuttle Mission STS-40
[NASA-TM-103822] N91-29210
IGNITION
Feasibility of a laser-ignited HMX deflagration-to-detonation transition device for the US Navy LITES Program
[DE91-015210] N91-29382
Diode laser ignition of explosive and pyrotechnic components
[DE90-012227] N91-29553
H-mode energy confinement scaling from the ASDEX, DIII-D, and jet tokamaks
[DE91-015145] N91-29957
ILLUSIONS
Human factors of night vision devices: Anecdotes from the field concerning visual illusions and other effects
[AD-A237641] N91-29735
IMAGE ANALYSIS
Multi-sensor image interpretation using laser radar and thermal images
[AD-A238245] N91-29576
Matching of complex 3-D surfaces using dynamic programming
[ERB-1022] N91-29743
A mixed limit theorem for stable random fields
[AD-A238222] N91-29840
ASAT monitoring project at LLNL
[DE91-013247] N91-29850
IMAGE CORRELATORS
Investigation of superresolution by incoherent to coherent conversion
[AD-A238111] N91-29544
IMAGE PROCESSING
Comparison of synthetic aperture radar autofocus techniques: Phase gradient vs subaperture
[DE91-014696] N91-29406
Detection of targets in terrain clutter by using multispectral infrared image processing
[AD-A237436] N91-29414
Full-field Fabry-Perot interferometer
[DE91-014610] N91-29540
VISAR: Line-imaging interferometer
[DE91-014749] N91-29542
Characterization of surface contaminants using infrared microspectroscopy
[DE91-009405] N91-29605
Algorithms for converting geodetic Earth location to satellite time and swath pixel coordinates for the DMSP satellite system
[AD-A237589] N91-29638
Multiple channel satellite analysis of cirrus
[AD-A238054] N91-29687
Matching of complex 3-D surfaces using dynamic programming
[ERB-1022] N91-29743
A fast, one pass algorithm to label objects and compute their features
[DE[illegible]] N91-29747
Stochastic simulation techniques for partition function approximation of Gibbs random field images
[AD-A238611] N91-29775
Theory and computer simulation of the interactional neural network
[NRC-30269] N91-29800
ASAT monitoring project at LLNL
[DE91-013247] N91-29850
A real time collimation sensor using a shear plate and a spatial light modulator
[DE90-011362] N91-29914
Development of reflective optical systems for XUV projection lithography
[DE91-013167] N91-29915
Multitarget tracking using optical processing
[AD-A237107] N91-29918
A vision system model
[AD-A238459] N91-29930
A survey of techniques in Aided Target Recognition (ATR) from digital and optical perspectives
[AD-A238644] N91-30052
IMAGE RECONSTRUCTION
Alignment of tomographic projections using an incomplete set of fiducial markers
[AD-A238536] N91-29772
IMAGE RESOLUTION
Investigation of superresolution by incoherent to coherent conversion
[AD-A238111] N91-29544
Matching of complex 3-D surfaces using dynamic programming
[ERB-1022] N91-29743
A mixed limit theorem for stable random fields
[AD-A238222] N91-29840
IMAGERY
Cognition and the brain
[AD-A237846] N91-29727
IMAGES
A survey of techniques in Aided Target Recognition (ATR) from digital and optical perspectives
[AD-A238644] N91-30052
IMAGING TECHNIQUES
Planetary instrument definition and development program: 'Miniature Monochromatic Imager'
[NASA-CR-186550] N91-29219
High-energy backscattered electron imaging of voids in aluminum metallizations
[DE91-014895] N91-29303
Mechanistic investigation of nanometer-scale/lithography at liquid-covered graphite surfaces
[AD-A237085] N91-29337
Hardware interface for high speed video imaging
[AD-D014902] N91-29400
Application of the nuclear microprobe to the imaging of single event upsets in integrated circuits
[DE91-014701] N91-29447
Use of electrical impedance imaging in two-phase, gas-liquid flows
[DE91-015914] N91-29531
Investigation of superresolution by incoherent to coherent conversion
[AD-A238111] N91-29544
Algorithms for converting geodetic Earth location to satellite time and swath pixel coordinates for the DMSP satellite system
[AD-A237589] N91-29638
DNA optical support program summary for 1989
[AD-A238397] N91-29679
Alignment of tomographic projections using an incomplete set of fiducial markers
[AD-A238536] N91-29772
ASAT monitoring project at LLNL
[DE91-013247] N91-29850
Development of optical subapertures
[AD-A237759] N91-29924
Plasma properties of hot coronal loops utilizing coordinated SMM and solar research rocket observations
[NASA-CR-186094] N91-29937
High-resolution Z-contrast imaging of superlattices and heterostructures
[DE91-015329] N91-29994
Responsivity uniformity enhancements for Backside-Illuminated Charge-Coupled Devices (BICCDs) by excimer laser-assisted etching
[AD-A237435] N91-29997
Diffraction-limited imaging of satellites using bispectral speckle interferometry
[DE91-015745] N91-30062
IMPACT
Experimental investigation of adiabatic shear banding at different impact velocities
[AD-A237901] N91-29625
IMPACT DAMAGE
Assessment of impact damage in toughened resin composites
[NAE-LTR-ST-1695] N91-29236
NASA workshop on impact damage to composites
[NASA-CP-10075] N91-29240
Impact characterization of graphite fiber reinforced thermoplastic laminates
[NIAR-91-16] N91-29241
Evaluation of Shadow Moire for surface deformation detection and measurement
[NAE-LTR-ST-1737] N91-29604
A simple model for low L/D penetration physics
[DE91-015747] N91-29633
IMPACT RESISTANCE
Assessment of impact damage in toughened resin composites
[NAE-LTR-ST-1695] N91-29236
Effect of fortifier on compression-after-impact strength of carbon fabric reinforced epoxy
[NAE-LTR-ST-1736] N91-29237
IMPACT TESTS
Launch capabilities to over 10 km/s
[DE91-014657] N91-29203
Whipple bumper shield simulations
[NASA-TM-105089] N91-29213
Dynamic behavior of fully dense molybdenum
[DE91-014902] N91-29304
High strain rate characterization of ceramics in shear
[AD-A238319] N91-29365
IMPACTORS
Launch capabilities to over 10 km/s
[DE91-014657] N91-29203
A simple model for low L/D penetration physics
[DE91-015747] N91-29633
IMPEDANCE
Numerical methods for scattering from electrically large objects
[AD-A238262] N91-29426
IMPLOSIONS
Computational simulations of plasma flow switches and imploding loads
[DE91-014768] N91-29480
Plasma and electrical diagnostics for Procyon experiments
[DE91-014736] N91-29952
Computational modeling of the Trailmaster Procyon system
[DE91-014765] N91-29955
IMPURITIES
Counterdoped high temperature, silicon array infrared detector
[AD-A238483] N91-29546
Fundamental studies of fusion plasmas
[DE91-015656] N91-29964
Impurity and neutral effects on the dissipative drift wave in tokamak edge plasmas
[DE91-015907] N91-29965
INCOMPRESSIBLE FLOW
Numerical simulation of a viscous vortex ring interaction with a density interface
[DE91-011532] N91-29489
Shock acceleration with turbulence minimization
[DE91-014741] N91-29505
INDEPENDENT VARIABLES
Robust design of multivariable control: An interval arithmetic approach
[AD-A238006] N91-29806
Singularities in Gaussian random fields
[AD-A238220] N91-29839
A goodness-of-fit test for a family of two parameter Weibulls with known shape using minimum distance estimation of parameters
[AD-A238633] N91-29847
INDIAN OCEAN
Hamiltonian 3-D ray tracing in the oceanic waveguide on the ellipsoidal earth
[AD-A237458] N91-29700
INDIUM ARSENIDES
Laser probing of the kinetics and dynamics of III -V semiconductor growth
[AD-A237795] N91-30009
INDIUM COMPOUNDS
Growth, nitrogen vacancy reduction and solid solution formation in cubic GaN thin films and the subsequent fabrication of superlattice structures using AlN and InN
[AD-A238521] N91-30021
INDIUM GALLIUM ARSENIDES
InP and InGaAs submicron gate microwave power transistors for 20 GHz applications
[AD-A238595] N91-29473
InGaAs/GaAs graded superlattices in photodetectors for wavelengths beyond 1 micron
[DE90-012073] N91-29969
Defect reductions in epitaxial growth using superlattice buffer layers
[AD-A237710] N91-30005
Uniaxial stress study of the quantum transitions in a strained layer (001) In0.2Ga0.8As/GaAs single quantum well
[DE91-014990] N91-30033
INDIUM PHOSPHIDES
Physics and applications of the lock-on effect
[DE91-014670] N91-29446
InP and InGaAs submicron gate microwave power transistors for 20 GHz applications
[AD-A238595] N91-29473

INDUCTION MOTORS
Maglev system concept using 20-K high-temperature superconductors and hyperconductors
[DE91-015714] N91-29860
INDUSTRIES
The Department of Energy's solar industrial program: New ideas for American industry
[DE91-002197] N91-29649
The Government-University-Industry Research Roundtable
[DE91-015795] N91-30044
INELASTIC SCATTERING
Inelastic deformation and fracture of glassy solids
[AD-A237290] N91-29344
Study of nuclear effects in the deuteron and extraction of neutron to proton stucture function ratio
[DE91-015484] N91-29873
Inelastic scattering in condensed matter with high intensity Moessbauer radiation
[DE91-014384] N91-29980
INERTIA
Solvent dynamical effects in electron transfer: The solvent inertial limit and the predicted influence of quantum effects
[AD-A237462] N91-29880
INERTIAL CONFINEMENT FUSION
Inertial fusion program and National Laser Users Facility program
[DE91-013164] N91-29556
Second Review of the Department of Energy's Inertial Confinement Fusion Program
[DE91-013157] N91-29945
INERTIAL FUSION (REACTOR)
Inertial fusion program and National Laser Users Facility program
[DE91-013164] N91-29556
INFERENCE
Limitations to the method of power spectrum analysis: Nonstationarity, biased estimators, and weak convergence to normality
[DE91-008583] N91-29812
Deduction and inference using conditional logic and probability
[AD-A237285] N91-29834
INFLATABLE STRUCTURES
Concentrator flight test experiment
[AD-A237390] N91-29647
INFORMATION MANAGEMENT
Configuration management concepts document. National PDES testbed report series
[PB91-194480] N91-29391
Information Systems Inventory (ISI)
[PB91-172940] N91-30055
Records management at the DOE national laboratories: Sandia National Laboratories
[DE91-015563] N91-30057
INFORMATION RETRIEVAL
User's guide to the (NCARAI) artificial intelligence technical library
[AD-A237270] N91-29802
INFORMATION SYSTEMS
Compilation and representation of intelligent electronic documents: An architecture for referenceability
[DE91-012635] N91-30045
Information Systems Inventory (ISI)
[PB91-172940] N91-30055
INFRARED ASTRONOMY
An investigation of Nova Persei (1901) and its environment N91-30059
INFRARED ASTRONOMY SATELLITE
An investigation of Nova Persei (1901) and its environment N91-30059
INFRARED DETECTORS
Counterdoped high temperature, silicon array infrared detector
[AD-A238483] N91-29546
ASAT monitoring project at LLNL
[DE91-013247] N91-29850
Molecular beam epitaxial growth and characterization of metastable compound semiconductors for infrared detector applications
[AD-A237797] N91-30010
INFRARED IMAGERY
Detection of targets in terrain clutter by using multispectral infrared image processing
[AD-A237436] N91-29414
Ocean thermal feature recognition, discrimination and tracking using infrared satellite imagery
[AD-A238138] N91-29703
INFRARED LASERS
Laser enhanced chemical reaction studies
[DE91-013021] N91-29555
INFRARED RADIATION
Counterdoped high temperature, silicon array infrared detector
[AD-A238483] N91-29546
Low-jitter, high-voltage, infrared, laser-triggered, vacuum switch
[DE91-014602] N91-29562
Multipixel multidimensional laser radar system theory
[AD-A238110] N91-29573
Characterization of surface contaminants using infrared microspectroscopy
[DE91-009405] N91-29605
Remote determination of soil moisture and evapotranspiration from thermal infrared measurements: Detection of a drying threshold
[PB91-195818] N91-29641
Worldwide maritime infrared atmospheric transmittance data
[AD-A237292] N91-29672
INFRARED SPECTRA
Synthesis and characterization of reduced tungsten sulfide cluster complexes
[DE91-014916] N91-29282
Infrared and Raman spectra of C60 and C70 solid films at room temperature
[AD-A237880] N91-29462
Atomic-resolution scanning tunneling microscopy and infrared spectroscopy as combined in-situ probes of electrochemical adlayer structure: Carbon monoxide on rhodium(111)
[AD-A237508] N91-29884
The influence of potential on metal-adsorbate structure: Solvent-independent nature of infrared spectra for Pt(111)/CO
[AD-A237509] N91-30004
INFRARED SPECTROMETERS
Structures, properties, and dynamics of metal clusters from infrared laser spectroscopy
[AD-A237669] N91-29570
INFRARED SPECTROSCOPY
Research in the physical sciences with application to the free electron laser
[AD-A237884] N91-29571
INJECTION MOLDING
Metal injection moulding: A brief review
[NAE-LTR-ST-531] N91-29289
Injection molding of engineering plastics
[AD-A238583] N91-29389
INJECTORS
Progress toward synergistic hypermixing nozzles
[NASA-TM-105169] N91-29150
INSPECTION
A novel epoxy lacquer for high strength steel in F-111 aircraft during overhaul
[AD-A236828] N91-29326
Neural networks and robotics applied to the non-destructive inspection of aircraft
[AD-A238312] N91-29609
INTEGRAL EQUATIONS
Numerical methods for scattering from electrically large objects
[AD-A238262] N91-29426
The boundary element method applied to the two dimensional Stefan moving boundary problem
[AD-A238458] N91-29828
INTEGRATED CIRCUITS
The magnetron-enhanced etching of double-level tungsten interconnect
[DE91-014984] N91-29306
Application of the nuclear microprobe to the imaging of single event upsets in integrated circuits
[DE91-014701] N91-29447
Analysis of FIN line feasibility for W-band attenuator applications
[AD-A237271] N91-29450
Failure mechanisms on GaAs integrated circuits: Electromigration on GaAs
[AD-A237352] N91-29451
Millimeter-wave characterization of GaAs devices and IC's
[AD-A237843] N91-29461
Stable integrated microwave to optical modulator
[AD-A238166] N91-29574
Monolithic integration of semiconductor and superconductor components
[AD-A237946] N91-30012
INTERCEPTION
Strategic defense initiative: Need to examine concurrency in development of brilliant pebbles
[AD-A238292] N91-29854
INTERFACES
The physics of pattern formation at liquid interfaces
[DE91-014529] N91-29504
Shock acceleration with turbulence minimization
[DE91-014741] N91-29505
A general graphical user interface for automatic reliability modeling
[NASA-TM-104068] N91-29745
A general lease-squares fitting package for the sun workstation
[AD-A238180] N91-29837
INTERFACIAL ENERGY
Effects of interfacial modification on diamond film adhesion
[AD-A237750] N91-29354
Connection between grain boundary structure and energy
[DE91-015558] N91-30030
INTERFACIAL TENSION
The physics of pattern formation at liquid interfaces
[DE91-014529] N91-29504
INTERFEROMETERS
VISAR: Line-imaging interferometer
[DE91-014749] N91-29542
A real time collimation sensor using a shear plate and a spatial light modulator
[DE90-011362] N91-29914
INTERFEROMETRY
Millimeter-accuracy satellite navigation
[AD-A237736] N91-29163
Study of particle correlations in high energy S + Pb and Pb + Pb interactions with a magnetic-interferometric-emulsion-chamber
[DE91-014355] N91-29897
INTERGALACTIC MEDIA
Dark matter in the universe
[DE91-014863] N91-30065
INTERIOR BALLISTICS
Basic simple modeling of balloting motion of railgun projectiles
[AD-A237938] N91-29205
An approximate analysis of balloting motion of railgun projectiles
[AD-A237942] N91-29206
Basic simple modeling of in-bore motion of railgun projectiles
[AD-A238064] N91-29207
Experimental hypervelocity firings using stick and granular propellant configurations
[AD-A238628] N91-29384
INTERMETALLICS
Intermetallics: Canadian perspective
[NAE-LTR-ST-1771] N91-29288
Micromechanisms of monotonic and cyclic subcritical crack growth in advanced high melting point low-ductility intermetallics
[AD-A238151] N91-29317
Mechanical properties of Fe3Al-based alloys
[DE91-015322] N91-29324
Development of nickel and iron aluminides and their applications
[DE91-015323] N91-29325
Environmental effects in niobium base alloys and other selected intermetallic compounds
[AD-A237535] N91-29658
The growth of ultrathin epitaxial intermetallic films
[AD-A237798] N91-30011
Intermetallic superconductors: The state of development in 1991
[DE91-014844] N91-30026
INTERNAL COMBUSTION ENGINES
International Union of Theoretical and Applied Mechanics (IUTAM) Symposium on Aerothermodynamics in Combustors
[AD-A237943] N91-29516
Conversion of methanol-fueled 16-valve, 4-cylinder engine to operation on gaseous 2H2/CO fuel
[PB91-195941] N91-29602
INTERNATIONAL COOPERATION
Digital SPC switching technology: Foreign technology assessment
[AD-A237258] N91-29449
INTERPOLATION
On the interpolation properties of feedforward layered neural networks
[AD-A238035] N91-29824
INTERSTITIALS
The atomic strain tensor
[AD-A237287] N91-29877
Superconducting superoxygenated La(2-x)Sr(x)CuO(4+delta): Search for phase separation
[DE91-015334] N91-29995
INVARIANCE
Invariant target recognition using self-organizing networks
[AD-A238252] N91-29807
Approximation from shift-invariant surfaces of L2(IRd)
[AD-A238165] N91-29826
INVENTORIES
Information Systems Inventory (ISI)
[PB91-172940] N91-30055
INVERSE KINEMATICS
Kinematics of serial manipulators and their parallel duals N91-29589

INVESTIGATION
Three case studies of management information systems
[AD-A238310] N91-30049
IODINE
Comparisons between scanning tunneling microscopy and outer-sphere electron-transfer rates at Pt(111) surfaces coated with ordered iodine adlayers
[AD-A237507] N91-29883
ION ATOM INTERACTIONS
Electron capture in very low energy collisions of multicharged ions with H and D in merged beams
[DE91-015617] N91-29909
Collisional processes of interest in MFE plasma research
[DE91-013023] N91-29943
ION BEAMS
Ion transmission studies of mulitple-sector isotope-ratio mass spectrometers
[DE91-014253] N91-29265
Measurement of longitudinal emittance growth using a laser-induced neutralization method
[DE91-013500] N91-29560
Electron-ion interaction cross sections determined by x ray spectroscopy on EBIT
[DE91-015786] N91-29903
Electromagnetic dissociation of Au and Co targets by relativistic heavy ions
[DE91-014915] N91-29906
Ion Implantation Technology: Proceedings of the 8th International Conference on Ion Implantation Technology
[AD-A237955] N91-30013
ION CYCLOTRON RADIATION
ICRF edge modeling
[DE91-014401] N91-29403
Fundamental studies of fusion plasmas
[DE91-015656] N91-29964
Anomalous ion heating from the dynamo in a reversed field pinch
[DE91-015586] N91-29966
ION DISTRIBUTION
Reactions of hydrogen atoms important to the decomposition of energetic materials
[AD-A238482] N91-29890
ION EMISSION
Lithium ion source for satellite charge control
[AD-A238272] N91-29470
ION ENGINES
Performance and optimization of a derated ion thruster for auxiliary propulsion
[NASA-TM-105144] N91-29229
ION EXTRACTION
Lithium ion source for satellite charge control
[AD-A238272] N91-29470
ION IMPACT
Negative ion formation with electron impact to simulants
[AD-A237478] N91-29881
ION IMPLANTATION
Ion Implantation Technology: Proceedings of the 8th International Conference on Ion Implantation Technology
[AD-A237955] N91-30013
Formation of CoSi2 in SIMOX wafers by high dose Co implantation
[DE91-015639] N91-30036
ION IRRADIATION
Application of the nuclear microprobe to the imaging of single event upsets in integrated circuits
[DE91-014701] N91-29447
Ion Implantation Technology: Proceedings of the 8th International Conference on Ion Implantation Technology
[AD-A237955] N91-30013
ION MICROSCOPES
Materials science applications of a 120 kV FEG TEM/STEM: Triskaidekaphilia
[DE91-010136] N91-29536
ION PROPULSION
Performance and optimization of a derated ion thruster for auxiliary propulsion
[NASA-TM-105144] N91-29229
ION SOURCES
Ion transmission studies of mulitple-sector isotope-ratio mass spectrometers
[DE91-014253] N91-29265
Lithium ion source for satellite charge control
[AD-A238272] N91-29470
Design aspects for a pulsed-mode, high-intensity, heavy negative ion source
[DE91-011094] N91-29864
The BNL toroidal volume H(-) source
[DE91-013592] N91-29947
ION TEMPERATURE
Anomalous ion heating from the dynamo in a reversed field pinch
[DE91-015586] N91-29966
ION TRAPS (INSTRUMENTATION)
Direct-sampling MS measurement of volatiles in environmental samples
[DE91-013417] N91-29653
Electron-ion interaction cross sections determined by x ray spectroscopy on EBIT
[DE91-015786] N91-29903
IONIC COLLISIONS
Strange quarks in nuclei
[DE91-015833] N91-29895
IONIC REACTIONS
Role of the solvent in kinetics of heterogeneous electron and ion transfer reactions
[AD-A237168] N91-29876
IONOSPHERIC DRIFT
Magnetospheric structure and dynamics: A multisatellite approach
[AD-A237674] N91-29676
IONOSPHERIC PROPAGATION
Impact of ionospheric scintillations on space-based surveillance radars
[AD-A237673] N91-29417
IONS
Electronic and ionic transport in processable conducting polymers
[AD-A238175] N91-29362
Physical properties and structure of ion-containing polymers
[AD-A238196] N91-29363
Charge motion effects in ionic clusters
[AD-A238178] N91-29886
Analytical calculation of neutral transport and its effect on ions
[DE91-015908] N91-29896
IRIDIUM
Electrical, magnetic, and spectroscopic properties of tetrathiafulvalene charge transfer compounds with iron, ruthenium, rhodium, and iridium halides
[AD-A237607] N91-29273
IRON
Deactivation by carbon of iron catalysts for indirect liquefaction
[DE91-011276] N91-29285
Effect of hydrogen on the electronic structure of a grain boundary in iron
[AD-A237499] N91-30002
IRON ALLOYS
Postirradiation deformation of ferritic Fe-Cr binary alloys
[DE91-014856] N91-29295
Mechanical properties of Fe3Al-based alloys
[DE91-015322] N91-29324
Development of nickel and iron aluminides and their applications
[DE91-015323] N91-29325
IRON COMPOUNDS
Electrical, magnetic, and spectroscopic properties of tetrathiafulvalene charge transfer compounds with iron, ruthenium, rhodium, and iridium halides
[AD-A237607] N91-29273
The growth of ultrathin epitaxial intermetallic films
[AD-A237798] N91-30011
IRON OXIDES
ANL's development of conductive ceramic components for MCFC
[DE91-015557] N91-29336
IRRADIATION
Ceramic decomposition under irradiation
[DE91-015061] N91-29372
ISENTROPIC PROCESSES
Adiabatic two-phase flow frictional pressure drop. Part 2: A generalized method for data correlation
[DE91-014462] N91-29501
ISOCYANATES
Studies of polymers for shock absorption applications
[AD-A237925] N91-29358
ISOLATION
Integrated structural damping and control system design for high-order flexible systems N91-29617
ISOMERS
Conformational characteristics of the polycarbonate 4,4'-isopropylidenediphenol
[AD-A237334] N91-29347
ISOPROPYL COMPOUNDS
Conformational characteristics of the polycarbonate 4,4'-isopropylidenediphenol
[AD-A237334] N91-29347
ISOTOPES
The mixed metallic-ionic clusters of the silver/silver iodide
[AD-A237883] N91-29314
Inelastic scattering in condensed matter with high intensity Moessbauer radiation
[DE91-014384] N91-29980
ISOTROPY
Compendium of material test results on HY-100 and pseudo HY-100 metals in support of US Navy programs
[DE91-013134] N91-29292
ITERATION
Barrier methods for large-scale quadratic programming
[AD-A238554] N91-29773
ITERATIVE SOLUTION
The parallel BFGS method for unconstrained minimization
[DE91-015784] N91-29798

J

JAMMING
A study of space communications spread-spectrum systems, phase 5 and 6. Part 2: Coding and modulation
[QU-90-2-PT-2] N91-29396
The study of space communications spread spectrum systems. Part 3: Uplink synchronization in an EHF frequency-hopped satellite system
[QU-90-3-PT-3] N91-29397
Coding for frequency hopped spread spectrum satellite communications
[ECE-89-1] N91-29398
Signal processing in impulsive electromagnetic interference
[AD-A237612] N91-29416
JET ENGINES
Micromechanisms of monotonic and cyclic subcritical crack growth in advanced high melting point low-ductility intermetallics
[AD-A238151] N91-29317
JET FLOW
Hypervelocity impact jet formation
[DE91-014651] N91-29619
JET MIXING FLOW
Progress toward synergistic hypermixing nozzles
[NASA-TM-105169] N91-29150
JOINTS (JUNCTIONS)
Ultrasonic evaluation of elastic and interfacial properties of composite materials and laminates N91-29238
Test results for composite specimens and elements containing joints and cutouts
[NASA-CR-178246] N91-29254
Kinematics of serial manipulators and their parallel duals N91-29589
Investigation of ultrasonic evaluation of solid-state metal bond
[DE91-014996] N91-29606
JOSEPHSON JUNCTIONS
Nonlinear dynamics of Josephson junction parametric amplifier arrays
[AD-A237451] N91-29454
Superconducting instrumentation for precision measurement and control
[DE91-014650] N91-29541
JUDGMENTS
Comparison of four methods for aggregating judgments from multiple experts
[DE91-013522] N91-30043
JUPITER RED SPOT
Statistical mechanics of two-dimensional Euler equations and Jupiter's Great Red Spot N91-29498

K

K-EPSILON TURBULENCE MODEL
Modification of the 'TEACH' computer code for use in a study of swirling turbulent flows
[DE91-010492] N91-29496
KALMAN FILTERS
Evaluation of a pre-production version of Canadian Marconi CMA-786 GPS receiver
[NAE-LTR-FR-106] N91-29158
Use of an extended Kalman filter
[AD-A238639] N91-29474
Multipixel multidimensional laser radar system theory
[AD-A238110] N91-29573
An alternative algorithm for discrete-time filtering
[AD-A238443] N91-29827
KAONS
High energy physics at Tufts University
[DE91-015055] N91-29908
KINEMATICS
Modeling of a 3-D light-weight space manipulator
[AD-A236823] N91-29586
A general purpose, comprehensive dynamics simulation of serial robot manipulators N91-29587
Singularity avoidance and the kinematics of an eight-revolute-joint manipulator N91-29588
Quasistatic manipulation with compliance and friction N91-29591

KINETIC ENERGY
Energy generation by a shock crossing a perturbed interface
[DE91-015678] N91-29530
Modeling a rain-induced mixed layer
[AD-A238022] N91-29702
KINETICS
Effect of alumina particle additions on the aging kinetics of 6061 aluminum matrix composites
[AD-A238052] N91-29246
Problems in nonlinear continuum dynamics
[AD-A237844] N91-29512
Experimental study of gas kinetics of a fast-axial flow kilowatt CO2 laser
[AD-A237178] N91-29565
Temperature dependence of proton electroreduction kinetics at gold(111) and (210) surfaces
[AD-A237460] N91-29879
KLYSTRONS
The APS radio frequency test stand control system
[DE91-015711] N91-29434
KNOWLEDGE BASES (ARTIFICIAL INTELLIGENCE)
Topographic map reading
[AD-A238026] N91-29640
Expert systems on multiprocessor architectures, volume 3
[AD-A238048] N91-29788
Expert systems on multiprocessor architectures, volume 4
[AD-A238049] N91-29789
KOLMOGOROFF THEORY
Analysis of nonGaussian, nonlinear time series with long-memory
[AD-A237847] N91-29822
KRYPTON FLUORIDE LASERS
Experimental and analytical study of laser-triggering in the Rimfire switch
[DE91-014662] N91-29483

L

LABORATORIES
Study of activation of metal samples from LDEF-1 and Spacelab-2
[NASA-CR-184171] N91-29297
NRL review, 1989-1990
[AD-A238612] N91-29856
Records management at the DOE national laboratories: Sandia National Laboratories
[DE91-015563] N91-30057
Technology transfer: A new program between Sandia National Laboratories and the University of New Mexico
[DE91-015439] N91-30058
LABORATORY EQUIPMENT
Load tables for the Avery and Gilmore standard force machines corrected for gravity, 1989
[NAE-LTR-ST-1703] N91-29535
LACQUERS
A novel epoxy lacquer for high strength steel in F-111 aircraft during overhaul
[AD-A236828] N91-29326
LAGEOS (SATELLITE)
Seasonal air and water mass redistribution and its effect on satellite and polar motion N91-29202
LAGRANGE MULTIPLIERS
Motion planning for manipulators with excessive degrees of freedom N91-29592
LAMINAR FLOW
Theoretical study of the flow in a rotating duct. Experimental study through flow visualization in a curved duct
[RAE-TRANS-2189] N91-29493
Effects of 1, 2, 3, and 4 Hz imposed bulk flow oscillations on transition in a straight channel with 40 to 1 aspect ratio
[AD-A237988] N91-29517
Separation-bubble velocity measurements using an oscillating-hot-wire system
[AD-A237997] N91-29518
Numerical prediction of turbulent oscillating flow and associated heat transfer
[NASA-CR-187177] N91-29524
LAMINATES
Ultrasonic evaluation of elastic and interfacial properties of composite materials and laminates N91-29238
Effect of fiber-matrix debonding on notched strength of titanium metal matrix composites
[NASA-TM-104131] N91-29239
Impact characterization of graphite fiber reinforced thermoplastic laminates
[NIAR-91-16] N91-29241
Composite specimen design analysis. Volume 2: Experimental efforts
[AD-A238277] N91-29247
Test results for composite specimens and elements containing joints and cutouts
[NASA-CR-178246] N91-29254
Properties and adhesion of polyimides in microelectronic devices
[AD-A238204] N91-29364
Review of literature on the damage, loss of stiffness, and residual strength of graphite/epoxy laminates subjected to cyclic loading
[NAE-LTR-ST(CR)-1711] N91-29611
Modeling and response analysis of thin-walled beam structures constructed of advanced composite materials N91-29615
LANDING AIDS
Mobile Microwave Landing System (MMLS) user interface
[AD-A237470] N91-29162
LANDING GEAR
Aircraft operations from runways with inclined ramps (ski-jump)
[AD-A237265] N91-29171
LANDSAT 5
A practical example of forest mapping and timber volume estimation using LANDSAT-5 TM imagery
[INPE-5244-PRE/1675] N91-29635
LANGUAGE PROGRAMMING
Negation in knowledge graphs
[PB91-185421] N91-29776
LAP JOINTS
A layered beam theory for single lap joints
[AD-A237324] N91-29607
LARGE SPACE STRUCTURES
Experimental verification of an innovative performance-validation methodology for large space systems
[AD-A237864] N91-29214
LASER APPLICATIONS
Light scattering characterization of polymer additives and correlation of molecular properties of polymer fluids
[AD-A238547] N91-29367
Feasibility of a laser-ignited HMX deflagration-to-detonation transition device for the US Navy LITES Program
[DE91-015210] N91-29382
Quaternary pulse position modulation electronics for free-space laser communications
[NASA-TM-104502] N91-29405
Full-field Fabry-Perot interferometer
[DE91-014610] N91-29540
Laser enhanced chemical reaction studies
[DE91-013021] N91-29555
Laser triggered spark gap modeling
[DE91-014831] N91-29557
Measurement of longitudinal emittance growth using a laser-induced neutralization method
[DE91-013500] N91-29560
Characterization of a sub-picosecond dye laser for the study of atom-perturber collisions
[AD-A238099] N91-29572
Short-pulse glass slab amplifier
[DE91-015385] N91-29580
The effect of three levels of laser glare on the speed and accuracy of target location performance when viewing a briefly presented visual array
[AD-A238565] N91-29736
Semiconductor deposition and etching interactions of laser-generated translationally hot atoms and radicals
[AD-A238198] N91-30015
LASER BEAMS
Laser surface modification for selective electroplating of metal: A 2.5 m/s laser direct-write process
[DE91-014988] N91-29322
The development of a fiber-optic readout pressure transducer
[AD-A238393] N91-29545
Adjustable magnification anamorphic beam expander
[DE91-014110] N91-29561
Second-harmonic generation of TEA CO2 10.6 micrometer laser light in AgGaS2 crystals
[AD-A237169] N91-29564
The laser ablation of aluminum at 193, 248, and 351 nm
[AD-A237574] N91-29569
High-intensity and high-energy laser interactions with single droplets
[AD-A238197] N91-29575
Degradation of brightness by resonant particle effects
[DE91-015181] N91-29578
Development of laser optics for the AWA photocathode
[DE91-015552] N91-29581
Nonlinear optical interactions involving the real Gaussian field
[DE91-015052] N91-29936
LASER CAVITIES
The MIT short-wavelength laser project
[DE91-015357] N91-29582
LASER FUSION
Inertial fusion program and National Laser Users Facility program
[DE91-013164] N91-29556
Measurements of the ion acoustic decay instability and the resultant thermal and suprathermal electron heating in laser-plasma interaction experiments
[DE90-012477] N91-29941
Stagnation and interpenetration of laser-created colliding plasmas
[DE91-013244] N91-29946
LASER HEATING
Semiconductor deposition and etching interactions of laser-generated translationally hot atoms and radicals
[AD-A238198] N91-30015
LASER INDUCED FLUORESCENCE
Laser probing of the kinetics and dynamics of III -V semiconductor growth
[AD-A237795] N91-30009
LASER INTERFEROMETRY
Growth, characterization, and device development in monocrystalline diamond films
[AD-A237463] N91-30000
LASER MATERIALS
Kinetics of dark reaction in chemical laser gases
[DE91-015320] N91-29579
LASER MODE LOCKING
Physics and applications of the lock-on effect
[DE91-014670] N91-29446
Short-pulse glass slab amplifier
[DE91-015385] N91-29580
LASER MODES
Blackbody pumped CO2 lasers using Gaussian and waveguide cavities
[DE91-012494] N91-29559
LASER OUTPUTS
Blackbody pumped CO2 lasers using Gaussian and waveguide cavities
[DE91-012494] N91-29559
Second-harmonic generation of TEA CO2 10.6 micrometer laser light in AgGaS2 crystals
[AD-A237169] N91-29564
Development of low-threshold value, high-power semiconductor laser
[AD-A237183] N91-29566
LASER PLASMA INTERACTIONS
High-intensity and high-energy laser interactions with single droplets
[AD-A238197] N91-29575
Measurements of the ion acoustic decay instability and the resultant thermal and suprathermal electron heating in laser-plasma interaction experiments
[DE90-012477] N91-29941
Stagnation and interpenetration of laser-created colliding plasmas
[DE91-013244] N91-29946
LASER PLASMAS
SDIO Laser Propulsion Workshop
[DE90-011758] N91-29550
Photoelectron and photoionization pumping of XUV lasers by laser-produced plasmas N91-29558
High-intensity and high-energy laser interactions with single droplets
[AD-A238197] N91-29575
Stagnation and interpenetration of laser-created colliding plasmas
[DE91-013244] N91-29946
LASER PROPULSION
SDIO Laser Propulsion Workshop
[DE90-011758] N91-29550
Program and applications for a near-term laser launch system
[DE90-011760] N91-29551
LASER PUMPING
Photoelectron and photoionization pumping of XUV lasers by laser-produced plasmas N91-29558
Blackbody pumped CO2 lasers using Gaussian and waveguide cavities
[DE91-012494] N91-29559
Characterization of a sub-picosecond dye laser for the study of atom-perturber collisions
[AD-A238099] N91-29572
LASER RANGE FINDERS
Seasonal air and water mass redistribution and its effect on satellite and polar motion N91-29202
LASER SPECTROMETERS
Diagnostic support services for LLNL (Lawrence Livermore National Laboratory) NOVA laser experiments
[DE90-012125] N91-29552
LASER SPECTROSCOPY
Fundamental studies of chemical vapor deposition diamond growth processes
[DE91-015324] N91-29374

Structures, properties, and dynamics of metal clusters from infrared laser spectroscopy
[AD-A237669] N91-29570
Research in the physical sciences with application to the free electron laser
[AD-A237884] N91-29571

LASER TARGET INTERACTIONS
Semiconductor deposition and etching interactions of laser-generated translationally hot atoms and radicals
[AD-A238198] N91-30015

LASER TARGETS
SDIO Laser Propulsion Workshop
[DE90-011758] N91-29550
Chinese physics lasers (selected articles)
[AD-A237263] N91-29567
The laser ablation of aluminum at 193, 248, and 351 nm
[AD-A237574] N91-29569

LASER WEAPONS
Plan for a laser weapon verification research program
[DE90-012123] N91-29848

LASERS
Diagnostic support services for LLNL (Lawrence Livermore National Laboratory) NOVA laser experiments
[DE90-012125] N91-29552
Ablation of material by front surface spallation
[DE91-014773] N91-29563
A real time collimation sensor using a shear plate and a spatial light modulator
[DE90-011362] N91-29914

LATTICE PARAMETERS
Calculation of intra-rare Earth binary phase diagrams
[DE91-014950] N91-29267

LATTICE VIBRATIONS
High resolution electron energy loss studies of surface vibrations
[DE91-014539] N91-30024

LATTICES (MATHEMATICS)
The design of a real-time adaptive filter development system
[AD-A237134] N91-29448

LAUNCHING
Launch capabilities to over 10 km/s
[DE91-014657] N91-29203
SDIO Laser Propulsion Workshop
[DE90-011758] N91-29550

LEAD (METAL)
Study of particle correlations in high energy S + Pb and Pb + Pb interactions with a magnetic-interferometric-emulsion-chamber
[DE91-014355] N91-29897

LEAD ACID BATTERIES
Performance and life evaluation of advanced battery technologies for electric vehicle applications
[DE91-015671] N91-29482

LEAD ALLOYS
Lead-free solders for electronics applications: Wetting analysis
[DE91-014900] N91-29320

LEAD ZIRCONATE TITANATES
Aspects of fatigue and rapid depolarization in the film PZT capacitors
[DE91-014904] N91-29484

LEADING EDGES
Near-stall loss measurements in a CD compressor cascade with exploratory leading edge flow control
[AD-A237497] N91-29509

LEAKAGE
A technique for measuring the solubilities of gases in liquids
[AD-A238071] N91-29278

LEAST SQUARES METHOD
Finite element-based system identification from experimental modal analysis results N91-29618
Piecework linear least-squares approximation planar curves including computer programs
[NRC-31069] N91-29811
Parameter estimation via nonlinear differential correction least square method
[NAL-PD-FC-9110] N91-29814
Least-squares learning and approximation of posterior probabilities on classification problems by neural network models
[AD-A237140] N91-29833
A general lease-squares fitting package for the sun workstation
[AD-A238180] N91-29837

LEVITATION
Maglev system concept using 20-K high-temperature superconductors and hyperconductors
[DE91-015714] N91-29860

LIAPUNOV FUNCTIONS
A survey of nonlinear dynamics (chaos theory)
[AD-A237802] N91-29821

LIBRARIES
ZLIB: A numerical library for differential algebra and Lie algebraic treatment of beam dynamics
[DE91-014875] N91-29746
User's guide to the (NCARAI) artificial intelligence technical library
[AD-A237270] N91-29802

LIE GROUPS
ZLIB: A numerical library for differential algebra and Lie algebraic treatment of beam dynamics
[DE91-014875] N91-29746
The 't Hooft's solution for arbitrary semisimple Lie group
[DE91-617572] N91-29813

LIFE (DURABILITY)
Development of the microstructure based stochastic life prediction models
[AD-A237768] N91-29312
Measurement of lithium cycling efficiency in organic electrolytes
[AD-A237632] N91-29457

LIFT
Preliminary flight-determined subsonic lift and drag characteristics of the X-29A forward-swept-wing airplane
[NASA-TM-100409] N91-29177

LIGANDS
Solvent-dependent redox thermodynamics of metal amine complexes. The delineation of specific solvation effects
[AD-A237503] N91-29272

LIGHT (VISIBLE RADIATION)
Spatial propagation of squeezed light in a degenerate parametric amplifier
[DE91-014989] N91-30039

LIGHT AIRCRAFT
NAE Twin Otter operations in the 1988 Eulerian model evaluation field study
[NAE-LTR-FR-107] N91-29651

LIGHT BEAMS
Experimental study of gas kinetics of a fast-axial flow kilowatt CO2 laser
[AD-A237178] N91-29565
Review of nondiffracting Bessel beams
[NASA-CR-187188] N91-29917
Optical soliton source
[AD-D014942] N91-29933

LIGHT EMISSION
High-intensity and high-energy laser interactions with single droplets
[AD-A238197] N91-29575
DNA optical support program summary for 1989
[AD-A238397] N91-29679

LIGHT GAS GUNS
Launch capabilities to over 10 km/s
[DE91-014657] N91-29203

LIGHT MODULATION
Stable integrated microwave to optical modulator
[AD-A238166] N91-29574
A real time collimation sensor using a shear plate and a spatial light modulator
[DE90-011362] N91-29914

LIGHT SCATTERING
Light scattering characterization of polymer additives and correlation of molecular properties of polymer fluids
[AD-A238547] N91-29367

LIGHT SOURCES
Diagnostic support services for LLNL (Lawrence Livermore National Laboratory) NOVA laser experiments
[DE90-012125] N91-29552

LIGHT TRANSMISSION
Fast acting optical deflection
[AD-A237904] N91-29927

LIMITER CIRCUITS
Spike leakage and burnout of silicon PIN diode microwave limiters
[AD-A238392] N91-29471

LINE SPECTRA
Second-harmonic generation of TEA CO2 10.6 micrometer laser light in AgGaS2 crystals
[AD-A237169] N91-29564

LINEAR ACCELERATORS
A high power cross-field amplifier at X-Band
[DE91-013277] N91-29441
REX: A 5-MV pulsed-power source for driving high-brightness electron beam diodes
[DE91-014604] N91-29443
Degradation of brightness by resonant particle effects
[DE91-015181] N91-29578
Control of energy sweep and transverse beam motion in induction linacs
[DE91-015177] N91-29911
A mesoscopic linear accelerator driven by superintense subpicosecond laser pulses
[DE91-015941] N91-29913

LINEAR EQUATIONS
A new look at the Tobak-Schiff model of nonplanar aircraft dynamics
[NAE-LTR-UA-101] N91-29168
Piecework linear least-squares approximation planar curves including computer programs
[NRC-31069] N91-29811

LINEAR INTEGRATED CIRCUITS
An alternative to operational amplifiers
[AD-A237439] N91-29453

LINEAR PROGRAMMING
The optimal location of GEODSS sensors in Canada
[AD-A238444] N91-29216
Coding for spread-spectrum channels in the presence of jamming
[AD-A238233] N91-29425
Primal-dual methods for linear programming
[AD-A237418] N91-29756

LINEAR QUADRATIC GAUSSIAN CONTROL
Effects of colocation and non-colocation of sensors and actuators on flexible structures
[AD-A238457] N91-29844

LINEAR SYSTEMS
The 't Hooft's solution for arbitrary semisimple Lie group
[DE91-617572] N91-29813

LIQUEFACTION
Deactivation by carbon of iron catalysts for indirect liquefaction
[DE91-011276] N91-29285

LIQUID AIR
An experimental study of plunging liquid jet induced air carryunder and dispersion
[AD-A237757] N91-29511

LIQUID ALLOYS
High temperature mass spectrometric study of the thermodynamics of liquid nickel-aluminium alloys at 2000 K
[MRL-TR-91-15] N91-29290

LIQUID COOLING
International aviation (selected articles)
[AD-A237232] N91-29142

LIQUID CRYSTALS
Adaptive liquid crystal TV based joint transform correlator as applied to real-time pattern recognition
[AD-A238576] N91-29931

LIQUID FLOW
Numerical and physical modelling of bubbly flow phenomena
[DE91-013646] N91-29492

LIQUID FUELS
Investigation of the combustion of liquid fuels in Rijke type pulse combustors
[DE90-012490] N91-29381
Electro-rheology fluids and liquid fuel flow
[AD-A238600] N91-29520

LIQUID HYDROGEN
NASA cryogenic fluid management space experiment efforts, 1960-1990
[NASA-TM-103752] N91-30073

LIQUID METALS
Secondary stability and three-dimensional natural convection in a shallow cavity N91-29495

LIQUID PHASES
A model of multicomponent droplet evaporation with liquid phase reactions
[DE90-012535] N91-29257
Approximate multiphase flow modeling by characteristic methods
[PB91-190959] N91-29526

LIQUID ROCKET PROPELLANTS
Design issues for propulsion systems using metallized propellants
[NASA-TM-105190] N91-29220

LIQUID SODIUM
Materials research for sodium engine development
[DE91-015715] N91-29378

LIQUID SURFACES
Mechanistic investigation of nanometer-scale/lithography at liquid-covered graphite surfaces
[AD-A237085] N91-29337

LIQUID-GAS MIXTURES
Use of electrical impedance imaging in two-phase, gas-liquid flows
[DE91-015914] N91-29531

LIQUID-LIQUID INTERFACES
Picosecond studies of chemical intermediates
[AD-A237859] N91-29275
Electrified microscopic and conventional interfaces between two immiscible electrolyte solutions
[AD-A237695] N91-29459

LIQUID-SOLID INTERFACES
Molecular dynamics simulation of the effect of interfaces in melting and solid-state amorphization
[DE91-015550] N91-29284

Theoretical studies of solid-fluid phase equilibria
[DE91-014811] N91-29287
A study of the liquid-solid interface during rapid resolidification of cooper-titanium using molecular dynamics
[AD-A238634] N91-30022

LIQUID-VAPOR INTERFACES
Picosecond studies of chemical intermediates
[AD-A237859] N91-29275

LIQUIDS
A technique for measuring the solubilities of gases in liquids
[AD-A238071] N91-29278
First principles simulations of metallic alloys and liquids
[DE91-015171] N91-29323
The physics of pattern formation at liquid interfaces
[DE91-014529] N91-29504

LITHIUM
Lithium combustion: A review
[AD-A238154] N91-29279
Measurement of lithium cycling efficiency in organic electrolytes
[AD-A237632] N91-29457
Lithium ion source for satellite charge control
[AD-A238272] N91-29470

LITHIUM ALLOYS
An investigation of the as-quenched and early aging characteristics of a Al - 4.1 wt. percent Li binary alloy by x ray diffraction
[AD-A237598] N91-29311

LITHIUM COMPOUNDS
A calorimetric investigation of deuterated palladium electrodes
[AD-A237571] N91-29456

LITHIUM OXIDES
ANL's development of conductive ceramic components for MCFC
[DE91-015557] N91-29336

LITHOGRAPHY
Mechanistic investigation of nanometer-scale/lithography at liquid-covered graphite surfaces
[AD-A237085] N91-29337
Pulse induced nanlithography of graphite in H2O: A road to chemical linkages to the surface?
[AD-A237086] N91-29338
Development of reflective optical systems for XUV projection lithography
[DE91-013167] N91-29915

LOAD TESTING MACHINES
A full function checkout test for the NAE full scale structural test control and data acquisition system
[NAE-LTR-ST-1696] N91-29166

LOADING MOMENTS
Description of computer programs used to analyze and plot Spectrapot data files
[NAE-ST-557] N91-29744

LOADS (FORCES)
Load tables for the Avery and Gilmore standard force machines corrected for gravity, 1989
[NAE-LTR-ST-1703] N91-29535
Bearing tester data compilation analysis, and reporting and bearing math modeling
[NASA-CR-178883] N91-29603
Structural optimization with pseudo-load approach exploiting design length scales N91-29616

LOGIC CIRCUITS
The use of searching algorithms for the minimization of multi-valued logic functions
[AD-A238018] N91-29763

LOGIC PROGRAMMING
Transfer of 4GL application from INGRES to ORACLE
[AD-A238448] N91-29771

LOGISTICS
Evaluation of aircraft turbine engine redesigns
[AD-A237599] N91-29184

LONG DURATION EXPOSURE FACILITY
Study of activation of metal samples from LDEF-1 and Spacelab-2
[NASA-CR-184171] N91-29297
IDA studies on natural space environmental effects on materials for SDIO
[AD-A237974] N91-29660
Activation calculations for trapped protons below 200 MeV: Appendix
[NASA-CR-184170] N91-29865

LOW ALTITUDE
A program to operate and upgrade the GL low altitude lidar systems
[AD-A238081] N91-29423

LOW REYNOLDS NUMBER
Performance of an airfoil at low Reynolds number
[NAL-PD-CF-9102] N91-29145

LOW SPEED WIND TUNNELS
An assessment of the acoustic noise in the working section of the NAE 6 ft x 9 ft low speed wind tunnel
[NAE-LTR-ST-1744] N91-29196

LOW TEMPERATURE
Performance of asphalt concrete airport pavements during thaw weakening periods: A field study
[AD-A237441] N91-29198

LUBRICANT TESTS
Basic mechanisms of diesel lubrication correlation of bench and engine tests
[AD-A237685] N91-29596
Effect of two synthetic lubricants on life of AISI 9310 spur gears
[NASA-TM-104352] N91-29599

LUBRICANTS
Effect of two synthetic lubricants on life of AISI 9310 spur gears
[NASA-TM-104352] N91-29599

LUBRICATION
Basic mechanisms of diesel lubrication correlation of bench and engine tests
[AD-A237685] N91-29596

LUMINANCE
The effects of luminance boundaries on color perception
[AD-A237794] N91-29925

LUMINESCENCE
Electronic and ionic transport in processable conducting polymers
[AD-A238175] N91-29362

LUMINOUS INTENSITY
Degradation of brightness by resonant particle effects
[DE91-015181] N91-29578

LUMPED PARAMETER SYSTEMS
Equations of motion for a flexible spacecraft-lumped parameter idealization
[NASA-CR-188727] N91-29211

LUNAR BASES
Concepts for manned lunar habitats
[NASA-TM-104114] N91-30068

LUNAR ECLIPSES
Central solar eclipses of 1992. Annual solar eclipse of 4-5 January 1992, total solar eclipse of 30 June 1992
[AD-A237614] N91-30069

LUNAR EXPLORATION
Nuclear data needs for the space exploration initiative
[DE91-013231] N91-29200

LUNAR RESOURCES
Production and use of metals and oxygen for lunar propulsion
[NASA-TM-105195] N91-29222

M

MACHINE ORIENTED LANGUAGES
Negation in knowledge graphs
[PB91-185421] N91-29776

MACROMOLECULES
Deconvolution of x ray diffraction data to elucidate plastic deformation mechanisms in the uniaxial extension of bulk Nylon-6
[AD-A237332] N91-29623

MAGNETIC COILS
The ASTROMAG superconducting magnet facility configured for a free flying satellite
[DE91-014710] N91-29204
Minimization of refrigeration power requirements for mechanical supports in cryogenic systems
[DE91-015720] N91-29392

MAGNETIC COMPRESSION
Procyon experiments utilizing explosively-formed fuse opening switches
[DE91-014742] N91-29953

MAGNETIC COOLING
Monte Carlo and mean field calculations of the magnetocaloric effect of ferromagnetically interacting clusters
[DE91-014792] N91-29859

MAGNETIC DIFFUSION
Magnetic fluctuations due to thermally excited Alfven waves
[DE90-011790] N91-29940

MAGNETIC DISTURBANCES
Impacts of a nominal nuclear electromagnetic pulse on electric power systems
[DE91-012991] N91-29401

MAGNETIC DOMAINS
Singularities in Gaussian random fields
[AD-A238220] N91-29839

MAGNETIC EFFECTS
The effects of magnetic field errors on reversed field pinch plasma
[DE91-013636] N91-29948

MAGNETIC FIELD CONFIGURATIONS
The effects of magnetic field errors on reversed field pinch plasma
[DE91-013636] N91-29948

MAGNETIC FIELD RECONNECTION
Magnetospheric structure and dynamics: A multisatellite approach
[AD-A237674] N91-29676
Total magnetic reconnection during a tokamak major disruption
[DE91-013637] N91-29949

MAGNETIC FIELDS
Requirements for the observation of Fermi surfaces in disordered alloys
[DE91-014578] N91-29321
Superconductivity induced by very high magnetic fields: Thermodynamic and transport properties
[DE91-015327] N91-29481
The ac losses in type-2 superconductors
[DE91-015201] N91-29485
Cognition and the brain
[AD-A237846] N91-29727
Singularities in Gaussian random fields
[AD-A238220] N91-29839
Monte Carlo and mean field calculations of the magnetocaloric effect of ferromagnetically interacting clusters
[DE91-014792] N91-29859
Design aspects for a pulsed-mode, high-intensity, heavy negative ion source
[DE91-011094] N91-29864
Magnetic fluctuations due to thermally excited Alfven waves
[DE90-011790] N91-29940
The BNL toroidal volume H(-) source
[DE91-013592] N91-29947
The effects of magnetic field errors on reversed field pinch plasma
[DE91-013636] N91-29948
Edge electrostatic fluctuations and transport in the MST reversed field pinch
[DE91-015218] N91-29959
Low temperature flux creep in high-T(sub c) superconductors
[DE91-015193] N91-29988
Development of model based magnetic LP-LEC growth large diameter GaAs
[AD-A237456] N91-29998

MAGNETIC FLUX
Procyon experiments utilizing explosively-formed fuse opening switches
[DE91-014742] N91-29953
Low temperature flux creep in high-T(sub c) superconductors
[DE91-015193] N91-29988

MAGNETIC LEVITATION VEHICLES
Maglev system concept using 20-K high-temperature superconductors and hyperconductors
[DE91-015714] N91-29860

MAGNETIC PERMEABILITY
Laser-atom interaction at high intensities
[AD-A238231] N91-29887
Ac susceptibility of superconductive thin films
[DE91-015273] N91-29993
Anisotropic spin susceptibility of the (Y,Ca),(Ba, La)2Cu4O8 system
[DE91-014593] N91-30032

MAGNETIC PROPERTIES
Electrical, magnetic, and spectroscopic properties of tetrathiafulvalene charge transfer compounds with iron, ruthenium, rhodium, and iridium halides
[AD-A237607] N91-29273

MAGNETIC RELAXATION
Low temperature flux creep in high-T(sub c) superconductors
[DE91-015193] N91-29988

MAGNETIC RESONANCE
Intermetallic superconductors: The state of development in 1991
[DE91-014844] N91-30026

MAGNETIC STORMS
Magnetospheric structure and dynamics: A multisatellite approach
[AD-A237674] N91-29676

MAGNETO-OPTICS
Neural networks and robotics applied to the non-destructive inspection of aircraft
[AD-A238312] N91-29609
Major achievements during the first program year
[AD-A237171] N91-29919

MAGNETOHYDRODYNAMIC FLOW
Computational simulations of plasma flow switches and imploding loads
[DE91-014768] N91-29480

Procyon experiments utilizing explosively-formed fuse opening switches
[DE91-014742] N91-29953
Plasma flow switch experiments on the Pegasus facility
[DE91-014744] N91-29954
Towards a realistic plasma simulation code
[DE91-015698] N91-29967
Course lectures abstracts of participants fellows project reports
[AD-A237909] N91-30070

MAGNETOHYDRODYNAMIC GENERATORS
Interactions of turbulent eddies and combustion in an MHD second stage combustor
[DE91-015722] N91-29968

MAGNETOHYDRODYNAMIC STABILITY
Numerical simulation of self-field MPD thrusters
[NASA-CR-187168] N91-29832
Identification of, and transition to, the second region of ideal MHD stability in tokamaks
[DE90-010380] N91-29938
Magnetic fluctuations due to thermally excited Alfven waves
[DE90-011790] N91-29940
Measurements of the ion acoustic decay instability and the resultant thermal and suprathermal electron heating in laser-plasma interaction experiments
[DE90-012477] N91-29941
Total magnetic reconnection during a tokamak major disruption
[DE91-013637] N91-29949
Global confinement and discrete dynamo activity in the MST reversed field pinch
[DE91-015219] N91-29960
Impurity and neutral effects on the dissipative drift wave in tokamak edge plasmas
[DE91-015907] N91-29965
Course lectures abstracts of participants fellows project reports
[AD-A237909] N91-30070

MAGNETOHYDRODYNAMIC WAVES
Magnetic fluctuations due to thermally excited Alfven waves
[DE90-011790] N91-29940

MAGNETOHYDRODYNAMICS
Ceramic fabrication R/D
[DE91-014758] N91-29335
Computational modeling of the Trailmaster Procyon system
[DE91-014765] N91-29955
Establishment of an Institute for Fusion Studies
[DE91-014922] N91-29956

MAGNETOPAUSE
Magnetospheric structure and dynamics: A multisatellite approach
[AD-A237674] N91-29676

MAGNETOPLASMADYNAMICS
Numerical simulation of self-field MPD thrusters
[NASA-CR-187168] N91-29832

MAGNETOSHEATH
Magnetospheric structure and dynamics: A multisatellite approach
[AD-A237674] N91-29676

MAGNETOSTATICS
Major achievements during the first program year
[AD-A237171] N91-29919

MAGNETRONS
The magnetron-enhanced etching of double-level tungsten interconnect
[DE91-014984] N91-29306

MAINTAINABILITY
Slaying the software dragon: A look at how software engineering, the Ada programming language and process maturity are changing software development
[AD-A237156] N91-29751

MAINTENANCE
A novel epoxy lacquer for high strength steel in F-111 aircraft during overhaul
[AD-A236828] N91-29326

MAN MACHINE SYSTEMS
Compliant walker
[NASA-CASE-GSC-13348-2] N91-29714
Workshop on Automation and Robotics: Proceedings
[DE91-015175] N91-29801

MAN-COMPUTER INTERFACE
Mobile Microwave Landing System (MMLS) user interface
[AD-A237470] N91-29162
The PC Dugout micro-mainframe integration system: PAX implementation
[AD-A237480] N91-29758
A general lease-squares fitting package for the sun workstation
[AD-A238180] N91-29837

MANAGEMENT
Management of variation and TQM
[AD-A238399] N91-29843

MANAGEMENT INFORMATION SYSTEMS
Three case studies of management information systems
[AD-A238310] N91-30049
Records management at the DOE national laboratories: Sandia National Laboratories
[DE91-015563] N91-30057

MANAGEMENT PLANNING
Configuration management concepts document. National PDES testbed report series
[PB91-194480] N91-29391

MANAGEMENT SYSTEMS
Methodology investigation, aviation test management system concept development
[AD-A237349] N91-29172

MANEUVERABILITY
Agility: Presentation and flight test methods for the operational fighter pilot
[AD-A238456] N91-29174

MANGANESE OXIDES
ANL's development of conductive ceramic components for MCFC
[DE91-015557] N91-29336

MANIFOLDS (MATHEMATICS)
Computational methods for bifurcation problems with symmetries on the manifold
[AD-A237146] N91-29817

MANIPULATORS
Modeling of a 3-D light-weight space manipulator
[AD-A236823] N91-29586
A general purpose, comprehensive dynamics simulation of serial robot manipulators N91-29587
Singularity avoidance and the kinematics of an eight-revolute-joint manipulator N91-29588
Kinematics of serial manipulators and their parallel duals N91-29589
Performance models for robot manipulators N91-29590
Motion planning for manipulators with excessive degrees of freedom N91-29592
Global optimality, conservativity and singularity in redundancy resolution of robotic manipulators N91-29593
Experiments in adaptive control of cooperating manipulators N91-29594
Research and development at ORNL/CESAR towards cooperating robotic systems for hazardous environments
[DE91-015638] N91-29810

MANNED MARS MISSIONS
Nuclear data needs for the space exploration initiative
[DE91-013231] N91-29200

MANNED SPACECRAFT
Nuclear data needs for the space exploration initiative
[DE91-013231] N91-29200

MANUALS
The use and design of flightcrew checklists and manuals
[AD-A237206] N91-29733

MANUFACTURING
Annual Electronics Manufacturing Seminar proceedings
[AD-A238017] N91-29467
Management of variation and TQM
[AD-A238399] N91-29843

MAPPING
Application of the nuclear microprobe to the imaging of single event upsets in integrated circuits
[DE91-014701] N91-29447
A survey of techniques in Aided Target Recognition (ATR) from digital and optical perspectives
[AD-A238644] N91-30052

MAPS
Application of the nuclear microprobe to the imaging of single event upsets in integrated circuits
[DE91-014701] N91-29447

MARINE METEOROLOGY
Dependence of radar backscatter on the energetics of the air-sea interface
[AD-A237818] N91-29685
An expert system approach for prediction of maritime visibility obscuration
[AD-A238305] N91-29688

MARKERS
Alignment of tomographic projections using an incomplete set of fiducial markers
[AD-A238536] N91-29772

MARKET RESEARCH
Worldwide wind/diesel hybrid power system study: Potential applications and technical issues
[DE91-002160] N91-29643

MARKETING
The Department of Energy's solar industrial program: New ideas for American industry
[DE91-002197] N91-29649
The advanced software development and commercialization project
[DE91-015756] N91-29797
Marketing for collegiate aviation education
[NIAR-91-18] N91-30042
Technology transfer: A new program between Sandia National Laboratories and the University of New Mexico
[DE91-015439] N91-30058

MARKOV PROCESSES
A general graphical user interface for automatic reliability modeling
[NASA-TM-104068] N91-29745
Simulation methodology
[AD-A238113] N91-29765
Diffusion approximations for complex repair systems
[AD-A238100] N91-29836

MARS SURFACE
Investigations in Martian geology. Part 1: Nature of the mantling deposit in the heavily cratered terrain of northeastern Arabia, Mars. Part 2: Experimental studies of clean and dust-or-sand-covered ice sublimation under Mars-like conditions N91-30067

MARTENSITIC TRANSFORMATION
Lightweight disk alloy development
[AD-A237064] N91-29309

MARTINGALES
The asymptotic distributions of autoregressive coefficients
[AD-A238538] N91-29831

MASS DISTRIBUTION
Seasonal air and water mass redistribution and its effect on satellite and polar motion N91-29202

MASS FLOW
Experimental study of cross-stream mixing in a cylindrical duct
[NASA-TM-105180] N91-29187

MASS RATIOS
Experimental hypervelocity firings using stick and granular propellant configurations
[AD-A238628] N91-29384

MASS SPECTRA
Direct-sampling MS measurement of volatiles in environmental samples
[DE91-013417] N91-29653

MASS SPECTROMETERS
Ion transmission studies of mulitple-sector isotope-ratio mass spectrometers
[DE91-014253] N91-29265
The mixed metallic-ionic clusters of the silver/silver iodide
[AD-A237883] N91-29314
Direct-sampling MS measurement of volatiles in environmental samples
[DE91-013417] N91-29653

MASS SPECTROSCOPY
High temperature mass spectrometric study of the thermodynamics of liquid nickel-aluminium alloys at 2000 K
[MRL-TR-91-15] N91-29290
Fundamental studies of chemical vapor deposition diamond growth processes
[DE91-015324] N91-29374
Negative ion formation with electron impact to simulants
[AD-A237478] N91-29881
Fundamental studies of the extraction process in inductively coupled plasma mass spectrometry
[DE90-011733] N91-29939
High temperature Knudsen effusion-mass spectrometric studies of the Y-Ba-Cu-O system
[NIAR-91-23] N91-29981

MASS TRANSFER
Analysis of condensation and evaporation of ammonia/water mixtures in matrix heat-exchangers
[DE91-014461] N91-29500

MATHEMATICAL LOGIC
Deduction and inference using conditional logic and probability
[AD-A237285] N91-29834

MATHEMATICAL MODELS
A new look at the Tobak-Schiff model of nonplanar aircraft dynamics
[NAE-LTR-UA-101] N91-29168
Compressor fault modelling for engine health monitoring: Review and recommendations
[NRC-TR-ENG-004] N91-29178
Flutter consideration of a crash-test aircraft
[DE91-015094] N91-29192
Investigation of the flame-acoustic wave interaction during axial solid rocket instabilities
[AD-A237851] N91-29223

An overview of aerothermal modeling
[NRC-32088] N91-29258
Structure of icosahedral borides by Raman spectroscopy
[DE91-010872] N91-29260
Compendium of material test results on HY-100 and pseudo HY-100 metals in support of US Navy programs
[DE91-013134] N91-29292
Development of the microstructure based stochastic life prediction models
[AD-A237768] N91-29312
An atomistic model of the amorphous glassy polycarbonate of 4,4'-isopropylidenediphenol
[AD-A237291] N91-29345
Injection molding of engineering plastics
[AD-A238583] N91-29389
Impact of ionospheric scintillations on space-based surveillance radars
[AD-A237673] N91-29417
A circuit model for an inductive strip in homogeneous finline
[AD-A238001] N91-29466
Simulation of the growth of Mo/Si multilayers
[DE91-015679] N91-29486
Numerical and physical modelling of bubbly flow phenomena
[DE91-013646] N91-29492
A numerical study of flow past a cylindrical body N91-29497
Prediction of the pressure drop in transverse, repeated-rib tubes with numerical modeling
[DE91-014465] N91-29503
Approximate multiphase flow modeling by characteristic methods
[PB91-190959] N91-29526
Laser triggered spark gap modeling
[DE91-014831] N91-29557
Modeling of a 3-D light-weight space manipulator
[AD-A236823] N91-29586
Performance models for robot manipulators N91-29590
Bearing tester data compilation analysis, and reporting and bearing math modeling
[NASA-CR-178883] N91-29603
Hypervelocity impact jet formation
[DE91-014651] N91-29619
A simple model for low L/D penetration physics
[DE91-015747] N91-29633
Numerical modeling of turbulent dispersion around structures using a particle-in-cell method
[DE91-012035] N91-29652
Perturbation techniques for models of bursting electrical activity in pancreatic (beta)-cells
[DE91-013901] N91-29715
Quantum measurement and the mind-brain connection
[DE91-012343] N91-29723
Analysis of Naval aviation selection test data with nonlinear models. Part 1: Parameter estimation
[AD-A238244] N91-29728
Hyperdimensional data analysis and structural inference
[AD-A238097] N91-29764
A type calculus for mathematical programming modeling languages
[AD-A238160] N91-29766
Limitations to the method of power spectrum analysis: Nonstationarity, biased estimators, and weak convergence to normality
[DE91-008583] N91-29812
Use of the implicit-finite-difference method to implement the parabolic equation model
[AD-A237437] N91-29819
Differential equations and continuum mechanics
[AD-A237722] N91-29820
Monte Carlo and mean field calculations of the magnetocaloric effect of ferromagnetically interacting clusters
[DE91-014792] N91-29859
Chasing the x(sub f) dependence of J/psi production
[DE91-015136] N91-29899
Mixed valent and heavy fermons and related systems
[DE91-015454] N91-29900
A research program in experimental and theoretical high energy physics
[DE91-014728] N91-29907
Fluidlike studies of the sheath and presheath regions of a plasma
[DE91-013343] N91-29944
Comparison of four methods for aggregating judgments from multiple experts
[DE91-013522] N91-30043

MATHEMATICAL PROGRAMMING
The optimal location of GEODSS sensors in Canada
[AD-A238444] N91-29216
Implementation of an exact penalty function formulation to solve convex nonlinear programming problems
[AD-A237905] N91-29761
A type calculus for mathematical programming modeling languages
[AD-A238160] N91-29766

MEASURING INSTRUMENTS
NAE Twin Otter operations in FIFE 1989
[NASA-CR-188770] N91-29169
Wind and flux calculations of the NAE Twin Otter
[NAE-LTR-FR-109] N91-29189
Standard NIM instrumentation system
[DE90-010387] N91-29532
Theoretical high energy physics
[DE91-013639] N91-29905

MECHANICAL DEVICES
An investigation to determine the producibility of a 3-D braider and bias direction weaving loom
[NASA-CR-188741] N91-29390

MECHANICAL PROPERTIES
Studies of polymers for shock absorption applications
[AD-A237925] N91-29358
The effects of HMX particle size and binder stiffness on the burning mechanism and regression rate of a series of fast burning propellants
[DE91-015785] N91-29387
Differential equations and continuum mechanics
[AD-A237722] N91-29820

MELTING
Molecular dynamics simulation of the effect of interfaces in melting and solid-state amorphization
[DE91-015550] N91-29284
Thermophysical properties of POCO AXF-5Q graphite up to melting
[DE91-014751] N91-29334

MELTING POINTS
Studies of polymers for shock absorption applications
[AD-A237925] N91-29358

MELTS (CRYSTAL GROWTH)
A study of the liquid-solid interface during rapid resolidification of cooper-titanium using molecular dynamics
[AD-A238634] N91-30022

MEMORY (COMPUTERS)
Portable parallel programming
[DE91-015648] N91-29794

MENTAL PERFORMANCE
Cognition and the brain
[AD-A237846] N91-29727

MERCURY AMALGAMS
Role of the solvent in kinetics of heterogeneous electron and ion transfer reactions
[AD-A237168] N91-29876

MESOMETEOROLOGY
Mesoscale modeling of precipitation scavenging by a cold-frontal squall line
[DE91-015534] N91-29695
Parameterizations of microphysical processes for simulation of regional-scale clouds
[DE91-015554] N91-29696

MESON-NUCLEON INTERACTIONS
Nuclear theory progress report
[DE91-013908] N91-29866

MESOSCALE PHENOMENA
On the application of edge wave theory to terrain-bounded cold surges: A numerical study N91-29670
Mesoscale modeling of precipitation scavenging by a cold-frontal squall line
[DE91-015534] N91-29695
Parameterizations of microphysical processes for simulation of regional-scale clouds
[DE91-015554] N91-29696
Mesoscale characteristics and the role of deformation on ocean dynamics
[AD-A237577] N91-29701

MESSAGE PROCESSING
A high data rate communications system using long pulses
[AD-D014947] N91-29430
Research in mathematics and computer science: Calculation of the probability of undetected error for certain error detection codes, phase 2
[AD-A238234] N91-29768

METABOLITES
The role of microorganisms in marine corrosion
[AD-A237062] N91-29308

METAL BONDING
Investigation of ultrasonic evaluation of solid-state metal bond
[DE91-014996] N91-29606

METAL FATIGUE
Tutor aft fuselage and empennage full-scale test: Procedures for creating a damage log
[NAE-ST-576] N91-29167
Deformation and thermal fatigue in high temperature austenitic alloys
[DE91-014981] N91-29305
Development of the microstructure based stochastic life prediction models
[AD-A237768] N91-29312
Strengthening mechanisms, creep, and fatigue processes in dispersion hardened niobium alloy
[AD-A237784] N91-29313
Aspects of fatigue and rapid depolarization in the film PZT capacitors
[DE91-014904] N91-29484

METAL FIBERS
Advanced materials for space nuclear power systems
[NASA-TM-105171] N91-29298

METAL FILMS
A study of copper segregation in sputtered Al-Si-Cu films using Auger electron spectroscopy
[AD-A238130] N91-29316

METAL FOILS
The mixed metallic-ionic clusters of the silver/silver iodide
[AD-A237883] N91-29314
The relative stability and possible structural formulae of the negatively charged silver monoiodide clusters
[AD-A238398] N91-29888

METAL FUELS
Production and use of metals and oxygen for lunar propulsion
[NASA-TM-105195] N91-29222

METAL HYDRIDES
The interaction of hydrogen with metal alloys
[NASA-TP-3128] N91-29318

METAL IONS
Electrochemical contact adsorption site changes driven by field and charge fact and theory
[AD-A237127] N91-29269
Lithium ion source for satellite charge control
[AD-A238272] N91-29470
Ruddlesden-Popper phases A(n+1)M(n)O(3n+1): Structures and properties
[DE91-011748] N91-29973

METAL MATRIX COMPOSITES
Effect of fiber-matrix debonding on notched strength of titanium metal matrix composites
[NASA-TM-104131] N91-29239
Effect of alumina particle additions on the aging kinetics of 6061 aluminum matrix composites
[AD-A238052] N91-29246

METAL OXIDE SEMICONDUCTORS
Introduction of a current waveform, waveshaping technique to limit conduction loss in high-frequency dc-dc converters suitable for space power
[AD-A237903] N91-29465

METAL OXIDES
Production and use of metals and oxygen for lunar propulsion
[NASA-TM-105195] N91-29222
Developmental status and system studies of the monolithic solid oxide fuel cell
[DE91-014389] N91-29645
Ruddlesden-Popper phases A(n+1)M(n)O(3n+1): Structures and properties
[DE91-011748] N91-29973
Defect characterization of electronic conducting pseudo-perovskite systems
[DE91-014385] N91-29978
High-(Tc) superconductors: Fabricating technologies and future perspectives
[DE91-015553] N91-30029

METAL PARTICLES
Design issues for propulsion systems using metallized propellants
[NASA-TM-105190] N91-29220
Micromechanisms of monotonic and cyclic subcritical crack growth in advanced high melting point low-ductility intermetallics
[AD-A238151] N91-29317

METAL PLATES
Launch capabilities to over 10 km/s
[DE91-014657] N91-29203
Feasibility of a laser-ignited HMX deflagration-to-detonation transition device for the US Navy LITES Program
[DE91-015210] N91-29382
Thick-section weldments in 21-6-9 and 316LN stainless steel for fusion energy applications
[DE91-015307] N91-29963

METAL POWDER
Metal injection moulding: A brief review
[NAE-LTR-ST-531] N91-29289
Postshock spectral radiance measurements in nickel and nickel/aluminum powders
[DE91-014695] N91-29302

An evaluation of nickel-aluminum coatings fabricated with the plasma-spray process
[DE91-013208] N91-29328

METAL PROPELLANTS
Design issues for propulsion systems using metallized propellants
[NASA-TM-105190] N91-29220
Production and use of metals and oxygen for lunar propulsion
[NASA-TM-105195] N91-29222

METAL SURFACES
Biofouling and corrosion fouling of plain and enhanced aluminum surfaces
[DE91-014464] N91-29300
X ray reflectivity studies of Au surfaces
[DE91-015308] N91-29307
Laser surface modification for selective electroplating of metal: A 2.5 m/s laser direct-write process
[DE91-014988] N91-29322
Properties and adhesion of polyimides in microelectronic devices
[AD-A238204] N91-29364
Basic mechanisms of diesel lubrication correlation of bench and engine tests
[AD-A237685] N91-29596
Quantitative interpretation of auger lineshapes and electron/photon stimulated desorption
[AD-A237138] N91-29874

METAL WORKING
Metal injection moulding: A brief review
[NAE-LTR-ST-531] N91-29289

METAL-METAL BONDING
Microstructural development in HSLA-100 steel weld metals
[AD-A237931] N91-29315

METALLIC PLASMAS
Stagnation and interpenetration of laser-created colliding plasmas
[DE91-013244] N91-29946

METALLIZING
High-energy backscattered electron imaging of voids in aluminum metallizations
[DE91-014895] N91-29303
Comparison between the interfacial chemistry of metallized polyimides and polymide
[AD-A238400] N91-29366
The 2nd Workshop on High Temperture Electronics (Metallization and Packaging)
[DE91-014332] N91-29442

METALS
Compendium of material test results on HY-100 and pseudo HY-100 metals in support of US Navy programs
[DE91-013134] N91-29292
A brief overview of the activities and accomplishments of the Metals and Ceramics Division
[DE91-014955] N91-29296
Study of activation of metal samples from LDEF-1 and Spacelab-2
[NASA-CR-184171] N91-29297
Analysis of weld metal solidification and microstructures
[DE91-014574] N91-29301
Effects of doping on hybridization gapped materials
[DE91-014611] N91-29477
Structures, properties, and dynamics of metal clusters from infrared laser spectroscopy
[AD-A237669] N91-29570

METASTABLE ATOMS
Surface structure and surface order
[AD-A237466] N91-30001

METASTABLE STATE
Study of energy levels and decay mechanisms for Singlet Rydberg states of molecular nitrogen
[AD-A238156] N91-29885
Electron microscopy of thick 304 SS-copper multilayers
[DE91-011116] N91-29972
Molecular beam epitaxial growth and characterization of metastable compound semiconductors for infrared detector applications
[AD-A237797] N91-30010

METEOROLOGICAL PARAMETERS
Aircraft icing handbook, volume 3
[AD-A238041] N91-29156
Scattering and polarization measurements using the PL/OPA low altitude lidar
[AD-A238082] N91-29424
Criteria for assessing the role of transported ozone/precursors in ozone nonattainment areas
[PB91-195958] N91-29662

METEOROLOGICAL SATELLITES
Multiple channel satellite analysis of cirrus
[AD-A238054] N91-29687
Cloud data collection, composites and analysis for Whole-Sky Imager (WSI) studies
[AD-A238531] N91-29690

METEOROLOGICAL SERVICES
Toward a new National Weather Service: A first report
[PB91-184077] N91-29694

METEOROLOGY
Equatorial entrainment zone simulations
[AD-A237234] N91-29657
An observational study of the efficiency of activation of accumulation-mode particles in warm continental stratiform clouds
[DE91-013335] N91-29681
A global geographic information system data base of storm occurrences and other climatic phenomena affecting coastal zones
[DE91-014949] N91-29682

METHOD OF CHARACTERISTICS
Approximate multiphase flow modeling by characteristic methods
[PB91-190959] N91-29526

METHYL ALCOHOL
Overview of the technical implications of methanol and ethanol as highway motor vehicle fuels
[PB91-182881] N91-29385

METHYL COMPOUNDS
The mixed metallic-ionic clusters of the silver/silver iodide
[AD-A237883] N91-29314
Simulation of large deformation in glassy atactic polypropylene
[AD-A237223] N91-29340
Organo- borazines.3.homo- and copolymerization of p-vinylphenyl- cyclotri- borazines
[AD-A237881] N91-29357
Negative ion formation with electron impact to simulants
[AD-A237478] N91-29881

METROLOGY
Technical publication announcements covering center programs, July to September 1990, with 1991 CEEE events calendar
[PB91-184754] N91-29476

MICROANALYSIS
Application of the nuclear microprobe to the imaging of single event upsets in integrated circuits
[DE91-014701] N91-29447
Characterization of surface contaminants using infrared microspectroscopy
[DE91-009405] N91-29605

MICROBALANCES
Using quartz crystal microbalances to simultaneously sense mass accumulation and solution properties
[DE91-011501] N91-29537

MICROBIOLOGY
Subsurface Science Program
[DE91-015480] N91-29665
Microbiology and physiology of anaerobic fermentations of cellulose
[DE91-015239] N91-29712

MICROBURSTS (METEOROLOGY)
DAR(3)E-1 evaluation: Assessment of weather forecasts made using the DAR(3)E-1 workstation
[PB91-181701] N91-29693

MICROCOMPUTERS
QBDATAMT: A computer program to read Datamyte recorder data into an IBM PC or compatible computer
[NAE-LTR-ST-547] N91-29742
The PC Dugout micro-mainframe integration system: PAX implementation
[AD-A237480] N91-29758
High bandwidth diagnosis within the framework of a microcomputer-based intelligent tutoring system
[AD-A237959] N91-29805

MICROELECTRONICS
Properties and adhesion of polyimides in microelectronic devices
[AD-A238204] N91-29364
The 2nd Workshop on High Temperture Electronics (Metallization and Packaging)
[DE91-014332] N91-29442
Simulation of the growth of Mo/Si multilayers
[DE91-015679] N91-29486
Monolithic integration of semiconductor and superconductor components
[AD-A237946] N91-30012
Solid state research
[NASA-CR-188021] N91-30016

MICROMETEOROIDS
IDA studies on natural space environmental effects on materials for SDIO
[AD-A237974] N91-29660

MICROMETEOROLOGY
Parameterizations of microphysical processes for simulation of regional-scale clouds
[DE91-015554] N91-29696

MICROORGANISMS
Specific mutagenesis of a chlorophyll-binding protein
[DE91-014813] N91-29711

MICROPROCESSORS
Verification of the FtCayuga fault-tolerant microprocessor system. Volume 2: Formal specification and correctness theorems
[NASA-CR-187574] N91-29777
Verification of the FtCayuga fault-tolerant microprocessor system. Volume 1: A case study in theorem prover-based verification
[NASA-CR-4381] N91-29778

MICROSCOPY
Application of the nuclear microprobe to the imaging of single event upsets in integrated circuits
[DE91-014701] N91-29447
Characterization of surface contaminants using infrared microspectroscopy
[DE91-009405] N91-29605
A study of the relationship between macroscopic measures and physical processes occurring during N00014-89-J-1708
[AD-A238423] N91-29627
Development of model based magnetic LP-LEC growth large diameter GaAs
[AD-A237456] N91-29998

MICROSTRIP TRANSMISSION LINES
Analysis of FIN line feasibility for W-band attenuator applications
[AD-A237271] N91-29450

MICROSTRUCTURE
Rejuvenation of service exposed alloy 713C turbine blades
[NAE-LTR-ST-1716] N91-29179
The failure of components in power generation equipment
[NAE-LTR-ST-1774] N91-29180
Microstructural and strength stability of CVD SiC fibers in argon environment
[NASA-TM-103772] N91-29250
Characteristics of autoclave and in-reactor nodular corrosion of Zircaloys
[DE91-013600] N91-29294
Tensile properties and microstructure of Alloy 718 thermally aged to 50,000 h
[DE91-014099] N91-29299
Analysis of weld metal solidification and microstructures
[DE91-014574] N91-29301
Development of the microstructure based stochastic life prediction models
[AD-A237768] N91-29312
Deformation induced microstructural and microchemical changes during thermomechanical treatment
[DE91-014862] N91-29319
Annealing effects on the microstructure of titanium electrical contacts on diamond films
[DE91-010150] N91-29327
Phase transformations, ultrastructure, and properties of rigid-rod polymers
[AD-A238643] N91-29368
Investigation of ultrasonic evaluation of solid-state metal bond
[DE91-014996] N91-29606
Pressure effects in the microwave plasma growth of polycrystalline diamond
[AD-A237751] N91-30006
Air-sintering mechanisms of chromites
[DE91-015527] N91-30027
Uniaxial stress study of the quantum transitions in a strained layer (001) In0.2Ga0.8As/GaAs single quantum well
[DE91-014990] N91-30033
TEM characterization of grain boundaries in mixed bicrystal films of aluminum
[DE91-016267] N91-30038

MICROWAVE CIRCUITS
Millimeter-wave characterization of GaAs devices and IC's
[AD-A237843] N91-29461
InP and InGaAs submicron gate microwave power transistors for 20 GHz applications
[AD-A238595] N91-29473
High temperature superconductor analog electronics for millimeter-wavelength communications
[NASA-TM-105184] N91-29982

MICROWAVE EQUIPMENT
Spike leakage and burnout of silicon PIN diode microwave limiters
[AD-A238392] N91-29471
Stable integrated microwave to optical modulator
[AD-A238166] N91-29574
Degradation of brightness by resonant particle effects
[DE91-015181] N91-29578

MICROWAVE FREQUENCIES
Fabrication of silicon nitride ceramics by microwave heating
[DE91-015312] N91-29373

MICROWAVE IMAGERY
An AVHRR data set for the arctic leads ARI
[AD-A237221] N91-29637
MICROWAVE LANDING SYSTEMS
Flight evaluation of complex approaches in a Twin Otter aircraft using a microwave landing system
[NAE-LTR-FR-114] N91-29159
Mobile Microwave Landing System (MMLS) user interface
[AD-A237470] N91-29162
MICROWAVE OSCILLATORS
A compact 200 kV pulse transformer system
[DE91-014669] N91-29479
MICROWAVE TUBES
A compact 200 kV pulse transformer system
[DE91-014669] N91-29479
MICROWAVES
Synthesis of diamond films by microwave generated pulsed plasmas
[AD-A237228] N91-29341
Pressure effects in the microwave plasma growth of polycrystalline diamond
[AD-A237751] N91-30006
MIE SCATTERING
Scattering and polarization measurements using the PL/OPA low altitude lidar
[AD-A238082] N91-29424
MILITARY AVIATION
Methodology investigation, aviation test management system concept development
[AD-A237349] N91-29172
MILITARY OPERATIONS
Dependence of radar backscatter on the energetics of the air-sea interface
[AD-A237818] N91-29685
A framework for understanding the strategic defense initiatives' software debates
[AD-A237193] N91-29852
MILLIMETER WAVES
Analysis of FIN line feasibility for W-band attenuator applications
[AD-A237271] N91-29450
Millimeter-wave characterization of GaAs devices and IC's
[AD-A237843] N91-29461
High temperature superconductor analog electronics for millimeter-wavelength communications
[NASA-TM-105184] N91-29982
MILLING (MACHINING)
Properties of materials with a fine length scale: Mechanically alloyed metals and the high temperature superconductor Y1Ba2Cu3O7
[DE91-012538] N91-29975
MIMD (COMPUTERS)
Lazy task creation: A technique for increasing the granularity of parallel programs
[AD-A237477] N91-29781
MINERALS
NMR spectroscopy of experimentally shocked silicate minerals
[DE91-014897] N91-29898
MINIATURE ELECTRONIC EQUIPMENT
Properties and adhesion of polyimides in microelectronic devices
[AD-A238204] N91-29364
MINIATURIZATION
Planetary instrument definition and development program: 'Miniature Monochromatic Imager'
[NASA-CR-186550] N91-29219
MINKOWSKI SPACE
Sum of distances in normed spaces
[AD-A238066] N91-29825
MINUTEMAN ICBM
Acoustic tests on a new motor generator system for the Minuteman launch control centers at Alpha 01 and Sierra 00, Malmstrom AFB, Montana
[AD-A237944] N91-29648
MIRRORS
Preparation of damage resistant optical coatings on flat substrates
[DE91-013588] N91-29916
Fabrication of lightweight Si/SiC LIDAR mirrors
[NASA-CR-4389] N91-29935
Responsivity uniformity enhancements for Backside-Illuminated Charge-Coupled Devices (BICCDs) by excimer laser-assisted etching
[AD-A237435] N91-29997
MISSILE CONFIGURATIONS
Missile Datcom: User's manual
[AD-A237817] N91-29148
MISSILE CONTROL
Acoustic tests on a new motor generator system for the Minuteman launch control centers at Alpha 01 and Sierra 00, Malmstrom AFB, Montana
[AD-A237944] N91-29648
MISSILE DEFENSE
Ceramic fabrication R/D
[DE91-014758] N91-29335
SDI performance and START constraints: Modeling phase-1 defense engagements
[DE91-013305] N91-29849
MISSILE DESIGN
Missile Datcom: User's manual
[AD-A237817] N91-29148
MISSILE LAUNCHERS
Acoustic tests on a new motor generator system for the Minuteman launch control centers at Alpha 01 and Sierra 00, Malmstrom AFB, Montana
[AD-A237944] N91-29648
MISSILE TRACKING
NRL review, 1989-1990
[AD-A238612] N91-29856
Multitarget tracking using optical processing
[AD-A237107] N91-29918
MISSILE TRAJECTORIES
Explosively driven missile trajectory parameters for various fragment materials and velocities
[DE91-014330] N91-29631
Multitarget tracking using optical processing
[AD-A237107] N91-29918
MISSILES
Missile Datcom: User's manual
[AD-A237817] N91-29148
The functional dependence of trajectory dispersion on initial condition errors
[DE91-014661] N91-29151
Twenty first century space propulsion study addendum
[AD-A238011] N91-29225
Strategic defense initiative: Need to examine concurrency in development of brilliant pebbles
[AD-A238292] N91-29854
MISSING MASS (ASTROPHYSICS)
Dark matter in the universe
[DE91-014863] N91-30065
MISSION PLANNING
Resource envelope concepts for mission planning
[NASA-TP-3139] N91-29209
MIXED OXIDES
Defects and transport in mixed oxides
[DE91-014537] N91-29266
Photoemission and electronic structure studies of YBa2Cu3O(x)
[DE91-014469] N91-29979
Anisotropic spin susceptibility of the (Y,Ca),(Ba, La)2Cu4O8 system
[DE91-014593] N91-30032
MIXING
Experimental study of cross-stream mixing in a cylindrical duct
[NASA-TM-105180] N91-29187
Experimental and analytical study of rippled trailing edge airfoils for compressor application
[AD-A237425] N91-29508
Modeling a rain-induced mixed layer
[AD-A238022] N91-29702
MIXING LENGTH FLOW THEORY
Interactions of turbulent eddies and combustion in an MHD second stage combustor
[DE91-015722] N91-29968
MIXTURES
Adiabatic two-phase flow frictional pressure drop. Part 2: A generalized method for data correlation
[DE91-014462] N91-29501
Thermophysical properties of supercritical fluids and fluid mixtures
[DE91-015794] N91-30041
MOBILE COMMUNICATION SYSTEMS
Very low bit rate voice for packetized mobile applications
[DE91-015333] N91-29409
MOBILITY
Objective assessments of mobility with an early Unmanned Ground Vehicle (UGV) prototype viewing system
[AD-A237317] N91-29595
MODAL RESPONSE
Finite element-based system identification from experimental modal analysis results N91-29618
MODELS
A vision system model
[AD-A238459] N91-29930
MODULATION
Auditory processing of complex sounds across frequency channels
[AD-A238023] N91-29862
MODULATORS
Stable integrated microwave to optical modulator
[AD-A238166] N91-29574
MODULES
Concepts for manned lunar habitats
[NASA-TM-104114] N91-30068
MOIRE FRINGES
Evaluation of Shadow Moire for surface deformation detection and measurement
[NAE-LTR-ST-1737] N91-29604
MOIRE INTERFEROMETRY
Evaluation of Shadow Moire for surface deformation detection and measurement
[NAE-LTR-ST-1737] N91-29604
MOISTURE CONTENT
Remote determination of soil moisture and evapotranspiration from thermal infrared measurements: Detection of a drying threshold
[PB91-195818] N91-29641
MOLDS
Advances in the drained shaping of ceramics
[DE91-015429] N91-29376
MOLECULAR BEAM EPITAXY
InGaAs/GaAs graded superlattices in photodetectors for wavelengths beyond 1 micron
[DE90-012073] N91-29969
Molecular beam epitaxial growth and characterization of metastable compound semiconductors for infrared detector applications
[AD-A237797] N91-30010
The embedded electron-gas boundary: A new standard problem in surface physics
[AD-A238152] N91-30014
Pseudomorphic semiconducting heterostructures from combinations of AlN, GaN and seleced SiC polytypes: Theoretical advancement and its coordination with experimental studies of nucleation, growth, characterizaiton and device development
[AD-A238520] N91-30020
MOLECULAR BEAMS
Molecular beam studies of reaction dynamics
[DE90-011600] N91-29256
Hot atom reactive scattering and photodissociation experiments with acetylene and ethylene
[DE91-013755] N91-29264
Molecular beam studies of reaction dynamics
[DE91-014866] N91-29868
MOLECULAR CHAINS
Simulation of large deformation in glassy atactic polypropylene
[AD-A237223] N91-29340
Quasi-static modeling of chain-dynamics in the amorphous glassy polycarbonate of 4,4'-isopropyledenediphenol
[AD-A237289] N91-29343
Conformational characteristics of the polycarbonate 4,4'-isopropylidenediphenol
[AD-A237334] N91-29347
Deconvolution of x ray diffraction data to elucidate plastic deformation mechanisms in the uniaxial extension of bulk Nylon-6
[AD-A237332] N91-29623
MOLECULAR COLLISIONS
Hot atom reactive scattering and photodissociation experiments with acetylene and ethylene
[DE91-013755] N91-29264
Spin-Label-Spin-Probe. Studies of bimolecular encounters in micelles
[AD-A238546] N91-29891
MOLECULAR ENERGY LEVELS
Design, synthesis and characterization of novel polydiacetylenes using new analytical techniques
[AD-A237362] N91-29348
Laser enhanced chemical reaction studies
[DE91-013021] N91-29555
MOLECULAR EXCITATION
Laser enhanced chemical reaction studies
[DE91-013021] N91-29555
Study of energy levels and decay mechanisms for Singlet Rydberg states of molecular nitrogen
[AD-A238156] N91-29885
MOLECULAR GASES
Study of energy levels and decay mechanisms for Singlet Rydberg states of molecular nitrogen
[AD-A238156] N91-29885
The relationship between the density wave, molecular gas and star formation in M51 N91-30064
MOLECULAR INTERACTIONS
Hot atom reactive scattering and photodissociation experiments with acetylene and ethylene
[DE91-013755] N91-29264
Light scattering characterization of polymer additives and correlation of molecular properties of polymer fluids
[AD-A238547] N91-29367
MOLECULAR IONS
The relative stability and possible structural formulae of the negatively charged silver monoiodide clusters
[AD-A238398] N91-29888
MOLECULAR ORBITALS
Orbitals, correlation, valencies in high-T(sub c) superconductors
[DE91-618099] N91-29977

MOLECULAR ROTATION
Simulation of large deformation in glassy atactic polypropylene
[AD-A237223] N91-29340
MOLECULAR SPECTRA
Spin-Label-Spin-Probe. Studies of bimolecular encounters in micelles
[AD-A238546] N91-29891
MOLECULAR STRUCTURE
Simulation of the structure of dense, amorphous bisphenol-A polycarbonate
[AD-A237222] N91-29270
Synthesis and characterization of reduced tungsten sulfide cluster complexes
[DE91-014916] N91-29282
Catalytic hydrogenation of carbon monoxide
[DE91-015452] N91-29283
Theoretical studies of solid-fluid phase equilibria
[DE91-014811] N91-29287
Simulation of large deformation in glassy atactic polypropylene
[AD-A237223] N91-29340
An atomistic model of the amorphous glassy polycarbonate of 4,4'-isopropylidenediphenol
[AD-A237291] N91-29345
Conformational characteristics of the polycarbonate 4,4'-isopropylidenediphenol
[AD-A237334] N91-29347
Physical properties and structure of ion-containing polymers
[AD-A238196] N91-29363
Infrared and Raman spectra of C60 and C70 solid films at room temperature
[AD-A237880] N91-29462
Study of energy levels and decay mechanisms for Singlet Rydberg states of molecular nitrogen
[AD-A238156] N91-29885
Orbitals, correlation, valencies in high-T(sub c) superconductors
[DE91-618099] N91-29977
High-resolution Z-contrast imaging of superlattices and heterostructures
[DE91-015329] N91-29994
A study of the liquid-solid interface during rapid resolidification of cooper-titanium using molecular dynamics
[AD-A238634] N91-30022
MOLECULAR THEORY
Theoretical studies of solid-fluid phase equilibria
[DE91-014811] N91-29287
MOLECULAR WEIGHT
Mechanism of anionic ring-opening polymerization of silacyclopent 3-enes
[AD-A237538] N91-29353
MOLECULES
Infrared and Raman spectra of C60 and C70 solid films at room temperature
[AD-A237880] N91-29462
MOLTEN SALTS
Pyrite cathode material for a thermal battery
[AD-D014945] N91-29475
MOLYBDENUM
Dynamic behavior of fully dense molybdenum
[DE91-014902] N91-29304
Simulation of the growth of Mo/Si multilayers
[DE91-015679] N91-29486
MOMENTUM TRANSFER
Analytical calculation of neutral transport and its effect on ions
[DE91-015908] N91-29896
MONOMERS
Dual cure photocatalyst systems
[DE91-014174] N91-29369
Solvent effects on simple electron transfer reactions. A comparison of results in Debye and non-Debye solvents
[AD-A237157] N91-29875
MONOPOLE ANTENNAS
NIST calibration procedure for vertically polarized monopole antennas 30 kHz to 300 MHz
[PB91-185124] N91-29432
MONTE CARLO METHOD
Pressure measurements in a low-density nozzle plume for code verification
[NASA-TM-105170] N91-29228
Defects and transport in mixed oxides
[DE91-014537] N91-29266
Atomic approaches to defect thermochemistry
[AD-A238260] N91-29280
Equation of state for pure sodium chloride
[DE91-014618] N91-29286
The charge-exchange neutral problem and the code NEUTRAL
[AD-A237889] N91-29464
Stochastic simulation techniques for partition function approximation of Gibbs random field images
[AD-A238611] N91-29775
On the analysis of grouped survival data using cumulative occurrence/exposure rates
[AD-A238219] N91-29838
New modified Anderson-Darling and Cramer-von Mises goodness-of-fit tests for a normal distribution with specified parameters
[AD-A238630] N91-29846
A goodness-of-fit test for a family of two parameter Weibulls with known shape using minimum distance estimation of parameters
[AD-A238633] N91-29847
Monte Carlo and mean field calculations of the magnetocaloric effect of ferromagnetically interacting clusters
[DE91-014792] N91-29859
Single-scatter Monte Carlo compared to condensed history results for low energy electrons
[DE91-015176] N91-29869
Quantitative analysis of oxygen segregation on inversion domain boundaries in aluminum nitride
[DE91-010869] N91-29971
A study of the liquid-solid interface during rapid resolidification of cooper-titanium using molecular dynamics
[AD-A238634] N91-30022
MORPHOLOGY
Morphology of bulk Nylon 6 subjected to plane strain compression
[AD-A237331] N91-29622
Stochastic modelling of seafloor morphology
[AD-A237063] N91-29697
MOSSBAUER EFFECT
Inelastic scattering in condensed matter with high intensity Moessbauer radiation
[DE91-014384] N91-29980
MOTION STABILITY
Performance and stability in high speed articulated structures undergoing quick maneuvers: Theory and applications
[AD-A237857] N91-29597
MOTOR VEHICLES
Overview of the technical implications of methanol and ethanol as highway motor vehicle fuels
[PB91-182881] N91-29385
MOTORS
Acoustic tests on a new motor generator system for the Minuteman launch control centers at Alpha 01 and Sierra 00, Malmstrom AFB, Montana
[AD-A237944] N91-29648
MULTIPHASE FLOW
Numerical and physical modelling of bubbly flow phenomena
[DE91-013646] N91-29492
Approximate multiphase flow modeling by characteristic methods
[PB91-190959] N91-29526
MULTIPHOTON ABSORPTION
Reactions of small molecular systems
[DE91-014519] N91-29867
Atomic physics in strong fields
[DE91-015393] N91-29872
MULTIPLEXING
Quaternary pulse position modulation electronics for free-space laser communications
[NASA-TM-104502] N91-29405
Application of Multi-Frequency Modulation (MFM) for high-speed data communications to a voice frequency channel
[AD-A238019] N91-29422
MULTIPROCESSING (COMPUTERS)
APRIL: A processor architecture for multiprocessing
[AD-A237476] N91-29739
A common interface real-time multiprocessor operating system for embedded systems
[AD-A238445] N91-29770
A high-performance retargetable simulator for parallel architectures
[AD-A237354] N91-29779
Counting networks
[AD-A237475] N91-29780
The MIT Alewife machine: A large-scale distributed-memory multiprocessor
[AD-A237705] N91-29784
Expert systems on multiprocessor architectures. Volume 1: Summary
[AD-A238046] N91-29786
Expert systems on multiprocessor architectures. Volume 2: Technical reports
[AD-A238047] N91-29787
Expert systems on multiprocessor architectures, volume 3
[AD-A238048] N91-29788
Expert systems on multiprocessor architectures, volume 4
[AD-A238049] N91-29789
Visualizing performance of parallel programs
[DE91-014966] N91-29793
Portable parallel programming
[DE91-015648] N91-29794
Supernodal symbolic Cholesky factorization on a local-memory multiprocessor
[DE91-014967] N91-29796
Using the Harmony operating system: Release 3.0
[ERA-377] N91-29799
Parallelizing the spectral transform method
[DE91-013969] N91-29815
MULTISENSOR APPLICATIONS
Multi-sensor feature level fusion
[AD-A237106] N91-29411
Design and analysis of multi-sensor sequential detection system
[AD-A238012] N91-29543
Multi-sensor image interpretation using laser radar and thermal images
[AD-A238245] N91-29576
MULTISPECTRAL BAND SCANNERS
Detection of targets in terrain clutter by using multispectral infrared image processing
[AD-A237436] N91-29414
MULTISTATIC RADAR
Range-only multistatic radar system
[AD-D011645] N91-29399
MULTIVARIABLE CONTROL
A linear control design structure to maintain loop properties during limit operation in a multi-nozzle turbofan engine
[NASA-TM-105163] N91-29188
MULTIVARIATE STATISTICAL ANALYSIS
Development of a mixture for nonlinear wave propagation in fiber-reinforced composites
[AD-A237471] N91-29243
Robust design of multivariable control: An interval arithmetic approach
[AD-A238006] N91-29806
MUONS
Study of nuclear effects in the deuteron and extraction of neutron to proton stucture function ratio
[DE91-015484] N91-29873
MUTATIONS
Specific mutagenesis of a chlorophyll-binding protein
[DE91-014813] N91-29711
Stable isotope fractionation in photosynthesis: Analysis of autotrophic competence following transformation of the chloroplast genome of Chlamydomonas
[DE91-015792] N91-29713

N

N-TYPE SEMICONDUCTORS
Defect characterization of electronic conducting pseudo-perovskite systems
[DE91-014385] N91-29978
NAPHTHALENE
A theoretical and experimental study of unimolecular and biomolecular radical hydrogen transfer reactions
[DE91-012607] N91-29261
NARROWBAND
Synchrotron studies of narrow band materials
[DE91-014826] N91-30025
NATURAL GAS
Ultra-low NOx gas turbine combustor
[PB91-184994] N91-29601
NATURAL LANGUAGE (COMPUTERS)
Negation in knowledge graphs
[PB91-185421] N91-29776
NAVIER-STOKES EQUATION
Numerical simulation of a viscous vortex ring interaction with a density interface
[DE91-011532] N91-29489
Theoretical study of the flow in a rotating duct. Experimental study through flow visualization in a curved duct
[RAE-TRANS-2189] N91-29493
Computational and theoretical aspects of nonlinear partial differential equations
[AD-A238495] N91-29829
NAVIGATION
Vision-based navigation and parallel computing
[AD-A238570] N91-29164
NAVIGATION SATELLITES
GPS: Aspects of pseudo-range positioning offshore N91-29161
NAVY
NRL review, 1989-1990
[AD-A238612] N91-29856

NEAR INFRARED RADIATION
Development of model based magnetic LP-LEC growth large diameter GaAs
[AD-A237456] N91-29998
NEGATIVE IONS
Design aspects for a pulsed-mode, high-intensity, heavy negative ion source
[DE91-011094] N91-29864
Negative ion formation with electron impact to simulants
[AD-A237478] N91-29881
NEODYMIUM LASERS
Photoelectron and photoionization pumping of XUV lasers by laser-produced plasmas N91-29558
Low-jitter, high-voltage, infrared, laser-triggered, vacuum switch
[DE91-014602] N91-29562
Chinese physics lasers (selected articles)
[AD-A237263] N91-29567
The MIT short-wavelength laser project
[DE91-015357] N91-29582
NERVOUS SYSTEM
Studies in neural networks
[AD-A237452] N91-29717
Software development of the cochlear filter and eighth-nerve model
[AD-A237454] N91-29757
NETWORK CONTROL
Compensation of distributed delays in integrated communication and control systems
[NASA-CR-187136] N91-29193
Description of a computer fault detector and net isolator
[AD-A238387] N91-29428
Counting networks
[AD-A237475] N91-29780
NETWORK SYNTHESIS
Description of a computer fault detector and net isolator
[AD-A238387] N91-29428
NEURAL NETS
Neural networks and robotics applied to the non-destructive inspection of aircraft
[AD-A238312] N91-29609
Studies in neural networks
[AD-A237452] N91-29717
Hardware Implementation of Neuron Nets and Synapses Workshop
[AD-A237704] N91-29718
Analog computation in neural systems: Architectures and complexity
[AD-A237856] N91-29785
Theory and computer simulation of the interactional neural network
[NRC-30269] N91-29800
Workshop on Automation and Robotics: Proceedings
[DE91-015175] N91-29801
Engineering applications of neural computing: A state-of-the-art survey
[AD-A237628] N91-29803
Design and hardware implementation of neural systems
[AD-A237703] N91-29804
Invariant target recognition using self-organizing networks
[AD-A238252] N91-29807
An expert system approach to global fault detection and isolation design
[AD-A238494] N91-29808
On the interpolation properties of feedforward layered neural networks
[AD-A238035] N91-29824
Least-squares learning and approximation of posterior probabilities on classification problems by neural network models
[AD-A237140] N91-29833
A vision system model
[AD-A238459] N91-29930
NEURONS
Hardware Implementation of Neuron Nets and Synapses Workshop
[AD-A237704] N91-29718
NEUTRAL BEAMS
H-mode energy confinement scaling from the ASDEX, DIII-D, and jet tokamaks
[DE91-015145] N91-29957
NEUTRAL PARTICLES
Analytical calculation of neutral transport and its effect on ions
[DE91-015908] N91-29896
NEUTRINOS
Study of nuclear effects in the deuteron and extraction of neutron to proton stucture function ratio
[DE91-015484] N91-29873
Research in nuclear astrophysics: Stellar collapse and supernovae
[DE91-015449] N91-30066
NEUTRON DIFFRACTION
Superconducting superoxygenated La(2-x)Sr(x)CuO(4+delta): Search for phase separation
[DE91-015334] N91-29995
NEUTRON FLUX DENSITY
Parametric design calculations using Green's function to determine unique source
[DE91-014683] N91-29861
NEUTRON IRRADIATION
Postirradiation deformation of ferritic Fe-Cr binary alloys
[DE91-014856] N91-29295
NEUTRON STARS
Proton deceleration near the surface of an accreting neutron star N91-30063
Research in nuclear astrophysics: Stellar collapse and supernovae
[DE91-015449] N91-30066
NEUTRONS
Study of nuclear effects in the deuteron and extraction of neutron to proton stucture function ratio
[DE91-015484] N91-29873
Neutron dosimetry using optically stimulated luminescence
[DE91-015781] N91-29902
Inverse problem in neutron reflection
[DE91-014457] N91-29984
NEWTON METHODS
Primal-dual methods for linear programming
[AD-A237418] N91-29756
Barrier methods for large-scale quadratic programming
[AD-A238554] N91-29773
NEWTONIAN FLUIDS
Steady flow of a fluid-solid mixture between parallel plates
[DE91-013114] N91-29491
NICKEL
Postshock spectral radiance measurements in nickel and nickel/aluminum powders
[DE91-014695] N91-29302
NICKEL ALLOYS
Rejuvenation of service exposed alloy 713C turbine blades
[NAE-LTR-ST-1716] N91-29179
High temperature mass spectrometric study of the thermodynamics of liquid nickel-aluminium alloys at 2000 K
[MRL-TR-91-15] N91-29290
Tensile properties and microstructure of Alloy 718 thermally aged to 50,000 h
[DE91-014099] N91-29299
Lightweight disk alloy development
[AD-A237064] N91-29309
Development of nickel and iron aluminides and their applications
[DE91-015323] N91-29325
An evaluation of nickel-aluminum coatings fabricated with the plasma-spray process
[DE91-013208] N91-29328
NICKEL CADMIUM BATTERIES
Performance and life evaluation of advanced battery technologies for electric vehicle applications
[DE91-015671] N91-29482
NICKEL COMPOUNDS
The growth of ultrathin epitaxial intermetallic films
[AD-A237798] N91-30011
NICKEL IRON BATTERIES
Performance and life evaluation of advanced battery technologies for electric vehicle applications
[DE91-015671] N91-29482
NIGHT VISION
Human factors of night vision devices: Anecdotes from the field concerning visual illusions and other effects
[AD-A237641] N91-29735
NIOBIUM
Micromechanisms of monotonic and cyclic subcritical crack growth in advanced high melting point low-ductility intermetallics
[AD-A238151] N91-29317
ANL's development of conductive ceramic components for MCFC
[DE91-015557] N91-29336
NIOBIUM ALLOYS
Strengthening mechanisms, creep, and fatigue processes in dispersion hardened niobium alloy
[AD-A237784] N91-29313
Environmental effects in niobium base alloys and other selected intermetallic compounds
[AD-A237535] N91-29658
NITRAMINE PROPELLANTS
Spectral studies of solid propellant combustion. 3: Emission and absorption results for HMX2 propellant
[AD-A237958] N91-29276
NITRIC OXIDE
Analysis of the ultraviolet emissions of nitric oxide from mid-latitude rocket observations
[AD-A237340] N91-29673
NITROGEN
Arcjet thermal characteristics
[NASA-TM-105156] N91-29231
A technique for measuring the solubilities of gases in liquids
[AD-A238071] N91-29278
Qualitative investigation of cryogenic injected shock dissipation
[NASA-TM-105140] N91-29525
Study of elementary reactions and energy transfer processes involving the NH and CN free radicals
[AD-A238461] N91-29889
NITROGEN OXIDES
Experimental study of cross-stream mixing in a cylindrical duct
[NASA-TM-105180] N91-29187
Investigation of particulate formation during diesel spray combustion
[DE90-008282] N91-29255
A methodology for inhibiting the formation of pollutants in diesel engines
[DE90-011615] N91-29584
NOBLE METALS
Pyrite cathode material for a thermal battery
[AD-D014945] N91-29475
NODULES
Characteristics of autoclave and in-reactor nodular corrosion of Zircaloys
[DE91-013600] N91-29294
NOISE INTENSITY
Translation of airfoil trailing edge noise article from Revue d'Acoustique
[AD-A237811] N91-29143
NOISE MEASUREMENT
Acoustic tests on a new motor generator system for the Minuteman launch control centers at Alpha 01 and Sierra 00, Malmstrom AFB, Montana
[AD-A237944] N91-29648
NOISE SPECTRA
Translation of airfoil trailing edge noise article from Revue d'Acoustique
[AD-A237811] N91-29143
An assessment of the acoustic noise in the working section of the NAE 6 ft x 9 ft low speed wind tunnel
[NAE-LTR-ST-1744] N91-29196
Spectra and covariances for classical nonlinear signal processing problems involving class A non-Gaussian noise
[AD-A237388] N91-29413
Acoustic background noise variation in Air Force platforms and its effect on noise removal algorithms
[AD-A238279] N91-29863
NONDESTRUCTIVE TESTS
Workshop proceedings: Toughening Mechanisms in Quasi-Brittle Materials
[AD-A238289] N91-29248
Evaluation of Shadow Moire for surface deformation detection and measurement
[NAE-LTR-ST-1737] N91-29604
Ultrasonic evaluation of silicon nitride green bodies
[AD-A237924] N91-29608
Neural networks and robotics applied to the non-destructive inspection of aircraft
[AD-A238312] N91-29609
NDE of ceramics and ceramic composites
[NASA-TM-104520] N91-29610
NONFERROUS METALS
JPRS report: Science and technology. USSR: Materials science
[JPRS-UMS-91-001] N91-29291
NONLINEAR EQUATIONS
Computational and theoretical aspects of nonlinear partial differential equations
[AD-A238495] N91-29829
NONLINEAR OPTICS
Laser-atom interaction at high intensities
[AD-A238231] N91-29887
Nonlinear optical interactions involving the real Gaussian field
[DE91-015052] N91-29936
NONLINEAR PROGRAMMING
Implementation of an exact penalty function formulation to solve convex nonlinear programming problems
[AD-A237905] N91-29761
An exact two-matching based branch and bound algorithm for the symmetric traveling salesman problem
[AD-A237878] N91-29823
NONLINEAR SYSTEMS
A new look at the Tobak-Schiff model of nonplanar aircraft dynamics
[NAE-LTR-UA-101] N91-29168

Development of a mixture for nonlinear wave propagation in fiber-reinforced composites
[AD-A237471] N91-29243

Nonlinear spectroscopy of multicomponent droplets and two- and three-dimensional measurements in flames
[AD-A238028] N91-29277

Spectra and covariances for classical nonlinear signal processing problems involving class A non-Gaussian noise
[AD-A237388] N91-29413

Nonlinear computerized methodology. A: Angle of arrival estimation. B: Data modeling and identification
[AD-A237564] N91-29415

Nonlinear dynamics of Josephson junction parametric amplifier arrays
[AD-A237451] N91-29454

Millimeter-wave characterization of GaAs devices and IC's
[AD-A237843] N91-29461

Problems in nonlinear continuum dynamics
[AD-A237844] N91-29512

Analysis of Naval aviation selection test data with nonlinear models. Part 1: Parameter estimation
[AD-A238244] N91-29728

Parameter estimation via nonlinear differential correction least square method
[NAL-PD-FC-9110] N91-29814

A survey of nonlinear dynamics (chaos theory)
[AD-A237802] N91-29821

A general lease-squares fitting package for the sun workstation
[AD-A238180] N91-29837

Electro-optic line narrowing of optical parametric oscillators
[AD-D014944] N91-29934

Course lectures abstracts of participants fellows project reports
[AD-A237909] N91-30070

NONLINEARITY

Development of a mixture for nonlinear wave propagation in fiber-reinforced composites
[AD-A237471] N91-29243

Nonlinear spectroscopy of multicomponent droplets and two- and three-dimensional measurements in flames
[AD-A238028] N91-29277

Fission-fusion adaptivity in finite elements for nonlinear dynamics of shells
[AD-A238029] N91-29626

Analysis of nonGaussian, nonlinear time series with long-memory
[AD-A237847] N91-29822

NORMAL DENSITY FUNCTIONS

New modified Anderson-Darling and Cramer-von Mises goodness-of-fit tests for a normal distribution with specified parameters
[AD-A238630] N91-29846

NORTHERN HEMISPHERE

Performance report of the Wind Research Lab.
[AD-A238575] N91-29691

NOTCH TESTS

Effect of fiber-matrix debonding on notched strength of titanium metal matrix composites
[NASA-TM-104131] N91-29239

A study of the relationship between macroscopic measures and physical processes occurring during N00014-89-J-1708
[AD-A238423] N91-29627

NOTCHES

Effect of fiber-matrix debonding on notched strength of titanium metal matrix composites
[NASA-TM-104131] N91-29239

NOVAE

An investigation of Nova Persei (1901) and its environment N91-30059

NOZZLE FLOW

Pressure measurements in a low-density nozzle plume for code verification
[NASA-TM-105170] N91-29228

NOZZLE GEOMETRY

Progress toward synergistic hypermixing nozzles
[NASA-TM-105169] N91-29150

Divergence thrust loss calculations for convergent-divergent nozzles: Extensions to the classical case
[NASA-TM-105176] N91-29181

NUCLEAR ASTROPHYSICS

Research in nuclear astrophysics: Stellar collapse and supernovae
[DE91-015449] N91-30066

NUCLEAR DEFORMATION

Algebraic approaches to nuclear structure
[DE91-015214] N91-29870

Superdeformation: An experimental review
[DE91-015566] N91-29894

NUCLEAR ELECTRIC PROPULSION

Light weight space power reactors for nuclear electric propulsion
[DE91-014803] N91-29232

NUCLEAR EXPLOSION EFFECT

Impacts of a nominal nuclear electromagnetic pulse on electric power systems
[DE91-012991] N91-29401

NUCLEAR FUSION

Fusion reactor materials
[DE91-012984] N91-29942

Collisional processes of interest in MFE plasma research
[DE91-013023] N91-29943

Establishment of an Institute for Fusion Studies
[DE91-014922] N91-29956

NUCLEAR MAGNETIC RESONANCE

NMR characterization of porous ceramics
[DE91-015051] N91-29371

The 3-D NMR imaging: A chemical microscope for analysis of heterogeneous macromolecular networks
[DE91-015109] N91-29375

NMR spectroscopy of experimentally shocked silicate minerals
[DE91-014897] N91-29898

NUCLEAR MEDICINE

Reevaluation of S-values considering electron transport
[DE91-015428] N91-29893

NUCLEAR MODELS

Nuclear theory progress report
[DE91-013908] N91-29866

Electromagnetic dissociation of Au and Co targets by relativistic heavy ions
[DE91-014915] N91-29906

NUCLEAR PHYSICS

Nuclear theory progress report
[DE91-013908] N91-29866

Medium energy nuclear physics research
[DE91-015740] N91-29901

Establishment of an Institute for Fusion Studies
[DE91-014922] N91-29956

NUCLEAR POWER PLANTS

Standard NIM instrumentation system
[DE90-010387] N91-29532

NUCLEAR PROPULSION

Nuclear data needs for the space exploration initiative
[DE91-013231] N91-29200

NUCLEAR RADIATION

Ventilation kinetics testing of a steel frame/rubber fabric underground shelter
[AD-A237469] N91-29734

NUCLEAR REACTIONS

Medium energy nuclear physics research
[DE91-015740] N91-29901

Electromagnetic dissociation of Au and Co targets by relativistic heavy ions
[DE91-014915] N91-29906

NUCLEAR REACTORS

A methodology for developing physical system fault diagnostic aids
[DE91-015533] N91-29809

NUCLEAR SCATTERING

Electromagnetic dissociation of Au and Co targets by relativistic heavy ions
[DE91-014915] N91-29906

NUCLEAR STRUCTURE

Nuclear theory progress report
[DE91-013908] N91-29866

Algebraic approaches to nuclear structure
[DE91-015214] N91-29870

NUCLEATION

Analysis of weld metal solidification and microstructures
[DE91-014574] N91-29301

Pseudomorphic semiconducting heterostructures from combinations of AlN, GaN and seleced SiC polytypes: Theoretical advancement and its coordination with experimental studies of nucleation, growth, characterizaiton and device development
[AD-A238520] N91-30020

NUCLEONS

Study of nuclear effects in the deuteron and extraction of neutron to proton stucture function ratio
[DE91-015484] N91-29873

Research in nuclear astrophysics: Stellar collapse and supernovae
[DE91-015449] N91-30066

NUMERICAL ANALYSIS

Nonlinear dynamics of Josephson junction parametric amplifier arrays
[AD-A237451] N91-29454

Prediction of the pressure drop in transverse, repeated-rib tubes with numerical modeling
[DE91-014465] N91-29503

Three-dimensional vortex dynamics and interactions in near-wall turbulent boundary layers
[AD-A237413] N91-29507

Laser triggered spark gap modeling
[DE91-014831] N91-29557

Equatorial entrainment zone simulations
[AD-A237234] N91-29657

Analytical and numerical methods; advanced computer concepts
[DE91-014526] N91-29795

Diffusion approximations for complex repair systems
[AD-A238100] N91-29836

NUMERICAL CONTROL

Analyzing photographically recorded atomic emission spectra using an automated densitometer
[DE91-015368] N91-29871

NYLON (TRADEMARK)

Morphology of bulk Nylon 6 subjected to plane strain compression
[AD-A237331] N91-29622

Deconvolution of x ray diffraction data to elucidate plastic deformation mechanisms in the uniaxial extension of bulk Nylon-6
[AD-A237332] N91-29623

O

OBJECT PROGRAMS

Persistent data/knowledge base
[AD-A237498] N91-30048

OBLIQUE SHOCK WAVES

Exact and approximate solutions to the oblique shock equations for real-time applications
[NASA-CR-187173] N91-29147

OCCULTATION

An expert system approach for prediction of maritime visibility obscuration
[AD-A238305] N91-29688

OCEAN BOTTOM

Stochastic modelling of seafloor morphology
[AD-A237063] N91-29697

Sea level and bottom pressure measurements in the Northern Gulf of Alaska
[PB91-184135] N91-29705

OCEAN CURRENTS

Dimensionless parameters important to the prediction of vortex-induced vibration of long, flexible cylinders in ocean currents
[PB91-184713] N91-29630

Dependence of radar backscatter on the energetics of the air-sea interface
[AD-A237818] N91-29685

Mesoscale characteristics and the role of deformation on ocean dynamics
[AD-A237577] N91-29701

Fitting seasonal averages with a continuous function
[AD-A238300] N91-29704

OCEAN DYNAMICS

Relating ocean acoustic ambient to ocean surface dynamics
[AD-A237167] N91-29699

Mesoscale characteristics and the role of deformation on ocean dynamics
[AD-A237577] N91-29701

OCEAN MODELS

Fitting seasonal averages with a continuous function
[AD-A238300] N91-29704

OCEAN SURFACE

Dependence of radar backscatter on the energetics of the air-sea interface
[AD-A237818] N91-29685

Relating ocean acoustic ambient to ocean surface dynamics
[AD-A237167] N91-29699

Modeling a rain-induced mixed layer
[AD-A238022] N91-29702

Ocean thermal feature recognition, discrimination and tracking using infrared satellite imagery
[AD-A238138] N91-29703

Validation of the Schwartz and Hon algorithm at low grazing angles
[AD-A238162] N91-29767

OCEAN TEMPERATURE

Acoustic tomographic estimate of ocean advective heat flux: A numerical assessment in the Norwegian Sea
[AD-A237100] N91-29698

Mesoscale characteristics and the role of deformation on ocean dynamics
[AD-A237577] N91-29701

OCEAN THERMAL ENERGY CONVERSION

Biofouling and corrosion fouling of plain and enhanced aluminum surfaces
[DE91-014464] N91-29300

OCEANOGRAPHY
Modeling a rain-induced mixed layer
[AD-A238022] N91-29702
Sea level and bottom pressure measurements in the Northern Gulf of Alaska
[PB91-184135] N91-29705
Oceanographic data report Number 7: Data from the Delaware Estuary SCENIC cruises, April 1986 - September 1988
[PB91-183582] N91-29706
Oceanographic data report Number 8: Density profiles from the Delaware Estuary, October 1986 - September 1988
[PB91-183608] N91-29707
NRL review, 1991
[AD-A238665] N91-29857
OCEANS
GPS: Aspects of pseudo-range positioning offshore N91-29161
Seasonal air and water mass redistribution and its effect on satellite and polar motion N91-29202
OLFACTORY PERCEPTION
Studies in neural networks
[AD-A237452] N91-29717
ON-LINE SYSTEMS
On-line monitoring of volatile organic species
[DE91-014655] N91-29655
OPENINGS
Test results for composite specimens and elements containing joints and cutouts
[NASA-CR-178246] N91-29254
OPERATING SYSTEMS (COMPUTERS)
Operational concept document for the Next Generation Computer Resources (NGCR) operating systems interface standard baseline
[AD-A237501] N91-29782
Using the Harmony operating system: Release 3.0
[ERA-377] N91-29799
OPERATIONAL AMPLIFIERS
An alternative to operational amplifiers
[AD-A237439] N91-29453
OPERATIONS RESEARCH
Counting networks
[AD-A237475] N91-29780
OPTICAL COMMUNICATION
Quaternary pulse position modulation electronics for free-space laser communications
[NASA-TM-104502] N91-29405
Optical Multiple Access Network (OMAN) for advanced processing satellite applications
[NASA-TM-105167] N91-29431
VLSI circuit techniques and technologies for ultrahigh speed data conversion interfaces
[AD-A238115] N91-29468
Design of a stabilized, dc-powered analog laser diode driver
[AD-A238596] N91-29577
SAFENET 2 fiber optic implementation study
[AD-A238044] N91-29929
OPTICAL CORRELATORS
Multitarget tracking using optical processing
[AD-A237107] N91-29918
Adaptive liquid crystal TV based joint transform correlator as applied to real-time pattern recognition
[AD-A238576] N91-29931
OPTICAL COUPLING
Optical soliton source
[AD-D014942] N91-29933
OPTICAL DATA PROCESSING
Multitarget tracking using optical processing
[AD-A237107] N91-29918
OPTICAL DISKS
Legal and records management issue of optical disk storage media
[DE91-014898] N91-30046
OPTICAL EMISSION SPECTROSCOPY
Spectral studies of solid propellant combustion. 3: Emission and absorption results for HMX2 propellant
[AD-A237958] N91-29276
OPTICAL EQUIPMENT
Theoretical, experimental, and numerical studies on hybrid acoustooptic bistable devices
[AD-A237885] N91-29463
Optoelectronic Materials Center
[AD-A237663] N91-29922
The 23rd Optoelectronic Workshop: Optical System Assessment for Design and Simulated Annealing
[AD-A238588] N91-29932
Electro-optic line narrowing of optical parametric oscillators
[AD-D014944] N91-29934
OPTICAL FIBERS
Fatigue resistant optical fibers
[AD-A237568] N91-29921
Effect of cladding thickness on attenuation in uniformly curved single-mode optical fibers
[AD-A238034] N91-29928
OPTICAL MEASUREMENT
Experimental analysis of B-dot sensors
[AD-A238487] N91-29547
A survey of optical diagnostic methods for the study of fuel fouling
[AD-A237361] N91-29920
OPTICAL MEMORY (DATA STORAGE)
Legal and records management issue of optical disk storage media
[DE91-014898] N91-30046
OPTICAL PROPERTIES
Structure and stability of underpotentially depositied layers on Au(111) studied by optical second harmonic generation
[AD-A237087] N91-29268
Design, synthesis and characterization of novel polydiacetylenes using new analytical techniques
[AD-A237362] N91-29348
Preparation and properties of new inorganic glasses and gel-derived solids
[AD-A238095] N91-29360
Investigation of superresolution by incoherent to coherent conversion
[AD-A238111] N91-29544
A survey of optical diagnostic methods for the study of fuel fouling
[AD-A237361] N91-29920
Fast acting optical deflection
[AD-A237904] N91-29927
OPTICAL RADAR
Multi-sensor feature level fusion
[AD-A237106] N91-29411
A program to operate and upgrade the GL low altitude lidar systems
[AD-A238081] N91-29423
Scattering and polarization measurements using the PL/OPA low altitude lidar
[AD-A238082] N91-29424
Space-based Doppler lidar sampling strategies: Algorithm development and simulated observation experiments
[NASA-CR-184172] N91-29554
Multipixel multidimensional laser radar system theory
[AD-A238110] N91-29573
Multi-sensor image interpretation using laser radar and thermal images
[AD-A238245] N91-29576
Three-dimensional mapping of atmospheric boundary layer structure and winds with a high performance lidar
[AD-A238098] N91-29678
The nature of the propagation of sea breeze fronts in central California
[AD-A238635] N91-29692
Fabrication of lightweight Si/SiC LIDAR mirrors
[NASA-CR-4389] N91-29935
OPTICAL REFLECTION
Development of reflective optical systems for XUV projection lithography
[DE91-013167] N91-29915
OPTICAL THICKNESS
Effects of interfacial modification on diamond film adhesion
[AD-A237750] N91-29354
OPTIMAL CONTROL
Global optimality, conservativity and singularity in redundancy resolution of robotic manipulators N91-29593
Vibration control and optimization in composite structural elements by use of add-on viscoelastic materials
[AD-A238533] N91-29628
OPTIMIZATION
Boron nitride and silicon nitride systems
[AD-A238080] N91-29359
Minimization of refrigeration power requirements for mechanical supports in cryogenic systems
[DE91-015720] N91-29392
Global optimality, conservativity and singularity in redundancy resolution of robotic manipulators N91-29593
Structural optimization with pseudo-load approach exploiting design length scales N91-29616
Vibration control and optimization in composite structural elements by use of add-on viscoelastic materials
[AD-A238533] N91-29628
The parallel BFGS method for unconstrained minimization
[DE91-015784] N91-29798
On satellite constellation selection
[DE91-014562] N91-29851
ORBITAL LAUNCHING
Program and applications for a near-term laser launch system
[DE90-011760] N91-29551
ORBITS
On satellite constellation selection
[DE91-014562] N91-29851
ORDER-DISORDER TRANSFORMATIONS
Intermetallics: Canadian perspective
[NAE-LTR-ST-1771] N91-29288
Requirements for the observation of Fermi surfaces in disordered alloys
[DE91-014578] N91-29321
ORGANIC COMPOUNDS
Comparison between the interfacial chemistry of metallized polyimides and polymide
[AD-A238400] N91-29366
De Haas-van Alphen and Fermi surface studies of organic superconductors (ET)2X
[DE91-015137] N91-29987
ORGANIC LIQUIDS
Mechanistic investigation of nanometer-scale/lithography at liquid-covered graphite surfaces
[AD-A237085] N91-29337
ORGANIC MATERIALS
Methods to determine the compatibility and degradation of organic materials
[AD-A237940] N91-29234
ORGANIC SOLIDS
Preparation and properties of new inorganic glasses and gel-derived solids
[AD-A238095] N91-29360
ORGANIZATIONS
The Government-University-Industry Research Roundtable
[DE91-015795] N91-30044
ORGANOMETALLIC COMPOUNDS
Catalytic hydrogenation of carbon monoxide
[DE91-015452] N91-29283
Organometallic precursor routes to Si-C-Al-O-N ceramics
[AD-A237753] N91-29355
Dual cure photocatalyst systems
[DE91-014174] N91-29369
ORGANS
Reevaluation of S-values considering electron transport
[DE91-015428] N91-29893
ORIFICE FLOW
Experimental study of cross-stream mixing in a cylindrical duct
[NASA-TM-105180] N91-29187
ORTHOGONAL FUNCTIONS
Forcasting tropical cyclone recurvature using an empirical othogonal function representation of vorticity fields
[AD-A238489] N91-29689
OSCILLATING FLOW
Effects of 1, 2, 3, and 4 Hz imposed bulk flow oscillations on transition in a straight channel with 40 to 1 aspect ratio
[AD-A237988] N91-29517
Numerical prediction of turbulent oscillating flow and associated heat transfer
[NASA-CR-187177] N91-29524
OSCILLATIONS
Numerical prediction of turbulent oscillating flow and associated heat transfer
[NASA-CR-187177] N91-29524
Degradation of brightness by resonant particle effects
[DE91-015181] N91-29578
Total magnetic reconnection during a tokamak major disruption
[DE91-013637] N91-29949
OSCILLATORS
Nonlinear dynamics of Josephson junction parametric amplifier arrays
[AD-A237451] N91-29454
OVERPRESSURE
Ventilation kinetics testing of a steel frame/rubber fabric underground shelter
[AD-A237469] N91-29734
OXIDATION
Supersonic combustion of a transverse injected H2 jet in a radio frequency heated flow
[DE91-014739] N91-29281
Environmental effects in niobium base alloys and other selected intermetallic compounds
[AD-A237535] N91-29658
OXIDATION-REDUCTION REACTIONS
Solvent-dependent redox thermodynamics of metal amine complexes. The delineation of specific solvation effects
[AD-A237503] N91-29272
Catalytic hydrogenation of carbon monoxide
[DE91-015452] N91-29283
Role of the solvent in kinetics of heterogeneous electron and ion transfer reactions
[AD-A237168] N91-29876

Defect characterization of electronic conducting pseudo-perovskite systems
[DE91-014385] N91-29978

OXYGEN
Quantitative analysis of oxygen segregation on inversion domain boundaries in aluminum nitride
[DE91-010869] N91-29971
Superconducting superoxygenated La(2-x)Sr(x)CuO(4+delta): Search for phase separation
[DE91-015334] N91-29995

OXYGEN ATOMS
IDA studies on natural space environmental effects on materials for SDIO
[AD-A237974] N91-29660

OXYGEN IONS
Electronic and ionic transport in processable conducting polymers
[AD-A238175] N91-29362
Developmental status and system studies of the monolithic solid oxide fuel cell
[DE91-014389] N91-29645
Electron capture in very low energy collisions of multicharged ions with H and D in merged beams
[DE91-015617] N91-29909

OXYGEN PRODUCTION
Production and use of metals and oxygen for lunar propulsion
[NASA-TM-105195] N91-29222

OXYGENATION
Superconducting superoxygenated La(2-x)Sr(x)CuO(4+delta): Search for phase separation
[DE91-015334] N91-29995

OZONE
Protecting the ozone shield: A new public policy
[AD-A237640] N91-29659
Theoretical studies of long-range transport of oxidants
[PB91-182360] N91-29661
Criteria for assessing the role of transported ozone/precursors in ozone nonattainment areas
[PB91-195958] N91-29662
Effects of solar heating by aerosols and trace gases on the temperature structure constant
[AD-A237675] N91-29677

OZONE DEPLETION
Protecting the ozone shield: A new public policy
[AD-A237640] N91-29659

P

P-I-N JUNCTIONS
Spike leakage and burnout of silicon PIN diode microwave limiters
[AD-A238392] N91-29471

P-TYPE SEMICONDUCTORS
Defect characterization of electronic conducting pseudo-perovskite systems
[DE91-014385] N91-29978
Molecular beam epitaxial growth and characterization of metastable compound semiconductors for infrared detector applications
[AD-A237797] N91-30010

P-3 AIRCRAFT
P-3 SAR calibration activity at Andros Island
[AD-A237357] N91-29412

PACIFIC OCEAN
Tropical cyclone motion in the northwest Pacific Ocean, phase 1
[AD-A237455] N91-29683
Performance report of the Wind Research Lab.
[AD-A238575] N91-29691
Modeling a rain-induced mixed layer
[AD-A238022] N91-29702

PACKAGING
Silicon Wafer Advanced Packaging (SWAP). Multichip Module (MCM) foundry study, version 2
[AD-A237412] N91-29452

PACKET TRANSMISSION
Very low bit rate voice for packetized mobile applications
[DE91-015333] N91-29409

PAINTS
Energy conserving coating: Pigment research
[AD-A237841] N91-29356

PALLADIUM
A calorimetric investigation of deuterated palladium electrodes
[AD-A237571] N91-29456

PALLADIUM ALLOYS
Requirements for the observation of Fermi surfaces in disordered alloys
[DE91-014578] N91-29321

PANCREAS
Perturbation techniques for models of bursting electrical activity in pancreatic (beta)-cells
[DE91-013901] N91-29715

PANEL METHOD (FLUID DYNAMICS)
Unsteady compressible lifting surface analysis for rotary wings using velocity potential modes N91-29170

PAPERS
Publications of the Executive Office of the President, January 20, 1989 - March 31, 1991
[PB91-156828] N91-30056

PARABOLIC DIFFERENTIAL EQUATIONS
Use of the implicit-finite-difference method to implement the parabolic equation model
[AD-A237437] N91-29819

PARACHUTE DESCENT
Stabilized square parachute
[AD-D014946] N91-29149

PARACHUTES
International aviation (selected articles)
[AD-A237232] N91-29142
Stabilized square parachute
[AD-D014946] N91-29149

PARALLEL COMPUTERS
A common interface real-time multiprocessor operating system for embedded systems
[AD-A238445] N91-29770
Optimal iterative task scheduling for parallel simulations
[AD-A238631] N91-29791
Portable parallel programming
[DE91-015648] N91-29794

PARALLEL FLOW
Secondary stability and three-dimensional natural convection in a shallow cavity N91-29495

PARALLEL PLATES
Steady flow of a fluid-solid mixture between parallel plates
[DE91-013114] N91-29491

PARALLEL PROCESSING (COMPUTERS)
Vision-based navigation and parallel computing
[AD-A238570] N91-29164
Numerical propulsion system simulation: An interdisciplinary approach
[NASA-TM-105181] N91-29221
ZLIB: A numerical library for differential algebra and Lie algebraic treatment of beam dynamics
[DE91-014875] N91-29746
Hyperdimensional data analysis and structural inference
[AD-A238097] N91-29764
Simulation methodology
[AD-A238113] N91-29765
Asynchronous design for parallel processing architectures
[AD-A237696] N91-29783
Performance implications of synchronization support for parallel FORTRAN programs
[AD-A238493] N91-29790
The CYK-approach to serial and parallel parsing
[PB91-185447] N91-29792
Visualizing performance of parallel programs
[DE91-014966] N91-29793
Portable parallel programming
[DE91-015648] N91-29794
Analytical and numerical methods; advanced computer concepts
[DE91-014526] N91-29795
The parallel BFGS method for unconstrained minimization
[DE91-015784] N91-29798
Parallelizing the spectral transform method
[DE91-013969] N91-29815
Towards a realistic plasma simulation code
[DE91-015698] N91-29967

PARALLEL PROGRAMMING
A high-performance retargetable simulator for parallel architectures
[AD-A237354] N91-29779
Lazy task creation: A technique for increasing the granularity of parallel programs
[AD-A237477] N91-29781
Portable parallel programming
[DE91-015648] N91-29794

PARAMETER IDENTIFICATION
Analysis of Naval aviation selection test data with nonlinear models. Part 1: Parameter estimation
[AD-A238244] N91-29728

PARAMETERIZATION
Parameterizations of microphysical processes for simulation of regional-scale clouds
[DE91-015554] N91-29696

PARAMETRIC AMPLIFIERS
Nonlinear dynamics of Josephson junction parametric amplifier arrays
[AD-A237451] N91-29454
Electro-optic line narrowing of optical parametric oscillators
[AD-D014944] N91-29934
Spatial propagation of squeezed light in a degenerate parametric amplifier
[DE91-014989] N91-30039

PARSING ALGORITHMS
The CYK-approach to serial and parallel parsing
[PB91-185447] N91-29792

PARTIAL DIFFERENTIAL EQUATIONS
The 't Hooft's solution for arbitrary semisimple Lie group
[DE91-617572] N91-29813
Parallelizing the spectral transform method
[DE91-013969] N91-29815
Computational and theoretical aspects of nonlinear partial differential equations
[AD-A238495] N91-29829

PARTICLE ACCELERATION
The High Energy Solar Physics mission (HESP): Scientific objectives and technical description
[NASA-TM-105033] N91-29201
RF transfer in the coupled-cavity free-electron laser two-beam accelerator
[DE91-015676] N91-29583

PARTICLE ACCELERATOR TARGETS
Medium energy nuclear physics research
[DE91-015740] N91-29901
Electromagnetic dissociation of Au and Co targets by relativistic heavy ions
[DE91-014915] N91-29906

PARTICLE ACCELERATORS
Development of laser optics for the AWA photocathode
[DE91-015552] N91-29581

PARTICLE BEAMS
ZLIB: A numerical library for differential algebra and Lie algebraic treatment of beam dynamics
[DE91-014875] N91-29746

PARTICLE COLLISIONS
Laser enhanced chemical reaction studies
[DE91-013021] N91-29555
Collisional processes of interest in MFE plasma research
[DE91-013023] N91-29943

PARTICLE IN CELL TECHNIQUE
Electromagnetic PIC simulations using finite elements on unstructured grids
[DE91-015141] N91-29962

PARTICLE INTERACTIONS
Electronic and ionic transport in processable conducting polymers
[AD-A238175] N91-29362
Characterization of a sub-picosecond dye laser for the study of atom-perturber collisions
[AD-A238099] N91-29572
Single-scatter Monte Carlo compared to condensed history results for low energy electrons
[DE91-015176] N91-29869
Study of nuclear effects in the deuteron and extraction of neutron to proton stucture function ratio
[DE91-015484] N91-29873
Electron-ion interaction cross sections determined by x ray spectroscopy on EBIT
[DE91-015786] N91-29903

PARTICLE PRODUCTION
Chasing the x(sub f) dependence of J/psi production
[DE91-015136] N91-29899
High energy physics: Experimental, Theoretical, and Phenomenology Institute
[DE91-015737] N91-29912

PARTICLE SIZE DISTRIBUTION
The effects of HMX particle size and binder stiffness on the burning mechanism and regression rate of a series of fast burning propellants
[DE91-015785] N91-29387

PARTICLE THEORY
Study of nuclear effects in the deuteron and extraction of neutron to proton stucture function ratio
[DE91-015484] N91-29873

PARTICULATES
Investigation of particulate formation during diesel spray combustion
[DE90-008282] N91-29255

PARTITIONS (MATHEMATICS)
Stochastic simulation techniques for partition function approximation of Gibbs random field images
[AD-A238611] N91-29775

PARTONS
Study of nuclear effects in the deuteron and extraction of neutron to proton stucture function ratio
[DE91-015484] N91-29873

PATTERN RECOGNITION
Distance measures for speech recognition
[NAE-AN-57] N91-29394
Range-only multistatic radar system
[AD-D011645] N91-29399
The physics of pattern formation at liquid interfaces
[DE91-014529] N91-29504

Multi-sensor image interpretation using laser radar and thermal images
[AD-A238245] N91-29576
Three-dimensional visualization for evaluating automated, geomorphic pattern-recognition analyses of crustal structures
[DE91-012929] N91-29668
The functional architecture of visual object recognition
[AD-A238617] N91-29732
Matching of complex 3-D surfaces using dynamic programming
[ERB-1022] N91-29743
A fast, one pass algorithm to label objects and compute their features
[DE91-015441] N91-29747
A vision system model
[AD-A238459] N91-29930
Adaptive liquid crystal TV based joint transform correlator as applied to real-time pattern recognition
[AD-A238576] N91-29931

PATTERN REGISTRATION
An automated software system for updating digital terrain databases from all-source imagery, phase 1
[AD-A237105] N91-29748

PAVEMENTS
Performance of asphalt concrete airport pavements during thaw weakening periods: A field study
[AD-A237441] N91-29198

PEBBLE BED REACTORS
Light weight space power reactors for nuclear electric propulsion
[DE91-014803] N91-29232

PENETRATION
Modeling a rain-induced mixed layer
[AD-A238022] N91-29702

PERFORMANCE PREDICTION
A computer program for prediction of internal performance of a ramrocket
[AD-A238179] N91-29226
ALS rocket engine combustion devices design and demonstration
[NASA-CR-183824] N91-29233
Minimization of refrigeration power requirements for mechanical supports in cryogenic systems
[DE91-015720] N91-29392
Effect of geometric parameters on the performance of second throat annular steam ejectors
[AD-A238645] N91-29522
Micro SAINT modeling of physiological and human performance in the heat
[AD-A238659] N91-29719
Predicting performance breakdown in pilots through objective measures of stress sensitivity
[AD-A237540] N91-29725
Analysis of Naval aviation selection test data with nonlinear models. Part 1: Parameter estimation
[AD-A238244] N91-29728
Predicting performance breakdown in pilots through objective measures of stress sensitivity
[AD-A238597] N91-29731

PERFORMANCE TESTS
Environmental assessment for the FAA explosive detection system independent validation and verification program
[DE91-013190] N91-29152
Composite specimen design analysis. Volume 2: Experimental efforts
[AD-A238277] N91-29247
Long-term testing and evaluation of cathode components in a commercial aluminum cell, volume 1
[DE90-010896] N91-29436
Performance and life evaluation of advanced battery technologies for electric vehicle applications
[DE91-015671] N91-29482
Experimental and analytical study of rippled trailing edge airfoils for compressor application
[AD-A237425] N91-29508
Development and evaluation of a human performance assessment battery
[AD-A237391] N91-29724

PERMANENT MAGNETS
Major achievements during the first program year
[AD-A237171] N91-29919

PERMITTIVITY
Solvent effects on simple electron transfer reactions. A comparison of results in Debye and non-Debye solvents
[AD-A237157] N91-29875

PERMUTATIONS
Randomization procedures applied to analysis of ballistic data
[AD-A238389] N91-30050

PERSONNEL
Micro SAINT modeling of physiological and human performance in the heat
[AD-A238659] N91-29719
Management of variation and TQM
[AD-A238399] N91-29843

PERSONNEL MANAGEMENT
Management of variation and TQM
[AD-A238399] N91-29843

PERSPIRATION
Micro SAINT modeling of physiological and human performance in the heat
[AD-A238659] N91-29719

PERTURBATION
Seasonal air and water mass redistribution and its effect on satellite and polar motion N91-29202
Numerical study of non-impulsively started flow around a circular cylinder
[AD-A238051] N91-29519

PERTURBATION THEORY
Response and stability analysis of helicopter rotor blades using computerized symbolic manipulation
[AD-A238660] N91-29175
Perturbation techniques for models of bursting electrical activity in pancreatic (beta)-cells
[DE91-013901] N91-29715

PHARMACOLOGY
Differential equations and continuum mechanics
[AD-A237722] N91-29820

PHASE CONJUGATION
Investigation of superresolution by incoherent to coherent conversion
[AD-A238111] N91-29544

PHASE DIAGRAMS
Calculation of intra-rare Earth binary phase diagrams
[DE91-014950] N91-29267
Theoretical studies of solid-fluid phase equilibria
[DE91-014811] N91-29287
Growth condition dependence of RHEED pattern from GaAs(111)B surface
[DE91-014770] N91-29986

PHASE MODULATION
An optically activated modulator and GaAs-GaAlAs compound semiconductor channel waveguide
[AD-A238642] N91-30023

PHASE SHIFT
Comparison of synthetic aperture radar autofocus techniques: Phase gradient vs subaperture
[DE91-014696] N91-29406

PHASE SHIFT KEYING
The study of space communications spread spectrum systems. Part 1: Saw-based joint group demodulation of frequency shift keyed and differential phase shift keyed signals
[QU-90-1-PT-1] N91-29395
Application of Multi-Frequency Modulation (MFM) for high-speed data communications to a voice frequency channel
[AD-A238019] N91-29422

PHASE TRANSFORMATIONS
Picosecond studies of chemical intermediates
[AD-A237859] N91-29275
Equation of state for pure sodium chloride
[DE91-014618] N91-29286
Mechanisms of transformation toughening
[DE91-013151] N91-29293
Fabrication, phase transformation studies and characterization of SiC-AlN-Al2OC ceramics
[DE91-013296] N91-29329
Modelling of deformation textures evolution in semi-crystalline polymers
[AD-A237288] N91-29342
Phase transformations, ultrastructure, and properties of rigid-rod polymers
[AD-A238643] N91-29368
Singularities in Gaussian random fields
[AD-A238220] N91-29839
Ruddlesden-Popper phases A(n+1)M(n)O(3n+1): Structures and properties
[DE91-011748] N91-29973
Superconducting superoxygenated La(2-x)Sr(x)CuO(4+delta): Search for phase separation
[DE91-015334] N91-29995

PHASED ARRAYS
High temperature superconductor analog electronics for millimeter-wavelength communications
[NASA-TM-105184] N91-29982

PHENOLIC RESINS
Simulation of the structure of dense, amorphous bisphenol-A polycarbonate
[AD-A237222] N91-29270
An atomistic model of the amorphous glassy polycarbonate of 4,4'-isopropylidenediphenol
[AD-A237291] N91-29345

PHENYLS
Organo- borazines.3.homo- and copolymerization of p-vinylphenyl- cyclotri- borazines
[AD-A237881] N91-29357

PHOSPHATES
Short-pulse glass slab amplifier
[DE91-015385] N91-29580

PHOSPHORUS COMPOUNDS
Negative ion formation with electron impact to simulants
[AD-A237478] N91-29881

PHOTOCATHODES
Development of laser optics for the AWA photocathode
[DE91-015552] N91-29581

PHOTOCHEMICAL REACTIONS
Molecular beam studies of reaction dynamics
[DE90-011600] N91-29256
Dual cure photocatalyst systems
[DE91-014174] N91-29369
Ultraviolet reflector materials for solar detoxification of hazardous waste
[DE91-002196] N91-29663
Molecular beam studies of reaction dynamics
[DE91-014866] N91-29868

PHOTOCONDUCTIVITY
Persistent photoconductivity in II-VI mixed semiconductors related critical phenomena and applications
[AD-A237792] N91-29460
High gain photoconductive semiconductor switching
[DE91-014668] N91-29478

PHOTODIODES
Design of a stabilized, dc-powered analog laser diode driver
[AD-A238596] N91-29577

PHOTODISSOCIATION
Hot atom reactive scattering and photodissociation experiments with acetylene and ethylene
[DE91-013755] N91-29264

PHOTOELECTRIC EMISSION
Requirements for the observation of Fermi surfaces in disordered alloys
[DE91-014578] N91-29321
Photoemission and electronic structure studies of YBa2Cu3O(x)
[DE91-014469] N91-29979
Photoemission measurement of Fermi surface, band dispersion, and quasiparticle lifetime in YBa2Cu3O6.9
[DE91-015194] N91-29989
Synchrotron studies of narrow band materials
[DE91-014826] N91-30025

PHOTOELECTRON SPECTROSCOPY
Preparation and properties of new inorganic glasses and gel-derived solids
[AD-A238095] N91-29360

PHOTOELECTRONS
Photoelectron and photoionization pumping of XUV lasers by laser-produced plasmas N91-29558

PHOTOGRAPHS
Analyzing photographically recorded atomic emission spectra using an automated densitometer
[DE91-015368] N91-29871
Plasma properties of hot coronal loops utilizing coordinated SMM and solar research rocket observations
[NASA-CR-186094] N91-29937

PHOTOGRAPHY
Topographic map reading
[AD-A238026] N91-29640

PHOTOINTERPRETATION
Debris/ice/TPS assessment and photographic analysis for Shuttle Mission STS-40
[NASA-TM-103822] N91-29210

PHOTOIONIZATION
Fundamental studies of chemical vapor deposition diamond growth processes
[DE91-015324] N91-29374
Photoelectron and photoionization pumping of XUV lasers by laser-produced plasmas N91-29558
Laser-atom interaction at high intensities
[AD-A238231] N91-29887

PHOTOLUMINESCENCE
High gain photoconductive semiconductor switching
[DE91-014668] N91-29478

PHOTOLYSIS
Hot atom reactive scattering and photodissociation experiments with acetylene and ethylene
[DE91-013755] N91-29264
Research in the physical sciences with application to the free electron laser
[AD-A237884] N91-29571
Reactions of small molecular systems
[DE91-014519] N91-29867

PHOTOMAPS
Topographic map reading
[AD-A238026] N91-29640

PHOTOMETERS
The development of a fiber-optic readout pressure transducer
[AD-A238393] N91-29545
PHOTOMETRY
Plasma properties of hot coronal loops utilizing coordinated SMM and solar research rocket observations
[NASA-CR-186094] N91-29937
PHOTOMICROGRAPHY
Ultrasonic evaluation of silicon nitride green bodies
[AD-A237924] N91-29608
PHOTONICS
First International conference on Frontiers of Polmer Research
[AD-A238112] N91-29361
PHOTONS
Structure and stability of underpotentially depositied layers on Au(111) studied by optical second harmonic generation
[AD-A237087] N91-29268
Technical activities 1990, Electron and Optical Physics Div.
[PB91-194423] N91-29858
Quantitative interpretation of auger lineshapes and electron/photon stimulated desorption
[AD-A237138] N91-29874
PHOTOPRODUCTION
High energy physics at Tufts University
[DE91-015055] N91-29908
PHOTOSYNTHESIS
Hydrogen productivity by photosynthetic water splitting
[DE90-012211] N91-29380
Specific mutagenesis of a chlorophyll-binding protein
[DE91-014813] N91-29711
Stable isotope fractionation in photosynthesis: Analysis of autotrophic competence following transformation of the chloroplast genome of Chlamydomonas
[DE91-015792] N91-29713
PHOTOVOLTAIC CELLS
Tritium-field betacells
[DE91-014666] N91-29910
PHYSICAL EXERCISE
Physiological responses to intermittent exercise as modified by heat stress and protective clothing
[AD-A237447] N91-29716
PHYSICAL OPTICS
Adjustable magnification anamorphic beam expander
[DE91-014110] N91-29561
PHYSICAL PROPERTIES
Physical properties and structure of ion-containing polymers
[AD-A238196] N91-29363
PHYSIOLOGICAL EFFECTS
Biological interactions of extremely-low-frequency electric and magnetic fields
[DE90-011927] N91-29709
Data acquisition system for collecting biophysical and physiological data
[AD-A237654] N91-29710
Physiological responses to intermittent exercise as modified by heat stress and protective clothing
[AD-A237447] N91-29716
The functional architecture of visual object recognition
[AD-A238617] N91-29732
Human factors of night vision devices: Anecdotes from the field concerning visual illusions and other effects
[AD-A237641] N91-29735
PHYSIOLOGICAL RESPONSES
Physiological responses to intermittent exercise as modified by heat stress and protective clothing
[AD-A237447] N91-29716
PHYSIOLOGICAL TESTS
Performance of Marine AV-8B (Harrier) pilots on a cognitive/psychomotor test battery: Comparison and prediction
[AD-A238563] N91-29729
Performance of several different Naval aviator communities on a cognitive/psychomotor test battery: Pipeline comparison and prediciton
[AD-A238564] N91-29730
The functional architecture of visual object recognition
[AD-A238617] N91-29732
PHYSIOLOGY
Data acquisition system for collecting biophysical and physiological data
[AD-A237654] N91-29710
Microbiology and physiology of anaerobic fermentations of cellulose
[DE91-015239] N91-29712
Micro SAINT modeling of physiological and human performance in the heat
[AD-A238659] N91-29719
PICOSECOND PULSES
Physical concepts and modeling procedures for picosecond and subpicosecond distributed circuits
[AD-A238592] N91-29472
PIGMENTS
Energy conserving coating: Pigment research
[AD-A237841] N91-29356
PILOT PERFORMANCE
Predicting performance breakdown in pilots through objective measures of stress sensitivity
[AD-A237540] N91-29725
Analysis of Naval aviation selection test data with nonlinear models. Part 1: Parameter estimation
[AD-A238244] N91-29728
Performance of Marine AV-8B (Harrier) pilots on a cognitive/psychomotor test battery: Comparison and prediction
[AD-A238563] N91-29729
Performance of several different Naval aviator communities on a cognitive/psychomotor test battery: Pipeline comparison and prediciton
[AD-A238564] N91-29730
Predicting performance breakdown in pilots through objective measures of stress sensitivity
[AD-A238597] N91-29731
The effect of three levels of laser glare on the speed and accuracy of target location performance when viewing a briefly presented visual array
[AD-A238565] N91-29736
PILOT SELECTION
Analysis of Naval aviation selection test data with nonlinear models. Part 1: Parameter estimation
[AD-A238244] N91-29728
PINS
Heat transfer and pressure drop in a compact pin-fin heat exchanger with pin orientation at 18 deg to the flow direction
[NASA-CR-186544] N91-29527
PIONS
High energy physics at Tufts University
[DE91-015055] N91-29908
PIPES (TUBES)
Transient flowmeter calibration facility
[AD-D014937] N91-29523
PISTON ENGINES
Basic mechanisms of diesel lubrication correlation of bench and engine tests
[AD-A237685] N91-29596
PITTING
Pulse induced nanlithography of graphite in H2O: A road to chemical linkages to the surface?
[AD-A237086] N91-29338
PLANAR STRUCTURES
Piecework linear least-squares approximation planar curves including computer programs
[NRC-31069] N91-29811
PLANE STRAIN
Effect of a free surface on stress distribution in a bimaterial composite
[PB91-185116] N91-29251
Prediction of edge stresses in layered media using the surface integral-finite element technique N91-29614
Morphology of bulk Nylon 6 subjected to plane strain compression
[AD-A237331] N91-29622
PLANE STRESS
Prediction of edge stresses in layered media using the surface integral-finite element technique N91-29614
PLANETARY GEOLOGY
Investigations in Martian geology. Part 1: Nature of the mantling deposit in the heavily cratered terrain of northeastern Arabia, Mars. Part 2: Experimental studies of clean and dust-or-sand-covered ice sublimation under Mars-like conditions N91-30067
PLASMA ACCELERATORS
Vlasov simulations of very-large-amplitude wave generation in the plasma wakefield accelerator
[AD-A237428] N91-29961
PLASMA CHEMISTRY
Chemical waste disposal in space by plasma discharge
[NASA-CR-184169] N91-29737
PLASMA COMPOSITION
Impurity and neutral effects on the dissipative drift wave in tokamak edge plasmas
[DE91-015907] N91-29965
PLASMA CONTROL
Design aspects for a pulsed-mode, high-intensity, heavy negative ion source
[DE91-011094] N91-29864
Fluidlike studies of the sheath and presheath regions of a plasma
[DE91-013343] N91-29944
The effects of magnetic field errors on reversed field pinch plasma
[DE91-013636] N91-29948
Future explosive pulse-power technology for high-energy plasma physics experiments
[DE91-014601] N91-29951
H-mode energy confinement scaling from the ASDEX, DIII-D, and jet tokamaks
[DE91-015145] N91-29957
Global confinement and discrete dynamo activity in the MST reversed field pinch
[DE91-015219] N91-29960
PLASMA DECAY
High-intensity and high-energy laser interactions with single droplets
[AD-A238197] N91-29575
PLASMA DENSITY
Vlasov simulations of very-large-amplitude wave generation in the plasma wakefield accelerator
[AD-A237428] N91-29961
PLASMA DIAGNOSTICS
Thermochemistry of hydrocarbon decomposition and relationship to properties of PECVD diamond films
[AD-A237793] N91-29274
Collisional processes of interest in MFE plasma research
[DE91-013023] N91-29943
Total magnetic reconnection during a tokamak major disruption
[DE91-013637] N91-29949
Plasma and electrical diagnostics for Procyon experiments
[DE91-014736] N91-29952
PLASMA DRIFT
Impurity and neutral effects on the dissipative drift wave in tokamak edge plasmas
[DE91-015907] N91-29965
PLASMA FREQUENCIES
High-intensity and high-energy laser interactions with single droplets
[AD-A238197] N91-29575
PLASMA HEATING
Synthesis of diamond films by microwave generated pulsed plasmas
[AD-A237228] N91-29341
ICRF edge modeling
[DE91-014401] N91-29403
Measurements of the ion acoustic decay instability and the resultant thermal and suprathermal electron heating in laser-plasma interaction experiments
[DE90-012477] N91-29941
H-mode energy confinement scaling from the ASDEX, DIII-D, and jet tokamaks
[DE91-015145] N91-29957
Anomalous ion heating from the dynamo in a reversed field pinch
[DE91-015586] N91-29966
PLASMA JETS
Chemical waste disposal in space by plasma discharge
[NASA-CR-184169] N91-29737
Fundamental studies of the extraction process in inductively coupled plasma mass spectrometry
[DE90-011733] N91-29939
The effects of magnetic field errors on reversed field pinch plasma
[DE91-013636] N91-29948
PLASMA PHYSICS
The Research Laboratory of Electronics
[AD-A237670] N91-29458
Future explosive pulse-power technology for high-energy plasma physics experiments
[DE91-014601] N91-29951
Establishment of an Institute for Fusion Studies
[DE91-014922] N91-29956
Electromagnetic PIC simulations using finite elements on unstructured grids
[DE91-015141] N91-29962
PLASMA PROPULSION
Numerical simulation of self-field MPD thrusters
[NASA-CR-187168] N91-29832
PLASMA SHEATHS
Fluidlike studies of the sheath and presheath regions of a plasma
[DE91-013343] N91-29944
Fundamental studies of fusion plasmas
[DE91-015656] N91-29964
PLASMA SPRAYING
Thermochemistry of hydrocarbon decomposition and relationship to properties of PECVD diamond films
[AD-A237793] N91-29274
An evaluation of nickel-aluminum coatings fabricated with the plasma-spray process
[DE91-013208] N91-29328
PLASMA WAVES
Detection of coherent structures in the edge of the TEXT tokamak plasma
[DE91-015183] N91-29958

Vlasov simulations of very-large-amplitude wave generation in the plasma wakefield accelerator
[AD-A237428] N91-29961
Fundamental studies of fusion plasmas
[DE91-015656] N91-29964
Impurity and neutral effects on the dissipative drift wave in tokamak edge plasmas
[DE91-015907] N91-29965

PLASMAS (PHYSICS)
Computation of broadband, high-power electromagnetic pulse generation from an air gas avalanche switch
[DE91-015793] N91-29435
Computational simulations of plasma flow switches and imploding loads
[DE91-014768] N91-29480
Gaseous prebreakdown processes that are important for pulsed power switching
[DE91-015902] N91-29487
Analytical calculation of neutral transport and its effect on ions
[DE91-015908] N91-29896
Future explosive pulse-power technology for high-energy plasma physics experiments
[DE91-014601] N91-29951
Plasma and electrical diagnostics for Procyon experiments
[DE91-014736] N91-29952
Electromagnetic PIC simulations using finite elements on unstructured grids
[DE91-015141] N91-29962
Fundamental studies of fusion plasmas
[DE91-015656] N91-29964
Towards a realistic plasma simulation code
[DE91-015698] N91-29967
Pressure effects in the microwave plasma growth of polycrystalline diamond
[AD-A237751] N91-30006

PLASTIC DEFORMATION
Modelling of deformation textures evolution in semi-crystalline polymers
[AD-A237288] N91-29342
The molecular view of plastic deformation and precursor processes of crazing in glassy polypropylene and polycarbonate
[AD-A237333] N91-29346
Deconvolution of x ray diffraction data to elucidate plastic deformation mechanisms in the uniaxial extension of bulk Nylon-6
[AD-A237332] N91-29623

PLASTIC FLOW
Fundamental studies in dynamic plasticity
[AD-A237114] N91-29621

PLASTIC PROPERTIES
Mechanisms of transformation toughening
[DE91-013151] N91-29293
Elastic-plastic constitutive relations at large strain
[DE91-013195] N91-29612
Fundamental studies in dynamic plasticity
[AD-A237114] N91-29621
Fission-fusion adaptivity in finite elements for nonlinear dynamics of shells
[AD-A238029] N91-29626
Consolidation and plasticity of Bi-Sr-Ca-Cu-O superconductors
[DE91-015544] N91-30028

PLASTICIZERS
Report on using expert systems for computer-aided formulation and property estimation of propellants. 1: Expert system shell selection and initial package design
[AD-A237567] N91-29383
The effects of HMX particle size and binder stiffness on the burning mechanism and regression rate of a series of fast burning propellants
[DE91-015785] N91-29387
Ultrasonic evaluation of silicon nitride green bodies
[AD-A237924] N91-29608

PLASTICS
Injection molding of engineering plastics
[AD-A238583] N91-29389

PLATES (STRUCTURAL MEMBERS)
Whipple bumper shield simulations
[NASA-TM-105089] N91-29213
Electroforming thin channel heat exchangers
[DE91-015114] N91-29528

PLATING
Liquid honing evaluation
[DE91-015749] N91-29393

PLATINUM
X ray reflectivity studies of Au surfaces
[DE91-015308] N91-29307
A calorimetric investigation of deuterated palladium electrodes
[AD-A237571] N91-29456
Comparisons between scanning tunneling microscopy and outer-sphere electron-transfer rates at Pt(111) surfaces coated with ordered iodine adlayers
[AD-A237507] N91-29883
The influence of potential on metal-adsorbate structure: Solvent-independent nature of infrared spectra for Pt(111)/CO
[AD-A237509] N91-30004

PLATINUM ALLOYS
First principles simulations of metallic alloys and liquids
[DE91-015171] N91-29323

PLUG NOZZLES
Divergence thrust loss calculations for convergent-divergent nozzles: Extensions to the classical case
[NASA-TM-105176] N91-29181

PLUMES
Pressure measurements in a low-density nozzle plume for code verification
[NASA-TM-105170] N91-29228

PNEUMATIC PROBES
Near-stall loss measurements in a CD compressor cascade with exploratory leading edge flow control
[AD-A237497] N91-29509

POINT DEFECTS
Defects and transport in mixed oxides
[DE91-014537] N91-29266

POINTING CONTROL SYSTEMS
A simulation of the instrument pointing system for the Astro-1 mission
[NASA-TM-103547] N91-30061

POINTS (MATHEMATICS)
Computational methods for bifurcation problems with symmetries on the manifold
[AD-A237146] N91-29817

POLAR WANDERING (GEOLOGY)
Seasonal air and water mass redistribution and its effect on satellite and polar motion N91-29202

POLARIZATION (CHARGE SEPARATION)
Charge motion effects in ionic clusters
[AD-A238178] N91-29886

POLARIZATION (WAVES)
NIST calibration procedure for vertically polarized monopole antennas 30 kHz to 300 MHz
[PB91-185124] N91-29432

POLARIZATION CHARACTERISTICS
NIST calibration procedure for vertically polarized monopole antennas 30 kHz to 300 MHz
[PB91-185124] N91-29432
Charge motion effects in ionic clusters
[AD-A238178] N91-29886

POLARONS
Large bipolarons and superconductivity
[DE91-014699] N91-29985

POLICIES
Publications of the Executive Office of the President, January 20, 1989 - March 31, 1991
[PB91-156828] N91-30056

POLLUTION MONITORING
Methods for determination of low-molecular weight carbonyl compounds in the ambient atmosphere
[DE91-015188] N91-29656
A climatological model for risk computations incorporating site-specific dry deposition influences
[DE91-015536] N91-29667

POLLUTION TRANSPORT
A climatological model for risk computations incorporating site-specific dry deposition influences
[DE91-015536] N91-29667

POLOIDAL FLUX
Total magnetic reconnection during a tokamak major disruption
[DE91-013637] N91-29949

POLYACETYLENE
Design, synthesis and characterization of novel polydiacetylenes using new analytical techniques
[AD-A237362] N91-29348

POLYATOMIC MOLECULES
Molecular beam studies of reaction dynamics
[DE90-011600] N91-29256
Laser enhanced chemical reaction studies
[DE91-013021] N91-29555
Molecular beam studies of reaction dynamics
[DE91-014866] N91-29868

POLYCARBONATES
Simulation of the structure of dense, amorphous bisphenol-A polycarbonate
[AD-A237222] N91-29270
Quasi-static modeling of chain-dynamics in the amorphous glassy polycarbonate of 4,4'-isopropyledenediphenol
[AD-A237289] N91-29343
An atomistic model of the amorphous glassy polycarbonate of 4,4'-isopropylidenediphenol
[AD-A237291] N91-29345
The molecular view of plastic deformation and precursor processes of crazing in glassy polypropylene and polycarbonate
[AD-A237333] N91-29346
Conformational characteristics of the polycarbonate 4,4'-isopropylidenediphenol
[AD-A237334] N91-29347

POLYCRYSTALS
Effects of interfacial modification on diamond film adhesion
[AD-A237750] N91-29354
Pressure effects in the microwave plasma growth of polycrystalline diamond
[AD-A237751] N91-30006
Connection between grain boundary structure and energy
[DE91-015558] N91-30030

POLYETHYLENES
Precursors to Si-N-C-O ceramics: A reinvestigation of the poly methylvinyl silylethyl enediamine systems
[DE91-013722] N91-29333
Modelling of deformation textures evolution in semi-crystalline polymers
[AD-A237288] N91-29342
Electronic and ionic transport in processable conducting polymers
[AD-A238175] N91-29362

POLYIMIDE RESINS
Properties and adhesion of polyimides in microelectronic devices
[AD-A238204] N91-29364
Comparison between the interfacial chemistry of metallized polyimides and polymide
[AD-A238400] N91-29366

POLYIMIDES
Effect of excess oxydianiline on the properties of polyimide
[AD-A237467] N91-29351
Properties and adhesion of polyimides in microelectronic devices
[AD-A238204] N91-29364
Injection molding of engineering plastics
[AD-A238583] N91-29389

POLYMER CHEMISTRY
Design, synthesis and characterization of novel polydiacetylenes using new analytical techniques
[AD-A237362] N91-29348
Comparison between the interfacial chemistry of metallized polyimides and polymide
[AD-A238400] N91-29366
Research in the physical sciences with application to the free electron laser
[AD-A237884] N91-29571

POLYMER MATRIX COMPOSITES
NASA workshop on impact damage to composites
[NASA-CP-10075] N91-29240

POLYMER PHYSICS
First International conference on Frontiers of Polmer Research
[AD-A238112] N91-29361
Research in the physical sciences with application to the free electron laser
[AD-A237884] N91-29571

POLYMERIC FILMS
Effect of excess oxydianiline on the properties of polyimide
[AD-A237467] N91-29351
Phase transformations, ultrastructure, and properties of rigid-rod polymers
[AD-A238643] N91-29368

POLYMERIZATION
Precursors to Si-N-C-O ceramics: A reinvestigation of the poly methylvinyl silylethyl enediamine systems
[DE91-013722] N91-29333
Model filled polymers 8: Synthesis of crosslinked polymeric beads by seed polymerization
[AD-A237429] N91-29349
Mechanism of anionic ring-opening polymerization of silacyclopent 3-enes
[AD-A237538] N91-29353
Physical properties and structure of ion-containing polymers
[AD-A238196] N91-29363
Phase transformations, ultrastructure, and properties of rigid-rod polymers
[AD-A238643] N91-29368
Dual cure photocatalyst systems
[DE91-014174] N91-29369
The cure of rigid polyurethane encapsulating foam
[DE91-016059] N91-29379

POLYMERS
Physical properties and structure of ion-containing polymers
[AD-A238196] N91-29363
Dual cure photocatalyst systems
[DE91-014174] N91-29369

The 3-D NMR imaging: A chemical microscope for analysis of heterogeneous macromolecular networks
[DE91-015109] N91-29375
Polymer drag reduction of a zero pressure gradient boundary layer
[AD-A237572] N91-29510

POLYPROPYLENE
Simulation of large deformation in glassy atactic polypropylene
[AD-A237223] N91-29340
The molecular view of plastic deformation and precursor processes of crazing in glassy polypropylene and polycarbonate
[AD-A237333] N91-29346

POLYSTYRENE
Model filled polymer 7: Flow behavior of polymers containing monodisperse crosslinked polymeric beads
[AD-A237430] N91-29350
Model filled polymers 9: Synthesis of uniformly crosslinked polystyrene microbeads
[AD-A237472] N91-29352

POLYURETHANE FOAM
The cure of rigid polyurethane encapsulating foam
[DE91-016059] N91-29379

POLYURETHANE RESINS
Studies of polymers for shock absorption applications
[AD-A237925] N91-29358

POROSITY
NMR characterization of porous ceramics
[DE91-015051] N91-29371
Advances in the drained shaping of ceramics
[DE91-015429] N91-29376

POSITION (LOCATION)
GPS: Aspects of pseudo-range positioning offshore N91-29161
Algorithms for converting geodetic Earth location to satellite time and swath pixel coordinates for the DMSP satellite system
[AD-A237589] N91-29638

POSITION SENSING
Evaluation of a pre-production version of Canadian Marconi CMA-786 GPS receiver
[NAE-LTR-FR-106] N91-29158

POSITIONING
GPS: Aspects of pseudo-range positioning offshore N91-29161

POTASSIUM OXIDES
Synthesis and superconductivity in Ba(1-x)K(x)BiO3
[DE91-015254] N91-29992

POTASSIUM PHOSPHATES
Optical and environmentally protective coatings for Potassium Dihydrogen Phosphate (KDP) harmonic converter crystals
[DE91-015296] N91-30034
Influence of diamond turning and surface cleaning processes on the degradation of KDP crystal surfaces
[DE91-015300] N91-30035

POTENTIAL ENERGY
Simulation of the growth of Mo/Si multilayers
[DE91-015679] N91-29486

POWDER METALLURGY
Metal injection moulding: A brief review
[NAE-LTR-ST-531] N91-29289
Powder metallurgy technology (selected articles)
[AD-A237176] N91-29310
Development of nickel and iron aluminides and their applications
[DE91-015323] N91-29325

POWDERED ALUMINUM
Design issues for propulsion systems using metallized propellants
[NASA-TM-105190] N91-29220
Slag and thermal environment of a spinning rocket motor
[AD-A238557] N91-29227

POWER AMPLIFIERS
A high power cross-field amplifier at X-Band
[DE91-013277] N91-29441

POWER CONDITIONING
Introduction of a current waveform, waveshaping technique to limit conduction loss in high-frequency dc-dc converters suitable for space power
[AD-A237903] N91-29465

POWER CONVERTERS
Introduction of a current waveform, waveshaping technique to limit conduction loss in high-frequency dc-dc converters suitable for space power
[AD-A237903] N91-29465

POWER SPECTRA
A survey of nonlinear dynamics (chaos theory)
[AD-A237802] N91-29821

PRECIPITATION (METEOROLOGY)
An observational study of the efficiency of activation of accumulation-mode particles in warm continental stratiform clouds
[DE91-013335] N91-29681
An investigation of the ERICA IOP-2 cyclone using the NORAPS model
[AD-A237683] N91-29684
Mesoscale modeling of precipitation scavenging by a cold-frontal squall line
[DE91-015534] N91-29695
Parameterizations of microphysical processes for simulation of regional-scale clouds
[DE91-015554] N91-29696

PRECIPITATION HARDENING
Strengthening mechanisms, creep, and fatigue processes in dispersion hardened niobium alloy
[AD-A237784] N91-29313

PRECISION
GPS: Aspects of pseudo-range positioning offshore N91-29161
Superconducting instrumentation for precision measurement and control
[DE91-014650] N91-29541

PREDICTION ANALYSIS TECHNIQUES
A computer program for prediction of internal performance of a ramrocket
[AD-A238179] N91-29226
Statistical characterization of graphite fiber for prediction of composite structure reliability
[AD-A238020] N91-29245
Compendium of material test results on HY-100 and pseudo HY-100 metals in support of US Navy programs
[DE91-013134] N91-29292
Development of the microstructure based stochastic life prediction models
[AD-A237768] N91-29312
Solvent dynamical effects in electron transfer: The solvent inertial limit and the predicted influence of quantum effects
[AD-A237462] N91-29880

PREDICTIONS
Prediction of edge stresses in layered media using the surface integral-finite element technique N91-29614

PREMIXED FLAMES
Combustion stability limits and planar imaging of swirl-stabilized flames N91-29262

PRESIDENTIAL REPORTS
Publications of the Executive Office of the President, January 20, 1989 - March 31, 1991
[PB91-156828] N91-30056

PRESSURE CHAMBERS
Kinetics of dark reaction in chemical laser gases
[DE91-015320] N91-29579

PRESSURE DROP
Heat transfer and pressure drop in a compact pin-fin heat exchanger with pin orientation at 18 deg to the flow direction
[NASA-CR-186544] N91-29527

PRESSURE EFFECTS
Numerical and physical modelling of bubbly flow phenomena
[DE91-013646] N91-29492
Pressure effects in the microwave plasma growth of polycrystalline diamond
[AD-A237751] N91-30006

PRESSURE GAGES
Experimental hypervelocity firings using stick and granular propellant configurations
[AD-A238628] N91-29384

PRESSURE GRADIENTS
Adiabatic two-phase flow frictional pressure drop. Part 1: Critical parameters and friction factors for air-water mixture
[DE91-014463] N91-29502
Polymer drag reduction of a zero pressure gradient boundary layer
[AD-A237572] N91-29510
Identification of, and transition to, the second region of ideal MHD stability in tokamaks
[DE90-010380] N91-29938

PRESSURE MEASUREMENT
Pressure measurements in a low-density nozzle plume for code verification
[NASA-TM-105170] N91-29228
The development of a fiber-optic readout pressure transducer
[AD-A238393] N91-29545
Sea level and bottom pressure measurements in the Northern Gulf of Alaska
[PB91-184135] N91-29705

PRESSURE PULSES
Performance of multiple stream pulsed jet combustion systems
[DE91-012338] N91-29259

PRESSURE RATIO
Effect of geometric parameters on the performance of second throat annular steam ejectors
[AD-A238645] N91-29522

PRESSURE REDUCTION
Adiabatic two-phase flow frictional pressure drop. Part 2: A generalized method for data correlation
[DE91-014462] N91-29501
Prediction of the pressure drop in transverse, repeated-rib tubes with numerical modeling
[DE91-014465] N91-29503

PRESSURE SENSORS
Performance of multiple stream pulsed jet combustion systems
[DE91-012338] N91-29259
The development of a fiber-optic readout pressure transducer
[AD-A238393] N91-29545

PRESSURE VESSELS
Pressure vessel burst test program
[AD-A237845] N91-29624

PRINTED CIRCUITS
Liquid honing evaluation
[DE91-015749] N91-29393

PROBABILITY DENSITY FUNCTIONS
First principles simulations of metallic alloys and liquids
[DE91-015171] N91-29323

PROBABILITY DISTRIBUTION FUNCTIONS
Anisotropic tensile probabilistic failure criterion for composites
[AD-A237601] N91-29244
An alternative algorithm for discrete-time filtering
[AD-A238443] N91-29827

PROBABILITY THEORY
Design and analysis of multi-sensor sequential detection system
[AD-A238012] N91-29543
Research in mathematics and computer science: Calculation of the probability of undetected error for certain error detection codes, phase 2
[AD-A238234] N91-29768
Least-squares learning and approximation of posterior probabilities on classification problems by neural network models
[AD-A237140] N91-29833
Deduction and inference using conditional logic and probability
[AD-A237285] N91-29834
The utility of elliptical and circular confidence regions for HFDF receivers
[AD-A238390] N91-29842

PROBLEM SOLVING
Analytical and numerical methods; advanced computer concepts
[DE91-014526] N91-29795
High bandwidth diagnosis within the framework of a microcomputer-based intelligent tutoring system
[AD-A237959] N91-29805

PROCEDURES
Composite specimen design analysis. Volume 2: Experimental efforts
[AD-A238277] N91-29247

PROCESS CONTROL (INDUSTRY)
An investigation to determine the producibility of a 3-D braider and bias direction weaving loom
[NASA-CR-188741] N91-29390
Long-term testing and evaluation of cathode components in a commercial aluminum cell, volume 1
[DE90-010896] N91-29436
Management of variation and TQM
[AD-A238399] N91-29843
Atomic layer epitaxy group IV materials: Surface processes, thin films, devices and their characterization
[AD-A238506] N91-30019

PROCESS HEAT
The Department of Energy's solar industrial program: New ideas for American industry
[DE91-002197] N91-29649

PRODUCT DEVELOPMENT
A brief overview of the activities and accomplishments of the Metals and Ceramics Division
[DE91-014955] N91-29296
Configuration management concepts document. National PDES testbed report series
[PB91-194480] N91-29391

PRODUCTION
Proceedings of the First Switch Tube Advanced Technology Meeting
[DE91-012634] N91-29440

PRODUCTION ENGINEERING
Production and use of metals and oxygen for lunar propulsion
[NASA-TM-105195] N91-29222

PROGRAM VERIFICATION (COMPUTERS)
Supersonic combustion of a transverse injected H2 jet in a radio frequency heated flow
[DE91-014739] N91-29281

Alsys Limited, Alsycomp 017, version 5.2, MICRO VAX 2 under Micro VMS V5.3 (host) to INMOS T425 transputer implemented on a B403 TRAM (target), 901118N1.11064
[AD-A237411] N91-29738

The language for DENOTE (Denotational Semantics Translation Environment)
[AD-A237144] N91-29750

Analog design verification with PSpice and MICRO-CAP 3
[AD-A237922] N91-29762

Verification of the FtCayuga fault-tolerant microprocessor system. Volume 2: Formal specification and correctness theorems
[NASA-CR-187574] N91-29777

Verification of the FtCayuga fault-tolerant microprocessor system. Volume 1: A case study in theorem prover-based verification
[NASA-CR-4381] N91-29778

PROGRAMMING LANGUAGES

A prolog system for converting VHDL-based models to Generalized Extraction System (GES) rules
[AD-A238545] N91-29741

The language for DENOTE (Denotational Semantics Translation Environment)
[AD-A237144] N91-29750

A type calculus for mathematical programming modeling languages
[AD-A238160] N91-29766

Transfer of 4GL application from INGRES to ORACLE
[AD-A238448] N91-29771

Data abstraction, concurrency and synchronization in Sina
[PB91-185454] N91-30053

PROGRAMS

The Government-University-Industry Research Roundtable
[DE91-015795] N91-30044

Bulletin of the Division of Electrical Engineering, 1988-1989
[NRC-30458] N91-30071

NRC annual report, 1988/1989
[NRC-30398] N91-30072

PROJECT MANAGEMENT

Flight Research Laboratory. Institute for Aerospace Research
[CTN-91-60105] N91-29140

Methodology investigation, aviation test management system concept development
[AD-A237349] N91-29172

A brief overview of the activities and accomplishments of the Metals and Ceramics Division
[DE91-014955] N91-29296

Toward a new National Weather Service: A first report
[PB91-184077] N91-29694

Second Review of the Department of Energy's Inertial Confinement Fusion Program
[DE91-013157] N91-29945

PROJECTILES

A simple model for low L/D penetration physics
[DE91-015747] N91-29633

PROPELLANT ADDITIVES

Slag and thermal environment of a spinning rocket motor
[AD-A238557] N91-29227

PROPELLANT BINDERS

The effects of HMX particle size and binder stiffness on the burning mechanism and regression rate of a series of fast burning propellants
[DE91-015785] N91-29387

PROPELLANT COMBUSTION

Spectral studies of solid propellant combustion. 3: Emission and absorption results for HMX2 propellant
[AD-A237958] N91-29276

The effects of HMX particle size and binder stiffness on the burning mechanism and regression rate of a series of fast burning propellants
[DE91-015785] N91-29387

Interactions of turbulent eddies and combustion in an MHD second stage combustor
[DE91-015722] N91-29968

PROPELLER BLADES

The design and construction of a shiplaunched VTOL unmanned air vehicle
[AD-A238053] N91-29173

PROPELLERS

Acoustic background noise variation in Air Force platforms and its effect on noise removal algorithms
[AD-A238279] N91-29863

PROPULSION SYSTEM CONFIGURATIONS

Design issues for propulsion systems using metallized propellants
[NASA-TM-105190] N91-29220

Numerical propulsion system simulation: An interdisciplinary approach
[NASA-TM-105181] N91-29221

Twenty first century propulsion concept
[AD-A237853] N91-29224

PROPULSION SYSTEM PERFORMANCE

Numerical propulsion system simulation: An interdisciplinary approach
[NASA-TM-105181] N91-29221

A computer program for prediction of internal performance of a ramrocket
[AD-A238179] N91-29226

Performance and optimization of a derated ion thruster for auxiliary propulsion
[NASA-TM-105144] N91-29229

PROPYLENE OXIDE

Studies of polymers for shock absorption applications
[AD-A237925] N91-29358

PROTECTIVE CLOTHING

Physiological responses to intermittent exercise as modified by heat stress and protective clothing
[AD-A237447] N91-29716

PROTECTIVE COATINGS

Effect of alumina particle additions on the aging kinetics of 6061 aluminum matrix composites
[AD-A238052] N91-29246

Optical and environmentally protective coatings for Potassium Dihydrogen Phosphate (KDP) harmonic converter crystals
[DE91-015296] N91-30034

PROTEINS

Specific mutagenesis of a chlorophyll-binding protein
[DE91-014813] N91-29711

PROTOCOL (COMPUTERS)

Operational concept document for the Next Generation Computer Resources (NGCR) operating systems interface standard baseline
[AD-A237501] N91-29782

PROTONS

The 3-D NMR imaging: A chemical microscope for analysis of heterogeneous macromolecular networks
[DE91-015109] N91-29375

Activation calculations for trapped protons below 200 MeV: Appendix
[NASA-CR-184170] N91-29865

Study of nuclear effects in the deuteron and extraction of neutron to proton stucture function ratio
[DE91-015484] N91-29873

Proton deceleration near the surface of an accreting neutron star N91-30063

PROVING

A prolog system for converting VHDL-based models to Generalized Extraction System (GES) rules
[AD-A238545] N91-29741

Verification of the FtCayuga fault-tolerant microprocessor system. Volume 1: A case study in theorem prover-based verification
[NASA-CR-4381] N91-29778

Plan for a laser weapon verification research program
[DE90-012123] N91-29848

PSYCHOLOGICAL FACTORS

Combining CL (Confidence Limits) and PL (Partial Limits) displays
[AD-A238507] N91-29830

PSYCHOMOTOR PERFORMANCE

Performance of Marine AV-8B (Harrier) pilots on a cognitive/psychomotor test battery: Comparison and prediction
[AD-A238563] N91-29729

Performance of several different Naval aviator communities on a cognitive/psychomotor test battery: Pipeline comparison and prediciton
[AD-A238564] N91-29730

PSYCHOPHYSICS

Psychophysical studies of visual cortical function
[AD-A238663] N91-29720

PSYCHOPHYSIOLOGY

Institute for the Study of Human Capabilities: Summary descriptions of research for the period December 1989 through September 1990
[AD-A237767] N91-29726

PULSE COMMUNICATION

Signal processing in impulsive electromagnetic interference
[AD-A237612] N91-29416

PULSE COMPRESSION

A high data rate communications system using long pulses
[AD-D014947] N91-29430

PULSE DOPPLER RADAR

Impact of ionospheric scintillations on space-based surveillance radars
[AD-A237673] N91-29417

PULSE GENERATORS

Computation of broadband, high-power electromagnetic pulse generation from an air gas avalanche switch
[DE91-015793] N91-29435

REX: A 5-MV pulsed-power source for driving high-brightness electron beam diodes
[DE91-014604] N91-29443

Design and test of a continuous duty pulsed ac generator
[DE91-014664] N91-29445

Millimeter-wave characterization of GaAs devices and IC's
[AD-A237843] N91-29461

Future explosive pulse-power technology for high-energy plasma physics experiments
[DE91-014601] N91-29951

Procyon experiments utilizing explosively-formed fuse opening switches
[DE91-014742] N91-29953

Computational modeling of the Trailmaster Procyon system
[DE91-014765] N91-29955

PULSE POSITION MODULATION

Quaternary pulse position modulation electronics for free-space laser communications
[NASA-TM-104502] N91-29405

PULSED LASERS

High gain photoconductive semiconductor switching
[DE91-014668] N91-29478

Full-field Fabry-Perot interferometer
[DE91-014610] N91-29540

Blackbody pumped CO2 lasers using Gaussian and waveguide cavities
[DE91-012494] N91-29559

Evolution of a finite pulse of radiation in a high-power free-electron laser
[AD-A237427] N91-29568

The laser ablation of aluminum at 193, 248, and 351 nm
[AD-A237574] N91-29569

Characterization of a sub-picosecond dye laser for the study of atom-perturber collisions
[AD-A238099] N91-29572

Short-pulse glass slab amplifier
[DE91-015385] N91-29580

Development of laser optics for the AWA photocathode
[DE91-015552] N91-29581

A mesoscopic linear accelerator driven by superintense subpicosecond laser pulses
[DE91-015941] N91-29913

PULSED RADIATION

Pulse induced nanlithography of graphite in H2O: A road to chemical linkages to the surface?
[AD-A237086] N91-29338

PULSES

Investigation of the combustion of liquid fuels in Rijke type pulse combustors
[DE90-012490] N91-29381

REX: A 5-MV pulsed-power source for driving high-brightness electron beam diodes
[DE91-014604] N91-29443

A mesoscopic linear accelerator driven by superintense subpicosecond laser pulses
[DE91-015941] N91-29913

PYRITES

Pyrite cathode material for a thermal battery
[AD-D014945] N91-29475

PYROLYSIS

Investigation of particulate formation during diesel spray combustion
[DE90-008282] N91-29255

A model of multicomponent droplet evaporation with liquid phase reactions
[DE90-012535] N91-29257

Organometallic precursor routes to Si-C-Al-O-N ceramics
[AD-A237753] N91-29355

PYROLYTIC GRAPHITE

Mechanistic investigation of nanometer-scale/lithography at liquid-covered graphite surfaces
[AD-A237085] N91-29337

Pulse induced nanlithography of graphite in H2O: A road to chemical linkages to the surface?
[AD-A237086] N91-29338

PYROTECHNICS

Diode laser ignition of explosive and pyrotechnic components
[DE90-012227] N91-29553

PYRROLES

Electronic and ionic transport in processable conducting polymers
[AD-A238175] N91-29362

Q

QUADRATIC PROGRAMMING
Barrier methods for large-scale quadratic programming
[AD-A238554] N91-29773
QUALITY CONTROL
Digital SPC switching technology: Foreign technology assessment
[AD-A237258] N91-29449
Slaying the software dragon: A look at how software engineering, the Ada programming language and process maturity are changing software development
[AD-A237156] N91-29751
Management of variation and TQM
[AD-A238399] N91-29843
QUANTILES
Scrawl strips, and letter or B-letter strips: Depicting marginals of scatter plots
[AD-A238556] N91-29845
QUANTITATIVE ANALYSIS
Analyzing photographically recorded atomic emission spectra using an automated densitometer
[DE91-015368] N91-29871
Quantitative interpretation of auger lineshapes and electron/photon stimulated desorption
[AD-A237138] N91-29874
Quantitative analysis of oxygen segregation on inversion domain boundaries in aluminum nitride
[DE91-010869] N91-29971
QUANTUM CHROMODYNAMICS
Theoretical high energy physics
[DE90-012527] N91-29904
Theoretical high energy physics
[DE91-013639] N91-29905
QUANTUM EFFICIENCY
InGaAs/GaAs graded superlattices in photodetectors for wavelengths beyond 1 micron
[DE90-012073] N91-29969
QUANTUM ELECTRONICS
Research in the physical sciences with application to the free electron laser
[AD-A237884] N91-29571
The embedded electron-gas boundary: A new standard problem in surface physics
[AD-A238152] N91-30014
Solid state research
[NASA-CR-188021] N91-30016
QUANTUM MECHANICS
Quantum measurement and the mind-brain connection
[DE91-012343] N91-29723
A survey of nonlinear dynamics (chaos theory)
[AD-A237802] N91-29821
The Kramers problem: Fifty years of development
[DE91-617583] N91-29855
Electron tunneling microscopy
[AD-A237504] N91-30003
Supercoherent states and physical systems
[DE91-014598] N91-30040
QUANTUM NUMBERS
Algebraic approaches to nuclear structure
[DE91-015214] N91-29870
QUANTUM OPTICS
Spatial propagation of squeezed light in a degenerate parametric amplifier
[DE91-014989] N91-30039
QUANTUM THEORY
Quantum measurement and the mind-brain connection
[DE91-012343] N91-29723
Solvent dynamical effects in electron transfer: The solvent inertial limit and the predicted influence of quantum effects
[AD-A237462] N91-29880
A research program in experimental and theoretical high energy physics
[DE91-014728] N91-29907
QUANTUM WELLS
Stable integrated microwave to optical modulator
[AD-A238166] N91-29574
Device processing of II-VI semiconductor films and quantum well structures
[AD-A238460] N91-30017
Uniaxial stress study of the quantum transitions in a strained layer (001) In0.2Ga0.8As/GaAs single quantum well
[DE91-014990] N91-30033
QUARK MODELS
Study of nuclear effects in the deuteron and extraction of neutron to proton stucture function ratio
[DE91-015484] N91-29873
High energy physics at Tufts University
[DE91-015055] N91-29908
QUARKS
Strange quarks in nuclei
[DE91-015833] N91-29895
Chasing the x(sub f) dependence of J/psi production
[DE91-015136] N91-29899
QUARTZ
NMR spectroscopy of experimentally shocked silicate minerals
[DE91-014897] N91-29898
QUARTZ CRYSTALS
Using quartz crystal microbalances to simultaneously sense mass accumulation and solution properties
[DE91-011501] N91-29537
On the role of crystal defects as sources of resonator frequency instability
[AD-A238505] N91-30018
QUENCHING
An investigation of the as-quenched and early aging characteristics of a Al - 4.1 wt. percent Li binary alloy by x ray diffraction
[AD-A237598] N91-29311
QUEUEING THEORY
Diffusion approximations for complex repair systems
[AD-A238100] N91-29836

R

RADAR
A dihedral corner reflector model for full polarization calibration of RCS measurements
[DE91-013572] N91-29402
Nonlinear computerized methodology. A: Angle of arrival estimation. B: Data modeling and identification
[AD-A237564] N91-29415
Signal processing in impulsive electromagnetic interference
[AD-A237612] N91-29416
A Doppler bin blanking CFAR processor for airborne radars
[AD-A237890] N91-29418
Use of the implicit-finite-difference method to implement the parabolic equation model
[AD-A237437] N91-29819
NRL review, 1991
[AD-A238665] N91-29857
RADAR ATTENUATION
A program to operate and upgrade the GL low altitude lidar systems
[AD-A238081] N91-29423
RADAR CLUTTER MAPS
A Doppler bin blanking CFAR processor for airborne radars
[AD-A237890] N91-29418
RADAR CORNER REFLECTORS
A dihedral corner reflector model for full polarization calibration of RCS measurements
[DE91-013572] N91-29402
RADAR CROSS SECTIONS
Portable 45-gigahertz radar for glint and scintillation studies
[AD-A238005] N91-29421
Numerical methods for scattering from electrically large objects
[AD-A238262] N91-29426
RADAR DETECTION
Range-only multistatic radar system
[AD-D011645] N91-29399
A program to operate and upgrade the GL low altitude lidar systems
[AD-A238081] N91-29423
RADAR ECHOES
Range-only multistatic radar system
[AD-D011645] N91-29399
RADAR EQUIPMENT
Scattering and polarization measurements using the PL/OPA low altitude lidar
[AD-A238082] N91-29424
RADAR IMAGERY
Comparison of synthetic aperture radar autofocus techniques: Phase gradient vs subaperture
[DE91-014696] N91-29406
P-3 SAR calibration activity at Andros Island
[AD-A237357] N91-29412
A Doppler bin blanking CFAR processor for airborne radars
[AD-A237890] N91-29418
Portable 45-gigahertz radar for glint and scintillation studies
[AD-A238005] N91-29421
VLSI circuit techniques and technologies for ultrahigh speed data conversion interfaces
[AD-A238115] N91-29468
Multi-sensor image interpretation using laser radar and thermal images
[AD-A238245] N91-29576
RADAR NETWORKS
Range-only multistatic radar system
[AD-D011645] N91-29399
RADAR TRACKING
Space-based Doppler lidar sampling strategies: Algorithm development and simulated observation experiments
[NASA-CR-184172] N91-29554
RADIANCE
Postshock spectral radiance measurements in nickel and nickel/aluminum powders
[DE91-014695] N91-29302
RADIATION CHEMISTRY
Chemical waste disposal in space by plasma discharge
[NASA-CR-184169] N91-29737
RADIATION DAMAGE
Ceramic decomposition under irradiation
[DE91-015061] N91-29372
Spike leakage and burnout of silicon PIN diode microwave limiters
[AD-A238392] N91-29471
Protecting the ozone shield: A new public policy
[AD-A237640] N91-29659
RADIATION DETECTORS
The ASTROMAG superconducting magnet facility configured for a free flying satellite
[DE91-014710] N91-29204
A slit aperture for the Monitoring X ray Experiment (MOXE)
[DE91-013317] N91-29538
Neutron dosimetry using optically stimulated luminescence
[DE91-015781] N91-29902
RADIATION DOSAGE
Nuclear data needs for the space exploration initiative
[DE91-013231] N91-29200
Protecting the ozone shield: A new public policy
[AD-A237640] N91-29659
Reevaluation of S-values considering electron transport
[DE91-015428] N91-29893
Fusion reactor materials
[DE91-012984] N91-29942
RADIATION EFFECTS
Effects of high-intensity solar radiation on carbon fibers
[DE91-015485] N91-29252
Postirradiation deformation of ferritic Fe-Cr binary alloys
[DE91-014856] N91-29295
Materials science applications of a 120 kV FEG TEM/STEM: Triskaidekaphilia
[DE91-010136] N91-29536
Biological interactions of extremely-low-frequency electric and magnetic fields
[DE90-011927] N91-29709
Fusion reactor materials
[DE91-012984] N91-29942
Formation of CoSi2 in SIMOX wafers by high dose Co implantation
[DE91-015639] N91-30036
RADIATION MEASUREMENT
The ASTROMAG superconducting magnet facility configured for a free flying satellite
[DE91-014710] N91-29204
Study of activation of metal samples from LDEF-1 and Spacelab-2
[NASA-CR-184171] N91-29297
Analysis of radio frequency radiation from a propagating electron beam
[AD-A237941] N91-29419
Remote sensing of snow covers using the gamma ray technique
[AD-A238016] N91-29639
Neutron dosimetry using optically stimulated luminescence
[DE91-015781] N91-29902
RADIATION SOURCES
The APS radio frequency test stand control system
[DE91-015711] N91-29434
Control of energy sweep and transverse beam motion in induction linacs
[DE91-015177] N91-29911
Application of diffraction correction to blackbody sources
[AD-A237840] N91-29926
Plasma flow switch experiments on the Pegasus facility
[DE91-014744] N91-29954
RADIATION TRANSPORT
Description of the Strategic High-Altitude Atmospheric Radiation Code (SHARC)
[AD-A237089] N91-29671
RADICALS
A theoretical and experimental study of unimolecular and biomolecular radical hydrogen transfer reactions
[DE91-012607] N91-29261

Hot atom reactive scattering and photodissociation experiments with acetylene and ethylene
[DE91-013755] N91-29264

RADIO ANTENNAS
A new system for measurement of low frequency radio transmitting antenna parameters in near real time
[AD-A238555] N91-29429

RADIO ASTRONOMY
The Research Laboratory of Electronics
[AD-A237670] N91-29458

RADIO COMMUNICATION
High temperature superconductor analog electronics for millimeter-wavelength communications
[NASA-TM-105184] N91-29982

RADIO FREQUENCIES
Sliding mode controller of RF cavity tuning loop
[DE91-015461] N91-29410
Analysis of radio frequency radiation from a propagating electron beam
[AD-A237941] N91-29419
The APS radio frequency test stand control system
[DE91-015711] N91-29434
A compact 200 kV pulse transformer system
[DE91-014669] N91-29479
RF transfer in the coupled-cavity free-electron laser two-beam accelerator
[DE91-015676] N91-29583

RADIO FREQUENCY HEATING
Supersonic combustion of a transverse injected H2 jet in a radio frequency heated flow
[DE91-014739] N91-29281
Fabrication of silicon nitride ceramics by microwave heating
[DE91-015312] N91-29373
ICRF edge modeling
[DE91-014401] N91-29403

RADIO INTERFEROMETERS
Millimeter-accuracy satellite navigation
[AD-A237736] N91-29163

RADIO RECEIVERS
Evaluation of a pre-production version of Canadian Marconi CMA-786 GPS receiver
[NAE-LTR-FR-106] N91-29158

RADIO WAVES
Analysis of radio frequency radiation from a propagating electron beam
[AD-A237941] N91-29419

RADIOACTIVE DECAY
Superdeformation: An experimental review
[DE91-015566] N91-29894
High energy physics at Tufts University
[DE91-015055] N91-29908
Tritium-field betacells
[DE91-014666] N91-29910

RADIOACTIVE ISOTOPES
Reevaluation of S-values considering electron transport
[DE91-015428] N91-29893

RADIOACTIVE WASTES
Chemical waste disposal in space by plasma discharge
[NASA-CR-184169] N91-29737

RADIOGRAPHY
NDE of ceramics and ceramic composites
[NASA-TM-104520] N91-29610

RADIOISOTOPE BATTERIES
Tritium-field betacells
[DE91-014666] N91-29910

RADIOMETERS
Technical activities 1990, Electron and Optical Physics Div.
[PB91-194423] N91-29858

RADIOSONDES
The nature of the propagation of sea breeze fronts in central California
[AD-A238635] N91-29692
Validation of the Schwartz and Hon algorithm at low grazing angles
[AD-A238162] N91-29767

RAIL TRANSPORTATION
Maglev system concept using 20-K high-temperature superconductors and hyperconductors
[DE91-015714] N91-29860

RAILGUN ACCELERATORS
Basic simple modeling of balloting motion of railgun projectiles
[AD-A237938] N91-29205
An approximate analysis of balloting motion of railgun projectiles
[AD-A237942] N91-29206
Basic simple modeling of in-bore motion of railgun projectiles
[AD-A238064] N91-29207

RAINBOWS
Tropical cyclone motion in the northwest Pacific Ocean, phase 1
[AD-A237455] N91-29683

RAINDROPS
Modeling a rain-induced mixed layer
[AD-A238022] N91-29702

RAMAN SPECTRA
Structure of icosahedral borides by Raman spectroscopy
[DE91-010872] N91-29260
Infrared and Raman spectra of C60 and C70 solid films at room temperature
[AD-A237880] N91-29462
High-intensity and high-energy laser interactions with single droplets
[AD-A238197] N91-29575

RAMAN SPECTROSCOPY
Structure of icosahedral borides by Raman spectroscopy
[DE91-010872] N91-29260
Preparation and properties of new inorganic glasses and gel-derived solids
[AD-A238095] N91-29360

RAMPS (STRUCTURES)
Aircraft operations from runways with inclined ramps (ski-jump)
[AD-A237265] N91-29171

RANDOM PROCESSES
Stochastic simulation techniques for partition function approximation of Gibbs random field images
[AD-A238611] N91-29775

RANDOM SAMPLING
Comparison of four methods for aggregating judgments from multiple experts
[DE91-013522] N91-30043

RANDOM VARIABLES
Singularities in Gaussian random fields
[AD-A238220] N91-29839

RANDOM VIBRATION
Dimensionless parameters important to the prediction of vortex-induced vibration of long, flexible cylinders in ocean currents
[PB91-184713] N91-29630

RANGEFINDING
A Doppler bin blanking CFAR processor for airborne radars
[AD-A237890] N91-29418

RARE EARTH ELEMENTS
Calculation of intra-rare Earth binary phase diagrams
[DE91-014950] N91-29267

RATES (PER TIME)
Micromechanisms of monotonic and cyclic subcritical crack growth in advanced high melting point low-ductility intermetallics
[AD-A238151] N91-29317
Quaternary pulse position modulation electronics for free-space laser communications
[NASA-TM-104502] N91-29405

RATINGS
Methods for evaluating discomfort glare
[PB91-185132] N91-29722

RATIOS
Design and analysis of multi-sensor sequential detection system
[AD-A238012] N91-29543

RAWINSONDES
TOVS satellite soundings of the ERICA IOP-2 cyclone
[AD-A237998] N91-29686

RAY TRACING
Hamiltonian 3-D ray tracing in the oceanic waveguide on the ellipsoidal earth
[AD-A237458] N91-29700

REACTING FLOW
Experimental and analytical comparison of flowfields in a 110 N (25 lbf) H2/O2 rocket
[NASA-TM-105175] N91-29230

REACTION KINETICS
Molecular beam studies of reaction dynamics
[DE90-011600] N91-29256
Hot atom reactive scattering and photodissociation experiments with acetylene and ethylene
[DE91-013755] N91-29264
Catalytic hydrogenation of carbon monoxide
[DE91-015452] N91-29283
The cure of rigid polyurethane encapsulating foam
[DE91-016059] N91-29379
Cyclic voltammetric wave-shapes for microdisk electrodes: Coupled effects of solution resistance, double-layer capacitance, and finite electrochemical kinetics
[AD-A237505] N91-29455
Effects of doping on hybridization gapped materials
[DE91-014611] N91-29477
International Union of Theoretical and Applied Mechanics (IUTAM) Symposium on Aerothermodynamics in Combustors
[AD-A237943] N91-29516
Kinetics of dark reaction in chemical laser gases
[DE91-015320] N91-29579
Molecular beam studies of reaction dynamics
[DE91-014866] N91-29868
Role of the solvent in kinetics of heterogeneous electron and ion transfer reactions
[AD-A237168] N91-29876
The effects of donor-acceptor electronic interactions on the rates of gas-phase metallocene electron-exchange reactions
[AD-A237459] N91-29878
Electron-transfer reactions at metal-solution interfaces: An introduction to some contemporary issues
[AD-A237506] N91-29882
Defect characterization of electronic conducting pseudo-perovskite systems
[DE91-014385] N91-29978
Laser probing of the kinetics and dynamics of III -V semiconductor growth
[AD-A237795] N91-30009

REACTIVITY
Organo- borazines.3.homo- and copolymerization of p-vinylphenyl- cyclotri- borazines
[AD-A237881] N91-29357

REACTOR DESIGN
Light weight space power reactors for nuclear electric propulsion
[DE91-014803] N91-29232

REACTOR MATERIALS
Fusion reactor materials
[DE91-012984] N91-29942
Thick-section weldments in 21-6-9 and 316LN stainless steel for fusion energy applications
[DE91-015307] N91-29963

REACTOR PHYSICS
Parametric design calculations using Green's function to determine unique source
[DE91-014683] N91-29861

REACTOR SAFETY
A methodology for developing physical system fault diagnostic aids
[DE91-015533] N91-29809

READING
Topographic map reading
[AD-A238026] N91-29640

READOUT
The development of a fiber-optic readout pressure transducer
[AD-A238393] N91-29545

REAL TIME OPERATION
Exact and approximate solutions to the oblique shock equations for real-time applications
[NASA-CR-187173] N91-29147
The design of a real-time adaptive filter development system
[AD-A237134] N91-29448
Experiments in adaptive control of cooperating manipulators N91-29594
Real-time Ada design methodologies and their impact on performance
[AD-A237259] N91-29754
A common interface real-time multiprocessor operating system for embedded systems
[AD-A238445] N91-29770
A real time collimation sensor using a shear plate and a spatial light modulator
[DE90-011362] N91-29914
Adaptive liquid crystal TV based joint transform correlator as applied to real-time pattern recognition
[AD-A238576] N91-29931
Specification and verification of real-time constraints in coarse-grain dataflow
[AD-A237355] N91-30047

RECEIVERS
A high data rate communications system using long pulses
[AD-D014947] N91-29430
The utility of elliptical and circular confidence regions for HFDF receivers
[AD-A238390] N91-29842

RECOIL PROTONS
Neutron dosimetry using optically stimulated luminescence
[DE91-015781] N91-29902

RECONNAISSANCE
Topographic map reading
[AD-A238026] N91-29640

RECORDING INSTRUMENTS
Video frame store: An advanced solid state recorder
[DE91-015709] N91-29549

RECORDS MANAGEMENT
Legal and records management issue of optical disk storage media
| DE91-014898 | N91-30046
Records management at the DOE national laboratories: Sandia National Laboratories
| DE91-015563 | N91-30057
RECOVERY VEHICLES
Carina aerothermal test at Mach 8
| AD-A238561 | N91-29218
RECRYSTALLIZATION
A study of the liquid-solid interface during rapid resolidification of cooper-titanium using molecular dynamics
| AD-A238634 | N91-30022
REDUCED GRAVITY
Bubble generation and movement under microgravity conditions
| NAE-LTR-FR-110 | N91-29388
REDUCTION (CHEMISTRY)
Synthesis and characterization of reduced tungsten sulfide cluster complexes
| DE91-014916 | N91-29282
Role of the solvent in kinetics of heterogeneous electron and ion transfer reactions
| AD-A237168 | N91-29876
Temperature dependence of proton electroreduction kinetics at gold(111) and (210) surfaces
| AD-A237460 | N91-29879
REDUNDANCY
Force-reflecting control of a teleoperated system coupling a nonredundant master with a redundant slave
| DE90-012137 | N91-29585
Global optimality, conservativity and singularity in redundancy resolution of robotic manipulators N91-29593
Verification of the FtCayuga fault-tolerant microprocessor system. Volume 2: Formal specification and correctness theorems
| NASA-CR-187574 | N91-29777
REDUNDANCY ENCODING
Fault-tolerant computing: An overview
| NASA-CR-188793 | N91-29769
REENTRY VEHICLES
The functional dependence of trajectory dispersion on initial condition errors
| DE91-014661 | N91-29151
Measurement of a three-dimensional hypersonic density field using holographic interferometry N91-29539
REFLECTANCE
X ray reflectivity studies of Au surfaces
| DE91-015308 | N91-29307
Inverse problem in neutron reflection
| DE91-014457 | N91-29984
REFLECTION
Energy conserving coating: Pigment research
| AD-A237841 | N91-29356
A dihedral corner reflector model for full polarization calibration of RCS measurements
| DE91-013572 | N91-29402
REFLECTORS
Ultraviolet reflector materials for solar detoxification of hazardous waste
| DE91-002196 | N91-29663
REFRACTION
Electro-optic line narrowing of optical parametric oscillators
| AD-D014944 | N91-29934
REFRACTIVITY
Optical and environmentally protective coatings for Potassium Dihydrogen Phosphate (KDP) harmonic converter crystals
| DE91-015296 | N91-30034
REFRACTORY MATERIALS
Very high temperature fibers of TiC and TiB2
| AD-A237423 | N91-29242
Lightweight disk alloy development
| AD-A237064 | N91-29309
REFRIGERATING
Minimization of refrigeration power requirements for mechanical supports in cryogenic systems
| DE91-015720 | N91-29392
REGRESSION ANALYSIS
XTRAN: An atmospheric transmittance code based on XSCALE
| AD-A237624 | N91-29674
Analysis of Naval aviation selection test data with nonlinear models. Part 1: Parameter estimation
| AD-A238244 | N91-29728
Confidence bands for the median survival time as a function of the covariates in the Cox model
| AD-A237626 | N91-29835
REGULATIONS
Scientific and technical information handbook for technical report preparation
| AD-A238548 | N91-30051
REINFORCED PLASTICS
Impact characterization of graphite fiber reinforced thermoplastic laminates
| NIAR-91-16 | N91-29241
REINFORCING FIBERS
Effect of fortifier on compression-after-impact strength of carbon fabric reinforced epoxy
| NAE-LTR-ST-1736 | N91-29237
Effect of fiber-matrix debonding on notched strength of titanium metal matrix composites
| NASA-TM-104131 | N91-29239
Impact characterization of graphite fiber reinforced thermoplastic laminates
| NIAR-91-16 | N91-29241
Very high temperature fibers of TiC and TiB2
| AD-A237423 | N91-29242
RELATIVISTIC ELECTRON BEAMS
Experimental analysis of B-dot sensors
| AD-A238487 | N91-29547
RELATIVISTIC PLASMAS
Vlasov simulations of very-large-amplitude wave generation in the plasma wakefield accelerator
| AD-A237428 | N91-29961
RELIABILITY
Statistical characterization of graphite fiber for prediction of composite structure reliability
| AD-A238020 | N91-29245
Slaying the software dragon: A look at how software engineering, the Ada programming language and process maturity are changing software development
| AD-A237156 | N91-29751
RELIABILITY ANALYSIS
Description of a computer fault detector and net isolator
| AD-A238387 | N91-29428
A general graphical user interface for automatic reliability modeling
| NASA-TM-104068 | N91-29745
RELIABILITY ENGINEERING
Heuristic methods in applied probability
| AD-A238229 | N91-29841
RELIEF MAPS
Topographic map reading
| AD-A238026 | N91-29640
Three-dimensional visualization for evaluating automated, geomorphic pattern-recognition analyses of crustal structures
| DE91-012929 | N91-29668
REMOTE CONTROL
Objective assessments of mobility with an early Unmanned Ground Vehicle (UGV) prototype viewing system
| AD-A237317 | N91-29595
REMOTE MANIPULATOR SYSTEM
Force-reflecting control of a teleoperated system coupling a nonredundant master with a redundant slave
| DE90-012137 | N91-29585
REMOTE SENSING
Detection of targets in terrain clutter by using multispectral infrared image processing
| AD-A237436 | N91-29414
Using the TIMS to estimate evapotranspiration from a forest
| NASA-CR-188729 | N91-29636
Remote sensing of snow covers using the gamma ray technique
| AD-A238016 | N91-29639
Remote determination of soil moisture and evapotranspiration from thermal infrared measurements: Detection of a drying threshold
| PB91-195818 | N91-29641
Multiple channel satellite analysis of cirrus
| AD-A238054 | N91-29687
Toward a new National Weather Service: A first report
| PB91-184077 | N91-29694
Workshop on Automation and Robotics: Proceedings
| DE91-015175 | N91-29801
NRL review, 1989-1990
| AD-A238612 | N91-29856
REMOTE SENSORS
International aviation (selected articles)
| AD-A237175 | N91-29141
REMOTELY PILOTED VEHICLES
AEROWING - The software for aerodynamic analysis of a large aspect-ratio finite wing at low speeds
| NAL-PD-CF-9101 | N91-29146
REMOVAL
A novel epoxy lacquer for high strength steel in F-111 aircraft during overhaul
| AD-A236828 | N91-29326
RESEARCH
The Government-University-Industry Research Roundtable
| DE91-015795 | N91-30044
RESEARCH AND DEVELOPMENT
Commonwealth Advisory Aeronautical Research Council. First Canadian newsletter on systems, 1989
| NAE-LTR-FR-108 | N91-29139
Review of Canadian aeronautical fatigue work: 1987-1989
| NAE-LTR-ST-1706 | N91-29165
JPRS report: Science and technology. USSR: Materials science
| JPRS-UMS-91-001 | N91-29291
Proceedings of the First Switch Tube Advanced Technology Meeting
| DE91-012634 | N91-29440
The Research Laboratory of Electronics
| AD-A237670 | N91-29458
Intermetallic superconductors: The state of development in 1991
| DE91-014844 | N91-30026
Bulletin of the Division of Electrical Engineering, 1988-1989
| NRC-30458 | N91-30071
NRC annual report, 1988/1989
| NRC-30398 | N91-30072
RESEARCH FACILITIES
Flight Research Laboratory. Institute for Aerospace Research
| CTN-91-60105 | N91-29140
RESEARCH MANAGEMENT
A brief overview of the activities and accomplishments of the Metals and Ceramics Division
| DE91-014955 | N91-29296
The Research Laboratory of Electronics
| AD-A237670 | N91-29458
Nuclear theory progress report
| DE91-013908 | N91-29866
Theoretical high energy physics
| DE91-013639 | N91-29905
Optoelectronic Materials Center
| AD-A237663 | N91-29922
Second Review of the Department of Energy's Inertial Confinement Fusion Program
| DE91-013157 | N91-29945
Establishment of an Institute for Fusion Studies
| DE91-014922 | N91-29956
RESEARCH PROJECTS
Subsurface Science Program
| DE91-015480 | N91-29665
NW lab for integrated systems
| AD-A237118 | N91-29749
NRL review, 1989-1990
| AD-A238612 | N91-29856
Optoelectronic Materials Center
| AD-A237663 | N91-29922
RESEARCH VEHICLES
Validation of the Schwartz and Hon algorithm at low grazing angles
| AD-A238162 | N91-29767
RESIDUAL STRENGTH
Review of literature on the damage, loss of stiffness, and residual strength of graphite/epoxy laminates subjected to cyclic loading
| NAE-LTR-ST(CR)-1711 | N91-29611
RESIDUAL STRESS
Polymer drag reduction of a zero pressure gradient boundary layer
| AD-A237572 | N91-29510
RESINS
Injection molding of engineering plastics
| AD-A238583 | N91-29389
RESONANCE
Degradation of brightness by resonant particle effects
| DE91-015181 | N91-29578
RESONANT FREQUENCIES
Dimensionless parameters important to the prediction of vortex-induced vibration of long, flexible cylinders in ocean currents
| PB91-184713 | N91-29630
RESONATORS
On the role of crystal defects as sources of resonator frequency instability
| AD-A238505 | N91-30018
RESOURCES MANAGEMENT
Resource envelope concepts for mission planning
| NASA-TP-3139 | N91-29209
RESPONSE TIME (COMPUTERS)
Transfer of 4GL application from INGRES to ORACLE
| AD-A238448 | N91-29771
RETRACTABLE EQUIPMENT
Measurements of retractable gas-cooled 6061 aluminum electrical leads operating in a vacuum
| DE91-014617 | N91-29444
REUSABLE HEAT SHIELDING
Debris/ice/TPS assessment and photographic analysis for Shuttle Mission STS-40
| NASA-TM-103822 | N91-29210

Ablative heat shield studies for NASA Mars/Earth return entry vehicles
[AD-A238159] N91-29215
REVERSE FIELD PINCH
The effects of magnetic field errors on reversed field pinch plasma
[DE91-013636] N91-29948
Global confinement and discrete dynamo activity in the MST reversed field pinch
[DE91-015219] N91-29960
Anomalous ion heating from the dynamo in a reversed field pinch
[DE91-015586] N91-29966
REVISIONS
Standard NIM instrumentation system
[DE90-010387] N91-29532
A prolog system for converting VHDL-based models to Generalized Extraction System (GES) rules
[AD-A238545] N91-29741
REYNOLDS NUMBER
Adiabatic two-phase flow frictional pressure drop. Part 2: A generalized method for data correlation
[DE91-014462] N91-29501
REYNOLDS STRESS
Polymer drag reduction of a zero pressure gradient boundary layer
[AD-A237572] N91-29510
RHEOLOGY
Injection molding of engineering plastics
[AD-A238583] N91-29389
RHODIUM
Atomic-resolution scanning tunneling microscopy and infrared spectroscopy as combined in-situ probes of electrochemical adlayer structure: Carbon monoxide on rhodium(111)
[AD-A237508] N91-29884
RHODIUM COMPOUNDS
Electrical, magnetic, and spectroscopic properties of tetrathiafulvalene charge transfer compounds with iron, ruthenium, rhodium, and iridium halides
[AD-A237607] N91-29273
RIGID STRUCTURES
Equations of motion for a flexible spacecraft-lumped parameter idealization
[NASA-CR-188727] N91-29211
ROBOT ARMS
A general purpose, comprehensive dynamics simulation of serial robot manipulators N91-29587
Singularity avoidance and the kinematics of an eight-revolute-joint manipulator N91-29588
Kinematics of serial manipulators and their parallel duals N91-29589
Performance models for robot manipulators N91-29590
Quasistatic manipulation with compliance and friction N91-29591
Global optimality, conservativity and singularity in redundancy resolution of robotic manipulators N91-29593
ROBOT CONTROL
Research and development at ORNL/CESAR towards cooperating robotic systems for hazardous environments
[DE91-015638] N91-29810
ROBOT DYNAMICS
Modeling of a 3-D light-weight space manipulator
[AD-A236823] N91-29586
Performance models for robot manipulators N91-29590
Research and development at ORNL/CESAR towards cooperating robotic systems for hazardous environments
[DE91-015638] N91-29810
ROBOT SENSORS
Vision-based navigation and parallel computing
[AD-A238570] N91-29164
ROBOTICS
Modeling of a 3-D light-weight space manipulator
[AD-A236823] N91-29586
Singularity avoidance and the kinematics of an eight-revolute-joint manipulator N91-29588
Kinematics of serial manipulators and their parallel duals N91-29589
Performance models for robot manipulators N91-29590
Quasistatic manipulation with compliance and friction N91-29591
Global optimality, conservativity and singularity in redundancy resolution of robotic manipulators N91-29593
Experiments in adaptive control of cooperating manipulators N91-29594
Neural networks and robotics applied to the non-destructive inspection of aircraft
[AD-A238312] N91-29609
Theory and computer simulation of the interactional neural network
[NRC-30269] N91-29800
Workshop on Automation and Robotics: Proceedings
[DE91-015175] N91-29801
Research and development at ORNL/CESAR towards cooperating robotic systems for hazardous environments
[DE91-015638] N91-29810
ROBOTS
Vision-based navigation and parallel computing
[AD-A238570] N91-29164
Force-reflecting control of a teleoperated system coupling a nonredundant master with a redundant slave
[DE90-012137] N91-29585
Modeling of a 3-D light-weight space manipulator
[AD-A236823] N91-29586
A general purpose, comprehensive dynamics simulation of serial robot manipulators N91-29587
Kinematics of serial manipulators and their parallel duals N91-29589
Quasistatic manipulation with compliance and friction N91-29591
Experiments in adaptive control of cooperating manipulators N91-29594
ROBUSTNESS (MATHEMATICS)
Compensation of distributed delays in integrated communication and control systems
[NASA-CR-187136] N91-29193
Effects of colocation and non-colocation of sensors and actuators on flexible structures
[AD-A238457] N91-29844
ROCKET ENGINE CASES
Slag and thermal environment of a spinning rocket motor
[AD-A238557] N91-29227
ROCKET ENGINES
A computer program for prediction of internal performance of a ramrocket
[AD-A238179] N91-29226
Slag and thermal environment of a spinning rocket motor
[AD-A238557] N91-29227
ALS rocket engine combustion devices design and demonstration
[NASA-CR-183824] N91-29233
International Union of Theoretical and Applied Mechanics (IUTAM) Symposium on Aerothermodynamics in Combustors
[AD-A237943] N91-29516
ROCKET SOUNDING
Analysis of the ultraviolet emissions of nitric oxide from mid-latitude rocket observations
[AD-A237340] N91-29673
ROCKS
Workshop proceedings: Toughening Mechanisms in Quasi-Brittle Materials
[AD-A238289] N91-29248
RODS
Effects of anisotropy on dynamic tensile behavior
[DE91-014748] N91-29632
ROOM TEMPERATURE
Compendium of material test results on HY-100 and pseudo HY-100 metals in support of US Navy programs
[DE91-013134] N91-29292
ROTARY WINGS
Unsteady compressible lifting surface analysis for rotary wings using velocity potential modes N91-29170
Response and stability analysis of helicopter rotor blades using computerized symbolic manipulation
[AD-A238660] N91-29175
ROTATING BODIES
Theoretical study of the flow in a rotating duct. Experimental study through flow visualization in a curved duct
[RAE-TRANS-2189] N91-29493
ROTATING FLUIDS
Theoretical study of the flow in a rotating duct. Experimental study through flow visualization in a curved duct
[RAE-TRANS-2189] N91-29493
ROTATING STALLS
Modification of axial-flow compressor stall margin by variation of stationary blade setting angles
[AD-A238406] N91-29186
ROTOR AERODYNAMICS
Calculated performance of the NASA Lewis icing research tunnel
[NASA-TM-105173] N91-29199
ROTORS
Calculated performance of the NASA Lewis icing research tunnel
[NASA-TM-105173] N91-29199
Design and test of a continuous duty pulsed ac generator
[DE91-014664] N91-29445
RUBBER
Ventilation kinetics testing of a steel frame/rubber fabric underground shelter
[AD-A237469] N91-29734
RUN TIME (COMPUTERS)
Using the Harmony operating system: Release 3.0
[ERA-377] N91-29799
RUNWAYS
Aircraft operations from runways with inclined ramps (ski-jump)
[AD-A237265] N91-29171
RUPTURING
Pressure vessel burst test program
[AD-A237845] N91-29624
RURAL AREAS
Theoretical studies of long-range transport of oxidants
[PB91-182360] N91-29661
RUTHENIUM
Electrical, magnetic, and spectroscopic properties of tetrathiafulvalene charge transfer compounds with iron, ruthenium, rhodium, and iridium halides
[AD-A237607] N91-29273

S

SAFETY DEVICES
Environmental assessment for the FAA explosive detection system independent validation and verification program
[DE91-013190] N91-29152
Laboratory evaluation of portable and walk-through explosives vapour detectors
[NAE-LTR-UA-104] N91-29533
SAFETY FACTORS
Methods to determine the compatibility and degradation of organic materials
[AD-A237940] N91-29234
SALINITY
Oceanographic data report Number 8: Density profiles from the Delaware Estuary, October 1986 - September 1988
[PB91-183608] N91-29707
SAMPLES
Oceanographic data report Number 8: Density profiles from the Delaware Estuary, October 1986 - September 1988
[PB91-183608] N91-29707
SAN ANDREAS FAULT
Regional tectonic deformation in Southern California, inferred from terrestrial geodesy and the global positioning system N91-29669
SATELLITE COMMUNICATION
The study of space communications spread spectrum systems. Part 1: Saw-based joint group demodulation of frequency shift keyed and differential phase shift keyed signals
[QU-90-1-PT-1] N91-29395
A study of space communications spread-spectrum systems, phase 5 and 6. Part 2: Coding and modulation
[QU-90-2-PT-2] N91-29396
The study of space communications spread spectrum systems. Part 3: Uplink synchronization in an EHF frequency-hopped satellite system
[QU-90-3-PT-3] N91-29397
Coding for frequency hopped spread spectrum satellite communications
[ECE-89-1] N91-29398
Combinatorial FSK modulation for power-efficient high-rate communications
[NASA-TM-105188] N91-29404
SATELLITE IMAGERY
A practical example of forest mapping and timber volume estimation using LANDSAT-5 TM imagery
[INPE-5244-PRE/1675] N91-29635
Ocean thermal feature recognition, discrimination and tracking using infrared satellite imagery
[AD-A238138] N91-29703
Diffraction-limited imaging of satellites using bispectral speckle interferometry
[DE91-015745] N91-30062
SATELLITE NAVIGATION SYSTEMS
Millimeter-accuracy satellite navigation
[AD-A237736] N91-29163
SATELLITE ORBITS
Seasonal air and water mass redistribution and its effect on satellite and polar motion N91-29202
SATELLITE SOUNDING
TOVS satellite soundings of the ERICA IOP-2 cyclone
[AD-A237998] N91-29686
SATELLITE-BORNE PHOTOGRAPHY
Ocean thermal feature recognition, discrimination and tracking using infrared satellite imagery
[AD-A238138] N91-29703
SATELLITES
On satellite constellation selection
[DE91-014562] N91-29851
SCALE MODELS
Carina aerothermal test at Mach 8
[AD-A238561] N91-29218

SCANNERS
Materials science applications of a 120 kV FEG TEM/STEM: Triskaidekaphilia
[DE91-010136] N91-29536
Stochastic modelling of seafloor morphology
[AD-A237063] N91-29697
SCANNING
Algorithms for converting geodetic Earth location to satellite time and swath pixel coordinates for the DMSP satellite system
[AD-A237589] N91-29638
Temperature dependence of proton electroreduction kinetics at gold(111) and (210) surfaces
[AD-A237460] N91-29879
SCANNING TUNNELING MICROSCOPY
Comparisons between scanning tunneling microscopy and outer-sphere electron-transfer rates at Pt(111) surfaces coated with ordered iodine adlayers
[AD-A237507] N91-29883
Atomic-resolution scanning tunneling microscopy and infrared spectroscopy as combined in-situ probes of electrochemical adlayer structure: Carbon monoxide on rhodium(111)
[AD-A237508] N91-29884
Scanning tunneling microscopy studies of the surfaces of a-Si:H and a-SiGe:H films
[DE91-002169] N91-29983
SCATTERING
Penn State/ONR Mid Frequency Workshop
[AD-A237982] N91-29420
Chasing the x(sub f) dependence of J/psi production
[DE91-015136] N91-29899
A real time collimation sensor using a shear plate and a spatial light modulator
[DE90-011362] N91-29914
Inverse problem in neutron reflection
[DE91-014457] N91-29984
SCATTERING COEFFICIENTS
Scattering and polarization measurements using the PL/OPA low altitude lidar
[AD-A238082] N91-29424
SCATTERING CROSS SECTIONS
Numerical methods for scattering from electrically large objects
[AD-A238262] N91-29426
Collisional processes of interest in MFE plasma research
[DE91-013023] N91-29943
SCHEDULES
Central solar eclipses of 1992. Annual solar eclipse of 4-5 January 1992, total solar eclipse of 30 June 1992
[AD-A237614] N91-30069
SCHEDULING
Performance implications of synchronization support for parallel FORTRAN programs
[AD-A238493] N91-29790
SCHROEDINGER EQUATION
Inverse problem in neutron reflection
[DE91-014457] N91-29984
Spatial propagation of squeezed light in a degenerate parametric amplifier
[DE91-014989] N91-30039
SCINTILLATION
Impact of ionospheric scintillations on space-based surveillance radars
[AD-A237673] N91-29417
Portable 45-gigahertz radar for glint and scintillation studies
[AD-A238005] N91-29421
Hyperdimensional data analysis and structural inference
[AD-A238097] N91-29764
SEA BREEZE
The nature of the propagation of sea breeze fronts in central California
[AD-A238635] N91-29692
SEA LEVEL
Sea level and bottom pressure measurements in the Northern Gulf of Alaska
[PB91-184135] N91-29705
SEA WATER
The role of microorganisms in marine corrosion
[AD-A237062] N91-29308
Oceanographic data report Number 8: Density profiles from the Delaware Estuary, October 1986 - September 1988
[PB91-183608] N91-29707
SEDIMENTS
Stochastic modelling of seafloor morphology
[AD-A237063] N91-29697
SEEDS
Model filled polymers 8: Synthesis of crosslinked polymeric beads by seed polymerization
[AD-A237429] N91-29349
SELF ABSORPTION
Study of activation of metal samples from LDEF-1 and Spacelab-2
[NASA-CR-184171] N91-29297
Inelastic scattering in condensed matter with high intensity Moessbauer radiation
[DE91-014384] N91-29980
SELF ORGANIZING SYSTEMS
Invariant target recognition using self-organizing networks
[AD-A238252] N91-29807
SELF SEALING
Quick disconnect pressure cap
[AD-D014936] N91-29598
SEMANTICS
The language for DENOTE (Denotational Semantics Translation Environment)
[AD-A237144] N91-29750
The 6th Workshop on the Mathematical Foundations of Programming Semantics
[AD-A237754] N91-29760
SEMICONDUCTING FILMS
Persistent photoconductivity in II-VI mixed semiconductors related critical phenomena and applications
[AD-A237792] N91-29460
Device processing of II-VI semiconductor films and quantum well structures
[AD-A238460] N91-30017
SEMICONDUCTOR DEVICES
Failure mechanisms on GaAs integrated circuits: Electromigration on GaAs
[AD-A237352] N91-29451
Persistent photoconductivity in II-VI mixed semiconductors related critical phenomena and applications
[AD-A237792] N91-29460
Device processing of II-VI semiconductor films and quantum well structures
[AD-A238460] N91-30017
An optically activated modulator and GaAs-GaAlAs compound semiconductor channel waveguide
[AD-A238642] N91-30023
SEMICONDUCTOR DIODES
Spike leakage and burnout of silicon PIN diode microwave limiters
[AD-A238392] N91-29471
Adjustable magnification anamorphic beam expander
[DE91-014110] N91-29561
Tritium-field betacells
[DE91-014666] N91-29910
SEMICONDUCTOR LASERS
Physics and applications of the lock-on effect
[DE91-014670] N91-29446
Diode laser ignition of explosive and pyrotechnic components
[DE90-012227] N91-29553
Adjustable magnification anamorphic beam expander
[DE91-014110] N91-29561
Development of low-threshold value, high-power semiconductor laser
[AD-A237183] N91-29566
Stable integrated microwave to optical modulator
[AD-A238166] N91-29574
Design of a stabilized, dc-powered analog laser diode driver
[AD-A238596] N91-29577
SEMICONDUCTORS (MATERIALS)
Effects of high-intensity solar radiation on carbon fibers
[DE91-015485] N91-29252
Atomic approaches to defect thermochemistry
[AD-A238260] N91-29280
ANL's development of conductive ceramic components for MCFC
[DE91-015557] N91-29336
Ceramic decomposition under irradiation
[DE91-015061] N91-29372
The 2nd Workshop on High Temperture Electronics (Metallization and Packaging)
[DE91-014332] N91-29442
Persistent photoconductivity in II-VI mixed semiconductors related critical phenomena and applications
[AD-A237792] N91-29460
Technical publication announcements covering center programs, July to September 1990, with 1991 CEEE events calendar
[PB91-184754] N91-29476
High gain photoconductive semiconductor switching
[DE91-014668] N91-29478
Research in the physical sciences with application to the free electron laser
[AD-A237884] N91-29571
User's manual for DIODE
[AD-A237190] N91-29752
Dielectric function of semiconductor superlattice
[DE91-617788] N91-29976
Vibrational, mechanical, and thermal properties of III-V semiconductors
[AD-A237785] N91-30008
Laser probing of the kinetics and dynamics of III -V semiconductor growth
[AD-A237795] N91-30009
Monolithic integration of semiconductor and superconductor components
[AD-A237946] N91-30012
Semiconductor deposition and etching interactions of laser-generated translationally hot atoms and radicals
[AD-A238198] N91-30015
Pseudomorphic semiconducting heterostructures from combinations of AlN, GaN and seleced SiC polytypes: Theoretical advancement and its coordination with experimental studies of nucleation, growth, characterizaiton and device development
[AD-A238520] N91-30020
Uniaxial stress study of the quantum transitions in a strained layer (001) In0.2Ga0.8As/GaAs single quantum well
[DE91-014990] N91-30033
SENSITIVITY
An elevated temperature titration calorimeter
[DE91-015765] N91-29548
SENSORS
Telescope and sensor interface preliminary requirements report for the PORTS chamber
[AD-A237755] N91-29923
SENSORY DISCRIMINATION
The functional architecture of visual object recognition
[AD-A238617] N91-29732
SEPARATED FLOW
Experimental and analytical study of rippled trailing edge airfoils for compressor application
[AD-A237425] N91-29508
SEQUENCING
A high data rate communications system using long pulses
[AD-D014947] N91-29430
SEQUENTIAL ANALYSIS
Design and analysis of multi-sensor sequential detection system
[AD-A238012] N91-29543
SERVICE LIFE
Tutor aft fuselage and empennage full-scale test: Procedures for creating a damage log
[NAE-ST-576] N91-29167
The failure of components in power generation equipment
[NAE-LTR-ST-1774] N91-29180
Materials research for sodium engine development
[DE91-015715] N91-29378
Chinese physics lasers (selected articles)
[AD-A237263] N91-29567
Probabilistic lifetime strength of aerospace materials via computational simulation
[NASA-CR-187178] N91-29629
SERVOMECHANISMS
Force-reflecting control of a teleoperated system coupling a nonredundant master with a redundant slave
[DE90-012137] N91-29585
SET THEORY
Implementation of an exact penalty function formulation to solve convex nonlinear programming problems
[AD-A237905] N91-29761
SHAFTS (MACHINE ELEMENTS)
Unsteady force calculations in turbomachinery
[AD-A237937] N91-29515
SHAPES
Advances in the drained shaping of ceramics
[DE91-015429] N91-29376
SHEAR FLOW
Three-dimensional vortex dynamics and interactions in near-wall turbulent boundary layers
[AD-A237413] N91-29507
SHEAR PROPERTIES
Experimental investigation of adiabatic shear banding at different impact velocities
[AD-A237901] N91-29625
SHEAR STRESS
Composite specimen design analysis. Volume 2: Experimental efforts
[AD-A238277] N91-29247
Polymer drag reduction of a zero pressure gradient boundary layer
[AD-A237572] N91-29510
Morphology of bulk Nylon 6 subjected to plane strain compression
[AD-A237331] N91-29622
SHELLS (STRUCTURAL FORMS)
Fission-fusion adaptivity in finite elements for nonlinear dynamics of shells
[AD-A238029] N91-29626

SHELTERS
Ventilation kinetics testing of a steel frame/rubber fabric underground shelter
[AD-A237469] N91-29734
SHIPS
The design and construction of a shiplaunched VTOL unmanned air vehicle
[AD-A238053] N91-29173
SHOCK ABSORBERS
Studies of polymers for shock absorption applications
[AD-A237925] N91-29358
SHOCK LOADS
The use of high velocity launchers for scientific and engineering studies
[DE91-015564] N91-29208
SHOCK TESTS
NMR spectroscopy of experimentally shocked silicate minerals
[DE91-014897] N91-29898
SHOCK WAVE PROFILES
Hydrogen-fueled scramjet investigation
[AD-A237569] N91-29183
SHOCK WAVE PROPAGATION
Exact and approximate solutions to the oblique shock equations for real-time applications
[NASA-CR-187173] N91-29147
Qualitative investigation of cryogenic injected shock dissipation
[NASA-TM-105140] N91-29525
A simple model for low L/D penetration physics
[DE91-015747] N91-29633
SHOCK WAVES
Translation of airfoil trailing edge noise article from Revue d'Acoustique
[AD-A237811] N91-29143
Postshock spectral radiance measurements in nickel and nickel/aluminum powders
[DE91-014695] N91-29302
Shock acceleration with turbulence minimization
[DE91-014741] N91-29505
Shockwave considerations for sub-grid closure modeling in turbulent large eddy simulations
[DE91-015142] N91-29506
Qualitative investigation of cryogenic injected shock dissipation
[NASA-TM-105140] N91-29525
Energy generation by a shock crossing a perturbed interface
[DE91-015678] N91-29530
Deformation behavior of pre-shocked copper as a function of strain rate and temperature
[DE91-015180] N91-29620
Analytical and numerical methods; advanced computer concepts
[DE91-014526] N91-29795
SHORT WAVE RADIATION
The MIT short-wavelength laser project
[DE91-015357] N91-29582
SIDE-LOOKING RADAR
Stochastic modelling of seafloor morphology
[AD-A237063] N91-29697
SIDES
Ventilation kinetics testing of a steel frame/rubber fabric underground shelter
[AD-A237469] N91-29734
SIGNAL DETECTION
Signal processing in impulsive electromagnetic interference
[AD-A237612] N91-29416
Design and analysis of multi-sensor sequential detection system
[AD-A238012] N91-29543
The effects of luminance boundaries on color perception
[AD-A237794] N91-29925
SIGNAL DETECTORS
Experimental analysis of B-dot sensors
[AD-A238487] N91-29547
SIGNAL MEASUREMENT
A new system for measurement of low frequency radio transmitting antenna parameters in near real time
[AD-A238555] N91-29429
SIGNAL PROCESSING
The study of space communications spread spectrum systems. Part 1: Saw-based joint group demodulation of frequency shift keyed and differential phase shift keyed signals
[QU-90-1-PT-1] N91-29395
The study of space communications spread spectrum systems. Part 3: Uplink synchronization in an EHF frequency-hopped satellite system
[QU-90-3-PT-3] N91-29397
Hardware interface for high speed video imaging
[AD-D014902] N91-29400
Combinatorial FSK modulation for power-efficient high-rate communications
[NASA-TM-105188] N91-29404
Spectra and covariances for classical nonlinear signal processing problems involving class A non-Gaussian noise
[AD-A237388] N91-29413
Detection of targets in terrain clutter by using multispectral infrared image processing
[AD-A237436] N91-29414
Nonlinear computerized methodology. A: Angle of arrival estimation. B: Data modeling and identification
[AD-A237564] N91-29415
Signal processing in impulsive electromagnetic interference
[AD-A237612] N91-29416
Physical concepts and modeling procedures for picosecond and subpicosecond distributed circuits
[AD-A238592] N91-29472
Technical publication announcements covering center programs, July to September 1990, with 1991 CEEE events calendar
[PB91-184754] N91-29476
Software development of the cochlear filter and eighth-nerve model
[AD-A237454] N91-29757
Auditory processing of complex sounds across frequency channels
[AD-A238023] N91-29862
Device processing of II-VI semiconductor films and quantum well structures
[AD-A238460] N91-30017
SIGNAL RECEPTION
Scattering and polarization measurements using the PL/OPA low altitude lidar
[AD-A238082] N91-29424
SIGNAL TO NOISE RATIOS
A Doppler bin blanking CFAR processor for airborne radars
[AD-A237890] N91-29418
Application of Multi-Frequency Modulation (MFM) for high-speed data communications to a voice frequency channel
[AD-A238019] N91-29422
SIGNAL TRANSMISSION
A new system for measurement of low frequency radio transmitting antenna parameters in near real time
[AD-A238555] N91-29429
Technical publication announcements covering center programs, July to September 1990, with 1991 CEEE events calendar
[PB91-184754] N91-29476
SILANES
Precursors to Si-N-C-O ceramics: A reinvestigation of the poly methylvinyl silylethyl enediamine systems
[DE91-013722] N91-29333
Scanning tunneling microscopy studies of the surfaces of a-Si:H and a-SiGe:H films
[DE91-002169] N91-29983
SILICATES
NMR spectroscopy of experimentally shocked silicate minerals
[DE91-014897] N91-29898
SILICIDES
Environmental effects in niobium base alloys and other selected intermetallic compounds
[AD-A237535] N91-29658
Formation of CoSi2 in SIMOX wafers by high dose Co implantation
[DE91-015639] N91-30036
SILICON
Silicon Wafer Advanced Packaging (SWAP). Multichip Module (MCM) foundry study, version 2
[AD-A237412] N91-29452
Counterdoped high temperature, silicon array infrared detector
[AD-A238483] N91-29546
Fabrication of lightweight Si/SiC LIDAR mirrors
[NASA-CR-4389] N91-29935
Epitaxial growth of single crystal diamond on silicon
[AD-A237758] N91-30007
Atomic layer epitaxy group IV materials: Surface processes, thin films, devices and their characterization
[AD-A238506] N91-30019
SILICON CARBIDES
An analysis of the wear behavior of SiC whisker reinforced alumina from 25 to 1200 C
[NASA-TM-104489] N91-29235
Microstructural and strength stability of CVD SiC fibers in argon environment
[NASA-TM-103772] N91-29250
Synthesis of multifilament silicon carbide fibers by chemical vapor deposition
[NASA-CR-188725] N91-29331
Precursors to Si-N-C-O ceramics: A reinvestigation of the poly methylvinyl silylethyl enediamine systems
[DE91-013722] N91-29333
Ceramic fabrication R/D
[DE91-014758] N91-29335
NMR characterization of porous ceramics
[DE91-015051] N91-29371
Fabrication of lightweight Si/SiC LIDAR mirrors
[NASA-CR-4389] N91-29935
SILICON FILMS
A study of copper segregation in sputtered Al-Si-Cu films using Auger electron spectroscopy
[AD-A238130] N91-29316
SILICON NITRIDES
Precursors to Si-N-C-O ceramics: A reinvestigation of the poly methylvinyl silylethyl enediamine systems
[DE91-013722] N91-29333
Boron nitride and silicon nitride systems
[AD-A238080] N91-29359
Fabrication of silicon nitride ceramics by microwave heating
[DE91-015312] N91-29373
Ultrasonic evaluation of silicon nitride green bodies
[AD-A237924] N91-29608
SILICON OXIDES
Optical and environmentally protective coatings for Potassium Dihydrogen Phosphate (KDP) harmonic converter crystals
[DE91-015296] N91-30034
SILVER ALLOYS
Requirements for the observation of Fermi surfaces in disordered alloys
[DE91-014578] N91-29321
SILVER IODIDES
The mixed metallic-ionic clusters of the silver/silver iodide
[AD-A237883] N91-29314
The relative stability and possible structural formulae of the negatively charged silver monoiodide clusters
[AD-A238398] N91-29888
SIMULATION
Whipple bumper shield simulations
[NASA-TM-105089] N91-29213
The evolution and structure of homogeneous stably stratified sheared turbulence N91-29499
A general purpose, comprehensive dynamics simulation of serial robot manipulators N91-29587
An investigation of the ERICA IOP-2 cyclone using the NORAPS model
[AD-A237683] N91-29684
Stochastic simulation techniques for partition function approximation of Gibbs random field images
[AD-A238611] N91-29775
The 23rd Optoelectronic Workshop: Optical System Assessment for Design and Simulated Annealing
[AD-A238588] N91-29932
SIMULATORS
A general purpose, comprehensive dynamics simulation of serial robot manipulators N91-29587
A high-performance retargetable simulator for parallel architectures
[AD-A237354] N91-29779
SINGLE CRYSTALS
Very high temperature fibers of TiC and TiB2
[AD-A237423] N91-29242
Structure and stability of underpotentially depositied layers on Au(111) studied by optical second harmonic generation
[AD-A237087] N91-29268
Growth, characterization, and device development in monocrystalline diamond films
[AD-A237463] N91-30000
Epitaxial growth of single crystal diamond on silicon
[AD-A237758] N91-30007
Molecular beam epitaxial growth and characterization of metastable compound semiconductors for infrared detector applications
[AD-A237797] N91-30010
Pseudomorphic semiconducting heterostructures from combinations of AlN, GaN and seleced SiC polytypes: Theoretical advancement and its coordination with experimental studies of nucleation, growth, characterizaiton and device development
[AD-A238520] N91-30020
Formation of CoSi2 in SIMOX wafers by high dose Co implantation
[DE91-015639] N91-30036
SINGLE EVENT UPSETS
Application of the nuclear microprobe to the imaging of single event upsets in integrated circuits
[DE91-014701] N91-29447
SINGULARITY (MATHEMATICS)
Global optimality, conservativity and singularity in redundancy resolution of robotic manipulators N91-29593

Performance and stability in high speed articulated structures undergoing quick maneuvers: Theory and applications
[AD-A237857] N91-29597

SINTERING
NMR characterization of porous ceramics
[DE91-015051] N91-29371
Air-sintering mechanisms of chromites
[DE91-015527] N91-30027

SLABS
Short-pulse glass slab amplifier
[DE91-015385] N91-29580
Test of Newtonian gravity using DSV sea cliff
[AD-A238558] N91-29680

SLAGS
Slag and thermal environment of a spinning rocket motor
[AD-A238557] N91-29227

SLIDING
An analysis of the wear behavior of SiC whisker reinforced alumina from 25 to 1200 C
[NASA-TM-104489] N91-29235
Sliding mode controller of RF cavity tuning loop
[DE91-015461] N91-29410

SLIP CASTING
Advances in the drained shaping of ceramics
[DE91-015429] N91-29376

SLITS
A slit aperture for the Monitoring X ray Experiment (MOXE)
[DE91-013317] N91-29538

SMOKE
A wind tunnel smoke generator
[NAE-LTR-LA-312] N91-29195

SNOW
An AVHRR data set for the arctic leads ARI
[AD-A237221] N91-29637

SNOW COVER
Remote sensing of snow covers using the gamma ray technique
[AD-A238016] N91-29639

SODIUM CARBONATES
Corrosion behavior of continuous-filament-wound ceramic composite tubes
[DE91-014959] N91-29370

SODIUM CHLORIDES
Equation of state for pure sodium chloride
[DE91-014618] N91-29286

SODIUM SULFUR BATTERIES
Performance and life evaluation of advanced battery technologies for electric vehicle applications
[DE91-015671] N91-29482

SOFTENING
A model of multicomponent droplet evaporation with liquid phase reactions
[DE90-012535] N91-29257

SOFTWARE ENGINEERING
Assessment team report on flight-critical systems research at NASA Langley Research Center
[NASA-CR-181850] N91-29176

SOFTWARE TOOLS
The APS radio frequency test stand control system
[DE91-015711] N91-29434
An automated software system for updating digital terrain databases from all-source imagery, phase 1
[AD-A237105] N91-29748
Proceedings of the 1st Workshop on Proximity Graphs
[AD-A237250] N91-29818

SOIL MOISTURE
Remote determination of soil moisture and evapotranspiration from thermal infrared measurements: Detection of a drying threshold
[PB91-195818] N91-29641

SOLAR ATMOSPHERE
The High Energy Solar Physics mission (HESP): Scientific objectives and technical description
[NASA-TM-105033] N91-29201

SOLAR CELLS
Tritium-field betacells
[DE91-014666] N91-29910

SOLAR COLLECTORS
Concentrator flight test experiment
[AD-A237390] N91-29647
The Department of Energy's solar industrial program: New ideas for American industry
[DE91-002197] N91-29649
Ultraviolet reflector materials for solar detoxification of hazardous waste
[DE91-002196] N91-29663

SOLAR ECLIPSES
Central solar eclipses of 1992. Annual solar eclipse of 4-5 January 1992, total solar eclipse of 30 June 1992
[AD-A237614] N91-30069

SOLAR ENERGY
Effects of high-intensity solar radiation on carbon fibers
[DE91-015485] N91-29252
Ultraviolet reflector materials for solar detoxification of hazardous waste
[DE91-002196] N91-29663

SOLAR ENERGY CONVERSION
The Department of Energy's solar industrial program: New ideas for American industry
[DE91-002197] N91-29649

SOLAR FLARES
The High Energy Solar Physics mission (HESP): Scientific objectives and technical description
[NASA-TM-105033] N91-29201

SOLAR FURNACES
Effects of high-intensity solar radiation on carbon fibers
[DE91-015485] N91-29252
The Department of Energy's solar industrial program: New ideas for American industry
[DE91-002197] N91-29649

SOLAR HEATING
Effects of solar heating by aerosols and trace gases on the temperature structure constant
[AD-A237675] N91-29677

SOLAR MAXIMUM MISSION
Plasma properties of hot coronal loops utilizing coordinated SMM and solar research rocket observations
[NASA-CR-186094] N91-29937

SOLAR PHYSICS
The High Energy Solar Physics mission (HESP): Scientific objectives and technical description
[NASA-TM-105033] N91-29201

SOLAR RADIATION
Effects of high-intensity solar radiation on carbon fibers
[DE91-015485] N91-29252
Equatorial entrainment zone simulations
[AD-A237234] N91-29657
IDA studies on natural space environmental effects on materials for SDIO
[AD-A237974] N91-29660
A manual method for determining the fractional stability category
[AD-A237627] N91-29675

SOLAR SAILS
Twenty first century space propulsion study addendum
[AD-A238011] N91-29225

SOLAR SPECTRA
Plasma properties of hot coronal loops utilizing coordinated SMM and solar research rocket observations
[NASA-CR-186094] N91-29937

SOLDERED JOINTS
Lead-free solders for electronics applications: Wetting analysis
[DE91-014900] N91-29320

SOLDERING
JPRS report: Science and technology. USSR: Materials science
[JPRS-UMS-91-001] N91-29291
Annual Electronics Manufacturing Seminar proceedings
[AD-A238017] N91-29467

SOLDERS
Lead-free solders for electronics applications: Wetting analysis
[DE91-014900] N91-29320

SOLID ELECTROLYTES
Materials research for sodium engine development
[DE91-015715] N91-29378
Electrocatalytic study of ammonia synthesis and methane dimerization in high temperature solid electrolyte cells
[DE90-012496] N91-29437
Developmental status and system studies of the monolithic solid oxide fuel cell
[DE91-014389] N91-29645

SOLID MECHANICS
NIKE2D: A nonlinear, implicit, two-dimensional finite element code for solid mechanics
[DE91-015734] N91-29634

SOLID PHASES
Air-sintering mechanisms of chromites
[DE91-015527] N91-30027

SOLID PROPELLANT COMBUSTION
Slag and thermal environment of a spinning rocket motor
[AD-A238557] N91-29227

SOLID PROPELLANT IGNITION
Slag and thermal environment of a spinning rocket motor
[AD-A238557] N91-29227

SOLID PROPELLANT ROCKET ENGINES
Investigation of the flame-acoustic wave interaction during axial solid rocket instabilities
[AD-A237851] N91-29223

SOLID PROPELLANTS
Investigation of the flame-acoustic wave interaction during axial solid rocket instabilities
[AD-A237851] N91-29223

SOLID SOLUTIONS
Growth, nitrogen vacancy reduction and solid solution formation in cubic GaN thin films and the subsequent fabrication of superlattice structures using AlN and InN
[AD-A238521] N91-30021

SOLID STATE
Molecular dynamics simulation of the effect of interfaces in melting and solid-state amorphization
[DE91-015550] N91-29284
Design, synthesis and characterization of novel polydiacetylenes using new analytical techniques
[AD-A237362] N91-29348
Superconducting instrumentation for precision measurement and control
[DE91-014650] N91-29541
Investigation of ultrasonic evaluation of solid-state metal bond
[DE91-014996] N91-29606
NRL review, 1989-1990
[AD-A238612] N91-29856
Mixed valent and heavy ferimons and related systems
[DE91-015454] N91-29900
Solid state research
[NASA-CR-188021] N91-30016

SOLID STATE DEVICES
Video frame store: An advanced solid state recorder
[DE91-015709] N91-29549
Responsivity uniformity enhancements for Backside-Illuminated Charge-Coupled Devices (BICCDs) by excimer laser-assisted etching
[AD-A237435] N91-29997

SOLID STATE LASERS
VISAR: Line-imaging interferometer
[DE91-014749] N91-29542
A mesoscopic linear accelerator driven by superintense subpicosecond laser pulses
[DE91-015941] N91-29913

SOLID STATE PHYSICS
The Research Laboratory of Electronics
[AD-A237670] N91-29458

SOLID-SOLID INTERFACES
Molecular dynamics simulation of the effect of interfaces in melting and solid-state amorphization
[DE91-015550] N91-29284
Annealing effects on the microstructure of titanium electrical contacts on diamond films
[DE91-010150] N91-29327
Electron microscopy of thick 304 SS-copper multilayers
[DE91-011116] N91-29972

SOLIDIFICATION
Analysis of weld metal solidification and microstructures
[DE91-014574] N91-29301
Method of obtaining current-conducting polymeric materials
[AD-A237174] N91-29339

SOLITARY WAVES
Optical soliton source
[AD-D014942] N91-29933

SOLUBILITY
A technique for measuring the solubilities of gases in liquids
[AD-A238071] N91-29278
Electrified microscopic and conventional interfaces between two immiscible electrolyte solutions
[AD-A237695] N91-29459

SOLVATION
Electrochemical contact adsorption site changes driven by field and charge fact and theory
[AD-A237127] N91-29269
Solvent-dependent redox thermodynamics of metal amine complexes. The delineation of specific solvation effects
[AD-A237503] N91-29272
Discreteness-of-solvent effects in Marcus equations in the mean spherical approximation
[AD-A237133] N91-29996
The influence of potential on metal-adsorbate structure: Solvent-independent nature of infrared spectra for Pt(111)/CO
[AD-A237509] N91-30004

SOLVENTS
Solvent-dependent redox thermodynamics of metal amine complexes. The delineation of specific solvation effects
[AD-A237503] N91-29272

A novel epoxy lacquer for high strength steel in F-111 aircraft during overhaul
[AD-A236828] N91-29326
Solvent effects on simple electron transfer reactions. A comparison of results in Debye and non-Debye solvents
[AD-A237157] N91-29875
Role of the solvent in kinetics of heterogeneous electron and ion transfer reactions
[AD-A237168] N91-29876
Solvent dynamical effects in electron transfer: The solvent inertial limit and the predicted influence of quantum effects
[AD-A237462] N91-29880
The influence of potential on metal-adsorbate structure: Solvent-independent nature of infrared spectra for Pt(111)/CO
[AD-A237509] N91-30004

SONAR
Nonlinear computerized methodology. A: Angle of arrival estimation. B: Data modeling and identification
[AD-A237564] N91-29415
Stochastic modelling of seafloor morphology
[AD-A237063] N91-29697

SONOBUOYS
Stabilized square parachute
[AD-D014946] N91-29149

SOUND PROPAGATION
Penn State/ONR Mid Frequency Workshop
[AD-A237982] N91-29420

SOUND TRANSMISSION
Modification of programs CHIEF and CID to compute sound radiation from an arbitrary body with mixed boundary conditions
[AD-A237502] N91-29759

SOUND WAVES
Investigation of the flame-acoustic wave interaction during axial solid rocket instabilities
[AD-A237851] N91-29223
On-line monitoring of volatile organic species
[DE91-014655] N91-29655
Modification of programs CHIEF and CID to compute sound radiation from an arbitrary body with mixed boundary conditions
[AD-A237502] N91-29759

SOUNDING ROCKETS
Plasma properties of hot coronal loops utilizing coordinated SMM and solar research rocket observations
[NASA-CR-186094] N91-29937

SOUTHERN HEMISPHERE
Lowell proper motion survey: Southern Hemisphere (Giclas, Burnham, and Thomas 1978). Documentation for the machine-readable version
[NASA-TM-105069] N91-30060

SPACE BASED RADAR
Impact of ionospheric scintillations on space-based surveillance radars
[AD-A237673] N91-29417
Space-based Doppler lidar sampling strategies: Algorithm development and simulated observation experiments
[NASA-CR-184172] N91-29554

SPACE DEBRIS
IDA studies on natural space environmental effects on materials for SDIO
[AD-A237974] N91-29660

SPACE ERECTABLE STRUCTURES
Concentrator flight test experiment
[AD-A237390] N91-29647

SPACE PERCEPTION
A program to operate and upgrade the GL low altitude lidar systems
[AD-A238081] N91-29423
Human factors of night vision devices: Anecdotes from the field concerning visual illusions and other effects
[AD-A237641] N91-29735

SPACE POWER REACTORS
Nuclear data needs for the space exploration initiative
[DE91-013231] N91-29200
Light weight space power reactors for nuclear electric propulsion
[DE91-014803] N91-29232
Advanced materials for space nuclear power systems
[NASA-TM-105171] N91-29298
The 0-G experiments with advanced ceramic fabric wick structures
[DE91-015531] N91-29377

SPACE SHUTTLES
Debris/ice/TPS assessment and photographic analysis for Shuttle Mission STS-40
[NASA-TM-103822] N91-29210

SPACE STATIONS
Resource envelope concepts for mission planning
[NASA-TP-3139] N91-29209
Whipple bumper shield simulations
[NASA-TM-105089] N91-29213

SPACE TECHNOLOGY EXPERIMENTS
NASA cryogenic fluid management space experiment efforts, 1960-1990
[NASA-TM-103752] N91-30073

SPACE TRANSPORTATION SYSTEM FLIGHTS
Debris/ice/TPS assessment and photographic analysis for Shuttle Mission STS-40
[NASA-TM-103822] N91-29210

SPACE WEAPONS
SDI performance and START constraints: Modeling phase-1 defense engagements
[DE91-013305] N91-29849
A framework for understanding the strategic defense initiatives' software debates
[AD-A237193] N91-29852
Report to the Congress on the Strategic Defense Initiative, 1991
[AD-A237658] N91-29853

SPACE-TIME FUNCTIONS
Sum of distances in normed spaces
[AD-A238066] N91-29825

SPACEBORNE EXPERIMENTS
A slit aperture for the Monitoring X ray Experiment (MOXE)
[DE91-013317] N91-29538
NASA cryogenic fluid management space experiment efforts, 1960-1990
[NASA-TM-103752] N91-30073

SPACEBORNE PHOTOGRAPHY
Planetary instrument definition and development program: 'Miniature Monochromatic Imager'
[NASA-CR-186550] N91-29219

SPACECRAFT CHARGING
Lithium ion source for satellite charge control
[AD-A238272] N91-29470

SPACECRAFT COMMUNICATION
Quaternary pulse position modulation electronics for free-space laser communications
[NASA-TM-104502] N91-29405

SPACECRAFT CONFIGURATIONS
Operational procedures for powering up, powering down, and configuring the qualification model of the FLTSATCOM satellite
[AD-A238485] N91-29217

SPACECRAFT CONSTRUCTION MATERIALS
Probabilistic lifetime strength of aerospace materials via computational simulation
[NASA-CR-187178] N91-29629

SPACECRAFT MODELS
Operational procedures for powering up, powering down, and configuring the qualification model of the FLTSATCOM satellite
[AD-A238485] N91-29217
Carina aerothermal test at Mach 8
[AD-A238561] N91-29218

SPACECRAFT POWER SUPPLIES
Advanced materials for space nuclear power systems
[NASA-TM-105171] N91-29298
Introduction of a current waveform, waveshaping technique to limit conduction loss in high-frequency dc-dc converters suitable for space power
[AD-A237903] N91-29465

SPACECRAFT PROPULSION
Numerical propulsion system simulation: An interdisciplinary approach
[NASA-TM-105181] N91-29221
Twenty first century space propulsion study addendum
[AD-A238011] N91-29225
Performance and optimization of a derated ion thruster for auxiliary propulsion
[NASA-TM-105144] N91-29229

SPACECRAFT SHIELDING
Nuclear data needs for the space exploration initiative
[DE91-013231] N91-29200
Whipple bumper shield simulations
[NASA-TM-105089] N91-29213

SPACECRAFT STRUCTURES
Experimental demonstration of a classical approach for flexible space structure control: NASA CSI testbeds
[NASA-CR-188724] N91-29212

SPACECREWS
Concepts for manned lunar habitats
[NASA-TM-104114] N91-30068

SPACELAB
Study of activation of metal samples from LDEF-1 and Spacelab-2
[NASA-CR-184171] N91-29297
Activation calculations for trapped protons below 200 MeV: Appendix
[NASA-CR-184170] N91-29865

SPALLATION
Ablation of material by front surface spallation
[DE91-014773] N91-29563

SPARK GAPS
Experimental and analytical study of laser-triggering in the Rimfire switch
[DE91-014662] N91-29483
Gaseous prebreakdown processes that are important for pulsed power switching
[DE91-015902] N91-29487
Laser triggered spark gap modeling
[DE91-014831] N91-29557

SPATIAL DISTRIBUTION
A method of investigating scales of motion in a turbulent wake
[AD-A237923] N91-29514
Eye movements and spatial pattern vision
[AD-A238664] N91-29721
On satellite constellation selection
[DE91-014562] N91-29851

SPATIAL RESOLUTION
The 3-D NMR imaging: A chemical microscope for analysis of heterogeneous macromolecular networks
[DE91-015109] N91-29375

SPECIFIC HEAT
Singularities in Gaussian random fields
[AD-A238220] N91-29839
Specific heat of YBaCu3O7: Volume fraction of superconductivity; parameters characteristic of the ideal superconducting state
[DE91-011827] N91-29974
Thermophysical properties of supercritical fluids and fluid mixtures
[DE91-015794] N91-30041

SPECIFIC IMPULSE
Design issues for propulsion systems using metallized propellants
[NASA-TM-105190] N91-29220
Experimental and analytical comparison of flowfields in a 110 N (25 lbf) H2/O2 rocket
[NASA-TM-105175] N91-29230

SPECIFICATIONS
Standard NIM instrumentation system
[DE90-010387] N91-29532
Verification of the FtCayuga fault-tolerant microprocessor system. Volume 2: Formal specification and correctness theorems
[NASA-CR-187574] N91-29777

SPECKLE INTERFEROMETRY
Diffraction-limited imaging of satellites using bispectral speckle interferometry
[DE91-015745] N91-30062

SPECKLE PATTERNS
Development of optical subapertures
[AD-A237759] N91-29924

SPECTRA
Characterization of surface contaminants using infrared microspectroscopy
[DE91-009405] N91-29605

SPECTRAL BANDS
Spectral studies of solid propellant combustion. 3: Emission and absorption results for HMX2 propellant
[AD-A237958] N91-29276
Second-harmonic generation of TEA CO2 10.6 micrometer laser light in AgGaS2 crystals
[AD-A237169] N91-29564

SPECTRAL EMISSION
Spectral studies of solid propellant combustion. 3: Emission and absorption results for HMX2 propellant
[AD-A237958] N91-29276

SPECTRAL THEORY
Translation of airfoil trailing edge noise article from Revue d'Acoustique
[AD-A237811] N91-29143

SPECTROGRAPHS
Planetary instrument definition and development program: 'Miniature Monochromatic Imager'
[NASA-CR-186550] N91-29219

SPECTROMETERS
Characterization of surface contaminants using infrared microspectroscopy
[DE91-009405] N91-29605

SPECTROSCOPIC ANALYSIS
NMR spectroscopy of experimentally shocked silicate minerals
[DE91-014897] N91-29898

SPECTROSCOPIC TELESCOPES
A real time collimation sensor using a shear plate and a spatial light modulator
[DE90-011362] N91-29914

SPECTROSCOPY
Electrical, magnetic, and spectroscopic properties of tetrathiafulvalene charge transfer compounds with iron, ruthenium, rhodium, and iridium halides
[AD-A237607] N91-29273
Nonlinear spectroscopy of multicomponent droplets and two- and three-dimensional measurements in flames
[AD-A238028] N91-29277

Characterization of surface contaminants using infrared microspectroscopy
[DE91-009405] N91-29605
Study of particle correlations in high energy S + Pb and Pb + Pb interactions with a magnetic-interferometric-emulsion-chamber
[DE91-014355] N91-29897
High resolution electron energy loss studies of surface vibrations
[DE91-014539] N91-30024

SPECTRUM ANALYSIS
Spectral estimation techniques with emphasis on short data records: A primer
[AD-A237486] N91-29271
Postshock spectral radiance measurements in nickel and nickel/aluminum powders
[DE91-014695] N91-29302
Limitations to the method of power spectrum analysis: Nonstationarity, biased estimators, and weak convergence to normality
[DE91-008583] N91-29812
Parallelizing the spectral transform method
[DE91-013969] N91-29815

SPEECH
Very low bit rate voice for packetized mobile applications
[DE91-015333] N91-29409
Research and development for Digital Voice Processing (DVP)
[AD-A238280] N91-29427

SPEECH BASEBAND COMPRESSION
Research and development for Digital Voice Processing (DVP)
[AD-A238280] N91-29427

SPEECH RECOGNITION
Distance measures for speech recognition
[NAE-AN-57] N91-29394

SPHERES
Numerical and physical modelling of bubbly flow phenomena
[DE91-013646] N91-29492

SPIN DYNAMICS
Singularities in Gaussian random fields
[AD-A238220] N91-29839
Epitaxial growth of single crystal diamond on silicon
[AD-A237758] N91-30007

SPIN RESONANCE
Spin-Label-Spin-Probe. Studies of bimolecular encounters in micelles
[AD-A238546] N91-29891

SPIRAL GALAXIES
The relationship between the density wave, molecular gas and star formation in M51 N91-30064

SPRAYED COATINGS
An evaluation of nickel-aluminum coatings fabricated with the plasma-spray process
[DE91-013208] N91-29328

SPRAYERS
An evaluation of nickel-aluminum coatings fabricated with the plasma-spray process
[DE91-013208] N91-29328
A methodology for inhibiting the formation of pollutants in diesel engines
[DE90-011615] N91-29584

SPREAD SPECTRUM TRANSMISSION
The study of space communications spread spectrum systems. Part 1: Saw-based joint group demodulation of frequency shift keyed and differential phase shift keyed signals
[QU-90-1-PT-1] N91-29395
A study of space communications spread-spectrum systems, phase 5 and 6. Part 2: Coding and modulation
[QU-90-2-PT-2] N91-29396
Coding for spread-spectrum channels in the presence of jamming
[AD-A238233] N91-29425

SPUTTERING
The mixed metallic-ionic clusters of the silver/silver iodide
[AD-A237883] N91-29314
A study of copper segregation in sputtered Al-Si-Cu films using Auger electron spectroscopy
[AD-A238130] N91-29316
Design aspects for a pulsed-mode, high-intensity, heavy negative ion source
[DE91-011094] N91-29864

SQUALLS
Mesoscale modeling of precipitation scavenging by a cold-frontal squall line
[DE91-015534] N91-29695

SQUEEZED STATES (QUANTUM THEORY)
Spatial propagation of squeezed light in a degenerate parametric amplifier
[DE91-014989] N91-30039

STABILITY
Secondary stability and three-dimensional natural convection in a shallow cavity N91-29495
A manual method for determining the fractional stability category
[AD-A237627] N91-29675

STABILITY TESTS
Response and stability analysis of helicopter rotor blades using computerized symbolic manipulation
[AD-A238660] N91-29175
Performance and stability in high speed articulated structures undergoing quick maneuvers: Theory and applications
[AD-A237857] N91-29597
Effects of anisotropy on dynamic tensile behavior
[DE91-014748] N91-29632

STABLE OSCILLATIONS
The relative stability and possible structural formulae of the negatively charged silver monoiodide clusters
[AD-A238398] N91-29888

STAINLESS STEELS
Thick-section weldments in 21-6-9 and 316LN stainless steel for fusion energy applications
[DE91-015307] N91-29963
Electron microscopy of thick 304 SS-copper multilayers
[DE91-011116] N91-29972

STANDARDS
Standard NIM instrumentation system
[DE90-010387] N91-29532
Load tables for the Avery and Gilmore standard force machines corrected for gravity, 1989
[NAE-LTR-ST-1703] N91-29535
Ada 9X requirements rationale
[AD-A237350] N91-29755
Scientific and technical information handbook for technical report preparation
[AD-A238548] N91-30051

STAR FORMATION
The relationship between the density wave, molecular gas and star formation in M51 N91-30064
Research in nuclear astrophysics: Stellar collapse and supernovae
[DE91-015449] N91-30066

STATIC MODELS
Simulation of the structure of dense, amorphous bisphenol-A polycarbonate
[AD-A237222] N91-29270
Simulation of large deformation in glassy atactic polypropylene
[AD-A237223] N91-29340
Quasi-static modeling of chain-dynamics in the amorphous glassy polycarbonate of 4,4'-isopropyledenediphenol
[AD-A237289] N91-29343
An atomistic model of the amorphous glassy polycarbonate of 4,4'-isopropylidenediphenol
[AD-A237291] N91-29345

STATISTICAL ANALYSIS
Signal processing in impulsive electromagnetic interference
[AD-A237612] N91-29416
Atmospheric methane concentrations: The NOAA/CMDL global cooperative flask sampling network, 1983 - 1988
[DE91-014942] N91-29664
Stochastic modelling of seafloor morphology
[AD-A237063] N91-29697
Simulation methodology
[AD-A238113] N91-29765
Limitations to the method of power spectrum analysis: Nonstationarity, biased estimators, and weak convergence to normality
[DE91-008583] N91-29812
Analysis of nonGaussian, nonlinear time series with long-memory
[AD-A237847] N91-29822
On the analysis of grouped survival data using cumulative occurrence/exposure rates
[AD-A238219] N91-29838
Comparison of four methods for aggregating judgments from multiple experts
[DE91-013522] N91-30043

STATISTICAL CORRELATION
Combining CL (Confidence Limits) and PL (Partial Limits) displays
[AD-A238507] N91-29830

STATISTICAL DISTRIBUTIONS
Limitations to the method of power spectrum analysis: Nonstationarity, biased estimators, and weak convergence to normality
[DE91-008583] N91-29812
A mixed limit theorem for stable random fields
[AD-A238222] N91-29840
Scrawl strips, and letter or B-letter strips: Depicting marginals of scatter plots
[AD-A238556] N91-29845
A goodness-of-fit test for a family of two parameter Weibulls with known shape using minimum distance estimation of parameters
[AD-A238633] N91-29847
Randomization procedures applied to analysis of ballistic data
[AD-A238389] N91-30050

STATISTICAL MECHANICS
Statistical mechanics of two-dimensional Euler equations and Jupiter's Great Red Spot N91-29498

STATISTICAL TESTS
Design and analysis of multi-sensor sequential detection system
[AD-A238012] N91-29543
On the analysis of grouped survival data using cumulative occurrence/exposure rates
[AD-A238219] N91-29838
New modified Anderson-Darling and Cramer-von Mises goodness-of-fit tests for a normal distribution with specified parameters
[AD-A238630] N91-29846

STATOR BLADES
Near-stall loss measurements in a CD compressor cascade with exploratory leading edge flow control
[AD-A237497] N91-29509

STATORS
Design and test of a continuous duty pulsed ac generator
[DE91-014664] N91-29445

STEADY FLOW
Steady flow of a fluid-solid mixture between parallel plates
[DE91-013114] N91-29491
Numerical study of non-impulsively started flow around a circular cylinder
[AD-A238051] N91-29519

STEADY STATE
Solutions of two-dimensional Euler equations with multigrid acceleration
[NAL-PD-CF-9006] N91-29494
Numerical simulation of self-field MPD thrusters
[NASA-CR-187168] N91-29832

STEAM
Effect of geometric parameters on the performance of second throat annular steam ejectors
[AD-A238645] N91-29522

STEELS
Explosively driven missile trajectory parameters for various fragment materials and velocities
[DE91-014330] N91-29631

STELLAR MOTIONS
Lowell proper motion survey: Southern Hemisphere (Giclas, Burnham, and Thomas 1978). Documentation for the machine-readable version
[NASA-TM-105069] N91-30060

STIFFNESS
Review of literature on the damage, loss of stiffness, and residual strength of graphite/epoxy laminates subjected to cyclic loading
[NAE-LTR-ST(CR)-1711] N91-29611
Vibration control and optimization in composite structural elements by use of add-on viscoelastic materials
[AD-A238533] N91-29628

STIFFNESS MATRIX
Equations of motion for a flexible spacecraft-lumped parameter idealization
[NASA-CR-188727] N91-29211

STIRLING ENGINES
Numerical prediction of turbulent oscillating flow and associated heat transfer
[NASA-CR-187177] N91-29524

STOCHASTIC PROCESSES
Development of the microstructure based stochastic life prediction models
[AD-A237768] N91-29312
Stochastic modelling of seafloor morphology
[AD-A237063] N91-29697
Simulation methodology
[AD-A238113] N91-29765
Stochastic simulation techniques for partition function approximation of Gibbs random field images
[AD-A238611] N91-29775
Analysis of nonGaussian, nonlinear time series with long-memory
[AD-A237847] N91-29822
An alternative algorithm for discrete-time filtering
[AD-A238443] N91-29827
The asymptotic distributions of autoregressive coefficients
[AD-A238538] N91-29831

Least-squares learning and approximation of posterior probabilities on classification problems by neural network models
[AD-A237140] N91-29833
Heuristic methods in applied probability
[AD-A238229] N91-29841

STOICHIOMETRY
Defects and transport in mixed oxides
[DE91-014537] N91-29266

STORAGE RINGS (PARTICLE ACCELERATORS)
Technical activities 1990, Electron and Optical Physics Div.
[PB91-194423] N91-29858

STORMS (METEOROLOGY)
DAR(3)E-1 evaluation: Assessment of weather forecasts made using the DAR(3)E-1 workstation
[PB91-181701] N91-29693

STRAIN DISTRIBUTION
Effect of fortifier on compression-after-impact strength of carbon fabric reinforced epoxy
[NAE-LTR-ST-1736] N91-29237

STRAIN GAGES
Instrumentation for ASE experiments in the dynamic wind tunnel
[PD-FC-9112] N91-29197
Strain gauge cabling, conditioning, and sensitivity calculations for the CT-114 (Tutor) aircraft aft fuselage and empennage full-scale fatigue test
[NAE-LTR-ST-1758] N91-29534
Description of computer programs used to analyze and plot Spectrapot data files
[NAE-ST-557] N91-29744

STRAIN HARDENING
Fundamental studies in dynamic plasticity
[AD-A237114] N91-29621

STRAIN RATE
Strengthening mechanisms, creep, and fatigue processes in dispersion hardened niobium alloy
[AD-A237784] N91-29313
High strain rate characterization of ceramics in shear
[AD-A238319] N91-29365
Deformation behavior of pre-shocked copper as a function of strain rate and temperature
[DE91-015180] N91-29620
Fundamental studies in dynamic plasticity
[AD-A237114] N91-29621

STRATEGY
SDI performance and START constraints: Modeling phase-1 defense engagements
[DE91-013305] N91-29849

STRATIFICATION
The evolution and structure of homogeneous stably stratified sheared turbulence N91-29499

STRATOSPHERE RADIATION
Protecting the ozone shield: A new public policy
[AD-A237640] N91-29659

STRATUS CLOUDS
An observational study of the efficiency of activation of accumulation-mode particles in warm continental stratiform clouds
[DE91-013335] N91-29681

STREAK CAMERAS
VISAR: Line-imaging interferometer
[DE91-014749] N91-29542

STREAMS
Experimental study of cross-stream mixing in a cylindrical duct
[NASA-TM-105180] N91-29187

STRESS (PHYSIOLOGY)
Physiological responses to intermittent exercise as modified by heat stress and protective clothing
[AD-A237447] N91-29716

STRESS (PSYCHOLOGY)
Predicting performance breakdown in pilots through objective measures of stress sensitivity
[AD-A237540] N91-29725
Predicting performance breakdown in pilots through objective measures of stress sensitivity
[AD-A238597] N91-29731

STRESS ANALYSIS
An analysis of the wear behavior of SiC whisker reinforced alumina from 25 to 1200 C
[NASA-TM-104489] N91-29235
Effect of fiber-matrix debonding on notched strength of titanium metal matrix composites
[NASA-TM-104131] N91-29239
Determining stresses in composites
[AD-A238618] N91-29249
Microtube strip heat exchanger
[DE91-015223] N91-29529
A layered beam theory for single lap joints
[AD-A237324] N91-29607
Prediction of edge stresses in layered media using the surface integral-finite element technique N91-29614
Probabilistic lifetime strength of aerospace materials via computational simulation
[NASA-CR-187178] N91-29629

STRESS CYCLES
Experimental stress measurements for the modified Indal Series 6400 VAWT
[NAE-LTR-LA-310] N91-29642

STRESS DISTRIBUTION
Effect of a free surface on stress distribution in a bimaterial composite
[PB91-185116] N91-29251

STRESS INTENSITY FACTORS
Prediction of edge stresses in layered media using the surface integral-finite element technique N91-29614

STRESS MEASUREMENT
Experimental stress measurements for the modified Indal Series 6400 VAWT
[NAE-LTR-LA-310] N91-29642
Description of computer programs used to analyze and plot Spectrapot data files
[NAE-ST-557] N91-29744

STRESS RELAXATION
The growth of ultrathin epitaxial intermetallic films
[AD-A237798] N91-30011

STRESS TENSORS
The atomic strain tensor
[AD-A237287] N91-29877
Fluidlike studies of the sheath and presheath regions of a plasma
[DE91-013343] N91-29944

STRESS-STRAIN RELATIONSHIPS
Elastic-plastic constitutive relations at large strain
[DE91-013195] N91-29612

STRESSES
Anisotropic tensile probabilistic failure criterion for composites
[AD-A237601] N91-29244
A layered beam theory for single lap joints
[AD-A237324] N91-29607

STRETCHING
Effects of anisotropy on dynamic tensile behavior
[DE91-014748] N91-29632

STRONTIUM COMPOUNDS
Consolidation and plasticity of Bi-Sr-Ca-Cu-O superconductors
[DE91-015544] N91-30028

STRUCTURAL ANALYSIS
Compendium of material test results on HY-100 and pseudo HY-100 metals in support of US Navy programs
[DE91-013134] N91-29292
Modeling and response analysis of thin-walled beam structures constructed of advanced composite materials N91-29615
Vibration control and optimization in composite structural elements by use of add-on viscoelastic materials
[AD-A238533] N91-29628
Dimensionless parameters important to the prediction of vortex-induced vibration of long, flexible cylinders in ocean currents
[PB91-184713] N91-29630

STRUCTURAL DESIGN
A brief overview of the activities and accomplishments of the Metals and Ceramics Division
[DE91-014955] N91-29296
Structural optimization with pseudo-load approach exploiting design length scales N91-29616

STRUCTURAL ENGINEERING
Engineering applications of neural computing: A state-of-the-art survey
[AD-A237628] N91-29803

STRUCTURAL MEMBERS
Review of Canadian aeronautical fatigue work: 1987-1989
[NAE-LTR-ST-1706] N91-29165

STRUCTURAL STABILITY
Experimental demonstration of a classical approach for flexible space structure control: NASA CSI testbeds
[NASA-CR-188724] N91-29212

STRUCTURAL VIBRATION
Equations of motion for a flexible spacecraft-lumped parameter idealization
[NASA-CR-188727] N91-29211
Structural optimization with pseudo-load approach exploiting design length scales N91-29616
Integrated structural damping and control system design for high-order flexible systems N91-29617
Finite element-based system identification from experimental modal analysis results N91-29618

STUDENTS
Marketing for collegiate aviation education
[NIAR-91-18] N91-30042

STYRENES
Organo- borazines.3.homo- and copolymerization of p-vinylphenyl- cyclotri- borazines
[AD-A237881] N91-29357

SUBROUTINE LIBRARIES (COMPUTERS)
Portable parallel programming
[DE91-015648] N91-29794

SUBROUTINES
ZLIB: A numerical library for differential algebra and Lie algebraic treatment of beam dynamics
[DE91-014875] N91-29746

SUBSONIC FLOW
Subsonic aerodynamic coefficients of the SDM at angles of attack up to 90 deg
[NAE-LTR-UA-93] N91-29144
Preliminary flight-determined subsonic lift and drag characteristics of the X-29A forward-swept-wing airplane
[NASA-TM-100409] N91-29177

SUBSTRATES
Determining stresses in composites
[AD-A238618] N91-29249
Development of low-threshold value, high-power semiconductor laser
[AD-A237183] N91-29566
Preparation of damage resistant optical coatings on flat substrates
[DE91-013588] N91-29916
Inverse problem in neutron reflection
[DE91-014457] N91-29984
Growth condition dependence of RHEED pattern from GaAs(111)B surface
[DE91-014770] N91-29986

SULFUR
Study of particle correlations in high energy S + Pb and Pb + Pb interactions with a magnetic-interferometric-emulsion-chamber
[DE91-014355] N91-29897

SULFUR FLUORIDES
Experimental and analytical study of laser-triggering in the Rimfire switch
[DE91-014662] N91-29483
Laser triggered spark gap modeling
[DE91-014831] N91-29557

SULFUR ISOTOPES
Study of particle correlations in high energy S + Pb and Pb + Pb interactions with a magnetic-interferometric-emulsion-chamber
[DE91-014355] N91-29897

SUPERCOMPUTERS
ZLIB: A numerical library for differential algebra and Lie algebraic treatment of beam dynamics
[DE91-014875] N91-29746
NRL review, 1989-1990
[AD-A238612] N91-29856

SUPERCONDUCTING FILMS
High temperature superconductor analog electronics for millimeter-wavelength communications
[NASA-TM-105184] N91-29982
Ac susceptibility of superconductive thin films
[DE91-015273] N91-29993

SUPERCONDUCTING MAGNETS
The ASTROMAG superconducting magnet facility configured for a free flying satellite
[DE91-014710] N91-29204
Minimization of refrigeration power requirements for mechanical supports in cryogenic systems
[DE91-015720] N91-29392
Measurements of retractable gas-cooled 6061 aluminum electrical leads operating in a vacuum
[DE91-014617] N91-29444
Cognition and the brain
[AD-A237846] N91-29727
Intermetallic superconductors: The state of development in 1991
[DE91-014844] N91-30026

SUPERCONDUCTING SUPER COLLIDER
Sliding mode controller of RF cavity tuning loop
[DE91-015461] N91-29410
ZLIB: A numerical library for differential algebra and Lie algebraic treatment of beam dynamics
[DE91-014875] N91-29746

SUPERCONDUCTIVITY
Synthesis and characterization of reduced tungsten sulfide cluster complexes
[DE91-014916] N91-29282
Superconductivity induced by very high magnetic fields: Thermodynamic and transport properties
[DE91-015327] N91-29481
The ac losses in type-2 superconductors
[DE91-015201] N91-29485
Superconducting instrumentation for precision measurement and control
[DE91-014650] N91-29541
Theoretical high energy physics
[DE90-012527] N91-29904
Specific heat of YBaCu3O7: Volume fraction of superconductivity; parameters characteristic of the ideal superconducting state
[DE91-011827] N91-29974

Large bipolarons and superconductivity
| DE91-014699 | N91-29985
Synthesis and superconductivity in Ba(1-x)K(x)BiO3
| DE91-015254 | N91-29992
Superconducting superoxygenated La(2-x)Sr(x)CuO(4 + delta): Search for phase separation
| DE91-015334 | N91-29995
Intermetallic superconductors: The state of development in 1991
| DE91-014844 | N91-30026

SUPERCONDUCTORS
Superconductivity induced by very high magnetic fields: Thermodynamic and transport properties
| DE91-015327 | N91-29481
The ac losses in type-2 superconductors
| DE91-015201 | N91-29485
Inelastic scattering in condensed matter with high intensity Moessbauer radiation
| DE91-014384 | N91-29980
De Haas-van Alphen and Fermi surface studies of organic superconductors (ET)2X
| DE91-015137 | N91-29987
Epitaxial growth of single crystal diamond on silicon
| AD-A237758 | N91-30007
Monolithic integration of semiconductor and superconductor components
| AD-A237946 | N91-30012
Intermetallic superconductors: The state of development in 1991
| DE91-014844 | N91-30026
Anisotropic spin susceptibility of the (Y,Ca),(Ba, La)2Cu4O8 system
| DE91-014593 | N91-30032

SUPERCRITICAL FLUIDS
Thermophysical properties of supercritical fluids and fluid mixtures
| DE91-015794 | N91-30041

SUPERCRITICAL PRESSURES
Equation of state for pure sodium chloride
| DE91-014618 | N91-29286

SUPERFLUIDITY
Mixed valent and heavy ferimons and related systems
| DE91-015454 | N91-29900

SUPERHIGH FREQUENCIES
A high power cross-field amplifier at X-Band
| DE91-013277 | N91-29441
InP and InGaAs submicron gate microwave power transistors for 20 GHz applications
| AD-A238595 | N91-29473

SUPERLATTICES
Research in the physical sciences with application to the free electron laser
| AD-A237884 | N91-29571
InGaAs/GaAs graded superlattices in photodetectors for wavelengths beyond 1 micron
| DE90-012073 | N91-29969
Dielectric function of semiconductor superlattice
| DE91-617788 | N91-29976
High-resolution Z-contrast imaging of superlattices and heterostructures
| DE91-015329 | N91-29994
Defect reductions in epitaxial growth using superlattice buffer layers
| AD-A237710 | N91-30005
Growth, nitrogen vacancy reduction and solid solution formation in cubic GaN thin films and the subsequent fabrication of superlattice structures using AlN and InN
| AD-A238521 | N91-30021

SUPERNOVAE
Research in nuclear astrophysics: Stellar collapse and supernovae
| DE91-015449 | N91-30066

SUPERSONIC COMBUSTION
Supersonic combustion of a transverse injected H2 jet in a radio frequency heated flow
| DE91-014739 | N91-29281

SUPERSONIC COMBUSTION RAMJET ENGINES
Hydrogen-fueled scramjet investigation
| AD-A237569 | N91-29183

SUPERSONIC FLOW
Exact and approximate solutions to the oblique shock equations for real-time applications
| NASA-CR-187173 | N91-29147
Hydrogen-fueled scramjet investigation
| AD-A237569 | N91-29183
Supersonic combustion of a transverse injected H2 jet in a radio frequency heated flow
| DE91-014739 | N91-29281
Fundamental studies of the extraction process in inductively coupled plasma mass spectrometry
| DE90-011733 | N91-29939

SUPERSONIC JET FLOW
Progress toward synergistic hypermixing nozzles
| NASA-TM-105169 | N91-29150

SUPERSYMMETRY
Supercoherent states and physical systems
| DE91-014598 | N91-30040

SURFACE CRACKS
The molecular view of plastic deformation and precursor processes of crazing in glassy polypropylene and polycarbonate
| AD-A237333 | N91-29346

SURFACE DEFECTS
Temperature dependence of proton electroreduction kinetics at gold(111) and (210) surfaces
| AD-A237460 | N91-29879
Surface structure and surface order
| AD-A237466 | N91-30001

SURFACE FINISHING
Influence of diamond turning and surface cleaning processes on the degradation of KDP crystal surfaces
| DE91-015300 | N91-30035

SURFACE LAYERS
Temperature dependence of proton electroreduction kinetics at gold(111) and (210) surfaces
| AD-A237460 | N91-29879

SURFACE PROPERTIES
Effect of a free surface on stress distribution in a bimaterial composite
| PB91-185116 | N91-29251
Molecular dynamics simulation of the effect of interfaces in melting and solid-state amorphization
| DE91-015550 | N91-29284
Mechanistic investigation of nanometer-scale/lithography at liquid-covered graphite surfaces
| AD-A237085 | N91-29337
Effect of two synthetic lubricants on life of AISI 9310 spur gears
| NASA-TM-104352 | N91-29599
Relating ocean acoustic ambient to ocean surface dynamics
| AD-A237167 | N91-29699
Scanning tunneling microscopy studies of the surfaces of a-Si:H and a-SiGe:H films
| DE91-002169 | N91-29983
Growth condition dependence of RHEED pattern from GaAs(111)B surface
| DE91-014770 | N91-29986
High resolution electron energy loss studies of surface vibrations
| DE91-014539 | N91-30024

SURFACE REACTIONS
Pulse induced nanlithography of graphite in H2O: A road to chemical linkages to the surface?
| AD-A237086 | N91-29338
Atomic-resolution scanning tunneling microscopy and infrared spectroscopy as combined in-situ probes of electrochemical adlayer structure: Carbon monoxide on rhodium(111)
| AD-A237508 | N91-29884
Electron tunneling microscopy
| AD-A237504 | N91-30003

SURFACE ROUGHNESS
Influence of diamond turning and surface cleaning processes on the degradation of KDP crystal surfaces
| DE91-015300 | N91-30035

SURFACE STABILITY
TOVS satellite soundings of the ERICA IOP-2 cyclone
| AD-A237998 | N91-29686

SURFACE TEMPERATURE
Using the TIMS to estimate evapotranspiration from a forest
| NASA-CR-188729 | N91-29636
Remote determination of soil moisture and evapotranspiration from thermal infrared measurements: Detection of a drying threshold
| PB91-195818 | N91-29641
Multiple channel satellite analysis of cirrus
| AD-A238054 | N91-29687
The nature of the propagation of sea breeze fronts in central California
| AD-A238635 | N91-29692

SURFACE VEHICLES
Objective assessments of mobility with an early Unmanned Ground Vehicle (UGV) prototype viewing system
| AD-A237317 | N91-29595
Maglev system concept using 20-K high-temperature superconductors and hyperconductors
| DE91-015714 | N91-29860

SURFACE WAVES
Modeling a rain-induced mixed layer
| AD-A238022 | N91-29702

SURGES
A compact 200 kV pulse transformer system
| DE91-014669 | N91-29479
On the application of edge wave theory to terrain-bounded cold surges: A numerical study N91-29670

SURVEYS
GPS: Aspects of pseudo-range positioning offshore N91-29161
A survey of optical diagnostic methods for the study of fuel fouling
| AD-A237361 | N91-29920

SURVIVAL
Confidence bands for the median survival time as a function of the covariates in the Cox model
| AD-A237626 | N91-29835

SURVIVAL EQUIPMENT
Donning times and flotation characteristics of infant life preservers: Four representative types
| AD-A237120 | N91-29153

SWEPT FORWARD WINGS
Preliminary flight-determined subsonic lift and drag characteristics of the X-29A forward-swept-wing airplane
| NASA-TM-100409 | N91-29177

SWIRLING
Combustion stability limits and planar imaging of swirl-stabilized flames N91-29262
Modification of the 'TEACH' computer code for use in a study of swirling turbulent flows
| DE91-010492 | N91-29496

SWITCHES
High gain photoconductive semiconductor switching
| DE91-014668 | N91-29478
Computational simulations of plasma flow switches and imploding loads
| DE91-014768 | N91-29480
Low-jitter, high-voltage, infrared, laser-triggered, vacuum switch
| DE91-014602 | N91-29562
A general graphical user interface for automatic reliability modeling
| NASA-TM-104068 | N91-29745
Plasma flow switch experiments on the Pegasus facility
| DE91-014744 | N91-29954

SWITCHING
Physics and applications of the lock-on effect
| DE91-014670 | N91-29446
High gain photoconductive semiconductor switching
| DE91-014668 | N91-29478
Gaseous prebreakdown processes that are important for pulsed power switching
| DE91-015902 | N91-29487
The MIT Alewife machine: A large-scale distributed-memory multiprocessor
| AD-A237705 | N91-29784
Electro-optic line narrowing of optical parametric oscillators
| AD-D014944 | N91-29934

SWITCHING CIRCUITS
Optical Multiple Access Network (OMAN) for advanced processing satellite applications
| NASA-TM-105167 | N91-29431
Digital SPC switching technology: Foreign technology assessment
| AD-A237258 | N91-29449
The charge-exchange neutral problem and the code NEUTRAL
| AD-A237889 | N91-29464

SWITCHING THEORY
Application of Multi-Frequency Modulation (MFM) for high-speed data communications to a voice frequency channel
| AD-A238019 | N91-29422

SYMBOLIC PROGRAMMING
A Workshop on the Integration of Numerical and Symbolic Computing Methods
| AD-A238601 | N91-29774

SYNAPSES
Hardware Implementation of Neuron Nets and Synapses Workshop
| AD-A237704 | N91-29718

SYNCHRONISM
Hardware interface for high speed video imaging
| AD-D014902 | N91-29400
APRIL: A processor architecture for multiprocessing
| AD-A237476 | N91-29739
Verification of the FtCayuga fault-tolerant microprocessor system. Volume 1: A case study in theorem prover-based verification
| NASA-CR-4381 | N91-29778
Asynchronous design for parallel processing architectures
| AD-A237696 | N91-29783
Performance implications of synchronization support for parallel FORTRAN programs
| AD-A238493 | N91-29790
Data abstraction, concurrency and synchronization in Sina
| PB91-185454 | N91-30053

SYNCHROTRON RADIATION
The APS radio frequency test stand control system
[DE91-015711] N91-29434
Synchrotron studies of narrow band materials
[DE91-014826] N91-30025
SYNCHROTRONS
Technical activities 1990, Electron and Optical Physics Div.
[PB91-194423] N91-29858
Synchrotron studies of narrow band materials
[DE91-014826] N91-30025
SYNTHESIS (CHEMISTRY)
A theoretical and experimental study of unimolecular and biomolecular radical hydrogen transfer reactions
[DE91-012607] N91-29261
Synthesis and characterization of reduced tungsten sulfide cluster complexes
[DE91-014916] N91-29282
Synthesis of multifilament silicon carbide fibers by chemical vapor deposition
[NASA-CR-188725] N91-29331
Organometallic precursor routes to Si-C-Al-O-N ceramics
[AD-A237753] N91-29355
Boron nitride and silicon nitride systems
[AD-A238080] N91-29359
Synthesis and superconductivity in Ba(1-x)K(x)BiO3
[DE91-015254] N91-29992
SYNTHETIC APERTURE RADAR
Comparison of synthetic aperture radar autofocus techniques: Phase gradient vs subaperture
[DE91-014696] N91-29406
P-3 SAR calibration activity at Andros Island
[AD-A237357] N91-29412
Portable 45-gigahertz radar for glint and scintillation studies
[AD-A238005] N91-29421
SYSTEM FAILURES
A methodology for developing physical system fault diagnostic aids
[DE91-015533] N91-29809
SYSTEM IDENTIFICATION
Finite element-based system identification from experimental modal analysis results N91-29618
SYSTEMS ANALYSIS
Multipixel multidimensional laser radar system theory
[AD-A238110] N91-29573
An expert system approach to global fault detection and isolation design
[AD-A238494] N91-29808
SYSTEMS ENGINEERING
Commonwealth Advisory Aeronautical Research Council. First Canadian newsletter on systems, 1989
[NAE-LTR-FR-108] N91-29139
Assessment team report on flight-critical systems research at NASA Langley Research Center
[NASA-CR-181850] N91-29176
Analog computation in neural systems: Architectures and complexity
[AD-A237856] N91-29785
Design and hardware implementation of neural systems
[AD-A237703] N91-29804
SYSTEMS INTEGRATION
Assessment team report on flight-critical systems research at NASA Langley Research Center
[NASA-CR-181850] N91-29176
A Workshop on the Integration of Numerical and Symbolic Computing Methods
[AD-A238601] N91-29774
Telescope and sensor interface preliminary requirements report for the PORTS chamber
[AD-A237755] N91-29923
SYSTEMS MANAGEMENT
The PC Dugout micro-mainframe integration system: PAX implementation
[AD-A237480] N91-29758

T

TABLES (DATA)
Activation calculations for trapped protons below 200 MeV: Appendix
[NASA-CR-184170] N91-29865
Lowell proper motion survey: Southern Hemisphere (Giclas, Burnham, and Thomas 1978). Documentation for the machine-readable version
[NASA-TM-105069] N91-30060
TAIL ASSEMBLIES
Tutor aft fuselage and empennage full-scale test: Procedures for creating a damage log
[NAE-ST-576] N91-29167
Strain gauge cabling, conditioning, and sensitivity calculations for the CT-114 (Tutor) aircraft aft fuselage and empennage full-scale fatigue test
[NAE-LTR-ST-1758] N91-29534
TAKEOFF
Aircraft operations from runways with inclined ramps (ski-jump)
[AD-A237265] N91-29171
The design and construction of a shiplaunched VTOL unmanned air vehicle
[AD-A238053] N91-29173
TAKEOFF RUNS
Aircraft operations from runways with inclined ramps (ski-jump)
[AD-A237265] N91-29171
TARGET ACQUISITION
Detection of targets in terrain clutter by using multispectral infrared image processing
[AD-A237436] N91-29414
Use of an extended Kalman filter
[AD-A238639] N91-29474
TARGET RECOGNITION
Multi-sensor feature level fusion
[AD-A237106] N91-29411
The effect of three levels of laser glare on the speed and accuracy of target location performance when viewing a briefly presented visual array
[AD-A238565] N91-29736
Invariant target recognition using self-organizing networks
[AD-A238252] N91-29807
A survey of techniques in Aided Target Recognition (ATR) from digital and optical perspectives
[AD-A238644] N91-30052
TARGETS
A Doppler bin blanking CFAR processor for airborne radars
[AD-A237890] N91-29418
Hypervelocity impact jet formation
[DE91-014651] N91-29619
SDI performance and START constraints: Modeling phase-1 defense engagements
[DE91-013305] N91-29849
TASK COMPLEXITY
Optimal iterative task scheduling for parallel simulations
[AD-A238631] N91-29791
TEA LASERS
Second-harmonic generation of TEA CO2 10.6 micrometer laser light in AgGaS2 crystals
[AD-A237169] N91-29564
TECHNOLOGIES
JPRS report: Science and technology. USSR: Materials science
[JPRS-UMS-91-001] N91-29291
TECHNOLOGY ASSESSMENT
Metal injection moulding: A brief review
[NAE-LTR-ST-531] N91-29289
Digital SPC switching technology: Foreign technology assessment
[AD-A237258] N91-29449
Engineering applications of neural computing: A state-of-the-art survey
[AD-A237628] N91-29803
Intermetallic superconductors: The state of development in 1991
[DE91-014844] N91-30026
High-(Tc) superconductors: Fabricating technologies and future perspectives
[DE91-015553] N91-30029
TECHNOLOGY TRANSFER
A brief overview of the activities and accomplishments of the Metals and Ceramics Division
[DE91-014955] N91-29296
Technology transfer: A new program between Sandia National Laboratories and the University of New Mexico
[DE91-015439] N91-30058
TECHNOLOGY UTILIZATION
Worldwide wind/diesel hybrid power system study: Potential applications and technical issues
[DE91-002160] N91-29643
Second Review of the Department of Energy's Inertial Confinement Fusion Program
[DE91-013157] N91-29945
TECTONICS
Regional tectonic deformation in Southern California, inferred from terrestrial geodesy and the global positioning system N91-29669
TELECOMMUNICATION
Signal processing in impulsive electromagnetic interference
[AD-A237612] N91-29416
Coding for spread-spectrum channels in the presence of jamming
[AD-A238233] N91-29425
A high data rate communications system using long pulses
[AD-D014947] N91-29430
Digital SPC switching technology: Foreign technology assessment
[AD-A237258] N91-29449
TELEPHONY
Application of Multi-Frequency Modulation (MFM) for high-speed data communications to a voice frequency channel
[AD-A238019] N91-29422
TELESCOPES
Telescope and sensor interface preliminary requirements report for the PORTS chamber
[AD-A237755] N91-29923
TELEVISION SYSTEMS
Adaptive liquid crystal TV based joint transform correlator as applied to real-time pattern recognition
[AD-A238576] N91-29931
TEMPERATURE
Studies of polymers for shock absorption applications
[AD-A237925] N91-29358
Singularities in Gaussian random fields
[AD-A238220] N91-29839
TEMPERATURE CONTROL
Design of a stabilized, dc-powered analog laser diode driver
[AD-A238596] N91-29577
TEMPERATURE DEPENDENCE
Equation of state for pure sodium chloride
[DE91-014618] N91-29286
Deformation behavior of pre-shocked copper as a function of strain rate and temperature
[DE91-015180] N91-29620
Effects of solar heating by aerosols and trace gases on the temperature structure constant
[AD-A237675] N91-29677
Temperature dependence of proton electroreduction kinetics at gold(111) and (210) surfaces
[AD-A237460] N91-29879
High temperature thermoelectric properties of boron carbide
[DE91-015848] N91-30037
TEMPERATURE EFFECTS
Intermetallics: Canadian perspective
[NAE-LTR-ST-1771] N91-29288
Strengthening mechanisms, creep, and fatigue processes in dispersion hardened niobium alloy
[AD-A237784] N91-29313
Energy conserving coating: Pigment research
[AD-A237841] N91-29356
Environmental effects in niobium base alloys and other selected intermetallic compounds
[AD-A237535] N91-29658
TEMPERATURE GRADIENTS
Effects of high-intensity solar radiation on carbon fibers
[DE91-015485] N91-29252
TEMPERATURE MEASUREMENT
Thermophysical properties of POCO AXF-5Q graphite up to melting
[DE91-014751] N91-29334
TENSILE PROPERTIES
Effects of high-intensity solar radiation on carbon fibers
[DE91-015485] N91-29252
Tensile properties and microstructure of Alloy 718 thermally aged to 50,000 h
[DE91-014099] N91-29299
Effects of anisotropy on dynamic tensile behavior
[DE91-014748] N91-29632
TENSILE STRENGTH
Anisotropic tensile probabilistic failure criterion for composites
[AD-A237601] N91-29244
Microstructural and strength stability of CVD SiC fibers in argon environment
[NASA-TM-103772] N91-29250
Mechanical properties of Fe3Al-based alloys
[DE91-015322] N91-29324
Environmental effects in niobium base alloys and other selected intermetallic compounds
[AD-A237535] N91-29658
TENSILE TESTS
Compendium of material test results on HY-100 and pseudo HY-100 metals in support of US Navy programs
[DE91-013134] N91-29292
Modelling of deformation textures evolution in semi-crystalline polymers
[AD-A237288] N91-29342
TENSOR ANALYSIS
Determining stresses in composites
[AD-A238618] N91-29249
The atomic strain tensor
[AD-A237287] N91-29877

TERMINAL BALLISTICS
A simple model for low L/D penetration physics
[DE91-015747] N91-29633
TERNARY ALLOYS
Properties of materials with a fine length scale: Mechanically alloyed metals and the high temperature superconductor Y1Ba2Cu3O7
[DE91-012538] N91-29975
TERRAIN
Detection of targets in terrain clutter by using multispectral infrared image processing
[AD-A237436] N91-29414
TEST EQUIPMENT
Cable tester
[AD-D014904] N91-29438
TEST STANDS
The APS radio frequency test stand control system
[DE91-015711] N91-29434
TETHERING
Twenty first century space propulsion study addendum
[AD-A238011] N91-29225
TEXTILES
An investigation to determine the producibility of a 3-D braider and bias direction weaving loom
[NASA-CR-188741] N91-29390
THEMATIC MAPPING
A practical example of forest mapping and timber volume estimation using LANDSAT-5 TM imagery
[INPE-5244-PRE/1675] N91-29635
THEORETICAL PHYSICS
Research in elementary particle physics
[DE91-015359] N91-29892
Theoretical high energy physics
[DE90-012527] N91-29904
Theoretical high energy physics
[DE91-013639] N91-29905
A research program in experimental and theoretical high energy physics
[DE91-014728] N91-29907
Establishment of an Institute for Fusion Studies
[DE91-014922] N91-29956
THERMAL ABSORPTION
A survey of optical diagnostic methods for the study of fuel fouling
[AD-A237361] N91-29920
THERMAL ANALYSIS
Arcjet thermal characteristics
[NASA-TM-105156] N91-29231
Organo- borazines.3.homo- and copolymerization of p-vinylphenyl- cyclotri- borazines
[AD-A237881] N91-29357
THERMAL BATTERIES
Pyrite cathode material for a thermal battery
[AD-D014945] N91-29475
THERMAL CONDUCTIVITY
High temperature thermoelectric properties of boron carbide
[DE91-015848] N91-30037
THERMAL EMISSION
Thermal emittance enhancement of graphite-copper composites for high temperature space based radiators
[NASA-TM-105178] N91-29332
Lithium ion source for satellite charge control
[AD-A238272] N91-29470
Multi-sensor image interpretation using laser radar and thermal images
[AD-A238245] N91-29576
THERMAL ENVIRONMENTS
Slag and thermal environment of a spinning rocket motor
[AD-A238557] N91-29227
Micro SAINT modeling of physiological and human performance in the heat
[AD-A238659] N91-29719
THERMAL EXPANSION
Application of ceramics to industrial gas turbines
[DE91-013140] N91-29330
THERMAL FATIGUE
Deformation and thermal fatigue in high temperature austenitic alloys
[DE91-014981] N91-29305
THERMAL PROTECTION
Donning times and flotation characteristics of infant life preservers: Four representative types
[AD-A237120] N91-29153
Debris/ice/TPS assessment and photographic analysis for Shuttle Mission STS-40
[NASA-TM-103822] N91-29210
THERMAL STABILITY
Tensile properties and microstructure of Alloy 718 thermally aged to 50,000 h
[DE91-014099] N91-29299
THERMISTORS
Design of a stabilized, dc-powered analog laser diode driver
[AD-A238596] N91-29577
THERMOCHEMISTRY
Thermochemistry of hydrocarbon decomposition and relationship to properties of PECVD diamond films
[AD-A237793] N91-29274
Lithium combustion: A review
[AD-A238154] N91-29279
Atomic approaches to defect thermochemistry
[AD-A238260] N91-29280
THERMODYNAMIC EQUILIBRIUM
Description of the Strategic High-Altitude Atmospheric Radiation Code (SHARC)
[AD-A237089] N91-29671
Surface structure and surface order
[AD-A237466] N91-30001
THERMODYNAMIC PROPERTIES
A computer program for prediction of internal performance of a ramrocket
[AD-A238179] N91-29226
Picosecond studies of chemical intermediates
[AD-A237859] N91-29275
High temperature mass spectrometric study of the thermodynamics of liquid nickel-aluminium alloys at 2000 K
[MRL-TR-91-15] N91-29290
Superconductivity induced by very high magnetic fields: Thermodynamic and transport properties
[DE91-015327] N91-29481
Ocean thermal feature recognition, discrimination and tracking using infrared satellite imagery
[AD-A238138] N91-29703
Study of energy levels and decay mechanisms for Singlet Rydberg states of molecular nitrogen
[AD-A238156] N91-29885
Vibrational, mechanical, and thermal properties of III-V semiconductors
[AD-A237785] N91-30008
Determination of thermodynamic and kinetic properties of grain boundaries using high temperature calorimetry
[DE91-015571] N91-30031
THERMODYNAMICS
Solvent-dependent redox thermodynamics of metal amine complexes. The delineation of specific solvation effects
[AD-A237503] N91-29272
Synthesis of multifilament silicon carbide fibers by chemical vapor deposition
[NASA-CR-188725] N91-29331
Numerical prediction of turbulent oscillating flow and associated heat transfer
[NASA-CR-187177] N91-29524
Measurement of a three-dimensional hypersonic density field using holographic interferometry N91-29539
THERMOELECTRIC GENERATORS
Materials research for sodium engine development
[DE91-015715] N91-29378
THERMOELECTRICITY
High temperature thermoelectric properties of boron carbide
[DE91-015848] N91-30037
THERMOGRAVIMETRY
TGA experimental data analyzed by transpiration theory
[NIAR-91-21] N91-29263
THERMOLUMINESCENCE
Neutron dosimetry using optically stimulated luminescence
[DE91-015781] N91-29902
THERMOMECHANICAL TREATMENT
Deformation induced microstructural and microchemical changes during thermomechanical treatment
[DE91-014862] N91-29319
THERMONUCLEAR REACTIONS
Establishment of an Institute for Fusion Studies
[DE91-014922] N91-29956
Research in nuclear astrophysics: Stellar collapse and supernovae
[DE91-015449] N91-30066
THERMOPHYSICAL PROPERTIES
The use of high velocity launchers for scientific and engineering studies
[DE91-015564] N91-29208
Thermophysical properties of POCO AXF-5Q graphite up to melting
[DE91-014751] N91-29334
Thermophysical properties of supercritical fluids and fluid mixtures
[DE91-015794] N91-30041
THERMOPLASTICITY
Impact characterization of graphite fiber reinforced thermoplastic laminates
[NIAR-91-16] N91-29241
THERMOREGULATION
Micro SAINT modeling of physiological and human performance in the heat
[AD-A238659] N91-29719
THICKNESS
Effect of cladding thickness on attenuation in uniformly curved single-mode optical fibers
[AD-A238034] N91-29928
THIN FILMS
Determining stresses in composites
[AD-A238618] N91-29249
Thermochemistry of hydrocarbon decomposition and relationship to properties of PECVD diamond films
[AD-A237793] N91-29274
Synthesis of diamond films by microwave generated pulsed plasmas
[AD-A237228] N91-29341
Effect of excess oxydianiline on the properties of polyimide
[AD-A237467] N91-29351
Effects of interfacial modification on diamond film adhesion
[AD-A237750] N91-29354
Ceramic decomposition under irradiation
[DE91-015061] N91-29372
Fundamental studies of chemical vapor deposition diamond growth processes
[DE91-015324] N91-29374
Infrared and Raman spectra of C60 and C70 solid films at room temperature
[AD-A237880] N91-29462
Aspects of fatigue and rapid depolarization in the film PZT capacitors
[DE91-014904] N91-29484
Simulation of the growth of Mo/Si multilayers
[DE91-015679] N91-29486
Scanning tunneling microscopy studies of the surfaces of a-Si:H and a-SiGe:H films
[DE91-002169] N91-29983
Inverse problem in neutron reflection
[DE91-014457] N91-29984
Ac susceptibility of superconductive thin films
[DE91-015273] N91-29993
Center for thin film studies
[AD-A237457] N91-29999
Growth, characterization, and device development in monocrystalline diamond films
[AD-A237463] N91-30000
The growth of ultrathin epitaxial intermetallic films
[AD-A237798] N91-30011
Atomic layer epitaxy group IV materials: Surface processes, thin films, devices and their characterization
[AD-A238506] N91-30019
Growth, nitrogen vacancy reduction and solid solution formation in cubic GaN thin films and the subsequent fabrication of superlattice structures using AlN and InN
[AD-A238521] N91-30021
TEM characterization of grain boundaries in mixed bicrystal films of aluminum
[DE91-016267] N91-30038
THIN WALLS
Modeling and response analysis of thin-walled beam structures constructed of advanced composite materials N91-29615
THREE DIMENSIONAL BODIES
Matching of complex 3-D surfaces using dynamic programming
[ERB-1022] N91-29743
Analytical calculation of neutral transport and its effect on ions
[DE91-015908] N91-29896
THREE DIMENSIONAL BOUNDARY LAYER
Three-dimensional mapping of atmospheric boundary layer structure and winds with a high performance lidar
[AD-A238098] N91-29678
THREE DIMENSIONAL FLOW
Three-dimensional vortex dynamics and interactions in near-wall turbulent boundary layers
[AD-A237413] N91-29507
THREE DIMENSIONAL MODELS
Theoretical studies of long-range transport of oxidants
[PB91-182360] N91-29661
Three-dimensional visualization for evaluating automated, geomorphic pattern-recognition analyses of crustal structures
[DE91-012929] N91-29668
The atomic strain tensor
[AD-A237287] N91-29877
THREE DIMENSIONAL MOTION
Conformal FDTD modeling wake fields
[DE91-015129] N91-29407
THRESHOLDS (PERCEPTION)
The effects of luminance boundaries on color perception
[AD-A237794] N91-29925
THROATS
Effect of geometric parameters on the performance of second throat annular steam ejectors
[AD-A238645] N91-29522

THROTTLING
Controlling crippled aircraft-with throttles
[NASA-TM-104238] N91-29191
THRUST
Divergence thrust loss calculations for convergent-divergent nozzles: Extensions to the classical case
[NASA-TM-105176] N91-29181
THRUST CONTROL
Controlling crippled aircraft-with throttles
[NASA-TM-104238] N91-29191
A simulation evaluation of a four-engine jet transport using engine thrust modulation for flightpath control
[NASA-TM-4324] N91-29194
THRUST MEASUREMENT
The design and construction of a shiplaunched VTOL unmanned air vehicle
[AD-A238053] N91-29173
THRUSTORS
Performance and optimization of a derated ion thruster for auxiliary propulsion
[NASA-TM-105144] N91-29229
THUNDERSTORMS
DAR(3)E-1 evaluation: Assessment of weather forecasts made using the DAR(3)E-1 workstation
[PB91-181701] N91-29693
TIDES
Oceanographic data report Number 7: Data from the Delaware Estuary SCENIC cruises, April 1986 - September 1988
[PB91-183582] N91-29706
TILTED PROPELLERS
The design and construction of a shiplaunched VTOL unmanned air vehicle
[AD-A238053] N91-29173
TIME DEPENDENCE
The boundary element method applied to the two dimensional Stefan moving boundary problem
[AD-A238458] N91-29828
H-mode energy confinement scaling from the ASDEX, DIII-D, and jet tokamaks
[DE91-015145] N91-29957
TIME DISCRIMINATION
Ocean thermal feature recognition, discrimination and tracking using infrared satellite imagery
[AD-A238138] N91-29703
TIME DIVISION MULTIPLEXING
The study of space communications spread spectrum systems. Part 1: Saw-based joint group demodulation of frequency shift keyed and differential phase shift keyed signals
[QU-90-1-PT-1] N91-29395
TIME MEASUREMENT
Ocean thermal feature recognition, discrimination and tracking using infrared satellite imagery
[AD-A238138] N91-29703
TIME OF FLIGHT SPECTROMETERS
Reactions of small molecular systems
[DE91-014519] N91-29867
TIME SERIES ANALYSIS
Analysis of nonGaussian, nonlinear time series with long-memory
[AD-A237847] N91-29822
The asymptotic distributions of autoregressive coefficients
[AD-A238538] N91-29831
TIME SHARING
Performance implications of synchronization support for parallel FORTRAN programs
[AD-A238493] N91-29790
TIN ALLOYS
Lead-free solders for electronics applications: Wetting analysis
[DE91-014900] N91-29320
TIROS N SERIES SATELLITES
TOVS satellite soundings of the ERICA IOP-2 cyclone
[AD-A237998] N91-29686
TITANIUM
Effect of fiber-matrix debonding on notched strength of titanium metal matrix composites
[NASA-TM-104131] N91-29239
Annealing effects on the microstructure of titanium electrical contacts on diamond films
[DE91-010150] N91-29327
Long-term testing and evaluation of cathode components in a commercial aluminum cell, volume 1
[DE90-010896] N91-29436
Effects of anisotropy on dynamic tensile behavior
[DE91-014748] N91-29632
TITANIUM ALLOYS
First principles simulations of metallic alloys and liquids
[DE91-015171] N91-29323
TITANIUM BORIDES
Very high temperature fibers of TiC and TiB2
[AD-A237423] N91-29242
TITANIUM CARBIDES
Very high temperature fibers of TiC and TiB2
[AD-A237423] N91-29242
TITRATION
An elevated temperature titration calorimeter
[DE91-015765] N91-29548
TOKAMAK DEVICES
ICRF edge modeling
[DE91-014401] N91-29403
Identification of, and transition to, the second region of ideal MHD stability in tokamaks
[DE90-010380] N91-29938
Total magnetic reconnection during a tokamak major disruption
[DE91-013637] N91-29949
Advanced divertor experiments on DIII-D
[DE91-011138] N91-29950
H-mode energy confinement scaling from the ASDEX, DIII-D, and jet tokamaks
[DE91-015145] N91-29957
Detection of coherent structures in the edge of the TEXT tokamak plasma
[DE91-015183] N91-29958
Thick-section weldments in 21-6-9 and 316LN stainless steel for fusion energy applications
[DE91-015307] N91-29963
Fundamental studies of fusion plasmas
[DE91-015656] N91-29964
Impurity and neutral effects on the dissipative drift wave in tokamak edge plasmas
[DE91-015907] N91-29965
TOLUENE
A theoretical and experimental study of unimolecular and biomolecular radical hydrogen transfer reactions
[DE91-012607] N91-29261
TOMOGRAPHY
A study of the relationship between macroscopic measures and physical processes occurring during N00014-89-J-1708
[AD-A238423] N91-29627
Alignment of tomographic projections using an incomplete set of fiducial markers
[AD-A238536] N91-29772
TOPOGRAPHY
Topographic map reading
[AD-A238026] N91-29640
Three-dimensional visualization for evaluating automated, geomorphic pattern-recognition analyses of crustal structures
[DE91-012929] N91-29668
Stochastic modelling of seafloor morphology
[AD-A237063] N91-29697
Cognition and the brain
[AD-A237846] N91-29727
TORCHES
An evaluation of nickel-aluminum coatings fabricated with the plasma-spray process
[DE91-013208] N91-29328
TOROIDAL PLASMAS
The BNL toroidal volume H(-) source
[DE91-013592] N91-29947
The effects of magnetic field errors on reversed field pinch plasma
[DE91-013636] N91-29948
Advanced divertor experiments on DIII-D
[DE91-011138] N91-29950
TOUGHNESS
Mechanisms of transformation toughening
[DE91-013151] N91-29293
Lightweight disk alloy development
[AD-A237064] N91-29309
TRACE ELEMENTS
Methods for determination of low-molecular weight carbonyl compounds in the ambient atmosphere
[DE91-015188] N91-29656
TRAILING EDGES
Translation of airfoil trailing edge noise article from Revue d'Acoustique
[AD-A237811] N91-29143
Experimental and analytical study of rippled trailing edge airfoils for compressor application
[AD-A237425] N91-29508
TRAJECTORIES
The functional dependence of trajectory dispersion on initial condition errors
[DE91-014661] N91-29151
Bubble generation and movement under microgravity conditions
[NAE-LTR-FR-110] N91-29388
TRAJECTORY ANALYSIS
Use of an extended Kalman filter
[AD-A238639] N91-29474
Explosively driven missile trajectory parameters for various fragment materials and velocities
[DE91-014330] N91-29631
TRAJECTORY CONTROL
Motion planning for manipulators with excessive degrees of freedom N91-29592
TRAJECTORY PLANNING
Performance models for robot manipulators N91-29590
Research and development at ORNL/CESAR towards cooperating robotic systems for hazardous environments
[DE91-015638] N91-29810
TRANSCONDUCTANCE
Molecular beam epitaxial growth and characterization of metastable compound semiconductors for infrared detector applications
[AD-A237797] N91-30010
TRANSFER FUNCTIONS
On the interpolation properties of feedforward layered neural networks
[AD-A238035] N91-29824
TRANSFORMATIONS (MATHEMATICS)
Analytical and numerical methods; advanced computer concepts
[DE91-014526] N91-29795
TRANSFORMERS
A compact 200 kV pulse transformer system
[DE91-014669] N91-29479
TRANSITION FLOW
Effects of 1, 2, 3, and 4 Hz imposed bulk flow oscillations on transition in a straight channel with 40 to 1 aspect ratio
[AD-A237988] N91-29517
TRANSITION METALS
Properties of materials with a fine length scale: Mechanically alloyed metals and the high temperature superconductor Y1Ba2Cu3O7
[DE91-012538] N91-29975
TRANSITION TEMPERATURE
Specific heat of YBaCu3O7: Volume fraction of superconductivity; parameters characteristic of the ideal superconducting state
[DE91-011827] N91-29974
De Haas-van Alphen and Fermi surface studies of organic superconductors (ET)2X
[DE91-015137] N91-29987
TRANSLATING
The language for DENOTE (Denotational Semantics Translation Environment)
[AD-A237144] N91-29750
TRANSLATIONAL MOTION
Equations of motion for a flexible spacecraft-lumped parameter idealization
[NASA-CR-188727] N91-29211
TRANSMITTANCE
Description of the Strategic High-Altitude Atmospheric Radiation Code (SHARC)
[AD-A237089] N91-29671
Worldwide maritime infrared atmospheric transmittance data
[AD-A237292] N91-29672
XTRAN: An atmospheric transmittance code based on XSCALE
[AD-A237624] N91-29674
TRANSMITTER RECEIVERS
A high data rate communications system using long pulses
[AD-D014947] N91-29430
TRANSMITTERS
Combinatorial FSK modulation for power-efficient high-rate communications
[NASA-TM-105188] N91-29404
A high data rate communications system using long pulses
[AD-D014947] N91-29430
Design of a stabilized, dc-powered analog laser diode driver
[AD-A238596] N91-29577
TRANSPIRATION
TGA experimental data analyzed by transpiration theory
[NIAR-91-21] N91-29263
TRANSPORT AIRCRAFT
Composite transport wing technology development: Design development tests and advanced structural concepts
[NASA-CR-4177] N91-29253
Test results for composite specimens and elements containing joints and cutouts
[NASA-CR-178246] N91-29254
TRANSPORT PROPERTIES
Electronic and ionic transport in processable conducting polymers
[AD-A238175] N91-29362
Superconductivity induced by very high magnetic fields: Thermodynamic and transport properties
[DE91-015327] N91-29481

Analytical calculation of neutral transport and its effect on ions
[DE91-015908] N91-29896
Thermophysical properties of supercritical fluids and fluid mixtures
[DE91-015794] N91-30041

TRANSPORT THEORY
TGA experimental data analyzed by transpiration theory
[NIAR-91-21] N91-29263
Parametric design calculations using Green's function to determine unique source
[DE91-014683] N91-29861

TRAPPED PARTICLES
Activation calculations for trapped protons below 200 MeV: Appendix
[NASA-CR-184170] N91-29865

TRAVELING SALESMAN PROBLEM
An exact two-matching based branch and bound algorithm for the symmetric traveling salesman problem
[AD-A237878] N91-29823

TRIENES
Mechanism of anionic ring-opening polymerization of silacyclopent 3-enes
[AD-A237538] N91-29353

TRIGGER CIRCUITS
Physics and applications of the lock-on effect
[DE91-014670] N91-29446
Experimental and analytical study of laser-triggering in the Rimfire switch
[DE91-014662] N91-29483

TROPICAL REGIONS
Equatorial entrainment zone simulations
[AD-A237234] N91-29657
A global geographic information system data base of storm occurrences and other climatic phenomena affecting coastal zones
[DE91-014949] N91-29682

TROPICAL STORMS
Tropical cyclone motion in the northwest Pacific Ocean, phase 1
[AD-A237455] N91-29683

TROPOSPHERE
Methods for determination of low-molecular weight carbonyl compounds in the ambient atmosphere
[DE91-015188] N91-29656
Use of the implicit-finite-difference method to implement the parabolic equation model
[AD-A237437] N91-29819

TUBE HEAT EXCHANGERS
Prediction of the pressure drop in transverse, repeated-rib tubes with numerical modeling
[DE91-014465] N91-29503

TUBES
Proceedings of the First Switch Tube Advanced Technology Meeting
[DE91-012634] N91-29440
Measurements of retractable gas-cooled 6061 aluminum electrical leads operating in a vacuum
[DE91-014617] N91-29444
Microtube strip heat exchanger
[DE91-015223] N91-29529

TUNGSTEN
The magnetron-enhanced etching of double-level tungsten interconnect
[DE91-014984] N91-29306
Low-jitter, high-voltage, infrared, laser-triggered, vacuum switch
[DE91-014602] N91-29562

TUNGSTEN COMPOUNDS
Synthesis and characterization of reduced tungsten sulfide cluster complexes
[DE91-014916] N91-29282

TURBINE BLADES
Rejuvenation of service exposed alloy 713C turbine blades
[NAE-LTR-ST-1716] N91-29179
Modification of axial-flow compressor stall margin by variation of stationary blade setting angles
[AD-A238406] N91-29186
Application of ceramics to industrial gas turbines
[DE91-013140] N91-29330
Theoretical study of the flow in a rotating duct. Experimental study through flow visualization in a curved duct
[RAE-TRANS-2189] N91-29493
Analysis of a teetered, variable-speed rotor
[DE91-002190] N91-29646

TURBINE PUMPS
Bearing tester data compilation analysis, and reporting and bearing math modeling
[NASA-CR-178883] N91-29603

TURBINES
Lightweight disk alloy development
[AD-A237064] N91-29309

TURBOCOMPRESSORS
Compressor fault modelling for engine health monitoring: Review and recommendations
[NRC-TR-ENG-004] N91-29178

TURBOFAN ENGINES
A linear control design structure to maintain loop properties during limit operation in a multi-nozzle turbofan engine
[NASA-TM-105163] N91-29188

TURBOFANS
Calculated performance of the NASA Lewis icing research tunnel
[NASA-TM-105173] N91-29199

TURBOMACHINERY
Unsteady force calculations in turbomachinery
[AD-A237937] N91-29515

TURBULENCE
Shock acceleration with turbulence minimization
[DE91-014741] N91-29505

TURBULENT BOUNDARY LAYER
Three-dimensional vortex dynamics and interactions in near-wall turbulent boundary layers
[AD-A237413] N91-29507
Polymer drag reduction of a zero pressure gradient boundary layer
[AD-A237572] N91-29510

TURBULENT FLOW
Theoretical study of the flow in a rotating duct. Experimental study through flow visualization in a curved duct
[RAE-TRANS-2189] N91-29493
Modification of the 'TEACH' computer code for use in a study of swirling turbulent flows
[DE91-010492] N91-29496
Shockwave considerations for sub-grid closure modeling in turbulent large eddy simulations
[DE91-015142] N91-29506
Three-dimensional vortex dynamics and interactions in near-wall turbulent boundary layers
[AD-A237413] N91-29507
Effects of 1, 2, 3, and 4 Hz imposed bulk flow oscillations on transition in a straight channel with 40 to 1 aspect ratio
[AD-A237988] N91-29517
Numerical prediction of turbulent oscillating flow and associated heat transfer
[NASA-CR-187177] N91-29524
Energy generation by a shock crossing a perturbed interface
[DE91-015678] N91-29530
Numerical modeling of turbulent dispersion around structures using a particle-in-cell method
[DE91-012035] N91-29652
Detection of coherent structures in the edge of the TEXT tokamak plasma
[DE91-015183] N91-29958
Interactions of turbulent eddies and combustion in an MHD second stage combustor
[DE91-015722] N91-29968

TURBULENT HEAT TRANSFER
Numerical prediction of turbulent oscillating flow and associated heat transfer
[NASA-CR-187177] N91-29524

TURBULENT JETS
Performance of multiple stream pulsed jet combustion systems
[DE91-012338] N91-29259

TURBULENT MIXING
Energy generation by a shock crossing a perturbed interface
[DE91-015678] N91-29530

TURBULENT WAKES
A method of investigating scales of motion in a turbulent wake
[AD-A237923] N91-29514

TWO DIMENSIONAL FLOW
Solutions of two-dimensional Euler equations with multigrid acceleration
[NAL-PD-CF-9006] N91-29494
A numerical study of flow past a cylindrical body
N91-29497

TWO DIMENSIONAL MODELS
NIKE2D: A nonlinear, implicit, two-dimensional finite element code for solid mechanics
[DE91-015734] N91-29634
Numerical simulation of self-field MPD thrusters
[NASA-CR-187168] N91-29832

TWO PHASE FLOW
Steady flow of a fluid-solid mixture between parallel plates
[DE91-013114] N91-29491
Adiabatic two-phase flow frictional pressure drop. Part 2: A generalized method for data correlation
[DE91-014462] N91-29501
Adiabatic two-phase flow frictional pressure drop. Part 1: Critical parameters and friction factors for air-water mixture
[DE91-014463] N91-29502
An experimental study of plunging liquid jet induced air carryunder and dispersion
[AD-A237757] N91-29511
Use of electrical impedance imaging in two-phase, gas-liquid flows
[DE91-015914] N91-29531

TYPHOONS
Tropical cyclone motion in the northwest Pacific Ocean, phase 1
[AD-A237455] N91-29683

U

U.S.S.R.
JPRS report: Science and technology. USSR: Materials science
[JPRS-UMS-91-001] N91-29291

ULTRAHIGH VACUUM
Effect of excess oxydianiline on the properties of polyimide
[AD-A237467] N91-29351

ULTRASONIC TESTS
Ultrasonic evaluation of elastic and interfacial properties of composite materials and laminates N91-29238
Investigation of ultrasonic evaluation of solid-state metal bond
[DE91-014996] N91-29606
Ultrasonic evaluation of silicon nitride green bodies
[AD-A237924] N91-29608
NDE of ceramics and ceramic composites
[NASA-TM-104520] N91-29610

ULTRAVIOLET EMISSION
Analysis of the ultraviolet emissions of nitric oxide from mid-latitude rocket observations
[AD-A237340] N91-29673

ULTRAVIOLET RADIATION
Ultraviolet reflector materials for solar detoxification of hazardous waste
[DE91-002196] N91-29663

ULTRAVIOLET SPECTRA
Analysis of the ultraviolet emissions of nitric oxide from mid-latitude rocket observations
[AD-A237340] N91-29673

UNDERGROUND EXPLOSIONS
Second Review of the Department of Energy's Inertial Confinement Fusion Program
[DE91-013157] N91-29945

UNDERWATER ACOUSTICS
Relating ocean acoustic ambient to ocean surface dynamics
[AD-A237167] N91-29699

UNDERWATER STRUCTURES
Penn State/ONR Mid Frequency Workshop
[AD-A237982] N91-29420

UNITED STATES
Methodology investigation, aviation test management system concept development
[AD-A237349] N91-29172
Publications of the Executive Office of the President, January 20, 1989 - March 31, 1991
[PB91-156828] N91-30056

UNIVERSITIES
Marketing for collegiate aviation education
[NIAR-91-18] N91-30042

UNIX (OPERATING SYSTEM)
The use of searching algorithms for the minimization of multi-valued logic functions
[AD-A238018] N91-29763

UNSTEADY FLOW
Unsteady force calculations in turbomachinery
[AD-A237937] N91-29515
Transient flowmeter calibration facility
[AD-D014937] N91-29523

URANIUM
Explosively driven missile trajectory parameters for various fragment materials and velocities
[DE91-014330] N91-29631

URUGUAY
A practical example of forest mapping and timber volume estimation using LANDSAT-5 TM imagery
[INPE-5244-PRE/1675] N91-29635

USER MANUALS (COMPUTER PROGRAMS)
NIKE2D: A nonlinear, implicit, two-dimensional finite element code for solid mechanics
[DE91-015734] N91-29634
User's manual for DIODE
[AD-A237190] N91-29752

USER REQUIREMENTS
Ada 9X requirements rationale
[AD-A237350] N91-29755

UTILITIES
Electric rate structures for thermal energy storage evaluation
[DE91-013168] N91-29644

V

VACANCIES (CRYSTAL DEFECTS)
Effect of hydrogen on the electronic structure of a grain boundary in iron
[AD-A237499] N91-30002
VACUUM CHAMBERS
Twenty first century propulsion concept
[AD-A237853] N91-29224
Telescope and sensor interface preliminary requirements report for the PORTS chamber
[AD-A237755] N91-29923
VALENCE
Mixed valent and heavy ferimons and related systems
[DE91-015454] N91-29900
VAPOR DEPOSITION
Thermochemistry of hydrocarbon decomposition and relationship to properties of PECVD diamond films
[AD-A237793] N91-29274
The mixed metallic-ionic clusters of the silver/silver iodide
[AD-A237883] N91-29314
Synthesis of multifilament silicon carbide fibers by chemical vapor deposition
[NASA-CR-188725] N91-29331
Synthesis of diamond films by microwave generated pulsed plasmas
[AD-A237228] N91-29341
Effect of excess oxydianiline on the properties of polyimide
[AD-A237467] N91-29351
Fundamental studies of chemical vapor deposition diamond growth processes
[DE91-015324] N91-29374
Electroforming thin channel heat exchangers
[DE91-015114] N91-29528
Design and hardware implementation of neural systems
[AD-A237703] N91-29804
Preparation of damage resistant optical coatings on flat substrates
[DE91-013588] N91-29916
Fabrication of lightweight Si/SiC LIDAR mirrors
[NASA-CR-4389] N91-29935
Scanning tunneling microscopy studies of the surfaces of a-Si:H and a-SiGe:H films
[DE91-002169] N91-29983
Semiconductor deposition and etching interactions of laser-generated translationally hot atoms and radicals
[AD-A238198] N91-30015
VAPOR PHASES
A technique for measuring the solubilities of gases in liquids
[AD-A238071] N91-29278
The effects of donor-acceptor electronic interactions on the rates of gas-phase metallocene electron-exchange reactions
[AD-A237459] N91-29878
VAPOR PRESSURE
Equation of state for pure sodium chloride
[DE91-014618] N91-29286
VAPORIZERS
Development of an explosive vapor generator
[DE91-015700] N91-29386
VAPORIZING
High temperature Knudsen effusion-mass spectrometric studies of the Y-Ba-Cu-O system
[NIAR-91-23] N91-29981
Semiconductor deposition and etching interactions of laser-generated translationally hot atoms and radicals
[AD-A238198] N91-30015
VAPORS
Analysis of condensation and evaporation of ammonia/water mixtures in matrix heat-exchangers
[DE91-014461] N91-29500
VARIANCE (STATISTICS)
Acoustic background noise variation in Air Force platforms and its effect on noise removal algorithms
[AD-A238279] N91-29863
VARIATIONS
Management of variation and TQM
[AD-A238399] N91-29843
VECTOR SPACES
Approximation from shift-invariant surfaces of L2(IRd)
[AD-A238165] N91-29826
VEGETATIVE INDEX
Remote determination of soil moisture and evapotranspiration from thermal infrared measurements: Detection of a drying threshold
[PB91-195818] N91-29641
VELOCITY
Shock acceleration with turbulence minimization
[DE91-014741] N91-29505
Experimental investigation of adiabatic shear banding at different impact velocities
[AD-A237901] N91-29625
Explosively driven missile trajectory parameters for various fragment materials and velocities
[DE91-014330] N91-29631
VELOCITY DISTRIBUTION
Polymer drag reduction of a zero pressure gradient boundary layer
[AD-A237572] N91-29510
An experimental study of plunging liquid jet induced air carryunder and dispersion
[AD-A237757] N91-29511
The laser ablation of aluminum at 193, 248, and 351 nm
[AD-A237574] N91-29569
Chemical waste disposal in space by plasma discharge
[NASA-CR-184169] N91-29737
Proton deceleration near the surface of an accreting neutron star N91-30063
VELOCITY MEASUREMENT
Full-field Fabry-Perot interferometer
[DE91-014610] N91-29540
Experimental study of gas kinetics of a fast-axial flow kilowatt CO2 laser
[AD-A237178] N91-29565
VERTICAL TAKEOFF AIRCRAFT
The design and construction of a shiplaunched VTOL unmanned air vehicle
[AD-A238053] N91-29173
VERY LARGE SCALE INTEGRATION
A prolog system for converting VHDL-based models to Generalized Extraction System (GES) rules
[AD-A238545] N91-29741
NW lab for integrated systems
[AD-A237118] N91-29749
A vision system model
[AD-A238459] N91-29930
VERY LOW FREQUENCIES
A new system for measurement of low frequency radio transmitting antenna parameters in near real time
[AD-A238555] N91-29429
VESTS
International aviation (selected articles)
[AD-A237232] N91-29142
VIBRATION
Dimensionless parameters important to the prediction of vortex-induced vibration of long, flexible cylinders in ocean currents
[PB91-184713] N91-29630
High resolution electron energy loss studies of surface vibrations
[DE91-014539] N91-30024
VIBRATION DAMPING
Integrated structural damping and control system design for high-order flexible systems N91-29617
Vibration control and optimization in composite structural elements by use of add-on viscoelastic materials
[AD-A238533] N91-29628
VIBRATION ISOLATORS
Integrated structural damping and control system design for high-order flexible systems N91-29617
VIBRATION MODE
Structural optimization with pseudo-load approach exploiting design length scales N91-29616
Finite element-based system identification from experimental modal analysis results N91-29618
VIBRATIONAL SPECTRA
Atomic-resolution scanning tunneling microscopy and infrared spectroscopy as combined in-situ probes of electrochemical adlayer structure: Carbon monoxide on rhodium(111)
[AD-A237508] N91-29884
Vibrational, mechanical, and thermal properties of III-V semiconductors
[AD-A237785] N91-30008
VIDEO DISKS
Video frame store: An advanced solid state recorder
[DE91-015709] N91-29549
VIDEO EQUIPMENT
A real time collimation sensor using a shear plate and a spatial light modulator
[DE90-011362] N91-29914
VIDEO SIGNALS
Hardware interface for high speed video imaging
[AD-D014902] N91-29400
VIEWING
Objective assessments of mobility with an early Unmanned Ground Vehicle (UGV) prototype viewing system
[AD-A237317] N91-29595
VIKING LANDER SPACECRAFT
Concepts for manned lunar habitats
[NASA-TM-104114] N91-30068
VISCOELASTICITY
Dynamic behavior of fully dense molybdenum
[DE91-014902] N91-29304
Vibration control and optimization in composite structural elements by use of add-on viscoelastic materials
[AD-A238533] N91-29628
VISCOUS FLOW
Performance of an airfoil at low Reynolds number
[NAL-PD-CF-9102] N91-29145
Numerical simulation of a viscous vortex ring interaction with a density interface
[DE91-011532] N91-29489
Secondary stability and three-dimensional natural convection in a shallow cavity N91-29495
VISIBILITY
An expert system approach for prediction of maritime visibility obscuration
[AD-A238305] N91-29688
VISION
Psychophysical studies of visual cortical function
[AD-A238663] N91-29720
Design and hardware implementation of neural systems
[AD-A237703] N91-29804
A vision system model
[AD-A238459] N91-29930
VISUAL ACUITY
Institute for the Study of Human Capabilities: Summary descriptions of research for the period December 1989 through September 1990
[AD-A237767] N91-29726
VISUAL PERCEPTION
The functional architecture of visual object recognition
[AD-A238617] N91-29732
The effect of three levels of laser glare on the speed and accuracy of target location performance when viewing a briefly presented visual array
[AD-A238565] N91-29736
The effects of luminance boundaries on color perception
[AD-A237794] N91-29925
VLASOV EQUATIONS
Vlasov simulations of very-large-amplitude wave generation in the plasma wakefield accelerator
[AD-A237428] N91-29961
Towards a realistic plasma simulation code
[DE91-015698] N91-29967
VOICE COMMUNICATION
Very low bit rate voice for packetized mobile applications
[DE91-015333] N91-29409
A high data rate communications system using long pulses
[AD-D014947] N91-29430
VOICE DATA PROCESSING
Research and development for Digital Voice Processing (DVP)
[AD-A238280] N91-29427
VOIDS
High-energy backscattered electron imaging of voids in aluminum metallizations
[DE91-014895] N91-29303
VOLT-AMPERE CHARACTERISTICS
Annealing effects on the microstructure of titanium electrical contacts on diamond films
[DE91-010150] N91-29327
VOLTAGE CONVERTERS (DC TO DC)
Introduction of a current waveform, waveshaping technique to limit conduction loss in high-frequency dc-dc converters suitable for space power
[AD-A237903] N91-29465
VOLTERRA EQUATIONS
The boundary element method applied to the two dimensional Stefan moving boundary problem
[AD-A238458] N91-29828
VORTEX RINGS
Numerical simulation of a viscous vortex ring interaction with a density interface
[DE91-011532] N91-29489
VORTEX SHEDDING
Numerical study of non-impulsively started flow around a circular cylinder
[AD-A238051] N91-29519
Dimensionless parameters important to the prediction of vortex-induced vibration of long, flexible cylinders in ocean currents
[PB91-184713] N91-29630
VORTICES
Numerical simulation of a viscous vortex ring interaction with a density interface
[DE91-011532] N91-29489

Theoretical study of the flow in a rotating duct. Experimental study through flow visualization in a curved duct
[RAE-TRANS-2189] N91-29493
Interactions of turbulent eddies and combustion in an MHD second stage combustor
[DE91-015722] N91-29968

VORTICITY
Forcasting tropical cyclone recurvature using an empirical othogonal function representation of vorticity fields
[AD-A238489] N91-29689

W

WAFERS
Silicon Wafer Advanced Packaging (SWAP). Multichip Module (MCM) foundry study, version 2
[AD-A237412] N91-29452
Development of model based magnetic LP-LEC growth large diameter GaAs
[AD-A237456] N91-29998
Formation of CoSi2 in SIMOX wafers by high dose Co implantation
[DE91-015639] N91-30036

WAKES
Conformal FDTD modeling wake fields
[DE91-015129] N91-29407
Visualization of wake fields
[DE91-015130] N91-29408

WALKING
Compliant walker
[NASA-CASE-GSC-13348-2] N91-29714

WALL FLOW
Progress toward synergistic hypermixing nozzles
[NASA-TM-105169] N91-29150
Secondary stability and three-dimensional natural convection in a shallow cavity N91-29495

WALLS
Computational simulations of plasma flow switches and imploding loads
[DE91-014768] N91-29480
Kinetics of dark reaction in chemical laser gases
[DE91-015320] N91-29579

WARFARE
A framework for understanding the strategic defense initiatives' software debates
[AD-A237193] N91-29852

WARNING SYSTEMS
Video frame store: An advanced solid state recorder
[DE91-015709] N91-29549

WASTE DISPOSAL
The observational approach in environmental restoration
[DE91-015528] N91-29666

WASTE TREATMENT
Ultraviolet reflector materials for solar detoxification of hazardous waste
[DE91-002196] N91-29663
The observational approach in environmental restoration
[DE91-015528] N91-29666

WASTE UTILIZATION
The observational approach in environmental restoration
[DE91-015528] N91-29666

WATER
Donning times and flotation characteristics of infant life preservers: Four representative types
[AD-A237120] N91-29153
Seasonal air and water mass redistribution and its effect on satellite and polar motion N91-29202
Mechanistic investigation of nanometer-scale/lithography at liquid-covered graphite surfaces
[AD-A237085] N91-29337
Pulse induced nanlithography of graphite in H2O: A road to chemical linkages to the surface?
[AD-A237086] N91-29338
Hydrogen productivity by photosynthetic water splitting
[DE90-012211] N91-29380
Analysis of condensation and evaporation of ammonia/water mixtures in matrix heat-exchangers
[DE91-014461] N91-29500
Adiabatic two-phase flow frictional pressure drop. Part 1: Critical parameters and friction factors for air-water mixture
[DE91-014463] N91-29502

WATER SPLITTING
Hydrogen productivity by photosynthetic water splitting
[DE90-012211] N91-29380

WATER VAPOR
Using the TIMS to estimate evapotranspiration from a forest
[NASA-CR-188729] N91-29636

WATERSHEDS
Using the TIMS to estimate evapotranspiration from a forest
[NASA-CR-188729] N91-29636

WAVE ATTENUATION
Effect of cladding thickness on attenuation in uniformly curved single-mode optical fibers
[AD-A238034] N91-29928

WAVE DIFFRACTION
Review of nondiffracting Bessel beams
[NASA-CR-187188] N91-29917

WAVE DISPERSION
Magnetic fluctuations due to thermally excited Alfven waves
[DE90-011790] N91-29940

WAVE EQUATIONS
Review of nondiffracting Bessel beams
[NASA-CR-187188] N91-29917

WAVE EXCITATION
High-intensity and high-energy laser interactions with single droplets
[AD-A238197] N91-29575

WAVE GENERATION
Vlasov simulations of very-large-amplitude wave generation in the plasma wakefield accelerator
[AD-A237428] N91-29961

WAVE INTERACTION
Investigation of the flame-acoustic wave interaction during axial solid rocket instabilities
[AD-A237851] N91-29223

WAVE PROPAGATION
Investigation of the flame-acoustic wave interaction during axial solid rocket instabilities
[AD-A237851] N91-29223
Development of a mixture for nonlinear wave propagation in fiber-reinforced composites
[AD-A237471] N91-29243
Analysis of radio frequency radiation from a propagating electron beam
[AD-A237941] N91-29419
A mesoscopic linear accelerator driven by superintense subpicosecond laser pulses
[DE91-015941] N91-29913
Review of nondiffracting Bessel beams
[NASA-CR-187188] N91-29917
Optical soliton source
[AD-D014942] N91-29933
Magnetic fluctuations due to thermally excited Alfven waves
[DE90-011790] N91-29940
Spatial propagation of squeezed light in a degenerate parametric amplifier
[DE91-014989] N91-30039

WAVEGUIDE LASERS
Blackbody pumped CO2 lasers using Gaussian and waveguide cavities
[DE91-012494] N91-29559
An optically activated modulator and GaAs-GaAlAs compound semiconductor channel waveguide
[AD-A238642] N91-30023

WAVEGUIDES
A high power cross-field amplifier at X-Band
[DE91-013277] N91-29441
A circuit model for an inductive strip in homogeneous finline
[AD-A238001] N91-29466
Hamiltonian 3-D ray tracing in the oceanic waveguide on the ellipsoidal earth
[AD-A237458] N91-29700
A mesoscopic linear accelerator driven by superintense subpicosecond laser pulses
[DE91-015941] N91-29913
Major achievements during the first program year
[AD-A237171] N91-29919

WEAK INTERACTIONS (FIELD THEORY)
High energy physics: Experimental, Theoretical, and Phenomenology Institute
[DE91-015737] N91-29912

WEAR
An analysis of the wear behavior of SiC whisker reinforced alumina from 25 to 1200 C
[NASA-TM-104489] N91-29235

WEATHER
Worldwide maritime infrared atmospheric transmittance data
[AD-A237292] N91-29672

WEATHER FORECASTING
Space-based Doppler lidar sampling strategies: Algorithm development and simulated observation experiments
[NASA-CR-184172] N91-29554
An investigation of the ERICA IOP-2 cyclone using the NORAPS model
[AD-A237683] N91-29684
An expert system approach for prediction of maritime visibility obscuration
[AD-A238305] N91-29688
Forcasting tropical cyclone recurvature using an empirical othogonal function representation of vorticity fields
[AD-A238489] N91-29689
DAR(3)E-1 evaluation: Assessment of weather forecasts made using the DAR(3)E-1 workstation
[PB91-181701] N91-29693
Toward a new National Weather Service: A first report
[PB91-184077] N91-29694

WEAVING
An investigation to determine the producibility of a 3-D braider and bias direction weaving loom
[NASA-CR-188741] N91-29390

WEIBULL DENSITY FUNCTIONS
A goodness-of-fit test for a family of two parameter Weibulls with known shape using minimum distance estimation of parameters
[AD-A238633] N91-29847

WEIGHT (MASS)
Load tables for the Avery and Gilmore standard force machines corrected for gravity, 1989
[NAE-LTR-ST-1703] N91-29535

WEIGHTLESSNESS
The 0-G experiments with advanced ceramic fabric wick structures
[DE91-015531] N91-29377

WELDABILITY
Analysis of weld metal solidification and microstructures
[DE91-014574] N91-29301

WELDED JOINTS
Analysis of weld metal solidification and microstructures
[DE91-014574] N91-29301
Microstructural development in HSLA-100 steel weld metals
[AD-A237931] N91-29315
Thick-section weldments in 21-6-9 and 316LN stainless steel for fusion energy applications
[DE91-015307] N91-29963

WELDING
JPRS report: Science and technology. USSR: Materials science
[JPRS-UMS-91-001] N91-29291
Thick-section weldments in 21-6-9 and 316LN stainless steel for fusion energy applications
[DE91-015307] N91-29963

WHISKER COMPOSITES
An analysis of the wear behavior of SiC whisker reinforced alumina from 25 to 1200 C
[NASA-TM-104489] N91-29235

WHITE NOISE
Acoustic background noise variation in Air Force platforms and its effect on noise removal algorithms
[AD-A238279] N91-29863

WICKS
The 0-G experiments with advanced ceramic fabric wick structures
[DE91-015531] N91-29377

WIGGLER MAGNETS
Evolution of a finite pulse of radiation in a high-power free-electron laser
[AD-A237427] N91-29568

WIND (METEOROLOGY)
Seasonal air and water mass redistribution and its effect on satellite and polar motion N91-29202
Numerical modeling of turbulent dispersion around structures using a particle-in-cell method
[DE91-012035] N91-29652
The nature of the propagation of sea breeze fronts in central California
[AD-A238635] N91-29692
Investigations in Martian geology. Part 1: Nature of the mantling deposit in the heavily cratered terrain of northeastern Arabia, Mars. Part 2: Experimental studies of clean and dust-or-sand-covered ice sublimation under Mars-like conditions N91-30067

WIND EFFECTS
Seasonal air and water mass redistribution and its effect on satellite and polar motion N91-29202

WIND MEASUREMENT
NAE Twin Otter operations in the 1988 Eulerian model evaluation field study
[NAE-LTR-FR-107] N91-29651

WIND PROFILES
NAE Twin Otter operations in the 1988 Eulerian model evaluation field study
[NAE-LTR-FR-107] N91-29651

WIND SHEAR
Equatorial entrainment zone simulations
[AD-A237234] N91-29657

WIND TUNNEL APPARATUS
A wind tunnel smoke generator
[NAE-LTR-LA-312] N91-29195
Instrumentation for ASE experiments in the dynamic wind tunnel
[PD-FC-9112] N91-29197
WIND TUNNEL TESTS
Subsonic aerodynamic coefficients of the SDM at angles of attack up to 90 deg
[NAE-LTR-UA-93] N91-29144
A wind tunnel smoke generator
[NAE-LTR-LA-312] N91-29195
Instrumentation for ASE experiments in the dynamic wind tunnel
[PD-FC-9112] N91-29197
Carina aerothermal test at Mach 8
[AD-A238561] N91-29218
WIND TUNNELS
Instrumentation for ASE experiments in the dynamic wind tunnel
[PD-FC-9112] N91-29197
Horizontal axis wind turbine post stall airfoil characteristics synthesization
[DE91-002198] N91-29650
WIND TURBINES
Hierarchic extensions in the static and dynamic analysis of elastic beams N91-29613
Experimental stress measurements for the modified Indal Series 6400 VAWT
[NAE-LTR-LA-310] N91-29642
Analysis of a teetered, variable-speed rotor
[DE91-002190] N91-29646
Horizontal axis wind turbine post stall airfoil characteristics synthesization
[DE91-002198] N91-29650
WIND VELOCITY
Wind and flux calculations of the NAE Twin Otter
[NAE-LTR-FR-109] N91-29189
Space-based Doppler lidar sampling strategies: Algorithm development and simulated observation experiments
[NASA-CR-184172] N91-29554
WINDPOWER UTILIZATION
Worldwide wind/diesel hybrid power system study: Potential applications and technical issues
[DE91-002160] N91-29643
Analysis of a teetered, variable-speed rotor
[DE91-002190] N91-29646
WINDPOWERED GENERATORS
Experimental stress measurements for the modified Indal Series 6400 VAWT
[NAE-LTR-LA-310] N91-29642
WINGS
AEROWING - The software for aerodynamic analysis of a large aspect-ratio finite wing at low speeds
[NAL-PD-CF-9101] N91-29146
Composite transport wing technology development: Design development tests and advanced structural concepts
[NASA-CR-4177] N91-29253
A novel epoxy lacquer for high strength steel in F-111 aircraft during overhaul
[AD-A236828] N91-29326
WIRE
Fabrication and wire extrusion of ceramic superconductors
[DE91-015207] N91-29991
WORKING FLUIDS
Light weight space power reactors for nuclear electric propulsion
[DE91-014803] N91-29232
Application of ceramics to industrial gas turbines
[DE91-013140] N91-29330
WORKLOADS (PSYCHOPHYSIOLOGY)
Physiological responses to intermittent exercise as modified by heat stress and protective clothing
[AD-A237447] N91-29716
Predicting performance breakdown in pilots through objective measures of stress sensitivity
[AD-A237540] N91-29725
WORKSTATIONS
A general lease-squares fitting package for the sun workstation
[AD-A238180] N91-29837
WURTZITE
Vibrational, mechanical, and thermal properties of III-V semiconductors
[AD-A237785] N91-30008

X

X RAY APPARATUS
A slit aperture for the Monitoring X ray Experiment (MOXE)
[DE91-013317] N91-29538
X RAY ASTRONOMY
A slit aperture for the Monitoring X ray Experiment (MOXE)
[DE91-013317] N91-29538
X RAY DIFFRACTION
Synthesis and characterization of reduced tungsten sulfide cluster complexes
[DE91-014916] N91-29282
An investigation of the as-quenched and early aging characteristics of a Al - 4.1 wt. percent Li binary alloy by x ray diffraction
[AD-A237598] N91-29311
Corrosion behavior of continuous-filament-wound ceramic composite tubes
[DE91-014959] N91-29370
Deconvolution of x ray diffraction data to elucidate plastic deformation mechanisms in the uniaxial extension of bulk Nylon-6
[AD-A237332] N91-29623
X RAY IMAGERY
Plasma properties of hot coronal loops utilizing coordinated SMM and solar research rocket observations
[NASA-CR-186094] N91-29937
X RAY LASERS
The MIT short-wavelength laser project
[DE91-015357] N91-29582
X RAY SCATTERING
X ray reflectivity studies of Au surfaces
[DE91-015308] N91-29307
X RAY SOURCES
Future explosive pulse-power technology for high-energy plasma physics experiments
[DE91-014601] N91-29951
Plasma and electrical diagnostics for Procyon experiments
[DE91-014736] N91-29952
Computational modeling of the Trailmaster Procyon system
[DE91-014765] N91-29955
Proton deceleration near the surface of an accreting neutron star N91-30063
X RAY SPECTRA
Electron-ion interaction cross sections determined by x ray spectroscopy on EBIT
[DE91-015786] N91-29903
X RAY SPECTROSCOPY
Preparation and properties of new inorganic glasses and gel-derived solids
[AD-A238095] N91-29360
Electron-ion interaction cross sections determined by x ray spectroscopy on EBIT
[DE91-015786] N91-29903
X RAYS
A slit aperture for the Monitoring X ray Experiment (MOXE)
[DE91-013317] N91-29538
Photoelectron and photoionization pumping of XUV lasers by laser-produced plasmas N91-29558
Technical activities 1990, Electron and Optical Physics Div.
[PB91-194423] N91-29858
Computational modeling of the Trailmaster Procyon system
[DE91-014765] N91-29955
X-29 AIRCRAFT
Preliminary flight-determined subsonic lift and drag characteristics of the X-29A forward-swept-wing airplane
[NASA-TM-100409] N91-29177

Y

YTTRIUM OXIDES
Photoemission and electronic structure studies of YBa2Cu3O(x)
[DE91-014469] N91-29979
High temperature Knudsen effusion-mass spectrometric studies of the Y-Ba-Cu-O system
[NIAR-91-23] N91-29981
Photoemission measurement of Fermi surface, band dispersion, and quasiparticle lifetime in YBa2Cu3O6.9
[DE91-015194] N91-29989
Anisotropic spin susceptibility of the (Y,Ca),(Ba, La)2Cu4O8 system
[DE91-014593] N91-30032

Z

ZETA PINCH
Procyon experiments utilizing explosively-formed fuse opening switches
[DE91-014742] N91-29953
ZINCBLENDE
Vibrational, mechanical, and thermal properties of III-V semiconductors
[AD-A237785] N91-30008
ZIRCALOYS (TRADEMARK)
Characteristics of autoclave and in-reactor nodular corrosion of Zircaloys
[DE91-013600] N91-29294
ZIRCONIUM OXIDES
Corrosion behavior of continuous-filament-wound ceramic composite tubes
[DE91-014959] N91-29370

Typical Personal Author Index Listing

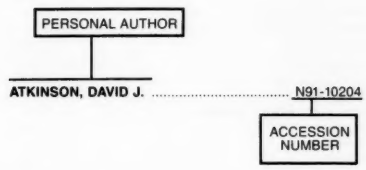

Listings in this index are arranged alphabetically by personal author. The accession number denotes the number by which the citation is identified.

A

AAMODT, R. E. N91-29964
ABBOTT, L. F. N91-29892
ABDELMALEK, N. N. N91-29811
ABERNATHY, D. L. N91-29307
ADAMS, DONALD F. N91-29247
ADAMS, P. A. N91-29534
ADAMS, REGINALD C. N91-29852
ADOLF, D. N91-29379
AGARWAL, ANANT N91-29739
N91-29784
AGGARWAL, J. K. N91-29576
AGIM, Y. Z. N91-29940
AGUIAR, H. N91-29444
AHZI, S. N91-29342
AITKEN, J. N91-29160
AITKEN, JOHN N91-29388
AKABANI, G. N91-29893
AKLONIS, J. J. N91-29349
N91-29350
N91-29352
AKLUFI, M. N91-29341
AKSAY, I. A. N91-29376
AKSIT, M. N91-30053
ALBERT, TERENCE R. N91-29448
ALBIN, GARY N91-29278
ALBRITTON, J. R. N91-29946
ALESSI, J. G. N91-29947
ALEXANDER, D. J. N91-29963
ALEXANDER, MILLARD H. N91-29889
ALLEM, R. N91-29179
ALLEN, CHRISTOPHER W. N91-29357
ALLEN, JONATHAN N91-29458
ALLEN, M. S. N91-30058
ALLEN, S. M. N91-29808
ALLEN, SUSAN M. N91-29246
ALLISTON-GREINER, A. F. N91-29596
ALMAGRI, A. N91-29960
ALMAGRI, A. F. N91-29948
ALTON, G. D. N91-29864
ALTUNISIK, ADNAN N91-29771
AMBROSIANO, J. N91-29962
AMIROUCHE, FARID M. N91-29597
ANDERKO, A. N91-29286
ANDERSON, B. N91-29954
ANDERSON, B. G. N91-29952
ANDERSON, D. V. N91-29967
ANDERSON, H. U. N91-29978
ANDERSON, J. V. N91-29649
ANDERSON, T. J. N91-29183
ANDERSON, T. W. N91-29831
ANG, J. A. N91-29619
ANIK, SADUN N91-29790
ANSON, D. N91-29330
ANTOLOVICH, STEPHEN D. N91-29627
ANTONIAK, Z. I. N91-29377
AREND, LAWRENCE E. N91-29721
ARGON, A. S. N91-29342
N91-29343
N91-29344
N91-29345
ARGON, ALI S. N91-29270
N91-29340
N91-29346
N91-29347
N91-29622
N91-29623
ARKO, A. J. N91-29979
N91-29989
ARMAN, B. N91-29500
N91-29503
ARMSTRONG, JEFFREY H. N91-29509
ARREGUIN, STEVE N91-29233
ASAY, J. R. N91-29203
N91-29208
ASELAGE, T. L. N91-29260
N91-30037
ASPNES, JAMES N91-29780
ASSADI, S. N91-29959
N91-29960
ATTERIDGE, D. G. N91-29319
AUCHAMPAUGH, G. N91-29200
AULD, B. A. N91-29472
AUTREY, T. N91-29261
AVERY, MARK N91-29452

B

BABCOCK, S. N91-29585
BACA, W. E. N91-29910
BACHMANN, KLAUS J. N91-30000
BAI, T. N91-29381
BAILLIE, S. W. N91-29190
BAIRD, JAMES K. N91-29737
BAK, MICHAEL N91-29614
BAKER, JOHN A. N91-29546
BALACHANDRAN, U. N91-29991
BALDESCHWIELER, JOHN D. N91-30003
BALDWIN, D. E. N91-29956
BALDWIN, R. H. N91-29324
BALES, BARNEY L. N91-29891
BALKO, B. A. N91-29264
BALLINGER, C. T. N91-29869
BANERJEE, P. N91-29769
BANERJEE, PARTHA P. N91-29463
BANGERT, JOHN A. N91-30069
BANGMIN, ZHANG N91-29564
BANKS, DAVID J. N91-29421
BARBEE, T. W., JR. N91-29972
BARBER, T. J. N91-29183
BARBER, THOMAS J. N91-29508
BARGER, V. N91-29912
BARKER, L. M. N91-29203
BARNES, G. A. N91-29562
BAROCK, RICHARD T. N91-29698
BARTHOLOMEW, C. H. N91-29285
BARTLETT, R. J. N91-29979
BARTSCH, R. R. N91-29954
BARTY, CHRISTOPHER PETER JAMES N91-29558
BASSO, G. N91-29196
BAST, CALLIE C. N91-29629
BASU, S. N91-29582
BATES, J. L. N91-30027
BATES, J. M. N91-29377
BATES, L. B. N91-29522
BATY, R. S. N91-29151
BEAVIS, L. N91-29440
BECK, N. J. N91-29584
BECKMAN, T. M. N91-29382
BECKSTEAD, J. N91-29960
BEDAIR, SALAH N91-30005
N91-30019
BEIERSDORFER, P. N91-29903
BELL, J. B. N91-29489
BELYTSCHKO, TED N91-29626
BENAK, T. N91-29236
BENEDEK, R. N91-29989
BENNETT, L. H. N91-29859
BENSADOUN, M. J. N91-29444
BENSINGER, J. R. N91-29892
BENTLEY, J. N91-29536
BERG, RICHARD L. N91-29198
BERGER, R. L. N91-29946
BERNHARDT, A. F. N91-29322
BERNSTEIN, L. S. N91-29671
BERSCH, CHARLES F. N91-29660
BERTON, JEFFREY J. N91-29181
BESTUL, THOR N91-29164
BEYERS, M. E. N91-29144
N91-29168
BHARGAVA, V. K. N91-29398
BHASIN, K. B. N91-29982
BHATT, RAMAKRISHNA T. N91-29250
BICKFORD, MARK N91-29777
N91-29778
BIENDENDER, M. D. N91-29473
BIGELOW, C. A. N91-29239
BIRDWELL, K. R. N91-29682
BLACK, F. M. N91-29385
BLACKBURN, M. J. N91-29309
BLAIR, D. S. N91-29605
BLAKE, IAN F. N91-29398
BLAKE, WILLIAM B. N91-29148
BLAKENEY, ROBERT D. N91-29768
BLANCHETTE, BRYAN M. N91-29173
BLOCKER, C. A. N91-29892
BLOOM, D. M. N91-29472
BLOOM, DAVID M. N91-29461
BLOWER, DAVID J. N91-29728
BLUM, ASHER S. N91-29850
BLUM, L. N91-29996
BLUMENTHAL, RIK N91-29338
BOAT, R. M. N91-29540
BOCZAR, BRUCE P. N91-29934
BODEK, A. N91-29873
BODT, BARRY A. N91-30050
BOEDEKER, L. R. N91-29255
BOERCKER, D. B. N91-29486
BOGRAD, S. J. N91-29705
BOND, WIE N91-29212
BONK, J. J. N91-29401
BONK, ROBERT B. N91-29234
BOOKER, J. M. N91-30043
BOQUIST, WALLACE P. N91-29679
BOSCH, R. N91-29946
BOSLOUGH, M. B. N91-29302
N91-29898
BOTTO, R. E. N91-29375
BOULANGER, P. N91-29800
BOULANGER, PIERRE N91-29743
BOWEN, BRENT D. N91-30042
BOWERS, R. N91-29954
BOWERS, R. L. N91-29480
N91-29955
BOYCE, LOLA N91-29629
BOYD, IAIN D. N91-29228
BOYNTON, J. E. N91-29713
BRACKETT, R. A. N91-29534
BRADUNAS, JOHN J. N91-29577
BRANDIS, R. N91-29147
BRANDON, S. L. N91-29292
BRANDON, S. T. N91-29962
BRAUD, J. P. N91-29582
BROADFOOT, A. L. N91-29219
BROCK, D. N91-29341
BROWN, A. P. N91-29336
BROWN, D. R. N91-29644
BROWN, FRANK M. N91-29741
BROWN, TODD R. N91-29195
BROWNELL, J. H. N91-29480
N91-29953
N91-29955
BRUECK, S. R. N91-29922
BRUEMMER, S. M. N91-29319
BRUNS, KEVIN D. N91-29148
BRYANT, GEORGE G. N91-29921
BUBBTRAM, M. T. N91-29445
BUCHENAUER, D. N91-29950
BUCKINGHAM, A. C. N91-29506
BUDINGER, J. M. N91-29405
BUDINGER, JAMES M. N91-29404
BUNNEY, L. E. N91-29414
BURCHAM, FRANK W., JR. N91-29191
N91-29194
BURKE, E. W. N91-29530
BURKE, T. N91-29446
BURR, DEBORAH N91-29835

BUTTERFIELD, A. J. N91-30068
BYRNE, CATHERINE A. N91-29358

C

CAGLAYAN, A. K. N91-29808
CAIN, M. N91-29624
CAIRNS, MARY M. N91-29693
CALABRESE, P. G. N91-29834
CALFO, R. M. N91-29445
CALIANNO, CARL N91-29149
CALLOWAY, T. M. N91-29406
CALVIN, M. D. N91-29896
CAMAIONI, D. M N91-29261
CAMERINI, U. N91-29912
CAMERON, A. N91-29596
CAMERON, D. N91-29596
CAMPUZANO, J. C. N91-29989
CANAVAN, G. H. N91-29851
CANFIELD, P. C. N91-29477
CANFIELD, T. N91-29797
CAPORASO, G. J. N91-29578
CARLIN, C. M. N91-29351
CARLIN, M. J. N91-29833
CARLSMITH, D. N91-29912
CARLSON, K. D. N91-29987
CARLSON, R. L. N91-29443
CARLSON, T. N. N91-29641
CARNELL, D. G. N91-29432
CARTER, J. G. N91-29881
CARTER, L. L. N91-29861
CASASENT, DAVID N91-29918
CASTEN, R. F. N91-29870
CATTO, P. J. N91-29964
CAUBLE, R. N91-29903
CAULEY, M. A. N91-29405
CHABOT, KATHLEEN A. N91-29234
CHAIKEN, DAVID N91-29784
CHAMIS, CHRISTOS C. N91-29221
CHANG, I-SHIH N91-29227
CHANG, J. J. C. N91-29559
CHANG, M. S. N91-29710
CHANG, QUAN-MING N91-29543
CHANG, R. P. N91-29462
CHANG, RICHARD K. N91-29277
N91-29575
CHANG, S. C. N91-29879
N91-29883
N91-29884
N91-30004
CHANG, S. L. N91-29968
CHANTRENNE, S. N91-29903
CHARTAS, G. N91-29960
CHAUDHURI, J. N91-29241
CHEN, CHI-SHAO N91-29657
CHEN, JIAHN-HORNG N91-29497
CHEN, M. N91-29903
CHEN, RAY N91-30023
CHEN, SOW-HSIN N91-29984
CHEN, T. F. N91-29192
CHEN, Y. J. N91-29578
CHENEY, M. N91-29531
CHENG, BILL H. N91-29513
CHHABILDAS, L. C. N91-29203
N91-29208
N91-29213
N91-29304
CHIANG, Y. M. N91-30031
CHIAPPETTA, L. N91-29183
CHICK, L. A. N91-30027
CHILDRESS, C. N91-29379
CHIPMAN, D. W. N91-29708
CHISHOLM, M. F. N91-29994
CHOE, G. H. N91-29241
CHOPPIN, G. R. N91-29548
CHRISTIANSEN, W. H. N91-29559
CHRISTOPHOROU, L. G. N91-29881
CHU, BEN N91-29367
CHU, CHEN-CHAU N91-29576
CHU, SHIH-I N91-29872
CHU, SZU H. N91-29205
N91-29206
N91-29207
CHUNG, H. M. N91-29294
CHURCH, K. D. N91-29436
CHYU, M. C. N91-29392
CIFUENTES, L. A. N91-29706
CLAPP, P. C. N91-29309
CLARK, C. W. N91-29858
N91-29887
CLARK, M. C. N91-29479
CLAUSING, R. E. N91-29327
CLAYTON, MICHAEL J. N91-29673
CLEM, J. R. N91-29485
CLEMENCE, ROBERT D., JR. N91-29766
CLIFTON, R. J. N91-29621
CLYNE, R. J. N91-29649
COATS, R. S. N91-29433
COCHRANE, J. C. N91-29952
COCHRANE, J. C., JR. N91-29954
COHEN, DONALD S. N91-29820
COHEN, J. B. N91-29249
COHEN, P. I. N91-30011
COHEN, R. E. N91-29622
N91-29623
COHEN, R. M. N91-29571
COLBECK, SAMUEL C. N91-29639
COLE, A. G. N91-29578
COLEMAN, M. N91-29624
COLLIGON, J. S. N91-30013
COLTON, MARIE C. N91-29685
COLVIN, JAMES E. N91-29222
CONLEY, JOSEPH L. N91-29194
COOK, J. V. N91-29750
COOPER, JILL M. N91-29332
COOPER, M. F. N91-29377
COSGROVE, JOSEPH E. N91-30007
COSTANTINO, M. S. N91-29387
COTTON, W. R. N91-29695
COUNSELMAN, C. C. N91-29163
CRABTREE, G. W. N91-29987
N91-29988
CRANE, J. ALLEN N91-29714
CRANNELL, CAROL N91-29201
CRESPODASILVA, MARCELO R. N91-29175
CROCKER, N. N91-29960
CROLL, JOHN B. N91-29139
N91-29159
CROTINGER, J. A. N91-29958
CROWLEY, JOHN S. N91-29735
CROWLEY, W. P. N91-29530
CROWN, JOHN S. N91-29847
CRUZ, J. E. N91-29432
CUDZINOVIC, M. N91-29960
CUI, JIYA N91-29182
CULLEN, D. E. N91-29869
CUNNINGHAM, C. N91-29849
CURLANDER, J. N91-29748
CURRAN, FRANCIS M. N91-29231
CUTLER, L. N91-29179
CYGAN, R. T. N91-29898

D

DAGDIGIAN, PAUL J. N91-29889
DAHMEN, U. N91-30038
DALBEY, S. N91-29647
DALY, R. T. N91-29434
DANDREA, J. A. N91-29736
DANFORD, M. D. N91-29318
DANIEL, B. R. N91-29381
DANIEL, BRADY R. N91-29223
DANIELS, R. C. N91-29682
DAS-GUPTA, D. K. N91-29927
DASU, S. N91-29873
DATSKOS, P. G. N91-29881
DAUM, P. H. N91-29681
DAVENPORT, J. W. N91-29323
DAVID, S. A. N91-29301
DAVIDSON, GILBERT N91-29423
DAVIDSON, R. F. N91-29632
DAVIS, D. O. N91-29150
DAVIS, J. BRADLEY N91-29210
DAVIS, JOHN N91-29201
DAVIS, LARRY S. N91-29164
DAVIS, ROBERT F. N91-30000
N91-30019
N91-30020
N91-30021
DAVIS, W. T. N91-30068
DEAN, JANET S. N91-29513
DEARHOLT, DONALD W. N91-29818
DEBOO, J. C. N91-29957
DEBOOR, CARL N91-29826
DECORSO, M. N91-29330
DEGROAT, JOANNE E. N91-29741
DEGROOT, J. S. N91-29941
DEJONGHE, L. C. N91-29317
DELAGRANGE, ARTHUR D. N91-29453
DELAMERTER, N. D. N91-29946
DELLACORTE, CHRISTOPHER N91-29235
DELLAROCAS, CHRYSANTHOS N. N91-29779
DELUCA, W. H. N91-29482
DEMENTHON, DANIEL N91-29164
DENATALE, J. F. N91-29354
N91-30006
DENHARTOG, D. N91-29960
DENHARTOG, D. J. N91-29959
DENNIS, BRIAN N91-29201
DEPIERO, F. N91-29585
DERAAD, LESTER L., JR. N91-29417
DEREZ, L. K. N91-29339
DEUTSCH, I. H. N91-30039
DEVIETTI, T. L. N91-29736
DEVORE, RONALD A. N91-29826
DEWITT, KENNETH J. N91-29228
DEXTER, R. N91-29960
DIAMOND, P. H. N91-29958
DICK, DAVID R. N91-29751
DICKINSON, BRADLEY W. N91-29785
DIECKMAN, S. N91-29378
DIECKMAN, S. L. N91-29375
DIECKMANN, R. N91-29266
DING, ZHENG-YOU N91-29352
DINGER, ROBERT J. N91-29421
DINGHUA, WANG N91-29564
DINGUS, R. S. N91-29563
DIPPOLITO, D. A. N91-29964
DIXON, DAVID S. N91-29439
DOBSON, JOHN N91-30014
DOERR, STEPHEN EUGENE N91-29539
DONGHAI, ZHU N91-29566
DORIS, S. N91-29378
DORRIS, S. E. N91-29991
DOSS, HANI N91-29835
DOTY, F. D. N91-29529
DOVER, C. B. N91-29895
DOW, JOHN N91-30008
DOWNEY, J. W. N91-29979
DOYLE, B. L. N91-29447
DRAKE, J. B. N91-29815
DREWETT, ADRIAN A. N91-29161
DROPPO, J. G., JR. N91-29667
DUBACH, J. F. N91-29901
DUBUS, B. N91-29759
DUFF, J. W. N91-29671
DUKES, MICHAEL A. N91-29741
DULING, I. N. N91-29933
DUNCAN, R. V. N91-29541
DUNHAM, JANET R. N91-29176
DUNN, J. E. N91-29203
DUPONT, LUC N91-29611
DURAND, B. N91-29912
DURAND, L. N91-29912
DUSEK, J. T. N91-29991
DUTOYA, DENIS N91-29493
DWORSKI, GEORGE N91-29700
DYE, RAYMOND H. N91-29862
DYKSTRA, PHILLIP C. N91-29514

E

EARLEY, L. M. N91-29562
EASTER, R. C. N91-29695
EASTMAN, J. A. N91-30031
ECKERLE, W. J. N91-29183
EDWARDS, G. N91-30035
EICHEL, P. H. N91-29406
EISENBERG, ADI N91-29363
EISENTHAL, K. B. N91-29275
EKLUND, WAYNE N91-29714
EKMANN, J. M. N91-29496
EL-MASRY, N. N91-30005
EL-SAYED, A. N91-29314
ELIAS, LORNE N91-29533
ELLIOTT, D. S. N91-29936
ELLIS, DAVID L. N91-29298
ELORANTA, EDWIN W. N91-29678
ELSAYED, MOSTAFA A. N91-29888
EMIN, D. N91-29260
N91-29985
EMMITT, G. D. N91-29554
EMSLIE, GORDON N91-29201
ENGELBERT, CARL R. N91-29245
ENGELMANN, B. N91-29634
ENGELMORE, ROBERT N91-29786
N91-29787
N91-29788
N91-29789
ENGUIST, BJORN N91-29426
EPPLEY, K. N91-29441
ERM, LINCOLN P. N91-29226
ERMAK, D. L. N91-29654
ERWIN, A. N91-29912
ESAREY, ERIC N91-29961
ESCHBACH, P. A. N91-29902
ESCOBAR, S. R. N91-29561
ESKEW, MARK N91-29452
ESKEWM, R. T., JR. N91-29925
ETHERIDGE, J. A. N91-29793
EVANS, J. R. N91-29414
EVANS, N. D. N91-29327
EWICK, D. W. N91-29382

F

FAGERQUIST, CLIFTON K. N91-29314
N91-29888
FAILOR, B. H. N91-29946
FAIRLIE, GREGORY W. N91-29153
FAIRMAN, TERRY M. N91-29648
FARAH, MARTHA J. N91-29732
FARRAR, BETH N91-29807
FARSAIE, ALI N91-29807
FATYGA, B. W. N91-30040
FAUBERT, D. N91-29418
FAULKNER, J. S. N91-29321
FAWCETT, W. R. N91-29875
N91-29876
N91-29996
FEBER, R. C. N91-29579
FEDERER, J. I. N91-29370
FEDORCHAK, SCOTT A. N91-29572
FEENSTRA, R. N91-29993
FEIGELMAN, M. V. N91-29988
FEIGENBAUM, EDWARD A. N91-29786
N91-29787
N91-29788
N91-29789
FEIKEMA, DOUGLAS ALAN N91-29262
FEINSTEIN, J. N91-29441
FELCHER, G. P. N91-29984
FENG, K. N91-29333
FENNER, DAVID B. N91-30007
FERNANDO, G. W. N91-29323
FERRIS, K. F. N91-29261
FERRO, P. D. N91-29305
FETTERER, F. M. N91-29637
FIALA, ALAN D. N91-30069
FIEDLER, S. L. N91-29794
FIFER, ROBERT A. N91-29383
FILHO, PEDRO HERNANDEZ N91-29635
FILIPPAS, A. V. N91-29958
FINDLEY, C. N91-29954
FINDLEY, C. E. N91-29952
FISCHMAN, KURT N91-29449
FISHER, A. T. N91-29536
FISHER, R. A. N91-29974
FISK, Z. N91-29477
FITCH, J. P. N91-30062
FLANNAGAN, M. N91-29722
FLINTOFF, J. F. N91-29354
FLYNN, G. N91-29555
FOGEL, M. L. N91-29706
FOLEY, M. G. N91-29668
FOLLSTAEDT, D. M. N91-29303
FONG, E. N. N91-30054
FOO, CHEK-PENG N91-29590
FORBES, GREGORY N91-29932
FORD, DEBRA M. N91-29689
FORGUES, PIERRE J. N91-29216
FORKAPA, MARK J. N91-29332
FORSYTH, E. B. N91-30026
FORWARD, ROBERT L. N91-29225
FOSS, COLBY A., JR. N91-29875
N91-29876
FOSTER, JOHN E. N91-29229
FOUTTER, R. R. N91-29920
FOWLER, CHRISTOPHER W. N91-29761
FOX, DANIEL N. N91-29704
FRANCE, D. M. N91-29501
N91-29502
FRANZ, J. A. N91-29261
FREAR, D. R. N91-29320
FREDRICKSON, KENT A. N91-29519
FREDRICKSON, LYLE J. N91-29768
FREEMAN, G. B. N91-29252
FREISER, B. S. N91-29878
FRENCH, D. C. N91-29375
FRETHEIM, ERIK J. N91-29930
FRIESE, G. N91-29647
FROESCHNER, K. E. N91-29633
FRY, W. N91-29912
FRYE, G. C. N91-29537
N91-29655
FU, C. Y. N91-29306
FUCHS, B. N91-30035
FUCHS, W. K. N91-29769
FUJIMURA, K. N91-29810
FUJITA, T. T. N91-29691
FULLER, J. J. N91-29807
FULLER, SCOTT J. N91-29311
FULLERTON, C. GORDON N91-29191
FUNKHOUSER, GORDON E. N91-29153
FURNISH, M. D. N91-29208
N91-29304

G

GAGLIARDI, ROBERT M. N91-29431
GAGNON, DAVID R. N91-29421
GAI, W. N91-29581
GALESKI, A. N91-29622
N91-29623
GALLAGHER, A. N91-29983
GAO, X. N91-29884
GAO, Y. N91-29970
GARCIA, R. N91-29560
GARNER, RICHARD C. N91-29423
N91-29424
GARRETT, S. M. N91-29644
GARRISON, J. C. N91-30039
GARVIN, CHARLES G. N91-30052
GATES, STEPHEN N91-29211
GATEWOOD, P. D. N91-29427
GAUDERT, P. C. N91-29237
GELLATLY, A. W. N91-29722
GELLERMAN, W. N91-29571
GELLES, D. S. N91-29295
GENTILE, F. T. N91-29345
GENTILE, FRANK T. N91-29270
GENTLEMAN, W. M. N91-29799
GEORGE, M. J. N91-29542
GEORGE, THOMAS F. N91-29886
GESHKENBEIN, V. B. N91-29988
GHANDEHARI, MOSTAFA N91-29825
GIBBS, D. N91-29307
GIBELING, JEFFERY C. N91-29313
GIBSON, J. H. N91-29444
GIESEKE, B. G. N91-29324
GILAT, AMOS N91-29365
GILL, PHILIP E. N91-29756
GILLANI, N. V. N91-29681
GILLHAM, N. W. N91-29713
GILLIE, K. R. N91-29482
GILMAN, SOL N91-29456
GILYARD, GLENN B. N91-29194
GINERIS, DENISE N91-29412
GLASS, J. T. N91-29327
GLASS, JEFFREY T. N91-30000
GLEICHER, G. J. N91-29261
GLOVER, DANIEL N91-30073
GLYNN, PETER W. N91-29765
GOCHEV, A. N91-29880
GOEBEL, C. N91-29912
GOELA, JITENDRA S. N91-29935
GOETZ, J. A. N91-29949
GOFF, JOHN A. N91-29697
GOFORTH, J. H. N91-29952
N91-29953
N91-29955
GOLDSTONE, J. A. N91-29995
GONZALEZ, J. A. N91-29476
GONZALEZ, RICHARD R. N91-29716
GOODELL, PHILLIPS W. N91-30042
GOODMAN, D. M. N91-30062
GOODS, S. H. N91-29910
GOODWIN, G. M. N91-29963
GOPALSAMI, N. N91-29375
N91-29378
GORD, J. R. N91-29878
GORDON, J. N91-29185
GORETTA, K. C. N91-29991
N91-30028
N91-30029
GOROCH, A. K. N91-29638
GOULD, M. J. N91-30068
GOULD, R. N91-29236
N91-29237
GOURDIN, W. H. N91-29620
GOUTSIAS, JOHN N91-29775
GOVINDARAJAN, R. N91-29663
GRANSTAFF, V. E. N91-29537
GRAY, G. T., III N91-29304
GREEN, L. G. N91-29387
GREEN, M. A. N91-29204
N91-29316
N91-29444
GREENBAUM, E. N91-29380
GREENE, A. N91-29954
GREENE, A. E. N91-29480
N91-29952
N91-29953
N91-29955
GREENWOOD, DAN N91-29609
GREENWOOD, J. A. N91-29596
GREGAR, J. S. N91-29378
GREINER, N. R. N91-29579
GRIFFIN, CHARLES F. N91-29253
GRIFFIN, G. R. N91-29730
GROBSTEIN, TONI L. N91-29298
GROTH, MARY F. N91-29222
GRUBER, O. N91-29957
GRUEBEL, G. N91-29307
GRUNINGER, J. H. N91-29671
GRUNZE, M. N91-29364
N91-29366
GU, C. N91-29979
GUIDEZ, JOEL N91-29493
GUIVENS, NORMAN R., JR. N91-29924
GULLIVER, T. A. N91-29398
GUTIERREZ, ROBERTO N91-29202

H

HAAR, THOMAS H. N91-29690
HAERENDEL, GERHARD N91-29201
HAFIZI, B. N91-29568
HAGELSTEIN, P. N91-29580
N91-29582
HAHN, C. N91-29366
HAJELA, P. N91-29628
HALL, R. C. N91-30045
HALLQUIST, J. O. N91-29634
HALPERIN, W. P. N91-29371
HALSTEAD, ROBERT H., JR. N91-29781
HALZEN, F. N91-29912
HAMELIN, A. N91-29879
HAMILTON, M. L. N91-29295
HAMM, MICHAEL K. N91-29215
HAMMOND, M. G. N91-29218
HANDSCHUH, R. F. N91-29600
HARARY, FRANK W. N91-29818
HARDWICK, C. D. N91-29158
HARELAND, W. A. N91-29871
HARFOUSH, F. N91-29407
N91-29408
HARITONIDIS, JOSEPH H. N91-29545
HARJES, H. C. N91-29445
HARKER, A. B. N91-29354
N91-30006
HARRIS, WILLIAM T. N91-30069
HARTLEY, T. T. N91-29147
HARVILL, K. A. N91-30054
HARVILL, WILLIAM E. N91-29253
HATFIELD, WILLIAM E. N91-29273
HAUSER, S. G. N91-29649
HAVENER, C. C. N91-29909
HAWKINS, J. D. N91-29637
HAWLEY, A. V. N91-29254
HAYNES, M. P. N91-29812
HAZELTINE, R. D. N91-29896
HE, JIANLIANG N91-29860
HEALEY, J. V. N91-29521
HEALEY, R. J. N91-29671
HEATH, M. T. N91-29793
HEATHERLY, L. N91-29374
HEATON, R. C. N91-29579
HEBEN, MICHAEL J. N91-29337
N91-29338
HEGEMIER, G. A. N91-29243
HEINE, D. L. N91-29444
HEINRICH, A. N91-29154
N91-29155
N91-29156
HELGESON, W. D. N91-29446
N91-29478
HEMMENT, P. L. N91-30013
HEMSING, W. F. N91-29540
N91-29542
HENDRICKS, R. C. N91-29525
HENRY, DANA S. N91-30047
HENRY, FRANK N91-29452
HENSHAW, PHILIP D. N91-29924
HENSINGER, D. M. N91-29259
HEPP, ALOYSIUS F. N91-29222
HERD, R. S. N91-29399
HERLIHY, MAURICE N91-29780
HERRMANN, W. N91-29612
HERRON, C. B. N91-29926
HERTEL, E. S. N91-29213
HEWER, G. A. N91-29928
HEWITT, R. L. N91-29166
HICKS, JOHN W. N91-29177
HICKS, R. S. N91-29901
HIGGINBOTHAM, SCOTT A. N91-29210
HIGLE, JULIA L. N91-29841
HILDEBRAND, JOHN A. N91-29680
HILL, D. A. N91-29432
HILL, D. N. N91-29950
HILL, S. A. N91-29213
HINGST, W. R. N91-29150
HINKS, D. G. N91-29992
HIXSON, R. S. N91-29334
HLAVACEK, VLADIMIR N91-29331
HOCH, M. P. N91-29706
HOCHHAUS, R. N91-29916

HOFF, L. E. N91-29414
HOFFMAN, N. M. N91-29505
HOKIN, S. N91-29959
N91-29960
HOLDEMAN, J. D. N91-29187
HOLLAND, JAMES A., II N91-29703
HOLLY, D. N91-29960
HOLT, MARLA J. N91-30042
HOLT, STEVEN E. N91-29499
HOM, K. N91-29259
N91-29584
HONG, BIN N91-29817
HONG, WILLIAM S. N91-29660
HORN, K. M. N91-29447
HORST, ALBERT W. N91-29384
HORST, R. N91-29769
HOSKING, F. M. N91-29320
HOUSTON, PAUL L. N91-29890
HOWE, S. D. N91-29200
HOWELL, PAUL R. N91-29315
HOWES, NORMAN R. N91-29754
HOWITT, D. G. N91-29372
HSIEH, DONOVAN N91-30048
HSU, R. N91-29306
HUANG, K. G. N91-29307
HUANG, X. Z. N91-29144
HUCKABINE, THOMAS N91-29177
HUDSON, HIGH N91-29201
HUEY, CECIL O., JR. N91-29390
HUGHES, T. W. N91-29595
HUGHES, W. J. N91-29676
HUGHES, WILLIAM E., JR. N91-29843
HULL, DAVID R. N91-29250
HULL, J. R. N91-29392
N91-29860
N91-29991
N91-30029
HUMMEL, J. R. N91-29677
HUNDLEY, M. F. N91-29477
HUNT, M. J. N91-29394
HUNTLEY, M. S., JR. N91-29733
HUPP, J. T. N91-29272
HUR, HONG B. N91-29702
HURFORD, GORDON N91-29201
HURST, G. B. N91-29653
HUTNIK, H. N91-29343
HUTNIK, M. N91-29345
N91-29346
N91-29347
HUTNIK, MICHELLE N91-29270
HWANG, C. C. N91-29496
HWU, WEN-MEI W. N91-29790
HYLAND, DAVID C. N91-29214
HYPES, W. D. N91-30068

I

IBELE, W. E. N91-29524
IBRAHIM, K. Y. N91-29209
IGLEHART, DONALD L. N91-29765
N91-29836
IMMARIGEON, J.-P. N91-29179
N91-29180
N91-29288
N91-29289
IMPELLUSO, T. J. N91-29243
INGERSOLL, D. N91-29386
INGRAHAM, RICHARD L. N91-29821
INTERRANTE, LEONARD V. N91-29355
IRONS, G. N91-29328
ISAAC, G. A. N91-29681
ISMAIL, SHAIK N91-29814
IVANCIC, WILLIAM D. N91-29431
IYER, R. K. N91-29769

J

JACKSON, LOGAN A. N91-29357
JACOB, D. J. N91-29661
JAEGER, H. N91-29334
JAGGI, NARENDRA K. N91-29520
JAKOWATZ, C. V., JR. N91-29406
JANOO, VINCENT C. N91-29198
JANSEN, J. N91-29585
JANSSENS, R. V. F. N91-29894
JAPEL, EDWARD J. N91-29758
JARRELL, D. B. N91-29809
JEBASINSKI, R. N91-30036
JELSMA, LAWRENCE F. N91-29850
JENDRZEJCZYK, J. A. N91-29501
N91-29502
JENNINGS, G. N91-29989
JEONG, Y. H. N91-29294
JESSON, D. E. N91-29994
JESSOP, E. S. N91-29387
JIANG, X. N91-30004
JING, HONGXING N91-29460
JING, ZHONGQI N91-29772
JOBE, D. O. N91-29487
JOHANSSON, E. M. N91-30062
JOHNSON, B. L., III N91-29643
JOHNSON, G. N91-29491
JOHNSON, G. A. N91-29473
JOHNSON, K. F. N91-29560
JOHNSON, KIRK N91-29784
JOHNSON, W. S. N91-29239
JONES, O. C. N91-29531
JOO, L. A. N91-29436
JORGENSEN, G. N91-29663
JORGENSEN, J. D. N91-29973
JORSTAD, NORMAN D. N91-29449
JOW, T. R. N91-29456
JOYCE, GLENN N91-29961
JOYCE, J. J. N91-29979
JUNGST, R. G. N91-29553
JUNIPER, MICHAEL D. N91-29448
JURGENS, T. N91-29407
N91-29408

K

KAHYA, GOKSEL N91-29846
KALADI, VASUDEVAN MUNDAKIZHI N91-29170
KALYON, DILHAN M. N91-29389
KAO, IMIN N91-29591
KAPLAN, STEVEN L. N91-29752
KAPOOR, V. J. N91-29473
KAPPES, M. M. N91-29462
KAPUR, DEEPAK N91-29774
KARDAUN, O. N91-29957
KARE, J. T. N91-29550
N91-29551
KARR, T. J. N91-29848
KASCHNITZ, E. N91-29334
KASISCHKE, ERIC N91-29412
KATNIK, GREGORY N. N91-29210
KATZ, S. B. N91-29391
KAUFFMAN, R. N91-29946
KAUFMAN, LLOYD N91-29727
KAUL, ROGER N91-29471
KAUPPILA, T. J. N91-29443
KAUSHIK, S. N91-29582
KAWABE, M. N91-29707
KAZAKOS, DEMETRIOS N91-29543
KEANE, C. J. N91-29946
KEATING, JEROME P. N91-29629
KEESLER, JEFF A. N91-29247
KEIPERT, S. J. N91-29369
KENIK, E. A. N91-29536
KENNEDY, R. M. N91-29699
KERCHNER, H. R. N91-29993
KERELIUK, S. N91-29190
KERLEY, G. I. N91-29203
KERLEY, JAMES J. N91-29714
KERSLAKE, S. D. N91-29405
KERSTEN, R. T. N91-29916
KESMODEL, L. L. N91-30024
KEVORKIAN, J. N91-29715
KHOMSKII, D. I. N91-29977
KIEFER, M. L. N91-29433
KIGGANS, J. O. N91-29373
KILLINGER, A. N91-29366
KIM, J. S. N91-29973
KIM, SUK C. N91-29230
KIM, YOUNG CHEOL N91-29975
KIM, YOUNG I. N91-29273
KING, C. B. N91-30068
KING, D. B. N91-29442
KING, W. R. N91-29643
KIRKPATRICK, R. J. N91-29898
KIRSCH, L. E. N91-29892
KIRWAN, ALBERT D., JR. N91-29701
KLEPACZKO, J. R. N91-29625
KLEPPER, C. C. N91-29950
KLEPPNER, DANIEL N91-29458
KLIMA, STANLEY J. N91-29610
KNAPP, D. N91-29903
KNAPP, J. A. N91-29303
KNEPTON, J. C. N91-29736
KNIBLOE, J. R. N91-29328
KNITTLE, C. D. N91-29409
KO, K. N91-29441
KOBER, W. N91-29748
KOEHLER, W. J. N91-29524
KOLB, G. J. N91-29252
KOMOROWSKI, J. P. N91-29604
KOMOROWSKI, JERZY P. N91-29611
KONIGES, A. E. N91-29958
KOOS, D. A. N91-29268
KORTH, G. E. N91-29299
KOSHIZUKA, N. N91-30032
KOSKIE, JOHN E. N91-29510
KOSTELECKY, V. A. N91-30040
KOSUGE, M. N91-30032
KOTANEN, A. R. N91-29604
KOTH, HOWARD E. N91-29517
KOUL, A. K. N91-29179
N91-29180
KOZLOWSKI, M. R. N91-30035
KRAIMER, M. R. N91-29434
KRALL, JONATHAN N91-29961
KRAMER, D. P. N91-29382
KRANING, KENNETH K., II N91-29716
KRANZ, DAVID N91-29739
N91-29781
N91-29784
KRASKO, GENRICH L. N91-30002
KREGEL, MARK D. N91-29428
KRESS, R. N91-29585
KRIZ, DENNIS N91-29352
KRIZ, R. D. N91-29251
KROLL, N. N91-29441
KRONAUER, RICHARD E. N91-29925
KRUSE, H. N91-29954
KRUSE, H. W. N91-29952
N91-29953
KRUSE, V. J. N91-29401
KU, WALTER H. N91-29448
KUBIATOWICZ, JOHN N91-29739
N91-29784
KUCERA, G. H. N91-29336
KULAGA, J. E. N91-29482
KUMAR, A. N91-29494
KUPPERMAN, D. S. N91-29378
KURIEN, T. V. N91-29839
N91-29840
KUZAN, JOHN D. N91-29514
KUZAY, T. M. N91-29392
KWEI, G. H. N91-29995

L

LACERDA, A. N91-29477
LACOMBE, DONALD J. N91-29451
LAFARGE, R. A. N91-29151
LAFOLLETTE, P. A. N91-29427
LAFOLLETTE, PHILIP A. N91-29863
LAI, M. K. Y. N91-29258
LAIRD, C. E. N91-29297
N91-29865
LALCHANDANI, ATAM N91-29836
LALLY, RICHARD W. N91-29419
LAM, Y. M. N91-29396
LAMB, BRIAN N91-29417
LAMERS, PAUL N91-29397
LAN, J. S. N91-29861
LANAGAN, M. T. N91-29991
N91-30029
LANDIS, GEOFFREY A. N91-29222
LANG, P. M. N91-29664
LANGDON, WILLIAM R. N91-29174
LAPOINTE, MICHAEL R. N91-29832
N91-29917
LARSEN, E. B. N91-29432
LASSILA, D. H. N91-29620
LAST, ISIDORE N91-29886
LATTIMER, J. M. N91-30066
LAUE, H. J. N91-29265
LAURICH, B. K. N91-29986
LAW, B. N91-29306
LAW, C. C. N91-29309
LAWLER, GREGORY M. N91-29767
LAWRENCE, T. W. N91-30062
LAWSON, H., JR. N91-29217
LAWSON, R. N. N91-29479
LAX, P. D. N91-29795
LAY, P. A. N91-29272
LAZARETH, O. N91-29232
LE, JEANETTE N91-29194
LEAITCH, W. R. N91-29681
LEBLANC, J. N91-29427
LEBO, M. E. N91-29706
N91-29707
LEE, B. J. N91-29944
LEE, DAVID CHUNG LIANG N91-29635
LEE, HEOW-PUEH N91-29592
LEE, IN YOUNG N91-29696
LEE, J. Y. N91-29973
LEE, K. L. N91-29292
LEE, R. L. N91-29652
LEE, RICHARD S. N91-29516
LEE, S. N91-29237
LEE, T. N91-29441
LEE, T. D. N91-29904
N91-29905

LEE, W. C. N91-29844
LEE, Y. T. N91-29256
LEE, YUAN T. N91-29868
LEES, DAVID E. N91-29924
LEFEBVRE, C. N91-29394
LEFEBVRE, PAUL N91-29523
LEITH, EMMETT N. N91-29544
LEONE, J. M., JR. N91-29652
LEONE, STEPHEN R. N91-30009
N91-30015
LES, JOHN M. N91-29464
LESPERANCE, G. N91-29179
LEVIN, JEFF A. N91-29768
LEVIN, S. N91-29444
LEWIS, NATHAN S. N91-29337
N91-29338
LEZNOV, A. N. N91-29813
LI, CHE-YU N91-29305
LI, G. N91-29398
LI, W. N91-29986
LIAO, Y. N91-30031
LICEAGA, CARLOS A. N91-29745
LIGHTFOOT, P. N91-29973
LILIENTAL-WEBER, Z. N91-29969
LIM, BENG-HONG N91-29739
LIM, HEOUNGBIN N91-29939
LIMON, M. N91-29444
LIN, J. T. N91-29531
LIN, ROBERT N91-29201
LINCOLN, R. C. N91-29910
LINDE, G. J. N91-29430
LINDEMUTH, I. R. N91-29951
N91-29953
LINDSAY, A. C. N91-29837
LING, JAMES N91-29201
LINNE, DIANE L. N91-29222
LISCINSKY, D. S. N91-29187
LIST, R. S. N91-29989
LITCHFIELD, J. K. N91-29475
LITVIN, F. L. N91-29600
LIU, R. N91-29979
LIU, S. N91-29462
LIZANICH, P. J. N91-29405
LO, CHI-KAI N91-29587
LOCHNER, J. C. N91-29538
LOEHNER, R. N91-29962
LOGAN, J. A. N91-29661
LOISEL, CRAIG L. N91-30022
LONG, GREGORY LYNN N91-29588
LONG, MARSHALL B. N91-29277
LOTTES, S. A. N91-29968
LOUBRIEL, G. M. N91-29446
N91-29478
LOVELACE, THOMAS B. N91-29629
LOVELESS, R. N91-29912
LUCK, ROGELIO N91-29193
LUDEWIG, H. N91-29232
LUDOVICE, P. J. N91-29345
LUDOVICE, PETER J. N91-29270
LUNG, TERESA F. N91-29740
LUNT, TERESA N91-30048

M

MA, G. H. M. N91-29327
MA, SHENMIN N91-29352
MACCAGNO, T. M. N91-29179
MACHADO, PETER N91-29598
MACHI, T. N91-30032
MACKAY, S. A. N91-29799
MACKENZIE, C. W. N91-29535
N91-29744
MACKENZIE, COLIN W. N91-29742
MACKENZIE, JOHN D. N91-29360
MACPHERSON, J. I. N91-29169
N91-29651
MACPHERSON, J. IAN N91-29189
MADAN, R. C. N91-29254
MAHAJAN, S. N91-29494
MAHAJAN, S. M. N91-29965
MAHDAVI, M. A. N91-29950
MAHER, J. V. N91-29504
MAILHIOT, C. N91-30033
MAJUMDAR, S. N91-29378
MAKOWSKI, M. A. N91-29583
MALBA, V. N91-29322
MALONE, K. T. N91-29409
MANN, R. C. N91-29810
MANTL, S. N91-30036
MANZ, PAUL C. N91-29659
MARBOE, R. C. N91-29143
MARCUS, D. L. N91-29489
MARIAM, Y. H. N91-29333
MARIELLA, R., JR. N91-29969
MARK, J. E. N91-29361
MARRS, R. N91-29903
MARSH, S. P. N91-29951
N91-29953
MART, PETER L. N91-29290
MARTIN, J. C. N91-29602
MARTIN, JORGE M. N91-29824
MARTIN, S. J. N91-29537
N91-29655
MARTIN, T. H. N91-29487
MARTIN, W. R. N91-29869
MARYNICK, DENNIS S. N91-29362
MASOUDI, M. N91-29491
MASSOUDI, M. N91-29496
MATHEWS, A. R. N91-29540
N91-29542
MATHUR, M. P. N91-29491
MATTERN, DUANE N91-29188
MATTOR, N. N91-29966
MAUDLIN, P. J. N91-29632
MAUPIN, G. D. N91-30027
MAXSON, J. A. N91-29259
N91-29584
MAYHALL, D. J. N91-29435
MCALPINE, N. S. N91-29272
MCDANIEL, B. N91-29647
MCELIECE, ROBERT J. N91-29425
MCILRATH, T. J. N91-29887
MCKEAGUE, IAN W. N91-29838
MCKENNA, FRANK P. N91-29725
MCKERNAN, SCOTT J. N91-29244
MCLANE, PETER J. N91-29395
MCLAUGHLIN, D. L. N91-29446
N91-29478
MCLOUGHLIN, FRANK ANTHONY N91-29617
MCMANIS, G. W. N91-29880
MCMICHAEL, R. D. N91-29859
MCNICHOLL, PATRICK J. N91-29423
MCWHORTER, ALAN L. N91-30016
MEERSON, B. N91-29913
MEIER, G. H. N91-29658
MEILUNAS, R. J. N91-29462
MEISSNER, DANA L. N91-29228
MELNIKOV, V. O. N91-29855
MELNITZKY, S. N91-29334
MENDEZ, ANTONIO J. N91-29431
MENG, TERESA H. N91-29783
MERCER, JAMES A. N91-29700
MERKLE, K. L. N91-29970
N91-29990
N91-30030
MESTHA, L. K. N91-29410
MEYER, F. W. N91-29909
MICHAEL, J. R. N91-29971
MICHARD, PIERRE-JAQUES N91-29493
MICHELOTTI, L. N91-29816
MIDDLETON, DAVID N91-29413
MILBURN, R. H. N91-29908
MILLER, D. L. N91-29753
N91-29823
MILLER, DOUGLAS P. N91-29465
MILLER, JONATHAN N91-29498
MILLER, RONALD J. N91-29684
MILLER, RONALD W. N91-29513
MILLER, S. D. N91-29902
MILLER, S. L. N91-29484
MINKOFF, M. N91-29797
MINTS, WILLIAM N91-29278
MISKIMEN, R. A. N91-29901
MISLOVE, MICHAEL W. N91-29760
MISRA, PRADEEP N91-29806
MITCHELL, RALPH N91-29308
MIYAKATE, T. N91-30032
MIZUNO, K. N91-29941
MOCHRIE, S. G. J. N91-29307
MOENY, W. M. N91-29557
MOHAMED, J. H. N91-29405
MOHLER, R. R. N91-29415
MOHR, ERIC N91-29781
MOLINA, E. A. N91-29719
MOLNAR, J. A. N91-29450
MONSON, P. A. N91-29287
MONTANA, D. M. N91-29399
MONTANO, J. W. N91-29318
MOON, B. M. N91-30028
MOORE, JEFFREY MORGAN N91-30067
MOORE, MARVIN E. N91-29148
MOREY, W. A. N91-29719
MORGAN, ALI S. N91-29877
MORGAN, W. L. N91-29486
N91-29557
MORGAN, W. R. N91-29436
MORIN, BRUCE L. N91-29508
MORLAN, LINDA J. N91-29234
MOROSIN, B. N91-29995
MORRIS, E. G. N91-29436
MORRIS, JEFFREY B. N91-29383
MORRIS, M. N91-29554
MORRISON, PHILIP W., JR. N91-30007
MORSE, J. N91-29969
MORUA, MICHAEL L. N91-29466
MOSES, J. DANIEL N91-29937
MOSSAYEBI, F. N91-29147
MOTT, P. N91-29346
MOTT, PETER N91-29877
MOTT, PETER H. N91-29340
MOWATT, LARRY N91-29452
MUELLER, PAUL N91-29718
N91-29804
MUENDEL, M. N91-29580
N91-29582
MUGHABGHAB, S. N91-29232
MUIRA, R. M. N91-29715
MUKHERJEE, AMIYA K. N91-29313
MUKHTAROV, M. A. N91-29813
MURAKAMI, HIDENORI N91-29243
MURPHY, J. R. N91-29758
MURPHY, W. D. N91-29426
MURR, L. E. N91-29319
MURRAY, WALTER N91-29756
MURTHY, VASUDEVA S. N91-29589
MURUGESH, L. N91-29317
MUZACA, JAMES N91-29598
MYERS, DWIGHT L. N91-29981
MYLES, K. M. N91-29645
MYRA, J. R N91-29964

N

NAGY, L. A. N91-29405
NAINKA, C. N91-29366
NAKAYAMA, KEN N91-29720
NASBY, R. D. N91-29484
NASH, A. S. N91-30028
NASH, P. N91-30028
NASRALLAH, M. M. N91-29978
NAYANI, S. N91-29488
NEALY, J. E. N91-30068
NEGLEY, G. H. N91-29910
NELSON, E. N91-29441
NEMEC, PAUL T. N91-29842
NEUDORFL, PAVEL N91-29533
NEWELL, J. C. N91-29531
NEWMAN, L. N91-29656
NEWMAN, W. I. N91-29812
NEWNAM, B. E. N91-29915
NG, E. N91-29796
NG, YU-NING N91-29289
NGUYEN, V. K. N91-29196
NICHOLLS, M. N91-29695
NICHOLS, LESTER D. N91-29221
NICKEL, D. L. N91-29401
NIETO, M. M. N91-30040
NII, H. P. N91-29786
N91-29787
N91-29788
N91-29789
NIJHOLT, ANTON N91-29792
NOREM, J. N91-29581
NORTH, RICHARD C. N91-29448
NOTIS, M. R. N91-29971
NOVAES, RENE ANTONIO N91-29635
NOVINSON, THOMAS N91-29356
NOWICK, A. S. N91-30018
NUSBAUM, A. N91-30046
NUTTALL, ALBERT H. N91-29413
NYE, HOLLY L. N91-29547

O

OBOT, N. T. N91-29501
N91-29502
OCKO, B. M. N91-29307
OFFENBACHER, ELMER L. N91-29639
OKIISHI, THEODORE H. N91-29186
OLSON, C. G. N91-29979
OLSON, D. A. N91-29527
OLSON, G. B. N91-29293
OLSON, GREGORY B. N91-30002
OLSON, R. E. N91-29943
OMALLEY, M. W. N91-29446
N91-29478
ONEIL, D. J. N91-29252
ONNO, T. N91-29158
OONA, H. N91-29952
N91-29953
N91-29954
N91-29955
OPLINGER, DONALD W. N91-29607
OPPENHEIM, A. K. N91-29259
N91-29584

OREY, MICHAEL A. N91-29805
ORNELLAS, D. L. N91-29387
OSBORNE, T. N91-29950
OSMOND, C. B. N91-29713
OSTOWARI, C. N91-29650
OSTROM, R. N91-29983
OTTO, J. N91-29916
OUZTS, PETER N91-29188
OVACIK, L. N91-29531
OVERFELT, P. L. N91-29928
OWENS, F. J. N91-29929

P

PADMANABHAN, VISWA N91-29154
N91-29155
N91-29156
PAKEY, DONALD DEAN N91-30063
PALASZEWSKI, BRYAN N91-29220
PANCHAL, C. N91-29300
PANCHAL, C. B. N91-29500
PAQUET, V. N91-29916
PARAMESWARAN, V. N91-29814
PARAMESWARAN, V. R. N91-29288
N91-29289
PARK, EUGENE N91-29431
PARK, MOONSOO N91-29350
PARK, YOUNG T. N91-29353
PARKER, J. V. N91-29952
N91-29953
N91-29954
PARKER, T. E. N91-29920
PARKS, D. M. N91-29342
PARKS, EARL L. N91-29451
PARRIS, P. E. N91-29978
PASIK, M. F. N91-29433
PATANKAR, S. V. N91-29524
PATEL, J. H. N91-29769
PATTERSON, MICHAEL J. N91-29229
PAUL, A. C. N91-29578
PAULEY, K. A. N91-29377
PAULIKAS, A. P. N91-29979
PEAK, JAMES A. N91-29688
PEASE, D. M. N91-29309
PEI, S. N91-29973
PEKNY, J. F. N91-29753
N91-29823
PEMSLER, J. P. N91-29475
PENA, G. E. N91-29487
PENA, RICARDO N91-29674
N91-29675
PENKO, PAUL F. N91-29228
N91-29230
PENNA, P. J. N91-29642
PENNER, REGINALD M. N91-29337
N91-29338
PENNYCOOK, S. J. N91-29994
PEREIRA, JOHN J. N91-29686
PERKINS, K. N91-29232
PERKINS, S. T. N91-29869
PERNAROWSKI, M. N91-29715
PERUCCHINI, JEAN N91-29493
PESCHKE, W. T. N91-29183
PETERSON, D. N91-29954
PETERSON, D. L. N91-29480
N91-29955
PETERSON, G. A. N91-29901
PETHE, R. G. N91-29351
PETRIE, T. W. N91-29950
PETTIT, G. D. N91-30033
PHANEUF, R. A. N91-29909
PHELPS, D. K. N91-29878
PHILLIPS, N. E. N91-29974
PHILLIPS, T. N91-29903
PHILPOTT, MICHAEL R. N91-29269
PICARD, R. R. N91-30043
PICCIOLO, J. J. N91-29991
N91-30029
PICK, HERBERT L., JR. N91-29640
PICK, MONIQUE N91-29201
PINADUWAGE, L. A. N91-29881
PING, MENG N91-29565
PIOTROWSKI, G. K. N91-29602
PIPKIN, F. M. N91-29885
PITZER, K. S. N91-29286
PLANO, LINDA S. N91-29274
PLASKACZ, E. N91-29797
PLICHTA, EDWARD J. N91-29456
PLOHR, BRADLEY K. N91-29829
POE, C. C., JR. N91-29240
POEPPEL, R. B. N91-29991
POINTON, T. D. N91-29433
POLITIS, C. N91-29975
POLLAINE, S. M. N91-29946
POLLAK, F. H. N91-30033
POMERANTZ, MARTIN N91-29362
PONCELEON, DULCE B. N91-29756
N91-29773
PONZONI, FLAVIO JORGE N91-29635
POON, C. N91-29236
N91-29237
POORNIMA, L. N91-29197
PORADA, E. N91-29800
POSTON, J. W., SR. N91-29893
POTAMIANOS, GERASIMOS N91-29775
POTTLACHER, G. N91-29334
POURAHMADI, MOSHEN N91-29822
POWELL, J. R. N91-29232
PRAGER, S. C. N91-29940
N91-29959
N91-29966
PRASAD, PARAS N. N91-29361
PRELEC, K. N91-29947
PREMAGEETHA, B. K. N91-29146
PREMALATHA N91-29145
PRICE, LARRY D. N91-29184
PRIEBE, C. E. N91-29833
PRIEDHORSKY, W. C. N91-29538
PROSPERETTI, A. N91-29492
PROVORSE, JOHN N91-29154
N91-29155
N91-29156
PRUESSNER, MANFRED K. N91-29271
PRUETT, N. J. N91-30057
PRZYSTUPA, MAREK A. N91-29312

Q

QIAN, G. X. N91-29323
QIANG, H. N91-30033
QIN, GUOYI N91-29976
QUALLS, G. D. N91-30068
QUINN, JANET N91-29608
QUINN, R. D. N91-29666
QUINTENZ, J. P. N91-29433

R

RAAYMAKERS, CONNIE L. N91-29758
RABAS, T. N91-29503
RAJAGOPAL, K. R. N91-29491
RAJESHWAR, KRISHNAN N91-29362
RAKOCZY, J. N91-30061
RAMAKER, DAVID E. N91-29874
RAMAMOORTHY, P. N91-29145
N91-29146
RAMESH, K. S. N91-29330
RAMMAGE, ROBERT L. N91-29438
RAMSEY, J. M. N91-29374
RAND, RICHARD JOHN N91-30064
RAO, K. T. N91-29317
RAOL, J. R. N91-29814
RAPP, DOUGLAS N91-29220
RAPTIS, A. C. N91-29378
RASOLT, M. N91-29481
RATHKOPF, J. A. N91-29869
RAWLINS, W. T. N91-29920
RAY, ASOK N91-29193
REDDIX, M. D. N91-29736
REDDY, J. N. N91-29488
REDDY, K. C. N91-29488
REED, BRIAN D. N91-29230
REED, K. N91-29903
REESON, K. J. N91-30013
REID, WARREN D. N91-29290
REIFF, W. M. N91-29973
REINOVSKY, R. E. N91-29951
N91-29953
REMPEL, T. D. N91-29959
REVANKAR, VITHAL N91-29331
REYNOLDS, JOHN R. N91-29362
RHEEM, K. S. N91-29294
RHEIN, ROBET A. N91-29279
RICCO, A. J. N91-29537
RICE, JAMES P. N91-29786
N91-29787
N91-29788
N91-29789
RICHMOND, G. L. N91-29268
RICKEL, D. G. N91-29952
N91-29953
N91-29955
RIDLON, R. N. N91-29443
RIOUX, M. N91-29800
RITZ, CH. P. N91-29958
ROBBINS, FREDERICK W. N91-29384
ROBERTS, J. M. N91-29656
ROBERTS, JOHN ANTHONY N91-30059
ROBERTSON, D. C. N91-29671
ROBINSON, F. L. N91-29606
ROCK, S. E. N91-29873
RODACY, P. J. N91-29386
RODERICK, N. F. N91-29480
RODGERS, M. S. N91-29484
RODRIGUEZ, A. E. N91-29483
N91-29557
RODWAY, D. C. N91-29316
ROGERS, STEPHEN B. N91-29672
ROGL, PETER N91-29359
ROHWEIN, G. J. N91-29479
ROKHLIN, VLADIMIR N91-29426
ROMANOFSKY, R. R. N91-29405
N91-29982
ROMIG, A. D., JR. N91-29303
RON, AMOS N91-29826
ROSS, RICHARD N91-29154
N91-29155
N91-29156
ROTH, J. D. N91-30004
ROTTMAN, MICHAEL S. N91-29770
ROWLANDS, D. E. N91-29185
ROY, CLERMONT N91-29611
RUKAVINA, JOHN P. N91-29186
RUSSELL, D. A. N91-29964
RUSSELL, S. M. N91-29309
RUSSELL, STEPHEN D. N91-29997
RUSSO, J. M. N91-29641
RUTH, CARL R. N91-29384
RUTLEDGE, SHARON K. N91-29332
RUXIANG, WANG N91-29565
RYTER, F. N91-29957

S

SAADATMAND, K. N91-29560
SABBAGH, S. A. N91-29938
SACHS, FREDERICK N91-29772
SADLER, PORTER N91-29452
SAKAUE, KATSUHIKO N91-29743
SALAS, F. J. N91-29553
SALMON, J. T. N91-29914
SALMON, RICK N91-30070
SALOVEY, R. N91-29349
N91-29350
N91-29352
SALSMAN, CHARLES P. N91-29422
SALZBERG, A. P. N91-29569
SANCHEZ, JUAN J. N91-29474
SANDER, O. R. N91-29560
SANDOVAL, D. N91-29560
SANDOVAL, W. F. N91-29579
SANDY, A. R. N91-29307
SANKOVIC, JOHN M. N91-29231
SARGESON, A. M. N91-29272
SARIC, WILLIAM S. N91-29518
SARTOR, JOANN M. N91-29791
SASS, DAVID N91-29400
SASSCER, D. N91-29300
SATER, JANET M. N91-29660
SATTORD, L. K. N91-29455
SAUNDERS, MICHAEL A. N91-29756
SAYKALLY, RICHARD J. N91-29570
SCAMMON, R. J. N91-29563
SCHADE, NICHOLAS N91-29439
SCHAEFER, R. M. N91-29602
SCHAFFER, M. J. N91-29950
SCHARDT, B. C. N91-29883
N91-29884
SCHEFTER, M. N91-29396
SCHERBARTH, D. W. N91-29445
SCHETZINA, J. F. N91-30017
SCHIFERT, S. K. N91-29632
SCHIHANG, SHU N91-29566
SCHILLING, C. H. N91-29376
SCHIRBER, J. E. N91-29995
SCHISSEL, D. P. N91-29957
SCHLECHT, RICHARD G. N91-29242
SCHLOTTMANN, P. N91-29900
SCHMIDT, E. N91-29232
SCHMIDT, K. N91-30036
SCHMIDT, WAYNE J. N91-29758
SCHNEIDER, M. N91-29903
SCHNEIDER, STEVEN J. N91-29230
SCHNEPS, J. N91-29908
SCHNITZER, H. J. N91-29892
SCHOWALTER, L. J. N91-29986
SCHROEDER, THOMAS A. N91-29683
SCHROT, JOHN N91-29724
SCHUPP, G. N91-29980
SCHUSTER, JULIUS C. N91-29359
SCHWANK, J. R. N91-29484
SCHWARTZ, S. E. N91-29681
SCHWELLENBACH, D. N91-29906
SCOFIELD, J. N91-29903

SCOTT, D. J. N91-29445
SCOTT, R. F. N91-29237
SEALY, B. J. N91-30013
SEAMEN, J. F. N91-29487
SEDGEWICK, J. M. N91-29644
SEIDEL, D. B. N91-29433
SEITZINGER, ALAN T. N91-29734
SEKA, W. N91-29941
SELLE, J. E. N91-29267
SENGERS, J. V. N91-30041
SENSHARMA, DILIP K. N91-29314
N91-29888
SEOL, S. Y. N91-29392
SEPANSKI, R. J. N91-29664
SESHADRI, K. N91-29197
SETHURAMAN, J. N91-29840
SETHURAMAN, JAYARAM N91-29839
SEVERT, C. W. N91-29442
SEVINSKY, T. P. N91-29929
SEXTON, DOUGLAS A. N91-29997
SEXTON, F. W. N91-29447
SEZEN, Y. N91-29257
SHAH, SURENDRA P. N91-29248
SHALKHAUSER, M. J. N91-29405
SHAMMA, S. N91-29719
SHANNON, ROBERT R. N91-29999
SHAPIRO, JEFFREY H. N91-29573
SHARMA, DINKBAR N91-29725
SHARP, D. N91-29624
SHARP, J. H. N91-29707
SHAVER, B. N91-29167
SHAVER, B. E. N91-29166
SHAVIT, NIR N91-29780
SHAW, R. W. N91-29374
SHEEN, DAN N91-29412
SHEFT, STANLEY N91-29862
SHELLMAN, C. H. N91-29819
SHEN, ZHENGKANG N91-29669
SHEPARD, STEVEN N91-29400
SHEPPARD, C. L. N91-30054
SHERMAN, BRADLEY D. N91-29431
SHETTLE, E. P. N91-29677
SHI, DONGLU N91-30029
SHI, H. N91-29979
SHIH, W. H. N91-29376
SHIMABUKURO, R. L. N91-29833
SHIMSKI, JOHN N91-29599
SHINAS, M. N91-29560
SHOEMAKER, P. A. N91-29833
SHOFNER, WILLIAM P. N91-29862
SHULL, R. D. N91-29859
SHULL, R. N. N91-29729
N91-29730
SHUMAN, A. N91-29440
SHUTT, J. D. N91-29252
SHUYUN, MA N91-29565
SHUZHI, ZHANG N91-29566
SIDERS, C. M. N91-29759
SIEWIOREK, DANIEL P. N91-29176
N91-29745
SIKKA, V. K. N91-29324
N91-29325
SIMMONS, STANLEY J. N91-29397
SIMONSEN, L. C. N91-30068
SIMPSON, D. L. N91-29165
SINGH, J. P. N91-29378
N91-29991
N91-30029
SIVAK, M. N91-29722
SJOREEN, T. P. N91-30036
SLANE, STEVEN N91-29456
N91-29457
SLANINA, J. T. N91-29393
SLEMROD, MARSHALL N91-29512
SMAGA, J. A. N91-29482
SMITH-WACKERLE, V. L. N91-29328
SMITH, C. R. N91-29507
SMITH, D. L. N91-29986
SMITH, J. R. N91-29548
SMITH, KENNETH O. N91-29601
SMOOT, G. F. N91-29204
N91-29444
SMYTH, J. D. N91-29666
SNYDER, LARRY N91-29749
SOLANO, E. R. N91-29896
SONG, OHSEOP N91-29615
SONG, TAE I. N91-29470
SONI, N. J. N91-29405
SORENSEN, K. W. N91-29402
SPAIN, E. H. N91-29595
SPANDE, ROBERT N91-29932
SPARLIN, D. M. N91-29978
SPARROW, VICTOR W. N91-29420
SPIVAKOVSKY, C. M. N91-29661
SPRAGINS, C. W. N91-29959
SPRANGLE, P. N91-29568
SRIVAS, MANDAYAM N91-29777
N91-29778
STAMBAUGH, R. D. N91-29950
STANION, K. N91-30035
STANNY, R. N91-29719
STAPP, H. P. N91-29723
STEELE, L. P. N91-29664
STEFFANI, C. P. N91-29528
STEINBERG, D. J. N91-29304
STEINFINK, H. N91-29973
STEPHEN, K. W. N91-29710
STEPHENS, K. G. N91-30013
STEPHENS, S. E. N91-29522
STEWART, D. A. N91-29799
STEWART, D. V. N91-29436
STEWART, H. E. N91-29584
STILL, C. H. N91-29798
STOCK, STUART R. N91-29627
STOCKER, A. N91-29748
STOCKS, G. M. N91-29321
STOFFELS, J. J. N91-29265
STOICOVICIU, L. N91-29879
STORCH, JOEL N91-29211
STOUKIDES, M. N91-29437
STOVER, J. B. N91-29405
STOY, STAN L. N91-29148
STRAPP, J. W. N91-29681
STRATTON, R. C. N91-29809
STRIKWERDA, JOHN C. N91-29829
STRINGFELLOW, G. B. N91-29571
STROMEYER, C. F., III N91-29925
STRUNSKUS, T. N91-29366
SUDOL, EUGENE G., JR. N91-29184
SULLIVAN, J. H. N91-29579
SUMIDA, P. T. N91-29254
SUN, C. T. N91-29628
SUN, LIQING N91-29349
N91-29350
SUNDBERG, R. L. N91-29671
SUTER, U. W. N91-29343
N91-29345
N91-29346
N91-29347
SUTER, ULRICH W. N91-29270
N91-29340
SUTTER, ULRICH W. N91-29877
SUZUKI, H. N91-29531
SWARTZENDRUBER, L. J. N91-29859
SWINDEMAN, R. W. N91-29305
SWINNEA, J. S. N91-29973

T

TABEREAUX, A. N91-29436
TACHIBANA, T. N91-29327
TAI, K. N91-30032
TAJIMA, T. N91-29913
TAKAHASHI, TARO N91-29708
TAKAHASHI, YOSHIYUKI N91-29897
TALLANT, D. R. N91-29260
TALLEY, ROBERT L. N91-29224
TAN, ROBERT J. N91-29471
TANAKA, S. N91-30032
TANG, C. M. N91-29568
TANGLER, J. L. N91-29650
TANNENBAUM, D. N91-29983
TAO, RONGJIA N91-29520
TAO, W. C. N91-29387
TARDELLI, J. D. N91-29427
TARDIFF, LISA N91-29608
TAUBER, D. N91-29582
TAYLOR, A. P. N91-29986
TAYLOR, E. R., JR. N91-29401
TAYLOR, MALCOLM S. N91-30050
TAYLOR, P. C. N91-29571
TAYLOR, RAYMOND L. N91-29935
TEAGUE, M. W. N91-29276
TENFORDE, T. S. N91-29709
TENNANT, R. A. N91-29281
TERRY, P. W. N91-29966
TERRY, ROBERT E. N91-29464
TERWILLIGER, C. D. N91-30031
TERZIAN, Y. N91-29812
TESKEY, ROBERT N91-29636
TEWARY, V. K. N91-29251
THAI, JULIE N91-29278
THAI, TAN N91-29549
N91-29747
THEBERGE, MARC W. N91-30049
THEOBALD, D. L. N91-29653
THOMAS, EDWIN L. N91-29368
THOMAS, I. N91-30035
THOMAS, I. M. N91-30034
THOMAS, J. N91-29748
THOME, F. V. N91-29442
THOMPSEN, C. N91-29647
THOMPSON, A. W. N91-29658
THOMPSON, C. V. N91-29653
THOMPSON, G. L. N91-29753
N91-29823
THOMPSON, J. D. N91-29477
THOMPSON, J. R. N91-29975
THOMPSON, P. A. N91-29406
THOMPSON, W., JR. N91-29759
THOMPSON, WILLIAM B. N91-29640
THOMSON, J. O. N91-29993
TIEDERMAN, WILLIAM G. N91-29510
TIEGS, T. N. N91-29373
TIETSWORTH, S. C. N91-29429
TILLEY, JEFFREY SCOTT N91-29670
TING, A. N91-29568
TITRAN, ROBERT H. N91-29298
TOEPPEN, J. S. N91-29914
TOKAZ, J. C. N91-29209
TOMENO, I. N91-30032
TOURYAN, K. J. N91-29483
N91-29557
TOWNSEND, DENNIS P. N91-29599
TOWNSEND, V. W. N91-29929
TRAYNOR, PETER T. N91-29395
TREMBACK, C. N91-29695
TRESANSKY, GEORGE N91-29278
TREW, R. J. N91-30000
TRIPATHI, A. N91-30053
TRIPATHY, SUKANT N91-29348
TROEDSON, S. C. N91-29837
TROWBRIDGE, CHRISTIAN A. N91-29423
TROYER, DAVID E. N91-29672
TRUAX, D. R. N91-30040
TRUCANO, T. G. N91-29203
TRUE, B. N91-29187
TRYBUS, C. L. N91-29299
TSAI, CHEN S. N91-29919
TUKEY, JOHN W. N91-29830
N91-29845
TULCHINSKIY, B. S. N91-29339
TUMMILLO, A. F. N91-29482
TURMAN, B. N. N91-29483
TURNER, ELIJAH W. N91-29171
TURNER, JOHN W. N91-29733
TURNER, M. S. N91-30065
TURNER, W. C. N91-29578
N91-29911
TURYK, P. J. N91-29178

U

UBBINK, W. H. N91-29237
UENO, HIROSHI N91-29586
UMEZAWA, A. N91-29988
UNERTL, W. N. N91-29351
N91-30001
UNSEREN, M. A. N91-29810

V

VAIRAVAMURTHY, A. N91-29656
VALANJU, P. M. N91-29896
VANBRONKHORST, ERIK N91-29421
VANDENAVYLE, J. A. N91-29303
VANDENBERG, H. N91-29776
VANDERAAR, MARK J. N91-29404
VANDERHOFF, JOHN A. N91-29276
VANDIVER, J. K. N91-29630
VANVECHTEN, JAMES A. N91-29280
VANYSEK, PETR N91-29459
VARACALLE, D. J., JR. N91-29328
VARY, ALEX N91-29610
VASSILIOU, MARIUS S. N91-29426
VEAL, B. W. N91-29979
N91-29989
VEITCH, JAMES G. N91-29845
VENTURINI, E. L. N91-29995
VERMA, S. K. N91-29162
VERMAAS, W. F.J. N91-29711
VIANCO, P. T. N91-29320
VIGIL, M. G. N91-29631
VINOKUR, V. M. N91-29988
VINSON, J. R. N91-29241
VIRKAR, A. N. N91-29329
VISWANATHAN, V. K. N91-29915
VITEK, J. M. N91-29301
VITERBI, ANDREW J. N91-29768
VITERNA, LARRY A. N91-29199
VOGT, R. N91-29899
VOIGT, J. A. N91-29995
VONG, F. C. N91-29434
VOSIKA, DONALD C. N91-29828
VRANOS, A. N91-29187

VRCKOVNIK, G. N91-29418
VUKELICH, STEVEN R. N91-29148

W

WAGER, JOHN F. N91-29280
WAGNER, F. N91-29957
WAGNER, PAUL K. N91-29404
WAHLBECK, P. G. N91-29263
WAHLBECK, PHILLIP G. N91-29981
WAKE, L. V. N91-29326
WALKER, CHARLES W., JR. N91-29456
WALKER, D. W. N91-29815
WALKER, J. N91-29549
WALKER, J. D. N91-29507
WALKER, S. N. N91-29646
WALKO, R. N91-29695
WALKO, R. J. N91-29910
WALL, M. A. N91-29972
WALLACE, W. N91-29180
N91-29288
WALSH, D. S. N91-29447
WALTER, C. M. N91-29427
WALTER, J. A. N91-29328
WAMBSGANSS, M. W. N91-29501
N91-29502
WANG, H. H. N91-29987
WANG, HONGXIN N91-29569
WANG, Q. N91-29398
WANG, TZYY-MING N91-29495
WANG, WEICHENG DAVID N91-29238
WANG, WEN I. N91-30010
WANG, Z. L. N91-29536
WANG, ZHAOYU N91-29593
WANTUCK, P. J. N91-29281
WARD, ALFORD L. N91-29471
N91-29752
WARD, K. J. N91-29605
WARGO, L. N91-30051
WARNES, R. H. N91-29540
N91-29542
WARREN, WAYNE H., JR. N91-30060
WATANABE, H. H. N91-29281
WATERS, W. M. N91-29430
WATSON, CHARLES S. N91-29726
WATSON, R. E. N91-29323
N91-29859
WATSON, ROBERT A. N91-29613
WATTS, ALAN W. N91-29763
WATTS, DAVID EDWARD N91-29618
WAYLAND, B. B. N91-29283
WEAVER, J. W. N91-29526
WEAVER, M. J. N91-29272
N91-29455
N91-29878
N91-29879
N91-29880
N91-29882
N91-29883
N91-29884
N91-30004
WEBB, B. J. N91-29377
WEBER, T. L. N91-29646
WEBER, WILLIAM P. N91-29353
WEBSTER, C. E. N91-29482
WEEKS, B. N91-29398
WEGMAN, EDWARD J. N91-29764
WEILER, J. D. N91-29209
WEIN, M. N91-29799
WEINER, BRAD R. N91-29569
WEINERT, M. N91-29323
WEINTRAUB, D. J. N91-29722
WEISS, D. L. N91-29955
WEST, M. N91-30061
WESTERVELT, JAMES D. N91-29803
WESTLEY, R. N91-29196
WESTMACOTT, K. H. N91-30038
WESTWOOD, A. D. N91-29971
WEYER, R. M. N91-29143
WHEELER, R. N91-30028
WHITELAW, J. H. N91-29516
WHITTEMORE, G. R. N91-29540
N91-29542
WHITTEN, W. B. N91-29374
WHORTON, M. N91-30061
WIDAY, DAVID N91-29451
WIEGEL, J. N91-29712
WIEMAN, SHARON A. N91-29687
WIESENFELD, KURT N91-29454
WILDERMAN, S. J. N91-29869
WILEY, CATHY J. N91-29802
WILLIAMS, J. M. N91-29987
WILLIAMSON, SAMUEL J. N91-29727
WILLIS, J. O. N91-30032
WILSON, R. E. N91-29646
WINKLER, M. A. N91-29334
WISE, LARRY N91-29172
WISE, M. B. N91-29653
WITEBSKY, C. N91-29444
WITHAM, MELODY N91-29762
WITT, AUGUST F. N91-29998
WITTIG, C. N91-29867
WITTKE, P. H. N91-29396
WOFSY, S. C. N91-29661
WOLF, D. N91-29284
N91-29990
N91-30030
WOLF, JACK K. N91-29768
WONG, K. C. N91-29707
WOOD, S. A. N91-29554
WOOD, W. E. N91-29319
WOODALL, J. M. N91-30033
WOOLEY, BRUCE A. N91-29468
WORLEY, P. H. N91-29815
WOSNITZA, J. N91-29987
WRIGHT, C. A. N91-29571
WU, C. T. N91-30028
N91-30029
WU, W. N91-30029
WU, XIPING N91-29803
WUNG, T.-S. N91-29516

X

XIAO, Q. F. N91-29986
XU, D. N91-30029
XU, MING N91-29988
XU, YANGSHENG N91-29586

Y

YAHIL, A. N91-30066
YAMADA, HIROMITSU N91-29743
YAN, YITON T. N91-29746
YANG, K. N91-29986
YAU, S. L. N91-29883
N91-29884
YEE, J. H. N91-29435
YELON, W. B. N91-29980
YETTER, JOSEPH A., JR. N91-29692
YEUNG, K. S. N91-29410
YEVICH, R. M. N91-29661
YIP, S. N91-29284
YOST, B. N91-29305
YOST, WILLIAM A. N91-29862
YOUNG, R. P. N91-29926
YOUNGDAHL, C. A. N91-29991
N91-30029
YU, FRANCIS T. N91-29931
YUAN, V. W. N91-29560
YUDONG, LI N91-29566
YUNGUI, GAO N91-29565

Z

ZABIN, SERENA M. N91-29416
ZACCARDELLI, E. N91-29647
ZANONATO, P. L. N91-29548
ZANUTTA, ROBERTO ERNESTO N91-29594
ZEHNER, D. M. N91-29307
ZEITZ, FREDERICK H., III N91-29827
ZHANG, JIANHONG N91-29616
ZHANG, MEI-JIE N91-29838
ZHANG, XIANG N91-29282
ZHANG, Y. N91-29600
ZHANG, Y. Z. N91-29965
ZHOU, STEPHEN Q. N91-29353
ZHOU, XIAO-LIN N91-29984
ZHU, GENXING N91-29496
ZIERKE, WILLIAM C. N91-29515
ZINN, B. T. N91-29381
ZINN, BEN T. N91-29223
ZITTER, ROBERT N. N91-29520
ZOU, DEZHONG N91-29349
ZUKAS, WALTER X. N91-29358
ZUMGERGE, MARK A. N91-29680
ZUMWALT, GLEN N91-29154
N91-29155
N91-29156
ZUTAVERN, F. J. N91-29446
N91-29478

Typical Corporate Source Index Listing

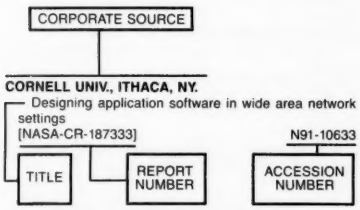

Listings in this index are arranged alphabetically by corporate source. The title of the document provides the user with a brief description of the subject matter. The report number helps to indicate the type of document cited (e.g., NASA report, translation, NASA contractor report). The accession number denotes the number by which the citation is identified. The titles are arranged under each corporate source in ascending accession number order.

A

ADVANCED FUEL RESEARCH, INC., EAST HARTFORD, CT.
Epitaxial growth of single crystal diamond on silicon
[AD-A237758] N91-30007

ADVANCED RESEARCH AND APPLICATIONS CORP., SUNNYVALE, CA.
Diagnostic support services for LLNL (Lawrence Livermore National Laboratory) NOVA laser experiments
[DE90-012125] N91-29552

AEROJET-GENERAL CORP., EL MONTE, CA.
Ada 9X requirements rationale
[AD-A237350] N91-29755

AEROJET TECHSYSTEMS CO., SACRAMENTO, CA.
ALS rocket engine combustion devices design and demonstration
[NASA-CR-183824] N91-29233

AERONAUTICAL RESEARCH LABS., MELBOURNE (AUSTRALIA).
An improved method of investigation of compressor blade fit using holographic interferometry
[AD-A238182] N91-29185
A computer program for prediction of internal performance of a ramrocket
[AD-A238179] N91-29226

AEROSPACE CORP., EL SEGUNDO, CA.
Slag and thermal environment of a spinning rocket motor
[AD-A238557] N91-29227
The language for DENOTE (Denotational Semantics Translation Environment)
[AD-A237144] N91-29750

AIR FORCE INST. OF TECH., WRIGHT-PATTERSON AFB, OH.
Agility: Presentation and flight test methods for the operational fighter pilot
[AD-A238456] N91-29174
Generalized simplified analytic solution of optimum cycle parameters for land and aircraft gas turbine engines and its applications
[AD-A237414] N91-29182
The optimal location of GEODSS sensors in Canada
[AD-A238444] N91-29216
A prolog system for converting VHDL-based models to Generalized Extraction System (GES) rules
[AD-A238545] N91-29741
A common interface real-time multiprocessor operating system for embedded systems
[AD-A238445] N91-29770
Transfer of 4GL application from INGRES to ORACLE
[AD-A238448] N91-29771
Optimal iterative task scheduling for parallel simulations
[AD-A238631] N91-29791
An alternative algorithm for discrete-time filtering
[AD-A238443] N91-29827
The boundary element method applied to the two dimensional Stefan moving boundary problem
[AD-A238458] N91-29828
The utility of elliptical and circular confidence regions for HFDF receivers
[AD-A238390] N91-29842
Effects of colocation and non-colocation of sensors and actuators on flexible structures
[AD-A238457] N91-29844
New modified Anderson-Darling and Cramer-von Mises goodness-of-fit tests for a normal distribution with specified parameters
[AD-A238630] N91-29846
A goodness-of-fit test for a family of two parameter Weibulls with known shape using minimum distance estimation of parameters
[AD-A238633] N91-29847
A vision system model
[AD-A238459] N91-29930
A study of the liquid-solid interface during rapid resolidification of cooper-titanium using molecular dynamics
[AD-A238634] N91-30022

AIR FORCE OCCUPATIONAL AND ENVIRONMENTAL HEALTH LAB., BROOKS AFB, TX.
Acoustic tests on a new motor generator system for the Minuteman launch control centers at Alpha 01 and Sierra 00, Malmstrom AFB, Montana
[AD-A237944] N91-29648

AIR FORCE SYSTEMS COMMAND, EGLIN AFB, FL.
Scientific and technical information handbook for technical report preparation
[AD-A238548] N91-30051

AIR FORCE SYSTEMS COMMAND, WRIGHT-PATTERSON AFB, OH.
International aviation (selected articles)
[AD-A237175] N91-29141
International aviation (selected articles)
[AD-A237232] N91-29142
Powder metallurgy technology (selected articles)
[AD-A237176] N91-29310
Method of obtaining current-conducting polymeric materials
[AD-A237174] N91-29339
Second-harmonic generation of TEA CO2 10.6 micrometer laser light in AgGaS2 crystals
[AD-A237169] N91-29564
Experimental study of gas kinetics of a fast-axial flow kilowatt CO2 laser
[AD-A237178] N91-29565
Development of low-threshold value, high-power semiconductor laser
[AD-A237183] N91-29566
Chinese physics lasers (selected articles)
[AD-A237263] N91-29567

AKRON UNIV., OH.
Exact and approximate solutions to the oblique shock equations for real-time applications
[NASA-CR-187173] N91-29147

ALABAMA UNIV., HUNTSVILLE.
Chemical waste disposal in space by plasma discharge
[NASA-CR-184169] N91-29737
Study of particle correlations in high energy S + Pb and Pb + Pb interactions with a magnetic-interferometric-emulsion-chamber
[DE91-014355] N91-29897

ALLIED-SIGNAL AEROSPACE CO., KANSAS CITY, MO.
Liquid honing evaluation
[DE91-015749] N91-29393
Investigation of ultrasonic evaluation of solid-state metal bond
[DE91-014996] N91-29606

AMERICAN SCIENCE AND ENGINEERING, INC., CAMBRIDGE, MA.
Plasma properties of hot coronal loops utilizing coordinated SMM and solar research rocket observations
[NASA-CR-186094] N91-29937

AMES LAB., IA.
Synthesis and characterization of reduced tungsten sulfide cluster complexes
[DE91-014916] N91-29262
The ac losses in type-2 superconductors
[DE91-015201] N91-29485
Electromagnetic dissociation of Au and Co targets by relativistic heavy ions
[DE91-014915] N91-29906
Fundamental studies of the extraction process in inductively coupled plasma mass spectrometry
[DE90-011733] N91-29939

ANALYTIC SCIENCES CORP., ARLINGTON, VA.
Report to the Congress on the Strategic Defense Initiative, 1991
[AD-A237658] N91-29853

ARCON CORP., WALTHAM, MA.
Research and development for Digital Voice Processing (DVP)
[AD-A238280] N91-29427
Acoustic background noise variation in Air Force platforms and its effect on noise removal algorithms
[AD-A238279] N91-29863

ARGONNE NATIONAL LAB., IL.
Molecular dynamics simulation of the effect of interfaces in melting and solid-state amorphization
[DE91-015550] N91-29284
Characteristics of autoclave and in-reactor nodular corrosion of Zircaloys
[DE91-013600] N91-29294
Biofouling and corrosion fouling of plain and enhanced aluminum surfaces
[DE91-014464] N91-29300
ANL's development of conductive ceramic components for MCFC
[DE91-015557] N91-29336
The 3-D NMR imaging: A chemical microscope for analysis of heterogeneous macromolecular networks
[DE91-015109] N91-29375
Materials research for sodium engine development
[DE91-015715] N91-29378
Minimization of refrigeration power requirements for mechanical supports in cryogenic systems
[DE91-015720] N91-29392
The APS radio frequency test stand control system
[DE91-015711] N91-29434
Performance and life evaluation of advanced battery technologies for electric vehicle applications
[DE91-015671] N91-29482
Analysis of condensation and evaporation of ammonia/water mixtures in matrix heat-exchangers
[DE91-014461] N91-29500
Adiabatic two-phase flow frictional pressure drop. Part 2: A generalized method for data correlation
[DE91-014462] N91-29501
Adiabatic two-phase flow frictional pressure drop. Part 1: Critical parameters and friction factors for air-water mixture
[DE91-014463] N91-29502
Prediction of the pressure drop in transverse, repeated-rib tubes with numerical modeling
[DE91-014465] N91-29503
Development of laser optics for the AWA photocathode
[DE91-015552] N91-29581
Developmental status and system studies of the monolithic solid oxide fuel cell
[DE91-014389] N91-29645
Parameterizations of microphysical processes for simulation of regional-scale clouds
[DE91-015554] N91-29696
The advanced software development and commercialization project
[DE91-015756] N91-29797
Maglev system concept using 20-K high-temperature superconductors and hyperconductors
[DE91-015714] N91-29860
Superdeformation: An experimental review
[DE91-015566] N91-29894
Interactions of turbulent eddies and combustion in an MHD second stage combustor
[DE91-015722] N91-29968

High resolution electron microscopy of grain boundaries
| DE91-010593 | N91-29970
Ruddlesden-Popper phases A(n + 1)M(n)O(3n + 1): Structures and properties
| DE91-011748 | N91-29973
Photoemission and electronic structure studies of YBa2Cu3O(x)
| DE91-014469 | N91-29979
Inverse problem in neutron reflection
| DE91-014457 | N91-29984
De Haas-van Alphen and Fermi surface studies of organic superconductors (ET)2X
| DE91-015137 | N91-29987
Low temperature flux creep in high-T(sub c) superconductors
| DE91-015193 | N91-29988
Photoemission measurement of Fermi surface, band dispersion, and quasiparticle lifetime in YBa2Cu3O6.9
| DE91-015194 | N91-29989
Correlations between grain boundary structure and energy
| DE91-015204 | N91-29990
Fabrication and wire extrusion of ceramic superconductors
| DE91-015207 | N91-29991
Synthesis and superconductivity in Ba(1-x)K(x)BiO3
| DE91-015254 | N91-29992
Consolidation and plasticity of Bi-Sr-Ca-Cu-O superconductors
| DE91-015544 | N91-30028
High-(Tc) superconductors: Fabricating technologies and future perspectives
| DE91-015553 | N91-30029
Connection between grain boundary structure and energy
| DE91-015558 | N91-30030
Determination of thermodynamic and kinetic properties of grain boundaries using high temperature calorimetry
| DE91-015571 | N91-30031

ARIZONA STATE UNIV., TEMPE.
Experimental demonstration of a classical approach for flexible space structure control: NASA CSI testbeds
| NASA-CR-188724 | N91-29212
Separation-bubble velocity measurements using an oscillating-hot-wire system
| AD-A237997 | N91-29518
Specific mutagenesis of a chlorophyll-binding protein
| DE91-014813 | N91-29711
Investigations in Martian geology. Part 1: Nature of the mantling deposit in the heavily cratered terrain of northeastern Arabia, Mars. Part 2: Experimental studies of clean and dust-or-sand-covered ice sublimation under Mars-like conditions N91-30067

ARIZONA UNIV., TUCSON.
Planetary instrument definition and development program: 'Miniature Monochromatic Imager'
| NASA-CR-186550 | N91-29219
Heuristic methods in applied probability
| AD-A238229 | N91-29841
Center for thin film studies
| AD-A237457 | N91-29999

ARMY AEROMEDICAL RESEARCH LAB., FORT RUCKER, AL.
Human factors of night vision devices: Anecdotes from the field concerning visual illusions and other effects
| AD-A237641 | N91-29735

ARMY ARMAMENT RESEARCH, DEVELOPMENT AND ENGINEERING CENTER, PICATINNY ARSENAL, NJ.
Basic simple modeling of balloting motion of railgun projectiles
| AD-A237938 | N91-29205
An approximate analysis of balloting motion of railgun projectiles
| AD-A237942 | N91-29206
Basic simple modeling of in-bore motion of railgun projectiles
| AD-A238064 | N91-29207
Methods to determine the compatibility and degradation of organic materials
| AD-A237940 | N91-29234

ARMY AVIATION TEST BOARD, FORT RUCKER, AL.
Methodology investigation, aviation test management system concept development
| AD-A237349 | N91-29172

ARMY COLD REGIONS RESEARCH AND ENGINEERING LAB., HANOVER, NH.
Performance of asphalt concrete airport pavements during thaw weakening periods: A field study
| AD-A237441 | N91-29198
Remote sensing of snow covers using the gamma ray technique
| AD-A238016 | N91-29639

ARMY CONSTRUCTION ENGINEERING RESEARCH LAB., CHAMPAIGN, IL.
The PC Dugout micro-mainframe integration system: PAX implementation
| AD-A237480 | N91-29758
Engineering applications of neural computing: A state-of-the-art survey
| AD-A237628 | N91-29803

ARMY LAB. COMMAND, FORT MONMOUTH, NJ.
A calorimetric investigation of deuterated palladium electrodes
| AD-A237571 | N91-29456
Measurement of lithium cycling efficiency in organic electrolytes
| AD-A237632 | N91-29457
Protecting the ozone shield: A new public policy
| AD-A237640 | N91-29659

ARMY LAB. COMMAND, WATERTOWN, MA.
Studies of polymers for shock absorption applications
| AD-A237925 | N91-29358
Ultrasonic evaluation of silicon nitride green bodies
| AD-A237924 | N91-29608
Fatigue resistant optical fibers
| AD-A237568 | N91-29921
Effect of hydrogen on the electronic structure of a grain boundary in iron
| AD-A237499 | N91-30002

ARMY LAB. COMMAND, WHITE SANDS MISSILE RANGE, NM.
XTRAN: An atmospheric transmittance code based on XSCALE
| AD-A237624 | N91-29674
A manual method for determining the fractional stability category
| AD-A237627 | N91-29675

ARMY MATERIALS TECHNOLOGY LAB., WATERTOWN, MA.
A layered beam theory for single lap joints
| AD-A237324 | N91-29607

ARMY RESEARCH INST. OF ENVIRONMENTAL MEDICINE, NATICK, MA.
Data acquisition system for collecting biophysical and physiological data
| AD-A237654 | N91-29710
Physiological responses to intermittent exercise as modified by heat stress and protective clothing
| AD-A237447 | N91-29716

ARMY STRATEGIC DEFENSE COMMAND, HUNTSVILLE, AL.
Management of variation and TQM
| AD-A238399 | N91-29843

ARNOLD ENGINEERING DEVELOPMENT CENTER, ARNOLD AIR FORCE STATION, TN.
Carina aerothermal test at Mach 8
| AD-A238561 | N91-29218
Effect of geometric parameters on the performance of second throat annular steam ejectors
| AD-A238645 | N91-29522
Application of diffraction correction to blackbody sources
| AD-A237840 | N91-29926

B

BALLISTIC RESEARCH LABS., ABERDEEN PROVING GROUND, MD.
Spectral studies of solid propellant combustion. 3: Emission and absorption results for HMX2 propellant
| AD-A237958 | N91-29276
Report on using expert systems for computer-aided formulation and property estimation of propellants. 1: Expert system shell selection and initial package design
| AD-A237567 | N91-29383
Experimental hypervelocity firings using stick and granular propellant configurations
| AD-A238628 | N91-29384
Description of a computer fault detector and net isolator
| AD-A238387 | N91-29428
A method of investigating scales of motion in a turbulent wake
| AD-A237923 | N91-29514
Randomization procedures applied to analysis of ballistic data
| AD-A238389 | N91-30050

BATTELLE COLUMBUS LABS., OH.
Application of ceramics to industrial gas turbines
| DE91-013140 | N91-29330

BATTELLE MEMORIAL INST., RESEARCH TRIANGLE PARK, NC.
The development of a fiber-optic readout pressure transducer
| AD-A238393 | N91-29545

BOSTON UNIV., MA.
Magnetospheric structure and dynamics: A multisatellite approach
| AD-A237674 | N91-29676

BRANDEIS UNIV., WALTHAM, MA.
Research in elementary particle physics
| DE91-015359 | N91-29892

BRIGHAM YOUNG UNIV., PROVO, UT.
Deactivation by carbon of iron catalysts for indirect liquefaction
| DE91-011276 | N91-29285

BROOKHAVEN NATIONAL LAB., UPTON, NY.
Light weight space power reactors for nuclear electric propulsion
| DE91-014803 | N91-29232
First principles simulations of metallic alloys and liquids
| DE91-015171 | N91-29323
Methods for determination of low-molecular weight carbonyl compounds in the ambient atmosphere
| DE91-015188 | N91-29656
An observational study of the efficiency of activation of accumulation-mode particles in warm continental stratiform clouds
| DE91-013335 | N91-29681
Monte Carlo and mean field calculations of the magnetocaloric effect of ferromagnetically interacting clusters
| DE91-014792 | N91-29859
Algebraic approaches to nuclear structure
| DE91-015214 | N91-29870
Strange quarks in nuclei
| DE91-015833 | N91-29895
The BNL toroidal volume H(-) source
| DE91-013592 | N91-29947
Intermetallic superconductors: The state of development in 1991
| DE91-014844 | N91-30026

BROWN UNIV., PROVIDENCE, RI.
A model of multicomponent droplet evaporation with liquid phase reactions
| DE90-012535 | N91-29257
Fundamental studies in dynamic plasticity
| AD-A237114 | N91-29621
A research program in experimental and theoretical high energy physics
| DE91-014728 | N91-29907

C

CALIFORNIA INST. OF TECH., PASADENA.
Mechanistic investigation of nanometer-scale/lithography at liquid-covered graphite surfaces
| AD-A237085 | N91-29337
Pulse induced nanlithography of graphite in H2O: A road to chemical linkages to the surface?
| AD-A237086 | N91-29338
Coding for spread-spectrum channels in the presence of jamming
| AD-A238233 | N91-29425
Statistical mechanics of two-dimensional Euler equations and Jupiter's Great Red Spot N91-29498
Studies in neural networks
| AD-A237452 | N91-29717
Differential equations and continuum mechanics
| AD-A237722 | N91-29820
Electron tunneling microscopy
| AD-A237504 | N91-30003
The relationship between the density wave, molecular gas and star formation in M51 N91-30064

CALIFORNIA STATE UNIV., NORTHRIDGE.
Spin-Label-Spin-Probe. Studies of bimolecular encounters in micelles
| AD-A238546 | N91-29891

CALIFORNIA UNIV., BERKELEY.
Micromechanisms of monotonic and cyclic subcritical crack growth in advanced high melting point low-ductility intermetallics
| AD-A238151 | N91-29317
Structures, properties, and dynamics of metal clusters from infrared laser spectroscopy
| AD-A237669 | N91-29570
Software development of the cochlear filter and eighth-nerve model
| AD-A237454 | N91-29757

CALIFORNIA UNIV., BERKELEY. LAWRENCE BERKELEY LAB.
The ASTROMAG superconducting magnet facility configured for a free flying satellite
| DE91-014710 | N91-29204
Molecular beam studies of reaction dynamics
| DE90-011600 | N91-29256

Performance of multiple stream pulsed jet combustion systems
[DE91-012338] N91-29259
Hot atom reactive scattering and photodissociation experiments with acetylene and ethylene
[DE91-013755] N91-29264
Equation of state for pure sodium chloride
[DE91-014618] N91-29286
Measurements of retractable gas-cooled 6061 aluminum electrical leads operating in a vacuum
[DE91-014617] N91-29444
A methodology for inhibiting the formation of pollutants in diesel engines
[DE90-011615] N91-29584
Quantum measurement and the mind-brain connection
[DE91-012343] N91-29723
Molecular beam studies of reaction dynamics
[DE91-014866] N91-29868
Specific heat of YBaCu3O7: Volume fraction of superconductivity; parameters characteristic of the ideal superconducting state
[DE91-011827] N91-29974
TEM characterization of grain boundaries in mixed bicrystal films of aluminum
[DE91-016267] N91-30038

CALIFORNIA UNIV., DAVIS.
Strengthening mechanisms, creep, and fatigue processes in dispersion hardened niobium alloy
[AD-A237784] N91-29313
Ceramic decomposition under irradiation
[DE91-015061] N91-29372
Solvent effects on simple electron transfer reactions. A comparison of results in Debye and non-Debye solvents
[AD-A237157] N91-29875
Role of the solvent in kinetics of heterogeneous electron and ion transfer reactions
[AD-A237168] N91-29876
Measurements of the ion acoustic decay instability and the resultant thermal and suprathermal electron heating in laser-plasma interaction experiments
[DE90-012477] N91-29941
Discreteness-of-solvent effects in Marcus equations in the mean spherical approximation
[AD-A237133] N91-29996

CALIFORNIA UNIV., IRVINE.
Major achievements during the first program year
[AD-A237171] N91-29919

CALIFORNIA UNIV., LOS ANGELES.
Development of the microstructure based stochastic life prediction models
[AD-A237768] N91-29312
The mixed metallic-ionic clusters of the silver/silver iodide
[AD-A237883] N91-29314
Preparation and properties of new inorganic glasses and gel-derived solids
[AD-A238095] N91-29360
Regional tectonic deformation in Southern California, inferred from terrestrial geodesy and the global positioning system N91-29669
The relative stability and possible structural formulae of the negatively charged silver monoiodide clusters
[AD-A238398] N91-29888

CALIFORNIA UNIV., SAN DIEGO, LA JOLLA.
Development of a mixture for nonlinear wave propagation in fiber-reinforced composites
[AD-A237471] N91-29243

CALIFORNIA UNIV., SANTA BARBARA.
The embedded electron-gas boundary: A new standard problem in surface physics
[AD-A238152] N91-30014

CALSPAN-BUFFALO UNIV. RESEARCH CENTER, NY.
Discretionary security for object-oriented database systems
[AD-A237573] N91-29740

CALSPAN FIELD SERVICES, INC., ARNOLD AFS, TN.
Carina aerothermal test at Mach 8
[AD-A238561] N91-29218

CAMBRIDGE UNIV. (ENGLAND).
Basic mechanisms of diesel lubrication correlation of bench and engine tests
[AD-A237685] N91-29596

CARNEGIE-MELLON UNIV., PITTSBURGH, PA.
Modeling of a 3-D light-weight space manipulator
[AD-A236823] N91-29586
Environmental effects in niobium base alloys and other selected intermetallic compounds
[AD-A237535] N91-29658
The functional architecture of visual object recognition
[AD-A238617] N91-29732
An exact algorithm for funding undirected Hamiltonian cycles based on a two-matching problem relaxation
[AD-A237241] N91-29753
An exact two-matching based branch and bound algorithm for the symmetric traveling salesman problem
[AD-A237878] N91-29823
Multitarget tracking using optical processing
[AD-A237107] N91-29918

CHARLES RIVER ANALYTICS, INC., CAMBRIDGE, MA.
An expert system approach to global fault detection and isolation design
[AD-A238494] N91-29808

CHEMICAL RESEARCH AND DEVELOPMENT CENTER, ABERDEEN PROVING GROUND, MD.
Ventilation kinetics testing of a steel frame/rubber fabric underground shelter
[AD-A237469] N91-29734

CHICAGO UNIV., IL.
Performance report of the Wind Research Lab.
[AD-A238575] N91-29691

CLARK-ATLANTA UNIV., GA.
Precursors to Si-N-C-O ceramics: A reinvestigation of the poly methylvinyl silylethyl enediamine systems
[DE91-013722] N91-29333

CLEMSON UNIV., SC.
An investigation to determine the producibility of a 3-D braider and bias direction weaving loom
[NASA-CR-188741] N91-29390

COLORADO UNIV., BOULDER.
Semiconductor deposition and etching interactions of laser-generated translationally hot atoms and radicals
[AD-A238198] N91-30015

COLUMBIA UNIV., NEW YORK, NY.
Picosecond studies of chemical intermediates
[AD-A237859] N91-29275
Laser enhanced chemical reaction studies
[DE91-013021] N91-29555
Theoretical high energy physics
[DE90-012527] N91-29904
Theoretical high energy physics
[DE91-013639] N91-29905
Identification of, and transition to, the second region of ideal MHD stability in tokamaks
[DE90-010380] N91-29938
Molecular beam epitaxial growth and characterization of metastable compound semiconductors for infrared detector applications
[AD-A237797] N91-30010
On the role of crystal defects as sources of resonator frequency instability
[AD-A238505] N91-30018

CONNECTICUT UNIV., STORRS.
Global optimality, conservativity and singularity in redundancy resolution of robotic manipulators N91-29593
Prediction of edge stresses in layered media using the surface integral-finite element technique N91-29614

CORNELL UNIV., ITHACA, NY.
Defects and transport in mixed oxides
[DE91-014537] N91-29266
Deformation and thermal fatigue in high temperature austenitic alloys
[DE91-014981] N91-29305
Reactions of hydrogen atoms important to the decomposition of energetic materials
[AD-A238482] N91-29890

COUNCIL FOR NATIONAL ACADEMIC AWARDS (ENGLAND).
An investigation of Nova Persei (1901) and its environment N91-30059

CRYSTALLUME, MENLO PARK, CA.
Thermochemistry of hydrocarbon decomposition and relationship to properties of PECVD diamond films
[AD-A237793] N91-29274

CVD, INC., WOBURN, MA.
Fabrication of lightweight Si/SiC LIDAR mirrors
[NASA-CR-4389] N91-29935

D

DAVID TAYLOR RESEARCH CENTER, BETHESDA, MD.
An evaluation of the NEKTON program
[AD-A237888] N91-29513

DEFENCE RESEARCH ESTABLISHMENT, OTTAWA (ONTARIO).
A Doppler bin blanking CFAR processor for airborne radars
[AD-A237890] N91-29418

DELAWARE UNIV., NEWARK.
Ocean thermal feature recognition, discrimination and tracking using infrared satellite imagery
[AD-A238138] N91-29703
Oceanographic data report Number 7: Data from the Delaware Estuary SCENIC cruises, April 1986 - September 1988
[PB91-183582] N91-29706
Oceanographic data report Number 8: Density profiles from the Delaware Estuary, October 1986 - September 1988
[PB91-183608] N91-29707

DEPARTMENT OF ENERGY, IDAHO FALLS, ID.
Environmental assessment for the FAA explosive detection system independent validation and verification program
[DE91-013190] N91-29152

DEPARTMENT OF ENERGY, WASHINGTON, DC.
Subsurface Science Program
[DE91-015480] N91-29665

DEPARTMENT OF THE AIR FORCE, WASHINGTON, DC.
Slaying the software dragon: A look at how software engineering, the Ada programming language and process maturity are changing software development
[AD-A237156] N91-29751

DEPARTMENT OF THE ARMY, WASHINGTON, DC.
Range-only multistatic radar system
[AD-D011645] N91-29399

DEPARTMENT OF THE NAVY, WASHINGTON, DC.
Stabilized square parachute
[AD-D014946] N91-29149
Hardware interface for high speed video imaging
[AD-D014902] N91-29400
A high data rate communications system using long pulses
[AD-D014947] N91-29430
Cable tester
[AD-D014904] N91-29438
Universal ground adapter assembly
[AD-D014908] N91-29439
Pyrite cathode material for a thermal battery
[AD-D014945] N91-29475
Transient flowmeter calibration facility
[AD-D014937] N91-29523
Quick disconnect pressure cap
[AD-D014936] N91-29598
Optical soliton source
[AD-D014942] N91-29933
Electro-optic line narrowing of optical parametric oscillators
[AD-D014944] N91-29934

DEPARTMENT OF TRANSPORTATION, CAMBRIDGE, MA.
The use and design of flightcrew checklists and manuals
[AD-A237206] N91-29733

DOTY SCIENTIFIC, INC., COLUMBIA, SC.
Microtube strip heat exchanger
[DE91-015223] N91-29529

DOUGLAS AIRCRAFT CO., INC., LONG BEACH, CA.
Test results for composite specimens and elements containing joints and cutouts
[NASA-CR-178246] N91-29254

DRAPER (CHARLES STARK) LAB., INC., CAMBRIDGE, MA.
Equations of motion for a flexible spacecraft-lumped parameter idealization
[NASA-CR-188727] N91-29211

DU PONT DE NEMOURS (E. I.) AND CO., WILMINGTON, DE.
An exact algorithm for funding undirected Hamiltonian cycles based on a two-matching problem relaxation
[AD-A237241] N91-29753
An exact two-matching based branch and bound algorithm for the symmetric traveling salesman problem
[AD-A237878] N91-29823

DUKE UNIV., DURHAM, NC.
Stable isotope fractionation in photosynthesis: Analysis of autotrophic competence following transformation of the chloroplast genome of Chlamydomonas
[DE91-015792] N91-29713

E

EDGERTON, GERMESHAUSEN AND GRIER, INC., IDAHO FALLS, ID.
Tensile properties and microstructure of Alloy 718 thermally aged to 50,000 h
[DE91-014099] N91-29299
An evaluation of nickel-aluminum coatings fabricated with the plasma-spray process
[DE91-013208] N91-29328

EG AND G MOUND APPLIED TECHNOLOGIES, MIAMISBURG, OH.
Feasibility of a laser-ignited HMX deflagration-to-detonation transition device for the US Navy LITES Program
[DE91-015210] N91-29382

EG AND G ROCKY FLATS, INC., GOLDEN, CO.
Calculation of intra-rare Earth binary phase diagrams
[DE91-014950] N91-29267

ELECTRONICS RESEARCH LAB., ADELAIDE (AUSTRALIA).
A general lease-squares fitting package for the sun workstation
[AD-A238180] N91-29837
ELECTROTECHNICAL LAB., IBARAKI (JAPAN).
Matching of complex 3-D surfaces using dynamic programming
[ERB-1022] N91-29743
ENVIRONMENTAL PROTECTION AGENCY, ADA, OK.
Approximate multiphase flow modeling by characteristic methods
[PB91-190959] N91-29526
ENVIRONMENTAL PROTECTION AGENCY, ANN ARBOR, MI.
Conversion of methanol-fueled 16-valve, 4-cylinder engine to operation on gaseous 2H2/CO fuel
[PB91-195941] N91-29602
ENVIRONMENTAL PROTECTION AGENCY, RESEARCH TRIANGLE PARK, NC.
Overview of the technical implications of methanol and ethanol as highway motor vehicle fuels
[PB91-182881] N91-29385
Criteria for assessing the role of transported ozone/precursors in ozone nonattainment areas
[PB91-195958] N91-29662
ENVIRONMENTAL PROTECTION AGENCY, WASHINGTON, DC.
Information Systems Inventory (ISI)
[PB91-172940] N91-30055
ENVIRONMENTAL RESEARCH INST. OF MICHIGAN, ANN ARBOR.
P-3 SAR calibration activity at Andros Island
[AD-A237357] N91-29412
EXECUTIVE OFFICE OF THE PRESIDENT, WASHINGTON, DC.
Publications of the Executive Office of the President, January 20, 1989 - March 31, 1991
[PB91-156828] N91-30056

F

FEDERAL AVIATION ADMINISTRATION, WASHINGTON, DC.
Donning times and flotation characteristics of infant life preservers: Four representative types
[AD-A237120] N91-29153
FERMI NATIONAL ACCELERATOR LAB., BATAVIA, IL.
Conformal FDTD modeling wake fields
[DE91-015129] N91-29407
Visualization of wake fields
[DE91-015130] N91-29408
A note on the automated differentiation of implicit functions
[DE91-015104] N91-29816
Dark matter in the universe
[DE91-014863] N91-30065
FLORIDA STATE UNIV., TALLAHASSEE.
On the analysis of grouped survival data using cumulative occurrence/exposure rates
[AD-A238219] N91-29838
Singularities in Gaussian random fields
[AD-A238220] N91-29839
A mixed limit theorem for stable random fields
[AD-A238222] N91-29840
FLORIDA UNIV., GAINESVILLE.
Vibration control and optimization in composite structural elements by use of add-on viscoelastic materials
[AD-A238533] N91-29628
FORWARD UNLTD., OXNARD, CA.
Twenty first century space propulsion study addendum
[AD-A238011] N91-29225

G

GATES LEARJET CORP., WICHITA, KS.
Aircraft icing handbook, volume 1
[AD-A238039] N91-29154
Aircraft icing handbook, volume 2
[AD-A238040] N91-29155
Aircraft icing handbook, volume 3
[AD-A238041] N91-29156
GENERAL ACCOUNTING OFFICE, WASHINGTON, DC.
Strategic defense initiative: Need to examine concurrency in development of brilliant pebbles
[AD-A238292] N91-29854
GENERAL ATOMIC CO., SAN DIEGO, CA.
H-mode energy confinement scaling from the ASDEX, DIII-D, and jet tokamaks
[DE91-015145] N91-29957
GENERAL ATOMICS TECHNOLOGIES CORP., SAN DIEGO, CA.
Advanced divertor experiments on DIII-D
[DE91-011138] N91-29950
GENERAL ELECTRIC CO., FAIRFIELD, CT.
Silicon Wafer Advanced Packaging (SWAP). Multichip Module (MCM) foundry study, version 2
[AD-A237412] N91-29452
GENERAL ELECTRIC CO., SCHENECTADY, NY.
Portable parallel programming
[DE91-015648] N91-29794
GENERAL ELECTRIC CO., SYRACUSE, NY.
Failure mechanisms on GaAs integrated circuits: Electromigration on GaAs
[AD-A237352] N91-29451
GENERAL PHYSICS CORP., CAPE CANAVERAL AFS, FL.
Pressure vessel burst test program
[AD-A237845] N91-29624
GEORGE MASON UNIV., FAIRFAX, VA.
Hyperdimensional data analysis and structural inference
[AD-A238097] N91-29764
GEORGE WASHINGTON UNIV., WASHINGTON, DC.
Quantitative interpretation of auger lineshapes and electron/photon stimulated desorption
[AD-A237138] N91-29874
GEORGIA INST. OF TECH., ATLANTA.
Unsteady compressible lifting surface analysis for rotary wings using velocity potential modes N91-29170
Investigation of the flame-acoustic wave interaction during axial solid rocket instabilities
[AD-A237851] N91-29223
Investigation of the combustion of liquid fuels in Rijke type pulse combustors
[DE90-012490] N91-29381
Signal processing in impulsive electromagnetic interference
[AD-A237612] N91-29416
Nonlinear dynamics of Josephson junction parametric amplifier arrays
[AD-A237451] N91-29454
A study of the relationship between macroscopic measures and physical processes occurring during N00014-89-J-1708
[AD-A238423] N91-29627
GEORGIA UNIV., ATHENS.
Using the TIMS to estimate evapotranspiration from a forest
[NASA-CR-188729] N91-29636
Microbiology and physiology of anaerobic fermentations of cellulose
[DE91-015239] N91-29712
High bandwidth diagnosis within the framework of a microcomputer-based intelligent tutoring system
[AD-A237959] N91-29805
GREAT LAKES RESEARCH CORP., ELIZABETHTON, TN.
Long-term testing and evaluation of cathode components in a commercial aluminum cell, volume 1
[DE90-010896] N91-29436
GRUMMAN AEROSPACE CORP., PRINCETON, NJ.
ICRF edge modeling
[DE91-014401] N91-29403

H

HARRIS CORP., MELBOURNE, FL.
Experimental verification of an innovative performance-validation methodology for large space systems
[AD-A237864] N91-29214
HARRY DIAMOND LABS., ADELPHI, MD.
Spike leakage and burnout of silicon PIN diode microwave limiters
[AD-A238392] N91-29471
User's manual for DIODE
[AD-A237190] N91-29752
A survey of techniques in Aided Target Recognition (ATR) from digital and optical perspectives
[AD-A238644] N91-30052
HARVARD UNIV., CAMBRIDGE, MA.
The role of microorganisms in marine corrosion
[AD-A237062] N91-29308
Theoretical studies of long-range transport of oxidants
[PB91-182360] N91-29661
Study of energy levels and decay mechanisms for Singlet Rydberg states of molecular nitrogen
[AD-A238156] N91-29885
The effects of luminance boundaries on color perception
[AD-A237794] N91-29925
HAWAII UNIV., MANOA.
Tropical cyclone motion in the northwest Pacific Ocean, phase 1
[AD-A237455] N91-29683
HONEYWELL, INC., BLOOMINGTON, MN.
Monolithic integration of semiconductor and superconductor components
[AD-A237946] N91-30012

I

IBM FEDERAL SYSTEMS DIV., MANASSAS, VA.
SAFENET 2 fiber optic implementation study
[AD-A238044] N91-29929
IBM RESEARCH LAB., SAN JOSE, CA.
Electrochemical contact adsorption site changes driven by field and charge fact and theory
[AD-A237127] N91-29269
IDAHO NATIONAL ENGINEERING LAB., IDAHO FALLS.
Environmental assessment for the FAA explosive detection system independent validation and verification program
[DE91-013190] N91-29152
ILLINOIS UNIV., CHICAGO.
Performance and stability in high speed articulated structures undergoing quick maneuvers: Theory and applications
[AD-A237857] N91-29597
ILLINOIS UNIV., URBANA.
Fault-tolerant computing: An overview
[NASA-CR-188793] N91-29769
Performance implications of synchronization support for parallel FORTRAN programs
[AD-A238493] N91-29790
ILLINOIS UNIV., URBANA-CHAMPAIGN.
Proton deceleration near the surface of an accreting neutron star N91-30063
INDAL TECHNOLOGIES, INC., MISSISSAUGA (ONTARIO).
Experimental stress measurements for the modified Indal Series 6400 VAWT
[NAE-LTR-LA-310] N91-29642
INDIANA UNIV., BLOOMINGTON.
Institute for the Study of Human Capabilities: Summary descriptions of research for the period December 1989 through September 1990
[AD-A237767] N91-29726
High resolution electron energy loss studies of surface vibrations
[DE91-014539] N91-30024
INSTITUTE FOR DEFENSE ANALYSES, ALEXANDRIA, VA.
Digital SPC switching technology: Foreign technology assessment
[AD-A237258] N91-29449
IDA studies on natural space environmental effects on materials for SDIO
[AD-A237974] N91-29660
Real-time Ada design methodologies and their impact on performance
[AD-A237259] N91-29754
INSTITUTO DE PESQUISAS ESPACIAIS, SAO JOSE DOS CAMPOS (BRAZIL).
A practical example of forest mapping and timber volume estimation using LANDSAT-5 TM imagery
[INPE-5244-PRE/1675] N91-29635
INTERNATIONAL CENTRE FOR THEORETICAL PHYSICS, TRIESTE (ITALY).
The 't Hooft's solution for arbitrary semisimple Lie group
[DE91-617572] N91-29813
The Kramers problem: Fifty years of development
[DE91-617583] N91-29855
Dielectric function of semiconductor superlattice
[DE91-617788] N91-29976
Orbitals, correlation, valencies in high-T(sub c) superconductors
[DE91-618099] N91-29977
IOWA STATE UNIV. OF SCIENCE AND TECHNOLOGY, AMES.
Modification of axial-flow compressor stall margin by variation of stationary blade setting angles
[AD-A238406] N91-29186

J

JAYCOR, VIENNA, VA.
User's guide to the (NCARAI) artificial intelligence technical library
[AD-A237270] N91-29802
JOHNS HOPKINS UNIV., BALTIMORE, MD.
Numerical and physical modelling of bubbly flow phenomena
[DE91-013646] N91-29492
Stochastic simulation techniques for partition function approximation of Gibbs random field images
[AD-A238611] N91-29775

Study of elementary reactions and energy transfer processes involving the NH and CN free radicals
[AD-A238461] N91-29889

JOINT INST. FOR LAB. ASTROPHYSICS, BOULDER, CO.
Laser probing of the kinetics and dynamics of III -V semiconductor growth
[AD-A237795] N91-30009

JOINT PUBLICATIONS RESEARCH SERVICE, ARLINGTON, VA.
JPRS report: Science and technology. USSR: Materials science
[JPRS-UMS-91-001] N91-29291

K

KAMAN SCIENCES CORP., COLORADO SPRINGS, CO.
Telescope and sensor interface preliminary requirements report for the PORTS chamber
[AD-A237755] N91-29923

KANSAS STATE UNIV., MANHATTAN.
Persistent photoconductivity in II-VI mixed semiconductors related critical phenomena and applications
[AD-A237792] N91-29460

KANSAS UNIV., LAWRENCE.
Atomic physics in strong fields
[DE91-015393] N91-29872

L

L'GARDE, INC., TUSTIN, CA.
Concentrator flight test experiment
[AD-A237390] N91-29647

LAMONT-DOHERTY GEOLOGICAL OBSERVATORY, PALISADES, NY.
CO2 measurements along the WOCE P-16 and 19 sections in the South Pacific Ocean: A joint LDGO/WHOI program
[DE91-015742] N91-29708

LASERGENICS CORP., SAN JOSE, CA.
Very high temperature fibers of TiC and TiB2
[AD-A237423] N91-29242

LAWRENCE LIVERMORE NATIONAL LAB., CA.
Flutter consideration of a crash-test aircraft
[DE91-015094] N91-29192
The magnetron-enhanced etching of double-level tungsten interconnect
[DE91-014984] N91-29306
Laser surface modification for selective electroplating of metal: A 2.5 m/s laser direct-write process
[DE91-014988] N91-29322
The effects of HMX particle size and binder stiffness on the burning mechanism and regression rate of a series of fast burning propellants
[DE91-015785] N91-29387
Computation of broadband, high-power electromagnetic pulse generation from an air gas avalanche switch
[DE91-015793] N91-29435
Simulation of the growth of Mo/Si multilayers
[DE91-015679] N91-29486
Numerical simulation of a viscous vortex ring interaction with a density interface
[DE91-011532] N91-29489
Shockwave considerations for sub-grid closure modeling in turbulent large eddy simulations
[DE91-015142] N91-29506
Electroforming thin channel heat exchangers
[DE91-015114] N91-29528
Energy generation by a shock crossing a perturbed interface
[DE91-015678] N91-29530
An elevated temperature titration calorimeter
[DE91-015765] N91-29548
SDIO Laser Propulsion Workshop
[DE90-011758] N91-29550
Program and applications for a near-term laser launch system
[DE90-011760] N91-29551
Blackbody pumped CO2 lasers using Gaussian and waveguide cavities
[DE91-012494] N91-29559
Adjustable magnification anamorphic beam expander
[DE91-014110] N91-29561
Degradation of brightness by resonant particle effects
[DE91-015181] N91-29578
RF transfer in the coupled-cavity free-electron laser two-beam accelerator
[DE91-015676] N91-29583
Deformation behavior of pre-shocked copper as a function of strain rate and temperature
[DE91-015180] N91-29620
A simple model for low L/D penetration physics
[DE91-015747] N91-29633
NIKE2D: A nonlinear, implicit, two-dimensional finite element code for solid mechanics
[DE91-015734] N91-29634
Numerical modeling of turbulent dispersion around structures using a particle-in-cell method
[DE91-012035] N91-29652
Atmospheric dispersion models for dense gas releases
[DE91-015144] N91-29654
The parallel BFGS method for unconstrained minimization
[DE91-015784] N91-29798
Workshop on Automation and Robotics: Proceedings
[DE91-015175] N91-29801
Plan for a laser weapon verification research program
[DE90-012123] N91-29848
SDI performance and START constraints: Modeling phase-1 defense engagements
[DE91-013305] N91-29849
ASAT monitoring project at LLNL
[DE91-013247] N91-29850
Single-scatter Monte Carlo compared to condensed history results for low energy electrons
[DE91-015176] N91-29869
Chasing the x(sub f) dependence of J/psi production
[DE91-015136] N91-29899
Electron-ion interaction cross sections determined by x ray spectroscopy on EBIT
[DE91-015786] N91-29903
Control of energy sweep and transverse beam motion in induction linacs
[DE91-015177] N91-29911
A real time collimation sensor using a shear plate and a spatial light modulator
[DE90-011362] N91-29914
Preparation of damage resistant optical coatings on flat substrates
[DE91-013588] N91-29916
Stagnation and interpenetration of laser-created colliding plasmas
[DE91-013244] N91-29946
Detection of coherent structures in the edge of the TEXT tokamak plasma
[DE91-015183] N91-29958
Electromagnetic PIC simulations using finite elements on unstructured grids
[DE91-015141] N91-29962
Towards a realistic plasma simulation code
[DE91-015698] N91-29967
InGaAs/GaAs graded superlattices in photodetectors for wavelengths beyond 1 micron
[DE90-012073] N91-29969
Electron microscopy of thick 304 SS-copper multilayers
[DE91-011116] N91-29972
Uniaxial stress study of the quantum transitions in a strained layer (001) In0.2Ga0.8As/GaAs single quantum well
[DE91-014990] N91-30033
Optical and environmentally protective coatings for Potassium Dihydrogen Phosphate (KDP) harmonic converter crystals
[DE91-015296] N91-30034
Influence of diamond turning and surface cleaning processes on the degradation of KDP crystal surfaces
[DE91-015300] N91-30035
Spatial propagation of squeezed light in a degenerate parametric amplifier
[DE91-014989] N91-30039
Diffraction-limited imaging of satellites using bispectral speckle interferometry
[DE91-015745] N91-30062

LEHIGH UNIV., BETHLEHEM, PA.
Three-dimensional vortex dynamics and interactions in near-wall turbulent boundary layers
[AD-A237413] N91-29507

LOCKHEED AERONAUTICAL SYSTEMS CO., BURBANK, CA.
Composite transport wing technology development: Design development tests and advanced structural concepts
[NASA-CR-4177] N91-29253

LODESTAR RESEARCH CORP., BOULDER, CO.
Fundamental studies of fusion plasmas
[DE91-015656] N91-29964

LOS ALAMOS NATIONAL LAB., NM.
Nuclear data needs for the space exploration initiative
[DE91-013231] N91-29200
Supersonic combustion of a transverse injected H2 jet in a radio frequency heated flow
[DE91-014739] N91-29281
Thermophysical properties of POCO AXF-5Q graphite up to melting
[DE91-014751] N91-29334
REX: A 5-MV pulsed-power source for driving high-brightness electron beam diodes
[DE91-014604] N91-29443
Effects of doping on hybridization gapped materials
[DE91-014611] N91-29477
Computational simulations of plasma flow switches and imploding loads
[DE91-014768] N91-29480
Shock acceleration with turbulence minimization
[DE91-014741] N91-29505
A slit aperture for the Monitoring X ray Experiment (MOXE)
[DE91-013317] N91-29538
Full-field Fabry-Perot interferometer
[DE91-014610] N91-29540
VISAR: Line-imaging interferometer
[DE91-014749] N91-29542
Measurement of longitudinal emittance growth using a laser-induced neutralization method
[DE91-013500] N91-29560
Low-jitter, high-voltage, infrared, laser-triggered, vacuum switch
[DE91-014602] N91-29562
Ablation of material by front surface spallation
[DE91-014773] N91-29563
Kinetics of dark reaction in chemical laser gases
[DE91-015320] N91-29579
Effects of anisotropy on dynamic tensile behavior
[DE91-014748] N91-29632
Limitations to the method of power spectrum analysis: Nonstationarity, biased estimators, and weak convergence to normality
[DE91-008583] N91-29812
On satellite constellation selection
[DE91-014562] N91-29851
Development of reflective optical systems for XUV projection lithography
[DE91-013167] N91-29915
Future explosive pulse-power technology for high-energy plasma physics experiments
[DE91-014601] N91-29951
Plasma and electrical diagnostics for Procyon experiments
[DE91-014736] N91-29952
Procyon experiments utilizing explosively-formed fuse opening switches
[DE91-014742] N91-29953
Plasma flow switch experiments on the Pegasus facility
[DE91-014744] N91-29954
Computational modeling of the Trailmaster Procyon system
[DE91-014765] N91-29955
Growth condition dependence of RHEED pattern from GaAs(111)B surface
[DE91-014770] N91-29986
Anisotropic spin susceptibility of the (Y,Ca),(Ba, La)2Cu4O8 system
[DE91-014593] N91-30032
Supercoherent states and physical systems
[DE91-014598] N91-30040
Comparison of four methods for aggregating judgments from multiple experts
[DE91-013522] N91-30043

LOWELL UNIV., MA.
Design, synthesis and characterization of novel polydiacetylenes using new analytical techniques
[AD-A237362] N91-29348

LOYOLA UNIV., CHICAGO, IL.
Auditory processing of complex sounds across frequency channels
[AD-A238023] N91-29862

M

MAINE UNIV., ORONO.
Effect of excess oxydianiline on the properties of polyimide
[AD-A237467] N91-29351
Properties and adhesion of polyimides in microelectronic devices
[AD-A238204] N91-29364
Comparison between the interfacial chemistry of metallized polyimides and polymide
[AD-A238400] N91-29366
Surface structure and surface order
[AD-A237466] N91-30001

MARYLAND UNIV., COLLEGE PARK.
Vision-based navigation and parallel computing
[AD-A238570] N91-29164
Laser-atom interaction at high intensities
[AD-A238231] N91-29887
Thermophysical properties of supercritical fluids and fluid mixtures
[DE91-015794] N91-30041

MASSACHUSETTS INST. OF TECH., CAMBRIDGE.
Millimeter-accuracy satellite navigation
[AD-A237736] N91-29163
Simulation of the structure of dense, amorphous bisphenol-A polycarbonate
[AD-A237222] N91-29270
Simulation of large deformation in glassy atactic polypropylene
[AD-A237223] N91-29340
Modelling of deformation textures evolution in semi-crystalline polymers
[AD-A237288] N91-29342
Quasi-static modeling of chain-dynamics in the amorphous glassy polycarbonate of 4,4'-isopropyledenediphenol
[AD-A237289] N91-29343
Inelastic deformation and fracture of glassy solids
[AD-A237290] N91-29344
An atomistic model of the amorphous glassy polycarbonate of 4,4'-isopropylidenediphenol
[AD-A237291] N91-29345
The molecular view of plastic deformation and precursor processes of crazing in glassy polypropylene and polycarbonate
[AD-A237333] N91-29346
Conformational characteristics of the polycarbonate 4,4'-isopropylidenediphenol
[AD-A237334] N91-29347
The Research Laboratory of Electronics
[AD-A237670] N91-29458
Characterization of a sub-picosecond dye laser for the study of atom-perturber collisions
[AD-A238099] N91-29572
Multipixel multidimensional laser radar system theory
[AD-A238110] N91-29573
Short-pulse glass slab amplifier
[DE91-015385] N91-29580
The MIT short-wavelength laser project
[DE91-015357] N91-29582
Morphology of bulk Nylon 6 subjected to plane strain compression
[AD-A237331] N91-29622
Deconvolution of x ray diffraction data to elucidate plastic deformation mechanisms in the uniaxial extension of bulk Nylon-6
[AD-A237332] N91-29623
Dimensionless parameters important to the prediction of vortex-induced vibration of long, flexible cylinders in ocean currents
[PB91-184713] N91-29630
APRIL: A processor architecture for multiprocessing
[AD-A237476] N91-29739
A high-performance retargetable simulator for parallel architectures
[AD-A237354] N91-29779
Counting networks
[AD-A237475] N91-29780
Lazy task creation: A technique for increasing the granularity of parallel programs
[AD-A237477] N91-29781
The MIT Alewife machine: A large-scale distributed-memory multiprocessor
[AD-A237705] N91-29784
The atomic strain tensor
[AD-A237287] N91-29877
Development of model based magnetic LP-LEC growth large diameter GaAs
[AD-A237456] N91-29998
Specification and verification of real-time constraints in coarse-grain dataflow
[AD-A237355] N91-30047

MASSACHUSETTS INST. OF TECH., LEXINGTON.
Solid state research
[NASA-CR-188021] N91-30016

MASSACHUSETTS UNIV., AMHERST.
Theoretical studies of solid-fluid phase equilibria
[DE91-014811] N91-29287
Phase transformations, ultrastructure, and properties of rigid-rod polymers
[AD-A238643] N91-29368
Medium energy nuclear physics research
[DE91-015740] N91-29901

MATERIALS RESEARCH LABS., ASCOT VALE (AUSTRALIA).
A novel epoxy lacquer for high strength steel in F-111 aircraft during overhaul
[AD-A236828] N91-29326

MATERIALS RESEARCH LABS., MELBOURNE (AUSTRALIA).
High temperature mass spectrometric study of the thermodynamics of liquid nickel-aluminium alloys at 2000 K
[MRL-TR-91-15] N91-29290

MATERIALS SCIENCES CORP., BLUE BELL, PA.
Composite specimen design analysis. Volume 2: Experimental efforts
[AD-A238277] N91-29247

MCDONNELL-DOUGLAS MISSILE SYSTEMS CO., SAINT LOUIS, MO.
Missile Datcom: User's manual
[AD-A237817] N91-29148

MCGILL UNIV., MONTREAL (QUEBEC).
Physical properties and structure of ion-containing polymers
[AD-A238196] N91-29363

METSAT, INC., FORT COLLINS, CO.
Cloud data collection, composites and analysis for Whole-Sky Imager (WSI) studies
[AD-A238531] N91-29690

METZ UNIV. (FRANCE).
Experimental investigation of adiabatic shear banding at different impact velocities
[AD-A237901] N91-29625

MICHIGAN UNIV., ANN ARBOR.
Combustion stability limits and planar imaging of swirl-stabilized flames N91-29262
Investigation of superresolution by incoherent to coherent conversion
[AD-A238111] N91-29544
Performance models for robot manipulators N91-29590
Structural optimization with pseudo-load approach exploiting design length scales N91-29616
Methods for evaluating discomfort glare
[PB91-185132] N91-29722
Synchrotron studies of narrow band materials
[DE91-014826] N91-30025

MIDWEST RESEARCH INST., GOLDEN, CO.
Worldwide wind/diesel hybrid power system study: Potential applications and technical issues
[DE91-002160] N91-29643
Analysis of a teetered, variable-speed rotor
[DE91-002190] N91-29646
The Department of Energy's solar industrial program: New ideas for American industry
[DE91-002197] N91-29649
Horizontal axis wind turbine post stall airfoil characteristics synthesization
[DE91-002198] N91-29650
Ultraviolet reflector materials for solar detoxification of hazardous waste
[DE91-002196] N91-29663
Scanning tunneling microscopy studies of the surfaces of a-Si:H and a-SiGe:H films
[DE91-002169] N91-29983

MINNESOTA MINING AND MFG. CO., SAINT PAUL.
Dual cure photocatalyst systems
[DE91-014174] N91-29369

MINNESOTA UNIV., MINNEAPOLIS.
Numerical prediction of turbulent oscillating flow and associated heat transfer
[NASA-CR-187177] N91-29524
Topographic map reading
[AD-A238026] N91-29640
The growth of ultrathin epitaxial intermetallic films
[AD-A237798] N91-30011
Data abstraction, concurrency and synchronization in Sina
[PB91-185454] N91-30053

MISSOURI UNIV., COLUMBIA.
Inelastic scattering in condensed matter with high intensity Moessbauer radiation
[DE91-014384] N91-29980

MISSOURI UNIV., ROLLA.
Collisional processes of interest in MFE plasma research
[DE91-013023] N91-29943
Defect characterization of electronic conducting pseudo-perovskite systems
[DE91-014385] N91-29978

MITRE CORP., BEDFORD, MA.
Mobile Microwave Landing System (MMLS) user interface
[AD-A237470] N91-29162

MSE, INC., BUTTE, MT.
Ceramic fabrication R/D
[DE91-014758] N91-29335

N

NATIONAL ACADEMY OF ENGINEERING, WASHINGTON, DC.
The Government-University-Industry Research Roundtable
[DE91-015795] N91-30044

NATIONAL ACADEMY OF SCIENCES - NATIONAL RESEARCH COUNCIL, WASHINGTON, DC.
Toward a new National Weather Service: A first report
[PB91-184077] N91-29694
Second Review of the Department of Energy's Inertial Confinement Fusion Program
[DE91-013157] N91-29945
The Government-University-Industry Research Roundtable
[DE91-015795] N91-30044

NATIONAL AERONAUTICAL ESTABLISHMENT, OTTAWA (ONTARIO).
Commonwealth Advisory Aeronautical Research Council. First Canadian newsletter on systems, 1989
[NAE-LTR-FR-108] N91-29139
Flight Research Laboratory. Institute for Aerospace Research
[CTN-91-60105] N91-29140
Subsonic aerodynamic coefficients of the SDM at angles of attack up to 90 deg
[NAE-LTR-UA-93] N91-29144
Evaluation of a pre-production version of Canadian Marconi CMA-786 GPS receiver
[NAE-LTR-FR-106] N91-29158
Flight evaluation of complex approaches in a Twin Otter aircraft using a microwave landing system
[NAE-LTR-FR-114] N91-29159
NAE participation in the United States FAA vertical separation study
[NAE-LTR-FR-105] N91-29160
Review of Canadian aeronautical fatigue work: 1987-1989
[NAE-LTR-ST-1706] N91-29165
A full function checkout test for the NAE full scale structural test control and data acquisition system
[NAE-LTR-ST-1696] N91-29166
Tutor aft fuselage and empennage full-scale test: Procedures for creating a damage log
[NAE-ST-576] N91-29167
A new look at the Tobak-Schiff model of nonplanar aircraft dynamics
[NAE-LTR-UA-101] N91-29168
NAE Twin Otter operations in FIFE 1989
[NASA-CR-188770] N91-29169
Rejuvenation of service exposed alloy 713C turbine blades
[NAE-LTR-ST-1716] N91-29179
The failure of components in power generation equipment
[NAE-LTR-ST-1774] N91-29180
Wind and flux calculations of the NAE Twin Otter
[NAE-LTR-FR-109] N91-29189
A wind tunnel smoke generator
[NAE-LTR-LA-312] N91-29195
An assessment of the acoustic noise in the working section of the NAE 6 ft x 9 ft low speed wind tunnel
[NAE-LTR-ST-1744] N91-29196
Assessment of impact damage in toughened resin composites
[NAE-LTR-ST-1695] N91-29236
Effect of fortifier on compression-after-impact strength of carbon fabric reinforced epoxy
[NAE-LTR-ST-1736] N91-29237
Intermetallics: Canadian perspective
[NAE-LTR-ST-1771] N91-29288
Metal injection moulding: A brief review
[NAE-LTR-ST-531] N91-29289
Bubble generation and movement under microgravity conditions
[NAE-LTR-FR-110] N91-29388
Distance measures for speech recognition
[NAE-AN-57] N91-29394
Laboratory evaluation of portable and walk-through explosives vapour detectors
[NAE-LTR-UA-104] N91-29533
Strain gauge cabling, conditioning, and sensitivity calculations for the CT-114 (Tutor) aircraft aft fuselage and empennage full-scale fatigue test
[NAE-LTR-ST-1758] N91-29534
Load tables for the Avery and Gilmore standard force machines corrected for gravity, 1989
[NAE-LTR-ST-1703] N91-29535
Evaluation of Shadow Moire for surface deformation detection and measurement
[NAE-LTR-ST-1737] N91-29604
Review of literature on the damage, loss of stiffness, and residual strength of graphite/epoxy laminates subjected to cyclic loading
[NAE-LTR-ST(CR)-1711] N91-29611
Experimental stress measurements for the modified Indal Series 6400 VAWT
[NAE-LTR-LA-310] N91-29642
NAE Twin Otter operations in the 1988 Eulerian model evaluation field study
[NAE-LTR-FR-107] N91-29651

QBDATAMT: A computer program to read Datamyte recorder data into an IBM PC or compatible computer
[NAE-LTR-ST-547] N91-29742
Description of computer programs used to analyze and plot Spectrapot data files
[NAE-ST-557] N91-29744

NATIONAL AERONAUTICAL LAB., BANGALORE (INDIA).

Performance of an airfoil at low Reynolds number
[NAL-PD-CF-9102] N91-29145
AEROWING - The software for aerodynamic analysis of a large aspect-ratio finite wing at low speeds
[NAL-PD-CF-9101] N91-29146
Instrumentation for ASE experiments in the dynamic wind tunnel
[PD-FC-9112] N91-29197
Solutions of two-dimensional Euler equations with multigrid acceleration
[NAL-PD-CF-9006] N91-29494
Parameter estimation via nonlinear differential correction least square method
[NAL-PD-FC-9110] N91-29814

NATIONAL AERONAUTICS AND SPACE ADMINISTRATION. GODDARD SPACE FLIGHT CENTER, GREENBELT, MD.

The High Energy Solar Physics mission (HESP): Scientific objectives and technical description
[NASA-TM-105033] N91-29201
Compliant walker
[NASA-CASE-GSC-13348-2] N91-29714
Lowell proper motion survey: Southern Hemisphere (Giclas, Burnham, and Thomas 1978). Documentation for the machine-readable version
[NASA-TM-105069] N91-30060

NATIONAL AERONAUTICS AND SPACE ADMINISTRATION. HUGH L. DRYDEN FLIGHT RESEARCH FACILITY, EDWARDS, CA.

Preliminary flight-determined subsonic lift and drag characteristics of the X-29A forward-swept-wing airplane
[NASA-TM-100409] N91-29177
Controlling crippled aircraft-with throttles
[NASA-TM-104238] N91-29191
A simulation evaluation of a four-engine jet transport using engine thrust modulation for flightpath control
[NASA-TM-4324] N91-29194

NATIONAL AERONAUTICS AND SPACE ADMINISTRATION. JOHN F. KENNEDY SPACE CENTER, COCOA BEACH, FL.

Debris/ice/TPS assessment and photographic analysis for Shuttle Mission STS-40
[NASA-TM-103822] N91-29210

NATIONAL AERONAUTICS AND SPACE ADMINISTRATION. LANGLEY RESEARCH CENTER, HAMPTON, VA.

Effect of fiber-matrix debonding on notched strength of titanium metal matrix composites
[NASA-TM-104131] N91-29239
NASA workshop on impact damage to composites
[NASA-CP-10075] N91-29240
A general graphical user interface for automatic reliability modeling
[NASA-TM-104068] N91-29745
Concepts for manned lunar habitats
[NASA-TM-104114] N91-30068

NATIONAL AERONAUTICS AND SPACE ADMINISTRATION. LEWIS RESEARCH CENTER, CLEVELAND, OH.

Progress toward synergistic hypermixing nozzles
[NASA-TM-105169] N91-29150
Divergence thrust loss calculations for convergent-divergent nozzles: Extensions to the classical case
[NASA-TM-105176] N91-29181
Experimental study of cross-stream mixing in a cylindrical duct
[NASA-TM-105180] N91-29187
A linear control design structure to maintain loop properties during limit operation in a multi-nozzle turbofan engine
[NASA-TM-105163] N91-29188
Calculated performance of the NASA Lewis icing research tunnel
[NASA-TM-105173] N91-29199
Design issues for propulsion systems using metallized propellants
[NASA-TM-105190] N91-29220
Numerical propulsion system interdisciplinary approach
[NASA-TM-105181] N91-29221
Production and use of metals and oxygen for lunar propulsion
[NASA-TM-105195] N91-29222
Pressure measurements in a low-density nozzle plume for code verification
[NASA-TM-105170] N91-29228
Performance and optimization of a derated ion thruster for auxiliary propulsion
[NASA-TM-105144] N91-29229
Experimental and analytical comparison of flowfields in a 110 N (25 lbf) H2/O2 rocket
[NASA-TM-105175] N91-29230
Arcjet thermal characteristics
[NASA-TM-105156] N91-29231
An analysis of the wear behavior of SiC whisker reinforced alumina from 25 to 1200 C
[NASA-TM-104489] N91-29235
Microstructural and strength stability of CVD SiC fibers in argon environment
[NASA-TM-103772] N91-29250
Advanced materials for space nuclear power systems
[NASA-TM-105171] N91-29298
Thermal emittance enhancement of graphite-copper composites for high temperature space based radiators
[NASA-TM-105178] N91-29332
Combinatorial FSK modulation for power-efficient high-rate communications
[NASA-TM-105188] N91-29404
Quaternary pulse position modulation electronics for free-space laser communications
[NASA-TM-104502] N91-29405
Optical Multiple Access Network (OMAN) for advanced processing satellite applications
[NASA-TM-105167] N91-29431
Qualitative investigation of cryogenic injected shock dissipation
[NASA-TM-105140] N91-29525
Effect of two synthetic lubricants on life of AISI 9310 spur gears
[NASA-TM-104352] N91-29599
Local synthesis and tooth contact analysis of face-milled spiral bevel gears
[NASA-TM-105182] N91-29600
NDE of ceramics and ceramic composites
[NASA-TM-104520] N91-29610
High temperature superconductor analog electronics for millimeter-wavelength communications
[NASA-TM-105184] N91-29982
NASA cryogenic fluid management space experiment efforts, 1960-1990
[NASA-TM-103752] N91-30073

NATIONAL AERONAUTICS AND SPACE ADMINISTRATION. MARSHALL SPACE FLIGHT CENTER, HUNTSVILLE, AL.

Resource envelope concepts for mission planning
[NASA-TP-3139] N91-29209
Whipple bumper shield simulations
[NASA-TM-105089] N91-29213
The interaction of hydrogen with metal alloys
[NASA-TP-3128] N91-29318
A simulation of the instrument pointing system for the Astro-1 mission
[NASA-TM-103547] N91-30061

NATIONAL BUREAU OF STANDARDS, WASHINGTON, DC.

Standard NIM instrumentation system
[DE90-010387] N91-29532

NATIONAL COMPUTING CENTRE LTD., MANCHESTER (ENGLAND).

Alsys Limited, Alsycomp 017, version 5.2, MICRO VAX 2 under Micro VMS V5.3 (host) to INMOS T425 transputer implemented on a B403 TRAM (target), 901118N1.11064
[AD-A237411] N91-29738

NATIONAL INST. OF STANDARDS AND TECHNOLOGY, BOULDER, CO.

Effect of a free surface on stress distribution in a bimaterial composite
[PB91-185116] N91-29251
NIST calibration procedure for vertically polarized monopole antennas 30 kHz to 300 MHz
[PB91-185124] N91-29432
Heat transfer and pressure drop in a compact pin-fin heat exchanger with pin orientation at 18 deg to the flow direction
[NASA-CR-186544] N91-29527

NATIONAL INST. OF STANDARDS AND TECHNOLOGY, GAITHERSBURG, MD.

Configuration management concepts document. National PDES testbed report series
[PB91-194480] N91-29391
Technical publication announcements covering center programs, July to September 1990, with 1991 CEEE events calendar
[PB91-184754] N91-29476
Technical activities 1990, Electron and Optical Physics Div.
[PB91-194423] N91-29858
Guide to design, implementation and management of distributed databases
[PB91-187567] N91-30054

NATIONAL OCEANIC AND ATMOSPHERIC ADMINISTRATION, BOULDER, CO.

DAR(3)E-1 evaluation: Assessment of weather forecasts made using the DAR(3)E-1 workstation
[PB91-181701] N91-29693

NATIONAL OCEANIC AND ATMOSPHERIC ADMINISTRATION, SEATTLE, WA.

Sea level and bottom pressure measurements in the Northern Gulf of Alaska
[PB91-184135] N91-29705

NATIONAL RESEARCH COUNCIL OF CANADA, OTTAWA (ONTARIO).

Compressor fault modelling for engine health monitoring: Review and recommendations
[NRC-TR-ENG-004] N91-29178
An investigation into the use of side-arm control for civil rotorcraft applications
[AD-A226628] N91-29190
An overview of aerothermal modeling
[NRC-32088] N91-29258
Computational fluid dynamics at NRC: A directory of practitioners and activities
[NRC-TTP-02-89] N91-29490
Matching of complex 3-D surfaces using dynamic programming
[ERB-1022] N91-29743
Using the Harmony operating system: Release 3.0
[ERA-377] N91-29799
Theory and computer simulation of the interactional neural network
[NRC-30269] N91-29800
Piecework linear least-squares approximation planar curves including computer programs
[NRC-31069] N91-29811
Bulletin of the Division of Electrical Engineering, 1988-1989
[NRC-30458] N91-30071
NRC annual report, 1988/1989
[NRC-30398] N91-30072

NATIONAL TAIWAN UNIV., TAIPEI.

International Union of Theoretical and Applied Mechanics (IUTAM) Symposium on Aerothermodynamics in Combustors
[AD-A237943] N91-29516

NATIONAL TRANSPORTATION SAFETY BOARD, WASHINGTON, DC.

Aircraft accident reports: Brief format US civil and foreign aviation issue Number 1 of 1989 accidents
[PB90-916901] N91-29157

NAVAL AEROSPACE MEDICAL RESEARCH LAB., PENSACOLA, FL.

Micro SAINT modeling of physiological and human performance in the heat
[AD-A238659] N91-29719
Analysis of Naval aviation selection test data with nonlinear models. Part 1: Parameter estimation
[AD-A238244] N91-29728
Performance of Marine AV-8B (Harrier) pilots on a cognitive/psychomotor test battery: Comparison and prediction
[AD-A238563] N91-29729
Performance of several different Naval aviator communities on a cognitive/psychomotor test battery: Pipeline comparison and prediciton
[AD-A238564] N91-29730
The effect of three levels of laser glare on the speed and accuracy of target location performance when viewing a briefly presented visual array
[AD-A238565] N91-29736

NAVAL CIVIL ENGINEERING LAB., PORT HUENEME, CA.

Energy conserving coating: Pigment research
[AD-A237841] N91-29356

NAVAL MEDICAL RESEARCH AND DEVELOPMENT COMMAND, BETHESDA, MD.

Development and evaluation of a human performance assessment battery
[AD-A237391] N91-29724

NAVAL MEDICAL RESEARCH INST., BETHESDA, MD.

A technique for measuring the solubilities of gases in liquids
[AD-A238071] N91-29278

NAVAL OBSERVATORY, WASHINGTON, DC.

Central solar eclipses of 1992. Annual solar eclipse of 4-5 January 1992, total solar eclipse of 30 June 1992
[AD-A237614] N91-30069

NAVAL OCEAN SYSTEMS CENTER, SAN DIEGO, CA.

Synthesis of diamond films by microwave generated pulsed plasmas
[AD-A237228] N91-29341
Detection of targets in terrain clutter by using multispectral infrared image processing
[AD-A237436] N91-29414
A new system for measurement of low frequency radio transmitting antenna parameters in near real time
[AD-A238555] N91-29429

The design of a real-time adaptive filter development system
[AD-A237134] N91-29448
InP and InGaAs submicron gate microwave power transistors for 20 GHz applications
[AD-A238595] N91-29473
Objective assessments of mobility with an early Unmanned Ground Vehicle (UGV) prototype viewing system
[AD-A237317] N91-29595
Use of the implicit-finite-difference method to implement the parabolic equation model
[AD-A237437] N91-29819
Least-squares learning and approximation of posterior probabilities on classification problems by neural network models
[AD-A237140] N91-29833
Deduction and inference using conditional logic and probability
[AD-A237285] N91-29834
Responsivity uniformity enhancements for Backside-Illuminated Charge-Coupled Devices (BICCDs) by excimer laser-assisted etching
[AD-A237435] N91-29997

NAVAL OCEANOGRAPHIC AND ATMOSPHERIC RESEARCH LAB., BAY SAINT LOUIS, MS.
An AVHRR data set for the arctic leads ARI
[AD-A237221] N91-29637
Algorithms for converting geodetic Earth location to satellite time and swath pixel coordinates for the DMSP satellite system
[AD-A237589] N91-29638
Dependence of radar backscatter on the energetics of the air-sea interface
[AD-A237818] N91-29685
An expert system approach for prediction of maritime visibility obscuration
[AD-A238305] N91-29688
Fitting seasonal averages with a continuous function
[AD-A238300] N91-29704

NAVAL POSTGRADUATE SCHOOL, MONTEREY, CA.
The design and construction of a shiplaunched VTOL unmanned air vehicle
[AD-A238053] N91-29173
Evaluation of aircraft turbine engine redesigns
[AD-A237599] N91-29184
Ablative heat shield studies for NASA Mars/Earth return entry vehicles
[AD-A238159] N91-29215
Operational procedures for powering up, powering down, and configuring the qualification model of the FLTSATCOM satellite
[AD-A238485] N91-29217
Anisotropic tensile probabilistic failure criterion for composites
[AD-A237601] N91-29244
Statistical characterization of graphite fiber for prediction of composite structure reliability
[AD-A238020] N91-29245
Effect of alumina particle additions on the aging kinetics of 6061 aluminum matrix composites
[AD-A238052] N91-29246
An investigation of the as-quenched and early aging characteristics of a Al - 4.1 wt. percent Li binary alloy by x ray diffraction
[AD-A237598] N91-29311
Analysis of radio frequency radiation from a propagating electron beam
[AD-A237941] N91-29419
Application of Multi-Frequency Modulation (MFM) for high-speed data communications to a voice frequency channel
[AD-A238019] N91-29422
Introduction of a current waveform, waveshaping technique to limit conduction loss in high-frequency dc-dc converters suitable for space power
[AD-A237903] N91-29465
A circuit model for an inductive strip in homogeneous finline
[AD-A238001] N91-29466
Lithium ion source for satellite charge control
[AD-A238272] N91-29470
Use of an extended Kalman filter
[AD-A238639] N91-29474
Near-stall loss measurements in a CD compressor cascade with exploratory leading edge flow control
[AD-A237497] N91-29509
Effects of 1, 2, 3, and 4 Hz imposed bulk flow oscillations on transition in a straight channel with 40 to 1 aspect ratio
[AD-A237988] N91-29517
Numerical study of non-impulsively started flow around a circular cylinder
[AD-A238051] N91-29519
Control of flow over a backward facing step
[AD-A238638] N91-29521
Experimental analysis of B-dot sensors
[AD-A238487] N91-29547
Design of a stabilized, dc-powered analog laser diode driver
[AD-A238596] N91-29577
Equatorial entrainment zone simulations
[AD-A237234] N91-29657
Analysis of the ultraviolet emissions of nitric oxide from mid-latitude rocket observations
[AD-A237340] N91-29673
An investigation of the ERICA IOP-2 cyclone using the NORAPS model
[AD-A237683] N91-29684
TOVS satellite soundings of the ERICA IOP-2 cyclone
[AD-A237998] N91-29686
Multiple channel satellite analysis of cirrus
[AD-A238054] N91-29687
Forcasting tropical cyclone recurvature using an empirical othogonal function representation of vorticity fields
[AD-A238489] N91-29689
The nature of the propagation of sea breeze fronts in central California
[AD-A238635] N91-29692
Acoustic tomographic estimate of ocean advective heat flux: A numerical assessment in the Norwegian Sea
[AD-A237100] N91-29698
Modeling a rain-induced mixed layer
[AD-A238022] N91-29702
The use of searching algorithms for the minimization of multi-valued logic functions
[AD-A238018] N91-29763
A type calculus for mathematical programming modeling languages
[AD-A238160] N91-29766
Validation of the Schwartz and Hon algorithm at low grazing angles
[AD-A238162] N91-29767
Sum of distances in normed spaces
[AD-A238066] N91-29825
A framework for understanding the strategic defense initiatives' software debates
[AD-A237193] N91-29852
Three case studies of management information systems
[AD-A238310] N91-30049

NAVAL RESEARCH LAB., WASHINGTON, DC.
Analysis of FIN line feasibility for W-band attenuator applications
[AD-A237271] N91-29450
The charge-exchange neutral problem and the code NEUTRAL
[AD-A237889] N91-29464
Evolution of a finite pulse of radiation in a high-power free-electron laser
[AD-A237427] N91-29568
Modification of programs CHIEF and CID to compute sound radiation from an arbitrary body with mixed boundary conditions
[AD-A237502] N91-29759
NRL review, 1989-1990
[AD-A238612] N91-29856
NRL review, 1991
[AD-A238665] N91-29857
Vlasov simulations of very-large-amplitude wave generation in the plasma wakefield accelerator
[AD-A237428] N91-29961

NAVAL SURFACE WARFARE CENTER, DAHLGREN, VA.
Worldwide maritime infrared atmospheric transmittance data
[AD-A237292] N91-29672
Invariant target recognition using self-organizing networks
[AD-A238252] N91-29807

NAVAL SURFACE WARFARE CENTER, SILVER SPRING, MD.
Spectral estimation techniques with emphasis on short data records: A primer
[AD-A237486] N91-29271
An alternative to operational amplifiers
[AD-A237439] N91-29453

NAVAL UNDERWATER SYSTEMS CENTER, NEW LONDON, CT.
Spectra and covariances for classical nonlinear signal processing problems involving class A non-Gaussian noise
[AD-A237388] N91-29413

NAVAL UNDERWATER SYSTEMS CENTER, NEWPORT, RI.
Relating ocean acoustic ambient to ocean surface dynamics
[AD-A237167] N91-29699
Operational concept document for the Next Generation Computer Resources (NGCR) operating systems interface standard baseline
[AD-A237501] N91-29782

NAVAL WEAPONS CENTER, CHINA LAKE, CA.
Lithium combustion: A review
[AD-A238154] N91-29279
Portable 45-gigahertz radar for glint and scintillation studies
[AD-A238005] N91-29421
Annual Electronics Manufacturing Seminar proceedings
[AD-A238017] N91-29467
Analog design verification with PSpice and MICRO-CAP 3
[AD-A237922] N91-29762
On the interpolation properties of feedforward layered neural networks
[AD-A238035] N91-29824
Effect of cladding thickness on attenuation in uniformly curved single-mode optical fibers
[AD-A238034] N91-29928

NETROLOGIC, INC., SAN DIEGO, CA.
Neural networks and robotics applied to the non-destructive inspection of aircraft
[AD-A238312] N91-29609

NEW MEXICO STATE UNIV., LAS CRUCES.
Proceedings of the 1st Workshop on Proximity Graphs
[AD-A237250] N91-29818
A survey of nonlinear dynamics (chaos theory)
[AD-A237802] N91-29821

NEW MEXICO UNIV., ALBUQUERQUE.
Optoelectronic Materials Center
[AD-A237663] N91-29922

NEW YORK UNIV., NEW YORK.
Cognition and the brain
[AD-A237846] N91-29727
Analytical and numerical methods; advanced computer concepts
[DE91-014526] N91-29795

NEWCASTLE-UPON-TYNE UNIV. (ENGLAND).
GPS: Aspects of pseudo-range positioning offshore
N91-29161

NORTH CAROLINA STATE UNIV., RALEIGH.
Growth, characterization, and device development in monocrystalline diamond films
[AD-A237463] N91-30000
Defect reductions in epitaxial growth using superlattice buffer layers
[AD-A237710] N91-30005
Device processing of II-VI semiconductor films and quantum well structures
[AD-A238460] N91-30017
Atomic layer epitaxy group IV materials: Surface processes, thin films, devices and their characterization
[AD-A238506] N91-30019
Pseudomorphic semiconducting heterostructures from combinations of AlN, GaN and seleced SiC polytypes: Theoretical advancement and its coordination with experimental studies of nucleation, growth, characterizaiton and device development
[AD-A238520] N91-30020
Growth, nitrogen vacancy reduction and solid solution formation in cubic GaN thin films and the subsequent fabrication of superlattice structures using AlN and InN
[AD-A238521] N91-30021

NORTH CAROLINA UNIV., CHAPEL HILL.
Electrical, magnetic, and spectroscopic properties of tetrathiafulvalene charge transfer compounds with iron, ruthenium, rhodium, and iridium halides
[AD-A237607] N91-29273

NORTHWESTERN UNIV., EVANSTON, IL.
Workshop proceedings: Toughening Mechanisms in Quasi-Brittle Materials
[AD-A238289] N91-29248
Determining stresses in composites
[AD-A238618] N91-29249
Mechanisms of transformation toughening
[DE91-013151] N91-29293
NMR characterization of porous ceramics
[DE91-015051] N91-29371
Infrared and Raman spectra of C60 and C70 solid films at room temperature
[AD-A237880] N91-29462
Fission-fusion adaptivity in finite elements for nonlinear dynamics of shells
[AD-A238029] N91-29626

NOTRE DAME UNIV., IN.
Vibrational, mechanical, and thermal properties of III-V semiconductors
[AD-A237785] N91-30008

O

OAK RIDGE NATIONAL LAB., TN.
A brief overview of the activities and accomplishments of the Metals and Ceramics Division
[DE91-014955] N91-29296
Analysis of weld metal solidification and microstructures
[DE91-014574] N91-29301
Deformation and thermal fatigue in high temperature austenitic alloys
[DE91-014981] N91-29305
X ray reflectivity studies of Au surfaces
[DE91-015308] N91-29307
Requirements for the observation of Fermi surfaces in disordered alloys
[DE91-014578] N91-29321
Mechanical properties of Fe3Al-based alloys
[DE91-015322] N91-29324
Development of nickel and iron aluminides and their applications
[DE91-015323] N91-29325
Annealing effects on the microstructure of titanium electrical contacts on diamond films
[DE91-010150] N91-29327
Corrosion behavior of continuous-filament-wound ceramic composite tubes
[DE91-014959] N91-29370
Fabrication of silicon nitride ceramics by microwave heating
[DE91-015312] N91-29373
Fundamental studies of chemical vapor deposition diamond growth processes
[DE91-015324] N91-29374
Hydrogen productivity by photosynthetic water splitting
[DE90-012211] N91-29380
Impacts of a nominal nuclear electromagnetic pulse on electric power systems
[DE91-012991] N91-29401
Superconductivity induced by very high magnetic fields: Thermodynamic and transport properties
[DE91-015327] N91-29481
Materials science applications of a 120 kV FEG TEM/STEM: Triskaidekaphilia
[DE91-010136] N91-29536
Force-reflecting control of a teleoperated system coupling a nonredundant master with a redundant slave
[DE90-012137] N91-29585
Direct-sampling MS measurement of volatiles in environmental samples
[DE91-013417] N91-29653
Atmospheric methane concentrations: The NOAA/CMDL global cooperative flask sampling network, 1983 - 1988
[DE91-014942] N91-29664
A global geographic information system data base of storm occurrences and other climatic phenomena affecting coastal zones
[DE91-014949] N91-29682
Visualizing performance of parallel programs
[DE91-014966] N91-29793
Supernodal symbolic Cholesky factorization on a l ocal-memory multiprocessor
[DE91-014967] N91-29796
Research and development at ORNL/CESAR towards cooperating robotic systems for hazardous environments
[DE91-015638] N91-29810
Parallelizing the spectral transform method
[DE91-013969] N91-29815
Design aspects for a pulsed-mode, high-intensity, heavy negative ion source
[DE91-011094] N91-29864
Negative ion formation with electron impact to simulants
[AD-A237478] N91-29881
Electron capture in very low energy collisions of multicharged ions with H and D in merged beams
[DE91-015617] N91-29909
Fusion reactor materials
[DE91-012984] N91-29942
Thick-section weldments in 21-6-9 and 316LN stainless steel for fusion energy applications
[DE91-015307] N91-29963
Properties of materials with a fine length scale: Mechanically alloyed metals and the high temperature superconduitor Y1Ba2Cu3O7
[DE91-012538] N91-29975
Ac susceptibility of superconductive thin films
[DE91-015273] N91-29993
High-resolution Z-contrast imaging of superlattices and heterostructures
[DE91-015329] N91-29994
Formation of CoSi2 in SIMOX wafers by high dose Co implantation
[DE91-015639] N91-30036

OHIO STATE UNIV., COLUMBUS.
Ultrasonic evaluation of elastic and interfacial properties of composite materials and laminates N91-29238
High strain rate characterization of ceramics in shear
[AD-A238319] N91-29365
Secondary stability and three-dimensional natural convection in a shallow cavity N91-29495
Kinematics of serial manipulators and their parallel duals N91-29589

OLD DOMINION UNIV., NORFOLK, VA.
Mesoscale characteristics and the role of deformation on ocean dynamics
[AD-A237577] N91-29701

ORA CORP., ITHACA, NY.
Verification of the FtCayuga fault-tolerant microprocessor system. Volume 2: Formal specification and correctness theorems
[NASA-CR-187574] N91-29777
Verification of the FtCayuga fault-tolerant microprocessor system. Volume 1: A case study in theorem prover-based verification
[NASA-CR-4381] N91-29778

OREGON GRADUATE INST. OF SCIENCE AND TECHNOLOGY, BEAVERTON.
Deformation induced microstructural and microchemical changes during thermomechanical treatment
[DE91-014862] N91-29319

OREGON STATE UNIV., CORVALLIS.
Atomic approaches to defect thermochemistry
[AD-A238260] N91-29280
Nonlinear computerized methodology. A: Angle of arrival estimation. B: Data modeling and identification
[AD-A237564] N91-29415

OREGON UNIV., EUGENE.
Structure and stability of underpotentially depositied layers on Au(111) studied by optical second harmonic generation
[AD-A237087] N91-29268

P

PACIFIC NORTHWEST LAB., RICHLAND, WA.
A theoretical and experimental study of unimolecular and biomolecular radical hydrogen transfer reactions
[DE91-012607] N91-29261
Ion transmission studies of mulitple-sector isotope-ratio mass spectrometers
[DE91-014253] N91-29265
Postirradiation deformation of ferritic Fe-Cr binary alloys
[DE91-014856] N91-29295
Advances in the drained shaping of ceramics
[DE91-015429] N91-29376
The 0-G experiments with advanced ceramic fabric wick structures
[DE91-015531] N91-29377
Electric rate structures for thermal energy storage evaluation
[DE91-013168] N91-29644
The observational approach in environmental restoration
[DE91-015528] N91-29666
A climatological model for risk computations incorporating site-specific dry deposition influences
[DE91-015536] N91-29667
Three-dimensional visualization for evaluating automated, geomorphic pattern-recognition analyses of crustal structures
[DE91-012929] N91-29668
Mesoscale modeling of precipitation scavenging by a cold-frontal squall line
[DE91-015534] N91-29695
Biological interactions of extremely-low-frequency electric and magnetic fields
[DE90-011927] N91-29709
A methodology for developing physical system fault diagnostic aids
[DE91-015533] N91-29809
Reevaluation of S-values considering electron transport
[DE91-015428] N91-29893
Neutron dosimetry using optically stimulated luminescence
[DE91-015781] N91-29902
Air-sintering mechanisms of chromites
[DE91-015527] N91-30027

PENNSYLVANIA STATE UNIV., UNIVERSITY PARK.
Translation of airfoil trailing edge noise article from Revue d'Acoustique
[AD-A237811] N91-29143
Compensation of distributed delays in integrated communication and control systems
[NASA-CR-187136] N91-29193
Microstructural development in HSLA-100 steel weld metals
[AD-A237931] N91-29315
Penn State/ONR Mid Frequency Workshop
[AD-A237982] N91-29420
A numerical study of flow past a cylindrical body N91-29497
Unsteady force calculations in turbomachinery
[AD-A237937] N91-29515
Remote determination of soil moisture and evapotranspiration from thermal infrared measurements: Detection of a drying threshold
[PB91-195818] N91-29641
On the application of edge wave theory to terrain-bounded cold surges: A numerical study N91-29670
Adaptive liquid crystal TV based joint transform correlator as applied to real-time pattern recognition
[AD-A238576] N91-29931

PENNSYLVANIA UNIV., PHILADELPHIA.
Catalytic hydrogenation of carbon monoxide
[DE91-015452] N91-29263
A general purpose, comprehensive dynamics simulation of serial robot manipulators N91-29587
Singularity avoidance and the kinematics of an eight-revolute-joint manipulator N91-29588
Hardware Implementation of Neuron Nets and Synapses Workshop
[AD-A237704] N91-29718
Design and hardware implementation of neural systems
[AD-A237703] N91-29804

PHOTOMETRICS, INC., WOBURN, MA.
A program to operate and upgrade the GL low altitude lidar systems
[AD-A238081] N91-29423
Scattering and polarization measurements using the PL/OPA low altitude lidar
[AD-A238082] N91-29424

PHYSICAL OPTICS CORP., TORRANCE, CA.
An optically activated modulator and GaAs-GaAlAs compound semiconductor channel waveguide
[AD-A238642] N91-30023

PHYSICAL SCIENCES, INC., ANDOVER, MA.
A survey of optical diagnostic methods for the study of fuel fouling
[AD-A237361] N91-29920

PITTSBURGH ENERGY TECHNOLOGY CENTER, PA.
Steady flow of a fluid-solid mixture between parallel plates
[DE91-013114] N91-29491
Modification of the 'TEACH' computer code for use in a study of swirling turbulent flows
[DE91-010492] N91-29496

PITTSBURGH UNIV., PA.
The physics of pattern formation at liquid interfaces
[DE91-014529] N91-29504
Environmental effects in niobium base alloys and other selected intermetallic compounds
[AD-A237535] N91-29658
Computational methods for bifurcation problems with symmetries on the manifold
[AD-A237146] N91-29817

PRATT AND WHITNEY AIRCRAFT, WEST PALM BEACH, FL.
Lightweight disk alloy development
[AD-A237064] N91-29309

PRINCETON UNIV., NJ.
Analog computation in neural systems: Architectures and complexity
[AD-A237856] N91-29785
Combining CL (Confidence Limits) and PL (Partial Limits) displays
[AD-A238507] N91-29830
Scrawl strips, and letter or B-letter strips: Depicting marginals of scatter plots
[AD-A238556] N91-29845

PUERTO RICO UNIV., RIO PIEDRAS.
The laser ablation of aluminum at 193, 248, and 351 nm
[AD-A237574] N91-29569

PURDUE UNIV., WEST LAFAYETTE, IN.
Solvent-dependent redox thermodynamics of metal amine complexes. The delineation of specific solvation effects
[AD-A237503] N91-29272
Cyclic voltammetric wave-shapes for microdisk electrodes: Coupled effects of solution resistance, double-layer capacitance, and finite electrochemical kinetics
[AD-A237505] N91-29455
Polymer drag reduction of a zero pressure gradient boundary layer
[AD-A237572] N91-29510
Finite element-based system identification from experimental modal analysis results N91-29618

An exact algorithm for funding undirected Hamiltonian cycles based on a two-matching problem relaxation
[AD-A237241] N91-29753

An exact two-matching based branch and bound algorithm for the symmetric traveling salesman problem
[AD-A237878] N91-29823

The effects of donor-acceptor electronic interactions on the rates of gas-phase metallocene electron-exchange reactions
[AD-A237459] N91-29878

Temperature dependence of proton electroreduction kinetics at gold(111) and (210) surfaces
[AD-A237460] N91-29879

Solvent dynamical effects in electron transfer: The solvent inertial limit and the predicted influence of quantum effects
[AD-A237462] N91-29880

Electron-transfer reactions at metal-solution interfaces: An introduction to some contemporary issues
[AD-A237506] N91-29882

Comparisons between scanning tunneling microscopy and outer-sphere electron-transfer rates at Pt(111) surfaces coated with ordered iodine adlayers
[AD-A237507] N91-29883

Atomic-resolution scanning tunneling microscopy and infrared spectroscopy as combined in-situ probes of electrochemical adlayer structure: Carbon monoxide on rhodium(111)
[AD-A237508] N91-29884

Nonlinear optical interactions involving the real Gaussian field
[DE91-015052] N91-29936

The influence of potential on metal-adsorbate structure: Solvent-independent nature of infrared spectra for Pt(111)/CO
[AD-A237509] N91-30004

Q

QATAR UNIV., DOHA.

The failure of components in power generation equipment
[NAE-LTR-ST-1774] N91-29180

QUALCOMM, INC., SAN DIEGO, CA.

Research in mathematics and computer science: Calculation of the probability of undetected error for certain error detection codes, phase 2
[AD-A238234] N91-29768

QUEENS UNIV., KINGSTON (ONTARIO).

The study of space communications spread spectrum systems. Part 1: Saw-based joint group demodulation of frequency shift keyed and differential phase shift keyed signals
[QU-90-1-PT-1] N91-29395

A study of space communications spread-spectrum systems, phase 5 and 6. Part 2: Coding and modulation
[QU-90-2-PT-2] N91-29396

The study of space communications spread spectrum systems. Part 3: Uplink synchronization in an EHF frequency-hopped satellite system
[QU-90-3-PT-3] N91-29397

R

R AND D ASSOCIATES, LOS ANGELES, CA.

Impact of ionospheric scintillations on space-based surveillance radars
[AD-A237673] N91-29417

READING UNIV. (ENGLAND).

Predicting performance breakdown in pilots through objective measures of stress sensitivity
[AD-A237540] N91-29725

Predicting performance breakdown in pilots through objective measures of stress sensitivity
[AD-A238597] N91-29731

RENSSELAER POLYTECHNIC INST., TROY, NY.

Response and stability analysis of helicopter rotor blades using computerized symbolic manipulation
[AD-A238660] N91-29175

Organometallic precursor routes to Si-C-Al-O-N ceramics
[AD-A237753] N91-29355

An experimental study of plunging liquid jet induced air carryunder and dispersion
[AD-A237757] N91-29511

Use of electrical impedance imaging in two-phase, gas-liquid flows
[DE91-015914] N91-29531

Implementation of an exact penalty function formulation to solve convex nonlinear programming problems
[AD-A237905] N91-29761

RESEARCH TRIANGLE INST., RESEARCH TRIANGLE PARK, NC.

Assessment team report on flight-critical systems research at NASA Langley Research Center
[NASA-CR-181850] N91-29176

RETINA FOUNDATION, BOSTON, MA.

Eye movements and spatial pattern vision
[AD-A238664] N91-29721

ROCHESTER UNIV., NY.

Inertial fusion program and National Laser Users Facility program
[DE91-013164] N91-29556

The 23rd Optoelectronic Workshop: Optical System Assessment for Design and Simulated Annealing
[AD-A238588] N91-29932

ROCKWELL INTERNATIONAL CORP., ANAHEIM, CA.

Multi-sensor feature level fusion
[AD-A237106] N91-29411

ROCKWELL INTERNATIONAL SCIENCE CENTER, THOUSAND OAKS, CA.

Effects of interfacial modification on diamond film adhesion
[AD-A237750] N91-29354

Numerical methods for scattering from electrically large objects
[AD-A238262] N91-29426

Electrodeposition of high temperature superconductors
[AD-A238227] N91-29469

Pressure effects in the microwave plasma growth of polycrystalline diamond
[AD-A237751] N91-30006

ROYAL AIRCRAFT ESTABLISHMENT, FARNBOROUGH (ENGLAND).

Theoretical study of the flow in a rotating duct. Experimental study through flow visualization in a curved duct
[RAE-TRANS-2189] N91-29493

ROYAL SIGNALS AND RADAR ESTABLISHMENT, MALVERN (ENGLAND).

A study of copper segregation in sputtered Al-Si-Cu films using Auger electron spectroscopy
[AD-A238130] N91-29316

S

SANDIA NATIONAL LABS., ALBUQUERQUE, NM.

The functional dependence of trajectory dispersion on initial condition errors
[DE91-014661] N91-29151

Launch capabilities to over 10 km/s
[DE91-014657] N91-29203

The use of high velocity launchers for scientific and engineering studies
[DE91-015564] N91-29208

Effects of high-intensity solar radiation on carbon fibers
[DE91-015485] N91-29252

Structure of icosahedral borides by Raman spectroscopy
[DE91-010872] N91-29260

Postshock spectral radiance measurements in nickel and nickel/aluminum powders
[DE91-014695] N91-29302

High-energy backscattered electron imaging of voids in aluminum metallizations
[DE91-014895] N91-29303

Dynamic behavior of fully dense molybdenum
[DE91-014902] N91-29304

Lead-free solders for electronics applications: Wetting analysis
[DE91-014900] N91-29320

The cure of rigid polyurethane encapsulating foam
[DE91-016059] N91-29379

Development of an explosive vapor generator
[DE91-015700] N91-29386

A dihedral corner reflector model for full polarization calibration of RCS measurements
[DE91-013572] N91-29402

Comparison of synthetic aperture radar autofocus techniques: Phase gradient vs subaperture
[DE91-014696] N91-29406

Very low bit rate voice for packetized mobile applications
[DE91-015333] N91-29409

A method for computing fields near the origin of a cylindrical coordinate system in time domain finite-difference electromagnetic simulations
[DE91-015431] N91-29433

Proceedings of the First Switch Tube Advanced Technology Meeting
[DE91-012634] N91-29440

The 2nd Workshop on High Temperture Electronics (Metallization and Packaging)
[DE91-014332] N91-29442

Design and test of a continuous duty pulsed ac generator
[DE91-014664] N91-29445

Physics and applications of the lock-on effect
[DE91-014670] N91-29446

Application of the nuclear microprobe to the imaging of single event upsets in integrated circuits
[DE91-014701] N91-29447

High gain photoconductive semiconductor switching
[DE91-014668] N91-29478

A compact 200 kV pulse transformer system
[DE91-014669] N91-29479

Experimental and analytical study of laser-triggering in the Rimfire switch
[DE91-014662] N91-29483

Aspects of fatigue and rapid depolarization in the film PZT capacitors
[DE91-014904] N91-29484

Gaseous prebreakdown processes that are important for pulsed power switching
[DE91-015902] N91-29487

Using quartz crystal microbalances to simultaneously sense mass accumulation and solution properties
[DE91-011501] N91-29537

Superconducting instrumentation for precision measurement and control
[DE91-014650] N91-29541

Video frame store: An advanced solid state recorder
[DE91-015709] N91-29549

Diode laser ignition of explosive and pyrotechnic components
[DE90-012227] N91-29553

Laser triggered spark gap modeling
[DE91-014831] N91-29557

Characterization of surface contaminants using infrared microspectroscopy
[DE91-009405] N91-29605

Elastic-plastic constitutive relations at large strain
[DE91-013195] N91-29612

Hypervelocity impact jet formation
[DE91-014651] N91-29619

Explosively driven missile trajectory parameters for various fragment materials and velocities
[DE91-014330] N91-29631

On-line monitoring of volatile organic species
[DE91-014655] N91-29655

A fast, one pass algorithm to label objects and compute their features
[DE91-015441] N91-29747

Analyzing photographically recorded atomic emission spectra using an automated densitometer
[DE91-015368] N91-29871

NMR spectroscopy of experimentally shocked silicate minerals
[DE91-014897] N91-29898

Tritium-field betacells
[DE91-014666] N91-29910

Quantitative analysis of oxygen segregation on inversion domain boundaries in aluminum nitride
[DE91-010869] N91-29971

Large bipolarons and superconductivity
[DE91-014699] N91-29985

Superconducting superoxygenated La(2-x)Sr(x)CuO(4+delta): Search for phase separation
[DE91-015334] N91-29995

High temperature thermoelectric properties of boron carbide
[DE91-015848] N91-30037

Compilation and representation of intelligent electronic documents: An architecture for referenceability
[DE91-012635] N91-30045

Legal and records management issue of optical disk storage media
[DE91-014898] N91-30046

Records management at the DOE national laboratories: Sandia National Laboratories
[DE91-015563] N91-30057

Technology transfer: A new program between Sandia National Laboratories and the University of New Mexico
[DE91-015439] N91-30058

SANDIA NATIONAL LABS., LIVERMORE, CA.

Compendium of material test results on HY-100 and pseudo HY-100 metals in support of US Navy programs
[DE91-013134] N91-29292

SCRIPPS INSTITUTION OF OCEANOGRAPHY, LA JOLLA, CA.

Test of Newtonian gravity using DSV sea cliff
[AD-A238558] N91-29680

SIMPSON WEATHER ASSOCIATES, INC., CHARLOTTESVILLE, VA.

Space-based Doppler lidar sampling strategies: Algorithm development and simulated observation experiments
[NASA-CR-184172] N91-29554

SMITH-KETTLEWELL INST. OF VISUAL SCIENCES, SAN FRANCISCO, CA.
Psychophysical studies of visual cortical function
[AD-A238663] N91-29720
SOLAR TURBINES, INC. SAN DIEGO, CA.
Ultra-low NOx gas turbine combustor
[PB91-184994] N91-29601
SOUTH CAROLINA UNIV., COLUMBIA.
Approximation from shift-invariant surfaces of L2(IRd)
[AD-A238165] N91-29826
SPARTA, INC., LEXINGTON, MA.
Effects of solar heating by aerosols and trace gases on the temperature structure constant
[AD-A237675] N91-29677
Development of optical subapertures
[AD-A237759] N91-29924
SPECTRA RESEARCH SYSTEMS, INC., HUNTSVILLE, AL.
Bearing tester data compilation analysis, and reporting and bearing math modeling
[NASA-CR-178883] N91-29603
SPECTRAL SCIENCES, INC., BURLINGTON, MA.
Description of the Strategic High-Altitude Atmospheric Radiation Code (SHARC)
[AD-A237089] N91-29671
SRI INTERNATIONAL CORP., MENLO PARK, CA.
Discretionary security for object-oriented database systems
[AD-A237573] N91-29740
Persistent data/knowledge base
[AD-A237498] N91-30048
STANFORD LINEAR ACCELERATOR CENTER, CA.
A high power cross-field amplifier at X-Band
[DE91-013277] N91-29441
Study of nuclear effects in the deuteron and extraction of neutron to proton stucture function ratio
[DE91-015484] N91-29873
STANFORD UNIV., CA.
Millimeter-wave characterization of GaAs devices and IC's
[AD-A237843] N91-29461
VLSI circuit techniques and technologies for ultrahigh speed data conversion interfaces
[AD-A238115] N91-29468
Physical concepts and modeling procedures for picosecond and subpicosecond distributed circuits
[AD-A238592] N91-29472
The evolution and structure of homogeneous stably stratified sheared turbulence N91-29499
Photoelectron and photoionization pumping of XUV lasers by laser-produced plasmas N91-29558
Quasistatic manipulation with compliance and friction N91-29591
Motion planning for manipulators with excessive degrees of freedom N91-29592
Experiments in adaptive control of cooperating manipulators N91-29594
Integrated structural damping and control system design for high-order flexible systems N91-29617
Primal-dual methods for linear programming
[AD-A237418] N91-29756
Simulation methodology
[AD-A238113] N91-29765
Barrier methods for large-scale quadratic programming
[AD-A238554] N91-29773
Asynchronous design for parallel processing architectures
[AD-A237696] N91-29783
Expert systems on multiprocessor architectures. Volume 1: Summary
[AD-A238046] N91-29786
Expert systems on multiprocessor architectures. Volume 2: Technical reports
[AD-A238047] N91-29787
Expert systems on multiprocessor architectures, volume 3
[AD-A238048] N91-29788
Expert systems on multiprocessor architectures, volume 4
[AD-A238049] N91-29789
The asymptotic distributions of autoregressive coefficients
[AD-A238538] N91-29831
Confidence bands for the median survival time as a function of the covariates in the Cox model
[AD-A237626] N91-29835
Diffusion approximations for complex repair systems
[AD-A238100] N91-29836
STATE UNIV. OF NEW YORK, ALBANY.
A Workshop on the Integration of Numerical and Symbolic Computing Methods
[AD-A238601] N91-29774
STATE UNIV. OF NEW YORK, BUFFALO.
Synthesis of multifilament silicon carbide fibers by chemical vapor deposition
[NASA-CR-188725] N91-29331
First International conference on Frontiers of Polmer Research
[AD-A238112] N91-29361
Alignment of tomographic projections using an incomplete set of fiducial markers
[AD-A238536] N91-29772
Charge motion effects in ionic clusters
[AD-A238178] N91-29886
STATE UNIV. OF NEW YORK, STONY BROOK.
Light scattering characterization of polymer additives and correlation of molecular properties of polymer fluids
[AD-A238547] N91-29367
Research in nuclear astrophysics: Stellar collapse and supernovae
[DE91-015449] N91-30066
STEVENS INST. OF TECH., HOBOKEN, NJ.
Injection molding of engineering plastics
[AD-A238583] N91-29389
SUPERCONDUCTING SUPER COLLIDER LAB., DALLAS, TX.
Sliding mode controller of RF cavity tuning loop
[DE91-015461] N91-29410
ZLIB: A numerical library for differential algebra and Lie algebraic treatment of beam dynamics
[DE91-014875] N91-29746
SURREY UNIV., GUILDFORD (ENGLAND).
Ion Implantation Technology: Proceedings of the 8th International Conference on Ion Implantation Technology
[AD-A237955] N91-30013
SVERDRUP TECHNOLOGY, INC., ARNOLD AFS, TN.
Effect of geometric parameters on the performance of second throat annular steam ejectors
[AD-A238645] N91-29522
SVERDRUP TECHNOLOGY, INC., BROOK PARK, OH.
Numerical simulation of self-field MPD thrusters
[NASA-CR-187168] N91-29832
Review of nondiffracting Bessel beams
[NASA-CR-187188] N91-29917
SYRACUSE UNIV., NY.
Theoretical, experimental, and numerical studies on hybrid acoustooptic bistable devices
[AD-A237885] N91-29463

T

TECHNISCHE HOGESCHOOL TWENTE, ENSCHEDE (NETHERLANDS).
Negation in knowledge graphs
[PB91-185421] N91-29776
The CYK-approach to serial and parallel parsing
[PB91-185447] N91-29792
Data abstraction, concurrency and synchronization in Sina
[PB91-185454] N91-30053
TECHNOLOGY INTERNATIONAL CORP., BEDFORD, MA.
DNA optical support program summary for 1989
[AD-A238397] N91-29679
TEMPLE UNIV., PHILADELPHIA, PA.
Mixed valent and heavy ferimons and related systems
[DE91-015454] N91-29900
TENNESSEE UNIV. SPACE INST., TULLAHOMA.
A finite element solver for 3-D compressible viscous flows
[NASA-CR-184175] N91-29488
TEXAS INSTRUMENTS, INC., DALLAS.
Silicon Wafer Advanced Packaging (SWAP). Multichip Module (MCM) foundry study, version 2
[AD-A237412] N91-29452
TEXAS UNIV., ARLINGTON.
Electronic and ionic transport in processable conducting polymers
[AD-A238175] N91-29362
TEXAS UNIV., AUSTIN.
Seasonal air and water mass redistribution and its effect on satellite and polar motion N91-29202
Measurement of a three-dimensional hypersonic density field using holographic interferometry N91-29539
Multi-sensor image interpretation using laser radar and thermal images
[AD-A238245] N91-29576
Analytical calculation of neutral transport and its effect on ions
[DE91-015908] N91-29896
A mesoscopic linear accelerator driven by superintense subpicosecond laser pulses
[DE91-015941] N91-29913
Establishment of an Institute for Fusion Studies
[DE91-014922] N91-29956
Impurity and neutral effects on the dissipative drift wave in tokamak edge plasmas
[DE91-015907] N91-29965
TEXAS UNIV., SAN ANTONIO.
Probabilistic lifetime strength of aerospace materials via computational simulation
[NASA-CR-187178] N91-29629
TUFTS UNIV., MEDFORD, MA.
Electrocatalytic study of ammonia synthesis and methane dimerization in high temperature solid electrolyte cells
[DE90-012496] N91-29437
High energy physics at Tufts University
[DE91-015055] N91-29908
TULANE UNIV., NEW ORLEANS, LA.
The 6th Workshop on the Mathematical Foundations of Programming Semantics
[AD-A237754] N91-29760

U

UNITED TECHNOLOGIES RESEARCH CENTER, EAST HARTFORD, CT.
Hydrogen-fueled scramjet investigation
[AD-A237569] N91-29183
Investigation of particulate formation during diesel spray combustion
[DE90-008282] N91-29255
Experimental and analytical study of rippled trailing edge airfoils for compressor application
[AD-A237425] N91-29508
UNIVERSAL ENERGY SYSTEMS, INC., DAYTON, OH.
Counterdoped high temperature, silicon array infrared detector
[AD-A238483] N91-29546
UNIVERSITY COLL. OF NORTH WALES, BANGOR.
Fast acting optical deflection
[AD-A237904] N91-29927
UNIVERSITY OF EASTERN KENTUCKY, RICHMOND.
Study of activation of metal samples from LDEF-1 and Spacelab-2
[NASA-CR-184171] N91-29297
Activation calculations for trapped protons below 200 MeV: Appendix
[NASA-CR-184170] N91-29865
UNIVERSITY OF NORTHERN ILLINOIS, DE KALB.
Electrified microscopic and conventional interfaces between two immiscible electrolyte solutions
[AD-A237695] N91-29459
Analysis of nonGaussian, nonlinear time series with long-memory
[AD-A237847] N91-29822
UNIVERSITY OF SOUTHERN CALIFORNIA, LOS ANGELES.
Model filled polymers 8: Synthesis of crosslinked polymeric beads by seed polymerization
[AD-A237429] N91-29349
Model filled polymer 7: Flow behavior of polymers containing monodisperse crosslinked polymeric beads
[AD-A237430] N91-29350
Model filled polymers 9: Synthesis of uniformly crosslinked polystyrene microbeads
[AD-A237472] N91-29352
Mechanism of anionic ring-opening polymerization of silacyclopent 3-enes
[AD-A237538] N91-29353
Reactions of small molecular systems
[DE91-014519] N91-29867
UNIVERSITY OF SOUTHERN ILLINOIS, CARBONDALE.
Electro-rheology fluids and liquid fuel flow
[AD-A238600] N91-29520
UTAH UNIV., SALT LAKE CITY.
Fabrication, phase transformation studies and characterization of SiC-AlN-Al2OC ceramics
[DE91-013296] N91-29329
Research in the physical sciences with application to the free electron laser
[AD-A237884] N91-29571

V

VERITAY TECHNOLOGY, INC., AMHERST, NY.
Twenty first century propulsion concept
[AD-A237853] N91-29224
VERMONT UNIV., BURLINGTON.
Organo- borazines.3.homo- and copolymerization of p-vinylphenyl- cyclotri- borazines
[AD-A237881] N91-29357
VEXCEL CORP., BOULDER, CO.
An automated software system for updating digital terrain databases from all-source imagery, phase 1
[AD-A237105] N91-29748
VICTORIA UNIV. (BRITISH COLUMBIA).
Coding for frequency hopped spread spectrum satellite communications
[ECE-89-1] N91-29398

VIRGINIA POLYTECHNIC INST. AND STATE UNIV., BLACKSBURG.
Modeling and response analysis of thin-walled beam structures constructed of advanced composite materials N91-29615

VIRGINIA UNIV., CHARLOTTESVILLE.
Design and analysis of multi-sensor sequential detection system
[AD-A238012] N91-29543

W

WASHINGTON UNIV., SEATTLE.
Hierarchic extensions in the static and dynamic analysis of elastic beams N91-29613
Hamiltonian 3-D ray tracing in the oceanic waveguide on the ellipsoidal earth
[AD-A237458] N91-29700
Perturbation techniques for models of bursting electrical activity in pancreatic (beta)-cells
[DE91-013901] N91-29715
NW lab for integrated systems
[AD-A237118] N91-29749
Nuclear theory progress report
[DE91-013908] N91-29866

WESTINGHOUSE DEFENSE AND ELECTRONIC SYSTEMS CENTER, BALTIMORE, MD.
Stable integrated microwave to optical modulator
[AD-A238166] N91-29574

WESTINGHOUSE HANFORD CO., RICHLAND, WA.
Parametric design calculations using Green's function to determine unique source
[DE91-014683] N91-29861

WICHITA STATE UNIV., KS.
Impact characterization of graphite fiber reinforced thermoplastic laminates
[NIAR-91-16] N91-29241
TGA experimental data analyzed by transpiration theory
[NIAR-91-21] N91-29263
High temperature Knudsen effusion-mass spectrometric studies of the Y-Ba-Cu-O system
[NIAR-91-23] N91-29981
Marketing for collegiate aviation education
[NIAR-91-18] N91-30042

WIEN UNIV. (AUSTRIA).
Boron nitride and silicon nitride systems
[AD-A238080] N91-29359

WISCONSIN UNIV., MADISON.
Problems in nonlinear continuum dynamics
[AD-A237844] N91-29512
Three-dimensional mapping of atmospheric boundary layer structure and winds with a high performance lidar
[AD-A238098] N91-29678
Approximation from shift-invariant surfaces of L2(IRd)
[AD-A238165] N91-29826
Computational and theoretical aspects of nonlinear partial differential equations
[AD-A238495] N91-29829
High energy physics: Experimental, Theoretical, and Phenomenology Institute
[DE91-015737] N91-29912
Magnetic fluctuations due to thermally excited Alfven waves
[DE90-011790] N91-29940
Fluidlike studies of the sheath and presheath regions of a plasma
[DE91-013343] N91-29944
The effects of magnetic field errors on reversed field pinch plasma
[DE91-013636] N91-29948
Total magnetic reconnection during a tokamak major disruption
[DE91-013637] N91-29949
Edge electrostatic fluctuations and transport in the MST reversed field pinch
[DE91-015218] N91-29959
Global confinement and discrete dynamo activity in the MST reversed field pinch
[DE91-015219] N91-29960
Anomalous ion heating from the dynamo in a reversed field pinch
[DE91-015586] N91-29966

WOODS HOLE OCEANOGRAPHIC INST., MA.
Stochastic modelling of seafloor morphology
[AD-A237063] N91-29697
Course lectures abstracts of participants fellows project reports
[AD-A237909] N91-30070

WRIGHT RESEARCH DEVELOPMENT CENTER, WRIGHT-PATTERSON AFB, OH.
Aircraft operations from runways with inclined ramps (ski-jump)
[AD-A237265] N91-29171

WRIGHT STATE UNIV., DAYTON, OH.
Robust design of multivariable control: An interval arithmetic approach
[AD-A238006] N91-29806

WYOMING UNIV., LARAMIE.
Composite specimen design analysis. Volume 2: Experimental efforts
[AD-A238277] N91-29247

Y

YALE UNIV., NEW HAVEN, CT.
Nonlinear spectroscopy of multicomponent droplets and two- and three-dimensional measurements in flames
[AD-A238028] N91-29277
High-intensity and high-energy laser interactions with single droplets
[AD-A238197] N91-29575

Typical Contract Number Index Listing

Listings in this index are arranged alphanumerically by contract number. Under each contract number the accession numbers denoting documents that have been produced as a result of research done under that contract are arranged in ascending order. The accession number denotes the number by which the citation is identified.

AF PROJ. 2301 ..... N91-29881
N91-29887
AF PROJ. 2302 ..... N91-29248
AF PROJ. 2303 ..... N91-29355
N91-29360
AF PROJ. 2304 ..... N91-29425
N91-29512
N91-29785
N91-29820
N91-29822
N91-29841
AF PROJ. 2306 ..... N91-29280
N91-29313
N91-29317
N91-29460
N91-30005
N91-30008
N91-30009
N91-30010
N91-30011
AF PROJ. 2307 ..... N91-29507
AF PROJ. 2308 ..... N91-29223
N91-29277
AF PROJ. 2313 ..... N91-29640
N91-29720
N91-29721
N91-29727
N91-29862
N91-29925
AF PROJ. 2401 ..... N91-29171
AF PROJ. 3484 ..... N91-29726
N91-29999
AF PROJ. 6096 ..... N91-29741
AF-AFOSR-0014-88 ..... N91-29275
AF-AFOSR-0040-88 ..... N91-29838
N91-29840
AF-AFOSR-0052-90 ..... N91-29774
AF-AFOSR-0063-89 ..... N91-30008
AF-AFOSR-0065-89 ..... N91-29507
AF-AFOSR-0066-88 ..... N91-29360
AF-AFOSR-0076-88 ..... N91-29841
AF-AFOSR-0089-87 ..... N91-29726
AF-AFOSR-0098-88 ..... N91-29887
AF-AFOSR-0100-88 ..... N91-29277
AF-AFOSR-0126-88 ..... N91-30010
AF-AFOSR-0160-88 ..... N91-30005
AF-AFOSR-0166-90 ..... N91-30009
AF-AFOSR-0167-90 ..... N91-29317
AF-AFOSR-0187-88 ..... N91-29640
AF-AFOSR-0221-89 ..... N91-29839
AF-AFOSR-0221-90 ..... N91-29727
AF-AFOSR-0227-88 ..... N91-29785
AF-AFOSR-0247-88 ..... N91-29425
AF-AFOSR-0269-88 ..... N91-29820
AF-AFOSR-0284-88 ..... N91-29822
AF-AFOSR-0290-89 ..... N91-29223
AF-AFOSR-0290-90 ..... N91-29248
AF-AFOSR-0304-89 ..... N91-29925
AF-AFOSR-0309-89 ..... N91-29280
AF-AFOSR-0315-87 ..... N91-29512
AF-AFOSR-0318-90 ..... N91-29460
AF-AFOSR-0326-88 ..... N91-29720
AF-AFOSR-0335-89 ..... N91-29862
AF-AFOSR-0377-89 ..... N91-29721
AF-AFOSR-0439-89 ..... N91-29355
AF-AFOSR-0455-89 ..... N91-29826
AF-AFOSR-0494-89 ..... N91-30011
ARPA ORDER 7526 ..... N91-29922
ARPA ORDER 7549 ..... N91-29452
DA PROJ. 1L1-61102-AH-43 ..... N91-29276
N91-29384
N91-30050
DA PROJ. 1L1-61102-AH-45 ..... N91-29250
DA PROJ. 1L1-61102-BH-57 ..... N91-29596
N91-29927
DA PROJ. 1L1-62111-AH-71 ..... N91-29675
DA PROJ. 1L1-62120-A-140 ..... N91-29752
DA PROJ. 1L1-62211-A-47A N91-29599
N91-29600
DA PROJ. 1L1-62618-AH-80 ..... N91-29514
DA PROJ. 1L1-611102-H-47 ..... N91-29456
DA PROJ. 1L6-65502-MM-40 ..... N91-29247
DA PROJ. 2Q1-61102-B-74-F N91-29725
DA PROJ. 3M1-62787-A-878 ..... N91-29710
DA PROJ. 3M4-63807-D-993 ..... N91-29724
DA PROJ. 3M4-637648995 ..... N91-29719
DA PROJ. 4A1-61102-AT-23 ..... N91-29803
DA PROJ. 4A7-62730-AT-42 ..... N91-29639
DA PROJ. 4A7-62784-AT-42 ..... N91-29639
DAAB07-88-C-F205 ..... N91-29411
DAAG29-82-K-0178 ..... N91-29845
DAAL03-G-90-0090 ..... N91-29826
DAAL03-86-D-0001 ..... N91-29545
N91-29821
DAAL03-86-G-0048 ..... N91-29389
DAAL03-86-K-0024 ..... N91-29678
DAAL03-86-K-0073 ..... N91-29845
DAAL03-86-K-0173 ..... N91-29932
DAAL03-87-K-0018 ..... N91-29829
DAAL03-87-K-0065 ..... N91-29363
DAAL03-87-K-0087 ..... N91-29764
DAAL03-87-K-0111 ..... N91-29468
DAAL03-87-K-0116 ..... N91-29175
DAAL03-87-K-0117 ..... N91-29573
DAAL03-87-K-0136 ..... N91-29367
DAAL03-87-K-0147 ..... N91-29931
DAAL03-87-K-0153 ..... N91-30017
DAAL03-88-K-0006 ..... N91-29891
DAAL03-88-K-0013 ..... N91-29628
DAAL03-88-K-0031 ..... N91-29889
DAAL03-88-K-0034 ..... N91-29890
DAAL03-88-K-0040 ..... N91-29575
DAAL03-88-K-0045 ..... N91-29830
DAAL03-88-K-0063 ..... N91-29765
N91-29836
DAAL03-88-K-0072 ..... N91-30015
DAAL03-88-K-0177 ..... N91-29544
DAAL03-89-K-0033 ..... N91-29831
DAAL03-89-K-0064 ..... N91-29772
DAAL03-90-G-0103 ..... N91-29838
N91-29839
N91-29840
DAAL03-91-G-0050 ..... N91-29576
DAAL03-91-G-0057 ..... N91-29361
DAAL04-87-C-0064 ..... N91-29247
DACA76-88-C-0008 ..... N91-29164
DACA76-90-C-0013 ..... N91-29748
DAJA45-86-C-0007 ..... N91-29596
DAJA45-88-C-0024 ..... N91-29725
N91-29731
DAJA45-90-C-0002 ..... N91-29359
DAJA45-90-C-0005 ..... N91-29927
DAJA45-90-C-0052 ..... N91-29625
DAJA45-90-M-0185 ..... N91-30013
DARPA ORDER 6155 ..... N91-29658
DE-AC01-89DP-20154 ..... N91-29945
DE-AC02-76CH-00016 ..... N91-29232
N91-29307
N91-29323
N91-29656
N91-29681
N91-29859
N91-29870
N91-29895
N91-29947
N91-30026
DE-AC02-76CH-03000 ..... N91-29407
N91-29408
N91-29816
N91-30065
DE-AC02-76ER-00881 ..... N91-29912
DE-AC02-76ER-02271 ..... N91-29904
N91-29905
DE-AC02-76ER-03077 ..... N91-29795
DE-AC02-76ER-03130 ..... N91-29907
DE-AC02-76ER-03230 ..... N91-29892
DE-AC02-83CH-10093 ..... N91-29643
N91-29646
N91-29649
N91-29650
N91-29663
N91-29983
DE-AC02-83ER-40085 ..... N91-29908
DE-AC02-84ER-40125 ..... N91-30040
DE-AC02-89CE-40878 ..... N91-29330
DE-AC02-89ER-40486 ..... N91-29410
N91-29746
DE-AC03-76SF-00098 ..... N91-29204
N91-29256
N91-29259
N91-29264
N91-29286
N91-29444
N91-29584
N91-29723
N91-29868
N91-29974
N91-30038
DE-AC03-76SF-00515 ..... N91-29441
N91-29873
DE-AC03-89ER-51114 ..... N91-29950
N91-29957
DE-AC04-76DP-00613 ..... N91-29393
N91-29606
DE-AC04-76DP-00789 ..... N91-29151
N91-29203
N91-29208
N91-29213
N91-29252
N91-29260
N91-29302
N91-29303
N91-29304
N91-29320
N91-29379
N91-29386
N91-29402
N91-29406
N91-29409
N91-29433
N91-29440
N91-29442
N91-29445
N91-29446
N91-29447
N91-29478
N91-29479
N91-29483
N91-29484
N91-29487
N91-29537
N91-29541
N91-29549
N91-29553
N91-29557
N91-29605
N91-29612
N91-29619
N91-29631
N91-29655
N91-29747
N91-29871
N91-29898
N91-29910
N91-29950
N91-29971
N91-29985

N91-29995
N91-30037
N91-30045
N91-30046
N91-30057
N91-30058
DE-AC04-76DP-03533 ..... N91-29650
DE-AC04-76DR-00789 ..... N91-29292
DE-AC04-87AL-43058 ..... N91-29255
DE-AC04-88DP-43495 ..... N91-29382
DE-AC05-76OR-00033 ..... N91-29327
DE-AC05-84OR-21400 ..... N91-29296
N91-29301
N91-29305
N91-29307
N91-29321
N91-29324
N91-29325
N91-29327
N91-29370
N91-29373
N91-29374
N91-29380
N91-29401
N91-29481
N91-29536
N91-29585
N91-29653
N91-29664
N91-29682
N91-29793
N91-29796
N91-29810
N91-29815
N91-29864
N91-29909
N91-29942
N91-29950
N91-29963
N91-29975
N91-29993
N91-29994
N91-30036
DE-AC06-76RL-01830 ..... N91-29261
N91-29265
N91-29295
N91-29376
N91-29377
N91-29644
N91-29666
N91-29667
N91-29668
N91-29695
N91-29709
N91-29809
N91-29893
N91-29902
N91-30027
DE-AC06-86NE-37963 ..... N91-29319
DE-AC06-87RL-10930 ..... N91-29861
DE-AC07-76ID-01570 ..... N91-29152
N91-29299
N91-29328
DE-AC07-87ID-12689 ..... N91-29436
DE-AC07-88ID-12692 ..... N91-29369
DE-AC07-88ID-12735 ..... N91-29335
DE-AC12-76SN-00052 ..... N91-29794
DE-AC34-90DP-62349 ..... N91-29267
DE-AI03-86SF-16310 ..... N91-29298
DE-AI05-83ER-40017 ..... N91-29961
DE-AS04-85AL-31881 ..... N91-29381
DE-AS08-87NV-10652 ..... N91-29941
DE-FC03-85DP-40200 ..... N91-29556
DE-FG01-90CE-15440 ..... N91-29529
DE-FG02-84ER-45131 ..... N91-29504
DE-FG02-84ER-45147 ..... N91-30024
DE-FG02-84ER-53175 ..... N91-29943
DE-FG02-85ER-13396 ..... N91-29753
DE-FG02-85ER-45200 ..... N91-29980
DE-FG02-85ER-45219 ..... N91-29978
DE-FG02-85ER-45222 ..... N91-29989
DE-FG02-85ER-53198 ..... N91-29948
N91-29949
N91-29959
N91-29960
DE-FG02-85ER-53212 ..... N91-29940
N91-29966
DE-FG02-86ER-13576 ..... N91-29936
DE-FG02-86ER-13615 ..... N91-29283
DE-FG02-86ER-45251 ..... N91-29371
DE-FG02-86ER-53218 ..... N91-29944
DE-FG02-86ER-53222 ..... N91-29938
DE-FG02-86ER-53236 ..... N91-29403
DE-FG02-87ER-40317 ..... N91-30066
DE-FG02-87ER-45286 ..... N91-29329
DE-FG02-87ER-45307 ..... N91-30031
DE-FG02-87ER-45333 ..... N91-29999
DE-FG02-88ER-13937 ..... N91-29555
DE-FG02-88ER-40415 ..... N91-29901
DE-FG02-88ER-45357 ..... N91-29995
DE-FG02-88ER-45365 ..... N91-29293
DE-FG02-88ER-53263 ..... N91-29964
DE-FG02-89CE-90048 ..... N91-29437
DE-FG02-89ER-14012 ..... N91-29580
N91-29582
DE-FG02-89ER-14031 ..... N91-29711
DE-FG02-89ER-14043 ..... N91-29492
DE-FG02-89ER-53291 ..... N91-29966
DE-FG02-89ER-53297 ..... N91-29938
DE-FG02-90ER-14150 ..... N91-29287
DE-FG02-90ER-14159 ..... N91-29872
DE-FG02-90ER-45416 ..... N91-30025
DE-FG02-90ER-60983 ..... N91-29708
DE-FG03-85ER-13363 ..... N91-29867
DE-FG03-86ER-45279 ..... N91-29372
DE-FG05-80ET-53088 ..... N91-29896
N91-29913
N91-29956
N91-29965
DE-FG05-87ER-45306 ..... N91-29333
DE-FG05-88ER-13902 ..... N91-30041
DE-FG05-88ER-40467 ..... N91-29897
DE-FG05-88ER-53266 ..... N91-29965
DE-FG05-88ER-60707 ..... N91-29893
DE-FG05-89ER-14005 ..... N91-29713
DE-FG05-89ER-75498 ..... N91-30044
DE-FG06-86ER-25019 ..... N91-29715
DE-FG06-88ER-40427 ..... N91-29866
DE-FG07-90ER-13032 ..... N91-29531
DE-FG09-86ER-13614 ..... N91-29712
DE-FG22-85PC-80527 ..... N91-29257
DE-FG22-86PC-90533 ..... N91-29285
DI-14-08-0001-G1490 ..... N91-29641
DNA001-88-C-0033 ..... N91-29679
DNA001-88-C-0046 ..... N91-29417
DSS-36001-8-3528/01-SS N91-29395
N91-29396
N91-29397
DSS-36001-8-3529/01-SS N91-29398
DTFA-01-84-2-02038 ..... N91-29198
DTFA03-85-C-00007 ..... N91-29154
N91-29155
N91-29156
F04611-87-C-0029 ..... N91-29225
F04611-87-C-0072 ..... N91-29647
F04611-89-C-0023 ..... N91-29224
F04701-88-C-0089 ..... N91-29227
N91-29750
F19628-85-C-0104 ..... N91-30018
F19628-86-C-0057 ..... N91-29427
F19628-86-C-0102 ..... N91-29423
N91-29424
F19628-86-K-0009 ..... N91-29163
F19628-86-K-0040 ..... N91-29219
F19628-87-C-0130 ..... N91-29671
F19628-87-K-0031 ..... N91-29885
F19628-88-C-0038 ..... N91-29677
F19628-88-C-0190 ..... N91-29863
F19628-89-0001-5420 ..... N91-29162
F19628-90-C-0002 ..... N91-30016
F19628-90-K-0003 ..... N91-29676
F30602-81-C-0169 ..... N91-29543
F30602-85-C-0012 ..... N91-29786
N91-29787
N91-29788
N91-29789
F30602-88-C-0052 ..... N91-29451
F30602-88-C-0142 ..... N91-30048
F30602-88-D-0026 ..... N91-29740
F30602-88-D-0027 ..... N91-29463
F33615-86-C-2695 ..... N91-29183
F33615-86-C-5037 ..... N91-29309
F33615-86-C-5091 ..... N91-29546
F33615-87-C-2739 ..... N91-29186
F33615-87-C-3604 ..... N91-29148
F33615-88-C-3605 ..... N91-29806
F33615-88-C-5478 ..... N91-29242
F33615-89-C-3606 ..... N91-29808
F33615-90-C-2068 ..... N91-29920
F49620-87-C-0106 ..... N91-29998
F49620-87-C-0108 ..... N91-29214
F49620-88-C-0011 ..... N91-29626
F49620-88-C-0013 ..... N91-29658
F49620-89-C-0009 ..... N91-29274
F49620-89-C-0048 ..... N91-29426
F49620-89-C-0073 ..... N91-29368
F49620-89-C-0114 ..... N91-29597
F49620-90-C-0017 ..... N91-29768
F49620-90-C-0068 ..... N91-30023
GRI-5083-251-1000 ..... N91-29601
MDA903-89-C-0003 ..... N91-29449
N91-29660
MDA972-90-C-0045 ..... N91-29452
MDA972-90-C-0046 ..... N91-29922
MIPR-FY1455-88-N065 ..... N91-29881
NAGW-1034 ..... N91-29636
NAG1-613 ..... N91-29769
NAG1-965 ..... N91-29212
NAG1-1083 ..... N91-29212
NAG3-823 ..... N91-29193
NAG3-863 ..... N91-29331
NAG3-867 ..... N91-29629
NAG3-904 ..... N91-29147
NAG3-1024 ..... N91-29524
NAG3-1263 ..... N91-29600
NAG5-637 ..... N91-29219
NASW-4245 ..... N91-29219
NAS1-17699 ..... N91-29253
NAS1-17701 ..... N91-29254
NAS1-17964 ..... N91-29176
NAS1-18476 ..... N91-29935
NAS1-18972 ..... N91-29777
N91-29778
NAS3-25266 ..... N91-29188
N91-29230
N91-29404
N91-29832
N91-29917
NAS3-25967 ..... N91-29187
NAS5-30141 ..... N91-29937
NAS8-36183 ..... N91-29603
NAS8-36555 ..... N91-29488
NAS8-36649 ..... N91-29297
N91-29865
NAS8-37195 ..... N91-29737
NAS8-37779 ..... N91-29554
NAS8-38080 ..... N91-29233
NAS9-16023 ..... N91-29211
NA86AA-D-SG040 ..... N91-29706
N91-29707
NA86AA-D-SG089 ..... N91-29630
NCC1-128 ..... N91-29390
NOAA-50-DGNW-0-00041 ..... N91-29694
NR PROJ. BR0-2301 ..... N91-29513
NR PROJ. RM3-5-G-80 ..... N91-29688
NR PROJ. RM3-5-G-84 ..... N91-29704
NR PROJ. RR0-1404 ..... N91-29824
NR PROJ. RR0-4108 ..... N91-29459
NR PROJ. RR0-4206 ..... N91-29732
NR PROJ. RR0-5202 ..... N91-29824
NSF ATM-88-14440 ..... N91-29219
NSF CCR-89-07654 ..... N91-29817
NSF CCR-89-18729 ..... N91-29818
NSF DMS-89-22154 ..... N91-29826
NSF DMS-90-00053 ..... N91-29826
NSF DMS-91-02857 ..... N91-29826
NSF OCE-89-01012 ..... N91-30070
N00014-80-C-1116 ..... N91-29249
N00014-82-C-0583 ..... N91-29269
N00014-83-K-0183 ..... N91-29510
N00014-85-K-0198 ..... N91-29753
N91-29823
N00014-85-K-0381 ..... N91-29472
N00014-85-K-0527 ..... N91-29518
N00014-86-C-0463 ..... N91-29690
N00014-86-C-0663 ..... N91-29508
N00014-86-K-0214 ..... N91-30003
N00014-86-K-0686 ..... N91-30021
N00014-86-K-0710 ..... N91-29571
N00014-86-K-0768 ..... N91-29342
N91-29343
N91-29344
N91-29345
N91-29346
N91-29347
N91-29622
N91-29623
N91-29877
N00014-87-K-0118 ..... N91-29621
N00014-87-K-0176 ..... N91-29243
N00014-87-K-0270 ..... N91-29570
N00014-87-K-0377 ..... N91-29717
N00014-87-K-0780 ..... N91-29804
N00014-87-K-0825 ..... N91-29739
N91-29781
N91-29784
N00014-88-C-0745 ..... N91-29929
N00014-88-J-1050 ..... N91-29718
N00014-88-K-0249 ..... N91-29683
N00014-88-K-0302 ..... N91-29349
N91-29350
N91-29352
N00014-88-K-0453 ..... N91-29749
N00014-88-K-0482 ..... N91-29337
N91-29338
N00014-88-K-0494 ..... N91-29454
N00014-88-K-0733 ..... N91-29365
N00014-89-J-1041 ..... N91-29357

N00014-89-J-1103 ..... N91-29874
N00014-89-J-1261 ..... N91-29268
N00014-89-J-1314 ..... N91-29351
N91-29364
N91-29366
N91-30001
N00014-89-J-1350 ..... N91-29314
N91-29888
N00014-89-J-1530 ..... N91-30014
N00014-89-J-1595 ..... N91-29701
N00014-89-J-1627 ..... N91-29835
N00014-89-J-1708 ..... N91-29627
N00014-89-J-1734 ..... N91-29273
N00014-89-J-1829 ..... N91-29569
N00014-89-J-1842 ..... N91-29461
N00014-89-J-1848 ..... N91-29462
N00014-89-J-1958 ..... N91-29315
N00014-89-J-1961 ..... N91-29353
N00014-89-J-1979 ..... N91-29700
N00014-89-J-1988 ..... N91-29779
N91-30047
N00014-89-J-3016 ..... N91-29732
N00014-89-J-3036 ..... N91-29783
N00014-90-C-0073 ..... N91-29574
N00014-90-C-0117 ..... N91-29412
N00014-90-C-0199 ..... N91-29924
N00014-90-C-0225 ..... N91-29469
N00014-90-C-0226 ..... N91-30012
N00014-90-C-1343 ..... N91-29826
N00014-90-J-1025 ..... N91-29817
N00014-90-J-1148 ..... N91-29348
N00014-90-J-1193 ..... N91-29886
N00014-90-J-1235 ..... N91-29875
N91-29876
N91-29996
N00014-90-J-1236 ..... N91-29415
N00014-90-J-1242 ..... N91-29756
N91-29773
N00014-90-J-1270 ..... N91-29769
N00014-90-J-1320 ..... N91-29362
N00014-90-J-1323 ..... N91-29818
N00014-90-J-1345 ..... N91-29775
N00014-90-J-1427 ..... N91-30020
N00014-90-J-1526 ..... N91-29691
N00014-90-J-1604 ..... N91-30000
N00014-90-J-1809 ..... N91-29760
N00014-90-J-4039 ..... N91-29919
N00014-90-J-4041 ..... N91-29520
N00014-90J-1063 ..... N91-29680
N00014-91-C-0095 ..... N91-29609
N00014-91-C-0101 ..... N91-30007
N00014-91-J-1046 ..... N91-29780
N00014-91-J-1058 ..... N91-29459
N00014-91-J-1271 ..... N91-29511
N00014-91-J-1299 ..... N91-29312
N00014-91-J-1333 ..... N91-29757
N00014-91-J-1334 ..... N91-29416
N00014-91-J-1409 ..... N91-29272
N91-29455
N91-29878
N91-29879
N91-29880
N91-29882
N91-29883
N91-29884
N91-30004
N00014-91-J-1416 ..... N91-30019
N00014-91-J-1459 ..... N91-29420
N00039-88-C-0051 ..... N91-29143
SDI084-88-C-0018 ..... N91-29853
W-31-109-ENG-38 ..... N91-29284
N91-29294
N91-29300
N91-29336
N91-29375
N91-29378
N91-29392
N91-29434
N91-29482
N91-29500
N91-29501
N91-29502
N91-29503
N91-29581
N91-29645
N91-29696
N91-29797
N91-29860
N91-29894
N91-29968
N91-29970
N91-29973
N91-29979
N91-29984
N91-29987
N91-29988

W-7405-ENG-36 ..... N91-29989
N91-29990
N91-29991
N91-29992
N91-30028
N91-30029
N91-30030
N91-30031
N91-29200
N91-29281
N91-29334
N91-29443
N91-29477
N91-29480
N91-29505
N91-29538
N91-29540
N91-29542
N91-29560
N91-29562
N91-29563
N91-29579
N91-29632
N91-29812
N91-29851
N91-29915
N91-29951
N91-29952
N91-29953
N91-29954
N91-29955
N91-29986
N91-30032
N91-30040
N91-30043

W-7405-ENG-48 ..... N91-29192
N91-29306
N91-29322
N91-29387
N91-29435
N91-29486
N91-29489
N91-29506
N91-29528
N91-29530
N91-29548
N91-29550
N91-29551
N91-29552
N91-29559
N91-29561
N91-29578
N91-29583
N91-29620
N91-29633
N91-29634
N91-29652
N91-29654
N91-29798
N91-29801
N91-29848
N91-29849
N91-29850
N91-29869
N91-29899
N91-29903
N91-29911
N91-29914
N91-29916
N91-29946
N91-29950
N91-29958
N91-29962
N91-29967
N91-29969
N91-29972
N91-30033
N91-30034
N91-30035
N91-30039
N91-30062

W-7405-ENG-82 ..... N91-29282
N91-29485
N91-29906
N91-29939
321-01-00 ..... N91-29431
326-84-32-20 ..... N91-30068
474-12-10 ..... N91-29199
505-62-40 ..... N91-29147
N91-29150
505-62-50 ..... N91-29188
505-62-52 ..... N91-29525
505-63-1A N91-29235
505-63-5B N91-29629
505-63-01-06 ..... N91-29253
505-63-36 ..... N91-29599

505-63-50-04 ..... N91-29600
N91-29239
N91-29240
505-64-00 ..... N91-29194
505-64-10-05 ..... N91-29777
N91-29778
505-66-21-02 ..... N91-29745
505-66-21-03 ..... N91-29176
505-66-71 ..... N91-29193
506-41-11 ..... N91-29222
506-42-00 ..... N91-29220
506-42-31 ..... N91-29228
N91-29229
N91-29230
N91-29231
N91-29832
N91-29917
506-44-21 ..... N91-29982
506-48-00 ..... N91-30073
509-10-03 ..... N91-29221
510-01-01 ..... N91-29250
510-01-50 ..... N91-29610
533-02-31 ..... N91-29191
533-02-51 ..... N91-29177
534-06-13-35 ..... N91-29254
537-01-22 ..... N91-29181
537-02-21 ..... N91-29187
590-13-11 ..... N91-29332
N91-29524
650-60-21 ..... N91-29404
N91-29405
992-35-15-06 ..... N91-29935

Typical Report Number Index Listing

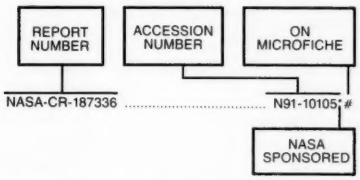

Listings in this index are arranged alphanumerically by report number. The accession number denotes the number by which the citation is identified. An asterisk (*) indicates that the item is a NASA report. A pound sign (#) indicates that the item is available on microfiche.

ACEE-30-FR-3610 ..... N91-29254* #

AD-A210128 ..... N91-29148 #
AD-A226628 ..... N91-29190 #
AD-A236823 ..... N91-29586 #
AD-A236828 ..... N91-29326 #
AD-A237062 ..... N91-29308 #
AD-A237063 ..... N91-29697 #
AD-A237064 ..... N91-29309 #
AD-A237085 ..... N91-29337 #
AD-A237086 ..... N91-29338 #
AD-A237087 ..... N91-29268 #
AD-A237089 ..... N91-29671 #
AD-A237100 ..... N91-29698 #
AD-A237105 ..... N91-29748 #
AD-A237106 ..... N91-29411 #
AD-A237107 ..... N91-29918 #
AD-A237114 ..... N91-29621 #
AD-A237118 ..... N91-29749 #
AD-A237120 ..... N91-29153 #
AD-A237127 ..... N91-29269 #
AD-A237133 ..... N91-29996 #
AD-A237134 ..... N91-29448 #
AD-A237138 ..... N91-29874 #
AD-A237140 ..... N91-29833 #
AD-A237144 ..... N91-29750 #
AD-A237146 ..... N91-29817 #
AD-A237156 ..... N91-29751 #
AD-A237157 ..... N91-29875 #
AD-A237167 ..... N91-29699 #
AD-A237168 ..... N91-29876 #
AD-A237169 ..... N91-29564 #
AD-A237171 ..... N91-29919 #
AD-A237174 ..... N91-29339 #
AD-A237175 ..... N91-29141 #
AD-A237176 ..... N91-29310 #
AD-A237178 ..... N91-29565 #
AD-A237183 ..... N91-29566 #
AD-A237190 ..... N91-29752 #
AD-A237193 ..... N91-29852 #
AD-A237206 ..... N91-29733 #
AD-A237221 ..... N91-29637 #
AD-A237222 ..... N91-29270 #
AD-A237223 ..... N91-29340 #
AD-A237228 ..... N91-29341 #
AD-A237232 ..... N91-29142 #
AD-A237234 ..... N91-29657 #
AD-A237241 ..... N91-29753 #
AD-A237250 ..... N91-29818 #
AD-A237258 ..... N91-29449 #
AD-A237259 ..... N91-29754 #
AD-A237263 ..... N91-29567 #
AD-A237265 ..... N91-29171 #
AD-A237270 ..... N91-29802 #
AD-A237271 ..... N91-29450 #
AD-A237285 ..... N91-29834 #
AD-A237287 ..... N91-29877 #
AD-A237288 ..... N91-29342 #
AD-A237289 ..... N91-29343 #
AD-A237290 ..... N91-29344 #
AD-A237291 ..... N91-29345 #
AD-A237292 ..... N91-29672 #
AD-A237317 ..... N91-29595 #
AD-A237324 ..... N91-29607 #
AD-A237331 ..... N91-29622 #
AD-A237332 ..... N91-29623 #
AD-A237333 ..... N91-29346 #
AD-A237334 ..... N91-29347 #
AD-A237340 ..... N91-29673 #
AD-A237349 ..... N91-29172 #
AD-A237350 ..... N91-29755 #
AD-A237352 ..... N91-29451 #
AD-A237354 ..... N91-29779 #
AD-A237355 ..... N91-30047 #
AD-A237357 ..... N91-29412 #
AD-A237361 ..... N91-29920 #
AD-A237362 ..... N91-29348 #
AD-A237388 ..... N91-29413 #
AD-A237390 ..... N91-29647 #
AD-A237391 ..... N91-29724 #
AD-A237411 ..... N91-29738 #
AD-A237412 ..... N91-29452 #
AD-A237413 ..... N91-29507 #
AD-A237414 ..... N91-29182 #
AD-A237418 ..... N91-29756 #
AD-A237423 ..... N91-29242 #
AD-A237425 ..... N91-29508 #
AD-A237427 ..... N91-29568 #
AD-A237428 ..... N91-29961 #
AD-A237429 ..... N91-29349 #
AD-A237430 ..... N91-29350 #
AD-A237435 ..... N91-29997 #
AD-A237436 ..... N91-29414 #
AD-A237437 ..... N91-29819 #
AD-A237439 ..... N91-29453 #
AD-A237441 ..... N91-29198 #
AD-A237447 ..... N91-29716 #
AD-A237451 ..... N91-29454 #
AD-A237452 ..... N91-29717 #
AD-A237454 ..... N91-29757 #
AD-A237455 ..... N91-29683 #
AD-A237456 ..... N91-29998 #
AD-A237457 ..... N91-29999 #
AD-A237458 ..... N91-29700 #
AD-A237459 ..... N91-29878 #
AD-A237460 ..... N91-29879 #
AD-A237462 ..... N91-29880 #
AD-A237463 ..... N91-30000 #
AD-A237466 ..... N91-30001 #
AD-A237467 ..... N91-29351 #
AD-A237469 ..... N91-29734 #
AD-A237470 ..... N91-29162 #
AD-A237471 ..... N91-29243 #
AD-A237472 ..... N91-29352 #
AD-A237475 ..... N91-29780 #
AD-A237476 ..... N91-29739 #
AD-A237477 ..... N91-29781 #
AD-A237478 ..... N91-29881 #
AD-A237480 ..... N91-29758 #
AD-A237486 ..... N91-29271 #
AD-A237497 ..... N91-29509 #
AD-A237498 ..... N91-30048 #
AD-A237499 ..... N91-30002 #
AD-A237501 ..... N91-29782 #
AD-A237502 ..... N91-29759 #
AD-A237503 ..... N91-29272 #
AD-A237504 ..... N91-30003 #
AD-A237505 ..... N91-29455 #
AD-A237506 ..... N91-29882 #
AD-A237507 ..... N91-29883 #
AD-A237508 ..... N91-29884 #
AD-A237509 ..... N91-30004 #
AD-A237535 ..... N91-29658 #
AD-A237538 ..... N91-29353 #
AD-A237540 ..... N91-29725 #
AD-A237564 ..... N91-29415 #
AD-A237567 ..... N91-29383 #
AD-A237568 ..... N91-29921 #
AD-A237569 ..... N91-29183 #
AD-A237571 ..... N91-29456 #
AD-A237572 ..... N91-29510 #
AD-A237573 ..... N91-29740 #
AD-A237574 ..... N91-29569 #
AD-A237577 ..... N91-29701 #
AD-A237589 ..... N91-29638 #
AD-A237598 ..... N91-29311 #
AD-A237599 ..... N91-29184 #
AD-A237601 ..... N91-29244 #
AD-A237607 ..... N91-29273 #
AD-A237612 ..... N91-29416 #
AD-A237614 ..... N91-30069 #
AD-A237624 ..... N91-29674 #
AD-A237626 ..... N91-29835 #
AD-A237627 ..... N91-29675 #
AD-A237628 ..... N91-29803 #
AD-A237632 ..... N91-29457 #
AD-A237640 ..... N91-29659 #
AD-A237641 ..... N91-29735 #
AD-A237654 ..... N91-29710 #
AD-A237658 ..... N91-29853 #
AD-A237663 ..... N91-29922 #
AD-A237669 ..... N91-29570 #
AD-A237670 ..... N91-29458 #
AD-A237673 ..... N91-29417 #
AD-A237674 ..... N91-29676 #
AD-A237675 ..... N91-29677 #
AD-A237683 ..... N91-29684 #
AD-A237685 ..... N91-29596 #
AD-A237695 ..... N91-29459 #
AD-A237696 ..... N91-29783 #
AD-A237703 ..... N91-29804 #
AD-A237704 ..... N91-29718 #
AD-A237705 ..... N91-29784 #
AD-A237710 ..... N91-30005 #
AD-A237722 ..... N91-29820 #
AD-A237736 ..... N91-29163 #
AD-A237750 ..... N91-29354 #
AD-A237751 ..... N91-30006 #
AD-A237753 ..... N91-29355 #
AD-A237754 ..... N91-29760 #
AD-A237755 ..... N91-29923 #
AD-A237757 ..... N91-29511 #
AD-A237758 ..... N91-30007 #
AD-A237759 ..... N91-29924 #
AD-A237767 ..... N91-29726 #
AD-A237768 ..... N91-29312 #
AD-A237784 ..... N91-29313 #
AD-A237785 ..... N91-30008 #
AD-A237792 ..... N91-29460 #
AD-A237793 ..... N91-29274 #
AD-A237794 ..... N91-29925 #
AD-A237795 ..... N91-30009 #
AD-A237797 ..... N91-30010 #
AD-A237798 ..... N91-30011 #
AD-A237802 ..... N91-29821 #
AD-A237811 ..... N91-29143 #
AD-A237817 ..... N91-29148 #
AD-A237818 ..... N91-29685 #
AD-A237840 ..... N91-29926 #
AD-A237841 ..... N91-29356 #
AD-A237843 ..... N91-29461 #
AD-A237844 ..... N91-29512 #
AD-A237845 ..... N91-29624 #
AD-A237846 ..... N91-29727 #
AD-A237847 ..... N91-29822 #
AD-A237851 ..... N91-29223 #
AD-A237853 ..... N91-29224 #
AD-A237856 ..... N91-29785 #
AD-A237857 ..... N91-29597 #
AD-A237859 ..... N91-29275 #
AD-A237864 ..... N91-29214 #
AD-A237878 ..... N91-29823 #
AD-A237880 ..... N91-29462 #
AD-A237881 ..... N91-29357 #
AD-A237883 ..... N91-29314 #
AD-A237884 ..... N91-29571 #
AD-A237885 ..... N91-29463 #
AD-A237888 ..... N91-29513 #
AD-A237889 ..... N91-29464 #
AD-A237890 ..... N91-29418 #
AD-A237901 ..... N91-29625 #
AD-A237903 ..... N91-29465 #
AD-A237904 ..... N91-29927 #
AD-A237905 ..... N91-29761 #
AD-A237909 ..... N91-30070 #
AD-A237922 ..... N91-29762 #
AD-A237923 ..... N91-29514 #

AD-A237924 N91-29608 #
AD-A237925 N91-29358 #
AD-A237931 N91-29315 #
AD-A237937 N91-29515 #
AD-A237938 N91-29205 #
AD-A237940 N91-29234 #
AD-A237941 N91-29419 #
AD-A237942 N91-29206 #
AD-A237943 N91-29516 #
AD-A237944 N91-29648 #
AD-A237946 N91-30012 #
AD-A237955 N91-30013 #
AD-A237958 N91-29276 #
AD-A237959 N91-29805 #
AD-A237974 N91-29660 #
AD-A237982 N91-29420 #
AD-A237988 N91-29517 #
AD-A237997 N91-29518 #
AD-A237998 N91-29686 #
AD-A238001 N91-29466 #
AD-A238005 N91-29421 #
AD-A238006 N91-29806 #
AD-A238011 N91-29225 #
AD-A238012 N91-29543 #
AD-A238016 N91-29639 #
AD-A238017 N91-29467 #
AD-A238018 N91-29763 #
AD-A238019 N91-29422 #
AD-A238020 N91-29245 #
AD-A238022 N91-29702 #
AD-A238023 N91-29862 #
AD-A238026 N91-29640 #
AD-A238028 N91-29277 #
AD-A238029 N91-29626 #
AD-A238034 N91-29928 #
AD-A238035 N91-29824 #
AD-A238039 N91-29154 #
AD-A238040 N91-29155 #
AD-A238041 N91-29156 #
AD-A238044 N91-29929 #
AD-A238046 N91-29786 #
AD-A238047 N91-29787 #
AD-A238048 N91-29788 #
AD-A238049 N91-29789 #
AD-A238051 N91-29519 #
AD-A238052 N91-29246 #
AD-A238053 N91-29173 #
AD-A238054 N91-29687 #
AD-A238064 N91-29207 #
AD-A238066 N91-29825 #
AD-A238071 N91-29278 #
AD-A238080 N91-29359 #
AD-A238081 N91-29423 #
AD-A238082 N91-29424 #
AD-A238095 N91-29360 #
AD-A238097 N91-29764 #
AD-A238098 N91-29678 #
AD-A238099 N91-29572 #
AD-A238100 N91-29836 #
AD-A238110 N91-29573 #
AD-A238111 N91-29544 #
AD-A238112 N91-29361 #
AD-A238113 N91-29765 #
AD-A238115 N91-29468 #
AD-A238130 N91-29316 #
AD-A238138 N91-29703 #
AD-A238151 N91-29317 #
AD-A238152 N91-30014 #
AD-A238154 N91-29279 #
AD-A238156 N91-29885 #
AD-A238159 N91-29215 #
AD-A238160 N91-29766 #
AD-A238162 N91-29767 #
AD-A238165 N91-29826 #
AD-A238166 N91-29574 #
AD-A238175 N91-29362 #
AD-A238178 N91-29886 #
AD-A238179 N91-29226 #
AD-A238180 N91-29837 #
AD-A238182 N91-29185 #
AD-A238196 N91-29363 #
AD-A238197 N91-29575 #
AD-A238198 N91-30015 #
AD-A238204 N91-29364 #
AD-A238219 N91-29838 #
AD-A238220 N91-29839 #
AD-A238222 N91-29840 #
AD-A238227 N91-29469 #
AD-A238229 N91-29841 #
AD-A238231 N91-29887 #
AD-A238233 N91-29425 #
AD-A238234 N91-29768 #
AD-A238244 N91-29728 #
AD-A238245 N91-29576 #
AD-A238252 N91-29807 #
AD-A238260 N91-29280 #
AD-A238262 N91-29426 #
AD-A238266 N91-29769* #
AD-A238272 N91-29470 #
AD-A238277 N91-29247 #
AD-A238279 N91-29863 #
AD-A238280 N91-29427 #
AD-A238289 N91-29248 #
AD-A238292 N91-29854 #
AD-A238300 N91-29704 #
AD-A238305 N91-29688 #
AD-A238310 N91-30049 #
AD-A238312 N91-29609 #
AD-A238319 N91-29365 #
AD-A238387 N91-29428 #
AD-A238389 N91-30050 #
AD-A238390 N91-29842 #
AD-A238392 N91-29471 #
AD-A238393 N91-29545 #
AD-A238397 N91-29679 #
AD-A238398 N91-29888 #
AD-A238399 N91-29843 #
AD-A238400 N91-29366 #
AD-A238406 N91-29186 #
AD-A238423 N91-29627 #
AD-A238427 N91-30016* #
AD-A238443 N91-29827 #
AD-A238444 N91-29216 #
AD-A238445 N91-29770 #
AD-A238448 N91-29771 #
AD-A238456 N91-29174 #
AD-A238457 N91-29844 #
AD-A238458 N91-29828 #
AD-A238459 N91-29930 #
AD-A238460 N91-30017 #
AD-A238461 N91-29889 #
AD-A238482 N91-29890 #
AD-A238483 N91-29546 #
AD-A238485 N91-29217 #
AD-A238487 N91-29547 #
AD-A238489 N91-29689 #
AD-A238493 N91-29790 #
AD-A238494 N91-29808 #
AD-A238495 N91-29829 #
AD-A238505 N91-30018 #
AD-A238506 N91-30019 #
AD-A238507 N91-29830 #
AD-A238520 N91-30020 #
AD-A238521 N91-30021 #
AD-A238531 N91-29690 #
AD-A238533 N91-29628 #
AD-A238536 N91-29772 #
AD-A238538 N91-29831 #
AD-A238545 N91-29741 #
AD-A238546 N91-29891 #
AD-A238547 N91-29367 #
AD-A238548 N91-30051 #
AD-A238554 N91-29773 #
AD-A238555 N91-29429 #
AD-A238556 N91-29845 #
AD-A238557 N91-29227 #
AD-A238558 N91-29680 #
AD-A238561 N91-29218 #
AD-A238563 N91-29729 #
AD-A238564 N91-29730 #
AD-A238565 N91-29736 #
AD-A238570 N91-29164 #
AD-A238575 N91-29691 #
AD-A238576 N91-29931 #
AD-A238583 N91-29389 #
AD-A238588 N91-29932 #
AD-A238592 N91-29472 #
AD-A238595 N91-29473 #
AD-A238596 N91-29577 #
AD-A238597 N91-29731 #
AD-A238600 N91-29520 #
AD-A238601 N91-29774 #
AD-A238611 N91-29775 #
AD-A238612 N91-29856 #
AD-A238617 N91-29732 #
AD-A238618 N91-29249 #
AD-A238628 N91-29384 #
AD-A238630 N91-29846 #
AD-A238631 N91-29791 #
AD-A238633 N91-29847 #
AD-A238634 N91-30022 #
AD-A238635 N91-29692 #
AD-A238638 N91-29521 #
AD-A238639 N91-29474 #
AD-A238642 N91-30023 #
AD-A238643 N91-29368 #
AD-A238644 N91-30052 #
AD-A238645 N91-29522 #
AD-A238659 N91-29719 #
AD-A238660 N91-29175 #
AD-A238663 N91-29720 #
AD-A238664 N91-29721 #
AD-A238665 N91-29857 #
AD-D011645 N91-29399
AD-D014902 N91-29400 #
AD-D014904 N91-29438 #
AD-D014908 N91-29439
AD-D014936 N91-29598 #
AD-D014937 N91-29523 #
AD-D014942 N91-29933 #
AD-D014944 N91-29934 #
AD-D014945 N91-29475 #
AD-D014946 N91-29149 #
AD-D014947 N91-29430 #
AD-E040005 N91-29637 #
AD-E040019 N91-29688 #
AD-E040041 N91-29704 #
AD-E040060 N91-29638 #
AD-E040062 N91-29685 #
AD-E501393 N91-29449 #
AD-E501397 N91-29754 #
AD-E501404 N91-29660 #
AEDC-TR-91-2 N91-29522 #
AEDC-TR-91-4 N91-29926 #
AEDC-TSR-91-V12 N91-29218 #
AFDTC-PAMPHLET-83-2 N91-30051 #
AFDTC-TM-91-01 N91-30051 #
AFIT/DS/ENG/91-1 N91-29930 #
AFIT/GA/ENY/91M-01 N91-29844 #
AFIT/GAE/ENY/91M-2 N91-29174 #
AFIT/GCE/ENG/91M-01 N91-29771 #
AFIT/GCE/ENG/91M-04 N91-29770 #
AFIT/GCS/ENC/91M-1 N91-29828 #
AFIT/GCS/ENG/91M-03 N91-29791 #
AFIT/GE/ENG-91J-06 N91-29827 #
AFIT/GNE/ENP/91M-4 N91-30022 #
AFIT/GOR/ENC/91M-3 N91-29846 #
AFIT/GOR/ENC/91M-4 N91-29847 #
AFIT/GSO/ENS/91M-1 N91-29216 #
AFIT/GST/ENS/91M-2 N91-29842 #
AFOSR-91-0232TR N91-29214 #
AFOSR-91-0504TR N91-29507 #
AFOSR-91-0535TR N91-29597 #
AFOSR-91-0544TR N91-29925 #
AFOSR-91-0546TR N91-29248 #
AFOSR-91-0549TR N91-29275 #
AFOSR-91-0554TR N91-29785 #
AFOSR-91-0556TR N91-29774 #
AFOSR-91-0557TR N91-29820 #
AFOSR-91-0564TR N91-29726 #
AFOSR-91-0565TR N91-29999 #
AFOSR-91-0566TR N91-30010 #
AFOSR-91-0568TR N91-29658 #
AFOSR-91-0569TR N91-29274 #
AFOSR-91-0571TR N91-29727 #
AFOSR-91-0572TR N91-30009 #
AFOSR-91-0574TR N91-29280 #
AFOSR-91-0575TR N91-30011 #
AFOSR-91-0576TR N91-29317 #
AFOSR-91-0580TR N91-29998 #
AFOSR-91-0582TR N91-29460 #
AFOSR-91-0583TR N91-30008 #
AFOSR-91-0584TR N91-30005 #
AFOSR-91-0586TR N91-29355 #
AFOSR-91-0590TR N91-29640 #
AFOSR-91-0593TR N91-29887 #
AFOSR-91-0594TR N91-29512 #
AFOSR-91-0596TR N91-29768 #
AFOSR-91-0599TR N91-29277 #
AFOSR-91-0600TR N91-29223 #
AFOSR-91-0602TR N91-29626 #
AFOSR-91-0604TR N91-29862 #
AFOSR-91-0612TR N91-29426 #
AFOSR-91-0614TR N91-29360 #
AFOSR-91-0615TR N91-29841 #
AFOSR-91-0616TR N91-29425 #
AFOSR-91-0617TR N91-29822 #
AFOSR-91-0639TR N91-29720 #
AFOSR-91-0651TR N91-29721 #
AFOSR-91-0664TR N91-30023 #

AFOSR-91-0666TR ..... N91-29368 #

AIAA-91-1997 ..... N91-29188* #
AIAA-91-2110 ..... N91-29228* #
AIAA-91-2264 ..... N91-29150* #
AIAA-91-2341 ..... N91-29832* #
AIAA-91-2350 ..... N91-29229* #
AIAA-91-2393 ..... N91-29281 #
AIAA-91-2456 ..... N91-29231* #
AIAA-91-2459 ..... N91-29187* #
AIAA-91-3471 ..... N91-29405* #
AIAA-91-3481 ..... N91-29222* #
AIAA-91-3484 ..... N91-29220* #
AIAA-91-3527 ..... N91-29332* #
AIAA-91-3530 ..... N91-29298* #
AIAA-91-3532 ..... N91-29404* #
AIAA-91-3538 ..... N91-30073* #
AIAA-91-3554 ..... N91-29221* #
AIAA-91-3592 ..... N91-29982* #

AL-TR-90-066 ..... N91-29647 #
AL-TR-91-0061 ..... N91-29648 #

ANL-HEP-CP-91-43 ..... N91-29581 #

ANL/CP-68452 ..... N91-29991 #
ANL/CP-69633 ..... N91-29294 #
ANL/CP-71552 ..... N91-30028 #
ANL/CP-71621 ..... N91-29500 #
ANL/CP-71781 ..... N91-29300 #
ANL/CP-71904 ..... N91-29990 #
ANL/CP-72035 ..... N91-29968 #
ANL/CP-72217 ..... N91-29860 #
ANL/CP-72267 ..... N91-30031 #
ANL/CP-72346 ..... N91-29645 #
ANL/CP-72361 ..... N91-29284 #
ANL/CP-72528-PT-1 ..... N91-29502 #
ANL/CP-72529-PT-2 ..... N91-29501 #
ANL/CP-72768 ..... N91-29970 #
ANL/CP-72825 ..... N91-29973 #
ANL/CP-72919 ..... N91-29482 #
ANL/CP-73053 ..... N91-30029 #
ANL/CP-73108 ..... N91-29378 #
ANL/CP-73141 ..... N91-29503 #
ANL/CP-73155 ..... N91-29336 #
ANL/CP-73209 ..... N91-29392 #
ANL/CP-73289 ..... N91-29696 #
ANL/CP-73327-REV ..... N91-30030 #
ANL/CP-73357 ..... N91-29979 #
ANL/CP-7[illegible]370 ..... N91-29894 #
ANL/CP-73387 ..... N91-29984 #
ANL/CP-73426 ..... N91-29987 #
ANL/CP-73493 ..... N91-29992 #
ANL/CP-73507 ..... N91-29989 #
ANL/CP-73508 ..... N91-29988 #
ANL/CP-73512 ..... N91-29434 #
ANL/CP-73537 ..... N91-29375 #

ANL/TM-488 ..... N91-29797 #

APL-UW-TR-8929 ..... N91-29700 #

AR-006-366 ..... N91-29290 #

ARAED-TR-91012 ..... N91-29234 #

ARFSD-TR-90028 ..... N91-29207 #
ARFSD-TR-90029 ..... N91-29205 #
ARFSD-TR-90030 ..... N91-29206 #

ARI-RN-91-39 ..... N91-29731 #
ARI-RN-91-40 ..... N91-29725 #
ARI-RN-91-45 ..... N91-29805 #

ARL-PROP-TM-452 ..... N91-29226 #

ARL-STRUC-TM-577 ..... N91-29185 #

ARL/PSU/TR-91-008 ..... N91-29515 #

ARO-23217.4-GS ..... N91-29678 #
ARO-23360.17-MA ..... N91-29845 #
ARO-23810.7-MS ..... N91-29389 #
ARO-23933.10-MA ..... N91-29829 #
ARO-24073.11-CH ..... N91-29363 #
ARO-24105.19-MA ..... N91-29764 #
ARO-24456.5-EG ..... N91-29175 #
ARO-24559.15-CH ..... N91-29367 #
ARO-24626.211-PH-UIR ..... N91-29932 #
ARO-24844.8-CH ..... N91-29891 #
ARO-25146.28-PH ..... N91-29931 #
ARO-25156.12-EL ..... N91-29468 #
ARO-25299.12-PH ..... N91-29573 #
ARO-25375.7-PH ..... N91-30015 #
ARO-25425.21-CH ..... N91-29889 #
ARO-25502.1-CH ..... N91-29890 #
ARO-25541.1-PH ..... N91-30017 #
ARO-25670.8-GS ..... N91-29575 #
ARO-25839.36-MA ..... N91-29765 #
ARO-25839.42-MA ..... N91-29836 #
ARO-25896.1-PH ..... N91-29544 #
ARO-26098.21-MA ..... N91-29830 #
ARO-26099.4-LS ..... N91-29772 #
ARO-26394.5-MA ..... N91-29831 #
ARO-27868.3-MA ..... N91-29838 #
ARO-27868.4-MA ..... N91-29839 #
ARO-27868.5-MA ..... N91-29840 #
ARO-28258.4-PH ..... N91-29576 #
ARO-28836.1-MS-CF ..... N91-29361 #

ASE-5600 ..... N91-29937* #

ASL-CR-91-0001-1 ..... N91-29821 #

ASL-TR-0294 ..... N91-29674 #
ASL-TR-0296 ..... N91-29675 #

ASTROMAG-034 ..... N91-29204 #
ASTROMAG-035 ..... N91-29444 #

AVSCOM-TR-91-C-011 ..... N91-29599* #
AVSCOM-TR-91-C-014 ..... N91-29250* #
AVSCOM-TR-91-C-039 ..... N91-29600* #

BDX-613-3962 ..... N91-29606 #

BNL-45445 ..... N91-29947 #
BNL-46115 ..... N91-29681 #
BNL-46235 ..... N91-29232 #
BNL-46239 ..... N91-29323 #
BNL-46244 ..... N91-29656 #
BNL-46259 ..... N91-30026 #
BNL-46279 ..... N91-29870 #
BNL-46292 ..... N91-29859 #
BNL-46322 ..... N91-29895 #

BR-302896 ..... N91-29493 #

BRL-CR-665 ..... N91-29545 #

BRL-MR-3911 ..... N91-29276 #
BRL-MR-3921 ..... N91-29384 #
BRL-MR-3922 ..... N91-29514 #

BRL-TR-3239 ..... N91-29383 #
BRL-TR-3240 ..... N91-29428 #
BRL-TR-3245 ..... N91-30050 #

CERL-SR-N-91/22 ..... N91-29803 #

CERL-TR-P-91/34 ..... N91-29758 #

CMS-TSR-92-2 ..... N91-29826 #

CMU-RI-TR-91-08 ..... N91-29586 #

CONF-891153-2 ..... N91-29991 #
CONF-900466-53 ..... N91-29969 #
CONF-900530-9 ..... N91-29914
CONF-900623-26 ..... N91-29295 #
CONF-900705-4 ..... N91-29380 #
CONF-900780-6 ..... N91-29585 #
CONF-900802-20 ..... N91-29333 #
CONF-900813-2 ..... N91-29973 #
CONF-900862-2 ..... N91-29723 #
CONF-901107-1 ..... N91-29294 #
CONF-901141-6 ..... N91-30065 #
CONF-901263-9-VUGRAPHS ..... N91-29580 #
CONF-901285-4 ..... N91-29369 #
CONF-901285-5 ..... N91-29655 #
CONF-910123-17 ..... N91-29605 #
CONF-910123-31 ..... N91-29559 #
CONF-910190-3 ..... N91-29974 #
CONF-910274 ..... N91-29801 #
CONF-910322-2 ..... N91-29994 #
CONF-910397-1 ..... N91-29376 #
CONF-910402-17 ..... N91-29261 #
CONF-910406-24 ..... N91-29986 #
CONF-910406-26 ..... N91-29303 #
CONF-910406-27 ..... N91-29990 #
CONF-910406-30 ..... N91-29284 #
CONF-910406-31 ..... N91-30037 #
CONF-910406-32 ..... N91-30038 #
CONF-910414-37 ..... N91-29861 #
CONF-910430-17 ..... N91-30031 #
CONF-910432-1 ..... N91-29668 #
CONF-910503-13 ..... N91-29200 #
CONF-910505-4 ..... N91-29864 #
CONF-910505-115 ..... N91-29441 #
CONF-910505-173 ..... N91-29560 #
CONF-910505-182 ..... N91-29947 #
CONF-910505-335 ..... N91-29746 #
CONF-910505-359 ..... N91-29407 #
CONF-910505-360 ..... N91-29408 #
CONF-910505-364 ..... N91-29911 #
CONF-910505-366 ..... N91-29578 #
CONF-910505-383 ..... N91-29410 #
CONF-910505-386 ..... N91-29581 #
CONF-910505-387 ..... N91-29583 #
CONF-910529-4 ..... N91-29893 #
CONF-910580-3 ..... N91-30036 #
CONF-910605-1 ..... N91-29281 #
CONF-910606-1 ..... N91-29869 #
CONF-910609-10 ..... N91-29950 #
CONF-910609-18 ..... N91-29957 #
CONF-910609-19 ..... N91-29958 #
CONF-910614-5 ..... N91-29299 #
CONF-910617-3 ..... N91-29373 #
CONF-910626-2 ..... N91-29232 #
CONF-910635-3 ..... N91-29444 #
CONF-910635-7 ..... N91-29993 #
CONF-910635-8 ..... N91-29963 #
CONF-910640-10 ..... N91-29952 #
CONF-910640-11 ..... N91-29446 #
CONF-910640-12 ..... N91-29478 #
CONF-910640-13 ..... N91-29479 #
CONF-910640-15 ..... N91-29955 #
CONF-910640-17 ..... N91-29953 #
CONF-910640-19 ..... N91-29443 #
CONF-910640-21 ..... N91-29562 #
CONF-910640-22 ..... N91-29951 #
CONF-910640-23 ..... N91-29954 #
CONF-910640-24 ..... N91-29480 #
CONF-910640-25 ..... N91-29483 #
CONF-910640-27 ..... N91-29445 #
CONF-910640-29 ..... N91-29435 #
CONF-910640-30 ..... N91-29487 #
CONF-910651-2-REV-1 ..... N91-29489 #
CONF-910654-3 ..... N91-29620 #
CONF-910659-5-REV-1 ..... N91-29652 #
CONF-910661-1 ..... N91-29541 #
CONF-910720-1 ..... N91-29506 #
CONF-910736-2 ..... N91-30032 #
CONF-910736-3 ..... N91-29985 #
CONF-910736-5 ..... N91-29995 #
CONF-910739-19 ..... N91-29503 #
CONF-910739-20 ..... N91-29300 #
CONF-910739-21-PT-1 ..... N91-29502 #
CONF-910739-22-PT-2 ..... N91-29501 #
CONF-910739-23 ..... N91-29500 #
CONF-910739-26 ..... N91-29377 #
CONF-910739-27 ..... N91-29531 #
CONF-910746-1 ..... N91-29909 #
CONF-910746-2 ..... N91-29903 #
CONF-910774-4 ..... N91-29409 #
CONF-910774-5 ..... N91-30058 #
CONF-910774-9 ..... N91-29549 #
CONF-910774-15 ..... N91-29386 #
CONF-910795-1 ..... N91-29481 #
CONF-910801-8 ..... N91-29910 #
CONF-910801-10 ..... N91-29378 #
CONF-910801-11 ..... N91-29860 #
CONF-910801-12 ..... N91-29392 #
CONF-910801-14-DRAFT ..... N91-29968 #
CONF-910801-15 ..... N91-29649 #
CONF-910847-2 ..... N91-29151 #
CONF-910859-1 ..... N91-29812 #
CONF-910870-7 ..... N91-29536 #
CONF-910870-8 ..... N91-29327 #
CONF-910870-10 ..... N91-29971 #
CONF-910872-1 ..... N91-29970 #
CONF-910872-3 ..... N91-29972 #
CONF-910885-1 ..... N91-29260 #
CONF-910903-1 ..... N91-29477 #
CONF-910903-3 ..... N91-29859 #
CONF-910909-8 ..... N91-29324 #
CONF-8405153-6 ..... N91-29650 #
CONF-8810506-1 ..... N91-29550 #
CONF-8906408 ..... N91-29442 #
CONF-8909334-1 ..... N91-29709 #
CONF-9002115-1 ..... N91-29584 #
CONF-9006187-1 ..... N91-29256 #
CONF-9006190-2 ..... N91-29553 #
CONF-9008162-3 ..... N91-29656 #
CONF-9010247-4 ..... N91-29849 #
CONF-9011119-4 ..... N91-29387 #
CONF-9011207-1 ..... N91-29328 #
CONF-9101102-3 ..... N91-29336 #
CONF-9102106-2 ..... N91-29259 #
CONF-9103112-2 ..... N91-29979 #
CONF-9103112-3 ..... N91-29989 #
CONF-9103184-1 ..... N91-30040 #
CONF-9103184-2-REV-1 ..... N91-30039 #
CONF-9103186-1 ..... N91-29898 #
CONF-9104158-4 ..... N91-29815 #
CONF-9104158-5 ..... N91-29798 #
CONF-9104192-12 ..... N91-29563 #
CONF-9104203-3 ..... N91-29915 #

CONF-9104238-2 ..... N91-29850 #
CONF-9104241-3-REV-1 ..... N91-29946 #
CONF-9104271-1 ..... N91-29984 #
CONF-9104274-1 ..... N91-29484 #
CONF-9105106-12 ..... N91-29899 #
CONF-9105106-16 ..... N91-29873 #
CONF-9105106-20 ..... N91-29895 #
CONF-9105133-2 ..... N91-30026 #
CONF-9105147-1 ..... N91-29485 #
CONF-9105151-6 ..... N91-29321 #
CONF-9105151-8 ..... N91-29987 #
CONF-9105151-9 ..... N91-29988 #
CONF-9105162-4 ..... N91-29868 #
CONF-9105181-13 ..... N91-29653 #
CONF-9105182-1 ..... N91-29975 #
CONF-9105197-2 ..... N91-29447 #
CONF-9105202-7 ..... N91-29323 #
CONF-9105216-1 ..... N91-29265 #
CONF-9105224-1 ..... N91-29306 #
CONF-9105226-1 ..... N91-29992 #
CONF-9105227-1 ..... N91-29375 #
CONF-9105233-1 ..... N91-30029 #
CONF-9106101-1-REV ..... N91-30030 #
CONF-9106116-4 ..... N91-29537 #
CONF-9106118-4 ..... N91-29402 #
CONF-9106122-3 ..... N91-29434 #
CONF-9106134-1 ..... N91-29204 #
CONF-9106176-2 ..... N91-29286 #
CONF-9106176-3 ..... N91-29334 #
CONF-9106196-2 ..... N91-29870 #
CONF-9106196-3 ..... N91-29894 #
CONF-9106222-1 ..... N91-29505 #
CONF-9106222-3 ..... N91-29530 #
CONF-9106229-1 ..... N91-29301 #
CONF-9106231-1 ..... N91-29322 #
CONF-9106235-3 ..... N91-29902 #
CONF-9106236-1 ..... N91-29990 #
CONF-9106238-1 ..... N91-29528 #
CONF-9106241-1 ..... N91-29307 #
CONF-9106244-2 ..... N91-30028 #
CONF-9107104-5 ..... N91-29681 #
CONF-9107104-9 ..... N91-29667 #
CONF-9107104-12 ..... N91-29695 #
CONF-9107105-17 ..... N91-29612 #
CONF-9107105-33 ..... N91-29203 #
CONF-9107105-35 ..... N91-29302 #
CONF-9107105-36 ..... N91-29619 #
CONF-9107105-38 ..... N91-29632 #
CONF-9107105-39 ..... N91-29542 #
CONF-9107105-42 ..... N91-29540 #
CONF-9107105-44 ..... N91-29304 #
CONF-9107105-45 ..... N91-29213* #
CONF-9107106-1 ..... N91-29645 #
CONF-9107106-2 ..... N91-30027 #
CONF-9107114-3 ..... N91-29654 #
CONF-9107115-1 ..... N91-29538 #
CONF-9107115-5 ..... N91-29406 #
CONF-9107115-7 ..... N91-30035 #
CONF-9107115-8 ..... N91-30034 #
CONF-9107115-9 ..... N91-29663 #
CONF-9107115-10 ..... N91-29374 #
CONF-9107115-11 ..... N91-29747 #
CONF-9107115-13 ..... N91-29486 #
CONF-9107135-1 ..... N91-30033 #
CONF-9107138-1 ..... N91-29208 #
CONF-9107139-1 ..... N91-29666 #
CONF-9107141-1 ..... N91-29809 #
CONF-9107142-1 ..... N91-29696 #
CONF-9107144-1 ..... N91-29810 #
CONF-9108100-2 ..... N91-30043 #
CONF-9108109-1 ..... N91-30046 #
CONF-9108110-1 ..... N91-29320 #
CONF-9108111-1 ..... N91-29325 #
CONF-9108113-1 ..... N91-30057 #
CONF-9108115-1 ..... N91-29482 #
CONF-9109108-1 ..... N91-29962 #
CONF-9109108-2 ..... N91-29433 #
CONF-9109108-3 ..... N91-29967 #

CONTRIB-1277 ..... N91-29705 #

COO-2271-113 ..... N91-29904 #
COO-2271-114 ..... N91-29905 #

CRC-APRAC-AP-9-A ..... N91-29661 #

CRDEC-TR-278 ..... N91-29734 #

CRHC-91-21 ..... N91-29790 #
CRHC-91-22 ..... N91-29769* #

CRL-MCCS-91-224 ..... N91-29818 #

CRREL-91-7 ..... N91-29198 #
CRREL-91-9 ..... N91-29639 #

CSDL-R-1582 ..... N91-29211* #

CTN-91-60005 ..... N91-29195 #
CTN-91-60006 ..... N91-29144 #
CTN-91-60007 ..... N91-29196 #
CTN-91-60008 ..... N91-29394 #
CTN-91-60011 ..... N91-29288 #
CTN-91-60012 ..... N91-30071 #
CTN-91-60013 ..... N91-30072 #
CTN-91-60015 ..... N91-29533 #
CTN-91-60016 ..... N91-29799 #
CTN-91-60018 ..... N91-29490 #
CTN-91-60021 ..... N91-29534 #
CTN-91-60022 ..... N91-29388 #
CTN-91-60023 ..... N91-29742 #
CTN-91-60024 ..... N91-29165 #
CTN-91-60025 ..... N91-29236 #
CTN-91-60027 ..... N91-29651 #
CTN-91-60028 ..... N91-29535 #
CTN-91-60029 ..... N91-29166 #
CTN-91-60030 ..... N91-29158 #
CTN-91-60033 ..... N91-29604 #
CTN-91-60034 ..... N91-29178 #
CTN-91-60036 ..... N91-29743 #
CTN-91-60039 ..... N91-29179 #
CTN-91-60042 ..... N91-29800 #
CTN-91-60047 ..... N91-29744 #
CTN-91-60061 ..... N91-29167 #
CTN-91-60073 ..... N91-29611 #
CTN-91-60074 ..... N91-29395 #
CTN-91-60075 ..... N91-29396 #
CTN-91-60076 ..... N91-29397 #
CTN-91-60078 ..... N91-29398 #
CTN-91-60080 ..... N91-29189 #
CTN-91-60081 ..... N91-29237 #
CTN-91-60082 ..... N91-29168 #
CTN-91-60083 ..... N91-29139 #
CTN-91-60091 ..... N91-29289 #
CTN-91-60098 ..... N91-29811 #
CTN-91-60099 ..... N91-29180 #
CTN-91-60100 ..... N91-29190 #
CTN-91-60102 ..... N91-29169* #
CTN-91-60103 ..... N91-29159 #
CTN-91-60104 ..... N91-29258 #
CTN-91-60105 ..... N91-29140 #
CTN-91-60115 ..... N91-29642 #
CTN-91-60124 ..... N91-29160 #

CTS-19-90 ..... N91-29849 #

CVD-TR-9081 ..... N91-29935* #

DEL-SG-06-90 ..... N91-29706 #
DEL-SG-07-90 ..... N91-29707 #

DE90-008282 ..... N91-29255 #
DE90-010380 ..... N91-29938 #
DE90-010387 ..... N91-29532 #
DE90-010896 ..... N91-29436 #
DE90-011362 ..... N91-29914
DE90-011600 ..... N91-29256 #
DE90-011615 ..... N91-29584 #
DE90-011733 ..... N91-29939 #
DE90-011758 ..... N91-29550 #
DE90-011760 ..... N91-29551 #
DE90-011790 ..... N91-29940 #
DE90-011927 ..... N91-29709 #
DE90-012073 ..... N91-29969 #
DE90-012123 ..... N91-29848 #
DE90-012125 ..... N91-29552 #
DE90-012137 ..... N91-29585 #
DE90-012211 ..... N91-29380 #
DE90-012227 ..... N91-29553 #
DE90-012477 ..... N91-29941 #
DE90-012490 ..... N91-29381 #
DE90-012496 ..... N91-29437 #
DE90-012527 ..... N91-29904 #
DE90-012535 ..... N91-29257 #
DE91-002160 ..... N91-29643 #
DE91-002169 ..... N91-29983 #
DE91-002190 ..... N91-29646 #
DE91-002196 ..... N91-29663 #
DE91-002197 ..... N91-29649 #
DE91-002198 ..... N91-29650 #
DE91-008583 ..... N91-29812 #
DE91-009405 ..... N91-29605 #
DE91-010136 ..... N91-29536 #
DE91-010150 ..... N91-29327 #
DE91-010492 ..... N91-29496 #
DE91-010593 ..... N91-29970 #
DE91-010869 ..... N91-29971 #
DE91-010872 ..... N91-29260 #
DE91-011094 ..... N91-29864 #
DE91-011116 ..... N91-29972 #
DE91-011138 ..... N91-29950 #
DE91-011276 ..... N91-29285 #

DE91-011501 ..... N91-29537 #
DE91-011532 ..... N91-29489 #
DE91-011748 ..... N91-29973 #
DE91-011827 ..... N91-29974 #
DE91-012035 ..... N91-29652 #
DE91-012338 ..... N91-29259 #
DE91-012343 ..... N91-29723 #
DE91-012494 ..... N91-29559 #
DE91-012538 ..... N91-29975 #
DE91-012607 ..... N91-29261 #
DE91-012634 ..... N91-29440 #
DE91-012635 ..... N91-30045 #
DE91-012929 ..... N91-29668 #
DE91-012984 ..... N91-29942 #
DE91-012991 ..... N91-29401 #
DE91-013021 ..... N91-29555 #
DE91-013023 ..... N91-29943 #
DE91-013114 ..... N91-29491 #
DE91-013134 ..... N91-29292 #
DE91-013140 ..... N91-29330 #
DE91-013151 ..... N91-29293 #
DE91-013157 ..... N91-29945 #
DE91-013164 ..... N91-29556 #
DE91-013167 ..... N91-29915 #
DE91-013168 ..... N91-29644 #
DE91-013190 ..... N91-29152 #
DE91-013195 ..... N91-29612 #
DE91-013208 ..... N91-29328 #
DE91-013231 ..... N91-29200 #
DE91-013244 ..... N91-29946 #
DE91-013247 ..... N91-29850 #
DE91-013277 ..... N91-29441 #
DE91-013296 ..... N91-29329 #
DE91-013305 ..... N91-29849 #
DE91-013317 ..... N91-29538 #
DE91-013335 ..... N91-29681 #
DE91-013343 ..... N91-29944 #
DE91-013417 ..... N91-29653 #
DE91-013500 ..... N91-29560 #
DE91-013522 ..... N91-30043 #
DE91-013572 ..... N91-29402 #
DE91-013588 ..... N91-29916 #
DE91-013592 ..... N91-29947 #
DE91-013600 ..... N91-29294 #
DE91-013636 ..... N91-29948 #
DE91-013637 ..... N91-29949 #
DE91-013639 ..... N91-29905 #
DE91-013646 ..... N91-29492 #
DE91-013722 ..... N91-29333 #
DE91-013755 ..... N91-29264 #
DE91-013901 ..... N91-29715 #
DE91-013908 ..... N91-29866 #
DE91-013969 ..... N91-29815 #
DE91-014099 ..... N91-29299 #
DE91-014110 ..... N91-29561 #
DE91-014174 ..... N91-29369 #
DE91-014253 ..... N91-29265 #
DE91-014330 ..... N91-29631 #
DE91-014332 ..... N91-29442 #
DE91-014355 ..... N91-29897 #
DE91-014384 ..... N91-29980 #
DE91-014385 ..... N91-29978 #
DE91-014389 ..... N91-29645 #
DE91-014401 ..... N91-29403 #
DE91-014457 ..... N91-29984 #
DE91-014461 ..... N91-29500 #
DE91-014462 ..... N91-29501 #
DE91-014463 ..... N91-29502 #
DE91-014464 ..... N91-29300 #
DE91-014465 ..... N91-29503 #
DE91-014469 ..... N91-29979 #
DE91-014519 ..... N91-29867 #
DE91-014526 ..... N91-29795 #
DE91-014529 ..... N91-29504 #
DE91-014537 ..... N91-29266 #
DE91-014539 ..... N91-30024 #
DE91-014562 ..... N91-29851 #
DE91-014574 ..... N91-29301 #
DE91-014578 ..... N91-29321 #
DE91-014593 ..... N91-30032 #
DE91-014598 ..... N91-30040 #
DE91-014601 ..... N91-29951 #
DE91-014602 ..... N91-29562 #
DE91-014604 ..... N91-29443 #
DE91-014610 ..... N91-29540 #
DE91-014611 ..... N91-29477 #
DE91-014617 ..... N91-29444 #
DE91-014618 ..... N91-29286 #
DE91-014650 ..... N91-29541 #
DE91-014651 ..... N91-29619 #
DE91-014655 ..... N91-29655 #
DE91-014657 ..... N91-29203 #
DE91-014661 ..... N91-29151 #
DE91-014662 ..... N91-29483 #
DE91-014664 ..... N91-29445 #
DE91-014666 ..... N91-29910 #

DE91-014668 ..... N91-29478 #
DE91-014669 ..... N91-29479 #
DE91-014670 ..... N91-29446 #
DE91-014683 ..... N91-29861 #
DE91-014695 ..... N91-29302 #
DE91-014696 ..... N91-29406 #
DE91-014699 ..... N91-29985 #
DE91-014701 ..... N91-29447 #
DE91-014710 ..... N91-29204 #
DE91-014728 ..... N91-29907 #
DE91-014736 ..... N91-29952 #
DE91-014739 ..... N91-29281 #
DE91-014741 ..... N91-29505 #
DE91-014742 ..... N91-29953 #
DE91-014744 ..... N91-29954 #
DE91-014748 ..... N91-29632 #
DE91-014749 ..... N91-29542 #
DE91-014751 ..... N91-29334 #
DE91-014758 ..... N91-29335 #
DE91-014765 ..... N91-29955 #
DE91-014768 ..... N91-29480 #
DE91-014770 ..... N91-29986 #
DE91-014773 ..... N91-29563 #
DE91-014792 ..... N91-29859 #
DE91-014803 ..... N91-29232 #
DE91-014811 ..... N91-29287 #
DE91-014813 ..... N91-29711 #
DE91-014826 ..... N91-30025 #
DE91-014831 ..... N91-29557 #
DE91-014844 ..... N91-30026 #
DE91-014856 ..... N91-29295 #
DE91-014862 ..... N91-29319 #
DE91-014863 ..... N91-30065 #
DE91-014866 ..... N91-29868 #
DE91-014875 ..... N91-29746 #
DE91-014895 ..... N91-29303 #
DE91-014896 ..... N91-29213* #
DE91-014897 ..... N91-29898 #
DE91-014898 ..... N91-30046 #
DE91-014900 ..... N91-29320 #
DE91-014902 ..... N91-29304 #
DE91-014904 ..... N91-29484 #
DE91-014915 ..... N91-29906 #
DE91-014916 ..... N91-29282 #
DE91-014922 ..... N91-29956 #
DE91-014942 ..... N91-29664 #
DE91-014949 ..... N91-29682 #
DE91-014950 ..... N91-29267 #
DE91-014955 ..... N91-29296 #
DE91-014959 ..... N91-29370 #
DE91-014966 ..... N91-29793 #
DE91-014967 ..... N91-29796 #
DE91-014981 ..... N91-29305 #
DE91-014984 ..... N91-29306 #
DE91-014988 ..... N91-29322 #
DE91-014989 ..... N91-30039 #
DE91-014990 ..... N91-30033 #
DE91-014996 ..... N91-29606 #
DE91-015051 ..... N91-29371 #
DE91-015052 ..... N91-29936 #
DE91-015055 ..... N91-29908 #
DE91-015061 ..... N91-29372 #
DE91-015094 ..... N91-29192 #
DE91-015104 ..... N91-29816 #
DE91-015109 ..... N91-29375 #
DE91-015114 ..... N91-29528 #
DE91-015129 ..... N91-29407 #
DE91-015130 ..... N91-29408 #
DE91-015136 ..... N91-29899 #
DE91-015137 ..... N91-29987 #
DE91-015141 ..... N91-29962 #
DE91-015142 ..... N91-29506 #
DE91-015144 ..... N91-29654 #
DE91-015145 ..... N91-29957 #
DE91-015171 ..... N91-29323 #
DE91-015175 ..... N91-29801 #
DE91-015176 ..... N91-29869 #
DE91-015177 ..... N91-29911 #
DE91-015180 ..... N91-29620 #
DE91-015181 ..... N91-29578 #
DE91-015183 ..... N91-29958 #
DE91-015188 ..... N91-29656 #
DE91-015193 ..... N91-29988 #
DE91-015194 ..... N91-29989 #
DE91-015201 ..... N91-29485 #
DE91-015204 ..... N91-29990 #
DE91-015207 ..... N91-29991 #
DE91-015210 ..... N91-29382 #
DE91-015214 ..... N91-29870 #
DE91-015218 ..... N91-29959 #
DE91-015219 ..... N91-29960 #
DE91-015223 ..... N91-29529 #
DE91-015239 ..... N91-29712 #
DE91-015254 ..... N91-29992 #
DE91-015273 ..... N91-29993 #
DE91-015296 ..... N91-30034 #
DE91-015300 ..... N91-30035 #
DE91-015307 ..... N91-29963 #
DE91-015308 ..... N91-29307 #
DE91-015312 ..... N91-29373 #
DE91-015320 ..... N91-29579 #
DE91-015322 ..... N91-29324 #
DE91-015323 ..... N91-29325 #
DE91-015324 ..... N91-29374 #
DE91-015327 ..... N91-29481 #
DE91-015329 ..... N91-29994 #
DE91-015333 ..... N91-29409 #
DE91-015334 ..... N91-29995 #
DE91-015357 ..... N91-29582 #
DE91-015359 ..... N91-29892 #
DE91-015368 ..... N91-29871 #
DE91-015385 ..... N91-29580 #
DE91-015393 ..... N91-29872 #
DE91-015428 ..... N91-29893 #
DE91-015429 ..... N91-29376 #
DE91-015431 ..... N91-29433 #
DE91-015439 ..... N91-30058 #
DE91-015441 ..... N91-29747 #
DE91-015449 ..... N91-30066 #
DE91-015452 ..... N91-29283 #
DE91-015454 ..... N91-29900 #
DE91-015461 ..... N91-29410 #
DE91-015480 ..... N91-29665 #
DE91-015484 ..... N91-29873 #
DE91-015485 ..... N91-29252 #
DE91-015527 ..... N91-30027 #
DE91-015528 ..... N91-29666 #
DE91-015531 ..... N91-29377 #
DE91-015533 ..... N91-29809 #
DE91-015534 ..... N91-29695 #
DE91-015536 ..... N91-29667 #
DE91-015544 ..... N91-30028 #
DE91-015550 ..... N91-29284 #
DE91-015552 ..... N91-29581 #
DE91-015553 ..... N91-30029 #
DE91-015554 ..... N91-29696 #
DE91-015557 ..... N91-29336 #
DE91-015558 ..... N91-30030 #
DE91-015563 ..... N91-30057 #
DE91-015564 ..... N91-29208 #
DE91-015566 ..... N91-29894 #
DE91-015571 ..... N91-30031 #
DE91-015586 ..... N91-29966 #
DE91-015617 ..... N91-29909 #
DE91-015638 ..... N91-29810 #
DE91-015639 ..... N91-30036 #
DE91-015648 ..... N91-29794 #
DE91-015656 ..... N91-29964 #
DE91-015671 ..... N91-29482 #
DE91-015676 ..... N91-29583 #
DE91-015678 ..... N91-29530 #
DE91-015679 ..... N91-29486 #
DE91-015698 ..... N91-29967 #
DE91-015700 ..... N91-29386 #
DE91-015709 ..... N91-29549 #
DE91-015711 ..... N91-29434 #
DE91-015714 ..... N91-29860 #
DE91-015715 ..... N91-29378 #
DE91-015720 ..... N91-29392 #
DE91-015722 ..... N91-29968 #
DE91-015734 ..... N91-29634 #
DE91-015737 ..... N91-29912 #
DE91-015740 ..... N91-29901 #
DE91-015742 ..... N91-29708 #
DE91-015745 ..... N91-30062 #
DE91-015747 ..... N91-29633 #
DE91-015749 ..... N91-29393 #
DE91-015756 ..... N91-29797 #
DE91-015765 ..... N91-29548 #
DE91-015781 ..... N91-29902 #
DE91-015784 ..... N91-29798 #
DE91-015785 ..... N91-29387 #
DE91-015786 ..... N91-29903 #
DE91-015792 ..... N91-29713 #
DE91-015793 ..... N91-29435 #
DE91-015794 ..... N91-30041 #
DE91-015795 ..... N91-30044 #
DE91-015833 ..... N91-29695 #
DE91-015848 ..... N91-30037 #
DE91-015902 ..... N91-29487 #
DE91-015907 ..... N91-29965 #
DE91-015908 ..... N91-29896 #
DE91-015914 ..... N91-29531 #
DE91-015941 ..... N91-29913 #
DE91-016059 ..... N91-29379 #
DE91-016267 ..... N91-30038 #
DE91-617572 ..... N91-29813 #
DE91-617583 ..... N91-29855 #
DE91-617788 ..... N91-29976 #
DE91-618099 ..... N91-29977 #

DNA-TR-90-78 ..... N91-29417 #
DNA-TR-90-115 ..... N91-29679 #

DODA-AR-006-128 ..... N91-29185 #
DODA-AR-006-362 ..... N91-29326 #
DODA-AR-006-481 ..... N91-29837 #
DODA-AR-006-599 ..... N91-29226 #

DOE/AL-31881/T2 ..... N91-29381 #
DOE/AL-43058/T1 ..... N91-29255 #

DOE/CE-15440/T3 ..... N91-29529 #
DOE/CE-40878/1 ..... N91-29330 #
DOE/CE-90048/1 ..... N91-29437 #

DOE/DP-20154/T1 ..... N91-29945 #
DOE/DP-40200/146 ..... N91-29556 #

DOE/EA-0507 ..... N91-29152 #

DOE/ER-0457T ..... N91-29532 #
DOE/ER-0501T ..... N91-29665 #
DOE/ER-00881/T2 ..... N91-29912 #
DOE/ER-02271/T5 ..... N91-29904 #
DOE/ER-02271/114 ..... N91-29905 #
DOE/ER-03077/284 ..... N91-29795 #
DOE/ER-03130/821 ..... N91-29907 #
DOE/ER-03230/T10 ..... N91-29892 #
DOE/ER-13363/T2 ..... N91-29867 #
DOE/ER-13576/1 ..... N91-29936 #
DOE/ER-13614/4 ..... N91-29712 #
DOE/ER-13615/5 ..... N91-29283 #
DOE/ER-13902/3 ..... N91-30041 #
DOE/ER-13937/3 ..... N91-29555 #
DOE/ER-14005/T1 ..... N91-29713 #
DOE/ER-14012/2 ..... N91-29582 #
DOE/ER-14031/3 ..... N91-29711 #
DOE/ER-14043/2 ..... N91-29492 #
DOE/ER-14150/1 ..... N91-29287 #
DOE/ER-14159/1 ..... N91-29872 #
DOE/ER-25019/21 ..... N91-29715 #
DOE/ER-40085/23 ..... N91-29908 #
DOE/ER-40317/5 ..... N91-30066 #
DOE/ER-40415/18 ..... N91-29901 #
DOE/ER-40427/11-N91 ..... N91-29866 #
DOE/ER-40467/6 ..... N91-29897 #
DOE/ER-45131/9 ..... N91-29504 #
DOE/ER-45147/6 ..... N91-30024 #
DOE/ER-45200/7 ..... N91-29980 #
DOE/ER-45219/5 ..... N91-29978 #
DOE/ER-45251/3 ..... N91-29371 #
DOE/ER-45279/T2 ..... N91-29372 #
DOE/ER-45286/4 ..... N91-29329 #
DOE/ER-45306/5 ..... N91-29333 #
DOE/ER-45333/1 ..... N91-29900 #
DOE/ER-45357/5 ..... N91-29266 #
DOE/ER-45365/2 ..... N91-29293 #
DOE/ER-45416/1 ..... N91-30025 #
DOE/ER-53175/6 ..... N91-29943 #
DOE/ER-53198/163 ..... N91-29949 #
DOE/ER-53198/171 ..... N91-29948 #
DOE/ER-53198/173 ..... N91-29960 #
DOE/ER-53198/174 ..... N91-29959 #
DOE/ER-53212/152 ..... N91-29940 #
DOE/ER-53212/177 ..... N91-29966 #
DOE/ER-53222/101 ..... N91-29938 #
DOE/ER-53236/11 ..... N91-29403 #
DOE/ER-53263/16 ..... N91-29964 #
DOE/ER-60983/2 ..... N91-29708 #
DOE/ER-75498/T2 ..... N91-30044 #

DOE/ET-53088/7 ..... N91-29956 #
DOE/ET-53088/489 ..... N91-29896 #
DOE/ET-53088/500 ..... N91-29965 #
DOE/ET-53088/504 ..... N91-29913 #

DOE/ID-12689/1-VOL-1-ADD ..... N91-29436 #
DOE/ID-12735/T15 ..... N91-29335 #

DOE/NASA/16310-16 ..... N91-29298* #

DOE/NE-37963/15 ..... N91-29319 #

DOE/NV-10652/T1 ..... N91-29941 #

DOE/PC-80527/T2 ..... N91-29257 #
DOE/PC-90533/16 ..... N91-29285 #

DOE/PETC-TR/91/3 ..... N91-29496 #
DOE/PETC-TR/91/7 ..... N91-29491 #

DOT/FAA/AM-91/6 ..... N91-29153 #
DOT/FAA/AM-91/7 ..... N91-29733 #

DOT/FAA/CT-88/8-1-VOL-1 ..... N91-29154 #
DOT/FAA/CT-88/8-2-VOL-2 ..... N91-29155 #
DOT/FAA/CT-88/8-3-VOL-3 ..... N91-29156 #

DOT/FAA/RD-91/16 ..... N91-29198 #

DREO-1073 ..... N91-29418 #

DRIC-BR-301751 ..... N91-29316 #

DTRC/CMLD-90/014 ..... N91-29513 #

E-5957 ..... N91-29250* #
E-6004 ..... N91-29599* #
E-6005 ..... N91-30073* #
E-6244 ..... N91-29525* #
E-6337 ..... N91-29235* #
E-6349 ..... N91-29600* #
E-6359 ..... N91-29221* #
E-6362 ..... N91-29405* #
E-6390 ..... N91-29610* #
E-6419 ..... N91-29229* #
E-6440 ..... N91-29832* #
E-6442 ..... N91-29231* #
E-6452 ..... N91-29188* #
E-6458 ..... N91-29431* #
E-6461 ..... N91-29150* #
E-6463 ..... N91-29228* #
E-6464 ..... N91-29298* #
E-6469 ..... N91-29199* #
E-6471 ..... N91-29230* #
E-6472 ..... N91-29181* #
E-6475 ..... N91-29332* #
E-6478 ..... N91-29187* #
E-6480 ..... N91-29917* #
E-6481 ..... N91-29982* #
E-6490 ..... N91-29404* #
E-6492 ..... N91-29220* #
E-6496 ..... N91-29222* #

ECE-89-1 ..... N91-29398 #

EGG-M-90293 ..... N91-29299 #
EGG-M-90391 ..... N91-29328 #
EGG-M-90520 ..... N91-29369 #

EPA/AA/CTAB-91/01 ..... N91-29602 #

EPA/450/4-91/015 ..... N91-29662 #
EPA/600/D-91/076 ..... N91-29385 #
EPA/600/2-91/015 ..... N91-29526 #

ERA-377 ..... N91-29799 #

ERB-966 ..... N91-29799 #
ERB-1020 ..... N91-29811 #
ERB-1021 ..... N91-29800 #
ERB-1022 ..... N91-29743 #

ERIM-226900-1-T ..... N91-29412 #

ERL-0544-GD ..... N91-29837 #

ESD-PUBL-3642 ..... N91-29664 #

ESD-TR-90-152 ..... N91-30016* #
ESD-TR-91-205 ..... N91-29162 #

ESDP-3656 ..... N91-29682 #

ESMC-TR-91-1 ..... N91-29624 #

ETL-0572 ..... N91-29164 #
ETL-0584 ..... N91-29748 #

FNAL-TM-1742 ..... N91-29816 #

FNAL/C-91/78-A ..... N91-30065 #
FNAL/C-91/144 ..... N91-29408 #
FNAL/C-91/145 ..... N91-29407 #

FSL-5 ..... N91-29693 #

FSU-STATISTICS-M832 ..... N91-29840 #
FSU-STATISTICS-M836 ..... N91-29839 #
FSU-STATISTICS-M840 ..... N91-29838 #

FTD-ID(RS)T-0470-91 ..... N91-29339 #
FTD-ID(RS)T-0533-90 ..... N91-29141 #
FTD-ID(RS)T-0647-90 ..... N91-29182 #
FTD-ID(RS)T-0691-90 ..... N91-29142 #
FTD-ID(RS)T-0720-90 ..... N91-29565 #
FTD-ID(RS)T-0742-90 ..... N91-29564 #
FTD-ID(RS)T-0811-90 ..... N91-29567 #
FTD-ID(RS)T-1058-90 ..... N91-29310 #
FTD-ID(RS)T-1135-90 ..... N91-29566 #

F06-9-1 ..... N91-29224 #

GA-A-20480 ..... N91-29950 #

GA-A-20548 ..... N91-29957 #

GAO/NSIAD-91-154 ..... N91-29854 #

GL-TR-90-0315 ..... N91-29671 #
GL-TR-90-0349 ..... N91-29677 #

GRI-90/0158 ..... N91-29601 #

H-1431 ..... N91-29177* #
H-1741 ..... N91-29194* #
H-1747 ..... N91-29191* #

HDL-PR-91-1 ..... N91-30052 #

HDL-SR-91-1 ..... N91-29752 #

HDL-TR-2195 ..... N91-29471 #

IAR-AN-67 ..... N91-29190 #

IC-90/163 ..... N91-29813 #
IC-90/227 ..... N91-29976 #
IC-90/262 ..... N91-29855 #
IC-90/266 ..... N91-29977 #

ICMA-91-163 ..... N91-29817 #

IDA-P-2432 ..... N91-29660 #
IDA-P-2488 ..... N91-29754 #
IDA-P-2498 ..... N91-29449 #

IDA/HQ-90-35736 ..... N91-29660 #
IDA/HQ-90-36322 ..... N91-29449 #
IDA/HQ-91-37919 ..... N91-29754 #

IFSR-489 ..... N91-29896 #
IFSR-500 ..... N91-29965 #
IFSR-504 ..... N91-29913 #

INPE-5244-PRE/1675 ..... N91-29635 #

IS-M-669 ..... N91-29485 #

IS-T-1414 ..... N91-29939 #
IS-T-1500 ..... N91-29906 #
IS-T-1534 ..... N91-29282 #

ISBN-0-662-56720-X ..... N91-30072 #

ISSN-0169-2690 ..... N91-29776 #
ISSN-0706-568X ..... N91-30071 #
ISSN-0923-1714 ..... N91-29792 #

JPRS-UMS-91-001 ..... N91-29291 #

KAPL-4728 ..... N91-29794 #

KCP-613-4394 ..... N91-29393 #

K91-21U(R) ..... N91-29923 #

LA-UR-91-477 ..... N91-29812 #
LA-UR-91-1439 ..... N91-29915 #
LA-UR-91-1512 ..... N91-30043 #
LA-UR-91-1523 ..... N91-29560 #
LA-UR-91-1595 ..... N91-29200 #
LA-UR-91-1654 ..... N91-29538 #
LA-UR-91-1911 ..... N91-29563 #
LA-UR-91-1919 ..... N91-29986 #
LA-UR-91-1924 ..... N91-29480 #
LA-UR-91-1946 ..... N91-29955 #
LA-UR-91-1954 ..... N91-29334 #
LA-UR-91-1973 ..... N91-29542 #
LA-UR-91-1976 ..... N91-29632 #
LA-UR-91-1983 ..... N91-29954 #
LA-UR-91-1992 ..... N91-29953 #
LA-UR-91-1993 ..... N91-29505 #
LA-UR-91-1995 ..... N91-29281 #
LA-UR-91-2007 ..... N91-29952 #
LA-UR-91-2014 ..... N91-29477 #
LA-UR-91-2020 ..... N91-29540 #
LA-UR-91-2050 ..... N91-29443 #
LA-UR-91-2052 ..... N91-29562 #
LA-UR-91-2054 ..... N91-29951 #
LA-UR-91-2074 ..... N91-30040 #
LA-UR-91-2096 ..... N91-30032 #

LA-12018-MS ..... N91-29579 #
LA-12059-MS ..... N91-29851 #

LBL-28270 ..... N91-29584 #
LBL-28713-ABS ..... N91-29256 #
LBL-29594 ..... N91-29723 #
LBL-30021 ..... N91-29259 #
LBL-30435 ..... N91-29974 #

LBL-30436-ABS ..... N91-29868 #
LBL-30655 ..... N91-29264 #
LBL-30694 ..... N91-30038 #
LBL-30773 ..... N91-29204 #
LBL-30785 ..... N91-29444 #
LBL-30861 ..... N91-29286 #

LRC-91-28 ..... N91-29964 #

LTR-90-SD-011 ..... N91-29647 #

LTR90-009 ..... N91-29677 #

M-664 ..... N91-29318* #
M-666 ..... N91-29209* #

MEMO-INF-90-13 ..... N91-29792 #
MEMO-INF-90-15 ..... N91-30053 #

MEMO-893 ..... N91-29776 #

MIT/LCS/TM-449 ..... N91-29781 #
MIT/LCS/TM-450 ..... N91-29739 #
MIT/LCS/TM-451 ..... N91-29780 #

MIT/LCS/TR-454 ..... N91-29784 #
MIT/LCS/TR-487 ..... N91-30047 #
MIT/LCS/TR-505 ..... N91-29779 #

MITSG-91-13 ..... N91-29630 #

MLM-3691 ..... N91-29382 #

MPL-U-48/91 ..... N91-29680 #

MRL-TN-590 ..... N91-29326 #

MRL-TR-91-15 ..... N91-29290 #

MSC-TFR-2110/1705-VOL-2 ..... N91-29247 #

MSRR-565 ..... N91-29753 #
MSRR-566 ..... N91-29823 #

MTL-TR-91-5-VOL-2 ..... N91-29247 #
MTL-TR-91-7 ..... N91-29921 #
MTL-TR-91-18 ..... N91-30002 #
MTL-TR-91-19 ..... N91-29608 #
MTL-TR-91-21 ..... N91-29358 #
MTL-TR-91-23 ..... N91-29607 #

MTR-11051 ..... N91-29162 #

NAE-AN-57 ..... N91-29394 #

NAE-LTR-FR-105 ..... N91-29160 #
NAE-LTR-FR-106 ..... N91-29158 #
NAE-LTR-FR-107 ..... N91-29651 #
NAE-LTR-FR-108 ..... N91-29139 #
NAE-LTR-FR-109 ..... N91-29189 #
NAE-LTR-FR-110 ..... N91-29388 #
NAE-LTR-FR-113 ..... N91-29169* #
NAE-LTR-FR-114 ..... N91-29159 #

NAE-LTR-LA-310 ..... N91-29642 #
NAE-LTR-LA-312 ..... N91-29195 #

NAE-LTR-ST(CR)-1711 ..... N91-29611 #

NAE-LTR-ST-531 ..... N91-29289 #
NAE-LTR-ST-547 ..... N91-29742 #
NAE-LTR-ST-1695 ..... N91-29236 #
NAE-LTR-ST-1696 ..... N91-29166 #
NAE-LTR-ST-1703 ..... N91-29535 #
NAE-LTR-ST-1706 ..... N91-29165 #
NAE-LTR-ST-1716 ..... N91-29179 #
NAE-LTR-ST-1736 ..... N91-29237 #
NAE-LTR-ST-1737 ..... N91-29604 #
NAE-LTR-ST-1744 ..... N91-29196 #
NAE-LTR-ST-1758 ..... N91-29534 #
NAE-LTR-ST-1771 ..... N91-29288 #
NAE-LTR-ST-1774 ..... N91-29180 #

NAE-LTR-UA-93 ..... N91-29144 #
NAE-LTR-UA-101 ..... N91-29168 #
NAE-LTR-UA-104 ..... N91-29533 #

NAE-ST-557 ..... N91-29744 #
NAE-ST-576 ..... N91-29167 #

NAL-PD-CF-9006 ..... N91-29494 #
NAL-PD-CF-9101 ..... N91-29146 #
NAL-PD-CF-9102 ..... N91-29145 #

NAL-PD-FC-9110 ..... N91-29814 #

NAMRL-MONOGRAPH-42 ..... N91-29719 #

NAMRL-TM-90-2 ..... N91-29728 #

NAMRL-1359 ..... N91-29736 #
NAMRL-1361 ..... N91-29730 #
NAMRL-1362 ..... N91-29729 #

NAS 1.15:4324 ..... N91-29194* #
NAS 1.15:100409 ..... N91-29177* #
NAS 1.15:103547 ..... N91-30061* #
NAS 1.15:103752 ..... N91-30073* #
NAS 1.15:103772 ..... N91-29250* #
NAS 1.15:103822 ..... N91-29210* #
NAS 1.15:104068 ..... N91-29745* #
NAS 1.15:104114 ..... N91-30068* #
NAS 1.15:104131 ..... N91-29239* #
NAS 1.15:104238 ..... N91-29191* #
NAS 1.15:104352 ..... N91-29599* #
NAS 1.15:104489 ..... N91-29235* #
NAS 1.15:104502 ..... N91-29405* #
NAS 1.15:104520 ..... N91-29610* #
NAS 1.15:105033 ..... N91-29201* #
NAS 1.15:105069 ..... N91-30060* #
NAS 1.15:105089 ..... N91-29213* #
NAS 1.15:105140 ..... N91-29525* #
NAS 1.15:105144 ..... N91-29229* #
NAS 1.15:105156 ..... N91-29231* #
NAS 1.15:105163 ..... N91-29188* #
NAS 1.15:105167 ..... N91-29431* #
NAS 1.15:105169 ..... N91-29150* #
NAS 1.15:105170 ..... N91-29228* #
NAS 1.15:105171 ..... N91-29298* #
NAS 1.15:105173 ..... N91-29199* #
NAS 1.15:105175 ..... N91-29230* #
NAS 1.15:105176 ..... N91-29181* #
NAS 1.15:105178 ..... N91-29332* #
NAS 1.15:105180 ..... N91-29187* #
NAS 1.15:105181 ..... N91-29221* #
NAS 1.15:105182 ..... N91-29600* #
NAS 1.15:105184 ..... N91-29982* #
NAS 1.15:105188 ..... N91-29404* #
NAS 1.15:105190 ..... N91-29220* #
NAS 1.15:105195 ..... N91-29222* #
NAS 1.26:4177 ..... N91-29253* #
NAS 1.26:4381 ..... N91-29778* #
NAS 1.26:4389 ..... N91-29935* #
NAS 1.26:178246 ..... N91-29254* #
NAS 1.26:178883 ..... N91-29603* #
NAS 1.26:181850 ..... N91-29176* #
NAS 1.26:183824 ..... N91-29233* #
NAS 1.26:184169 ..... N91-29737* #
NAS 1.26:184170 ..... N91-29865* #
NAS 1.26:184171 ..... N91-29297* #
NAS 1.26:184172 ..... N91-29554* #
NAS 1.26:184175 ..... N91-29488* #
NAS 1.26:186094 ..... N91-29937* #
NAS 1.26:186544 ..... N91-29527* #
NAS 1.26:186550 ..... N91-29219* #
NAS 1.26:187136 ..... N91-29193* #
NAS 1.26:187168 ..... N91-29832* #
NAS 1.26:187173 ..... N91-29147* #
NAS 1.26:187177 ..... N91-29524* #
NAS 1.26:187178 ..... N91-29629* #
NAS 1.26:187188 ..... N91-29917* #
NAS 1.26:187574 ..... N91-29777* #
NAS 1.26:188021 ..... N91-30016* #
NAS 1.26:188724 ..... N91-29212* #
NAS 1.26:188725 ..... N91-29331* #
NAS 1.26:188727 ..... N91-29211* #
NAS 1.26:188729 ..... N91-29636* #
NAS 1.26:188741 ..... N91-29390* #
NAS 1.26:188770 ..... N91-29169* #
NAS 1.26:188793 ..... N91-29769* #
NAS 1.55:10075 ..... N91-29240* #
NAS 1.60:3128 ..... N91-29318* #
NAS 1.60:3139 ..... N91-29209* #
NAS 1.71:GSC-13348-2 ..... N91-29714* #

NASA-CASE-GSC-13348-2 ..... N91-29714* #

NASA-CP-10075 ..... N91-29240* #

NASA-CR-4177 ..... N91-29253* #
NASA-CR-4381 ..... N91-29778* #
NASA-CR-4389 ..... N91-29935* #
NASA-CR-178246 ..... N91-29254* #
NASA-CR-178883 ..... N91-29603* #
NASA-CR-181850 ..... N91-29176* #
NASA-CR-183824 ..... N91-29233* #
NASA-CR-184169 ..... N91-29737* #
NASA-CR-184170 ..... N91-29865* #
NASA-CR-184171 ..... N91-29297* #
NASA-CR-184172 ..... N91-29554* #
NASA-CR-184175 ..... N91-29488* #
NASA-CR-186094 ..... N91-29937* #
NASA-CR-186544 ..... N91-29527* #
NASA-CR-186550 ..... N91-29219* #
NASA-CR-187136 ..... N91-29193* #
NASA-CR-187168 ..... N91-29832* #
NASA-CR-187173 ..... N91-29147* #
NASA-CR-187177 ..... N91-29524* #
NASA-CR-187178 ..... N91-29629* #
NASA-CR-187188 ..... N91-29917* #
NASA-CR-187574 ..... N91-29777* #
NASA-CR-188021 ..... N91-30016* #
NASA-CR-188724 ..... N91-29212* #
NASA-CR-188725 ..... N91-29331* #
NASA-CR-188727 ..... N91-29211* #
NASA-CR-188729 ..... N91-29636* #
NASA-CR-188741 ..... N91-29390* #
NASA-CR-188770 ..... N91-29169* #
NASA-CR-188793 ..... N91-29769* #

NASA-TM-4324 ..... N91-29194* #
NASA-TM-100409 ..... N91-29177* #
NASA-TM-103547 ..... N91-30061* #
NASA-TM-103752 ..... N91-30073* #
NASA-TM-103772 ..... N91-29250* #
NASA-TM-103822 ..... N91-29210* #
NASA-TM-104068 ..... N91-29745* #
NASA-TM-104114 ..... N91-30068* #
NASA-TM-104131 ..... N91-29239* #
NASA-TM-104238 ..... N91-29191* #
NASA-TM-104352 ..... N91-29599* #
NASA-TM-104489 ..... N91-29235* #
NASA-TM-104502 ..... N91-29405* #
NASA-TM-104520 ..... N91-29610* #
NASA-TM-105033 ..... N91-29201* #
NASA-TM-105069 ..... N91-30060* #
NASA-TM-105089 ..... N91-29213* #
NASA-TM-105140 ..... N91-29525* #
NASA-TM-105144 ..... N91-29229* #
NASA-TM-105156 ..... N91-29231* #
NASA-TM-105163 ..... N91-29188* #
NASA-TM-105167 ..... N91-29431* #
NASA-TM-105169 ..... N91-29150* #
NASA-TM-105170 ..... N91-29228* #
NASA-TM-105171 ..... N91-29298* #
NASA-TM-105173 ..... N91-29199* #
NASA-TM-105175 ..... N91-29230* #
NASA-TM-105176 ..... N91-29181* #
NASA-TM-105178 ..... N91-29332* #
NASA-TM-105180 ..... N91-29187* #
NASA-TM-105181 ..... N91-29221* #
NASA-TM-105182 ..... N91-29600* #
NASA-TM-105184 ..... N91-29982* #
NASA-TM-105188 ..... N91-29404* #
NASA-TM-105190 ..... N91-29220* #
NASA-TM-105195 ..... N91-29222* #

NASA-TP-3128 ..... N91-29318* #
NASA-TP-3139 ..... N91-29209* #

NAVSWC-MP-90-409 ..... N91-29672 #

NAVSWC-TR-90-180 ..... N91-29453 #
NAVSWC-TR-90-236 ..... N91-29271 #
NAVSWC-TR-90-418 ..... N91-29807 #

NCEL-TN-1831 ..... N91-29356 #

NDP-035 ..... N91-29682 #
NDP-038 ..... N91-29664 #

NIAR-91-16 ..... N91-29241 #
NIAR-91-18 ..... N91-30042 #
NIAR-91-21 ..... N91-29263 #
NIAR-91-23 ..... N91-29981 #

NIST/SP-500/185 ..... N91-30054 #
NIST/SP-802 ..... N91-29251 #

NIST/TN-1347 ..... N91-29432 #

NISTIR-3965 ..... N91-29527* #
NISTIR-4537 ..... N91-29476 #
NISTIR-4538 ..... N91-29391 #
NISTIR-4553 ..... N91-29858 #

NMRI-90-138 ..... N91-29278 #

NOAA-DR-ERL-PMEL-29 ..... N91-29705 #

NOAA-TR-ERL-443 ..... N91-29693 #

NOARL-PR-90-073-401 ..... N91-29688 #

NOARL-TN-105 ..... N91-29638 #
NOARL-TN-118 ..... N91-29637 #

NOARL-6 ..... N91-29685 #

NOBS-CIRC-176 ..... N91-30069 #

NORDA-246 ..... N91-29704 #

NOSC/TD-2103 ..... N91-29997 #

NOSC/TR-1404 ..... N91-29414 #
NOSC/TR-1413 ..... N91-29819 #

NPS-MA-91-001 ..... N91-29825 #
NPS-MA-001 ..... N91-29825 #

NPS-61-90-006 ..... N91-29767 #

NRC-TR-ENG-004 ..... N91-29178 #

NRC-TTP-02-89 ..... N91-29490 #

NRC-27469 ..... N91-29799 #
NRC-30081 ..... N91-29799 #
NRC-30144 ..... N91-29394 #
NRC-30269 ..... N91-29800 #
NRC-30398 ..... N91-30072 #
NRC-30411 ..... N91-29743 #
NRC-30458 ..... N91-30071 #
NRC-31069 ..... N91-29811 #
NRC-31204 ..... N91-29178 #
NRC-32088 ..... N91-29258 #
NRC-32133 ..... N91-29190 #

NRL-MR-6772 ..... N91-29961 #
NRL-MR-6779 ..... N91-29464 #
NRL-MR-6813 ..... N91-29759 #
NRL-MR-6842 ..... N91-29802 #
NRL-MR-6843 ..... N91-29450 #
NRL-MR-6844 ..... N91-29568 #

NRL-PUB-181-4830 ..... N91-29857 #

NRL-158-4831 ..... N91-29856 #

NSSDC/WDC-A-R/S-89-15 ..... N91-30060* #

NTSB/AAB-90/01 ..... N91-29157 #

NUSC-TD-6998 ..... N91-29782 #
NUSC-TD-8879 ..... N91-29699 #

NUSC-TR-8887 ..... N91-29413 #

NWC-TP-7075 ..... N91-29762 #
NWC-TP-7087 ..... N91-29279 #
NWC-TP-7094 ..... N91-29824 #
NWC-TP-7104 ..... N91-29928 #
NWC-TP-7121 ..... N91-29421 #

ORNL-6653 ..... N91-29296 #

ORNL/CDIAC-40 ..... N91-29682 #
ORNL/CDIAC-42 ..... N91-29664 #

ORNL/ER-0313/9 ..... N91-29942 #

ORNL/M-1389 ..... N91-29942 #

ORNL/SUB-83-43374/2 ..... N91-29401 #
ORNL/SUB-85-27488/05 ..... N91-29305 #

ORNL/TM-11691 ..... N91-29370 #
ORNL/TM-11813 ..... N91-29793 #
ORNL/TM-11836 ..... N91-29796 #

PB90-916901 ..... N91-29157 #
PB91-156828 ..... N91-30056 #
PB91-172940 ..... N91-30055 #
PB91-181701 ..... N91-29693 #
PB91-182360 ..... N91-29661 #
PB91-182881 ..... N91-29385 #
PB91-183582 ..... N91-29706 #
PB91-183608 ..... N91-29707 #
PB91-184077 ..... N91-29694 #
PB91-184135 ..... N91-29705 #
PB91-184713 ..... N91-29630 #
PB91-184754 ..... N91-29476 #
PB91-184994 ..... N91-29601 #
PB91-185116 ..... N91-29251 #
PB91-185124 ..... N91-29432 #
PB91-185132 ..... N91-29722 #
PB91-185421 ..... N91-29776 #
PB91-185447 ..... N91-29792 #
PB91-185454 ..... N91-30053 #
PB91-187567 ..... N91-30054 #
PB91-190959 ..... N91-29526 #
PB91-194423 ..... N91-29858 #
PB91-194464 ..... N91-29527* #
PB91-194480 ..... N91-29391 #

PB91-195818 ..... N91-29641 #
PB91-195941 ..... N91-29602 #
PB91-195958 ..... N91-29662 #

PD-FC-9112 ..... N91-29197 #

PHM-TR-91-06 ..... N91-29424 #
PHM-TR-91-10 ..... N91-29423 #

PL-TR-91-2013 ..... N91-29424 #
PL-TR-91-2039 ..... N91-29423 #
PL-TR-91-2063 ..... N91-29676 #
PL-TR-91-2087 ..... N91-29163 #
PL-TR-91-3009 ..... N91-29224 #
PL-TR-91-3022-ADD ..... N91-29225 #

PME-FM-91-1 ..... N91-29510 #

PNL-SA-17147 ..... N91-29709 #
PNL-SA-17478 ..... N91-29295 #
PNL-SA-18442 ..... N91-29668 #
PNL-SA-18817 ..... N91-29666 #
PNL-SA-18880 ..... N91-29377 #
PNL-SA-19111 ..... N91-29261 #
PNL-SA-19175 ..... N91-29265 #
PNL-SA-19212 ..... N91-30027 #
PNL-SA-19305 ..... N91-29809 #
PNL-SA-19548 ..... N91-29667 #
PNL-SA-19592 ..... N91-29902 #
PNL-SA-19712 ..... N91-29695 #
PNL-SA-19740 ..... N91-29893 #
PNL-SA-19754 ..... N91-29376 #

PNL-7697 ..... N91-29644 #

PSI-2143/TR-1115 ..... N91-29920 #

PSU-ARL-TM-91-120 ..... N91-29143 #

PWA-FR-21413 ..... N91-29309 #

QU-90-1-PT-1 ..... N91-29395 #
QU-90-2-PT-2 ..... N91-29396 #
QU-90-3-PT-3 ..... N91-29397 #

R/D-614B-MS-01 ..... N91-29625 #
R/D-5305-AN-01 ..... N91-29596 #
R/D-6310-MS-01 ..... N91-29927 #
R/D-6636-AN-02 ..... N91-29516 #

R/F-6461-EE-02 ..... N91-30013 #

RAE-TRANS-2189 ..... N91-29493 #

RDA-TR-161603-001 ..... N91-29417 #

REPT-88-1316-PI ..... N91-29544 #
REPT-535 ..... N91-29603* #
REPT-1990:4 ..... N91-30016* #

RFP-4423 ..... N91-29267 #

RL-TR-91-17 ..... N91-29740 #
RL-TR-91-72 ..... N91-30048 #
RL-TR-91-76-VOL-1 ..... N91-29786 #
RL-TR-91-81 ..... N91-29451 #
RL-TR-91-83 ..... N91-29463 #
RL-TR-91-92 ..... N91-29543 #
RL-TR-91-93 ..... N91-29427 #
RL-TR-91-95 ..... N91-30018 #
RL-TR-91-97 ..... N91-29863 #

RSRE-MEMO-4281 ..... N91-29316 #

R9004 ..... N91-29808 #

SAND-88-2554C ..... N91-29985 #
SAND-89-1371 ..... N91-29871 #
SAND-90-0641C ..... N91-29553 #
SAND-90-2172 ..... N91-29440 #
SAND-90-2813C ..... N91-29478 #
SAND-90-2815C ..... N91-29479 #
SAND-90-3000C ..... N91-29303 #
SAND-90-3020C ..... N91-29483 #
SAND-90-3072C ..... N91-29446 #
SAND-90-3073C ..... N91-29445 #
SAND-90-3080C ..... N91-30037 #
SAND-90-3125C ..... N91-29402 #
SAND-90-3150 ..... N91-30045 #
SAND-90-3190C ..... N91-29203 #
SAND-90-7034 ..... N91-29252 #
SAND-91-0031C ..... N91-29320 #
SAND-91-0057C ..... N91-29406 #
SAND-91-0062C ..... N91-29151 #
SAND-91-0064C ..... N91-29537 #
SAND-91-0081C ..... N91-29304 #

SAND-91-0122C ..... N91-29898 #
SAND-91-0146C ..... N91-29619 #
SAND-91-0162C ..... N91-29605 #
SAND-91-0236C ..... N91-29260 #
SAND-91-0237C ..... N91-29484 #
SAND-91-0277 ..... N91-29631 #
SAND-91-0328 ..... N91-29379 #
SAND-91-0370 ..... N91-29442 #
SAND-91-0659C ..... N91-29655 #
SAND-91-0711C ..... N91-29208 #
SAND-91-0725 ..... N91-29541 #
SAND-91-0760C ..... N91-29971 #
SAND-91-0773C ..... N91-29995 #
SAND-91-0799C ..... N91-29447 #
SAND-91-1102C ..... N91-29487 #
SAND-91-1169C ..... N91-29612 #
SAND-91-1197C ..... N91-29302 #
SAND-91-1227C ..... N91-29213* #
SAND-91-1324C ..... N91-29747 #
SAND-91-1364C ..... N91-29910 #
SAND-91-1370C ..... N91-30046 #
SAND-91-1514C ..... N91-29433 #
SAND-91-1565C ..... N91-29409 #
SAND-91-1570C ..... N91-30058 #
SAND-91-1581C ..... N91-30057 #
SAND-91-1589C ..... N91-29386 #
SAND-91-1667C ..... N91-29549 #
SAND-91-7065 ..... N91-29557 #
SAND-91-8213 ..... N91-29292 #

SC71004.FR ..... N91-29426 #

SERI-TP-250-4256 ..... N91-29649 #

SERI/TP-214-4409 ..... N91-29983 #
SERI/TP-257-3757 ..... N91-29643 #
SERI/TP-257-4366 ..... N91-29646 #
SERI/TP-257-4400 ..... N91-29650 #
SERI/TP-257-4418 ..... N91-29663 #

SLCET-TR-91-10 ..... N91-29659 #
SLCET-TR-91-15 ..... N91-29457 #
SLCET-TR-91-17 ..... N91-29456 #

SPARTA-LTR91-009 ..... N91-29924 #

SR-2 ..... N91-29424 #
SR-4 ..... N91-29671 #

SRS/STD-PR-535/11 ..... N91-29603* #

SR90-R-5357 ..... N91-29601 #

SSCL-452 ..... N91-29410 #
SSCL-464 ..... N91-29746 #

SSD-TR-90-49 ..... N91-29750 #
SSD-TR-91-15 ..... N91-29227 #

SSI-TR-176 ..... N91-29671 #

SU-GL-4840 ..... N91-29472 #
SU-GL-4841 ..... N91-29461 #

SU-RL-TR-91-76-VOL-2 ..... N91-29787 #
SU-RL-TR-91-76-VOL-3 ..... N91-29788 #
SU-RL-TR-91-76-VOL-4 ..... N91-29789 #

SU-SLAC-PUB-5559 ..... N91-29441 #
SU-SLAC-PUB-5598 ..... N91-29873 #

SU-SOL-91-2 ..... N91-29773 #
SU-SOL-91-3 ..... N91-29756 #

SU-TR-26 ..... N91-29831 #
SU-TR-443 ..... N91-29835 #

SWAP001-AC ..... N91-29452 #

TIC-864 ..... N91-29679 #

TR-GD-016 ..... N91-29258 #

TR-2 ..... N91-29569 #
TR-4 ..... N91-29462 #
TR-10 ..... N91-29875 #
TR-12 ..... N91-29338 #
TR-12 ..... N91-29876 #
TR-14 ..... N91-29996 #
TR-17 ..... N91-29357 #
TR-23 ..... N91-29877 #
TR-29 ..... N91-29269 #
TR-31 ..... N91-29249 #
TR-31 ..... N91-29362 #
TR-43 ..... N91-29273 #
TR-70 ..... N91-29314 #

TR-71 ..... N91-29888 #
TR-90-251-AFOSR ..... N91-29840 #
TR-90-256-AFOSR ..... N91-29839 #
TR-91-6-70 ..... N91-29576 #
TR-91-7 ..... N91-29701 #
TR-91-257-AFOSR ..... N91-29838 #
TR-98 ..... N91-29879 #
TR-99 ..... N91-29878 #
TR-101 ..... N91-29880 #
TR-102 ..... N91-29883 #
TR-103 ..... N91-29272 #
TR-104 ..... N91-29455 #
TR-105 ..... N91-29882 #
TR-106 ..... N91-29884 #
TR-107 ..... N91-30004 #
TR-0090(5920-07)-02 ..... N91-29750 #
TR-0091(6464-05)-1 ..... N91-29227 #

UCB/R/91/A1072 ..... N91-29317 #

UCID-21718 ..... N91-29551 #
UCID-21719 ..... N91-29550 #
UCID-21956 ..... N91-29848 #

UCRL-CR-103900 ..... N91-29552 #
UCRL-CR-107094 ..... N91-29916 #
UCRL-CR-107905 ..... N91-29548 #

UCRL-ID-105574 ..... N91-30062 #
UCRL-ID-106488 ..... N91-29561 #
UCRL-ID-107239 ..... N91-29192 #
UCRL-ID-107610 ..... N91-29633 #

UCRL-JC-104237 ..... N91-29559 #
UCRL-JC-104425-REV-1 ..... N91-29946 #
UCRL-JC-104515 ..... N91-29387 #
UCRL-JC-105183-REV-1 ..... N91-29489 #
UCRL-JC-105249 ..... N91-29435 #
UCRL-JC-105271-REV-1 ..... N91-29652 #
UCRL-JC-105487 ..... N91-29306 #
UCRL-JC-105558 ..... N91-29578 #
UCRL-JC-105566 ..... N91-29911 #
UCRL-JC-105604 ..... N91-29583 #
UCRL-JC-105835 ..... N91-30035 #
UCRL-JC-105836 ..... N91-30034 #
UCRL-JC-105843 ..... N91-29506 #
UCRL-JC-106130 ..... N91-29620 #
UCRL-JC-106375 ..... N91-29322 #
UCRL-JC-106498 ..... N91-29849 #
UCRL-JC-106546 ..... N91-30033 #
UCRL-JC-106765 ..... N91-29972 #
UCRL-JC-106819 ..... N91-29850 #
UCRL-JC-106908 ..... N91-29528 #
UCRL-JC-106950-REV-1 ..... N91-30039 #
UCRL-JC-107067 ..... N91-29869 #
UCRL-JC-107194 ..... N91-29958 #
UCRL-JC-107409 ..... N91-29530 #
UCRL-JC-107453 ..... N91-29798 #
UCRL-JC-107505 ..... N91-29899 #
UCRL-JC-107536 ..... N91-29654 #
UCRL-JC-107611 ..... N91-29903 #
UCRL-JC-107684 ..... N91-29962 #
UCRL-JC-107735 ..... N91-29967 #
UCRL-JC-107890 ..... N91-29486 #

UCRL-MA-105413 ..... N91-29634 #

UCRL-102524 ..... N91-29914
UCRL-102563 ..... N91-29969 #

UILU-ENG-91-1231 ..... N91-29790 #
UILU-ENG-91-2232 ..... N91-29769* #

UMTRI-91-13 ..... N91-29722 #

US-PATENT-APPL-SN-370234 ..... N91-29399
US-PATENT-APPL-SN-518619 ..... N91-29149 #
US-PATENT-APPL-SN-527966 ..... N91-29934 #
US-PATENT-APPL-SN-539954 ..... N91-29439
US-PATENT-APPL-SN-590182 ..... N91-29598 #
US-PATENT-APPL-SN-591924 ..... N91-29438 #
US-PATENT-APPL-SN-608764 ..... N91-29933 #
US-PATENT-APPL-SN-632707 ..... N91-29523 #
US-PATENT-APPL-SN-648696 ..... N91-29430 #
US-PATENT-APPL-SN-652156 ..... N91-29475 #
US-PATENT-APPL-SN-676669 ..... N91-29400 #
US-PATENT-APPL-SN-725111 ..... N91-29714* #

US-PATENT-CLASS-343-15 ..... N91-29399
US-PATENT-CLASS-439-100 ..... N91-29439

US-PATENT-4,499-468 ..... N91-29399
US-PATENT-5,007,847 ..... N91-29439

USAARL-91-15 ..... N91-29735 #

USARIEM-T9-91 ..... N91-29710 #

USARIEM-12-91 ..... N91-29716 #

USGS/G-1490 ..... N91-29641 #

UTRC/R89-957707 ..... N91-29508 #
UTRC/R90-957663-1 ..... N91-29183 #

UW-CMRG-R-90-101-VOL-2 ..... N91-29247 #

UW-CPTC-91-4 ..... N91-29944 #

WHC-SA-0986 ..... N91-29861 #

WHOI-90-24 ..... N91-29697 #
WHOI-91-03 ..... N91-30070 #

WL-TR-91-2019 ..... N91-29881 #
WL-TR-91-2064 ..... N91-29920 #
WL-TR-91-3007 ..... N91-29808 #
WL-TR-91-3039 ..... N91-29148 #
WL-TR-91-4041 ..... N91-29242 #
WL-TR-91-4048 ..... N91-29546 #
WL-TR-91-5018 ..... N91-29741 #

WP-1991-18 ..... N91-29753 #
WP-1991-21 ..... N91-29823 #

WRDC-TM-90-337-FIBE ..... N91-29171 #

WRDC-TR-90-2065 ..... N91-29183 #
WRDC-TR-90-3080 ..... N91-29806 #
WRDC-TR-90-4125 ..... N91-29309 #

WSU/DC/91/TR-53 ..... N91-29886 #

Appendix

NASA SCIENTIFIC AND TECHNICAL INFORMATION PROGRAM PRODUCTS AND SERVICES

The NASA Scientific and Technical Information (STI) Program provides for the collection and announcement of aerospace-related reports and literature obtained worldwide through agreements and exchanges. The result of the collection is the comprehensive NASA STI Database that covers aeronautics, space, and supporting disciplines.

The STI Database, documents generated or obtained by NASA, and products and services derived from or supporting the database are made available to the NASA research community and to the public. Descriptions and sources of these items are presented in the following pages.

Scientific and Technical Aerospace Reports (*STAR*) is an abstract journal, listing citations with abstracts for aerospace-related reports obtained from worldwide sources. *STAR* is issued on the 8th and 23rd of each month and announces current documents that have been entered into the NASA STI Database during the previous two weeks. The reports are of the following types:

- NASA, NASA contractor, and NASA grantee reports;
- Reports issued by other U.S. Government agencies, domestic and foreign institutions, universities, and private firms;
- Translations in report form;
- NASA-owned patents and patent applications;
- Other U.S. Government agency and foreign patents and patent applications;
- Domestic and foreign dissertations and theses.

Journal, book, and conference literature, journal translations, and certain foreign dissertations having the same subject scope as *STAR* are announced in a companion journal, *International Aerospace Abstracts* (*IAA*). *IAA* is issued on the 1st and 15th of each month and is available from the American Institute of Aeronautics and Astronautics, Technical Information Service, 555 West 57th Street, 12th Floor, New York, NY 10019.

ELIGIBILITY AND REGISTRATION FOR NASA STI PRODUCTS AND SERVICES

Organizations of the type listed below that have registered with NASA can receive products and services.

- NASA offices and installations, contractors, subcontractors, grantees, and consultants;
- Other U.S. Government agencies and their contractors;
- Libraries in the United States that have arrangements with NASA to maintain collections of NASA documents for public reference;
- Other organizations in the United States having a need for NASA documents in work related to aeronautics and space research;
- Organizations abroad that have established reciprocal documents exchange arrangements with NASA.

Only the central service points or central points of document acquisition and control within qualified organizations are eligible to register for NASA STI products and services. Domestic organizations that may be eligible to receive various classes of NASA publications and services should address their requests for registration or further information to:

NASA Center for AeroSpace Information
ATTN: Registration Services
P.O. Box 8757
BWI Airport, MD 21240
301-621-0153

Organizations abroad should direct requests to:

National Aeronautics and Space Administration
Director, Scientific and Technical Information Program
Code NTT
Washington, DC 20546
USA
703-271-5640

SUBJECT SCOPE

The subject scope of *STAR* and *IAA* includes all aspects of aeronautics and space research and development, supporting basic and applied research, and applications. Aerospace aspects of Earth resources, energy development, conservation, oceanography, environmental protection, urban transportation, and other topics of high national priority are also covered.

HOW TO USE *STAR* SUBJECT CATEGORIES

Abstracts in *STAR* are categorized by 10 major subject divisions that are divided further into 76 specific subject categories. The subject divisions and categories are listed in the Table of Contents together with a note for each that defines its scope and provides any cross-references. For example:

16 SPACE TRANSPORTATION
Includes passenger and cargo space transportation, e.g., shuttle operations; and space rescue techniques. For related information see also *03 Air Transportation and Safety* and *18 Spacecraft Design, Testing and Performance.* For space suits see *54 Man/System Technology and Life Support.*

CROSS-REFERENCES

Individual *STAR* abstracts are not ordinarily cross-referenced, except for certain conference reports or book translations that have had separate abstracts written for their component papers or chapters. Citations and abstracts of the components follow immediately after those of the parent document. When the subject content of a component differs sufficiently from the general content of the parent, a cross-reference citation also is printed at the end of the category to which it normally would have been assigned if it were independent.

DOCUMENTS ON MICROFICHE

Documents available on microfiche are designated by a pound sign (#) following the accession number.

LIMITED REPRODUCIBILITY

A note of limited reproducibility appears in the citation, if there are factors affecting the reproducibility of more than 20% of the document. These factors include faint or broken type, color photographs, black and white photographs, foldouts, dot matrix print, or some other factor that limits the reproducibility of the document. This notation also appears on the microfiche header with the specific factor checked off on a list visible in the second frame.

COLOR COPIES

An increasing number of NASA scientific and technical reports are being produced with color graphs, charts, illustrations, and photographs. An indication that a document has color pages follows the source and pricing (SAP) information in the *STAR* citation.

Registered users of the NASA Scientific and Technical Information Program will receive ordered documents with color at no additional cost, as long as stock copies of the document are available. Otherwise, an additional fee of $2.00 per color page will be charged. The NASA Center for AeroSpace Information staff will contact registered users to determine individual user's needs.

NASA PATENTS AND PATENT APPLICATIONS

Patents and patent applications owned by NASA are announced in *STAR* under appropriate subject categories and are referenced in the *STAR* indexes. In the Report/Accession Number Index, patents are indexed by the NASA Case Number, and the U.S. Patent Class. Patent applications are indexed by the NASA Case Number and the U.S. Patent Application Serial Number.

Printed copies of patents (which are not microfiched) are available for purchase from the U.S. Patent and Trademark Office.

NASA patent application specifications are sold in both paper copy and microfiche by the National Technical Information Service (NTIS). The US-Patent-Appl-SN-number should be used in ordering either paper copy or microfiche from NTIS.

When ordering patents, the U.S. Patent Number should be used, and payment must be remitted in advance, by money order or check payable to the Commissioner of Patents and Trademarks. Prepaid purchase coupons for ordering are also available from the U.S. Patent and Trademark Office.

The patents and patent applications announced in *STAR* are owned by NASA and are available for royalty-free licensing. Requests for licensing terms and further information should be addressed to:

National Aeronautics and Space Administration
Associate General Counsel for Intellectual Property
Code GP
Washington, DC 20546

SOURCES FOR DOCUMENTS

One or more sources from which a document announced in *STAR* is available to the public is given in each citation. The most commonly indicated sources and their acronyms or abbreviations are listed on page A-6. If the publication is available from a source other than those listed, the publisher and address will be displayed on the availability line or in combination with the corporate source line.

Avail: NTIS. Sold by the National Technical Information Service. Prices for hard copy (HC) and microfiche (MF) are indicated by a price code following the letters HC or MF in the *STAR* citation. Current values for the price codes are given in the tables on page A-7.

Initially distributed microfiche under the NTIS SRIM (Selected Research in Microfiche) is available at greatly reduced unit prices. For this service and for information concerning subscription to NASA printed reports, consult the NTIS Subscription Section, Springfield, VA 22161.

NOTE ON ORDERING DOCUMENTS: When ordering NASA publications (those followed by the * symbol), use the N accession number. NASA patent applications (only the specifications are offered) should be ordered by the US-Patent-Appl-SN number. Non-NASA publications (no asterisk) should be ordered by the AD, PB, or other *report number* shown on the last line of the citation, not by the N accession number. It is also advisable to cite the title and other bibliographic identification.

Avail: SOD (or GPO). Sold by the Superintendent of Documents, U.S. Government Printing Office, in hard copy. The current price and order number are given following the availability line. (NTIS will fill microfiche requests, as indicated above, for those documents identified by a # symbol.)

Avail: BLL (formerly NLL): British Library Lending Division, Boston Spa, Wetherby, Yorkshire, England. Photocopies available from this organization at the price shown. (If none is given, address inquiry to the BLL.)

Avail: DOE Depository Libraries. Organizations in U.S. cities and abroad that maintain collections of Department of Energy reports, usually in microfiche form, are listed in *Energy Research Abstracts.* Services available from the DOE and its depositories are described in a booklet, *DOE Technical Information Center - Its Functions and Services* (TID-4660), which may be obtained without charge from the DOE Technical Information Center.

Avail: ESDU. Pricing information on specific data, computer programs, and details on Engineering Sciences Data Unit (ESDU) topic categories can be obtained from ESDU International Ltd. Requesters in North America should use the Virginia address while all other requesters should use the London address, both of which are on page A-6.

Avail: Fachinformationszentrum, Karlsruhe. Sold by the Fachinformationszentrum Energie, Physik, Mathematik GMBH, Eggenstein Leopoldshafen, Federal Republic of Germany, at the price shown in deutschmarks (DM).

Avail: HMSO. Publications of Her Majesty's Stationery Office are sold in the U.S. by Pendragon House, Inc. (PHI), Redwood City, CA. The U.S. price (including a service and mailing charge) is given, or a conversion table may be obtained from PHI.

Avail: NASA Public Document Rooms. Documents so indicated may be examined at or purchased from the National Aeronautics and Space Administration, Public Documents Room (Room 126), 600 Independence Ave., S.W., Washington, DC 20546, or public document rooms located at NASA installations, and the NASA Pasadena Office at the Jet Propulsion Laboratory.

Avail: Univ. Microfilms. Documents so indicated are dissertations selected from *Dissertation Abstracts* and are sold by University Microfilms as xerographic copy (HC) and microfilm. All requests should cite the author and the Order Number as they appear in the citation.

Avail: US Patent and Trademark Office. Sold by Commissioner of Patents and Trademarks, U.S. Patent and Trademark Office, at the standard price of $1.50 each, postage free. (See discussion of NASA patents and patent applications below.)

Avail: (US Sales Only). These foreign documents are available to users within the United States from the National Technical Information Service (NTIS). They are available to users outside the United States through the International Nuclear Information Service (INIS) representative in their country, or by applying directly to the issuing organization.

Avail: USGS. Originals of many reports from the U.S. Geological Survey, which may contain color illustrations, or otherwise may not have the quality of illustrations preserved in the microfiche or facsimile reproduction, may be examined by the public at the libraries of the USGS field offices whose addresses are listed on page A-6. The libraries may be queried concerning the availability of specific documents and the possible utilization of local copying services, such as color reproduction.

Avail: Issuing Activity, or Corporate Author, or no indication of availability. Inquiries as to the availability of these documents should be addressed to the organization shown in the citation as the corporate author of the document.

FEDERAL DEPOSITORY LIBRARIES: To provide the general public with greater access to U.S. Government publications, Congress established the Federal Depository Library Program under the Government Printing Office (GPO), with 52 regional depositories responsible for permanent retention of material, inter-library loan, and reference services. (These libraries are not sales outlets.) At least one copy of nearly every NASA and NASA-sponsored publication, either in printed or microfiche format, is received and retained by the 52 regional depositories. A list of the regional GPO libraries, appears on page A-8. A local library can contact a regional depository library to help locate specific reports, or direct contact may be made by an individual.

PUBLIC COLLECTION OF NASA DOCUMENTS

An extensive collection of NASA and NASA-sponsored publications is maintianed by the British Library Lending Divison, Boston Spa, Wetherby, Yorkshire, England, for public access. The British Library Lending Division also has available many of the non-NASA publications cited in *STAR*.

European requesters may purchase facsimile copy or microfiche of NASA and NASA-sponsored documents, those identified by both the symbols # and * from ESA—Information Retrieval Service, European Space Agency, 8-10 rue Mario-Nikis, 75738 Paris CEDEX 15, France.

SUBMITTING DOCUMENTS

All users of this abstract service are urged to forward reports to be considered for announcement in *STAR*. This will aid NASA in its efforts to provide the fullest possible coverage of all scientific and technical publications that might support aeronautics and space research and development. If you have prepared relevant reports (other than those you will transmit to NASA, DOD, or DOE through the usual contract- or grant-reporting channels), please send them for consideration to the NASA Center for AeroSpace Information, P.O. Box 8757, BWI Airport, MD 21240.

Reprints of journal articles, book chapters, and conference papers are also welcome. These will be considered for announcement in *STAR*'s companion journal, *IAA*.

You may specify a particular source to be included in a report announcement if you wish; otherwise the report will be placed on a public sale at the National Technical Information Service. Copyrighted publications will be announced but not distributed or sold.

PURCHASE OF *STAR*

STAR is publicly available on annual subscription from the Superintendent of Documents, U.S. Government Printing Office, Washington, DC 20402.

STAR is available to registered users on annual subscription from the NASA Center for AeroSpace Information, ATTN: Registration Services, P.O. Box 8757, BWI Airport, MD 21240.

Microfiche of the abstract sections of *STAR* are available, on annual subscription only, from NTIS as PB91-911300, Attn: Subscriptions, 5285 Port Royal Road, Springfield, VA 22161. Annual subscription rates are $85.00 North America; $170.00 foreign. Abstract sections for previous years retroactive to 1964 are available at the current rates.

ADDRESSES OF ORGANIZATIONS

American Institute of Aeronautics and Astronautics
Technical Information Service
555 West 57th Street, 12th Floor
New York, New York 10019

British Library Lending Division,
Boston Spa, Wetherby, Yorkshire,
England

Commissioner of Patents and Trademarks
U.S. Patent and Trademark Office
Washington, DC 20231

Department of Energy
Technical Information Center
P.O. Box 62
Oak Ridge, Tennessee 37830

European Space Agency-Information Retrieval Service
ESRIN
Via Galileo Galilei
00044 Frascati (Rome) Italy

Engineering Sciences Data Unit International
P.O. Box 1633
Manassas, Virginia 22110

Engineering Sciences Data Unit International, Ltd.
251-259 Regent Street
London, W1R 7AD, England

Fachinformationszentrum Energie, Physik, Mathematik
GMBH
7514 Eggenstein Leopoldshafen
Federal Republic of Germany

Her Majesty's Stationery Office
P.O. Box 569, S.E. 1
London, England

NASA Center for AeroSpace Information
P.O. Box 8757
BWI Airport, Maryland 21240

National Aeronautics and Space Administration
Scientific and Technical Information Program (NTT)
Washington, DC 20546

National Technical Information Service
5285 Port Royal Road
Springfield, Virginia 22161

Pendragon House, Inc.
899 Broadway Avenue
Redwood City, California 94063

Superintendent of Documents
U.S. Government Printing Office
Washington, DC 20402

University Microfilms
A Xerox Company
300 North Zeeb Road
Ann Arbor, Michigan 48106

University Microfilms, Ltd.
Tylers Green
London, England

U.S. Geological Survey Library National Center
MS 950
12201 Sunrise Valley Drive
Reston, Virginia 22092

U.S. Geological Survey Library
2255 North Gemini Drive
Flagstaff, Arizona 86001

U.S. Geological Survey
345 Middlefield Road
Menlo Park, California 94025

U.S. Geological Survey Library
Box 25046
Denver Federal Center, MS914
Denver, Colorado 80225

NTIS PRICE SCHEDULES

(Effective October 1, 1991)

Schedule A
STANDARD PRICE DOCUMENTS AND MICROFICHE**

PRICE CODE	NORTH AMERICAN PRICE	FOREIGN PRICE
A01	$ 9.00	$ 18.00
A02	12.50	25.00
A03	17.00	34.00
A04-A05	19.00	38.00
A06-A09	26.00	52.00
A10-A13	35.00	70.00
A14-A17	43.00	86.00
A18-A21	50.00	100.00
A22-A25	59.00	118.00
A99	*	*
N01	60.00	120.00
N02	59.00	118.00
N03	20.00	40.00

Schedule E
EXCEPTION PRICE DOCUMENTS AND MICROFICHE**

PRICE CODE	NORTH AMERICAN PRICE	FOREIGN PRICE
E01	$11.00	$ 22.00
E02	14.00	28.00
E03	16.00	32.00
E04	19.00	38.00
E05	21.00	42.00
E06	24.00	48.00
E07	27.00	54.00
E08	30.00	60.00
E09	33.00	66.00
E10	36.00	72.00
E11	39.00	78.00
E12	43.00	86.00
E13	46.00	92.00
E14	50.00	100.00
E15	54.00	108.00
E16	59.00	118.00
E17	64.00	128.00
E18	69.00	138.00
E19	76.00	152.00
E20	88.00	176.00
E99	*	*

* Contact NTIS for price quote.

** Effective January 1, 1991, the microfiche copy of any new document entering the NTIS collection will be priced the same as the paper copy of the document.

IMPORTANT NOTICE

NTIS Shipping and Handling Charges

U.S., Canada, Mexico — ADD $3.00 per TOTAL ORDER

All Other Countries — ADD $4.00 per TOTAL ORDER

Exceptions — Does NOT apply to:

ORDERS REQUESTING NTIS RUSH HANDLING
ORDERS FOR SUBSCRIPTION OR STANDING ORDER PRODUCTS *ONLY*

NOTE: Each additional delivery address on an order requires a separate shipping and handling charge.

FEDERAL REGIONAL DEPOSITORY LIBRARIES

ALABAMA

AUBURN UNIV. AT MONTGOMERY LIBRARY
Documents Dept.
7300 University Drive
Montgomery, AL 36117-3596
(205) 244-3650 FAX: (205) 244-0678

UNIV. OF ALABAMA
Amelia Gayle Gorgas Library
Govt. Documents
Box 870266
Tuscaloosa, AL 35487-0266
(205) 348-6046 FAX: (205) 348-8833

ARIZONA

DEPT. OF LIBRARY, ARCHIVES, AND PUBLIC RECORDS
Federal Documents
Third Floor State Capitol
1700 West Washington
Phoenix, AZ 85007
(602) 542-4121 FAX: (602) 542-4400; 542-4500

ARKANSAS

ARKANSAS STATE LIBRARY
State Library Services
One Capitol Mall
Little Rock, AR 72201
(501) 682-2869

CALIFORNIA

CALIFORNIA STATE LIBRARY
Govt. Publications Section
914 Capitol Mall - P.O. Box 942837
Sacramento, CA 94237-0001
(916) 322-4572 FAX: (916) 324-8120

COLORADO

UNIV. OF COLORADO - BOULDER
Norlin Library
Govt. Publications
Campus Box 184
Boulder, CO 80309-0184
(303) 492-8834 FAX: (303) 492-2185

DENVER PUBLIC LIBRARY
Govt. Publications Dept. BS/GPD
1357 Broadway
Denver, CO 80203
(303) 571-2135

CONNECTICUT

CONNECTICUT STATE LIBRARY
231 Capitol Avenue
Hartford, CT 06106
(203) 566-4971 FAX: (203) 566-3322

FLORIDA

UNIV. OF FLORIDA LIBRARIES
Documents Dept.
Library West
Gainesville, FL 32611-2048
(904) 392-0366 FAX: (904) 392-7251

GEORGIA

UNIV. OF GEORGIA LIBRARIES
Govt. Documents Dept.
Jackson Street
Athens, GA 30602
(404) 542-8949 FAX: (404) 542-6522

HAWAII

UNIV. OF HAWAII
Hamilton Library
Govt. Documents Collection
2550 The Mall
Honolulu, HI 96822
(808) 948-8230 FAX: (808) 956-5968

IDAHO

UNIV. OF IDAHO LIBRARY
Documents Section
Moscow, ID 83843
(208) 885-6344 FAX: (208) 885-6817

ILLINOIS

ILLINOIS STATE LIBRARY
Reference Dept.
300 South Second
Springfield, IL 62701-1796
(217) 782-7596 FAX: (217) 524-0041

INDIANA

INDIANA STATE LIBRARY
Serials/Documents Section
140 North Senate Avenue
Indianapolis, IN 46204
(317) 232-3678 FAX: (317) 232-3728

IOWA

UNIV. OF IOWA LIBRARIES
Govt. Publications Dept.
Washington & Madison Streets
Iowa City, IA 52242
(319) 335-5926 FAX: (319) 335-5830

KANSAS

UNIV. OF KANSAS
Govt. Documents & Map Library
6001 Malatt Hall
Lawrence, KS 66045-2800
(913) 864-4660 FAX: (913) 864-5380

KENTUCKY

UNIV. OF KENTUCKY LIBRARIES
Govt. Publications/Maps Dept.
Lexington, KY 40506-0039
(606) 257-3139 FAX: (606) 257-1563; 257-8379

LOUISIANA

LOUISIANA STATE UNIV.
Middleton Library
Govt. Documents Dept.
Baton Rouge, LA 70803
(504) 388-2570 FAX: (504) 388-6992

LOUISIANA TECHNICAL UNIV.
Prescott Memorial Library
Govt. Documents Dept.
305 Wisteria Street
Ruston, LA 71270-9985
(318) 257-4962 FAX: (318) 257-2447

MAINE

TRI-STATE DOCUMENTS DEPOSITORY
Raymond H. Fogler Library
Govt. Documents & Microforms Dept.
Univ. of Maine
Orono, ME 04469
(207) 581-1680

MARYLAND

UNIV. OF MARYLAND
Hornbake Library
Govt. Documents/Maps Unit
College Park, MD 20742
(301) 454-3034 FAX: (301) 454-4985

MASSACHUSETTS

BOSTON PUBLIC LIBRARY
Govt. Documents Dept.
666 Boylston Street
Boston, MA 02117
(617) 536-5400 ext. 226
FAX: (617) 267-8273; 267-8248

MICHIGAN

DETROIT PUBLIC LIBRARY
5201 Woodward Avenue
Detroit, MI 48202-4093
(313) 833-1440; 833-1409
FAX: (313) 833-5039

LIBRARY OF MICHIGAN
Govt. Documents Unit
P.O. Box 30007
Lansing, MI 48909
(517) 373-0640 FAX: (517) 373-3381

MINNESOTA

UNIV. OF MINNESOTA
Wilson Library
Govt. Publications Library
309 19th Avenue South
Minneapolis, MN 55455
(612) 624-5073 FAX: (612) 626-9353

MISSISSIPPI

UNIV. OF MISSISSIPPI
J.D. Williams Library
Federal Documents Dept.
106 Old Gym Bldg.
University, MS 38677
(601) 232-5857 FAX: (601) 232-5453

MISSOURI

UNIV. OF MISSOURI - COLUMBIA
Ellis Library
Govt. Documents
Columbia, MO 65201
(314) 882-6733 FAX: (314) 882-8044

MONTANA

UNIV. OF MONTANA
Maureen & Mike Mansfield Library
Documents Div.
Missoula, MT 59812-1195
(406) 243-6700 FAX: (406) 243-2060

NEBRASKA

UNIV. OF NEBRASKA - LINCOLN
D.L. Love Memorial Library
Documents Dept.
Lincoln, NE 68588
(402) 472-2562

NEVADA

UNIV. OF NEVADA
Reno Library
Govt. Publications Dept.
Reno, NV 89557
(702) 784-6579 FAX: (702) 784-1751

NEW JERSEY

NEWARK PUBLIC LIBRARY
U.S. Documents Div.
5 Washington Street - P.O. Box 630
Newark, NJ 07101-0630
(201) 733-7812 FAX: (201) 733-5648

NEW MEXICO

UNIV. OF NEW MEXICO
General Library
Govt. Publications Dept.
Albuquerque, NM 87131-1466
(505) 277-5441 FAX: (505) 277-6019

NEW MEXICO STATE LIBRARY
325 Don Gaspar Avenue
Santa Fe, NM 87503
(505) 827-3826 FAX: (505) 827-3820

NEW YORK

NEW YORK STATE LIBRARY
Documents/Gift & Exchange Section
Federal Depository Program
Cultural Education Center
Albany, NY 12230
(518) 474-5563 FAX: (518) 474-5786

NORTH CAROLINA

UNIV. OF NORTH CAROLINA - CHAPEL HILL
CB#3912, Davis Library
BA/SS Dept.—Documents
Chapel Hill, NC 27599
(919) 962-1151 FAX: (919) 962-0484

NORTH DAKOTA

NORTH DAKOTA STATE UNIV. LIBRARY
Documents Office
Fargo, ND 58105
(701) 237-8886 FAX: (701) 237-7138
In cooperation with Univ. of North Dakota, Chester Fritz Library
Grand Forks

OHIO

STATE LIBRARY OF OHIO
Documents Dept.
65 South Front Street
Columbus, OH 43266
(614) 644-7051 FAX: (614) 752-9178

OKLAHOMA

OKLAHOMA DEPT. OF LIBRARIES
U.S. Govt. Information Div.
200 NE 18th Street
Oklahoma City, OK 73105-3298
(405) 521-2502, ext. 252, 253
FAX: (405) 525-7804

OKLAHOMA STATE UNIV.
Edmon Low Library
Documents Dept.
Stillwater, OK 74078
(405) 744-6546 FAX: (405) 744-5183

OREGON

PORTLAND STATE UNIV.
Millar Library
934 SW Harrison - P.O. Box 1151
Portland, OR 97207
(503) 725-3673 FAX: (503) 725-4527

PENNSYLVANIA

STATE LIBRARY OF PENN.
Govt. Publications Section
Walnut St. & Commonwealth Ave. - P.O. Box 1601
Harrisburg, PA 17105
(717) 787-3752

SOUTH CAROLINA

CLEMSON UNIV.
Cooper Library
Public Documents Unit
Clemson, SC 29634-3001
(803) 656-5174 FAX: (803) 656-3025
In cooperation with Univ. of South Carolina, Thomas Cooper Library, Columbia

TENNESSEE

MEMPHIS STATE UNIV. LIBRARIES
Govt. Documents
Memphis, TN 38152
(901) 678-2586 FAX: (901) 678-2511

TEXAS

TEXAS STATE LIBRARY
United States Documents
P.O. Box 12927 - 1201 Brazos
Austin, TX 78711
(512) 463-5455 FAX: (512) 463-5436

TEXAS TECH. UNIV. LIBRARY
Documents Dept.
Lubbock, TX 79409
(806) 742-2268 FAX: (806) 742-1920

UTAH

UTAH STATE UNIV.
Merrill Library & Learning Resources Center, UMC-3000
Documents Dept.
Logan, UT 84322-3000
(801) 750-2684 FAX: (801) 750-2677

VIRGINIA

UNIV. OF VIRGINIA
Alderman Library
Govt. Documents
Charlottesville, VA 22903-2498
(804) 924-3133 FAX: (804) 924-4337

WASHINGTON

WASHINGTON STATE LIBRARY
Document Section
MS AJ-11
Olympia, WA 98504-0111
(206) 753-4027 FAX: (206) 753-3546

WEST VIRGINIA

WEST VIRGINIA UNIV. LIBRARY
Govt. Documents Section
P.O. Box 6069
Morgantown, WV 26506
(304) 293-3640

WISCONSIN

ST. HIST. SOC. OF WISCONSIN LIBRARY
Govt. Publications Section
816 State Street
Madison, WI 53706
(608) 262-2781 FAX: (608) 262-4711
In cooperation with Univ. of Wisconsin-Madison, Memorial Library

MILWAUKEE PUBLIC LIBRARY
Documents Div.
814 West Wisconsin Avenue
Milwaukee, WI 53233
(414) 278-2167 FAX: (414) 278-2137

WYOMING

WYOMING STATE LIBRARY
Supreme Court & Library Bldg.
Govt. Publications
Cheyenne, WY 82002
(307) 777-5920 FAX: (307) 777-6289

National Aeronautics and
Space Administration
Code NTT
Washington, D.C.
20546

Official Business

Penalty for Private Use, $300

SPECIAL FOURTH-CLASS RATE
POSTAGE & FEES PAID
NASA
PERMIT No. G27

POSTMASTER: If Undeliverable (Section 158 Postal Manual) Do Not Return